PHOTOGRAPHIC SURFACE PHOTOMETRY OF GALAXIES IN THE VIRGO CLUSTER

Christopher W. Fraser

A Thesis Submitted for the Degree of PhD
at the
University of St Andrews

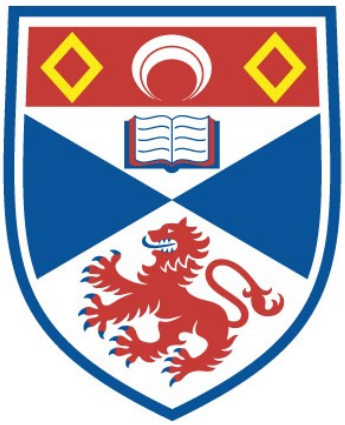

1971

PHOTOGRAPHIC SURFACE PHOTOMETRY OF GALAXIES IN THE VIRGO CLUSTER

by

Christopher W. Fraser

A thesis presented for the Degree of Doctor of Philosophy in the University of St Andrews.

March 1971.

ProQuest LLC.
789 East Eisenhower Parkway
P.O. Box 1346
Ann Arbor, MI 48106 – 1346

DECLARATION

I hereby declare that the following Thesis is based on the results of experiments carried out by me, that the Thesis is my own composition, and that it has not previously been presented for a Higher Degree. The research was carried out at the University Observatory, St Andrews.

CERTIFICATE

I certify that Christopher W. Fraser has spent nine terms at Research Work at the University Observatory, St Andrews, that he has fulfilled the conditions of Ordinance No. 16 (St Andrews) and that he is qualified to submit the accompanying Thesis in application for the Degree of Ph.D.

PREFACE

Surface photometry is one area of extragalactic studies in which information is urgently needed by optical as well as radio astronomers. The aim of this thesis is to supply some of the photometric parameters for 48 galaxies in two international colour systems. The reader will notice that descriptions are included of many detailed aspects of the work and little attention is paid to the more basic problems. This is because the discussion of the basic problems in photographic photometry of galaxies formed the contents of an M.Sc. thesis.

Volume one is devoted to a detailed description of the methods used for the reduction techniques together with a discussion of the results, while volumes two and three contain the photometric data. In this volume, the first chapter is concerned with previous investigations and the following chapter contains detailed descriptions of the instruments and methods used in the preliminary plate reductions. The subject of isophotometry is dealt with in the third chapter, while in the fourth and fifth chapters respectively, mention is made of the reduction techniques, together with conclusions which may be deduced from the photometric data. This information is

given in volume two for those galaxies with NGC Catalogue numbers from 4189 to 4459, while the data for objects from NGC 4461 to NGC 4762 are listed in the third volume of the thesis.

VOLUME ONE - CONTENTS

Chapter I

1.1 Introduction. The aim of the first chapter of this thesis is to make a critical examination of the observational techniques and reduction methods adopted by other authors whose work was closely related to the current investigation on surface photometry of galaxies. No attempt has been made to include every published work on the subject in this appraisal and therefore it is only to sections of those papers which are particularly relevant to the present work that minor criticisms will be given. However, in view of the special attention devoted to the sources of error which will be revealed throughout this study of the development of surface photometry, it should become apparent in succeeding chapters that the elimination of such errors in the present investigation ought to enable results of high photometric accuracy to be achieved.

1.2 Review. Following the pioneer investigations of Reynolds (1919), in which he found that the luminosity along the major axis of M31, could be represented by the expression

$$\text{Luminosity} = \frac{\text{Constant}}{(x + 1)^{\frac{1}{2}}}$$

for radial values of x less than 7' from the nucleus, the first investigator to obtain detailed information on galaxies was Hubble (1930). He obtained luminosity curves for fifteen elliptical galaxies and derived analytical expressions to represent the distribution of luminosity within the objects. The account which was given not only of the observational details but also the reduction techniques contained considerably more detail than is found in some of the more recent papers. In fact, modern papers on galaxy photometry now tend to omit certain details which, although clearly appreciated by the authors involved, could highlight and illustrate by their inclusion some of the more serious difficulties of the subject to readers who are not particularly well versed in this specialized field. However, it is as a result of the inclusion of some details that two major criticisms, first suggested by de Vaucouleurs (1948a), may be put forward.

The first concerns the observational procedure, in which a series of exposures usually ranging from 15 minutes to 5 seconds was made on <u>one</u> photographic plate at the Newtonian focus of the 100-inch Mount Wilson telescope. Let us suppose that five exposures, t_1 to t_5, were made for one galaxy. Under these conditions the first galaxy exposure is made up of three components:

a zero pre-exposure to the sky, an exposure t_1 to the sky plus galaxy, and a post-exposure $t_2 + t_3 + t_4 + t_5$ to the sky. The second galaxy exposure has the respective values t_1, t_2 and $t_3 + t_4 + t_5$ for the sky pre-exposure, the sky + galaxy exposure and the sky post-exposure. It becomes clear that the five galaxy exposures were made under different conditions. Consequently, microphotometer tracings across the image of the galaxy would not give an accurate representation of the luminosity distribution, since pre- and post-exposures produce changes in the latent images which in turn affect the response of the photographic plate, particularly when the plate has been exposed to very low levels of illumination.

Secondly, errors were introduced in the calibration of the plates. Before the actual calibration exposure, Hubble first subjected the plates to an exposure which would "simulate the sky-fog on the nebular plate". In the case of the first galaxy exposure, this system would have been acceptable had no errors been introduced by this method of pre-exposure, but the sky-fog exposure prior to calibration was always a pre-exposure, while in the actual observations, it was solely a pre-exposure on only one occasion out of five.

Nevertheless, Hubble's work was still of a sufficiently high standard to enable him to re-introduce Reynold's law (1913) for the brightness B of a point at a distance r from the centre of an elliptical galaxy in the form

$$B = B_o/(r + a)^2$$

where B_o is the central brightness and a is a scale parameter varying from one galaxy to another.

Redman was working on a similar problem in 1931, although his first paper on the subject was not published until 1936. He proposed and used two methods for the photometry: the first required one exposure to the galaxy followed by an extrafocal exposure to standard stars, while the second method, the better from the point of view of photometric accuracy due to the difficulties encountered with the former in detecting the outer regions of a galaxy, needed a set of exposures of the galaxy in order to record more adequately the very considerable intensity range from the centre to the faint outer regions. The main criticism of this work was that the calibration spots were superimposed on the sky-fog. Redman and Shirley (1938) thought that as both the calibration and galaxy exposures were superimposed on the sky fog, they claimed that this sky fog could then be omitted in subsequent measurements.

Redman and Shirley's observing and calibration conditions were similar to the first exposure of the set taken by Hubble in his work, where the sky-fog was only a pre-exposure just the same as the calibration pre-exposure. However, what both Redman and Hubble failed to recognize was that the pre-exposure of the sky-fog on the calibration areas would affect the shape of the resulting characteristic curve.

In 1948 de Vaucouleurs made a major contribution to the subject with papers (1948, 1948a) which included a very extensive and quantitative discussion of the types of errors which are expected in galaxy photometry, together with the measurements made of three galaxies. The results which had been obtained hitherto by other observers for the total magnitudes and luminosity profiles of several galaxies did not appear to be closely inter-related. This was because of difficulties with

a) accurate calibration techniques

b) determination of the precise level of the sky background.

de Vaucouleurs' values of magnitudes and profiles were supplemented by several other parameters, in particular the effective dimensions and effective luminosity profiles. The advantage of these 'effective' values was that

they gave intrinsic characteristics of the galaxy which were independent of the resolving power of the telescope used for the observations. These values were precise so long as the effective radius of the galaxy was considerably greater than the effective radius of the instrumental scattering function as determined from stellar images. Elliptical isophotes were assumed after microphotometer tracings across the main axes of the object had been taken; these isophotes were used in the calculation of the total luminosity of the system. The total integrated luminosity emitted between the centre of a galaxy with circular symmetry and an isophote of distance r from the centre is $L_r = 2\pi \int_0^r I(r)\ r\ dr$ and the total luminosity is $L_T = 2\pi \int_0^\infty I(r)\ r\ dr$. The fraction of the total luminosity emitted between the curve and r is defined by $k(r) = L_r/L_T$. For elliptical objects, both Redman and de Vaucouleurs obtained the integrated luminosity by integrations which were based upon the surface luminosity distribution along the major and minor axes of these objects. The function k(r) defines the relative integrated luminosity curve as a function of r, and the effective radius r_e, introduced by de Vaucouleurs (1948), is defined so that $k(r) = \frac{1}{2}$. i.e. one half of the total luminosity of the system is

emitted within this distance from the centre. de Vaucouleurs also deduced a relationship for elliptical galaxies for which the intensity at a distance r from the centre was proportional to the quarter power of that distance, namely

$$\log J = -3.33(\rho^{\frac{1}{4}} - 1) \text{ where}$$

$J = I/I_e$ and $\rho = r/r_e$, I_e being the intensity corresponding to r_e. This formula has the advantage over Hubble's relation that neither the integrated brightness nor the central intensity is infinite.

Bigay (1951) published work on galaxies and began his paper with a review of the four methods used prior to 1951 for photometry of galaxies. They were

1) direct comparison between the galaxy and standard stars on the same plates obtained on telescopes with short focal lengths
2) comparisons between stars and galaxy images on plates taken out of focus
3) photo-electric aperture measurements and
4) magnitudes deduced from photometric profiles.

After describing these methods in detail, Bigay gave the results of measurements of the magnitudes of 175 bright galaxies by a method which was novel at the

time, viz. Fabry photometry; this work dealt with integrated rather than surface photometry. Plotting the magnitudes which he obtained against other published magnitudes, as a test of the validity and accuracy of his results, he found that the correlation exhibited a scatter of one and a half magnitudes on the average.

Evans (1951, 1952) investigated some southern elliptical nebulae in 1951 by studying isophotes which had been assembled from microphotometer tracings. A large section of the work was devoted to the determination of the size of the errors which could occur if the estimate of the level of the sky background both on the galaxy profile and on the characteristic curve was not known with sufficient accuracy. It was found that for an error of 0.02^{m} in the determination of the magnitude of the sky background, the subsequent error in the calculated magnitude of the galaxy could be as large as 0.15^{m}. Evans noted that in NGC 1291, there appeared to be a steady rotation of the major axes of successive isophotes; this effect was particularly evident on two plates microphotometered at 90^{o} to each other. Evans highlighted certain points which are not detailed by other writers such as the quantitative determination of sky background errors,

while certain points which should have been included to retain the same consistency for detail, such as the design of a tube sensitometer, were noticeably absent. The writer has been informed on several occasions by Evans that his papers were often shortened at the suggestion of referees, and that but for these suggestions, he would have included a detailed description of a tube sensitometer.

In 1953 de Vaucouleurs published work on the distribution of mass and luminosity in elliptical galaxies. The methods used to obtain the luminosity distribution were similar to those used in 1948 and the results also confirmed the linear variation of intensity with the quarter power of distance.

The first photo-electric work on the subject came from Stebbins and Whitford (1937), who measured magnitudes of 175 galaxies brighter than fifteenth magnitude. These magnitudes were obtained using a Kunz photo-cell attached to the 60- or 100-inch Mount Wilson reflectors, together with four focal plane diaphragms giving field diameters of 42, 64, 128 and 163 arc sec on the 100-inch. These values were increased by a factor of 1.7 when used on the 60-inch telescope. When this work was carried out, the largest

aperture was considered sufficiently large to allow the total light of the majority of the chosen galaxies to be measured, this judgement being based upon the accepted measured dimensions of the objects at that time. However, it is now known from data on micro-photometer tracings of plates of galaxies obtained with modern emulsions (e.g. van den Bergh 1969) that the outer regions of galaxies extend considerably further than earlier dimensions had indicated. Consequently, the early work of Stebbins and Whitford would suffer from incomplete measurements of the total magnitudes for many of the systems. Aware of this difficulty, Stebbins and Whitford (1952) published a further set of 176 magnitudes of galaxies in the range $9.2 \leqslant m \leqslant 18.2$. This later work improved on the former in two ways, viz., the use of a 1P21 photomultiplier in place of the photo-cell, and the availability of a field diaphragm of 5.1 arc min on the 100-inch, or 8.7 arc min on the 60-inch telescope. However, even with this extra diaphragm, the possibility was still present of missing the faint outer extensions of giant elliptical systems.

Photo-electric scans were first attempted by van Houten, Oort and Hiltner in 1948, although their results were not published until 1954. A diaphragm could be

driven by a synchronous motor in an arbitrary direction in the Cassegrain focal plane of the McDonald 82-inch telescope, and tracings were made along the principal axes of the galaxy. The amplifier sensitivity was varied by the use of different grid leaks, but the determination of the relative sensitivities of these grid leaks proved difficult, due to the variation of their ratios with temperature and humidity. Furthermore, although the dark current was measured before and after each tracing, the value of the night sky for each galaxy was determined only once for each night. These difficulties lead to considerable errors in the results, and for this reason, the work could only be regarded as unsuccessful.

Further photo-electric work was published by Pettit (1954), who determined the magnitudes on the photographic scale and also the colour indices of galaxies with the 60- and 100-inch Mount Wilson telescopes between 1947 and 1954. The telescope observations were made using a refrigerated 1P21 photomultiplier, Schott BG 1 and GG 7 filters were used for the blue and yellow readings and the field apertures ranged in diameter from 0.2 to 8.6 arc min. The observational programme in 1947 and 1948 was confined to the 60-inch

telescope with the following two aims in view:

1) to measure galaxies of large angular diameters and
2) to provide standards on the international system for use on the 100-inch telescope where the polar calibration sequence was not available.

For the latter purpose, the central stars of Selected Areas in the 30° zone which passed near the zenith were chosen, enabling the extinction and reddening functions for each night to be obtained. A star was measured from a low altitude to the meridian on four occasions each night, to determine the colour equation and atmospheric extinction. The measurements of both the galaxy and the comparison star were reduced to the zenith before converting to magnitude. The magnitudes which were obtained depended on the free deflection minus the yellow (F-Y), the reduction to the zenith was made by plotting log (F-Y) against sec z for the Selected Area and the constant $\underline{a}$ determined in the extinction formula $C = a(\sec z - 1)$. Normally, the numerical value of $\underline{a}$ was approximately equal to 0.1, and when this value was substituted in the above equation, it gave a correction to C which in turn, when added to the observed log (F-Y), reduced all the deflections for the night to the zenith.

The next step in the magnitude determination involved the calibration of the instrument for the night. Since most of the objects studied were fainter than ninth magnitude, it was this value which was chosen as the basic brightness for the calibrations; this meant that log (F-Y) was determined for a ninth magnitude star at the zenith for the night. If North Polar Sequence stars were used, these would also require to be reduced to the zenith using the extinction formula, since their magnitudes were given for the zenith at Mount Wilson. The log (F-Y) for each such star, if it had been ninth magnitude, was obtained using the relation

$$\log (F-Y)_9 = \log (F-Y) + 0.4(m_{pg} - 9)$$

and so the magnitude for any object was given by the expression

$$m_{pg} = 10/4 \left[\log (F-Y)_9 - \log (F-Y) \right] + 9$$

The detailed description of this aspect of the work has been given because it highlights the contrast between some of the techniques used to obtain reasonably consistent photo-electric measurements in comparison with the more involved methods necessary

for successful photographic work, which will be described in the course of this thesis.

The accuracy of the results was checked by two methods. First, the internal agreement of repeated measurements which gave average departures of 0.07^m and secondly, agreement with other observers' measures. A comparison with the Shapley-Ames Catalogue showed that when the magnitudes were divided into four groups, the mean departures per group ranged from -0.3^m to $+0.1^m$, while comparison with Bigay's measurements showed a similar range from -0.10^m to $+0.13^m$. Such comparisons are not really justified, because the inherent difficulties of centring the galaxy in the apertures and of ensuring that the apertures are sufficiently large to allow the total luminosity of the galaxy to be measured, mean that a comparison is being made between an unknown luminosity measured photo-electrically, depending on the angular size and central brightness of an object, and a luminosity governed only by the limit to which measurements may be made above the threshold brightness on a photographic plate. Furthermore, Pettit does not state clearly how often or on what location measurements are made of the sky background. It is well known that where the galaxy and sky are

measured together, the sky can be contributing as much as 90% of the total light, and it is for this reason that measurements are made of the sky to the north, south, east and west of the galaxy, in order to minimize not only position errors but also the continual variation in the brightness of the sky background.

The results of Pettit's colour index work lead to the following formulae for the relationship between colour index and magnitude in the range $9 \leq m \leq 18$:-
For ellipticals,

$$C.I. = 0.04\ (m_{pg} - 9) + 0.84$$

while the corresponding equation for spirals was

$$C.I. = 0.08\ (m_{pg} - 9) + 0.50$$

thus making elliptical galaxies redder than spirals.

With the publication of Holmberg's classic paper (Holmberg 1958), there became available to other astronomers a comprehensive catalogue of magnitudes and colours of galaxies. The advantage of this work was that since each magnitude measured represented the light contained within a certain isophote corresponding to a surface luminosity which was more or less constant for the entire plate material, all the

magnitudes were comparable measurements forming a homogeneous system. The observational procedure employed was to take two exposures of equal duration on separate halves of the plate, one an in-focus exposure of the galaxy, the other an extra-focal exposure of the stars in a comparison field. Microphotometer tracings of the stars then furnished the relation between plate density and surface luminosity, hence making the calibrations "independent of artificial means such as tube sentitometers". The magnitudes were obtained from the numerical integration of parallel cross-sections across each object, together with one scan along the major axis. Since the observations dealt with surface objects, the results were almost independent of seeing conditions between the galaxy and calibration exposures. In addition, Holmberg pointed out that focussing and guiding errors in the telescope, which could lead to large errors in stellar photometry, do not arise in nebular work. Of course, this is only applicable when it is the total luminosity of the system which is being measured, and not detailed photometry of the nuclear regions, which could be affected by the instrumental scattering function. Furthermore, photo-electric observations

give good results for galaxies with a rather high surface brightness, where the relatively steep gradients make photographic work rather difficult. In contrast, with galaxies of low surface brightness, it is only by photographic methods that reliable results can be obtained, due to the difficulty of eliminating field stars in the aperture field when using photo-electric measurements. Another problem in photo-electric work, the variation in sky brightness, which is unimportant in photographic work since the galaxy plus sky are being observed simultaneously, could only be overcome successfully by an observational technique which would permit a continuous monitoring of the sky background. A twin telescope, such as the one at the Royal Observatory, Edinburgh, would be well suited to this requirement.

One minor criticism of Holmberg's work is that at the beginning of the observational programme, each plate was calibrated individually, the exposure of the galaxy being made on one half of the plate and the star field exposure on the other. However, towards the end of the work, the two plates facing each other within a sub-package were treated as one photometric unit. Although it was claimed that no noticeable

increase in the errors resulted from this procedure, it is, nevertheless, true that no two photographic emulsions can have truly identical calibration curves. The principal sources of error in the work were the following:-

1) A difference in the sky fog between the region surrounding the galaxy and the calibration field.
2) Changes in the sensitivity of the emulsion between the first and second exposures.
3) the smoothing effect obtained due to the use of too large a scanning aperture in the microphotometry and
4) incorrect extrapolation over the nebular regions for the background curves representing the sky-fog.

In comparisons with other observers' results, Holmberg pointed out one possible reason for the unexpectedly large errors which arose in Pettit's (1954) work. These errors were due partly to inaccurate magnitudes of the North Polar Sequence stars which were used to calibrate the photo-electric galaxy measurements and also to the high ultra-violet transmission of Pettit's BG 1 filter (de Vaucouleurs 1961a). Holmberg's comparison with Stebbins and Whitford's (1952) photo-electric work produced deviations which ranged from -0.29^m to $+0.17^m$ with a mean deviation of -0.03^m. A

possible source of error in the photo-electric work was the difficulty in locating the centres of the galaxies without a pronounced central core in the field apertures. Following these comparisons, Holmberg studied integrated colours of galaxies against their classification type, rather than studying colours at specific points within the galaxy.

The methods by which galaxy dimensions were measured, discussed in detail by de Vaucouleurs (1957) were standardized in a paper by the same writer published in 1959. Prior to these publications, the brightness dimensions referred to a given isophote of some specified brightness. The effective dimensions, defined previously (de Vaucouleurs 1948), had the advantage that only relative measurements of surface intensities with an arbitrary zero point were required for their calculation, whereas brightness dimensions required the absolute measurement of surface brightness in a given magnitude scale. For an elliptical system, the effective dimensions were D_e and d_e, giving an axial ratio of d_e/D_e. Photometric dimensions, which are in nature brightness dimensions, are determined by the threshold brightness $\underline{I}$ together with the law of luminosity distribution $I(r)$ in the image, while the

effective dimensions depend only upon the latter. The two laws for the luminosity distribution were summarized (de Vaucouleurs 1961c) in the following form:-

1) for ellipticals, the quarter power law (de Vaucouleurs 1948) was now written in the revised form:-

$$\log J = -3.33(\rho^{\frac{1}{4}} - 1) \quad \text{and}$$

2) for lenticulars and spirals the relation was

$$\log J = -0.729(\rho - 1).$$

The coefficients -3.33 and -0.729 are required by the form of the respective functions.

Another type of dimension, micrometric, was a direct micrometer measurement of photographic negatives. These dimensions, of course, refer to an unspecified mean brightness threshold depending upon the properties of the object, of the foreground and of the photographic plate itself, de Vaucouleurs decided after experiments that the most significant parameters were the major diameter D and the axial ratio d/D. If many independent measurements were available, together with correspondingly good calibrations, the corrected micrometric data could be used as distance indicators. A statistical analysis of apparent diameters (D) as a function of axis ratio D/d suggested that the relationship between the face-on

diameter and the observed diameter D is

$$\log D = \log D(0) + 0.4 \log D/d$$

where D(0) was the face-on diameter i.e. the diameter that would be observed if the axial ratio were equal to unity or if log D/d = 0. Consequently, a galaxy which was observed edge-on with an axial ratio R = d/D = 0.2 appeared with a maximum diameter almost twice the face-on diameter. This confirmed the observational evidence for the apparent excess of edge-on systems in statistical surveys. Recently, de Vaucouleurs et al. (1970) have found that the coefficient of log D/d is nearer the value 0.2. The principal aim in securing more consistent data on diameters was the need to improve the extrapolation correction, $m_r - m_t$, which must be applied to the integrated magnitude m_r within a distance r from the nucleus in order to calculate the total or asymptotic magnitude m_t.

Departing from the field of photographic photometry, de Vaucouleurs (1961a) published integrated colours in the UBV system for 148 galaxies observed photo-electrically in 1957 and 1958. After having determined (U-B) and (B-V) colours, the face-on colours (i.e. corrected for tilt effects), $(U-B)_o$ and $(B-V)_o$ were found to very as a function of morphological type and of the ratio

A/D(0), the field aperture to the face-on diameter. One of the advantages of these photo-electric measurements is that they can be used to fix the zero point of photographic measurements. By knowing the diameter 2r of the field aperture used in the photo-electric work, it is possible to establish the relationship between m_r, the measured magnitude with reference to the standard stars in the UBV system, and L_r, the integrated luminosity within the same radius derived from the photographic plate, in the form m_r = constant - 2.5 log L_r. This constant yields the zero point of the photographic photometry.

The colour indices quoted do not measure the local colour, C(r), at a given radius r from the centre of the galaxy, but the integrated colour out to a given radius r defined by the following equation

$$|C|_0^r = \int_0^r C(r).I(r).dr \; / \int_0^r I(r).r.dr$$

Clearly, if detailed knowledge of the law of luminosity distribution I(r) were available, it would be possible in principle, to derive C(r) itself from the integrated colours, although in practice, this is not the case due to the sensitivity of integral equations to accidental errors of measurement. When the face-on colours were plotted as a function of A/D(0) for several types of

galaxy, the general decrease of integrated colour indices outwards from the centre, together with the tendency to reach asymptotic values for ratios of $A/D(0) \geqslant 1.0$, is reversed and becomes an increase for Magellanic type spirals and irregulars. The range of values for the colour index was small for ellipticals and lenticulars and larger for the a, b and c stages of spirals. In comparison of his colours with other observational results, de Vaucouleurs pointed out when a comparison was made with Holmberg's (1958) values, asymptotic colours for which $A/D(0) > 1$ had to be used, because Holmberg's values were differences between the total photographic and photovisual magnitudes, as determined by the integration of microphotometric cross-sections.

The next two important papers to appear were by M.H. Liller (1960) and van Houten (1961). References to both papers appear to be relatively rare, and it is therefore considered prudent to make a more critical examination of these two papers in comparison with the more general background information which has been the object of this appraisal of published work in the field of galaxy photometry.

The most obvious source of error common to both papers, was the apparently indirect method of plate

calibration. Liller used two plate collections in a study of the distribution of intensity of elliptical galaxies in the Virgo cluster, one taken with the 24-36-inch Curtis Schmidt, the other taken with the 48-inch Mount Palomar Schmidt. The Curtis Schmidt plates were calibrated in a fairly conventional manner, and by a comparison between the intensities within galaxies common to both sets of plates, a calibration was obtained for the 48-inch Schmidt plates, which had previously been uncalibrated. The location in this manner of identical points within a galaxy on different plates is extremely difficult to achieve accurately, and the graph which Mrs Liller used to reinforce her argument that the calibration was satisfactory was derived from measurements of three objects. This graph was then used as a calibration standard for <u>all</u> the 48-inch plates. Isophotes for the galaxies were obtained with the Michigan isophotometer, and graphs were drawn of the ellipticity of the isophotes against distance from the centre. It was found that spiral galaxies exhibited a curve of increasing ellipticity from the centre outwards, while the curve for ellipticals rose to a maximum at a point approximately equal to half the value of the semi-major axis. Agreement with the quarter power law was obtained for most of the objects under investigation,

although some galaxies which did not satisfy the law were shown by de Vaucouleurs (1961c) to be SO types.

The year 1961 saw the publication of a very extensive study by van Houten of 20 galaxies photographed by Oort from 1936 onwards at Mount Wilson. Oort's original plates had sensitometer marks, together with the additional calibration of extrafocal exposures on Selected Area stars, but in the photometric reductions, both these calibration sources produced different results. The absolute calibration was to be provided by photo-electric observations of four galaxies, together with extra-focal exposures of standard stars. However, before the absolute calibration could be used, it was necessary to obtain the relative calibrations, and these were obtained with the following rather indirect technique.

The images of the extra-focal Selected Area stars which appeared as rings on the plate were scanned in two mutually perpendicular directions. Since coma was present, it was found that only those images in the centre of the field gave four deflections duitable for averaging and which could give a value for the density scale. Even if the abscissa of the characteristic curve, the intensity, had been known

with a high degree of accuracy, the possibility of errors in the curve would, nevertheless, have been considerable for two reasons. The first was the poor density measurements and secondly, more important, the intensity scale used by Seares in his 1930 catalogue of magnitudes of Selected Area stars. Although these magnitudes were known to have a scale error for stars fainter than magnitude 14^m, van Houten neglected this error in the construction of the calibration curves which he subsequently described as "not ambiguous". The general form of the curve was established after inspection of a mean curve determined in 1940 by Kleibrink; unfortunately, the blackening of the plates had changed during the intervening years. Finally, differences in the exposure times of the galaxy and standard stars introduced errors due to reciprocity failure, and the Schwarzschild exponent had to be calculated. It is surprising that any useful information whatever resulted from the photometry of plates which seemed beset by so many calibration difficulties. In addition, one of the sets of isophotes which were constructed for each galaxy contained deformations due to the fact that the plate had been broken, the pieces laid together on the microphotometer

and the isophotes assembled from the resulting tracings! Since the apertures used for the photo-electric observations were much larger than those used for the microphotometry, dispersion conditions had to be applied to the data before the relationship between the two systems could be established.

Part of the discussion of results concerned the variation of axial ratio with different isophotes. van Houten found that for NGC 4472, 4486, 4621 and 4649, the axial ratio of all isophotes was constant, but Oort (1940) de Vaucouleurs (1948, 1959a) and Liller (1960) had shown that there were variations in the ellipticities. This would suggest that the accuracy of van Houten's isophotes was not particularly high, especially since Liller's isophotes were obtained using the University of Michigan isophotometer, which was known to produce reliable results. van Houten tested the validity of the quarter power law for ellipticals, and the intensity distributions of the four galaxies already mentioned for which the axial ratio of the isophotes remained constant could be well represented by de Vaucouleurs' (1959) relation. However, this relationship, which was known to hold only for elliptical objects, was then tested for mixed edge-on systems and spirals. Surprisingly, the only agreement

obtained was for the minor axes of the bulges of spirals but van Houten still denounced the quarter power law on the basis of these comparisons.

Around the same time as de Vaucouleurs ' (1961) photo-electric work, Tifft (1961, 1963) was conducting an investigation into the colours of galaxies. The scope of the work involved four-colour photometry of about 50 galaxies, each galaxy usually being observed with three diaphragms. An important feature of the work was that, in addition to plotting diagrams for the variation of integrated colours against A/D(0), Tifft plotted diagrams for concentric ring measurements against A/D(0) to study the actual colour within the galaxy. There was no appreciable difference between the two diagrams, which agreed with the results of de Vaucouleurs (1961).

Shobbrook (1965), who made a similar investigation of 53 southern galaxies, also determined their total magnitudes. In order to obtain such magnitudes directly, it would have been necessary to take measurements through field diaphragms whose diameters were at least twice the accepted diameter of the galaxies. Naturally, this was found impossible for some of the larger brighter objects, but the problem

was supposedly overcome by a rather indirect method which involved the determination of the dependence of other observers' magnitude measurements upon the ratio A/D(0). Extrapolation then produced for different types of objects the magnitudes corresponding to the largest A/D(0) ratios required by the project.

Two papers have been published in recent years concerning the relationship, if any, between the ellipticity and diameters of elliptical galaxies. Edelen (1965) proposed that the mean linear diameter was a decreasing function of the ellipticity, and in contrast, Rood and Sastry (1967) found no relationship between the two quantities after an examination of 176 elliptical systems.

One publication closely related to the work of this thesis is that by Markaryan, Oganesyan and Arakelyan (1965). Blue and yellow observations were made of ten elliptical and lenticular galaxies in the Virgo cluster using the 40-inch Schmidt telescope at Byurakan Observatory. The reductions were performed on a microphotometer which had an attachment to permit an adjustment of 3 to 4 microns in two mutually perpendicular directions. Once more the calibrations were not of the accurary demanded by precise

photometry, because following the galaxy exposure, another plate from the same box was exposed for the same time as the galaxy to an out-of-focus North Polar Sequence, obtained by inserting a plane-parallel piece of glass in front of the emulsion, in order to furnish the calibration. Both plates were processed simultaneously to minimize errors. This calibration technique is similar to that used by Holmberg (1958). For each galaxy under study, a chart was assembled giving the brightness of the galaxy within grid squares of size 9.7 arc seconds. This information was used to draw graphs of the surface brightness and colour index distributions along the principal axes. Much larger variations of the colour index were found when compared with other results (e.g. de Vaucouleurs 1961a). However, there was a moderate degree of uncertainty in the establishment of the zero points of the colour curves. A continuation of this work examined the surface distribution of six spiral galaxies (Markaryan et a 1966). Rood and Baum (1967) have catalogued 315 galaxies in a 0.32 square degree field in the centre of the Coma cluster. In later work (Rood and Baum 1968), the detailed

reduction procedure for deriving brightness profiles for 32 objects was described. Due to the large sampling interval used in the microphotometer digitization, errors may be introduced with possible resolution difficulties. King (1961) has attempted to obtain empirical laws for stellar density distribution in globular clusters. This density for $r > 1'$ was found to be closely proportional to $\left[(1/r) - (1/r_o)\right]^2$ where r_o denotes the limiting radius at zero density. Later work (1962a) produced a law represented by three parameters: (1) a number factor (2) the size of the central core r_c and (3) the limiting radii r_o. The profile is characterized by a concentration ratio (defined by r_o/r_c) which may have values from 4 to 130 for the globular clusters. This same profile fits the dwarf ellipticals, where the ratios range from 3 to 10, but larger values are found for the giant ellipticals, with their higher central brightness. For the central regions, the surface density is given by $f = f(o)/\ 1 + (r/r_c)^2$, where f(o) denotes the central surface density (King 1962b); complete profiles for 9 globular clusters have been obtained (1966) using the above relations.

The first Atlas of photometric results for many galaxies was published by Sersic (1968); it gave photographs, descriptions and detailed surface photometry of 50

southern galaxies. Although the parameters in such a recent publication are not identical to the "standards" defined by de Vaucouleurs (1968a), there is still some similarity between the two systems. For example, if S(m) denotes the area of the galaxy brighter than magnitude m, then

$$S(m) = K(m - m'')^n$$

where m" defines the zero point and the exponent n ranges in value from 2 for late-type spirals to 8 for ellipticals; intermediate values of n denote mixtures of types. The value of n is related with the parameter m_o by the relation

$$m_o = m'' + 1.086\ n.$$

Possible errors in the Atlas may be found in galaxies with complex structures, since some of the isophotes were drawn "with the aid of photographs".

Kron and Papiashvili (1967) and Walker and Kron (1967) used the electronic camera in an investigation of M13 and M15, and obtained good agreement with the quarter power law (de Vaucouleurs 1948, 1959). The superb advantages of the instrument are its high storage capacity, relatively high quantum efficiency, low noise level, and, more recently (e.g. Ables & Kron 1967), with a suitable choice of emulsion and development conditions, its linear

response (some difficulties were present in original designs (Walker 1965) with non-linearity of response). Since the camera has electrostatic electron optics, the photo-cathode must be curved towards the photographic plate. Due to the small size of the cathode, the largest circular field available at the present time is 35 mm diameter. Larger fields may be possible with the Griboval camera which uses magnetic focussing.

In conclusion, six recent publications offer encouragement for workers in the future to improve upon the accuracy of previous measurements. In the first place, the characteristic curve has now been expressed in a linear form by de Vaucouleurs (1968). This relationship should enable more precise calibrations to be obtained for astronomical emulsions. Secondly, the use of the IIIaJ emulsion and a Wratten 2C or 4 filter (van den Bergh, 1969, Arp and Bertola 1969, 1971) has enabled faint outer regions of galaxies to be more easily detected than in the past. Such regions have been confirmed by de Vaucouleurs (1969, 1970c) for M87 and NGC 4889 using sensitive photo-electric methods. This wealth of information still available on these faint outer regions may herald the beginnings of significant advances in theories concerned with the structure and evolution of galaxies.

Chapter II

2.1 Introduction. While the last few decades have seen rapid advances in many fields of astronomical research, detailed surface photometry remains one field in which astronomers have seemed reluctant to devote the attention necessary to keep pace with the progress in other related topics in the study of galaxies. Only Oort (1940), de Vaucouleurs (1961b, 1963b, 1963c, 1964), de Vaucouleurs and Page (1962), van Houten (1961) and Liller (1960) have published and used detailed isophotal maps in their investigations.

Two possible explanations may be offered to account for the absence of regular publications in the subject. The first is that the reduction techniques necessary to produce reliable results are extremely involved and lengthy, a fact which does not suit the American publication system where frequent small articles often seem to be more important than less frequent but more substantial contributions. Secondly, no standard system of parameters for galaxies had been in existence before the ones proposed by de Vaucouleurs and now adopted by the Working Group on Galaxy Photometry.

This Group was formed at the 1961 I.A.U. Meeting in Berkeley, and before that date, comparisons of results were almost impossible, due to the different systems chosen by each observer. The present investigation was carried out following the recommendations of the Working Group. However, before undertaking a major programme on the surface photometry of galaxies in an attempt to bridge the existing gap in extra-galactic studies, a preliminary investigation was made into all the factors which could affect the accuracy of the results, and it is these factors which will be considered in turn throughout this chapter.

2.2 The Telescope. The Cassegrain Schmidt telescope available for use at the University Observatory, St Andrews was completed in 1963, and all the plate material used in the work was obtained with this instrument. The optical system and dimensions of the James Gregory Telescope, as it is called, are shown in figure 1. The primary and secondary mirrors are spheres of diameter 37 and 18 inches and radii of curvature 116 and 112 inches respectively, giving a nearly flat Petzval surface (Linfoot 1955). The aperture stop which is situated midway between the

primary mirror and the corrector plate is formed by an iris diaphragm, adjustable from 30 to 37 inches diameter.

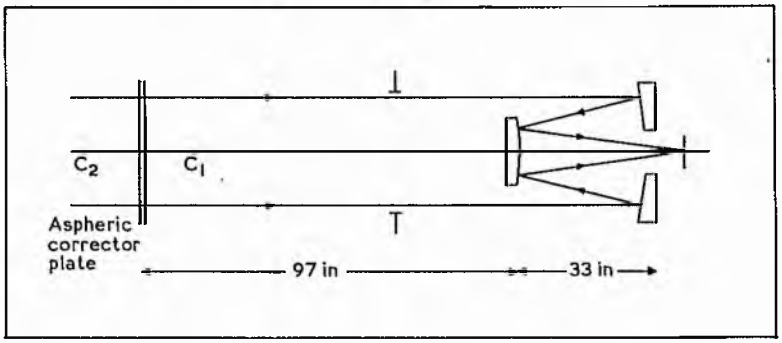

Figure 1 - Schematic diagram of James Gregory Telescope.

The large size of the secondary mirror is dictated by the requirement of an accessible focus with mirrors of similar radii, and the precise value of the Petzval curvature is chosen to balance out the field curvature due to the presence of a small amount of astigmatism (less than 1 arc sec at 2^{o} off axis), thus giving a flat best field. The focal ratio of the system is 2.9 giving a plate scale of 1 mm = 76.4 arc sec and using the 8 inch square photographic plates, a 4^{o} square field is produced.

After initial tests to determine the focus of the

telescope, it became apparent that a certain amount of spherical aberration was present, amounting to a circle of least confusion of under 8 arc sec, due to the corrector plate being too strong. It was pertinent to enquire what effects, if any, this would have on a programme of surface photometry. The luminosity distribution of a stellar image may be closely approximated (de Vaucouleurs 1948) by a unique Gauss function of the form

$$\frac{I(x)}{I(0)} = \exp -x^2/2\sigma^2$$

where I(x) represents the intensity at a radial distance x from the centre of the image, having a central intensity I(0). The dispersion of the stellar images for the James Gregory Telescope was found equal to 2.75 arc sec compared with 2.3 arc sec for the 30-inch Cambridge Telescope used by Redman and Shirley (1938). Clearly, image structure within 8 arc sec of the centre of a galaxy will suffer from distortion, but the overall luminosity distribution will not be affected. However, since surface photometry involves the determination of a mean profile, some selection effect must be employed for the present work. If at r = 6 arc sec, the specific intensity in the star image is I = I(0)/10, then for

such effects to be relatively unimportant in the smoothing of a galaxy profile, the galaxy should be detectable to at least 10 times this value, i.e. to a distance of 60 arc sec or a diameter of 2 arc min. Consequently, only those galaxies for which the value of log D(0) exceeded 1.3 in the Reference Catalogue (de Vaucouleurs and de Vaucouleurs 1964) were chosen. The comments on image structure for the James Gregory Telescope referred to the centre of the field. For wide field work the aperture stop should be set to 32 inches to eliminate vignetting, and initial tests using 4-inch square plates confirmed the acceptability of the images over the field. However, when the work was extended to the full field width of 4 degrees, it became necessary to reduce the aperture stop to its minimum value of 30 inches in order to improve the image quality at the edge of the field, and it was as this aperture that all the observational work was undertaken.

2.3 Calibration. Calibrations which under most conditions would appear to be satisfactory were the subject of some critical comments in the previous chapter. These comments were made for two important reasons. In the first place, it is believed that

the method used throughout the current work was extremely accurate, since it avoided many of the sources of uncertainty in previous work. Secondly, under conditions where a calibration exposure is made on a plate which may, but not necessarily so, have an emulsion sensitivity identical to that of another plate taken from the same box and used for the telescope exposure, it is still almost impossible to create identical processing conditions for both the telescope and calibration plates.

The calibrations in the present investigation were undertaken in the following manner. At one end of an optical bench of length four feet was a light source with a Wratten 78A filter to raise the colour temperature from 2360°K to 3200°K. At the other end, there was a plate holder assembly with several light baffles interposed between these two units to prevent reflections from the walls of the bench assembly. The mounting of the lamp was such that the plane of the filament lay along the line drawn from the wedge to the lamp filament in order to reduce to a minimum the effective area of the source as seen from the plate. The colour temperature filter was placed as close as possible to the lamp to achieve minimal variation of the intensity of illumination at the plate. For a

similar reason, the achromatic density wedge was almost in contact with the emulsion. All surfaces in the system were painted matt black.

This wedge was in the form of an achromatic prism mounted in one corner of a square metal plate. Between the clear glass strips at each end of the wedge, density steps with value 0.2, 0.4, 0.6, 0.8 and 1.0 were obtained by a rhodium plating technique. The width of each strip was 1.9 mm. Since the photographic emulsion responds to an intensity ratio far in excess of the 10:1 ratio produced by the wedge, it was necessary to increase the ratio by placing neutral density filters in the light beam. These filters were located so that they were not quite perpendicular to the beam in order to prevent the occurrence of multiple reflections, and also as close as possible to the light source to minimize any variations in the flux incident upon the wedge due to any non-uniformity in their transmission characteristics. During the telescope exposures, the four corners of the plate were masked off to leave the corners free for calibrations, which, throughout this work, were always made on the same plates as the galaxy images. The interposition of the filters in the calibration beam necessitated further exposures

in order to obtain other segments of the characteristic curve. Measurements of the calibrations performed in this way showed that the plate fog level adjacent to the wedge exposures remained extremely constant at the four corners. Since the calibration exposures were four times as long as the telescope exposure, it was decided to obtain a wedge with a larger density range so that the time devoted to calibration could be reduced without any loss of accuracy, so long as the fog level remained constant. A coating of rhodium producing a density of 1.0 and designated by the hatched area in figure 2 was made on the existing wedge assembly.

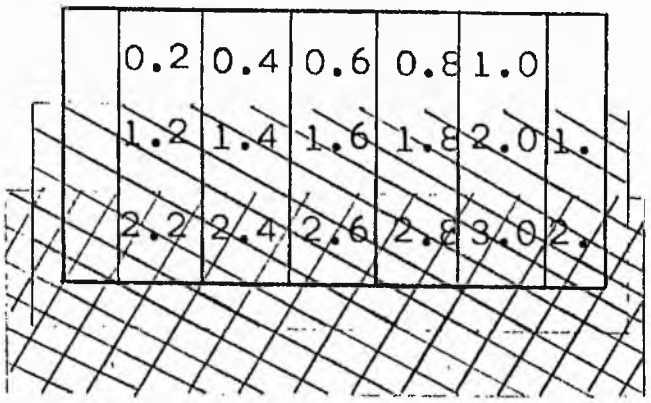

Figure 2 - Diagram of density wedge.

A further 1.0 coating, shown by crosses, was then evaporated on top of the 1.0 hatched area, thus

producing a wedge with a range of density of 3 and giving an effective transmission factor of one thousand. Using this wedge, it was possible to obtain the complete density range necessary for drawing the calibration curve with one exposure on one corner of the plate. However, both as a safeguard that the exposure and neutral density filter combination were suitably chosen to give the correct densities on the plate and also as a check on the initial exposure, a second exposure was made in the diametrically opposite corner of the plate. Following the calibrations, a time delay of at least three days was usually given to take account of latent image decay of both images. This interval concurs with, and in most cases betters a value given by de Vaucouleurs (1968) for $\Delta T/T < 0.1$ where ΔT is the age difference between the telescope and calibration exposures and T is the time delay between the latter exposure and the development. In the same paper, details were also given of the linear relationship between the intensity and the opacitance (equal to the opacity minus one) over the whole range of densities of practical interest in photographic photometry. All the characteristic curves in the work were originally drawn in the conventional H and D

S-shaped curve. However, these curves were constructed by drawing through a set of points a curve whose correct shape was not known a priori. When the writer became aware of the linearization method for drawing characteristic curves, the calibrations were carried out a second time using this new system. The remarkable differences between this method and the previous work emphasized the errors which could be introduced by drawing an arbitrary curve through a set of points. With the straight line, it was obvious whether or not any one point had an erroneous density value, whereas previously a polynomial curve was forced to fit all the data points. Another advantage of this new system is that since fewer data measurements are needed, such a refined density wedge as that used in this work is not really necessary in future calibrations.

2.4 Microphotometers. The original type of microphotometer available for use was a Hilger and Watts L470 scanning-type microphotometer. Basically, the operating pronciple of the instrument was as follows:- most of the available output from a light source passed through the plate and hence to a photomultiplier while the remainder passed directly to a second photo-

multiplier in order to take account of any variations in the illumination of the lamp. The net current from the two photo-tubes was fed to a Brown Recorder. The instrument thus measured transmission and not density.

Two major difficulties were present when initial scans across galaxies were made in the summer of 1965. In the first place, errors were introduced due to the fact that the drive motors on the microphotometer and the Brown Recorder did not rotate with a constant angular velocity. This resulted in distortions and scale errors in the scan abscissae. For isophotometric work, where many scans had to be taken across the object at well determined intercepts, a measuring screw was fitted to the plate table to provide the accuracy in y-spacing down to the necessary 5 micron stepping interval between the successive scans. The second and possibly the more important difficulty was the inherent drift present in the instrument. Due to the relatively slow response of the Brown Recorder, especially in regions where the density gradients are steep, individual scans had to be taken at slow driving speeds. Even in the course of one scan, it was possible to detect changes in the dark current reading before and after the scan. This change was almost certainly

caused by the non-uniformity of response of the two photo-tubes, thus making transmission measurements dependent upon intensity changes in the reference beam.

These two difficulties are overcome in the design of the Joyce Loebl microphotometer. A direct mechanical linkage between the plate and recording table ensures synchronization of table and pen positions, irrespective of the magnification ratio chosen. The ratios available range from 1 to 2000. Furthermore, the instrument incorporates a true double-beam system in which two light beams are taken from a single source, one to act as the measuring beam, the other as reference, and both beams terminate at the cathode of one photomultiplier, thus eliminating possible variations in the intensity of the source. Due to the limitations of the Hilger microphotometer, the University Observatory acquired in 1965 a Joyce Loebl microphotometer, which also incorporated the Isodensitracer attachment. A more detailed description of the instrument's isophotometric operation mode will be given in the next chapter which will concern isophotometers. For the moment, however, the microphotometric mode will now be described, together with the additions necessary for the digitization of the instrument, carried out during the summer of 1969.

All the cross-sectional scans across galaxies, which were necessary to obtain the profiles and calibrate the isophotes, were digitized and subsequent computer reduction of the information was used to obtain the luminosity profiles for each object.

The Joyce Loebl microphotometer is a double beam instrument of the null balancing type, balance being achieved by the servo-positioning in the reference beam of a linear density wedge. Linked directly to this wedge assembly is the recording pen. The machine will therefore measure density linearly within the range of the particular wedge in use. The instrument supplied to the University Observatory was also fitted with helical potentiometers to provide analogue outputs of both table position and density; both outputs were connected to digital voltmeters. The sampling interval was achieved in the following manner. From inspection of a typical cross-section, the noise pulses were found to occur on average every 1.5 arc sec on the plate. In order to retain all the available information, it was decided to sample every second of arc. Using the 50 times magnification arm, this would involve making 300 samples in the course of one scan. The digital voltmeter measuring the table position was a five digit ten volt full scale model, and with a

suitable choice of the voltage applied to the table potentiometer, it was possible to make the sampling interval correspond to 0.02 volts.

It was then only necessary to feed at each sample a triggering signal to the wedge digital voltmeter in order to perform the density digitization. This was achieved by fitting on a nor gate to each terminal of the digital voltmeter corresponding to an odd number in its second least significant digit. This had the effect of switching on a transistor every time an odd number was displayed, and of switching off the transistor when the display was even. When the transistor was switched on, the current supplied was used to drive the triggering signal for the digital voltmeter measuring density, thus performing the necessary digitization. At the same time, the voltage value corresponding to density was punched out on paper tape.

The basic idea of the system, although satisfactory in that it produced digitized pulses when commanded to do so, was nevertheless subject to a considerable number of spurious multiple density digitizations due to pick up of noise pulses. Let us consider in detail the effects produced by noise pulses which are ringing in nature, that is, cases where the amplitudes of the

pulses slowly decay with time. At a change-over from an even to an odd number, one digitization is produced. When noise pulses are present, the probability of the odd number going even again and producing a double digitization is highest exactly at a change-over, either from an even to an odd number or vice versa. This is because the table position is continuously moving away from or towards a change-over value, and at intermediate points the amplitudes of the pulses are not sufficiently large to swing the voltage to a change-over value. In order to overcome this problem, the average time between digitizations was calculated, and a monostable introduced to the electrical circuit in order to leave on a transistor, once switched, for the period of the duty cycle, irrespective of whether the input signal to the base of the transistor is attempting to reverse the switching, due to noise pulses. The circuit of the monostable was arranged so that the duty cycle was 80% of the sampling time interval. This arrangement largely overcame the difficulties experienced with multiple digitizations, but a further check was made during scanning, when it was a simple matter to detect audibly 50 punches per volt change in the table digital voltmeter corresponding to 50 required digitizations. Any scans in which extra pulses

happened to be produced were discarded and the scan re-run.

This description of the digitization procedure has been included because it only involved the expense of some £10 on the electronic components necessary to build the stabilized power supply for the potentiometers, the nor gate and the monostable. All the other equipment used in the system was supplied from stock already available in the University Observatory.

2.5 Processing Equipment. Basic to all successful photographic photometry is the meticulous care with which the processing of valuable plates must be undertaken. It is appropriate to consider each stage of the process in turn. In the first phase, each plate should be developed in fresh developer at a temperature of 68°F for five minutes. For a set of plates taken on different occasions, it is desirable to obtain identical development conditions. In this connexion, although time control is relatively easy to achieve, such control is not quite so easy with regard to temperature. The main requirement would be extremely accurate control over the darkroom temperature and the user should check the temperature of the solutions before commencing development. Perhaps the most suitable

system would be one in which control was made over both temperature and humidity, as suggested by Miller (1966).

Agitation of the plates also presents problems. In microphotometer scans across the initial wedge exposures, it was noticed that edge effects were present, even although the developing dish had been thoroughly rocked during development. These effects disappeared when brush development was used, and this method was used for all the plates processed in this investigation. The edge effects found in the previous plates were attributed to standing waves being set up in the developer, possibly caused by too rhythmic a rocking motion of the dish. Another source of uneven development was due to poor immersion of plates in the developing solution. For optimum results, the developer should, on immersion, make immediate contact with the entire emulsion surface and to aid this process, the plates were first immersed in water before immersion in the developer.

With regard to fixing and washing, the plates were fixed only for as long as necessary, because excessive fixing is liable to cause bleaching of the image. In a similar way, washing was accomplished in the minimum time in order to avoid the clumping of silver grains

which often occurs after long periods of washing. Throughout the present work, the plates were not washed continuously during the washing period, but this interval was subdivided into six equal washes, each of five minutes duration, interspersed with complete changes of water.

Chapter III

3.1 Introduction. One of the most important requirements for obtaining successful results in any photometric investigation of galaxies is the accuracy of the isophotal map which gives the distribution of relative intensity with the object. Isophotes may be produced in two different ways, one photographic, the other by mechanical means, and both systems will be considered in turn in the following sections.

3.2 Photographic methods. The first work using this method was done by van Hopf (1937), who constructed isophotes by sketching around the boundaries between the light and dark areas of a very high contrast print made from a galaxy negative. The high contrast removed the smooth intensity distribution inherent in most galactic images and the nett result was a fairly well-defined light galaxy on a dark background. This approximate method was superseded with the application to galaxy photometery of the Sabattier effect in 1963 by Richter and Hogner (1963). In view of the relative speed with which output may be obtained in comparison with more conventional techniques, this method appears well suited to the problems in galaxy photometry. This is true up to a point, but one important feature is the critical dependence of the

method upon the uniformity of illumination of the light source used for the exposures. A series of tests was made to assess the potentiality of the technique. The results of these tests are illustrated in figures 3 and 4, which represent the best isophotes which could be obtained for NGC 4258. However, experts in the technique seem to produce better results (e.g. Richter and Hogner 1964, 1965, 1966). The Sabattier process was used for the isophote shown in figure 3 while the variation of the original process proposed and used by Hodge and Brownlee (1966) was employed to produce figure 4. In this variation, several contact copies of a plate were made, each with a different exposure. Contact copies of copies were also made in order that pairs of negatives and positives of slightly different density may be selected and sandwiched together, when an enlargement from the composite should produce a clear sharp isophote.

Two features are apparent after an examination of figures 3 and 4. In the first place, isophotes as such are extremely difficult to produce, because the definition of the isophote seems to depend very critically on the exposure ratio between the negative/positive pair. In unfavourable cases, an area of approximately equal intensity is produced, not a clear

Figure 3 - Isophote of NGC 4258 obtained using the Sabbatier process.

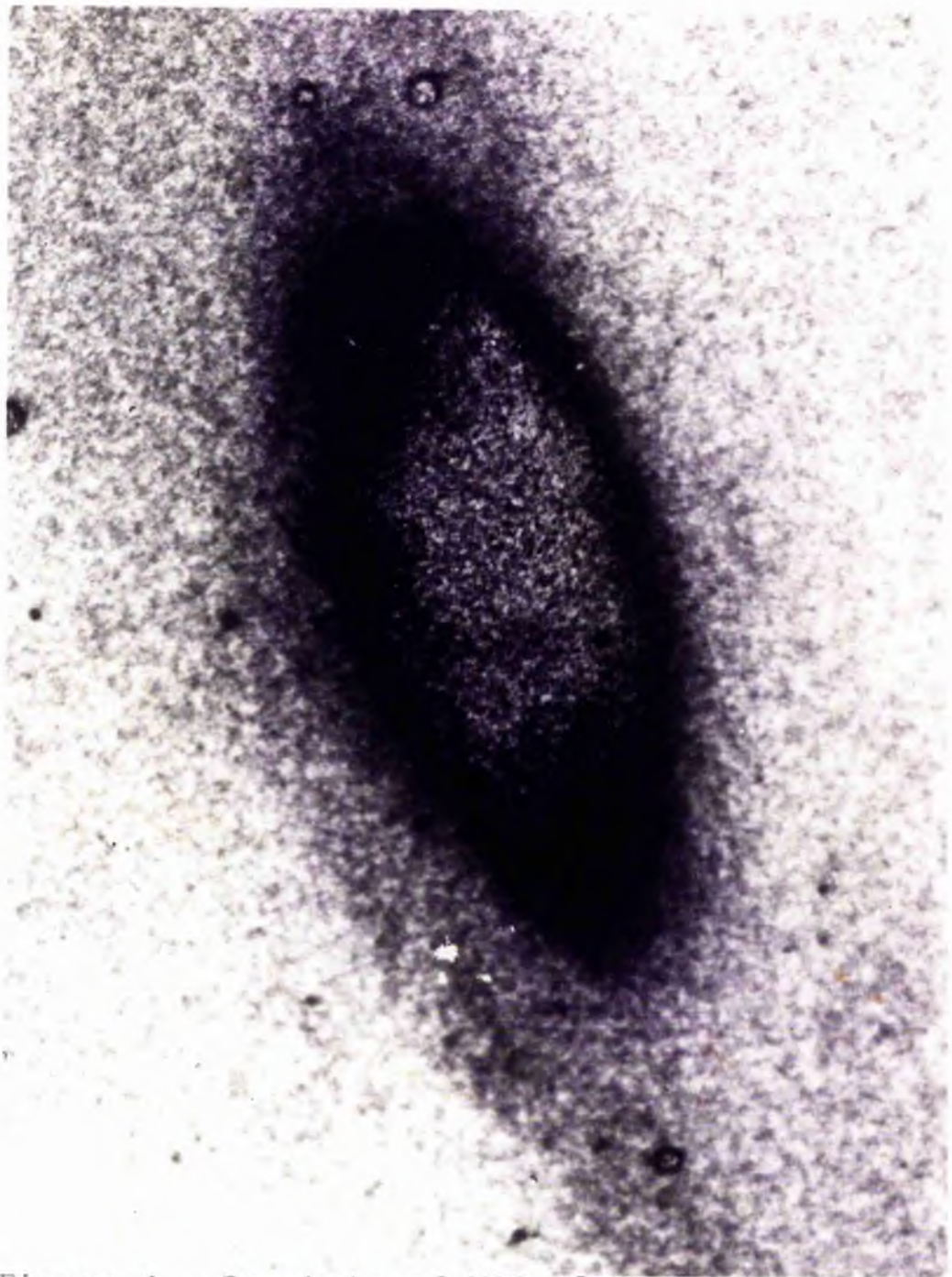

Figure 4 - Isophote of NGC 4258 obtained using the photographic method of Hodge and Brownlee.

sharp line. When high contrast photographic materials are used, and in cases when the exposure ratio is suitable for producing the required line, photographic effects then play a major role in determining the exact shape of the resulting isophote. Secondly, the magnifications which may be obtained with an enlarger are much smaller than those available on most micro-photometers. Accordingly, to achieve any degree of successful isophotometry by photographic means, it would be expedient for the original plates to be obtained on a telescope with a large plate scale. Tracings of NGC 4258 with the scanning type isophotometer at the University Observatory are shown in the figures 5 and 6. The visible distortion in the stellar images were produced by design and will be explained at a later stage in this chapter. Comparison with figures 3 and 4 should illustrate to the reader why the photographic methods were abandoned in favour of mechanical methods.

At the recent 1970 IAU General Assembly in Brighton, it was pointed out at the meeting of the Working Group on Photographic Materials that a new high contrast emulsion yielded favourable results when used in work on the Sabattier effect. In view of this new information, it is possible on the one hand that more accurate results

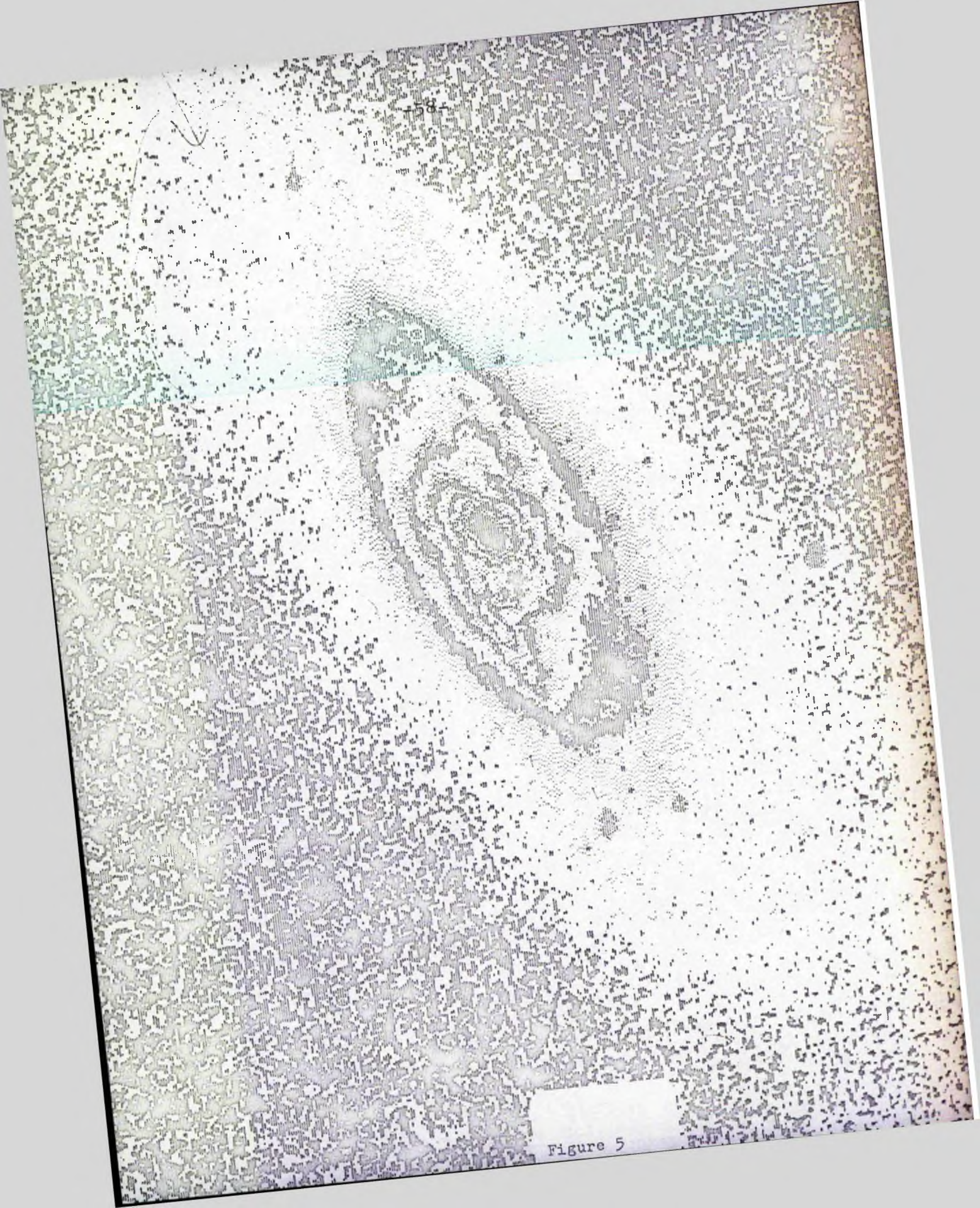

Figure 5

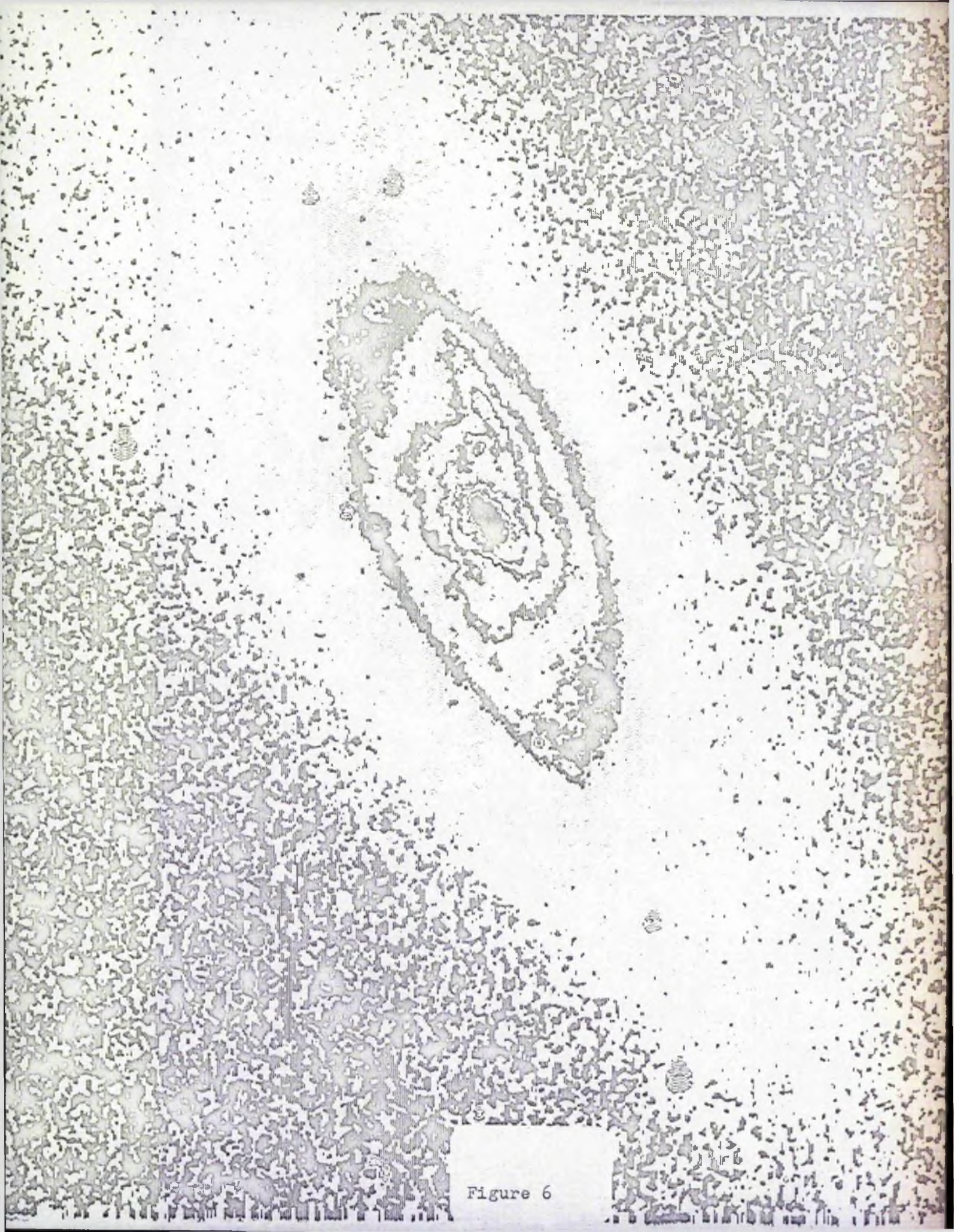

Figure 6

may be obtained in the future using photographic techniques, while on the other hand, it should be noted that all these isodensitometry techniques give curves of constant density and not the true isophotes corrected for plate errors, which can only be derived by more elaborate numerical mapping techniques (Jones et al. 1967).

3.3 Mechanical Methods. The simplest system for isophotometry using mechanical methods is the case where isophotes are constructed from microphotometric scans. For objects with fine structure, the process is extremely tedious and time consuming due to the small stepping increment required to record the details. Such a procedure was used by Holmberg (1958) and van Houten (1960). Holmberg, in particular, was successful in obtaining accurate results over the large sample of objects under study. The logical extension of this method would be complete digitization of the microphotometer output, subsequent computer reduction of the data followed by the production of isophotal contours.

As an alternative, adaption to an automatic scanning mode of a microphotometer fitted with some method for detecting and recording pre-defined densities would produce lines of equal density, which could then

readily have assigned to them their respective intensities. This scheme was used in principle by Mohler and Pierce (1957). However, the slow operating speed of their instrument due to the long time constant of the recorder combined with the large mass of the pen trip mechanism proved to be major disadvantages of this system. These difficulties were overcome by Koelbloed (1965), who designed an attachment for use with a normal microphotometer. The use of a high speed galvanometer together with teledelthos paper for the recording provided a much faster instrument than that of Mohler and Pierce. The writer used Koelbloed's instrument and considers it to have great possibilities as an isophotometer, even although it still lacks some of the refinements necessary to make it suitable for multiple applications. Further design improvements are in progress.

Perhaps the most simple and inexpensive method for obtaining isophotes is to follow, manually, points of constant deflection within an object using a microphotometer with precision x and y screws fitted to the plate carriage, noting the intermediate readings. This was done by de Vaucouleurs (1961b, 1963b, 1963c, 1964) and later adopted by Bertola (1966) in an investigation of

three late-type galaxies. It is surprising that such a method was chosen for objects with complex structure, rather than ellipticals or lenticulars, since a considerable amount of smoothing was effected in the delineation of the isophotes from the measured date points.

Automation of this principle was found in an isophotometer designed by Williams and Hiltner (1940). Its contour following mode of operation was known as hunting. Two limitations in the system were as follows:- first of all, the inability to record more than one isophote at a time and secondly, the inability to differentiate between a true isophote and such details as small islands or closed-loop isophotes within larger ones. Clearly these disadvantages only make the instrument suitable for isophotometry of systems without much fine structure. In addition, constant operator attendance would seem to be necessary.

de Vaucouleurs and Griboval (1965) have designed an isophotometer which can operate in two basic modes: (1) a contour following mode for simple closed loop isophotes and (2) a scanning mode to record more complex structures. This instrument combines the principle of the Michigan isophotometer together

with Koelbloed's design, and some illustrations are given for sample tracings. At the present time, there is a two dimensional digitized densitometer in the final stages of construction at the Department of Astronomy in the University of Texas at Austin.,

After due consideration had been given to the relative advantages of the different systems discussed in this chapter, it would appear that the basic essentials for an isophotometer are as follows:-

(1) electronic stability

(2) ability to scan rather than hunt in order to record all details

(3) versatility in the choice of magnification used for a particular tracing in order to study selected areas of a galaxy rather than the complete object

(4) fast operating speed.

These four requirements were fulfilled in the Joyce Loebl Microdensitometer with an Isodensitracer attachment (abbreviated in future to MDM and IDT). In view of the drift problems encountered with the Hilger microphotometer, together with the large time necessary to complete one scan, reliable construction of meaningful isophotes from the resulting tracings proved impossible. The MDM can scan fifty times more quickly than the Hilger micro-

photometer described in Section 2.4, and using the IDT attachment, a scan is produced not in the conventional y-deflection form, but as a coded x-direction line. Multiple scans, together with the appropriate table and plate increments, form an overall contour map of scanned area.

The scanning process is controlled by an electronic programmer. Upon completion of an x-scan, the table drive is reversed and at the same time two pre-selected pulse trains n_1 and n_2 are fed from the programmer, one to a stepping motor providing y-drive to the plate table and the other to a special recording pen stepping motor. This pen replaces the one linked to the linear density wedge in MDM work. The number of pulses n_1 fed into the plate table controls the scan spacing and the ratio $n_2 : n_1$ determined the y-magnification. Various magnifications may be obtained by selecting different settings of n_1 and n_2. When the plate table has returned to its starting value and the y-stepping process has been completed, the next scan commences. A driving pulley is used to provide movement to the density wedge during the servo-positioning routine. In the IDT attachment, a commutator ring, illustrated in figure 7, is screwed on top of the pulley and two

metallic contacts are located radially at the points indicated in the figure.

Figure 7 - Diagram of commutator ring.

As the wedge assembly moves during servo-positioning, the pulley rotates and the contacts either touch one of the two metallic areas of the ring or in certain positions, no contact is made at all. This sequence of operations is called the quantization of the wedge movement. Depending upon which of the two metallic contacts are being made at any particular instant will determine the mode in which the recording pen will write - either dots or continuous lines. The density quantization thus changes a normal microphotometer tracing into a coded line. As scanning

proceeds, a two dimensional density map consisting of spaces, dots or lines is produced, a transition from spaces to dots to lines corresponding to increasing density and vice-versa. The resulting isophotes are thus uniquely defined as those lines which may be drawn through the points where the pen mode changes. By dividing the complete density range of the wedge by the number of divisions of the commutator ring formed within this range, it is possible to calculate the density increment per change of pen mode. All the isophotes therefore have integral multiples of density above some reference level. After the principal axes of an object have been determined from the isophotes, microphotometric cross sections along these axes furnish the calibration of the isophotes.

Before making any tracings, it was first necessary to check the magnification ratios so that identical x and y ratios would produce a one to one correspondence. An elaborate set of dial test indicators was fitted to the instrument. Results of test tracings showed that, contrary to expectations, it was not in the stepping motors that the errors were larger, but in the ratio arm. The 100 times magnification, used for most galaxies with angular diameters less than 3 arc min,

was found to have a magnification of 105 while the 50 times arm gave a value nearer to 51. For the y-stepping motors, the errors were only around one half of one percent.

In their paper on the merits of photographic methods for producing isophotes, Hodge and Brownlee (1966) mentioned that distortions could occur with scanning type isophotometers, and also that the interpretation of small scale structures with dimensions similar in size to the step size in y is extremely difficult. Criticism of this statement in defence of the scanning type isophotometer formed the basis of a paper published by the writer (1966). Figure 8 shows isophotes of NGC 3389 obtained with the University of Michigan isophotometer. Clearly the interpretation in this case of some details would prove difficult, and it is possible that when Hodge and Brownlee made their critical comment on this matter, they had no knowledge of the existence of the Joyce Loebl instrument. In figure 9, isophotes with a density increment of 0.06 are shown for the same object. They were obtained on the Joyce Loebl machine from a plate taken with the James Gregory Telescope. The reader should have no difficulty in assessing the increase in detail of the latter diagram over the Michigan isophotes. This additional accuracy is

Figure 8 - Isophotes of NGC 3389 obtained with the University of Michigan isophotometer.

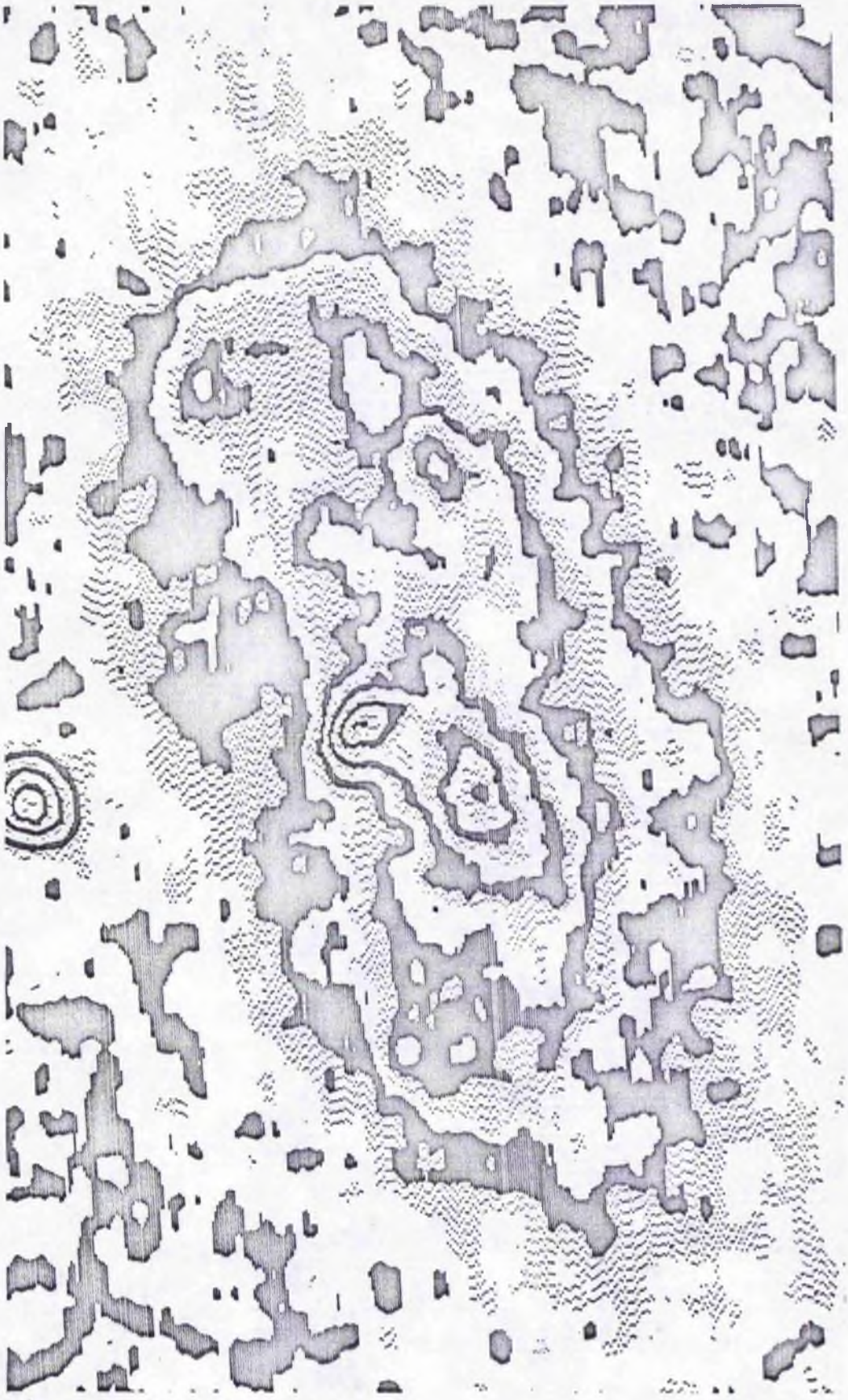

Figure 9 - Isophotes of NGC 3389 obtained with the Joyce Loebl Isodensitracer.

possible mainly due to the close y-spacing adopted. The minimum increment which may be made in the y direction is 1.25 microns on the plate table, corresponding to 0.095 arc sec on plates taken with the Gregory Telescope. As a further comparison, a plate of NGC 5566 was taken at St Andrews to provide the necessary source from which an IDT tracing could be obtained. Hodge and Brownlee had selected this object in order to obtain the isophotes shown in figure 10 which were supposed to demonstrate the high degree of accuracy possible with the photographic methods over other methods. The IDT tracing from the St Andrews plate is shown in figure 11 and inspection of this figure with the previous one should reinforce previous remarks. The other advantages of the Joyce Loebl instrument over other isophotometers, in particular ones of the scanning type, are as follows:-

1. Since the y-scanning steps may be extremely small, it is possible to make detailed investigation on small scale structures without the interpretative problems described by Hodge and Brownlee (1966). Any confusion which may arise may be resolved on the basis of rotating the plate through 90^{o} and repeating the tracing. Exact similarity of the isophotes is obtained after taking account of the slight magnification errors in the ratio arm.

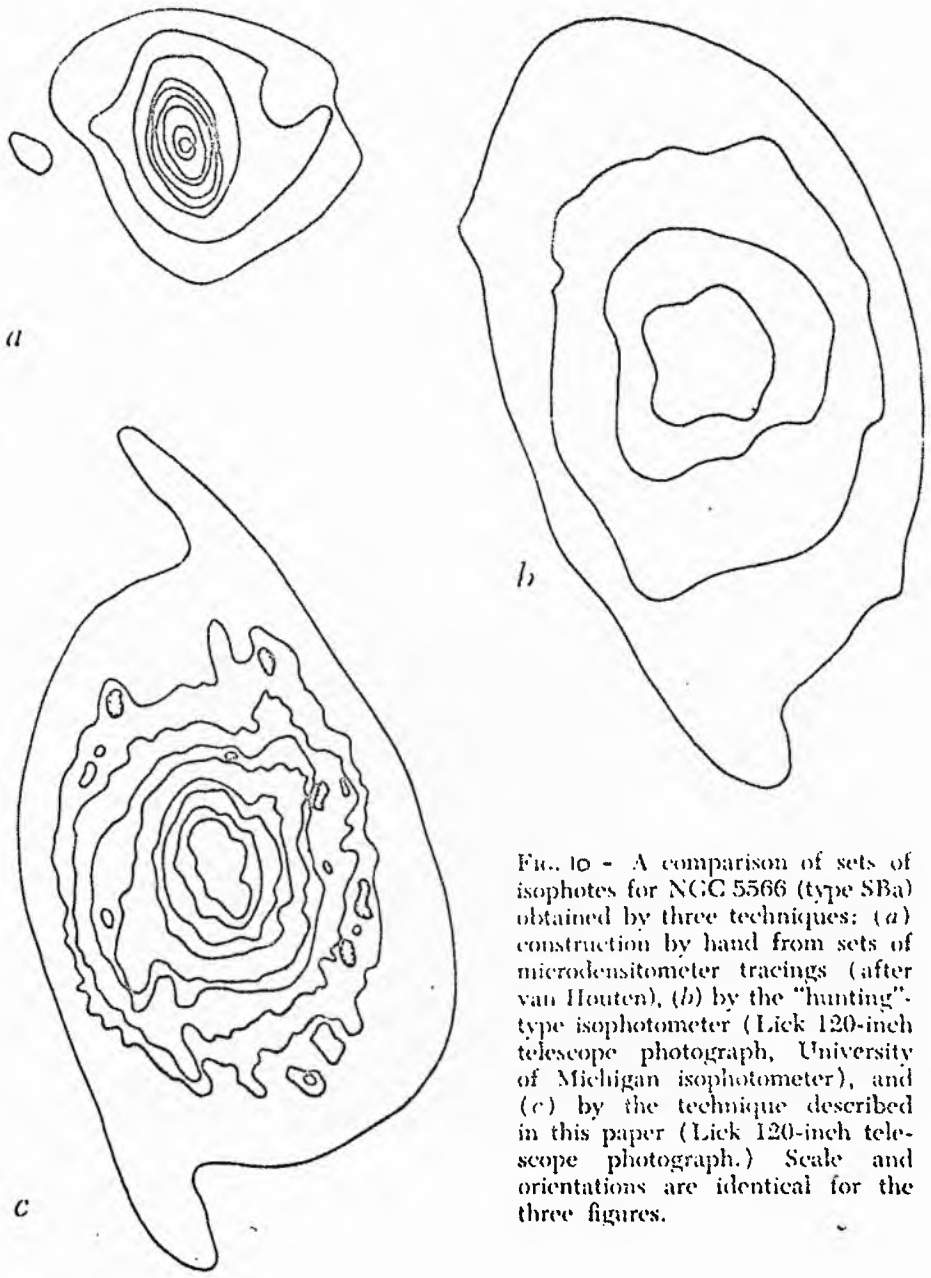

FIG. 10 - A comparison of sets of isophotes for NGC 5566 (type SBa) obtained by three techniques: (*a*) construction by hand from sets of microdensitometer tracings (after van Houten), (*b*) by the "hunting"-type isophotometer (Lick 120-inch telescope photograph, University of Michigan isophotometer), and (*c*) by the technique described in this paper (Lick 120-inch telescope photograph.) Scale and orientations are identical for the three figures.

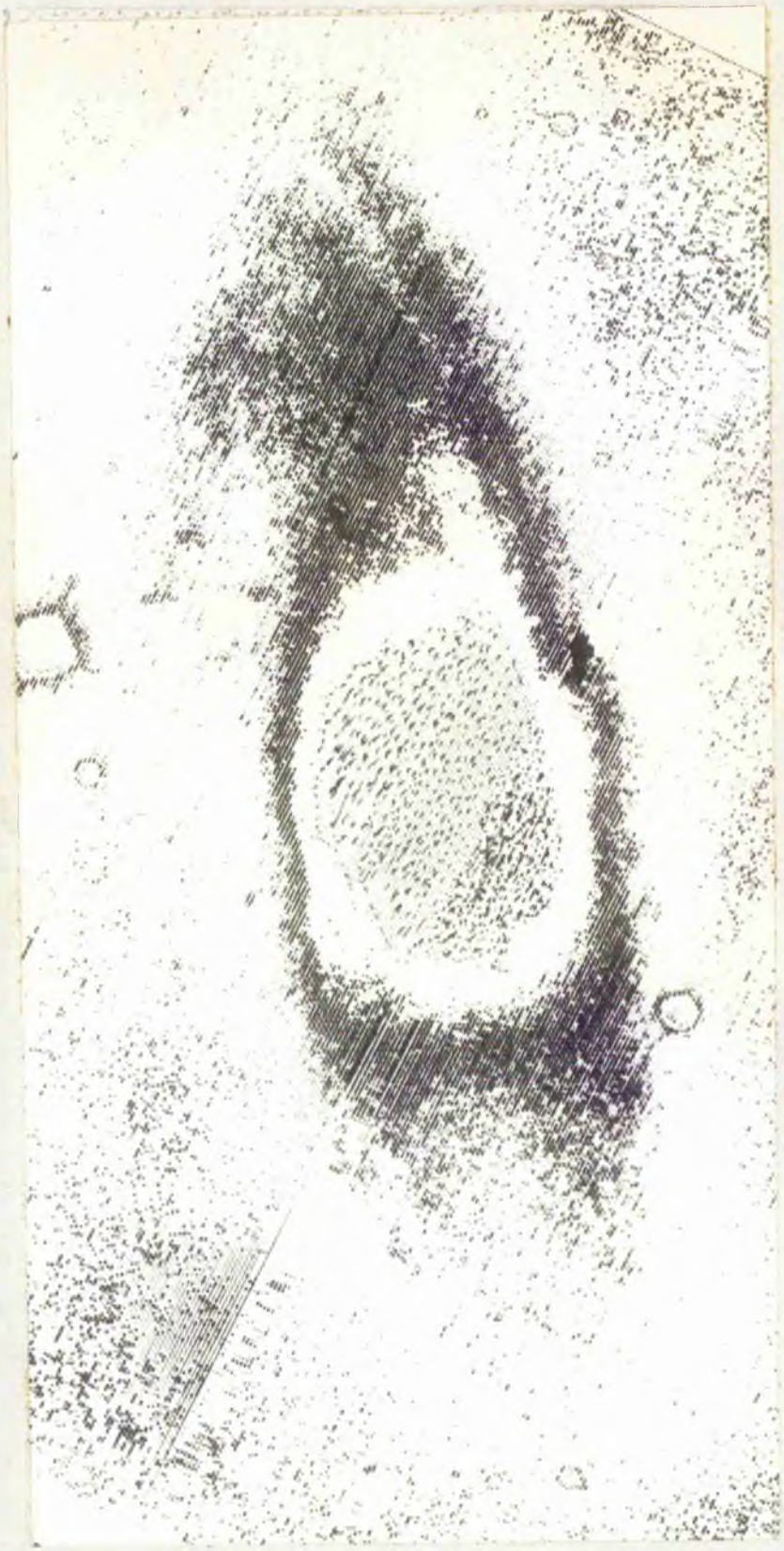

Figure 11 - Isophotes of faint outer regions of NGC 5566. The core is over-exposed.

2. Since the recording pen can write in three different modes, the difficulties formerly present in determining the sign of the density gradient are not now present. Clearly no ambiguity is found in cases where closed loop isophotes occur within larger ones.

3. The speed with which the tracings are produced is extremely rapid.

In this connexion, an examination will now be made of the distortions found in the stellar images in figures 5 and 6. The plate was rotated through 180° between each tracing. A useful design feature of the MDM is a differential control. This adjusts the speed of the recording table, which is driven by a servo motor. The control phase of this motor receives signals from an amplifier, the output of which varies inversely with the rate of change of density on the plate. Hence the recording pen will never overshoot in parts of the scan with high density gradients, since the table is then moving at its slowest speed. However, when used as an IDT, this valuable feature was inoperative, and great care was necessary in the selection of the maximum possible scanning speed consistent with the production

of distortion-free tracings. The largest density gradients encountered on a plate are in stellar images, and inspection of these images in figures 5 and 6 readily shows that the scanning speed was too fast, since the distortions are in the same direction, However, if the two tracings are superimposed, the isophotes within the galaxy match perfectly, indicating that although the scanning speed has obviously been too fast to produce symmetrical stellar images, this speed was nevertheless acceptable for accurate isophotometry of galaxies. Therefore it is proposed that so long as the stellar images are reasonably symmetrical, there is no reason for believing that asymmetry could be introduced in isophotes of galaxies. This condition formed the basis for the determination of the maximum speed at which scanning could proceed.

4. The higher accuracy in the detection of faint isophotes. Contrary to the operation of other scanning-type isophotometers where isophotes are obtained corresponding to certain pre-selected densities, the IDT provides a continuous digital record of density changes over the entire scanned area.

Initially the wedge base control is arranged so that the noise in the sky background makes the mode of the recording pen alternate between lines and spaces in approximately equal proportions.

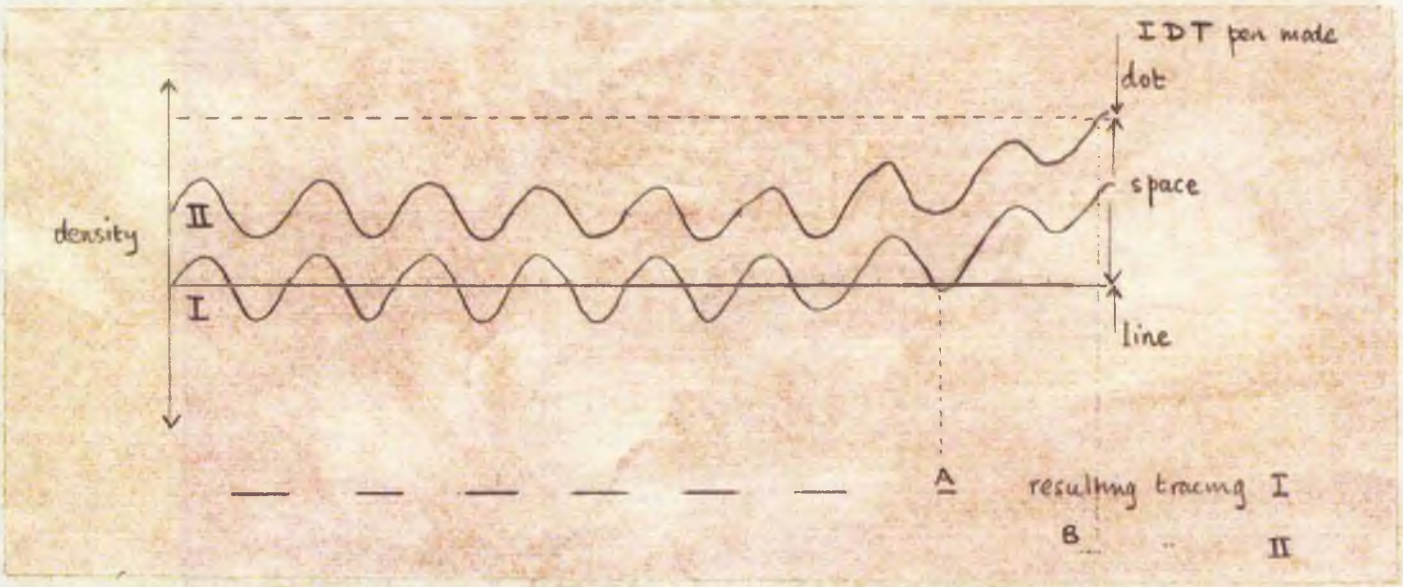

Figure 12 - Diagram illustrating base level setting for background.

In figure 12, the solid line represents the level of the background corresponding with the density transition level at which the IDT pen mode will change from lines to spaces. A typical density tracing is shown by line I while an identical tracing at a higher base control setting is indicated in line II. In case I , a density change in the back-

ground signal considerably smaller than the noise level will produce a marked change in the line to space ratio as indicated at A in the resulting tracing. Considering case II , the first indication of a density change will be shown at B when dots will appear on the tracing. Clearly the first case enables identification of a much fainter isophote level than the second. This system permits more accurate values for the contributions from the faint outer regions to the total luminosity of the galaxy under study, since fewer "average" isophotes derived from the radial scans across the object will be required.

A recent development in isophotometry by Bredohl (1970) has combined the detection of pre-selected density values with rapid speed of electronic raster scanning. A plate of a galaxy is placed in front of a television camera, and as the image is built up on a large screen, an identification mark is added on the screen every time the scanning video signal crosses a pre-selected reference level. This arrangement can produce detailed isophote maps of a galaxy in 10 minutes, but the limitation of the technique is similar to that encountered in equidensitometry, namely that regions of low density gradients tend to produce broad isophotes.

3.4 Smoothing Methods. In addition to photographic and mechanical systems isophotes may also be drawn on graph plotters after computer reduction of data. Various smoothing functions may be applied to the data in order to aid definition of the fainter isophotes and an investigation was made into the comparison between different smoothing techniques and the IDT tracings. The procedure followed for the construction of isophotes was to scan an area of the plate at least twice the apparent size of the galaxy under investigation so as to ensure that each scan extended well into the sky background, and then to sample the data at uniform intervals Δx along each scan to produce a data block for computer processing with on-line graph plotting. The plotting routine involved searching along every grid line forming the boundaries of each individual data block, locating a particular value of plate density and plotting a small straight line to the adjacent grid line thus forming a segment of the isophote corresponding to the chosen density. The shift Δy between successive scans should be less than Δy_o, the average size of the plate grain, for maximum effectiveness in sampling. In practice, however, this would produce a prohibitive amount of data and it is unfortunately necessary to

use a value of Δy which exceeds the optimum value sometimes by as much as a factor of ten.

The object selected was the E2 type galaxy NGC 4261 with an apparent size of 2.8 x 3.1 arc min. The scanning aperture used for the microphotometry was 50 x 50 microns, or 3.8 x 3.8 arc sec on the plate, and the scans were sampled for data points at every 100 microns in x, with the same value for the stepping increment in y. The total area scanned was 6.3 x 6.3 arc min for which 2,500 data points were obtained. This preliminary study, carried out in 1967, was one project which could have benefited from the modern digitization facilities available, but the basic results illustrated in the next set of figures would only be changed in minor details, not in general character, by such an improved system. The IDT tracing of NGC 4261 with which the smoothing results will be compared is shown in figure 13. The density increment for the isophotes is 0.06, twice that used for figure 14, which shows output for the same galaxy from computer graph plotter data reduction of the microphotometric scans. The density increment is small so that although the details in the background may be retained, it was necessary to restrict the maximum density plotted in order to avoid confusion

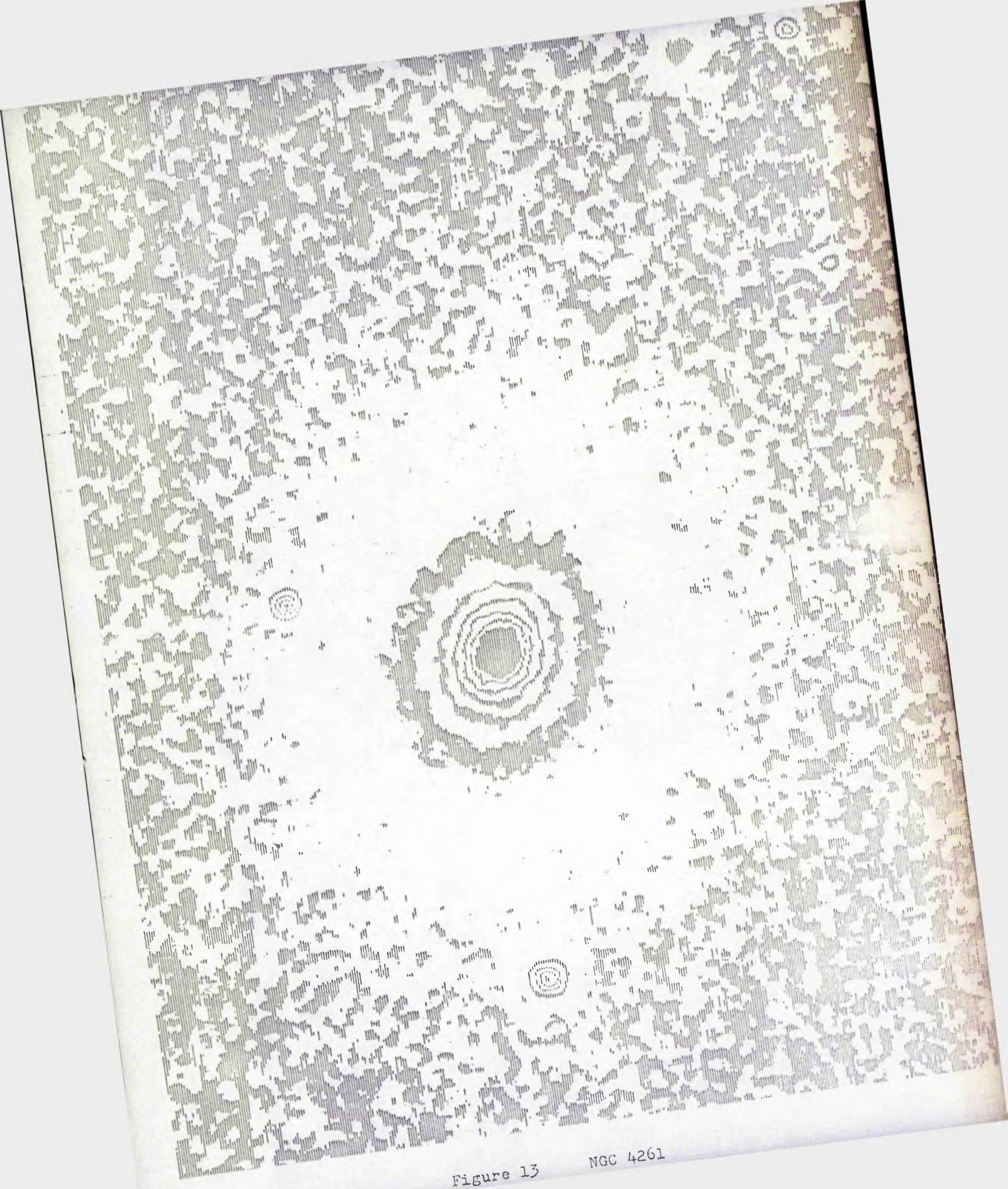

Figure 13 NGC 4261

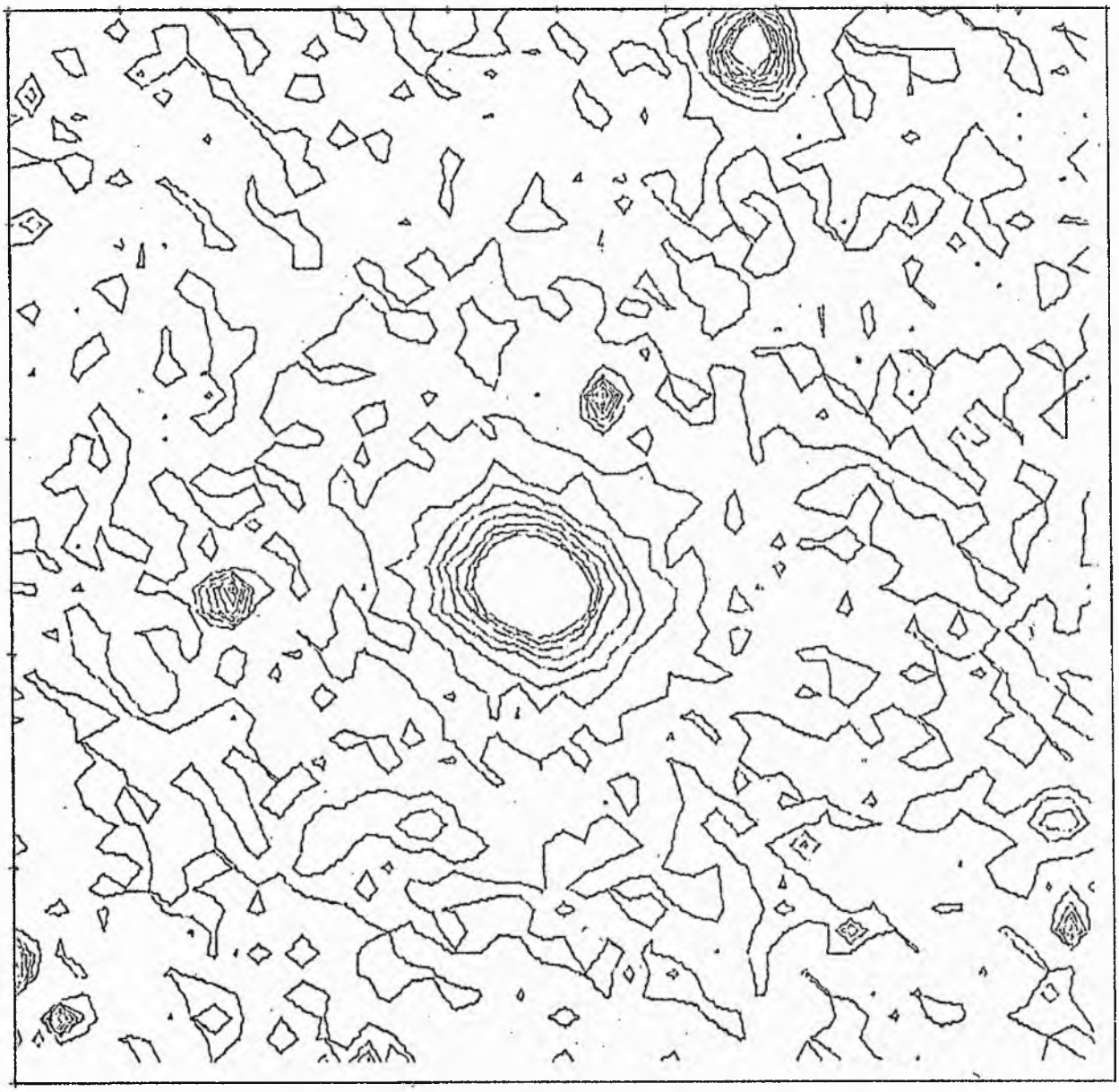

Figure 14 Computer output from microphotometric scans across NGC 4261

near the centre. It is clear from the figure that the output contains too much information on the random plate fluctuations compared with the galaxy. It is thus necessary to examine the methods of smoothing the data, especially in the outermost regions of the galaxy, which will remove the plate grain noise but yet retain information on the galaxy profile.

The array of data points in the form of a nine-point cross is shows in figure 15.

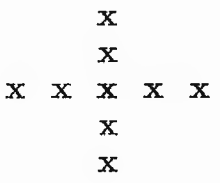

Figure 15 - Diagram of nine-point cross array of data points.

Let us consider the smoothing of the data first by rows and then by columns throughout the data block. It is assumed that the data are sufficiently close together to justify the hypothesis that the second derivative does not change much over the course of a few measurements.

Let us assume that the five horizontal data points of the cross designated by the co-ordinates x = -2, -1, 0, +1, +2 lie very nearly on a parabola of second order, represented theoretically by the expression

$$f(x) = a + bx + cx^2$$

By the principle of least squares, we have two sets of normal equations. These are

$$5a + 10c = \sum f$$
$$10a + 34x = \sum fx^2$$

It is the central value at x = 0 which is to be corrected, and the theoretical value at x = 0 is f(x) = a. Solution of the normal equation for a gives the following result for the smoothed value $\bar{f}_o$ at the centre of the row

$$70\ \bar{f}_o = 70f_o - 6\delta_x^4 f_o$$

or

$$\bar{f}_o = f_o - 3/35\delta_x^4 f_o$$

where δ_x^4 is the fourth central difference. After scanning the entire data block by rows, we may smooth the new data block of $\bar{f}_o$ values by columns to give

$$\bar{\bar{f}} = \bar{f}_o - 3/35\delta_y^4 \bar{f}_o$$

for the doubly smoothed central value of the nine-point cross. It may be shown that the procedure of smoothing by rows and then by columns is equivalent to smoothing firstly by columns and then by rows. However, this

double smoothing process is likely to be more severe than smoothing simultaneously by rows and columns. The smoothed central value for the nine-point cross for simultaneous smoothing is

$$\bar{f}_o = f_o - 3/53 \left(\delta_x^4 f_o + \delta_y^4 f_o \right)$$

Since it would appear to be rather artificial to use raw data in the form of a cross rather than a small block of data, the array shown in figure 16 in the form of a nine-point block was considered.

x x x
x x x
x x x

Figure 16 - Diagram for data array forming nine-point block.

For this array the central smoothed value is given by

$$\bar{f}_o = f_o - 1/9 \, \delta_y^2 \left(\delta_x^2 f_o \right)$$

Figures 17, 18 and 19 show the effects of smoothing by rows then columns. It is apparent that one application of this procedure immediately removes most of the ambiguity in the outer regions of the galaxy. However, successive applications of this process could produce distortions in the nuclear regions due to

oversmoothing. The effects of simultaneous smoothing by rows and columns in the nine-point cross are illustrated in figures 20, 21 and 22. This procedure is less severe and therefore less likely to produce distortion in isophotal contours. The third case is considered in figures 23, 24 and 25 and it is apparent that quite considerable distortions are introduced by this process, especially in high density gradient areas such as those found in stellar images.

If we compare the results of all the smoothing techniques with the IDT tracing of NGC 4261 illustrated in figure 13, it is apparent that the outermost isophote runs near to, or even intersects the two stars located closest to the galaxy. This dramatic agreement between figures 13, 18, 19, 21 and 22 illustrates the advantages of the smoothing of data. There is, however, a case against smoothing of data based on the view that some important information is lost in the process. For this reason, it would be preferable to preserve all the information as it is done in the IDT tracings. This point is demonstrated in a comparison of the IDT tracings of NGC 4261 (Figure 13) on the two-dimensional map with the computed contours from the unsmoothed data (Figure 14), when it is seen how some confusion and ambiguity is

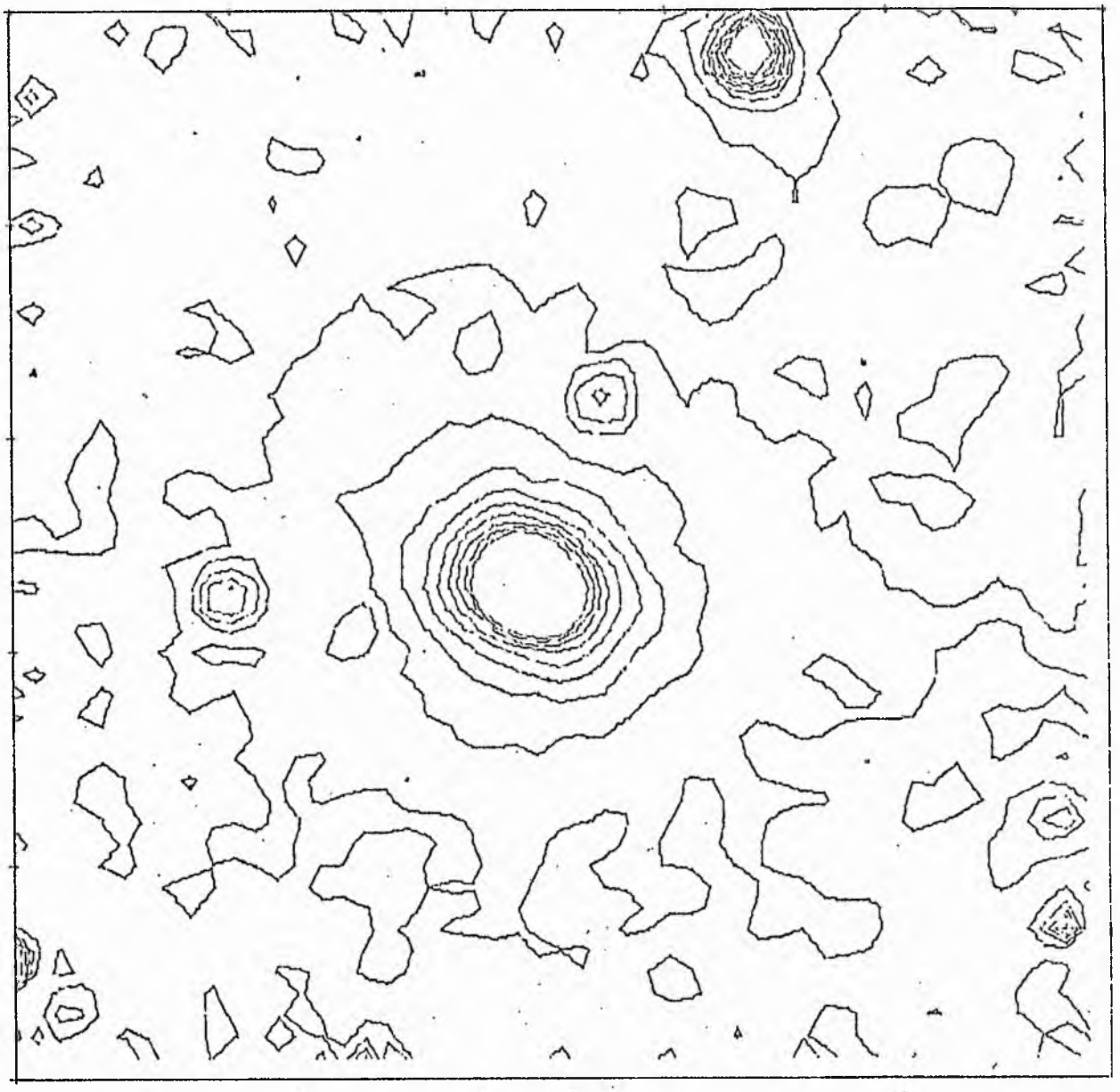

NINE POINT CROSS --- ROWS THEN COLUMNS

Figure 17 NGC 4261

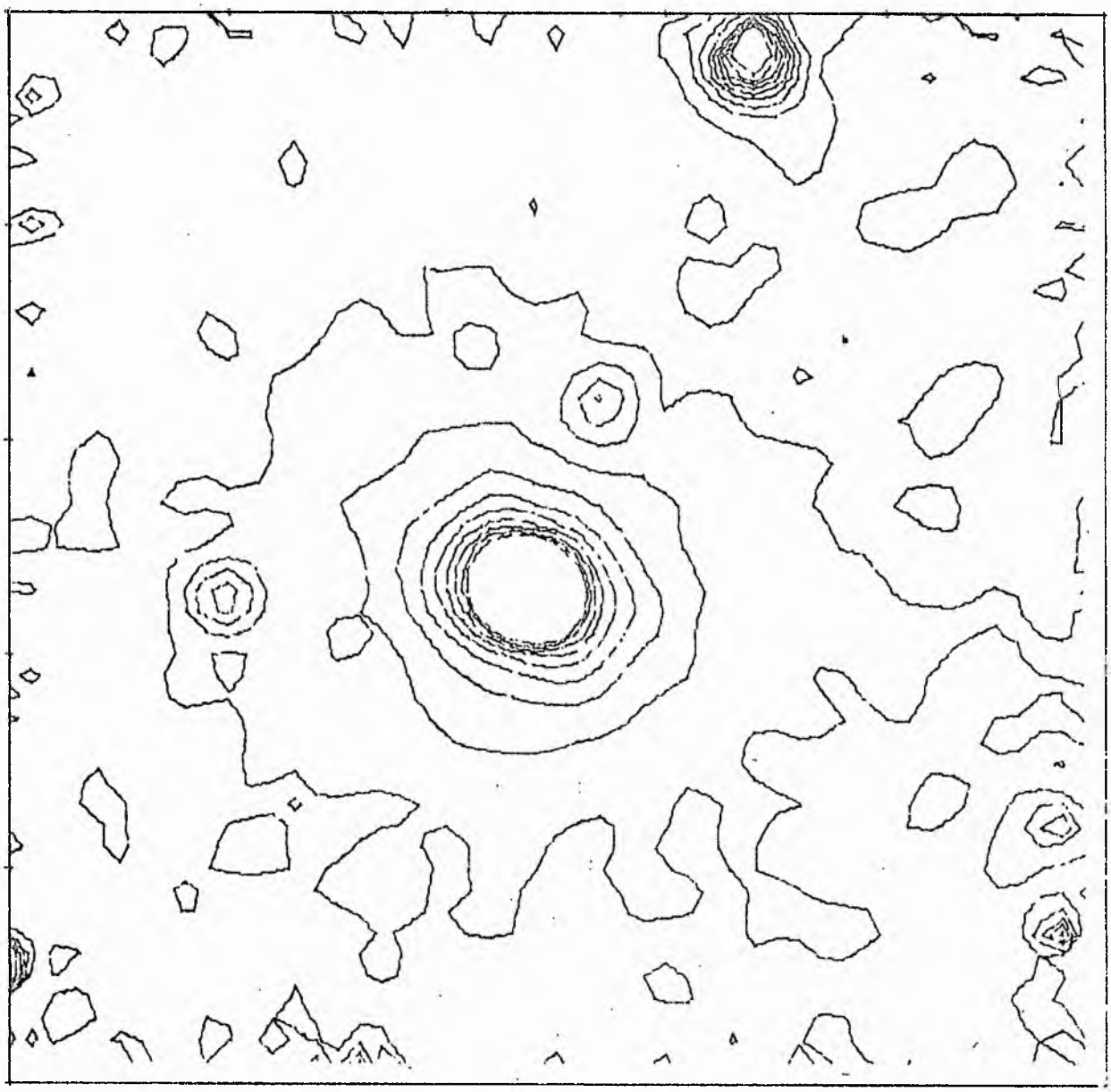

Figure 18 NGC 4261

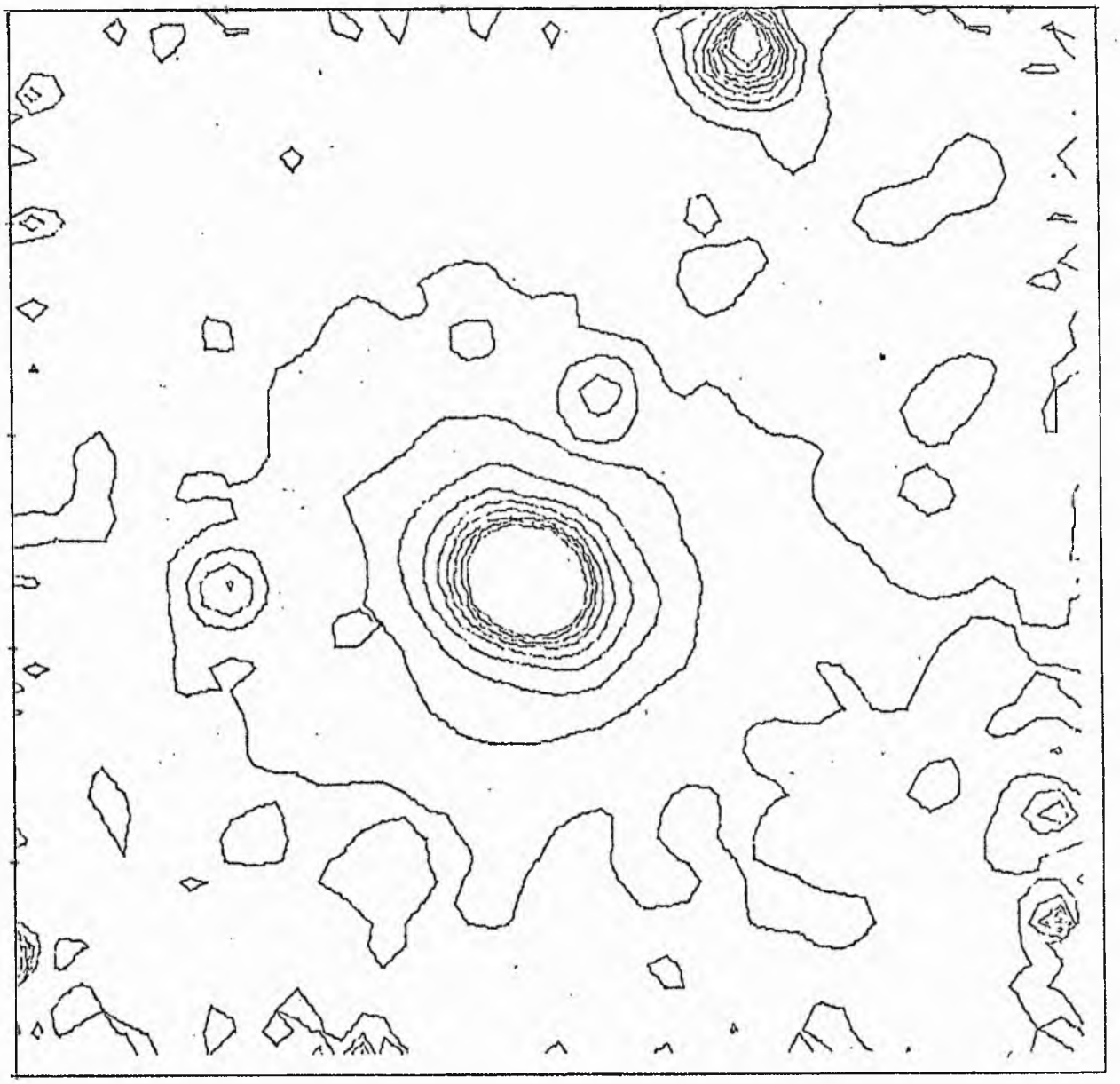

NINE POINT CROSS-ROWS THEN COLUMNS SMOOTHED 3 TIMES

Figure 19 NGC 4261

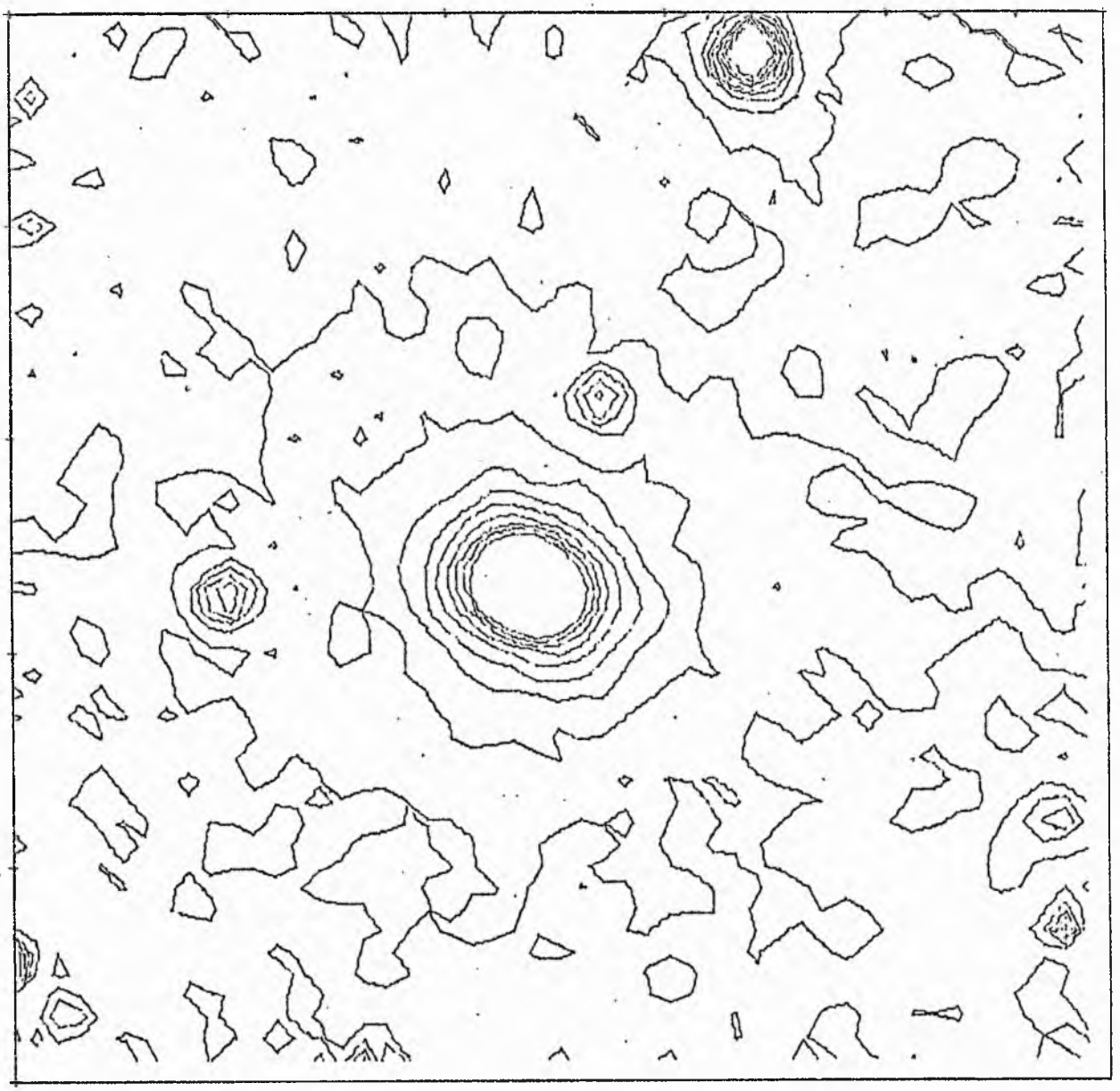

NINE POINT CROSS, SIMULTANEOUS IN X AND Y

Figure 20 NGC 4261

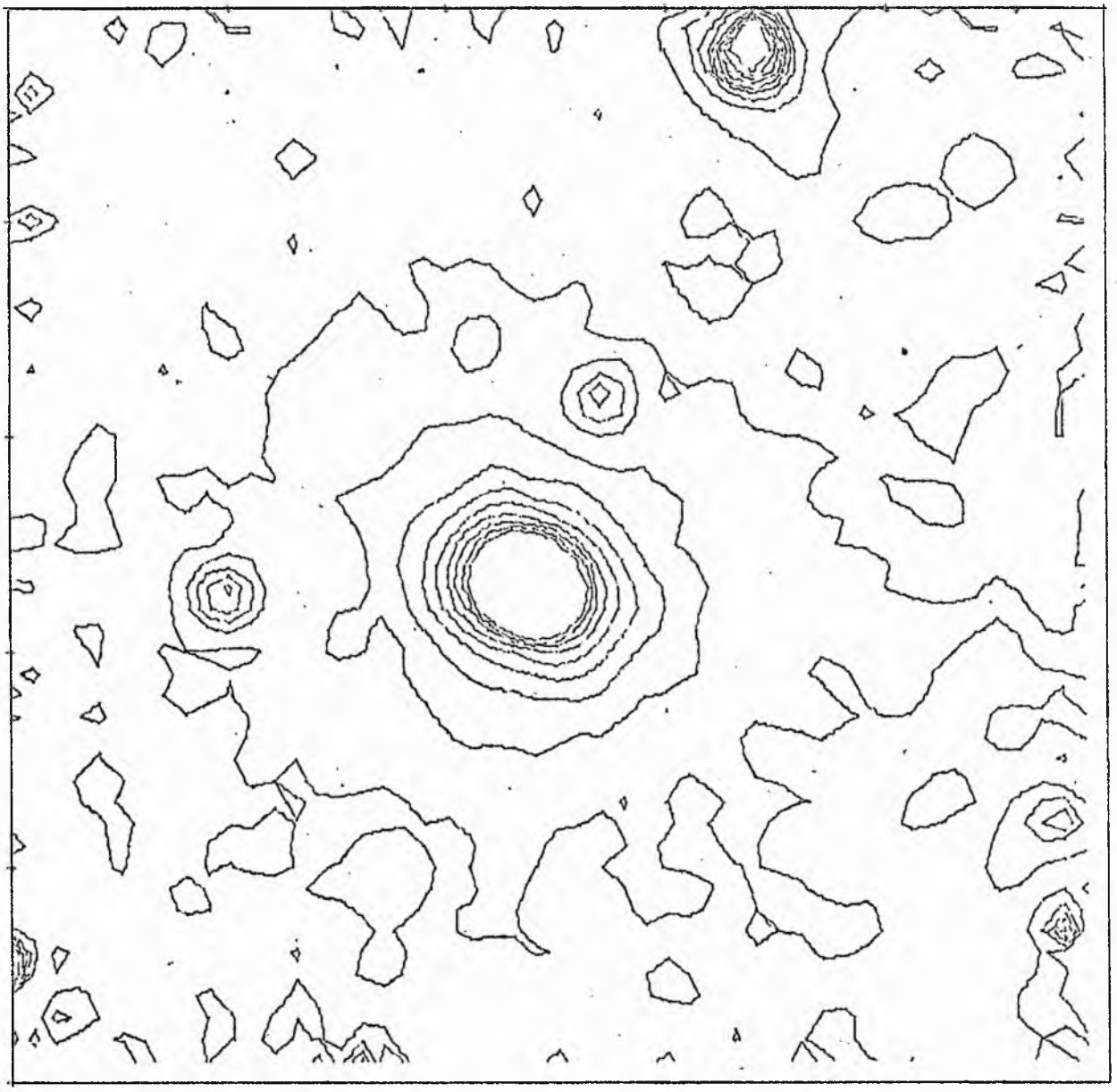

NINE POINT CROSS, SIMULTANEOUS IN X AND Y SMOOTHED 2 TIMES

Figure 21 NGC 4261

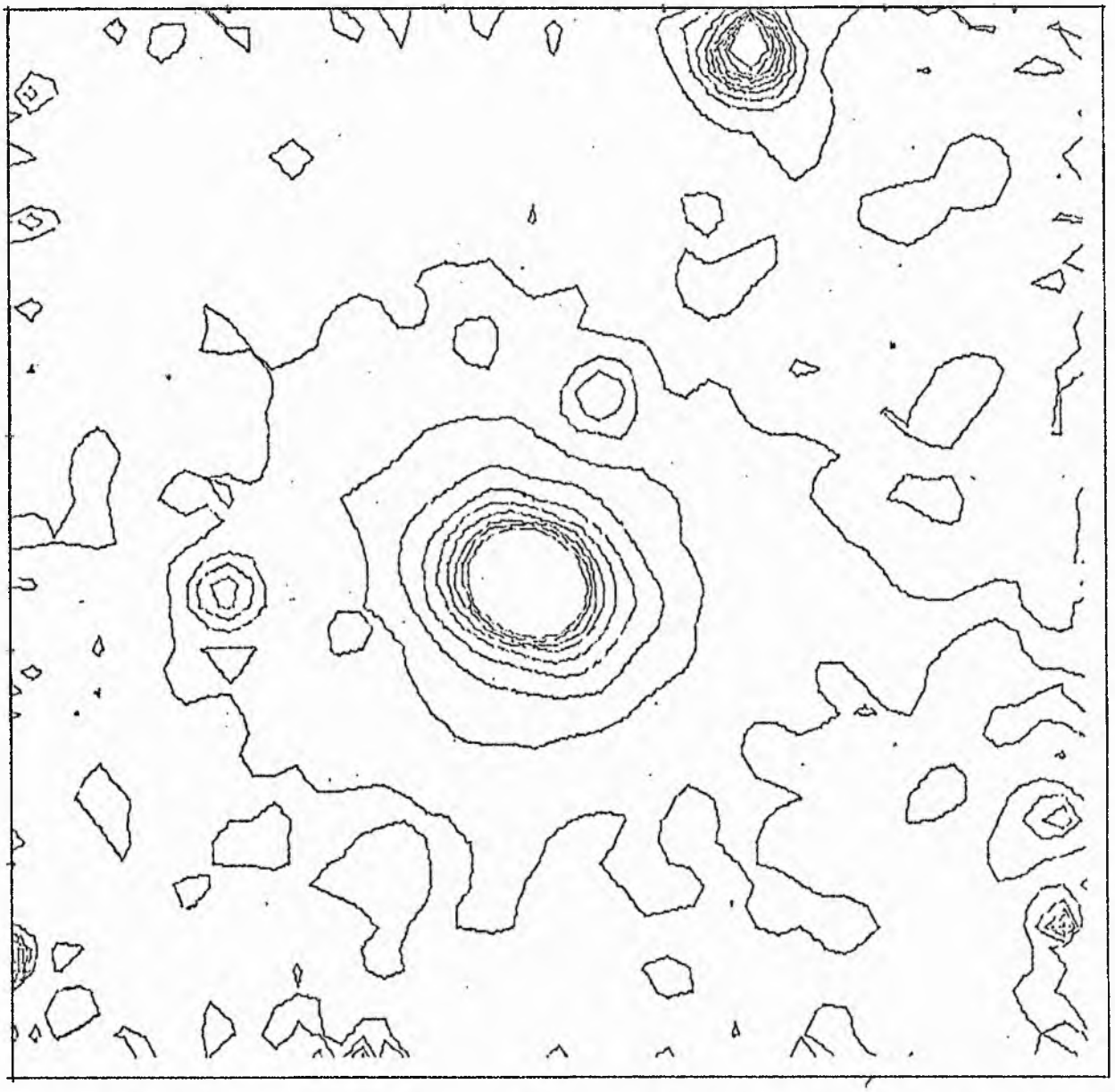

NINE POINT CROSS, SIMULTANEOUS IN X AND Y SMOOTHED 3 TIMES

Figure 22 NGC 4261

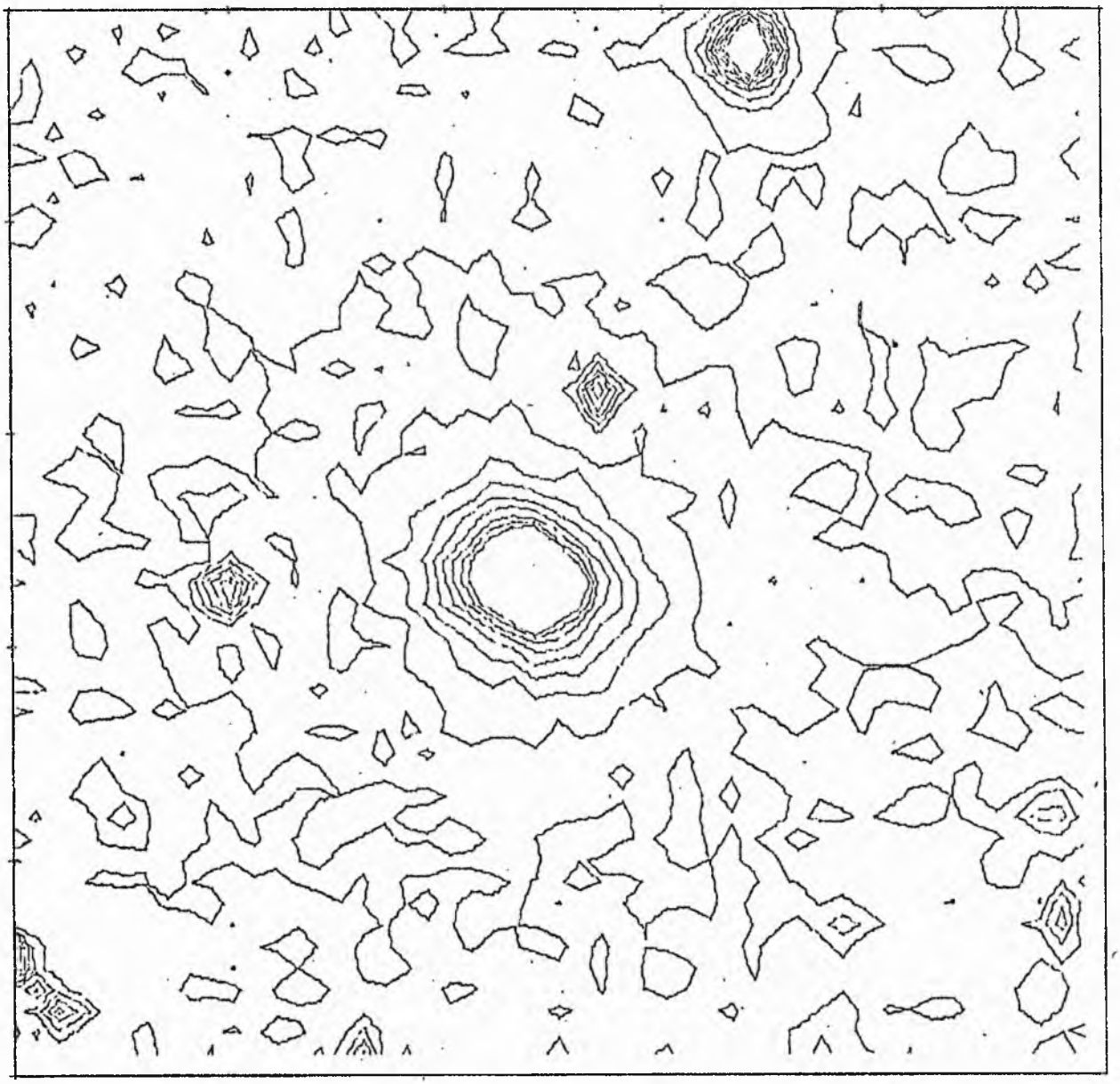

NINE POINT BLOCK

Figure 23 NGC 4261

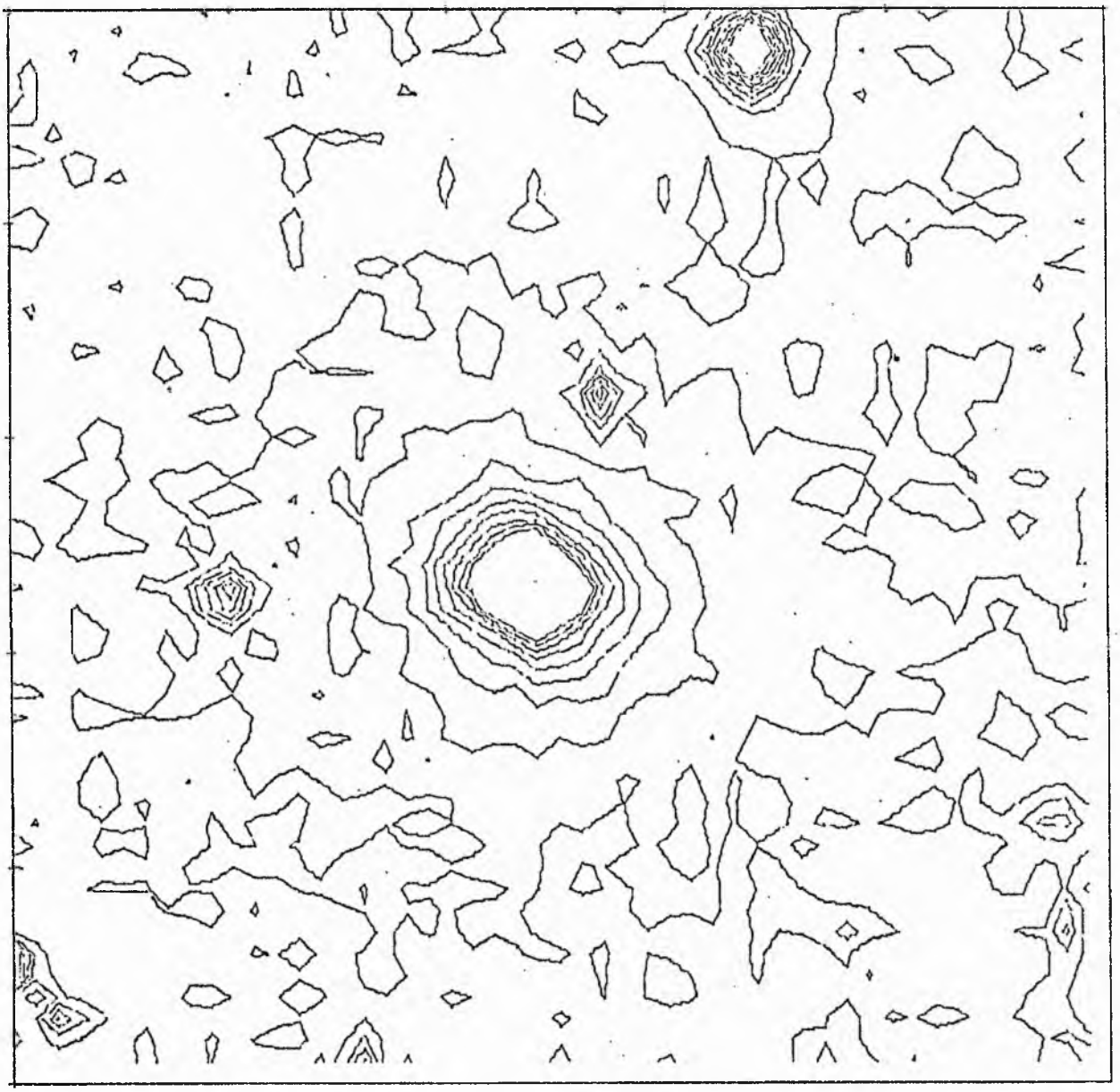

NINE POINT BLOCK SMOOTHED 2 TIMES

Figure 24 NGC 4261

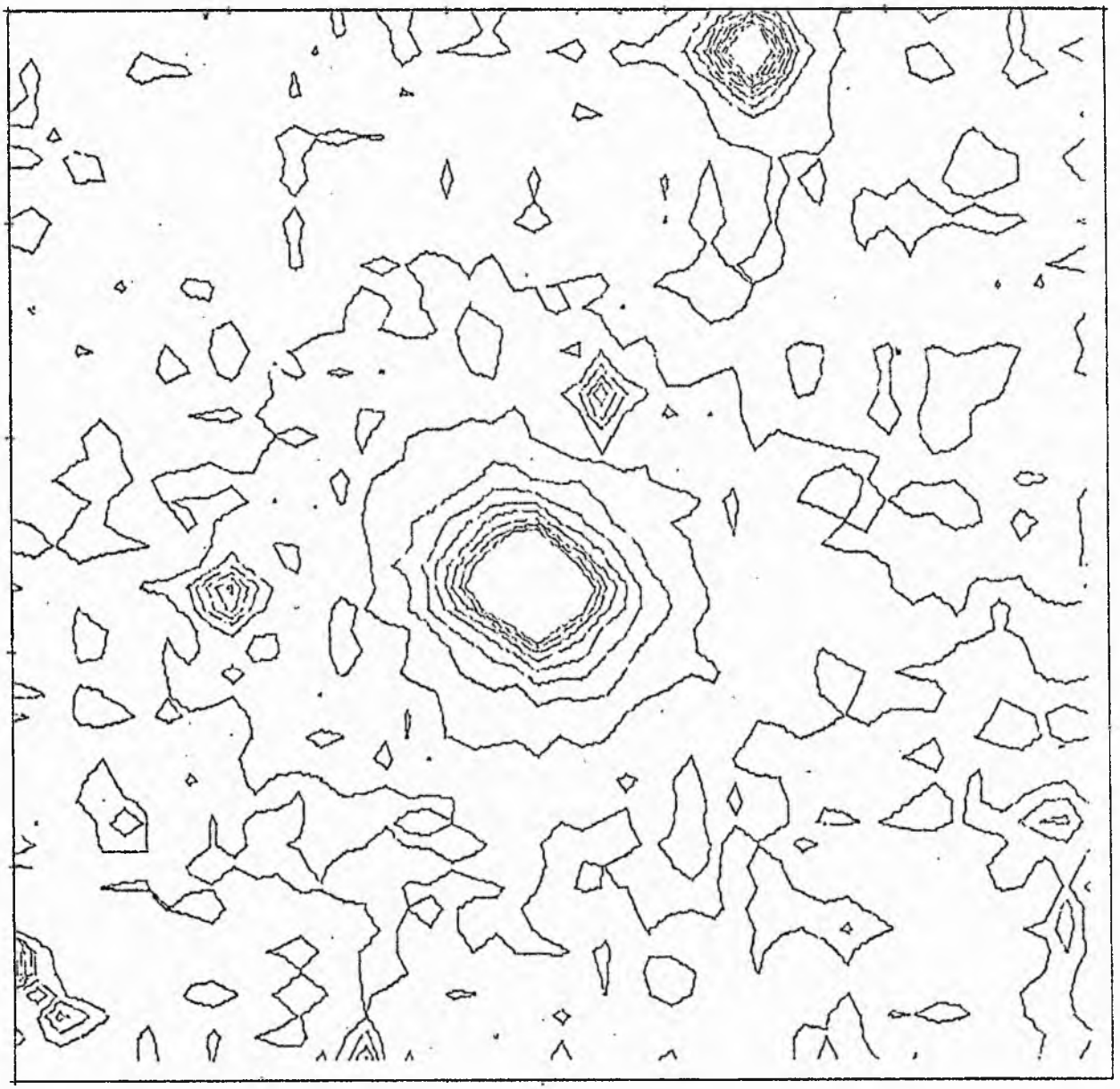

NINE POINT BLOCK SMOOTHED 3 TIMES

Figure 25 NGC 4261

present in regions of low density. However, the IDT tracing has the advantage that a far smaller stepping increment, of the order of magnitude of the plate grain, was used and all the information was retained and presented visually to the human eye, which is an excellent integrator. The mass of detail is easily averaged and the outermost isophote may easily be located at the changes in the line to space ratio of the background. The agreement with the smoother data for the nine-point cross shows that the principle of smoothing is successful when applied to the fainter isophotes so long as the remaining information is left unsmoothed in order to preserve resolution and detailed structure in the central regions. It is concluded that the coded IDT maps are vastly superior for the isophotometric studies, but in the absence of an isodensitracer, a large amount of useful information may be obtained with the application of appropriate smoothing techniques, with due consideration being given to their inherent nett gains and losses.

This work paralled a detailed investigation by W. Jones et al. (1967) on numerical mapping techniques. These techniques involved the determination of isophotes from a set of grid measurements. The sky background was

divided into two components, one to examine the overall variations of the background and the other to study point sources which could be removed from the background, such as stars, flaws in the emulsions etc. Least squares fits of different trigonometrical functions were performed on the data, and the smmothing corrections derived in this way were only applied up to a given intensity level, consistend with the conditions indicated in the previous paragraph.

The results of this investigation would appear impressive compared with the work carried out on NGC 4261. However, it should be stressed that the two projects were entirely different in character. On the one hand, the former study attempted to obtain a complete set of isophotes for an object, while the current work at St Andrews was only concerned with the determination of the outermost isophotes.

Chapter IV

4.1 Introduction. The aim of the current work has been to obtain detailed photometric parameters in two colours for a set of galaxies of different morphological types. In the past, workers have published their own parameters which were determined arbitrarily, but with the establishment of an IAU Working Group on Galaxy Photometry, the parameters have now been standardized. It is in these standard parameters that the results of this investigation will be presented. Although some of the parameters have been described in the first chapter of this thesis, the following list gives the full definitions and descriptions of the parameters (de Vaucouleurs 1961c) obtained for each galaxy. This photometric information will be presented in Volumes 2 and 3 of the thesis.

4.2 Parameters. It is convenient to subdivide the definitions for parameters into parts, depending upon galaxy type.

Case 1. Circular Case. Let the mean radial specific intensity distribution be $I(r)$ for a system with circular symmetry, such as an E0 galaxy. The integral luminosity emitted within radius r from the centre is then

$$L_r = 2\pi \int_o^r I(r)\ r\ dr \qquad (1)$$

and the total luminosity is

$$L_T = 2\pi \int_\bullet^\infty I(r)\ r\ dr \qquad (2)$$

giving a corresponding total magnitude of

$$m_T = c - 2.5 \log L_T. \qquad (3)$$

The fraction of the total luminosity emitted between 0 and r is

$$k(r) = L_r/L_T \qquad (4)$$

and the function k(r) defines the relative integrated luminosity profile of the galaxy, either as a function or $\underline{r}$ or, through the luminosity profile I(r), as a function of I . The value of L_T is calculated by extrapolation using I as the variable, as outlined by de Vaucouleurs (1960). The effective radius r_e of the galaxy is such that

$$k(r_e) = 1/2 \qquad (5)$$

Case 2. General Case. For a system without circular symmetry, such as an elliptical seen edge-on, a spiral, or even an irregular system with detached "islands", an

equivalent radius r^* may be defined by the relation

$$r^* = \sqrt{A/\pi} \qquad (6)$$

where A is the total area within a given isophote, including irregular structures. The equivalent luminosity profile $I(r^*)$, the equivalent relative integrated luminosity curve $k(r^*)$ and the equivalent effective radius r_e may then be defined as before.

If the unit of surface brightness of I is calibrated in photographic magnitudes per square minute, the luminosity profile may be placed on an absolute basis of specific intensity and the absolute value of specific intensity I_e along the effective isophote of area A_e corresponding to the equivalent effective radius r_e can be determined. If the absolute value of specific intensity is expressed in magnitude per unit solid angle μ, the value of μ_e corresponding to I_e may be used to calculate the average specific intensity I'_e or μ'_e inside the effective isophote from the relation

$$I'_e = L_e/A_e$$

$$= L_T/2A_e \qquad \text{from (4) and (5).}$$

Hence

$$I'_e = L_T/2\pi(r^*_e)^2. \qquad (7)$$

The corresponding relation for μ'_e is derived from equation (3) giving

$$\mu'_e = c - 2.5 \log I'_e$$

$$= c - 2.5 \log L_T + 5 \log r^*_e + 1.995$$

$$= m_T + 5 \log r^*_e + 1.995. \qquad (8).$$

It is important to notice that the effective parameters are independent of the observing conditions so long as the semi-minor axis is much greater than the instrumental profile. This was one reason for making the selection of galaxies, discussed in section 2.2., for the present investigation.

The luminosity distribution of galaxies can also be expressed in terms of the reduced, or dimensionless variables, as outlined in the first chapter. If $J = I/I_e$ and $\alpha = a/a_e$ or $\rho = r^*/r^*_e$, galaxies of the same type and orientation should be represented by the same reduced luminosity profile $J(\alpha)$ or $J(\rho)$.

In addition to the effective dimension r^*_e defined by $k(r^*_e) = 1/2$, it is in terms of this function that two further dimensions, r^*_1 and r^*_3, are introduced in order to define the concentration indices given by the expressions

$$C_{21} = r^*_e/r^*_1 \qquad \text{and}$$

$$C_{32} = r^*_3/r^*_e \qquad (9)$$

where $k(r_1) = 1/4$ and $k(r_3) = 3/4$.

In addition to the characteristic parameters just described, the study of surface photometry within an object is completed with the following supplementary tables and diagrams:-

(1) A set of isophote maps

(2) The luminosity profile log I(a) and Log I(b) along the respective major and minor axes.

(3) The relative integrated luminosity curve $k(r^*)$ and

(4) A table of the mean luminosity distribution I(r) and the integrated luminosity k(r) with arguments I and r^*.

4.3 Plate Material. The total number of galaxies with $m < 13$ for which plates have been obtained on the James Gregory Telescope was 106. The dates during which the observations were carried out are shown as follows:-

Dates	Number of Plates taken	Number of galaxies photographed.
March 1965 to May 1965	48	52
November 1965 to April 1966	71	46
November 1966 to March 1967	6	8
Total	125	106

However, for the reasons given in section 2.2, only 48 galaxies with face-on diameter $D(0) > 2$ arc min were chosen for detailed investigation. Observations were made in the international B and V system using the following plate/filter combinations:-

B system Kodak 103a0 and Schott GG 13

V system Kodak 103aD and Schott GG 14

All the plates were taken with Hour Angles less than 2^h from the meridian, so that over the range of declinations in the study ($16^\circ \leq \delta \leq 3^\circ$), the maximum and minimum values of sec z were 1.91 and 1.31 respectively, at the latitude $+56^\circ 20' 10''$ of the University Observatory.

In view of the small f/ratio of the telescope, it was necessary to maintain a strict check on the focus setting during observations. In this connexion, it is

interesting to note the effect on the focus setting of interposing a glass filter in front of the photographic emulsion. At the centre of the plate, the focus is pushed out by 0.2004t while at the edge of the field, the coefficient of t is 0.2036, where t is the thickness of the filter in use. The value of the coefficient is based upon values of the angles of incidence $\underline{i}$ of the convergent beam, which for the James Gregory Telescope were found to lie in the range $6^{\circ} \leq i \leq 9^{\circ}$. It should be noted that with a filter in use, there is a difference in focal setting equal to 0.0032t at full aperture between the centre and the edge of the field. This is another reason, in addition to that outlined in section 2.2 for using the minimum aperture of 30 inches.

In order to secure photometric information that is homogeneous, two exposures of 4 and 40 minutes were used throughout the work. The galaxy profiles obtained from the 40 minute exposures were supplemented in the central regions by profile sections derived from the 4 minute plate. The longer exposure, the maximum value possible, was dictated by the blackening of the sky background on the plate due mainly to urban lighting.

Nevertheless, this exposure was still sufficiently large to detect the faint outer regions. The plates chosen for the reduction had passed a very thorough series of tests, based upon image quality, emulsion defects, uniformity of background, and density of the calibration areas etc. One of the most common causes for plate rejection was the considerable difficulty encountered with the telescope sidereal drive during the 1965/66 observing season. Frequent audible bursts of hunting of the drive motor resulted in trailed images before it was possible to end the exposure by moving from the guiding eyepiece to the plate loading assembly area in order to close the dark slide.

4.4 Isophotes. The first stage in the overall reductions involved obtaining detailed B and V isophote maps for each of the 48 galaxies under study. Most of the advantages of the Joyce Loebl Isodensitracer have already been mentioned in the previous chapter, but before satisfactory tracings could be produced with regularity, it was necessary to make a few modifications to the instrument. To secure some degree of uniformity, all tracings were made with a density increment of 0.12, a scanning aperture of 50μ x 50μ or 3.8 x 3.8 arc sec., and depending upon the angular diameter of the object,

with a magnification of either 50 or 100 in order to fill the entire recording area. The base-line setting for the background was set up to produce approximately equal line to space ratios in order to assist with the determination of the fainter isophotes. After the initial setting sequence, it was possible to leave the machine unattended to trace the isophote maps automatically. However, three major system faults became apparent in the early tracings and they will be described at this point.

First of all, the recording pen supplied did not dot correctly and only lines and spaces could be seen on resulting tracings. The fault did not lie in the electronic circuits, since the pen was physically going through a dotting sequence, neither was it due to the ink flow of the biro pen since lines were being drawn with ease. After many tests, it was established that the quality of the dots depended upon the velocoty with which the pen made contact with the recording paper. Now with no signal input present on the pen solenoid, that is, in the clear mode, and also with the IDT pen assembly lowered as far as possible down to the recording paper, there was still a large gap between the pen tip and the recording paper surface through which the pen had to travel in order to dot. The velocity acquired by the pen when contact

was made with the paper was considered far too large, and an additional spacer was inserted in the solenoid/ pen-holder assembly in order to narrow the gap to about half its original value. This modification produced an immediate improvement in the dotting quality of the pen and the resulting tracings were acceptable for detailed measurements.

The second problem was only encountered after approximately the first ten tracings. For no obvious reason, the pen mode would change completely in the middle of a tracing, giving clear areas where there were previously dots, dots where there were lines and lines instead of spaces. Initially, such tracings were immediately stopped and a second trace taken. However, after this fault had occurred several times, a connexion was established between the fault and the lamp failure. The lamp life seemed to average out at about 40 hours, or the time to complete 10 tracings, and the fault was noted to occur about 5 hours before failure of the lamp.

The third problem, repeated breakages of the drive cord, arose as a consequence of the lamp failure. Should the lamp fail during an IDT tracing, the servo-positioning motor controlling the wedge movement tries to position the density wedge at infinite density. Since the maximum

density on the wedge has a finite value, the servo motor pushes the wedge to end-stops, and all the strain is then taken up on the drive cord, which fractures easily after a short time under tension. Such a problem does not arise in MDM operation because the operator is in constant attendance. The difficulty was overcome by fitting a silicon photo-sensitive diode inside the lamp-holder assembly, together with the necessary electronic circuit for switching off the servo amplifier when the diode detected the large change in light intensity at bulb failure.

Returning to the second problem it seemed strange that such sudden density jumps were present, especially since the optical system was designed to take account of any intensity changes in the reference supply. However, let us consider the effect of a slow variation in the intensity of the reference beam, while the measuring beam intensity remains constant. On IDT work, this variation would have remained unnoticed but for the obvious error in the visual display on the tracing. Of course, the sudden jump on the tracings would have been due to the magnitude of the difference in light output being by this stage large enough to move the commutator ring relative to the pen contacts, described on figure 7 in section 3.3., from the centre of the area in which they were originally

set up over to an adjacent area. However, having described in detail the effect, the cause must still be sought for the apparent variation in the reference source intensity. The clue to the solution lay in the very fact that such density jumps were found near the end of the usable life of the lamp. Figure 26 shows the plan view of the initial stages of the optical paths.

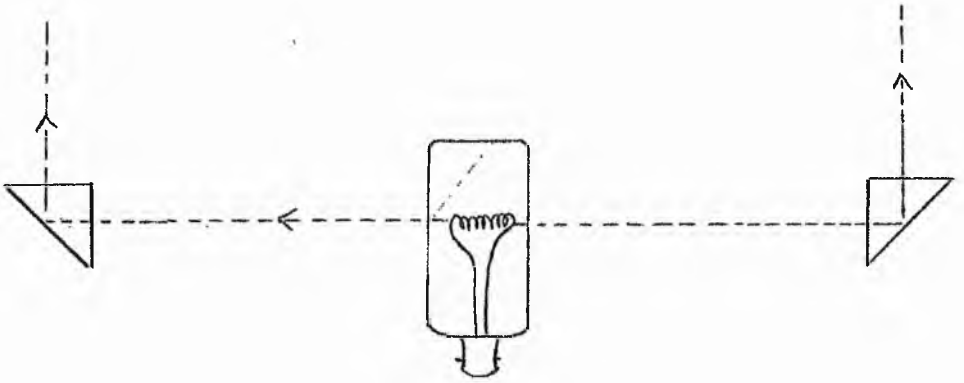

Figure 26 - Lamp and prism optical arrangement in Joyce Loebl. Although both prisms reflecting the respective reference and measuring beams are receiving light from an almost point source, namely the ends of the lamp filament, this point source is still different for each beam in that it is separated by the length of the filament. Now the effect of a variation of light output across the filament itself would be to produce a change in the intensity of the reference beam with respect to the measuring beam, thus removing the advantages of the long-term stability

found with the single lamp system. It is proposed that it is local variations in the resistance of the lamp filament which produced the different light outputs, and such resistance variations would be expected near the end of a lamp's working life.

The lamp fitted to the Joyce Loebl was originally a tungsten lamp with an average working life of 40 hours. Around the time of delivery of the instrument to the University Observatory, quartz-iodine lamps were becoming increasingly popular, in view of their high light output and apparently long life. Furthermore, when used as standard fittings in motor car headlights, they must be able to withstand multiple on-off switchings, something which is not recommended for the tungsten projector lamps. The lamp housing assembly was modified to accept the slightly different mounting of a quartz-iodine lamp, which was then fitted. In view of the relatively high light output of quartz-iodine compared with a tungsten source, this new lamp was slightly under-run, and this had the effect of prolonging its working life. Even the filament of the quartz-iodine lamp had much smaller dimensions than its tungsten counterpart. Tracings obtained since this modification have been completely free from drift problems, indicating that the tungsten lamp

filament must have suffered from resistance variations. The new quartz-iodine lamp has been in use now for over 1000 hours, and although the photo-diode lamp-failure detection circuit has not been required, it is a source of encouragement that this is the case.

The isophote maps produced were all measured with a planimeter, and appropriate scaling factors were used to transform the areas of each isophote to angular measurements. The planimeter was fitted with a special magnifying tracer to facilitate accurate measurements. From the isophote map, the major and minor axes are determined by plotting the length of the radius vector for each isophote against its corresponding position angle. The points of intersection with the principal axes are measured for each isophote to determine its ellipticity. Where the isophote intersects the axis in more than one point, the average value is taken. It now remains to calibrate each isophote, and this is done by means of microphotometric cross-sections.

4.5 Cross-sections and calibrations. Microphotometer scans were made in four directions across the centre of each galaxy, two directions being along the principal axes, and the other two at 45^{o} to these axes. In view of the recent digitization of the microphotometer, almost all the

reductions were carried out at the University Computing Laboratory, in which an IBM 360 Model 44 is available. At first, the scans were made with the same aperture as that used for the isophote maps, 50μ x 50μ, and they extended well beyond the measured major axis of each galaxy. However, after preliminary results on all the galaxies became available, some of the values for the effective radii seemed to be rather low. It became clear during discussions with Dr G. de Vaucouleurs, who visited the University Observatory prior to the 1970 IAU General Assembly in Brighton, that the scans may not have extended sufficiently far into the background and as a result, the sky background density level was too high, giving too low a value for the total luminosity of the object. Accordingly, all the original scans were re-run following the IAU meeting, but on this occasion the total length of scan was 31 arc min, giving an extension from the nucleus of 16.5 arc min into the background; the scanning aperture was 200μ x 50μ or 14.2 x 3.8 arc sec on the plate. These large scans enabled a much more precise assessment to be made of the sky background level. Measurements were made of the densities above the sky background at known

radial distances greater than those for which values had originally been obtained and this information, together with the revised sky background value was used to supplement the original digitized measurements.

The relative calibration was carried out by making scans across the wedge exposures with a projected scanning aperture equal to 0.4 x 0.1 mm. Since the calibration "curve" was being constructed in the linear form following de Vaucouleurs (1968), it was necessary to convert the densities measured on the tracing back to opacities. The continuous density wedges supplied with the MDM are of the linear type and have known factors for determining the relationship between the density of the wedge and distance on the recording paper. These MDM wedge factors were checked on the Hilger L470 machine and were found to be accurate within the limits of the calibration graphs supplied with each wedge. It is thus only necessary to measure distance on the tracings above a fixed reference level and multiply this distance by the wedge factor to ascertain the density level.

Let us suppose a particular step of the calibration wedge gives a density above the fog level of the plate $D = \log (\Delta_o/\delta)$ where Δ_o would be the equivalent deflection produced by the fog level in a transmission

measuring system and δ is the corresponding deflection produced by scanning across the step. Then the opacitance for this particular step is given by

$$\omega = \left(\frac{\Delta}{\delta} - 1 \right)$$

A graph of $\log \omega$ versus $\log I$ for all steps on the wedge exposure yields the value of n in the following relation for the characteristic curve

$$I = A\omega^{n}$$

At the same time as the calibration exposures were made, scans were taken at least 20 arc min to the north, south, east and west of the galaxy in order to determine the level of the sky background relative to the fog level on the plate. The average produces the required density level of the background D_s.

The reduction procedure for the cross-sections and isophote calibration was as follows:-

1) For all the digitized values in each scan, it was first necessary to transform the voltage measurements to density. Results of separate tracings produced a value of 0.2884 for the conversion factor for changing voltage to density. Since the least significant digit on the digital voltmeter measuring density was one hundredth

of a volt, the accuracy of the density measurement was 0.0028, or better than one per cent in transmission.

2) Each density value in its present form was related only to the arbitrary initial voltage setting on the digital voltmeter before the digitization scan commenced. A zero point conversion had to be applied to convert these arbitrary density measures to known densities above the plate fog. The average value of the first ten digitized points of the scan was calculated. At the same time as the digitization scans were in progress, a microphotometer tracing was also produced for checking purposes in the subsequent reductions. The average density level of that part of the tracing corresponding to the first ten scan values was determined and any necessary adjustment between this level and the true background level as determined from the later scans was noted. After applying this minor adjustment, the difference was calculated between the arbitrary density value of the background found from the digitized scans and the true density level D_s determined during the calibration traces. This difference was applied to every digitized density value to make the new values correspond with correct densities above the plate fog level.

3) Every density value was converted to a corresponding intensity above the plate fog level using the linear calibration curve. The intensity value of the sky background corresponding to density D_s is equal to i_s and the intensity of a point in the cross-section with a corrected digitized density value equal to D_{g+s} above the fog level is given by i_{g+s}, made up of an intensity i_s due to the sky background plus the intensity contribution i_g from the galaxy itself.

4) The next step is to assign to each relative intensity value on the digitized scan a position value relative to the centre of the galaxy. The precise position sampling interval during digitization was known in angular measure, and it only remained to find the centre of the cross-section from the array of digitized values. The radial distances $\underline{r}$ of each point from the centre were then computed, and with information on the intensity, it was then possible to output from the computer the luminosity profiles $\log I = f(r)$ either in numerical form on the line-printer or in graphical form on the plotter.

5) The intensity in the luminosity profile is given by the expression

$$I = \frac{i_{g+s}}{i_s} - 1$$

i.e. using the sky background intensity as a unit.

6) The values for the abscissae of the points of intersection of isophotes along each axis (+a and -a for major axis, $\pm$b for minor axis, $\pm$c and $\pm$d for the two axes at 45^{o}) were punched on cards and loaded in the computer. Interpolations on the luminosity profile appropriate to the axis gave values for log I, for the abscissae of each intersection of each axis with each isophote. The mean values were taken for each axis, then for each isophote and the $\overline{\log I}$ value obtained is plotted against $r^{*} = \sqrt{A/\pi}$ where A is the area measured by planimetry of the isophotes. A smooth curve drawn through the points yields that part of the equivalent luminosity profile within the outermost isophote. The remaining section is found after measuring on the luminosity profile graphs the abscissae where log I = -1.0, -1.2, -1.4, -1.6, -1.8 and -2.0. The equivalent radii were given by

$$r^{*} = \sqrt[4]{\bar{a}.\ \bar{b}.\ \bar{c}.\ \bar{d}.}$$

4.6 Integration. Values of r were measured from the equivalent luminosity profile for intervals in log I of 0.1 down to a threshold level of log I = -2.0. The

luminosity L_r within a radius $\underline{r}$ was found from the following expression

$$L_r = \pi \sum_{i=1}^{n} (r_{i+1}^2 - r_i^2) I_{i+\frac{1}{2}}$$

where $\underline{i}$ denotes the isophote under consideration.

This expression may also be written in the form

$$L_r = \pi \sum_{i=1}^{n} P_i$$

where each value of P is the luminous flux in an annulus of width $(r_{i+1} - r_i)$.

The selection of the rather small integration interval of 0.1 in log I produced a negligible error in the calibration of the total luminosity. This choice was based on results of a study by de Vaucouleurs (1948), in which it was found that the systematic errors which could be introduced in ΣP increased approximately with the square of the integration interval.

The total luminosity L_T is found by computing the extrapolation correction ΔP which allows for the contribution of the outermost parts of the galaxy below the threshold. The correction ΔP is obtained by plotting log $(P/\Delta I)$ versus log $\bar{I}$ and this curve is extrapolated to a value of $\bar{I}$ midway between I_1 = threshold value and I = 0 corresponding to $r = \infty$, i.e. $I_1/2$. With a threshold value of log I = -2.0, this gives $I_1 = 0.01$ and $\bar{I} = .005$. L_T is given by the expression

$$L_T = \Sigma P_i + \Delta P$$

Calculations of L_T are shown in the appendix where the integration tables of the mean luminosity distribution for each galaxy have been listed.

The absolute calibration has not been made with some of the unnecessarily complicated methods used in the past, e.g. extra-focal stellar images or north polar sequence transfer. Although these methods may have been successfully used by Holmberg (1958) and Markaryan (1965), they are nevertheless subject to many sources of error, such as variable absorption and changes in temperature and humidity. With the large number of photo-electric measurements listed in the Reference Catalogue (de Vaucouleurs and de Vaucouleurs 1964), it was possible to relate measurements of the integrated magnitude of a galaxy within some arbitrary fraction of the total flux received through field apertures of diameter $\underline{2r}$ placed in the focal plane of a telescope. If m_r is the tabulated magnitude in the B.G.C. with a given aperture radius $\underline{r}$ and L_r the integrated luminosity within the same radius, the relation

$$m_r = \text{constant} - 2.5 \log L_r$$

defines the conversion constant between relative and specific intensities (e.g. de Vaucouleurs et al. 1968). Several apertures were desirable to determine the constant more accurately, since both L_r and m_r are subject to errors. Values of L_r corresponding to each value of m_r and $\underline{r}$ listed in appendices II and III of the B.G.C. are obtained from the integration table of mean luminosity distribution, and for each pair of entries in the catalogue, a separate constant is produced.

Chapter V

5.1 Introduction. The photometric data obtained in the current investigation are listed in the subsequent volumes of the thesis. However, before a discussion of these results is given, it is first necessary to examine some of the more important sources of error in the work.

5.2 Errors. Errors may be divided into two categories. First of all, there are errors arising from those sections of the work concerned only with relative measurements, and secondly, there are errors arising from the photo-electric calibration process.

In the first case, many of the error sources introduced in the initial stages of the investigation by the use of the conventional H-D characteristic curve have been removed by the use of the 'linear' curve (de Vaucouleurs 1969). In addition, there are errors introduced when the sky background is not well-defined; these errors have been investigated by de Vaucouleurs (1948). Not only will the value of the total magnitude be affected by such poor determinations, but also the values of the parameters involving distance, such as the major axis at threshold, effective radius etc. Although Evans (1952) has already shown that,

depending on the magnitude of the sky background upon which the galaxy is superimposed, a background level error of $0^m.02$ could introduce an error of $0^m.15$ in the total magnitude of the galaxy, it would, nevertheless be interesting to convert the $0^m.02$ background magnitude difference into density on a typical microphotometer tracing and then compare such a density value with the typical conversions applied to the present data after the reduction of the additional large radial distance scans made following the IAU. Before proceeding, it is necessary to know the density value of the background to which the $0^m.02$ difference is to be applied. The usual density for the sky background on a 40^m exposure plate was about 0.45 above the plate fog level. This corresponds to $\omega = 1.818$, and $I = 0.1291$ if $n = 0.5$ in the equation

$$I = A\omega^n$$

A magnitude difference of $0^m.02$ leads to a new value of $\log I = 0.1321$ giving $\omega = 1.864$, equivalent to a density above the plate fog of 0.457. Thus a magnitude variation in the galaxy of $0^m.15$ would be produced by a density difference of only 0.007.

Another approach to the problem may be taken by

using numerical values for the intensities obtained from the integration tables of two luminosity distributions. With the largest density wedge supplied with the MDM, the density of 0.007 is equivalent to 0.54 mm on the chart. Tables 1 and 2 show intermediate computer reductions for the mean luminosity distribution of NGC 4486 prior to carrying out the photo-electric calibration. The first table gives the results obtained in the summer of 1970 while table 2 shows the final results for the luminosity distribution using the revised value for the sky background. The ratio of the respective total luminosities L_T in tables 2 and 1 is 1.64, corresponding to a magnitude difference of 0.41. With the large scanning aperture used in the additional cross-sections, it is a simple matter to measure, on the partly smoothed profile for those radial distances at which the erroneous background was taken, the density above the revised background level; in the case of NGC 4486, the density difference was found to be 0.18. Using the magnitude difference for this galaxy of $0^m.41$ from tables 1 and 2, equivalent to a background magnitude difference of 2.74 times Evans' value, the corresponding density difference should be 0.19. Although the actual value was 0.18 or 1.39 mm., the agreement

Table 1

MEAN LUMINOSITY DISTRIBUTION IN NGC 4486
B COLOR

LOG I	I	MEAN I	R	AREA	DEL A	P	SIGMA P	K(R)	RO	LOG J
1.47	29.512		0.0	0.0			0.0	0.0	0.0	1.593
		27.319			68.81	1879.5303				
1.40	25.119		4.68	68.81			1879.530	0.030	0.077	1.523
		22.536			81.20	1829.8232				
1.30	19.953		6.91	150.01			3709.354	0.060	0.114	1.423
		17.971			85.60	1532.3118				
1.20	15.849		8.66	235.61			5241.664	0.084	0.142	1.323
		14.219			108.78	1546.7246				
1.10	12.589		10.47	344.38			6788.387	0.109	0.172	1.223
		11.295			206.33	2330.4055				
1.00	10.000		13.24	550.71			9118.789	0.147	0.218	1.123
		8.972			215.79	1935.9453				
0.90	7.943		15.62	766.50			11054.734	0.178	0.257	1.023
		7.126			172.66	1230.4458				
0.80	6.310		17.29	939.16			12285.180	0.198	0.284	0.923
		5.661			332.60	1882.7546				
0.70	5.012		20.12	1271.76			14167.934	0.228	0.331	0.823
		4.496			401.72	1806.3184				
0.60	3.981		23.08	1673.48			15974.250	0.257	0.379	0.723
		3.572			532.70	1902.6340				
0.50	3.162		26.50	2206.18			17876.883	0.287	0.436	0.623
		2.837			603.79	1939.9692				
0.40	2.512		30.33	2889.98			19816.852	0.319	0.499	0.523
		2.254			644.10	1451.5198				
0.30	1.995		33.54	3534.07			21268.371	0.342	0.551	0.423
		1.790			1437.33	2572.9270				
0.20	1.585		36.78	4971.41			23841.297	0.383	0.654	0.323
		1.422			1710.93	2432.7786				
0.10	1.259		40.12	6682.34			26274.074	0.422	0.758	0.223
		1.129			1966.78	2221.3994				
-0.00	1.000		52.47	8649.12			28495.473	0.458	0.863	0.123
		0.897			2316.44	2078.2183				
-0.10	0.794		59.08	10965.55			30573.687	0.492	0.971	0.023
		0.713			3775.58	2690.6335				
-0.20	0.631		68.50	14741.14			33264.320	0.535	1.126	-0.077
		0.566			5713.37	3234.1687				
-0.30	0.501		80.69	20454.50			36498.488	0.587	1.327	-0.177
		0.450			5515.30	2479.9338				
-0.40	0.398		90.92	25969.80			38978.422	0.627	1.495	-0.277
		0.357			6039.50	2157.1091				
-0.50	0.316		100.94	32009.31			41135.527	0.661	1.659	-0.377
		0.284			6524.09	1850.9351				
-0.60	0.251		110.75	38533.40			42986.461	0.691	1.821	-0.477
		0.225			6962.24	1568.9890				
-0.70	0.200		120.34	45495.64			44555.449	0.716	1.978	-0.577
		0.179			7311.76	1308.8594				
-0.80	0.158		129.65	52807.40			45864.309	0.737	2.131	-0.677
		0.142			7629.58	1084.8550				
-0.90	0.126		138.70	60436.98			46949.160	0.755	2.280	-0.777
		0.113			1945.89	2200.8579				
-1.00	0.100		159.50	79922.87			49150.016	0.790	2.622	-0.877
		0.090			13234.25	1187.3303				
-1.10	0.079		172.20	93157.12			50337.344	0.809	2.831	-0.977
		0.071			19658.25	1400.9341				
-1.20	0.063		185.50	112815.37			51738.277	0.832	3.115	-1.077
		0.057			13477.44	762.9226				
-1.30	0.050		200.50	126292.81			52501.199	0.844	3.296	-1.177
		0.045			33741.44	1817.1807				
-1.40	0.040		225.70	160034.25			54018.379	0.869	3.710	-1.277
		0.036			31320.87	1118.6866				
-1.50	0.032		244.80	191355.12			55137.062	0.887	4.057	-1.377
		0.028			38516.00	1092.7385				
-1.60	0.025		270.50	229871.12			56229.801	0.904	4.447	-1.477
		0.023			46313.37	1043.7156				
-1.70	0.020		296.50	276184.50			57273.516	0.921	4.874	-1.577
		0.018			46520.69	832.7649				
-1.80	0.016		320.50	322705.19			58106.277	0.934	5.269	-1.677
		0.014			44748.06	636.2839				
-1.90	0.013		342.00	367453.25			58742.559	0.945	5.622	-1.777
		0.011			38808.25	546.9545				
-2.00	0.010		379.00	451261.50			59689.152	0.960	6.231	-1.877
							62189.000	(1)		

Table 2

REVISED MEAN LUMINOSITY DISTRIBUTION IN NGC 4486
B COLOUR

LOG I	I	MEAN I	R	AREA	DEL A	P	SIGMA P	K(R)	RO	LOG J
1.43	26.915		0.0	0.0			0.0	0.0	0.0	1.833
		26.017			58.90	1532.4402				
1.40	25.119		4.33	58.90			1532.440	0.02	0.04	1.803
		22.536			103.51	2332.5947				
1.30	19.953		7.19	162.41			3865.035	0.04	0.07	1.703
		17.901			110.48	1977.6392				
1.20	15.849		9.32	272.89			5842.672	0.06	0.09	1.603
		14.219			156.43	2224.3042				
1.10	12.589		11.69	429.32			8066.973	0.09	0.11	1.503
		11.295			195.26	2205.4043				
1.00	10.000		14.10	624.58			10272.375	0.11	0.14	1.403
		8.972			184.70	1657.0632				
0.90	7.943		16.05	809.28			11929.437	0.13	0.16	1.303
		7.126			277.58	1978.1682				
0.80	6.310		18.60	1086.86			13907.605	0.15	0.18	1.203
		5.661			269.70	1526.6997				
0.70	5.012		20.78	1356.57			15434.305	0.17	0.20	1.103
		4.496			437.94	1969.1885				
0.60	3.981		23.90	1794.51			17403.492	0.19	0.23	1.003
		3.572			540.03	1928.8147				
0.50	3.162		27.26	2334.54			19332.305	0.21	0.27	0.903
		2.837			717.73	2036.2593				
0.40	2.512		31.17	3052.27			21368.562	0.23	0.31	0.803
		2.254			1016.97	2291.8044				
0.30	1.995		35.99	4069.24			23660.363	0.26	0.35	0.703
		1.790			1594.58	2854.4138				
0.20	1.585		42.46	5663.82			26514.773	0.29	0.42	0.603
		1.422			1839.17	2615.1267				
0.10	1.259		48.87	7502.99			29129.898	0.32	0.48	0.503
		1.129			1941.66	2193.0305				
-0.00	1.000		54.83	9444.66			31322.926	0.34	0.54	0.403
		0.897			3572.52	3205.1267				
-0.10	0.794		64.37	13017.18			34528.051	0.38	0.63	0.303
		0.713			5720.75	4076.8423				
-0.20	0.631		77.23	18737.93			38604.891	0.42	0.76	0.203
		0.566			6348.33	3593.6016				
-0.30	0.501		89.36	25086.26			42198.492	0.46	0.88	0.103
		0.450			7209.09	3241.5413				
-0.40	0.398		101.39	32295.35			45440.031	0.50	1.00	0.003
		0.357			9165.54	3273.6248				
-0.50	0.316		114.88	41460.89			48713.652	0.53	1.13	-0.097
		0.284			11346.51	3219.0918				
-0.60	0.251		129.65	52807.40			51932.742	0.57	1.27	-0.197
		0.225			8179.85	1843.3857				
-0.70	0.200		139.33	60987.25			53776.125	0.59	1.37	-0.297
		0.179			11233.62	2010.9021				
-0.80	0.158		151.62	72220.87			55787.023	0.61	1.49	-0.397
		0.142			15374.00	2186.0396				
-0.90	0.126		166.98	87594.87			57973.062	0.64	1.64	-0.497
		0.113			19995.87	2258.4583				
-1.00	0.100		185.06	107590.75			60231.520	0.66	1.82	-0.597
		0.090			26620.44	2388.2922				
-1.10	0.079		206.69	134211.19			62619.809	0.69	2.03	-0.697
		0.071			42979.31	3062.8967				
-1.20	0.063		237.49	177190.50			65682.687	0.72	2.33	-0.797
		0.057			124638.44	7055.4570				
-1.30	0.050		309.96	301828.94			72738.125	0.80	3.04	-0.897
		0.045			83675.69	3762.4695				
-1.40	0.040		350.30	385504.62			76500.562	0.84	3.44	-0.997
		0.036			58758.81	2098.6855				
-1.50	0.032		376.05	444263.44			78599.187	0.86	3.69	-1.097
		0.028			45084.62	1279.0972				
-1.60	0.025		394.67	489348.06			79878.250	0.88	3.88	-1.197
		0.023			77834.69	1754.0781				
-1.70	0.020		424.90	567182.75			81632.312	0.90	4.17	-1.297
		0.018			99024.19	1772.6282				
-1.80	0.016		460.50	666206.94			83404.937	0.92	4.52	-1.397
		0.014			102193.31	1453.1125				
-1.90	0.013		494.56	768400.25			84858.000	0.93	4.86	-1.497
		0.011			64019.94	723.0901				
-2.00	0.010		514.75	832420.19			85581.062	0.94	5.06	-1.597
							91099.000	(1)		

between the current work and Evans' investigation emphasizes the importance of precise background determination, and also demonstrates the basic difficulties in measuring accurately on noisy tracings, distances of 0.2 mm. The determination of the background level has also been discussed qualitatively and quantitatively by de Vaucouleurs (1948). The two tables also show the dramatic difference in the values derived for r_e, viz., 61."83 and 101."4, indicating an increase of 64% after revision of the sky background level.

For the photo-electric calibration of the photographic measurements, remarks were passed in the previous chapter (section 4.6) on the convenience of such a system, since it removes some of the inherent difficulties present in the more indirect methods. However, it was found in the present work that some pairs of photo-electric results in the Reference Catalogue showed occasional large differences depending upon the observer. Let us consider the case of NGC 4649, whose photometric calibration is shown in table 3, where the magnitude data are taken from appendix I of the Reference Catalogue (G. and A. de Vaucouleurs 1964).

Table 3

Zero point of photographic photometry : NGC 4649

r	B(r)	L_r	Const.	Source of B(r)
32.2 arc sec	11.10	22614	21.99	A
122.2 " "	10.27	48313	21.98	B
122.2 " "	10.06	48313	21.77	C
286.5 " "	9.95	64318	21.97	G

Mean adopted constant in mag.sec.$^{-2}$ 21.98

The sources of the magnitudes, all transformed to the B system, are as follows:-

A - Stebbins & Whitford (1957); B - Stebbins & Whitford (1952); C - Pettit (1954); G - Holmberg (1958).

Clearly the value for the adopted constant should be averaged among A, B and G, since source C, using the same aperture as B, is obviously in error by a fifth of a magnitude. These errors in Pettit's work, detected by de Vaucouleurs (1963), have already been mentioned elsewhere in the thesis. For NGC 4649, the determination of the constant has been easy, but for many other galaxies, where there is a large scatter of constants about a mean, it is necessary to refer to the Introduction to the Reference Catalogue and also to de Vaucouleurs'

work (1963) in order to assess the accuracy of individual magnitude sources. Consider, for example, the following pair of values for NGC 4267. For an aperture radius of 65.6 arc sec, Bigay's (1951) magnitude transformed to the B system is 11.74 while at a radius of 72.1 arc sec, the B magnitude derived from Bigay's et al. work (1953, 1954, 1955) is 12.06. Before these measurements may be used in a zero point determination, there is already a magnitude difference of at least $0^{m}.32$, and although it is known that Bigay's magnitudes were poor at large apertures (de Vaucouleurs 1963), it is still difficult to decide which of these two measurements is the more likely to be accurate. In addition, if the luminosity profile of the galaxy is not correctly determined, the differences will be even greater. For more than half the galaxies studied, no more than two values appear in appendix II for the B-V colour and for 14 objects, there is only one value. Although for some galaxies it may be possible to construct colour curves within the galaxy if both the B and V calibrations are accurate, no attempt will be made in this thesis to construct colour curves of B-V within galaxies, since precise determination of the V

magnitude is impossible for many of the objects, due to inadequate calibration data. Further work to obtain good photo-electric measurements on galaxies is urgently required and this is one field where scope for research is still virtually unlimited.

Some of the calibration problems may well be removed with the introduction of the concept of "standard galaxies", in which well-determined profiles may be used to provide an internal photometric calibration, irrespective of whether the plate carries additional relative calibration areas. There are not yet sufficient photometric profiles of galaxies determined by direct photo-electric scanning methods to justify the establishment of such galaxies as standard objects, although unpublished data on NGC 3115, 3379 and 4486 are now available from de Vaucouleurs. However, using the integrated magnitude B(0) within an aperture of diameter equal to the face-on value D(0), and also the integrated luminosity law for normal ellipticals described in the Introduction to the Reference Catalogue, it is possible to derive the brightness distribution I(r) in magnitudes per square second. This method was outlined by G.de Vaucouleurs at the 1970 IAU meeting of the Working

Group on Galaxy Photometry and full details have now been circulated to members of the Group (de Vaucouleurs 1970).

The integrated luminosity law may be expressed as

$$B(0) - B(X) = \beta X(2X_o - X)$$

where for ellipticals, $\beta = 0.75$ and $X_o = +1$. $B(X)$ is the integrated magnitude within a circular aperture of diameter $A = 2r$ and X is equal to $\log A/D(0)$. The surface brightness $\mu(X)$ at X is given by

$$\mu(X) = -2.5 \log P.Q \quad \text{where}$$
$$P = (0.8)10^{-0.4B(0)}/\pi D(0)^2 \quad \text{and}$$
$$Q = 2\beta(X_o - X)/10^{2X - 0.4\beta' X(X_o - X)}.$$

The quantity P, derived from values of $B(0)$ and $D(0)$ listed in columns 16 and 12 respectively of the Reference Catalogue, fixes the zero point of the stellar magnitude scale and Q gives the shape of the luminosity distribution law.

This method was used to check measurements for NGC 4649, the galaxy whose photometric zero-point calibration was shown in table 3. Results of the calculations are shown in the following table.

Table 4

Use of integrated magnitude to calculate surface brightness in NGC 4649

X	r	P	Q	$\mu(X)_{calc.}$	μ_{obs}	O-C
-1.00	9.5 arc sec	1.93×10^{-6}	75.36	18.48	18.80	+0.32
0.11	122.2 "	"	0.860	23.35	23.49	+0.14
0.30	189.28 "	"	0.303	24.47	24.73	+0.26
0.60	378 "	"	0.044	26.57	26.75	+0.18

It is noted that even with the good calibration constants obtained in table 3 for the zero points of the photographic magnitudes, the surface brightness within the galaxy are about $0^m.22$ faint compared with the quantities derived in the above calculation. No error was present in the profile since a graph of values of log I against $\alpha^{\frac{1}{4}}$ agreed closely with the theoretical straight line equation for ellipticals. It is possible that the differences in O-C for NGC 4649 may be due in part to the overlap of this galaxy with NGC 4647. In cases where galaxies overlap, the isophotes of both galaxies are obtained on the same tracing and the corresponding areas within contours are measured on the assumption that the isophotes would have been symmetrical had the objects been isolated. It is thus a problem of deciding at what points the

isophotes depart from symmetry, although in this work, the presence of a detailed isophote map is a distinct advantage (cf. work of Holmberg 1958). The isophote calibration is established in a similar way, by using only one real half of a cross-sectional scan and assuming symmetry.

The calculation was repeated for NGC 4486, an isolated galaxy compared with the previous example, where B(0) = 10.3 and D(0) = 3'.715, and the results are shown in table 5.

Table 5

Calculation of distribution of surface brightness in NGC 4486

X	r	P	Q	$\mu(X)_{calc.}$	μ_{obs}	O-C
-0.87	15 arc sec	1.4×10^{-6}	50.0	19.27	19.53	+0.26
-0.18	75 "	"	3.30	22.23	22.46	+0.23
+0.13	150 "	"	.78	23.80	23.97	+0.17
+0.35	250 "	"	.24	25.13	25.08	-0.05
+0.55	400 "	"	.06	26.51	26.19	-0.32
+0.65	500 "	"	.03	27.29	26.86	-0.43

The systematic difference in the values of O-C with increasing radial distance from the centre of this galaxy can easily be explained in the following way. At small

values of r, the observed distribution of luminosity is faint due partly to the smoothing of the true profile by both the telescope and microphotometer instrumental functions. It is to be expected that the central depletion of intensity is replaced in the outer regions of the system, but not to the extent of a half magnitude nett difference from centre to edge. The major contribution to the observed increase in luminosity at large radial distances must be due to the detection and measurement of part of the outer corona which is now known to surround NGC 4486 (de Vaucouleurs 1969). For example, at 500 arc sec from the centre, the theoretical calculation for μ gives a value of 27.79, the observed value is 26.86 and where the photometry of the corona is complete, its contribution to the light of the galaxy raises the observed distribution at this distance, measured off de Vaucouleurs graph (1969) to a surface brightness of 25.3 mag sec^{-2}. In the Working Group Circular (de Vaucouleurs 1970), mention was not made of the range of values of X satisfying the integrated luminosity law; it is only applicable for $-1<X<+1$. However, although this method will prove extremely

useful in the future where elliptical galaxies are present on uncalibrated wide field plate collections, it must be stressed that recent developments in the detection of coronas around giant elliptical systems, such as M87, mean that results derived in this way should be checked carefully in case the unknown luminosity distribution contains light measurements from such outer extensions.

5.3 Results. Complete photometric data for the galaxies are listed in standard format, following the presentation adopted by de Vaucouleurs (1961b), and from the contents of volumes 2 and 3 of the thesis. In a large scale investigation of this nature, where many types of galaxies have been studied, it should be possible to derive relationships between some of the photometric parameters and the revised morphological type (de Vaucouleurs 1963).

First of all, let us compare and examine the data for the radial distribution of surface brightness I(r) in NGC 4535 (type SAB(s)c) with similar data by Sersic (1968) for M83, and also data for NGC 4459 (type SA(r)0) with measurements made by Liller (1960). These distributions, shown in figure 27, are typical

for the whole family of disk-like galaxies, including spirals and lenticulars (Sandage, Freeman and Stokes 1970). The measurements from the current work are indicated in the figure by crosses. de Vaucouleurs (1959a) has shown that the luminosity distribution for these objects consists of two main components, an inner spheroidal component which follows closely the law for ellipticals

$$\log I \propto r^{\frac{1}{4}}$$

and an outer exponential disk component

$$I(r) = I_o e^{-\alpha r}$$

containing a large fraction of the total luminosity. I_o is the central intensity of the disk component extrapolated to r = 0. This two-component nature of the disk systems distinguishes them from ellipticals, which have a single component given by the quarter power law (de Vaucouleurs 1959a). At large radial distances, the quarter power law distribution appears to be approximately exponential (Freeman 1970), so that the I(r) law is qualitatively similar to that shown in figure 27 for objects like NGC 4459, but the main difference between the distribution for elliptical

and disk galaxies is that the apparently exponential and non-exponential sections of the profiles for ellipticals are not independent.

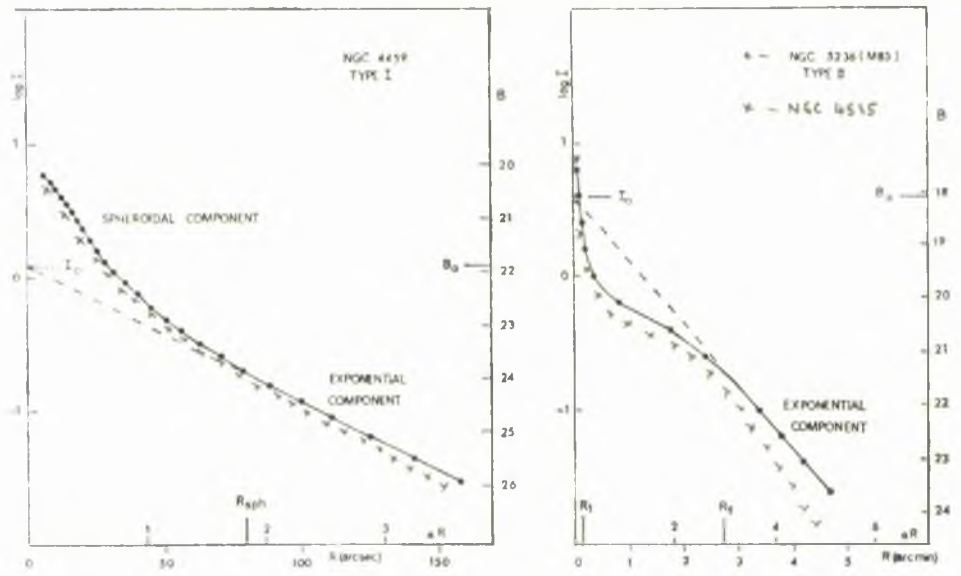

FIG. 27.—Radial luminosity distributions for NGC 4459 and M83. I is the surface brightness. Ordinates are log I and I in B-mag per square second of arc. R is distance from the nucleus along the major axis; the dimensionless radius αR is also shown. I_0, B_0 are the surface-brightness scale for the exponential disk, uncorrected for inclination and galactic absorption. R_1, R_2, and R_{sph} are defined in § III. *Filled circles*, observed points; crosses, St. Ambrus work.

A study was undertaken of the variation of the central surface brightness $B(0)_c$ with morphological type, since Freeman found, for 28 galaxies out of 36, that $B(0)_c$ was nearly constant at $21^m.65$ along the entire spiral sequence and showed no apparent dependence on morphological type. After extrapolating

the exponential disk component to r = 0 in order to derive the apparent intensity scale given by

$$B(0) = -2.5 \log I_o + \text{const.},$$

the intrinsic intensity scale is obtained by correcting B(0) for the inclination to the line of sight and also for galactic absorption. The corrected central brightness is derived from the relation

$$B(0)_c = B(0) + 2.5 \log R - 0.2 \operatorname{cosec} b^{II}$$

where R is the ratio of major to minor diameter of the disk, as derived from the isophotes and cross-sections of the galaxy; the coefficient of cosec b^{II} is that obtained by de Vaucouleurs and Malik (1969) while the values of b^{II} are obtained from the B.G.C. (G. & A. de Vaucouleurs 1964). Only those galaxies for which the exponential components were easily defined have been included in this study, and the results are given in table 6.

Figure 28 shows $B(0)_c$ against morphological type. Statistical analysis of the data is made possible by

TABLE 6

DATA FOR 19 GALAXIES

NGC	Classification stage	B(0)	log R	$B(0)_c$
4235	a	21.20	.49	22.32
4293	0/a	21.76	.22	22.22
4321	bc	21.08	.15	21.36
4382	0^+	21.96	.08	22.08
4394	bc	21.76	;05	21.80
4450	ab	21.50	.16	21.82
4477	0^o	22.02	.01	21.96
4501	b	22.50	.07	22.56
4535	c	21.46	.02	21.43
4536	bc	21.93	.14	22.34
4548	b	21.50	.00	21.51
4567	bc	22.30	.08	22.42
4569	ab	21.18	.31	21.84
4571	cd	21.62	.03	21.63
4578	0	22.40	.14	22.64
4579	b	20.86	.08	20.95
4698	ab	22.40	.10	22.56
4754	0^-	22.21	.11	22.37
4762	0^o	22.32	.44	22.40

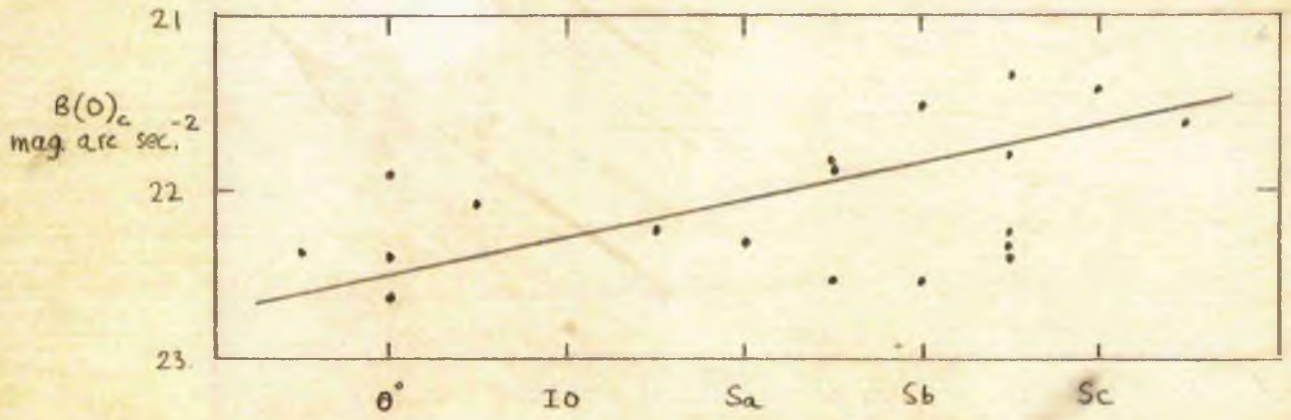

Figure 28 - $B(0)_c$ against morphological type.

assigning to each classification stage the following numerical scale

T	L^-	L^o	L^+	IO	SO/a	Sa	Sab	Sb	Sbc	Sc	Scd
n	1	2	3	4	5	6	7	8	9	10	11

This scale is similar to one quoted by de Vaucouleurs (1970b). Note that in Freeman's paper (1970), the scale given throughout for morphological type departs considerably from the above scheme, being much more condensed for all the lenticular stages. Least squares fitting of the data for figure 28 produces the

equation

$$B(0)_c = 22.76 - 0.11\ n,$$

where n denotes the Hubble type. This expression indicates that there is a systematic variation of $B(0)_c$ with morphological type, contrary to Freeman's (1970) results. The difference is greatest around the lenticular stage, and it may be due in part to possible errors in Liller's photometry (1960, 1966), which provided the source of Freeman's data on B(0) for lenticulars. A comparison of Liller's work with the writer's investigation will be given at a later stage.

The gradient G(a) = d log I/da has been plotted against revised morphological type in figure 29, and it is seen that the data exhibit the usual scatter since G(a) is proportional to the angular size of each object. A more meaningful relation may be obtained by normalizing the length scale to r_e and setting $y = \frac{r^*}{r_e}$. In figure 30, the gradient G(y) = d log I/dy is seen to vary with morphological type according to the relation

$$G(y) = -.22 + .05n\ .$$

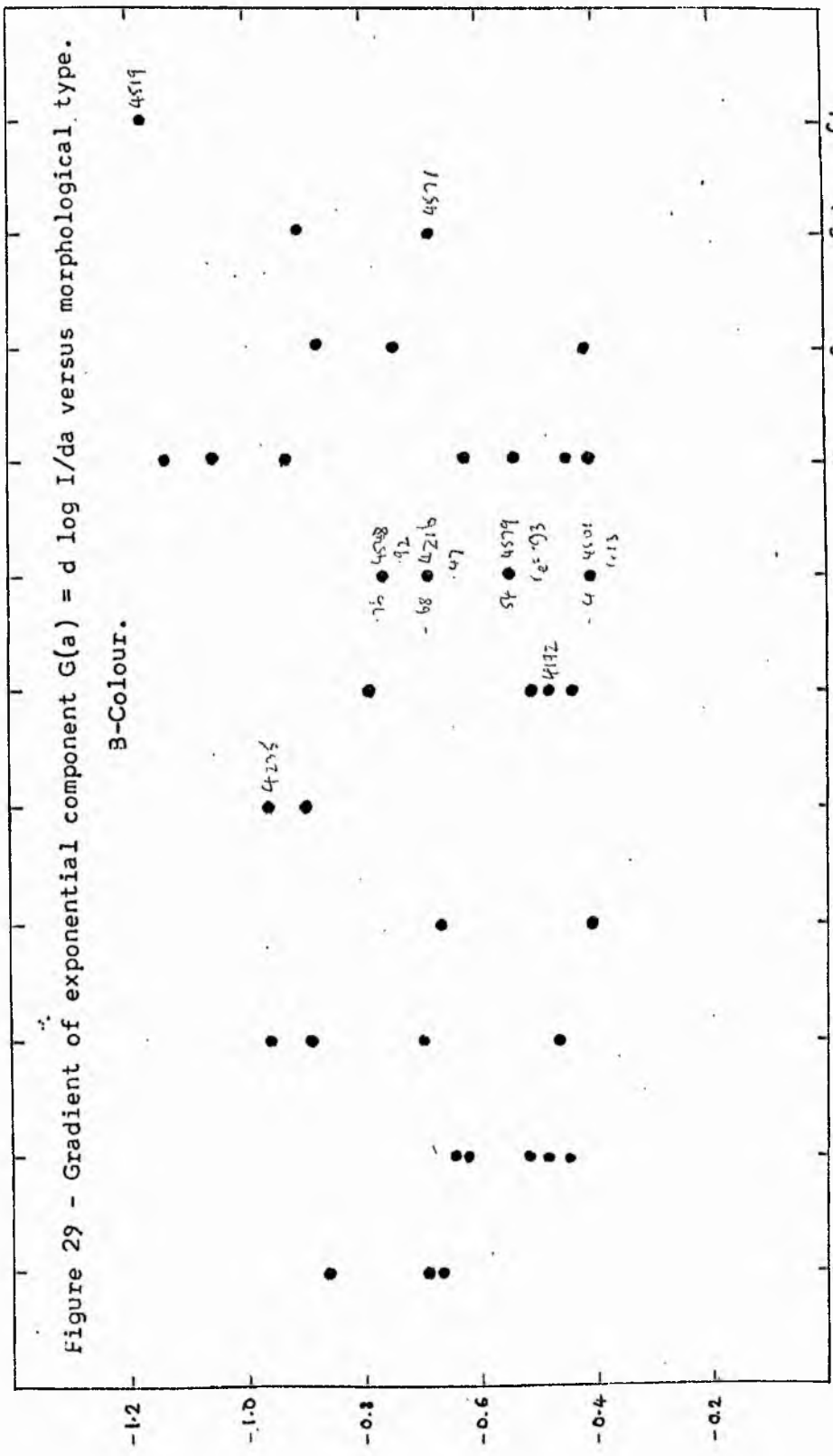

Figure 29 - Gradient of exponential component G(a) = d log I/da versus morphological type.
B-Colour.

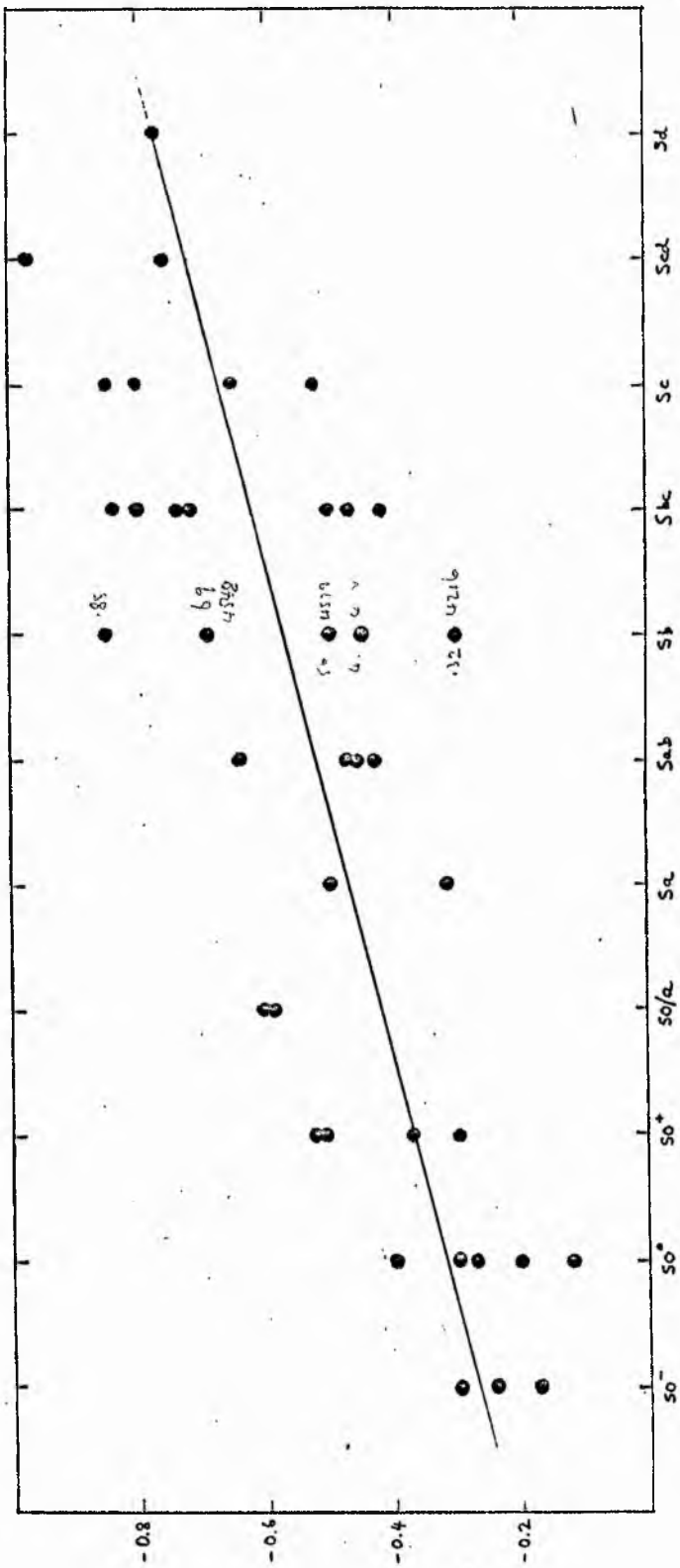

Figure 30 - Gradient of exponential component G(y) = d log I/dy versus morphological type where $y = r^*/r_e$. B-Colour.

This result will be verified after the concentration indices are plotted against morphological types, but for the present, the above relation agrees with the work of Freeman (1970) who found a mixture of values for G(a) in early types but predominantly high values for later types. However, in this investigation, two stage cd galaxies and one stage d object were the latest types to be observed, so it is not possible to verify completely Freeman's results for the late-type objects, although extrapolation of the least squares fit in figure 30 would indicate agreement in principle. Originally, plots were also made on this figure to test whether there was any correlation of gradient with families within each stage, but no correlation was noted.

A comparison of results in the current work with that of Mrs Liller (1960, 1966) can be made by using her values for either m_T, the total integrated magnitude including an extrapolation correction, or a_{25}, the semi-major axis of the isophote at a surface brightness of 25.0 mag.per square second of arc. Table 7 gives data for all the galaxies common to both investigations, while the filled circles in figure 31 illustrate graphically the respective values. The slope of the

Table 7

Comparison of different measurements of semi-major axis in arc min. at $\mu = 25$ mag.sec^{-2}.

NGC	a'_{25}(Liller)	a'/a	a(25)(Fraser)	NGC	a'_{25}	a'/a	a(25)	
4365	3.33	1.03	3.22	3.06	4486	4.28	1.10	3.90	5.36
4374	3.60	1.23	2.92	2.78	4552	2.81	1.13	2.48	2.62
4406	6.15	1.52	4.05	4.20	4649	4.63	1.13	4.08	3.81
4459	2.10	0.95	2.20	2.06	4526	3.78	1.16	3.25	3.55
4472	6.33	1.26	5.03	5.05	4578	1.66	0.99	1.67	1.78

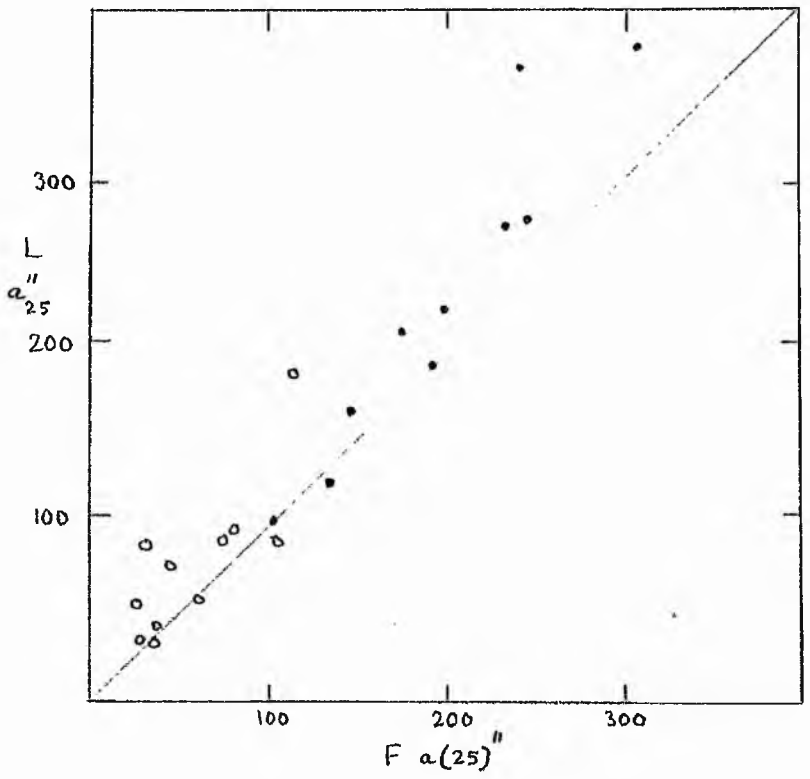

Figure 31 - Graphed Output of Table 7

give proper caption

no, there is a sept. curv. Plot a/a vs area'

graph departs only slightly from 45^{o} but in general the data show good agreement. The large discrepancy in the two values for NGC 4406 may be due to the fact that Liller finds its m_T to be exceptionally bright at 9.61, compared with Holmberg's and the writer's respective values of 10.1 and 10.04. The open circles in figure 31 show values for Liller's a_e and the writer's equivalent a_e; this quantity was derived from values of r_e and the measured axial ratio $q = b/a$ of the isophotes at r_e using the relation

$$a_e = r_e \sqrt{1/q_e}$$

Out of the 11 galaxies for which comparisons could be made, NGC 4459, 4461, 4486 and 4552 show particularly good agreement. In view of the fact that such good agreement was obtained for these four objects, for which the results were published by Mrs Liller in 1966, and since the measuring procedure in the current work has been uniform throughout, it is suggested that there may be errors in some of Mrs Liller's results, supported by the following three reasons.

First of all, it is possible that errors could have been introduced in the extrapolation procedure. Since the isophote levels reached down to a few per cent

of the sky background, it was necessary to extrapolate to an infinite radius for the undetected contributions of the galaxy, and in some cases such corrections could be significant. Furthermore, Liller (1966) pointed out that an error of only $0^m.1$ in the extrapolation yielding m_T would lead to an error of more than 10% in a_e. In addition, if m_T is erroneous, as may well have been the case for NGC 4406, the resultant error in a_e may be considerable.

Secondly, in the 1960 investigation, Mrs Liller smoothed all the isophotes and assumed them to be ellipses whereas in 1966, corrections were applied to any isophote which departed from an elliptical form.

Thirdly, Mrs Liller (1966) has pointed out that some of the 1960 calibrations were known to have zero point inaccuracies of as much as $0^m.5$ after check measurements were made on NGC 4486 using unpublished photo-electric data of Baum.

For these reasons, it would appear that the 1960 results would be more likely to have errors compared with the 1966 investigation. From the writer's work on the central brightness $B(0)_c$ of the disk component (see figure 28), it was found that the value for lenticulars would lie around $22^m.4$. Using Liller's 1960 data,

Freeman finds for 8 lenticular galaxies an average $B(0)_c$ of 21.51 while 4 objects in the 1966 investigation produced an average for $B(0)_c$ of 21.89. It is proposed that if the writer's values for lenticulars err on the faint side, then Freeman's results for the same stages will err on the bright side, thus contributing to the apparent constant value for $B(0)_c$ along the entire spiral sequence. If Liller's 1960 work is inaccurate and if the average $B(0)_c$ derived by Freeman from this data should in fact have been closer to 21.9, this would have the effect of producing a variation in $B(0)_c$ along the morphological sequence, similar in slope to the relation derived by the writer in figure 28.

The apparent ellipticity of the isophotes increases from the nucleus outwards beyond which a very slow decrease takes place in the outer regions; this is confirmation of results given by de Vaucouleurs (1959a, 1970a). Part of the observed decrease towards the centre is due to the instrumental smoothing which tends to produce circular isophotes irrespective of their true shapes. However, recent work by Arp and Bertola (1969) has shown that for M87, the ellipticity of outer isophotes is 0.5 compared with zero for the central isophotes.

Confirmation of such results should be obtained in future work using not only the IIIaJ emulsions now available (van den Bergh 1969),(Arp and Bertola 1969), but also with photo-electric techniques, such as those employed by de Vaucouleurs (1969). It is important to point out that Arp and Bertola, although they obtained plates with IIIaJ emulsion and published detailed isodensitracer photographs (1971) which [they claimed could] enable faint outer isophotes to be detected, this method has been employed by the writer in St Andrews for the past six years and its advantages in drawing isophotes were described in a paper published in 1967 (Fraser 1967).

One point concerning the ellipticities of isophotes is that there appears to be some ambiguity in the published literature about the definition of axial ratio and the resulting interpretation of ellipticity. This confusion originally lead to some difficulties in linking the writer's observed ellipticities with the published data.

The variation of concentration indices with morphological type has been analysed in both colours and the results shown in figures 32 to 35. It is seen that in all cases there is a systematic dependence of index along the Hubble sequence, the smaller indices

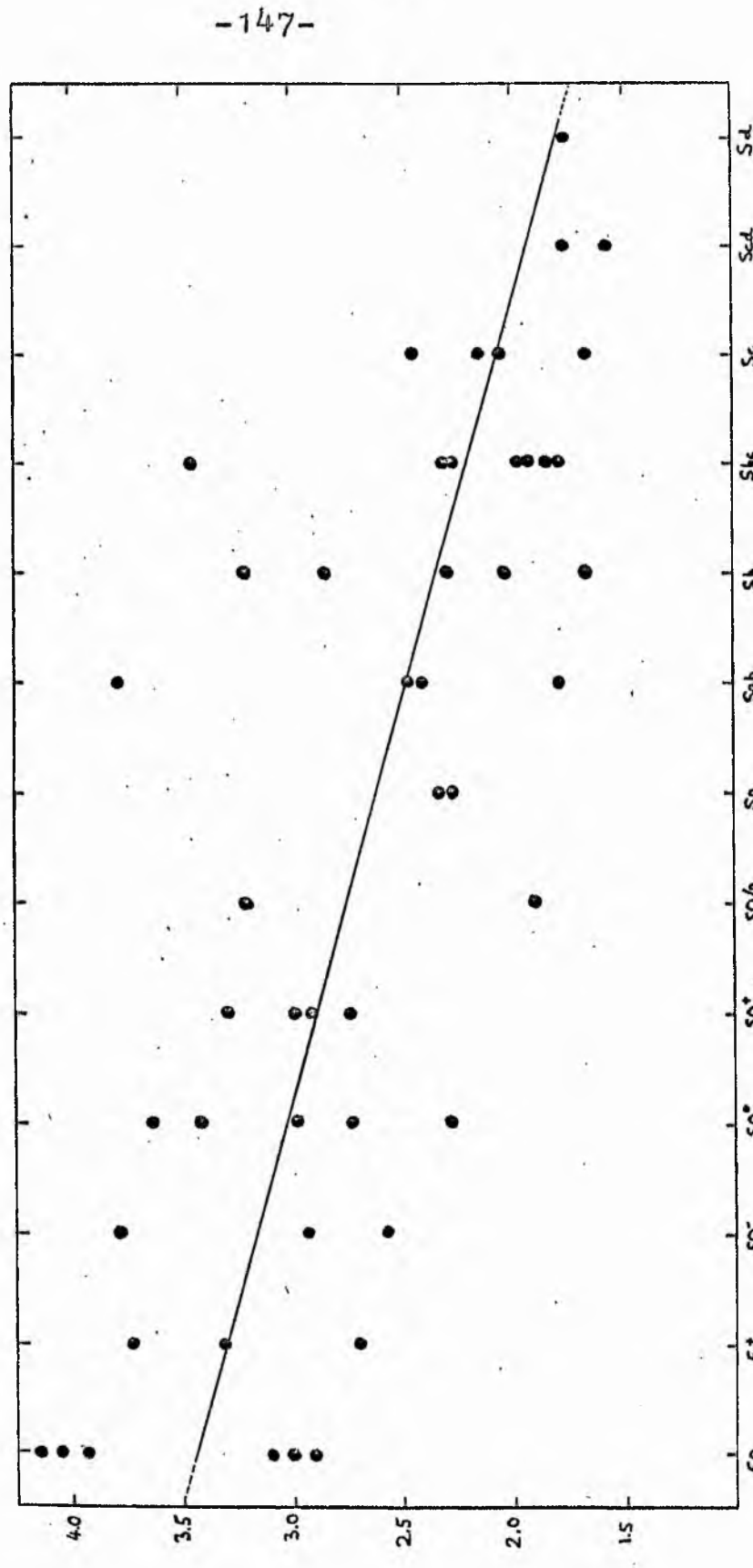

Figure 32 - Concentration index C_{21} versus morphological type. B-Colour.

compare HD1.

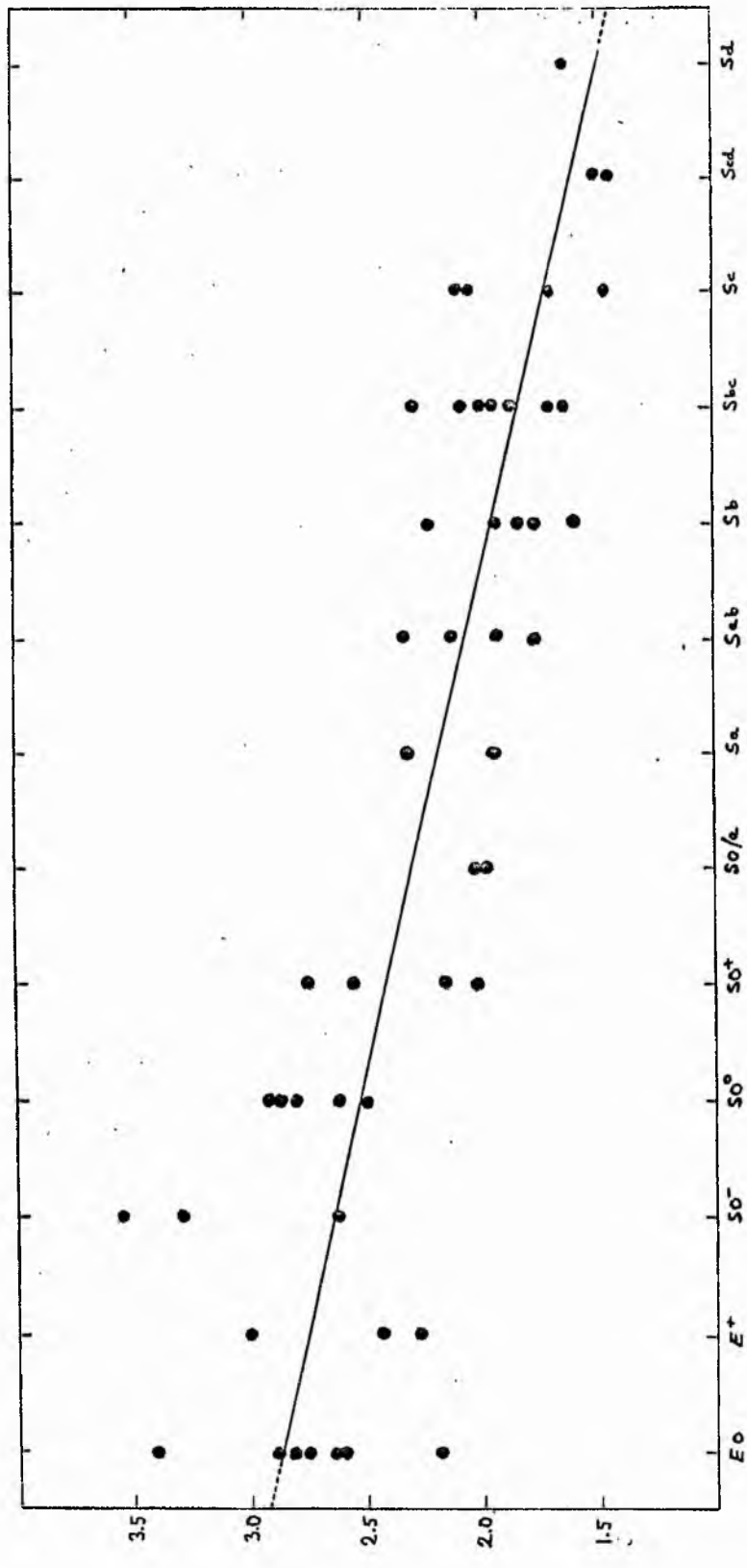

Figure 33 - Concentration index C_{32} versus morphological type. B-Colour.

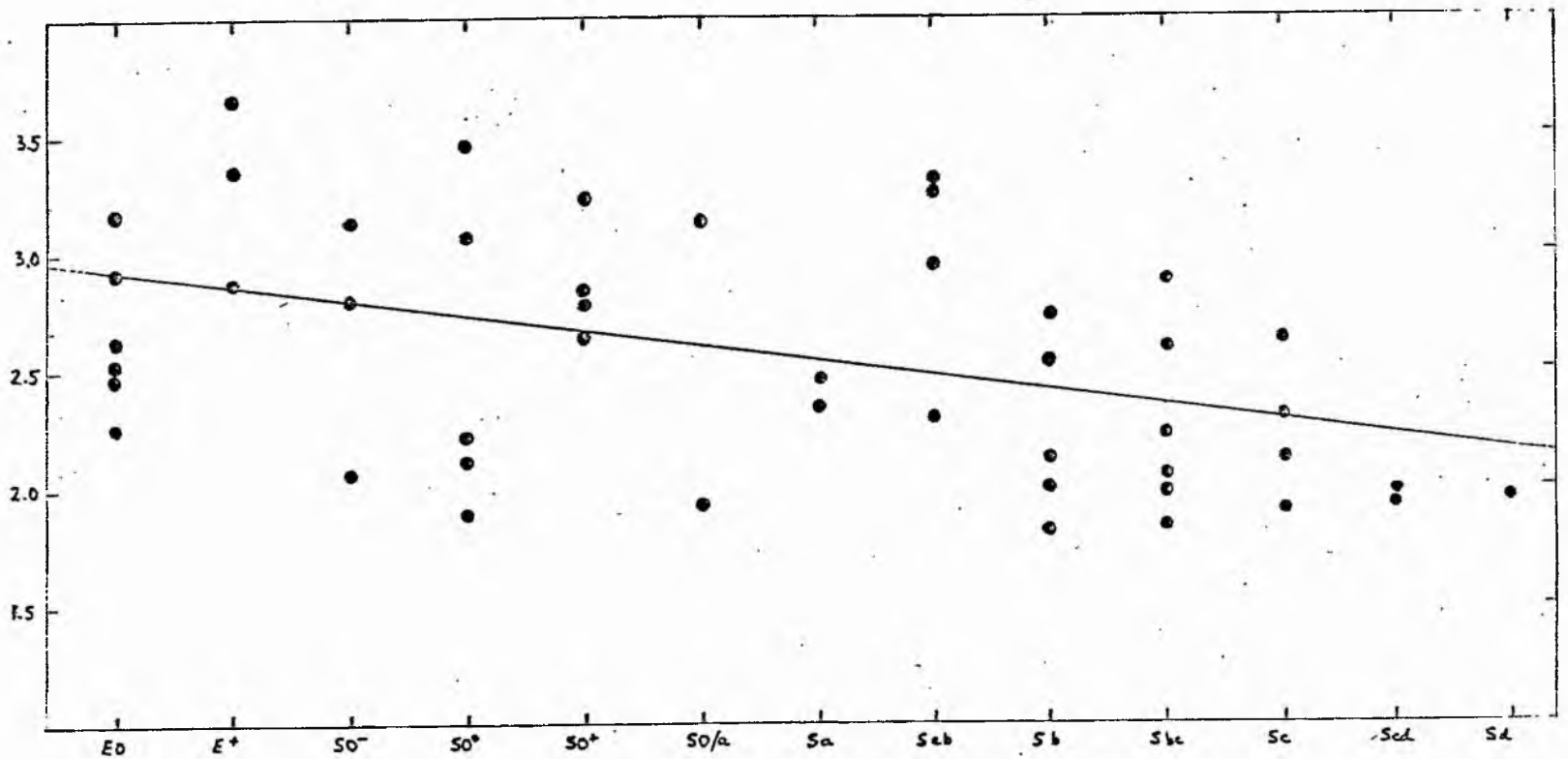

Figure 34 - Concentration index C_{21} versus morphological type. V-Colour.

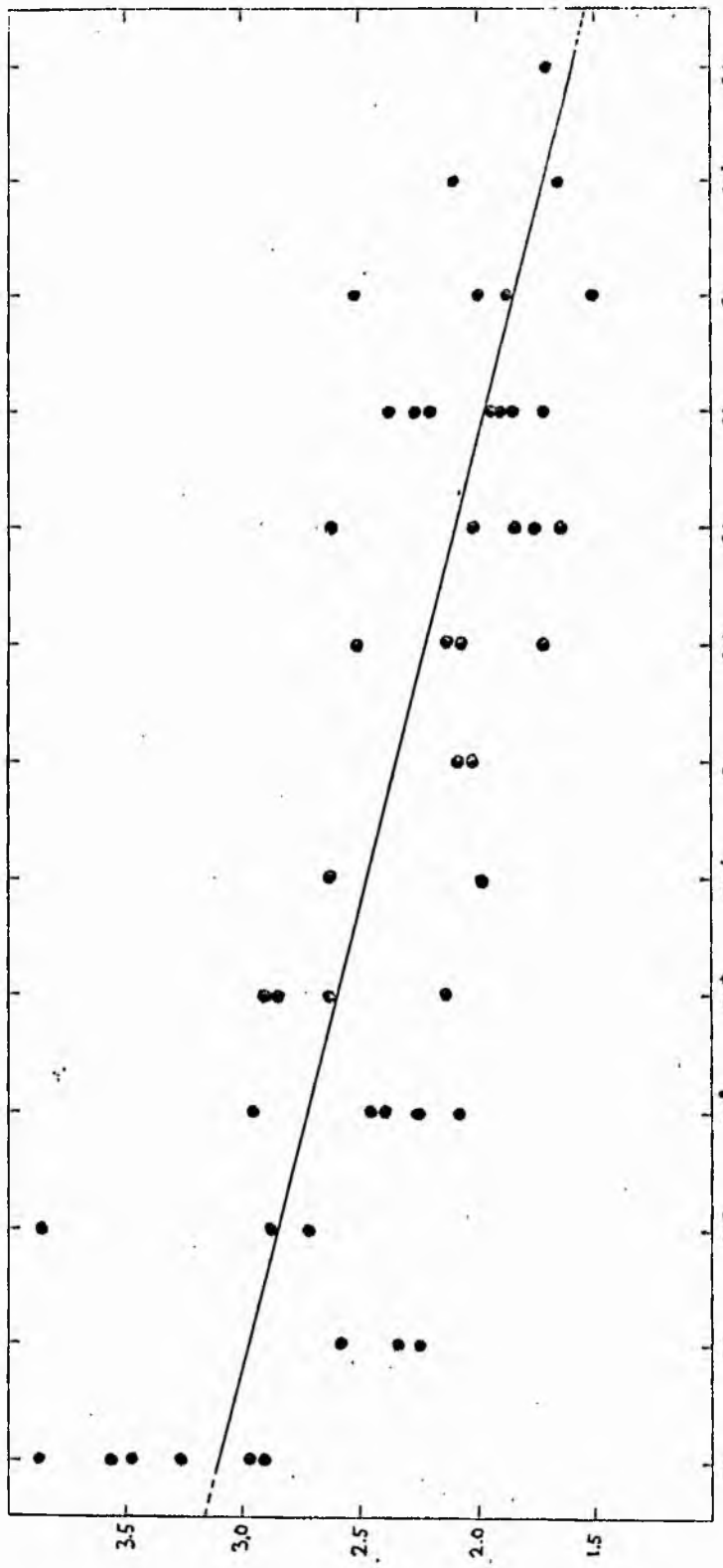

Figure 35 - Concentration index C_{32} versus morphological type. V-Colour.

being found with the late types and the S0 and E galaxies having all but the lowest values of concentration index. This is to be expected since the late types have compact nuclei and their boundaries are well defined by the spiral arms, thus making the ratios defined by the concentration indices all fairly small, while for ellipticals, which merge imperceptibly into the background at large radial distances, r_3, defined by $k(r_3) = \frac{3}{4}$, is much farther out in the ellipticals compared with r_e than it is in late spirals. Since the morphological sequence includes ellipticals on this occasion, the numerical values assigned to each stage are as follows:

$\mathfrak{H}$	E	E^+	L^-	L	L^+	S0/a	Sa	Sab	Sb	Sbc	Sc	Scd	Sd
n	1	2	3	4	5	6	7	8	9	10	11	12	13

A least squares fit to each set of data on figures 32 and 33 produced the following relationships for the B system:

$$C_{21}: \quad C.I. = 3.6 - 0.140\ n$$

$$C_{32}: \quad C.I. = 3.2 - 0.124\ n$$

where n denotes, as before, the Hubble type. Analyses for the data shown in figures 34 and 35 produced for the V system the following equations:

C_{21}: C.I. = 2.96 - 0.061 n

C_{32}: C.I. = 3.20 - 0.124 n.

The results (shown in figures 32 to 35) for the concentration indices may be compared with the trend shown in figure 30 for the gradients. For the lower gradients found in the outer envelopes of lenticulars, the concentration index should be numerically large compared with later type objects; similarly, low concentration indices should be produced by galaxies having high gradients. These inverse relationships are confirmed in the results shown in figures 30, 32, 33, 34 and 35. This classification work on luminosity is similar to Freeman's work (1970) on the angular sizes of different sections of a galaxy. Freeman's parameter gives the ratio of the apparent radius R_{sph} (defined in figure 27) of the spheroidal component to the radius of the disk at some consistent surface brightness. However, this ratio is shown to be only very weakly correlated with galaxy type, increasing from late to early types. The present work on the concentration indices, shown in figures 32 to 35, gives more dramatic relationships.

In case inclination effects were important in

determining the location of points in the four figures under discussion, an analysis was made of the relationship between concentration index and galactic inclination. For a galaxy, the inclination $\underline{i}$ of the axis of rotation to the line of sight is given by

$$\cos^2 i = (q^2 - q_o^2)/(1 - q_o^2) \quad \text{where } q = b/a.$$

The value of q_o has, in the past, been taken as 0.2 (Holmberg 1958), but it has recently been shown (de Vaucouleurs 1970a) that the value of q_o varies systematically along the Hubble sequence. However, it suffices to remark that q may be used as a measure of the inclination of a galaxy. Figure 36 shows the concentration indices versus varieties, families and apparent ellipticities within stages for each of the points plotted in figure 32. No systematic effects are noted, except perhaps a tendency for more of the larger ellipticities to be associated with the later types, indicating a decrease in concentration index with increase in angle of inclination. Note the cluster of SAB(rs) types at stage bc.

DOLS SOL. fig. 9

Just as the luminosity profile I(r) may be divided up into distinct components, it is also

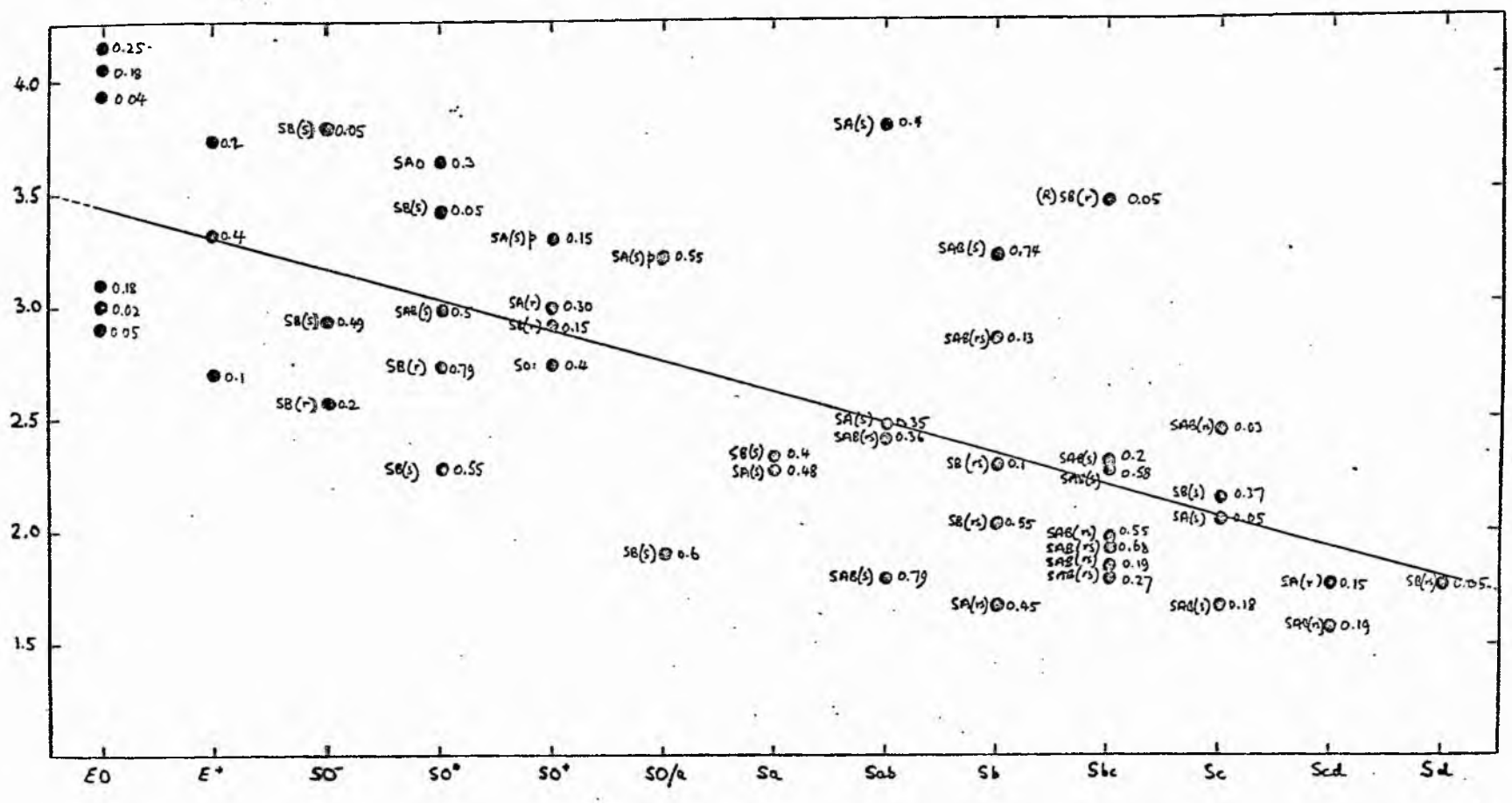

Figure 36 - Concentration index C_{21} (B-Colour), varieties, families and ellipticities versus stages of revised morphological sequence.

possible to subdivide the reduced luminosity profile. Such a profile for the B system photometry of NGC 4477 is shown in figure 37. It is seen that the graph may be divided into three components, a central, an intermediate and an outer. de Vaucouleurs (1959a) has already given equations for the reduced laws for ellipticals and the exponential law observed for late-type spirals, and pointed out that the ellipsoidal law seems to apply to the spheroidal component of early spirals. Instead of attempting to fit a truly exponential component to the central regions where the scale in ρ is small, the reduced law was plotted in terms of $\rho^{\frac{1}{4}}$, where a straight line fit was obtained for the first 16 data points, neglecting the first two which suffer from resolution difficulties and effects of smoothing functions. The equation for the line fit to the data was

$$\log J = 3.43 - 3.39\,\rho^{\frac{1}{4}},$$

indicating good agreement with de Vaucouleurs' (1959a) results. For the second component, the same straight line fitting technique was applied to the data and the result, shown in figure 37, produced for this second component the following equation

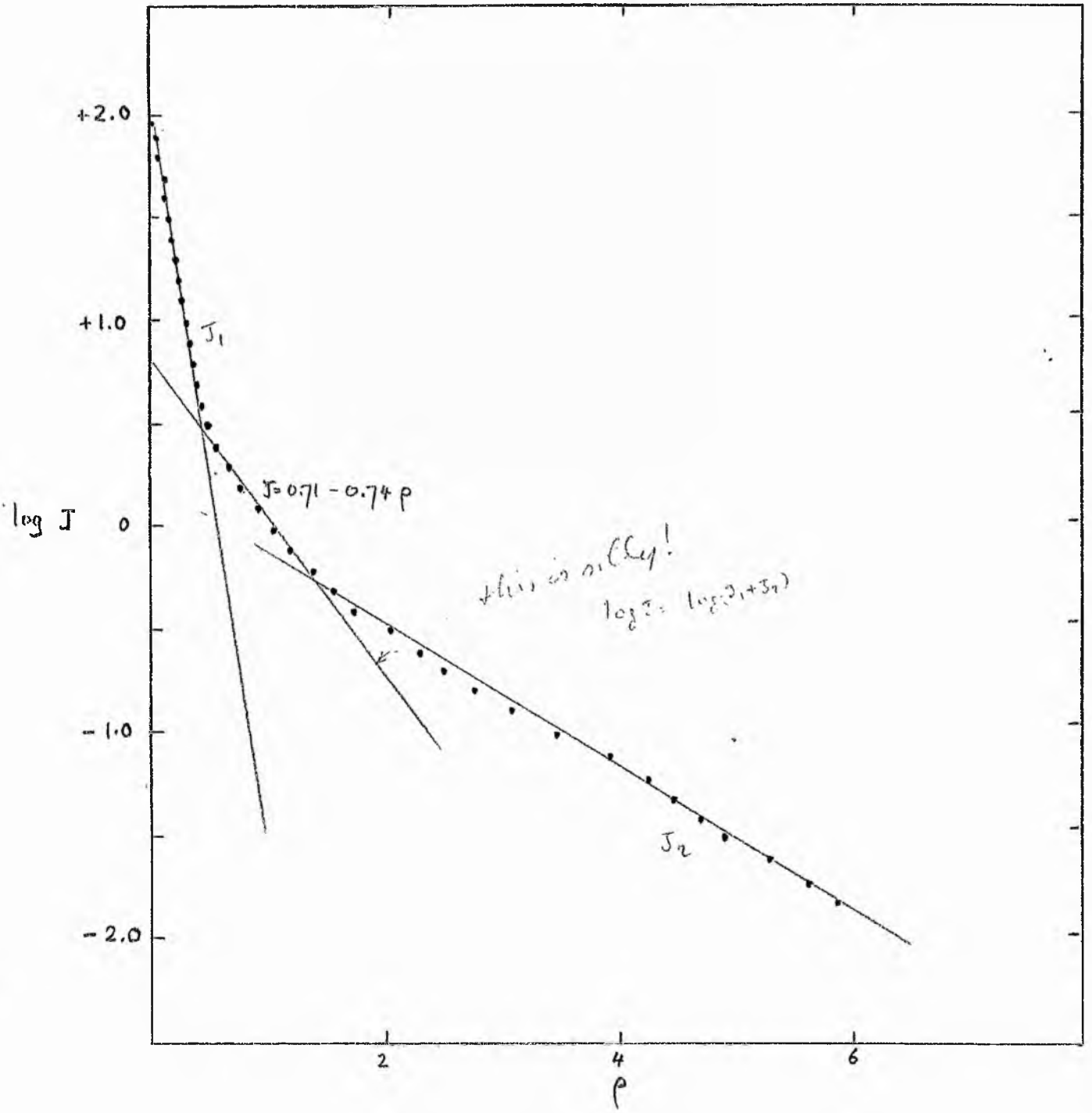

Figure 37 - Reduced luminosity profile of NGC 4477.

$$\log J = 0.71 - 0.74\rho .$$

This result is consistent with de Vaucouleurs' relation (1959a) which differs from the above only in the sense that each coefficient is equal to .729. This type of analysis has been carried out for all the galaxies in the work; the results for the measurements of the gradient for each component of the reduced luminosity profile are shown in figure 38. Examination of the data reveals one important feature, also exhibited in figure 37. The profile in most cases seems to consist, not of two distinct components, but three. As a general rule, the first or central component is consistent with the quarter power law for ellipticals, the second concurs with the exponential law for late-type spirals and the third component satisfies an equation of the type

$$\log J = -b(\rho - 1) \text{ where } b \doteq 0.3.$$

In cases where only two components are detected, the second of these obeys the exponential law for late-type systems. The detection of the third component in such galaxies as NGC 4216, 4293, 4382, 4461, 4477, 4501, 4519 and 4527 may be due to the large radial distances scanned on the plate. These distances are consistent with the measured principal axes at threshold being systematically greater than Holmberg's (1958) values

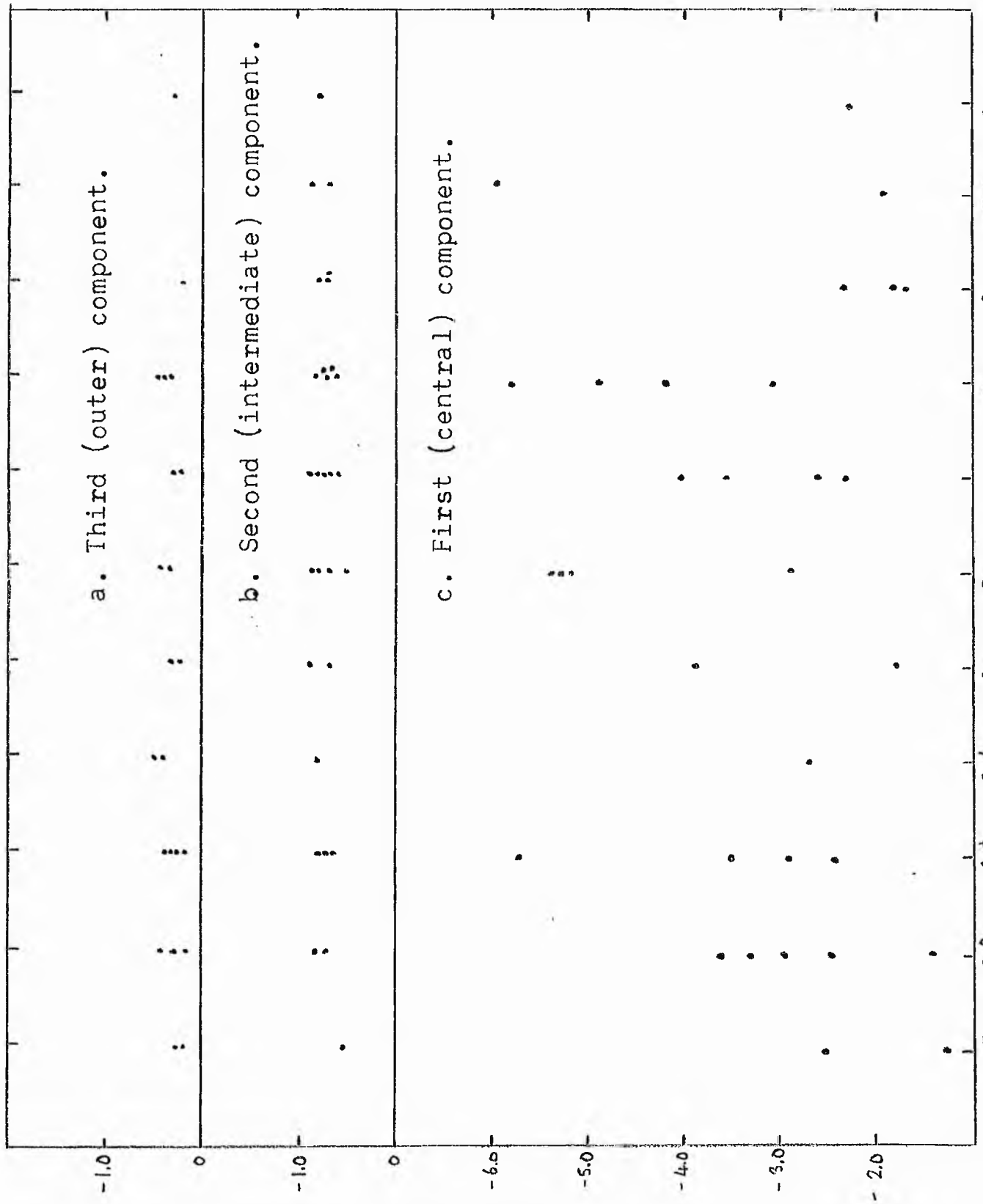

Figure 38.

Gradient of exponential components of reduced luminosity profile versus morphological type.

for NGC's 4216, 4382, 4501, 4519 and 4527; these are the only galaxies from the previous list common to both investigations. It may be possible that this third component could be more widely measured in future investigations. The question arose as to whether the presence of the third component in most, but not all, of the galaxies studied could be a selection effect, appearing only in the objects with small apparent magnitudes. However, a graph of the number of components versus the apparent magnitude showed that any correlation was extremely weak, if not altogether absent. The ratio of the number of galaxies with three components to those objects with two was about 2:1, all the component numbers being uniformly distributed in apparent magnitude. Comparison of the reduced luminosity profiles with other observers' results for galaxies in common is not possible, since previous investigations have not presented the photometric data in the "standard" form.

Heidmann (1967) has investigated the relationship between the intrinsic luminosity L of a galaxy and its diameter A up to a faint isophote and finds that

$$L \propto A^{q}$$

The exponent of A was found for spirals to be 2.8 using Holmberg's (1964) data and for ellipticals the corresponding q value was 1.9,, obtained from Liller's (1960, 1966) data. The difference in the values of q was not due to different values used for the brightness of the limiting isophote (26.5 and 26.0 mag.sec.$^{-2}$ respectively), since the same q value was obtained from Liller's data using either the 25 or 24 mag.sec.$^{-2}$ limiting isophote. In a similar investigation, Heidmann (1969) found a value for q of 1.8 for Rood and Baum's (1968) photometric data for galaxies in the Coma cluster.

Such a study was also possible for the present work, since one of the tabulated standard parameters was the major axis 2a(25) at μ = 25.0 mag.sec.$^{-2}$; the results of this investigation are shown in figure 39. Analysis of the data for all galaxy types grouped together produced the line, drawn in the figure, which has a slope q = 1.71. Since there were 27 spirals included, one should have expected the slope of the line to have been closed to the value of 2.8 found by Heidmann from Holmberg's (1964) data on spirals. After analysing the data on 27 spirals and 7 ellipticals separately, the resulting q values were 1.62 and 1.89 respectively.

a must be corrected to "face-on", also m.

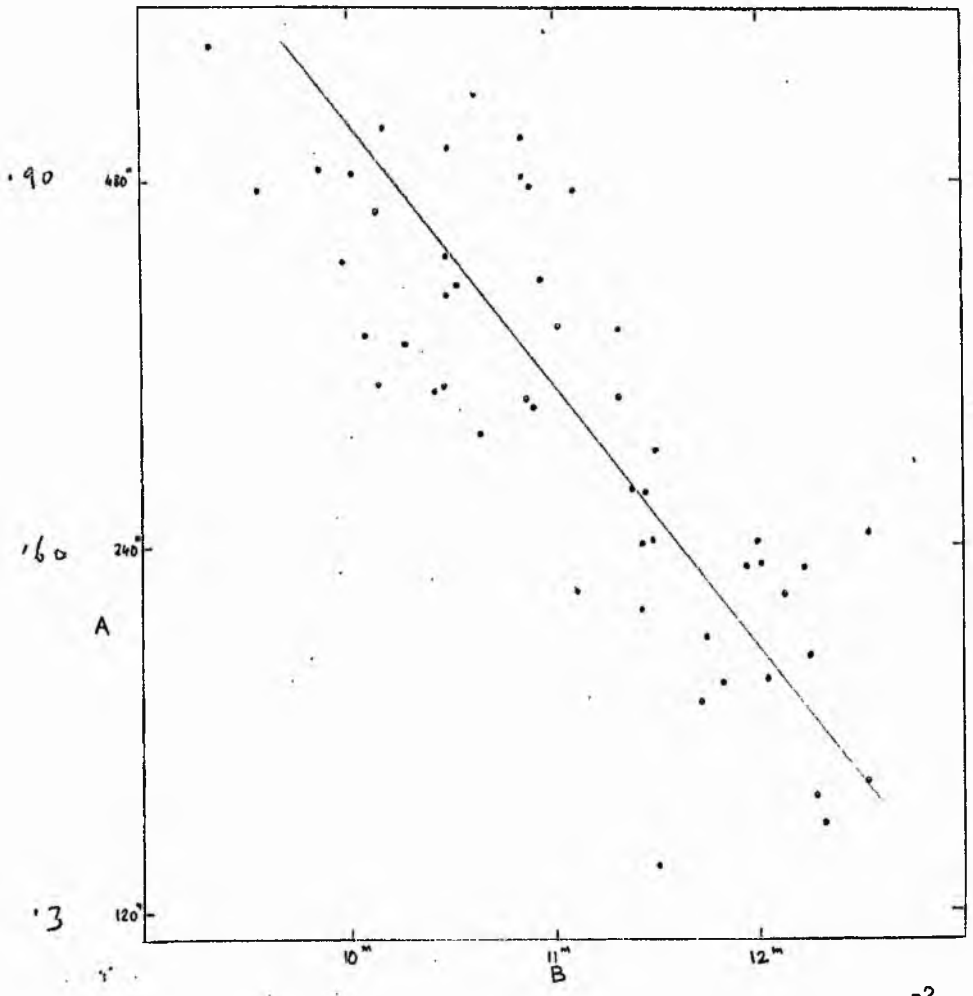

Figure 39 - Diameter A in arc sec of isophote 25 B mag sec^{-2} as a function of apparent total magnitude B.

The value for ellipticals is consistent with Heidmann's values for both the Virgo ellipticals and the Coma cluster galaxies, but there is disagreement in the results for spirals. It was mentioned in the previous section on the reduced luminosity profiles that the third component could be due to the large radial distances to which galaxies had been detected. In this connexion, some of the writer's diameters were found to be larger than Holmberg's 1958 values, from which Heidmann derived the q value for spirals of 2.8. It would only require a reduction of 20% in the diameter of the brighter galaxies (i.e. those around 10^m) on figure 39 to change the q value from 1.71 to 2.65. Accordingly, the observed slope of the data in the figure may be due to increased diameter measurements, but the study emphasizes the sensitivity of the q value in the luminosity-diameter relation to the methods in which the diameters are determined.

Several of the previous comparisons have depended upon the accuracy of Holmberg's photometry. For this reason it is interesting to compare the writer's r^* at $\mu_B = 26.5$, interpolated from the integration tables, with the corresponding quantity $\sqrt{ab}$ from Holmberg's

(1958) photometry. The results are shown in figure 40, where the mean systematic difference for 7 ellipticals and lenticulars is $\log r^{*} - \log \sqrt{ab} = +0.05$;

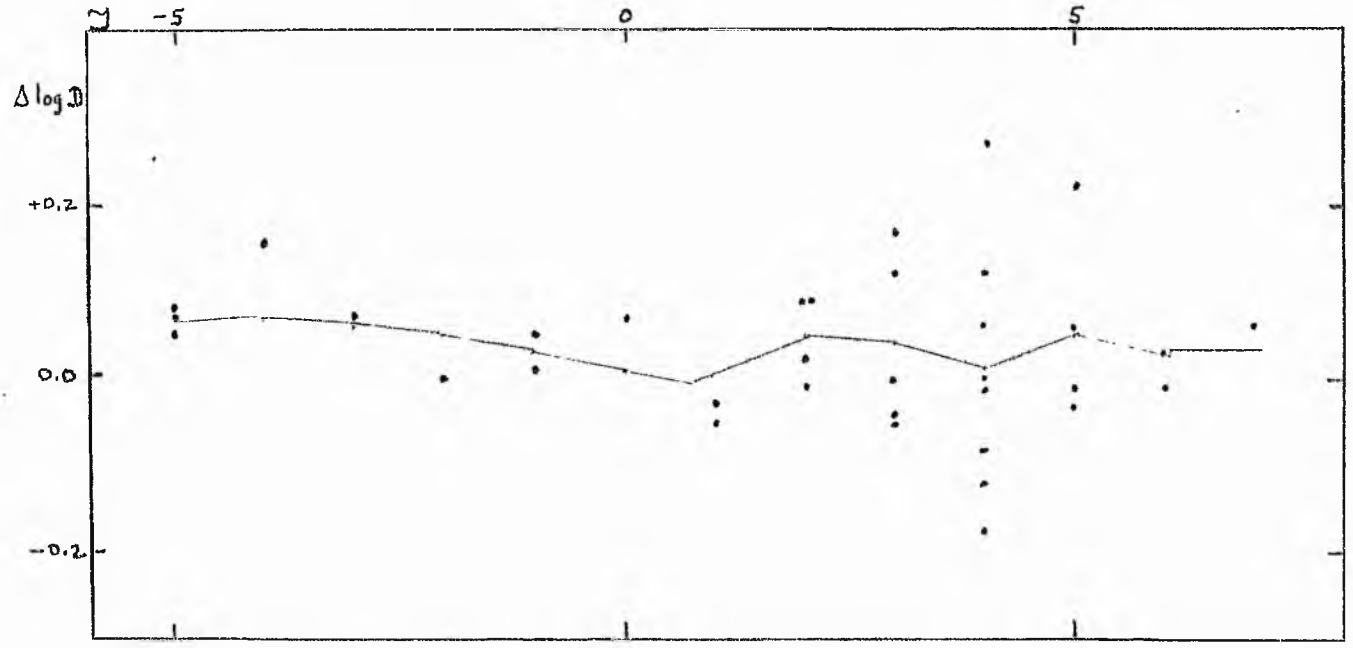

Figure 40 - Comparison with Holmberg's data at $\mu = 26.5$ mag.sec^{-2}.

the corresponding quantity for 27 spirals is +0.03, almost independent of morphological type. Near $\mu = 26.5$ the average slope of the luminosity curve is $\Delta \log D = 0.06 \Delta \mu$, so that either Holmberg's statement that his diameters refer to 26.5 is incorrect or there are errors in the present photometric work at this faint level.

In order to check Holmberg's photometry at $\mu = 26.5$, de Vaucouleurs' method (1970), which used the integrated magnitudes listed in the Reference Catalogue (already

described on page 128) has been applied to all the elliptical galaxies with axial ratios close to unity originally measured by Holmberg (1958). The calculated surface brightness for each galaxy listed in table 8 at μ = 26.5 is shown in the third column of the table, while in the fourth Holmberg's value of $\sqrt{ab}$ is given; the writer's measurements for r^{*} at μ = 26.5 are indicated in column five for objects in common.

Table 8

Values of radial distances at μ = 26.5 mag.sec.$^{-2}$

NGC	E type	r''_{calc}	r'_2/r_1	$r''(H) = \sqrt{ab}$	r^{*}'' (F)
4278	1-2	208	1.118	186	-
4283	0	91	1.338	68	-
4472	2	396	1.165	340	431 410
4486	0-1	(399)	1.243	321	439 460
4649	2	370	1.298	285	292 346
		Mean	1.232	$\rightarrow \Delta\log r = 0.090 \rightarrow \Delta\mu =$	

It is noted that in each case, Holmberg's values are systematically too low by an average of 22%. For three objects, the writer's average values are only 3% high; the difference may be due in the case of NGC 4649 to overlap with NGC 4647 and for NGC 4486, the large value for r^{*} could result from partial detection of

the outer corona. a point already discussed elsewhere in the thesis. However, there seems little doubt that Holmberg's measurements are in error; his assertion that the diameters refer to an approximate background level of $26^{m}.5$ for the (1958, 1964) 103a0 plates was based upon the assumption of a constant low density being produced by the sky background on standard exposure plates. In fact, since the background density of the standard photographic exposure "reduced the sky fog to a minimum", the background measurements were being made right at the toe of the calibration curve, in the area in which accurate density measurements are exceedingly difficult to achieve. Furthermore, when exposing each plate to the standard 10^{m} exposure, no effect was applied to take account of possible variations in the sky brightness throughout the entire investigation. In addition, the accurate measurement of the minor axis depends upon whether one of the 15 tracings was actually scanning the true axis itself or scanning parallel to it.

The present data has been used by de Vaucouleurs (1971) to calibrate the Reference Catalogue diameter i.e. to find the value of μ which statistically corresponds to the log D values. The results agree at μ = 24 to 25 mag.sec.$^{-2}$ with de Vaucouleurs' previous calibration using

the Mount Stromlo photometry.

In the future, it may be possible to derive further relationships between the parameters, morphological types and colours of galaxies following a more accurate calibration of the magnitudes. There is little doubt that many more investigations should be carried out using surface photometry to obtain standard parameters, since the results of such studies will assist our understanding of the structure and evolution of galaxies.

CONCLUDING REMARKS

This thesis is the first attempt to obtain detailed parameters for a large number of objects in two colours. One result of such an investigation is the streamlining of the photometric reductions for one galaxy. All the reductions are performed on the University of St Andrews IBM 360/44 computer and detailed parameters for one galaxy can be produced in five minutes. In the future, data reduction at the University Observatory will be greatly assisted by the use of a Honeywell 316 data processor, which will enable scanned information in IDT work to be read straight from the Joyce Loebl into the 360. Hence detailed maps of colour may be obtained if calibration standards were accurately set up.

Further work at St Andrews will use some plates of the Coma cluster of galaxies to be taken in 1971 with the 98" Isaac Newton Telescope, when it is hoped that the better plate scale, together with the improved computational facilities available, will enable more detailed results to be obtained for many elliptical and lenticular galaxies with a wide selection of luminosities. Of course, the need still exists for photo-electric observers to obtain further precise measurements to supplement former photographic studies.

ACKNOWLEDGEMENTS

The writer wishes to thank Professor D.W.N. Stibbs for the continual encouragement and advice which was willingly given during his supervision of the work for this thesis. In addition I am grateful to Professor Stibbs for arranging a visit to the University of Texas in 1968 to enable me to work with Dr G.de Vaucouleurs, from whom I had the opportunity to clarify many details of the photometric reductions, in addition to studying many other topics under his supervision. Acknowledgement is due to Mr D.M. Carr who carried out all the electronic modification on the Joyce Loebl, including the digitization facilities, and also to Dr I.G.van Breda, who designed the serializer which was used in the digitization work. The writer also acknowledges the photographic work carried out by Mr R. Dunlop, in particular his assistance in the large number of photographic reductions of computer output. Finally, thanks are due to other members of the academic and technical staff who offered advice on aspects of the work on numerous occasions.

Part of the work was performed during the writer's tenure of a Science Research Council Studentship. The support of the Carnegie Trust is also acknowledged for the tenure of a Senior Scholarship in 1966.

REFERENCES

Ables, H.D. and Kron, G.E. 1967, P.A.S.P., 79, 423.

Arp, H. and Bertola, F. 1969. Ap.Lett., 4,23.

———. 1971, Ap.J., 163, 195.

Bergh, S. van den 1969, Ap.Lett., 4, 117.

Bigay, J.H. 1951, Ann d'ap., 14, 319.

Bigay, J.H., Dumont, R., Lenouvel, F. and Lunel, M. 1953, Ann d'ap., 16, 133.

Bigay, J.H. and Dumont, R. 1954, Ann d'ap., 17,78.

———. 1955, Ann d'ap., 18, 141.

Bredohl, H.B. 1970, Astron. and Astroph., 7, 167.

Edelen, D.G.B. 1965, A.J., 70, 747.

Evans, D.S. 1951, M.N.R.A.S., 111, 526.

———. 1952, M.N.R.A.S., 112, 606.

Fraser, C.W. 1967, Observatory, 87, 29.

Freeman, K.C. 1970, Ap.J., 160, 811.

Heidmann, J. 1967, C.R.Acad.Sci., 265B, 866.

———. 1969, Ap.Lett., 3, 19.

Hodge, P.W. and Brownlee, D.E. 1966, P.A.S.P., 78, 125.

Holmberg, E. 1958, Medd.Lund.Obs., Ser.II, No. 136.

———. 1964, Ark.Astr., 3, 387.

Hopf, A.van 1937, Z.Ap., 14, 104.

Houten, C.J.van 1961, B.A.N., 16, 1.

Hubble, E. 1930, Ap.J., 71, 231.

Jones, W.B., Obitts, D.L., Gallet, R.M. and Vaucouleurs, G.de 1967, Publ.Dept. of Astron. Univ.Texas, Series II, Vol.1, No. 8.

Liller, M.H. 1960, Ap.J., 132, 306.

———. 1966, Ap.J., 146, 28.

Linfoot, E.H. 1955, Recent Advances in Optics (Oxford: O.U.P.).

King, I.R. 1961, A.J., 66, 47.

———. 1962a, A.J., 67, 224.

———. 1962b, A.J. 67, 471.

———. 1966, A.J., 71, 276.

Koelbloed, D. 1965, B.A.N., 18, 62.

Kron, G.E. and Papiashvili, I.I. 1967, P.A.S.P., 79, 9.

Markaryan, B.E., Oganesyan, E. and Arakelyan, S.N. 1965, Astrophysics, 1, 38.

Miller, W.C. 1966, P.A.S.P., 78, 228.

Mohler, O.C. and Pierce, A.K. 1957, Ap.J., 125, 285.

Oort, J.H. 1940, Ap.J., 91, 273.

Redman, R.O. and Shirley, E.C. 1936, M.N.R.A.S., 96, 588.

———. 1938, M.N.R.A.S., 98, 613,

Reynolds, J.H. 1913, M.N.R.A.S., 74, 132.

Richter, N. and Hogner, W. 1963, A.N. 287, 261.

———. 1964, Mitt Karl-Schwarzchild Obs., Tautenburg, No.10.

———. 1965, Mitt Karl-Schwarzchild Obs., Tautenburg, No. 23.

———. 1966, Mitt Karl-Schwarzchild Obs., Tautenburg, No. 32.

Rood, H.J. and Baum, W.A. 1967, A.J., 72, 398.

———. 1968, A.J., 73, 442.

Rood, H.J. and Sastry, C.V. 1967, A.J., 72, 233.

Sandage, A., Freeman, K.C. and Stokes, N.R. 1970,
Ap.J., 160, 831.

Sersic, J.L. 1968, 'Atlas de Galaxias Australes', Cordoba.

Shobbrook, R.R. 1965, M.N.R.A.S., 131, 293.

Stebbins, J. and Whitford, A.E. 1937, Ap.J., 86, 237.

———. 1952, Ap.J., 115, 284.

Tifft, W.G. 1961, A.J., 66, 390.

———. 1963, A.J., 68, 302.

Vaucouleurs, G.de 1948, Ann.d'ap., 11, 247.

———. 1948a, J.des Observ., 31, 113.

———. 1957, Ann.Obs.Houga, II, Part 1.

———. 1959, A.J., 64, 397.

———. 1959a, Hdb.d. Phys., 53, 275.

———. 1960, Ap.J., 131, 574.

———. 1961a, Ap.J. Supp., 5, 233.

———. 1961b, A.J., 133, 405.

———. 1961c, Problems of Extra-Galactic Research:
I.A.U. Symp. No. 15.

———. 1963, Ap.J. Supp., 8, 31.

———. 1963b, Ap.J., 137, 720.

———. 1963c, Ap.J., 138, 934.

———. 1964, Ap.J., 139, 899.

Vaucouleurs, G.de 1968, Applied Optics, 7, 1513.

———. 1968a, I.A.U. Comm. 28, Circular No. 6, Supp. I.

———. 1969, Ap.Lett., 4, 17.

———. 1970, I.A.U. Comm. 28, Circular No. 7a.

———. 1970a, Bull. A.A.S., 2, 308.

———. 1970b, Stars and Stellar Systems, Vol.9, Chap.17 (Chicago: Univ.Chicago Press).

———. 1970c, Ap.Lett., 5, 219.

———. 1971, private communication.

Vaucouleurs, G.de, Angione, R. and Fraser, C.W. 1968, Ap. Lett., 2, 141.

Vaucouleurs, G.de, Griboval, P. and White, T. 1965, P.A.S.P., 77, 115.

Vaucouleurs, G. de and Heidmann, J. and N. 1970, private communication.

Vaucouleurs, G.de and Page, J. 1962, Ap.J., 136, 107.

Vaucouleurs, G.de and Malik, G. 1969, M.N.R.A.S., 142, 387.

Vaucouleurs, G.de and A. de 1964, Reference Catalogue of Bright Galaxies (Austin: Univ.Texas Press).

Walker, M.F. 1965, informal meeting organized by Dr Merle Walker at Third Symposium on Photo-electronic Devices held in London.

Walker, M.F. and Kron, G.E. 1967, P.A.S.P., 79, 551.

Williams, R. and Hiltner, W.A. 1940, Pub.Univ.Mich.Obs., 8, 45.

PHOTOGRAPHIC SURFACE PHOTOMETRY OF GALAXIES IN THE VIRGO CLUSTER

by

Christopher W. Fraser

VOLUME TWO

PHOTOMETRIC DATA FOR GALAXIES

NGC 4189 to NGC 4559

EXPLANATORY NOTES FOR USE WITH THE PHOTOMETRIC DATA

The data for each galaxy occupy twelve pages, divided equally between the B and the V colours. The galaxies are listed in increasing order of NGC identification numbers and each page may be described as follows:-

1. Luminosity profile of major axis. The y-axis denotes log I, with the value of log I = -2.00 at the origin. Each division on the y-axis represents a value of +1.00 in log I. For the x-axis, which denotes distance r, the centre of the galaxy is plotted at the centre of the axis. Each division represents 50 arc sec.

2. Luminosity profile of minor axis. The units for the x and y axes are as before.

3. Equivalent luminosity profile. The y-axis denotes increasing log I, each division representing an integer value from a minimum at the origin of log I = -2.00. The distance r is given on the x-axis, from zero at the origin and increasing by 50 arc sec per division.

4. Relative integrated luminosity curve k(r) is plotted as ordinate, each positive division in y

representing a value of 0.1, and r*, as in case 3, denotes increasing distance r*, in 50 arc sec steps.

5. Table of mean luminosity distribution. The areas in column 5 are expressed in square seconds of arc, and in the last column, μ is in mag. sec^{-2}.

6. Table of photometric parameters. The units are as follows:-

a. The total luminosity is expressed in sky units per square minute.

b. The apparent central surface brightness is in mag. per square second, as are the surface brightnesses at k = $\frac{1}{4}$, $\frac{1}{2}$ and $\frac{3}{4}$.

c. The major axis and minor axis at threshold together with the major axis at μ = 25.0 mag.sec^{-2}, and the semi-major axis measurements at k = $\frac{1}{4}$, $\frac{1}{2}$ and $\frac{3}{4}$, are expressed in minutes of arc.

d. The gradient of the exponential component G(a) = d log I/da is expressed per minute of arc, as is the equivalent gradient of the exponential component G(r*) = d log I/dr*

e. The mean surface brightness is in magnitudes per square minute.

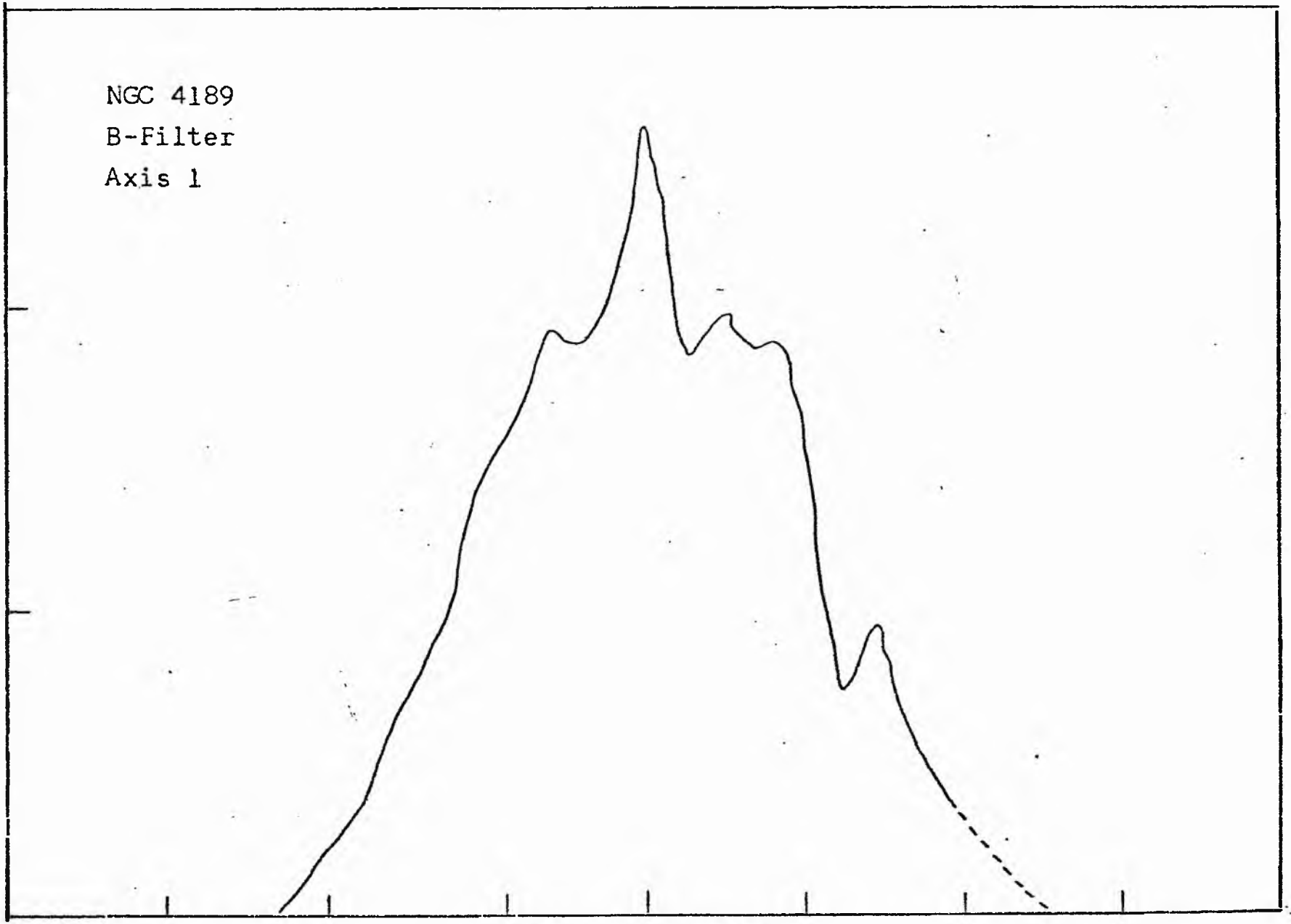

Luminosity profile

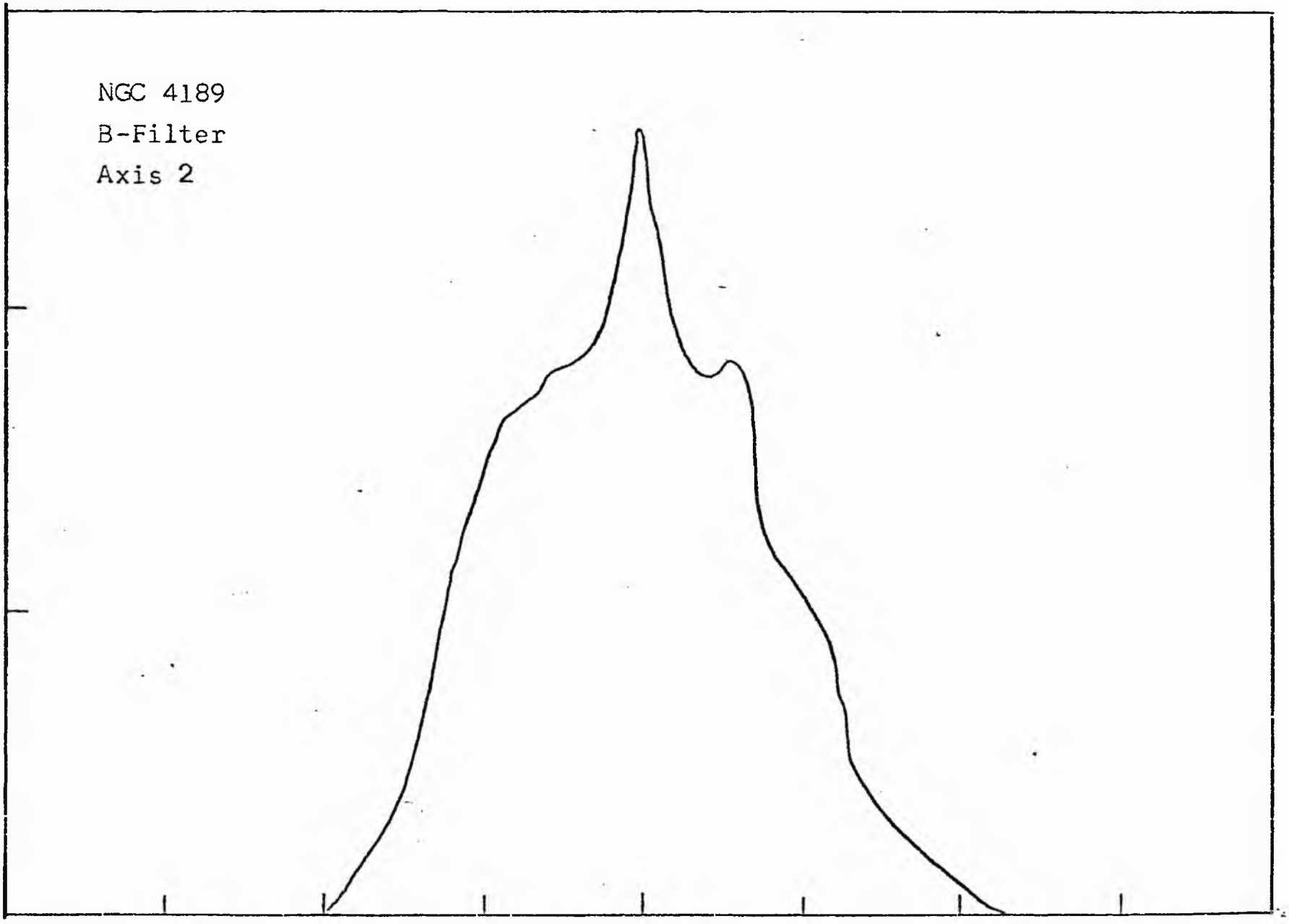
NGC 4189
B-Filter
Axis 2

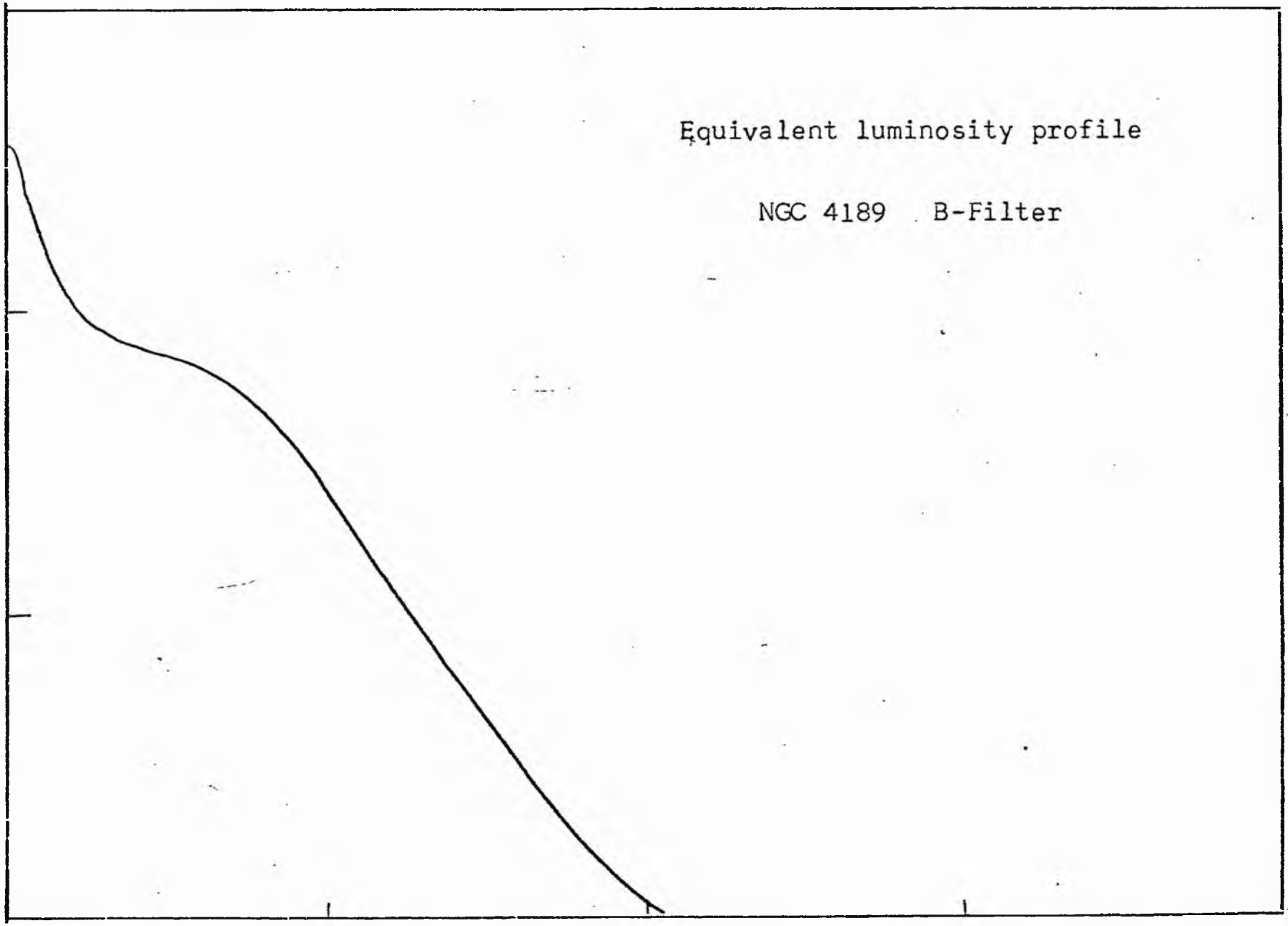
Equivalent luminosity profile
NGC 4189 B-Filter

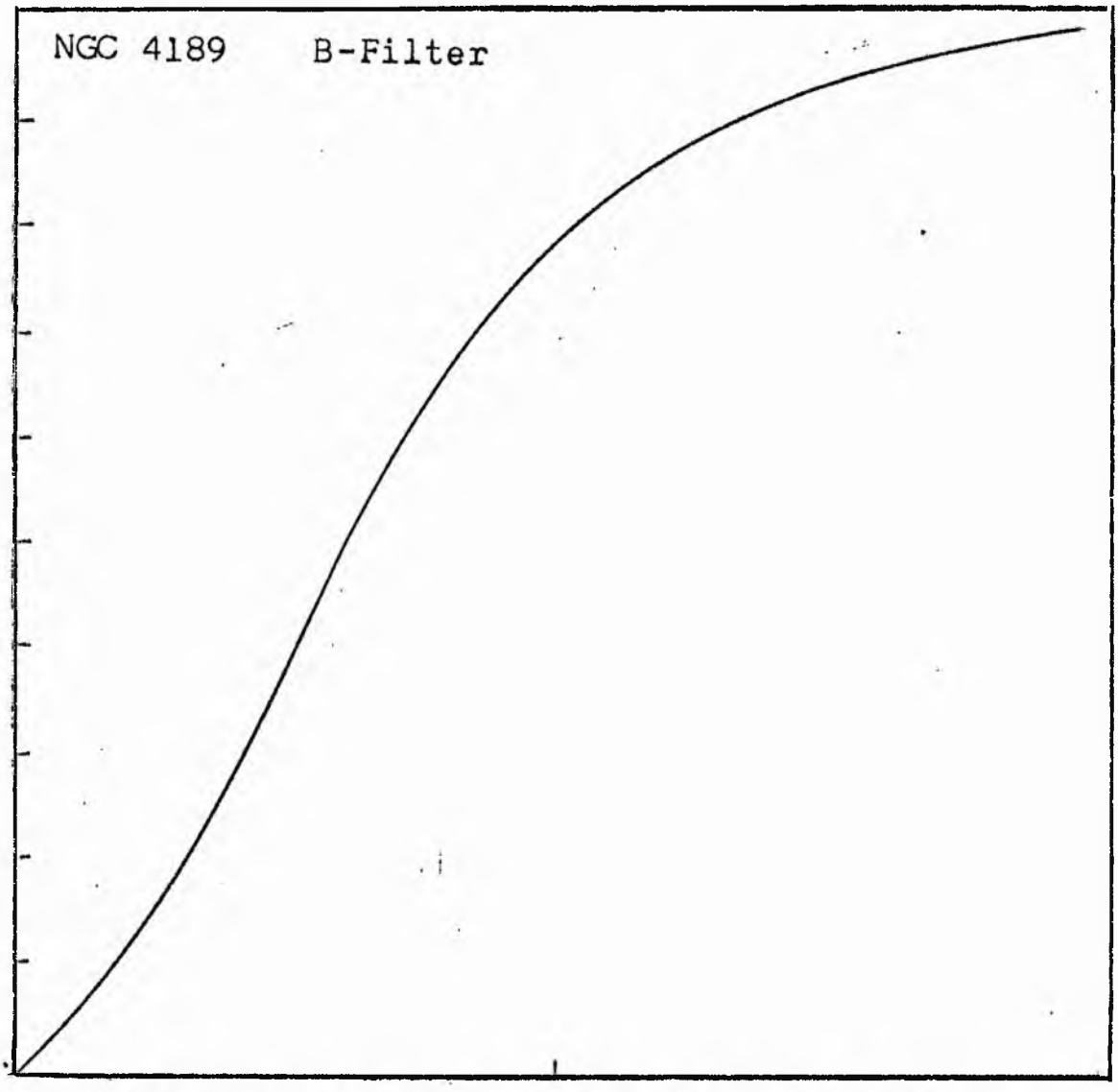

Relative integrated luminosity k(r) versus equivalent radius r*.

MEAN LUMINOSITY DISTRIBUTION IN NGC 4189
B COLOR

LOG I	I	T	R	AREA	ΔA	P	ΣP	K(R)	ρ	LOG J	μ
0.48	3.020		0.0	0.0			0.0	0.0	0.0	0.713	20.73
		2.765			20.27	56.0604					
0.40	2.512		2.44	20.27			96.06	0.01	0.07	0.633	20.93
		2.254			41.11	92.6379					
0.30	1.995		4.42	61.38			148.70	0.03	0.13	0.533	21.18
		1.790			71.77	128.4659					
0.20	1.585		6.51	133.14			277.16	0.05	0.19	0.433	21.43
		1.422			79.13	112.5176					
0.10	1.259		8.22	212.27			389.68	0.07	0.24	0.333	21.68
		1.129			93.77	105.9118					
0.00	1.000		9.87	306.04			495.59	0.08	0.29	0.233	21.93
		0.897			716.36	642.6917					
-0.10	0.794		18.04	1022.40			1138.28	0.19	0.53	0.133	22.18
		0.713			1831.48	1305.1909					
-0.20	0.631		30.14	2853.88			2443.48	0.42	0.88	0.033	22.43
		0.566			1426.05	807.2495					
-0.30	0.501		36.91	4279.94			3250.73	0.55	1.08	-0.067	22.68
		0.450			550.02	247.3149					
-0.40	0.398		39.21	4829.96			3498.04	0.59	1.15	-0.167	22.93
		0.357			1068.34	381.5776					
-0.50	0.316		43.33	5898.30			3879.62	0.66	1.27	-0.267	23.18
		0.284			1032.61	292.9609					
-0.60	0.251		46.97	6930.91			4172.58	0.71	1.37	-0.367	23.43
		0.225			1767.73	398.3706					
-0.70	0.200		52.62	8698.64			4570.95	0.78	1.54	-0.467	23.68
		0.179			1090.16	195.1466					
-0.80	0.158		55.82	9788.80			4766.09	0.81	1.63	-0.567	23.93
		0.142			1180.47	167.8527					
-0.90	0.126		59.09	10969.27			4933.94	0.84	1.73	-0.667	24.18
		0.113			1279.02	144.4607					
-1.00	0.100		62.44	12248.29			5078.40	0.86	1.83	-0.767	24.43
		0.090			1378.48	123.6725					
-1.10	0.079		65.86	13626.77			5202.07	0.88	1.93	-0.867	24.68
		0.071			1705.50	121.5418					
-1.20	0.063		69.86	15332.27			5323.61	0.90	2.04	-0.967	24.93
		0.057			1377.17	77.9581					
-1.30	0.050		72.93	16709.45			5401.57	0.92	2.13	-1.067	25.18
		0.045			1709.59	76.8716					
-1.40	0.040		76.57	18419.04			5478.44	0.93	2.24	-1.167	25.43
		0.036			1833.18	65.4756					
-1.50	0.032		80.29	20252.21			5543.91	0.94	2.35	-1.267	25.68
		0.028			1957.09	55.5247					
-1.60	0.025		84.08	22209.30			5599.43	0.95	2.46	-1.367	25.93
		0.023			2086.01	47.0101					
-1.70	0.020		87.94	24295.31			5646.44	0.96	2.57	-1.467	26.18
		0.018			2225.79	39.8438					
-1.80	0.016		91.88	26521.11			5686.29	0.97	2.69	-1.567	26.43
		0.014			2371.52	33.7213					
-1.90	0.013		95.90	28892.63			5720.00	0.97	2.81	-1.667	26.68
		0.011			2517.00	28.4290					
-2.00	0.010		99.99	31409.63			5748.43	0.98	2.92	-1.767	26.93
- ∞							5884.00	(1)			∞

42

24

PHOTOMETRIC PARAMETERS OF NGC 4189

B-FILTER

Total luminosity	L_T	= 1.63
Total apparent magnitude	m_T	= 12.53
Apparent central surface brightness	μ_o	= 20.73
Major axis at threshold	$2a_m$	= 4.01
Minor axis at threshold	$2b_m$	= 3.38
Major axis at μ=25.0 mag sec^{-2}	2a(25)	= 2.56
Luminosity within μ=25.0 mag sec^{-2}	k(25)	= 0.91
Gradient of exponential component	G(a)	= -1.72
Equivalent gradient of exponential comp.	G(r*)	= -1.57
Equivalent gradient of reduced exp. comp.	G(ρ)	= -0.89
Parameters at k = ¼ :		
Semi-major axis	a_1	= 0.32
Axis ratio	b/a	= 0.81
Equivalent radius	r_1*	= 0.36
Surface brightness	μ_1	= 22.24
Parameters at k = ½(effective) :		
Semi-major axis	a_e	= 0.71
Axis ratio	b/a	= 0.78
Equivalent radius	r_e*	= 0.57
Surface brightness	μ_e	= 22.55
Mean surface brightness	μ_e'	= 13.32
Parameters at k = ¾ :		
Semi-major axis	a_3	= 0.93
Axis ratio	b/a	= 0.78
Equivalent radius	r_3*	= 0.83
Surface brightness	μ_3	= 23.57
Concentration indices	C_{21}	= 1.58
	C_{32}	= 1.47

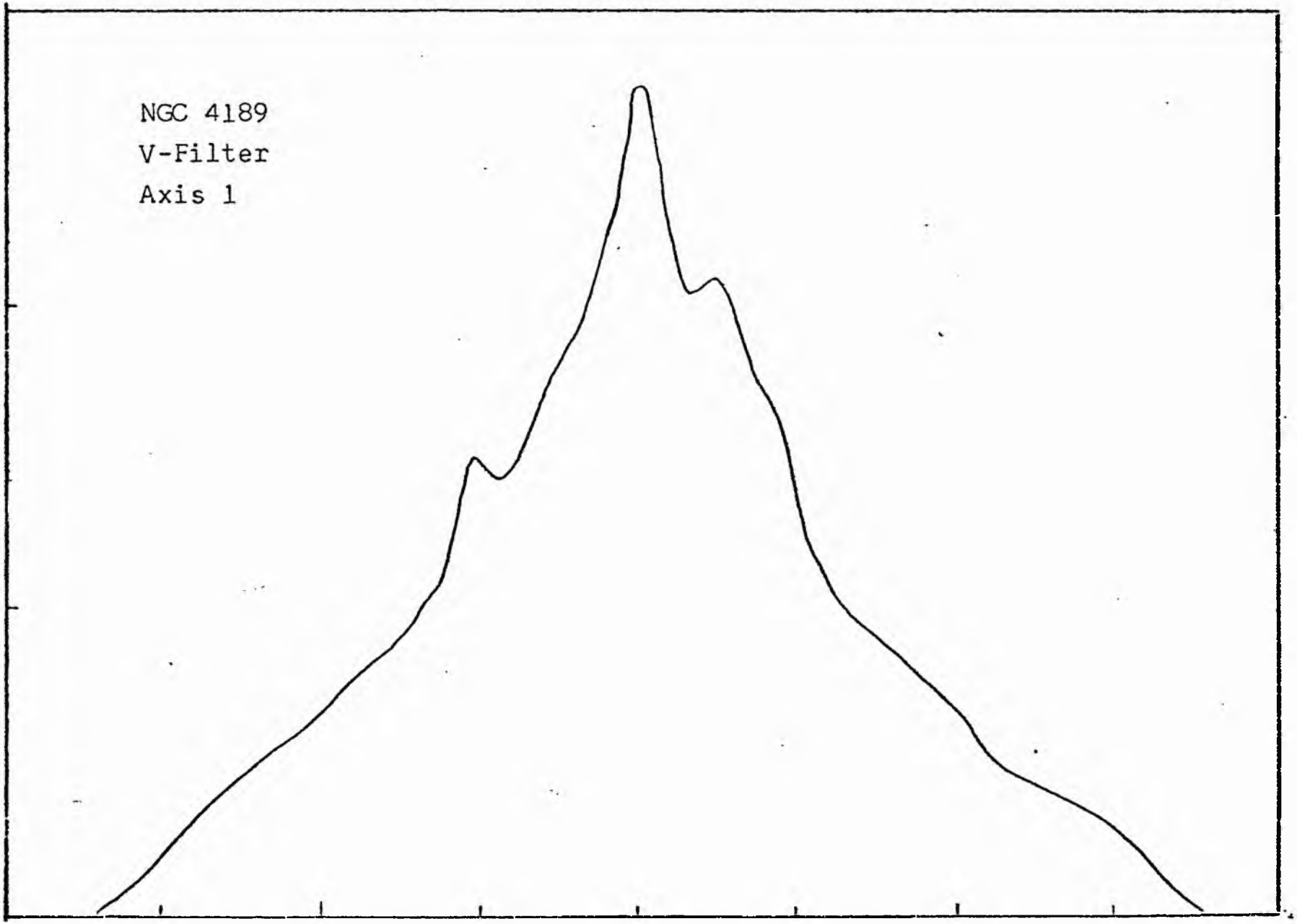
NGC 4189
V-Filter
Axis 1

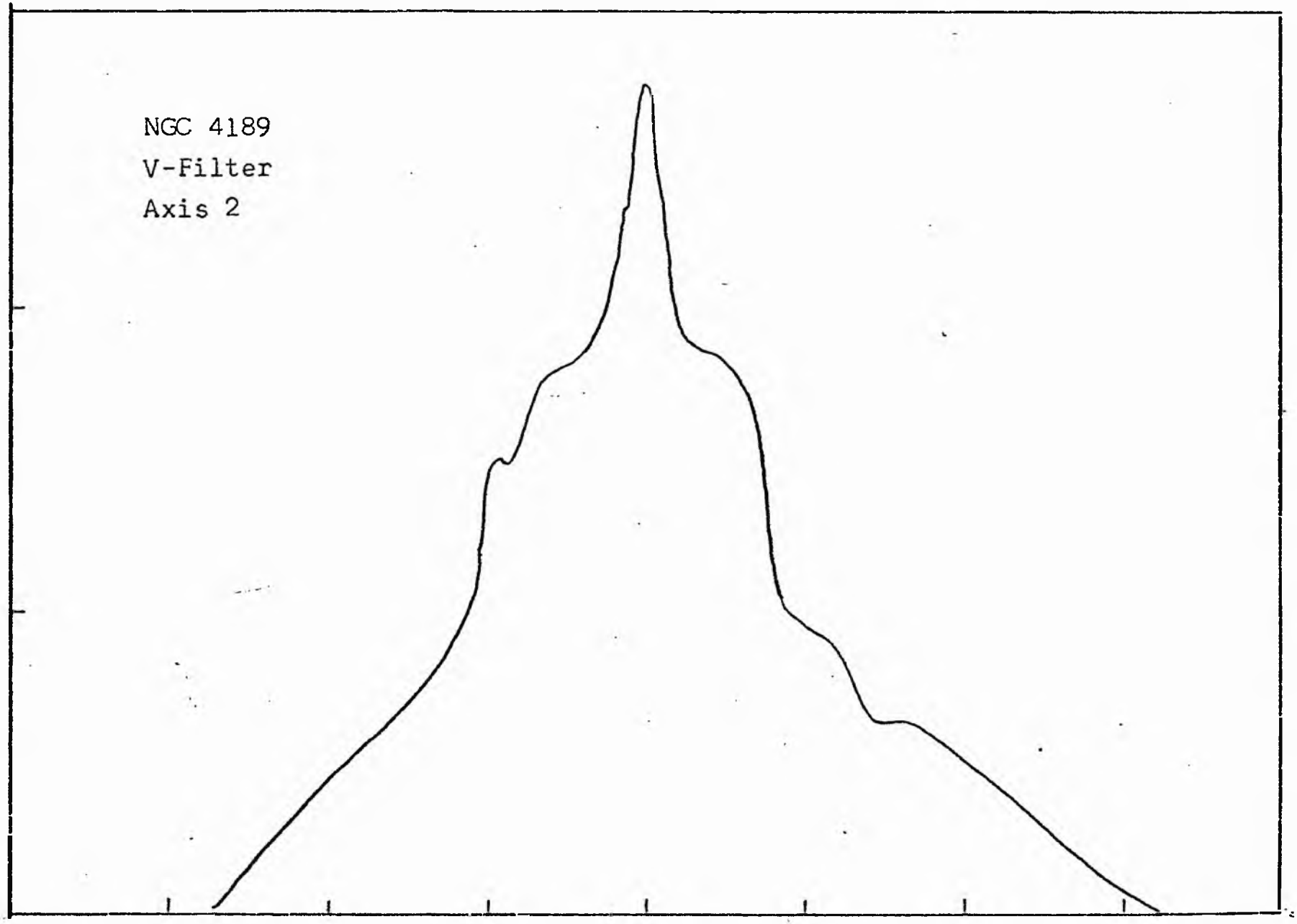
NGC 4189
V-Filter
Axis 2

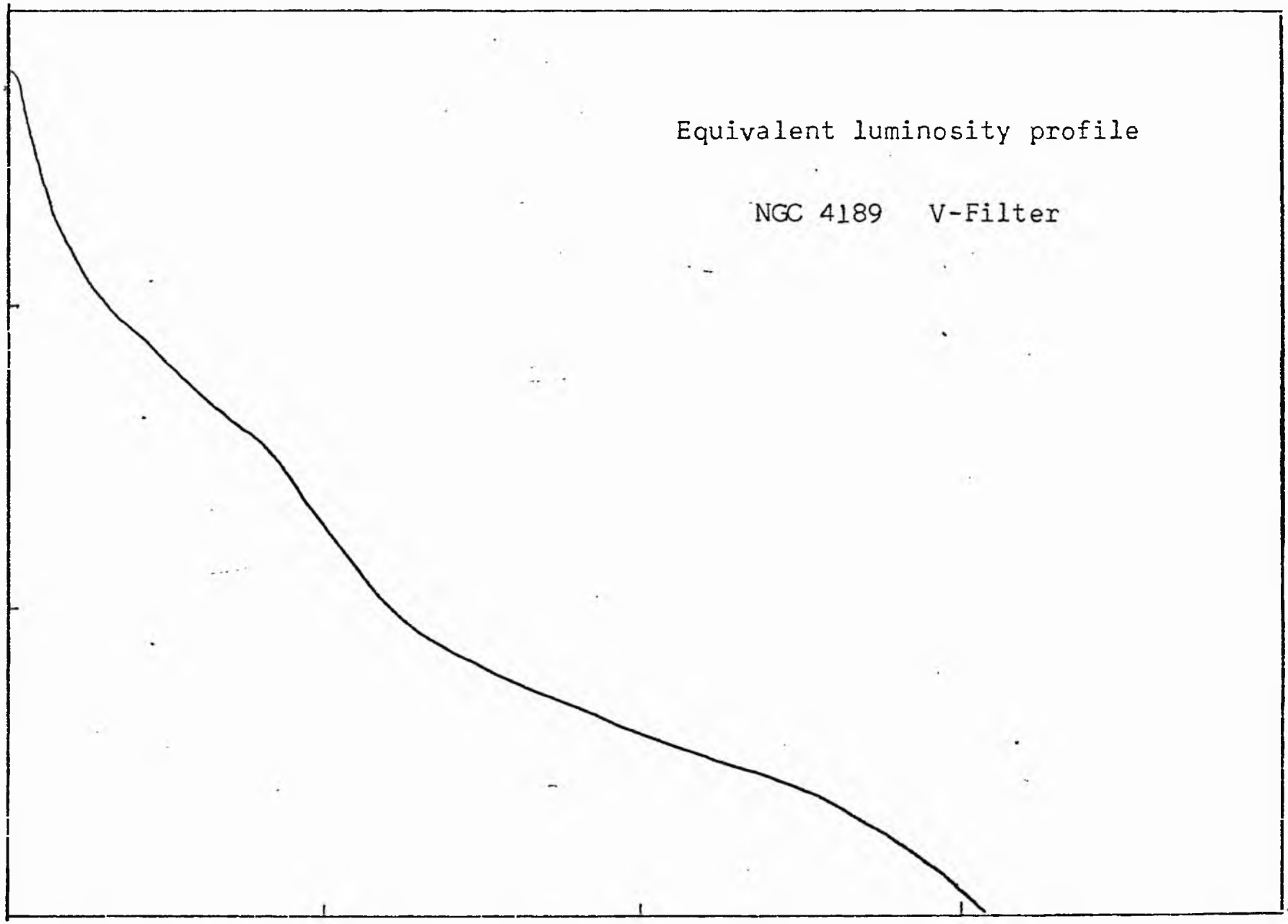
Equivalent luminosity profile
NGC 4189 V-Filter

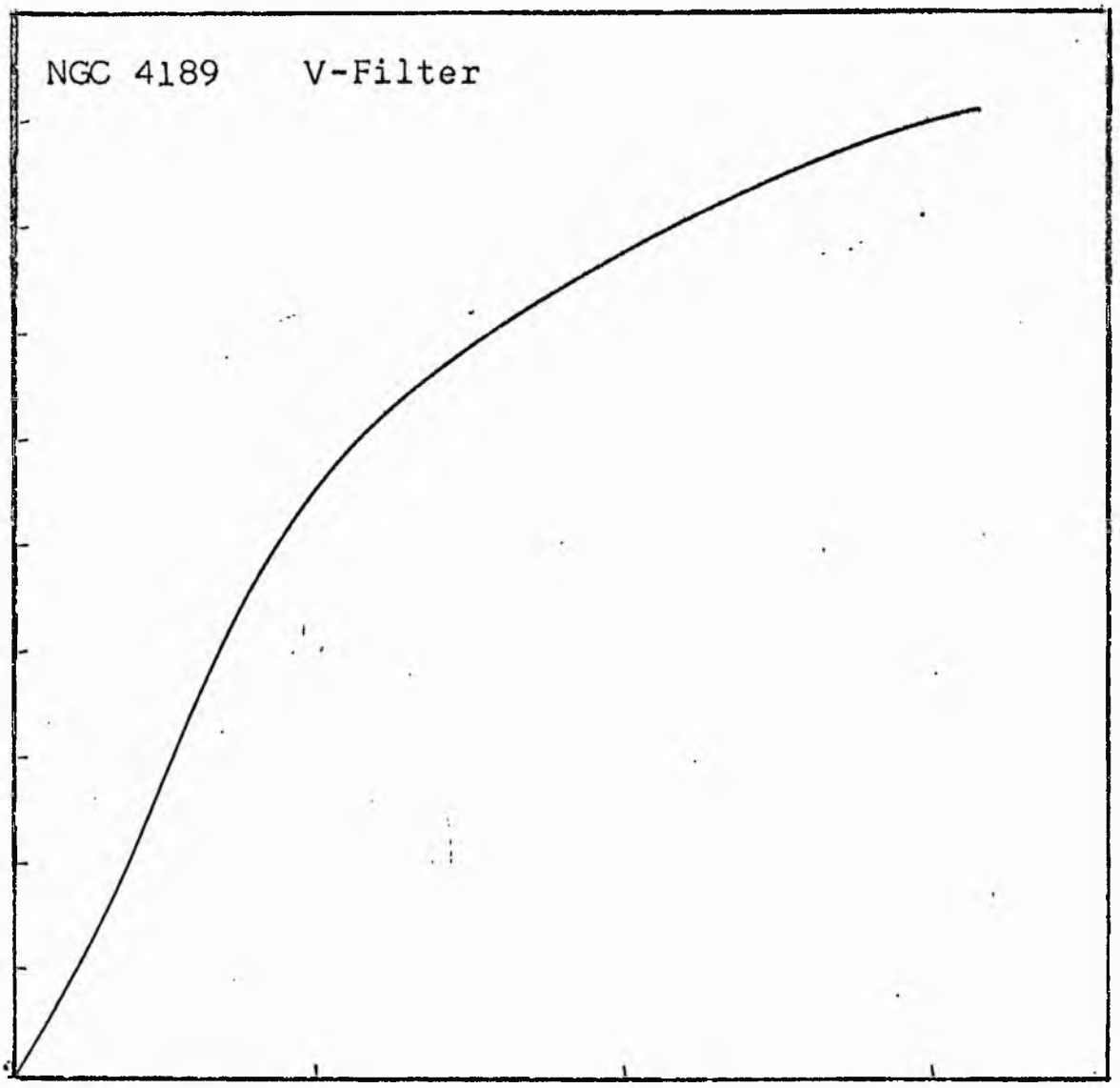

Relative integrated luminosity k(r) versus equivalent radius r*.

MEAN LUMINOSITY DISTRIBUTION IN NGC 4189
V COLOUR

LOG I	I	$\bar{I}$	R	AREA	Δ A	P	Σ P	K(R)	ρ	LOG J	μ
0.72	5.248		0.0	0.0			0.0	0.0	0.0	1.262	19.46
		5.130			10.99	56.3570					
0.70	5.012		1.87	10.99			56.36	0.01	0.04	1.242	19.51
		4.496			13.29	59.7745					
0.60	3.981		2.78	24.28			116.13	0.02	0.07	1.142	19.76
		3.572			31.14	111.2153					
0.50	3.162		4.20	55.42			227.35	0.03	0.10	1.042	20.01
		2.837			45.58	129.3171					
0.40	2.512		5.67	101.00			356.66	0.05	0.13	0.942	20.26
		2.254			57.82	130.2913					
0.30	1.995		7.11	158.81			486.96	0.06	0.17	0.842	20.51
		1.790			103.06	184.4840					
0.20	1.585		9.13	261.87			671.44	0.09	0.21	0.742	20.76
		1.422			183.76	261.2839					
0.10	1.259		11.91	445.63			932.72	0.12	0.28	0.642	21.01
		1.129			398.30	449.8684					
0.00	1.000		16.39	843.93			1382.59	0.18	0.39	0.542	21.26
		0.897			464.75	416.9600					
-0.10	0.794		20.41	1308.69			1799.55	0.23	0.48	0.442	21.51
		0.713			654.81	466.6462					
-0.20	0.631		25.00	1963.50			2266.2.	0.29	0.59	0.342	21.76
		0.566			835.73	473.0847					
-0.30	0.501		29.85	2799.23			2739.28	0.36	0.70	0.242	22.01
		0.450			1177.83	529.6062					
-0.40	0.398		35.58	3977.05			3268.89	0.43	0.84	0.142	22.26
		0.357			1191.22	425.4656					
-0.50	0.316		40.56	5168.27			3694.35	0.48	0.95	0.042	22.51
		0.284			1207.59	342.6035					
-0.60	0.251		45.05	6375.86			4036.96	0.52	1.06	-0.058	22.76
		0.225			1446.73	326.0317					
-0.70	0.200		49.90	7822.59			4362.99	0.57	1.17	-0.158	23.01
		0.179			371.13	66.4358					
-0.80	0.158		51.07	8193.73			4429.42	0.58	1.20	-0.258	23.26
		0.142			1069.22	152.0340					
-0.90	0.126		54.30	9262.95			4581.45	0.60	1.28	-0.358	23.51
		0.113			1896.48	214.2012					
-1.00	0.100		59.60	11159.43			4795.65	0.62	1.40	-0.458	23.76
		0.090			3281.95	294.4456					
-1.10	0.079		67.80	14441.39			5090.10	0.66	1.60	-0.558	24.01
		0.071			3944.00	281.0674					
-1.20	0.063		76.50	18385.39			5371.16	0.70	1.80	-0.658	24.26
		0.057			6611.12	374.2395					
-1.30	0.050		89.20	24996.51			5745.40	0.75	2.10	-0.758	24.51
		0.045			7330.70	329.6250					
-1.40	0.040		101.44	32327.21			6075.03	0.79	2.39	-0.858	24.76
		0.036			9003.86	321.5911					
-1.50	0.032		114.70	41331.07			6396.62	0.83	2.70	-0.958	25.01
		0.028			8434.07	239.2838					
-1.60	0.025		125.06	49765.14			6635.90	0.86	2.96	-1.058	25.26
		0.023			7583.72	170.9067					
-1.70	0.020		135.11	57348.86			6806.80	0.89	3.18	-1.158	25.51
		0.018			6418.23	114.8928					
-1.80	0.016		142.47	63767.09			6921.70	0.90	3.35	-1.258	25.76
		0.014			4916.16	69.9042					
-1.90	0.013		147.86	68683.25			6991.60	0.91	3.48	-1.358	26.01
		0.011			7085.94	80.0342					
-2.00	0.010		155.30	75769.19			7071.63	0.92	3.66	-1.458	26.26
$-\infty$							7691.00	1.1)			∞

PHOTOMETRIC PARAMETERS OF NGC 4189

V-FILTER

Total luminosity ..... L_I = 2.13

Total apparent magnitude ..... m_T = 11.54

Apparent central surface brightness ..... μ_o = 19.46

Major axis at threshold ..... $2a_m$ = 5.8

Minor axis at threshold ..... $2b_m$ = 3.83

Major axis at μ=25.0 mag sec^{-2} ..... 2a(25) = 4.1

Luminosity within μ=25.0 mag sec^{-2} ..... k(25) = 0.83

Gradient of exponential component ..... G(a) = -0.68

Equivalent gradient of exponential comp. .... G(r*) = -0.80

Equivalent gradient of reduced exp. comp. .... G(ρ) = -0.66

Parameters at k = ¼ :

- Semi-major axis ..... a_1 = 0.383
- Axis ratio ..... b/a = 0.69
- Equivalent radius ..... r_1* = 0.36
- Surface brightness ..... μ_1 = 21.59

Parameters at k = ½(effective) :

- Semi-major axis ..... a_e = 0.82
- Axis ratio ..... b/a = 0.87
- Equivalent radius ..... r_e* = 0.70
- Surface brightness ..... μ_e = 22.63
- Mean surface brightness ..... μ_e' = 12.76

Parameters at k = ¾ :

- Semi-major axis ..... a_3 = 1.75
- Axis ratio ..... b/a = 0.76
- Equivalent radius ..... r_3* = 1.50
- Surface brightness ..... μ_3 = 24.51

Concentration indices ..... C_{21} = 1.97, C_{32} = 2.12

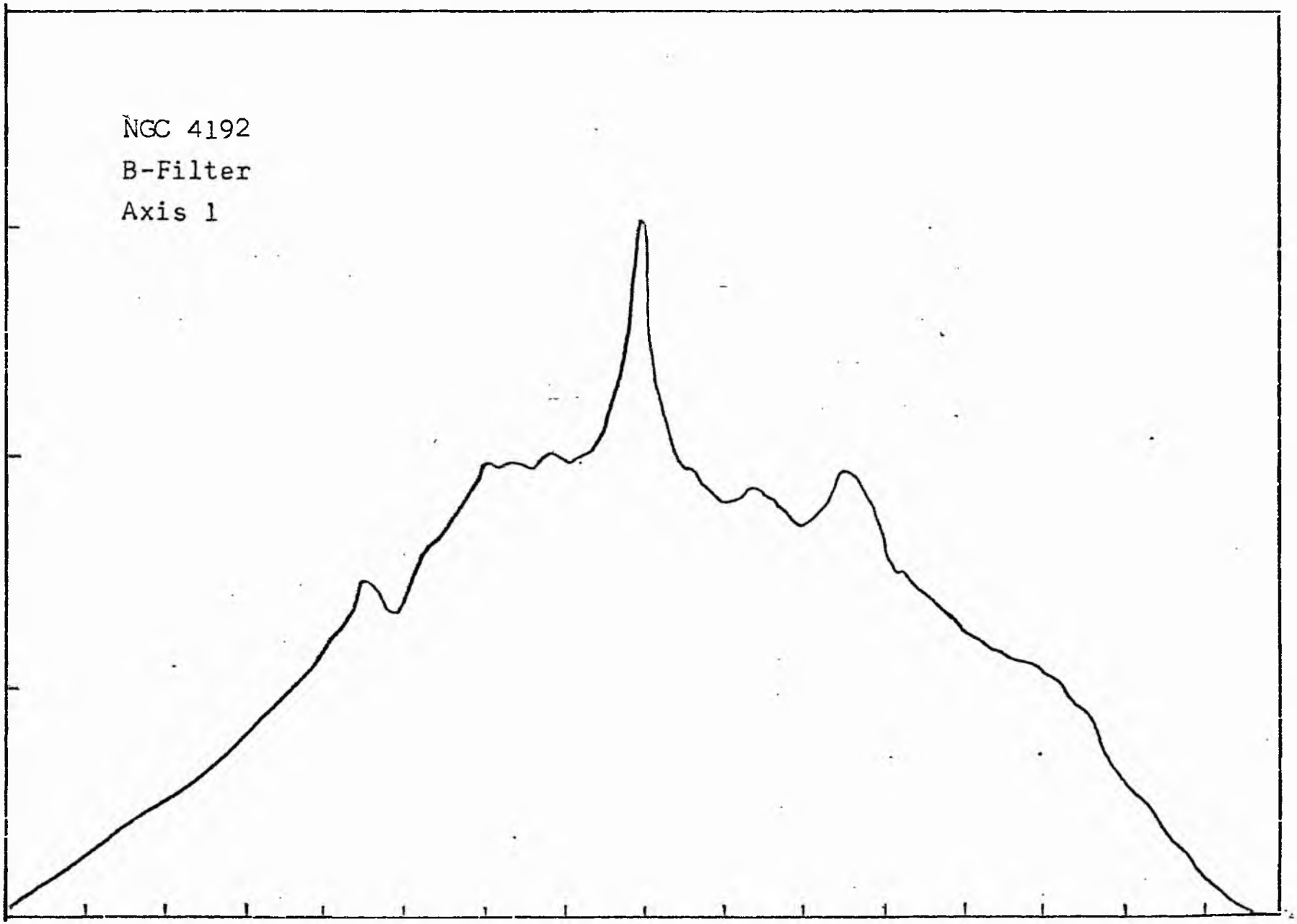
NGC 4192
B-Filter
Axis 1

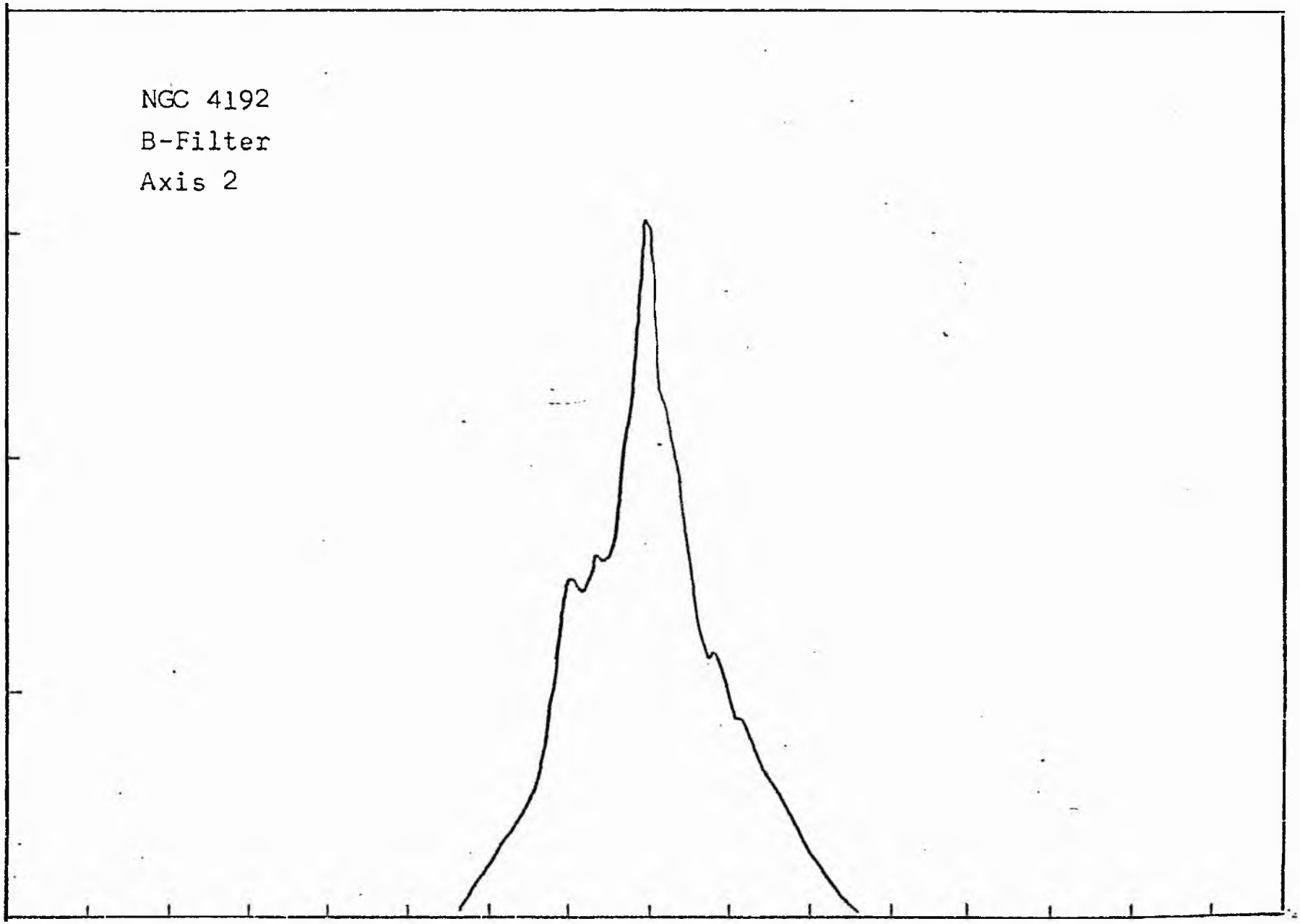
NGC 4192
B-Filter
Axis 2

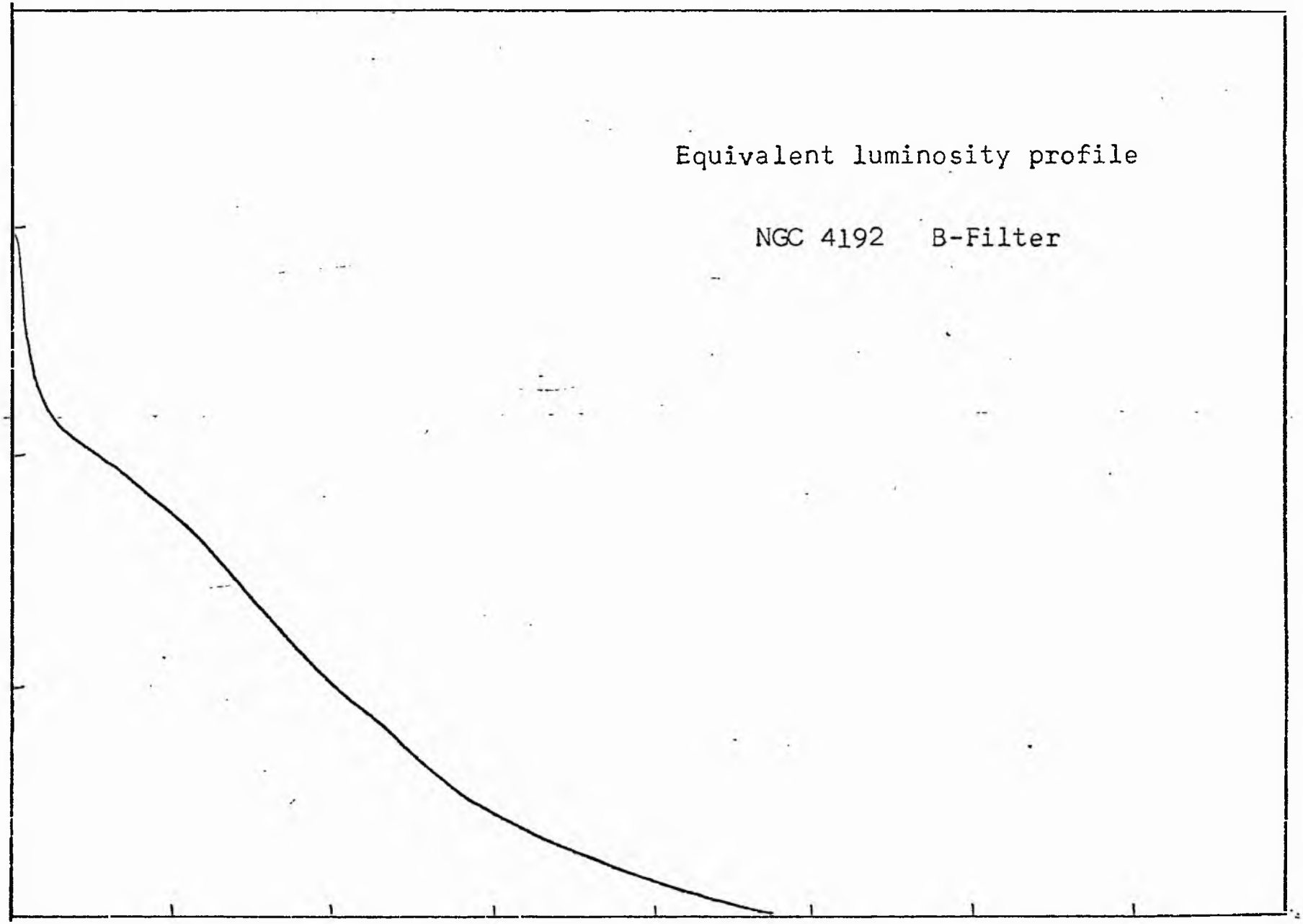
Equivalent luminosity profile
NGC 4192 B-Filter

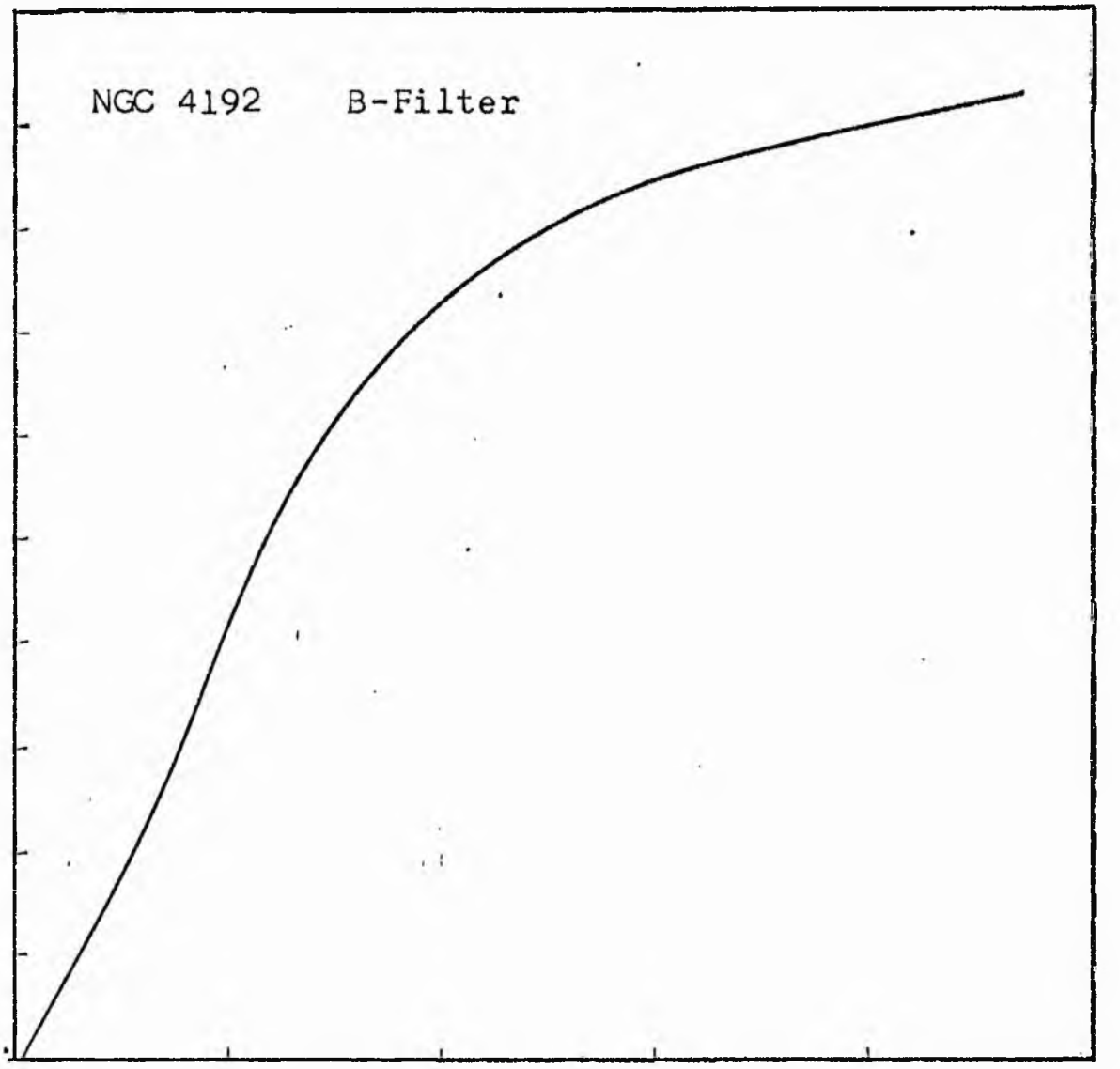

Relative integrated luminosity k(r) versus equivalent radius r*.

MEAN LUMINOSITY DISTRIBUTION IN NGC 4192
B COLOUR

LOG I	I	I	R	AREA	ΔA	P	ΣP	K(R)	ρ	LOG J	μ
0.99	9.772		0.0	0.0			0.0	0.0	0.0	1.323	19.14
		8.858			12.07	106.9026					
0.90	7.943		1.96	12.07			106.90	0.01	0.03	1.233	19.37
		7.126			25.76	183.5683					
0.80	6.310		3.47	37.83			290.47	0.01	0.06	1.133	19.62
		5.661			36.99	209.3760					
0.70	5.012		4.88	74.82			499.85	0.02	0.08	1.033	19.87
		4.496			86.24	387.7781					
0.60	3.981		7.16	161.06			887.62	0.04	0.12	0.933	20.12
		3.572			60.09	214.6134					
0.50	3.162		8.39	221.14			1102.24	0.05	0.14	0.833	20.37
		2.837			40.73	115.5545					
0.40	2.512		9.13	261.87			1217.79	0.06	0.15	0.733	20.62
		2.254			129.40	291.6084					
0.30	1.995		11.16	391.27			1509.40	0.07	0.19	0.633	20.87
		1.790			312.76	559.8687					
0.20	1.585		14.97	704.03			2069.27	0.10	0.25	0.533	21.12
		1.422			199.62	283.8379					
0.10	1.259		16.96	903.65			2353.11	0.11	0.28	0.433	21.37
		1.129			1596.44	1803.1194					
0.00	1.000		28.21	2500.09			4156.23	0.20	0.47	0.333	21.62
		0.897			2376.79	2132.3708					
-0.10	0.794		39.40	4876.88			6288.59	0.31	0.66	0.233	21.87
		0.713			2696.90	1921.9260					
-0.20	0.631		49.10	7573.78			8210.52	0.40	0.82	0.133	22.12
		0.566			2885.49	1633.3975					
-0.30	0.501		57.70	10459.27			9843.91	0.48	0.96	0.033	22.37
		0.450			2288.34	1028.9446					
-0.40	0.398		63.70	12747.61			10872.86	0.53	1.06	-0.067	22.62
		0.357			3000.06	1071.5244					
-0.50	0.316		70.80	15747.66			11944.38	0.58	1.18	-0.167	22.87
		0.284			3204.39	909.1118					
-0.60	0.251		77.67	18952.05			12853.49	0.63	1.30	-0.267	23.12
		0.225			3495.64	787.7688					
-0.70	0.200		84.53	22447.69			13641.25	0.67	1.41	-0.367	23.37
		0.179			2661.04	476.3474					
-0.80	0.158		89.40	25108.73			14117.60	0.69	1.49	-0.467	23.62
		0.142			3603.41	512.3723					
-0.90	0.126		95.60	28712.13			14629.97	0.71	1.60	-0.567	23.87
		0.113			6786.87	766.5532					
-1.00	0.100		106.30	35499.00			15396.52	0.75	1.77	-0.667	24.12
		0.090			4900.49	439.6558					
-1.10	0.079		113.40	40399.50			15836.17	0.77	1.89	-0.767	24.37
		0.071			3864.57	275.4065					
-1.20	0.063		118.70	44264.06			16111.58	0.79	1.98	-0.867	24.62
		0.057			6430.62	364.0212					
-1.30	0.050		127.03	50694.68			16475.60	0.80	2.12	-0.967	24.87
		0.045			7130.57	320.6262					
-1.40	0.040		135.67	57825.25			16796.22	0.82	2.26	-1.067	25.12
		0.036			9388.81	335.3406					
-1.50	0.032		146.27	67214.06			17131.56	0.84	2.44	-1.167	25.37
		0.028			12839.12	364.2598					
-1.60	0.025		159.63	80053.19			17495.82	0.85	2.66	-1.267	25.62
		0.023			14428.62	325.1631					
-1.70	0.020		173.42	94481.81			17820.98	0.87	2.89	-1.367	25.87
		0.018			29279.06	524.1243					
-1.80	0.016		198.48	123760.87			18345.10	0.90	3.31	-1.467	26.12
		0.014			23764.81	337.9187					
-1.90	0.013		216.70	147525.69			18683.02	0.91	3.62	-1.567	26.37
		0.011			25526.06	288.3115					
-2.00	0.010		234.70	173051.75			18971.33	0.93	3.92	-1.667	26.62
$-\infty$							20471.00	(1)			∞

PHOTOMETRIC PARAMETERS OF NGC 4192

B-FILTER

Total luminosity	L_T	= 5.68
Total apparent magnitude	m_T	= 10.86
Apparent central surface brightness	μ_o	= 19.14
Major axis at threshold	$2a_m$	= 13.3
Minor axis at threshold	$2b_m$	= 4.5
Major axis at μ=25.0 mag sec^{-2}	2a(25)	= 8.06
Luminosity within μ=25.0 mag sec^{-2}	k(25)	= 0.81
Gradient of exponential component	G(a)	= -0.47
Equivalent gradient of exponential comp.	G(r*)	= -0.85
Equivalent gradient of reduced exp. comp.	G(ρ)	= -0.84
Parameters at k = ¼ :		
Semi-major axis	a_1	= 1.46
Axis ratio	b/a	= 0.25
Equivalent radius	r_1*	= 0.56
Surface brightness	μ_1	= 21.74
Parameters at k = ½(effective) :		
Semi-major axis	a_e	= 2.25
Axis ratio	b/a	= 0.22
Equivalent radius	r_e*	= 0.99
Surface brightness	μ_e	= 22.47
Mean surface brightness	μ_e'	= 12.83
Parameters at k = ¾ :		
Semi-major axis	a_3	= 4.03
Axis ratio	b/a	= 0.24
Equivalent radius	r_3*	= 1.76
Surface brightness	μ_3	= 24.12
Concentration indices	C_{21}	= 1.79
	C_{32}	= 1.76

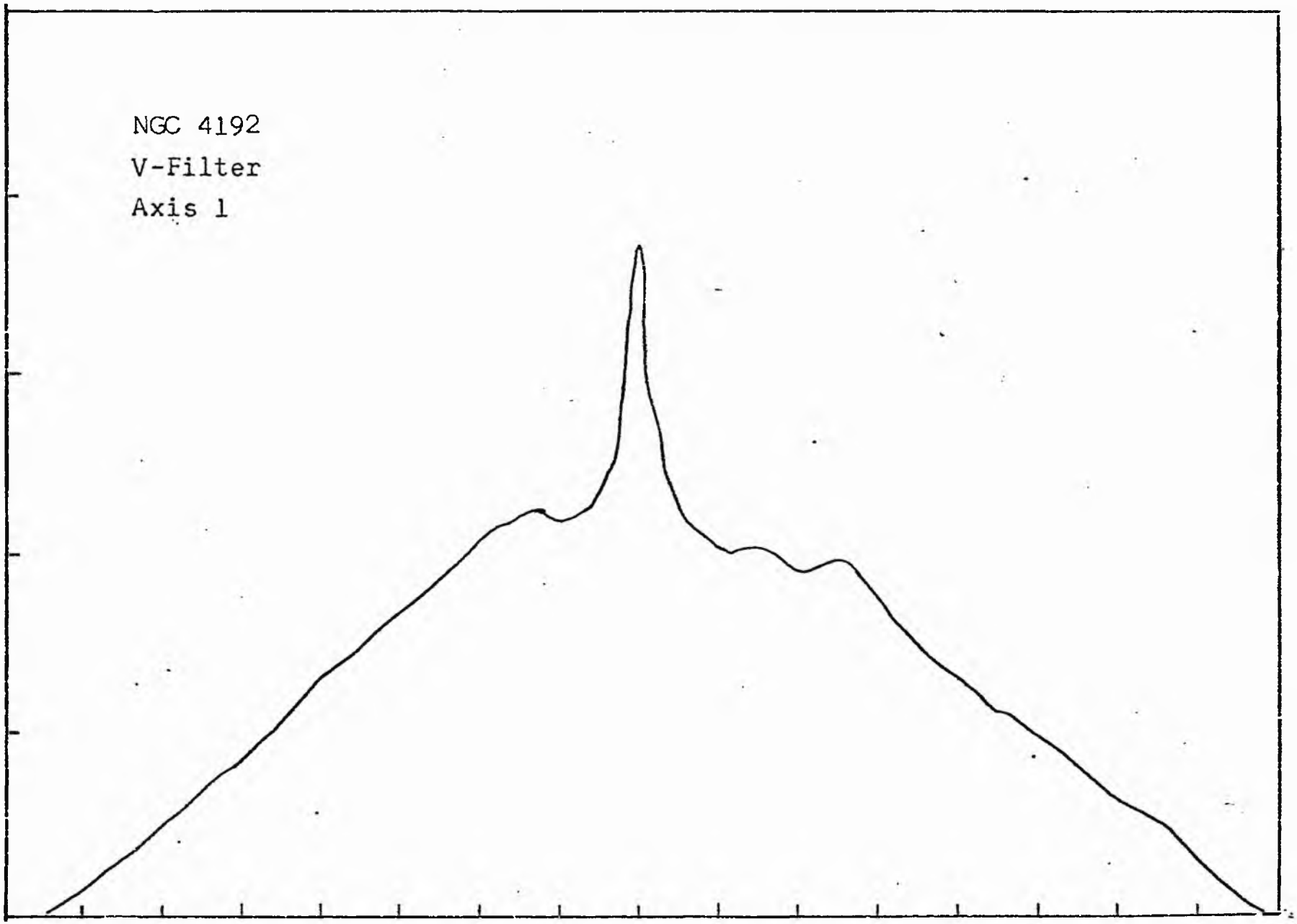
NGC 4192
V-Filter
Axis 1

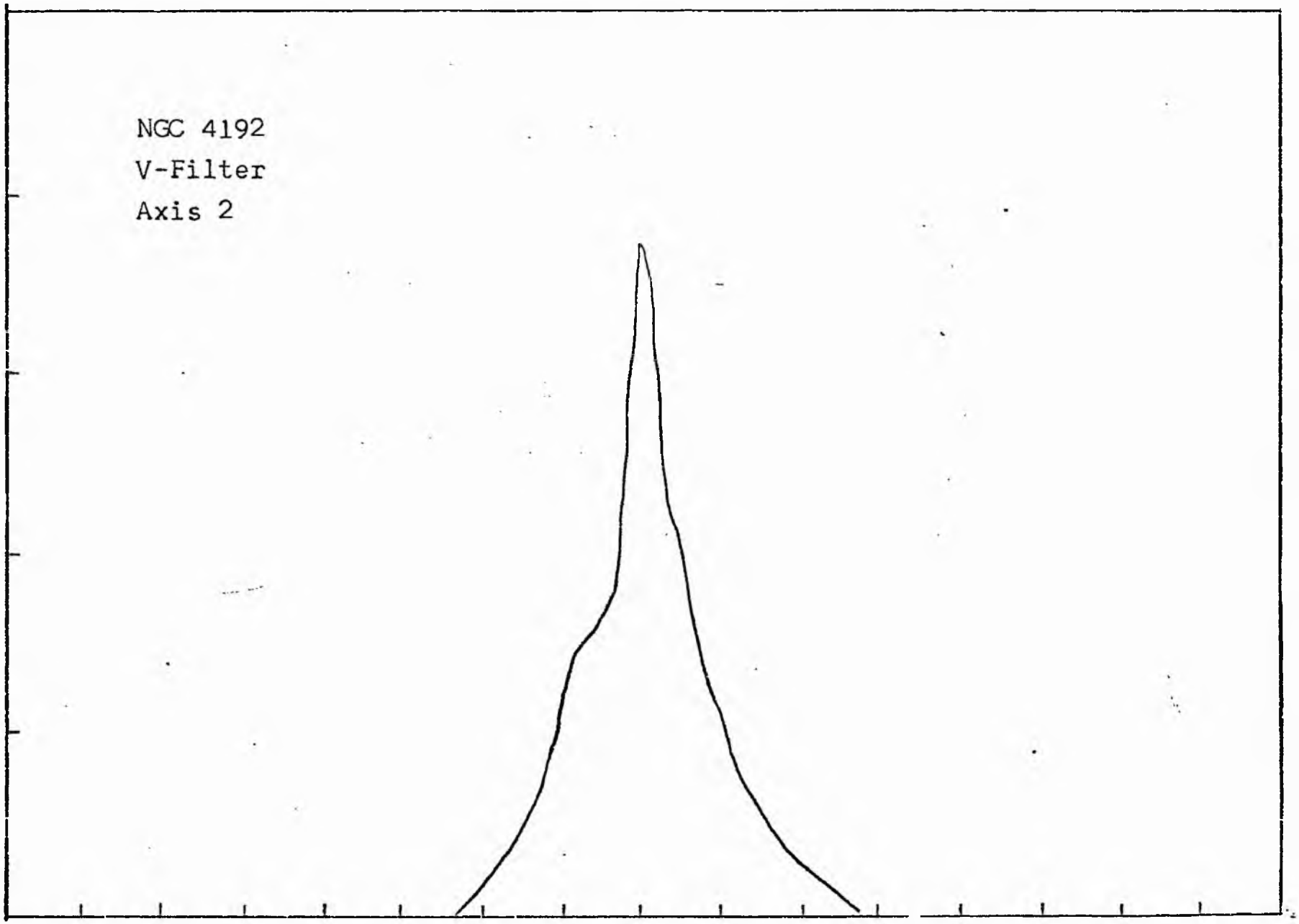
NGC 4192
V-Filter
Axis 2

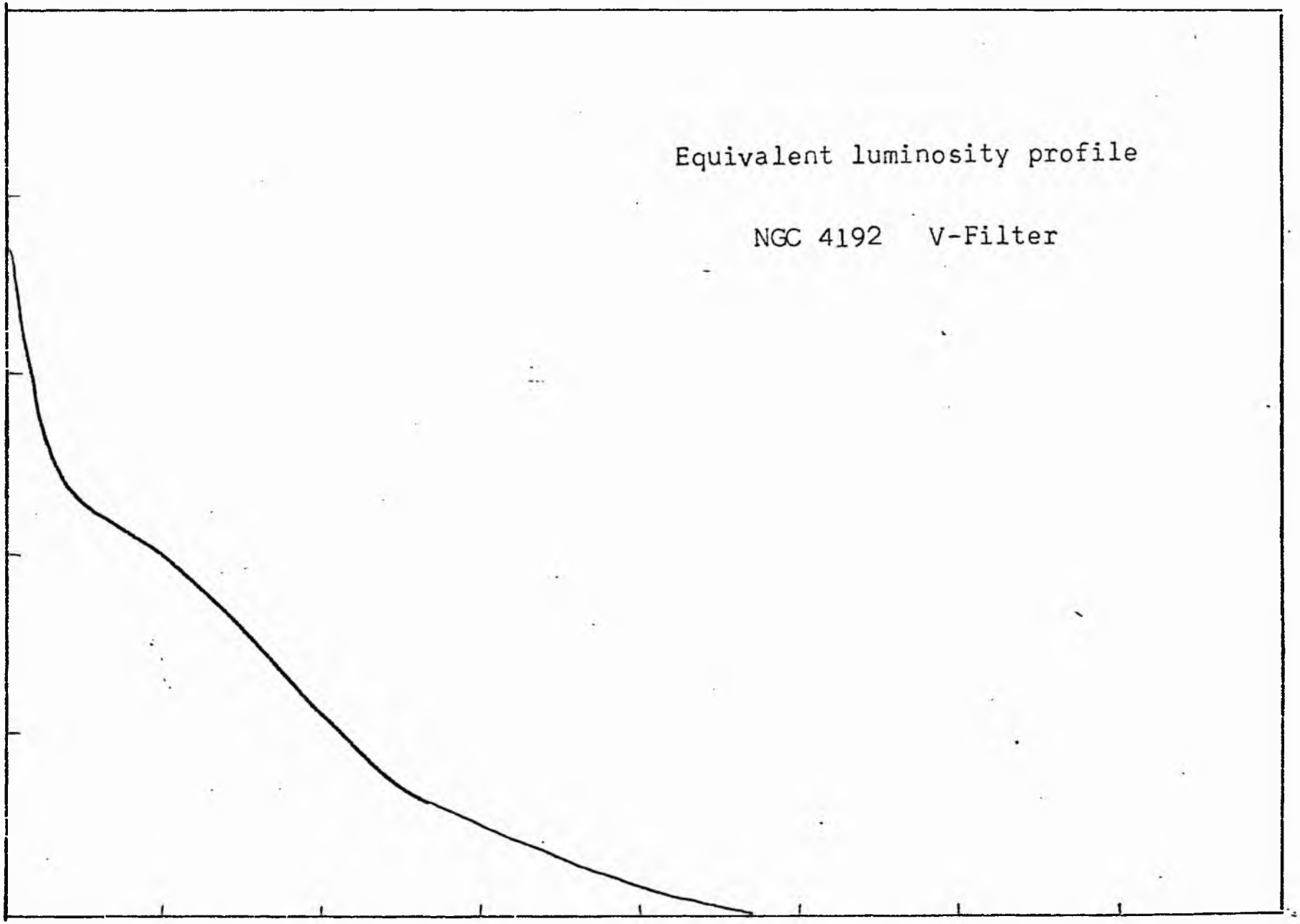
Equivalent luminosity profile
NGC 4192 V-Filter

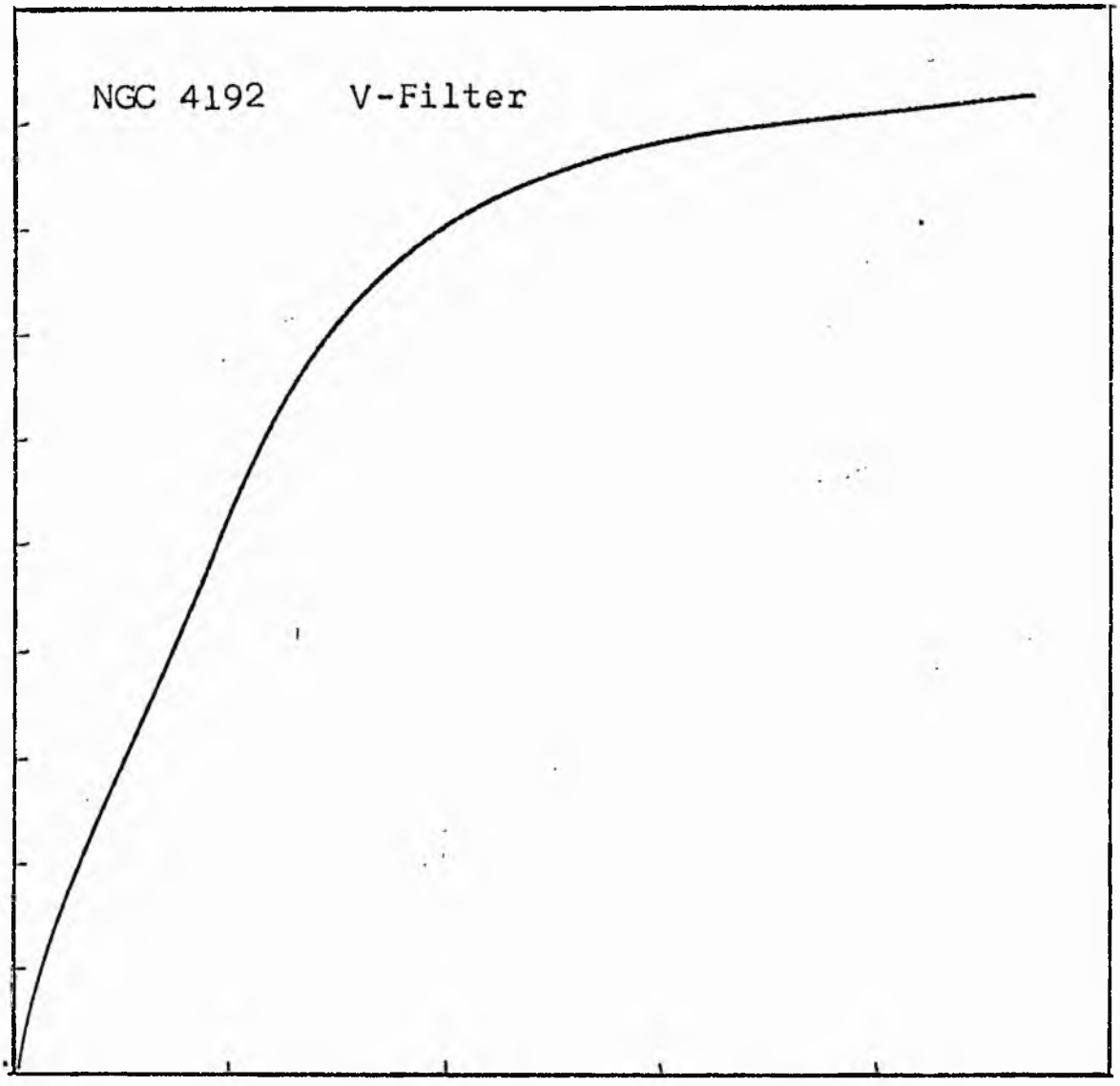

Relative integrated luminosity k(r) versus equivalent radius r*.

MEAN LUMINOSITY DISTRIBUTION IN NGC 4192
V COLOUR

LOG I	I	$\bar{I}$	R	AREA	Δ A	P	Σ P	K(R)	ρ	LOG J	μ
1.68	47.863		0.0	0.0			0.0	0.0	0.0	1.683	17.18
		43.837			8.04	352.5559					
1.60	39.811		1.60	8.04			352.56	0.01	0.03	1.603	17.38
		35.717			16.59	592.4534					
1.50	31.623		2.80	24.63			945.01	0.03	0.06	1.503	17.63
		28.371			16.08	456.3423					
1.40	25.119		3.60	40.72			1401.35	0.05	0.08	1.403	17.88
		22.536			22.34	503.4004					
1.30	19.953		4.48	63.05			1904.75	0.06	0.10	1.303	18.13
		17.901			21.90	391.9475					
1.20	15.849		5.20	84.95			2296.70	0.07	0.11	1.203	18.38
		14.219			47.78	679.4363					
1.10	12.589		6.50	132.73			2976.14	0.10	0.14	1.103	18.63
		11.295			85.26	962.9661					
1.00	10.000		8.33	217.99			3939.10	0.13	0.18	1.003	18.88
		8.972			34.78	312.0645					
0.90	7.943		8.97	252.78			4251.16	0.14	0.19	0.903	19.13
		7.126			16.03	114.2158					
0.80	6.310		9.25	268.80			4365.38	0.14	0.20	0.803	19.38
		5.661			94.25	533.5073					
0.70	5.012		10.75	363.05			4898.88	0.16	0.23	0.703	19.63
		4.496			116.89	525.5867					
0.60	3.981		12.36	479.94			5424.47	0.18	0.26	0.603	19.88
		3.572			156.21	557.9294					
0.50	3.162		14.23	636.15			5982.39	0.19	0.30	0.503	20.13
		2.837			240.01	680.9194					
0.40	2.512		16.70	876.16			6663.31	0.22	0.36	0.403	20.38
		2.254			469.98	1059.1333					
0.30	1.995		20.70	1346.14			7722.45	0.25	0.44	0.303	20.63
		1.790			1198.46	2145.3232					
0.20	1.585		28.46	2544.60			9867.77	0.32	0.61	0.203	20.88
		1.422			1960.87	2788.1697					
0.10	1.259		37.87	4505.47			12655.93	0.41	0.81	0.103	21.13
		1.129			2369.49	2676.2339					
-0.00	1.000		46.78	6874.96			15332.16	0.50	0.99	0.003	21.38
		0.897			2669.87	2395.2969					
-0.10	0.794		55.12	9544.83			17727.46	0.58	1.17	-0.097	21.63
		0.713			2632.95	1876.3430					
-0.20	0.631		62.26	12177.78			19603.80	0.64	1.32	-0.197	21.88
		0.566			1710.95	968.5139					
-0.30	0.501		66.49	13888.72			20572.31	0.67	1.41	-0.297	22.13
		0.450			2419.91	1088.1008					
-0.40	0.398		72.05	16308.63			21660.41	0.70	1.53	-0.397	22.38
		0.357			2594.65	926.7200					
-0.50	0.316		77.57	18903.28			22587.13	0.73	1.65	-0.497	22.63
		0.284			2765.21	784.5110					
-0.60	0.251		83.05	21668.50			23371.64	0.76	1.77	-0.597	22.88
		0.225			2937.24	661.9268					
-0.70	0.200		88.50	24605.74			24033.56	0.78	1.88	-0.697	23.13
		0.179			3094.34	553.9077					
-0.80	0.158		93.90	27700.07			24587.47	0.80	2.00	-0.797	23.38
		0.142			3252.61	462.4893					
-0.90	0.126		99.26	30952.68			25049.96	0.81	2.11	-0.897	23.63
		0.113			3406.84	384.7881					
-1.00	0.100		104.58	34359.52			25434.74	0.83	2.22	-0.997	23.88
		0.090			3563.95	319.7444					
-1.10	0.079		109.87	37923.47			25754.48	0.84	2.34	-1.097	24.13
		0.071			3703.61	263.9343					
-1.20	0.063		115.11	41627.07			26018.42	0.84	2.45	-1.197	24.38
		0.057			3845.89	217.7052					
-1.30	0.050		120.31	45472.96			26236.12	0.85	2.56	-1.297	24.63
		0.045			13353.94	600.4575					
-1.40	0.040		136.84	58826.90			26836.58	0.87	2.91	-1.397	24.88
		0.036			7416.54	264.8955					
-1.50	0.032		145.21	66243.44			27101.47	0.88	3.09	-1.497	25.13
		0.028			10504.62	298.0264					
-1.60	0.025		156.30	76748.06			27399.50	0.89	3.32	-1.597	25.38
		0.023			12237.19	275.7759					
-1.70	0.020		168.30	88985.25			27675.27	0.90	3.58	-1.697	25.63
		0.018			13936.44	249.4750					
-1.80	0.016		181.00	102921.69			27924.74	0.91	3.85	-1.797	25.88
		0.014			35226.94	500.8994					
-1.90	0.013		209.70	138148.62			28425.64	0.92	4.46	-1.897	26.13
		0.011			34019.44	384.2407					
-2.00	0.010		234.10	172168.06			28809.88	0.94	4.98	-1.997	26.38
- ∞							30809.00	(1)			∞

PHOTOMETRIC PARAMETERS OF NGC 4192

V-FILTER

Total luminosity ..... L_T = 8.55

Total apparent magnitude ..... m_T = 10.16

Apparent central surface brightness ..... μ_o = 17.18

Major axis at threshold ..... $2a_m$ = 13.00

Minor axis at threshold ..... $2b_m$ = 4.45'

Major axis at μ=25.0 mag sec^{-2} ..... 2a(25) = 10.7

Luminosity within μ=25.0 mag sec^{-2} ..... k(25) = 0.88

Gradient of exponential component ..... G(a) = -0.44

Equivalent gradient of exponential comp..... G(r*) = -1.03

Equivalent gradient of reduced exp. comp..... G(ρ) = -0.87

Parameters at k = ¼ :

- Semi-major axis ..... a_1 = 0.75
- Axis ratio ..... b/a = 0.51
- Equivalent radius ..... r_1* = 0.34
- Surface brightness ..... μ_1 = 20 63

Parameters at k = ½(effective) :

- Semi-major axis ..... a_e = 1.70
- Axis ratio ..... b/a = 0.21
- Equivalent radius ..... r_e* = 0.78
- Surface brightness ..... μ_e = 21.38
- Mean surface brightness ..... μ_e' = 11.61

Parameters at k = ¾ :

- Semi-major axis ..... a_3 = 3.07
- Axis ratio ..... b/a = 0.20
- Equivalent radius ..... r_3* = 1.35
- Surface brightness ..... μ_3 = 22.78

Concentration indices ..... C_{21} = 2.28, C_{32} = 1.72

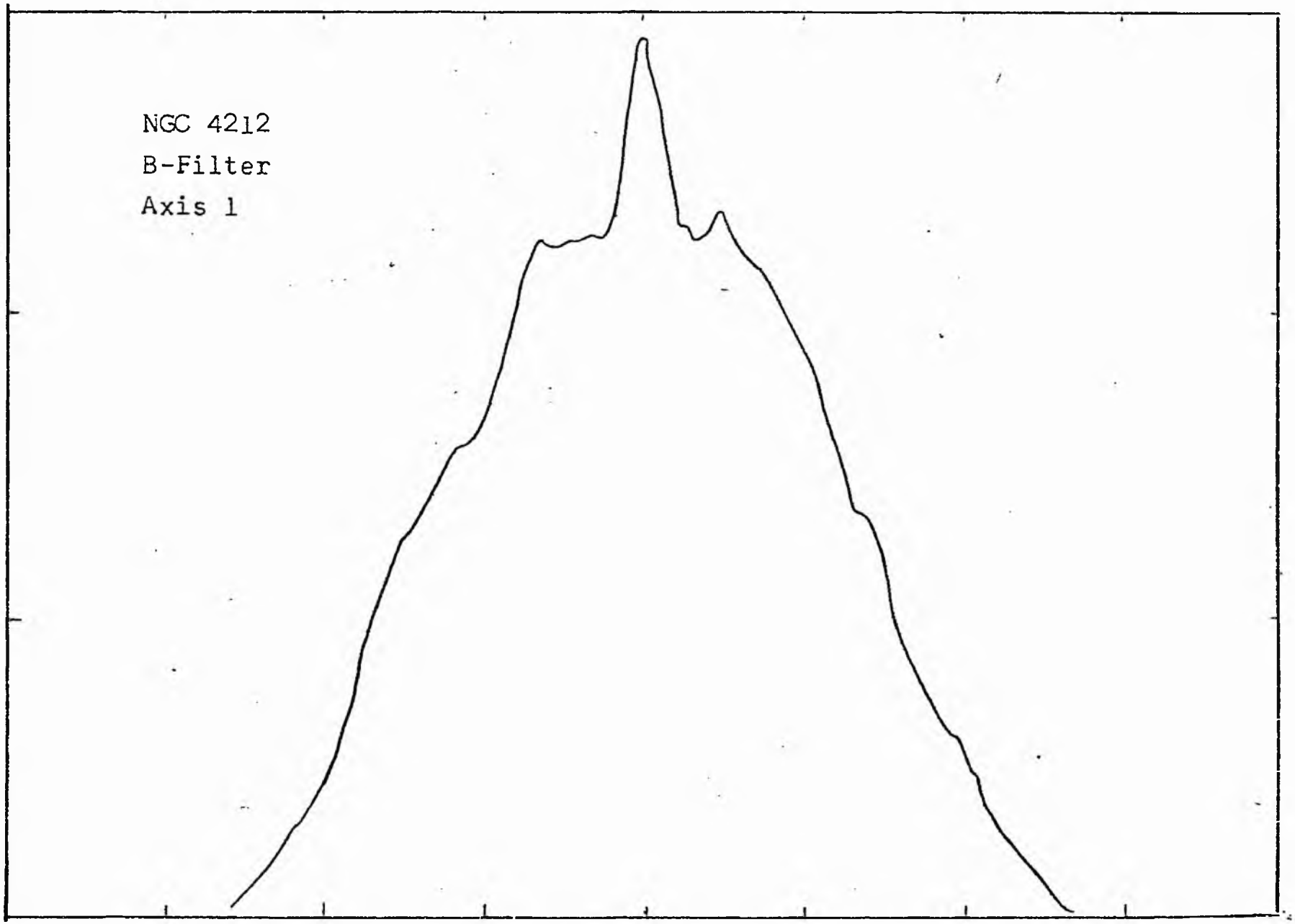
NGC 4212
B-Filter
Axis 1

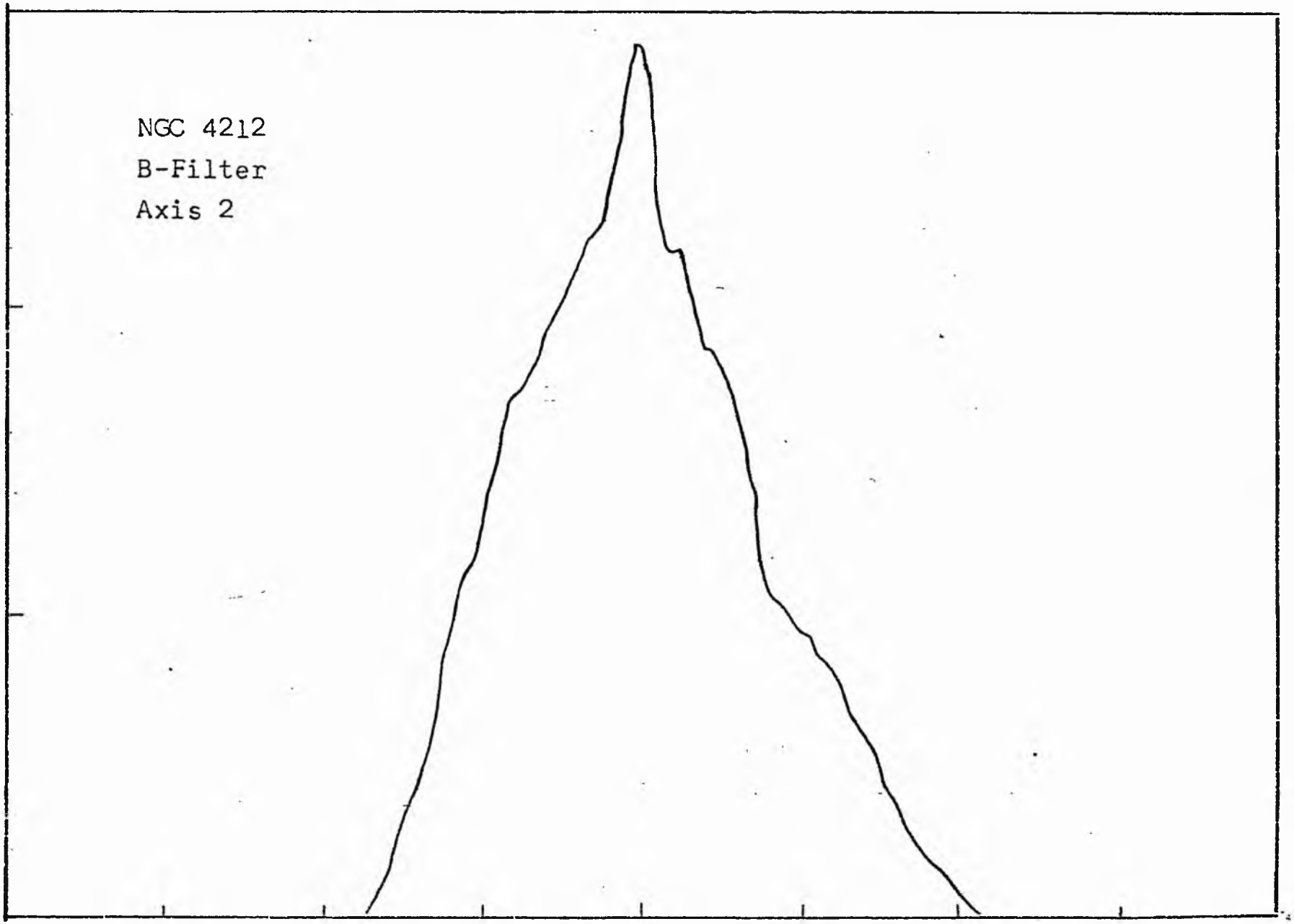
NGC 4212
B-Filter
Axis 2

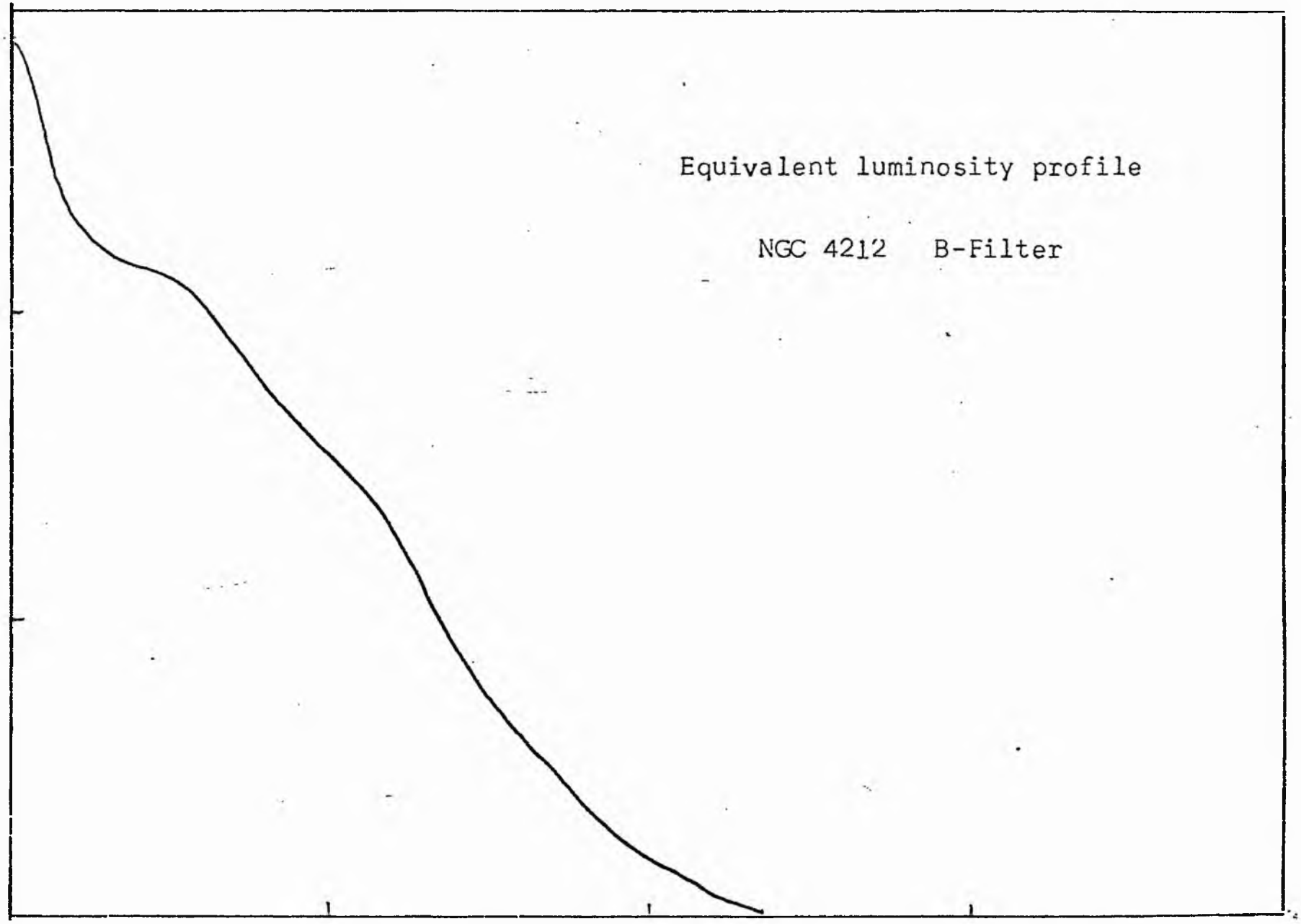
Equivalent luminosity profile
NGC 4212 B-Filter

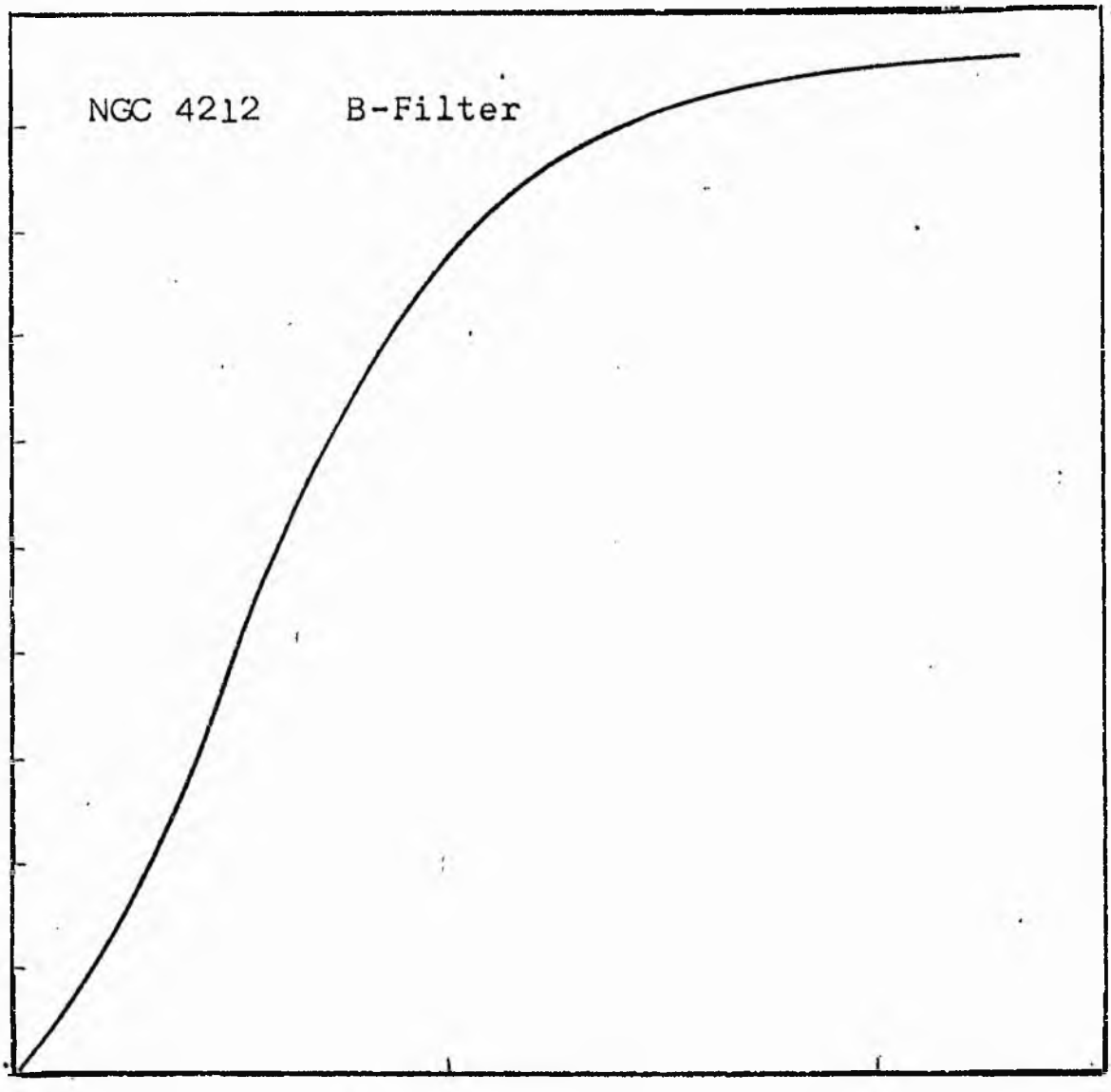

Relative integrated luminosity k(r) versus equivalent radius r*.

MEAN LUMINOSITY DISTRIBUTION IN NGC 4212
B COLOUR

LOG I	I	$\bar{I}$	R	AREA	ΔA	P	ΣP	K(R)	ρ	LOG J	μ
0.89	7.762		0.0	0.0			0.0	0.0	0.0	0.942	19.52
		7.036			10.29	72.4159					
0.80	6.310		1.81	10.29			72.42	0.01	0.06	0.852	19.75
		5.661			28.19	159.5889					
0.70	5.012		3.50	38.48			232.00	0.03	0.11	0.752	20.00
		4.496			43.23	194.3745					
0.60	3.981		5.10	81.71			426.38	0.05	0.17	0.652	20.25
		3.572			76.65	273.7861					
0.50	3.162		7.10	158.37			700.17	0.08	0.23	0.552	20.50
		2.837			42.69	121.1272					
0.40	2.512		8.00	201.06			821.29	0.09	0.26	0.452	20.75
		2.254			106.85	240.7838					
0.30	1.995		9.90	307.91			1062.08	0.11	0.32	0.352	21.00
		1.790			417.93	748.1206					
0.20	1.585		15.20	725.83			1810.20	0.20	0.50	0.252	21.25
		1.422			1301.00	1849.8987					
0.10	1.259		25.40	2026.83			3660.10	0.40	0.83	0.152	21.50
		1.129			560.87	633.4807					
0.00	1.000		28.70	2587.70			4293.57	0.46	0.94	0.052	21.75
		0.897			689.89	618.9463					
-0.10	0.794		32.30	3277.59			4912.52	0.53	1.06	-0.048	22.00
		0.713			726.34	517.6201					
-0.20	0.631		35.70	4003.93			5430.14	0.59	1.17	-0.148	22.25
		0.566			964.98	546.2476					
-0.30	0.501		39.77	4968.91			5976.38	0.65	1.30	-0.248	22.50
		0.450			1353.29	608.5029					
-0.40	0.398		44.86	6322.20			6584.88	0.71	1.47	-0.348	22.75
		0.357			1285.56	459.1602					
-0.50	0.316		49.21	7607.75			7044.04	0.76	1.61	-0.448	23.00
		0.284			1267.00	359.4587					
-0.60	0.251		53.15	8874.75			7403.50	0.80	1.74	-0.548	23.25
		0.225			1225.12	276.0896					
-0.70	0.200		56.70	10099.87			7679.59	0.83	1.85	-0.648	23.50
		0.179			1149.62	205.7914					
-0.80	0.158		59.84	11249.49			7885.37	0.85	1.96	-0.748	23.75
		0.142			1057.72	150.3982					
-0.90	0.126		62.59	12307.21			8035.77	0.87	2.05	-0.848	24.00
		0.113			937.44	105.8802					
-1.00	0.100		64.93	13244.65			8141.65	0.88	2.12	-0.948	24.25
		0.090			1039.55	93.2646					
-1.10	0.079		67.43	14284.20			8234.91	0.89	2.20	-1.048	24.50
		0.071			1197.70	85.3532					
-1.20	0.063		70.20	15481.89			8320.26	0.90	2.29	-1.148	24.75
		0.057			1954.73	110.6527					
-1.30	0.050		74.50	17436.62			8430.91	0.91	2.43	-1.248	25.00
		0.045			2319.23	104.2843					
-1.40	0.040		79.30	19755.86			8535.20	0.92	2.59	-1.348	25.25
		0.036			2200.60	78.5990					
-1.50	0.032		83.60	21956.46			8613.79	0.93	2.73	-1.448	25.50
		0.028			2593.70	73.5862					
-1.60	0.025		88.40	24550.16			8687.38	0.94	2.89	-1.548	25.75
		0.023			2679.93	60.3948					
-1.70	0.020		93.10	27230.09			8747.77	0.94	3.04	-1.648	26.00
		0.018			4500.79	80.5685					
-1.80	0.016		100.50	31730.87			8828.34	0.95	3.28	-1.748	26.25
		0.014			4506.64	64.0812					
-1.90	0.013		107.40	36237.51			8892.42	0.96	3.51	-1.848	26.50
		0.011			6254.68	70.6453					
-2.00	0.010		116.30	42492.19			8963.06	0.97	3.80	-1.948	26.75
- ∞							9263.00	(1)			∞

PHOTOMETRIC PARAMETERS OF NGC 4212

B-FILTER

Total luminosity	L_T	= 2.57
Total apparent magnitude	m_T	= 11.83
Apparent central surface brightness	μ_o	= 19.52
Major axis at threshold	$2a_m$	= 4.41
Minor axis at threshold	$2b_m$	= 3.03
Major axis at μ=25.0 mag sec^{-2}	2a(25)	= 3.08
Luminosity within μ=25.0 mag sec^{-2}	k(25)	= 0.91
Gradient of exponential component	G(a)	= -1.66
Equivalent gradient of exponential comp.	G(r*)	= -1.53
Equivalent gradient of reduced exp. comp.	G(ρ)	= -0.83
Parameters at k = ¼ :		
Semi-major axis	a_1	= 0.53
Axis ratio	b/a	= 0.62
Equivalent radius	r_1*	= 0.30
Surface brightness	μ_1	= 21.31
Parameters at k = ½(effective) :		
Semi-major axis	a_e	= 0.74
Axis ratio	b/a	= 0.53
Equivalent radius	r_e*	= 0.51
Surface brightness	μ_e	= 21.89
Mean surface brightness	μ_e'	= 12.36
Parameters at k = ¾ :		
Semi-major axis	a_3	= 1.05
Axis ratio	b/a	= 0.60
Equivalent radius	r_3*	= 0.80
Surface brightness	μ_3	= 22.93
Concentration indices	C_{21}	= 1.66
	C_{32}	= 1.58

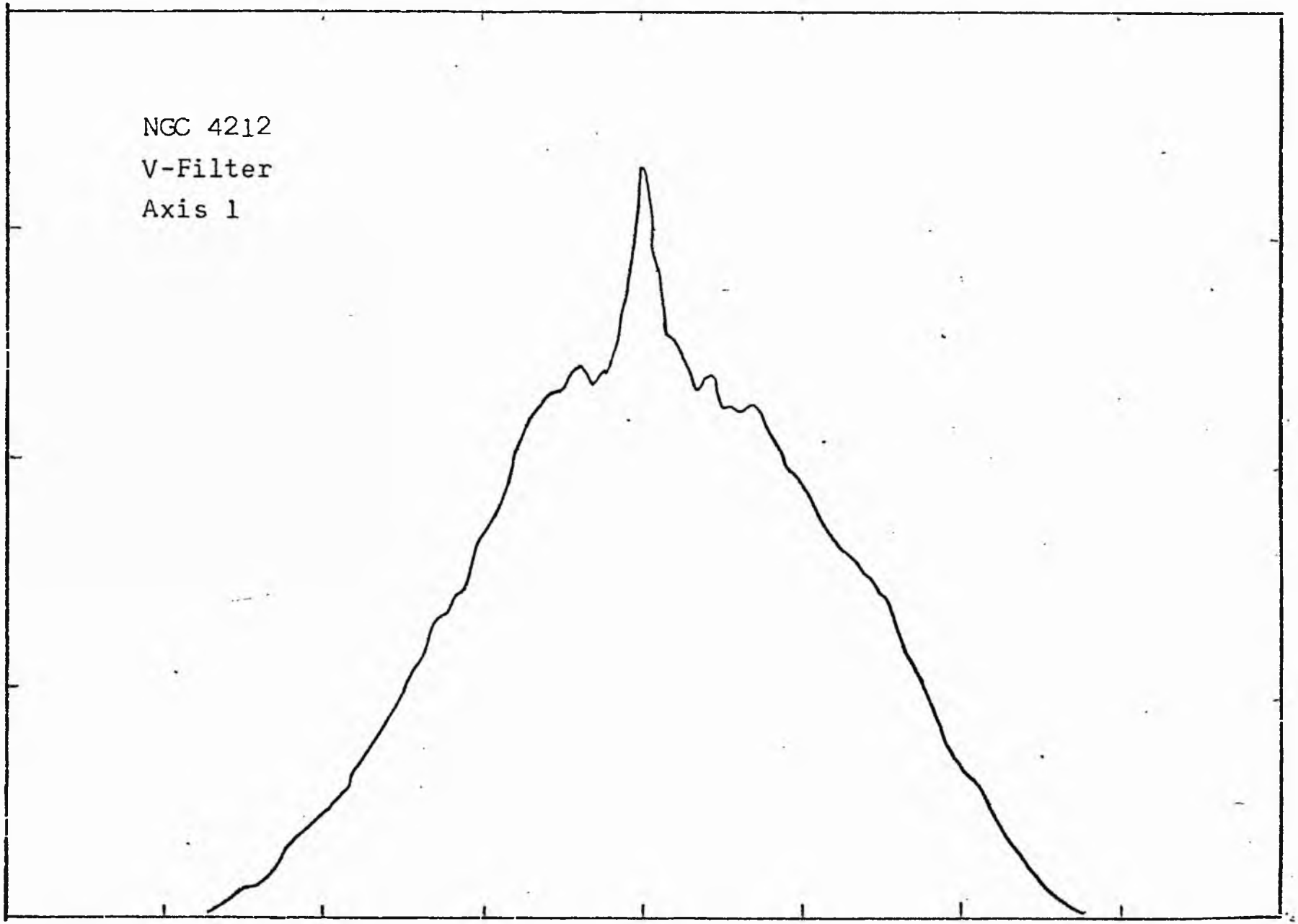
NGC 4212
V-Filter
Axis 1

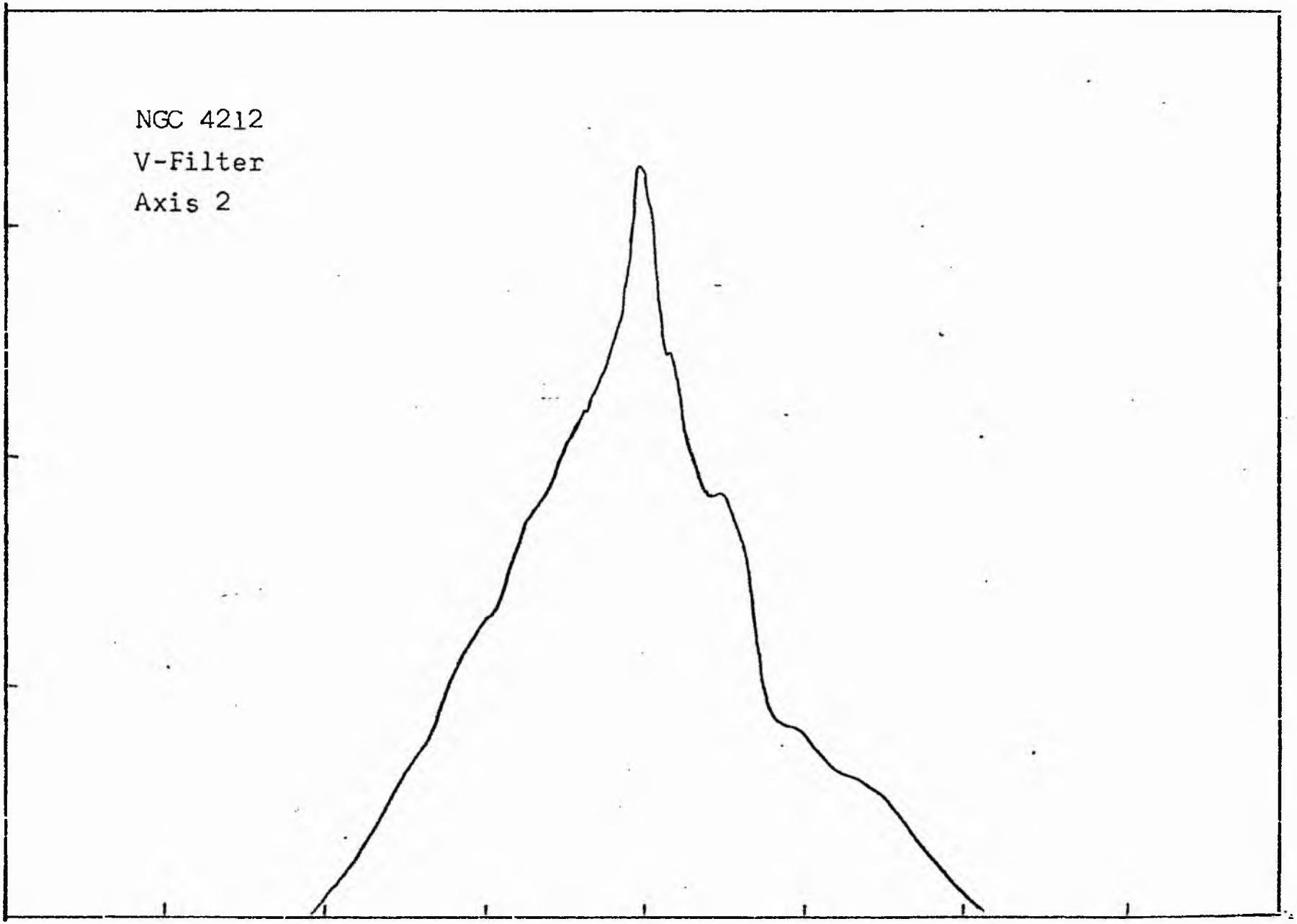
NGC 4212
V-Filter
Axis 2

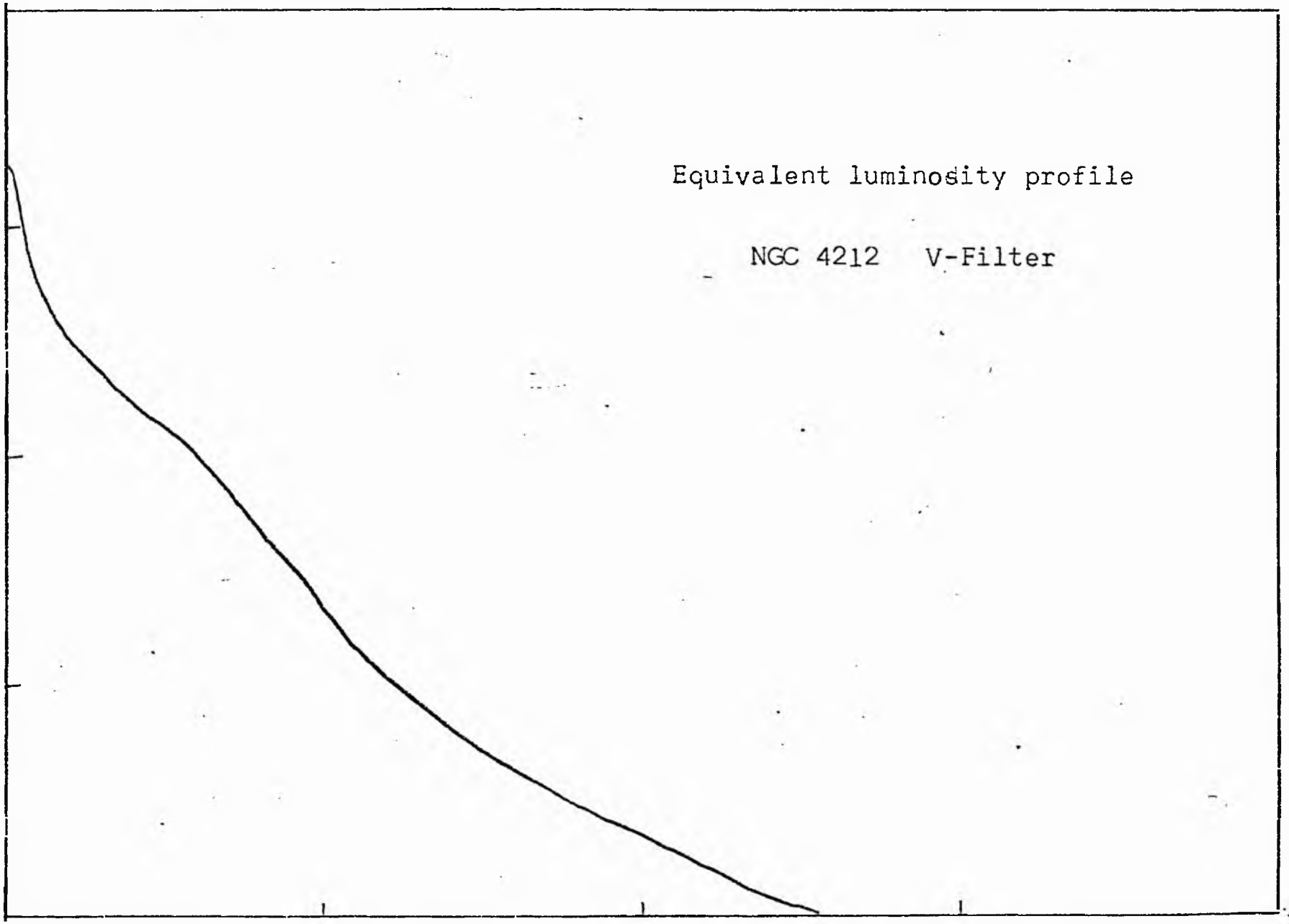
Equivalent luminosity profile
NGC 4212 V-Filter

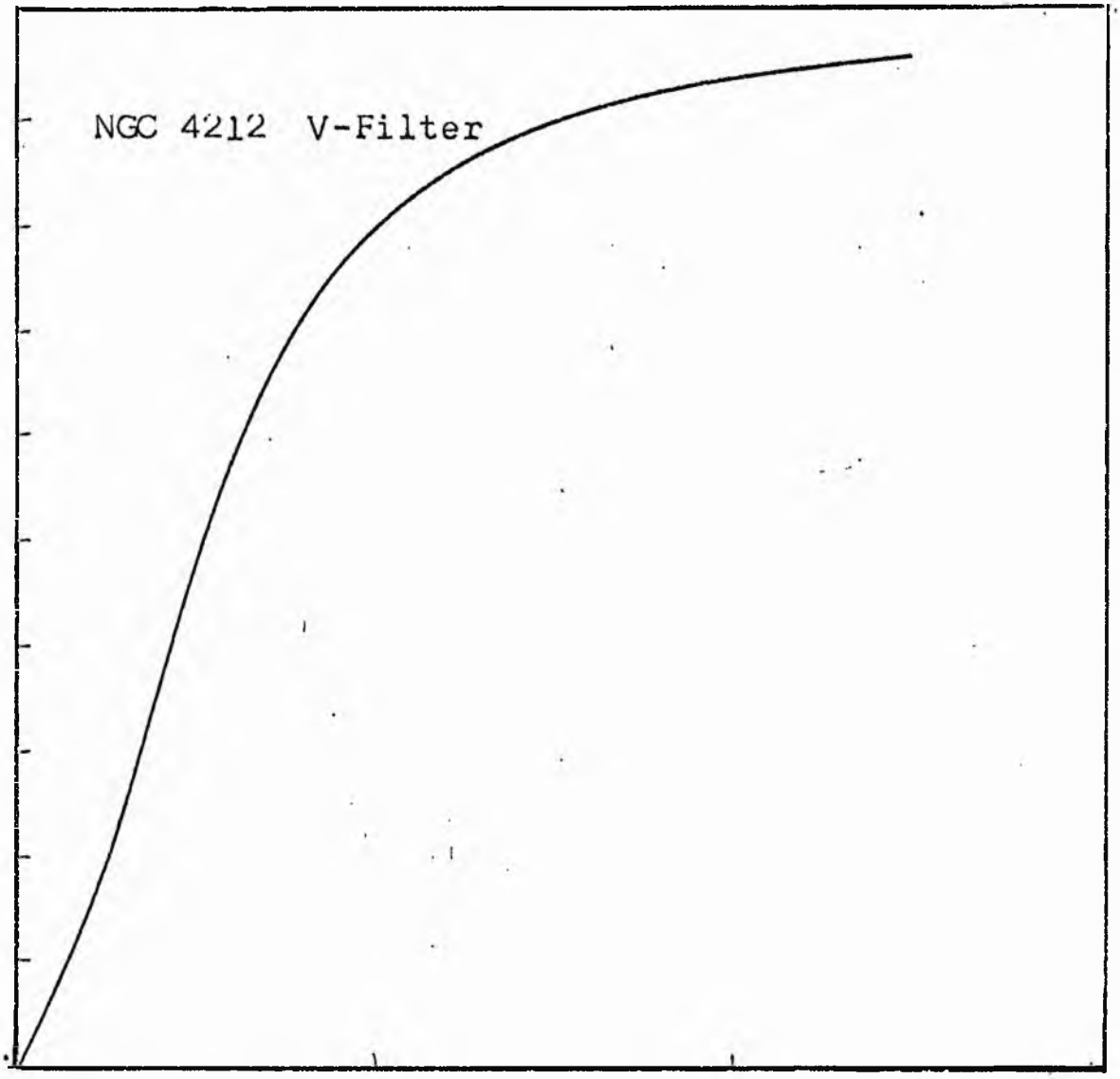

Relative integrated luminosity k(r) versus equivalent radius r*.

MEAN LUMINOSITY DISTRIBUTION IN NGC 4212
V COLOUR

LOG I	I	T	R	AREA	ΔA	P	ΣP	K(R)	ρ	LOG J	μ
1.27	18.621		0.0	0.0			0.0	0.0	0.0	1.117	18.03
		17.235			10.87	187.3199					
1.20	15.849		1.86	10.87			187.32	0.02	0.07	1.047	18.21
		14.219			2.46	35.0216					
1.10	12.589		2.06	13.33			222.34	0.02	0.08	0.947	18.46
		11.295			19.04	215.0446					
1.00	10.000		3.21	32.37			437.39	0.04	0.12	0.847	18.71
		8.972			25.18	225.8845					
0.90	7.943		4.28	57.55			663.27	0.06	0.16	0.747	18.96
		7.126			16.35	116.5110					
0.80	6.310		4.85	73.90			779.78	0.07	0.18	0.647	19.21
		5.661			54.78	310.1025					
0.70	5.012		6.40	128.68			1089.88	0.10	0.24	0.547	19.46
		4.496			35.09	157.7655					
0.60	3.981		7.22	163.77			1247.65	0.12	0.27	0.447	19.71
		3.572			137.34	490.5217					
0.50	3.162		9.79	301.10			1738.17	0.16	0.37	0.347	19.96
		2.837			189.77	538.3943					
0.40	2.512		12.50	490.87			2276.57	0.21	0.47	0.247	20.21
		2.254			385.28	868.2668					
0.30	1.995		16.70	876.16			3144.83	0.29	0.63	0.147	20.46
		1.790			791.53	1416.8955					
0.20	1.585		23.04	1667.69			4561.73	0.43	0.87	0.047	20.71
		1.422			755.02	1073.5723					
0.10	1.259		27.77	2422.71			5635.30	0.53	1.05	-0.053	20.96
		1.129			290.91	328.5728					
-0.00	1.000		29.39	2713.62			5963.87	0.56	1.11	-0.153	21.21
		0.897			621.04	557.1748					
-0.10	0.794		32.58	3334.66			6521.04	0.61	1.24	-0.253	21.46
		0.713			864.50	616.0762					
-0.20	0.631		36.56	4199.16			7137.11	0.67	1.39	-0.353	21.71
		0.566			802.29	454.1511					
-0.30	0.501		39.90	5001.44			7591.26	0.71	1.51	-0.453	21.96
		0.450			804.66	361.8113					
-0.40	0.398		42.99	5806.10			7953.07	0.75	1.63	-0.553	22.21
		0.357			726.40	259.4473					
-0.50	0.316		45.60	6532.50			8212.52	0.77	1.73	-0.653	22.46
		0.284			805.59	228.5536					
-0.60	0.251		48.33	7338.09			8441.07	0.79	1.83	-0.753	22.71
		0.225			801.17	180.5501					
-0.70	0.200		50.90	8139.27			8621.61	0.81	1.93	-0.853	22.96
		0.179			886.40	158.6723					
-0.80	0.158		53.60	9025.66			8780.29	0.82	2.03	-0.953	23.21
		0.142			721.09	102.5330					
-0.90	0.126		55.70	9746.76			8882.82	0.83	2.11	-1.053	23.46
		0.113			1487.70	168.0297					
-1.00	0.100		59.80	11234.45			9050.84	0.85	2.27	-1.153	23.71
		0.090			1714.05	153.7786					
-1.10	0.079		64.20	12948.50			9204.62	0.86	2.43	-1.253	23.96
		0.071			3473.50	247.5368					
-1.20	0.063		72.30	16422.00			9452.16	0.89	2.74	-1.353	24.21
		0.057			1915.34	108.4224					
-1.30	0.050		76.40	18337.34			9560.58	0.90	2.90	-1.453	24.46
		0.045			3357.26	150.9590					
-1.40	0.040		83.10	21694.60			9711.54	0.91	3.15	-1.553	24.71
		0.036			3752.30	134.0207					
-1.50	0.032		90.00	25446.90			9845.55	0.92	3.41	-1.653	24.96
		0.028			3265.23	92.6380					
-1.60	0.025		95.60	28712.13			9938.19	0.93	3.63	-1.753	25.21
		0.023			5071.57	114.2927					
-1.70	0.020		103.70	33783.71			10052.48	0.94	3.93	-1.853	25.46
		0.018			3131.76	56.0615					
-1.80	0.016		108.40	36915.47			10108.54	0.95	4.11	-1.953	25.71
		0.014			2986.81	42.4702					
-1.90	0.013		112.70	39902.28			10151.01	0.95	4.27	-2.053	25.96
		0.011			9185.11	103.7437					
-2.00	0.010		125.00	49087.39			10254.75	0.96	4.74	-2.153	26.21
- ∞							10674.00	(1)			∞

V-C35

PHOTOMETRIC PARAMETERS OF NGC 4212

V-FILTER

Total luminosity ..... L_T = 2.96

Total apparent magnitude ..... m_T = 11.14

Apparent central surface brightness ..... μ_o = 18.03

Major axis at threshold ..... $2a_m$ = 4.61

Minor axis at threshold ..... $2b_m$ = 3.65

Major axis at μ=25.0 mag sec^{-2} ..... 2a(25) = 3.56

Luminosity within μ=25.0 mag sec^{-2} ..... k(25) = 0.92

Gradient of exponential component ..... G(a) = -1.36

Equivalent gradient of exponential comp..... G(r*) = -1.66

Equivalent gradient of reduced exp. comp..... G(ρ) = -0.87

Parameters at k = ¼ :

- Semi-major axis ..... a_1 = 0.36
- Axis ratio ..... b/a = 0.54
- Equivalent radius ..... r_1* = 0.24
- Surface brightness ..... μ_1 = 20.33

Parameters at k = ½(effective) :

- Semi-major axis ..... a_e = 0.63
- Axis ratio ..... b/a = 0.51
- Equivalent radius ..... r_e* = 0.44
- Surface brightness ..... μ_e = 20.88
- Mean surface brightness ..... μ_e' = 11.33

Parameters at k = ¾ :

- Semi-major axis ..... a_3 = 0.97
- Axis ratio ..... b/a = 0.60
- Equivalent radius ..... r_3* = 0.72
- Surface brightness ..... μ_3 = 22.21

Concentration indices ..... C_{21} = 1.83, C_{32} = 1.65

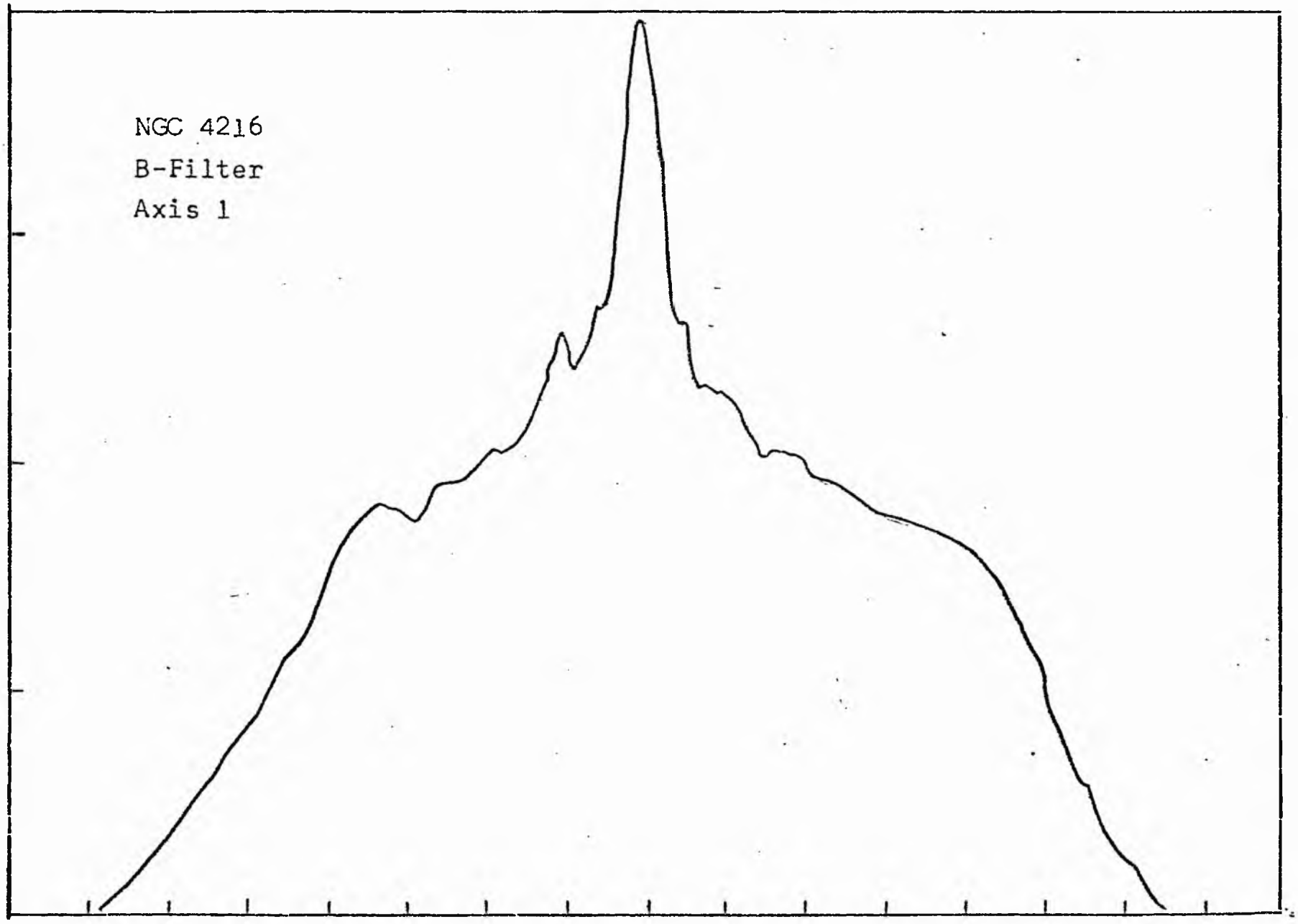
NGC 4216
B-Filter
Axis 1

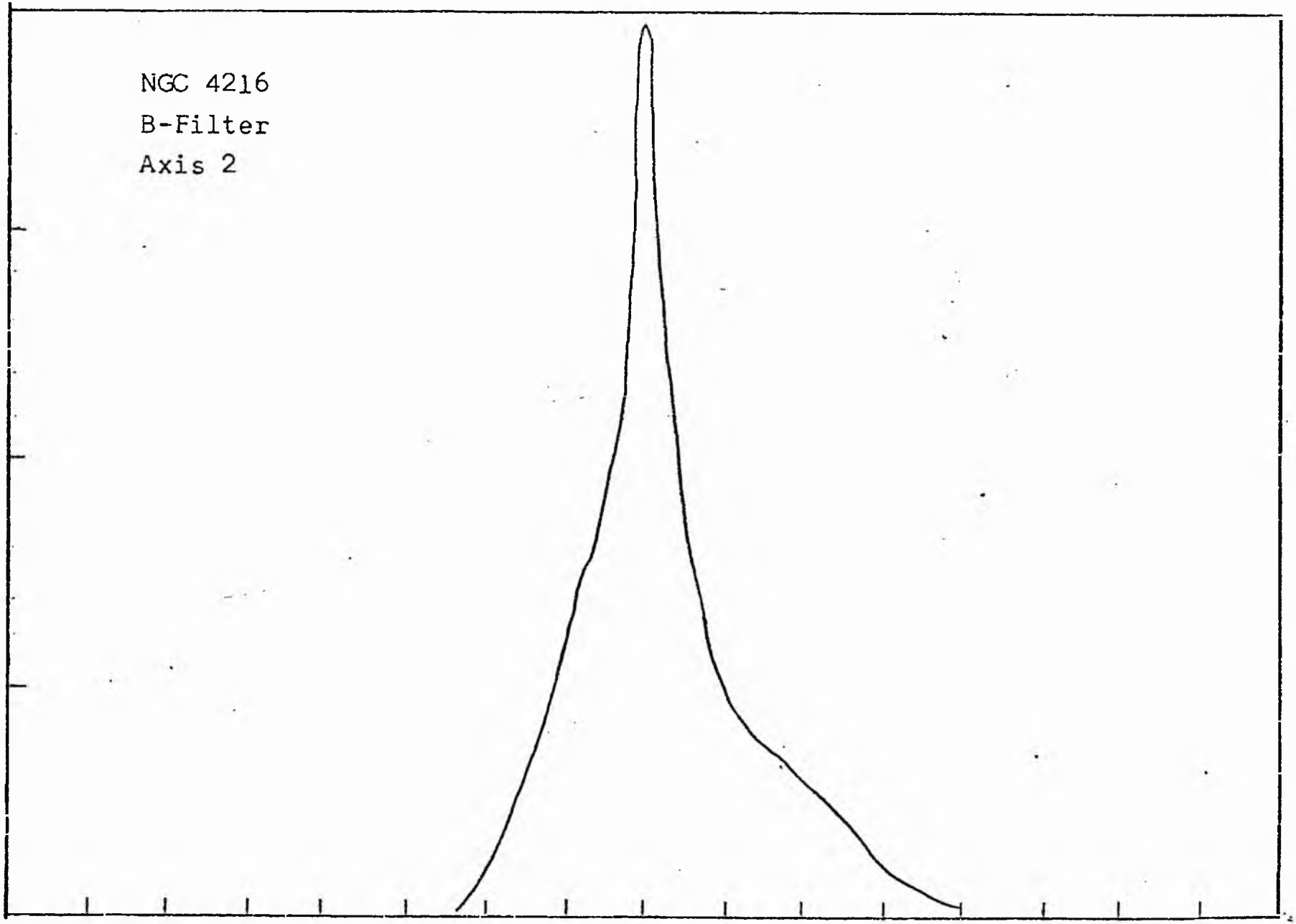
NGC 4216
B-Filter
Axis 2

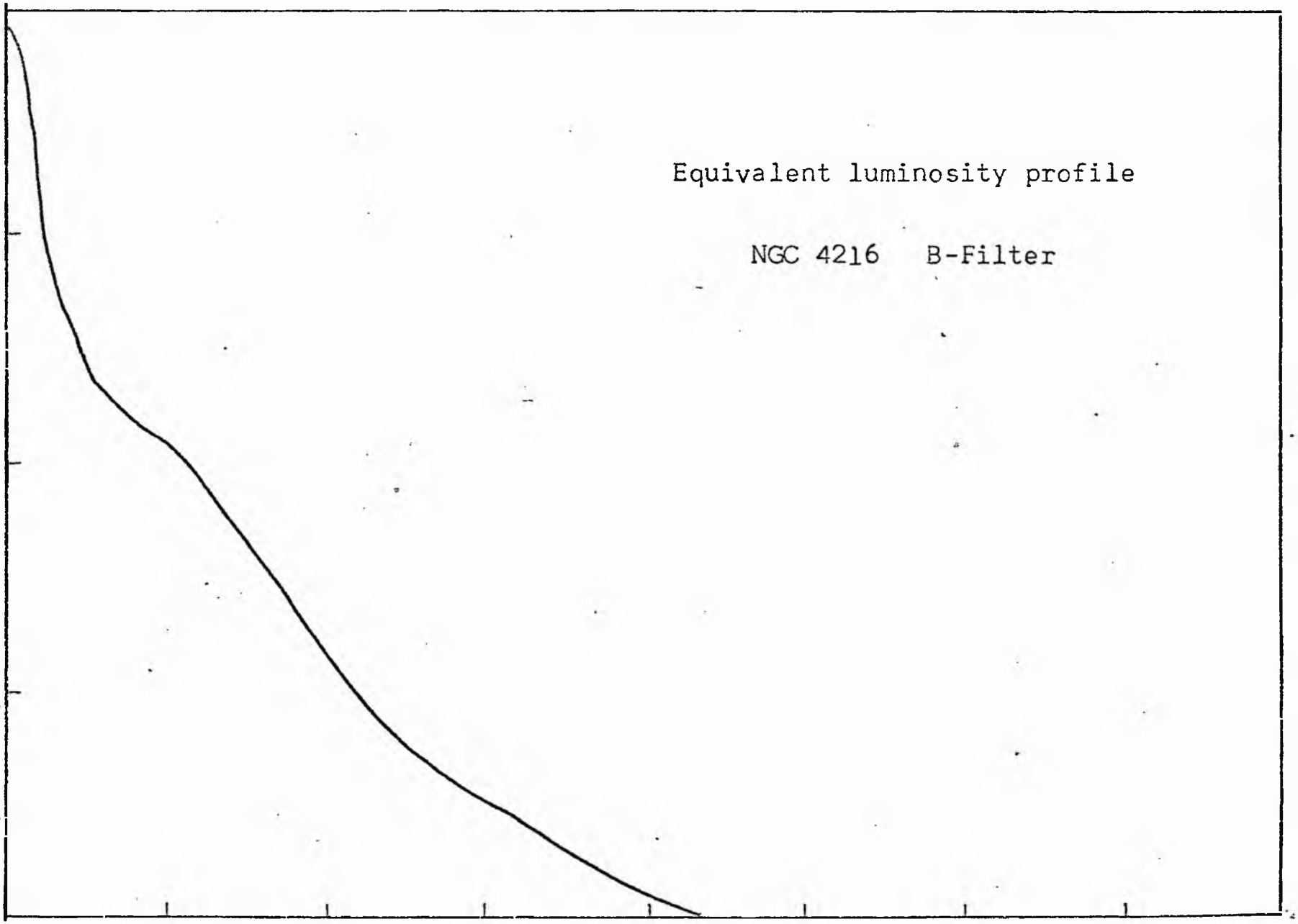
Equivalent luminosity profile
NGC 4216 B-Filter

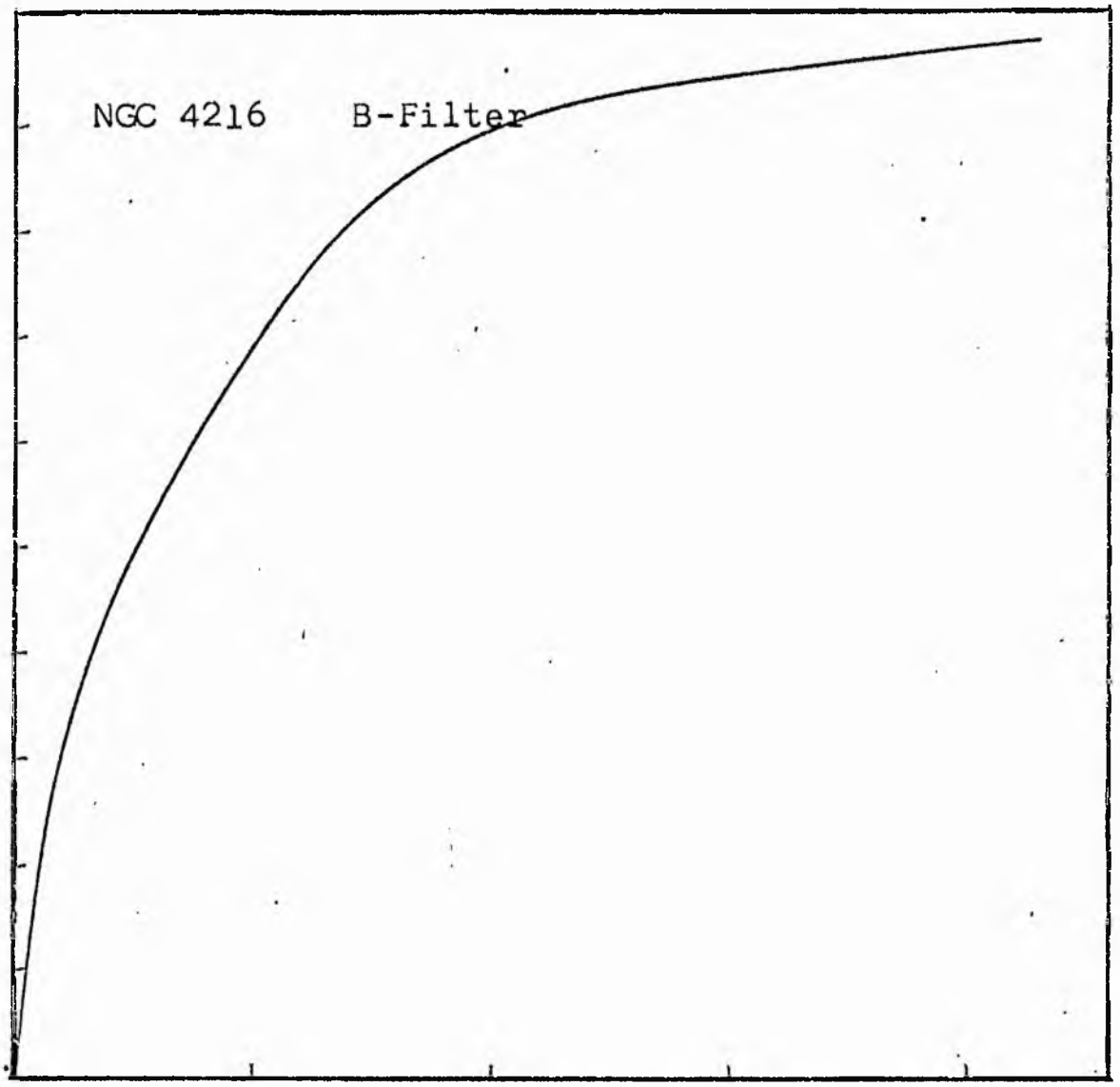

Relative integrated luminosity k(r) versus equivalent radius r*.

MEAN LUMINOSITY DISTRIBUTION IN NGC 4216
B COLOUR

LOG I	I	$\bar{I}$	R	AREA	ΔA	P.	ΣP	K(R)	ρ	LOG J	μ
1.95	89.125		0.0	0.0			0.0	0.0	0.0	1.669	17.69
		84.279			38.48	3243.4304					
1.90	79.433		3.50	38.48			3243.43	0.07	0.12	1.619	17.82
		71.264			14.33	1020.9026					
1.80	63.096		4.10	52.81			4264.33	0.09	0.15	1.519	18.07
		56.607			28.90	1636.0937					
1.70	50.119		5.10	81.71			5900.43	0.12	0.18	1.419	18.32
		44.965			55.13	2479.1204					
1.60	39.811		6.60	136.85			8379.54	0.18	0.23	1.319	18.57
		35.717			79.58	2842.2036					
1.50	31.623		8.30	216.42			11221.75	0.24	0.30	1.219	18.82
		28.371			15.93	451.8833					
1.40	25.119		8.60	232.35			11673.63	0.25	0.31	1.119	19.07
		22.536			45.24	1019.4863					
1.30	19.952		9.40	277.59			12693.11	0.27	0.33	1.019	19.32
		17.901			62.20	1113.4807					
1.20	15.849		10.40	339.79			13806.59	0.29	0.37	0.919	19.57
		14.219			68.49	973.8125					
1.10	12.589		11.40	408.28			14780.41	0.31	0.41	0.819	19.82
		11.295			90.48	1021.9036					
1.00	10.000		12.60	498.76			15802.31	0.33	0.45	0.719	20.07
		8.972			65.35	586.2488					
0.90	7.943		13.40	564.10			16388.55	0.35	0.48	0.619	20.32
		7.126			114.76	817.8394					
0.80	6.310		14.70	678.87			17206.39	0.36	0.52	0.519	20.57
		5.661			176.43	998.7236					
0.70	5.012		16.50	855.30			18205.11	0.39	0.59	0.419	20.82
		4.496			439.32	1975.3665					
0.60	3.981		20.30	1294.62			20180.48	0.43	0.72	0.319	21.07
		3.572			455.12	1625.5378					
0.50	3.162		23.60	1749.74			21806.01	0.46	0.84	0.219	21.32
		2.837			325.25	922.7539					
0.40	2.512		25.70	2074.99			22728.77	0.48	0.91	0.119	21.57
		2.254			335.52	756.1191					
0.30	1.995		27.70	2410.51			23484.88	0.50	0.99	0.019	21.82
		1.790			1843.95	3300.7947					
0.20	1.585		36.80	4254.46			26785.68	0.57	1.31	-0.081	22.07
		1.422			2252.27	3202.5049					
0.10	1.259		45.51	6506.74			29988.18	0.63	1.62	-0.181	22.32
		1.129			2378.04	2685.8826					
-0.00	1.000		53.18	8884.77			32674.06	0.69	1.89	-0.281	22.57
		0.897			2342.17	2101.2974					
-0.10	0.794		59.78	11226.95			34775.36	0.74	2.13	-0.381	22.82
		0.713			1044.90	744.6340					
-0.20	0.631		62.50	12271.84			35519.99	0.75	2.22	-0.481	23.07
		0.566			2902.83	1643.2007					
-0.30	0.501		69.50	15174.68			37163.19	0.79	2.47	-0.581	23.32
		0.450			3548.70	1595.6516					
-0.40	0.398		77.20	18723.37			38758.84	0.82	2.75	-0.681	23.57
		0.357			1990.52	710.9441					
-0.50	0.316		81.20	20713.89			39469.78	0.83	2.89	-0.781	23.82
		0.284			1770.98	502.4373					
-0.60	0.251		84.60	22484.87			39972.21	0.85	3.01	-0.881	24.07
		0.225			3131.95	705.8027					
-0.70	0.200		90.30	25616.82			40678.01	0.86	3.21	-0.981	24.32
		0.179			2497.79	447.1208					
-0.80	0.158		94.60	28114.61			41125.13	0.87	3.37	-1.081	24.57
		0.142			4378.53	622.5835					
-0.90	0.126		101.70	32493.14			41747.71	0.88	3.62	-1.181	24.82
		0.113			4626.94	522.5930					
-1.00	0.100		108.70	37120.08			42270.30	0.89	3.87	-1.281	25.07
		0.090			4138.95	371.3306					
-1.10	0.079		114.60	41259.03			42641.63	0.90	4.08	-1.381	25.32
		0.071			4281.99	305.1519					
-1.20	0.063		120.40	45541.02			42946.78	0.91	4.28	-1.481	25.57
		0.057			9613.57	544.1968					
-1.30	0.050		132.50	55154.59			43490.97	0.92	4.71	-1.581	25.82
		0.045			8818.57	396.5247					
-1.40	0.040		142.70	63973.16			43887.50	0.93	5.08	-1.681	26.07
		0.036			13266.77	473.8467					
-1.50	0.032		156.80	77239.94			44361.34	0.94	5.58	-1.781	26.32
		0.028			13979.81	396.6196					
-1.60	0.025		170.40	91219.75			44757.96	0.95	6.06	-1.881	26.57
		0.023			14680.00	330.8259					
-1.70	0.020		183.60	105899.75			45088.78	0.95	6.53	-1.981	26.82
		0.018			16517.87	295.6843					
-1.80	0.016		197.40	122417.62			45384.46	0.96	7.02	-2.081	27.07
		0.014			19311.37	274.5920					
-1.90	0.013		212.40	141729.00			45659.05	0.97	7.56	-2.181	27.32
		0.011			5932.87	67.0102					
-2.00	0.010		216.80	147661.87			45726.06	0.97	7.71	-2.281	27.57
$-\infty$							47276.00	(1)			∞

PHOTOMETRIC PARAMETERS OF NGC 4216

B-FILTER

Total luminosity	L_T	= 13.13
Total apparent magnitude	m_T	= 10.88
Apparent central surface brightness	μ_o	= 17.69
Major axis at threshold	$2a_m$	= 11.03
Minor axis at threshold	$2b_m$	= 5.02
Major axis at μ=25.0 mag sec^{-2}	2a(25)	= 7.95
Luminosity within μ=25.0 mag sec^{-2}	k(25)	= 0.89
Gradient of exponential component	G(a)	= -0.68
Equivalent gradient of exponential comp.	G(r*)	= -1.03
Equivalent gradient of reduced exp. comp.	G(ρ)	= -0.51
Parameters at k = ¼ :		
Semi-major axis	a_1	= 0.28
Axis ratio	b/a	= 0.70
Equivalent radius	r_1*	= 0.14
Surface brightness	μ_1	= 19.07
Parameters at k = ½(effective) :		
Semi-major axis	a_e	= 0.92
Axis ratio	b/a	= 0.33
Equivalent radius	r_e*	= 0.47
Surface brightness	μ_e	= 21.82
Mean surface brightness	μ_e'	= 11.22
Parameters at k = ¾ :		
Semi-major axis	a_3	= 2.2
Axis ratio	b/a	= 0.24
Equivalent radius	r_3*	= 1.03
Surface brightness	μ_3	= 23.07
Concentration indices	C_{21}	= 3.23
	C_{32}	= 2.21

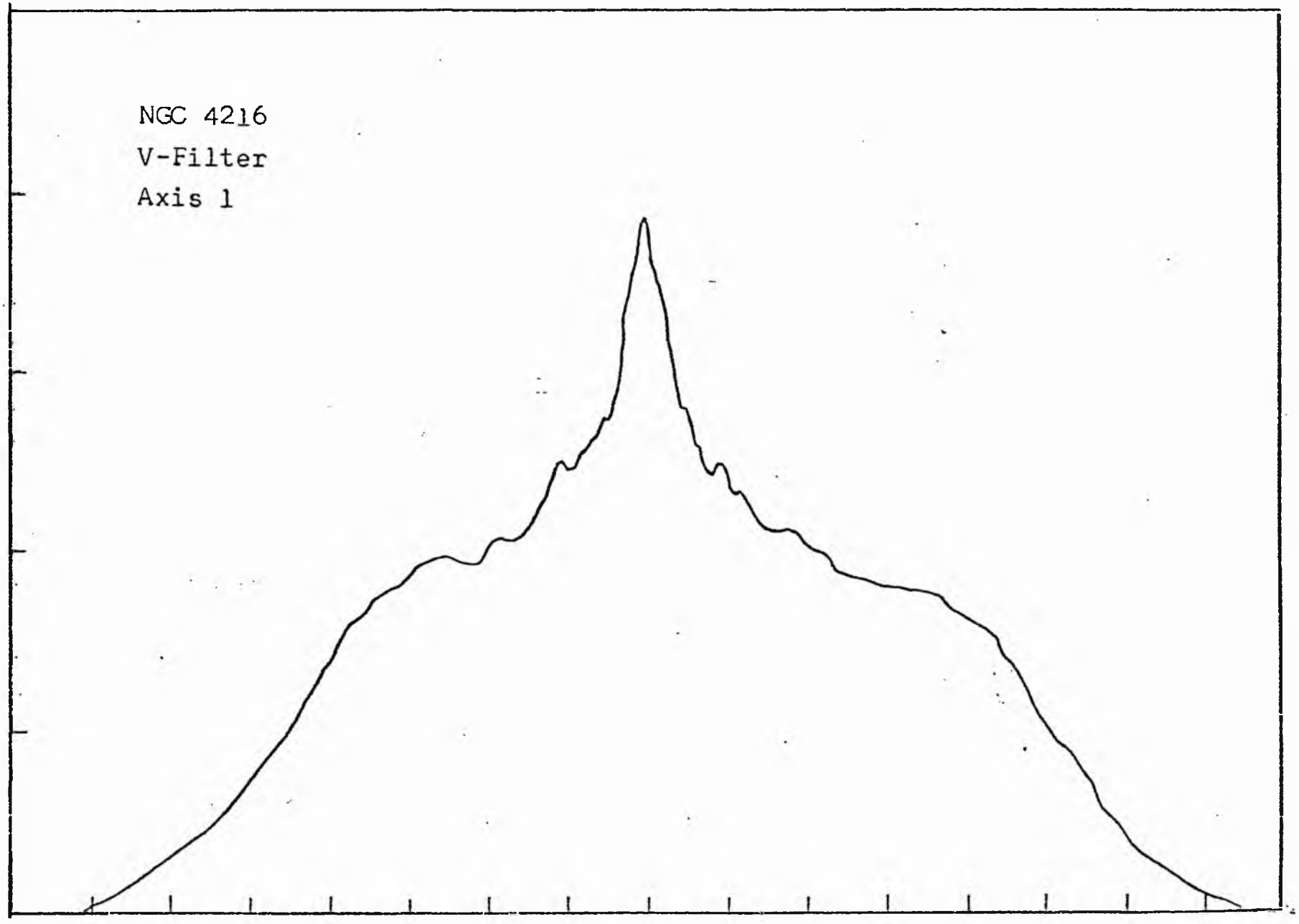
NGC 4216
V-Filter
Axis 1

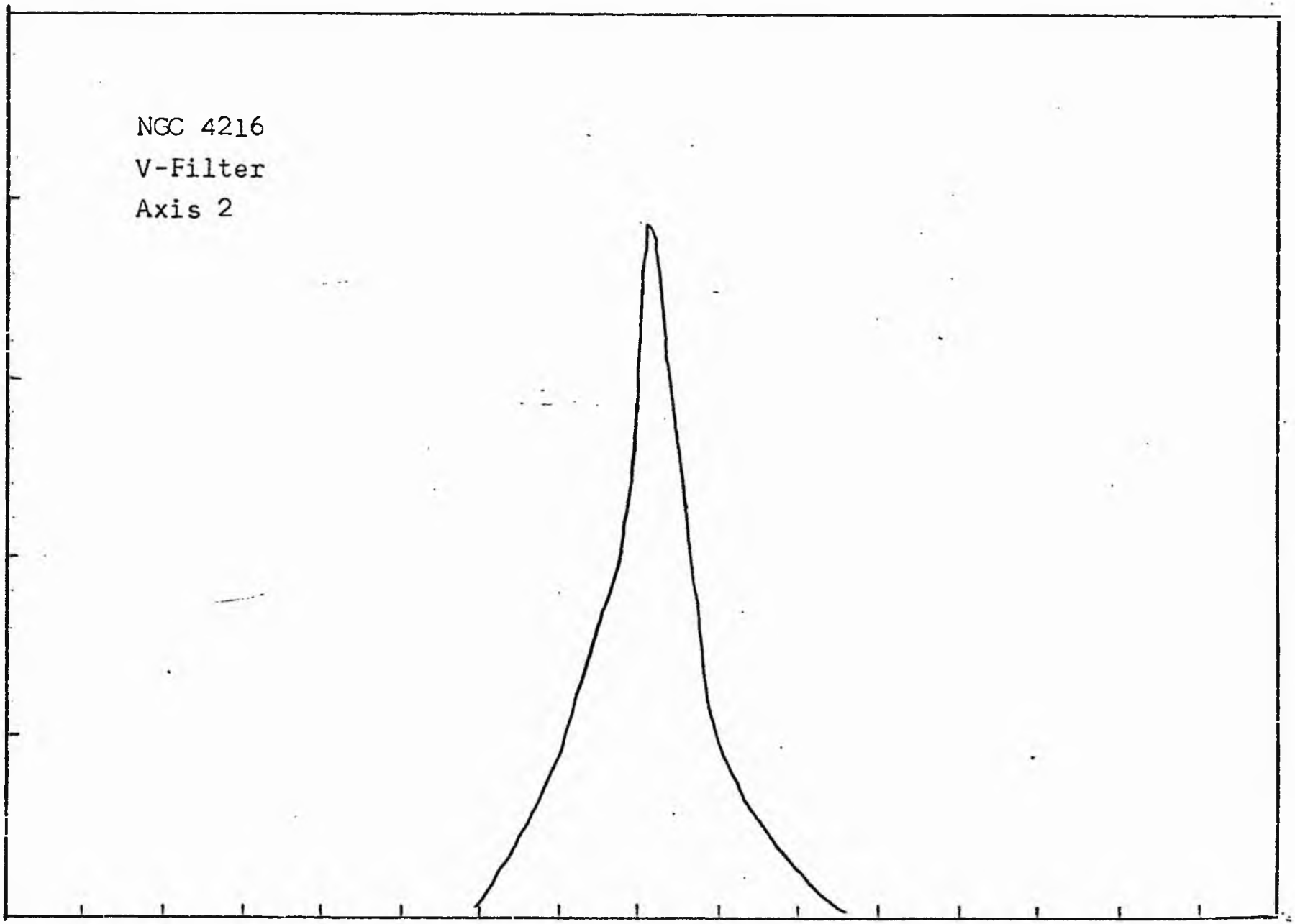
NGC 4216
V-Filter
Axis 2

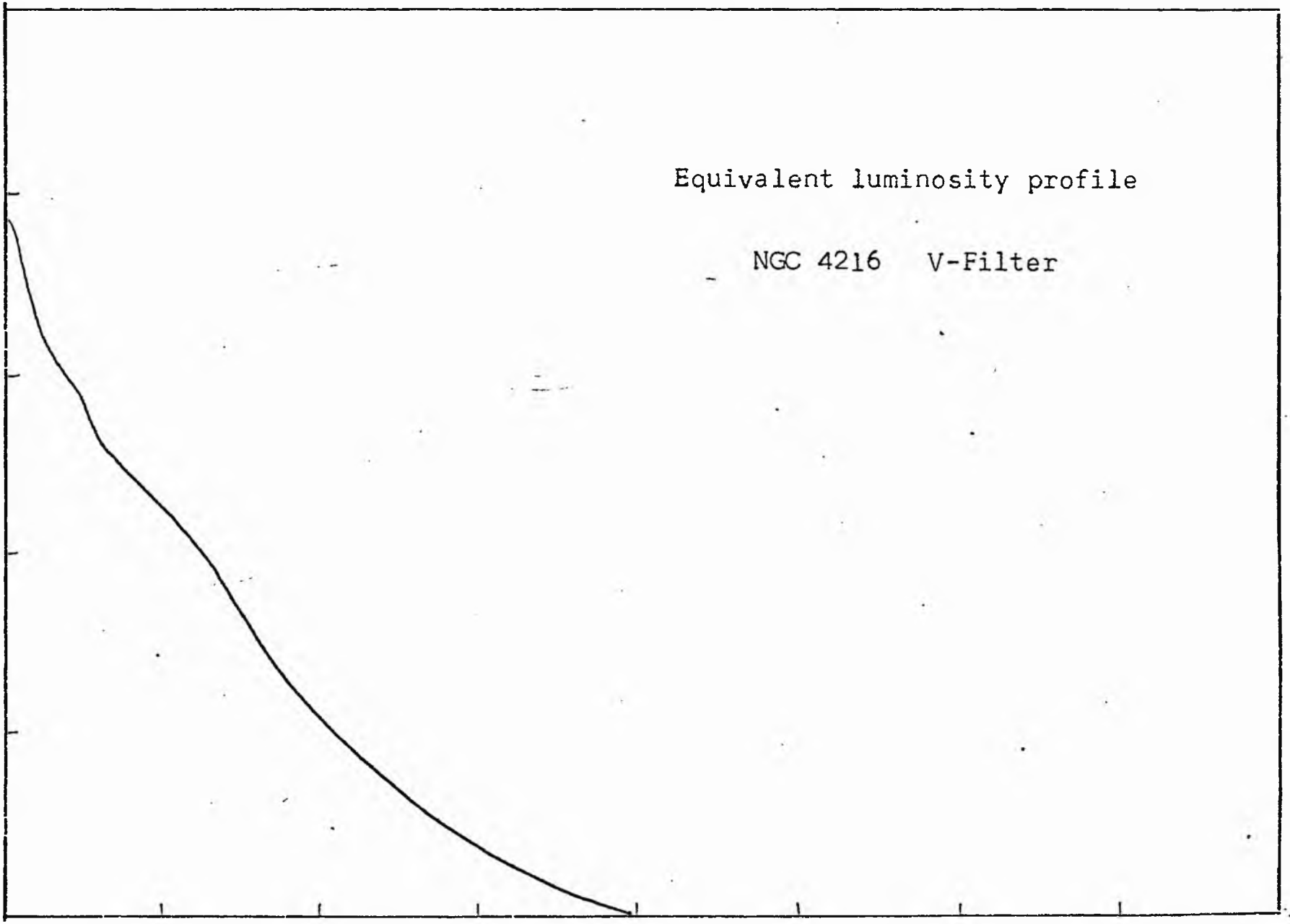
Equivalent luminosity profile
NGC 4216 V-Filter

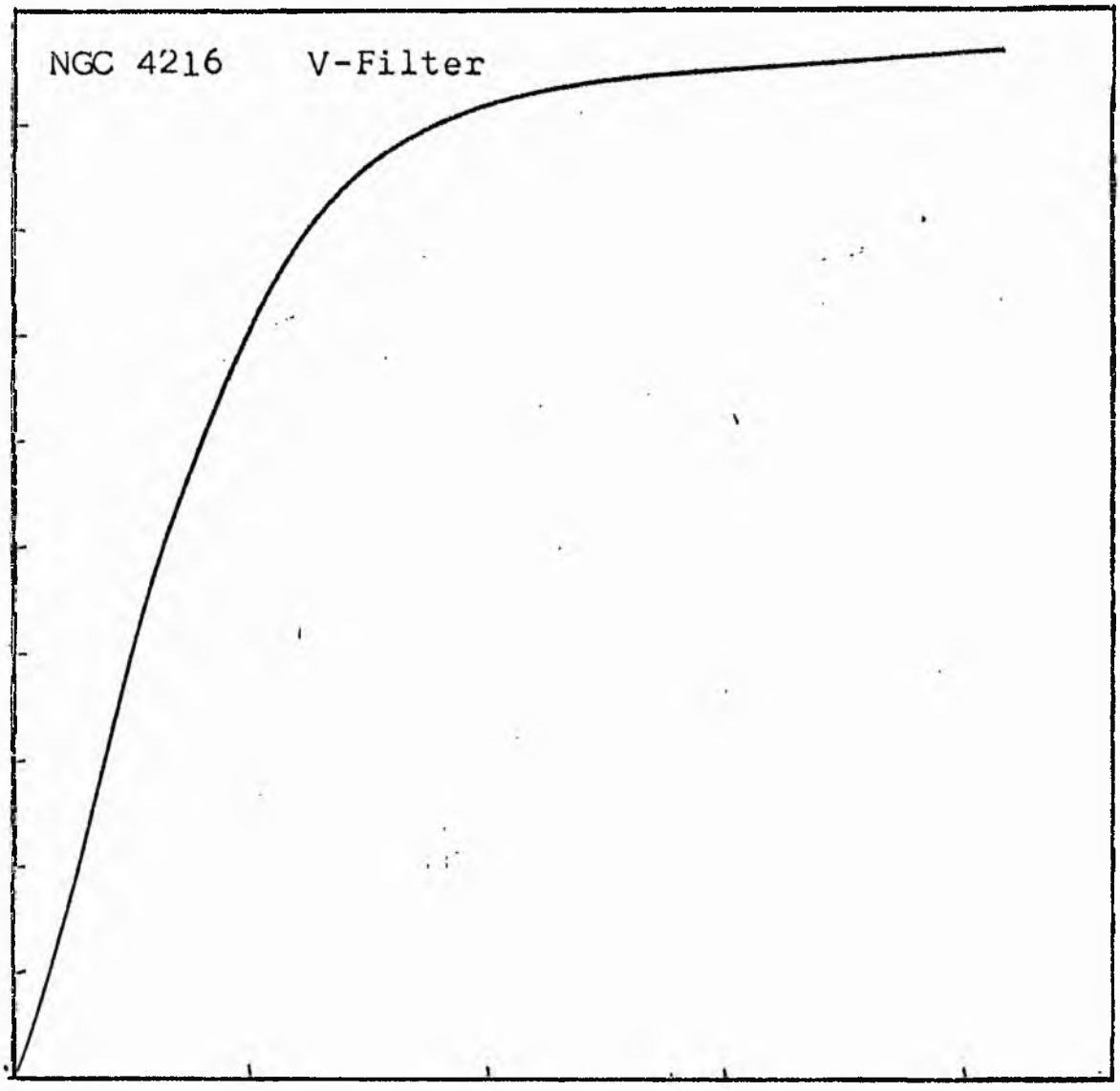

Relative integrated luminosity k(r) versus equivalent radius r*.

MEAN LUMINOSITY DISTRIBUTION IN NGC 4216
V COLOUR

LOG I	I	$\bar{I}$	R	AREA	ΔA	P	ΣP	KIRJ	ϱ	LOG J	μ
1.84	69.183		0.0	0.0			0.0	0.0	0.0	1.301	17.34
		66.139			4.52	299.2068					
1.80	63.096		1.20	4.52			299.21	0.01	0.04	1.261	17.44
		56.607			20.11	1138.1516					
1.70	50.119		2.80	24.63			1437.36	0.03	0.10	1.161	17.69
		44.965			28.18	1267.1038					
1.60	39.811		4.10	52.81			2704.46	0.05	0.14	1.061	17.94
		35.717			64.09	2289.0237					
1.50	31.623		6.10	116.90			4993.48	0.09	0.21	0.961	18.19
		28.371			45.96	1303.9592					
1.40	25.119		7.20	162.86			6297.44	0.11	0.25	0.861	18.44
		22.536			69.49	1566.0427					
1.30	19.952		8.60	232.35			7863.48	0.14	0.29	0.761	18.69
		17.901			114.01	2040.8257					
1.20	15.849		10.50	346.36			9904.30	0.18	0.36	0.661	18.94
		14.219			76.37	1085.9326					
1.10	12.589		11.60	422.73			10990.23	0.20	0.39	0.561	19.19
		11.295			190.38	2150.2888					
1.00	10.000		13.97	613.12			13140.52	0.24	0.48	0.461	19.44
		8.972			637.24	5717.0820					
0.90	7.943		19.95	1250.36			18857.60	0.34	0.68	0.361	19.69
		7.126			840.81	5991.8945					
0.80	6.310		25.80	2091.17			24849.50	0.45	0.88	0.261	19.94
		5.661			148.44	840.2800					
0.70	5.012		26.70	2239.61			25689.77	0.46	0.91	0.161	20.19
		4.496			258.71	1163.2756					
0.60	3.981		28.20	2498.32			26853.05	0.49	0.96	0.061	20.44
		3.572			501.30	1790.4778					
0.50	3.162		30.90	2999.62			28643.52	0.52	1.05	-0.039	20.69
		2.837			1074.14	3047.4058					
0.40	2.512		36.01	4073.76			31690.93	0.57	1.23	-0.139	20.94
		2.254			1781.06	4013.7212					
0.30	1.995		43.17	5854.82			35704.64	0.65	1.47	-0.239	21.19
		1.790			1905.19	3410.4160					
0.20	1.585		49.70	7760.02			39115.06	0.71	1.69	-0.339	21.44
		1.422			2197.85	3125.1226					
0.10	1.259		56.30	9957.87			42240.18	0.76	1.92	-0.439	21.69
		1.129			1465.24	1654.9243					
-0.00	1.000		60.30	11423.11			43895.10	0.79	2.05	-0.539	21.94
		0.897			1727.87	1550.1692					
-0.10	0.794		64.70	13150.98			45445.27	0.82	2.20	-0.639	22.19
		0.713			1590.16	1133.2083					
-0.20	0.631		68.50	14741.14			46578.48	0.84	2.33	-0.739	22.44
		0.566			1229.74	696.1155					
-0.30	0.501		71.30	15970.87			47274.59	0.85	2.43	-0.839	22.69
		0.450			1606.45	722.3286					
-0.40	0.398		74.80	17577.32			47996.92	0.87	2.55	-0.939	22.94
		0.357			1389.38	496.2390					
-0.50	0.316		77.70	18966.70			48493.16	0.88	2.64	-1.039	23.19
		0.284			1240.14	351.8369					
-0.60	0.251		80.20	20206.85			48844.99	0.88	2.73	-1.139	23.44
		0.225			2812.72	633.8630					
-0.70	0.200		85.60	23019.57			49478.85	0.89	2.91	-1.239	23.69
		0.179			2654.02	475.0872					
-0.80	0.158		90.40	25673.59			49953.94	0.90	3.08	-1.339	23.94
		0.142			3703.09	526.5430					
-0.90	0.126		96.70	29376.68			50480.48	0.91	3.29	-1.439	24.19
		0.113			4276.85	483.0513					
-1.00	0.100		103.50	33653.53			50963.53	0.92	3.52	-1.539	24.44
		0.090			4636.70	415.9861					
-1.10	0.079		110.40	38290.22			51379.52	0.93	3.76	-1.639	24.69
		0.071			3764.67	268.2859					
-1.20	0.063		115.70	42054.89			51647.80	0.93	3.94	-1.739	24.94
		0.057			6875.52	389.2036					
-1.30	0.050		124.80	48930.42			52037.00	0.94	4.25	-1.839	25.19
		0.045			4817.95	216.6380					
-1.40	0.040		130.80	53748.37			52253.64	0.94	4.45	-1.939	25.44
		0.036			5561.00	198.6211					
-1.50	0.032		137.40	59309.37			52452.26	0.95	4.68	-2.039	25.69
		0.028			11093.94	314.7449					
-1.60	0.025		149.70	70403.31			52767.00	0.95	5.10	-2.139	25.94
		0.023			9319.25	210.0171					
-1.70	0.020		159.30	79722.56			52977.02	0.96	5.42	-2.239	26.19
		0.018			18922.94	338.7371					
-1.80	0.016		177.20	98645.50			53315.75	0.96	6.03	-2.339	26.44
		0.014			17528.31	249.2385					
-1.90	0.013		192.30	116173.81			53564.99	0.97	6.55	-2.439	26.69
		0.011			16367.31	184.8642					
-2.00	0.010		205.40	132541.12			53749.86	0.97	6.99	-2.539	26.94
$-\infty$							55350.00	(1)			∞

PHOTOMETRIC PARAMETERS OF NGC 4216
V-FILTER

Total luminosity ..... L_T = 15.37
Total apparent magnitude ..... m_T = 10.09
Apparent central surface brightness ..... μ_o = 17.34
Major axis at threshold ..... $2a_m$ = 12.7
Minor axis at threshold ..... $2b_m$ = 4.23
Major axis at μ=25.0 mag sec^{-2} ..... 2a(25) = 8.67
Luminosity within μ=25.0 mag sec^{-2} ..... k(25) = 0.93
Gradient of exponential component ..... G(a) = -0.54
Equivalent gradient of exponential comp..... G(r*) = -1.06
Equivalent gradient of reduced exp. comp..... G(ρ) = -0.72
Parameters at k = ¼ :
- Semi-major axis ..... a_1 = 0.30
- Axis ratio ..... b/a = 0.66
- Equivalent radius ..... r_1* = 0.24
- Surface brightness ..... μ_1 = 19.46

Parameters at k = ½(effective) :
- Semi-major axis ..... a_e = 0.63
- Axis ratio ..... b/a = 0.39
- Equivalent radius ..... r_e* = 0.49
- Surface brightness ..... μ_e = 20.52
- Mean surface brightness ..... μ_e' = 10.53

Parameters at k = ¾ :
- Semi-major axis ..... a_3 = 1.36
- Axis ratio ..... b/a = 0.32
- Equivalent radius ..... r_3* = 0.91
- Surface brightness ..... μ_3 = 21.64

Concentration indices ..... C_{21} = 2.00, C_{32} = 1.86

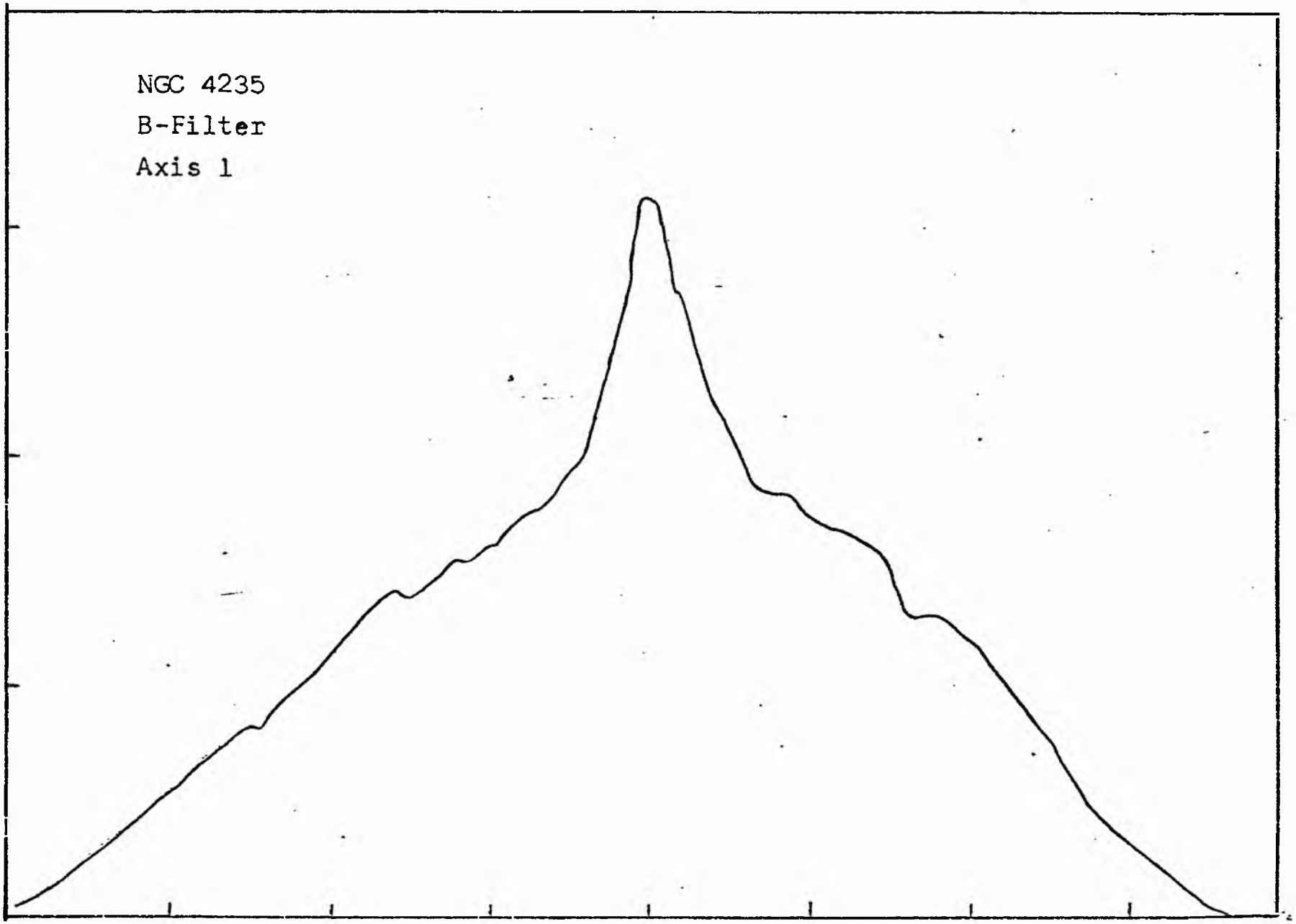
NGC 4235
B-Filter
Axis 1

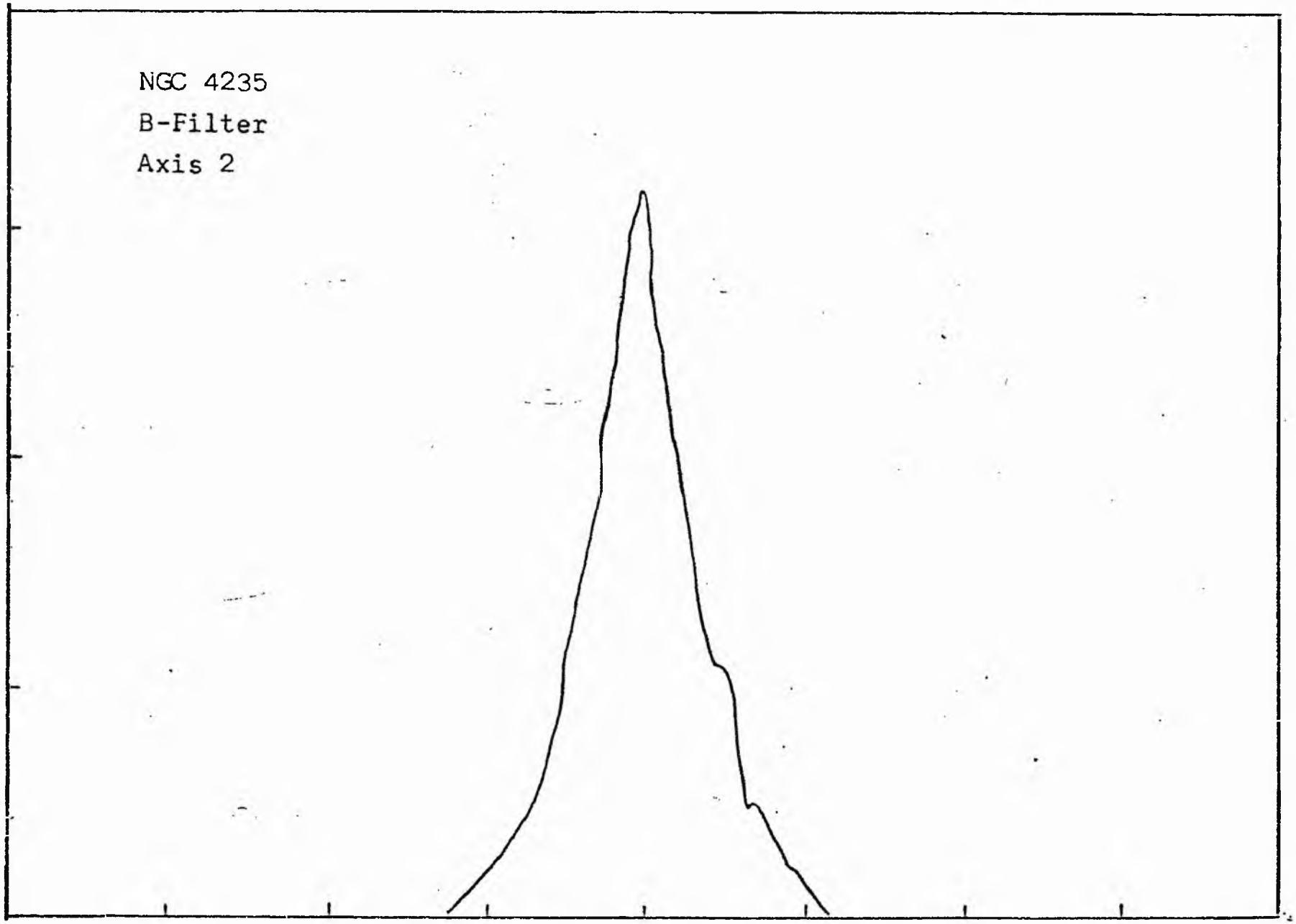
NGC 4235
B-Filter
Axis 2

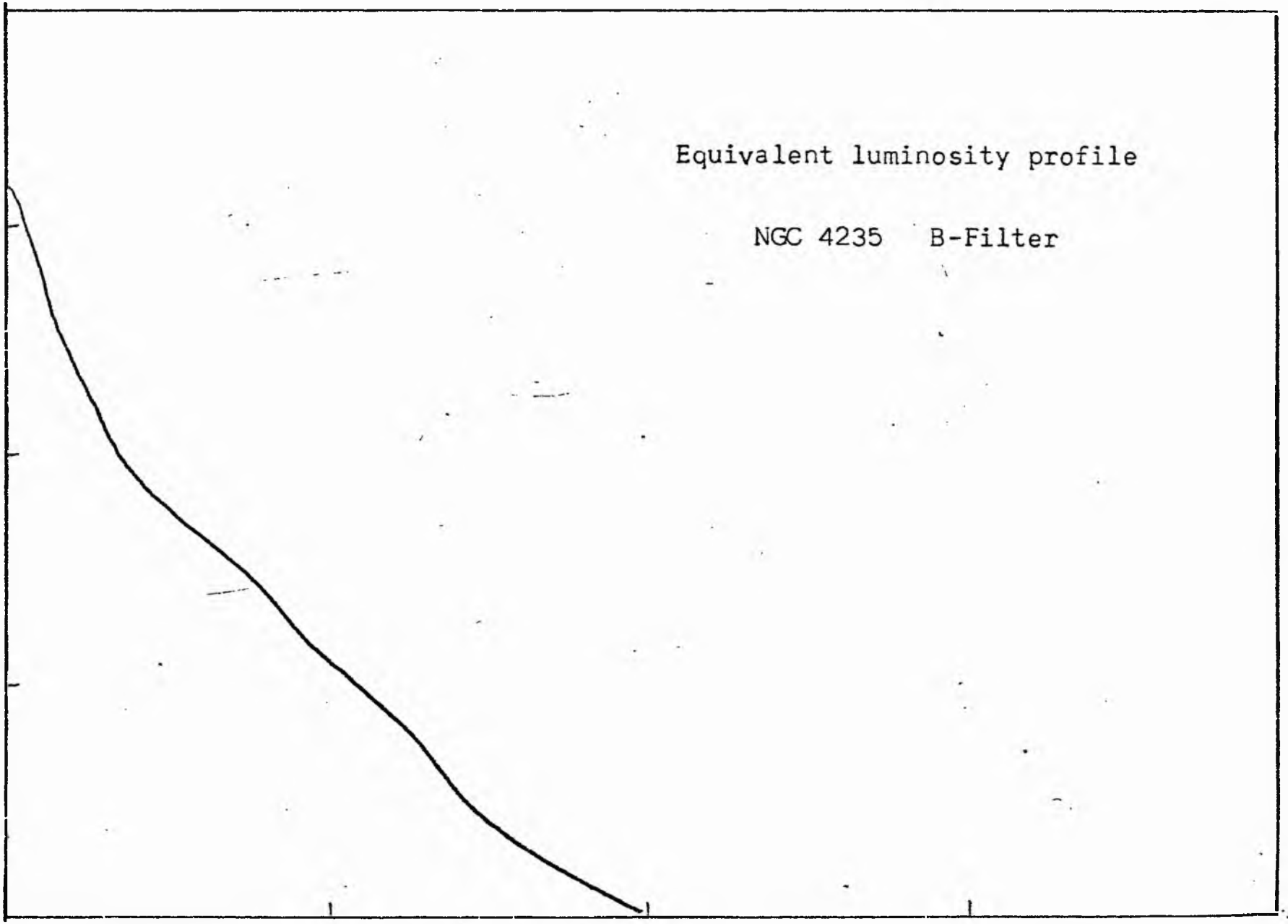
Equivalent luminosity profile
NGC 4235 B-Filter

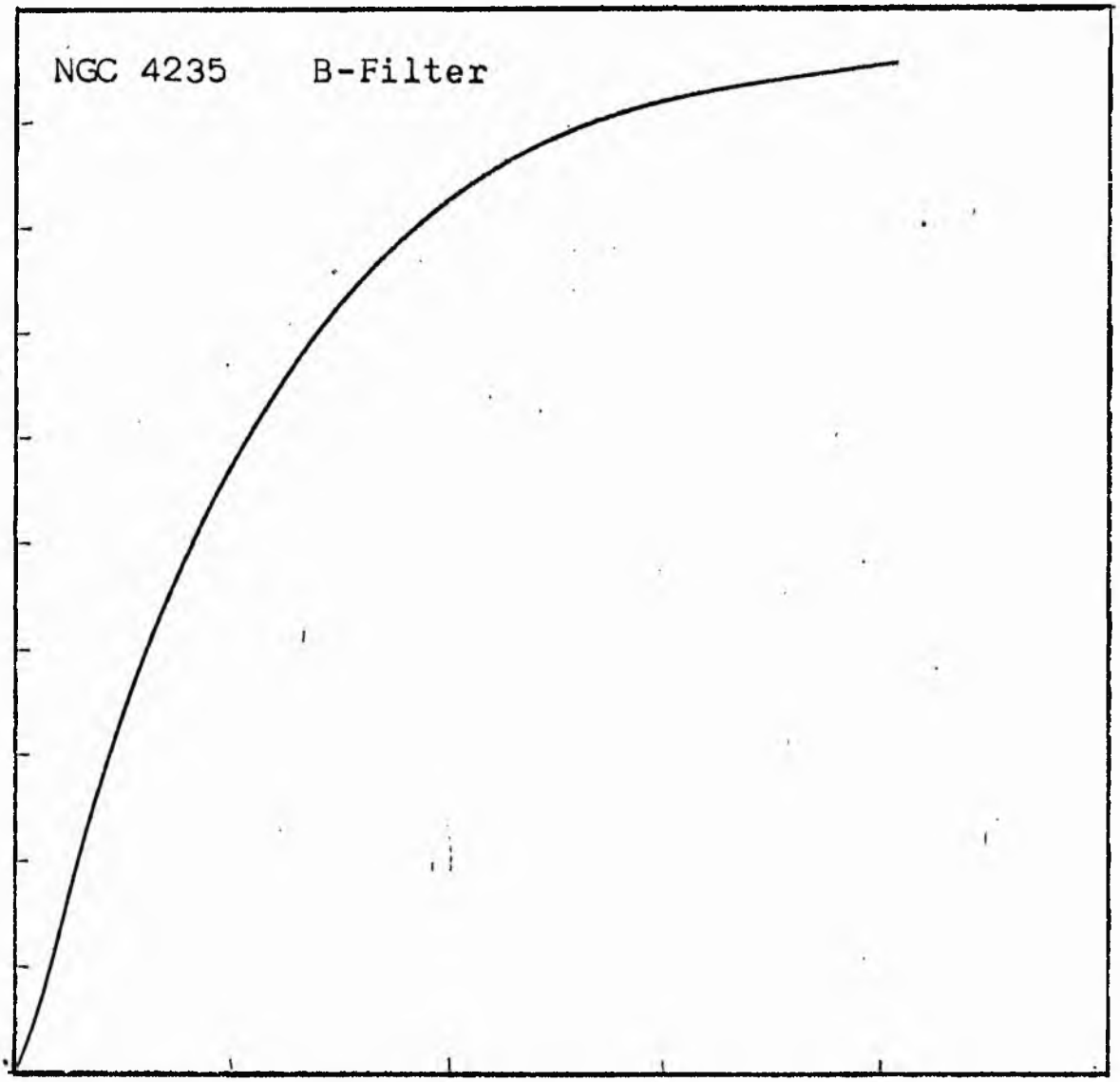

Relative integrated luminosity k(r) versus equivalent radius r*.

MEAN LUMINOSITY DISTRIBUTION IN NGC 4235
B COLOUR

LOG I	I	$\bar{I}$	R	AREA	ΔA	P	ΣP	K(R)	ρ	LOG J	μ
1.14	13.804		0.0	0.0			0.0	0.0	0.0	1.221	19.32
		13.197			16.33	215.5156					
1.10	12.589		2.28	16.33			215.52	0.03	0.11	1.181	19.42
		11.295			10.09	113.9573					
1.00	10.000		2.90	26.42			329.47	0.05	0.14	1.081	19.67
		8.972			65.19	584.8425					
0.90	7.943		5.40	91.61			914.32	0.14	0.26	0.981	19.92
		7.126			25.29	180.2258					
0.80	6.310		6.10	116.90			1094.54	0.16	0.30	0.881	20.17
		5.661			28.37	160.5861					
0.70	5.012		6.80	145.27			1255.13	0.19	0.33	0.781	20.42
		4.496			4.30	19.3528					
0.60	3.981		6.90	149.57			1274.48	0.19	0.34	0.681	20.67
		3.572			158.34	565.5239					
0.50	3.162		9.90	307.91			1840.00	0.27	0.48	0.581	20.92
		2.837			100.37	284.7688					
0.40	2.512		11.40	408.28			2124.77	0.31	0.55	0.481	21.17
		2.254			106.44	239.8635					
0.30	1.995		12.80	514.72			2364.64	0.35	0.62	0.381	21.42
		1.790			164.15	293.8381					
0.20	1.585		14.70	678.87			2658.47	0.39	0.71	0.281	21.67
		1.422			155.82	221.5636					
0.10	1.259		16.30	834.69			2880.04	0.43	0.79	0.181	21.92
		1.129			228.93	258.5654					
-0.00	1.000		18.40	1063.62			3138.60	0.46	0.89	0.081	22.17
		0.897			335.05	300.5950					
-0.10	0.794		21.10	1398.67			3439.20	0.51	1.03	-0.019	22.42
		0.713			487.07	347.1096					
-0.20	0.631		24.50	1885.74			3786.31	0.56	1.19	-0.119	22.67
		0.566			683.95	387.1675					
-0.30	0.501		28.60	2569.70			4173.47	0.62	1.39	-0.219	22.92
		0.450			748.61	336.6111					
-0.40	0.398		32.50	3318.31			4510.08	0.67	1.58	-0.319	23.17
		0.357			1076.02	384.3210					
-0.50	0.316		37.40	4394.33			4894.40	0.72	1.82	-0.419	23.42
		0.284			835.29	236.9774					
-0.60	0.251		40.80	5229.62			5131.38	0.76	1.98	-0.519	23.67
		0.225			742.42	167.3103					
-0.70	0.200		43.60	5972.04			5298.69	0.78	2.12	-0.619	23.92
		0.179			820.87	146.9417					
-0.80	0.158		46.50	6792.91			5445.63	0.81	2.26	-0.719	24.17
		0.142			998.36	141.9583					
-0.90	0.126		49.80	7791.27			5587.59	0.83	2.42	-0.819	24.42
		0.113			2308.60	260.7400					
-1.00	0.100		56.70	10099.87			5848.33	0.86	2.76	-0.919	24.67
		0.090			1285.38	115.3200					
-1.10	0.079		60.20	11385.25			5963.65	0.88	2.93	-1.019	24.92
		0.071			1282.43	91.3919					
-1.20	0.063		63.50	12667.69			6055.04	0.90	3.09	-1.119	25.17
		0.057			1225.22	69.3564					
-1.30	0.050		66.50	13892.91			6124.39	0.91	3.23	-1.219	25.42
		0.045			934.43	42.0165					
-1.40	0.040		68.70	14827.34			6166.41	0.91	3.34	-1.319	25.67
		0.036			1685.66	60.2066					
-1.50	0.032		72.50	16513.00			6226.61	0.92	3.53	-1.419	25.92
		0.028			1537.45	43.6191					
-1.60	0.025		75.80	18050.45			6270.23	0.93	3.69	-1.519	26.17
		0.023			2663.45	60.0233					
-1.70	0.020		81.20	20713.89			6330.25	0.94	3.95	-1.619	26.42
		0.018			3836.27	68.6728					
-1.80	0.016		88.40	24550.16			6398.92	0.95	4.30	-1.719	26.67
		0.014			3032.04	43.1134					
-1.90	0.013		93.70	27582.20			6442.04	0.95	4.56	-1.819	26.92
		0.011			4592.22	51.8681					
-2.00	0.010		101.20	32174.43			6493.90	0.96	4.92	-1.919	27.17
$-\infty$							6763.00	(1)			∞

PHOTOMETRIC PARAMETERS OF NGC 4235

B-FILTER

Total luminosity ..... L_T = 1.87

Total apparent magnitude ..... m_T = 12.6

Apparent central surface brightness ..... μ_o = 19.32

Major axis at threshold ..... $2a_m$ = 6.13

Minor axis at threshold ..... $2b_m$ = 1.96

Major axis at μ=25.0 mag sec^{-2} ..... 2a(25) = 4.1

Luminosity within μ=25.0 mag sec^{-2} ..... k(25) = 0.89

Gradient of exponential component ..... G(a) = -0.95

Equivalent gradient of exponential comp.... G(r*) = -1.62

Equivalent gradient of reduced exp. comp.... G(ρ) = -0.62

Parameters at k = ¼ :

- Semi-major axis ..... a_1 = 0.19
- Axis ratio ..... b/a = 0.65
- Equivalent radius ..... r_1* = 0.15
- Surface brightness ..... μ_1 = 20.88

Parameters at k = ½(effective) :

- Semi-major axis ..... a_e = 0.46
- Axis ratio ..... b/a = 0.55
- Equivalent radius ..... r_e* = 0.34
- Surface brightness ..... μ_e = 22.37
- Mean surface brightness ..... μ_e' = 12.24

Parameters at k = ¾ :

- Semi-major axis ..... a_3 = 1.37
- Axis ratio ..... b/a = 0.23
- Equivalent radius ..... r_3* = 0.66
- Surface brightness ..... μ_3 = 23.61

Concentration indices ..... C_{21} = 2.26, C_{32} = 1.94

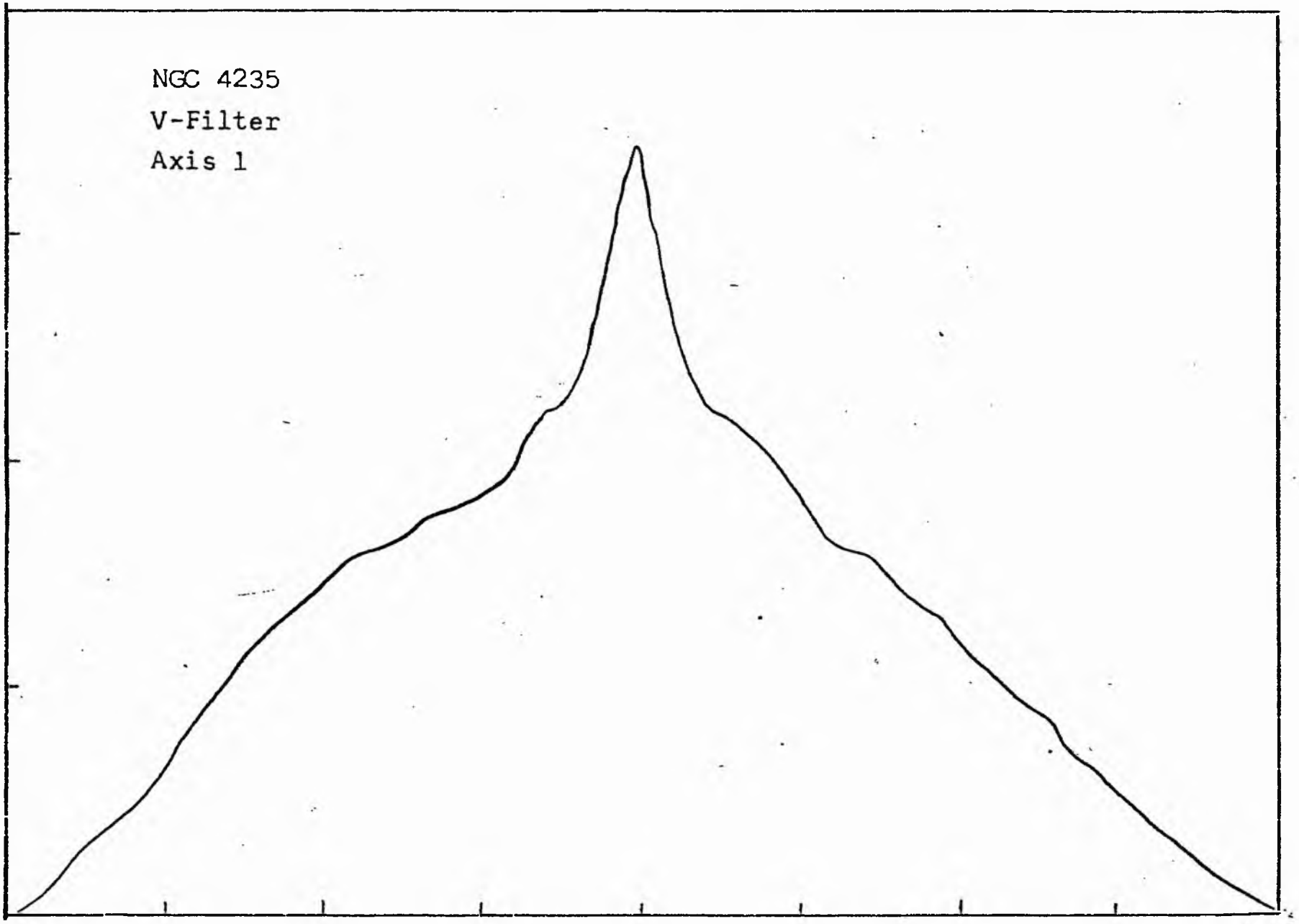
NGC 4235
V-Filter
Axis 1

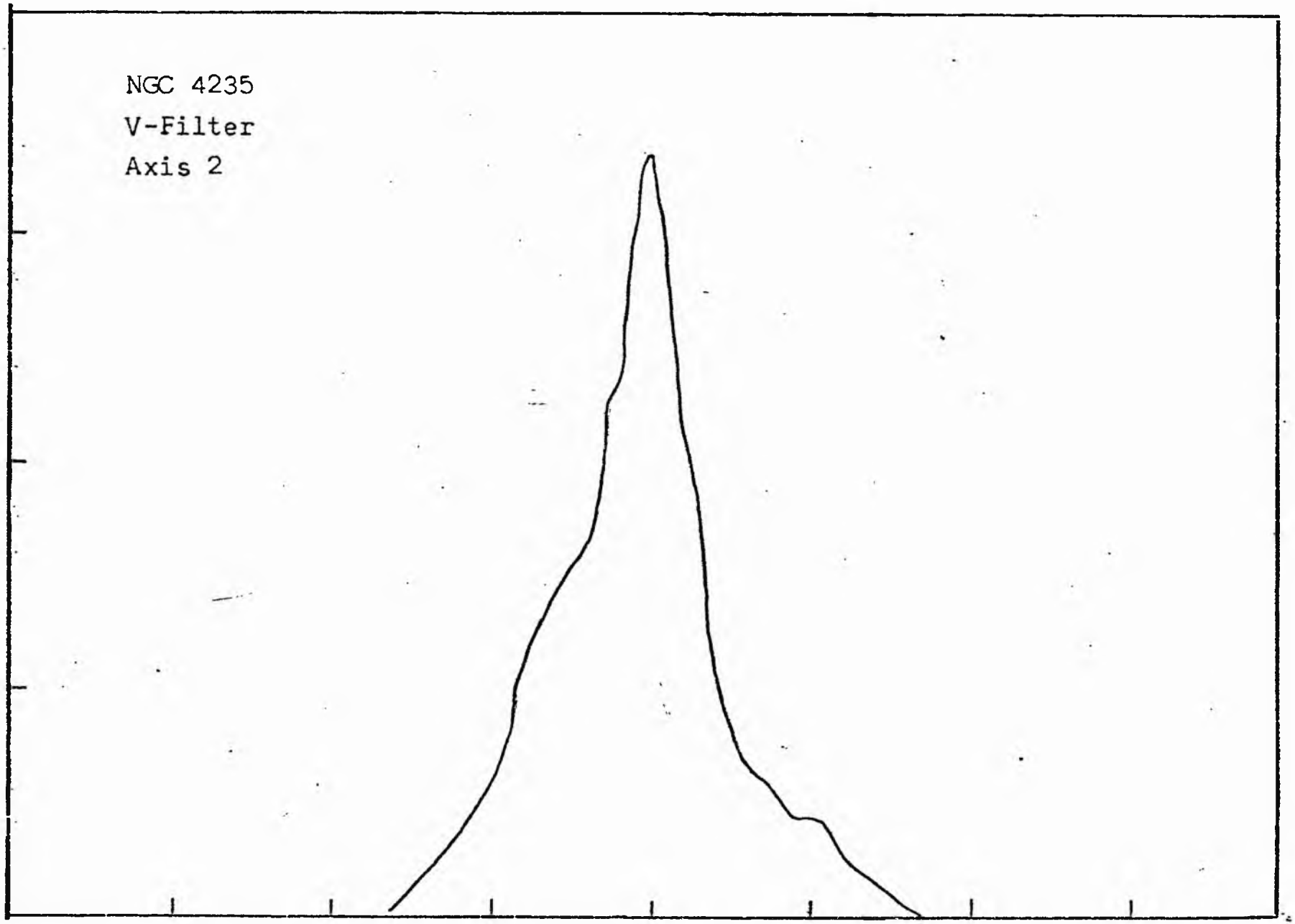
NGC 4235
V-Filter
Axis 2

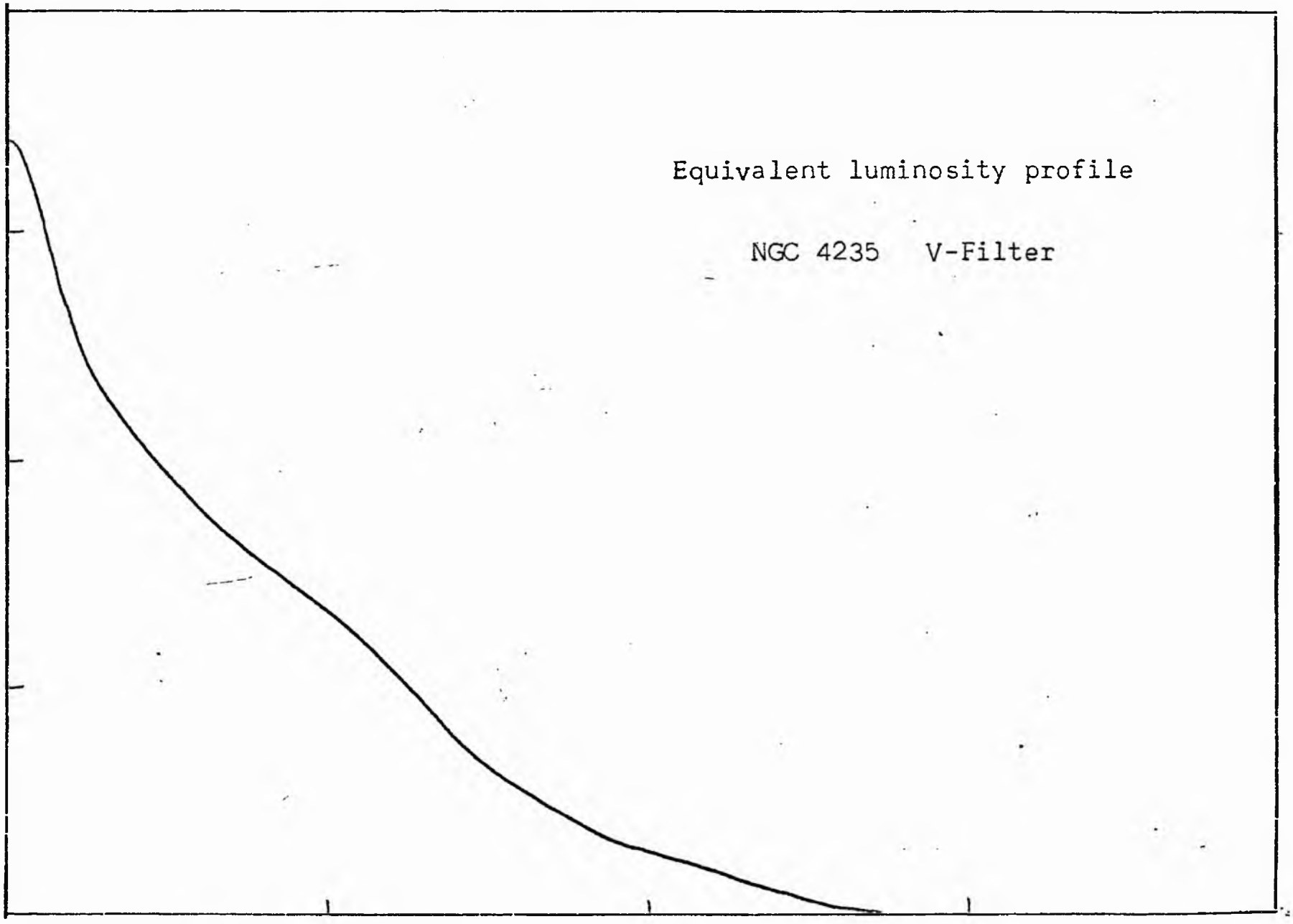
Equivalent luminosity profile
NGC 4235 V-Filter

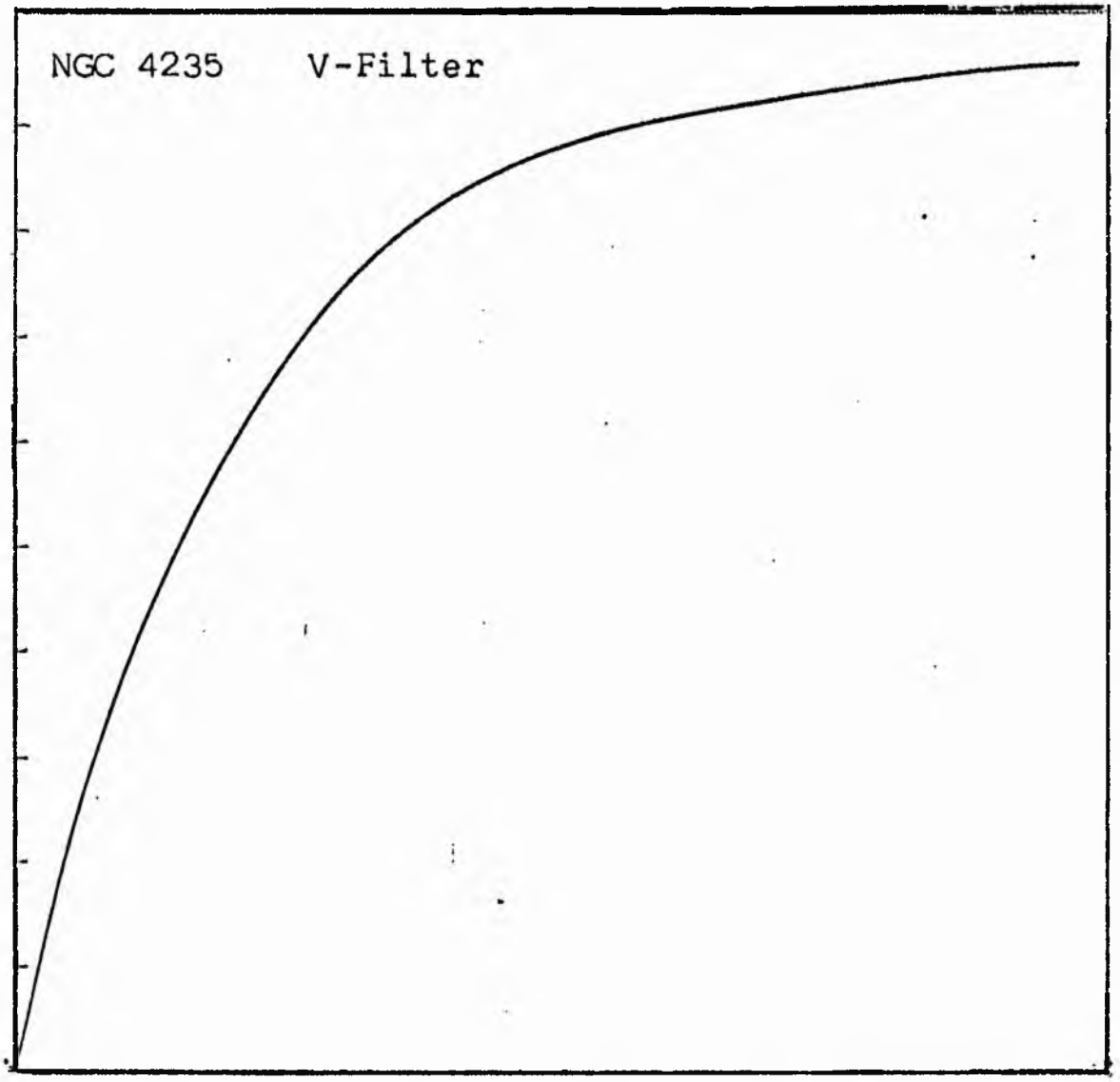

Relative integrated luminosity k(r) versus equivalent radius r*.

MEAN LUMINOSITY DISTRIBUTION IN NGC 4235
V COLOUR

LOG I	I	$\bar{I}$	R	AREA	ΔA	P	ΣP	K(R)	ρ	LOG J	μ
1.32	20.893		0.0	0.0			0.0	0.0	0.0	1.323	18.25
		20.423			18.70	381.9824					
1.30	19.953		2.44	18.70			381.98	0.04	0.11	1.303	18.30
		17.901			22.69	406.2148					
1.20	15.849		3.63	41.40			788.20	0.08	0.16	1.203	18.55
		14.219			24.22	344.3196					
1.10	12.589		4.57	65.61			1132.52	0.11	0.21	1.103	18.80
		11.295			40.07	452.5886					
1.00	10.000		5.80	105.68			1585.11	0.15	0.26	1.003	19.05
		8.972			37.46	336.0374					
0.90	7.943		6.75	143.14			1921.14	0.19	0.30	0.903	19.30
		7.126			21.54	153.4734					
0.80	6.310		7.24	164.67			2074.62	0.20	0.33	0.803	19.55
		5.661			86.97	492.3379					
0.70	5.012		8.95	251.65			2566.95	0.25	0.40	0.703	19.80
		4.496			88.15	396.3401					
0.60	3.981		10.40	339.79			2963.29	0.29	0.47	0.603	20.05
		3.572			68.49	244.6118					
0.50	3.162		11.40	408.28			3207.91	0.31	0.51	0.503	20.30
		2.837			98.43	279.2417					
0.40	2.512		12.70	506.71			3487.15	0.34	0.57	0.403	20.55
		2.254			144.73	326.1665					
0.30	1.995		14.40	651.44			3813.31	0.37	0.65	0.303	20.80
		1.790			435.42	779.4387					
0.20	1.585		18.60	1086.86			4592.75	0.44	0.84	0.203	21.05
		1.422			132.36	188.1982					
0.10	1.259		19.70	1219.22			4780.95	0.46	0.88	0.103	21.30
		1.129			329.08	371.6843					
-0.00	1.000		22.20	1548.30			5152.63	0.50	1.00	0.003	21.55
		0.897			542.87	487.0376					
-0.10	0.794		25.80	2091.17			5639.66	0.55	1.16	-0.097	21.80
		0.713			661.37	471.3184					
-0.20	0.631		29.60	2752.54			6110.98	0.59	1.33	-0.197	22.05
		0.566			760.50	430.4941					
-0.30	0.501		33.44	3513.03			6541.47	0.63	1.50	-0.297	22.30
		0.450			1131.50	508.7761					
-0.40	0.398		38.45	4644.54			7050.25	0.68	1.73	-0.397	22.55
		0.357			1319.29	471.2046					
-0.50	0.316		43.57	5963.82			7521.45	0.73	1.96	-0.497	22.80
		0.284			1067.80	302.9441					
-0.60	0.251		47.31	7031.62			7824.39	0.76	2.12	-0.597	23.05
		0.225			1584.56	357.0913					
-0.70	0.200		52.37	8616.18			8181.48	0.79	2.35	-0.697	23.30
		0.179			1123.57	201.1281					
-0.80	0.158		55.68	9739.76			8382.61	0.81	2.50	-0.797	23.55
		0.142			974.83	138.6115					
-0.90	0.126		58.40	10714.59			8521.21	0.83	2.62	-0.897	23.80
		0.113			1557.26	175.8864					
-1.00	0.100		62.50	12271.84			8697.10	0.84	2.81	-0.997	24.05
		0.090			1330.11	119.3327					
-1.10	0.079		65.80	13601.95			8816.43	0.85	2.95	-1.097	24.30
		0.071			1355.17	96.5753					
-1.20	0.063		69.00	14957.12			8913.00	0.86	3.10	-1.197	24.55
		0.057			1830.31	103.6090					
-1.30	0.050		73.10	16787.43			9016.61	0.87	3.28	-1.297	24.80
		0.045			1636.41	73.5812					
-1.40	0.040		76.58	18423.84			9090.19	0.88	3.44	-1.397	25.05
		0.036			3848.91	137.4712					
-1.50	0.032		84.20	22272.75			9227.66	0.89	3.78	-1.497	25.30
		0.028			3628.54	102.9454					
-1.60	0.025		90.80	25901.29			9330.60	0.90	4.08	-1.597	25.55
		0.023			5703.41	128.5316					
-1.70	0.020		100.30	31604.70			9459.13	0.92	4.50	-1.697	25.80
		0.018			6720.22	120.2984					
-1.80	0.016		110.45	38324.92			9579.43	0.93	4.96	-1.797	26.05
		0.014			7960.49	113.1922					
-1.90	0.013		121.38	46285.41			9692.62	0.94	5.45	-1.897	26.30
		0.011			7380.82	83.3646					
-2.00	0.010		130.70	53666.22			9775.98	0.95	5.87	-1.997	26.55
$-\infty$							10325.00	(1)			∞

PHOTOMETRIC PARAMETERS OF NGC 4235

V-FILTER

Total luminosity ..... L_T = 2.86

Total apparent magnitude ..... m_T = 11.52

Apparent central surface brightness ..... μ_o = 18.25

Major axis at threshold ..... $2a_m$ = 6.23

Minor axis at threshold ..... $2b_m$ = 2.98

Major axis at μ=25.0 mag sec^{-2} ..... 2a(25) = 4.81

Luminosity within μ=25.0 mag sec^{-2} ..... k(25) = 0.88

Gradient of exponential component ..... G(a) = -0.78

Equivalent gradient of exponential comp.... G(r*) = -1.46

Equivalent gradient of reduced exp. comp.... G(ρ) = -0.61

Parameters at k = ¼ :

- Semi-major axis ..... a_1 = 0.26
- Axis ratio ..... b/a = 0.56
- Equivalent radius ..... r_1* = 0.15
- Surface brightness ..... μ_1 = 19.80

Parameters at k = ½(effective) :

- Semi-major axis ..... a_e = 0.63
- Axis ratio ..... b/a = 0.36
- Equivalent radius ..... r_e* = 0.37
- Surface brightness ..... μ_e = 21.55
- Mean surface brightness ..... μ_e' = 11.37

Parameters at k = ¾ :

- Semi-major axis ..... a_3 = 1.52
- Axis ratio ..... b/a = 0.26
- Equivalent radius ..... r_3* = 0.77
- Surface brightness ..... μ_3 = 22.97

Concentration indices ..... C_{21} = 2.47, C_{32} = 2.08

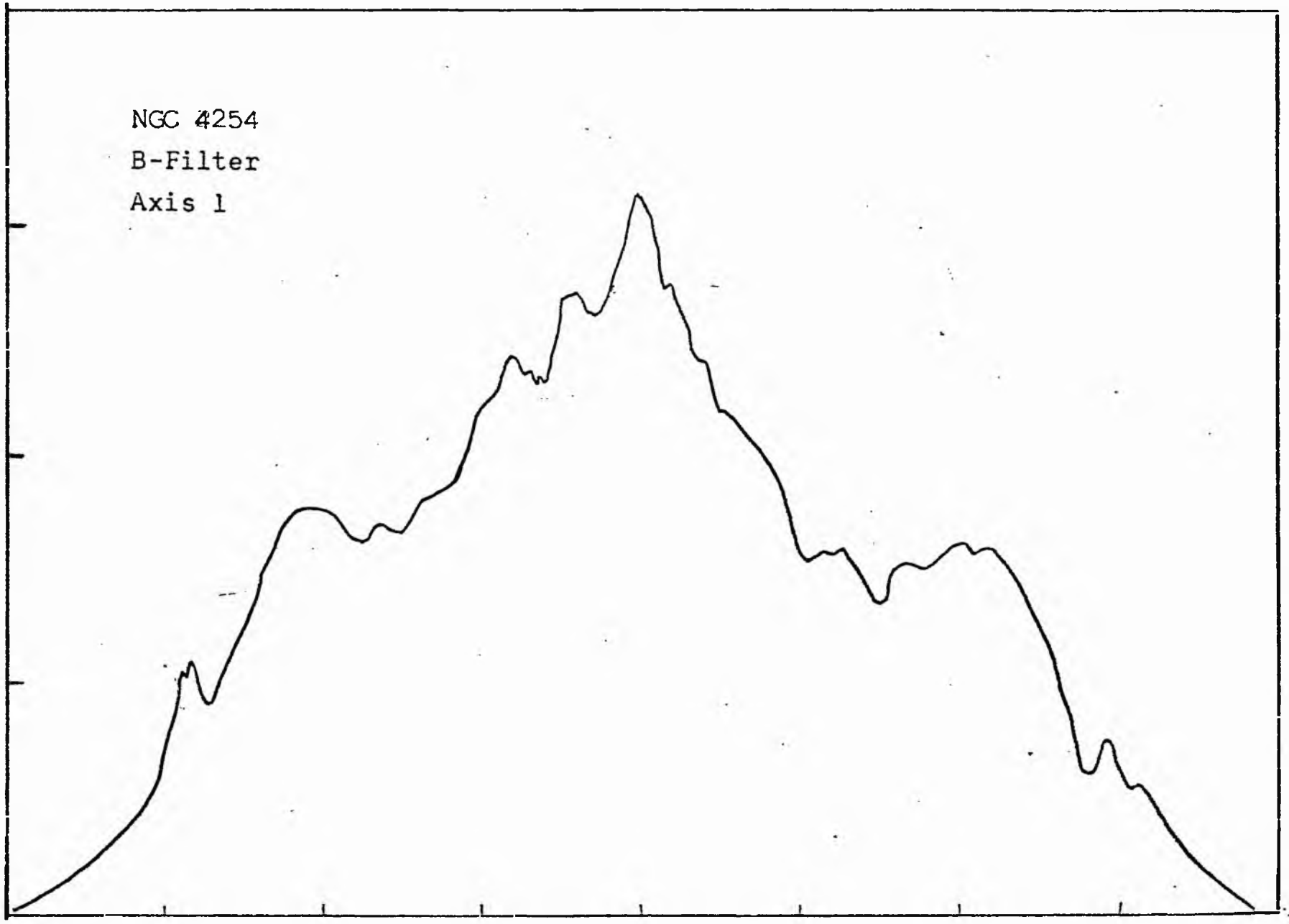
NGC 4254
B-Filter
Axis 1

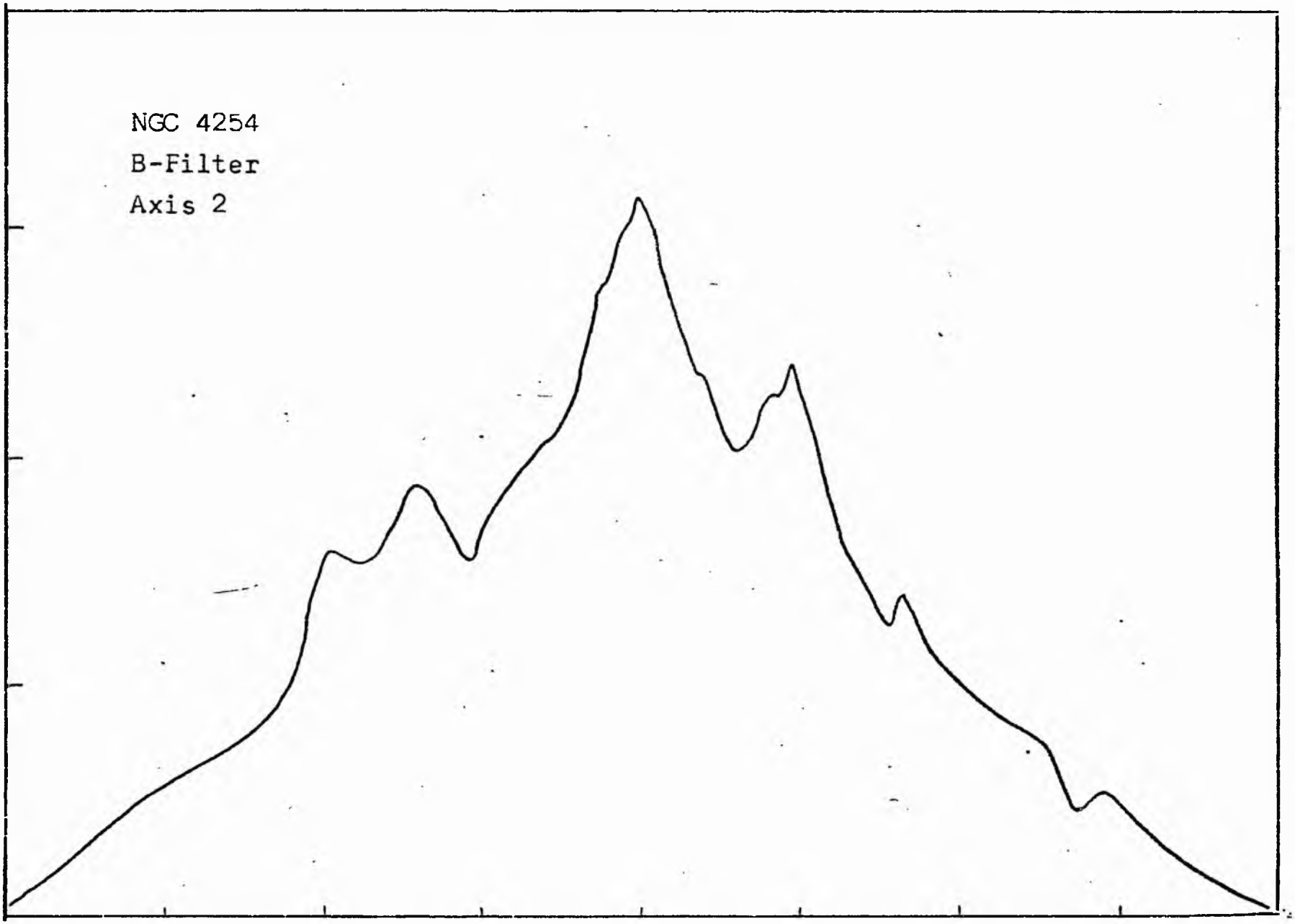
NGC 4254
B-Filter
Axis 2

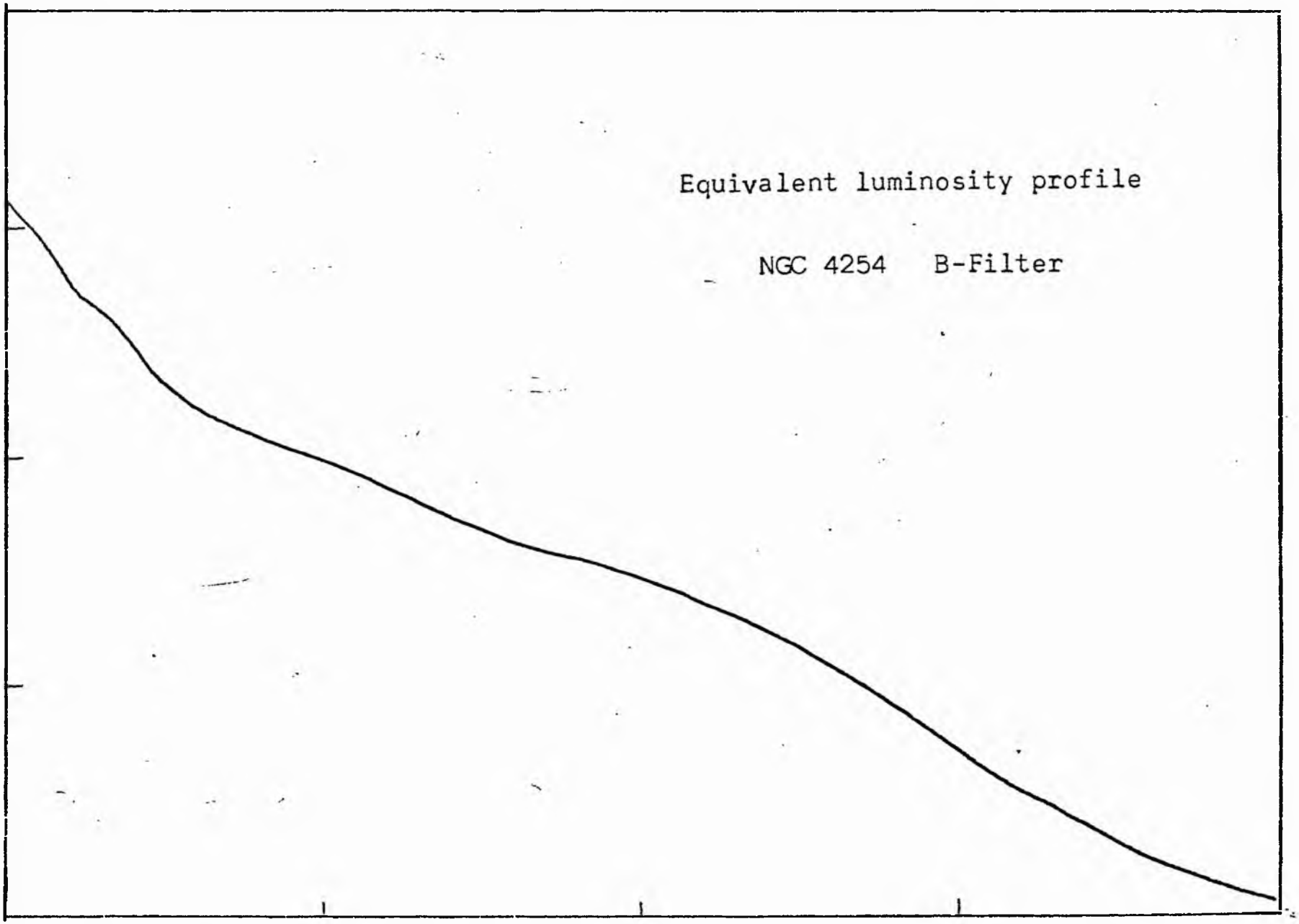
Equivalent luminosity profile
NGC 4254 B-Filter

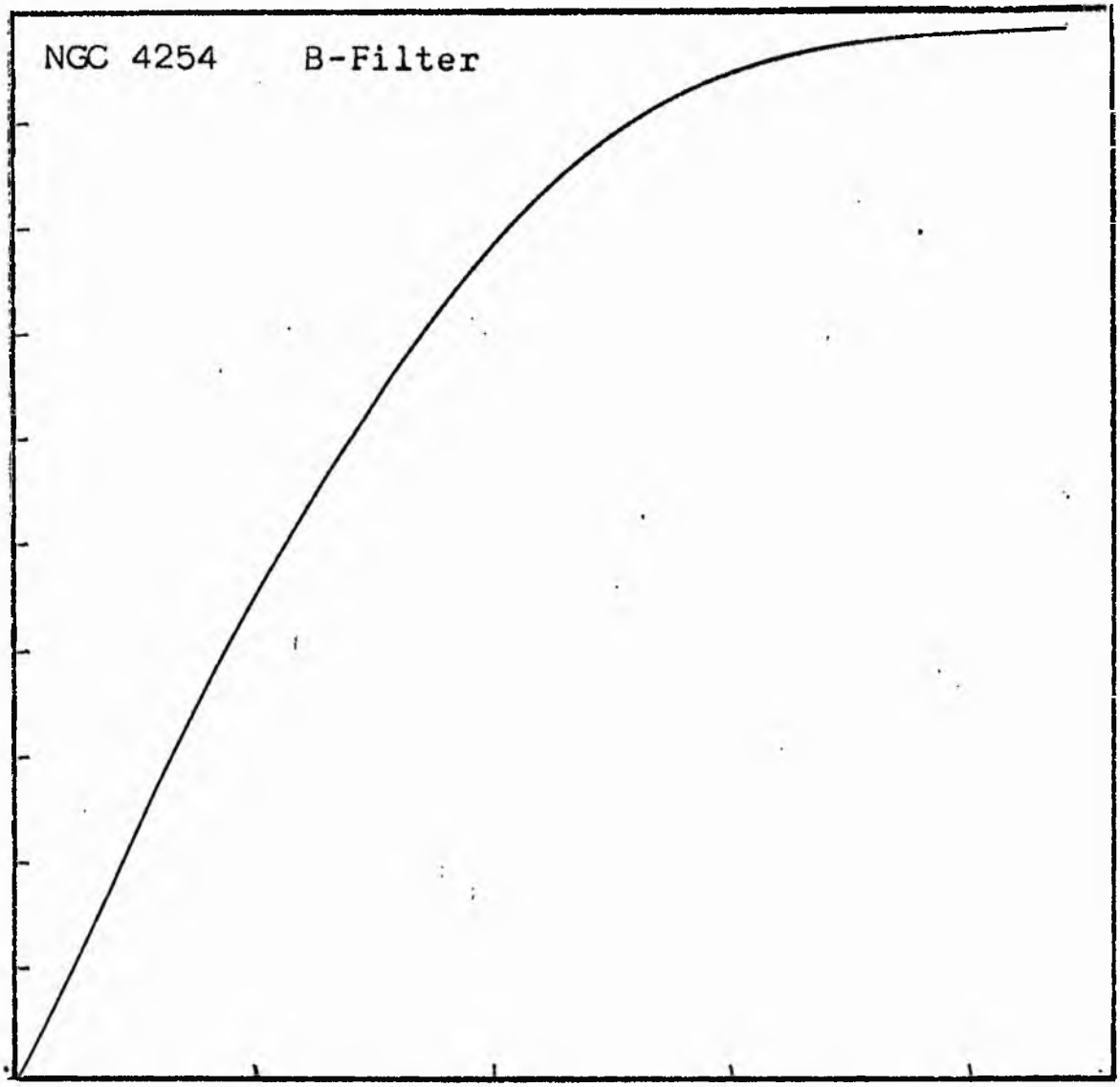

Relative integrated luminosity k(r) versus equivalent radius r*.

MEAN LUMINOSITY DISTRIBUTION IN NGC 4254
B COLOUR

LOG I	I	I	R	AREA	ΔA	P	ΣP	K(R)	ρ	LOG J	μ
1.06	11.482		0.0	0.0			0.0	0.0	0.0	1.171	19.14
		10.741			37.83	406.2966					
1.00	10.000		3.47	37.83			406.30	0.01	0.06	1.111	19.29
		8.972			82.94	744.0642					
0.90	7.943		6.20	120.76			1150.36	0.03	0.11	1.011	19.54
		7.126			145.14	1034.3401					
0.80	6.310		9.20	265.90			2184.70	0.06	0.17	0.911	19.79
		5.661			80.46	455.4407					
0.70	5.012		10.50	346.36			2640.14	0.08	0.19	0.811	20.04
		4.496			508.94	2288.4250					
0.60	3.981		16.50	855.30			4928.57	0.14	0.30	0.711	20.29
		3.572			426.60	1523.6626					
0.50	3.162		20.20	1281.89			6452.23	0.19	0.37	0.611	20.54
		2.837			308.54	875.3437					
0.40	2.512		22.50	1590.43			7327.57	0.21	0.41	0.511	20.79
		2.254			204.08	459.9009					
0.30	1.995		23.90	1794.51			7787.47	0.23	0.43	0.411	21.04
		1.793			976.66	1748.2952					
0.20	1.585		29.70	2771.17			9535.76	0.28	0.54	0.311	21.29
		1.422			2587.41	3679.6674					
0.10	1.259		41.30	5358.58			13214.83	0.38	0.75	0.211	21.54
		1.123			1522.26	1719.3340					
0.00	1.000		46.80	6880.84			14934.16	0.43	0.85	0.111	21.79
		0.897			2382.11	2137.1482					
-0.10	0.794		54.30	9262.95			17071.30	0.49	0.99	0.011	22.04
		0.713			2503.70	1784.2612					
-0.20	0.631		61.20	11766.64			18855.54	0.55	1.11	-0.089	22.29
		0.566			3892.17	2203.2490					
-0.30	0.501		70.60	15658.81			21058.79	0.61	1.28	-0.189	22.54
		0.450			7414.58	3333.9480					
-0.40	0.398		85.70	23073.39			24392.73	0.71	1.56	-0.289	22.79
		0.357			6364.07	2273.0420					
-0.50	0.316		96.80	29437.46			26665.77	0.77	1.76	-0.389	23.04
		0.284			6195.27	1757.6516					
-0.60	0.251		106.50	35632.73			28423.42	0.82	1.93	-0.489	23.29
		0.225			5770.43	1300.4126					
-0.70	0.200		114.80	41403.16			29723.83	0.86	2.08	-0.589	23.54
		0.179			5203.10	931.3975					
-0.80	0.158		121.80	46606.27			30655.23	0.89	2.21	-0.689	23.79
		0.142			4464.25	634.7776					
-0.90	0.126		127.50	51070.52			31290.00	0.91	2.32	-0.789	24.04
		0.113			3254.69	367.6060					
-1.00	0.100		131.50	54325.21			31657.61	0.92	2.39	-0.889	24.29
		0.090			4381.38	393.0825					
-1.10	0.079		136.70	58706.59			32050.69	0.93	2.48	-0.989	24.54
		0.071			5087.38	362.5498					
-1.20	0.063		142.50	63793.97			32413.24	0.94	2.59	-1.089	24.79
		0.057			6986.09	395.4656					
-1.30	0.050		150.10	70780.06			32808.70	0.95	2.73	-1.189	25.04
		0.045			8442.81	379.6311					
-1.40	0.040		158.80	79222.87			33188.33	0.96	2.88	-1.289	25.29
		0.036			4964.50	177.3172					
-1.50	0.032		163.70	84187.37			33365.65	0.97	2.97	-1.389	25.54
		0.028			5539.62	157.1652					
-1.60	0.025		169.00	89727.00			33522.81	0.97	3.07	-1.489	25.79
		0.023			5716.06	128.8171					
-1.70	0.020		174.30	95443.06			33651.63	0.97	3.17	-1.589	26.04
		0.018			3983.31	71.3053					
-1.80	0.016		177.90	99426.37			33722.93	0.98	3.23	-1.689	26.29
		0.014			22248.25	316.3542					
-1.90	0.013		196.80	121674.62			34039.29	0.99	3.57	-1.789	26.54
		0.011			6514.87	73.5842					
-2.00	0.010		202.00	128189.50			34112.87	0.99	3.67	-1.889	26.79
$-\infty$							34552.00	(1)			∞

PHOTOMETRIC PARAMETERS OF NGC 4254

B-FILTER

Total luminosity ..... L_T = 9.60

Total apparent magnitude ..... m_T = 10.46

Apparent central surface brightness ..... μ_o = 19.14

Major axis at threshold ..... $2a_m$ = 6.92

Minor axis at threshold ..... $2b_m$ = 6.58

Major axis at μ=25.0 mag sec^{-2} ..... 2a(25) = 5.20

Luminosity within μ=25.0 mag sec^{-2} ..... k(25) = 0.95

Gradient of exponential component ..... G(a) = -0.87

Equivalent gradient of exponential comp.... G(r*) = -0.66

Equivalent gradient of reduced exp. comp.... G(ρ) = -0.82

Parameters at k = ¼ :

- Semi-major axis ..... a_1 = 0.62
- Axis ratio ..... b/a = 0.65
- Equivalent radius ..... r_1* = 0.44
- Surface brightness ..... μ_1 = 21.14

Parameters at k = ½(effective) :

- Semi-major axis ..... a_e = 0.93
- Axis ratio ..... b/a = 0.98
- Equivalent radius ..... r_e* = 0.92
- Surface brightness ..... μ_e = 22.08
- Mean surface brightness ..... μ_e' = 12.25

Parameters at k = ¾ :

- Semi-major axis ..... a_3 = 1.62
- Axis ratio ..... b/a = 0.93
- Equivalent radius ..... r_3* = 1.55
- Surface brightness ..... μ_3 = 22.96

Concentration indices ..... C_{21} = 2.07, C_{32} = 1.69

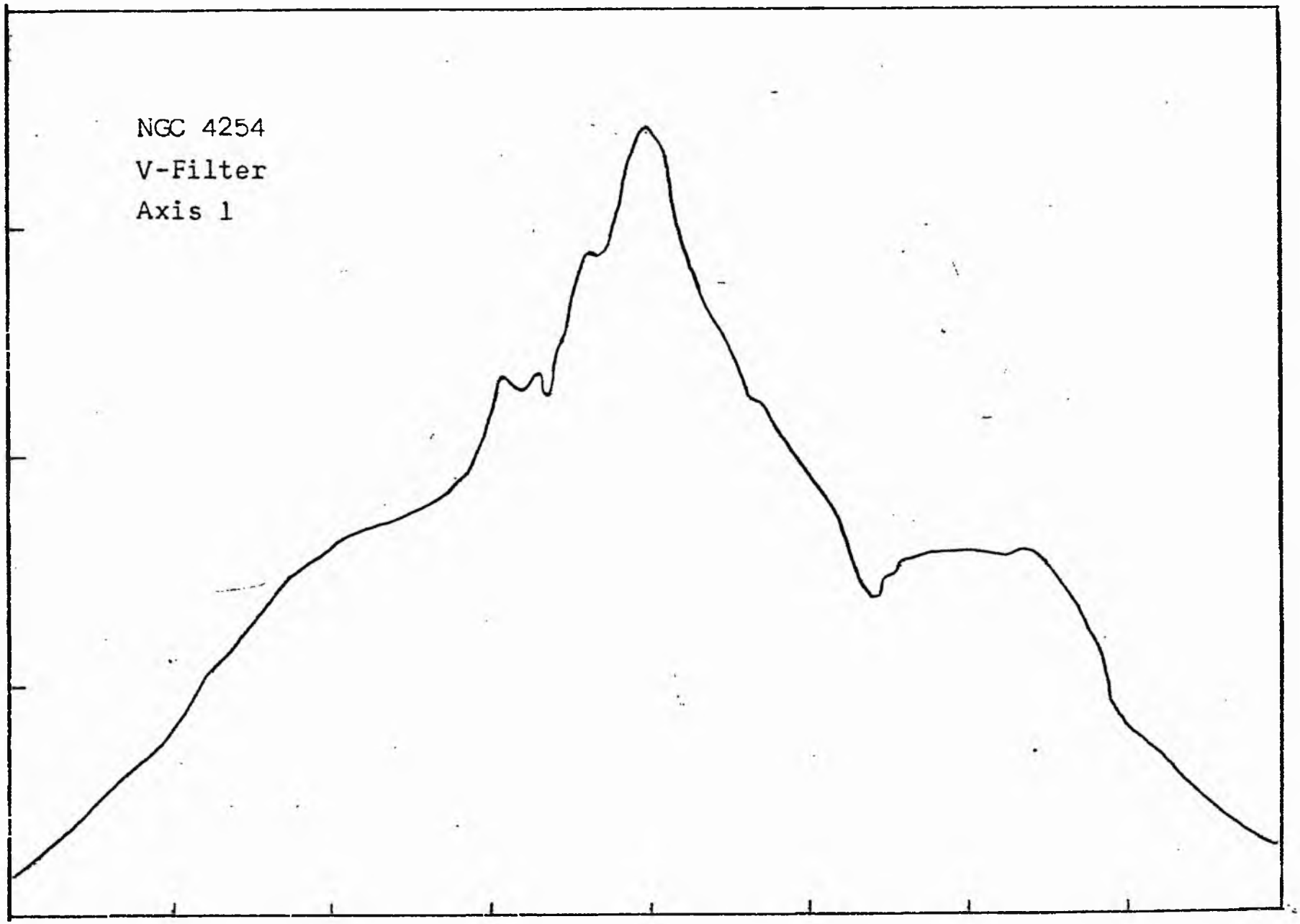
NGC 4254
V-Filter
Axis 1

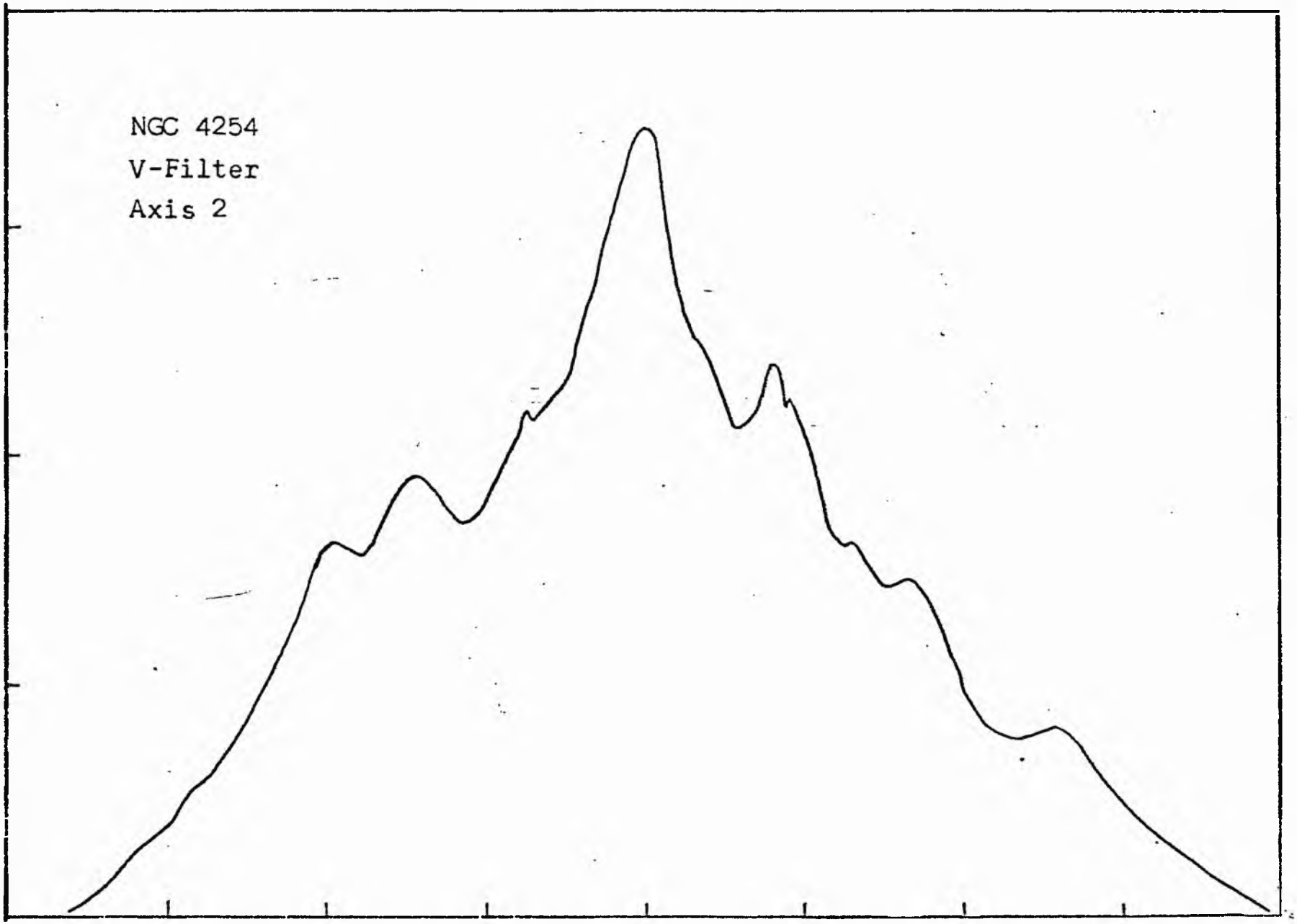
NGC 4254
V-Filter
Axis 2

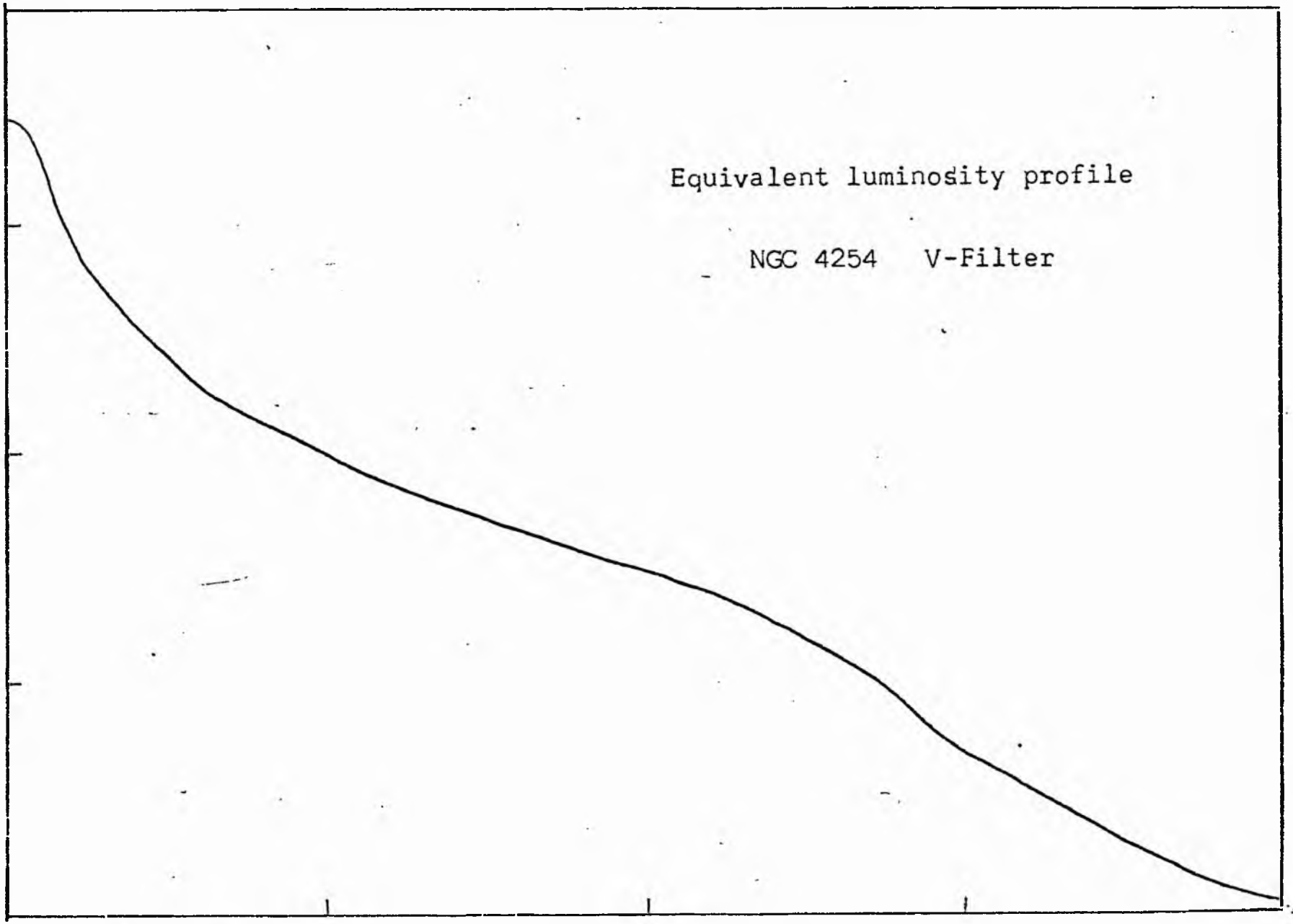
Equivalent luminosity profile
NGC 4254 V-Filter

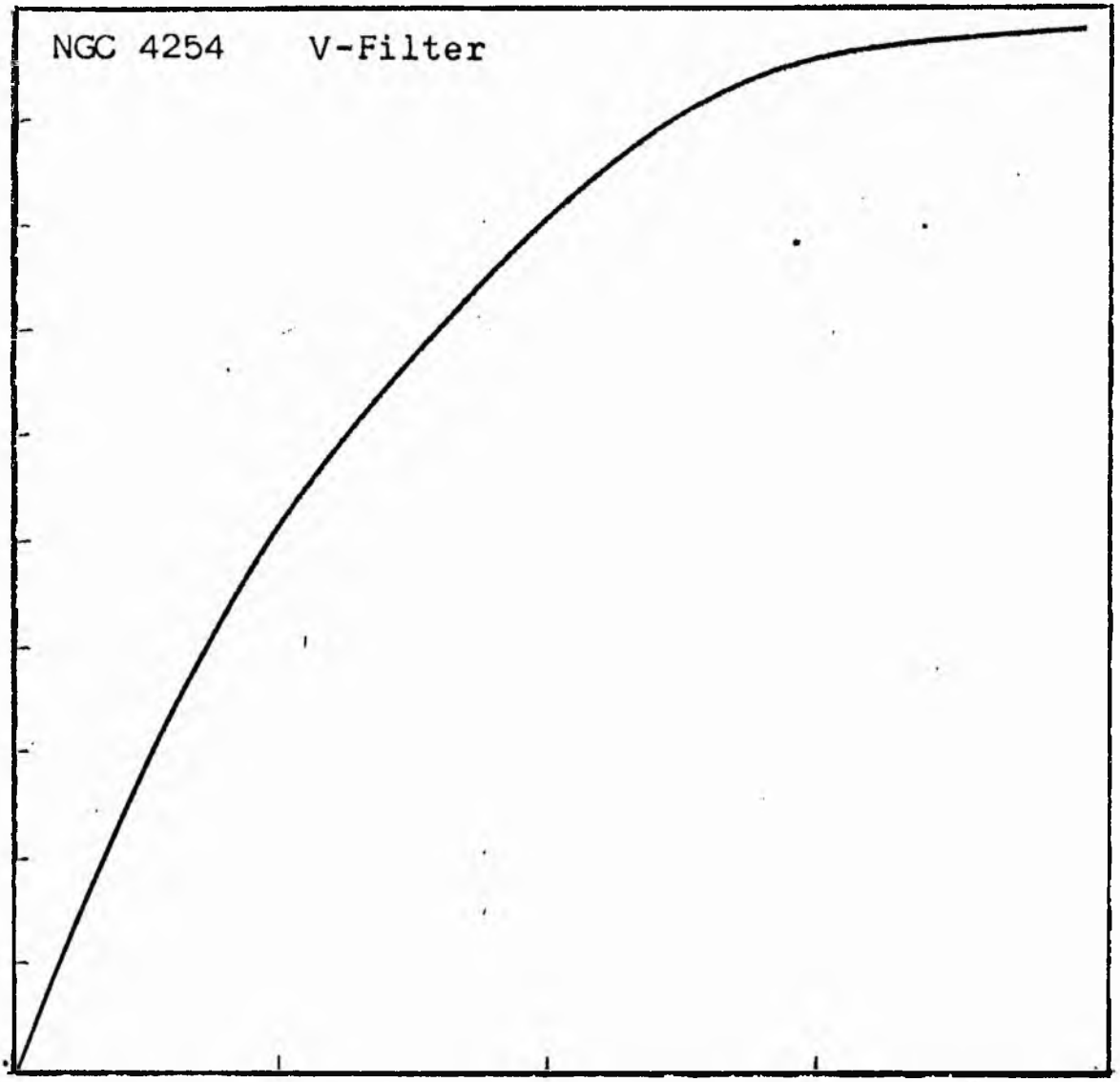

Relative integrated luminosity k(r) versus equivalent radius r*.

MEAN LUMINOSITY DISTRIBUTION IN NGC 4254
V COLOUR

LOG I	I	Ī	R	AREA	ΔA	P	ΣP	K(R)	ρ	LOG J	μ
1.42	26.303		0.0	0.0			0.0	0.0	0.0	1.328	18.00
		25.711			26.42	679.2971					
1.40	25.119		2.90	26.42			679.30	0.02	0.06	1.308	18.05
		22.536			61.83	1393.3930					
1.30	19.953		5.30	88.25			2072.60	0.05	0.11	1.208	18.30
		17.931			48.60	869.9832					
1.20	15.849		6.60	136.85			2942.58	0.07	0.14	1.108	18.55
		14.219			12.72	180.9152					
1.10	12.589		6.90	149.57			3123.50	0.07	0.15	1.008	18.80
		11.295			128.02	1445.9304					
1.00	10.000		9.40	277.59			4569.43	0.11	0.20	0.908	19.05
		8.972			152.46	1367.8232					
0.90	7.943		11.70	430.05			5937.25	0.14	0.25	0.808	19.30
		7.126			239.61	1707.5527					
0.80	6.310		14.60	669.66			7644.80	0.18	0.31	0.708	19.55
		5.661			325.72	1843.7944					
0.70	5.012		17.80	995.38			9488.59	0.22	0.38	0.608	19.80
		4.496			416.58	1873.1174					
0.60	3.981		21.20	1411.96			11361.71	0.26	0.45	0.508	20.05
		3.572			308.25	1100.9746					
0.50	3.162		23.40	1720.21			12462.68	0.29	0.50	0.408	20.30
		2.837			519.40	1473.5742					
0.40	2.512		26.70	2239.61			13936.25	0.32	0.57	0.308	20.55
		2.254			276.46	623.0183					
0.30	1.995		28.30	2516.07			14559.27	0.34	0.60	0.208	20.80
		1.790			2435.36	4359.4727					
0.20	1.585		39.70	4951.43			18918.74	0.44	0.85	0.108	21.05
		1.422			1870.72	2659.9890					
0.10	1.259		46.60	6822.15			21578.73	0.50	1.00	0.008	21.30
		1.129			567.66	641.1445					
-0.00	1.000		48.50	7389.81			22219.87	0.51	1.04	-0.092	21.55
		0.897			2217.46	1989.4204					
-0.10	0.794		55.30	9607.27			24209.29	0.56	1.18	-0.192	21.80
		0.713			3462.54	2467.5464					
-0.20	0.631		64.50	13069.81			26676.84	0.62	1.38	-0.292	22.05
		0.566			4696.02	2658.2783					
-0.30	0.501		75.20	17765.83			29335.11	0.68	1.61	-0.392	22.30
		0.450			7964.60	3581.2524					
-0.40	0.398		90.50	25730.43			32916.36	0.76	1.93	-0.492	22.55
		0.357			6571.29	2347.0466					
-0.50	0.316		101.40	32301.72			35263.41	0.81	2.17	-0.592	22.80
		0.284			8240.40	2337.8638					
-0.60	0.251		113.60	40542.12			37601.27	0.87	2.43	-0.692	23.05
		0.225			5529.99	1246.2214					
-0.70	0.200		121.10	46072.11			38847.49	0.90	2.59	-0.792	23.30
		0.179			5239.01	937.8218					
-0.80	0.158		127.80	51311.12			39785.31	0.92	2.73	-0.892	23.55
		0.142			4763.04	677.2593					
-0.90	0.126		133.60	56074.16			40462.57	0.93	2.86	-0.992	23.80
		0.113			4275.71	482.9248					
-1.00	0.100		138.60	60349.86			40945.49	0.95	2.96	-1.092	24.05
		0.093			1137.42	102.0452					
-1.10	0.079		139.90	61487.28			41047.53	0.95	2.99	-1.192	24.30
		0.071			4291.66	305.8423					
-1.20	0.063		144.70	65778.94			41353.37	0.96	3.09	-1.292	24.55
		0.057			4061.19	229.8932					
-1.30	0.050		149.10	69840.12			41583.26	0.96	3.19	-1.392	24.80
		0.045			4859.50	218.5070					
-1.40	0.040		154.20	74699.62			41801.77	0.97	3.30	-1.492	25.05
		0.036			6027.00	215.2661					
-1.50	0.032		160.30	80726.62			42017.03	0.97	3.43	-1.592	25.30
		0.028			7730.62	219.3258					
-1.60	0.025		167.80	88457.25			42236.36	0.98	3.59	-1.692	25.55
		0.023			4916.37	110.7952					
-1.70	0.020		172.40	93373.62			42347.15	0.98	3.68	-1.792	25.80
		0.018			6724.56	120.3761					
-1.80	0.016		178.50	100098.19			42467.52	0.98	3.81	-1.892	26.05
		0.014			9760.12	138.7817					
-1.90	0.013		187.00	109858.31			42606.30	0.98	4.00	-1.992	26.30
		0.011			11692.69	132.0662					
-2.00	0.010		196.70	121551.00			42738.37	0.99	4.20	-2.092	26.55
$-\infty$							43208.00	(1)			∞

PHOTOMETRIC PARAMETERS OF NGC 4254

V-FILTER

Total luminosity	L_T	= 12.01
Total apparent magnitude	m_T	= 9.96
Apparent central surface brightness	μ_o	= 18.00
Major axis at threshold	$2a_m$	= 7.02
Minor axis at threshold	$2b_m$	= 6.26
Major axis at μ=25.0 mag sec^{-2}	2a(25)	= 4.96
Luminosity within μ=25.0 mag sec^{-2}	k(25)	= 0.96
Gradient of exponential component	G(a)	= -0.89
Equivalent gradient of exponential comp.	G(r*)	= -0.68
Equivalent gradient of reduced exp. comp.	G(ρ)	= -0.71
Parameters at k = ¼ :		
Semi-major axis	a_1	= 0.28
Axis ratio	b/a	= 0.88
Equivalent radius	r_1*	= 0.34
Surface brightness	μ_1	= 19.99
Parameters at k = ½(effective) :		
Semi-major axis	a_e	= 0.73
Axis ratio	b/a	= 0.95
Equivalent radius	r_e*	= 0.78
Surface brightness	μ_e	= 21.30
Mean surface brightness	μ_e'	= 11.41
Parameters at k = ¾ :		
Semi-major axis	a_3	= 1.42
Axis ratio	b/a	= 1.12
Equivalent radius	r_3*	= 1.47
Surface brightness	μ_3	= 22.52
Concentration indices	C_{21}	= 2.32
	C_{32}	= 1.89

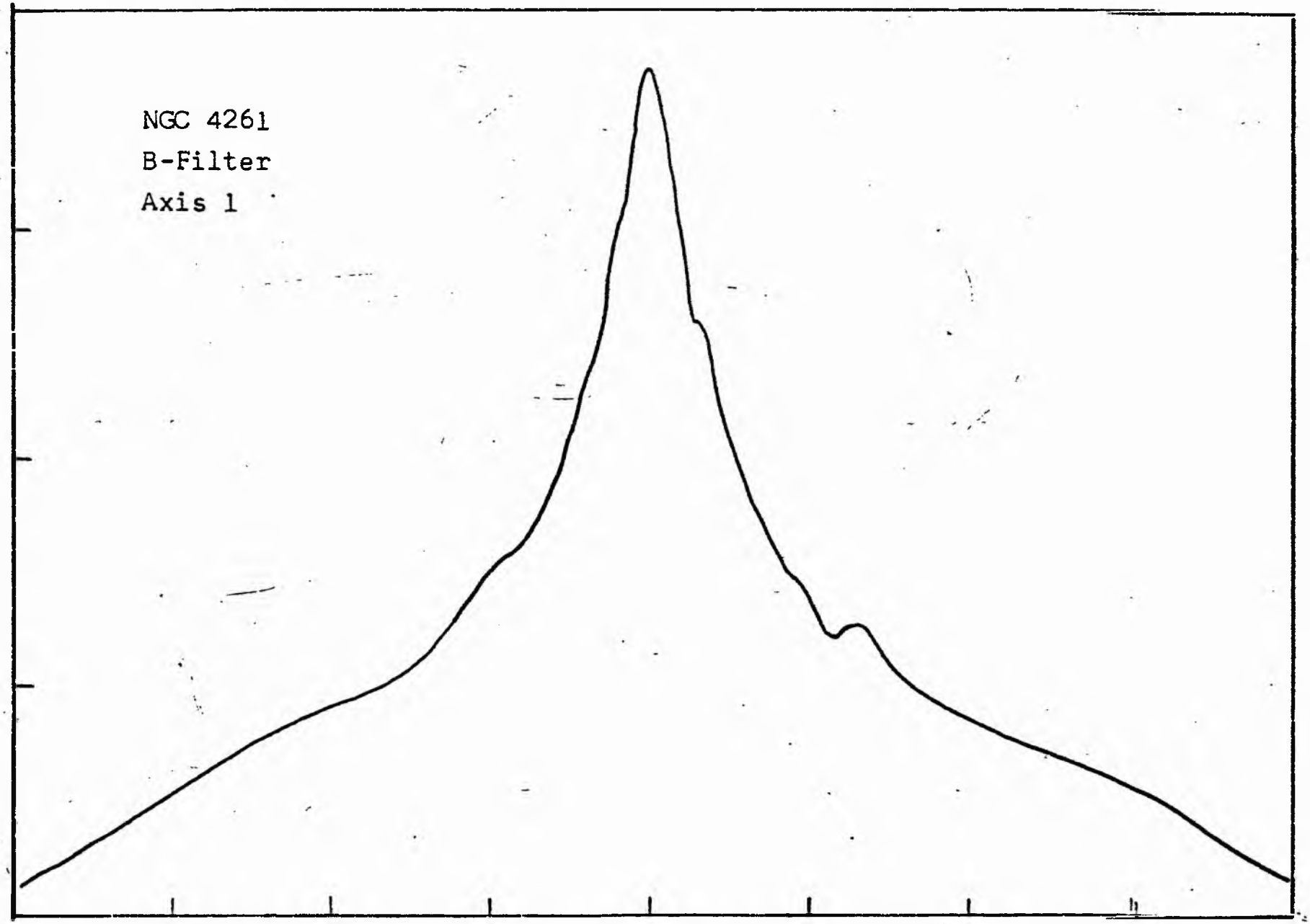
NGC 4261
B-Filter
Axis 1

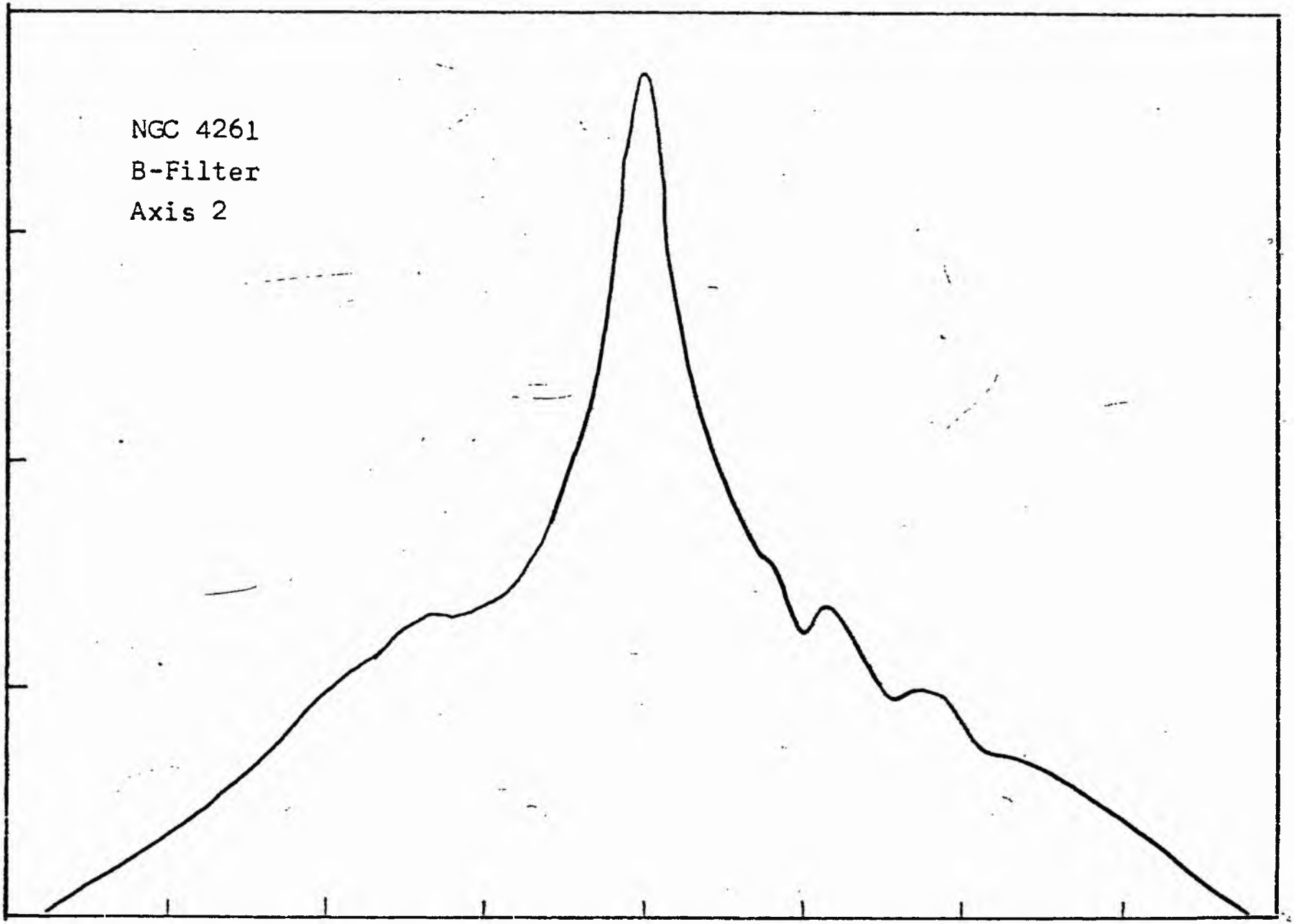
NGC 4261
B-Filter
Axis 2

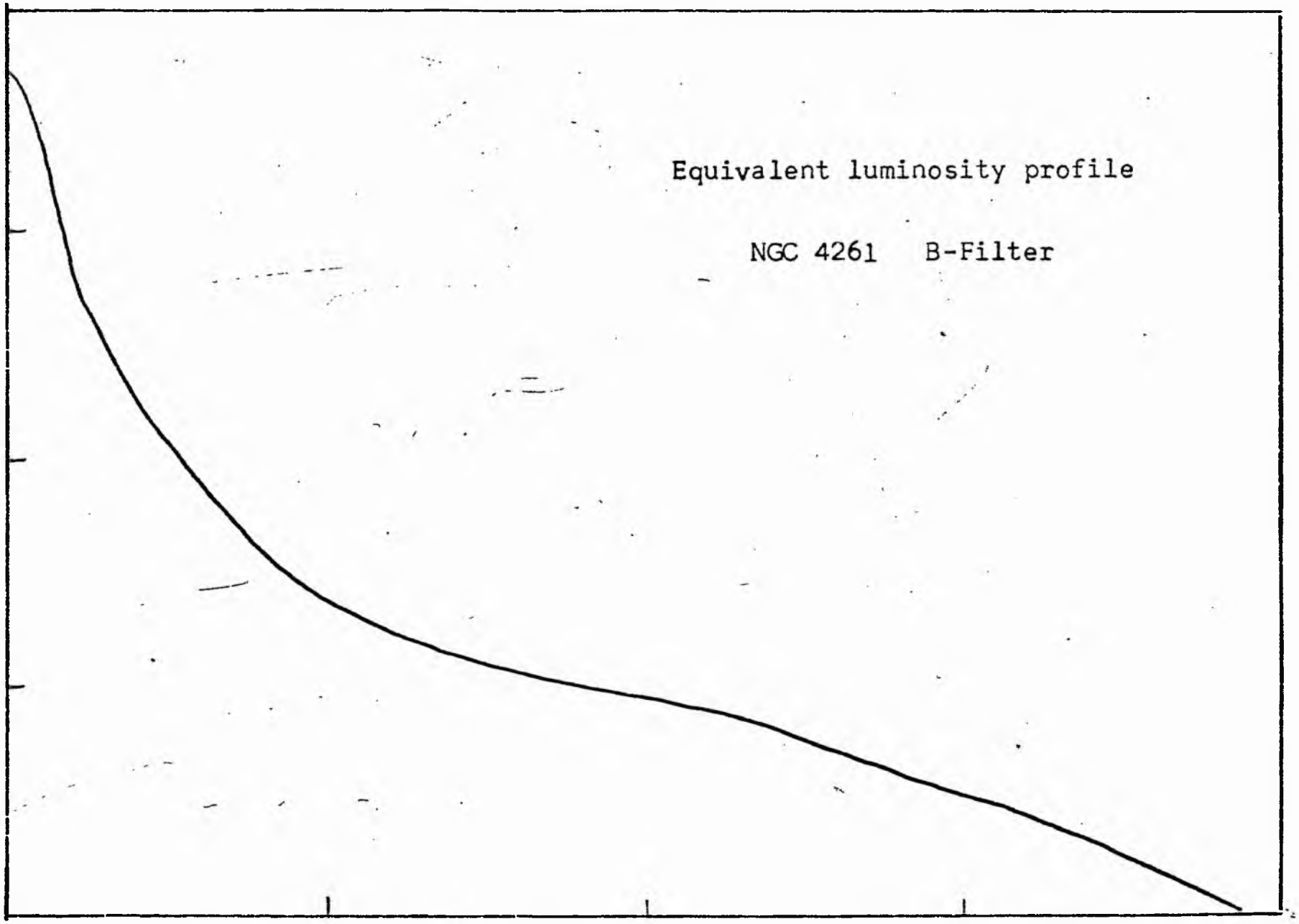
Equivalent luminosity profile
NGC 4261 B-Filter

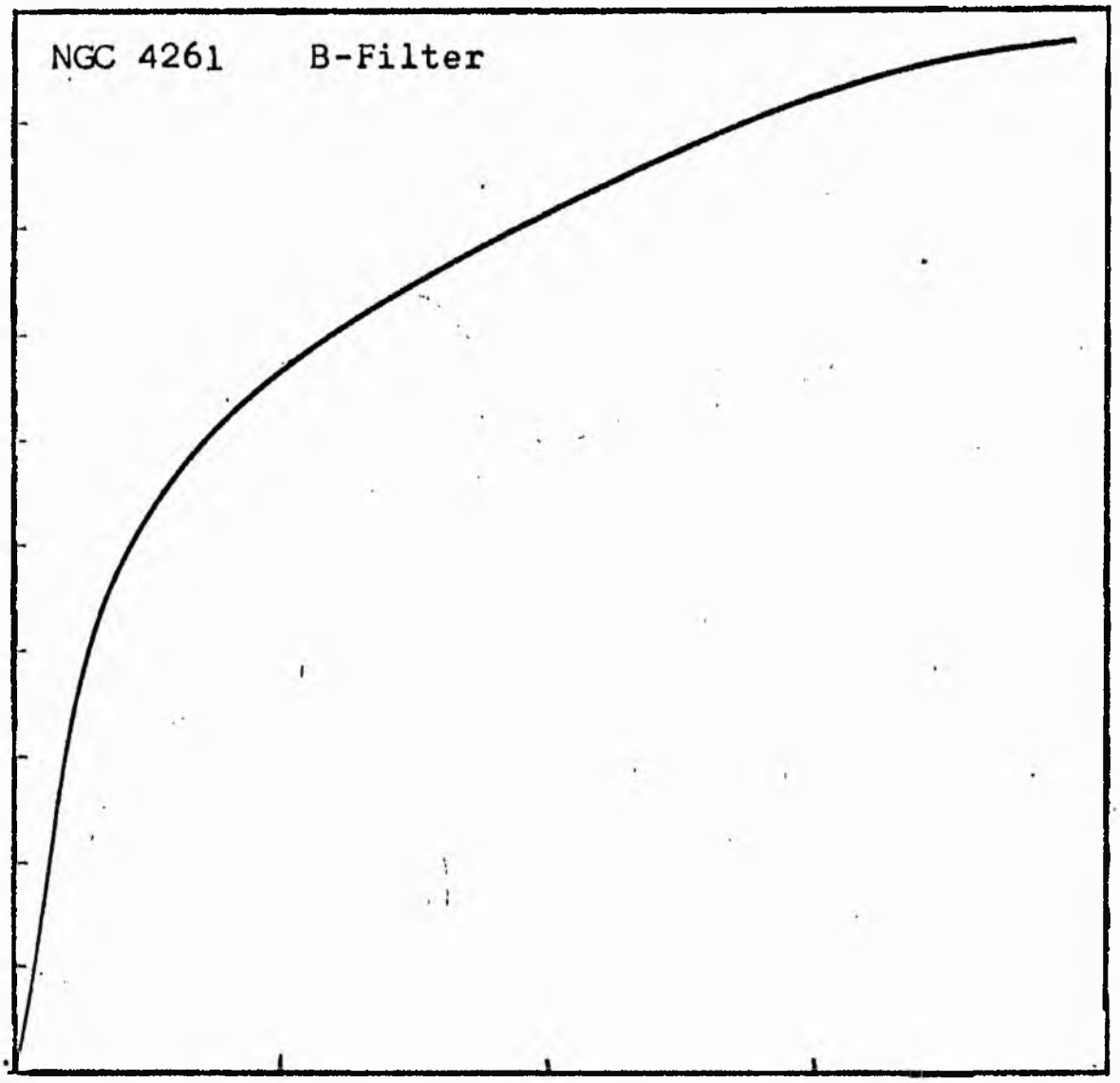

Relative integrated luminosity k(r) versus equivalent radius r*.

MEAN LUMINOSITY DISTRIBUTION IN NGC 4261
B COLOUR

LOG I	.I	$\bar{I}$	R	AREA	ΔA	P	ΣP	K(R)	ρ	LOG J	μ
1.68	47.863		0.0	0.0			0.0	0.0	0.0	1.509	18.01
		43.837			36.32	1592.0120					
1.60	39.811		3.40	36.32			1592.01	0.08	0.15	1.429	18.21
		35.717			19.10	682.2185					
1.50	31.623		4.20	55.42			2274.23	0.11	0.19	1.329	18.46
		28.371			36.19	1026.7700					
1.40	25.119		5.40	91.61			3301.00	0.16	0.24	1.229	18.71
		22.536			29.15	657.0039					
1.30	19.953		6.20	120.76			3958.00	0.20	0.28	1.129	18.96
		17.901			42.10	753.5723					
1.20	15.849		7.20	162.86			4711.57	0.23	0.32	1.029	19.21
		14.219			53.56	761.6287					
1.10	12.589		8.30	216.42			5473.20	0.27	0.37	0.929	19.46
		11.295			49.48	558.8547					
1.00	10.000		9.20	265.90			6032.05	0.30	0.41	0.829	19.71
		8.972			42.00	376.8325					
0.90	7.943		9.90	307.91			6408.88	0.32	0.45	0.729	19.96
		7.126			58.53	417.0935					
0.80	6.310		10.80	366.44			6825.97	0.34	0.49	0.629	20.21
		5.661			71.00	401.9089					
0.70	5.012		11.80	437.44			7227.88	0.36	0.53	0.529	20.46
		4.496			109.96	494.4102					
0.60	3.981		13.20	547.39			7722.29	0.38	0.59	0.429	20.71
		3.572			178.44	637.3342					
0.50	3.162		15.20	725.03			8359.62	0.41	0.68	0.329	20.96
		2.837			203.57	577.5549					
0.40	2.512		17.20	929.41			8937.18	0.44	0.77	0.229	21.21
		2.254			169.17	381.2449					
0.30	1.995		18.70	1098.58			9318.42	0.46	0.84	0.129	21.46
		1.790			340.14	608.8745					
0.20	1.585		21.40	1438.72			9927.29	0.49	0.96	0.029	21.71
		1.422			416.35	592.0144					
0.10	1.259		24.30	1855.08			10519.30	0.52	1.09	-0.071	21.96
		1.129			401.34	453.2942					
-0.00	1.000		26.80	2256.42			10972.59	0.54	1.21	-0.171	22.21
		0.897			552.20	495.4102					
-0.10	0.794		29.90	2808.61			11468.00	0.57	1.35	-0.271	22.46
		0.713			571.23	407.0840					
-0.20	0.631		32.80	3379.85			11875.09	0.59	1.48	-0.371	22.71
		0.566			737.02	417.2039					
-0.30	0.501		36.20	4116.87			12292.29	0.61	1.63	-0.471	22.96
		0.450			395.75	177.9453					
-0.40	0.398		37.90	4512.61			12470.23	0.62	1.71	-0.571	23.21
		0.357			1215.42	434.1057					
-0.50	0.316		42.70	5728.03			12904.34	0.64	1.92	-0.671	23.46
		0.284			1661.78	471.4578					
-0.60	0.251		48.50	7389.81			13375.80	0.66	2.18	-0.771	23.71
		0.225			2252.24	507.5566					
-0.70	0.200		55.40	9642.05			13883.35	0.69	2.49	-0.871	23.96
		0.179			2945.96	527.3484					
-0.80	0.158		63.30	12588.01			14410.70	0.71	2.85	-0.971	24.21
		0.142			4708.46	669.4973					
-0.90	0.126		74.20	17296.47			15080.20	0.75	3.34	-1.071	24.46
		0.113			7812.26	882.3625					
-1.00	0.100		89.40	25108.73			15962.55	0.79	4.03	-1.171	24.71
		0.090			9791.72	878.4763					
-1.10	0.079		105.40	34900.45			16841.03	0.83	4.75	-1.271	24.96
		0.071			10564.96	752.9031					
-1.20	0.063		120.30	45465.40			17593.93	0.87	5.42	-1.371	25.21
		0.057			8777.21	496.8538					
-1.30	0.050		131.40	54242.61			18090.78	0.90	5.92	-1.471	25.46
		0.045			9551.36	429.4751					
-1.40	0.040		142.50	63793.97			18520.25	0.92	6.42	-1.571	25.71
		0.036			10325.47	368.7935					
-1.50	0.032		153.60	74119.44			18889.05	0.94	6.92	-1.671	25.96
		0.028			8736.12	247.8524					
-1.60	0.025		162.40	82855.56			19136.90	0.95	7.31	-1.771	26.21
		0.023			8792.94	198.1567					
-1.70	0.020		170.80	91648.50			19335.05	0.96	7.69	-1.871	26.46
		0.018			8898.81	159.2969					
-1.80	0.016		178.90	100547.31			19494.35	0.97	8.06	-1.971	26.71
		0.014			8607.19	122.3875					
-1.90	0.013		186.40	109154.50			19616.74	0.97	8.39	-2.071	26.96
		0.011			10549.69	119.1560					
-2.00	0.010		195.20	119704.19			19735.89	0.98	8.79	-2.171	27.21
$-\infty$							20195.00	(1)			∞

PHOTOMETRIC PARAMETERS OF NGC 4261

B-FILTER

Total luminosity ..... L_T = 5.61

Total apparent magnitude ..... m_T = 11.45

Apparent central surface brightness ..... μ_o = 18.01

Major axis at threshold ..... $2a_m$ = 6.80

Minor axis at threshold ..... $2b_m$ = 6.32

Major axis at μ=25.0 mag sec^{-2} ..... 2a(25) = 4.01

Luminosity within μ=25.0 mag sec^{-2} ..... k(25) = 0.84

Gradient of exponential component ..... G(a) = -0.54

Equivalent gradient of exponential comp..... G(r*) = -0.51

Equivalent gradient of reduced exp. comp..... G(ρ) = -0.18

Parameters at k = ¼ :

- Semi-major axis ..... a_1 = 0.16
- Axis ratio ..... b/a = 1.20
- Equivalent radius ..... r_1* = 0.13
- Surface brightness ..... μ_1 = 19.33

Parameters at k = ½(effective) :

- Semi-major axis ..... a_e = 0.36
- Axis ratio ..... b/a = 0.95
- Equivalent radius ..... r_e* = 0.37
- Surface brightness ..... μ_e = 21.79
- Mean surface brightness ..... μ_e' = 11.30

Parameters at k = ¾ :

- Semi-major axis ..... a_3 = 1.23
- Axis ratio ..... b/a = 1.07
- Equivalent radius ..... r_3* = 1.26
- Surface brightness ..... μ_3 = 24.46

Concentration indices ..... C_{21} = 2.89, C_{32} = 3.39

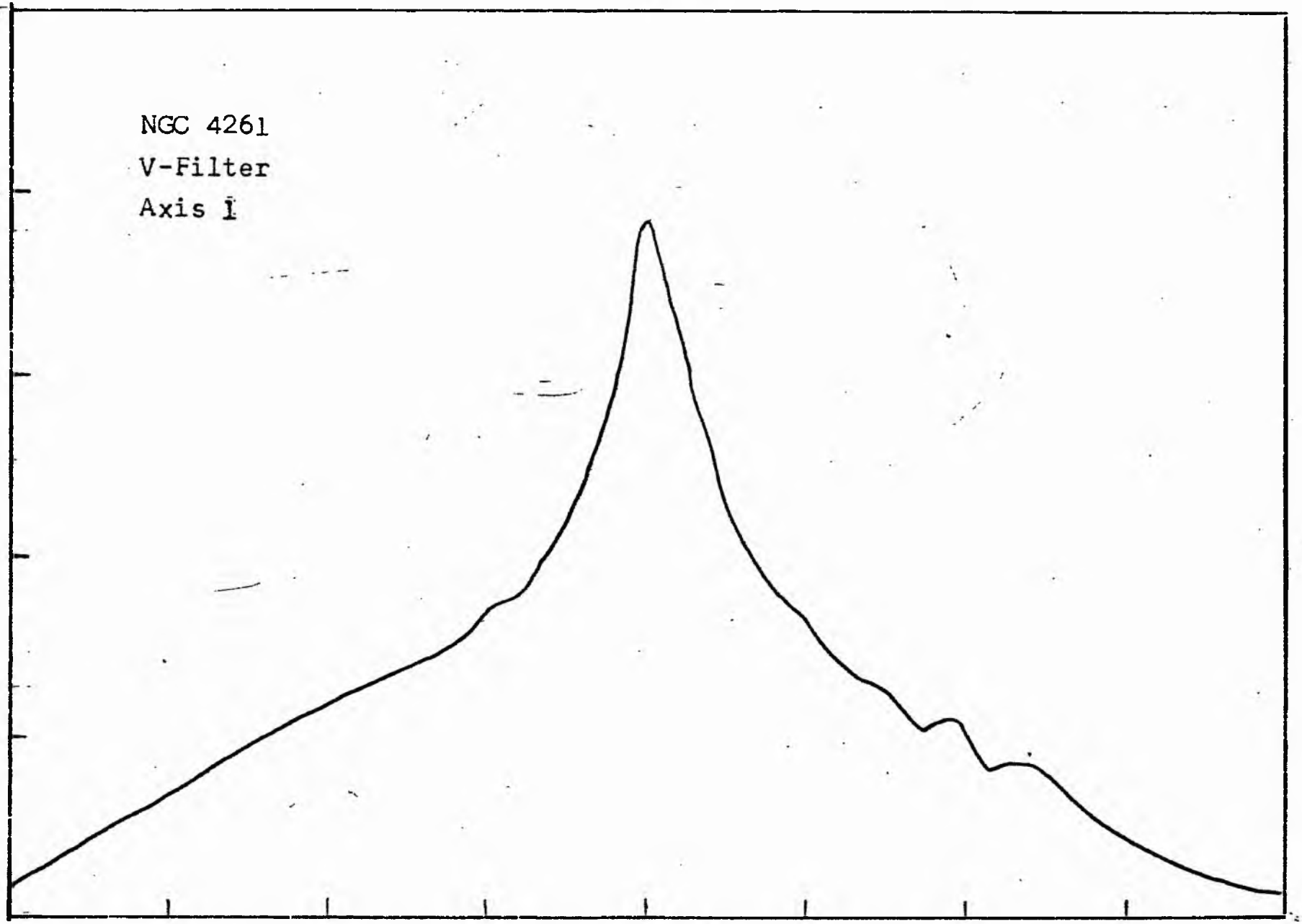
NGC 4261
V-Filter
Axis I

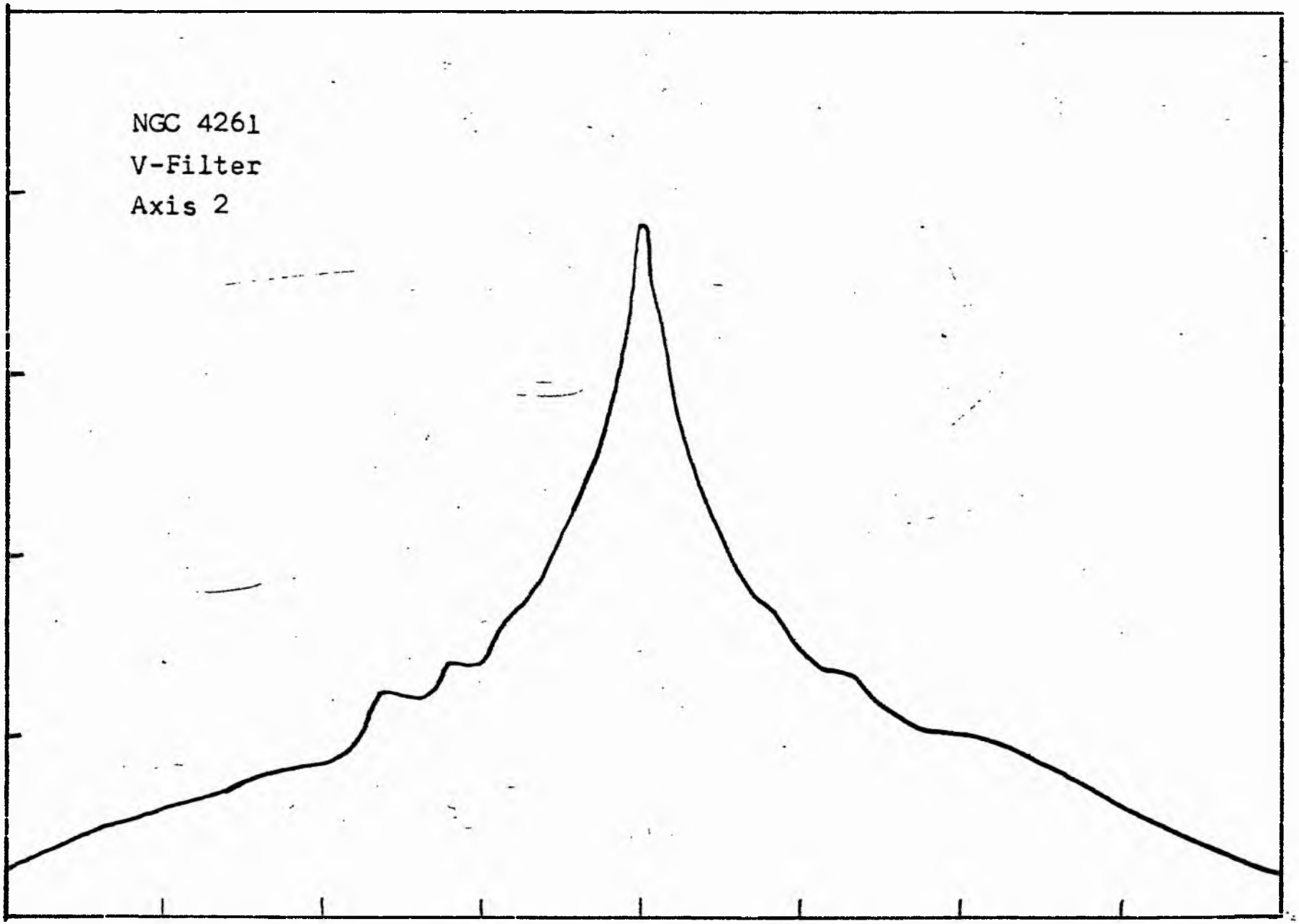
NGC 4261
V-Filter
Axis 2

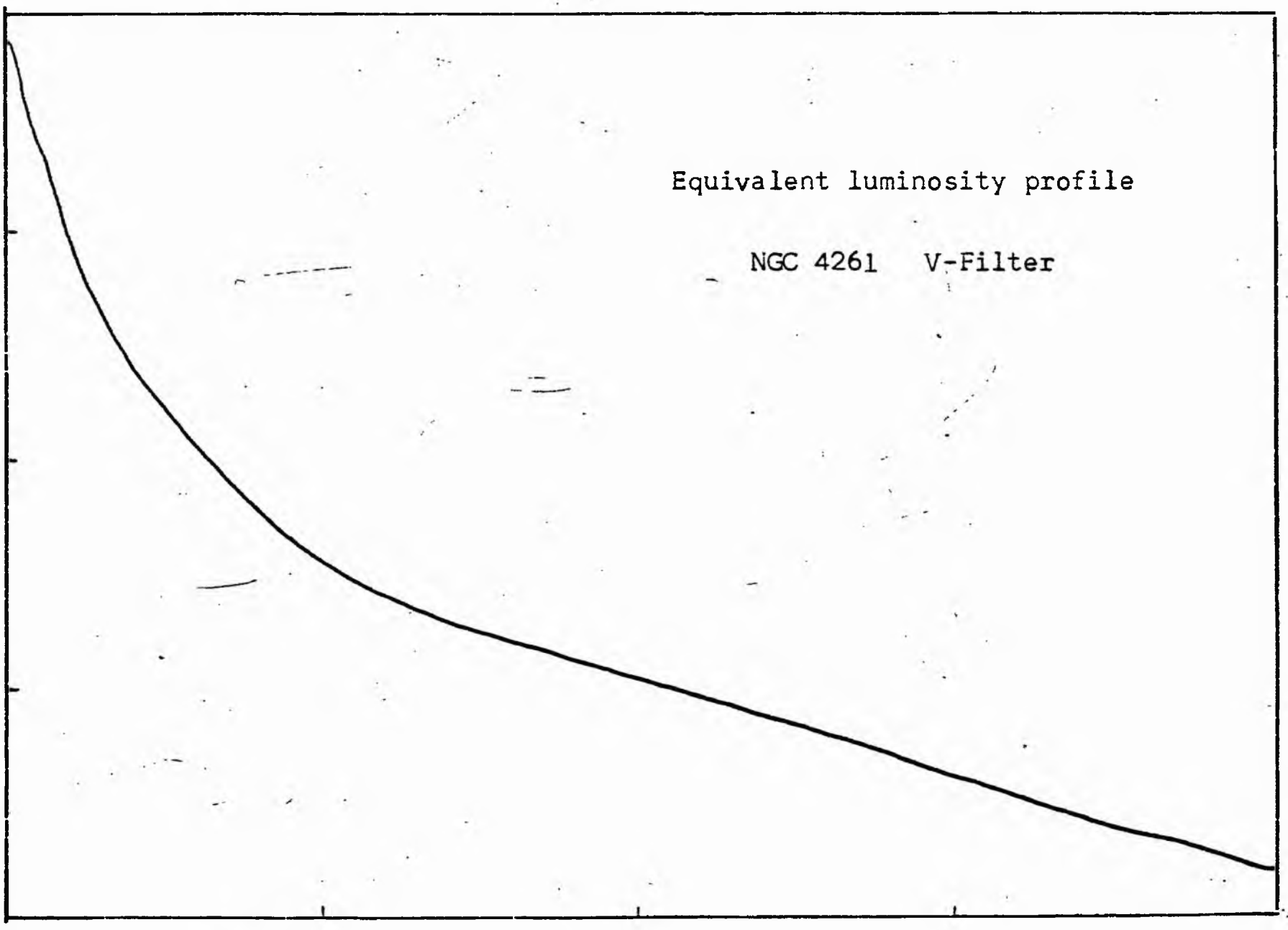
Equivalent luminosity profile
NGC 4261 V-Filter

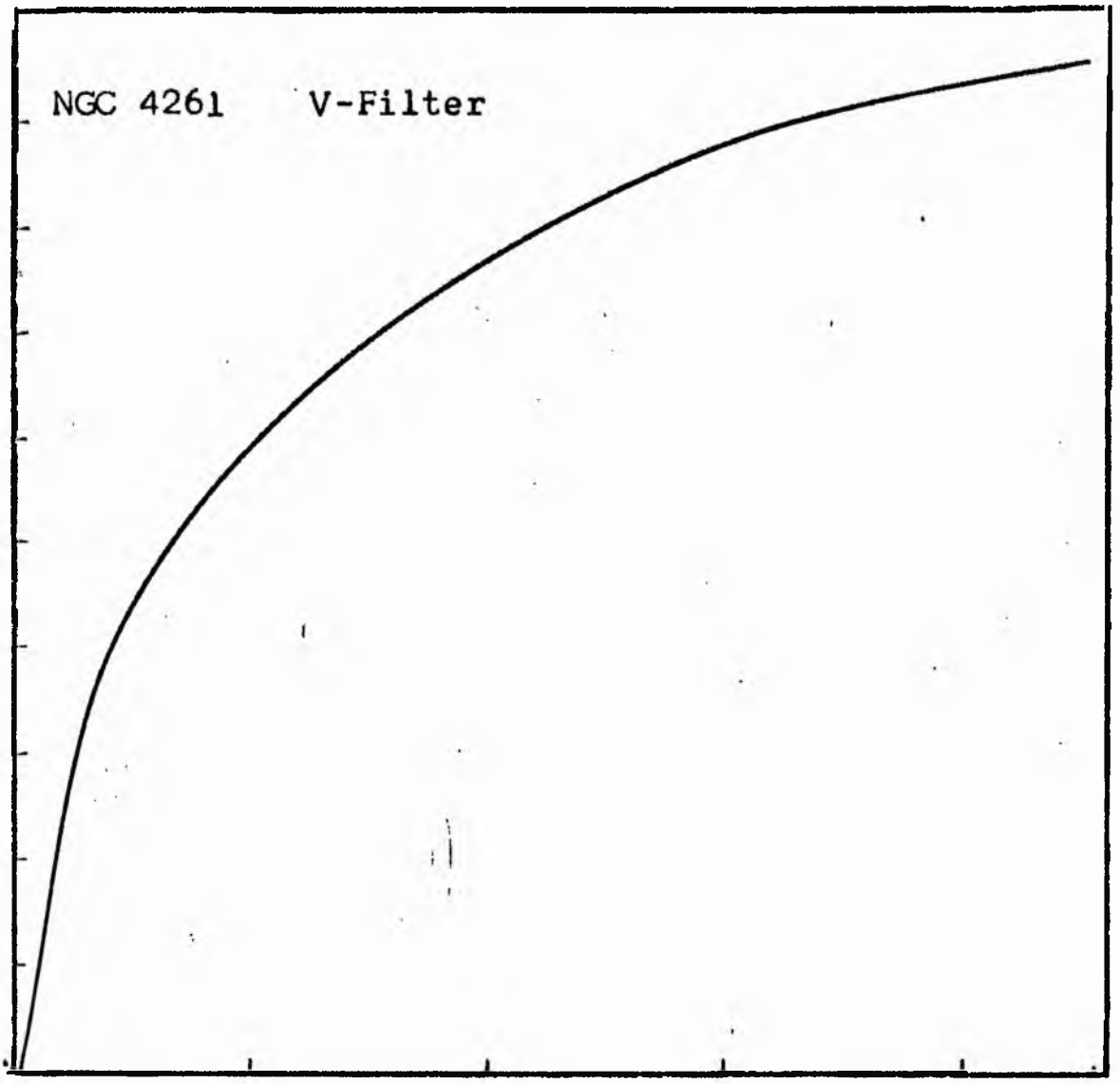

Relative integrated luminosity k(r) versus equivalent radius r*.

MEAN LUMINOSITY DISTRIBUTION IN NGC 4261
V COLOUR

LOG I	I	$\bar{I}$	R	AREA	ΔA	P	ΣP	K(R)	ρ	LOG J	μ
1.86	72.444		0.0	0.0			0.0	0.0	0.0	1.856	16.76
		67.770			0.28	19.1614					
1.80	63.096		0.30	0.28			19.16	0.00	0.01	1.796	16.91
		56.637			2.26	128.0422					
1.70	50.119		0.90	2.54			147.20	0.01	0.03	1.696	17.16
		44.965			3.61	162.4491					
1.60	39.811		1.40	6.16			309.65	0.01	0.04	1.596	17.41
		35.717			7.70	274.9070					
1.50	31.623		2.10	13.85			584.56	0.02	0.07	1.496	17.66
		28.371			55.54	1575.8018					
1.40	25.119		4.70	69.40			2160.36	0.08	0.15	1.396	17.91
		22.536			59.28	1335.9517					
1.30	19.952		6.40	128.68			3496.31	0.13	0.20	1.296	18.16
		17.901			62.45	1117.9819					
1.20	15.849		7.80	191.13			4614.29	0.18	0.25	1.196	18.41
		14.219			41.22	586.0732					
1.10	12.589		8.60	232.35			5200.36	0.20	0.27	1.096	18.66
		11.295			51.18	578.0134					
1.00	10.000		9.50	283.53			5778.37	0.22	0.30	0.996	18.91
		8.972			76.15	683.2056					
0.90	7.943		10.70	359.68			6461.58	0.25	0.34	0.896	19.16
		7.126			115.61	823.8835					
0.80	6.310		12.30	475.29			7285.46	0.28	0.39	0.796	19.41
		5.661			97.26	550.5781					
0.70	5.012		13.50	572.56			7836.04	0.30	0.43	0.696	19.66
		4.496			148.51	667.7700					
0.60	3.981		15.15	721.07			8503.81	0.33	0.48	0.596	19.91
		3.572			222.44	794.4880					
0.50	3.162		17.33	943.51			9298.29	0.36	0.55	0.496	20.16
		2.837			214.61	608.8513					
0.40	2.512		19.20	1158.12			9907.14	0.38	0.61	0.396	20.41
		2.254			401.37	904.4998					
0.30	1.995		22.28	1559.48			10811.64	0.41	0.70	0.296	20.66
		1.790			465.75	833.7273					
0.20	1.585		25.39	2025.23			11645.36	0.45	0.80	0.196	20.91
		1.422			528.31	751.2095					
0.10	1.259		28.51	2553.55			12396.57	0.47	0.90	0.096	21.16
		1.129			621.36	701.7939					
-0.00	1.000		31.79	3174.90			13098.36	0.50	1.00	-0.004	21.41
		0.897			713.23	639.8801					
-0.10	0.794		35.18	3888.14			13738.24	0.53	1.11	-0.104	21.66
		0.713			352.47	251.1836					
-0.20	0.631		36.74	4240.61			13989.43	0.54	1.16	-0.204	21.91
		0.566			1089.46	616.7112					
-0.30	0.501		41.19	5330.07			14606.14	0.56	1.30	-0.304	22.16
		0.450			1500.87	674.8560					
-0.40	0.398		46.63	6830.94			15280.99	0.58	1.47	-0.404	22.41
		0.357			2010.45	718.0623					
-0.50	0.316		53.05	8841.39			15999.05	0.61	1.68	-0.504	22.66
		0.284			2638.62	748.5947					
-0.60	0.251		60.45	11480.01			16747.64	0.64	1.91	-0.604	22.91
		0.225			3407.81	767.9709					
-0.70	0.200		68.84	14887.82			17515.61	0.67	2.17	-0.704	23.16
		0.179			6303.26	1128.3259					
-0.80	0.158		82.13	21191.09			18643.94	0.71	2.59	-0.804	23.41
		0.142			9936.46	1412.8662					
-0.90	0.126		99.54	31127.55			20056.80	0.77	3.14	-0.904	23.66
		0.113			7726.60	872.6860					
-1.00	0.100		111.21	38854.15			20929.48	0.80	3.51	-1.004	23.91
		0.090			8899.38	798.4175					
-1.10	0.079		123.29	47753.54			21727.90	0.83	3.89	-1.104	24.16
		0.071			8960.40	638.5547					
-1.20	0.063		134.36	56713.94			22366.45	0.86	4.24	-1.204	24.41
		0.057			8665.58	490.5339					
-1.30	0.050		144.26	65379.52			22856.98	0.87	4.56	-1.304	24.66
		0.045			10878.29	489.1394					
-1.40	0.040		155.80	76257.81			23346.12	0.89	4.92	-1.404	24.91
		0.036			13586.00	485.2483					
-1.50	0.032		169.11	89843.81			23831.37	0.91	5.34	-1.504	25.16
		0.028			11717.69	332.4412					
-1.60	0.025		179.80	101561.50			24163.80	0.92	5.68	-1.604	25.41
		0.023			10416.06	234.5995					
-1.70	0.020		188.79	111971.56			24398.40	0.93	5.96	-1.704	25.66
		0.018			9270.62	165.9523					
-1.80	0.016		196.45	121242.19			24564.35	0.94	6.20	-1.804	25.91
		0.014			20420.12	290.3577					
-1.90	0.013		212.35	141662.31			24854.71	0.95	6.71	-1.904	26.16
		0.011			17013.44	192.1620					
-2.00	0.010		224.74	158675.75			25046.87	0.96	7.10	-2.004	26.41
$-\infty$							26146.00	(1)			∞

PHOTOMETRIC PARAMETERS OF NGC 4261

V-FILTER

Total luminosity ..... L_T = 7.26

Total apparent magnitude ..... m_T = 10.37

Apparent central surface brightness ..... μ_o = 16.76

Major axis at threshold ..... $2a_m$ = 7.3

Minor axis at threshold ..... $2b_m$ = 7.22

Major axis at μ=25.0 mag sec^{-2} ..... 2a(25) = 5.2

Luminosity within μ=25.0 mag sec^{-2} ..... k(25) = 0.90

Gradient of exponential component ..... G(a) = -0.53

Equivalent gradient of exponential comp..... G(r*) = -0.53

Equivalent gradient of reduced exp. comp..... G(ρ) = -0.27

Parameters at k = ¼ :

- Semi-major axis ..... a_1 = 0.21
- Axis ratio ..... b/a = 0.96
- Equivalent radius ..... r_1* = 0.18
- Surface brightness ..... μ_1 = 19.16

Parameters at k = ½(effective) :

- Semi-major axis ..... a_e = 0.53
- Axis ratio ..... b/a = 0.87
- Equivalent radius ..... r_e* = 0.53
- Surface brightness ..... μ_e = 21.41
- Mean surface brightness ..... μ_e' = 10.87

Parameters at k = ¾ :

- Semi-major axis ..... a_3 = 1.59
- Axis ratio ..... b/a = 0.96
- Equivalent radius ..... r_3* = 1.56
- Surface brightness ..... μ_3 = 23.58

Concentration indices ..... C_{21} = 2.92, C_{32} = 2.96

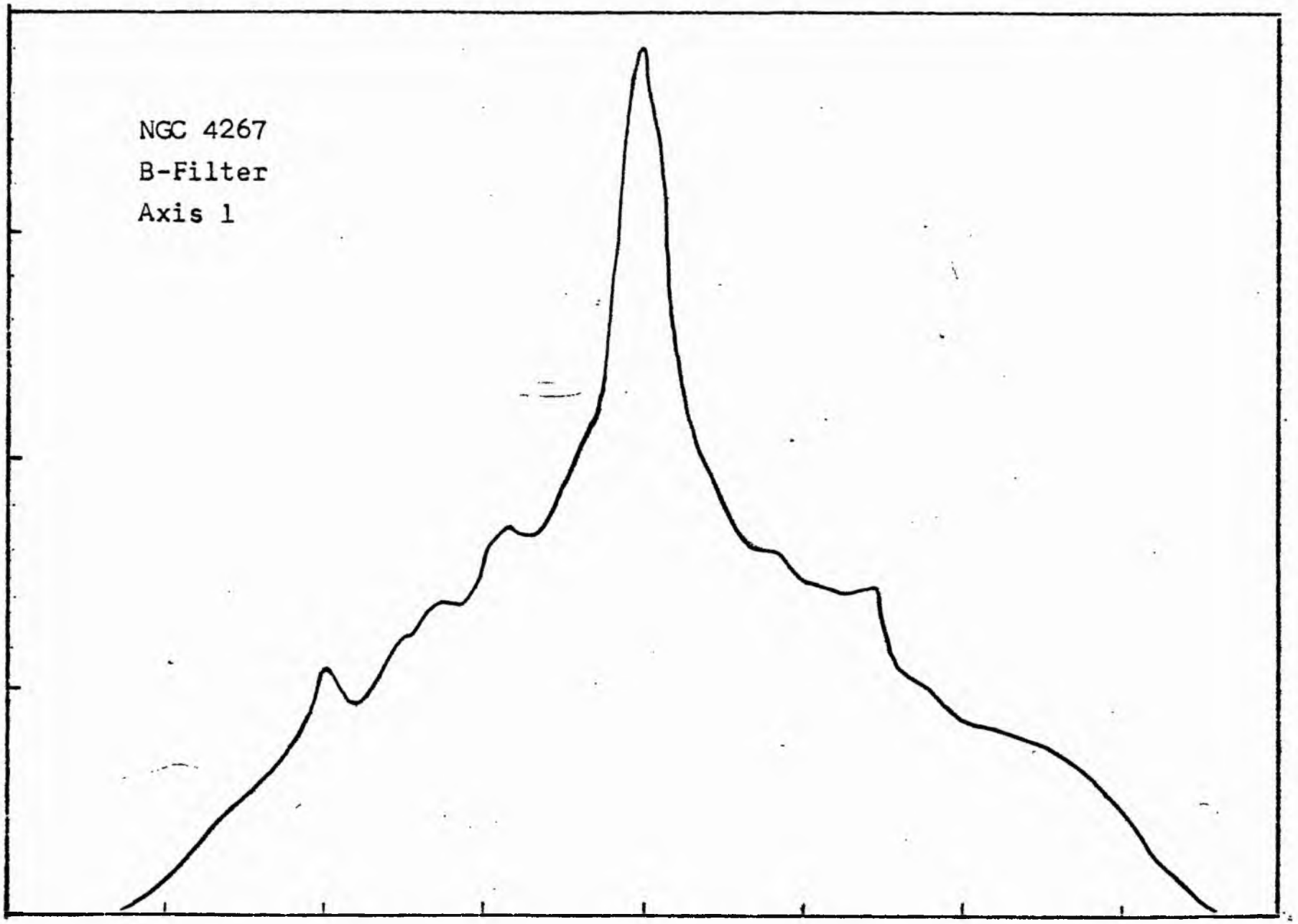
NGC 4267
B-Filter
Axis 1

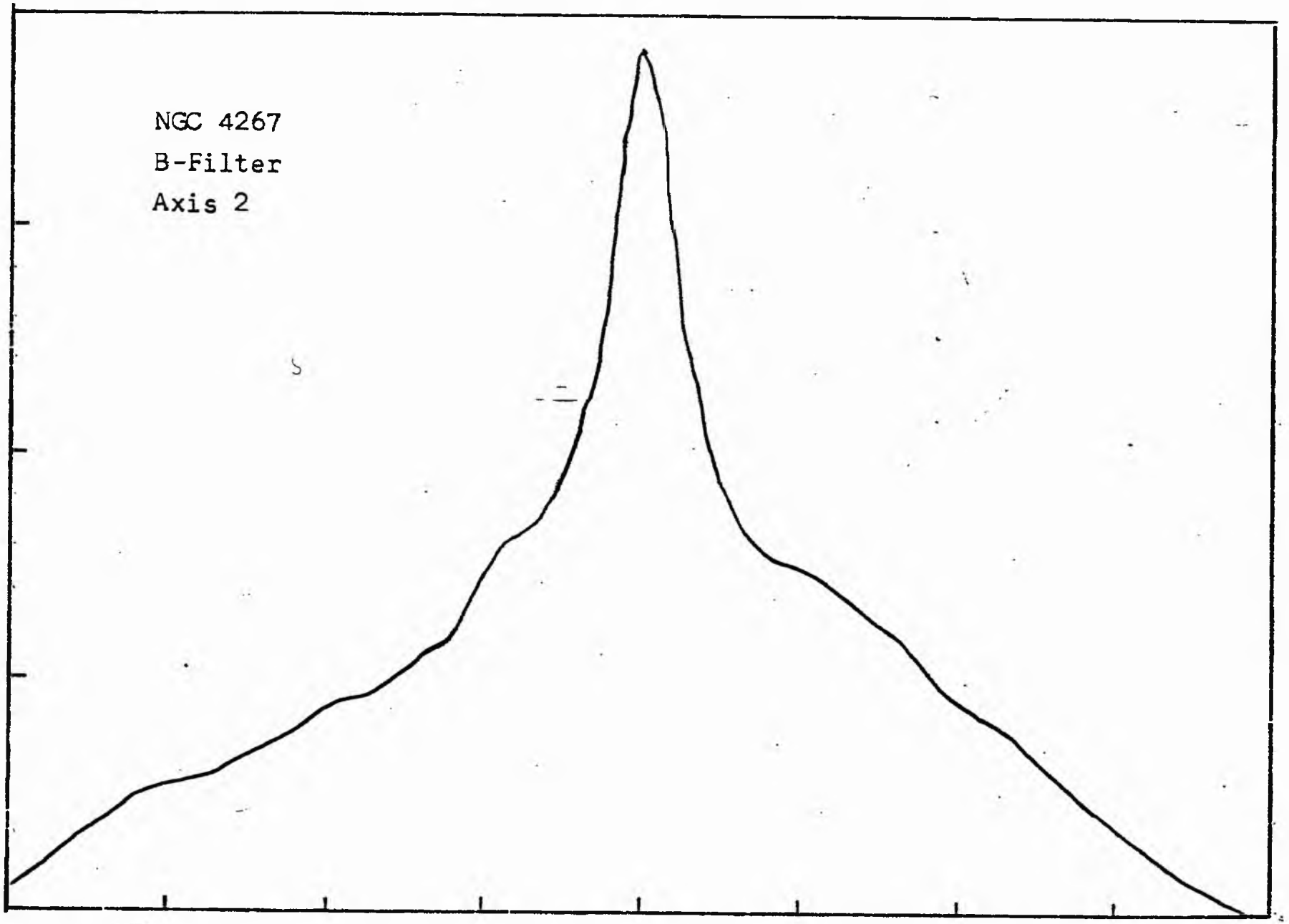
NGC 4267
B-Filter
Axis 2

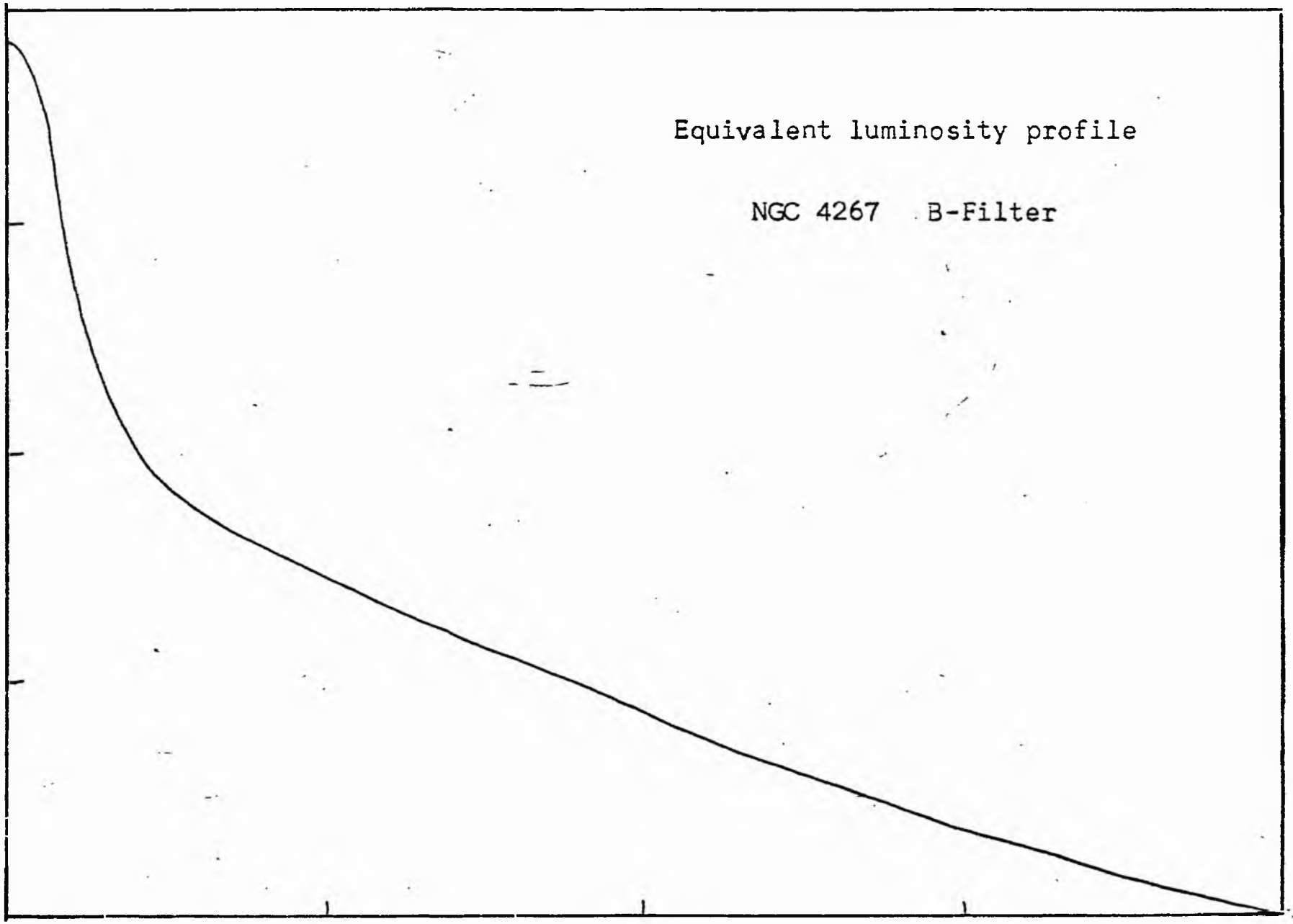
Equivalent luminosity profile
NGC 4267 B-Filter

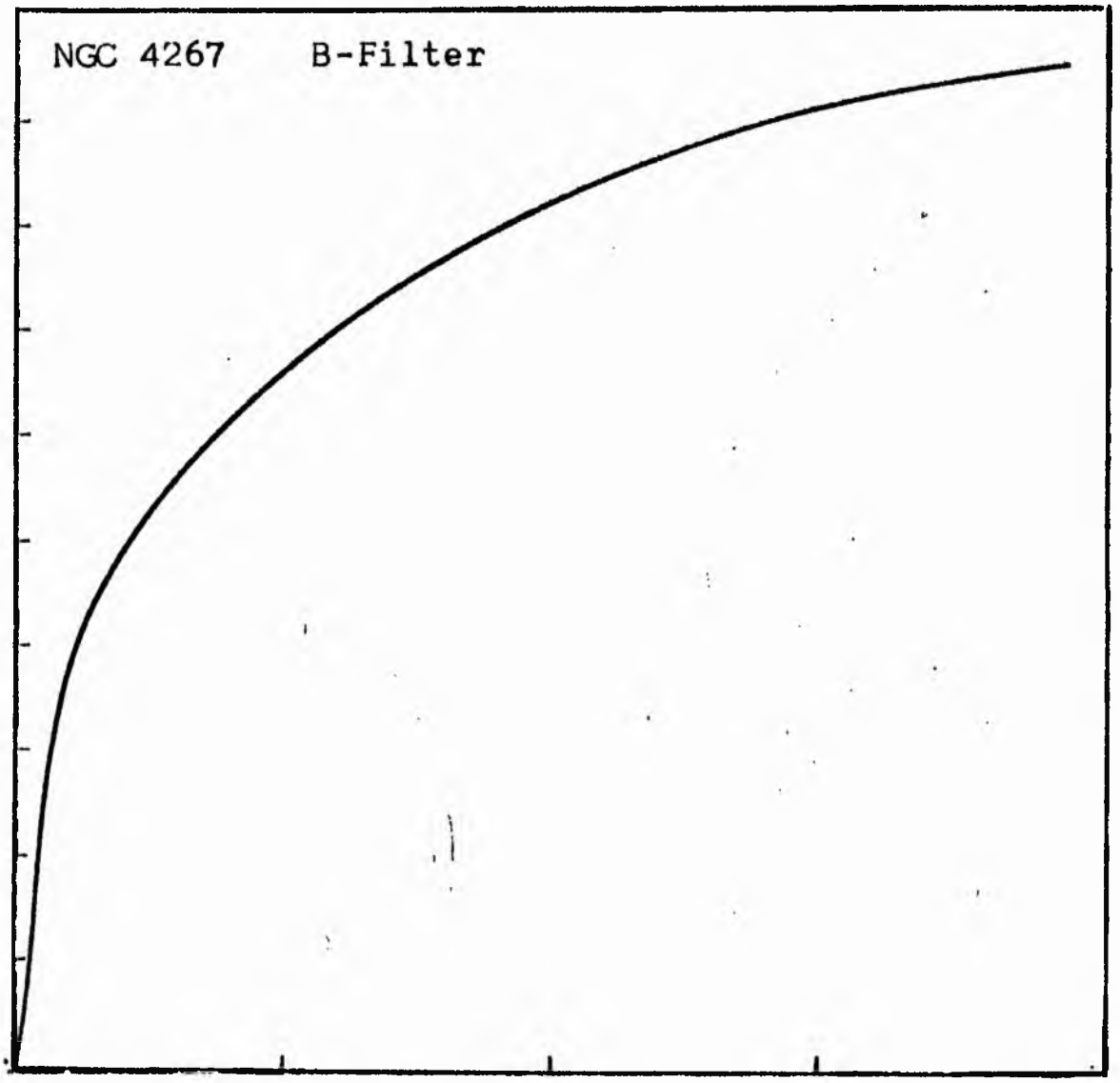

Relative integrated luminosity k(r) versus equivalent radius r*.

MEAN LUMINOSITY DISTRIBUTION IN NGC 4267
B COLOUR

LOG I	I	$\bar{I}$	R	AREA	ΔA	P	ΣP	KIRI	ρ	LOG J	μ
1.84	69.183		0.0	0.0			0.0	0.0	0.0	1.854	17.92
		66.139			23.59	1559.9487					
1.80	63.096		2.74	23.59			1559.95	0.07	0.13	1.814	18.02
		56.607			24.69	1397.5798					
1.70	50.119		3.92	48.27			2957.53	0.14	0.18	1.714	18.27
		44.965			30.89	1389.1543					
1.60	39.811		5.02	79.17			4346.68	0.21	0.23	1.614	18.52
		35.717			21.12	754.2656					
1.50	31.623		5.65	100.29			5100.95	0.24	0.26	1.514	18.77
		28.371			21.26	603.0383					
1.40	25.119		6.22	121.54			5703.98	0.27	0.29	1.414	19.02
		22.536			10.78	242.9564					
1.30	19.952		6.49	132.32			5946.93	0.29	0.30	1.314	19.27
		17.901			47.23	845.4319					
1.20	15.849		7.56	179.55			6792.36	0.33	0.35	1.214	19.52
		14.219			11.58	164.6723					
1.10	12.589		7.80	191.13			6957.04	0.33	0.36	1.114	19.77
		11.295			46.65	526.9197					
1.00	10.000		8.70	237.79			7483.95	0.36	0.40	1.014	20.02
		8.972			33.93	304.3955					
0.90	7.943		9.30	271.72			7788.35	0.37	0.43	0.914	20.27
		7.126			23.88	170.1507					
0.80	6.310		9.70	295.59			7958.50	0.38	0.45	0.814	20.52
		5.661			70.84	401.0193					
0.70	5.012		10.80	366.44			8359.51	0.40	0.50	0.714	20.77
		4.496			49.04	220.5064					
0.60	3.981		11.50	415.48			8580.02	0.41	0.53	0.614	21.02
		3.572			75.40	269.2957					
0.50	3.162		12.50	490.87			8849.31	0.42	0.58	0.514	21.27
		2.837			116.11	329.4204					
0.40	2.512		13.90	606.99			9178.73	0.44	0.64	0.414	21.52
		2.254			109.33	246.3756					
0.30	1.995		15.10	716.31			9425.10	0.45	0.70	0.314	21.77
		1.790			155.65	278.6250					
0.20	1.585		16.66	871.97			9703.73	0.47	0.77	0.214	22.02
		1.422			173.23	246.3200					
0.10	1.259		18.24	1045.20			9950.04	0.48	0.84	0.114	22.27
		1.129			362.77	409.7266					
-0.00	1.000		21.17	1407.96			10359.77	0.50	0.98	0.014	22.52
		0.897			595.00	533.8069					
-0.10	0.794		25.25	2002.96			10893.57	0.52	1.17	-0.086	22.77
		0.713			996.66	710.2583					
-0.20	0.631		30.90	2999.62			11603.83	0.56	1.43	-0.186	23.02
		0.566			1231.76	697.2578					
-0.30	0.501		36.70	4231.38			12301.09	0.59	1.70	-0.286	23.27
		0.450			1661.48	747.0750					
-0.40	0.398		43.31	5892.86			13048.16	0.63	2.00	-0.386	23.52
		0.357			2141.21	764.7659					
-0.50	0.316		50.57	8034.07			13812.93	0.66	2.34	-0.486	23.77
		0.284			2790.88	791.7913					
-0.60	0.251		58.70	10824.95			14604.72	0.70	2.71	-0.586	24.02
		0.225			3017.85	680.0901					
-0.70	0.200		66.38	13042.80			15284.81	0.73	3.07	-0.686	24.27
		0.179			3453.67	618.2295					
-0.80	0.158		74.20	17296.47			15903.04	0.76	3.43	-0.786	24.52
		0.142			3858.51	548.6418					
-0.90	0.126		82.06	21154.98			16451.68	0.79	3.79	-0.886	24.77
		0.113			3228.82	364.6816					
-1.00	0.100		88.10	24383.80			16816.36	0.81	4.07	-0.986	25.02
		0.090			4992.87	447.9409					
-1.10	0.079		96.70	29376.68			17264.29	0.83	4.47	-1.086	25.27
		0.071			6457.06	460.1565					
-1.20	0.063		106.80	35833.74			17724.45	0.85	4.94	-1.186	25.52
		0.057			8206.85	464.5662					
-1.30	0.050		118.40	44040.59			18189.01	0.87	5.47	-1.286	25.77
		0.045			8482.08	381.3945					
-1.40	0.040		129.30	52522.67			18570.41	0.89	5.98	-1.386	26.02
		0.036			9404.90	335.9128					
-1.50	0.032		140.40	61927.57			18906.32	0.91	6.49	-1.486	26.27
		0.028			10369.49	294.1917					
-1.60	0.025		151.70	72297.06			19200.51	0.92	7.01	-1.586	26.52
		0.023			13025.56	293.5417					
-1.70	0.020		164.80	85322.62			19494.05	0.94	7.62	-1.686	26.77
		0.018			11770.25	210.6978					
-1.80	0.016		175.80	97092.87			19704.74	0.95	8.13	-1.786	27.02
		0.014			10079.69	143.3250					
-1.90	0.013		184.70	107172.56			19848.07	0.95	8.54	-1.886	27.27
		0.011			8518.50	96.2141					
-2.00	0.010		191.90	115691.06			19944.28	0.96	8.87	-1.986	27.52
$-\infty$							20844.00	(1)			∞

PHOTOMETRIC PARAMETERS OF NGC 4267

B-FILTER

Total luminosity	L_T	= 5.79
Total apparent magnitude	m_T	= 11.72
Apparent central surface brightness	μ_o	= 17.92
Major axis at threshold	$2a_m$	= 5.93
Minor axis at threshold	$2b_m$	= 6.04
Major axis at μ=25.0 mag sec^{-2}	$2a(25)$	= 2.98
Luminosity within μ=25.0 mag sec^{-2}	$k(25)$	= 0.81
Gradient of exponential component	$G(a)$	= -0.68
Equivalent gradient of exponential comp.	$G(r^*)$	= -0.59
Equivalent gradient of reduced exp. comp.	$G(\rho)$	= -0.24

Parameters at k = ¼ :

Semi-major axis	a_1	= 0.13
Axis ratio	b/a	= 0.96
Equivalent radius	r_1^*	= 0.09
Surface brightness	μ_1	= 18.94

Parameters at k = ½(effective) :

Semi-major axis	a_e	= 0.32
Axis ratio	b/a	= 1.12
Equivalent radius	r_e^*	= 0.36
Surface brightness	μ_e	= 22.52
Mean surface brightness	μ_e'	= 11.52

Parameters at k = ¾ :

Semi-major axis	a_3	= 1.27
Axis ratio	b/a	= 0.86
Equivalent radius	r_3^*	= 1.17
Surface brightness	μ_3	= 24.46

Concentration indices	C_{21}	= 3.76
	C_{32}	= 3.27

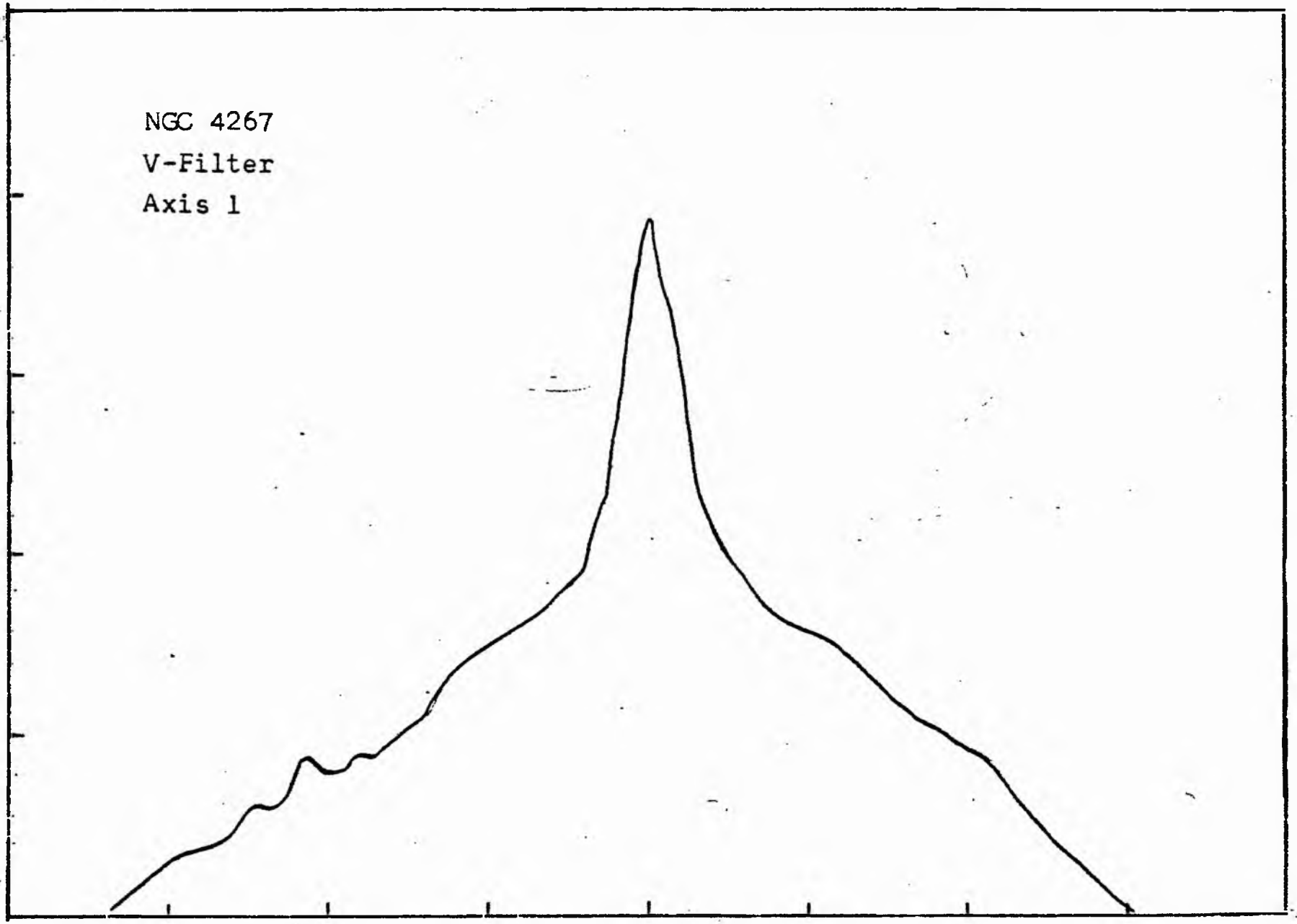
NGC 4267
V-Filter
Axis 1

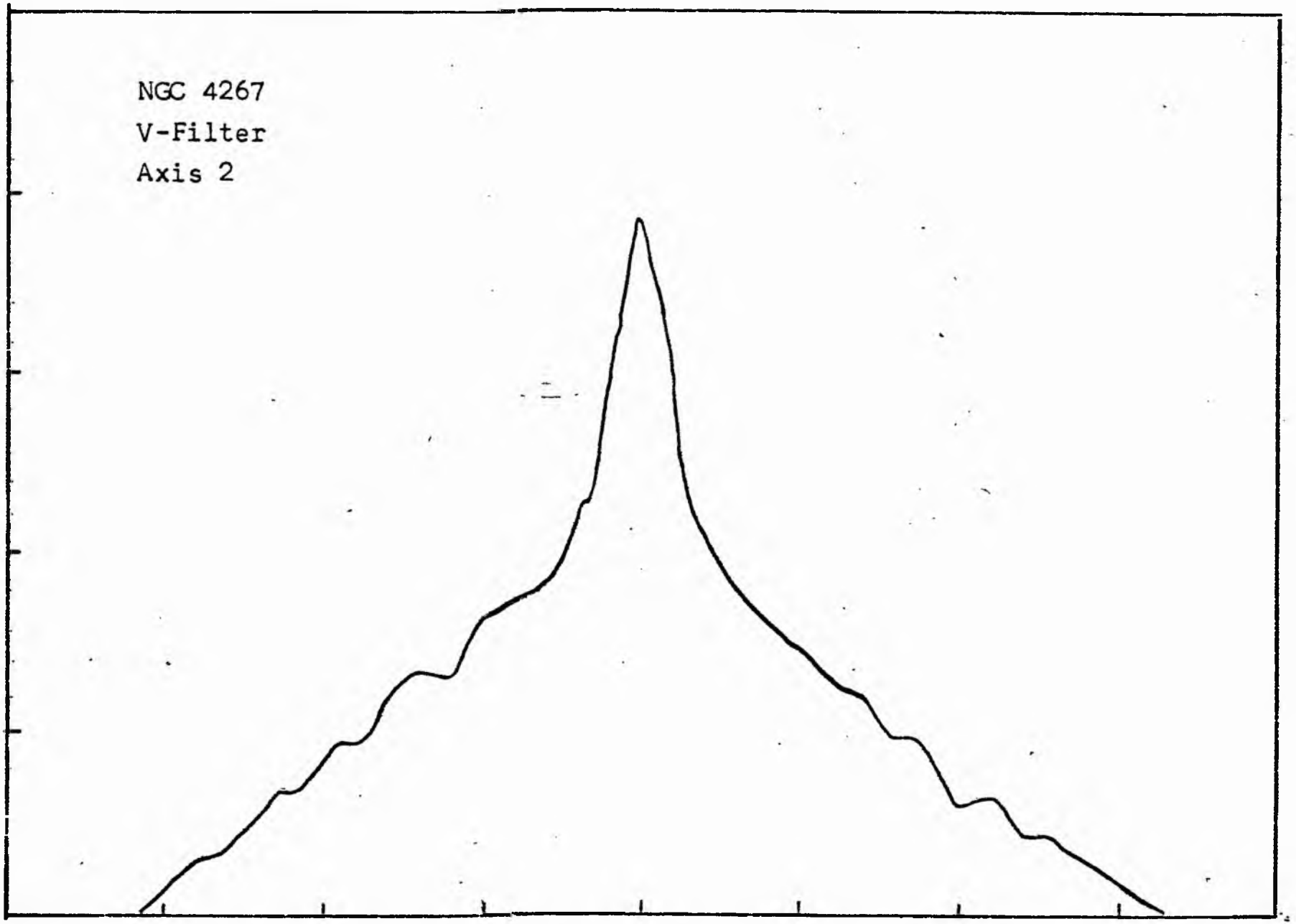
NGC 4267
V-Filter
Axis 2

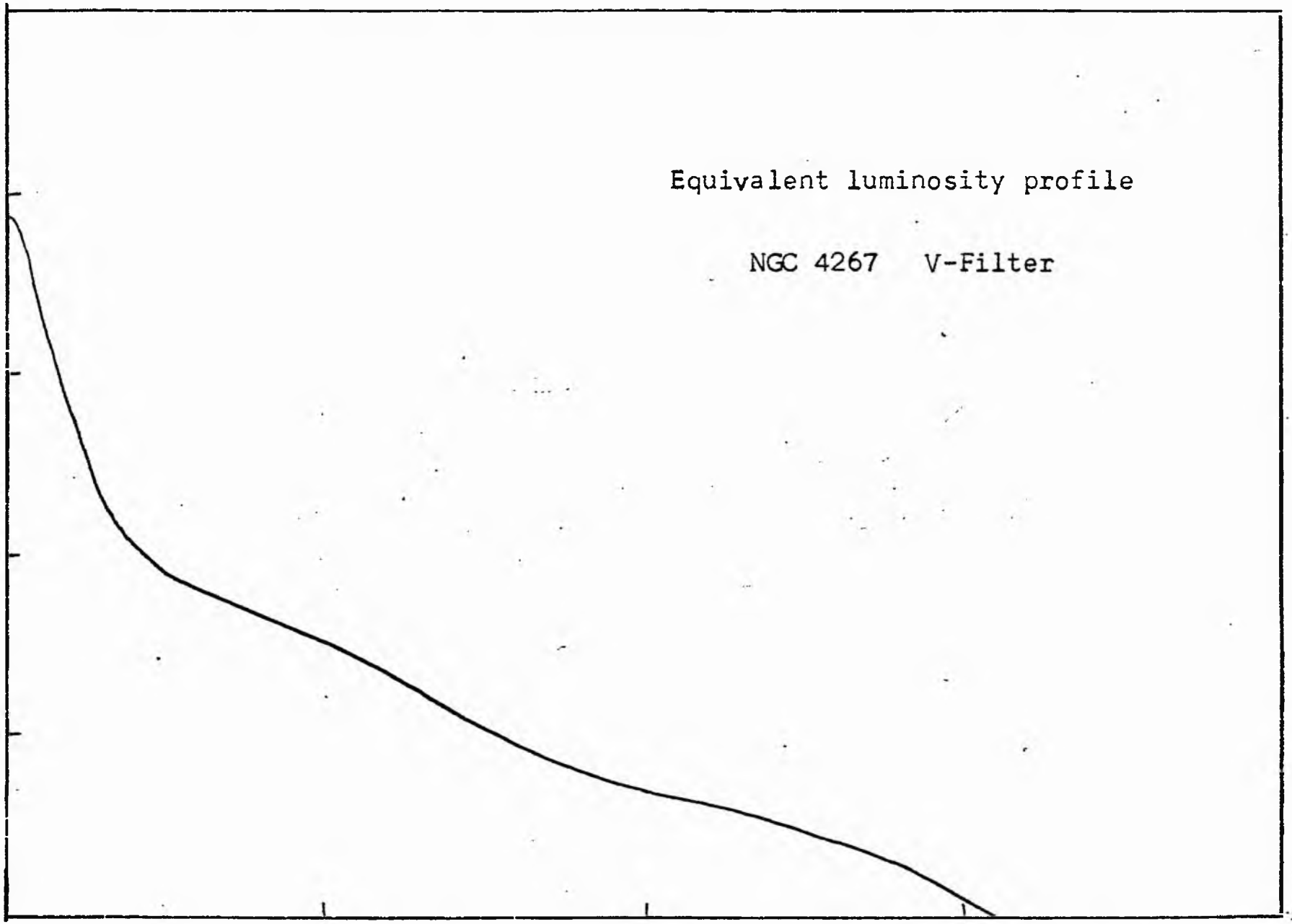
Equivalent luminosity profile
NGC 4267 V-Filter

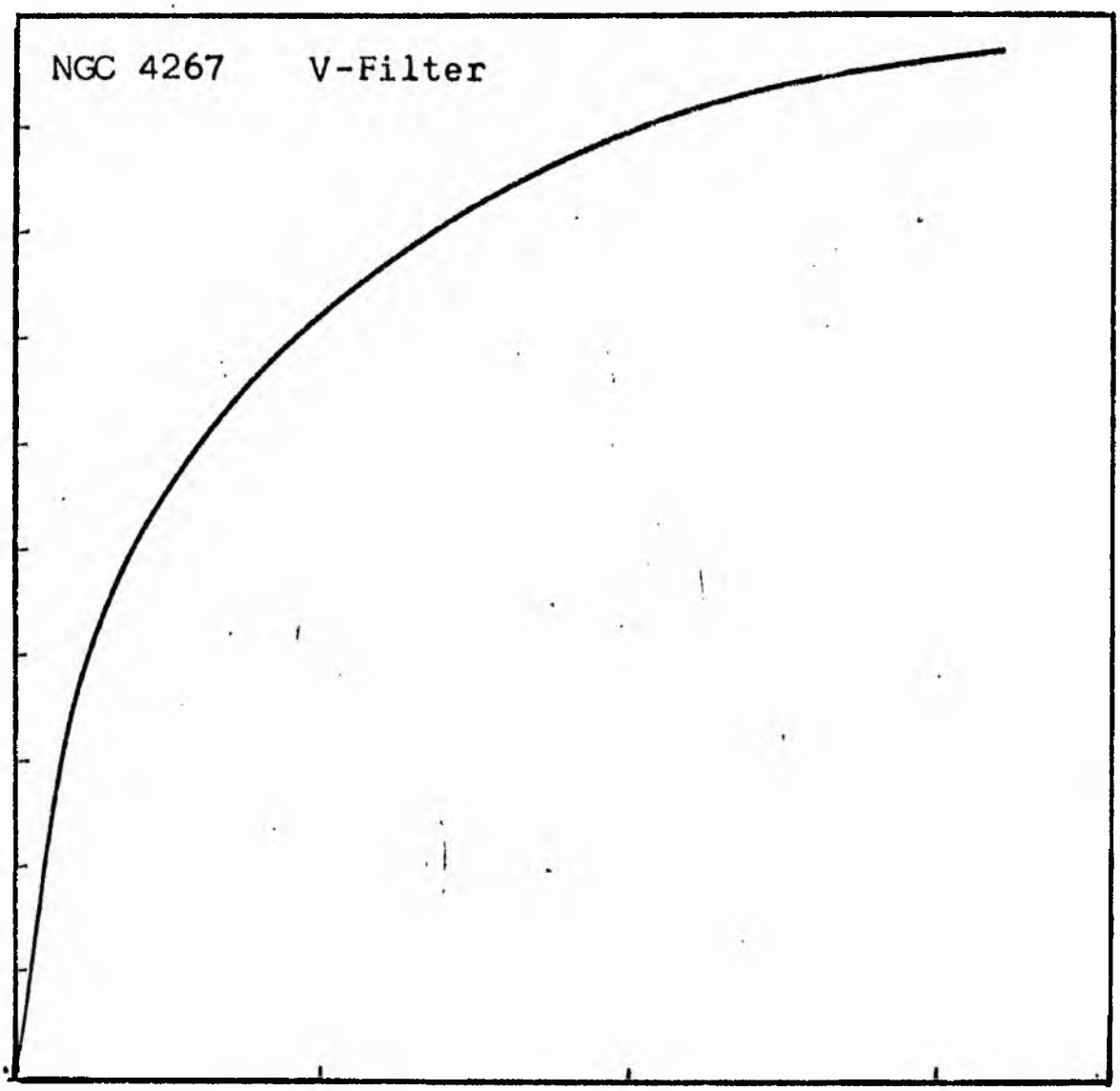

Relative integrated luminosity k(r) versus equivalent radius r*.

MEAN LUMINOSITY DISTRIBUTION IN NGC 4267
V COLOUR

LOG I	I	$\bar{I}$	R	AREA	ΔA	P	ΣP	K(R)	ρ	LOG J	μ
1.81	64.565		0.0	0.0			0.0	0.0	0.0	1.782	16.91
		63.830			1.54	98.2594					
1.80	63.096		0.70	1.54			98.26	0.01	0.04	1.772	16.94
		56.607			12.32	697.1182					
1.70	50.119		2.10	13.85			795.38	0.05	0.11	1.672	17.19
		44.965			22.46	1010.0115					
1.60	39.811		3.40	36.32			1805.39	0.11	0.17	1.572	17.44
		35.717			19.10	682.2170					
1.50	31.623		4.20	55.42			2487.61	0.15	0.21	1.472	17.69
		28.371			23.12	655.9910					
1.40	25.119		5.00	78.54			3143.60	0.19	0.25	1.372	17.94
		22.536			23.53	530.2739					
1.30	19.952		5.70	102.07			3673.87	0.23	0.29	1.272	18.19
		17.901			34.78	622.5383					
1.20	15.849		6.60	136.85			4296.41	0.26	0.34	1.172	18.44
		14.219			44.61	634.3171					
1.10	12.589		7.60	181.46			4930.72	0.30	0.39	1.072	18.69
		11.295			56.33	636.2068					
1.00	10.000		8.70	237.79			5566.93	0.34	0.44	0.972	18.94
		8.972			28.70	257.4438					
0.90	7.943		9.21	266.48			5824.37	0.36	0.47	0.872	19.19
		7.126			29.11	207.4459					
0.80	6.310		9.70	295.59			6031.81	0.37	0.49	0.772	19.44
		5.661			77.66	439.6089					
0.70	5.012		10.90	373.25			6471.42	0.40	0.56	0.672	19.69
		4.496			35.03	157.5048					
0.60	3.981		11.40	408.28			6628.92	0.41	0.58	0.572	19.94
		3.572			67.01	239.3369					
0.50	3.162		12.30	475.29			6868.26	0.42	0.63	0.472	20.19
		2.837			114.35	324.4292					
0.40	2.512		13.70	589.65			7192.68	0.44	0.70	0.372	20.44
		2.254			89.22	201.0651					
0.30	1.995		14.70	678.87			7393.75	0.45	0.75	0.272	20.69
		1.790			155.82	278.9302					
0.20	1.585		16.30	834.69			7672.68	0.47	0.83	0.172	20.94
		1.422			138.45	196.8622					
0.10	1.259		17.60	973.14			7869.54	0.48	0.90	0.072	21.19
		1.129			347.12	392.0520					
-0.00	1.000		20.50	1320.25			8261.59	0.51	1.04	-0.028	21.44
		0.897			643.24	577.0886					
-0.10	0.794		25.00	1963.50			8838.67	0.54	1.27	-0.128	21.69
		0.713			1094.66	780.0928					
-0.20	0.631		31.20	3058.15			9618.76	0.59	1.59	-0.228	21.94
		0.566			1598.47	904.8450					
-0.30	0.501		38.50	4656.62			10523.61	0.65	1.96	-0.328	22.19
		0.450			2253.65	1013.3416					
-0.40	0.398		46.90	6910.28			11536.95	0.71	2.39	-0.428	22.44
		0.357			1101.57	393.4409					
-0.50	0.316		50.50	8011.84			11930.38	0.73	2.57	-0.528	22.69
		0.284			1353.74	384.0652					
-0.60	0.251		54.60	9365.59			12314.45	0.76	2.78	-0.628	22.94
		0.225			1793.85	404.2544					
-0.70	0.200		59.60	11159.43			12718.70	0.78	3.04	-0.728	23.19
		0.179			2154.66	385.6985					
-0.80	0.158		65.10	13314.09			13104.39	0.80	3.32	-0.828	23.44
		0.142			2836.48	403.3186					
-0.90	0.126		71.70	16150.57			13507.71	0.83	3.65	-0.928	23.69
		0.113			2913.89	329.1113					
-1.00	0.100		77.90	19064.46			13836.82	0.85	3.97	-1.028	23.94
		0.090			3847.66	345.1973					
-1.10	0.079		85.40	22912.12			14182.02	0.87	4.35	-1.128	24.19
		0.071			4787.95	341.2087					
-1.20	0.063		93.90	27700.07			14523.22	0.89	4.78	-1.228	24.44
		0.057			5113.35	289.4519					
-1.30	0.050		102.20	32813.42			14812.67	0.91	5.21	-1.328	24.69
		0.045			5615.66	252.5066					
-1.40	0.040		110.60	38429.08			15065.18	0.92	5.64	-1.428	24.94
		0.036			6508.75	232.4719					
-1.50	0.032		119.60	44937.84			15297.64	0.94	6.09	-1.528	25.19
		0.028			6293.03	178.5388					
-1.60	0.025		127.70	51230.86			15476.18	0.95	6.51	-1.628	25.44
		0.023			5770.47	130.0423					
-1.70	0.020		134.70	57001.33			15606.22	0.96	6.86	-1.728	25.69
		0.018			4222.52	75.5868					
-1.80	0.016		139.60	61223.85			15681.80	0.96	7.11	-1.828	25.94
		0.014			5650.59	80.3468					
-1.90	0.013		145.90	66874.44			15762.15	0.97	7.43	-1.928	26.19
		0.011			6091.44	68.8011					
-2.00	0.010		152.40	72965.87			15830.95	0.97	7.77	-2.028	26.44
- ∞							16290.00	(1)			∞

PHOTOMETRIC PARAMETERS OF NGC 4267

V-FILTER

Total luminosity	L_T	= 4.53
Total apparent magnitude	m_T	= 10.91
Apparent central surface brightness	μ_o	= 16.91
Major axis at threshold	$2a_m$	= 5.56
Minor axis at threshold	$2b_m$	= 5.57
Major axis at μ=25.0 mag sec^{-2}	2a(25)	= 4.1
Luminosity within μ=25.0 mag sec^{-2}	k(25)	= 0.93
Gradient of exponential component	G(a)	= -0.97
Equivalent gradient of exponential comp.	G(r*)	= -0.89
Equivalent gradient of reduced exp. comp.	G(ρ)	= -0.30
Parameters at k = ¼ :		
Semi-major axis	a_1	= 0.16
Axis ratio	b/a	= 1.04
Equivalent radius	r_1*	= 0.10
Surface brightness	μ_1	= 18.36
Parameters at k = ½(effective) :		
Semi-major axis	a_e	= 0.38
Axis ratio	b/a	= 0.96
Equivalent radius	r_e*	= 0.33
Surface brightness	μ_e	= 21.36
Mean surface brightness	μ_e'	= 10.51
Parameters at k = ¾ :		
Semi-major axis	a_3	= 1.02
Axis ratio	b/a	= 0.92
Equivalent radius	r_3*	= 0.89
Surface brightness	μ_3	= 22.86
Concentration indices	C_{21}	= 3.13
	C_{32}	= 2.73

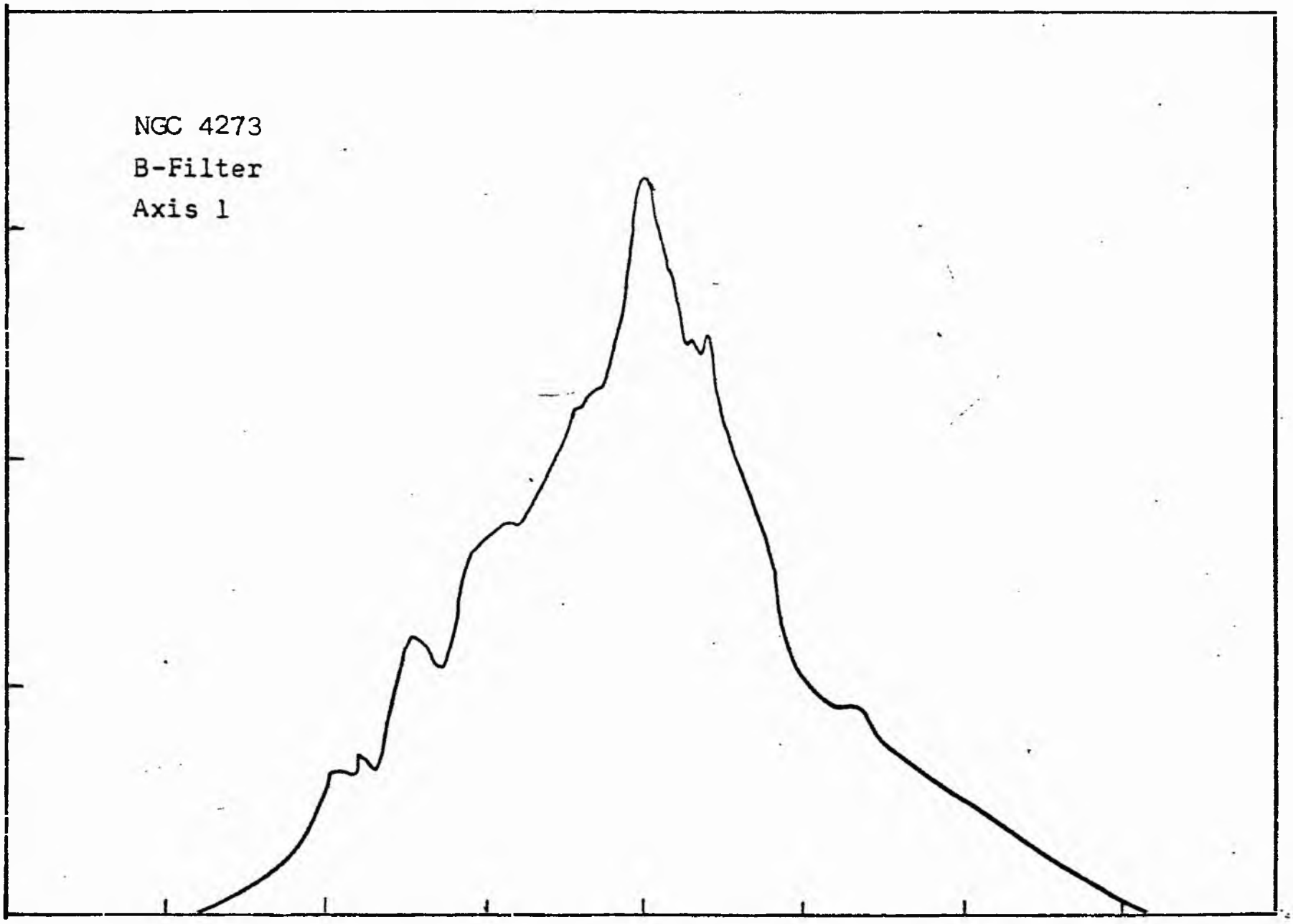
NGC 4273
B-Filter
Axis 1

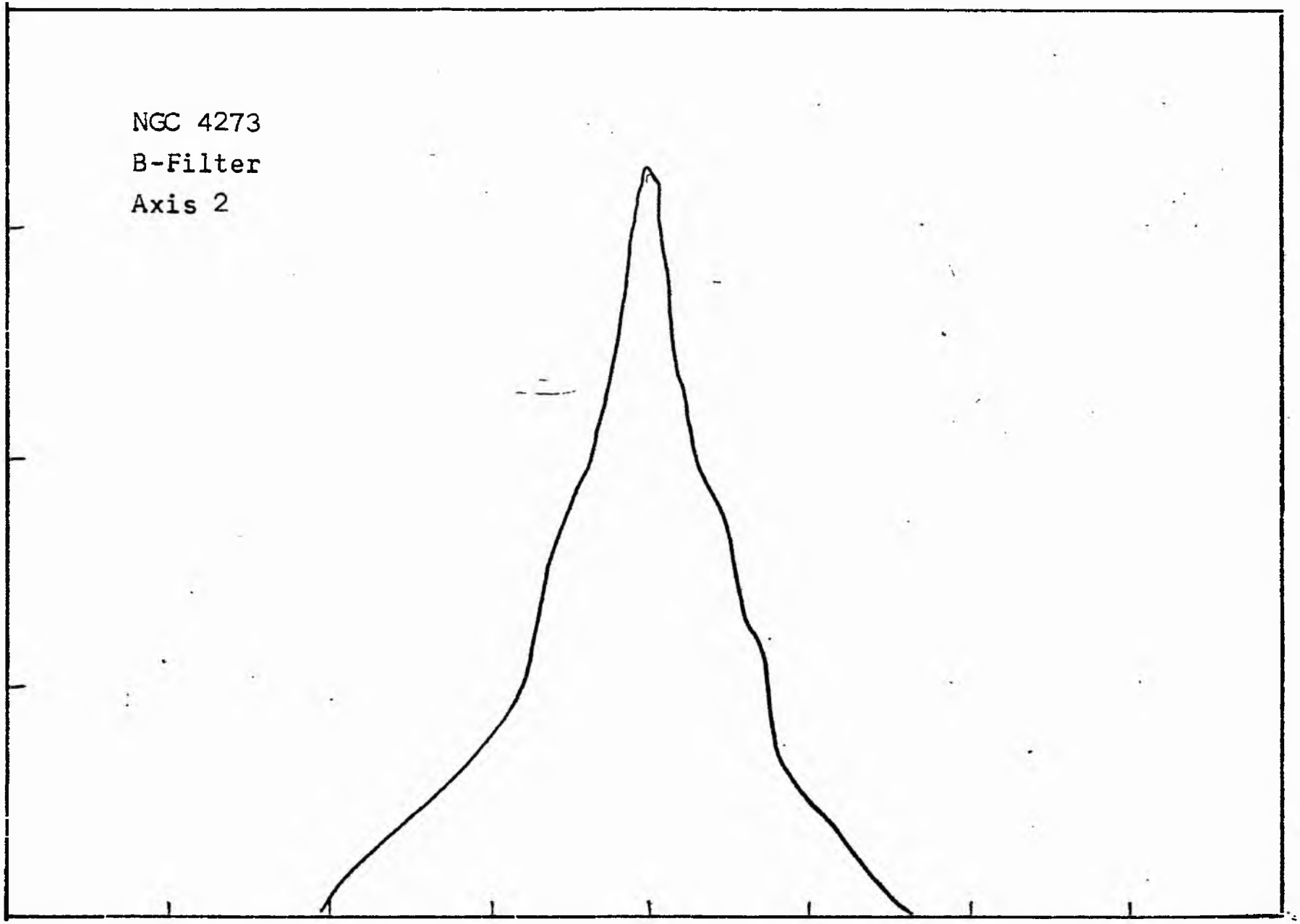
NGC 4273
B-Filter
Axis 2

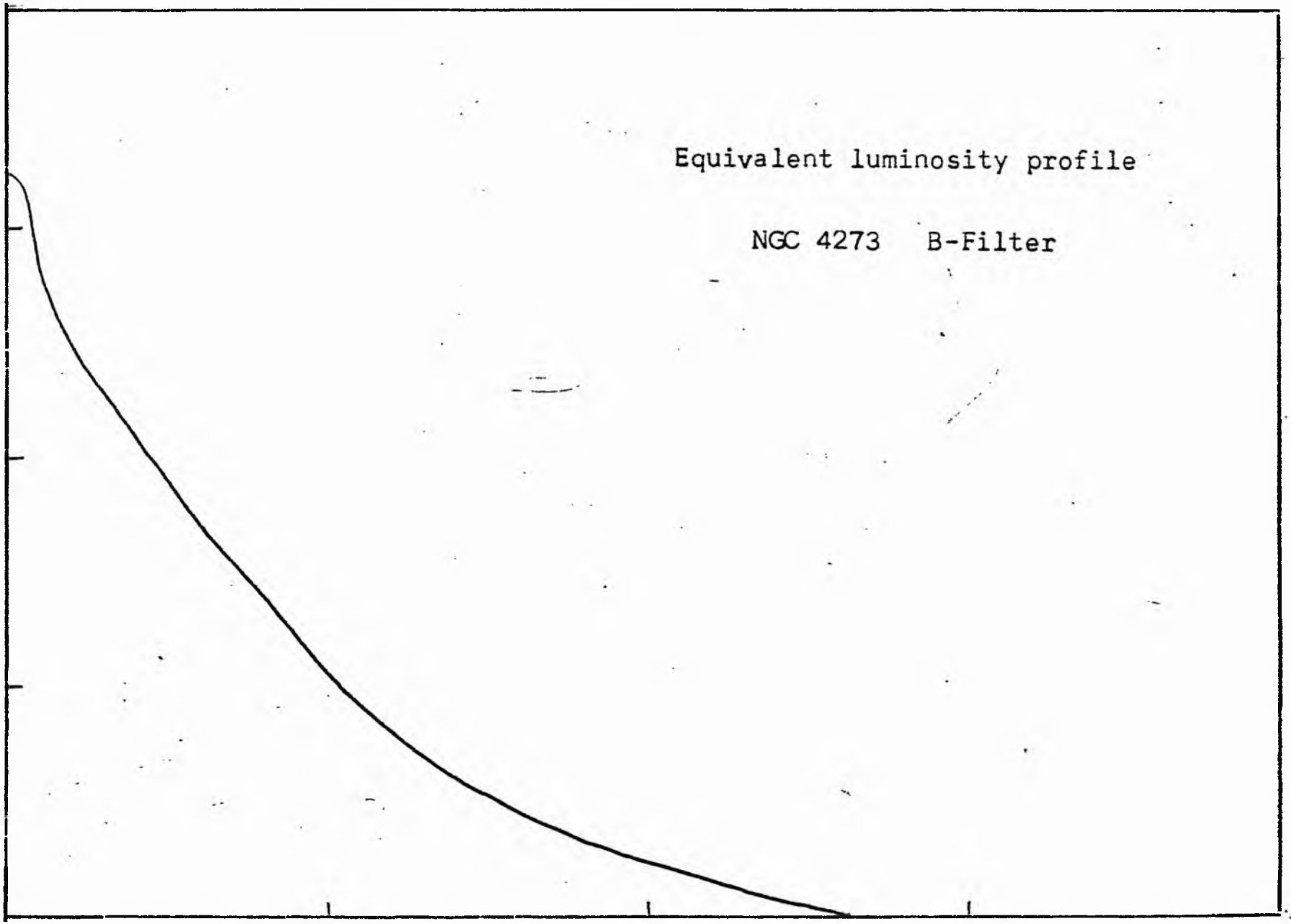
Equivalent luminosity profile
NGC 4273 B-Filter

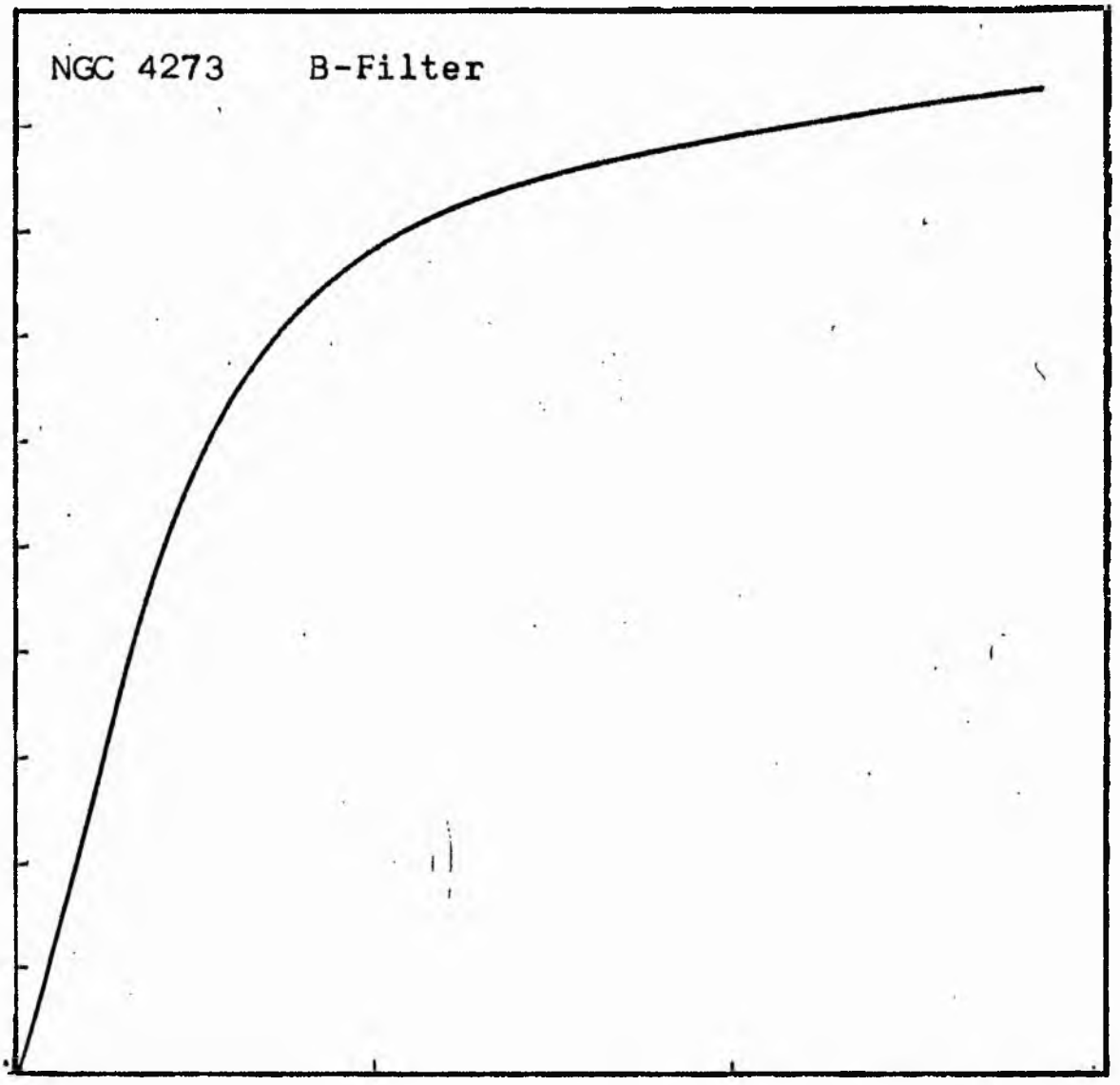

Relative integrated luminosity k(r) versus equivalent radius r*.

MEAN LUMINOSITY DISTRIBUTION IN NGC 4273
O COLOUR

LOG I	I	Ī	R	AREA	ΔA	P	ΣP	K(R)	ρ	LOG J	μ
1.29	19.498		0.0	0.0			0.0	0.0	0.0	1.217	18.09
		17.674			27.71	489.7666					
1.20	15.849		2.97	27.71			489.77	0.06	0.14	1.127	19.12
		14.219			3.07	43.5904					
1.10	12.589		3.13	30.78			533.36	0.06	0.15	1.027	19.37
		11.295			24.11	272.3494					
1.00	10.000		4.18	54.89			805.71	0.10	0.20	0.927	19.62
		8.972			21.46	192.5755					
0.90	7.943		4.93	76.36			998.29	0.12	0.24	0.827	19.87
		7.126			28.60	203.8120					
0.80	6.310		5.78	104.96			1202.10	0.14	0.28	0.727	20.12
		5.661			71.76	406.2073					
0.70	5.012		7.50	176.71			1608.31	0.19	0.36	0.627	20.37
		4.496			76.06	342.0042					
0.60	3.981		8.97	252.78			1950.31	0.23	0.44	0.527	20.62
		3.572			85.71	306.1401					
0.50	3.162		10.38	338.49			2256.45	0.27	0.50	0.427	20.87
		2.837			144.56	410.1350					
0.40	2.512		12.40	483.05			2666.59	0.32	0.60	0.327	21.12
		2.254			224.75	506.4897					
0.30	1.995		15.01	707.80			3173.08	0.38	0.73	0.227	21.37
		1.790			314.60	563.1624					
0.20	1.585		18.04	1022.40			3736.24	0.45	0.87	0.127	21.62
		1.422			243.04	345.5862					
0.10	1.259		20.07	1265.45			4081.83	0.49	0.97	0.027	21.87
		1.129			287.04	324.2021					
-0.00	1.000		22.23	1552.49			4406.03	0.53	1.08	-0.073	22.12
		0.897			234.52	210.4010					
-0.10	0.794		23.85	1787.01			4616.43	0.55	1.16	-0.173	22.37
		0.713			419.18	298.7227					
-0.20	0.631		26.50	2206.18			4915.15	0.59	1.29	-0.273	22.62
		0.566			542.63	307.1694					
-0.30	0.501		29.58	2748.82			5222.32	0.63	1.43	-0.373	22.87
		0.450			872.19	392.1772					
-0.40	0.398		33.95	3621.01			5614.49	0.67	1.65	-0.473	23.12
		0.357			749.86	267.8245					
-0.50	0.316		37.30	4370.86			5882.32	0.71	1.81	-0.573	23.37
		0.284			777.04	220.4536					
-0.60	0.251		40.48	5147.91			6102.77	0.73	1.96	-0.673	23.62
		0.225			766.74	172.7911					
-0.70	0.200		43.39	5914.65			6275.56	0.75	2.10	-0.773	23.87
		0.179			834.50	149.3820					
-0.80	0.158		46.35	6749.15			6424.94	0.77	2.25	-0.873	24.12
		0.142			701.73	99.7803					
-0.90	0.126		48.70	7450.88			6524.71	0.78	2.36	-0.973	24.37
		0.113			466.05	52.6392					
-1.00	0.100		50.20	7916.94			6577.35	0.79	2.43	-1.073	24.62
		0.090			1482.99	133.0485					
-1.10	0.079		54.70	9399.93			6710.40	0.80	2.65	-1.173	24.87
		0.071			1461.94	104.1842					
-1.20	0.063		58.80	10861.86			6814.58	0.82	2.85	-1.273	25.12
		0.057			2534.16	143.4520					
-1.30	0.050		65.30	13396.02			6958.03	0.83	3.17	-1.373	25.37
		0.045			2085.87	93.7910					
-1.40	0.040		70.20	15481.89			7051.82	0.85	3.40	-1.473	25.62
		0.036			3047.96	108.8639					
-1.50	0.032		76.80	18529.85			7160.68	0.86	3.72	-1.573	25.87
		0.028			3112.58	88.3072					
-1.60	0.025		83.00	21642.43			7248.99	0.87	4.03	-1.673	26.12
		0.023			6770.16	152.5719					
-1.70	0.020		95.10	28412.59			7401.56	0.89	4.61	-1.773	26.37
		0.018			7690.08	137.6598					
-1.80	0.016		107.20	36102.67			7539.21	0.90	5.20	-1.873	26.62
		0.014			6755.68	96.0607					
-1.90	0.013		116.80	42858.35			7635.27	0.92	5.66	-1.973	26.87
		0.011			8935.70	100.9266					
-2.00	0.010		128.40	51794.04			7736.20	0.93	6.23	-2.073	27.12
							8336.00	(1)			
$-\infty$											∞

PHOTOMETRIC PARAMETERS OF NGC 4273

B-FILTER

Total luminosity	L_T	= 2.31
Total apparent magnitude	m_T	= 12.32
Apparent central surface brightness	μ_o	= 18.89
Major axis at threshold	$2a_m$	= 5.13
Minor axis at threshold	$2b_m$	= 3.90
Major axis at μ=25.0 mag sec^{-2}	2a(25)	= 2.35
Luminosity within μ=25.0 mag sec^{-2}	k(25)	= 0.81
Gradient of exponential component	G(a)	= -1.58
Equivalent gradient of exponential comp.	G(r*)	= -2.08
Equivalent gradient of reduced exp. comp.	G(ρ)	= -0.74
Parameters at k = ¼ :		
Semi-major axis	a_1	= 0.22
Axis ratio	b/a	= 0.61
Equivalent radius	r_1*	= 0.16
Surface brightness	μ_1	= 20.74
Parameters at k = ½(effective) :		
Semi-major axis	a_e	= 0.43
Axis ratio	b/a	= 0.58
Equivalent radius	r_e*	= 0.34
Surface brightness	μ_e	= 21.95
Mean surface brightness	μ_e'	= 11.97
Parameters at k = ¾ :		
Semi-major axis	a_3	= 0.99
Axis ratio	b/a	= 0.57
Equivalent radius	r_3*	= 0.72
Surface brightness	μ_3	= 23.87
Concentration indices	C_{21}	= 2.15
	C_{32}	= 2.08

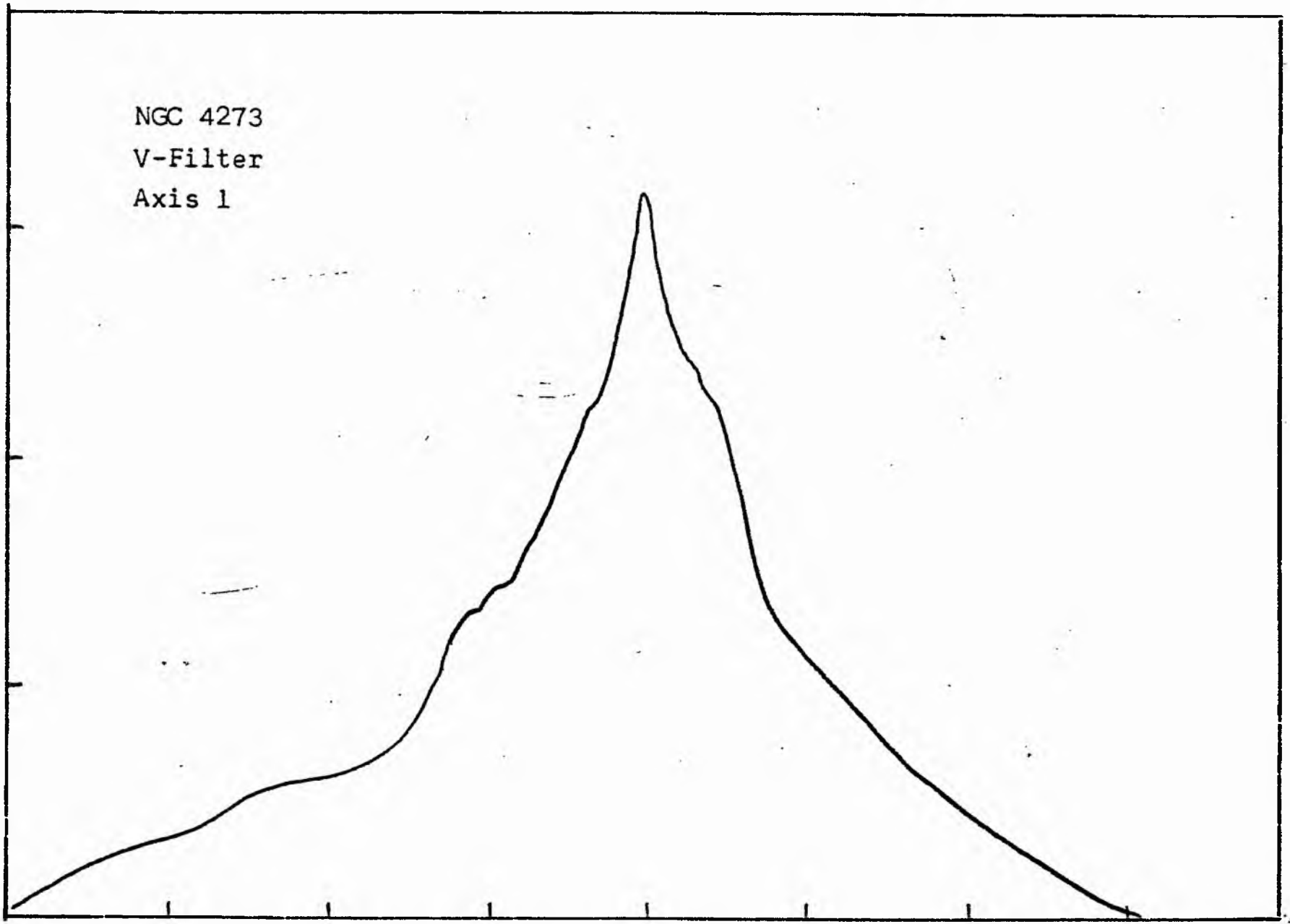
NGC 4273
V-Filter
Axis 1

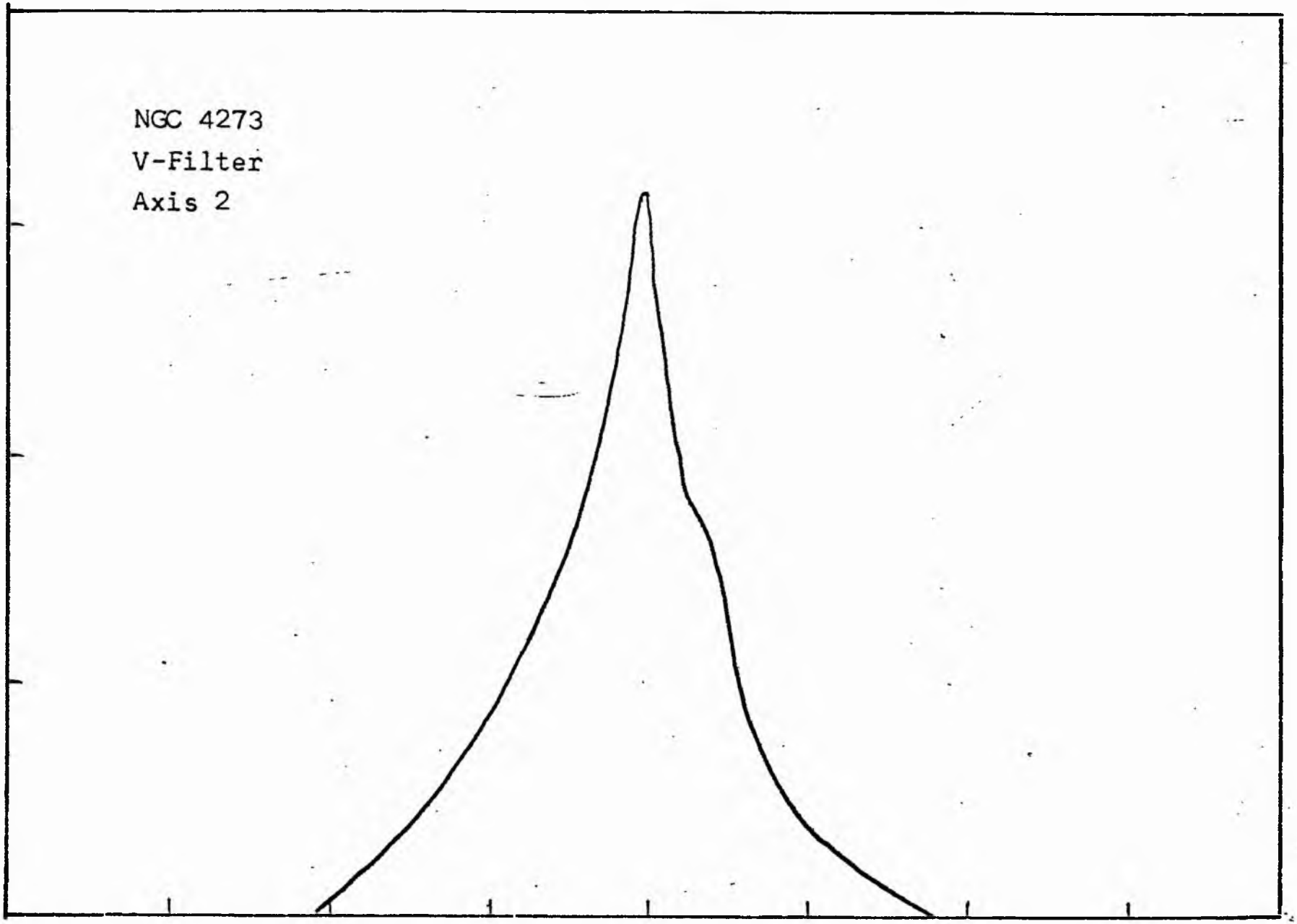
NGC 4273
V-Filter
Axis 2

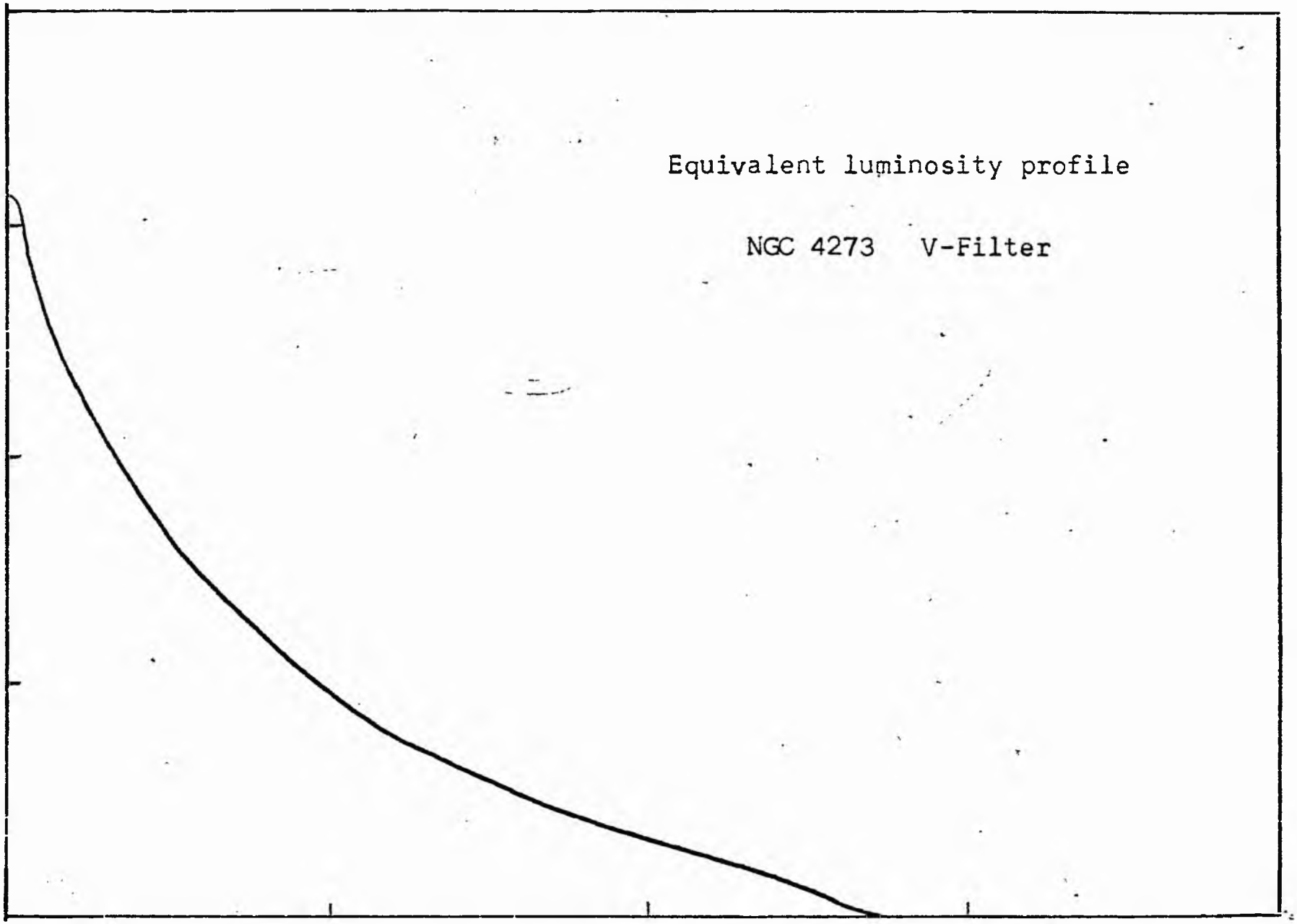
Equivalent luminosity profile
NGC 4273 V-Filter

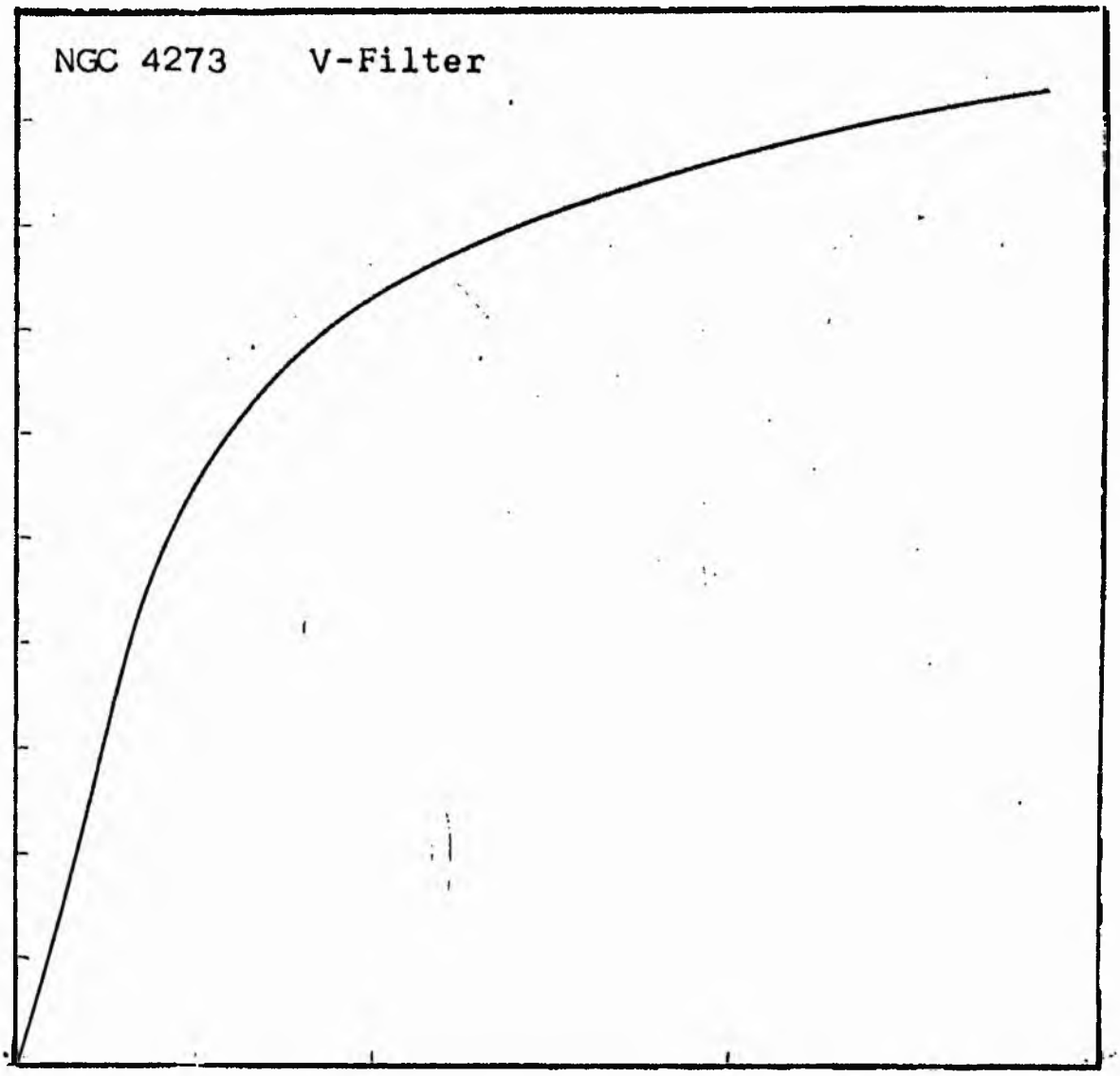

Relative integrated luminosity k(r) versus equivalent radius r*.

MEAN LUMINOSITY DISTRIBUTION IN NGC 4273
V COLOUR

LOG I	I	$\bar{I}$	R	AREA	ΔA	P	ΣP	K(R)	ρ	LOG J	μ
1.17	14.791		0.0	0.0			0.0	0.0	0.0	1.237	18.40
		13.690			12.07	165.2225					
1.10	12.589		1.96	12.07			165.22	0.02	0.09	1.167	18.58
		11.295			16.96	191.6084					
1.00	10.000		3.04	29.03			356.83	0.05	0.14	1.067	18.83
		8.972			31.79	285.1885					
0.90	7.943		4.40	60.82			642.02	0.09	0.21	0.967	19.08
		7.126			20.89	148.8820					
0.80	6.310		5.10	81.71			790.90	0.11	0.24	0.867	19.33
		5.661			23.97	135.6895					
0.70	5.012		5.80	105.68			926.59	0.13	0.27	0.767	19.58
		4.496			66.35	298.3423					
0.60	3.981		7.40	172.03			1224.93	0.18	0.35	0.667	19.83
		3.572			105.56	377.0164					
0.50	3.162		9.40	277.59			1601.95	0.23	0.44	0.567	20.08
		2.837			118.60	336.4895					
0.40	2.512		11.23	396.20			1938.44	0.28	0.53	0.467	20.33
		2.254			152.03	342.6001					
0.30	1.995		13.21	548.22			2281.04	0.33	0.62	0.367	20.58
		1.790			261.06	467.3174					
0.20	1.585		16.05	809.28			2748.36	0.39	0.75	0.267	20.83
		1.422			219.94	312.7278					
0.10	1.259		18.10	1029.22			3061.08	0.44	0.85	0.167	21.08
		1.129			226.16	255.4424					
-0.00	1.000		19.99	1255.38			3316.53	0.48	0.93	0.067	21.33
		0.897			241.74	216.8811					
-0.10	0.794		21.83	1497.12			3533.41	0.51	1.02	-0.033	21.58
		0.713			137.44	97.9439					
-0.20	0.631		22.81	1634.56			3631.35	0.52	1.07	-0.133	21.83
		0.566			338.37	191.5435					
-0.30	0.501		25.06	1972.93			3822.89	0.55	1.17	-0.233	22.08
		0.450			455.01	204.5961					
-0.40	0.398		27.80	2427.95			4027.49	0.58	1.30	-0.333	22.33
		0.357			595.02	212.5215					
-0.50	0.316		31.02	3022.96			4240.01	0.61	1.45	-0.433	22.58
		0.284			969.75	275.1272					
-0.60	0.251		35.65	3992.72			4515.14	0.65	1.67	-0.533	22.83
		0.225			688.12	155.0740					
-0.70	0.200		38.60	4680.84			4670.21	0.67	1.81	-0.633	23.08
		0.179			644.05	115.2908					
-0.80	0.158		41.17	5324.90			4785.50	0.69	1.93	-0.733	23.33
		0.142			1102.02	156.6973					
-0.90	0.126		45.23	6426.92			4942.19	0.71	2.12	-0.833	23.58
		0.113			1486.86	167.9357					
-1.00	0.100		50.19	7913.78			5110.12	0.73	2.35	-0.933	23.83
		0.090			1125.36	100.9636					
-1.10	0.079		53.64	9039.14			5211.09	0.75	2.51	-1.033	24.08
		0.071			1096.38	78.1331					
-1.20	0.063		56.80	10135.53			5289.22	0.76	2.66	-1.133	24.33
		0.057			3425.12	193.8872					
-1.30	0.050		65.70	13560.65			5483.11	0.79	3.07	-1.233	24.58
		0.045			2770.62	124.5809					
-1.40	0.040		72.10	16331.27			5607.68	0.80	3.37	-1.333	24.83
		0.036			6153.60	219.7877					
-1.50	0.032		84.60	22484.87			5827.47	0.84	3.96	-1.433	25.08
		0.028			3645.13	103.4161					
-1.60	0.025		91.20	26130.00			5930.88	0.85	4.27	-1.533	25.33
		0.023			5430.60	122.3837					
-1.70	0.020		100.23	31560.60			6053.27	0.87	4.69	-1.633	25.58
		0.018			6938.01	124.1971					
-1.80	0.016		110.70	38498.61			6177.46	0.89	5.18	-1.733	25.83
		0.014			7042.41	100.1378					
-1.90	0.013		120.40	45541.02			6277.60	0.90	5.63	-1.833	26.08
		0.011			8199.13	92.6072					
-2.00	0.010		130.79	53740.15			6370.20	0.91	6.12	-1.933	26.33
$-\infty$							6970.00	(1)			∞

PHOTOMETRIC PARAMETERS OF NGC 4273

V-FILTER

Total luminosity	L_T	= 1.94
Total apparent magnitude	m_T	= 11.72
Apparent central surface brightness	μ_o	= 18.40
Major axis at threshold	$2a_m$	= 6.05
Minor axis at threshold	$2b_m$	= 3.02
Major axis at μ=25.0 mag sec^{-2}	2a(25)	= 3.52
Luminosity within μ=25.0 mag sec^{-2}	k(25)	= 0.83
Gradient of exponential component	G(a)	= -1.31
Equivalent gradient of exponential comp.	G(r*)	= -1.71
Equivalent gradient of reduced exp. comp.	G(ρ)	= -0.79

Parameters at k = ¼ :

Semi-major axis	a_1	= 0.23
Axis ratio	b/a	= 0.57
Equivalent radius	r_1*	= 0.17
Surface brightness	μ_1	= 20.18

Parameters at k = ½(effective) :

Semi-major axis	a_e	= 0.45
Axis ratio	b/a	= 0.59
Equivalent radius	r_e*	= 0.36
Surface brightness	μ_e	= 21.50
Mean surface brightness	μ_e'	= 11.51

Parameters at k = ¾ :

Semi-major axis	a_3	= 1.12
Axis ratio	b/a	= 0.65
Equivalent radius	r_3*	= 0.90
Surface brightness	μ_3	= 24.08

Concentration indices	C_{21}	= 2.10
	C_{32}	= 2.54

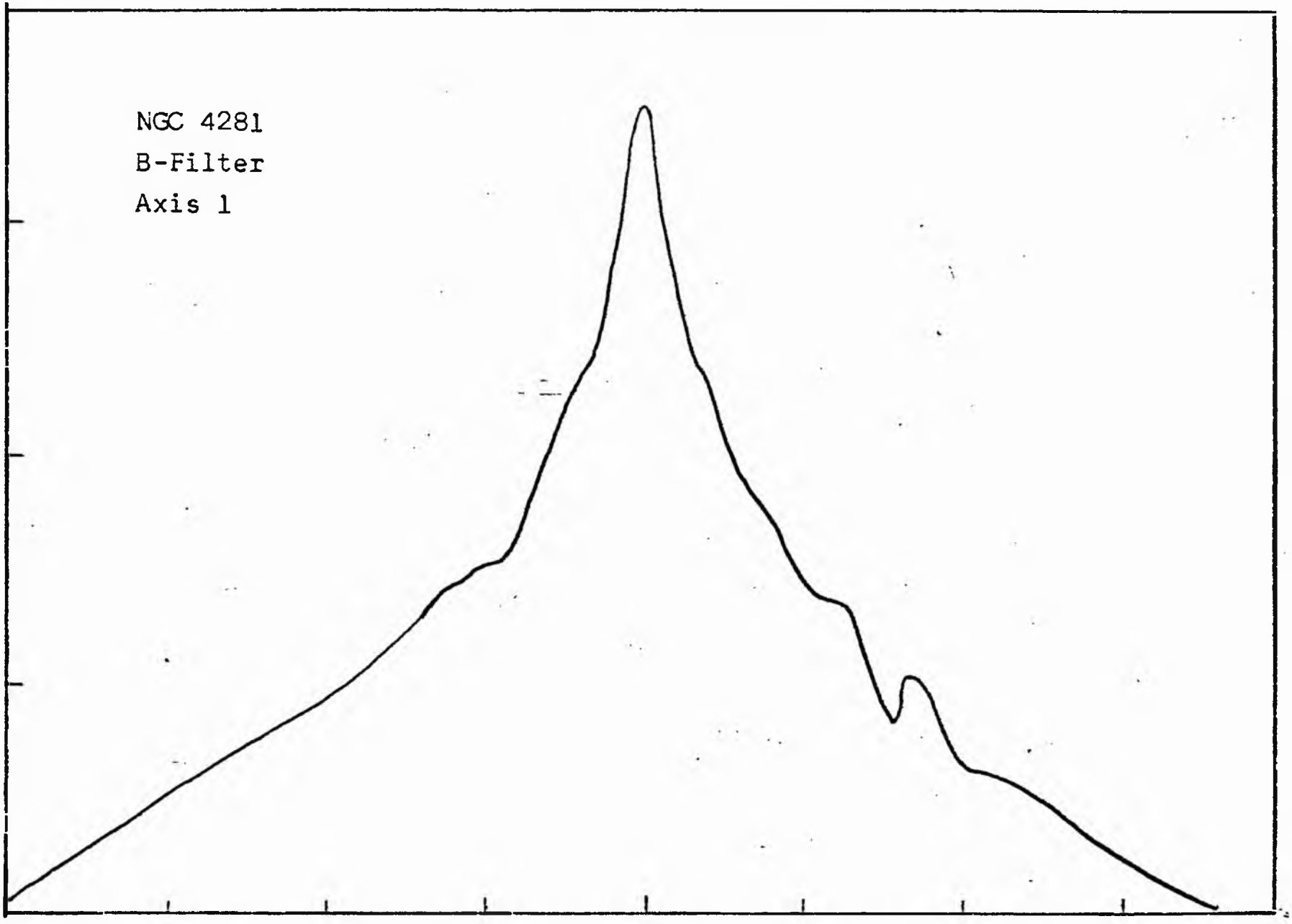
NGC 4281
B-Filter
Axis 1

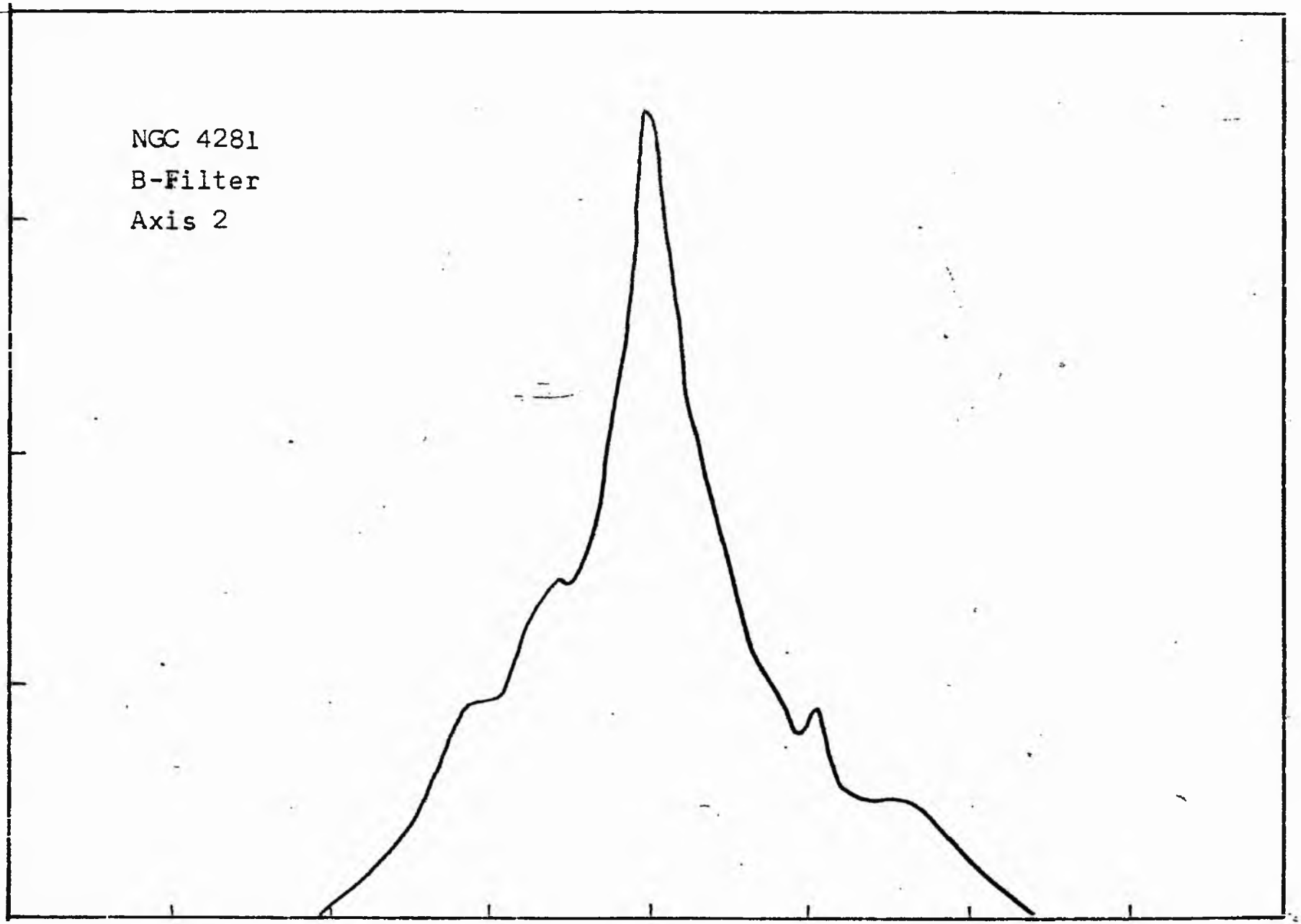
NGC 4281
B-Filter
Axis 2

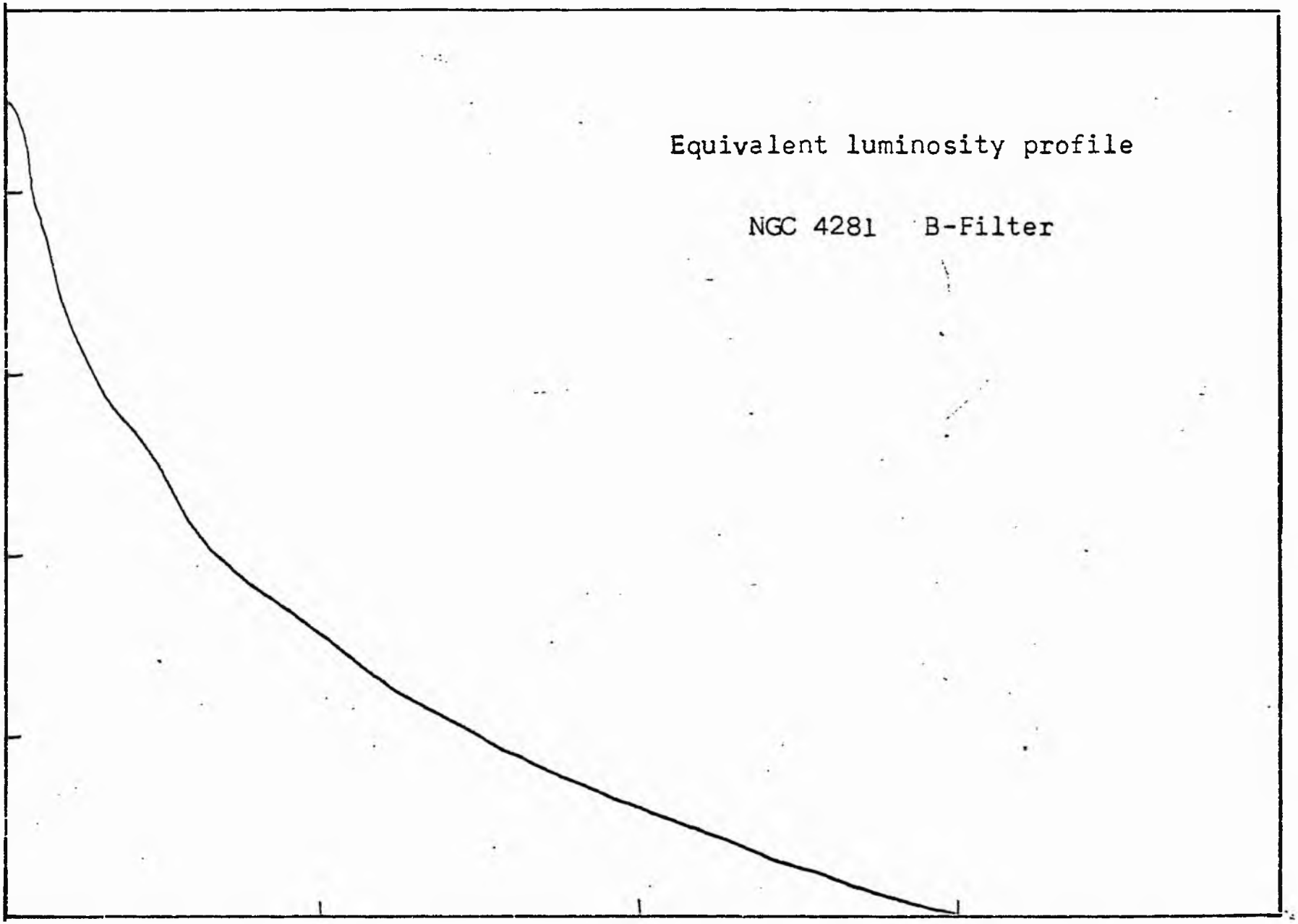
Equivalent luminosity profile
NGC 4281 B-Filter

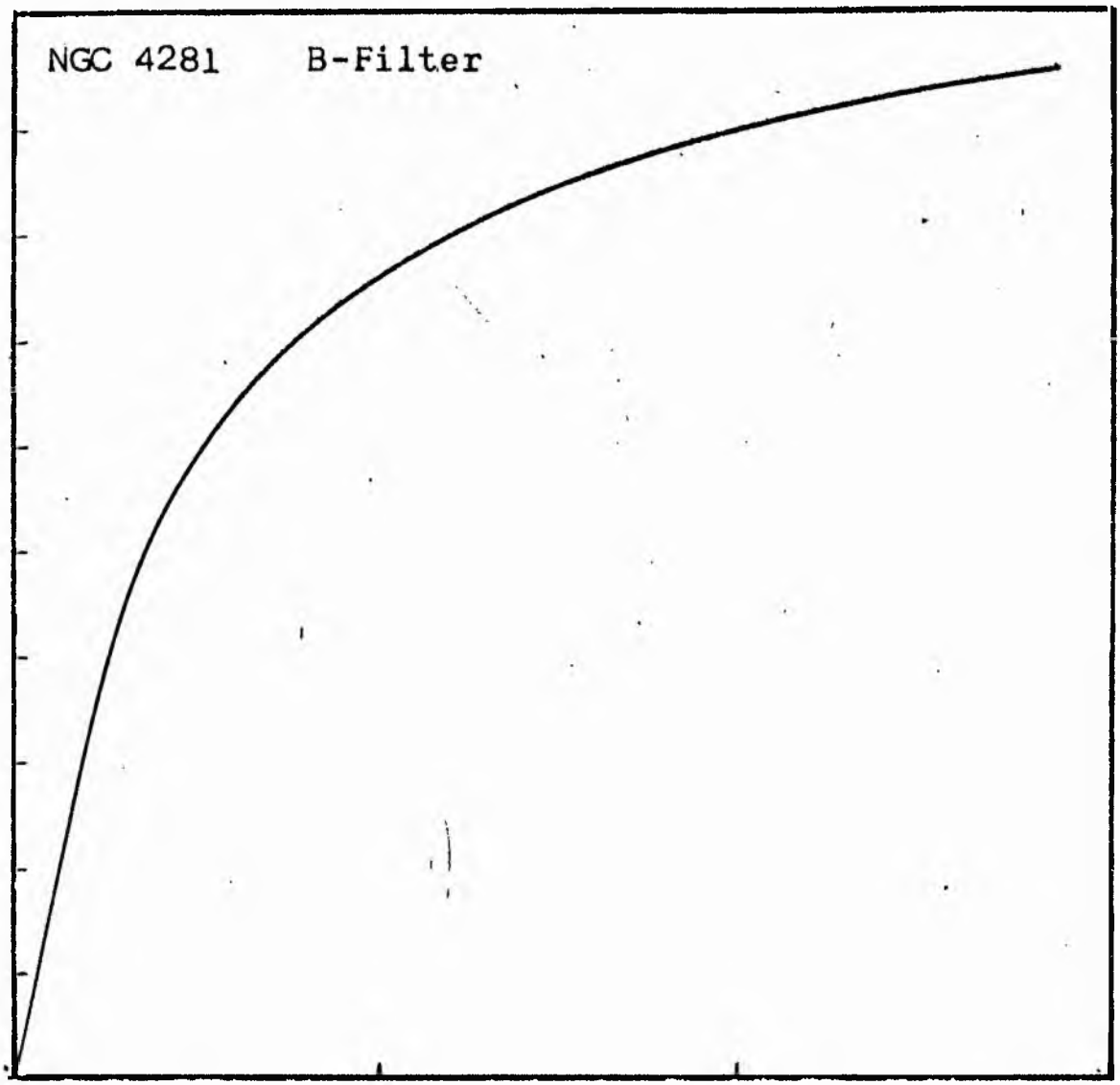

Relative integrated luminosity k(r) versus equivalent radius r*.

MEAN LUMINOSITY DISTRIBUTION IN NGC 4281
B COLOUR

LOG I	I	$\bar{I}$	R	AREA	ΔA	P	ΣP	K(R)	ρ	LOG J	μ
1.54	34.674		0.0	0.0			0.0	0.0	0.0	1.400	18.36
		33.148			16.62	550.8901					
1.50	31.623		2.30	16.62			550.89	0.05	0.12	1.360	18.46
		28.371			17.59	499.1250					
1.40	25.119		3.30	34.21			1050.02	0.10	0.17	1.260	18.71
		22.536			11.15	251.3326					
1.30	19.953		3.80	45.36			1301.35	0.12	0.20	1.160	18.96
		17.901			18.25	326.7358					
1.20	15.849		4.50	63.62			1628.08	0.16	0.23	1.060	19.21
		14.219			21.33	303.3118					
1.10	12.589		5.20	84.95			1931.40	0.18	0.27	0.960	19.46
		11.295			31.95	360.0616					
1.00	10.000		6.10	116.90			2292.26	0.22	0.32	0.860	19.71
		8.972			28.37	254.5112					
0.90	7.943		6.80	145.27			2546.77	0.24	0.35	0.760	19.96
		7.126			34.29	244.3367					
0.80	6.310		7.56	179.55			2791.10	0.27	0.39	0.660	20.21
		5.661			57.14	323.4626					
0.70	5.012		8.68	236.70			3114.57	0.30	0.45	0.560	20.46
		4.496			78.72	353.9695					
0.60	3.981		10.02	315.42			3468.54	0.33	0.52	0.460	20.71
		3.572			81.48	291.0337					
0.50	3.162		11.24	396.90			3759.57	0.36	0.58	0.360	20.96
		2.837			137.30	389.5308					
0.40	2.512		13.04	534.20			4149.10	0.40	0.68	0.260	21.21
		2.254			115.43	260.1306					
0.30	1.995		14.38	649.63			4409.23	0.42	0.75	0.160	21.46
		1.790			259.36	464.2654					
0.20	1.585		17.01	908.99			4873.49	0.46	0.88	0.060	21.71
		1.422			411.27	584.7817					
0.10	1.259		20.50	1320.25			5458.27	0.52	1.07	-0.040	21.96
		1.129			361.94	408.7976					
-0.00	1.000		23.14	1682.20			5867.07	0.56	1.20	-0.140	22.21
		0.897			264.06	236.9034					
-0.10	0.794		24.89	1946.25			6103.97	0.58	1.29	-0.240	22.46
		0.713			417.49	297.5229					
-0.20	0.631		27.43	2363.75			6401.49	0.61	1.43	-0.340	22.71
		0.566			459.92	260.3447					
-0.30	0.501		29.98	2823.66			6661.83	0.63	1.56	-0.440	22.96
		0.450			240.37	108.0818					
-0.40	0.398		31.23	3064.03			6769.91	0.64	1.62	-0.540	23.21
		0.357			734.00	262.1602					
-0.50	0.316		34.77	3798.03			7032.07	0.67	1.81	-0.640	23.46
		0.284			1012.23	287.1775					
-0.60	0.251		39.13	4810.27			7319.25	0.70	2.04	-0.740	23.71
		0.225			1355.07	305.3752					
-0.70	0.200		44.30	6165.34			7624.62	0.73	2.30	-0.840	23.96
		0.179			1780.01	318.6345					
-0.80	0.158		50.29	7945.35			7943.25	0.76	2.62	-0.940	24.21
		0.142			1454.58	206.8275					
-0.90	0.126		54.70	9399.93			8150.08	0.78	2.85	-1.040	24.46
		0.113			1425.03	160.9514					
-1.00	0.100		58.70	10824.95			8311.03	0.79	3.05	-1.140	24.71
		0.090			2984.51	267.7595					
-1.10	0.079		66.30	13809.46			8578.79	0.82	3.45	-1.240	24.96
		0.071			2977.97	212.2233					
-1.20	0.063		73.10	16787.43			8791.01	0.84	3.80	-1.340	25.21
		0.057			3419.42	193.5643					
-1.30	0.050		80.20	20206.85			8984.57	0.86	4.17	-1.440	25.46
		0.045			3245.01	145.9115					
-1.40	0.040		86.40	23451.86			9130.48	0.87	4.49	-1.540	25.71
		0.036			5320.39	190.0280					
-1.50	0.032		95.70	28772.24			9320.51	0.89	4.98	-1.640	25.96
		0.028			6128.20	173.8634					
-1.60	0.025		105.40	34900.45			9494.37	0.90	5.48	-1.740	26.21
		0.023			6791.76	153.0587					
-1.70	0.020		115.20	41692.20			9647.43	0.92	5.99	-1.840	26.46
		0.018			7709.04	138.0135					
-1.80	0.016		125.40	49402.04			9785.44	0.93	6.52	-1.940	26.71
		0.014			8448.79	120.1354					
-1.90	0.013		135.70	57850.82			9905.57	0.94	7.06	-2.040	26.96
		0.011			8474.74	95.7202					
-2.00	0.010		145.30	66325.56			10001.29	0.95	7.56	-2.140	27.21
$-\infty$							10501.00	(1)			∞

PHOTOMETRIC PARAMETERS OF NGC 4281

B-FILTER

Total luminosity	L_T	= 2.92
Total apparent magnitude	m_T	= 12.26
Apparent central surface brightness	μ_o	= 18.36
Major axis at threshold	$2a_m$	= 6.24
Minor axis at threshold	$2b_m$	= 3.65
Major axis at μ=25.0 mag sec^{-2}	$2a(25)$	= 3.28
Luminosity within μ=25.0 mag sec^{-2}	$k(25)$	= 0.83
Gradient of exponential component	$G(a)$	= -0.95
Equivalent gradient of exponential comp.	$G(r^*)$	= -1.02
Equivalent gradient of reduced exp. comp.	$G(\rho)$	= -0.79
Parameters at k = ¼ :		
Semi-major axis	a_1	= 0.18
Axis ratio	b/a	= 0.67
Equivalent radius	r_1^*	= 0.12
Surface brightness	μ_1	= 20.04
Parameters at k = ½(effective) :		
Semi-major axis	a_e	= 0.54
Axis ratio	b/a	= 0.41
Equivalent radius	r_e^*	= 0.32
Surface brightness	μ_e	= 21.88
Mean surface brightness	μ_e'	= 11.75
Parameters at k = ¾ :		
Semi-major axis	a_3	= 1.18
Axis ratio	b/a	= 0.47
Equivalent radius	r_3^*	= 0.82
Surface brightness	μ_3	= 24.13
Concentration indices	C_{21}	= 2.73
	C_{32}	= 2.55

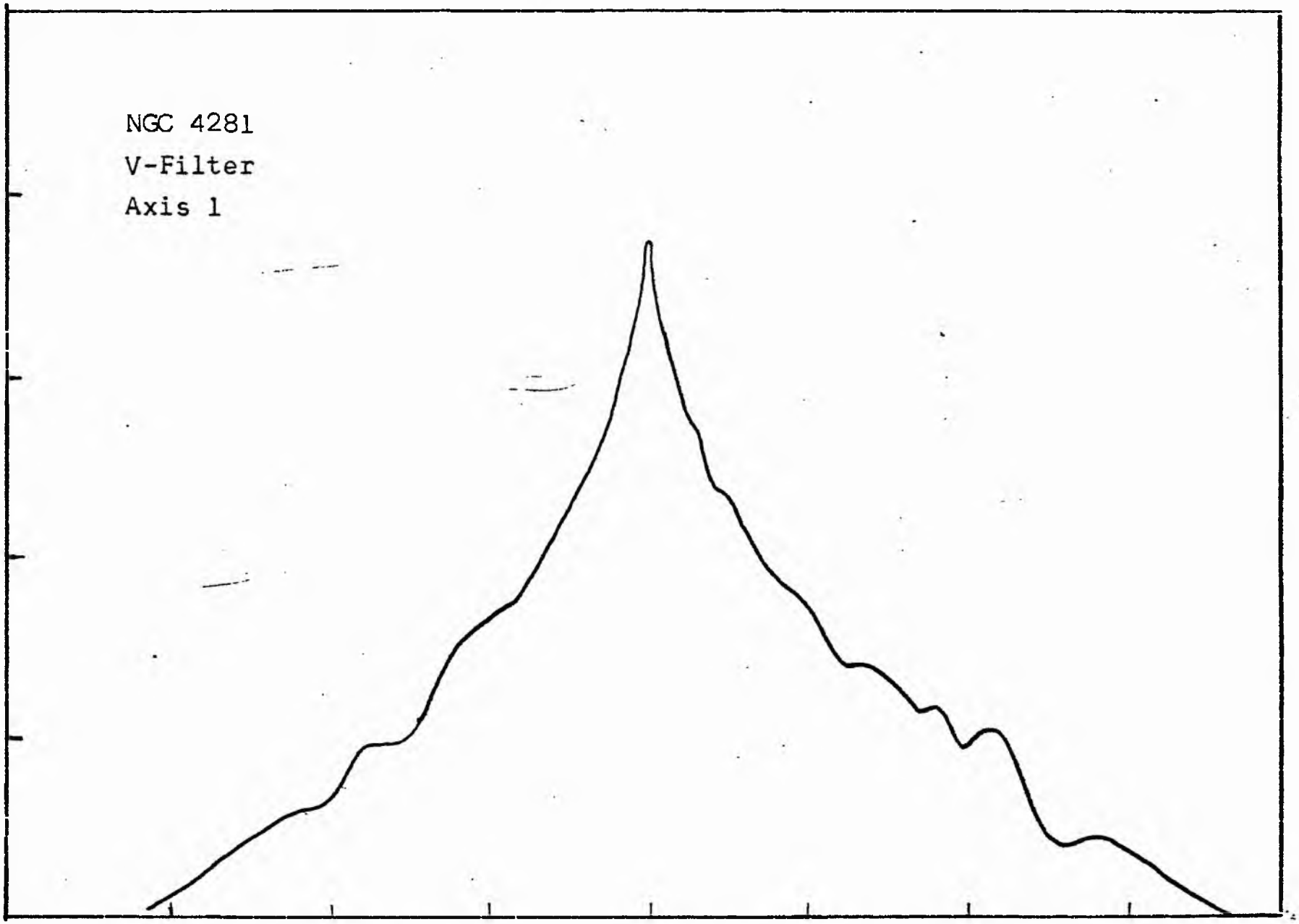
NGC 4281
V-Filter
Axis 1

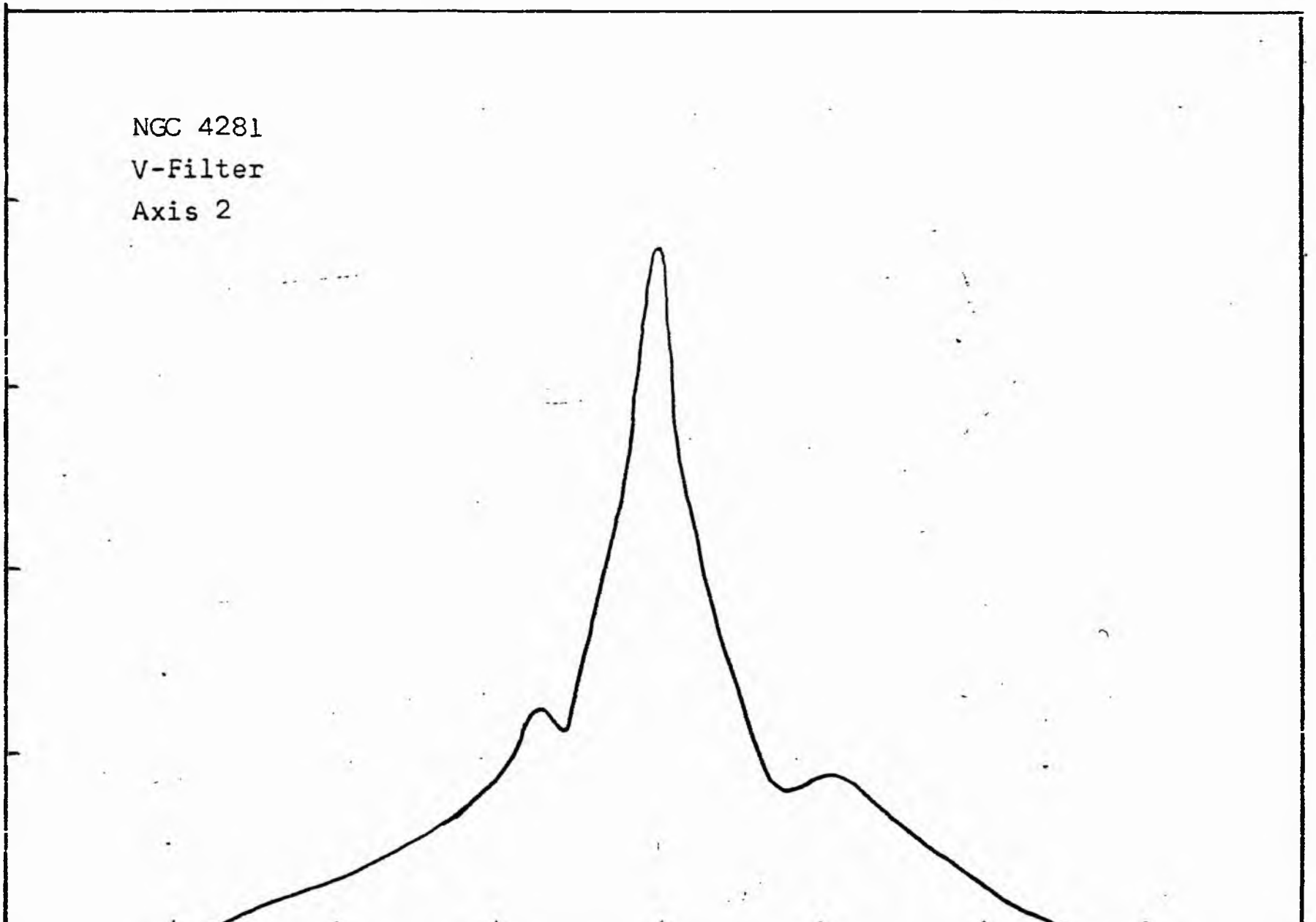
NGC 4281
V-Filter
Axis 2

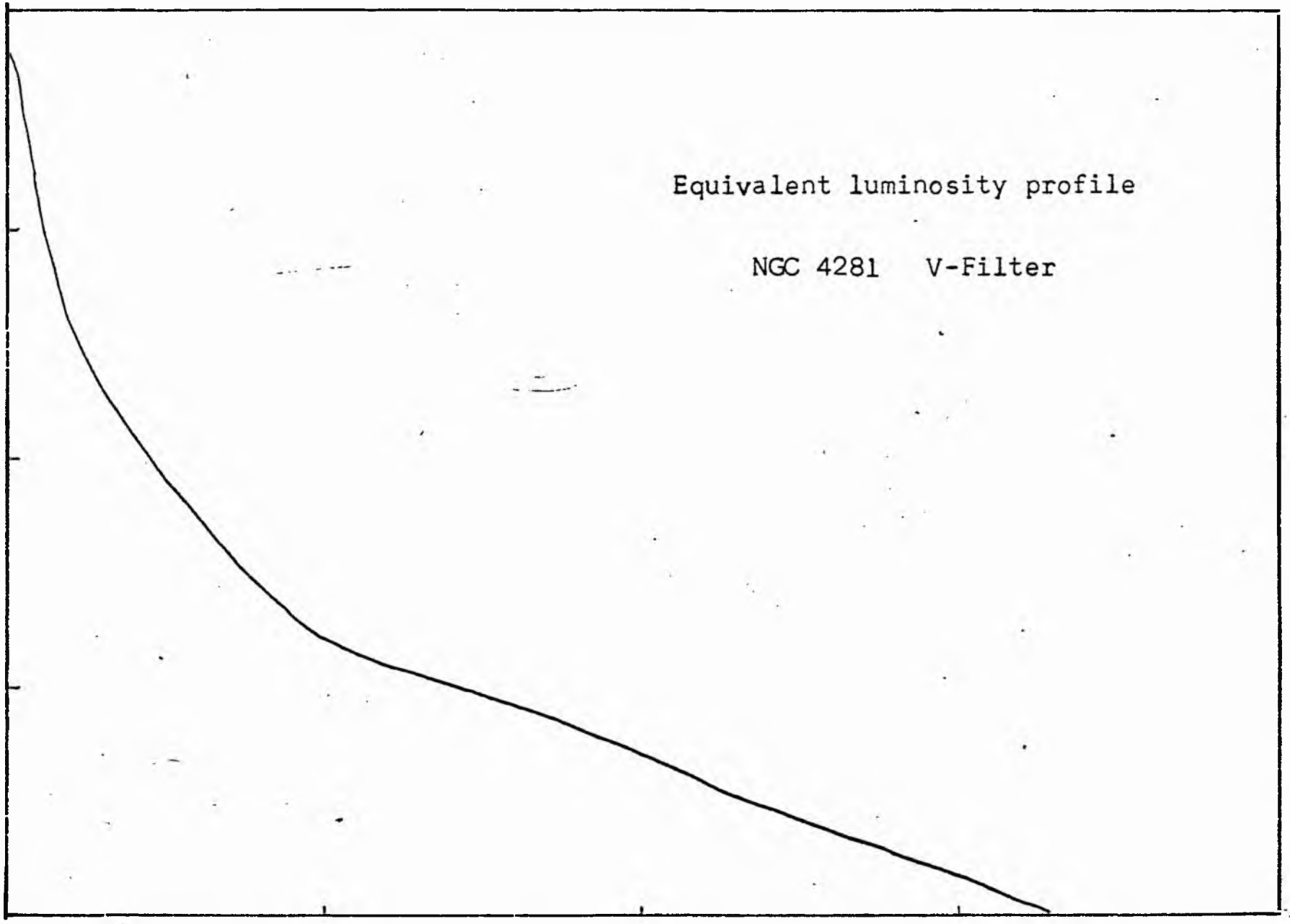
Equivalent luminosity profile
NGC 4281 V-Filter

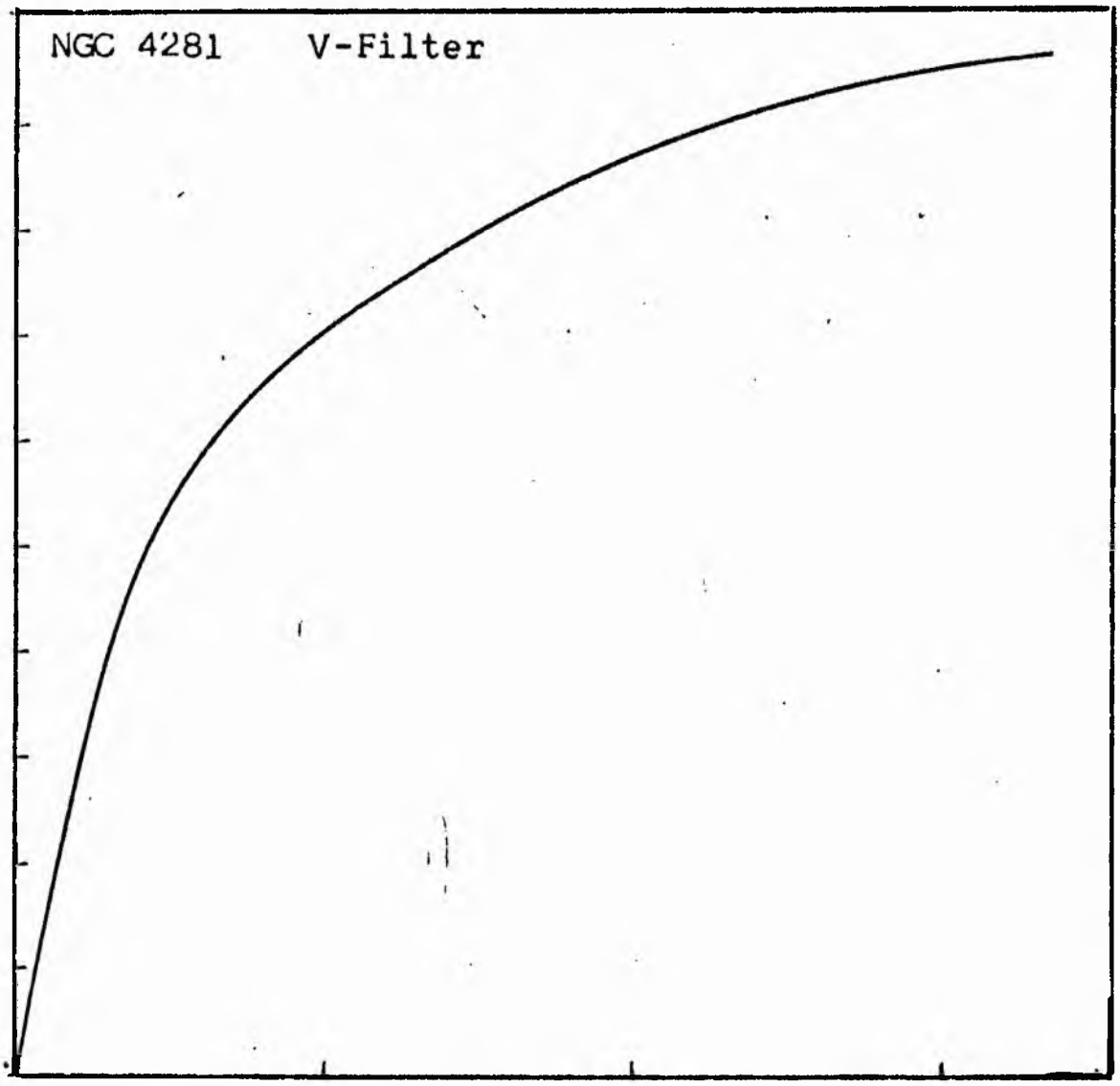

Relative integrated luminosity k(r) versus equivalent radius r*.

MEAN LUMINOSITY DISTRIBUTION IN NGC 4281
V COLOUR

LOG I	I	$\bar{I}$	R	AREA	$\triangle A$	P	ΣP	K(R)	ρ	LOG J	μ
1.78	60.256		0.0	0.0			0.0	0.0	0.0	1.665	17.07
		55.187			3.14	173.3760					
1.70	50.119		1.00	3.14			173.38	0.01	0.05	1.585	17.27
		44.965			5.94	266.9824					
1.60	39.811		1.70	9.08			440.36	0.03	0.08	1.485	17.52
		35.717			15.55	555.4253					
1.50	31.623		2.80	24.63			995.78	0.07	0.13	1.385	17.77
		28.371			13.85	393.0608					
1.40	25.119		3.50	38.48			1388.84	0.10	0.16	1.285	18.02
		22.536			14.33	322.8369					
1.30	19.953		4.10	52.81			1711.68	0.13	0.19	1.185	18.27
		17.901			10.81	193.4551					
1.20	15.849		4.50	63.62			1905.14	0.14	0.21	1.085	18.52
		14.219			45.74	650.3994					
1.10	12.589		5.90	109.36			2555.54	0.19	0.27	0.985	18.77
		11.295			40.65	459.0815					
1.00	10.000		6.91	150.01			3014.62	0.22	0.32	0.885	19.02
		8.972			33.85	303.6768					
0.90	7.943		7.65	183.85			3318.29	0.25	0.35	0.785	19.27
		7.126			41.53	295.9358					
0.80	6.310		8.47	225.38			3614.23	0.27	0.39	0.685	19.52
		5.661			51.62	292.2053					
0.70	5.012		9.39	277.00			3906.44	0.29	0.43	0.585	19.77
		4.496			100.37	451.3186					
0.60	3.981		10.96	377.37			4357.75	0.32	0.50	0.485	20.02
		3.572			126.15	450.5549					
0.50	3.162		12.66	503.52			4808.31	0.36	0.58	0.385	20.27
		2.837			166.14	471.3540					
0.40	2.512		14.60	669.66			5279.66	0.39	0.67	0.285	20.52
		2.254			227.61	512.9270					
0.30	1.995		16.90	897.27			5792.59	0.43	0.78	0.185	20.77
		1.790			301.00	538.8093					
0.20	1.585		19.53	1198.27			6331.39	0.47	0.90	0.085	21.02
		1.422			350.03	497.7134					
0.10	1.259		22.20	1548.30			6829.11	0.51	1.02	-0.015	21.27
		1.129			430.93	486.7183					
-0.00	1.000		25.10	1979.23			7315.82	0.54	1.15	-0.115	21.52
		0.897			396.60	355.8101					
-0.10	0.794		27.50	2375.83			7671.63	0.57	1.26	-0.215	21.77
		0.713			395.34	281.7324					
-0.20	0.631		29.70	2771.17			7953.36	0.59	1.36	-0.315	22.02
		0.566			385.79	218.3828					
-0.30	0.501		31.70	3156.95			8171.74	0.60	1.45	-0.415	22.27
		0.450			824.57	370.7649					
-0.40	0.398		35.60	3981.53			8542.50	0.63	1.63	-0.515	22.52
		0.357			723.60	258.4460					
-0.50	0.316		38.70	4705.13			8800.95	0.65	1.78	-0.615	22.77
		0.284			627.54	178.0362					
-0.60	0.251		41.20	5332.66			8978.98	0.66	1.89	-0.715	23.02
		0.225			1228.52	276.8547					
-0.70	0.200		45.70	6561.18			9255.83	0.68	2.10	-0.815	23.27
		0.179			2163.93	387.3586					
-0.80	0.158		52.70	8725.11			9643.19	0.71	2.42	-0.915	23.52
		0.142			4425.86	629.3152					
-0.90	0.126		64.70	13150.98			10272.50	0.76	2.97	-1.015	23.77
		0.113			3774.54	426.3186					
-1.00	0.100		73.40	16925.52			10698.82	0.79	3.37	-1.115	24.02
		0.090			5825.92	522.6797					
-1.10	0.079		85.10	22751.44			11221.50	0.83	3.90	-1.215	24.27
		0.071			5185.13	369.5139					
-1.20	0.063		94.30	27936.57			11591.01	0.86	4.33	-1.315	24.52
		0.057			3605.15	204.0776					
-1.30	0.050		100.20	31541.71			11795.08	0.87	4.60	-1.415	24.77
		0.045			6264.48	281.6814					
-1.40	0.040		109.70	37806.20			12076.76	0.89	5.03	-1.515	25.02
		0.036			6085.74	217.3638					
-1.50	0.032		118.20	43891.94			12294.12	0.91	5.42	-1.615	25.27
		0.028			8630.73	244.8623					
-1.60	0.025		129.30	52522.67			12538.98	0.93	5.93	-1.715	25.52
		0.023			6183.92	139.3601					
-1.70	0.020		136.70	58706.59			12678.34	0.94	6.27	-1.815	25.77
		0.018			6618.55	118.4781					
-1.80	0.016		144.20	65325.14			12796.82	0.95	6.62	-1.915	26.02
		0.014			13300.23	189.1190					
-1.90	0.013		158.20	78625.37			12985.94	0.96	7.26	-2.015	26.27
		0.011			6180.25	69.8043					
-2.00	0.010		164.30	84805.62			13055.74	0.97	7.54	-2.115	26.52
$-\infty$							13515.00	(1)			∞

PHOTOMETRIC PARAMETERS OF NGC 4281

V-FILTER

Total luminosity	L_T	= 3.75
Total apparent magnitude	m_T	= 11.19
Apparent central surface brightness	μ_o	= 17.07
Major axis at threshold	$2a_m$	= 5.96
Minor axis at threshold	$2b_m$	= 3.95
Major axis at μ=25.0 mag sec^{-2}	2a(25)	= 3.80
Luminosity within μ=25.0 mag sec^{-2}	k(25)	= 0.89
Gradient of exponential component	G(a)	= -0.88
Equivalent gradient of exponential comp.	G(r*)	= -0.76
Equivalent gradient of reduced exp. comp.	G(ρ)	= -0.80

Parameters at k = ¼ :

Semi-major axis	a_1	= 0.19
Axis ratio	b/a	= 0.69
Equivalent radius	r_1*	= 0.13
Surface brightness	μ_1	= 19.27

Parameters at k = ½(effective) :

Semi-major axis	a_e	= 0.37
Axis ratio	b/a	= 0.73
Equivalent radius	r_e*	= 0.36
Surface brightness	μ_e	= 21.21
Mean surface brightness	μ_e'	= 10.98

Parameters at k = ¾ :

Semi-major axis	a_3	= 1.26
Axis ratio	b/a	= 0.47
Equivalent radius	r_3*	= 1.03
Surface brightness	μ_3	= 23.72

Concentration indices	C_{21}	= 2.79
	C_{32}	= 2.85

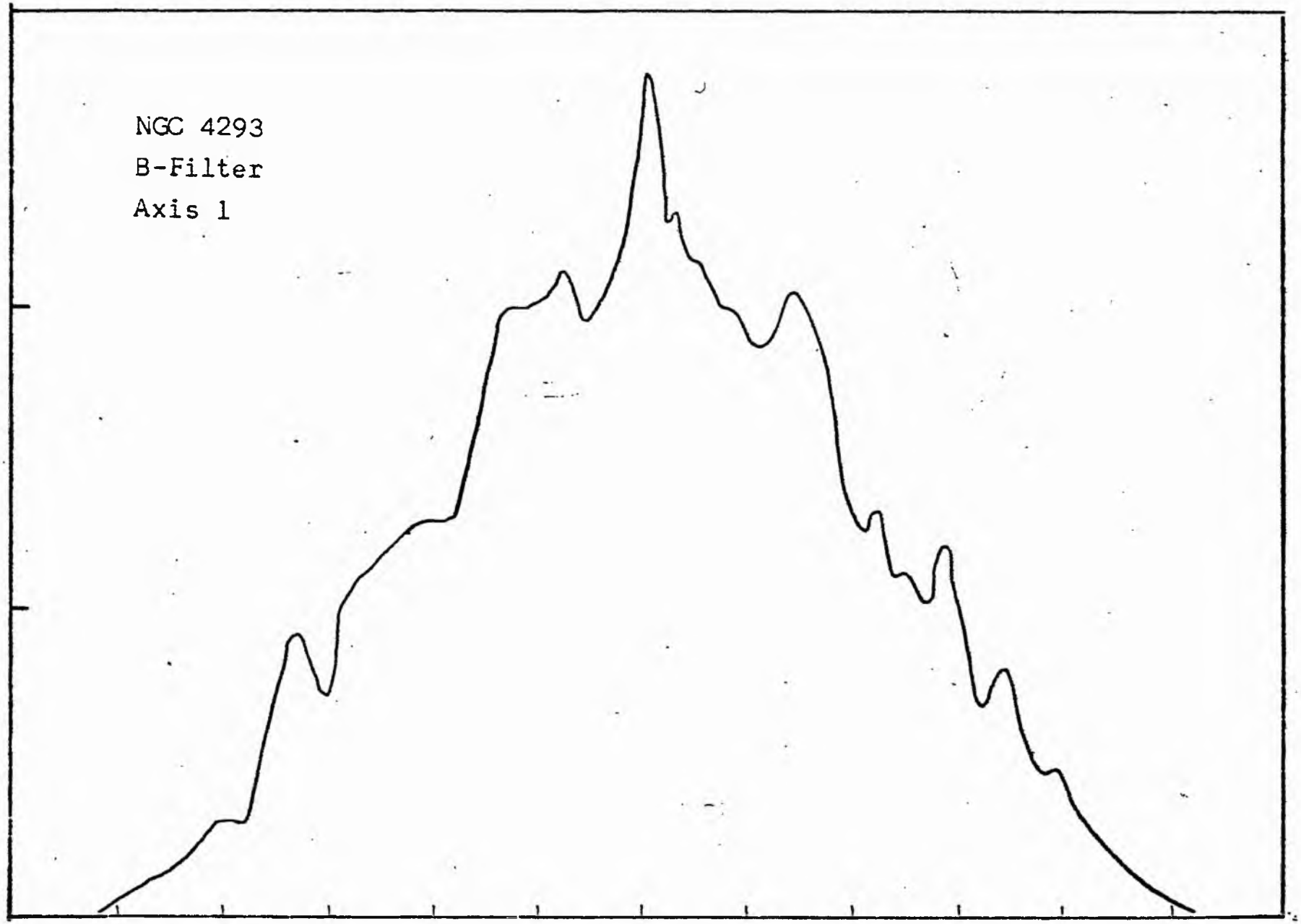
NGC 4293
B-Filter
Axis 1

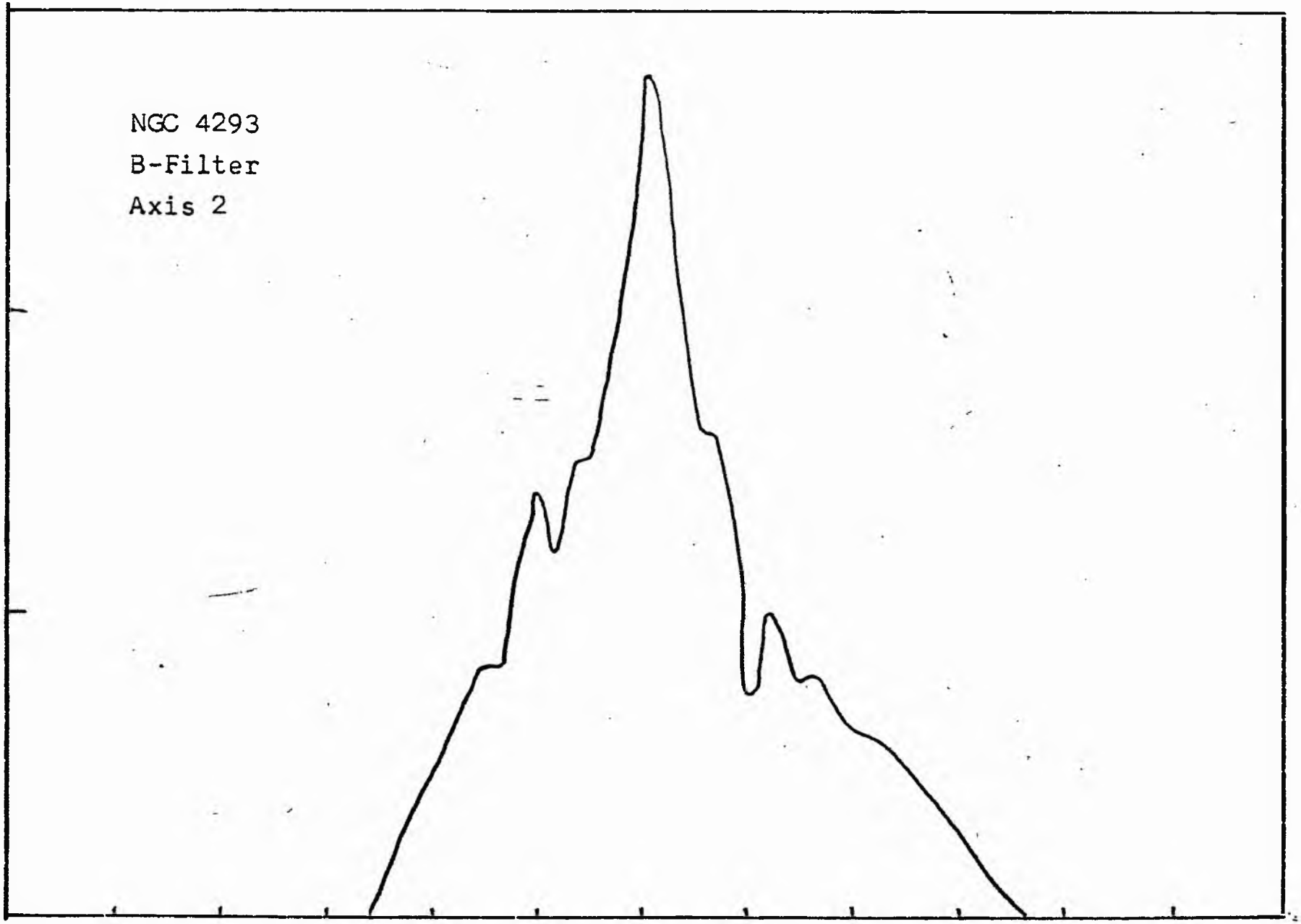
NGC 4293
B-Filter
Axis 2

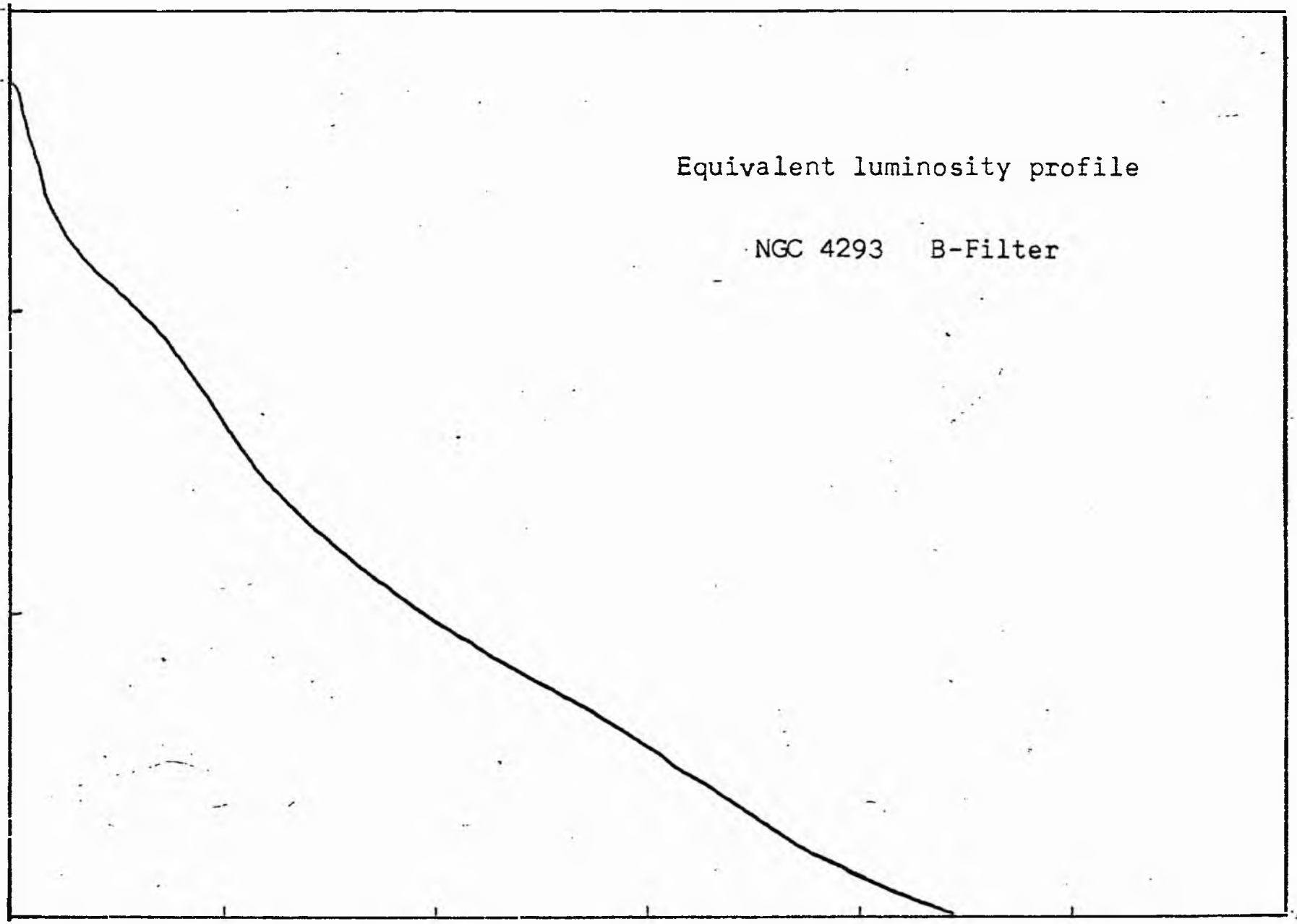
Equivalent luminosity profile
NGC 4293 B-Filter

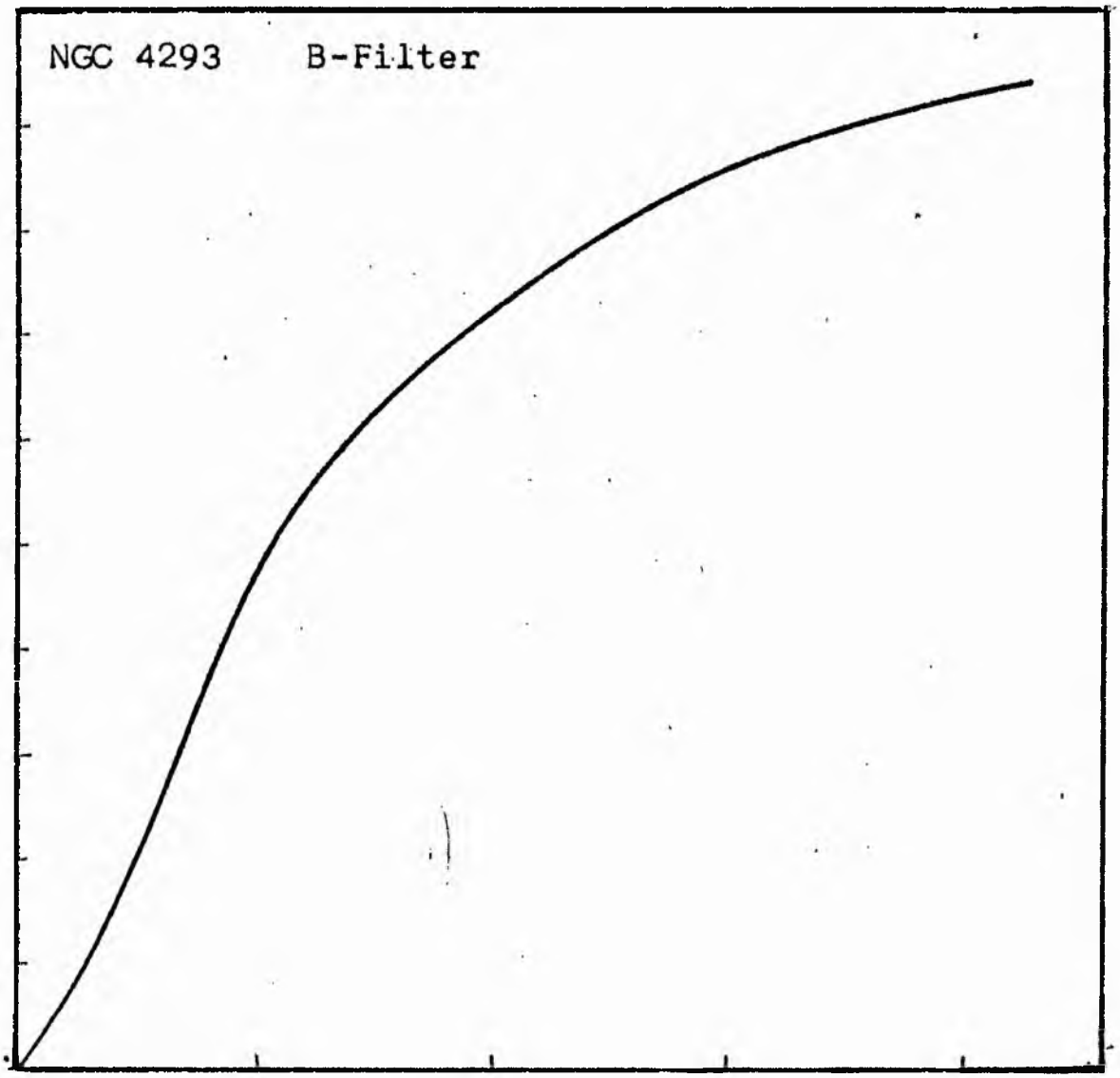

Relative integrated luminosity k(r) versus equivalent radius r*.

MEAN LUMINOSITY DISTRIBUTION IN NGC 4293
B COLOUR

LOG I	I	$\bar{I}$	R	AREA	ΔA	P	ΣP	K(R)	ρ	LOG J	μ
0.79	6.166		0.0	0.0			0.0	0.0	0.0	1.288	19.58
		5.589			22.23	124.2338					
0.70	5.012		2.66	22.23			124.23	0.01	0.05	1.198	19.81
		4.496			29.81	134.0465					
0.60	3.981		4.07	52.04			258.28	0.02	0.08	1.098	20.06
		3.572			75.44	269.4321					
0.50	3.162		6.37	127.48			527.71	0.03	0.12	0.998	20.31
		2.837			25.58	72.5826					
0.40	2.512		6.98	153.06			600.29	0.04	0.13	0.898	20.56
		2.254			173.79	391.6519					
0.30	1.995		10.20	326.85			991.95	0.06	0.19	0.798	20.81
		1.790			171.91	307.7265					
0.20	1.585		12.60	498.76			1299.68	0.08	0.23	0.698	21.06
		1.422			1035.62	1472.5649					
0.10	1.259		22.10	1534.38			2772.24	0.17	0.41	0.598	21.31
		1.129			1332.77	1505.3157					
0.00	1.000		30.21	2867.15			4277.55	0.27	0.56	0.498	21.56
		0.897			1357.31	1217.7275					
-0.10	0.794		36.67	4224.46			5495.28	0.34	0.68	0.398	21.81
		0.713			1269.91	904.9897					
-0.20	0.631		41.82	5494.37			6400.27	0.40	0.78	0.298	22.06
		0.566			1345.36	761.5730					
-0.30	0.501		46.66	6839.73			7161.84	0.45	0.87	0.198	22.31
		0.450			638.71	287.1965					
-0.40	0.398		48.79	7478.45			7449.04	0.46	0.91	0.098	22.56
		0.357			1689.22	603.3359					
-0.50	0.316		54.02	9167.67			8052.37	0.50	1.00	-0.002	22.81
		0.284			2255.44	639.8879					
-0.60	0.251		60.30	11423.11			8692.26	0.54	1.12	-0.102	23.06
		0.225			2933.21	661.0210					
-0.70	0.200		67.60	14356.32			9353.28	0.58	1.25	-0.202	23.31
		0.179			3770.41	674.9343					
-0.80	0.158		75.96	18126.73			10028.21	0.62	1.41	-0.302	23.56
		0.142			4763.93	677.3889					
-0.90	0.126		85.36	22890.66			10705.60	0.67	1.58	-0.402	23.81
		0.113			5045.90	569.9167					
-1.00	0.100		94.30	27936.57			11275.51	0.70	1.75	-0.502	24.06
		0.090			9183.51	823.9133					
-1.10	0.079		108.70	37120.08			12099.42	0.75	2.02	-0.602	24.31
		0.071			7540.14	537.3450					
-1.20	0.063		119.23	44660.22			12636.77	0.79	2.21	-0.702	24.56
		0.057			6330.21	358.3376					
-1.30	0.050		127.40	50990.43			12995.10	0.81	2.36	-0.802	24.81
		0.045			11733.62	527.6023					
-1.40	0.040		141.30	62724.05			13522.70	0.84	2.62	-0.902	25.06
		0.036			11395.39	407.0093					
-1.50	0.032		153.60	74119.44			13929.71	0.87	2.85	-1.002	25.31
		0.028			13181.87	373.9841					
-1.60	0.025		166.70	87301.31			14303.69	0.89	3.09	-1.102	25.56
		0.023			9129.94	205.7522					
-1.70	0.020		175.20	96431.25			14509.44	0.90	3.25	-1.202	25.81
		0.018			12606.12	225.6622					
-1.80	0.016		186.30	109037.37			14735.10	0.92	3.46	-1.302	26.06
		0.014			17129.44	243.5684					
-1.90	0.013		200.40	126166.81			14978.67	0.93	3.72	-1.402	26.31
		0.011			13302.56	150.2497					
-2.00	0.010		210.70	139469.37			15128.91	0.94	3.91	-1.502	26.56

PHOTOMETRIC PARAMETERS OF NGC 4293

B-FILTER

Total luminosity	L_T	= 4.47
Total apparent magnitude	m_T	= 11.04
Apparent central surface brightness	μ_o	= 19.58
Major axis at threshold	$2a_m$	= 8.20
Minor axis at threshold	$2b_m$	= 4.96
Major axis at μ=25.0 mag sec^{-2}	2a(25)	= 6.04
Luminosity within μ=25.0 mag sec^{-2}	k(25)	= 0.83
Gradient of exponential component	G(a)	= -0.66
Equivalent gradient of exponential comp.	G(r*)	= -0.57
Equivalent gradient of reduced exp. comp.	G(ρ)	= -0.75

Parameters at k = ¼ :

Semi-major axis	a_1	= 0.80
Axis ratio	b/a	= 0.26
Equivalent radius	r_1*	= 0.48
Surface brightness	μ_1	= 21.51

Parameters at k = ½(effective) :

Semi-major axis	a_e	= 1.70
Axis ratio	b/a	= 0.27
Equivalent radius	r_e*	= 0.90
Surface brightness	μ_e	= 22.81
Mean surface brightness	μ_e'	= 12.80

Parameters at k = ¾ :

Semi-major axis	a_3	= 2.70
Axis ratio	b/a	= 0.43
Equivalent radius	r_3*	= 1.80
Surface brightness	μ_3	= 24.31

Concentration indices	C_{21}	= 1.87
	C_{32}	= 2.00

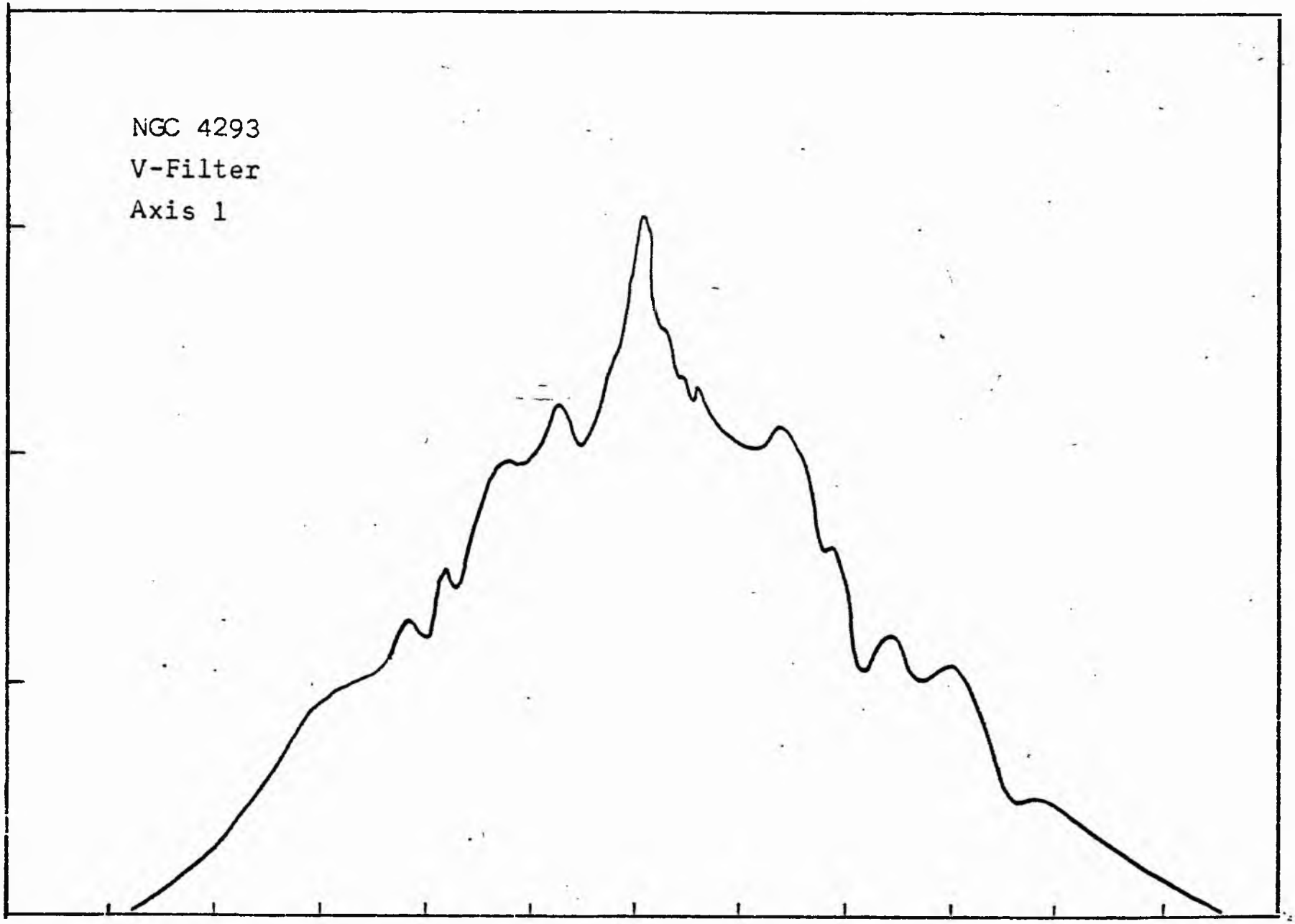
NGC 4293
V-Filter
Axis 1

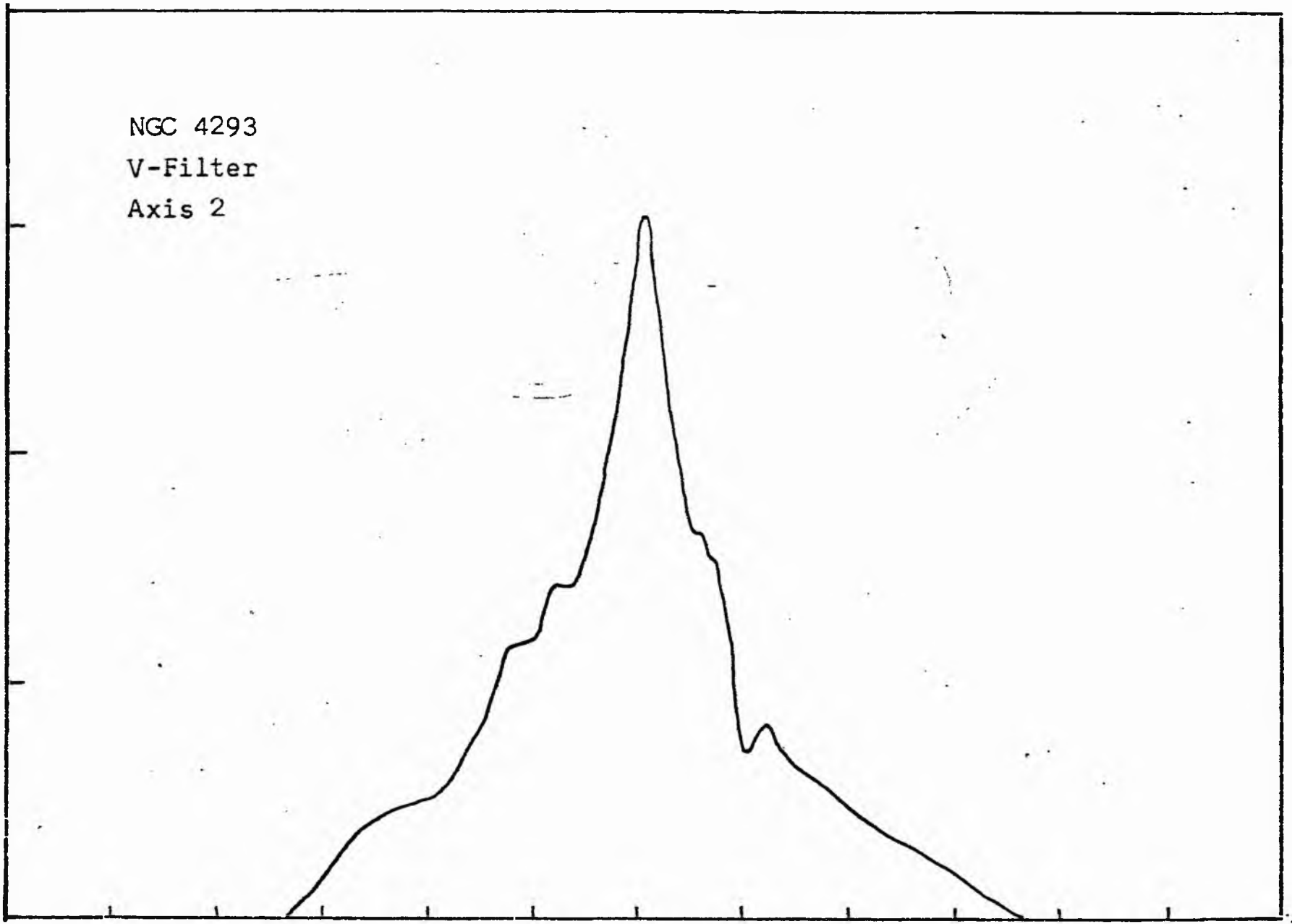
NGC 4293
V-Filter
Axis 2

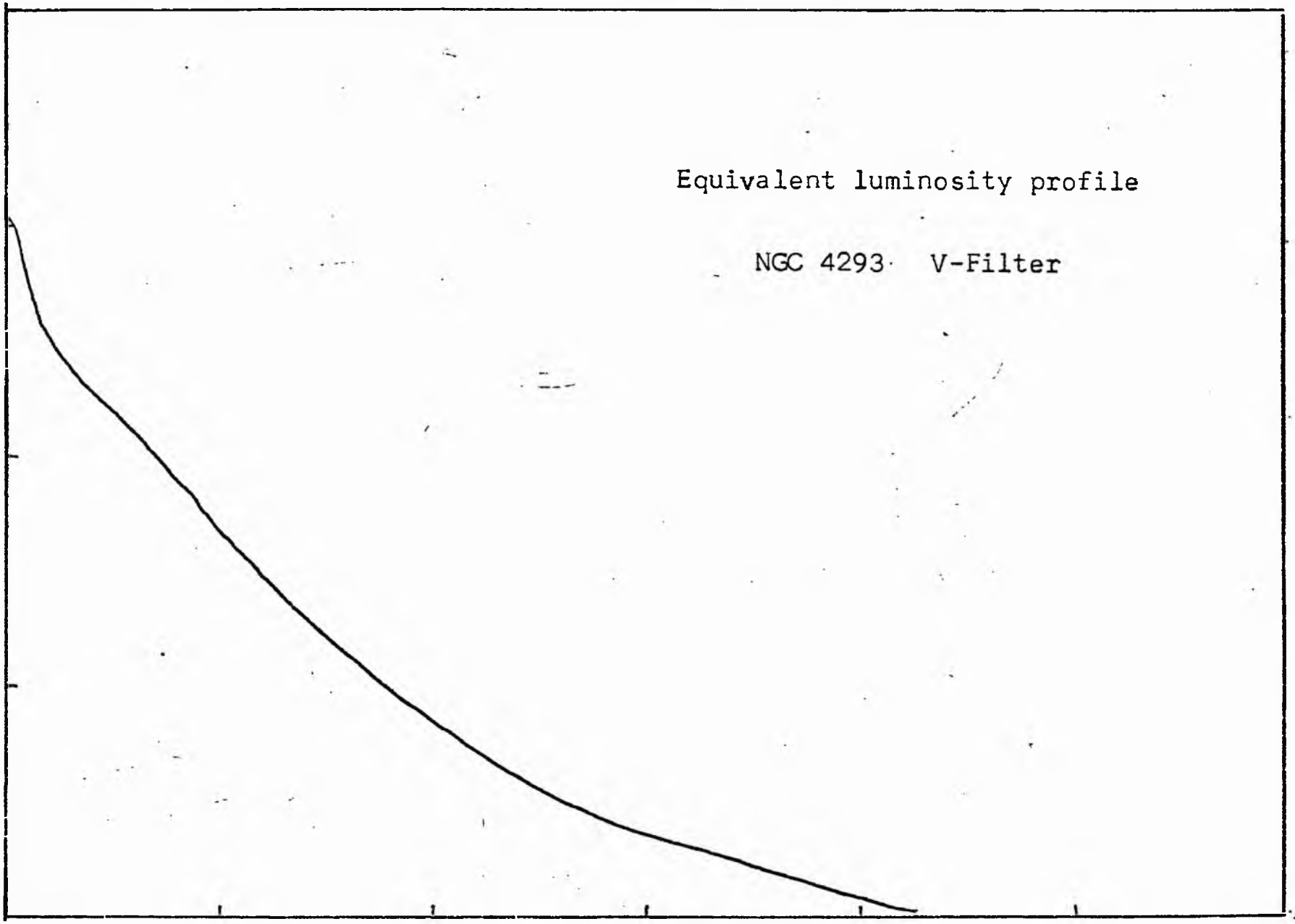
Equivalent luminosity profile
NGC 4293 V-Filter

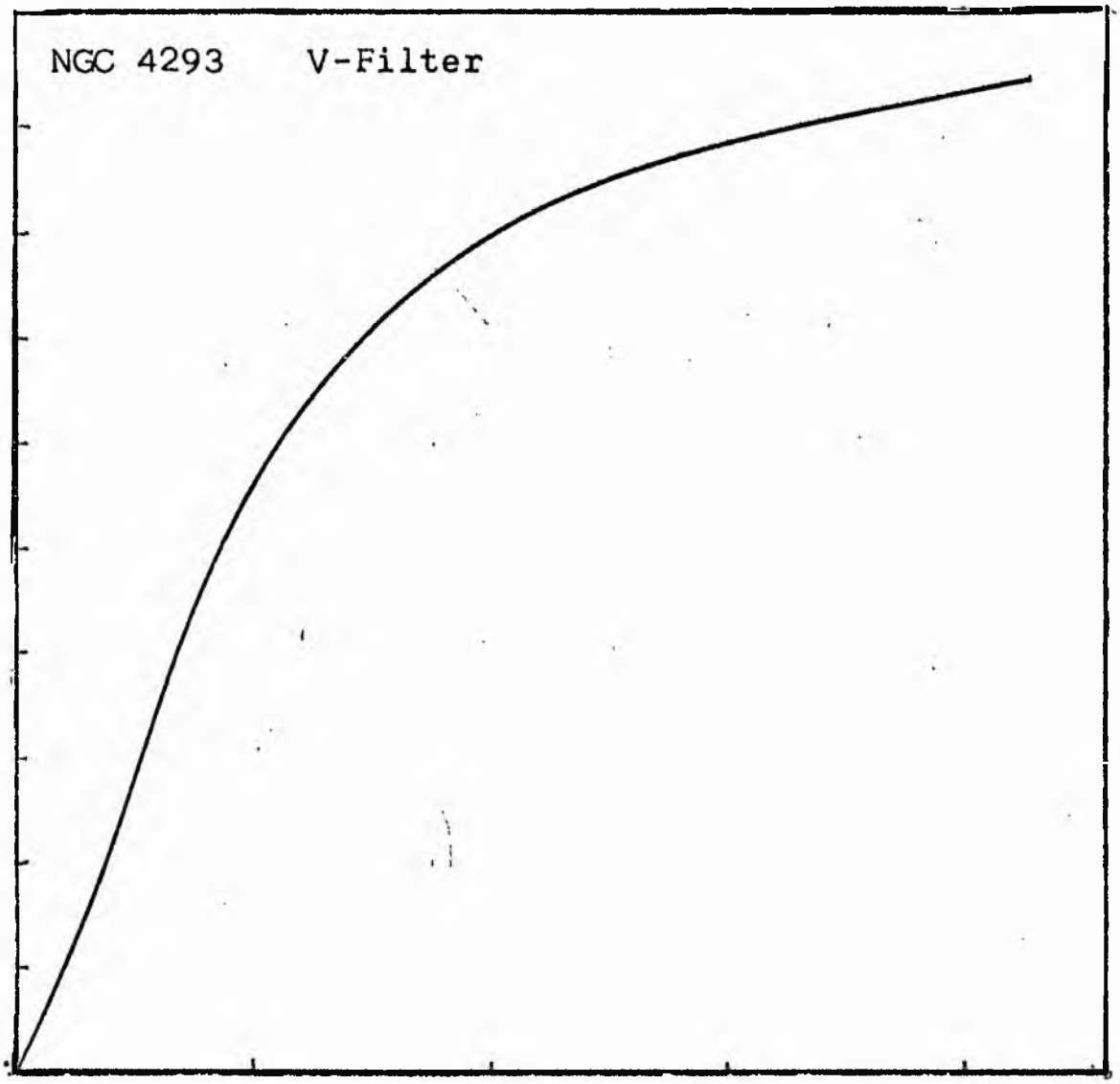

Relative integrated luminosity k(r) versus equivalent radius r*.

MEAN LUMINOSITY DISTRIBUTION IN NGC 4293
V COLOUR

LOG I	I	$\bar{I}$	R	AREA	Δ A	P	Σ P	K(R)	ρ	LOG J
1.04	10.965		0.0	0.0			0.0	0.0	0.0	1.206
		10.482			19.63	205.8211				
1.00	10.000		2.50	19.63			205.82	0.01	0.06	1.166
		8.972			33.69	302.2693				
0.90	7.943		4.12	53.33			508.09	0.03	0.10	1.066
		7.126			65.11	464.0022				
0.80	6.310		6.14	118.44			972.09	0.05	0.14	0.966
		5.661			42.17	238.7086				
0.70	5.012		7.15	160.61			1210.80	0.07	0.17	0.866
		4.496			91.04	409.3740				
0.60	3.981		8.95	251.65			1620.18	0.09	0.21	0.766
		3.572			114.79	409.9775				
0.50	3.162		10.80	366.44			2030.15	0.11	0.26	0.666
		2.837			148.28	420.6909				
0.40	2.512		12.80	514.72			2450.84	0.14	0.30	0.566
		2.254			230.34	519.0925				
0.30	1.995		15.40	745.06			2969.94	0.17	0.36	0.466
		1.790			1273.80	2280.1946				
0.20	1.585		25.35	2018.86			5250.13	0.29	0.60	0.366
		1.422			601.40	855.1379				
0.10	1.259		28.88	2620.26			6105.27	0.34	0.68	0.266
		1.129			968.82	1094.2476				
0.00	1.000		33.80	3589.08			7199.51	0.40	0.80	0.166
		0.897			1312.59	1177.6094				
-0.10	0.794		39.50	4901.67			8377.12	0.47	0.93	0.066
		0.713			1125.29	801.9265				
-0.20	0.631		43.80	6026.95			9179.05	0.51	1.03	-0.034
		0.566			1271.72	719.8848				
-0.30	0.501		48.20	7298.67			9898.93	0.55	1.14	-0.134
		0.450			649.84	292.1970				
-0.40	0.398		50.30	7948.51			10191.12	0.57	1.19	-0.234
		0.357			1833.27	654.7864				
-0.50	0.316		55.80	9781.78			10845.91	0.61	1.32	-0.334
		0.284			2568.73	728.7700				
-0.60	0.251		62.70	12350.51			11574.68	0.65	1.48	-0.434
		0.225			3308.30	745.5525				
-0.70	0.200		70.60	15658.81			12320.23	0.69	1.67	-0.534
		0.179			4346.96	778.1411				
-0.80	0.158		79.80	20005.77			13098.37	0.73	1.88	-0.634
		0.142			1950.68	277.3699				
-0.90	0.126		83.60	21956.46			13375.74	0.75	1.97	-0.734
		0.113			2593.70	292.9497				
-1.00	0.100		88.40	24550.16			13668.69	0.77	2.09	-0.834
		0.090			3982.05	357.2566				
-1.10	0.079		95.30	28532.21			14025.94	0.79	2.25	-0.934
		0.071			5906.20	420.9023				
-1.20	0.063		104.70	34438.41			14446.84	0.81	2.47	-1.034
		0.057			3436.74	194.5455				
-1.30	0.050		109.80	37875.15			14641.39	0.82	2.59	-1.134
		0.045			5277.25	237.2917				
-1.40	0.040		117.20	43152.40			14878.68	0.83	2.77	-1.234
		0.036			12002.19	428.6824				
-1.50	0.032		132.50	55154.59			15307.36	0.86	3.13	-1.334
		0.028			12916.91	366.4668				
-1.60	0.025		147.20	68071.50			15673.82	0.88	3.48	-1.434
		0.023			15397.44	346.9963				
-1.70	0.020		163.00	83468.94			16020.82	0.90	3.85	-1.534
		0.018			15399.31	275.6628				
-1.80	0.016		177.40	98868.25			16296.48	0.91	4.19	-1.634
		0.014			12522.81	178.0655				
-1.90	0.013		188.30	111391.06			16474.54	0.92	4.45	-1.734
		0.011			19349.44	218.5479				
-2.00	0.010		204.00	130740.50			16693.09	0.94	4.82	-1.834
$-\infty$							17843.00	(1)		

PHOTOMETRIC PARAMETERS OF NGC 4293

V-FILTER

Total luminosity ..... L_T = 4.96

Total apparent magnitude ..... m_T = ---

Apparent central surface brightness ..... μ_o = ---

Major axis at threshold ..... $2a_m$ = 8.15

Minor axis at threshold ..... $2b_m$ = 5.77

Major axis at μ=25.0 mag sec^{-2} ..... 2a(25) = ---

Luminosity within μ=25.0 mag sec^{-2} ..... k(25) = ---

Gradient of exponential component ..... G(a) = -0.61

Equivalent gradient of exponential comp..... G(r*) = -0.95

Equivalent gradient of reduced exp. comp..... G(ρ) = -0.73

Parameters at k = ¼ :

- Semi-major axis ..... a_1 = 0.54
- Axis ratio ..... b/a = 0.45
- Equivalent radius ..... r_1* = 0.36
- Surface brightness ..... μ_1 = ---

Parameters at k = ½(effective) :

- Semi-major axis ..... a_e = 1.19
- Axis ratio ..... b/a = 0.30
- Equivalent radius ..... r_e* = 0.71
- Surface brightness ..... μ_e = ---
- Mean surface brightness ..... μ_e' = ---

Parameters at k = ¾ :

- Semi-major axis ..... a_3 = 2.19
- Axis ratio ..... b/a = 0.41
- Equivalent radius ..... r_3* = 1.40
- Surface brightness ..... μ_3 = ---

Concentration indices ..... C_{21} = 1.93, C_{32} = 1.98

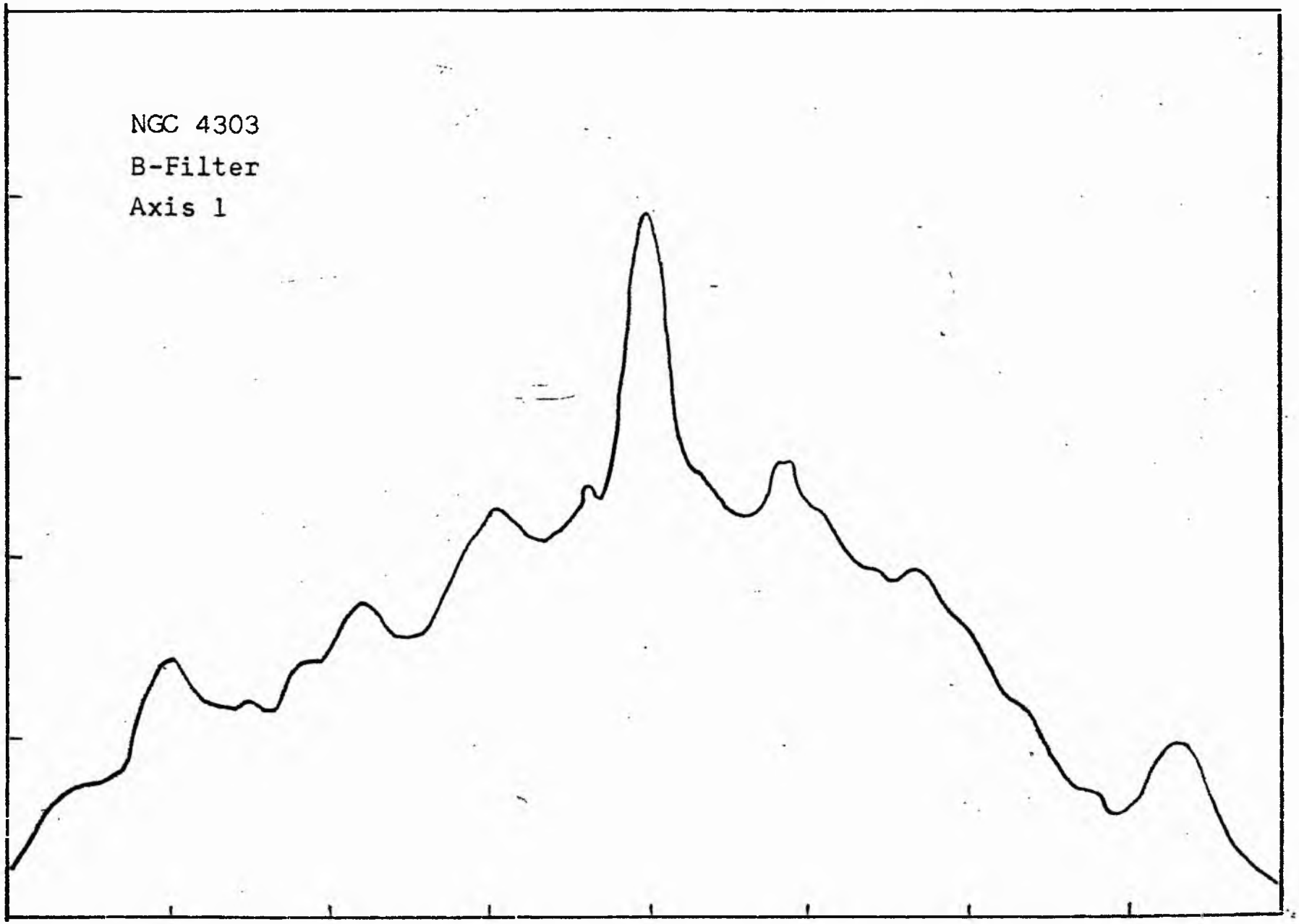
NGC 4303
B-Filter
Axis 1

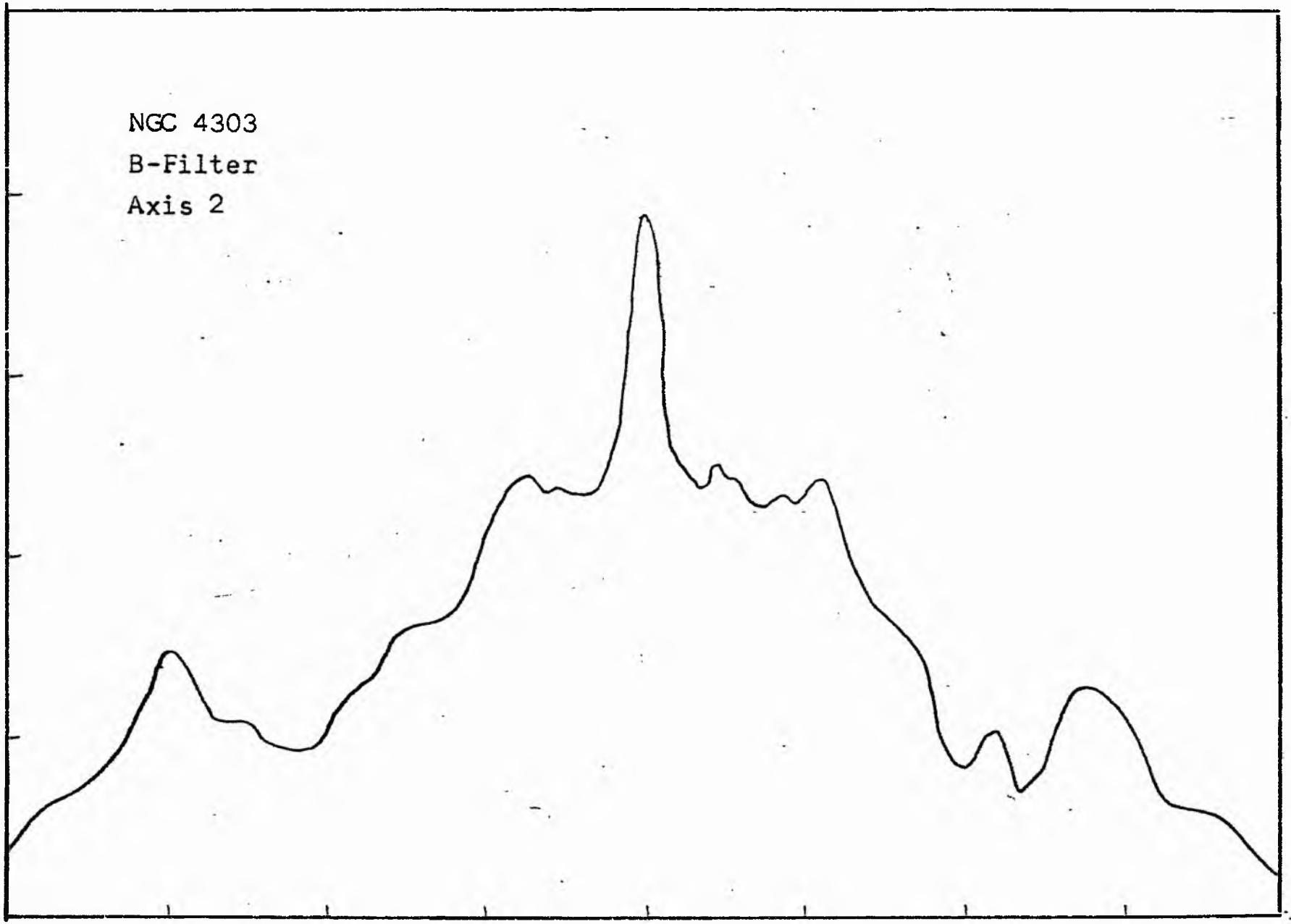
NGC 4303
B-Filter
Axis 2

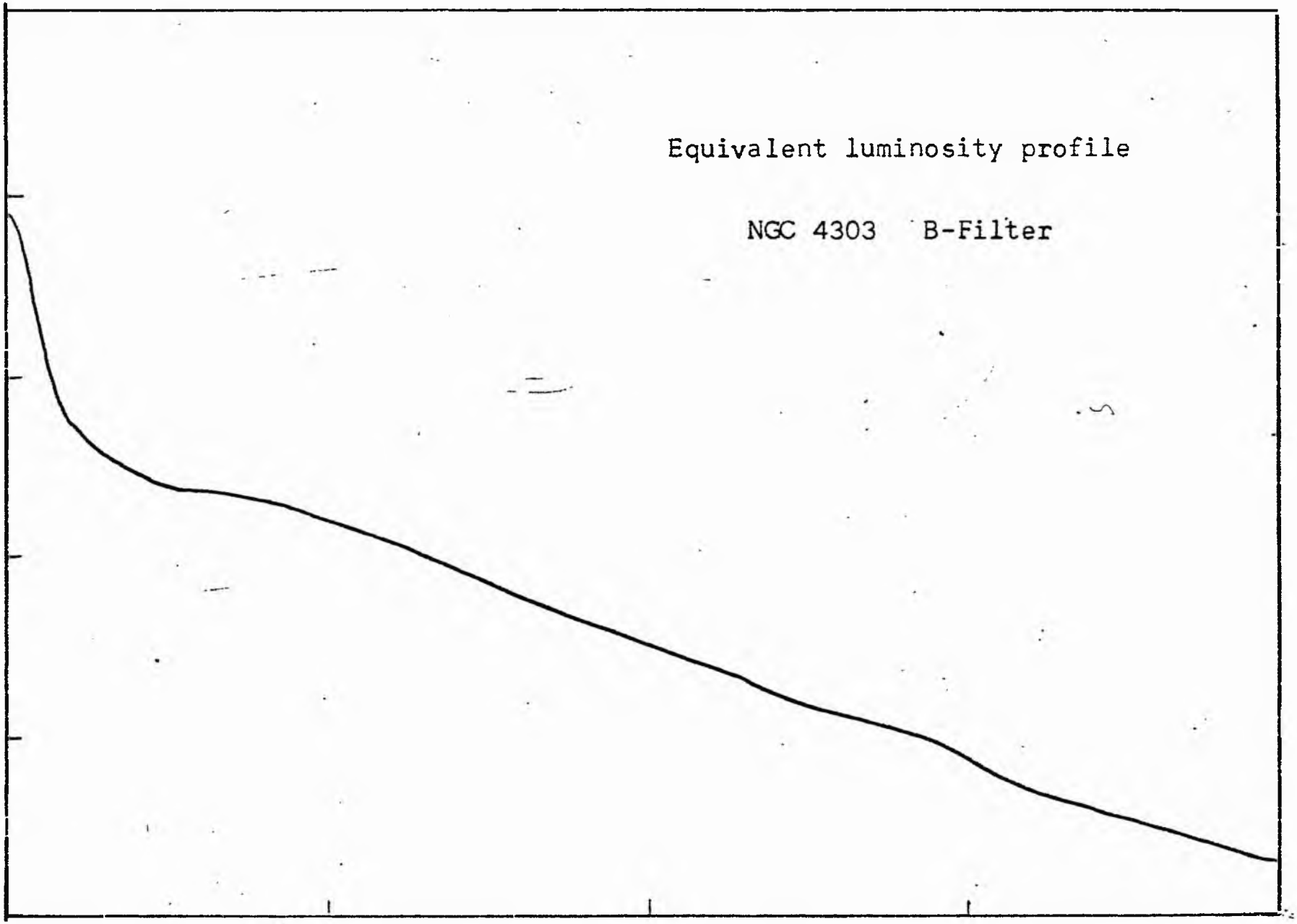
Equivalent luminosity profile
NGC 4303 B-Filter

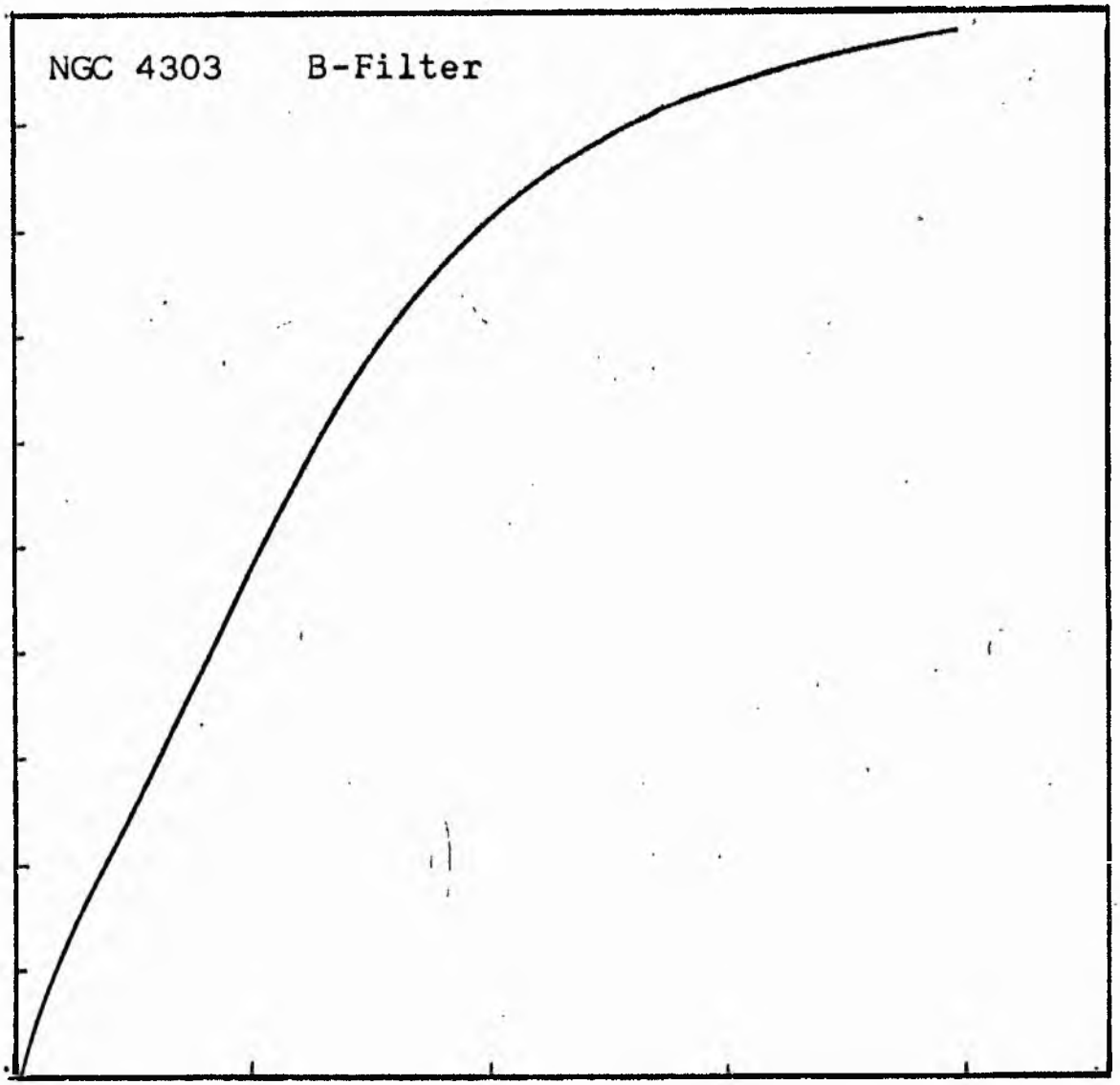

Relative integrated luminosity k(r) versus equivalent radius r*.

MEAN LUMINOSITY DISTRIBUTION IN NGC 4303
B COLOUR

LOG I	I	Ī	R	AREA	ΔA	P	ΣP	K(R)	ρ	LOG J	μ
1.92	83.176		0.0	0.0			0.0	0.0	0.0	1.725	17.07
		81.304			1.54	125.1585					
1.90	79.433		0.70	1.54			125.16	0.00	0.01	1.705	17.12
		71.264			4.62	329.1074					
1.80	63.096		1.40	6.16			454.27	0.01	0.03	1.605	17.37
		56.807			16.74	947.8679					
1.70	50.119		2.70	22.90			1402.13	0.03	0.05	1.505	17.62
		44.965			22.46	1010.0107					
1.60	39.811		3.80	45.36			2412.14	0.05	0.07	1.405	17.87
		35.717			19.67	702.6951					
1.50	31.623		4.55	65.04			3114.84	0.06	0.09	1.305	18.12
		28.371			7.34	208.3389					
1.40	25.119		4.80	72.38			3323.18	0.07	0.09	1.205	18.37
		22.536			22.65	510.4524					
1.30	19.952		5.50	95.03			3833.63	0.08	0.11	1.105	18.62
		17.901			24.56	439.7068					
1.20	15.849		6.17	119.60			4273.34	0.09	0.12	1.005	18.87
		14.219			55.24	785.4236					
1.10	12.589		7.46	174.83			5058.76	0.10	0.14	0.905	19.12
		11.295			16.30	184.0989					
1.00	10.000		7.80	191.13			5242.86	0.11	0.15	0.805	19.37
		8.972			20.11	180.3844					
0.90	7.943		8.20	211.24			5423.24	0.11	0.16	0.705	19.62
		7.126			72.29	515.1499					
0.80	6.310		9.50	283.53			5938.39	0.12	0.18	0.605	19.87
		5.661			146.52	829.4243					
0.70	5.012		11.70	430.05			6767.81	0.14	0.23	0.505	20.12
		4.496			248.81	1118.7769					
0.60	3.981		14.70	678.87			7886.58	0.16	0.28	0.405	20.37
		3.572			503.50	1798.3311					
0.50	3.162		19.40	1182.37			9684.91	0.20	0.38	0.305	20.62
		2.837			537.84	1525.8865					
0.40	2.512		23.40	1720.21			11210.79	0.23	0.45	0.205	20.87
		2.254			3483.81	7850.9570					
0.30	1.995		40.70	5204.02			19061.75	0.39	0.79	0.105	21.12
		1.790			3063.68	5484.1758					
0.20	1.585		51.30	8267.69			24545.93	0.50	0.99	0.005	21.37
		1.422			2083.10	2961.9541					
0.10	1.259		57.40	10350.79			27507.88	0.56	1.11	-0.095	21.62
		1.129			2759.57	3116.8049					
-0.00	1.000		64.60	13110.36			30624.68	0.62	1.25	-0.195	21.87
		0.897			2588.41	2322.2153					
-0.10	0.794		70.69	15698.77			32946.90	0.67	1.37	-0.295	22.12
		0.713			2753.96	1962.5796					
-0.20	0.631		76.64	18452.73			34909.48	0.71	1.48	-0.395	22.37
		0.566			2465.73	1395.7715					
-0.30	0.501		81.60	20918.46			36305.25	0.73	1.58	-0.495	22.62
		0.450			3233.40	1453.8804					
-0.40	0.398		87.68	24151.87			37759.12	0.76	1.70	-0.595	22.87
		0.357			8848.04	3160.2097					
-0.50	0.316		102.49	32999.90			40919.33	0.83	1.98	-0.695	23.12
		0.284			3305.13	937.6863					
-0.60	0.251		107.50	36305.03			41857.02	0.85	2.08	-0.795	23.37
		0.225			4882.04	1100.1960					
-0.70	0.200		114.50	41187.07			42957.21	0.87	2.22	-0.895	23.62
		0.179			5083.07	909.9043					
-0.80	0.158		121.36	46270.14			43867.11	0.89	2.35	-0.995	23.87
		0.142			12522.36	1780.5552					
-0.90	0.126		136.80	58792.50			45647.67	0.92	2.65	-1.095	24.12
		0.113			5899.96	666.3750					
-1.00	0.100		143.50	64692.46			46314.04	0.94	2.78	-1.195	24.37
		0.090			2733.16	245.2084					
-1.10	0.079		146.50	67425.62			46559.25	0.94	2.84	-1.295	24.62
		0.071			3448.81	245.7765					
-1.20	0.063		150.20	70874.44			46805.02	0.95	2.91	-1.395	24.87
		0.057			9148.69	517.8811					
-1.30	0.050		159.60	80023.12			47322.90	0.96	3.09	-1.495	25.12
		0.045			8645.19	388.7285					
-1.40	0.040		168.00	88668.31			47711.63	0.96	3.25	-1.595	25.37
		0.036			9088.50	324.6121					
-1.50	0.032		176.40	97756.81			48036.24	0.97	3.41	-1.695	25.62
		0.028			13279.62	376.7549					
-1.60	0.025		188.00	111036.44			48412.99	0.98	3.64	-1.795	25.87
		0.023			7566.50	170.5174					
-1.70	0.020		194.30	118602.94			48583.51	0.98	3.76	-1.895	26.12
		0.018			7563.87	135.4000					
-1.80	0.016		200.40	126166.81			48718.91	0.99	3.88	-1.995	26.37
		0.014			7797.75	110.8777					
-1.90	0.013		206.50	133964.56			48829.78	0.99	4.00	-2.095	26.62
		0.011			7631.00	86.1900					
-2.00	0.010		212.30	141595.56			48915.97	0.99	4.11	-2.195	26.87
-∞							49455.00	(1)			∞

PHOTOMETRIC PARAMETERS OF NGC 4303

B-FILTER

Total luminosity	L_T	= 13.74
Total apparent magnitude	m_T	= 10.13
Apparent central surface brightness	μ_o	= 17.07
Major axis at threshold	$2a_m$	= 7.18
Minor axis at threshold	$2b_m$	= 7.25
Major axis at μ=25.0 mag sec^{-2}	2a(25)	= 5.46
Luminosity within μ=25.0 mag sec^{-2}	k(25)	= 0.95
Gradient of exponential component	G(a)	= -0.93
Equivalent gradient of exponential comp.	G(r*)	= -0.76
Equivalent gradient of reduced exp. comp.	G(ρ)	= -0.71
Parameters at k = ¼ :		
Semi-major axis	a_1	= 0.36
Axis ratio	b/a	= 1.13
Equivalent radius	r_1*	= 0.44
Surface brightness	μ_1	= 20.90
Parameters at k = ½(effective) :		
Semi-major axis	a_e	= 0.77
Axis ratio	b/a	= 1.17
Equivalent radius	r_e*	= 0.86
Surface brightness	μ_e	= 21.37
Mean surface brightness	μ_e'	= 11.78
Parameters at k = ¾ :		
Semi-major axis	a_3	= 1.53
Axis ratio	b/a	= 0.77
Equivalent radius	r_3*	= 1.40
Surface brightness	μ_3	= 22.79
Concentration indices	C_{21}	= 1.97
	C_{32}	= 1.64

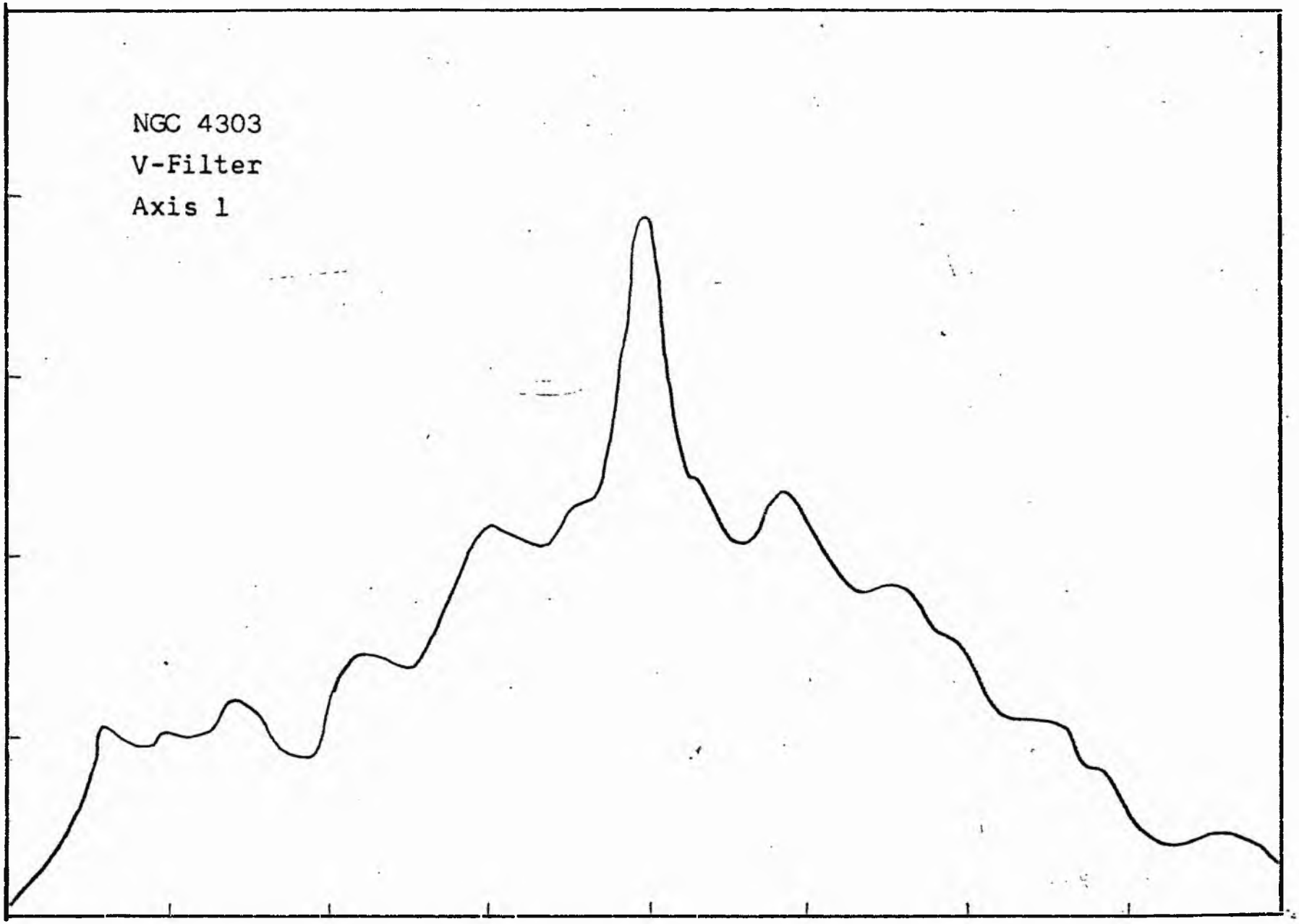
NGC 4303
V-Filter
Axis 1

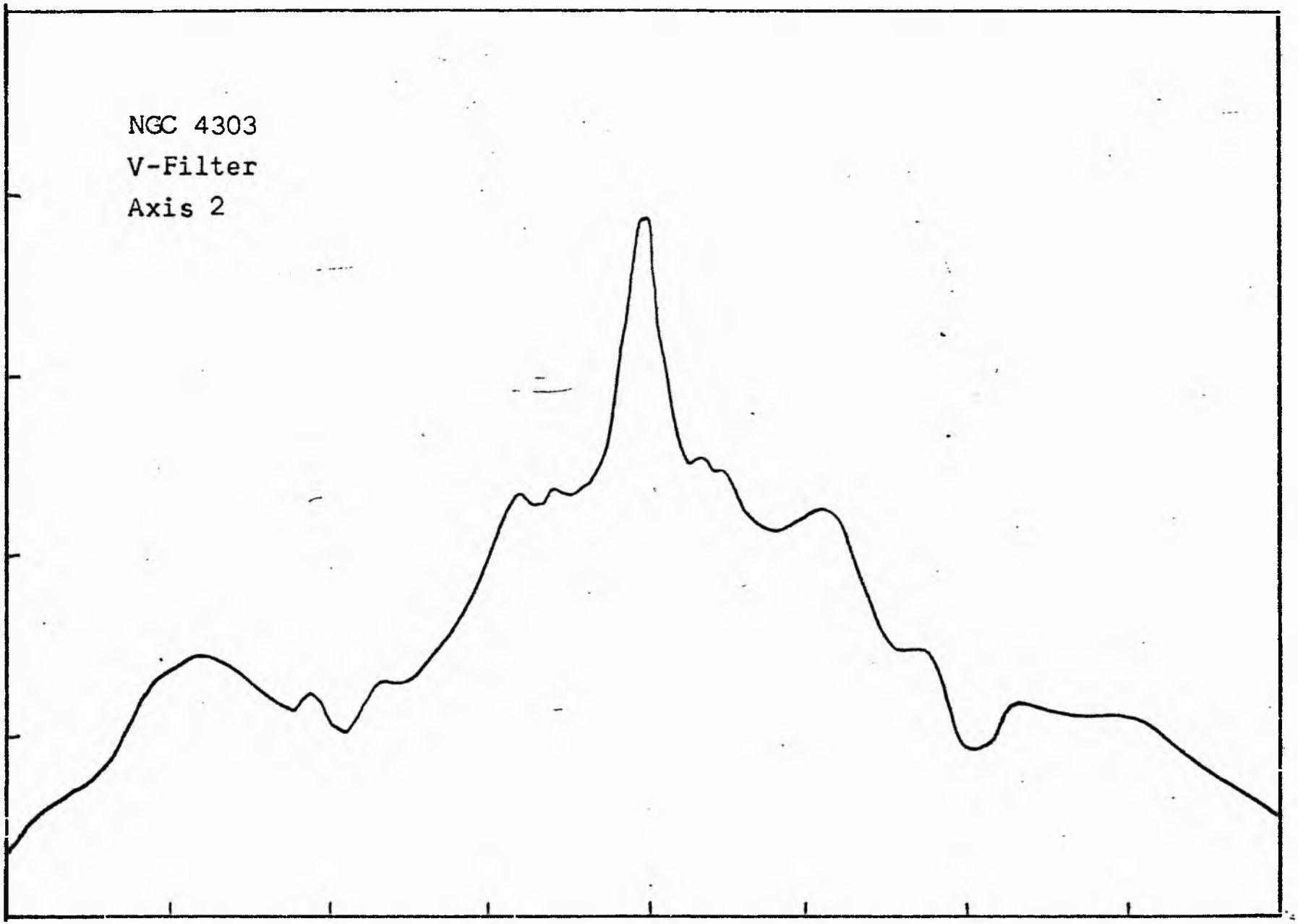
NGC 4303
V-Filter
Axis 2

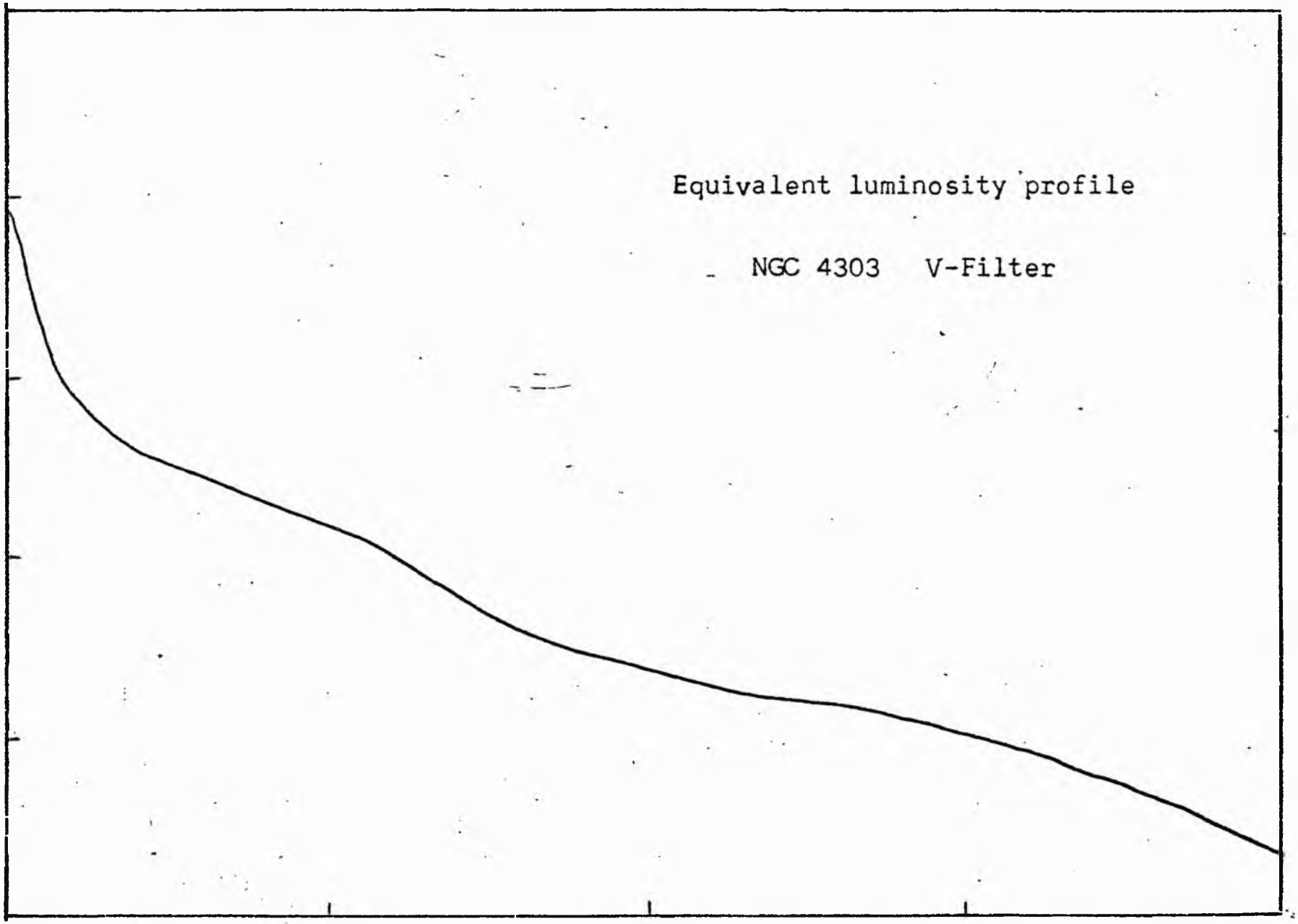
Equivalent luminosity profile
NGC 4303 V-Filter

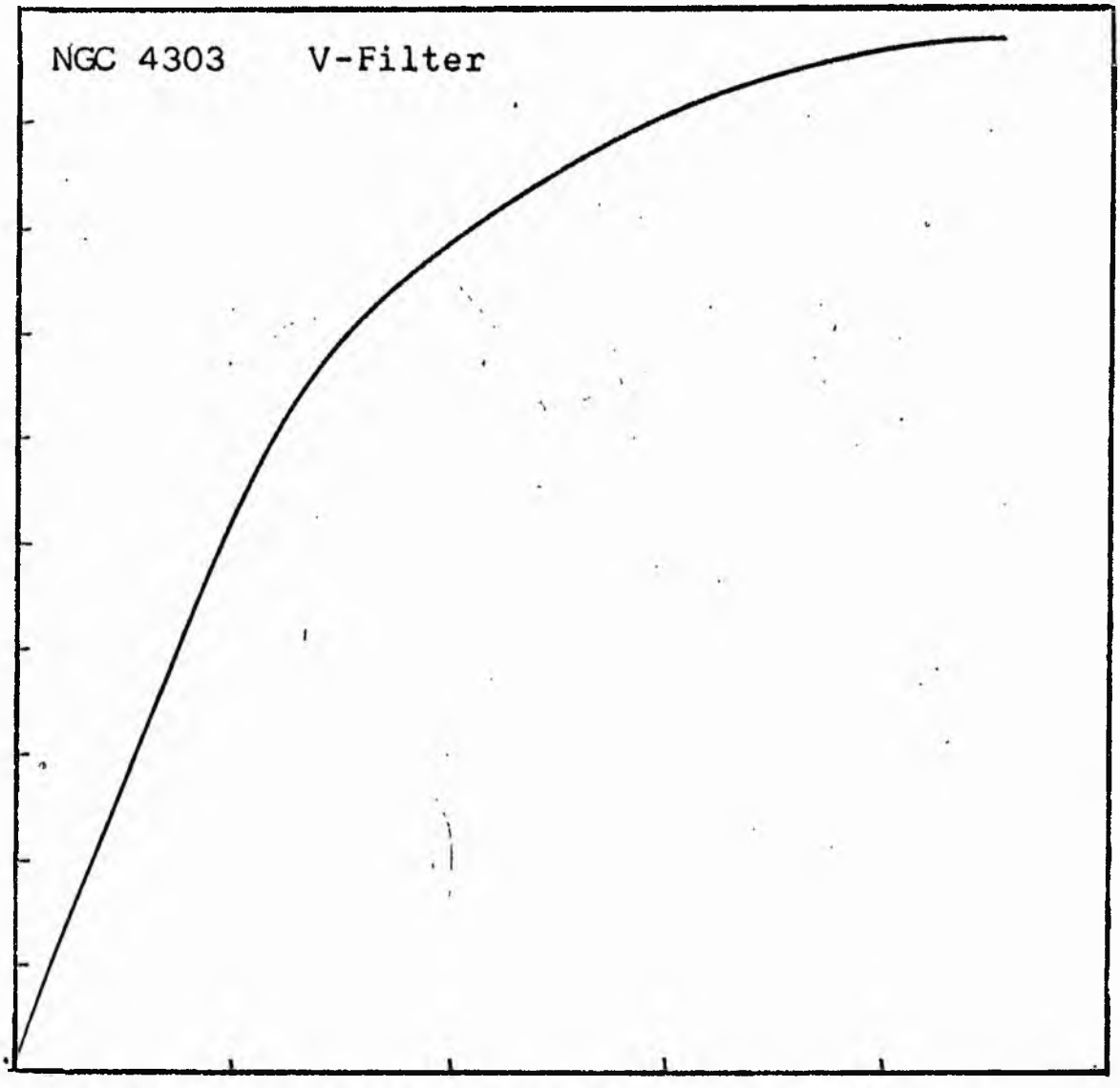

Relative integrated luminosity k(r) versus equivalent radius r*.

MEAN LUMINOSITY DISTRIBUTION IN NGC 4303
V COLOUR

LOG I	I	$\bar{I}$	R	AREA	ΔA	P	ΣP	K(R)	ρ	LOG J	μ
1.82	66.069		0.0	0.0			0.0	0.0	0.0	1.653	16.77
		64.582			2.01	129.8507					
1.80	63.096		0.80	2.01			129.85	0.00	0.02	1.633	16.82
		56.607			7.07	400.1316					
1.70	50.119		1.70	9.08			529.98	0.01	0.04	1.533	17.07
		44.965			4.78	214.7156					
1.60	39.811		2.10	13.85			744.70	0.02	0.04	1.433	17.32
		35.717			31.51	1125.4358					
1.50	31.623		3.80	45.36			1870.13	0.04	0.08	1.333	17.57
		28.371			7.45	211.2350					
1.40	25.119		4.10	52.81			2081.37	0.04	0.09	1.233	17.82
		22.536			19.57	441.0691					
1.30	19.952		4.80	72.38			2522.44	0.05	0.10	1.133	18.07
		17.901			29.69	531.4358					
1.20	15.849		5.70	102.07			3053.87	0.07	0.12	1.033	18.32
		14.219			74.64	1061.3655					
1.10	12.589		7.50	176.71			4115.24	0.09	0.16	0.933	18.57
		11.295			34.53	389.9556					
1.00	10.000		8.20	211.24			4505.19	0.10	0.17	0.833	18.82
		8.972			78.29	702.3691					
0.90	7.943		9.60	289.53			5207.56	0.11	0.20	0.733	19.07
		7.126			90.60	645.6738					
0.80	6.310		11.00	380.13			5853.23	0.13	0.23	0.633	19.32
		5.661			289.53	1638.9314					
0.70	5.012		14.60	669.66			7492.16	0.16	0.31	0.533	19.57
		4.496			452.55	2034.8420					
0.60	3.981		18.90	1122.21			9527.00	0.20	0.40	0.433	19.82
		3.572			810.00	2893.0181					
0.50	3.162		24.80	1932.20			12420.02	0.27	0.52	0.333	20.07
		2.837			1096.61	3111.1538					
0.40	2.512		31.05	3028.81			15531.17	0.33	0.65	0.233	20.32
		2.254			1460.01	3290.2251					
0.30	1.995		37.80	4488.83			18821.39	0.40	0.79	0.133	20.57
		1.790			2043.67	3658.3049					
0.20	1.585		45.60	6532.50			22479.70	0.48	0.96	0.033	20.82
		1.422			1735.19	2467.2666					
0.10	1.259		51.30	8267.69			24946.96	0.53	1.08	-0.067	21.07
		1.129			1903.56	2149.9829					
-0.00	1.000		56.90	10171.25			27096.94	0.58	1.19	-0.167	21.32
		0.897			2416.76	2168.2163					
-0.10	0.794		63.30	12588.01			29265.16	0.63	1.33	-0.267	21.57
		0.713			2499.45	1781.2021					
-0.20	0.631		69.30	15087.46			31046.36	0.66	1.45	-0.367	21.82
		0.566			2349.16	1329.7869					
-0.30	0.501		74.50	17436.62			32376.14	0.69	1.56	-0.467	22.07
		0.450			1093.23	491.5627					
-0.40	0.398		76.80	18529.85			32867.70	0.70	1.61	-0.567	22.32
		0.357			1677.00	598.9644					
-0.50	0.316		80.20	20206.85			33466.66	0.71	1.68	-0.667	22.57
		0.284			6673.41	1893.2881					
-0.60	0.251		92.50	26880.25			35359.95	0.76	1.94	-0.767	22.82
		0.225			9357.26	2108.7144					
-0.70	0.200		107.40	36237.51			37468.66	0.80	2.25	-0.867	23.07
		0.179			6988.56	1250.9988					
-0.80	0.158		117.30	43226.07			38719.66	0.83	2.46	-0.967	23.32
		0.142			13606.13	1934.6558					
-0.90	0.126		134.50	56832.20			40654.31	0.87	2.82	-1.067	23.57
		0.113			20407.74	2304.9656					
-1.00	0.100		156.80	77239.94			42959.27	0.92	3.29	-1.167	23.82
		0.090			6639.19	595.6418					
-1.10	0.079		163.40	83879.12			43554.91	0.93	3.43	-1.267	24.07
		0.071			7126.62	507.8723					
-1.20	0.063		170.20	91005.75			44062.79	0.94	3.57	-1.367	24.32
		0.057			7306.00	413.5718					
-1.30	0.050		176.90	98311.75			44476.36	0.95	3.71	-1.467	24.57
		0.045			7242.25	325.6458					
-1.40	0.040		183.30	105554.00			44802.00	0.96	3.84	-1.567	24.82
		0.036			3717.62	132.7817					
-1.50	0.032		186.50	109271.62			44934.78	0.96	3.91	-1.667	25.07
		0.028			4378.75	124.2291					
-1.60	0.025		190.20	113650.37			45059.01	0.96	3.99	-1.767	25.32
		0.023			13273.06	299.1194					
-1.70	0.020		201.00	126923.44			45358.12	0.97	4.21	-1.867	25.57
		0.018			8994.44	161.0083					
-1.80	0.016		208.00	135917.87			45519.13	0.97	4.36	-1.967	25.82
		0.014			11607.81	165.0537					
-1.90	0.013		216.70	147525.69			45684.18	0.98	4.54	-2.067	26.07
		0.011			14072.25	158.9422					
-2.00	0.010		226.80	161597.94			45843.12	0.98	4.75	-2.167	26.32
- ∞							46813.00	(1)			∞

PHOTOMETRIC PARAMETERS OF NGC 4303

V-FILTER

Total luminosity	L_T	= 13.00
Total apparent magnitude	m_T	= 9.64
Apparent central surface brightness	μ_o	= 16.77
Major axis at threshold	$2a_m$	= 7.12
Minor axis at threshold	$2b_m$	= 7.23
Major axis at μ=25.0 mag sec^{-2}	2a(25)	= 5.80
Luminosity within μ=25.0 mag sec^{-2}	k(25)	= 0.96
Gradient of exponential component	G(a)	= -0.84
Equivalent gradient of exponential comp.	G(r*)	= -0.73
Equivalent gradient of reduced exp. comp.	G(ρ)	= -0.78
Parameters at k = ¼ :		
Semi-major axis	a_1	= 0.23
Axis ratio	b/a	= 1.27
Equivalent radius	r_1*	= 0.39
Surface brightness	μ_1	= 19.99
Parameters at k = ½(effective) :		
Semi-major axis	a_e	= 0.67
Axis ratio	b/a	= 1.14
Equivalent radius	r_e*	= 0.80
Surface brightness	μ_e	= 20.97
Mean surface brightness	μ_e'	= 11.14
Parameters at k = ¾ :		
Semi-major axis	a_3	= 1.48
Axis ratio	b/a	= 0.85
Equivalent radius	r_3*	= 1.51
Surface brightness	μ_3	= 22.77
Concentration indices	C_{21}	= 2.04
	C_{32}	= 1.90

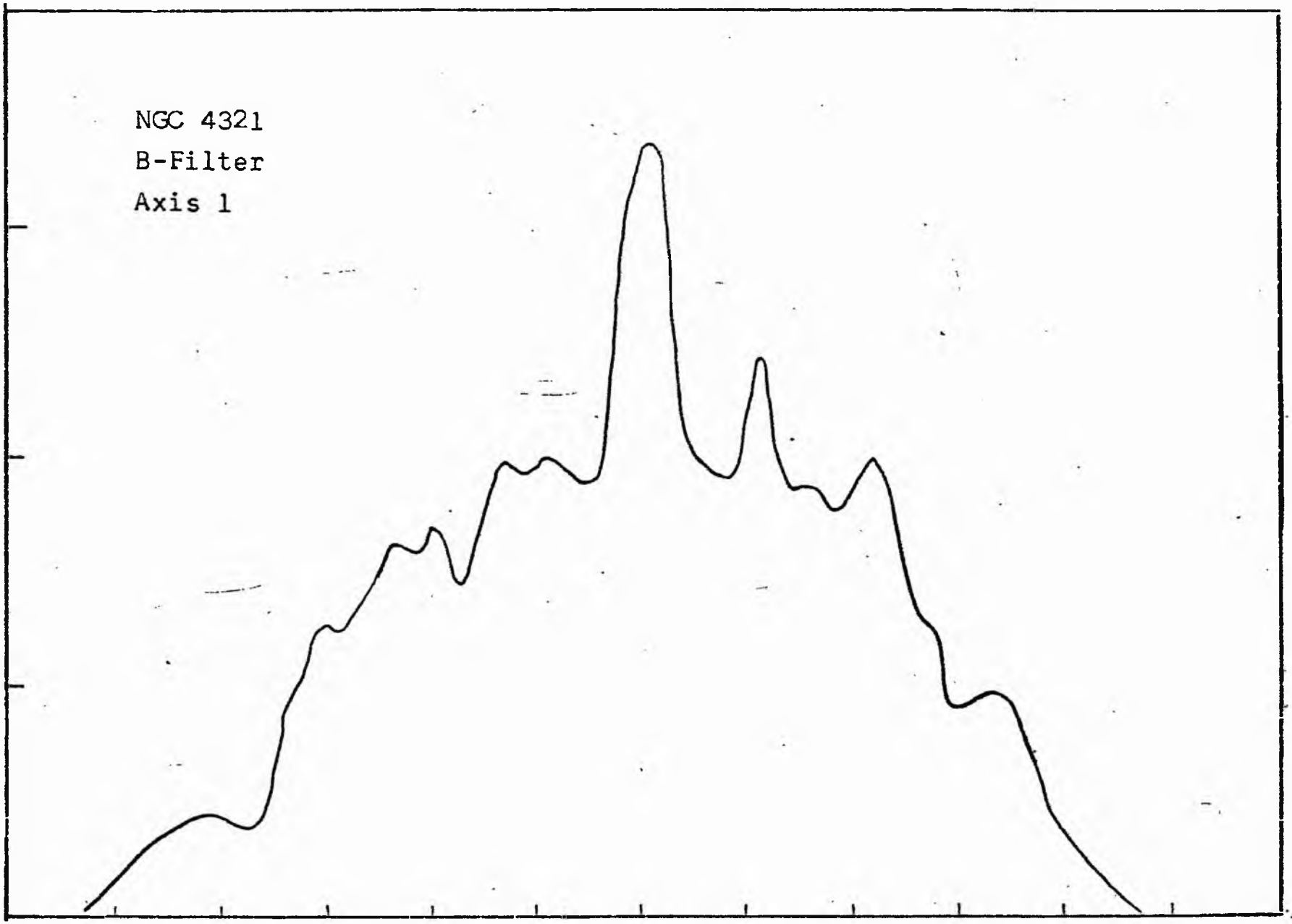
NGC 4321
B-Filter
Axis 1

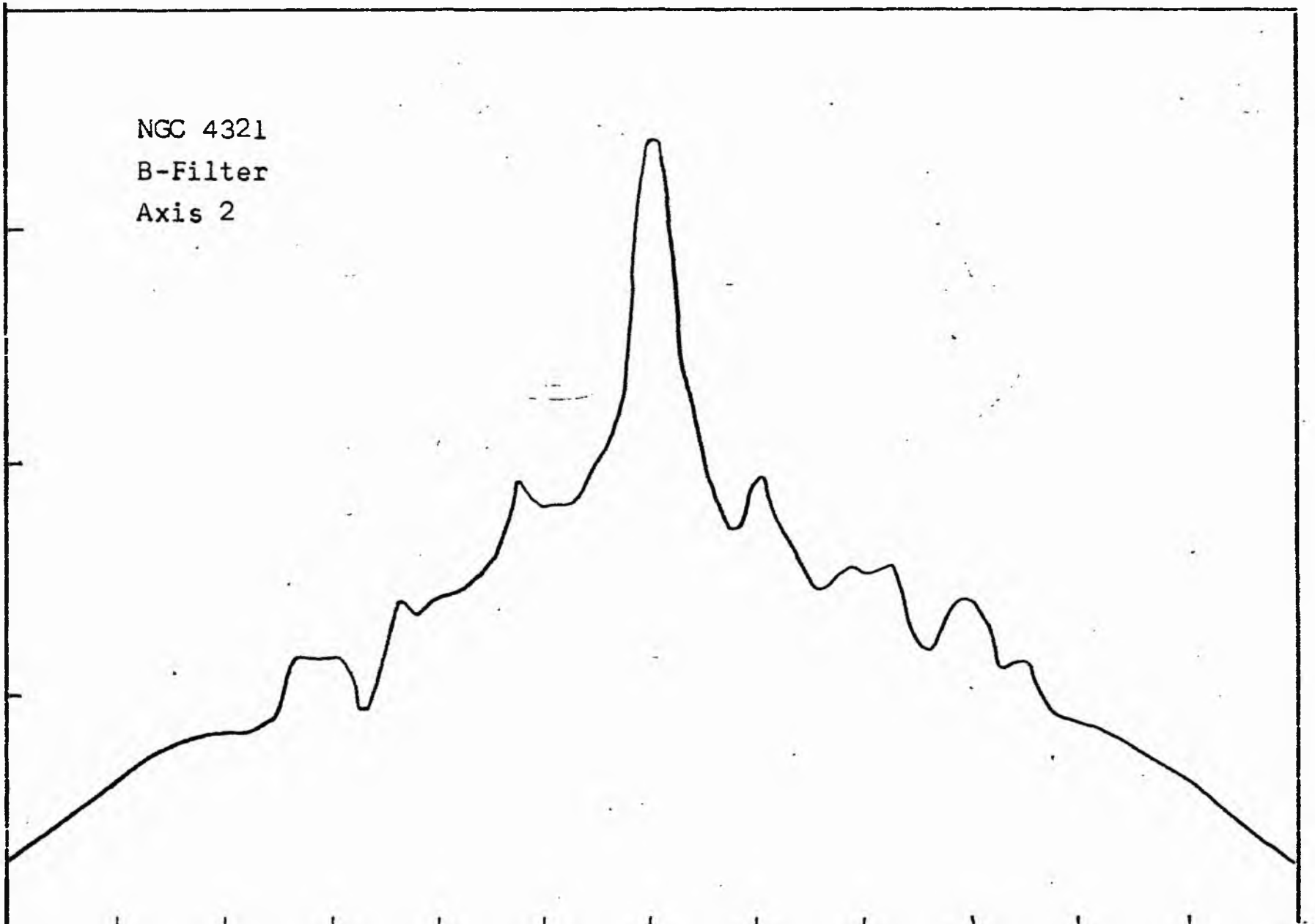
NGC 4321
B-Filter
Axis 2

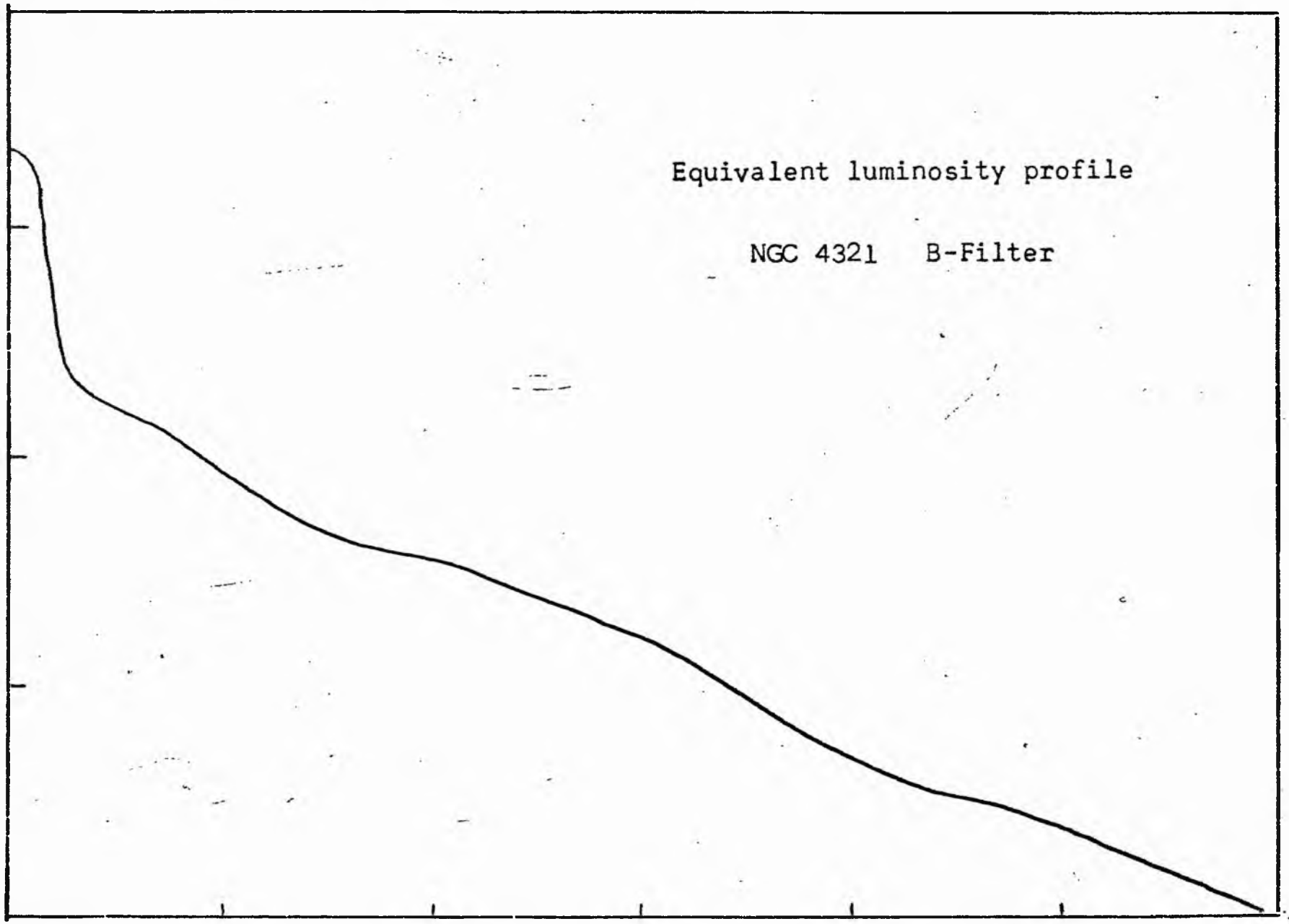
Equivalent luminosity profile
NGC 4321 B-Filter

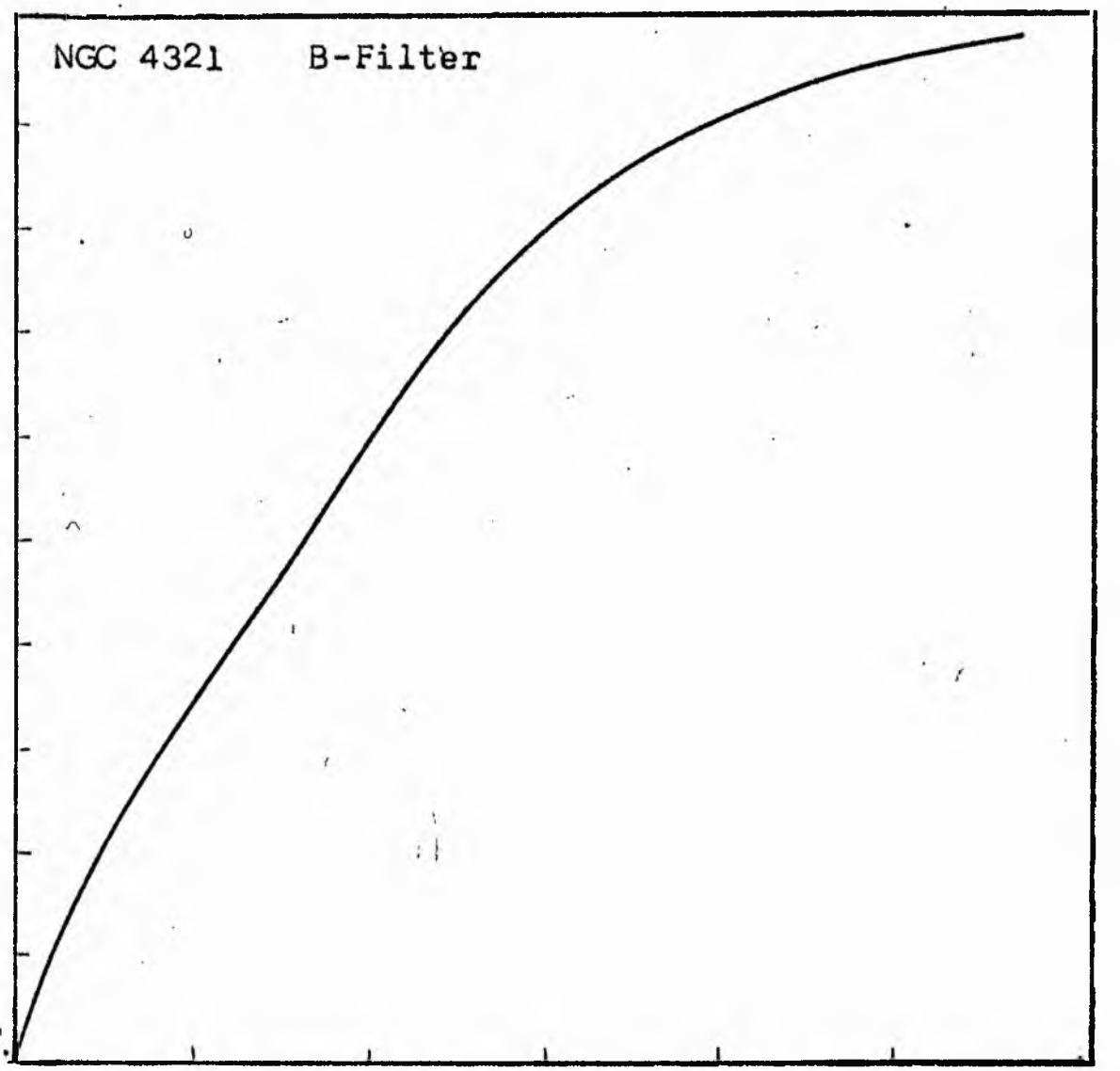

Relative integrated luminosity k(r) versus equivalent radius r*.

MEAN LUMINOSITY DISTRIBUTION IN NGC 4321
B COLOUR

LOG I	I	$\bar{I}$	R	AREA	ΔA	P	ΣP	K(R)	ρ	LOG J	μ
1.34	21.878		0.0	0.0			0.0	0.0	0.0	1.677	18.44
		20.919			129.08	2699.7598					
1.30	19.993		6.41	129.08			2699.76	0.06	0.08	1.637	18.54
		17.901			82.16	1470.6990					
1.20	15.849		8.20	211.24			4170.46	0.09	0.10	1.537	18.79
		14.219			15.74	223.7993					
1.10	12.589		8.50	226.98			4394.25	0.09	0.10	1.437	19.04
		11.295			21.87	246.9612					
1.00	10.000		8.90	248.85			4641.21	0.10	0.11	1.337	19.29
		8.972			71.63	642.6187					
0.90	7.943		10.10	320.47			5283.83	0.11	0.12	1.237	19.54
		7.126			52.78	376.1230					
0.80	6.310		10.90	373.25			5659.95	0.12	0.13	1.137	19.79
		5.661			20.83	117.9060					
0.70	5.012		11.20	394.08			5777.86	0.12	0.14	1.037	20.04
		4.496			43.35	194.9394					
0.60	3.981		11.80	437.44			5972.79	0.12	0.15	0.937	20.29
		3.972			69.27	247.4161					
0.50	3.162		12.70	506.71			6220.21	0.13	0.16	0.837	20.54
		2.837			49.01	139.0415					
0.40	2.512		13.30	555.72			6359.25	0.13	0.16	0.737	20.79
		2.254			218.66	492.7539					
0.30	1.995		15.70	774.37			6852.00	0.14	0.19	0.637	21.04
		1.790			1653.57	2960.0183					
0.20	1.585		27.80	2427.95			9812.02	0.20	0.34	0.537	21.29
		1.422			2374.95	3376.9502					
0.10	1.259		39.10	4802.89			13188.96	0.27	0.48	0.437	21.54
		1.129			2225.75	2513.8984					
-0.00	1.000		47.30	7028.65			15702.86	0.33	0.58	0.337	21.79
		0.897			1663.38	1492.3193					
-0.10	0.794		52.60	8692.03			17195.18	0.36	0.65	0.237	22.04
		0.713			2096.07	1493.7451					
-0.20	0.631		58.60	10788.10			18688.92	0.39	0.72	0.137	22.29
		0.566			6648.53	3763.5354					
-0.30	0.501		74.50	17436.62			22452.46	0.47	0.92	0.037	22.54
		0.450			11395.77	5124.0625					
-0.40	0.398		95.80	28832.40			27576.52	0.57	1.18	-0.063	22.79
		0.357			9866.21	3452.4495					
-0.50	0.316		110.70	38498.61			31028.97	0.65	1.36	-0.163	23.04
		0.284			11615.08	3295.2871					
-0.60	0.251		126.30	50113.70			34324.25	0.71	1.56	-0.263	23.29
		0.225			11197.90	2523.5254					
-0.70	0.200		139.70	61311.60			36847.78	0.77	1.72	-0.363	23.54
		0.179			14272.28	2554.8433					
-0.80	0.158		155.11	75583.87			39402.62	0.82	1.91	-0.463	23.79
		0.142			7680.37	1092.0776					
-0.90	0.126		162.80	83264.25			40494.69	0.84	2.01	-0.563	24.04
		0.113			5879.69	664.0884					
-1.00	0.100		168.45	89143.94			41158.78	0.86	2.08	-0.663	24.29
		0.090			10226.56	917.4912					
-1.10	0.079		177.85	99370.50			42076.27	0.88	2.19	-0.763	24.54
		0.071			10276.44	732.3445					
-1.20	0.063		186.82	109646.94			42808.61	0.89	2.30	-0.863	24.79
		0.057			6575.25	372.2078					
-1.30	0.050		192.34	116222.19			43180.82	0.90	2.37	-0.963	25.04
		0.045			33202.12	1492.9304					
-1.40	0.040		218.09	149424.31			44673.75	0.93	2.69	-1.063	25.29
		0.036			27781.12	992.2568					
-1.50	0.032		237.50	177205.44			45666.00	0.95	2.93	-1.163	25.54
		0.028			11830.75	335.6504					
-1.60	0.025		245.30	189036.19			46001.65	0.96	3.02	-1.263	25.79
		0.023			24480.37	551.6682					
-1.70	0.020		260.70	213516.56			46553.34	0.97	3.21	-1.363	26.04
		0.018			22858.06	409.1812					
-1.80	0.016		274.30	236374.62			46962.52	0.98	3.38	-1.463	26.29
		0.014			17191.75	244.4539					
-1.90	0.013		284.10	253566.37			47206.97	0.98	3.50	-1.563	26.54
		0.011			24109.94	272.3159					
-2.00	0.010		297.30	277676.31			47479.28	0.99	3.66	-1.663	26.79
-∞							48079.00	(1)			∞

PHOTOMETRIC PARAMETERS OF NGC 4321

B-FILTER

Total luminosity	L_T	= 13.35
Total apparent magnitude	m_T	= 10.08
Apparent central surface brightness	μ_o	= 18.44
Major axis at threshold	$2a_m$	= 8.28
Minor axis at threshold	$2b_m$	= 11.50
Major axis at μ=25.0 mag sec^{-2}	2a(25)	= 5.96
Luminosity within μ=25.0 mag sec^{-2}	k(25)	= 0.90
Gradient of exponential component	G(a)	= -0.63
Equivalent gradient of exponential comp.	G(r*)	= -0.48
Equivalent gradient of reduced exp. comp.	G(ρ)	= -0.69

Parameters at k = ¼ :

Semi-major axis	a_1	= 0.55
Axis ratio	b/a	= 0.48
Equivalent radius	r_1*	= 0.58
Surface brightness	μ_1	= 21.47

Parameters at k = ½(effective) :

Semi-major axis	a_e	= 1.68
Axis ratio	b/a	= 0.55
Equivalent radius	r_e*	= 1.35
Surface brightness	μ_e	= 22.61
Mean surface brightness	μ_e'	= 12.73

Parameters at k = ¾ :

Semi-major axis	a_3	= 2.25
Axis ratio	b/a	= 0.96
Equivalent radius	r_3*	= 2.25
Surface brightness	μ_3	= 23.42

Concentration indices	C_{21}	= 2.30
	C_{32}	= 1.67

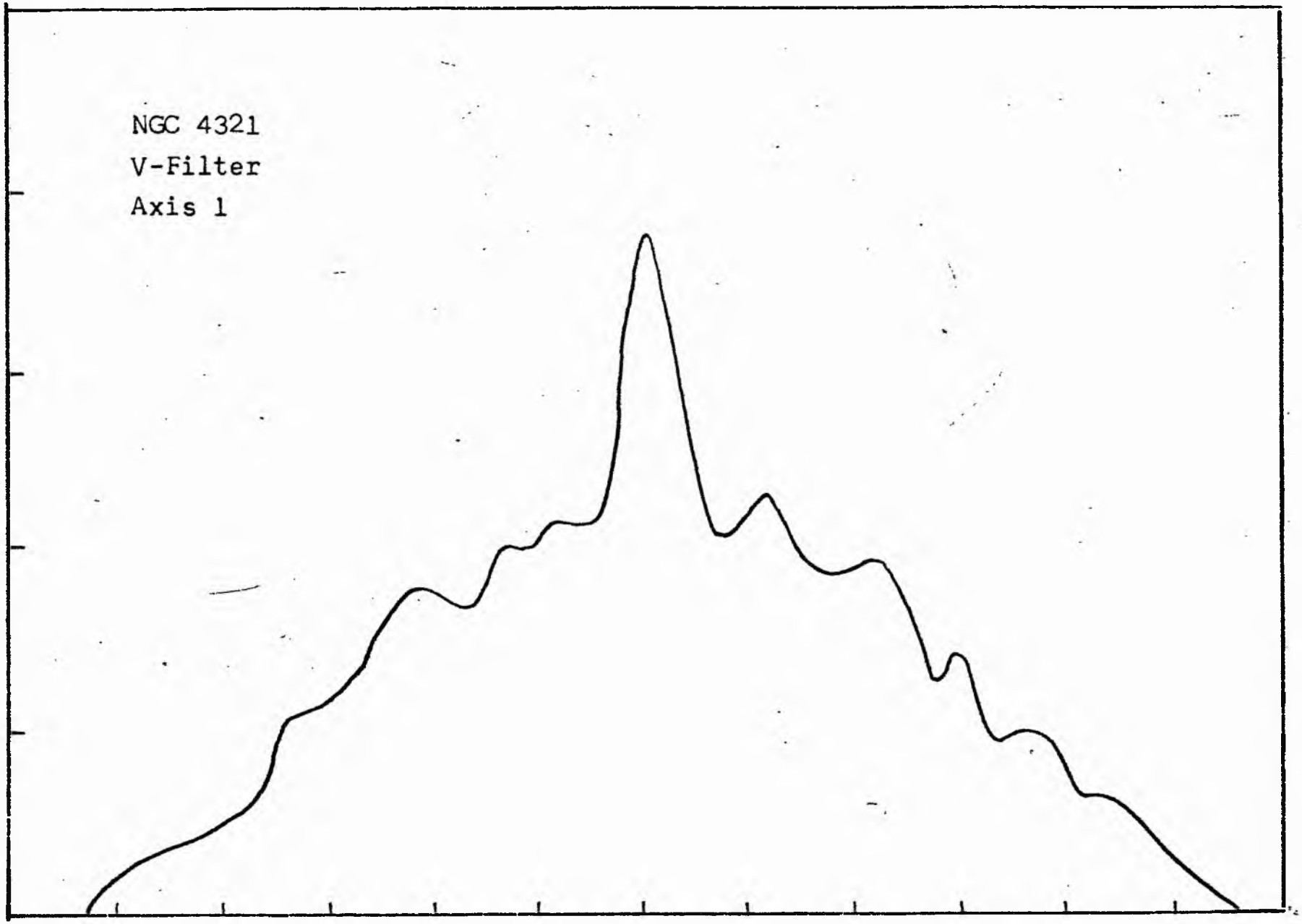
NGC 4321
V-Filter
Axis 1

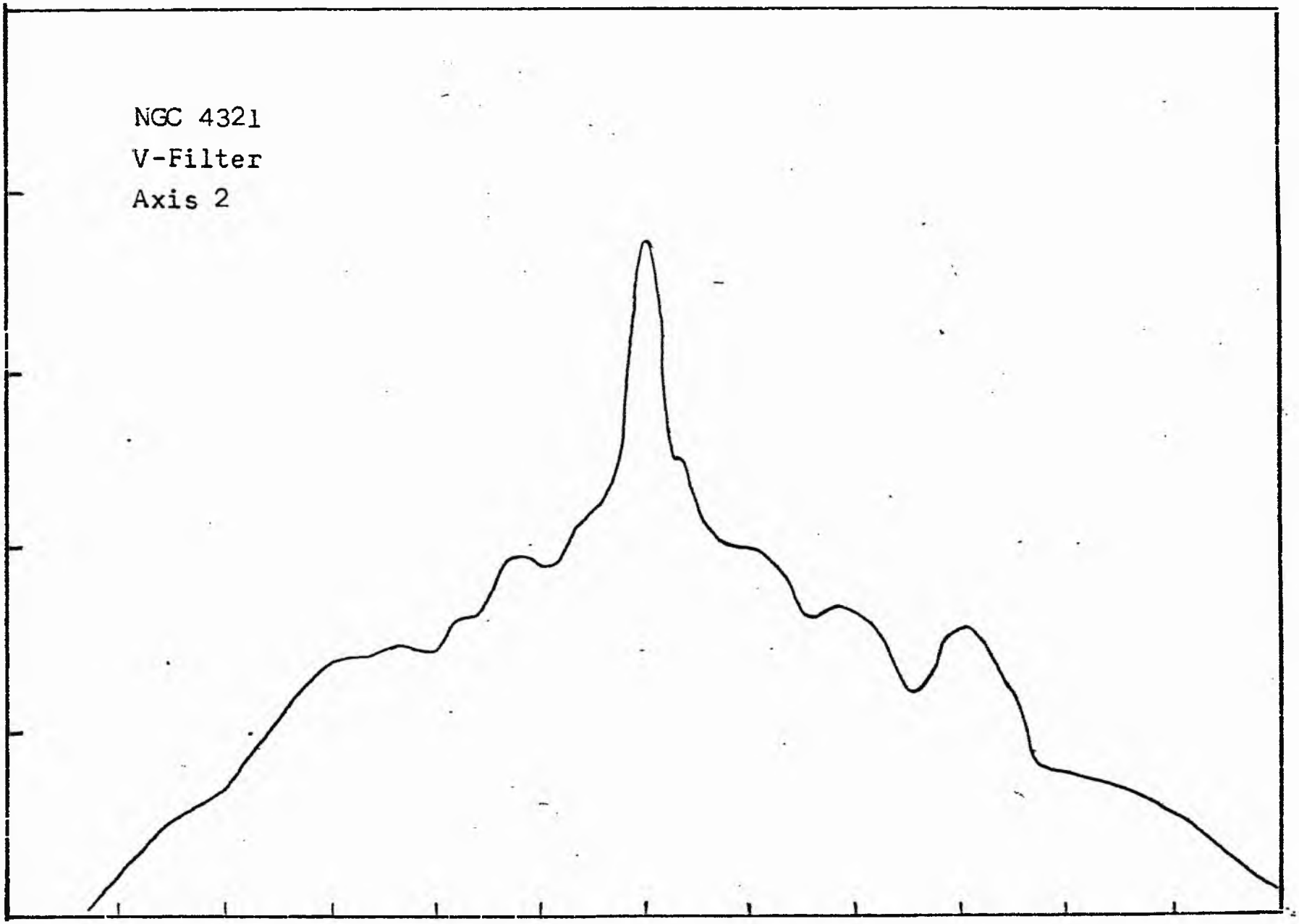
NGC 4321
V-Filter
Axis 2

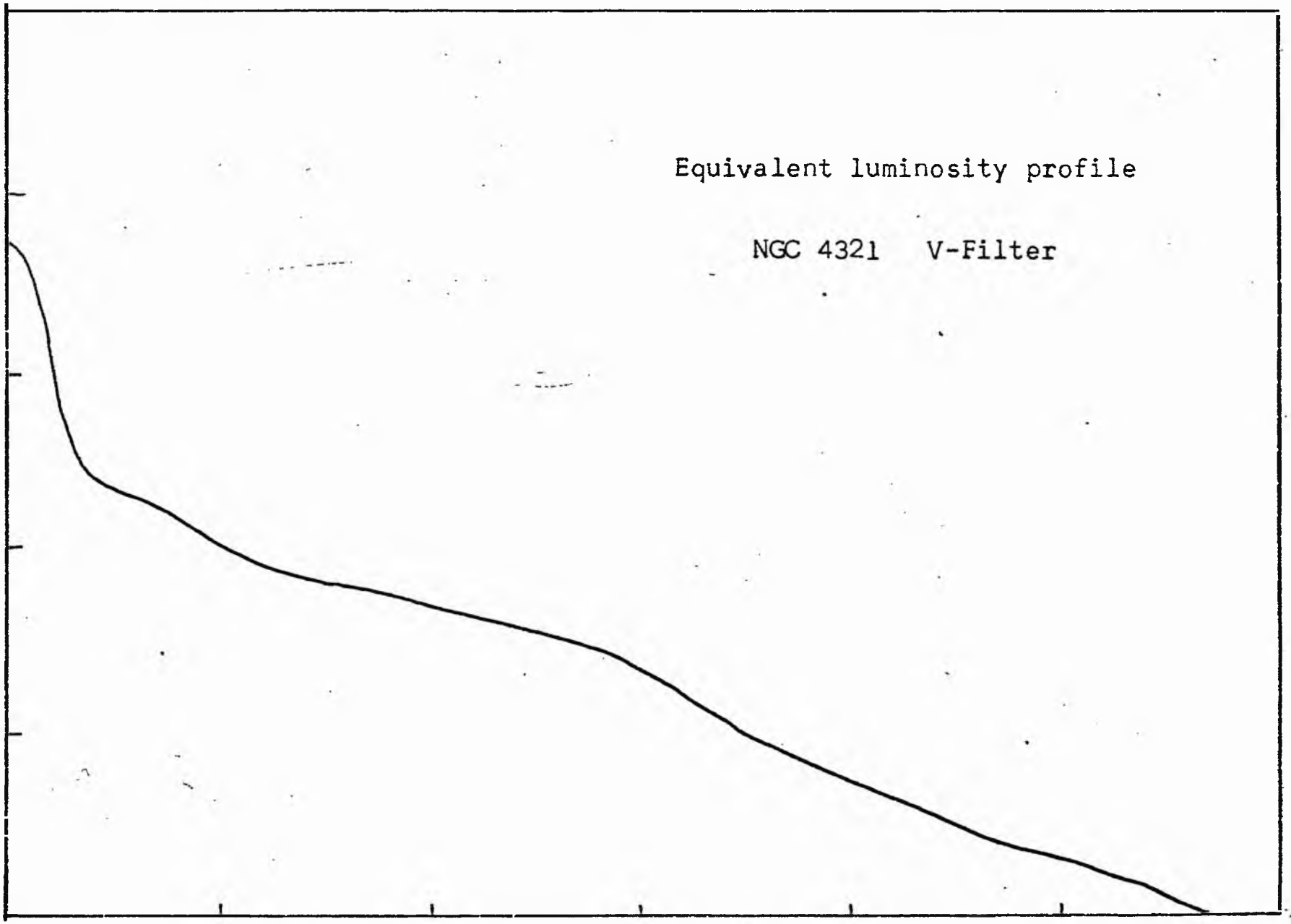
Equivalent luminosity profile
NGC 4321 V-Filter

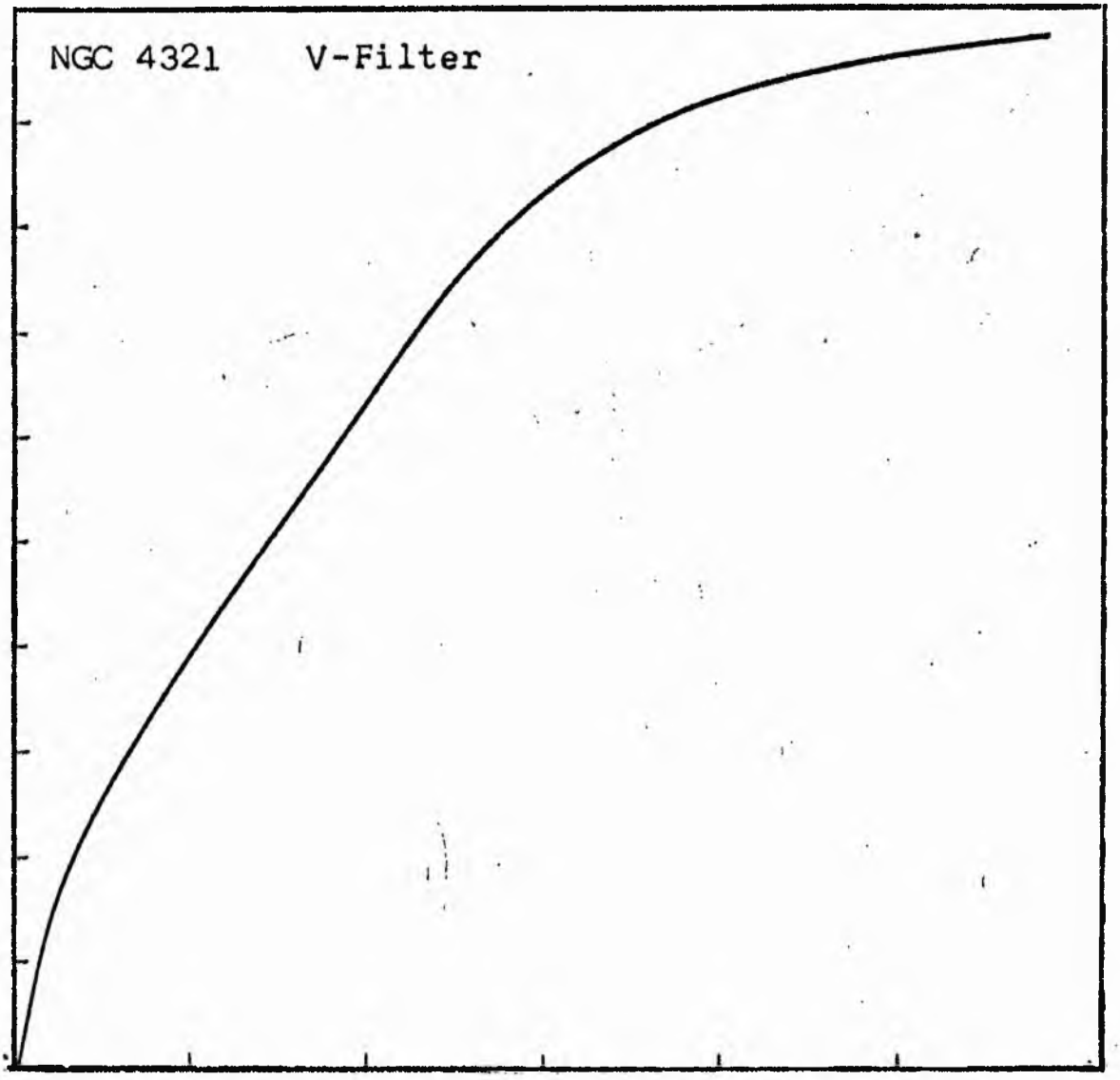

Relative integrated luminosity k(r) versus equivalent radius r*.

MEAN LUMINOSITY DISTRIBUTION IN NGC 4321
V COLOUR

LOG I	I	$\bar{I}$	R	AREA	ΔA	P	ΣP	K(R)	ρ	LOG J	μ
1.67	46.773		0.0	0.0			0.0	0.0	0.0	1.869	17.34
		43.292			55.42	2399.1418					
1.60	39.811		4.20	55.42			2399.14	0.04	0.06	1.799	17.52
		35.717			61.48	2195.8962					
1.50	31.623		6.10	116.90			4595.04	0.07	0.08	1.699	17.77
		28.371			126.39	3585.6711					
1.40	25.119		8.80	243.28			8180.70	0.13	0.12	1.599	18.02
		22.536			22.62	509.7437					
1.30	19.953		9.20	265.90			8690.45	0.14	0.13	1.499	18.27
		17.901			23.62	422.8994					
1.20	15.849		9.60	289.53			9113.34	0.15	0.13	1.399	18.52
		14.219			30.94	440.0012					
1.10	12.589		10.10	320.47			9553.34	0.16	0.14	1.299	18.77
		11.295			73.61	831.3657					
1.00	10.000		11.20	394.08			10384.71	0.17	0.15	1.199	19.02
		8.972			43.35	388.9539					
0.90	7.943		11.80	437.44			10773.66	0.18	0.16	1.099	19.27
		7.126			37.86	269.7778					
0.80	6.310		12.30	475.29			11043.44	0.18	0.17	0.999	19.52
		5.661			88.81	502.7412					
0.70	5.012		13.40	564.10			11546.18	0.19	0.18	0.899	19.77
		4.496			105.56	474.6340					
0.60	3.981		14.60	669.66			12020.81	0.20	0.20	0.799	20.02
		3.572			46.65	166.6269					
0.50	3.162		15.10	716.31			12187.43	0.20	0.21	0.699	20.27
		2.837			77.91	221.0398					
0.40	2.512		15.90	794.23			12408.47	0.20	0.22	0.599	20.52
		2.254			1976.94	4455.1562					
0.30	1.995		29.70	2771.17			16863.63	0.27	0.40	0.499	20.77
		1.790			2205.24	3947.5239					
0.20	1.585		39.80	4976.40			20811.15	0.34	0.54	0.399	21.02
		1.422			644.81	916.8599					
0.10	1.259		42.30	5621.21			21728.01	0.35	0.58	0.299	21.27
		1.129			1467.00	1656.9170					
-0.00	1.000		47.50	7088.22			23384.93	0.38	0.65	0.199	21.52
		0.897			1903.80	1708.0166					
-0.10	0.794		53.50	8992.02			25092.94	0.41	0.73	0.099	21.77
		0.713			8025.85	5719.5312					
-0.20	0.631		73.60	17017.87			30812.47	0.50	1.00	-0.001	22.02
		0.566			12116.28	6858.6562					
-0.30	0.501		96.30	29134.15			37671.13	0.61	1.31	-0.101	22.27
		0.450			10860.23	4883.2500					
-0.40	0.398		112.83	39994.38			42554.38	0.69	1.54	-0.201	22.52
		0.357			10508.92	3753.4287					
-0.50	0.316		126.79	50503.30			46307.80	0.75	1.73	-0.301	22.77
		0.284			8892.44	2522.8484					
-0.60	0.251		137.50	59395.74			48830.65	0.79	1.87	-0.401	23.02
		0.225			10257.13	2311.5122					
-0.70	0.200		148.90	69652.87			51142.16	0.83	2.03	-0.501	23.27
		0.179			7095.19	1270.0884					
-0.80	0.158		156.30	76748.06			52412.25	0.85	2.13	-0.601	23.52
		0.142			6413.94	912.0002					
-0.90	0.126		162.70	83162.00			53324.25	0.87	2.22	-0.701	23.77
		0.113			7384.50	834.0491					
-1.00	0.100		169.77	90546.50			54158.30	0.88	2.31	-0.801	24.02
		0.090			9383.50	841.8523					
-1.10	0.079		178.35	99930.00			55000.15	0.89	2.43	-0.901	24.27
		0.071			9376.81	668.2310					
-1.20	0.063		186.53	109306.81			55668.38	0.90	2.54	-1.001	24.52
		0.057			16130.75	913.1177					
-1.30	0.050		199.82	125437.56			56581.50	0.92	2.72	-1.101	24.77
		0.045			24055.31	1081.6426					
-1.40	0.040		218.14	149492.87			57663.14	0.94	2.97	-1.201	25.02
		0.036			20388.25	728.2048					
-1.50	0.032		232.54	169881.12			58391.34	0.95	3.17	-1.301	25.27
		0.028			15748.94	446.8127					
-1.60	0.025		243.08	185630.06			58838.15	0.96	3.31	-1.401	25.52
		0.023			10138.69	228.4844					
-1.70	0.020		249.63	195768.75			59066.64	0.96	3.40	-1.501	25.77
		0.018			20541.50	367.7114					
-1.80	0.016		262.40	216310.25			59434.35	0.97	3.57	-1.601	26.02
		0.014			21445.06	304.9319					
-1.90	0.013		275.10	237755.31			59739.28	0.97	3.75	-1.701	26.27
		0.011			25178.31	284.3826					
-2.00	0.010		289.30	262933.62			60023.66	0.98	3.94	-1.801	26.52
$-\infty$							61523.00	(1)			∞

PHOTOMETRIC PARAMETERS OF NGC 4321

V-FILTER

Total luminosity	L_T	= 17.09
Total apparent magnitude	m_T	= 9.56
Apparent central surface brightness	μ_o	= 17.34
Major axis at threshold	$2a_m$	= 8.50
Minor axis at threshold	$2b_m$	= 10.06
Major axis at μ=25.0 mag sec^{-2}	2a(25)	= 7.03
Luminosity within μ=25.0 mag sec^{-2}	k(25)	= 0.94
Gradient of exponential component	G(a)	= -0.51
Equivalent gradient of exponential comp.	G(r*)	= -0.54
Equivalent gradient of reduced exp. comp.	G(ρ)	= -0.72
Parameters at k = ¼ :		
Semi-major axis	a_1	= 0.47
Axis ratio	b/a	= 0.61
Equivalent radius	r_1*	= 0.42
Surface brightness	μ_1	= 20.69
Parameters at k = ½(effective) :		
Semi-major axis	a_e	= 1.62
Axis ratio	b/a	= 0.64
Equivalent radius	r_e*	= 1.22
Surface brightness	μ_e	= 22.02
Mean surface brightness	μ_e'	= 11.99
Parameters at k = ¾ :		
Semi-major axis	a_3	= 2.26
Axis ratio	b/a	= 0.86
Equivalent radius	r_3*	= 2.10
Surface brightness	μ_3	= 22.77
Concentration indices	C_{21}	= 2.89
	C_{32}	= 1.72

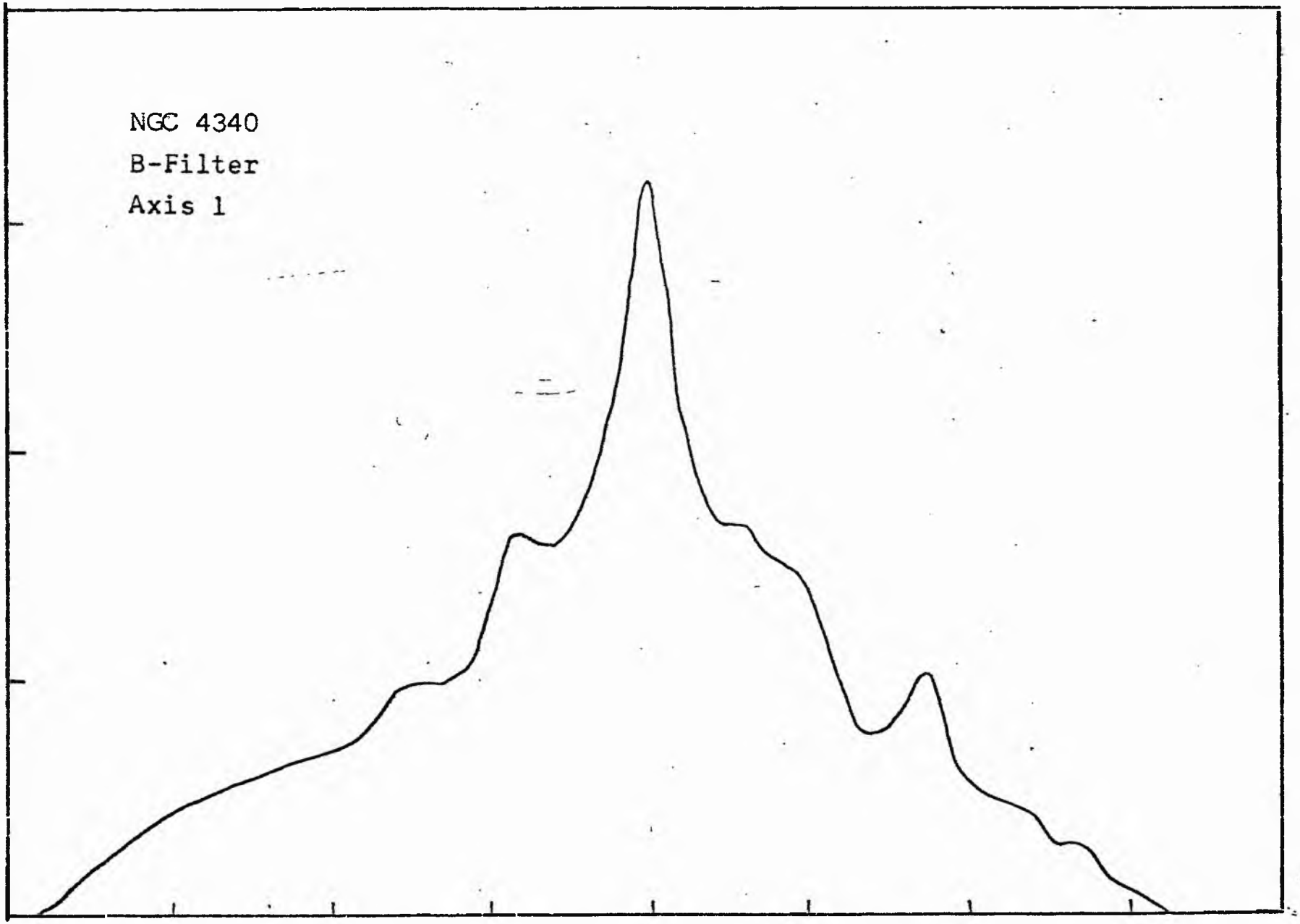
NGC 4340
B-Filter
Axis 1

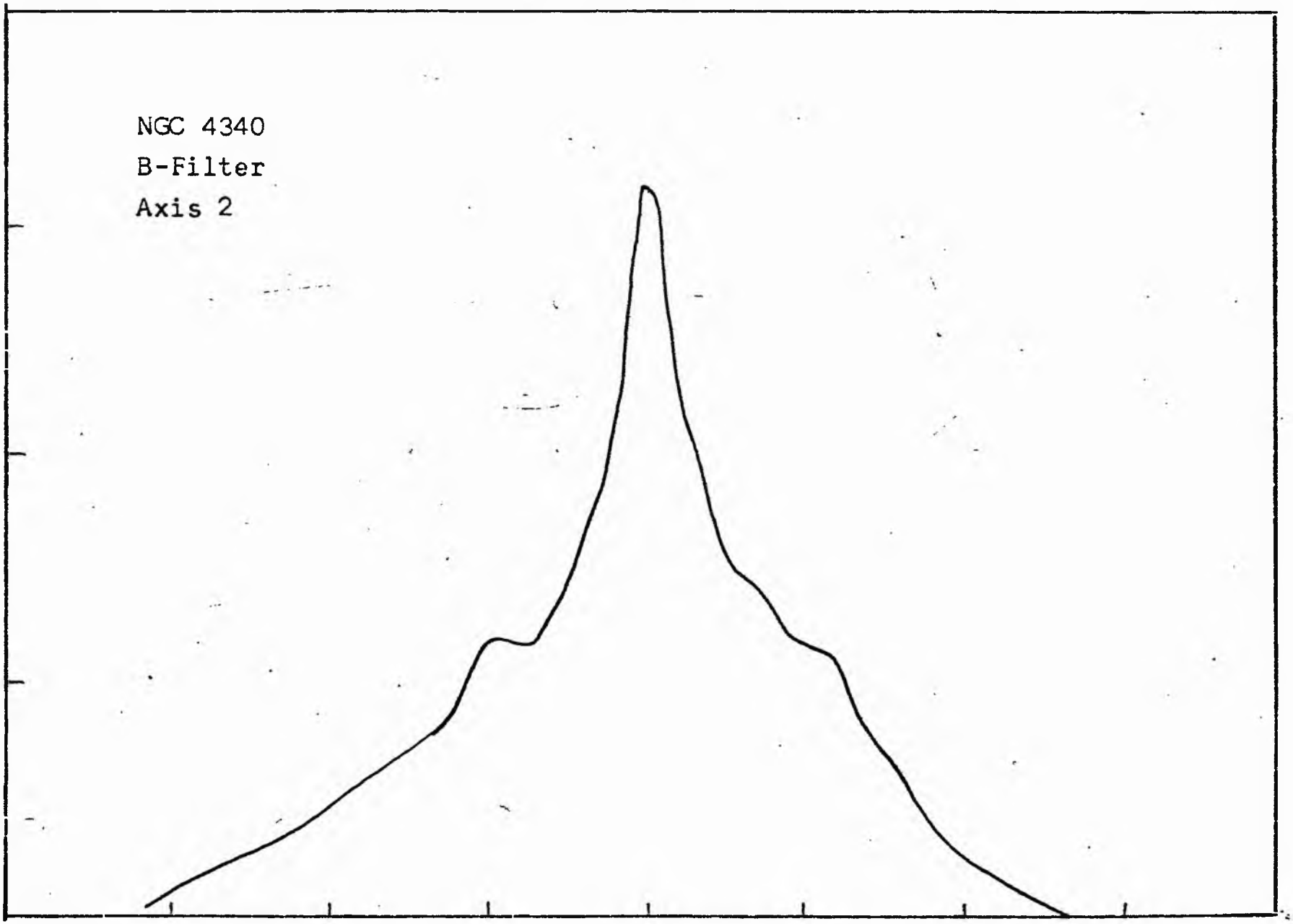
NGC 4340
B-Filter
Axis 2

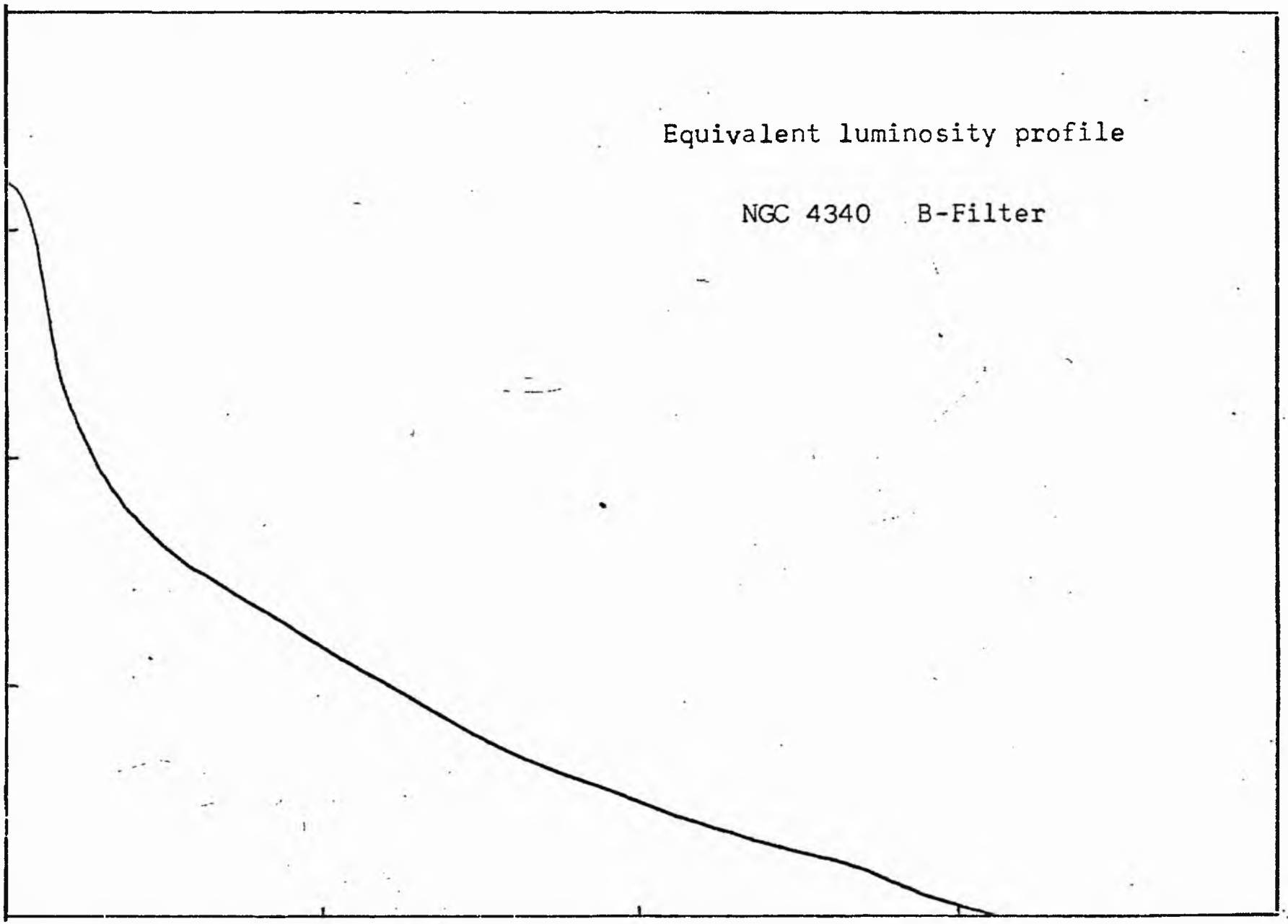
Equivalent luminosity profile
NGC 4340 B-Filter

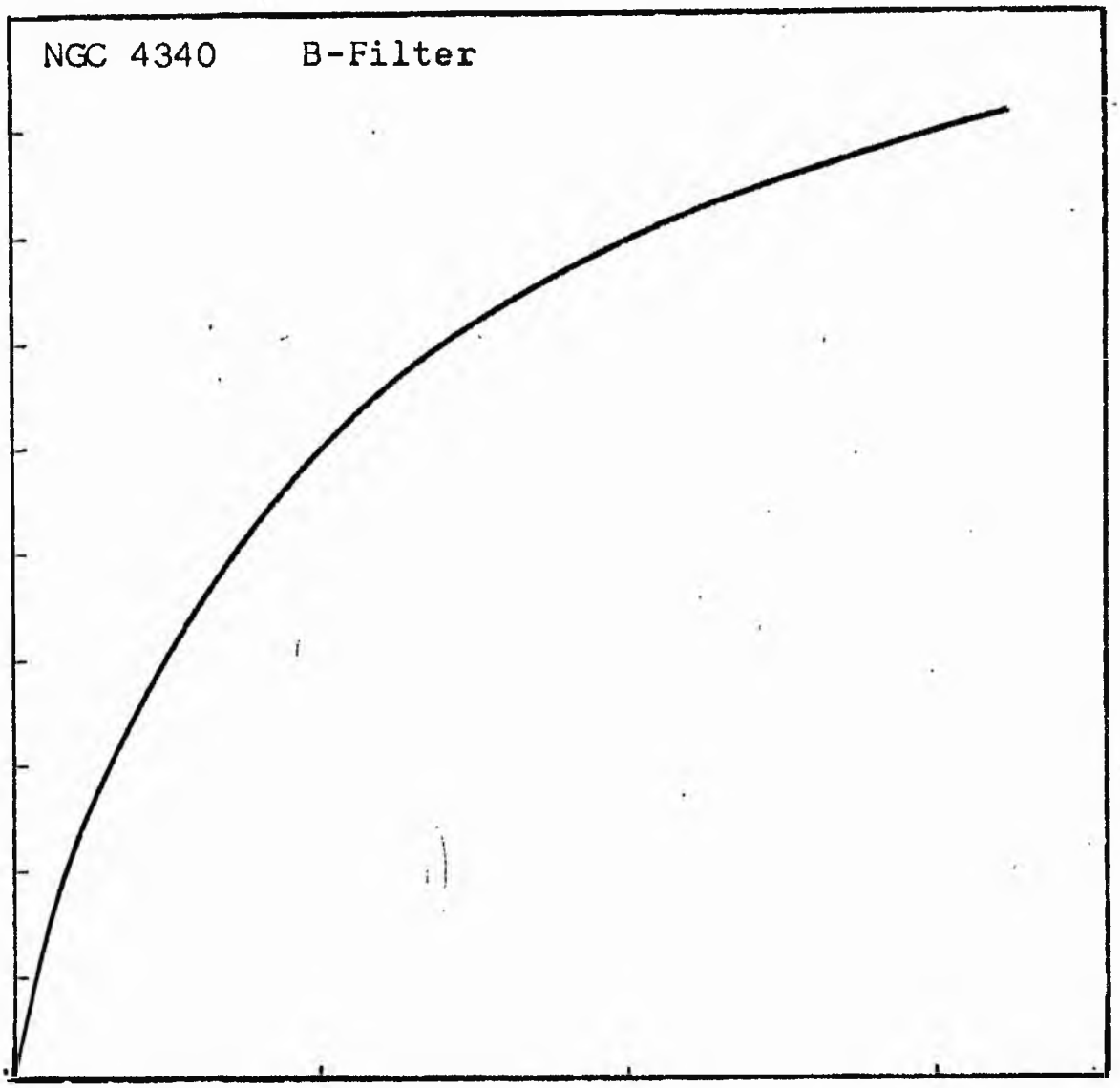

Relative integrated luminosity k(r) versus equivalent radius r*.

MEAN LUMINOSITY DISTRIBUTION IN NGC 4340
B COLOUR

LOG I	I	$\bar{I}$	R	AREA	ΔA	P	ΣP	K(R)	ρ	LOG J	μ
1.19	15.488		0.0	0.0			0.0	0.0	0.0	1.732	18.72
		14.039			26.42	370.9128					
1.10	12.589		2.90	26.42			370.91	0.05	0.08	1.642	18.95
		11.295			18.94	213.9627					
1.00	10.000		3.80	45.36			584.88	0.08	0.10	1.542	19.20
		8.972			18.25	163.7561					
0.90	7.943		4.50	63.62			748.63	0.10	0.12	1.442	19.45
		7.126			31.42	223.8829					
0.80	6.310		5.50	95.03			972.51	0.13	0.15	1.342	19.70
		5.661			14.33	81.0932					
0.70	5.012		5.90	109.36			1053.61	0.14	0.16	1.242	19.95
		4.496			58.06	261.0496					
0.60	3.981		7.30	167.42			1314.66	0.17	0.20	1.142	20.20
		3.572			18.85	67.3245					
0.50	3.162		7.70	186.27			1381.98	0.18	0.21	1.042	20.45
		2.837			24.98	70.8579					
0.40	2.512		8.20	211.24			1452.84	0.19	0.22	0.942	20.70
		2.254			48.91	110.2320					
0.30	1.995		9.10	260.16			1563.07	0.20	0.25	0.842	20.95
		1.790			207.44	371.3323					
0.20	1.585		12.20	467.59			1934.40	0.25	0.33	0.742	21.20
		1.422			96.51	137.2280					
0.10	1.259		13.40	564.10			2071.63	0.27	0.37	0.642	21.45
		1.129			133.36	150.6256					
-0.00	1.000		14.90	697.46			2222.26	0.29	0.41	0.542	21.70
		0.897			178.69	160.3174					
-0.10	0.794		16.70	876.16			2382.57	0.31	0.46	0.442	21.95
		0.713			210.71	150.1575					
-0.20	0.631		18.60	1086.86			2532.73	0.33	0.51	0.342	22.20
		0.566			475.42	269.1199					
-0.30	0.501		22.30	1562.28			2801.85	0.37	0.61	0.242	22.45
		0.450			1116.37	501.9707					
-0.40	0.398		29.20	2678.65			3303.82	0.43	0.80	0.142	22.70
		0.357			1038.99	371.0920					
-0.50	0.316		34.40	3717.63			3674.91	0.48	0.94	0.042	22.95
		0.284			1208.88	342.9700					
-0.60	0.251		39.60	4926.52			4017.88	0.53	1.08	-0.058	23.20
		0.225			1491.88	336.2068					
-0.70	0.200		45.20	6418.40			4354.09	0.57	1.24	-0.158	23.45
		0.179			1978.73	354.2080					
-0.80	0.158		51.70	8397.13			4708.30	0.62	1.41	-0.258	23.70
		0.142			1175.43	167.1349					
-0.90	0.126		55.20	9572.55			4875.43	0.64	1.51	-0.358	23.95
		0.113			1586.88	179.2321					
-1.00	0.100		59.60	11159.43			5054.66	0.66	1.63	-0.458	24.20
		0.090			2442.52	219.1343					
-1.10	0.079		65.80	13601.95			5273.79	0.69	1.80	-0.558	24.45
		0.071			3047.97	217.2121					
-1.20	0.063		72.80	16649.93			5491.00	0.72	1.99	-0.658	24.70
		0.057			3860.39	218.5267					
-1.30	0.050		80.80	20510.32			5709.53	0.75	2.21	-0.758	24.95
		0.045			4710.88	211.8244					
-1.40	0.040		89.60	25221.20			5921.35	0.77	2.45	-0.858	25.20
		0.036			6699.38	239.2815					
-1.50	0.032		100.80	31920.58			6160.63	0.81	2.76	-0.958	25.45
		0.028			9338.45	264.9414					
-1.60	0.025		114.60	41259.03			6425.57	0.84	3.13	-1.058	25.70
		0.023			9172.60	206.7132					
-1.70	0.020		126.70	50431.63			6632.29	0.87	3.46	-1.158	25.95
		0.018			9223.56	165.1106					
-1.80	0.016		137.80	59655.19			6797.39	0.89	3.77	-1.258	26.20
		0.014			8972.37	127.5804					
-1.90	0.013		147.80	68627.56			6924.97	0.91	4.04	-1.358	26.45
		0.011			7728.19	87.2881					
-2.00	0.010		155.90	76355.75			7012.26	0.92	4.26	-1.458	26.70
$-\infty$							7642.00	(1)			∞

PHOTOMETRIC PARAMETERS OF NGC 4340

B-FILTER

Total luminosity ..... L_T = 2.12

Total apparent magnitude ..... m_T = 11.99

Apparent central surface brightness ..... μ_o = 18.72

Major axis at threshold ..... $2a_m$ = 5.95

Minor axis at threshold ..... $2b_m$ = 4.70

Major axis at μ=25.0 mag sec^{-2} ..... 2a(25) = 4.05

Luminosity within μ=25.0 mag sec^{-2} ..... k(25) = 0.76

Gradient of exponential component ..... G(a) = -0.88

Equivalent gradient of exponential comp..... G(r*) = -0.67

Equivalent gradient of reduced exp. comp..... G(ρ) = -0.32

Parameters at k = ¼ :

- Semi-major axis ..... a_1 = 0.22
- Axis ratio ..... b/a = 1.07
- Equivalent radius ..... r_1* = 0.21
- Surface brightness ..... μ_1 = 20.95

Parameters at k = ½(effective) :

- Semi-major axis ..... a_e = 0.41
- Axis ratio ..... b/a = 0.96
- Equivalent radius ..... r_e* = 0.61
- Surface brightness ..... μ_e = 23.05
- Mean surface brightness ..... μ_e' = 12.91

Parameters at k = ¾ :

- Semi-major axis ..... a_3 = 1.73
- Axis ratio ..... b/a = 0.71
- Equivalent radius ..... r_3* = 1.31
- Surface brightness ..... μ_3 = 24.95

Concentration indices ..... C_{21} = 2.90, C_{32} = 2.14

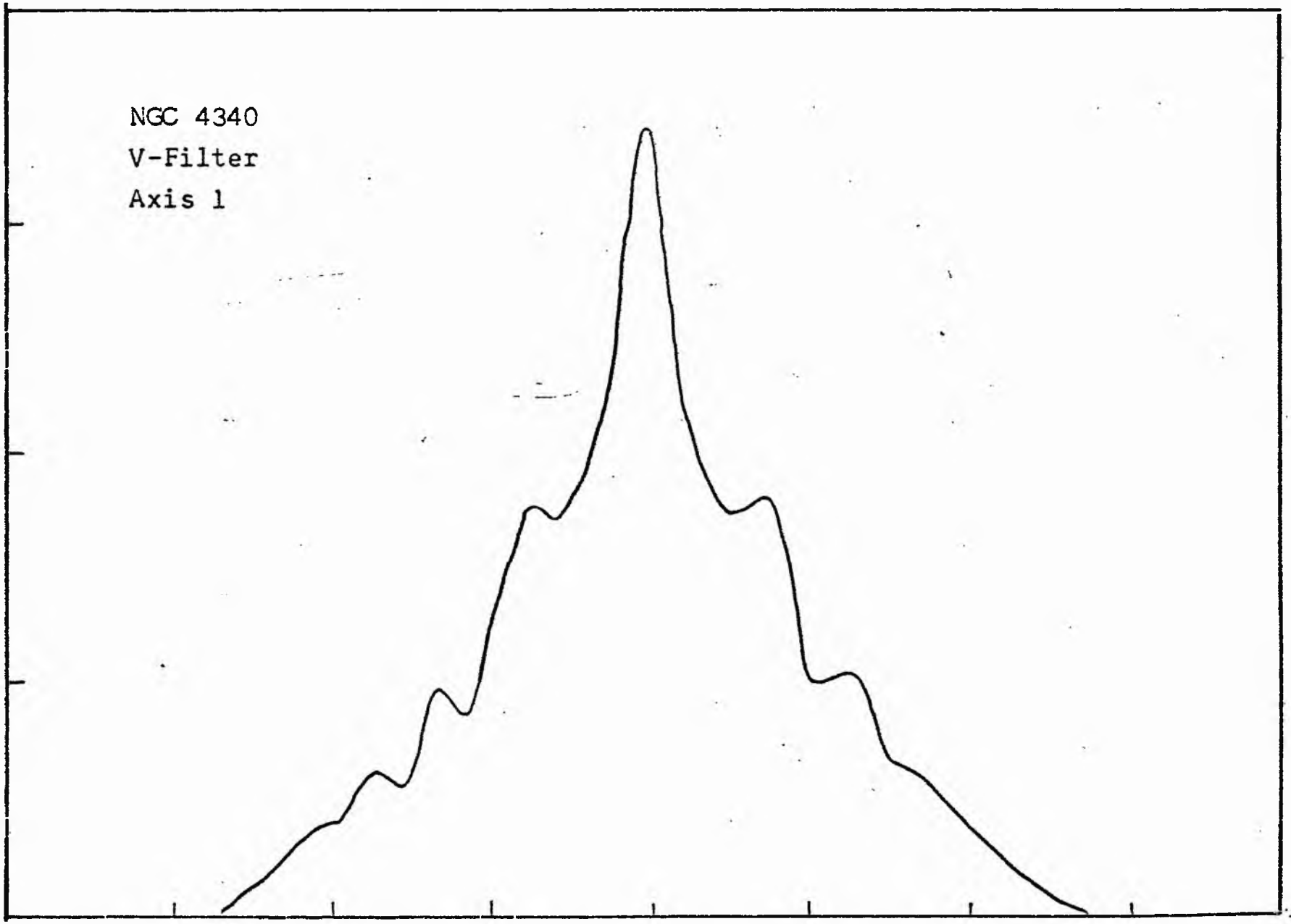
NGC 4340
V-Filter
Axis 1

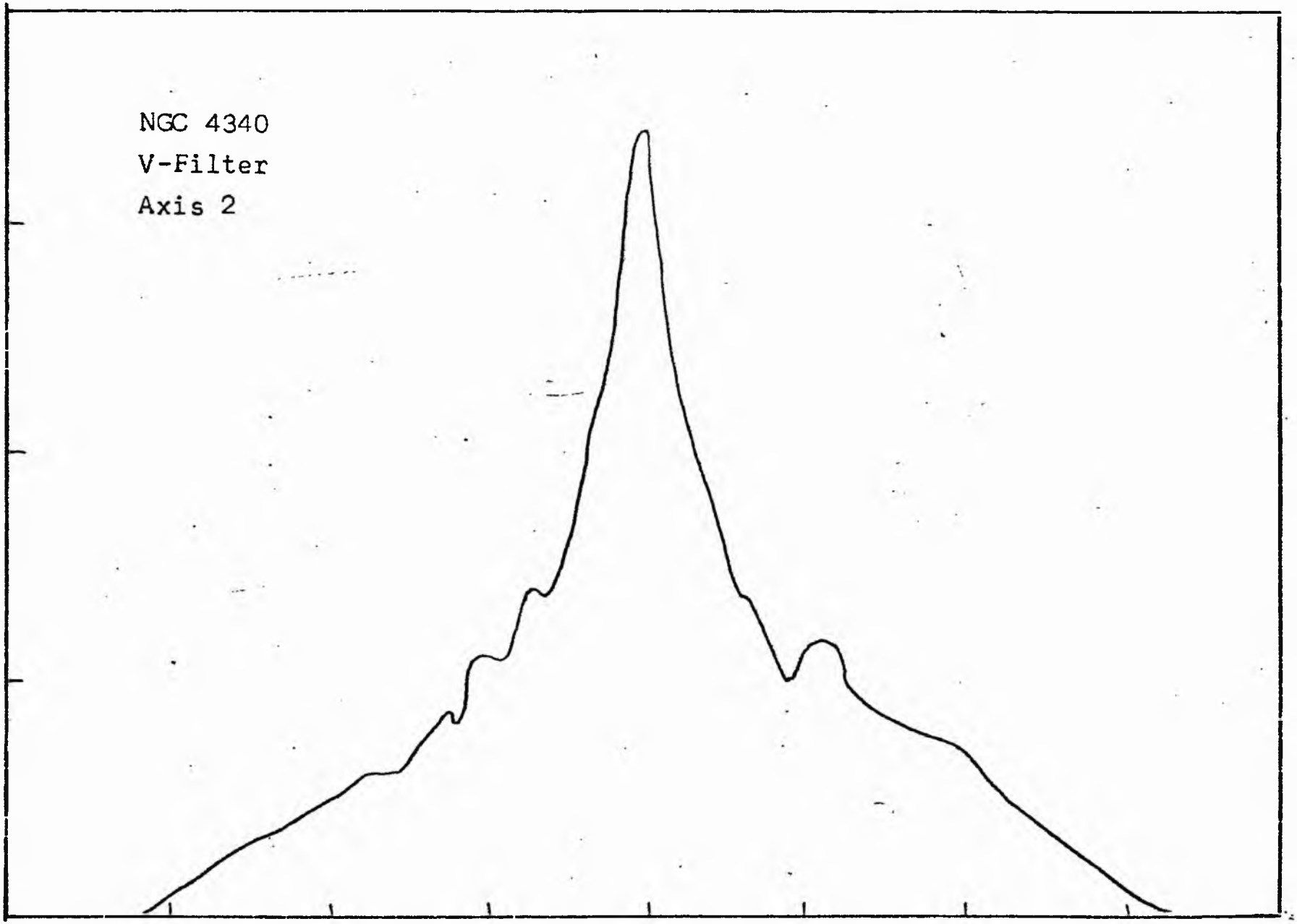
NGC 4340
V-Filter
Axis 2

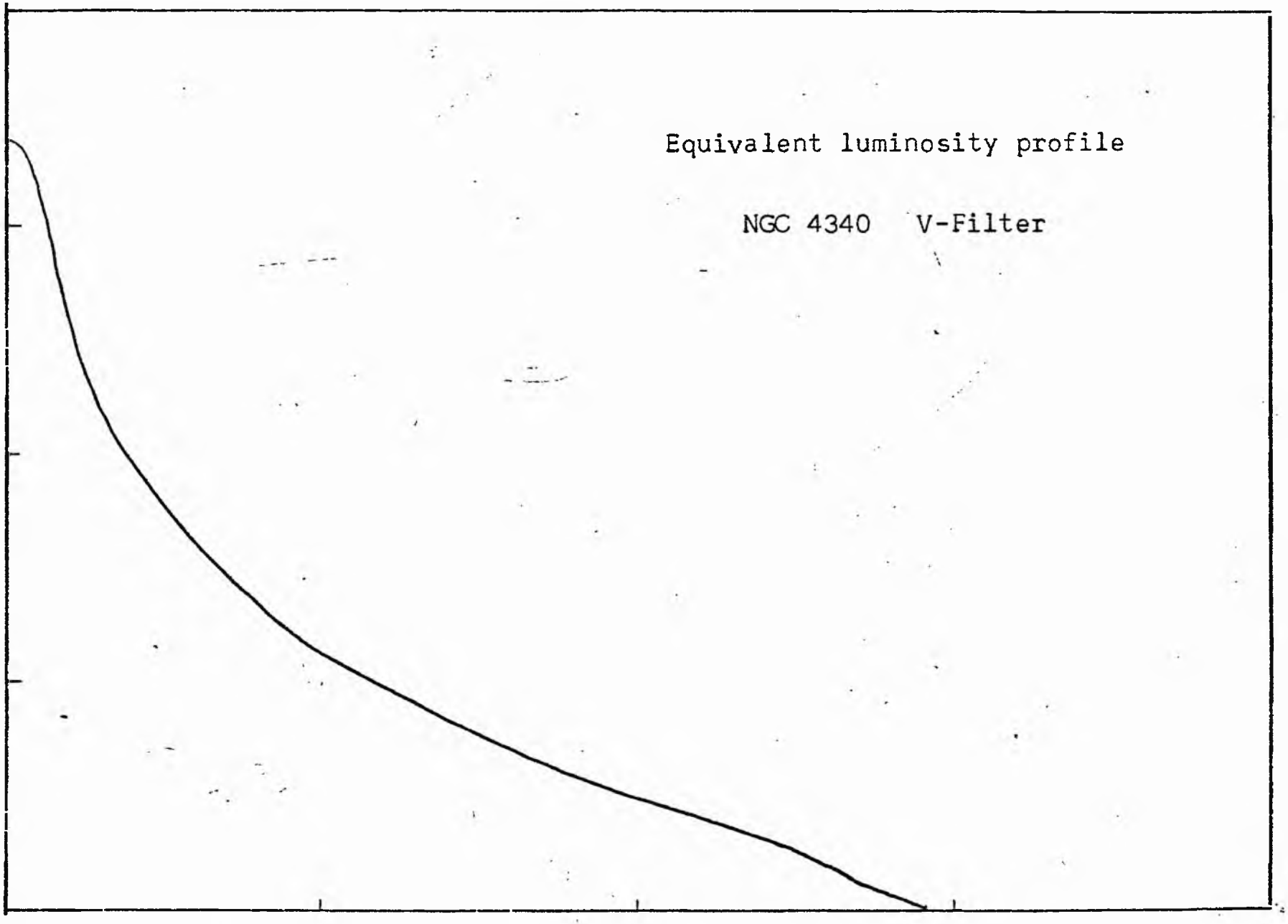
Equivalent luminosity profile
NGC 4340 V-Filter

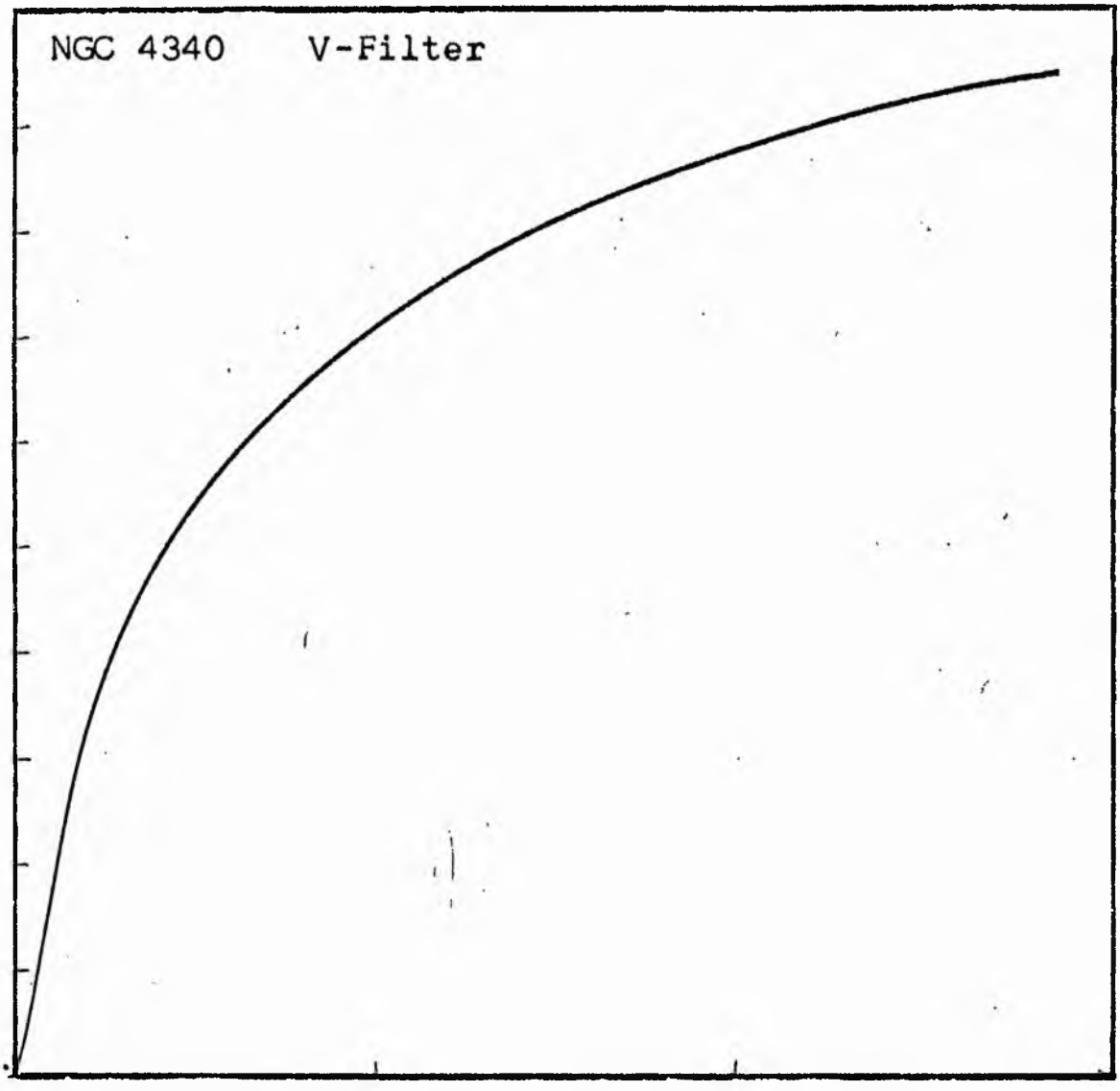

Relative integrated luminosity k(r) versus equivalent radius r*.

MEAN LUMINOSITY DISTRIBUTION IN NGC 4340
V COLOUR

LOG I	I	$\bar{I}$	R	AREA	ΔA	P	ΣP	K(R)	ρ	LOG J	μ
1.44	27.542		0.0	0.0			0.0	0.0	0.0	1.546	17.37
		26.331			9.08	239.0601					
1.40	25.119		1.70	9.08			239.06	0.03	0.08	1.506	17.47
		22.536			36.29	817.7158					
1.30	19.953		3.80	45.36			1056.78	0.12	0.19	1.406	17.72
		17.901			21.11	377.9106					
1.20	15.849		4.60	66.48			1434.69	0.16	0.23	1.306	17.97
		14.219			28.56	406.0547					
1.10	12.589		5.50	95.03			1840.74	0.20	0.27	1.206	18.22
		11.295			10.65	120.2868					
1.00	10.000		5.80	105.68			1961.03	0.22	0.29	1.106	18.47
		8.972			52.68	472.6646					
0.90	7.943		7.10	158.37			2433.69	0.27	0.35	1.006	18.72
		7.126			9.05	64.4780					
0.80	6.310		7.30	167.42			2498.17	0.27	0.36	0.906	18.97
		5.661			43.83	248.0818					
0.70	5.012		8.20	211.24			2746.25	0.30	0.40	0.806	19.22
		4.496			43.23	194.3744					
0.60	3.981		9.00	254.47			2940.63	0.32	0.44	0.706	19.47
		3.572			53.44	190.8632					
0.50	3.162		9.90	307.91			3131.49	0.34	0.49	0.606	19.72
		2.837			72.23	204.9085					
0.40	2.512		11.00	380.13			3336.40	0.37	0.54	0.506	19.97
		2.254			118.63	267.3328					
0.30	1.995		12.60	498.76			3603.73	0.40	0.62	0.406	20.22
		1.790			108.23	193.7360					
0.20	1.585		13.90	606.99			3797.47	0.42	0.68	0.306	20.47
		1.422			177.28	252.0753					
0.10	1.259		15.80	784.27			4049.54	0.44	0.78	0.206	20.72
		1.129			211.11	238.4436					
-0.00	1.000		17.80	995.38			4287.98	0.47	0.87	0.106	20.97
		0.897			286.51	257.0498					
-0.10	0.794		20.20	1281.89			4545.03	0.50	0.99	0.006	21.22
		0.713			365.59	260.5320					
-0.20	0.631		22.90	1647.48			4805.56	0.53	1.13	-0.094	21.47
		0.566			443.69	251.1573					
-0.30	0.501		25.80	2091.17			5056.72	0.55	1.27	-0.194	21.72
		0.450			514.59	231.3848					
-0.40	0.398		28.80	2605.76			5288.10	0.58	1.42	-0.294	21.97
		0.357			733.00	261.8020					
-0.50	0.316		32.60	3338.76			5549.90	0.61	1.60	-0.394	22.22
		0.284			846.63	240.1953					
-0.60	0.251		36.50	4185.39			5790.09	0.63	1.79	-0.494	22.47
		0.225			1044.23	235.3246					
-0.70	0.200		40.80	5229.62			6025.42	0.66	2.01	-0.594	22.72
		0.179			2190.70	392.1506					
-0.80	0.158		48.60	7420.31			6417.57	0.70	2.39	-0.694	22.97
		0.142			1774.53	252.3213					
-0.90	0.126		54.10	9194.84			6669.89	0.73	2.66	-0.794	23.22
		0.113			1964.59	221.8934					
-1.00	0.100		59.60	11159.43			6891.78	0.76	2.93	-0.894	23.47
		0.090			2442.52	219.1343					
-1.10	0.079		65.80	13601.95			7110.91	0.78	3.23	-0.994	23.72
		0.071			3369.71	240.1409					
-1.20	0.063		73.50	16971.67			7351.05	0.81	3.61	-1.094	23.97
		0.057			4410.80	249.6837					
-1.30	0.050		82.50	21382.46			7600.73	0.83	4.05	-1.194	24.22
		0.045			5964.75	268.2041					
-1.40	0.040		93.30	27347.21			7868.94	0.86	4.59	-1.294	24.47
		0.036			5852.62	209.0379					
-1.50	0.032		102.80	33199.84			8077.97	0.89	5.05	-1.394	24.72
		0.028			6067.67	172.1460					
-1.60	0.025		111.80	39267.50			8250.12	0.90	5.49	-1.494	24.97
		0.023			6273.52	141.3796					
-1.70	0.020		120.40	45541.02			8391.50	0.92	5.92	-1.594	25.22
		0.018			6253.02	111.9351					
-1.80	0.016		128.40	51794.04			8503.43	0.93	6.31	-1.694	25.47
		0.014			6227.42	88.5493					
-1.90	0.013		135.90	58021.46			8591.98	0.94	6.68	-1.794	25.72
		0.011			6041.38	68.2360					
-2.00	0.010		142.80	64062.85			8660.21	0.95	7.02	-1.894	25.97
$-\infty$							9120.00	(1)			∞

PHOTOMETRIC PARAMETERS OF NGC 4340

V-FILTER

Total luminosity ..... L_T = 2.53

Total apparent magnitude ..... m_T = 11.07

Apparent central surface brightness ..... μ_o = 17.37

Major axis at threshold ..... $2a_m$ = 4.49

Minor axis at threshold ..... $2b_m$ = 5.08

Major axis at μ=25.0 mag sec^{-2} ..... 2a(25) = 3.93

Luminosity within μ=25.0 mag sec^{-2} ..... k(25) = 0.91

Gradient of exponential component ..... G(a) = -1.22

Equivalent gradient of exponential comp..... G(r*) = -0.73

Equivalent gradient of reduced exp. comp..... G(ρ) = -0.24

Parameters at k = ¼ :

- Semi-major axis ..... a_1 = 0.15
- Axis ratio ..... b/a = 1.11
- Equivalent radius ..... r_1* = 0.12
- Surface brightness ..... μ_1 = 18.62

Parameters at k = ½(effective) :

- Semi-major axis ..... a_e = 0.36
- Axis ratio ..... b/a = 0.73
- Equivalent radius ..... r_e* = 0.34
- Surface brightness ..... μ_e = 21.22
- Mean surface brightness ..... μ_e' = 12.38

Parameters at k = ¾ :

- Semi-major axis ..... a_3 = 1.05
- Axis ratio ..... b/a = 0.98
- Equivalent radius ..... r_3* = 0.97
- Surface brightness ..... μ_3 = 23.39

Concentration indices ..... C_{21} = 2.83, C_{32} = 2.85

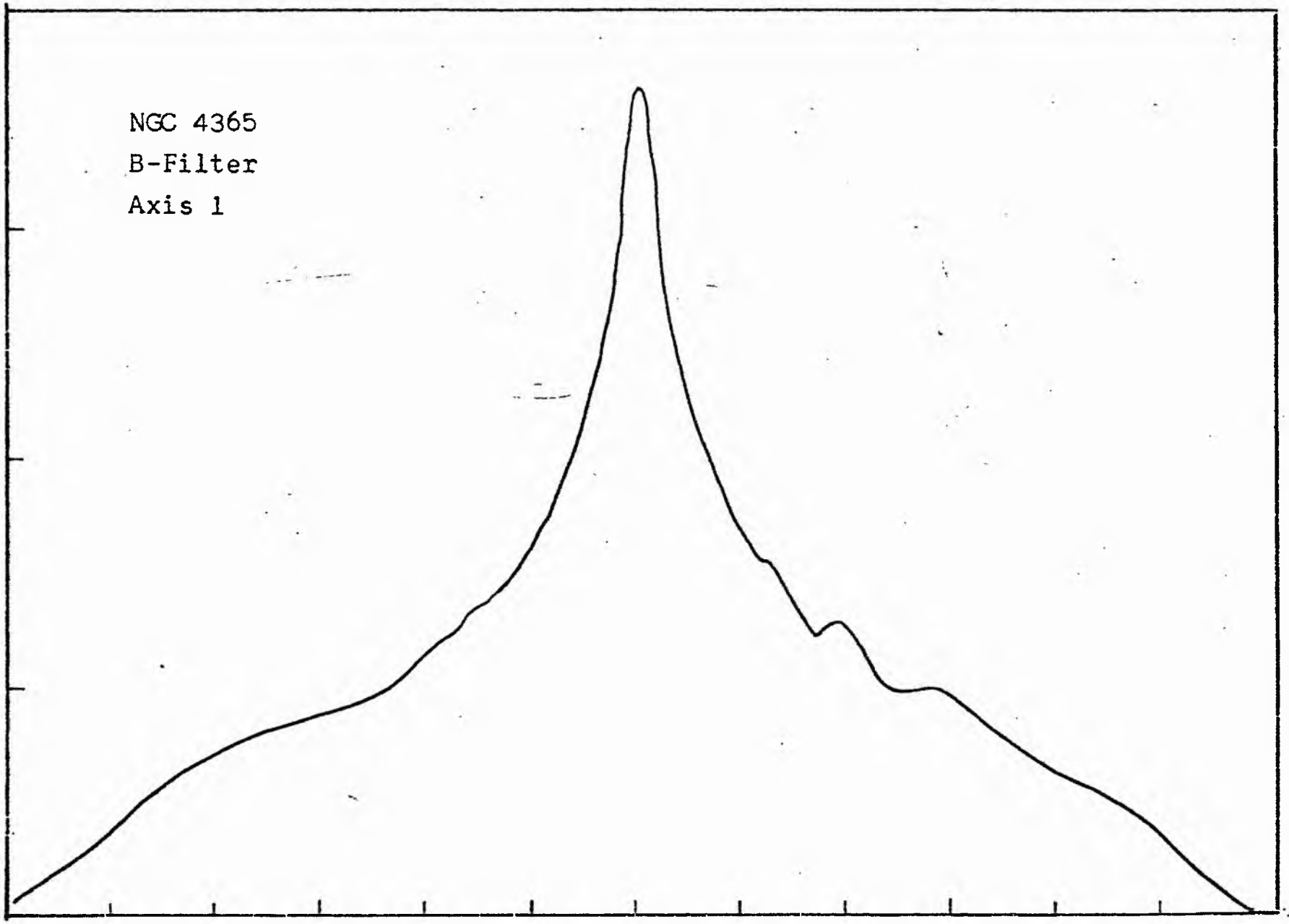
NGC 4365
B-Filter
Axis 1

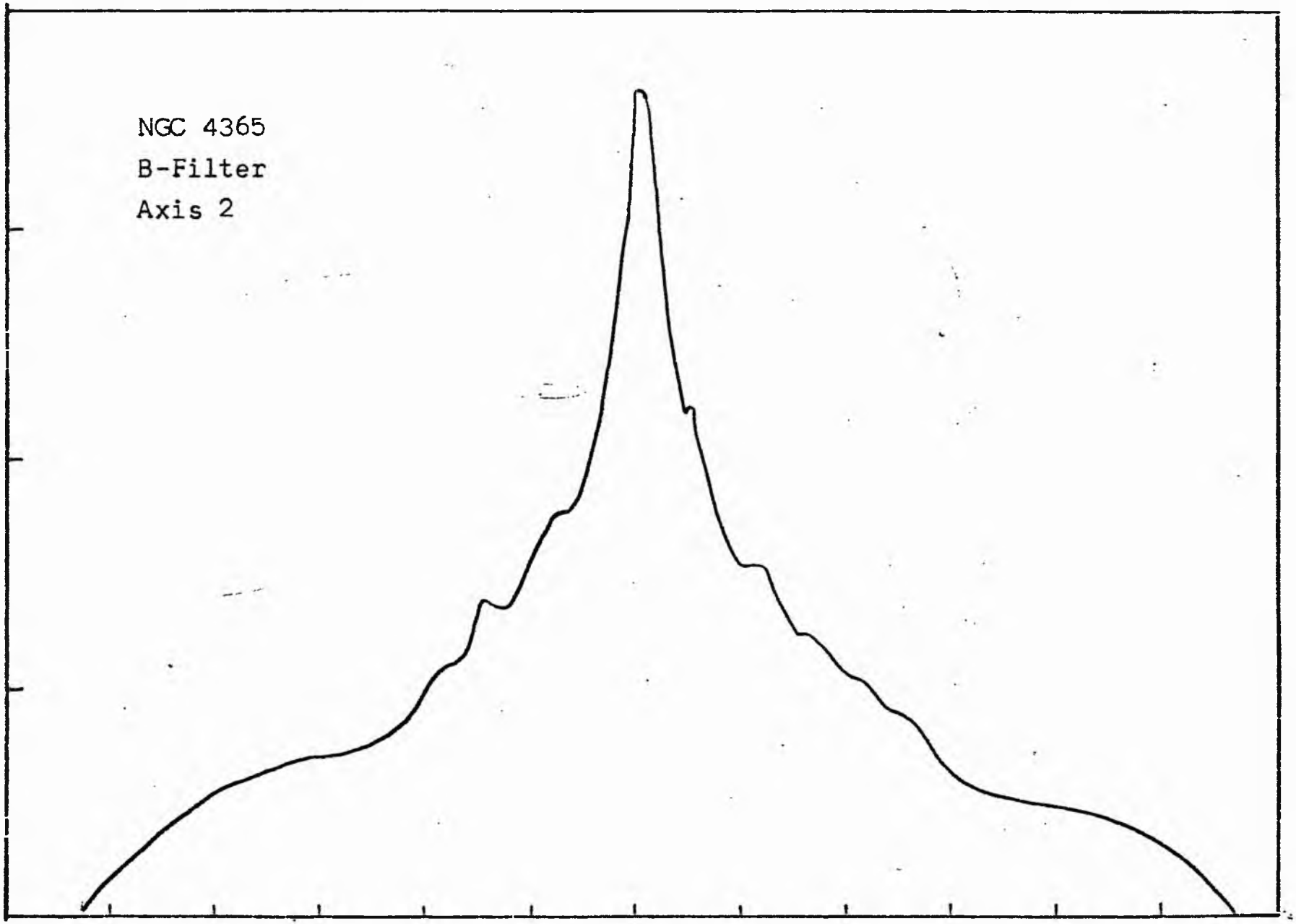
NGC 4365
B-Filter
Axis 2

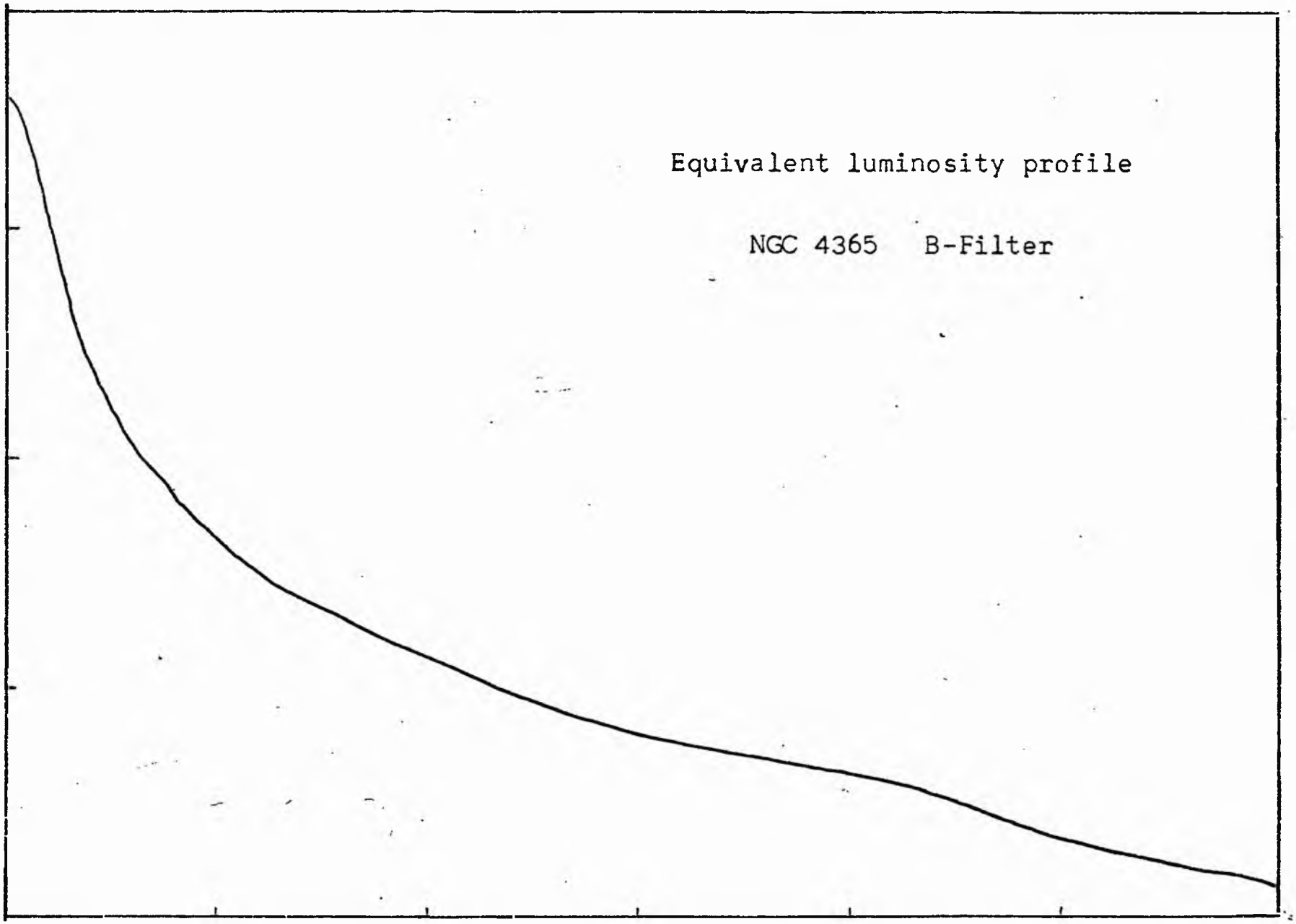
Equivalent luminosity profile
NGC 4365 B-Filter

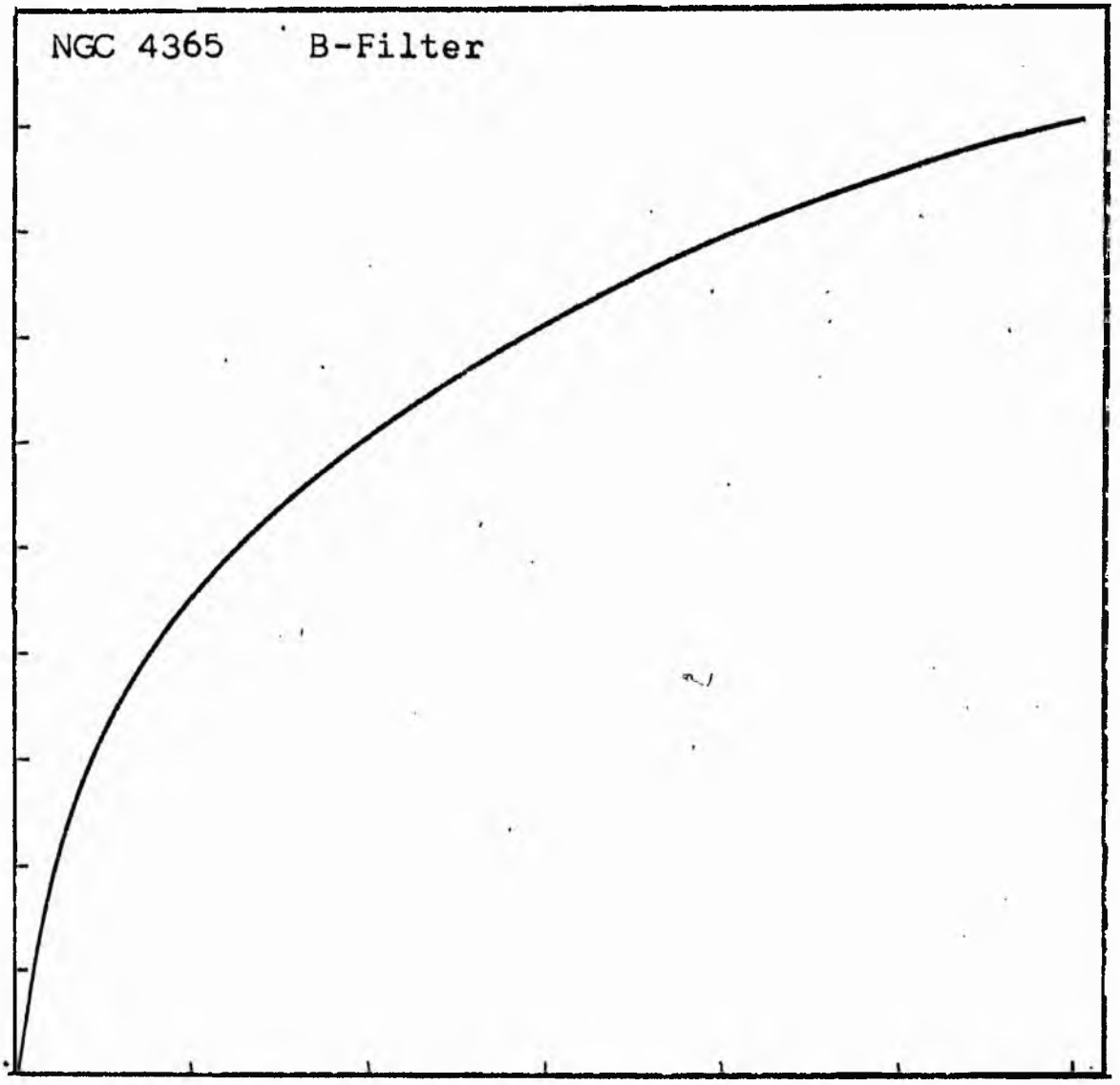

Relative integrated luminosity k(r) versus equivalent radius r*.

MEAN LUMINOSITY DISTRIBUTION IN NGC 4365
B COLOUR

LOG I	I	$\bar{I}$	R	AREA	ΔA	P	ΣP	K(R)	ρ	LOG J	μ
1.67	46.773		0.0	0.0			0.0	0.0	0.0	2.244	17.61
		43.292			19.63	850.0366					
1.60	39.811		2.50	19.63			850.04	0.03	0.04	2.174	17.79
		35.717			35.78	1278.0388					
1.50	31.623		4.20	55.42			2128.08	0.06	0.07	2.074	18.04
		28.371			37.90	1075.1223					
1.40	25.119		5.45	93.31			3203.20	0.09	0.09	1.974	18.29
		22.536			19.41	437.3618					
1.30	19.953		5.99	112.72			3640.56	0.11	0.09	1.874	18.54
		17.901			42.10	753.5876					
1.20	15.849		7.02	154.82			4394.14	0.13	0.11	1.774	18.79
		14.219			42.74	607.7178					
1.10	12.589		7.93	197.56			5001.86	0.15	0.12	1.674	19.04
		11.295			55.78	630.0161					
1.00	10.000		8.98	253.34			5631.87	0.17	0.14	1.574	19.29
		8.972			62.08	556.9353					
0.90	7.943		10.02	315.42			6188.81	0.18	0.16	1.474	19.54
		7.126			78.66	560.5920					
0.80	6.310		11.20	394.08			6749.40	0.20	0.18	1.374	19.79
		5.661			136.85	774.6533					
0.70	5.012		13.00	530.93			7524.05	0.22	0.20	1.274	20.04
		4.496			191.09	859.2217					
0.60	3.981		15.16	722.02			8383.27	0.25	0.24	1.174	20.29
		3.572			114.72	409.7397					
0.50	3.162		16.32	836.74			8793.01	0.26	0.26	1.074	20.54
		2.837			217.65	617.4866					
0.40	2.512		18.32	1054.39			9410.49	0.28	0.29	0.974	20.79
		2.254			304.79	686.8606					
0.30	1.995		20.80	1359.18			10097.35	0.30	0.33	0.874	21.04
		1.790			405.42	725.7358					
0.20	1.585		23.70	1764.60			10823.09	0.32	0.37	0.774	21.29
		1.422			508.69	723.3020					
0.10	1.259		26.90	2273.29			11546.39	0.34	0.42	0.674	21.54
		1.129			649.18	733.2205					
-0.00	1.000		30.50	2922.47			12279.61	0.36	0.48	0.574	21.79
		0.897			816.81	732.8125					
-0.10	0.794		34.50	3739.28			13012.42	0.39	0.54	0.474	22.04
		0.713			963.41	686.5669					
-0.20	0.631		38.69	4702.70			13698.98	0.41	0.61	0.374	22.29
		0.566			1434.84	812.2212					
-0.30	0.501		44.20	6137.54			14511.20	0.43	0.70	0.274	22.54
		0.450			1842.61	828.5186					
-0.40	0.398		50.40	7980.14			15339.72	0.45	0.79	0.174	22.79
		0.357			2479.12	885.4590					
-0.50	0.316		57.70	10459.27			16225.18	0.48	0.91	0.074	23.04
		0.284			3142.68	891.6016					
-0.60	0.251		65.80	13601.95			17116.78	0.51	1.04	-0.026	23.29
		0.225			7162.99	1614.2273					
-0.70	0.200		81.30	20764.95			18731.00	0.56	1.28	-0.126	23.54
		0.179			6057.21	1084.2834					
-0.80	0.158		92.40	26822.16			19815.29	0.59	1.45	-0.226	23.79
		0.142			6961.55	989.8655					
-0.90	0.126		103.70	33783.71			20805.15	0.62	1.63	-0.326	24.04
		0.113			8635.45	975.3391					
-1.00	0.100		116.20	42419.16			21780.48	0.65	1.83	-0.426	24.29
		0.090			11823.45	1060.7554					
-1.10	0.079		131.40	54242.61			22841.24	0.68	2.07	-0.526	24.54
		0.071			15223.27	1084.8738					
-1.20	0.063		148.70	69465.87			23926.11	0.71	2.34	-0.626	24.79
		0.057			31757.00	1797.6772					
-1.30	0.050		179.50	101222.87			25723.79	0.76	2.83	-0.726	25.04
		0.045			36794.06	1654.4382					
-1.40	0.040		209.60	138016.94			27378.22	0.81	3.30	-0.826	25.29
		0.036			22017.31	786.3899					
-1.50	0.032		225.70	160034.25			28164.61	0.83	3.55	-0.926	25.54
		0.028			21072.31	597.8420					
-1.60	0.025		240.10	181106.56			28762.45	0.85	3.78	-1.026	25.79
		0.023			22695.12	511.4548					
-1.70	0.020		254.70	203801.69			29273.90	0.87	4.01	-1.126	26.04
		0.018			54067.31	967.8542					
-1.80	0.016		286.50	257869.00			30241.75	0.90	4.51	-1.226	26.29
		0.014			14972.06	212.8911					
-1.90	0.013		294.70	272841.06			30454.64	0.90	4.64	-1.326	26.54
		0.011			7644.44	86.3420					
-2.00	0.010		298.80	280485.50			30540.98	0.91	4.70	-1.426	26.79
$-\infty$							33740.00	(1)			∞

PHOTOMETRIC PARAMETERS OF NGC 4365

B-FILTER

Total luminosity ..... L_T = 9.30

Total apparent magnitude ..... m_T = 10.47

Apparent central surface brightness ..... μ_o = 17.61

Major axis at threshold ..... $2a_m$ = 10.40

Minor axis at threshold ..... $2b_m$ = 9.37

Major axis at μ=25.0 mag sec^{-2} ..... 2a(25) = 6.43

Luminosity within μ=25.0 mag sec^{-2} ..... k(25) = 0.75

Gradient of exponential component ..... G(a) = -0.43

Equivalent gradient of exponential comp. .... G(r*) = -0.38

Equivalent gradient of reduced exp. comp. .... G(ρ) = -0.28

Parameters at k = ¼ :

- Semi-major axis ..... a_1 = 0.26
- Axis ratio ..... b/a = 0.69
- Equivalent radius ..... r_1* = 0.25
- Surface brightness ..... μ_1 = 20.29

Parameters at k = ½(effective) :

- Semi-major axis ..... a_e = 1.11
- Axis ratio ..... b/a = 0.95
- Equivalent radius ..... r_e* = 1.06
- Surface brightness ..... μ_e = 23.17
- Mean surface brightness ..... μ_e' = 12.59

Parameters at k = ¾ :

- Semi-major axis ..... a_3 = 3.06
- Axis ratio ..... b/a = 0.83
- Equivalent radius ..... r_3* = 2.87
- Surface brightness ..... μ_3 = 24.99

Concentration indices ..... C_{21} = 4.15, C_{32} = 2.71

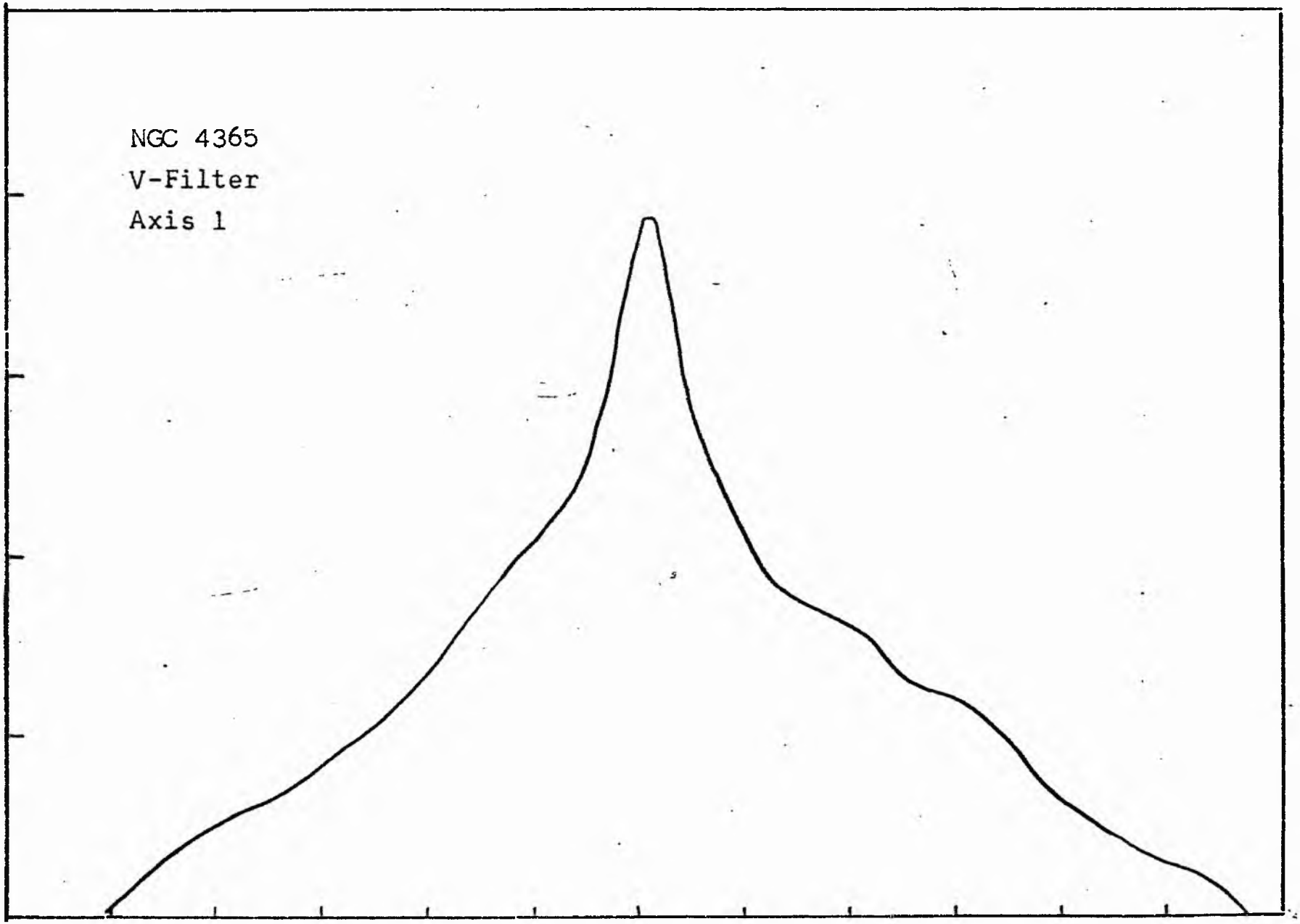
NGC 4365
V-Filter
Axis 1

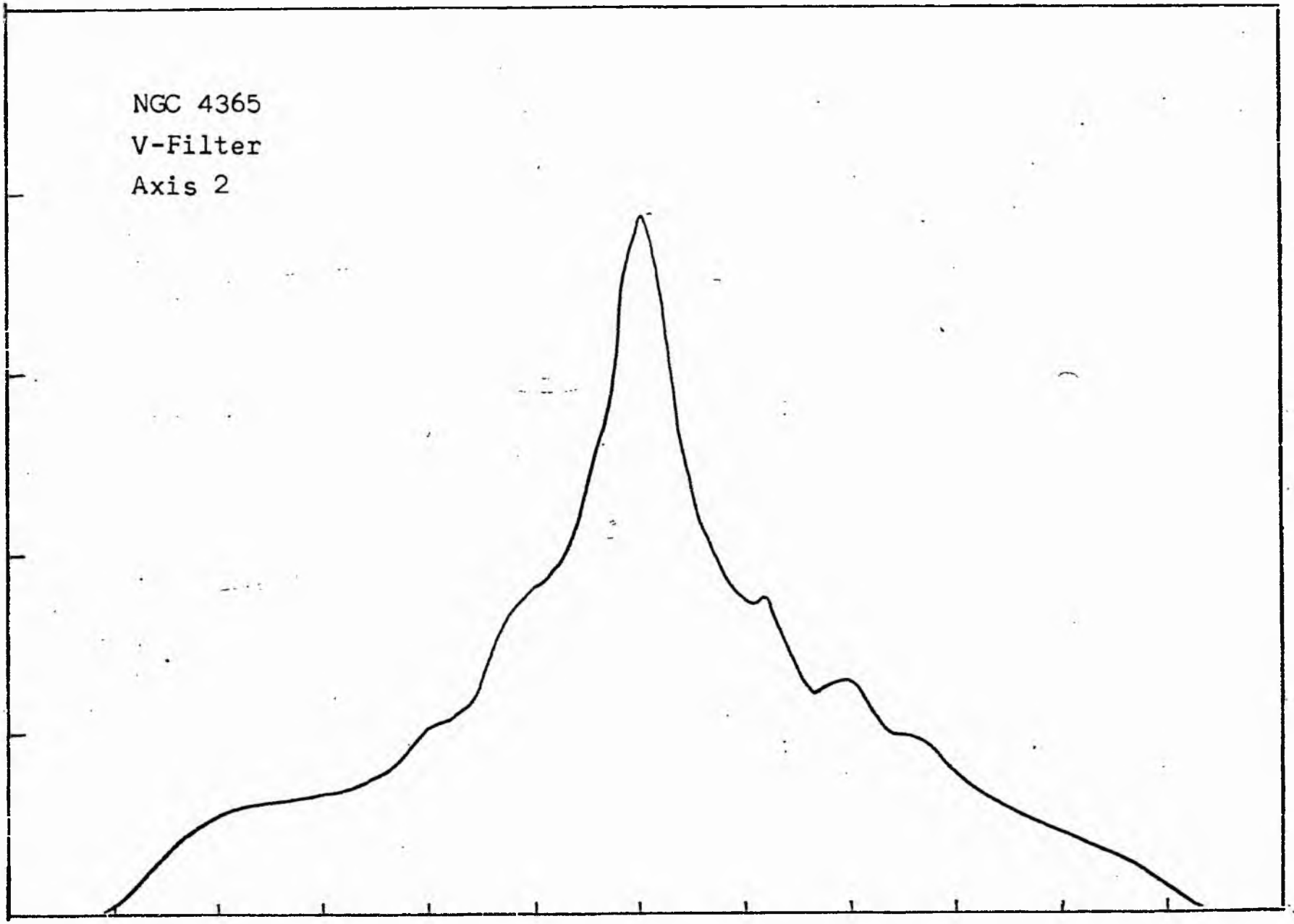
NGC 4365
V-Filter
Axis 2

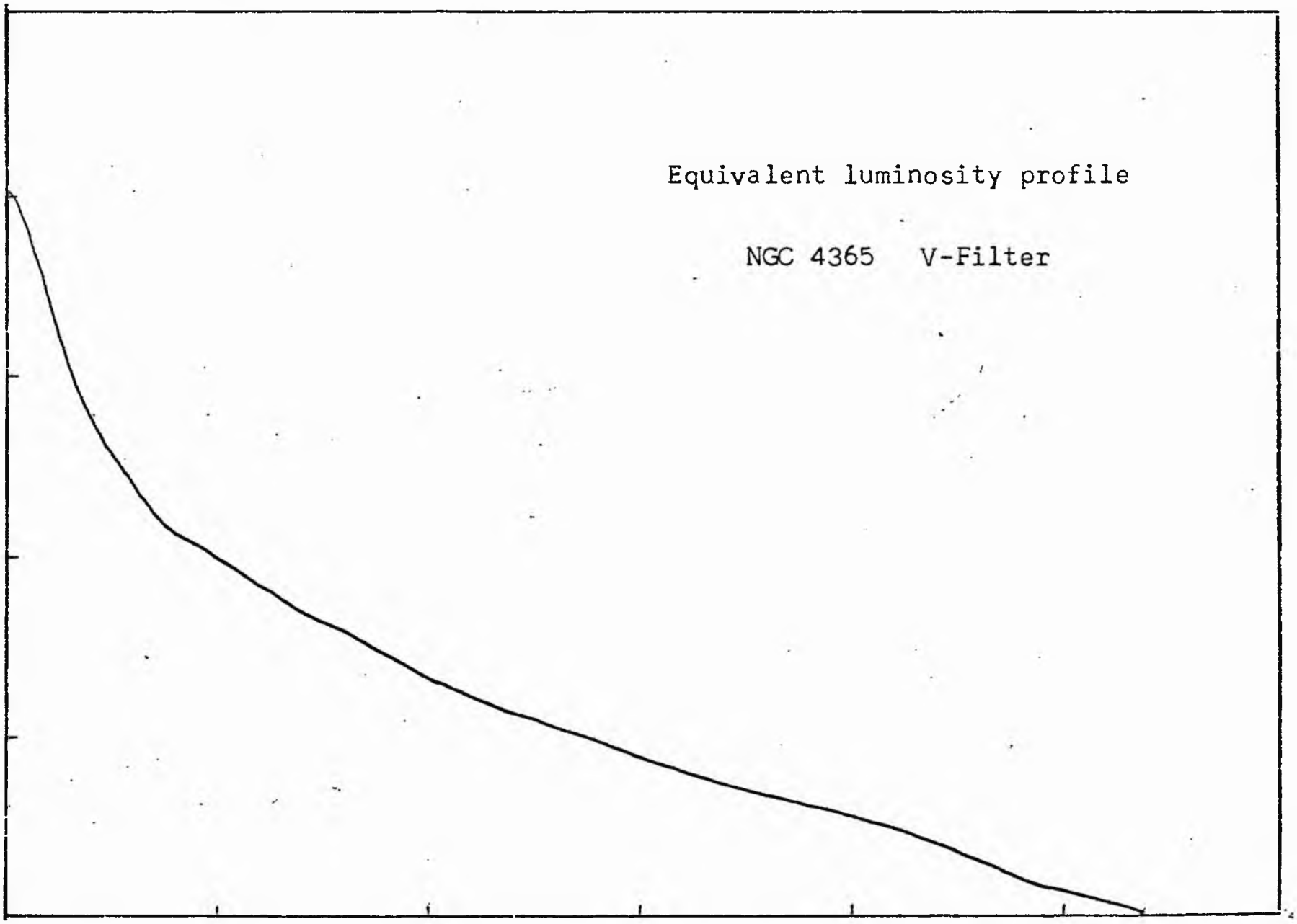
Equivalent luminosity profile
NGC 4365 V-Filter

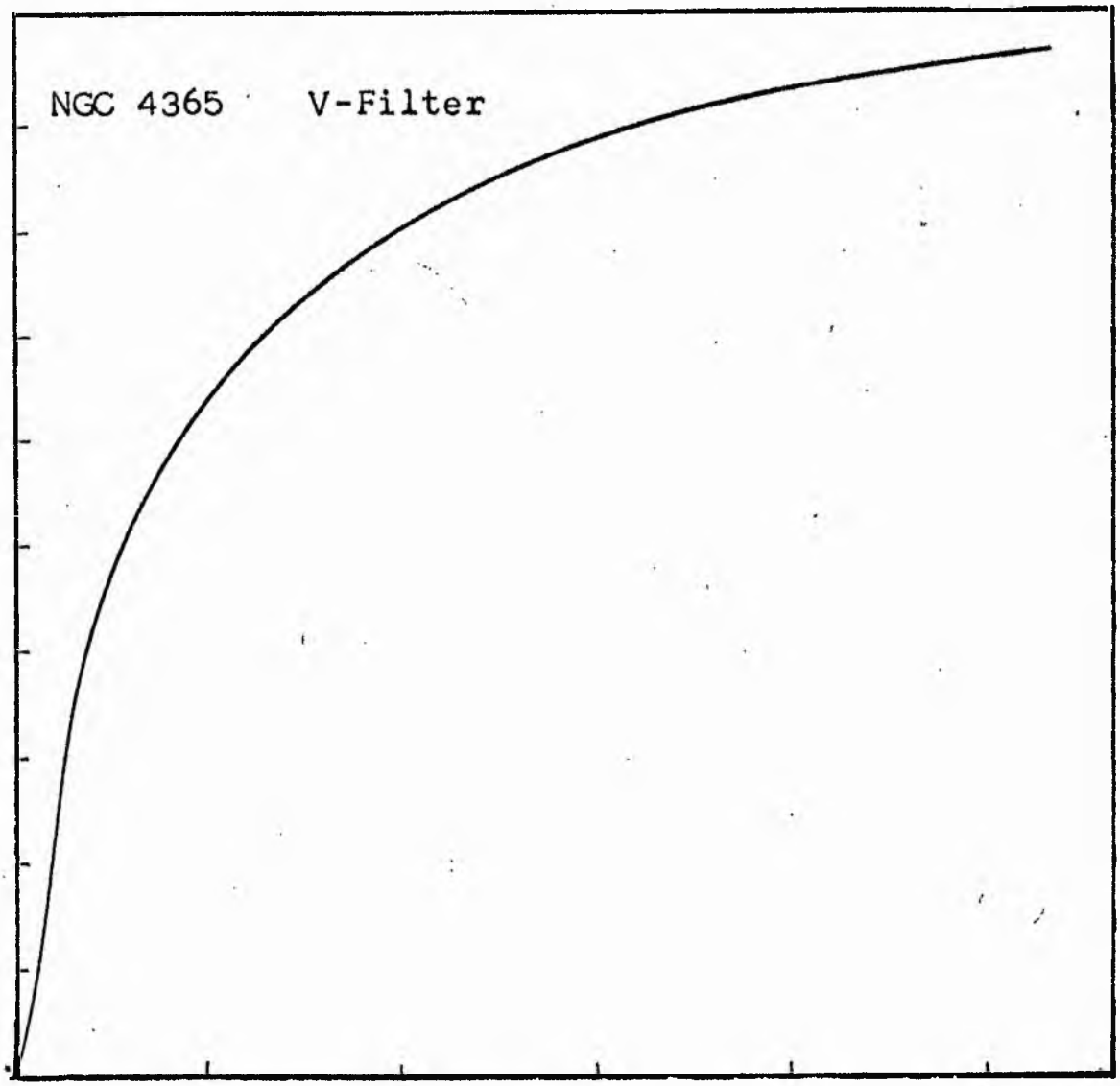

Relative integrated luminosity k(r) versus equivalent radius r*.

MEAN LUMINOSITY DISTRIBUTION IN NGC 4365
V COLOUR

LOG I	I	$\bar{I}$	R	AREA	ΔA	P	ΣP	K(R)	ρ	LOG J	μ
2.04	109.648		0.0	0.0			0.0	0.0	0.0	1.582	16.96
		104.824			5.31	556.5396					
2.00	100.000		1.30	5.31			556.54	0.01	0.05	1.542	17.06
		89.716			19.32	1733.3889					
1.90	79.433		2.80	24.63			2289.93	0.04	0.11	1.442	17.31
		71.264			16.08	1146.2812					
1.80	63.096		3.60	40.72			3436.21	0.06	0.14	1.342	17.56
		56.607			41.00	2320.7617					
1.70	50.119		5.10	81.71			5756.97	0.10	0.19	1.242	17.81
		44.965			72.23	3247.5791					
1.60	39.811		7.00	153.94			9004.55	0.16	0.26	1.142	18.06
		35.717			52.18	1863.7566					
1.50	31.623		8.10	206.12			10868.30	0.19	0.30	1.042	18.31
		28.371			140.24	3978.7231					
1.40	25.119		10.50	346.36			14847.02	0.26	0.39	0.942	18.56
		22.536			61.92	1395.4189					
1.30	19.952		11.40	408.28			16242.44	0.28.	0.43	0.842	18.81
		17.901			82.59	1478.4600					
1.20	15.849		12.50	490.87			17720.90	0.31	0.47	0.742	19.06
		14.219			124.00	1763.1394					
1.10	12.589		13.99	614.87			19484.04	0.34	0.53	0.642	19.31
		11.295			139.89	1580.0449					
1.00	10.000		15.50	754.77			21064.08	0.37	0.58	0.542	19.56
		8.972			174.64	1566.7996					
0.90	7.943		17.20	929.41			22630.87	0.40	0.65	0.442	19.81
		7.126			192.80	1373.9587					
0.80	6.310		18.90	1122.21			24004.83	0.42	0.71	0.342	20.06
		5.661			250.07	1415.5669					
0.70	5.012		20.90	1372.28			25420.40	0.44	0.79	0.242	20.31
		4.496			289.62	1302.2788					
0.60	3.981		23.00	1661.90			26722.68	0.47	0.86	0.142	20.56
		3.572			380.92	1360.5051					
0.50	3.162		25.50	2042.82			28083.18	0.49	0.96	0.042	20.81
		2.837			473.25	1342.6299					
0.40	2.512		28.30	2516.07			29425.81	0.51	1.06	-0.058	21.06
		2.254			640.89	1444.2749					
0.30	1.995		31.70	3156.95			30870.08	0.54	1.19	-0.158	21.31
		1.790			735.60	1316.7783					
0.20	1.585		35.20	3892.56			32186.86	0.56	1.32	-0.258	21.56
		1.422			548.90	780.4734					
0.10	1.259		37.60	4441.45			32967.33	0.58	1.41	-0.358	21.81
		1.129			1558.01	1759.7034					
-0.00	1.000		43.70	5999.46			34727.04	0.61	1.64	-0.458	22.06
		0.897			2300.49	2063.9041					
-0.10	0.794		51.40	8299.96			36790.94	0.64	1.93	-0.558	22.31
		0.713			3313.37	2361.2366					
-0.20	0.631		60.80	11613.33			39152.17	0.68	2.28	-0.658	22.56
		0.566			2828.05	1600.8716					
-0.30	0.501		67.80	14441.39			40753.04	0.71	2.55	-0.758	22.81
		0.450			2808.50	1262.8237					
-0.40	0.398		74.10	17249.88			42015.86	0.73	2.78	-0.858	23.06
		0.357			4654.09	1662.2771					
-0.50	0.316		83.50	21903.97			43678.14	0.76	3.14	-0.958	23.31
		0.284			2646.19	750.7415					
-0.60	0.251		88.40	24550.16			44428.87	0.78	3.32	-1.058	23.56
		0.225			4887.30	1101.3826					
-0.70	0.200		96.80	29437.46			45530.25	0.79	3.64	-1.158	23.81
		0.179			6800.05	1217.2544					
-0.80	0.158		107.40	36237.51			46747.51	0.82	4.03	-1.258	24.06
		0.142			9227.89	1312.1140					
-0.90	0.126		120.30	45465.40			48059.62	0.84	4.52	-1.358	24.31
		0.113			11535.93	1302.9333					
-1.00	0.100		134.70	57001.33			49362.55	0.86	5.06	-1.458	24.56
		0.090			6078.36	545.3262					
-1.10	0.079		141.70	63079.69			49907.87	0.87	5.32	-1.558	24.81
		0.071			11136.31	793.6191					
-1.20	0.063		153.70	74216.00			50701.49	0.89	5.77	-1.658	25.06
		0.057			13820.06	782.3142					
-1.30	0.050		167.40	88036.06			51483.80	0.90	6.29	-1.758	25.31
		0.045			19950.37	897.0632					
-1.40	0.040		185.40	107986.44			52380.87	0.91	6.96	-1.858	25.56
		0.036			24942.12	890.8528					
-1.50	0.032		205.70	132928.56			53271.72	0.93	7.73	-1.958	25.81
		0.028			10406.44	295.2397					
-1.60	0.025		213.60	143335.00			53566.96	0.94	8.02	-2.058	26.06
		0.023			14016.19	315.8665					
-1.70	0.020		223.80	157351.19			53882.82	0.94	8.41	-2.158	26.31
		0.018			18960.00	339.4006					
-1.80	0.016		236.90	176311.19			54222.22.	0.95	8.90	-2.258	26.56
		0.014			31834.06	452.6545					
-1.90	0.013		257.40	208145.25			54674.87	0.95	9.67	-2.358	26.81
		0.011			9155.56	103.4095					
-2.00	0.010		263.00	217300.81			54778.28	0.96	9.88	-2.458	27.06
- ∞							57278.00	(1)			∞

PHOTOMETRIC PARAMETERS OF NGC 4365

V-FILTER

Total luminosity	L_T	= 15.91
Total apparent magnitude	m_T	= 10.16
Apparent central surface brightness	μ_o	= 16.96
Major axis at threshold	$2a_m$	= 9.62
Minor axis at threshold	$2b_m$	= 8.83
Major axis at μ=25.0 mag sec^{-2}	$2a(25)$	= 5.37
Luminosity within μ=25.0 mag sec^{-2}	$k(25)$	= 0.88
Gradient of exponential component	$G(a)$	= -0.49
Equivalent gradient of exponential comp.	$G(r^*)$	= -0.55
Equivalent gradient of reduced exp. comp.	$G(\rho)$	= -0.24
Parameters at k = ¼ :		
Semi-major axis	a_1	= 0.22
Axis ratio	b/a	= 0.85
Equivalent radius	r_1^*	= 0.17
Surface brightness	μ_1	= 18.52
Parameters at k = ½(effective) :		
Semi-major axis	a_e	= 0.57
Axis ratio	b/a	= 0.74
Equivalent radius	r_e^*	= 0.44
Surface brightness	μ_e	= 20.93
Mean surface brightness	μ_e'	= 10.36
Parameters at k = ¾ :		
Semi-major axis	a_3	= 1.57
Axis ratio	b/a	= 0.77
Equivalent radius	r_3^*	= 1.32
Surface brightness	μ_3	= 23.24
Concentration indices	C_{21}	= 2.62
	C_{32}	= 2.97

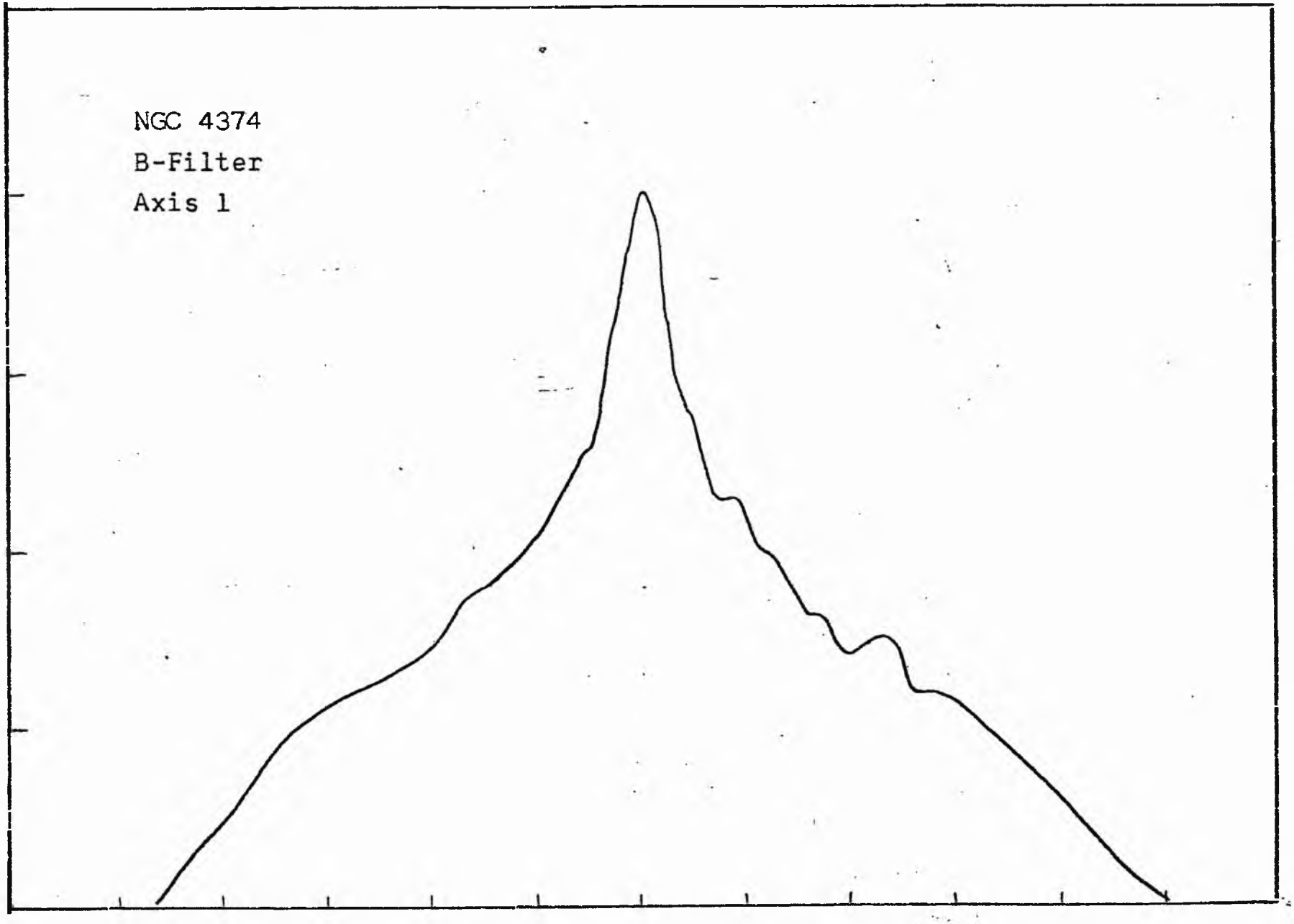
NGC 4374
B-Filter
Axis 1

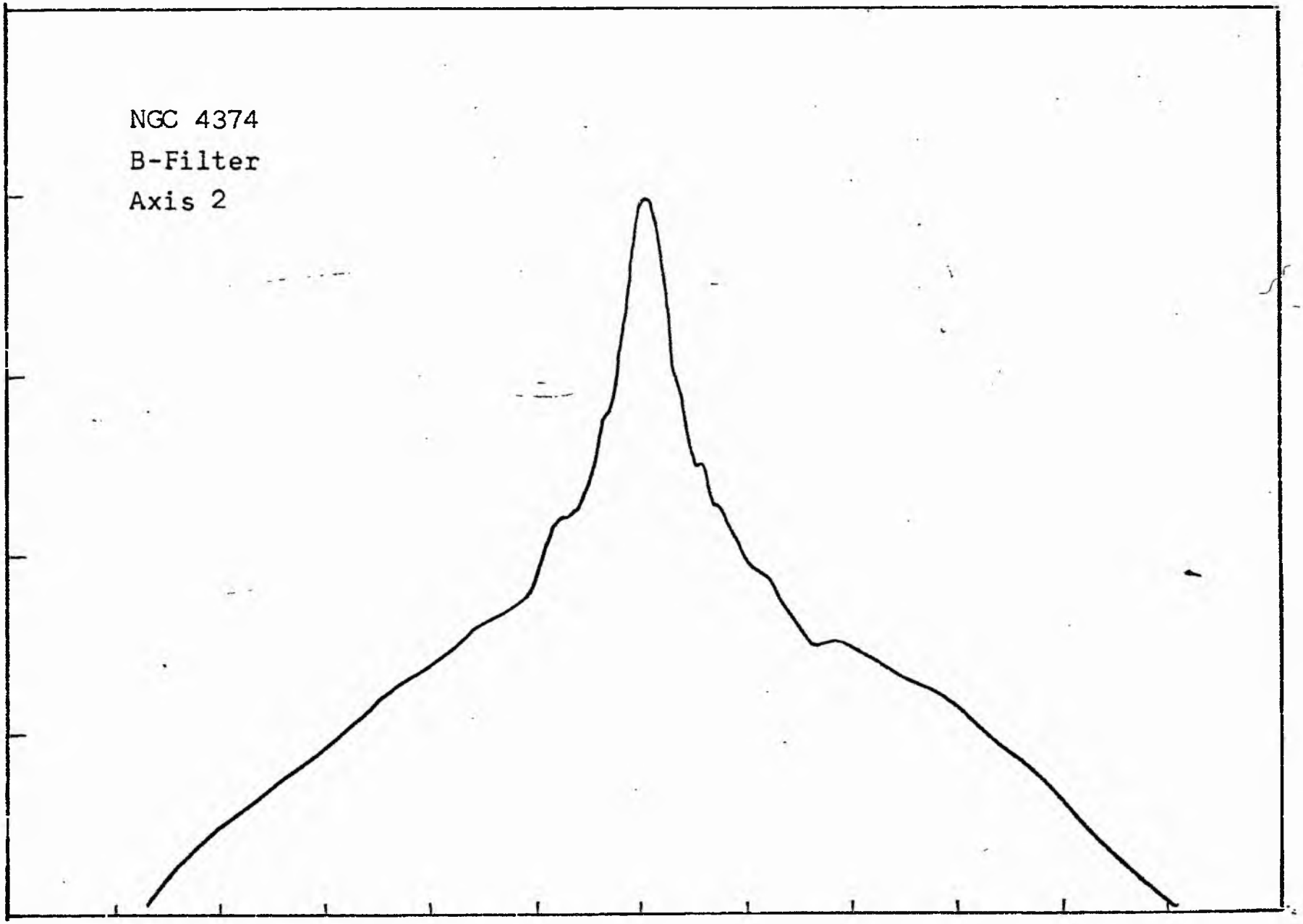
NGC 4374
B-Filter
Axis 2

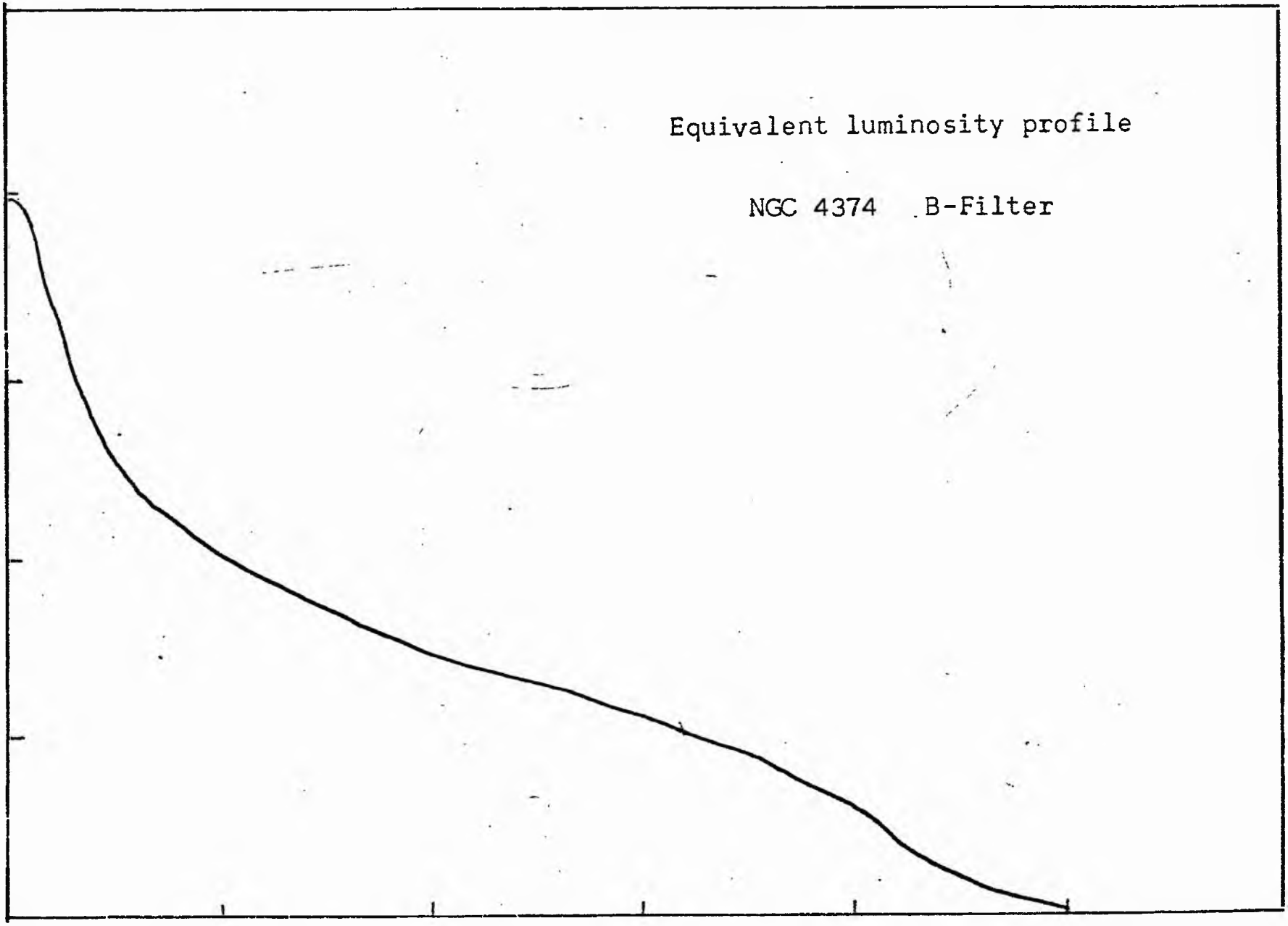
Equivalent luminosity profile
NGC 4374 B-Filter

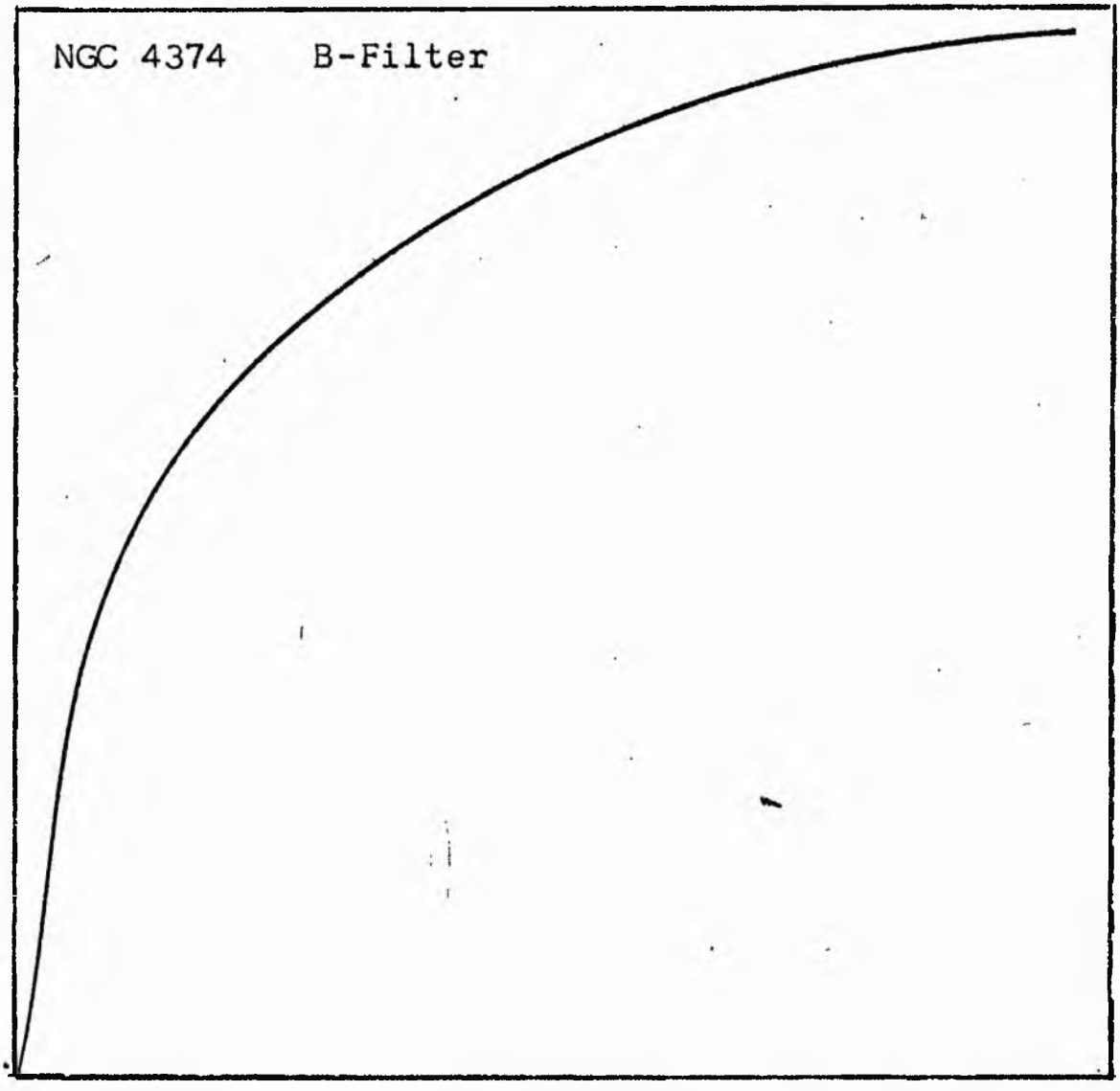

Relative integrated luminosity k(r) versus equivalent radius r*.

MEAN LUMINOSITY DISTRIBUTION IN NGC 4374
B COLOUR

LOG I	I	I	R	AREA	ΔA	P	ΣP	KIRI	ρ	LOG J	μ
1.93	85.114		0.0	0.0			0.0	0.0	0.0	1.445	17.51
		82.273			28.84	2372.9761					
1.90	79.433		3.03	28.84			2372.98	0.04	0.12	1.415	17.59
		71.264			109.25	7785.7500					
1.80	63.096		6.63	138.09			10158.72	0.15	0.25	1.315	17.84
		56.607			32.08	1816.1912					
1.70	50.119		7.36	170.18			11974.91	0.18	0.28	1.215	18.09
		44.965			48.86	2197.0085					
1.60	39.811		8.35	219.04			14171.92	0.21	0.32	1.115	18.34
		35.717			82.68	2953.0066					
1.50	31.623		9.80	301.72			17124.92	0.25	0.38	1.015	18.59
		28.371			64.72	1836.0586					
1.40	25.119		10.80	366.44			18960.98	0.28	0.41	0.915	18.84
		22.536			116.62	2628.0105					
1.30	19.952		12.40	483.05			21588.99	0.32	0.48	0.815	19.09
		17.901			89.50	1602.1780					
1.20	15.849		13.50	572.56			23191.16	0.34	0.52	0.715	19.34
		14.219			153.28	2179.4612					
1.10	12.589		15.20	725.83			25370.62	0.38	0.58	0.615	19.59
		11.295			171.44	1936.2830					
1.00	10.000		16.90	897.27			27306.91	0.40	0.65	0.515	19.84
		8.972			64.84	581.7498					
0.90	7.943		17.50	962.11			27888.65	0.41	0.67	0.415	20.09
		7.126			208.10	1482.9788					
0.80	6.310		19.30	1170.21			29371.63	0.44	0.74	0.315	20.34
		5.661			378.09	2140.2551					
0.70	5.012		22.20	1548.30			31511.88	0.47	0.85	0.215	20.59
		4.496			186.64	839.2261					
0.60	3.981		23.50	1734.94			32351.11	0.48	0.90	0.115	20.84
		3.572			340.05	1214.5210					
0.50	3.162		25.70	2074.99			33565.62	0.50	0.99	0.015	21.09
		2.837			423.33	1201.0125					
0.40	2.512		28.20	2498.32			34766.64	0.52	1.08	-0.085	21.34
		2.254			943.64	2126.5452					
0.30	1.995		33.10	3441.96			36893.18	0.55	1.27	-0.185	21.59
		1.790			1360.94	2436.1636					
0.20	1.585		39.10	4802.89			39329.34	0.58	1.50	-0.285	21.84
		1.422			1815.84	2581.9404					
0.10	1.259		45.90	6618.73			41911.28	0.62	1.76	-0.385	22.09
		1.129			1298.20	1466.2615					
-0.00	1.000		50.20	7916.94			43377.54	0.64	1.93	-0.485	22.34
		0.897			2182.93	1958.4355					
-0.10	0.794		56.70	10099.87			45335.97	0.67	2.18	-0.585	22.59
		0.713			2848.63	2030.0437					
-0.20	0.631		64.20	12948.50			47366.01	0.70	2.46	-0.685	22.84
		0.566			3564.49	2017.7454					
-0.30	0.501		72.50	16513.00			49383.75	0.73	2.78	-0.785	23.09
		0.450			4303.06	1934.8467					
-0.40	0.398		81.40	20816.06			51318.60	0.76	3.13	-0.885	23.34
		0.357			5028.22	1795.9045					
-0.50	0.316		90.70	25844.28			53114.50	0.79	3.48	-0.985	23.59
		0.284			6776.78	1922.6162					
-0.60	0.251		101.90	32621.06			55037.11	0.82	3.91	-1.085	23.84
		0.225			8637.97	1946.6191					
-0.70	0.200		114.60	41259.03			56983.73	0.84	4.40	-1.185	24.09
		0.179			10615.73	1900.2874					
-0.80	0.158		128.50	51874.77			58884.02	0.87	4.93	-1.285	24.34
		0.142			13813.23	1964.1042					
-0.90	0.126		144.60	65688.00			60848.12	0.90	5.55	-1.385	24.59
		0.113			12937.37	1461.2205					
-1.00	0.100		158.20	78625.37			62309.34	0.92	6.07	-1.485	24.84
		0.090			11953.12	1072.3875					
-1.10	0.079		169.80	90578.50			63381.72	0.94	6.52	-1.585	25.09
		0.071			10644.37	758.5615					
-1.20	0.063		179.50	101222.87			64140.28	0.95	6.89	-1.685	25.34
		0.057			9105.94	515.4612					
-1.30	0.050		187.40	110328.81			64655.74	0.96	7.19	-1.785	25.59
		0.045			7421.06	333.6860					
-1.40	0.040		193.60	117749.87			64989.43	0.96	7.43	-1.885	25.84
		0.036			8542.94	305.1262					
-1.50	0.032		200.50	126292.81			65294.55	0.97	7.70	-1.985	26.09
		0.028			8061.25	228.7049					
-1.60	0.025		206.80	134354.06			65523.25	0.97	7.94	-2.085	26.34
		0.023			8846.81	199.3703					
-1.70	0.020		213.50	143200.87			65722.56	0.97	8.20	-2.185	26.59
		0.018			8437.75	151.0432					
-1.80	0.016		219.70	151638.62			65873.56	0.98	8.43	-2.285	26.84
		0.014			21413.12	304.4773					
-1.90	0.013		234.70	173051.75			66178.00	0.98	9.01	-2.385	27.09
		0.011			18303.37	206.7315					
-2.00	0.010		246.80	191355.12			66384.69	0.98	9.48	-2.485	27.34
-∞							67484.00	1.0			∞

PHOTOMETRIC PARAMETERS OF NGC 4374

B-FILTER

Total luminosity	L_T	= 18.75
Total apparent magnitude	m_T	= 10.27
Apparent central surface brightness	μ_o	= 17.51
Major axis at threshold	$2a_m$	= 8.03
Minor axis at threshold	$2b_m$	= 7.70
Major axis at μ=25.0 mag sec^{-2}	2a(25)	= 5.85
Luminosity within μ=25.0 mag sec^{-2}	k(25)	= 0.95
Gradient of exponential component	G(a)	= -0.61
Equivalent gradient of exponential comp.	G(r*)	= -0.49
Equivalent gradient of reduced exp. comp.	G(ρ)	= -0.26

Parameters at k = ¼ :

Semi-major axis	a_1	= 0.22
Axis ratio	b/a	= 0.92
Equivalent radius	r_1*	= 0.16
Surface brightness	μ_1	= 18.59

Parameters at k = ½(effective) :

Semi-major axis	a_e	= 0.57
Axis ratio	b/a	= 0.79
Equivalent radius	r_e*	= 0.43
Surface brightness	μ_e	= 21.09
Mean surface brightness	μ_e'	= 10.41

Parameters at k = ¾ :

Semi-major axis	a_3	= 1.43
Axis ratio	b/a	= 0.95
Equivalent radius	r_3*	= 1.30
Surface brightness	μ_3	= 23.26
Concentration indices	C_{21}	= 2.69
	C_{32}	= 3.00

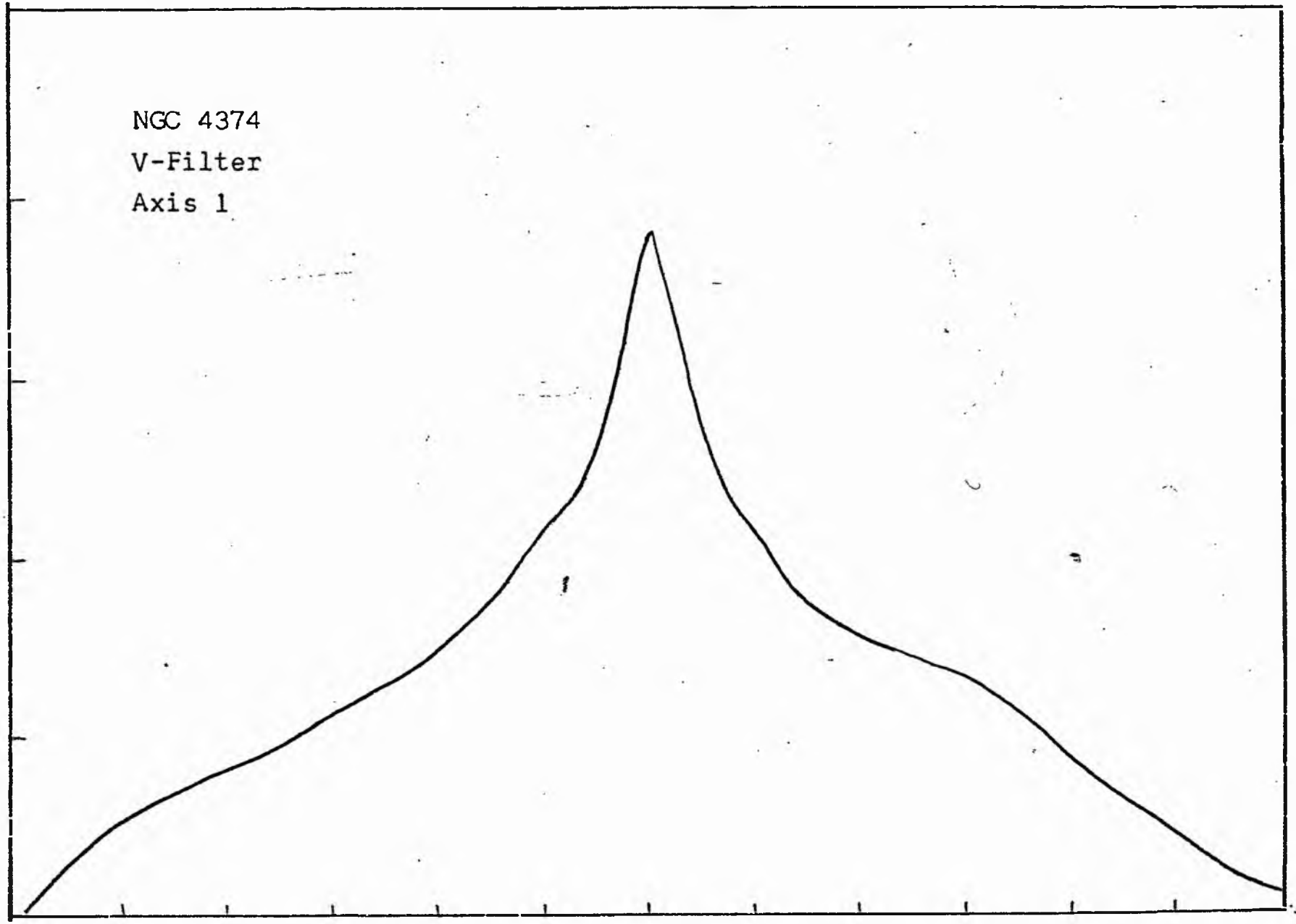
NGC 4374
V-Filter
Axis 1

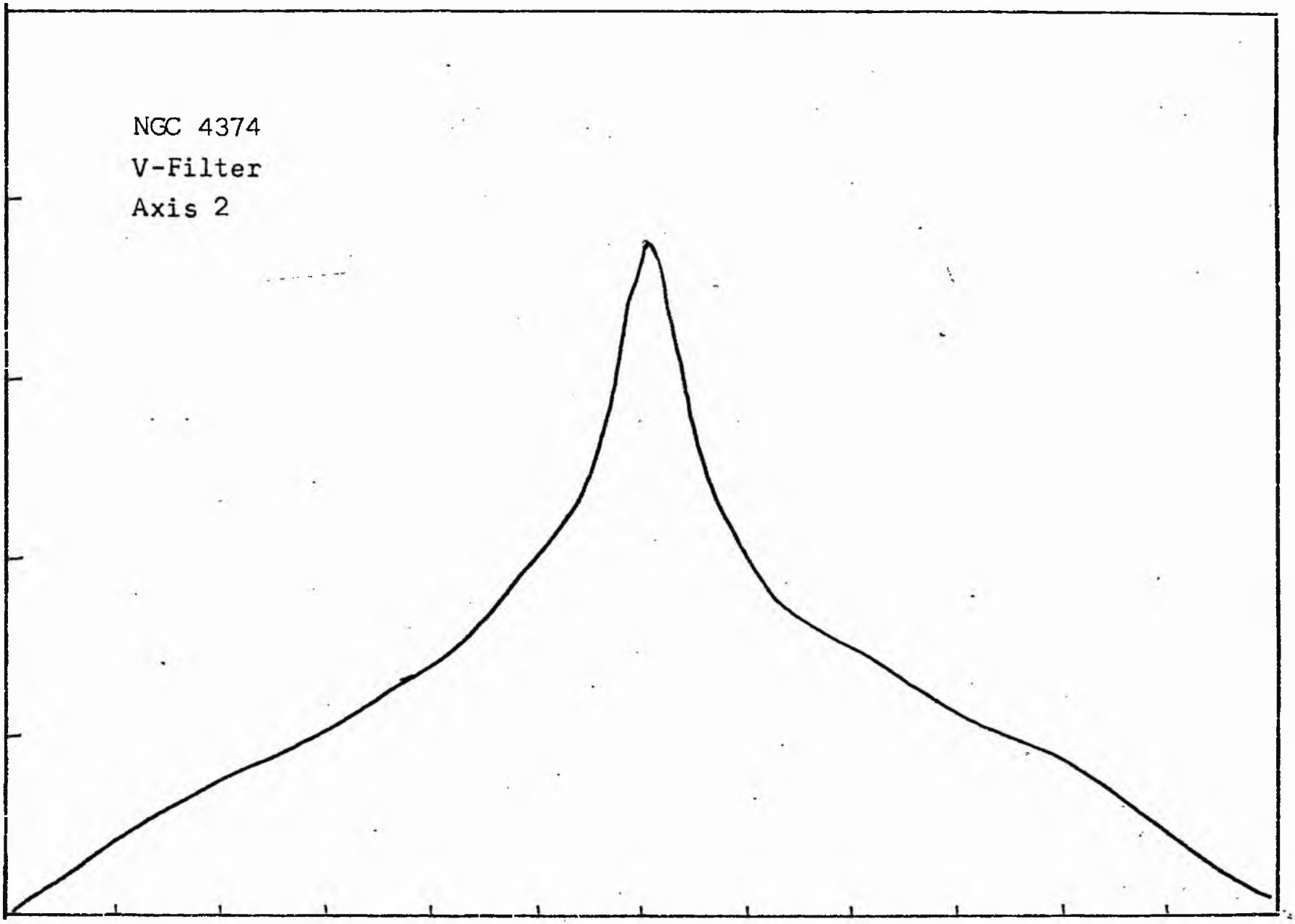
NGC 4374
V-Filter
Axis 2

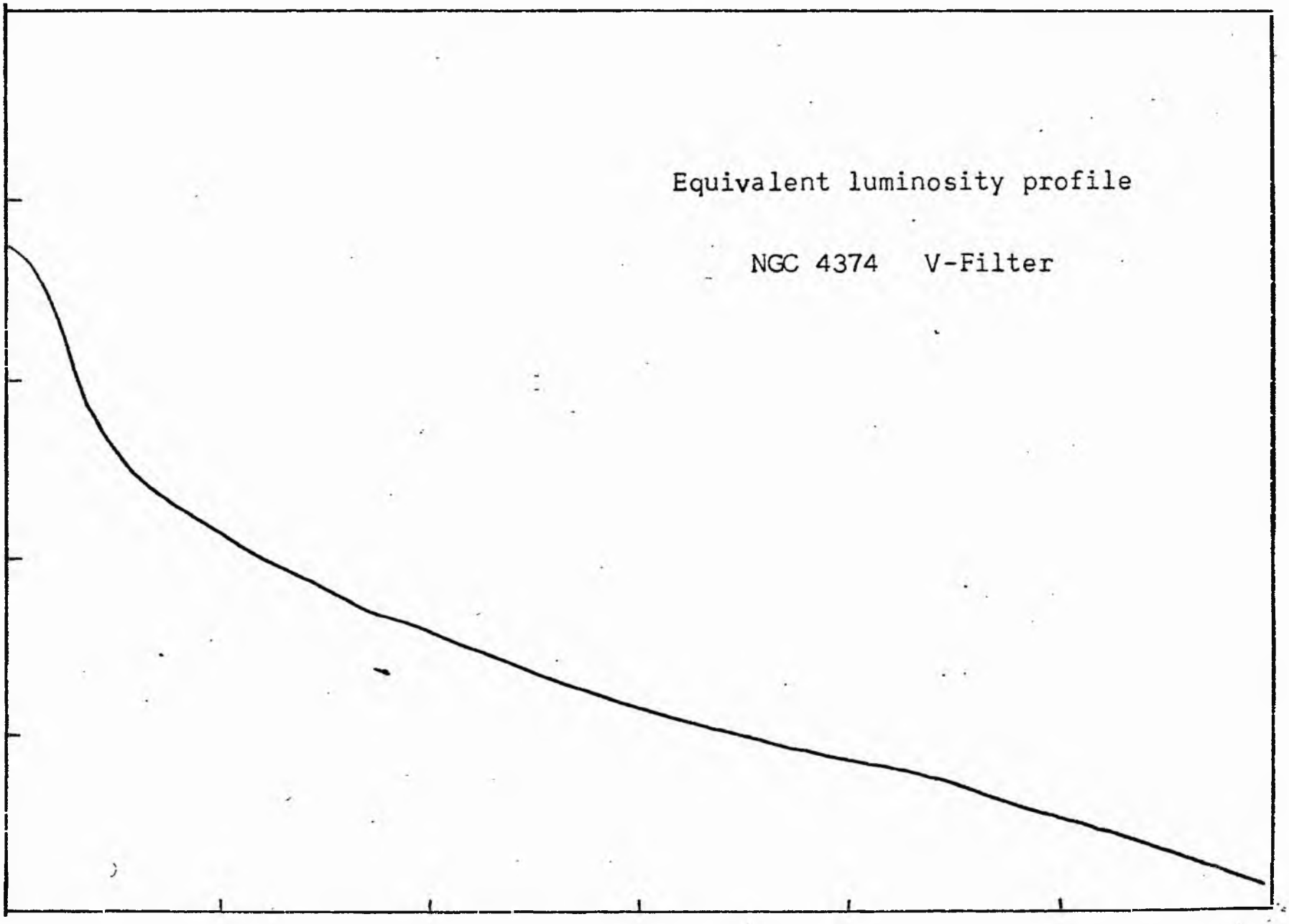
Equivalent luminosity profile
NGC 4374 V-Filter

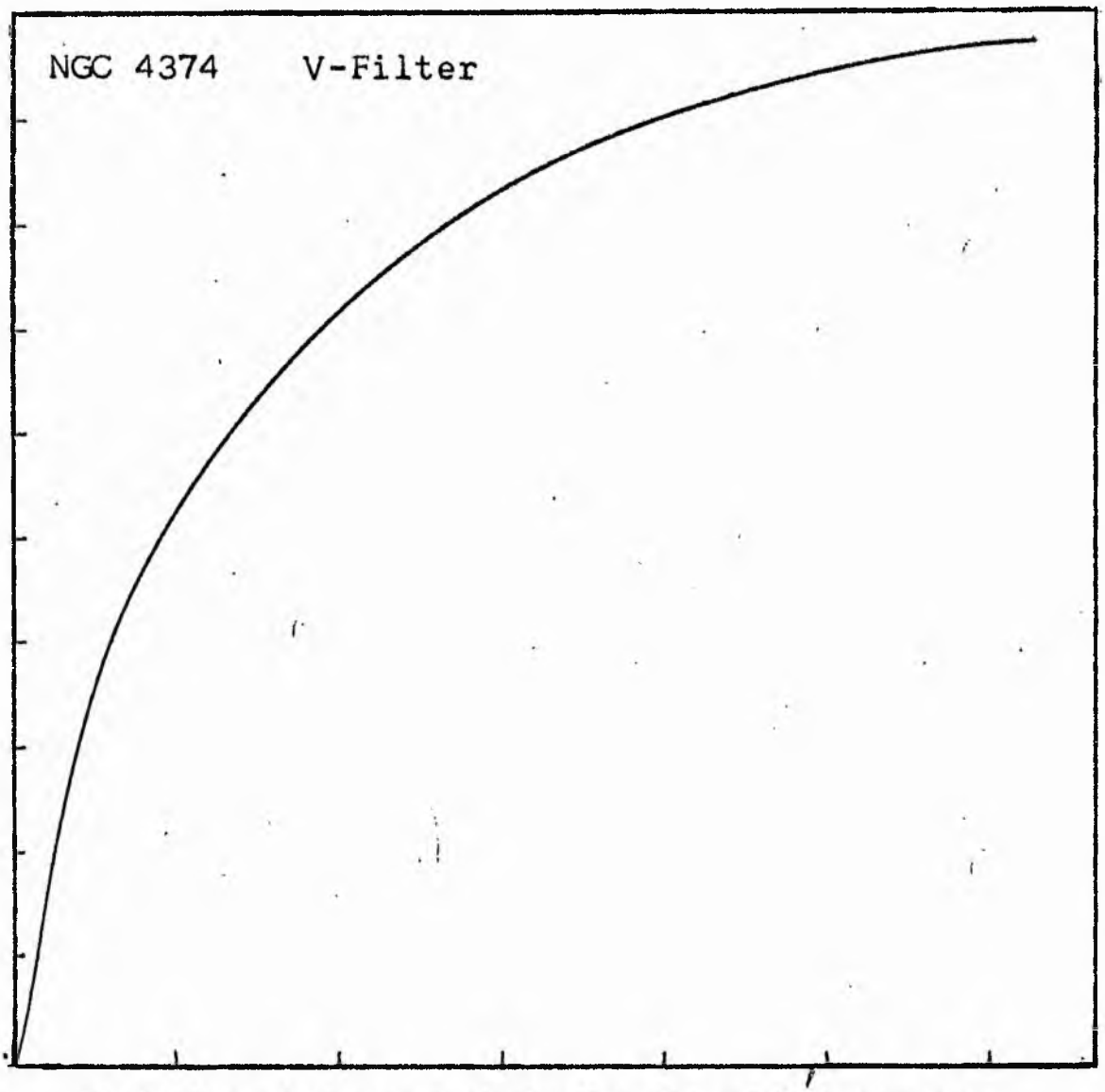

Relative integrated luminosity k(r) versus equivalent radius r*.

MEAN LUMINOSITY DISTRIBUTION IN NGC 4374
V COLOUR

LOG I	I	$\bar{I}$	R	AREA	ΔA	P	ΣP	K(R)	ρ	LOG J	μ
1.76	57.544		0.0	0.0			0.0	0.0	0.0	1.603	17.08
		53.831			0.50	27.0585					
1.70	50.119		0.40	0.50			27.06	0.00	0.01	1.543	17.23
		44.965			13.35	600.3574					
1.60	39.811		2.10	13.85			627.42	0.01	0.05	1.443	17.48
		35.717			74.39	2657.0657					
1.50	31.623		5.30	88.25			3284.48	0.04	0.12	1.343	17.73
		28.371			122.99	3489.4138					
1.40	25.119		8.20	211.24			6773.89	0.09	0.18	1.243	17.98
		22.536			303.48	6839.0664					
1.30	19.953		12.80	514.72			13612.96	0.19	0.28	1.143	18.23
		17.901			220.70	3950.6301					
1.20	15.849		15.30	735.42			17563.59	0.24	0.34	1.043	18.48
		14.219			78.92	1122.0969					
1.10	12.589		16.10	814.33			18685.68	0.26	0.35	0.943	18.73
		11.295			118.32	1336.3945					
1.00	10.000		17.23	932.65			20022.08	0.27	0.38	0.843	18.98
		8.972			190.74	1711.2588					
0.90	7.943		18.91	1123.39			21733.34	0.30	0.42	0.743	19.23
		7.126			288.56	2056.4023					
0.80	6.310		21.20	1411.96			23789.74	0.33	0.47	0.643	19.48
		5.661			322.99	1828.3347					
0.70	5.012		23.50	1734.94			25618.07	0.35	0.52	0.543	19.73
		4.496			356.22	1601.7356					
0.60	3.981		25.80	2091.17			27219.80	0.37	0.57	0.443	19.98
		3.572			182.12	650.4680					
0.50	3.162		26.90	2273.29			27870.27	0.38	0.59	0.343	20.23
		2.837			668.37	1896.2187					
0.40	2.512		30.60	2941.66			29766.49	0.41	0.67	0.243	20.48
		2.254			1382.46	3115.4543					
0.30	1.995		37.10	4324.12			32881.94	0.45	0.82	0.143	20.73
		1.790			1430.77	2561.1826					
0.20	1.585		42.80	5754.89			35443.12	0.48	0.94	0.043	20.98
		1.422			1973.93	2806.7283					
0.10	1.259		49.60	7728.82			38249.85	0.52	1.09	-0.057	21.23
		1.129			2335.46	2637.8015					
-0.00	1.000		56.60	10064.28			40887.65	0.56	1.25	-0.157	21.48
		0.897			3828.63	3434.8909					
-0.10	0.794		66.50	13892.91			44322.54	0.61	1.46	-0.257	21.73
		0.713			4300.71	3064.8528					
-0.20	0.631		76.10	18193.61			47387.39	0.65	1.67	-0.357	21.98
		0.566			4079.14	2309.0752					
-0.30	0.501		84.20	22272.75			49696.46	0.68	1.85	-0.457	22.23
		0.450			4433.41	1993.4631					
-0.40	0.398		92.20	26706.16			51689.93	0.71	2.03	-0.557	22.48
		0.357			6300.20	2250.2151					
-0.50	0.316		102.50	33006.36			53940.14	0.74	2.26	-0.657	22.73
		0.284			8252.67	2341.3413					
-0.60	0.251		114.60	41259.03			56281.48	0.77	2.52	-0.757	22.98
		0.225			9252.23	2085.0518					
-0.70	0.200		126.80	50511.27			58366.53	0.80	2.79	-0.857	23.23
		0.179			10012.88	1792.3765					
-0.80	0.158		138.80	60524.15			60158.91	0.82	3.05	-0.957	23.48
		0.142			11963.73	1701.1270					
-0.90	0.126		151.90	72487.87			61860.03	0.85	3.34	-1.057	23.73
		0.113			13769.19	1555.1733					
-1.00	0.100		165.70	86257.06			63415.20	0.87	3.65	-1.157	23.98
		0.090			18262.94	1638.4822					
-1.10	0.079		182.40	104520.00			65053.68	0.89	4.01	-1.257	24.23
		0.071			24559.50	1750.2131					
-1.20	0.063		202.70	129079.50			66803.87	0.91	4.46	-1.357	24.48
		0.057			18582.37	1051.8975					
-1.30	0.050		216.80	147661.87			67855.75	0.93	4.77	-1.457	24.73
		0.045			19831.50	891.7197					
-1.40	0.040		230.90	167493.37			68747.44	0.94	5.08	-1.557	24.98
		0.036			23861.75	852.2673					
-1.50	0.032		246.80	191355.12			69599.69	0.95	5.43	-1.657	25.23
		0.028			22161.44	628.7417					
-1.60	0.025		260.70	213516.56			70228.37	0.96	5.74	-1.757	25.48
		0.023			21653.25	487.9753					
-1.70	0.020		273.60	235169.81			70716.31	0.97	6.02	-1.857	25.73
		0.018			26493.06	474.2500					
-1.80	0.016		288.60	261662.87			71190.56	0.97	6.35	-1.957	25.98
		0.014			20515.00	291.7073					
-1.90	0.013		299.70	282177.87			71482.25	0.98	6.59	-2.057	26.23
		0.011			17590.12	198.6760					
-2.00	0.010		308.90	299768.00			71680.87	0.98	6.80	-2.157	26.48
- ∞							73130.00	(1)			∞

PHOTOMETRIC PARAMETERS OF NGC 4374

V-FILTER

Total luminosity	L_T	= 20.31
Total apparent magnitude	m_T	= 9.33
Apparent central surface brightness	μ_o	= 17.08
Major axis at threshold	$2a_m$	= 10.20
Minor axis at threshold	$2b_m$	= 10.12
Major axis at μ=25.0 mag sec^{-2}	2a(25)	= 7.72
Luminosity within μ=25.0 mag sec^{-2}	k(25)	= 0.94
Gradient of exponential component	G(a)	= -0.50
Equivalent gradient of exponential comp.	G(r*)	= -0.43
Equivalent gradient of reduced exp. comp.	G(ρ)	= -0.31
Parameters at k = ¼ :		
Semi-major axis	a_1	= 0.28
Axis ratio	b/a	= 1.05
Equivalent radius	r_1*	= 0.26
Surface brightness	μ_1	= 18.61
Parameters at k = ½(effective) :		
Semi-major axis	a_e	= 0.83
Axis ratio	b/a	= 0.90
Equivalent radius	r_e*	= 0.76
Surface brightness	μ_e	= 21.10
Mean surface brightness	μ_e'	= 10.78
Parameters at k = ¾ :		
Semi-major axis	a_3	= 1.80
Axis ratio	b/a	= 0.88
Equivalent radius	r_3*	= 1.78
Surface brightness	μ_3	= 22.81
Concentration indices	C_{21}	= 2.88
	C_{32}	= 2.35

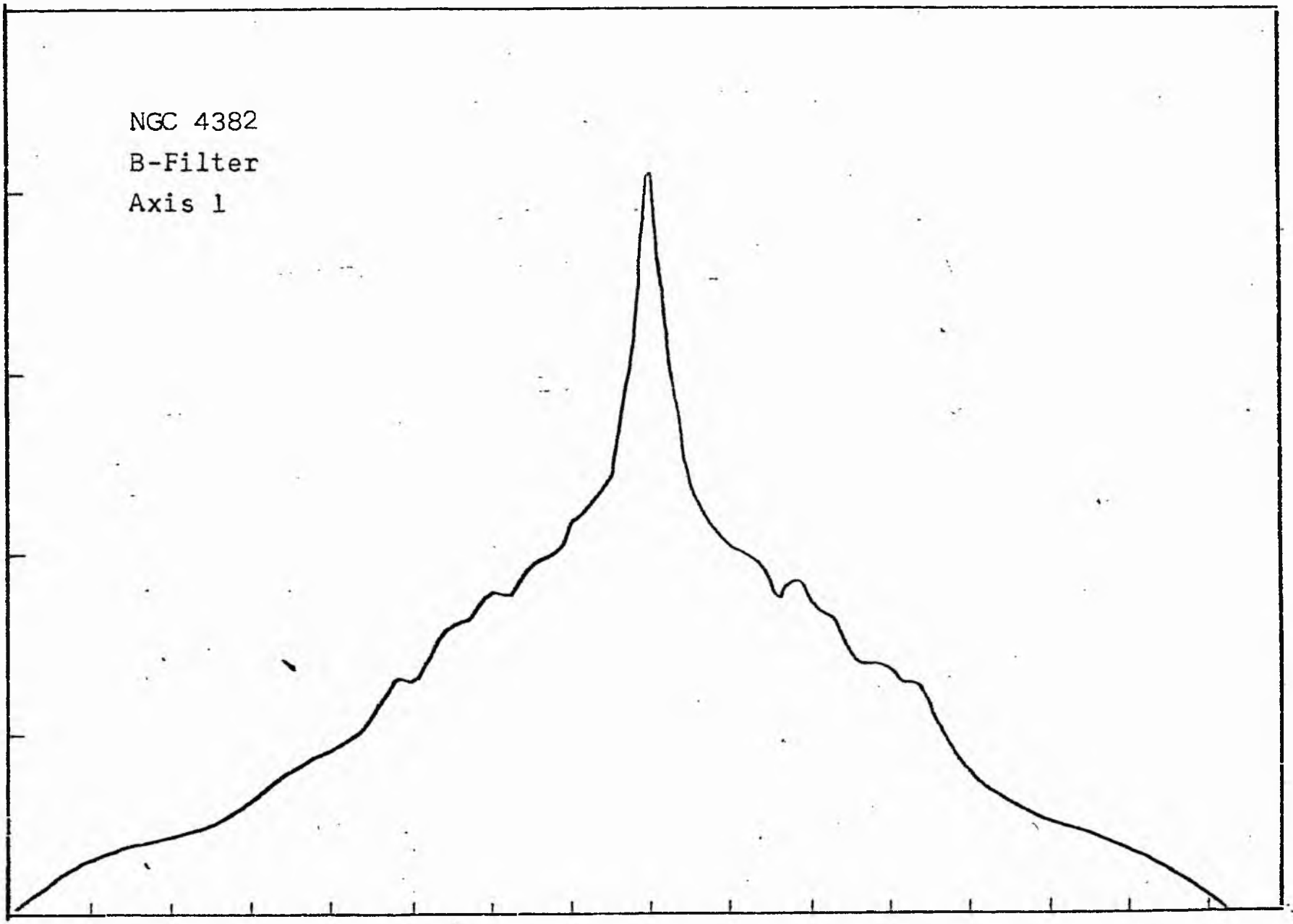
NGC 4382
B-Filter
Axis 1

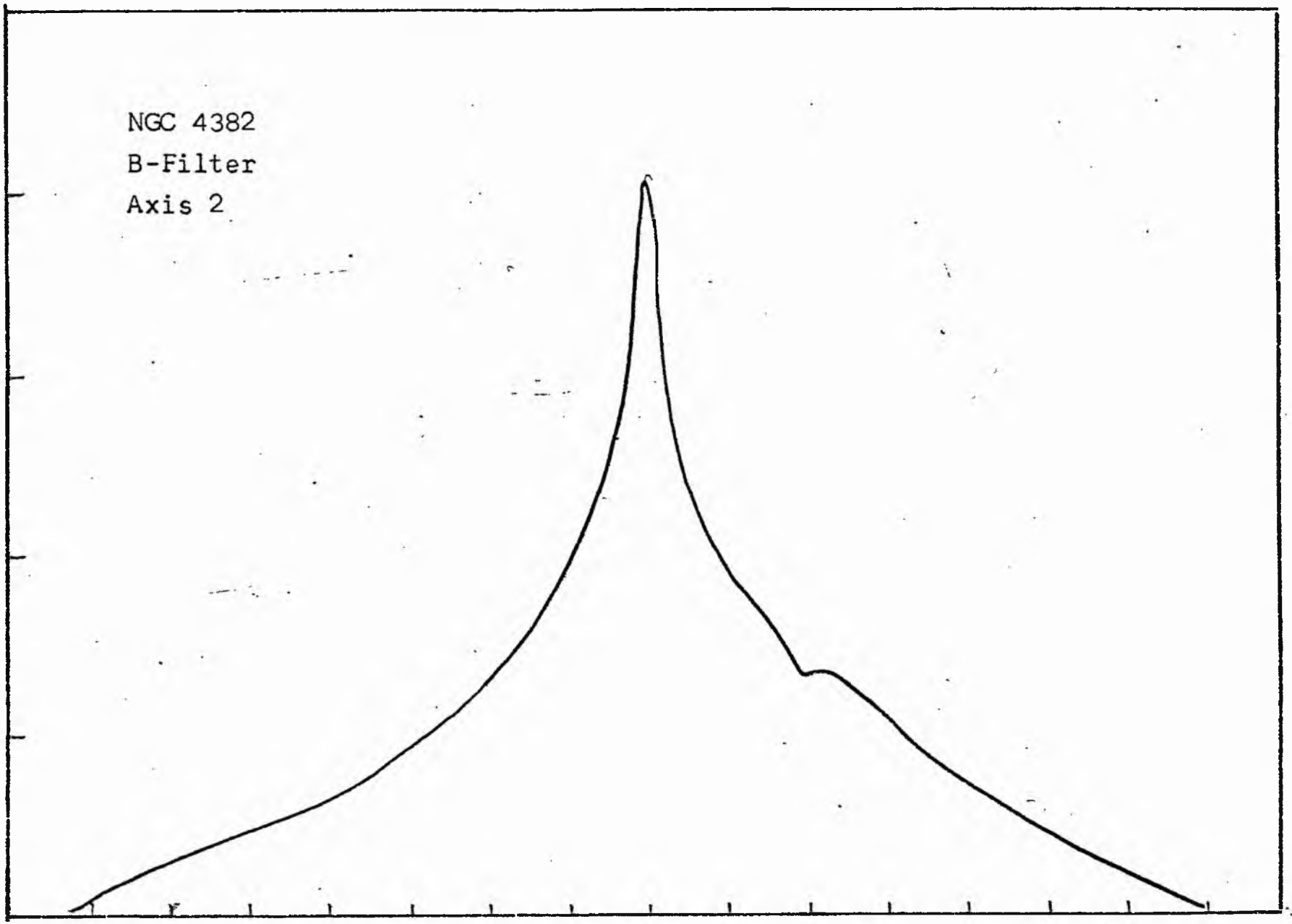
NGC 4382
B-Filter
Axis 2

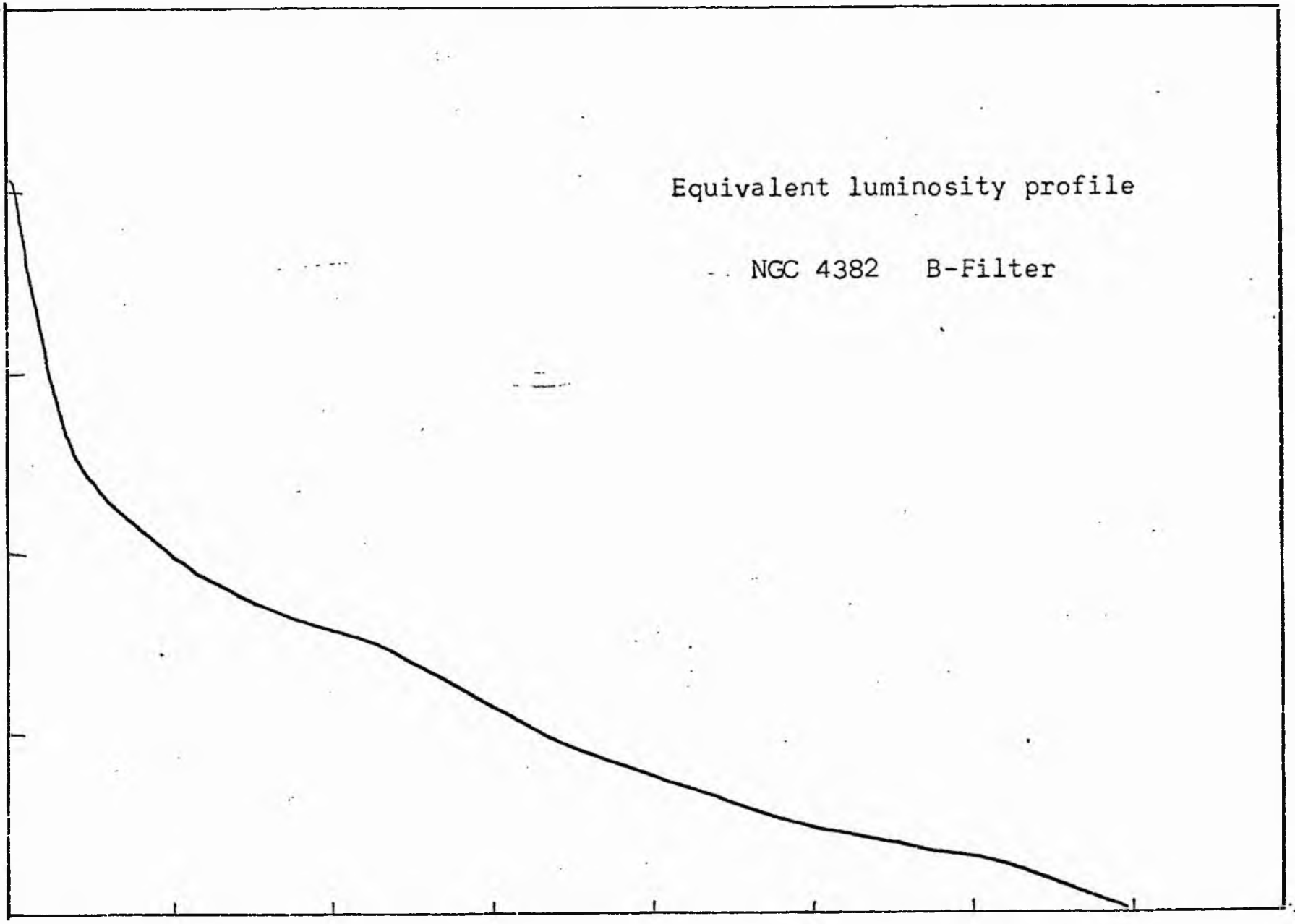
Equivalent luminosity profile
NGC 4382 B-Filter

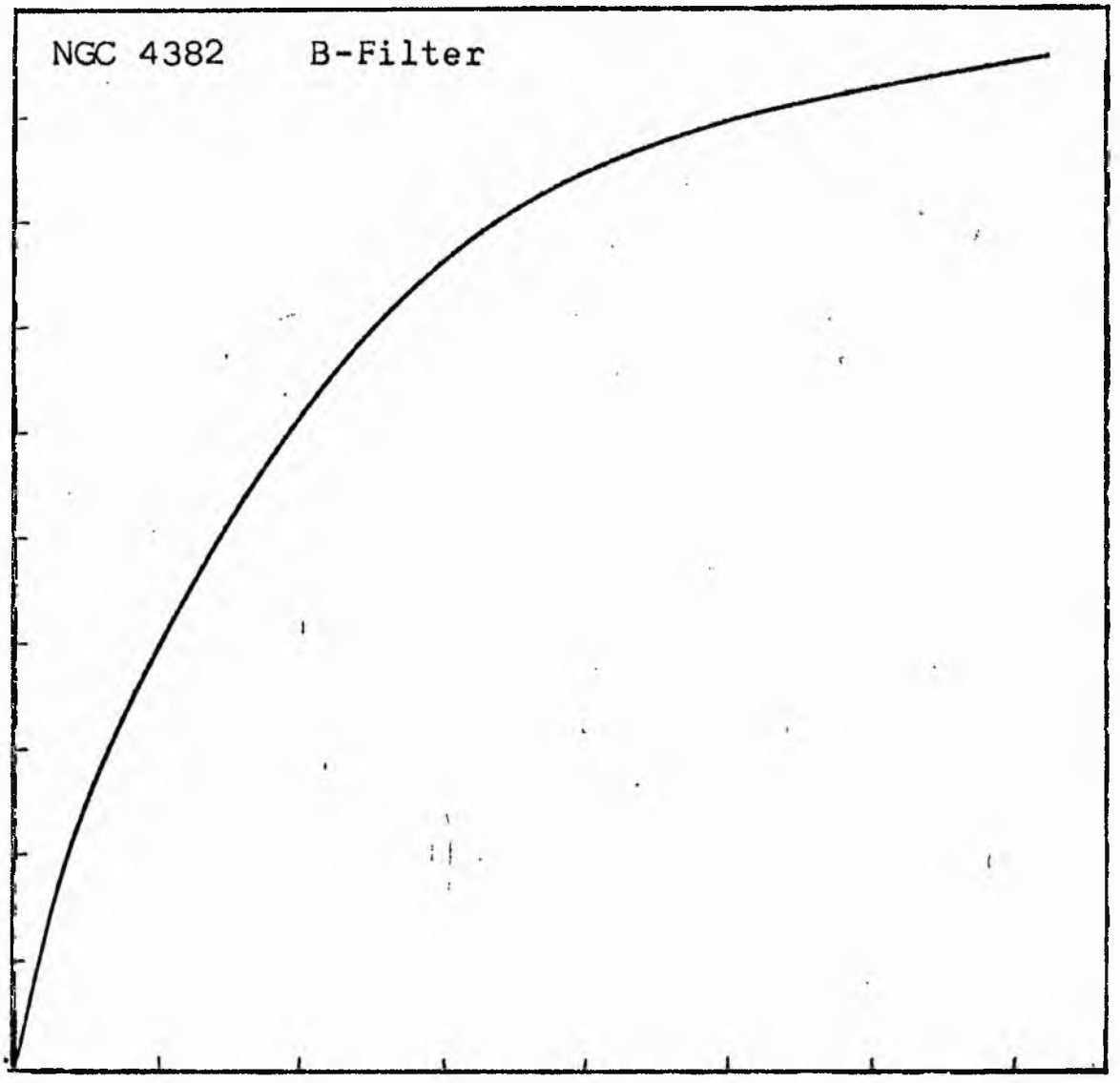

Relative integrated luminosity k(r) versus equivalent radius r*.

MEAN LUMINOSITY DISTRIBUTION IN NGC 4382
B COLOUR

LOG I	I	$\bar{I}$	A	AREA	ΔA	P	ΣP	K(R)	ρ	LOG J	μ
2.09	123.027		0.0	0.0			0.0	0.0	0.0	2.337	16.79
		111.513			2.54	283.7666					
2.00	100.000		0.90	2.54			283.77	0.00	0.01	2.247	17.02
		89.716			7.63	684.8999					
1.90	79.433		1.80	10.18			968.67	0.02	0.03	2.147	17.27
		71.264			14.45	1029.8608					
1.80	63.096		2.80	24.63			1998.53	0.03	0.04	2.047	17.52
		56.607			16.08	910.5227					
1.70	50.119		3.60	40.72			2909.05	0.05	0.05	1.947	17.77
		44.965			20.68	1289.7068					
1.60	39.811		4.70	69.40			4198.75	0.07	0.07	1.847	18.02
		35.717			31.24	1115.9648					
1.50	31.623		5.66	100.64			5314.72	0.09	0.08	1.747	18.27
		28.371			34.96	991.9441					
1.40	25.119		6.57	135.61			6306.66	0.10	0.09	1.647	18.52
		22.536			66.46	1497.7607					
1.30	19.952		8.02	202.07			7804.42	0.13	0.11	1.547	18.77
		17.901			23.31	417.3022					
1.20	15.849		8.47	225.38			8221.72	0.13	0.12	1.447	19.02
		14.219			25.15	357.5413					
1.10	12.589		8.93	250.53			8579.26	0.14	0.13	1.347	19.27
		11.295			59.52	627.0518					
1.00	10.000		9.87	306.04			9206.31	0.15	0.14	1.247	19.52
		0.972			153.92	1300.8696					
0.90	7.943		12.10	459.96			10587.18	0.17	0.17	1.147	19.77
		7.126			164.62	1173.1382					
0.80	6.310		14.10	624.58			11760.31	0.19	0.20	1.047	20.02
		5.661			190.76	1079.8442					
0.70	5.012		16.11	815.34			12840.16	0.21	0.23	0.947	20.27
		4.496			310.43	1395.8291					
0.60	3.981		18.93	1125.77			14235.98	0.23	0.27	0.847	20.52
		3.572			145.99	521.4175					
0.50	3.162		20.12	1271.76			14757.40	0.24	0.29	0.747	20.77
		2.837			513.75	1457.5364					
0.40	2.512		23.84	1785.51			16214.93	0.27	0.34	0.647	21.02
		2.254			768.04	1730.8201					
0.30	1.995		28.51	2553.55			17945.75	0.29	0.41	0.547	21.27
		1.790			1078.13	1929.9285					
0.20	1.585		34.00	3631.68			19875.68	0.33	0.49	0.447	21.52
		1.422			1852.18	2633.6152					
0.10	1.259		41.78	5483.86			22509.29	0.37	0.60	0.347	21.77
		1.129			2111.53	2384.8743					
-0.00	1.000		49.17	7595.39			24894.16	0.41	0.70	0.247	22.02
		0.897			1838.93	1649.8132					
-0.10	0.794		54.80	9434.32			26543.97	0.44	0.78	0.147	22.27
		0.713			3594.98	2561.9165					
-0.20	0.631		64.40	13029.30			29105.89	0.48	0.92	0.047	22.52
		0.566			6329.98	3583.2004					
-0.30	0.501		78.50	19359.28			32689.09	0.54	1.12	-0.053	22.77
		0.450			6942.92	3121.8423					
-0.40	0.398		91.50	26302.20			35810.93	0.59	1.31	-0.153	23.02
		0.357			10954.60	3912.6018					
-0.50	0.316		100.90	37256.80			39723.53	0.65	1.56	-0.253	23.27
		0.284			11126.26	3156.5908					
-0.60	0.251		124.10	48383.06			42880.12	0.70	1.78	-0.353	23.52
		0.225			10066.14	2260.4656					
-0.70	0.200		136.40	58449.20			45148.58	0.74	1.95	-0.453	23.77
		0.179			6694.87	1198.4265					
-0.80	0.158		144.00	65144.07			46347.01	0.76	2.06	-0.553	24.02
		0.142			9361.93	1331.1731					
-0.90	0.126		154.00	74506.00			47678.18	0.78	2.21	-0.653	24.27
		0.113			9887.25	1116.7219					
-1.00	0.100		163.90	84393.25			48794.90	0.80	2.35	-0.753	24.52
		0.090			13363.56	1198.9263					
-1.10	0.079		176.40	97756.81			49993.82	0.82	2.53	-0.853	24.77
		0.071			17693.19	1260.8887					
-1.20	0.063		191.70	115450.00			51254.71	0.84	2.75	-0.953	25.02
		0.057			18514.56	1048.0566					
-1.30	0.050		206.50	133964.56			52302.77	0.86	2.96	-1.053	25.27
		0.045			17012.12	800.9172					
-1.40	0.040		219.80	151776.69			53103.68	0.87	3.15	-1.153	25.52
		0.036			28726.94	1026.0342					
-1.50	0.032		239.70	180503.62			54129.71	0.89	3.43	-1.253	25.77
		0.028			50099.44	1444.0627					
-1.60	0.025		271.40	231403.06			55573.77	0.91	3.89	-1.353	26.02
		0.023			52283.56	1178.2537					
-1.70	0.020		300.50	283686.62			56752.02	0.93	4.30	-1.453	26.27
		0.018			52240.75	935.1553					
-1.80	0.016		327.00	335927.37			57687.18	0.95	4.68	-1.553	26.52
		0.014			38217.06	543.4158					
-1.90	0.013		345.10	374144.44			58230.59	0.95	4.94	-1.653	26.77
		0.011			15996.44	180.6753					
-2.00	0.010		352.40	390140.87			58411.26	0.96	5.05	-1.753	27.02
$-\infty$							61011.00	(1)			∞

PHOTOMETRIC PARAMETERS OF NGC 4382

B-FILTER

Total luminosity ..... L_T = 16.95

Total apparent magnitude ..... m_T = 9.98

Apparent central surface brightness ..... μ_o = 16.79

Major axis at threshold ..... $2a_m$ = 12.83

Minor axis at threshold ..... $2b_m$ = 10.64

Major axis at μ=25.0 mag sec^{-2} ..... $2a(25)$ = 6.85

Luminosity within μ=25.0 mag sec^{-2} ..... $k(25)$ = 0.84

Gradient of exponential component ..... $G(a)$ = -0.46

Equivalent gradient of exponential comp. ..... $G(r^*)$ = -0.43

Equivalent gradient of reduced exp. comp. ..... $G(\rho)$ = -0.63

Parameters at k = ¼ :

- Semi-major axis ..... a_1 = 0.40
- Axis ratio ..... b/a = 0.96
- Equivalent radius ..... r_1^* = 0.36
- Surface brightness ..... μ_1 = 20.84

Parameters at k = ½(effective) :

- Semi-major axis ..... a_e = 1.57
- Axis ratio ..... b/a = 0.66
- Equivalent radius ..... r_e^* = 1.16
- Surface brightness ..... μ_e = 22.60
- Mean surface brightness ..... μ_e' = 12.30

Parameters at k = ¾ :

- Semi-major axis ..... a_3 = 2.55
- Axis ratio ..... b/a = 0.76
- Equivalent radius ..... r_3^* = 2.34
- Surface brightness ..... μ_3 = 23.89

Concentration indices ..... C_{21} = 3.27, C_{32} = 2.01

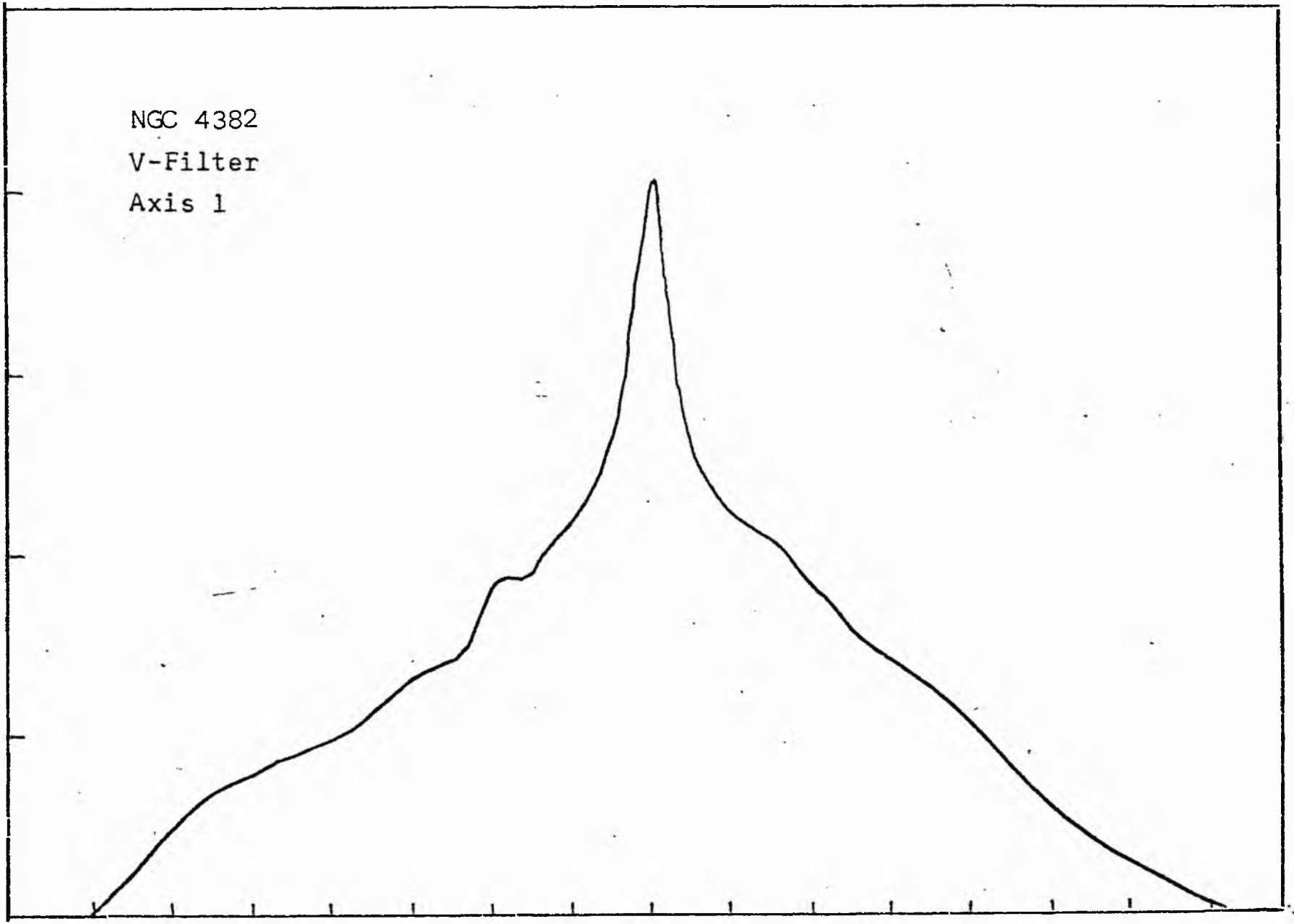
NGC 4382
V-Filter
Axis 1

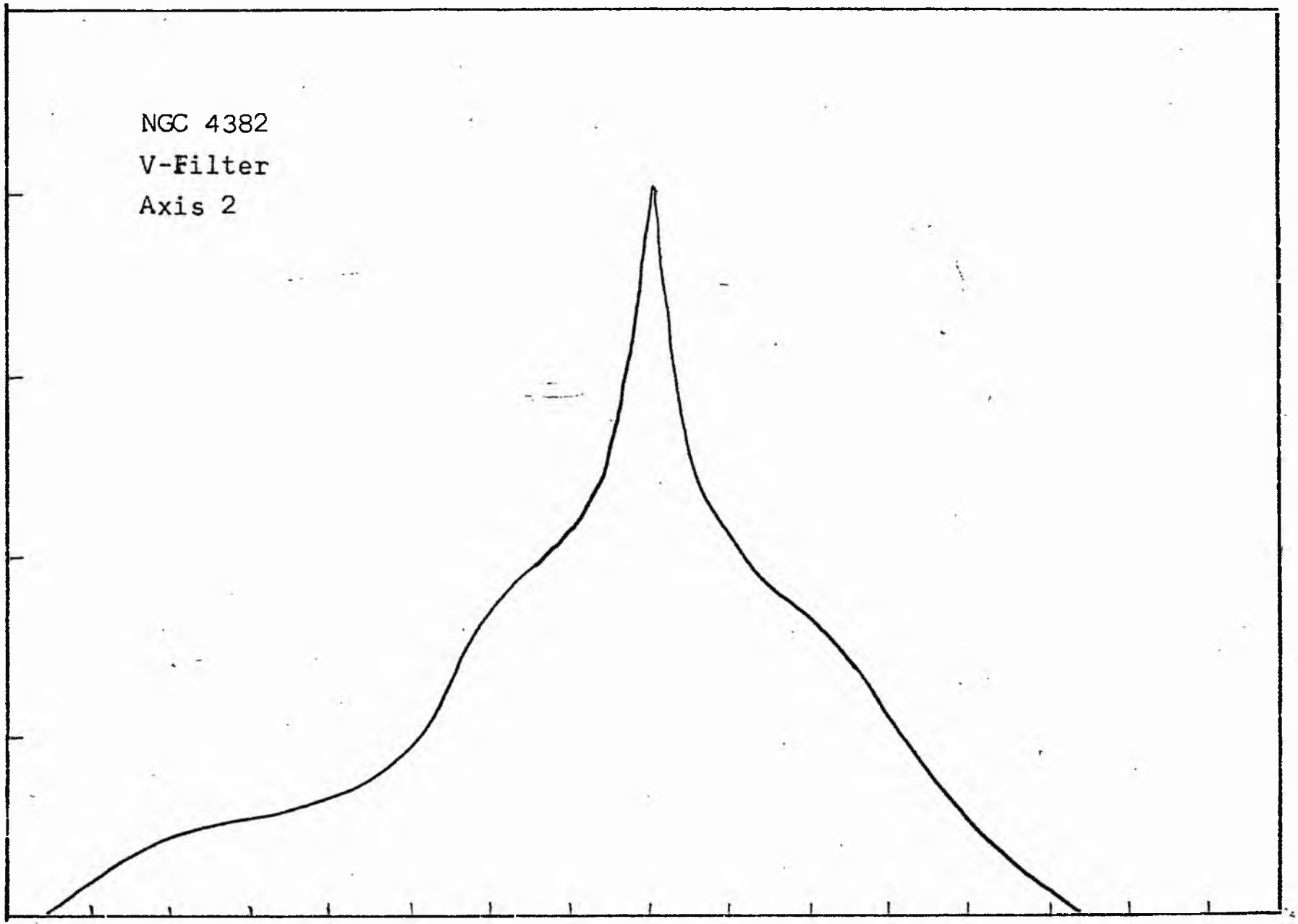
NGC 4382
V-Filter
Axis 2

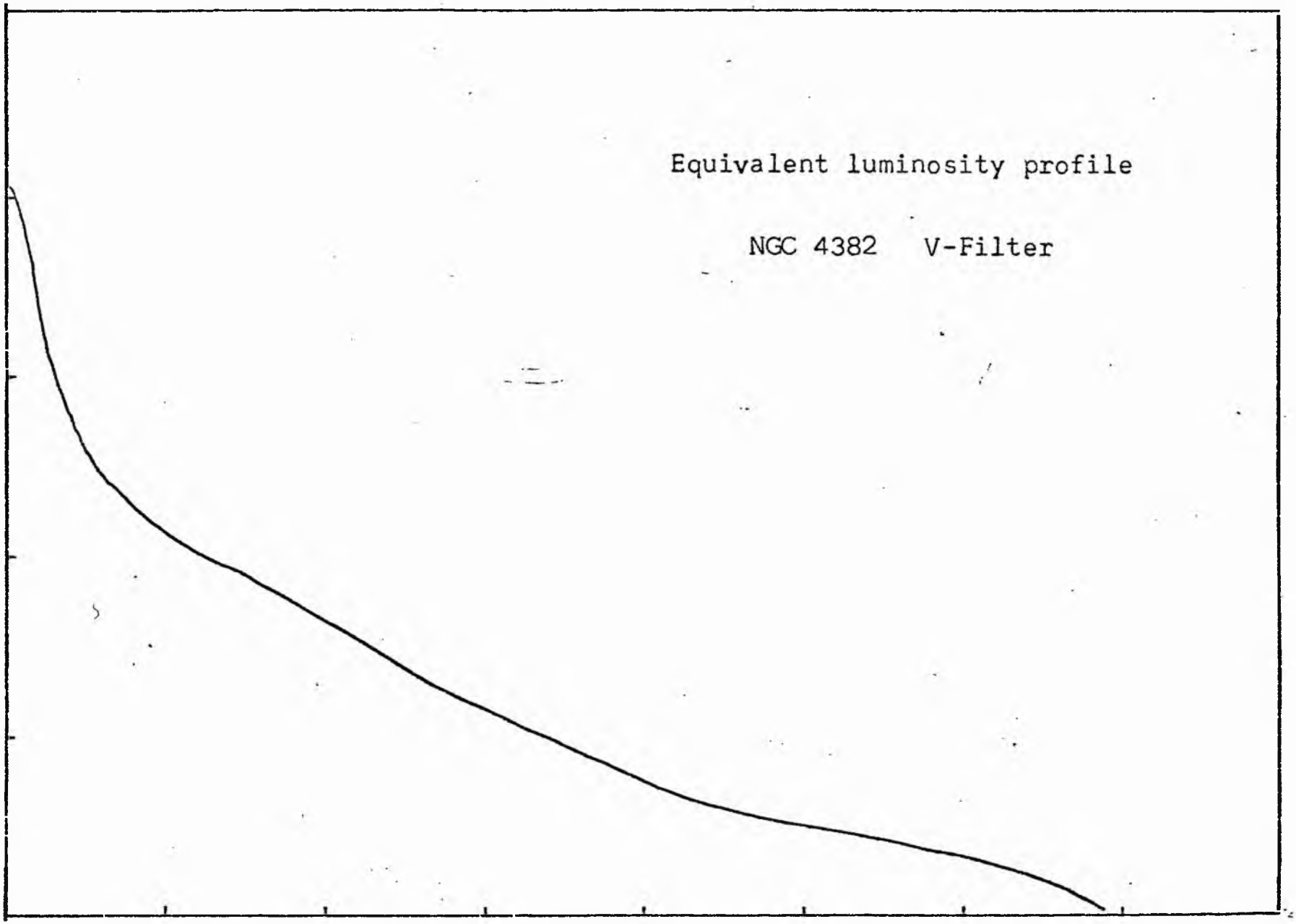
Equivalent luminosity profile
NGC 4382 V-Filter

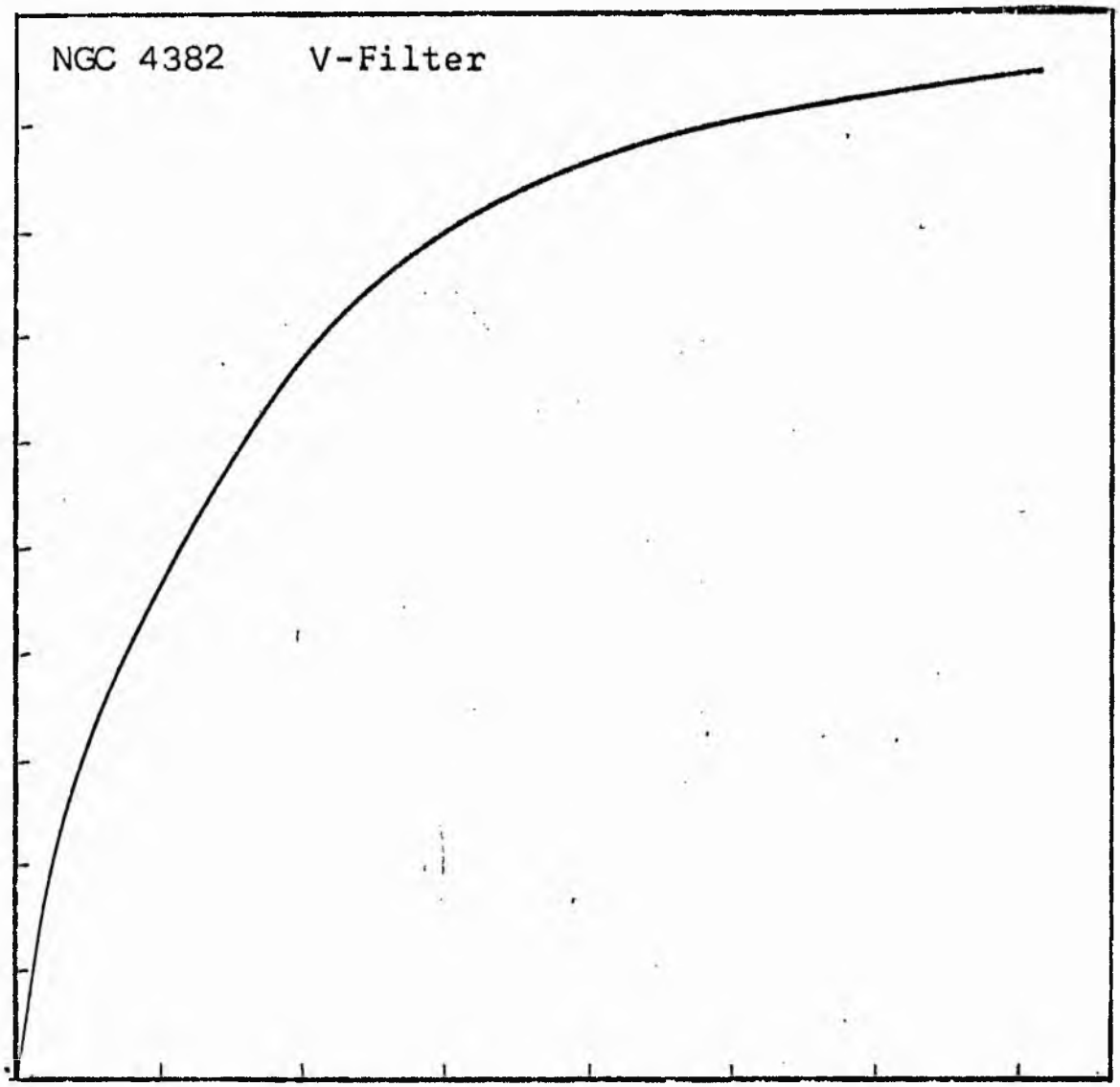

Relative integrated luminosity k(r) versus equivalent radius r*.

MEAN LUMINOSITY DISTRIBUTION IN NGC 4382
'V COLOUR

LOG I	I	$\bar{I}$	R	AREA	ΔA	P	ΣP	K(R)	ρ	LOG J	μ
2.08	120.226		0.0	0.0			0.0	0.0	0.0	2.037	16.28
		110.113			3.80	418.5754					
2.00	100.000		1.10	3.80			418.58	0.01	0.02	1.957	16.48
		89.716			12.82	1149.9556					
1.90	79.433		2.30	16.62			1568.53	0.02	0.04	1.857	16.73
		71.264			31.16	2220.9202					
1.80	63.096		3.90	47.78			3789.45	0.05	0.07	1.757	16.98
		56.607			30.76	1741.0186					
1.70	50.119		5.00	78.54			5530.47	0.07	0.09	1.657	17.23
		44.965			42.22	1898.5378					
1.60	39.811		6.20	120.76			7429.00	0.09	0.11	1.557	17.48
		35.717			73.32	2618.8665					
1.50	31.623		7.86	194.09			10047.87	0.12	0.14	1.457	17.73
		28.371			36.65	1039.7175					
1.40	25.119		8.57	230.73			11087.58	0.13	0.15	1.357	17.98
		22.536			118.93	2680.2275					
1.30	19.952		10.55	349.67			13767.81	0.17	0.18	1.257	18.23
		17.901			119.46	2138.4458					
1.20	15.849		12.22	469.13			15906.25	0.19	0.21	1.157	18.48
		14.219			106.82	1518.9312					
1.10	12.589		13.54	575.95			17425.18	0.21	0.24	1.057	18.73
		11.295			173.95	1964.7151					
1.00	10.000		15.45	749.91			19389.90	0.24	0.27	0.957	18.98
		8.972			194.69	1746.7041					
0.90	7.943		17.34	944.60			21136.60	0.26	0.30	0.857	19.23
		7.126			203.89	1452.9614					
0.80	6.310		19.12	1148.48			22589.56	0.27	0.33	0.757	19.48
		5.661			298.32	1688.6709					
0.70	5.012		21.46	1446.80			24278.23	0.29	0.37	0.657	19.73
		4.496			355.22	1597.2422					
0.60	3.981		23.95	1802.02			25875.47	0.31	0.42	0.557	19.98
		3.572			289.14	1032.7141					
0.50	3.162		25.80	2091.17			26908.18	0.33	0.45	0.457	20.23
		2.837			966.98	2743.3921					
0.40	2.512		31.20	3058.15			29651.57	0.36	0.54	0.357	20.48
		2.254			1305.68	2942.4365					
0.30	1.995		37.27	4363.84			32594.01	0.40	0.65	0.257	20.73
		1.790			1391.05	2490.0779					
0.20	1.585		42.80	5754.89			35084.08	0.43	0.74	0.157	20.98
		1.422			2545.07	3618.8269					
0.10	1.259		51.40	8299.96			38702.91	0.47	0.89	0.057	21.23
		1.129			3854.36	4353.3203					
-0.00	1.000		62.20	12154.32			43056.23	0.52	1.08	-0.043	21.48
		0.897			4404.26	3951.3135					
-0.10	0.794		72.60	16558.57			47007.54	0.57	1.26	-0.143	21.73
		0.713			4927.69	3511.6567					
-0.20	0.631		82.70	21486.26			50519.20	0.61	1.44	-0.243	21.98
		0.566			6568.95	3718.4707					
-0.30	0.501		94.50	28055.21			54237.66	0.66	1.64	-0.343	22.23
		0.450			8141.82	3660.9216					
-0.40	0.398		107.34	36197.03			57898.58	0.70	1.86	-0.443	22.48
		0.357			9890.30	3532.4707					
-0.50	0.316		121.12	46087.33			61431.05	0.74	2.10	-0.543	22.73
		0.284			5223.79	1482.0234					
-0.60	0.251		127.80	51311.12			62913.07	0.76	2.22	-0.643	22.98
		0.225			4679.13	1054.4707					
-0.70	0.200		133.50	55990.25			63967.54	0.78	2.32	-0.743	23.23
		0.179			9334.89	1671.0071					
-0.80	0.158		144.20	65325.14			65638.50	0.80	2.50	-0.843	23.48
		0.142			8794.30	1250.4612					
-0.90	0.126		153.60	74119.44			66888.94	0.81	2.67	-0.943	23.73
		0.113			24437.00	2760.0535					
-1.00	0.100		177.12	98556.44			69648.94	0.84	3.07	-1.043	23.98
		0.090			12751.81	1144.0425					
-1.10	0.079		188.23	111308.25			70792.94	0.86	3.27	-1.143	24.23
		0.071			17465.75	1244.6807					
-1.20	0.063		202.46	128774.00			72037.56	0.87	3.51	-1.243	24.48
		0.057			21487.37	1216.3391					
-1.30	0.050		218.70	150261.37			73253.87	0.89	3.80	-1.343	24.73
		0.045			27392.00	1231.6738					
-1.40	0.040		237.80	177653.37			74485.50	0.90	4.13	-1.443	24.98
		0.036			35208.19	1257.5237					
-1.50	0.032		260.30	212861.56			75743.00	0.92	4.52	-1.543	25.23
		0.028			43030.75	1220.8208					
-1.60	0.025		285.40	255892.31			76963.81	0.93	4.95	-1.643	25.48
		0.023			27039.12	619.3491					
-1.70	0.020		300.10	282931.44			77583.12	0.94	5.21	-1.743	25.73
		0.018			44219.12	791.5610					
-1.80	0.016		322.70	327150.56			78364.62	0.95	5.60	-1.843	25.98
		0.014			10628.19	151.1243					
-1.90	0.013		327.90	337778.75			78515.69	0.95	5.69	-1.943	26.23
		0.011			50151.00	566.4414					
-2.00	0.010		351.40	387929.75			79082.12	0.96	6.10	-2.043	26.48
- ∞							82482.00	(1)			∞

PHOTOMETRIC PARAMETERS OF NGC 4382

V-FILTER

Total luminosity	L_T	= 22.91
Total apparent magnitude	m_T	= 9.19
Apparent central surface brightness	μ_o	= 16.28
Major axis at threshold	$2a_m$	= 11.30
Minor axis at threshold	$2b_m$	= 10.62
Major axis at μ=25.0 mag sec^{-2}	2a(25)	= 8.72
Luminosity within μ=25.0 mag sec^{-2}	k(25)	= 0.90
Gradient of exponential component	G(a)	= -0.40
Equivalent gradient of exponential comp.	G(r*)	= -0.52
Equivalent gradient of reduced exp. comp.	G(ρ)	= -0.57
Parameters at k = ¼ :		
Semi-major axis	a_1	= 0.27
Axis ratio	b/a	= 1.05
Equivalent radius	r_1*	= 0.28
Surface brightness	μ_1	= 19.11
Parameters at k = ½(effective) :		
Semi-major axis	a_e	= 1.05
Axis ratio	b/a	= 0.89
Equivalent radius	r_e*	= 0.96
Surface brightness	μ_e	= 21.38
Mean surface brightness	μ_e'	= 11.05
Parameters at k = ¾ :		
Semi-major axis	a_3	= 2.45
Axis ratio	b/a	= 0.89
Equivalent radius	r_3*	= 2.05
Surface brightness	μ_3	= 22.85
Concentration indices	C_{21}	= 3.44
	C_{32}	= 2.14

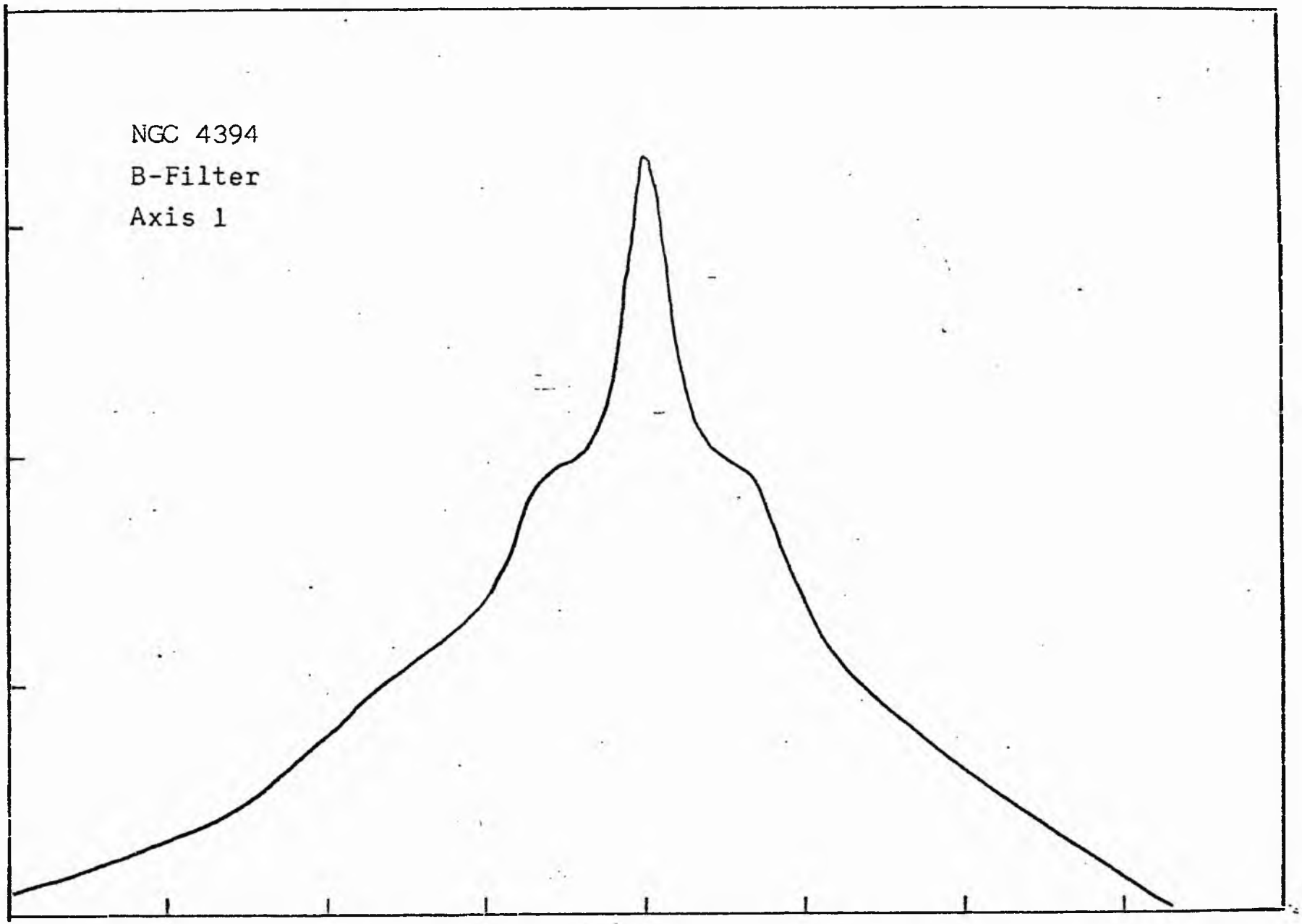
NGC 4394
B-Filter
Axis 1

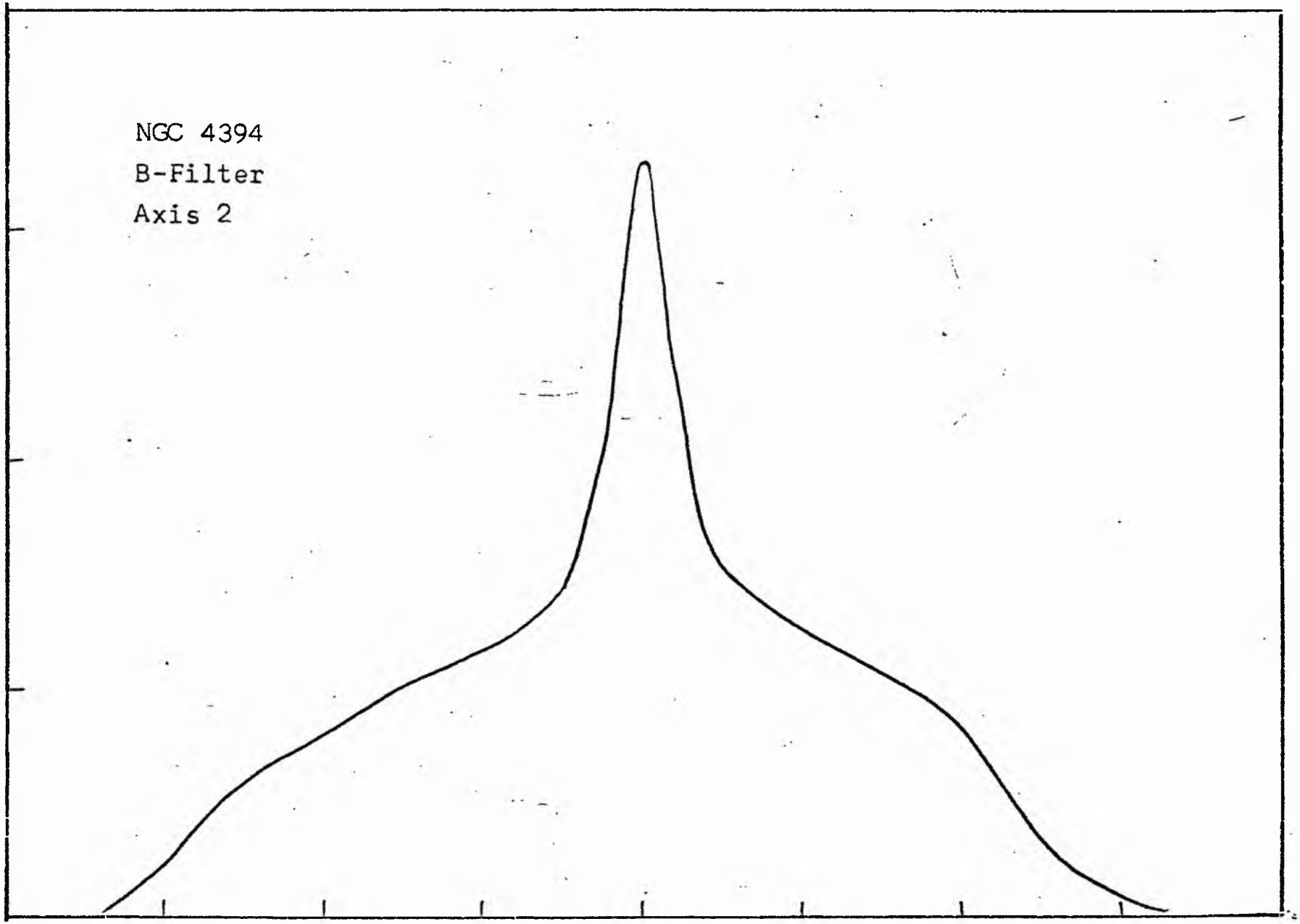
NGC 4394
B-Filter
Axis 2

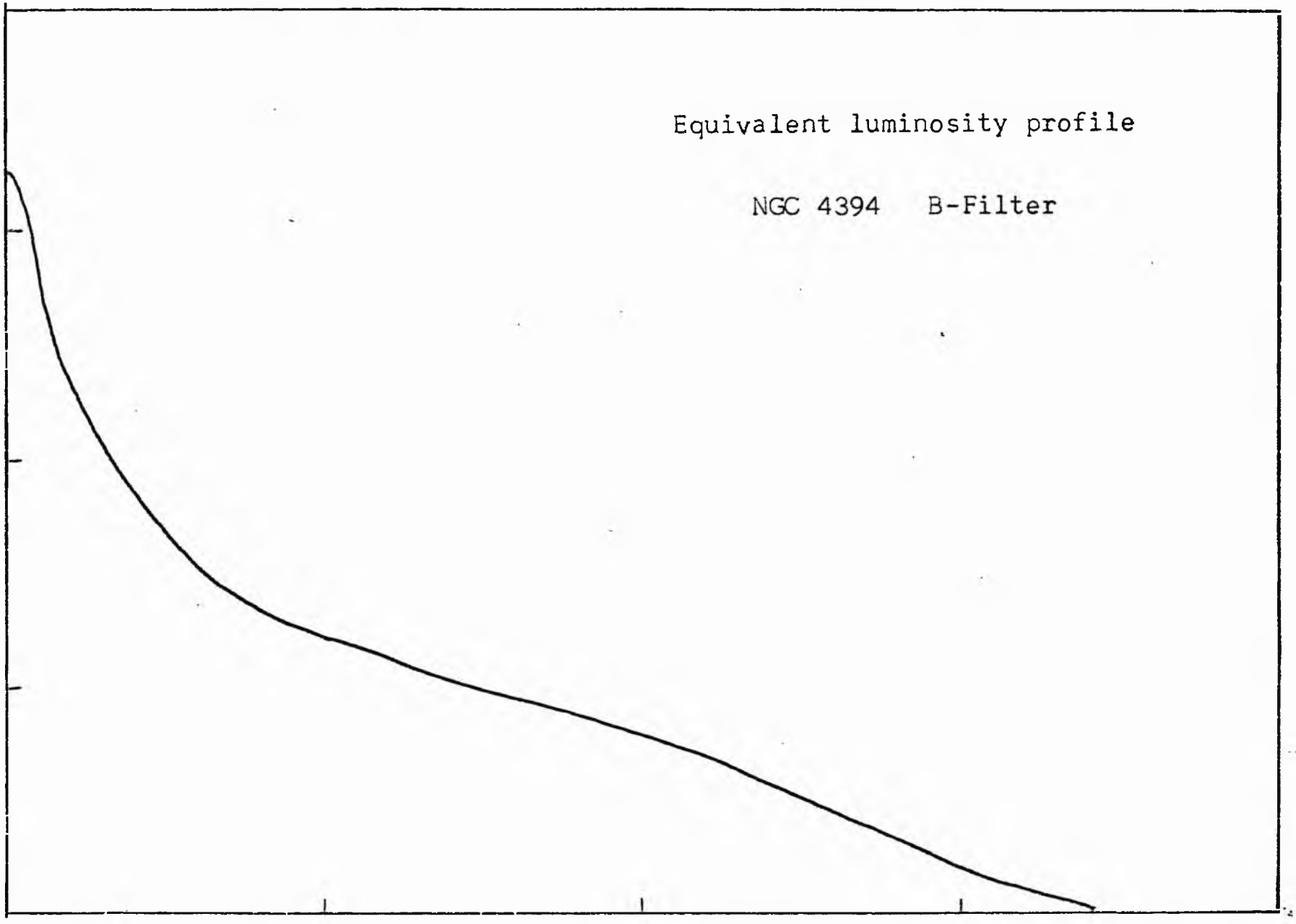
Equivalent luminosity profile
NGC 4394 B-Filter

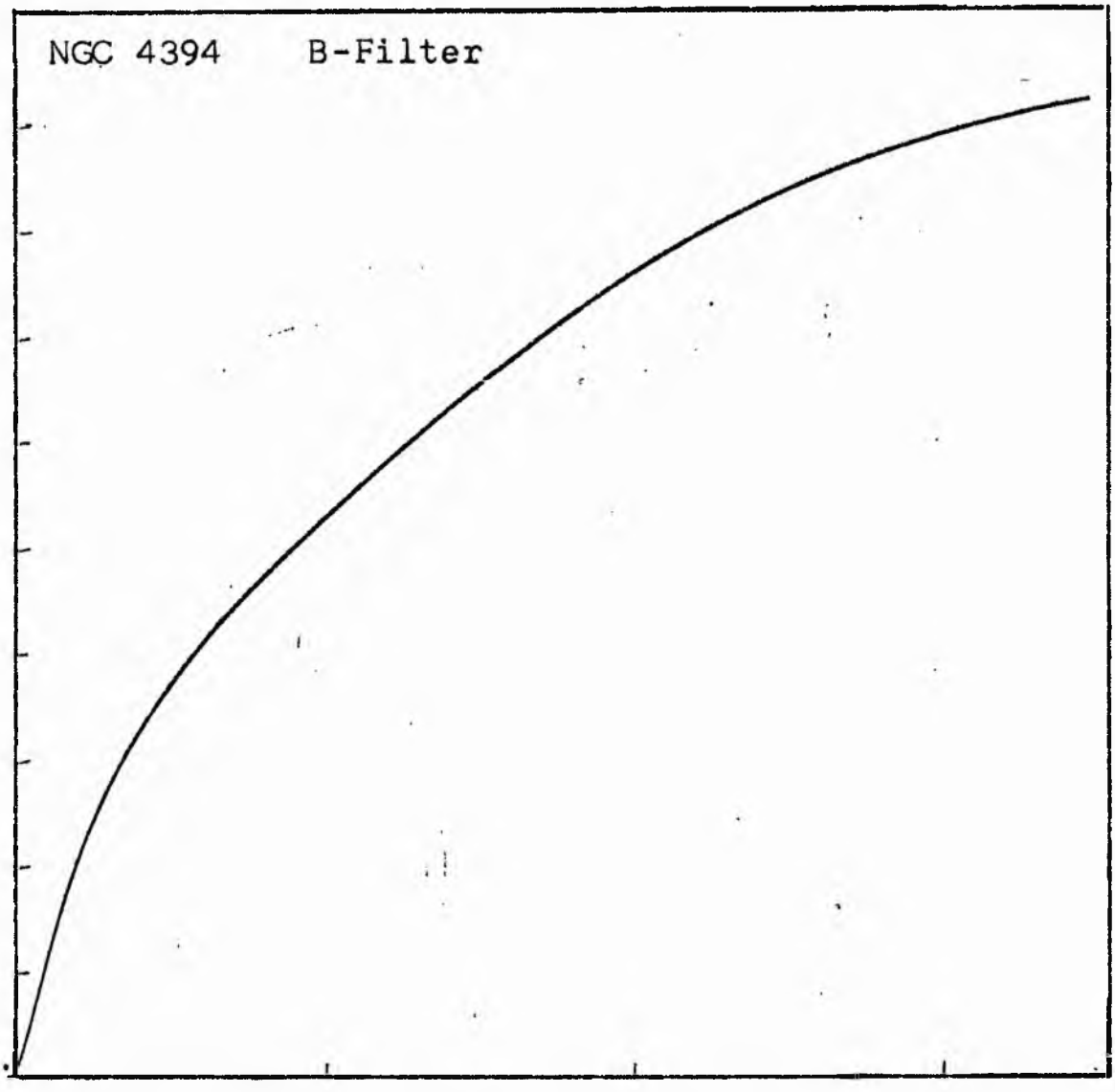

Relative integrated luminosity k(r) versus equivalent radius r*.

MEAN LUMINOSITY DISTRIBUTION IN NGC 4394
B COLOUR

LOG I	I	T	R	AREA	ΔA	P	ΣP	K(R)	ρ	LOG J	μ
1.28	19.055		0.0	0.0			0.0	0.0	0.0	2.037	18.26
		17.452			25.34	442.2065					
1.20	15.849		2.84	25.34			442.21	0.05	0.06	1.957	18.46
		14.219			15.38	218.6356					
1.10	12.589		3.60	40.72			660.84	0.07	0.08	1.857	18.71
		11.295			28.68	323.9600					
1.00	10.000		4.70	69.40			984.80	0.10	0.10	1.757	18.96
		8.972			18.85	169.1108					
0.90	7.943		5.30	88.25			1153.91	0.12	0.11	1.657	19.21
		7.126			17.44	124.2951					
0.80	6.310		5.80	105.68			1278.17	0.13	0.12	1.557	19.46
		5.661			15.08	85.3616					
0.70	5.012		6.20	120.76			1363.53	0.14	0.13	1.457	19.71
		4.496			37.60	169.0890					
0.60	3.981		7.10	158.37			1532.62	0.16	0.15	1.357	19.96
		3.572			39.69	141.7581					
0.50	3.162		7.94	198.06			1674.38	0.17	0.17	1.257	20.21
		2.837			56.98	161.6497					
0.40	2.512		9.01	255.03			1836.03	0.19	0.19	1.157	20.46
		2.254			90.01	202.8383					
0.30	1.995		10.48	345.04			2038.86	0.21	0.22	1.057	20.71
		1.790			165.66	296.5491					
0.20	1.585		12.75	510.71			2335.41	0.24	0.27	0.957	20.96
		1.422			198.98	282.9360					
0.10	1.259		15.03	709.69			2618.35	0.27	0.32	0.857	21.21
		1.129			230.56	260.4055					
-0.00	1.000		17.30	940.25			2878.75	0.29	0.37	0.757	21.46
		0.897			238.47	213.9454					
-0.10	0.794		19.37	1178.71			3092.70	0.32	0.41	0.657	21.71
		0.713			340.43	242.6066					
-0.20	0.631		21.99	1519.15			3335.31	0.34	0.47	0.557	21.96
		0.566			439.64	248.8656					
-0.30	0.501		24.97	1958.78			3584.17	0.37	0.53	0.457	22.21
		0.450			311.12	139.8958					
-0.40	0.398		26.88	2269.91			3724.07	0.38	0.57	0.357	22.46
		0.357			753.06	268.9678					
-0.50	0.316		31.02	3022.96			3993.04	0.41	0.66	0.257	22.71
		0.284			1093.90	310.3491					
-0.60	0.251		36.20	4116.87			4303.38	0.44	0.77	0.157	22.96
		0.225			1536.29	346.2141					
-0.70	0.200		42.42	5653.16			4649.59	0.48	0.91	0.057	23.21
		0.179			2841.71	508.6885					
-0.80	0.158		52.00	8494.87			5158.28	0.53	1.11	-0.043	23.46
		0.142			4292.79	610.3965					
-0.90	0.126		63.80	12787.66			5768.68	0.59	1.36	-0.143	23.71
		0.113			6032.86	681.3892					
-1.00	0.100		77.40	18820.52			6450.06	0.66	1.65	-0.243	23.96
		0.090			5785.22	519.0295					
-1.10	0.079		88.50	24605.74			6969.09	0.71	1.89	-0.343	24.21
		0.071			6371.89	454.0889					
-1.20	0.063		99.30	30977.62			7423.18	0.76	2.12	-0.443	24.46
		0.057			6828.57	386.5476					
-1.30	0.050		109.70	37806.20			7809.72	0.80	2.34	-0.543	24.71
		0.045			4832.29	217.2833					
-1.40	0.040		116.50	42638.48			8027.00	0.82	2.49	-0.643	24.96
		0.036			6684.79	238.7604					
-1.50	0.032		125.30	49323.28			8265.76	0.85	2.68	-0.743	25.21
		0.028			5748.09	163.0791					
-1.60	0.025		132.40	55071.36			8428.84	0.86	2.83	-0.843	25.46
		0.023			6679.91	150.5381					
-1.70	0.020		140.20	61751.27			8579.37	0.88	3.00	-0.943	25.71
		0.018			8652.04	154.8798					
-1.80	0.016		149.70	70403.31			8734.25	0.89	3.20	-1.043	25.96
		0.014			13578.50	193.0761					
-1.90	0.013		163.50	83981.81			8927.33	0.91	3.49	-1.143	26.21
		0.011			12009.62	135.6459					
-2.00	0.010		174.80	95991.44			9062.97	0.93	3.73	-1.243	26.46
-∞							9772.00	(1)			∞

PHOTOMETRIC PARAMETERS OF NGC 4394

B-FILTER

Total luminosity ..... L_T = 2.71

Total apparent magnitude ..... m_T = 11.48

Apparent central surface brightness ..... μ_o = 18.26

Major axis at threshold ..... $2a_m$ = 6.13

Minor axis at threshold ..... $2b_m$ = 5.56

Major axis at μ=25.0 mag sec^{-2} ..... $2a(25)$ = 4.03

Luminosity within μ=25.0 mag sec^{-2} ..... $k(25)$ = 0.84

Gradient of exponential component ..... $G(a)$ = -0.96

Equivalent gradient of exponential comp..... $G(r^*)$ = -0.65

Equivalent gradient of reduced exp. comp..... $G(\rho)$ = -0.50

Parameters at k = ¼ :

- Semi-major axis ..... a_1 = 0.23
- Axis ratio ..... b/a = 0.94
- Equivalent radius ..... r_1^* = 0.23
- Surface brightness ..... μ_1 = 21.04

Parameters at k = ½(effective) :

- Semi-major axis ..... a_e = 1.08
- Axis ratio ..... b/a = 0.62
- Equivalent radius ..... r_e^* = 0.78
- Surface brightness ..... μ_e = 23.31
- Mean surface brightness ..... μ_e' = 12.93

Parameters at k = ¾ :

- Semi-major axis ..... a_3 = 1.56
- Axis ratio ..... b/a = 1.04
- Equivalent radius ..... r_3^* = 1.62
- Surface brightness ..... μ_3 = 24.40

Concentration indices ..... C_{21} = 3.44, C_{32} = 2.07

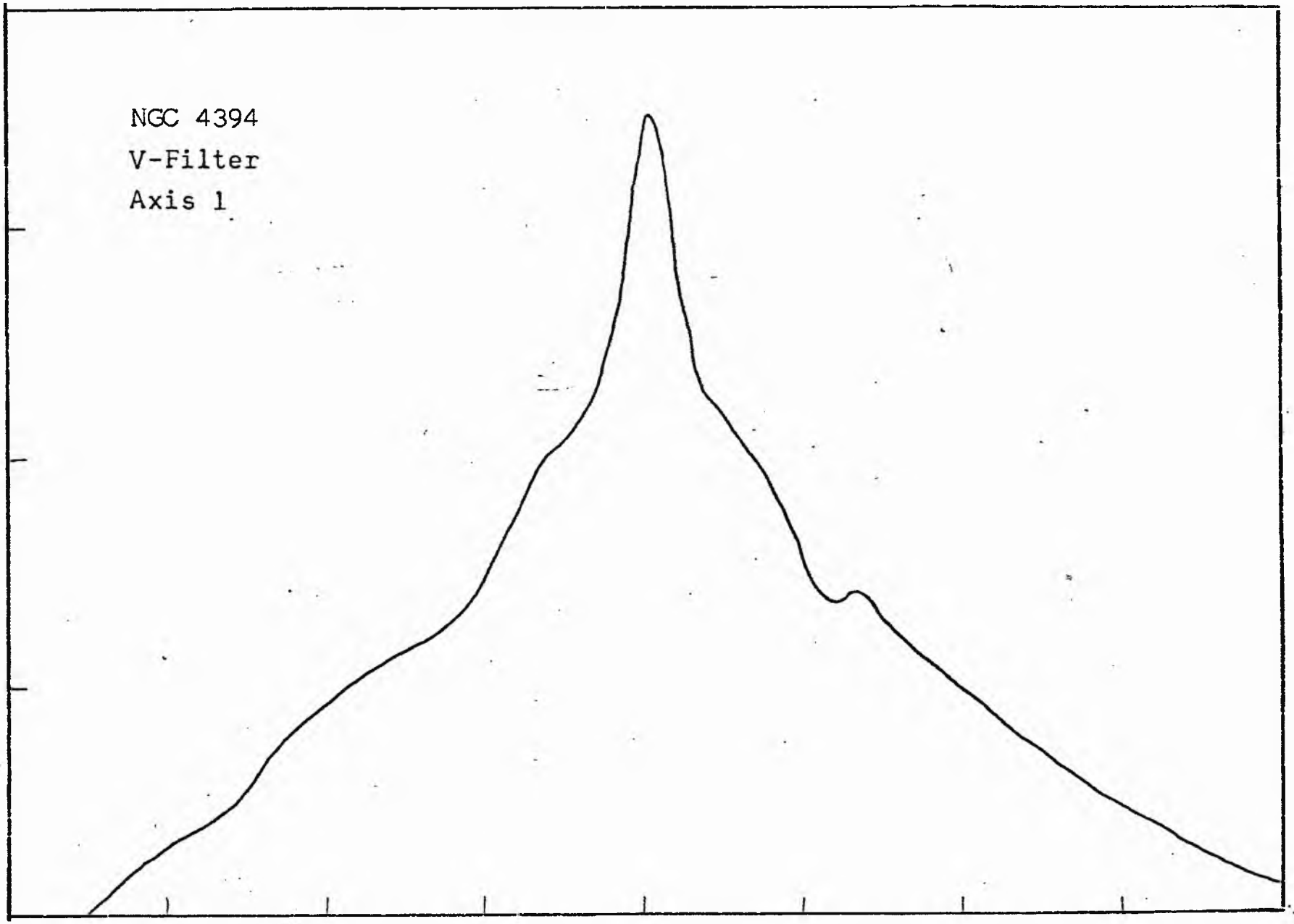
NGC 4394
V-Filter
Axis 1

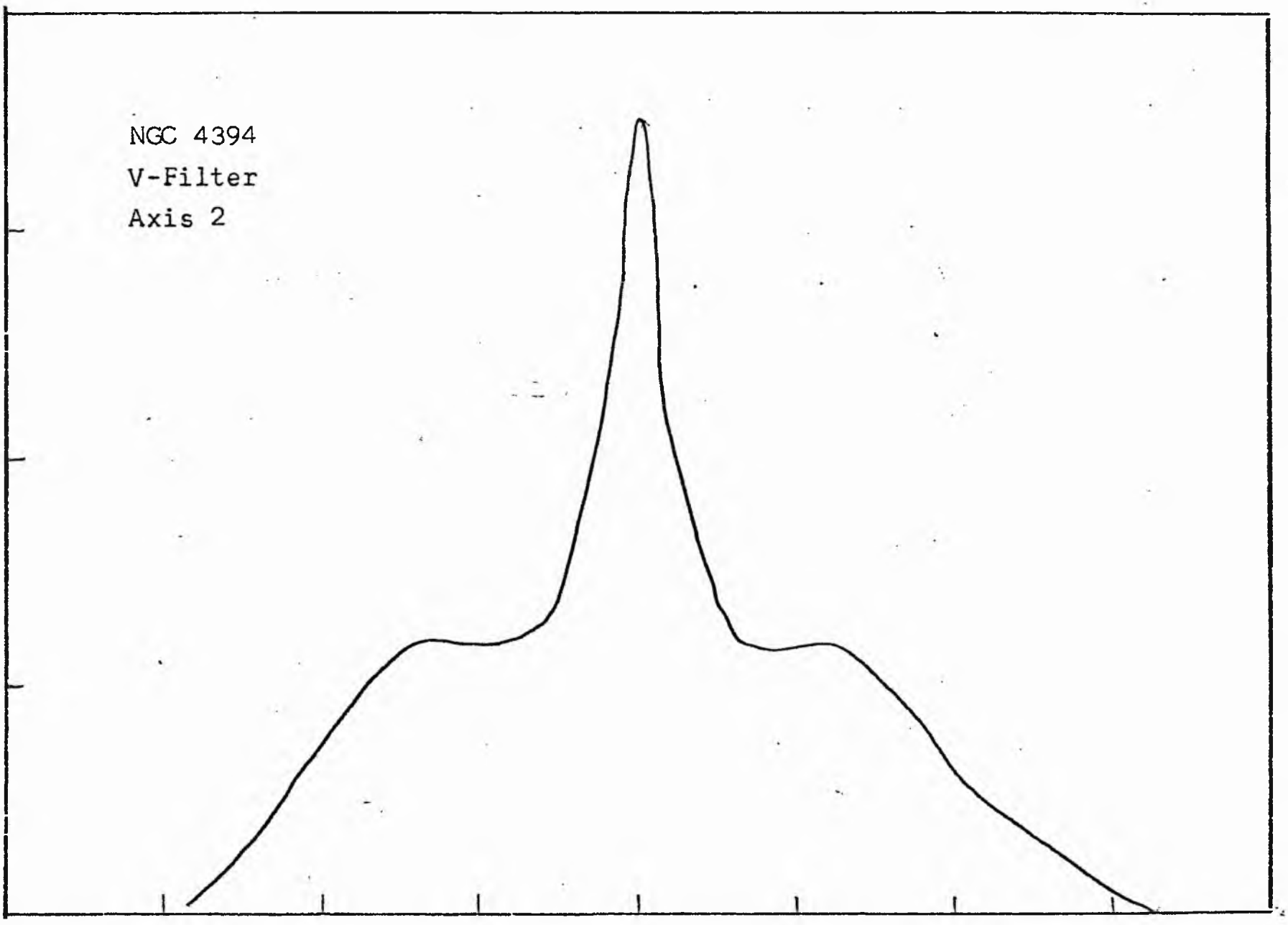
NGC 4394
V-Filter
Axis 2

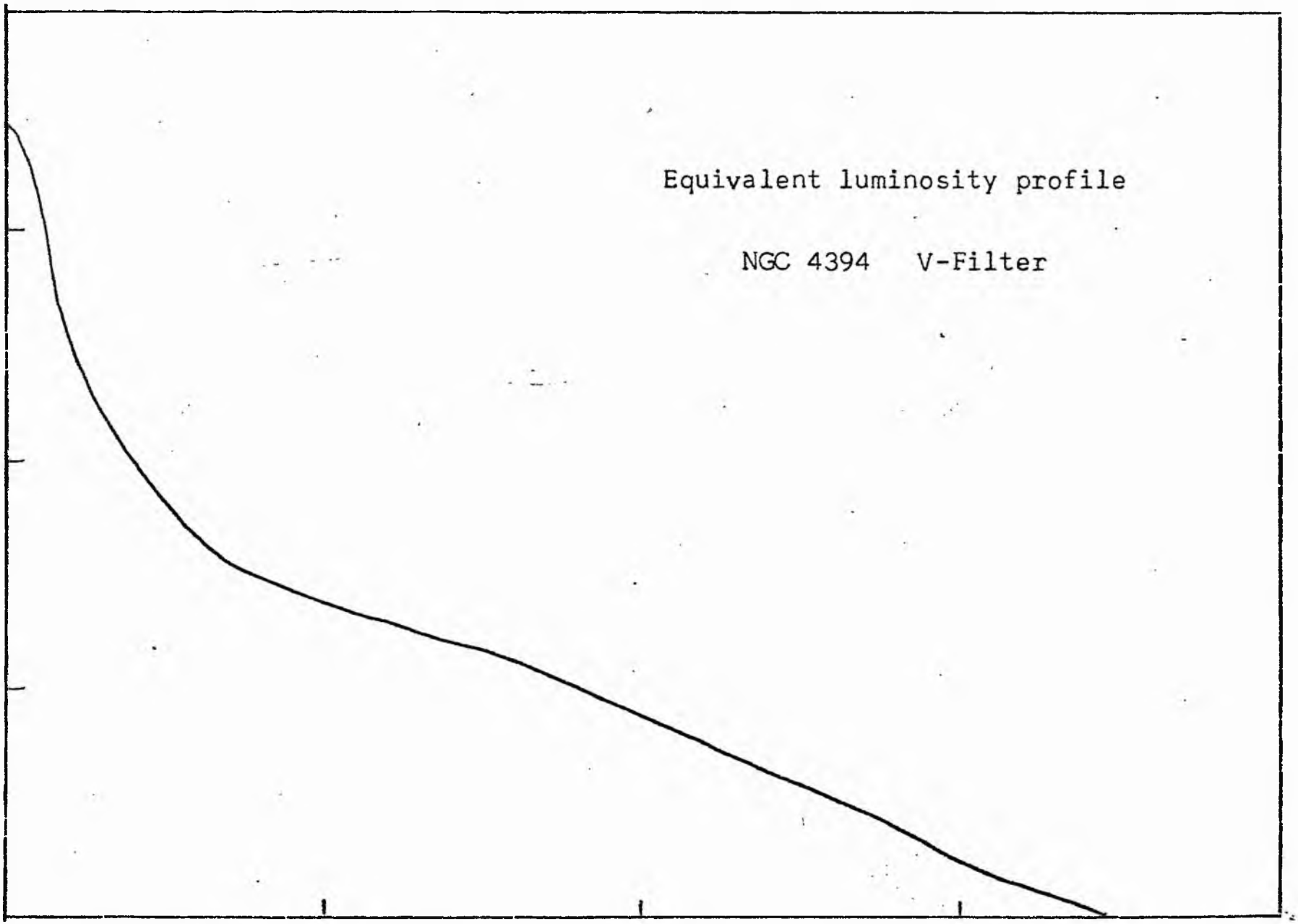
Equivalent luminosity profile
NGC 4394 V-Filter

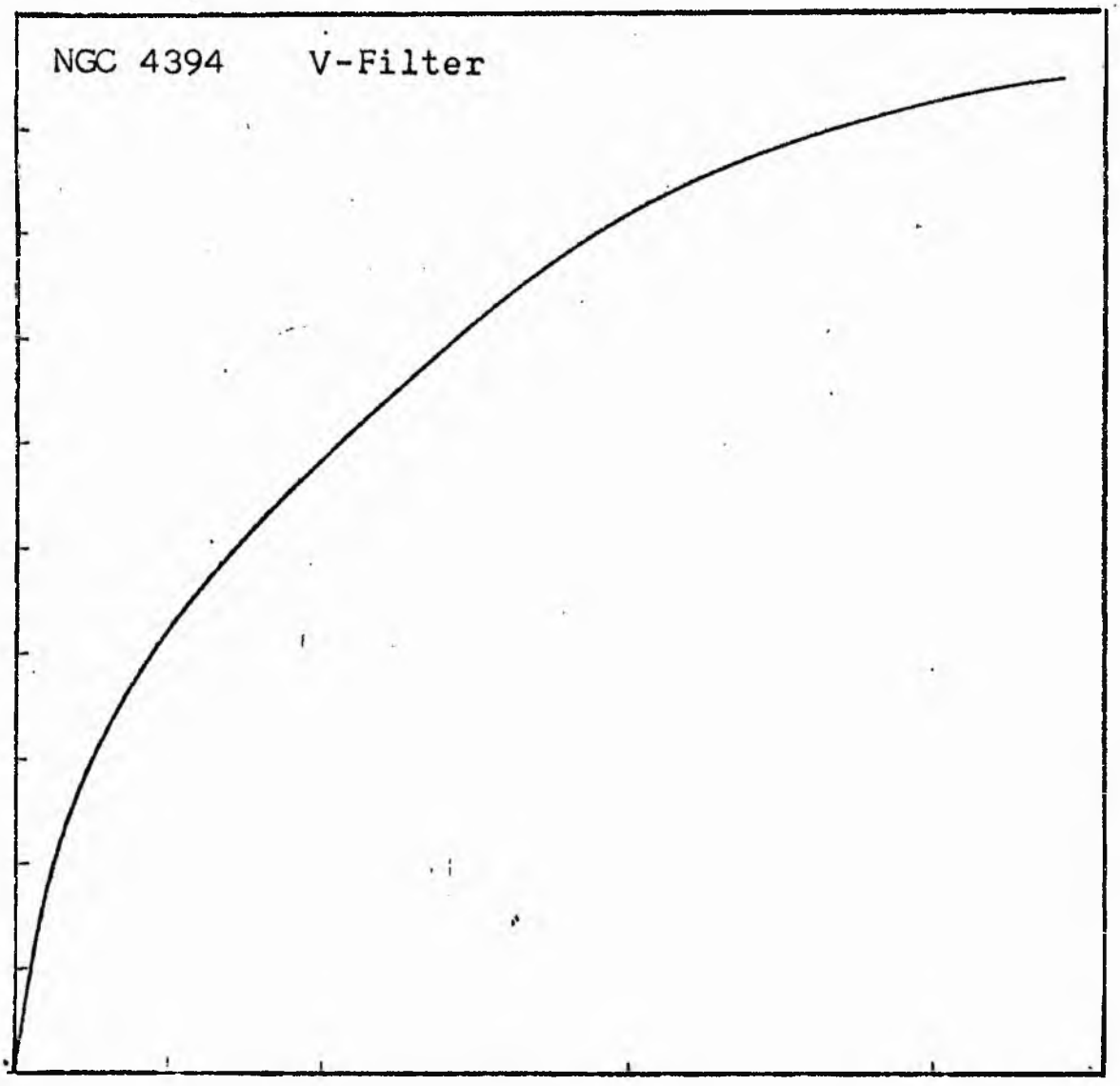

Relative integrated luminosity k(r) versus equivalent radius r*.

MEAN LUMINOSITY DISTRIBUTION IN NGC 4394
V COLOUR

LOG I	I	$\bar{I}$	R	AREA	ΔA	P	ΣP	K(R)	ρ	LOG J	μ
1.45	28.184		0.0	0.0			0.0	0.0	0.0	1.933	17.49
		26.651			17.65	470.2891					
1.40	25.119		2.37	17.65			470.29	0.04	0.06	1.883	17.62
		22.536			33.88	763.5972					
1.30	19.953		4.05	51.53			1233.89	0.10	0.11	1.783	17.87
		17.901			24.83	444.4058					
1.20	15.849		4.93	76.36			1678.29	0.13	0.13	1.683	18.12
		14.219			16.61	236.2483					
1.10	12.589		5.44	92.97			1914.54	0.15	0.15	1.583	18.37
		11.295			16.76	189.2840					
1.00	10.000		5.91	109.73			2103.82	0.16	0.16	1.483	18.62
		8.972			34.68	311.1721					
0.90	7.943		6.78	144.41			2415.00	0.19	0.18	1.383	18.87
		7.126			27.15	193.5172					
0.80	6.310		7.39	171.57			2608.51	0.20	0.20	1.283	19.12
		5.661			28.99	164.1075					
0.70	5.012		7.99	200.56			2772.62	0.21	0.22	1.183	19.37
		4.496			27.49	123.6068					
0.60	3.981		8.52	228.05			2896.23	0.22	0.23	1.083	19.62
		3.572			107.19	382.8337					
0.50	3.162		10.33	335.24			3279.06	0.25	0.28	0.983	19.87
		2.837			94.82	269.0015					
0.40	2.512		11.70	430.05			3548.06	0.27	0.32	0.883	20.12
		2.254			168.23	379.1226					
0.30	1.995		13.80	598.28			3927.19	0.30	0.37	0.783	20.37
		1.790			202.95	363.2944					
0.20	1.585		15.97	801.23			4290.48	0.33	0.43	0.683	20.62
		1.422			232.54	330.6448					
0.10	1.259		18.14	1033.77			4621.12	0.36	0.49	0.583	20.87
		1.129			243.05	274.5161					
-0.00	1.000		20.16	1276.82			4895.64	0.38	0.55	0.483	21.12
		0.897			352.01	315.8064					
-0.10	0.794		22.77	1628.83			5211.44	0.40	0.62	0.383	21.37
		0.713			446.16	317.9526					
-0.20	0.631		25.70	2074.99			5529.39	0.43	0.70	0.283	21.62
		0.566			368.70	208.7128					
-0.30	0.501		27.89	2443.69			5738.10	0.44	0.75	0.183	21.87
		0.450			594.88	267.4868					
-0.40	0.398		31.10	3038.58			6005.59	0.46	0.84	0.083	22.12
		0.357			1560.17	557.2400					
-0.50	0.316		38.26	4598.75			6562.82	0.51	1.04	-0.017	22.37
		0.284			2453.70	696.1331					
-0.60	0.251		47.38	7052.45			7258.96	0.56	1.28	-0.117	22.62
		0.225			4370.66	984.9597					
-0.70	0.200		60.30	11423.11			8243.91	0.64	1.63	-0.217	22.87
		0.179			3490.68	624.8574					
-0.80	0.158		68.90	14913.79			8868.77	0.69	1.86	-0.317	23.12
		0.142			3423.55	486.7969					
-0.90	0.126		76.40	18337.34			9355.57	0.72	2.07	-0.417	23.37
		0.113			5168.84	583.8013					
-1.00	0.100		86.50	23506.18			9939.37	0.77	2.34	-0.517	23.62
		0.090			5026.03	450.9177					
-1.10	0.079		95.30	28532.21			10390.28	0.80	2.58	-0.617	23.87
		0.071			5906.20	420.9016					
-1.20	0.063		104.70	34438.41			10811.18	0.84	2.83	-0.717	24.12
		0.057			4478.65	253.5246					
-1.30	0.050		111.30	38917.06			11064.70	0.86	3.01	-0.817	24.37
		0.045			5123.53	230.3791					
-1.40	0.040		118.40	44040.59			11295.08	0.87	3.20	-0.917	24.62
		0.036			4498.54	160.6742					
-1.50	0.032		124.30	48539.13			11455.75	0.89	3.36	-1.017	24.87
		0.028			8546.86	242.4833					
-1.60	0.025		134.80	57086.00			11698.23	0.91	3.65	-1.117	25.12
		0.023			7336.26	165.3295					
-1.70	0.020		143.20	64422.25			11863.56	0.92	3.87	-1.217	25.37
		0.018			7589.18	135.8537					
-1.80	0.016		151.40	72011.44			11999.41	0.93	4.10	-1.317	25.62
		0.014			10742.12	152.7450					
-1.90	0.013		162.30	82753.56			12152.16	0.94	4.39	-1.417	25.87
		0.011			8252.19	93.2065					
-2.00	0.010		170.20	91005.75			12245.36	0.95	4.60	-1.517	26.12
- ∞							12925.00	(1)			∞

PHOTOMETRIC PARAMETERS OF NGC 4394

V-FILTER

Total luminosity	L_T	= 3.59
Total apparent magnitude	m_T	= 10.84
Apparent central surface brightness	μ_o	= 17.49
Major axis at threshold	$2a_m$	= 6.37
Minor axis at threshold	$2b_m$	= 4.82
Major axis at μ=25.0 mag sec^{-2}	2a(25)	= 4.10
Luminosity within μ=25.0 mag sec^{-2}	k(25)	= 0.90
Gradient of exponential component	G(a)	= -0.58
Equivalent gradient of exponential comp.	G(r*)	= -0.68
Equivalent gradient of reduced exp. comp.	G(ρ)	= -0.45
Parameters at k = ¼ :		
Semi-major axis	a_1	= 0.28
Axis ratio	b/a	= 0.53
Equivalent radius	r_1*	= 0.17
Surface brightness	μ_1	= 19.87
Parameters at k = ½(effective) :		
Semi-major axis	a_e	= 0.85
Axis ratio	b/a	= 0.49
Equivalent radius	r_e*	= 0.62
Surface brightness	μ_e	= 22.32
Mean surface brightness	μ_e'	= 11.79
Parameters at k = ¾ :		
Semi-major axis	a_3	= 1.53
Axis ratio	b/a	= 0.78
Equivalent radius	r_3*	= 1.37
Surface brightness	μ_3	= 23.52
Concentration indices	C_{21}	= 3.66
	C_{32}	= 2.22

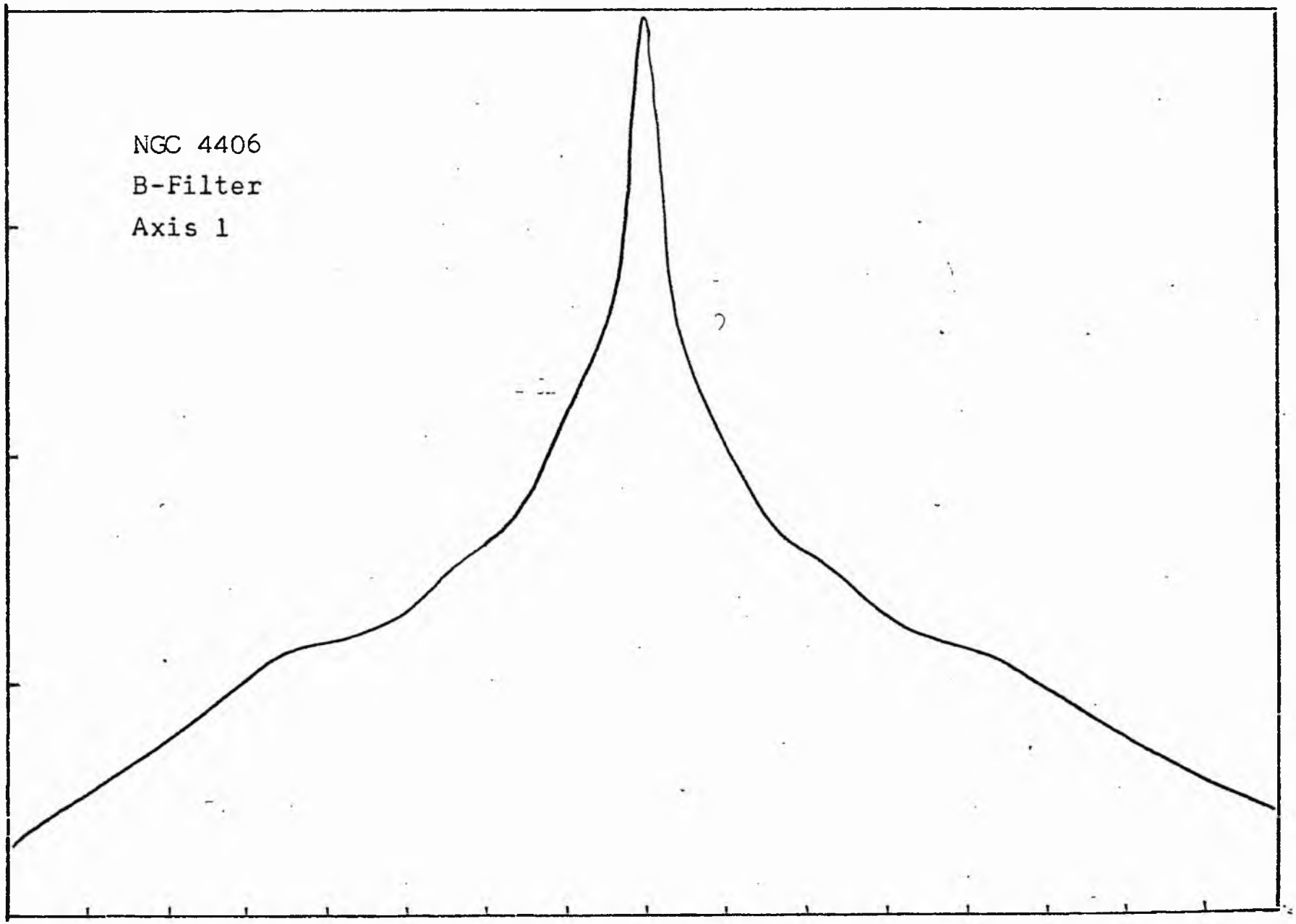
NGC 4406
B-Filter
Axis 1

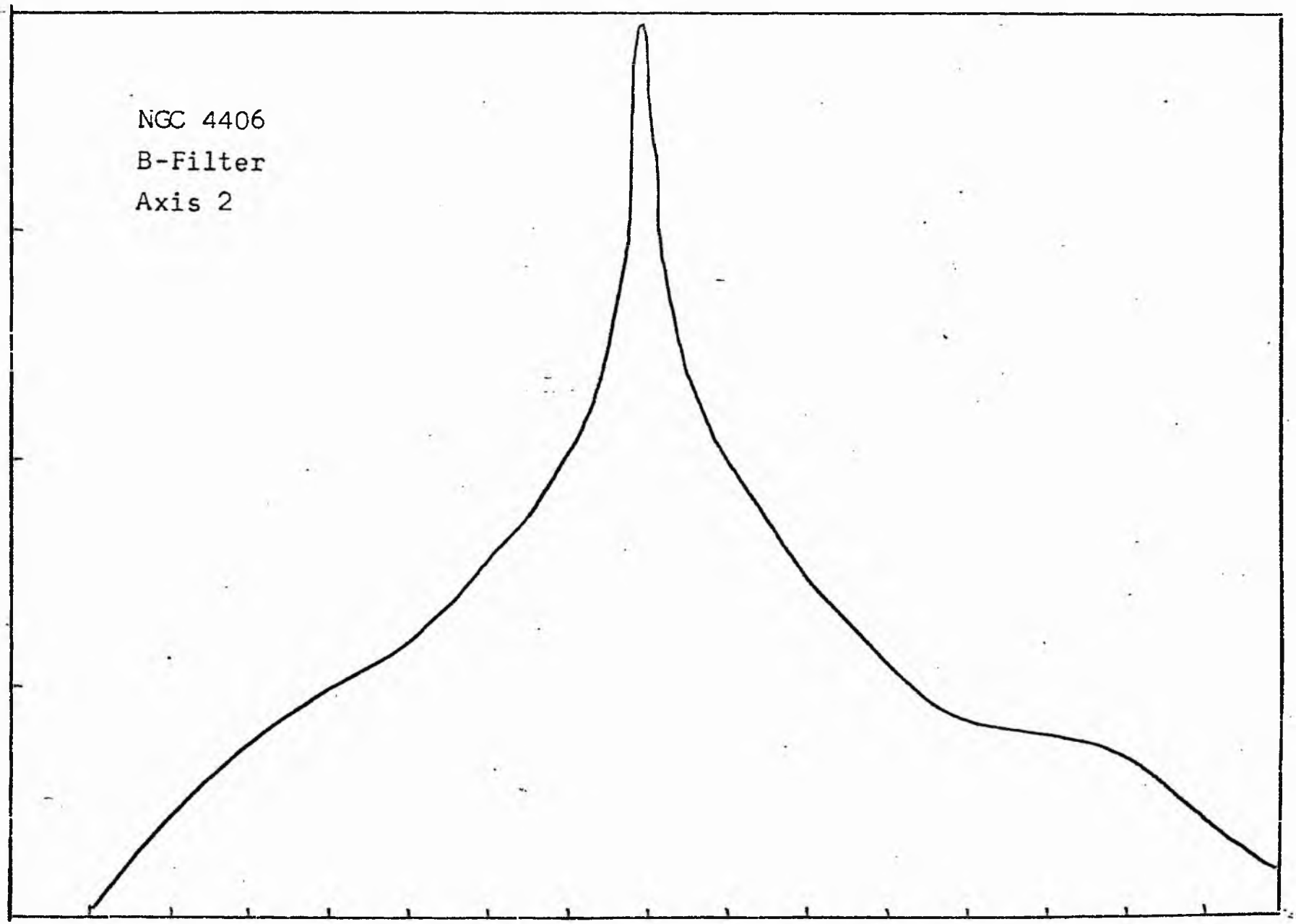
NGC 4406
B-Filter
Axis 2

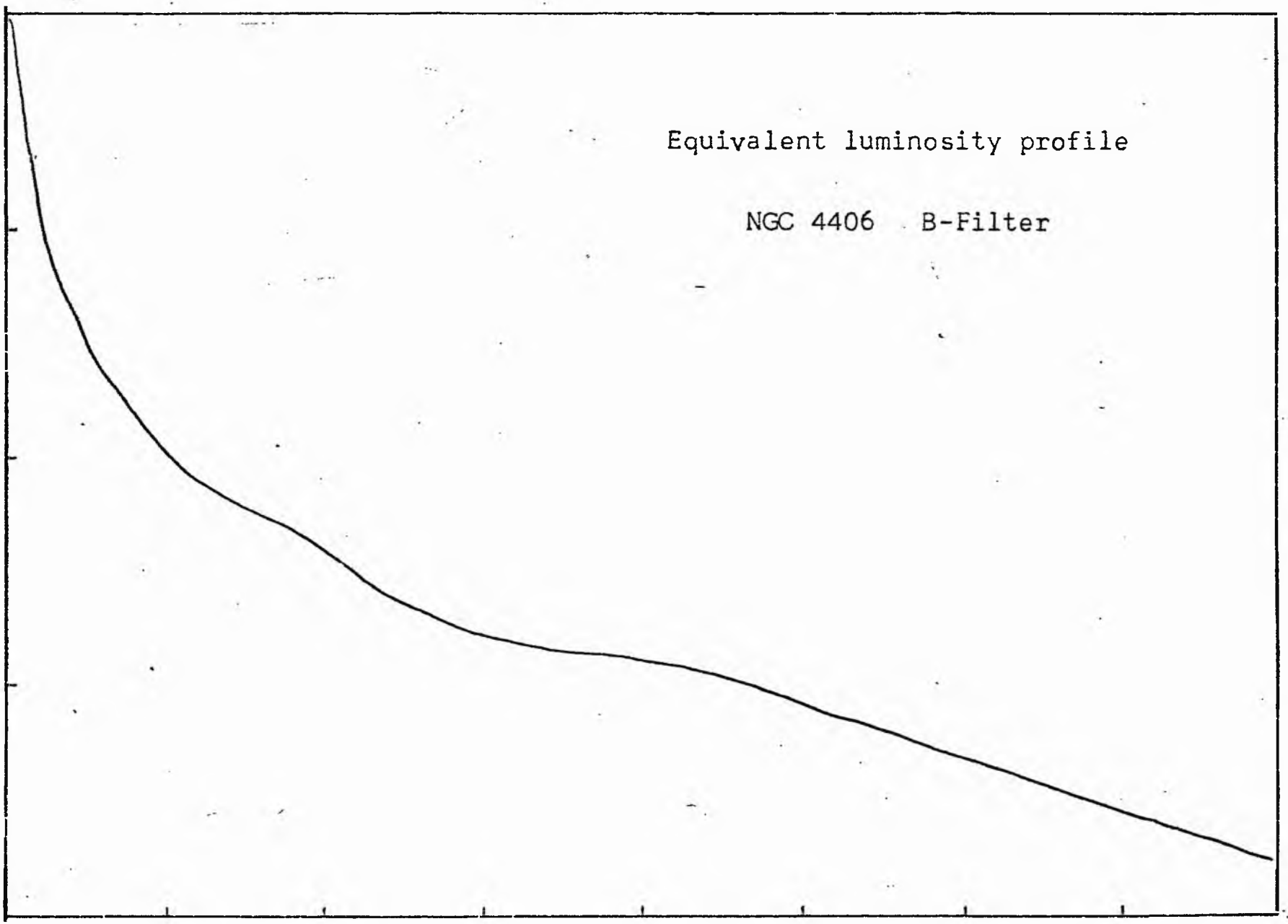
Equivalent luminosity profile
NGC 4406 B-Filter

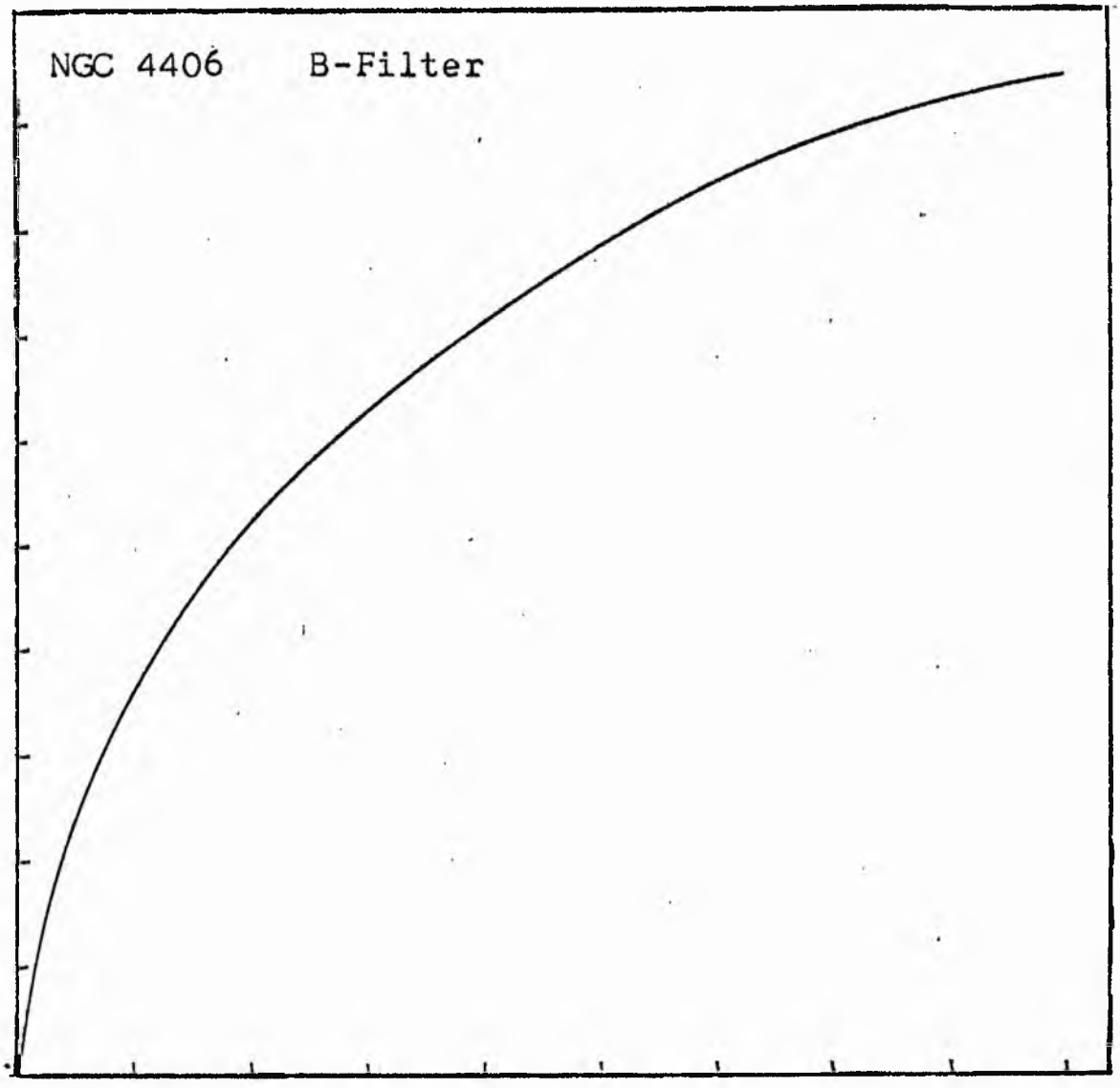

Relative integrated luminosity k(r) versus equivalent radius r*.

MEAN LUMINOSITY DISTRIBUTION IN NGC 4406
B COLOUR

LOG I	I	$\bar{I}$	R	AREA	ΔA	P	ΣP	K(R)	ρ	LOG J	μ
1.93	85.114		0.0	0.0			0.0	0.0	0.0	2.231	17.63
		82.273			30.19	2483.8848					
1.90	79.433		3.10	30.19			2483.88	0.03	0.03	2.201	17.71
		71.264			33.43	2382.1160					
1.80	63.096		4.50	63.62			4866.00	0.05	0.05	2.101	17.96
		56.607			38.45	2176.7158					
1.70	50.119		5.70	102.07			7042.71	0.08	0.06	2.001	18.21
		44.965			18.69	840.4990					
1.60	39.811		6.20	120.76			7883.21	0.09	0.07	1.901	18.46
		35.717			16.08	574.4995					
1.50	31.623		6.60	136.85			8457.71	0.09	0.07	1.801	18.71
		28.371			49.42	1402.0012					
1.40	25.119		7.70	186.27			9859.71	0.11	0.09	1.701	18.96
		22.536			91.33	2058.0872					
1.30	19.952		9.40	277.59			11917.79	0.13	0.10	1.601	19.21
		17.901			152.46	2729.1584					
1.20	15.849		11.70	430.05			14646.95	0.16	0.13	1.501	19.46
		14.219			14.83	210.8443					
1.10	12.589		11.90	444.88			14857.79	0.16	0.13	1.401	19.71
		11.295			153.40	1732.6230					
1.00	10.000		13.80	598.28			16590.41	0.18	0.15	1.301	19.96
		8.972			176.09	1579.7708					
0.90	7.943		15.70	774.37			18170.18	0.20	0.17	1.201	20.21
		7.126			60.32	429.8403					
0.80	6.310		16.30	834.69			18600.02	0.20	0.18	1.101	20.46
		5.661			228.93	1295.8884					
0.70	5.012		18.40	1063.62			19895.91	0.21	0.20	1.001	20.71
		4.496			470.77	2116.7747					
0.60	3.981		22.10	1534.38			22012.68	0.24	0.25	0.901	20.96
		3.572			589.33	2104.8901					
0.50	3.162		26.00	2123.72			24117.57	0.26	0.29	0.801	21.21
		2.837			647.45	1836.8535					
0.40	2.512		29.70	2771.17			25954.42	0.28	0.33	0.701	21.46
		2.254			924.88	2084.2781					
0.30	1.995		34.30	3696.05			28038.70	0.30	0.38	0.601	21.71
		1.790			1205.62	2158.1350					
0.20	1.585		39.50	4901.67			30196.83	0.33	0.44	0.501	21.96
		1.422			1832.93	2606.2349					
0.10	1.259		46.30	6734.59			32803.07	0.35	0.52	0.401	22.21
		1.129			2223.84	2511.7305					
-0.00	1.000		53.40	8958.44			35314.80	0.38	0.59	0.301	22.46
		0.897			3078.92	2762.2747					
-0.10	0.794		61.90	12037.36			38077.07	0.41	0.69	0.201	22.71
		0.713			5073.13	3615.3066					
-0.20	0.631		73.80	17110.49			41692.37	0.45	0.82	0.101	22.96
		0.566			8110.71	4591.2148					
-0.30	0.501		89.60	25221.20			46283.59	0.50	1.00	0.001	23.21
		0.450			8497.38	3820.7983					
-0.40	0.398		103.60	33718.58			50104.39	0.54	1.15	-0.099	23.46
		0.357			4433.04	1503.3204					
-0.50	0.316		110.20	38151.62			51607.71	0.56	1.23	-0.199	23.71
		0.284			8149.04	2311.9336					
-0.60	0.251		121.40	46300.66			53999.65	0.58	1.35	-0.299	23.96
		0.225			11464.93	2583.6902					
-0.70	0.200		135.60	57765.59			56583.34	0.61	1.51	-0.399	24.21
		0.179			16353.85	2927.4487					
-0.80	0.158		153.60	74119.44			59510.78	0.64	1.71	-0.499	24.46
		0.142			39172.69	5569.9648					
-0.90	0.126		189.90	113292.12			65080.75	0.70	2.12	-0.599	24.71
		0.113			62721.50	7084.1211					
-1.00	0.100		236.70	176013.62			72164.81	0.78	2.64	-0.699	24.96
		0.090			20807.37	1866.7559					
-1.10	0.079		250.30	196821.00			74031.56	0.80	2.79	-0.799	25.21
		0.071			38177.19	2720.6624					
-1.20	0.063		273.50	234998.19			76752.19	0.83	3.05	-0.899	25.46
		0.057			45111.87	2553.6548					
-1.30	0.050		290.60	280110.06			79305.81	0.86	3.33	-0.999	25.71
		0.045			42997.81	1933.3850					
-1.40	0.040		320.70	323107.87			81239.19	0.88	3.57	-1.099	25.96
		0.036			49953.12	1784.1658					
-1.50	0.032		344.60	373061.00			83023.31	0.90	3.84	-1.199	26.21
		0.028			61217.25	1736.7883					
-1.60	0.025		371.80	434278.25			84760.06	0.91	4.14	-1.299	26.46
		0.023			35991.50	811.0984					
-1.70	0.020		386.90	470269.75			85571.12	0.92	4.31	-1.399	26.71
		0.018			45538.94	815.1870					
-1.80	0.016		405.20	515808.69			86386.25	0.93	4.51	-1.499	26.96
		0.014			37576.62	534.3093					
-1.90	0.013		419.70	553385.31			86920.50	0.94	4.67	-1.599	27.21
		0.011			39989.31	451.6680					
-2.00	0.010		434.60	593374.62			87372.12	0.94	4.84	-1.699	27.46
$-\infty$							92672.00	(1)			∞

PHOTOMETRIC PARAMETERS OF NGC 4406

B-FILTER

Total luminosity	L_T	= 25.74
Total apparent magnitude	m_T	= 10.04
Apparent central surface brightness	μ_o	= 17.63
Major axis at threshold	$2a_m$	= 16.03
Minor axis at threshold	$2b_m$	= 12.42
Major axis at μ=25.0 mag sec^{-2}	2a(25)	= 8.10
Luminosity within μ=25.0 mag sec^{-2}	k(25)	= 0.78
Gradient of exponential component	G(a)	= -0.21
Equivalent gradient of exponential comp.	G(r*)	= -0.26
Equivalent gradient of reduced exp. comp.	G(ρ)	= -0.44
Parameters at k = ¼ :		
Semi-major axis	a_1	= 0.45
Axis ratio	b/a	= 0.81
Equivalent radius	r_1*	= 0.40
Surface brightness	μ_1	= 21.08
Parameters at k = ½(effective) :		
Semi-major axis	a_e	= 1.32
Axis ratio	b/a	= 1.04
Equivalent radius	r_e*	= 1.50
Surface brightness	μ_e	= 23.21
Mean surface brightness	μ_e'	= 12.92
Parameters at k = ¾ :		
Semi-major axis	a_3	= 3.86
Axis ratio	b/a	= 0.75
Equivalent radius	r_3*	= 3.64
Surface brightness	μ_3	= 24.87
Concentration indices	C_{21}	= 3.71
	C_{32}	= 2.43

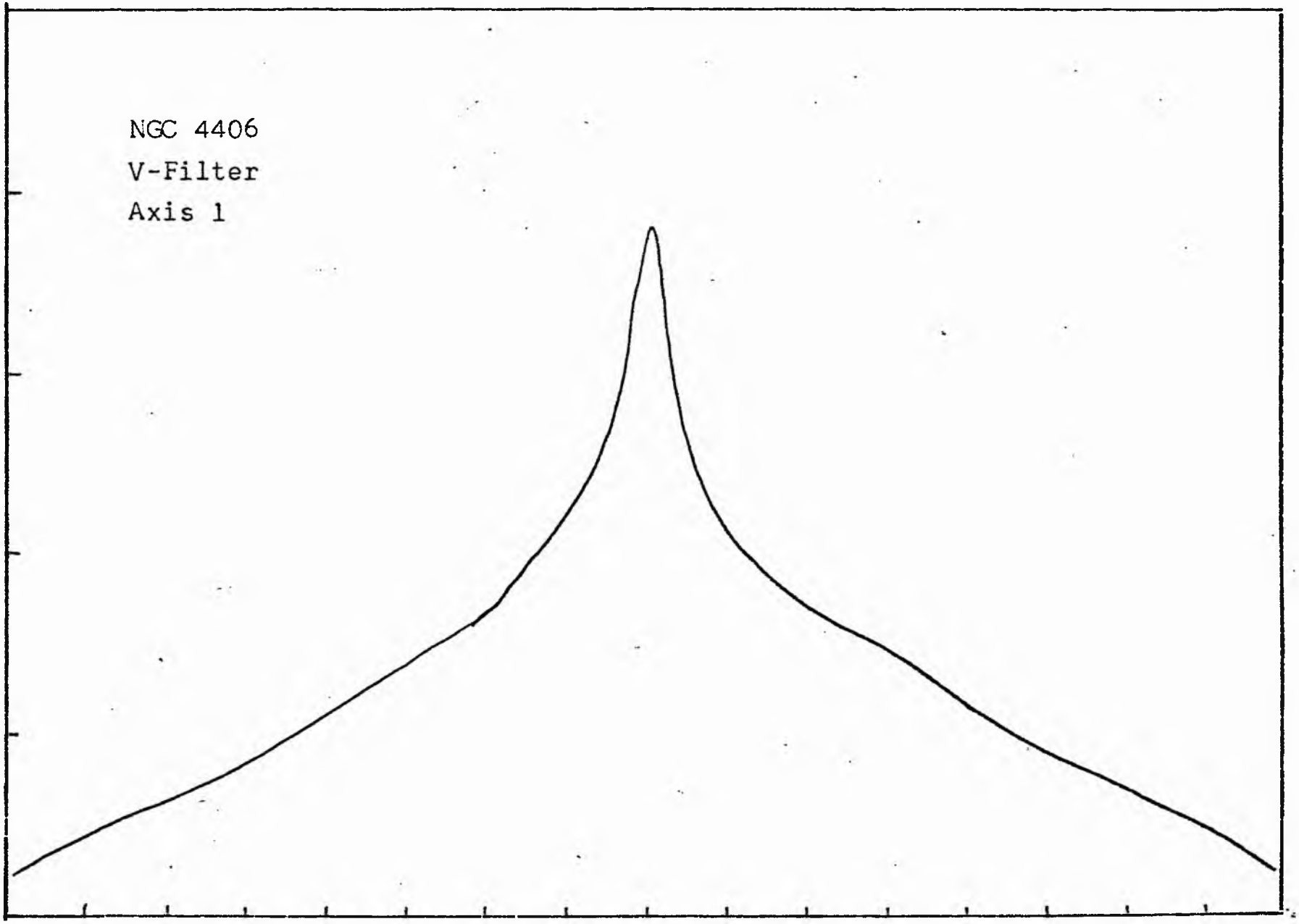
NGC 4406
V-Filter
Axis 1

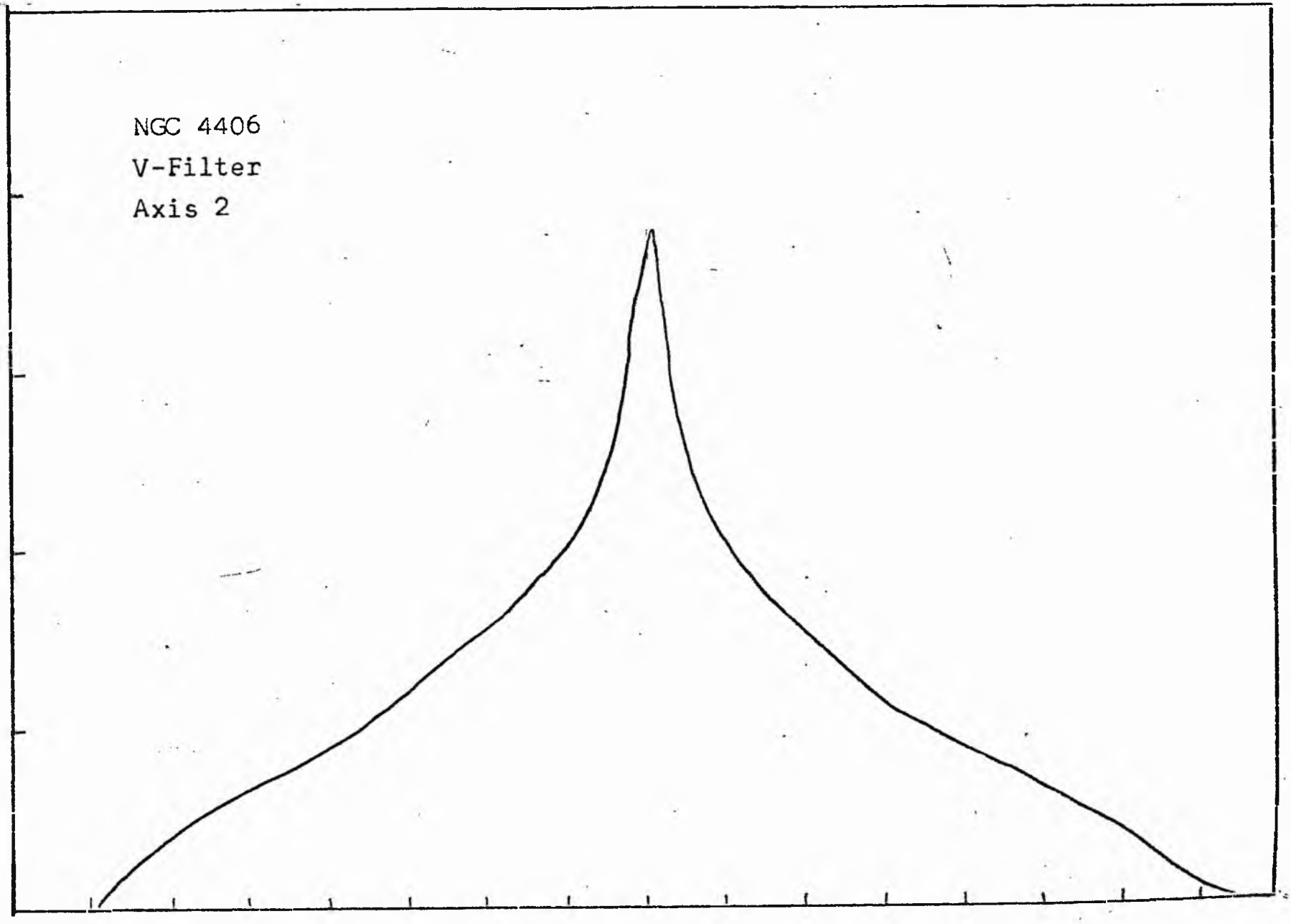
NGC 4406
V-Filter
Axis 2

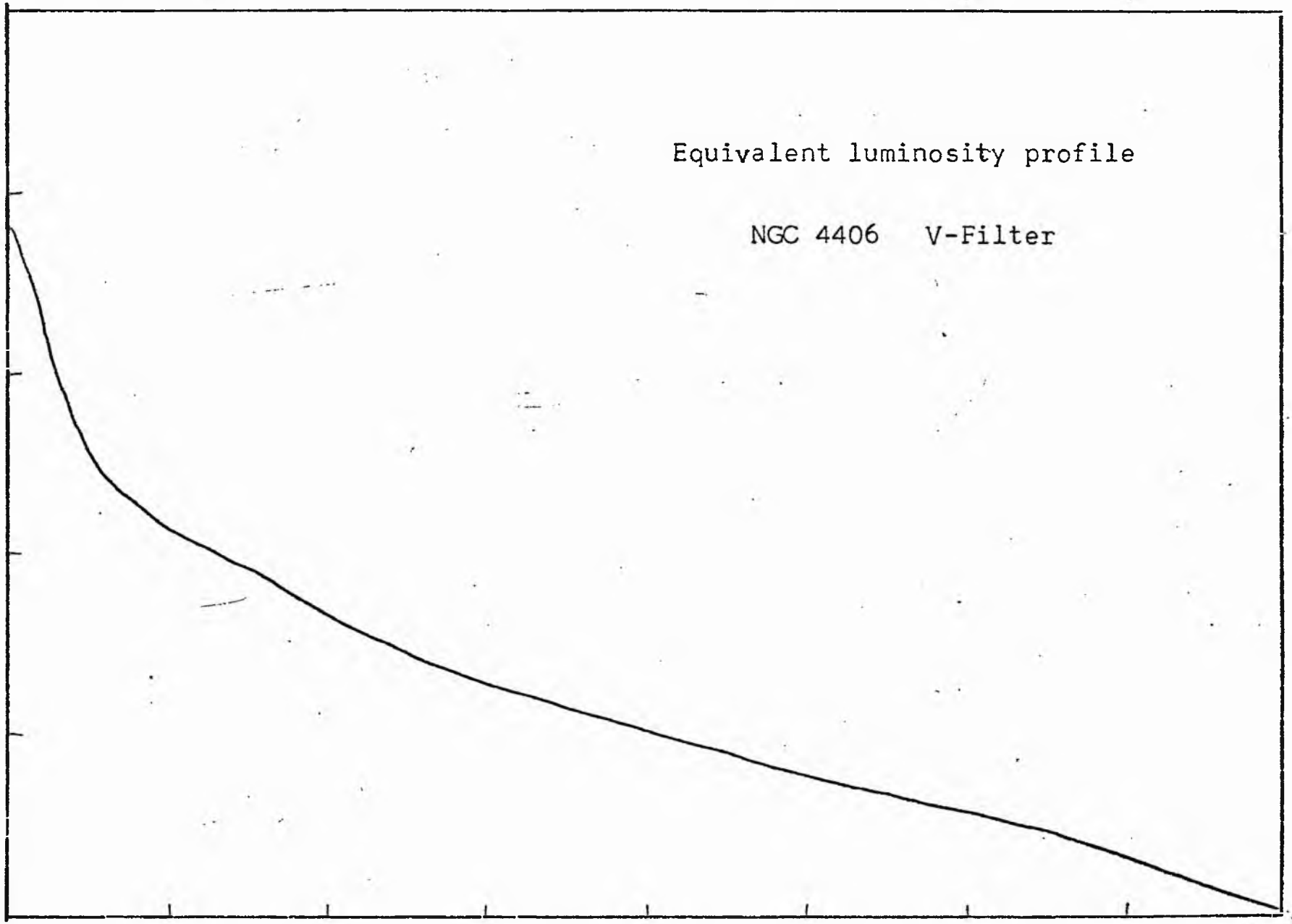
Equivalent luminosity profile
NGC 4406 V-Filter

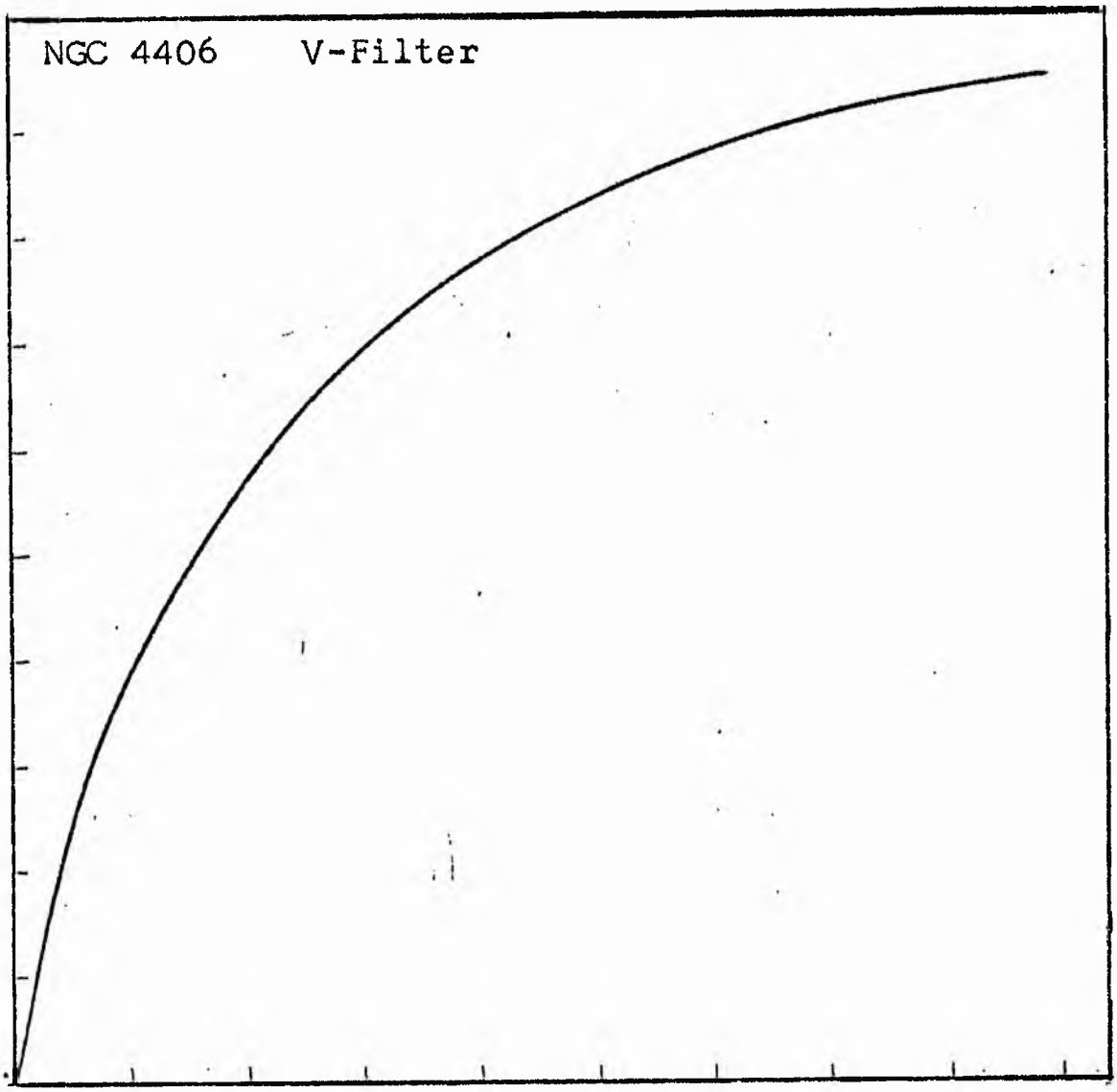

Relative integrated luminosity k(r) versus equivalent radius r*.

MEAN LUMINOSITY DISTRIBUTION IN NGC 4406
V COLOUR

LOG I	I	$\bar{I}$	R	AREA	ΔA	P	ΣP	K(R)	ρ	LOG J	μ
1.84	69.183		0.0	0.0			0.0	0.0	0.0	1.942	17.03
		66.139			8.04	531.9231					
1.80	63.096		1.60	8.04			531.92	0.01	0.02	1.902	17.13
		56.607			22.15	1253.7454					
1.70	50.119		3.10	30.19			1785.67	0.02	0.04	1.802	17.38
		44.965			25.23	1134.3193					
1.60	39.811		4.20	55.42			2919.99	0.03	0.06	1.702	17.63
		35.717			46.65	1666.2744					
1.50	31.623		5.70	102.07			4586.26	0.05	0.08	1.602	17.88
		28.371			135.72	3850.3762					
1.40	25.119		8.70	237.79			8436.64	0.09	0.12	1.502	18.13
		22.536			237.50	5352.3008					
1.30	19.952		12.30	475.29			13788.94	0.15	0.17	1.402	18.38
		17.901			72.10	1290.6296					
1.20	15.849		13.20	547.39			15079.57	0.16	0.18	1.302	18.63
		14.219			150.07	2133.8950					
1.10	12.589		14.90	697.46			17213.46	0.19	0.20	1.202	18.88
		11.295			47.60	537.5652					
1.00	10.000		15.40	745.06			17751.02	0.19	0.21	1.102	19.13
		8.972			131.10	1176.1577					
0.90	7.943		16.70	876.16			18927.18	0.21	0.23	1.002	19.38
		7.126			294.05	2095.5210					
0.80	6.310		19.30	1170.21			21022.70	0.23	0.26	0.902	19.63
		5.661			295.53	1672.8997					
0.70	5.012		21.60	1465.74			22695.60	0.25	0.29	0.802	19.88
		4.496			374.10	1682.1211					
0.60	3.981		24.20	1839.84			24377.72	0.26	0.33	0.702	20.13
		3.572			588.10	2100.5012					
0.50	3.162		27.80	2427.95			26478.22	0.29	0.38	0.602	20.38
		2.837			689.30	1955.5854					
0.40	2.512		31.50	3117.25			28433.80	0.31	0.43	0.502	20.63
		2.254			1137.22	2562.7896					
0.30	1.995		36.80	4254.46			30996.59	0.34	0.50	0.402	20.88
		1.790			1313.72	2351.6487					
0.20	1.585		42.10	5568.19			33348.24	0.36	0.57	0.302	21.13
		1.422			3156.93	4488.8281					
0.10	1.259		52.70	8725.11			37837.07	0.41	0.71	0.202	21.38
		1.129			2850.05	3219.0029					
-0.00	1.000		60.70	11575.16			41056.07	0.45	0.82	0.102	21.63
		0.897			5442.71	4882.9648					
-0.10	0.794		73.60	17017.87			45939.03	0.50	1.00	0.002	21.88
		0.713			8655.71	6168.3867					
-0.20	0.631		90.40	25673.59			52107.42	0.57	1.22	-0.098	22.13
		0.566			6247.00	3536.2256					
-0.30	0.501		100.80	31920.58			55643.64	0.60	1.36	-0.198	22.38
		0.450			6369.64	2864.0715					
-0.40	0.398		110.40	38290.22			58507.71	0.64	1.49	-0.298	22.63
		0.357			4494.77	1605.3762					
-0.50	0.316		116.70	42785.00			60113.09	0.65	1.58	-0.398	22.88
		0.284			8526.12	2418.9163					
-0.60	0.251		127.80	51311.12			62532.00	0.68	1.73	-0.498	23.13
		0.225			9300.28	2095.8745					
-0.70	0.200		138.90	60611.40			64627.87	0.70	1.88	-0.598	23.38
		0.179			18212.85	3260.2214					
-0.80	0.158		158.40	78824.25			67888.06	0.74	2.14	-0.698	23.63
		0.142			27075.50	3849.8662					
-0.90	0.126		183.60	105899.75			71737.87	0.78	2.49	-0.798	23.88
		0.113			20771.25	2346.0227					
-1.00	0.100		200.80	126671.00			74083.87	0.80	2.72	-0.898	24.13
		0.090			34784.50	3120.7288					
-1.10	0.079		226.70	161455.50			77204.56	0.84	3.07	-0.998	24.38
		0.071			31453.44	2241.5005					
-1.20	0.063		247.80	192908.94			79446.06	0.86	3.35	-1.098	24.63
		0.057			37471.87	2121.1763					
-1.30	0.050		270.80	230380.81			81567.19	0.89	3.67	-1.198	24.88
		0.045			29291.44	1317.0815					
-1.40	0.040		287.50	259672.25			82884.25	0.90	3.89	-1.298	25.13
		0.036			33917.25	1211.4155					
-1.50	0.032		305.70	293589.50			84095.62	0.91	4.14	-1.398	25.38
		0.028			43777.50	1242.0068					
-1.60	0.025		327.70	337367.00			85337.62	0.93	4.447	-1.498	25.63
		0.023			40690.69	916.9985					
-1.70	0.020		346.90	378057.69			86254.56	0.94	4.70	-1.598	25.88
		0.018			46926.56	840.0266					
-1.80	0.016		367.80	424984.25			87094.56	0.95	4.98	-1.698	26.13
		0.014			13040.00	185.4183					
-1.90	0.013		373.40	438024.25			87279.94	0.95	5.05	-1.798	26.38
		0.011			71691.69	809.7375					
-2.00	0.010		402.80	509715.94			88089.62	0.96	5.45	-1.898	26.63
- ∞							92089.00	1.00			∞

PHOTOMETRIC PARAMETERS OF NGC 4406

V-FILTER

Total luminosity	L_T	= 25.58
Total apparent magnitude	m_T	= 9.21
Apparent central surface brightness	μ_o	= 17.03
Major axis at threshold	$2a_m$	= 14.58
Minor axis at threshold	$2b_m$	= 11.70
Major axis at μ=25.0 mag sec^{-2}	2a(25)	= 9.81
Luminosity within μ=25.0 mag sec^{-2}	k(25)	= 0.89
Gradient of exponential component	G(a)	= -0.28
Equivalent gradient of exponential comp.	G(r*)	= -0.31
Equivalent gradient of reduced exp. comp.	G(ρ)	= -0.34
Parameters at k = ¼ :		
Semi-major axis	a_1	= 0.53
Axis ratio	b/a	= 0.66
Equivalent radius	r_1*	= 0.37
Surface brightness	μ_1	= 19.88
Parameters at k = ½(effective) :		
Semi-major axis	a_e	= 1.37
Axis ratio	b/a	= 0.69
Equivalent radius	r_e*	= 1.23
Surface brightness	μ_e	= 21.88
Mean surface brightness	μ_e'	= 11.65
Parameters at k = ¾ :		
Semi-major axis	a_3	= 3.08
Axis ratio	b/a	= 0.76
Equivalent radius	r_3*	= 2.76
Surface brightness	μ_3	= 23.69
Concentration indices	C_{21}	= 3.35
	C_{32}	= 2.24

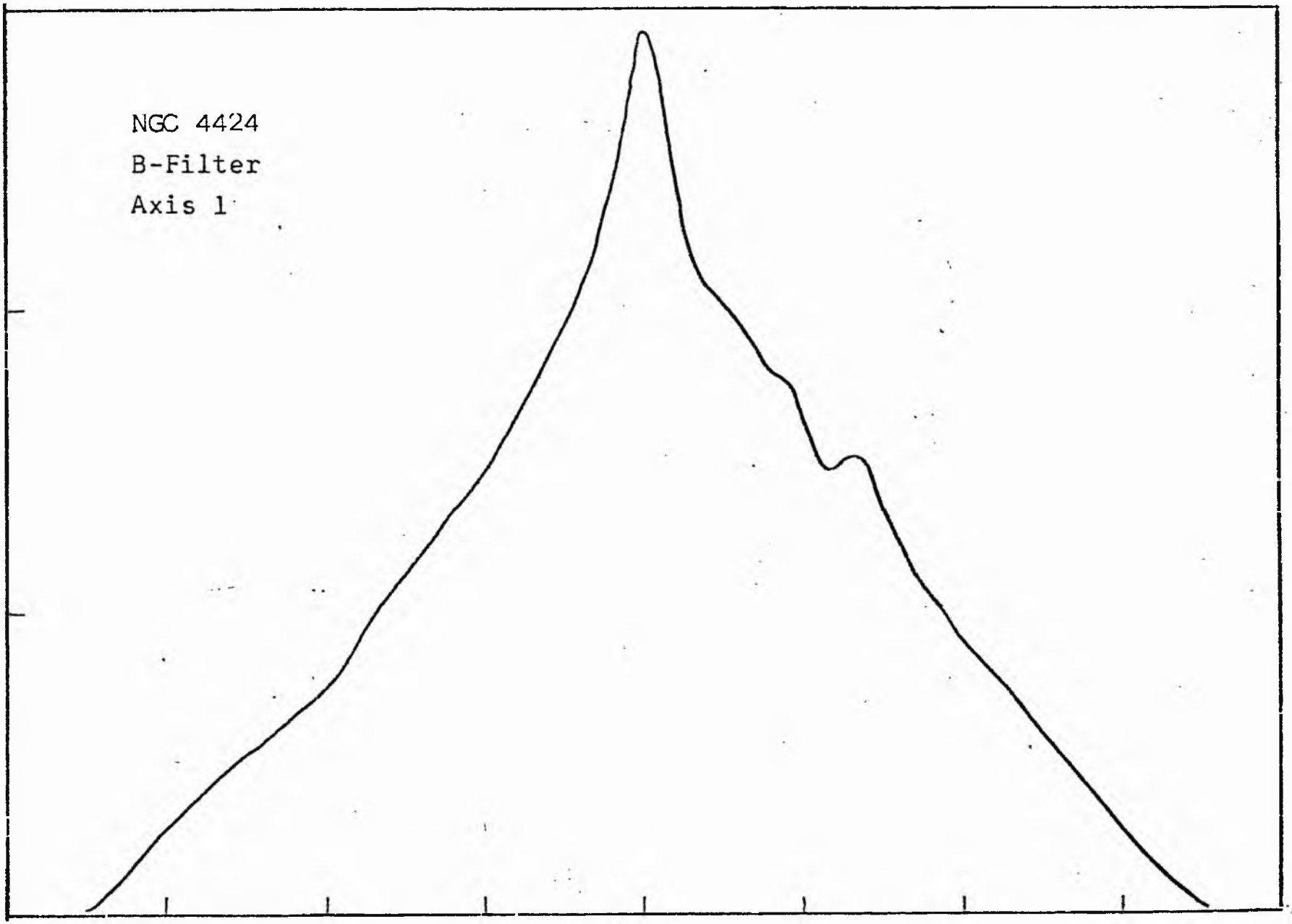
NGC 4424
B-Filter
Axis 1

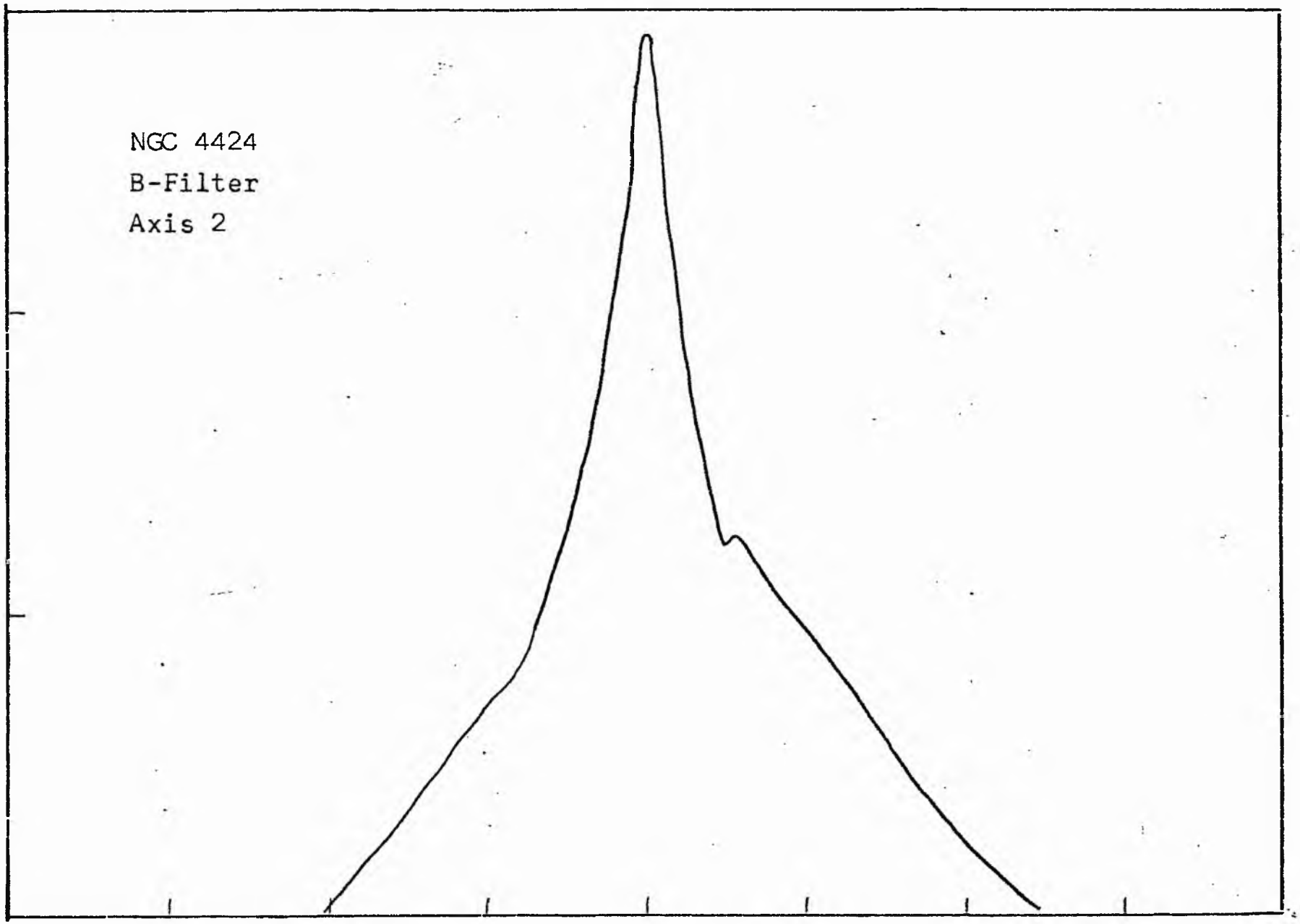
NGC 4424
B-Filter
Axis 2

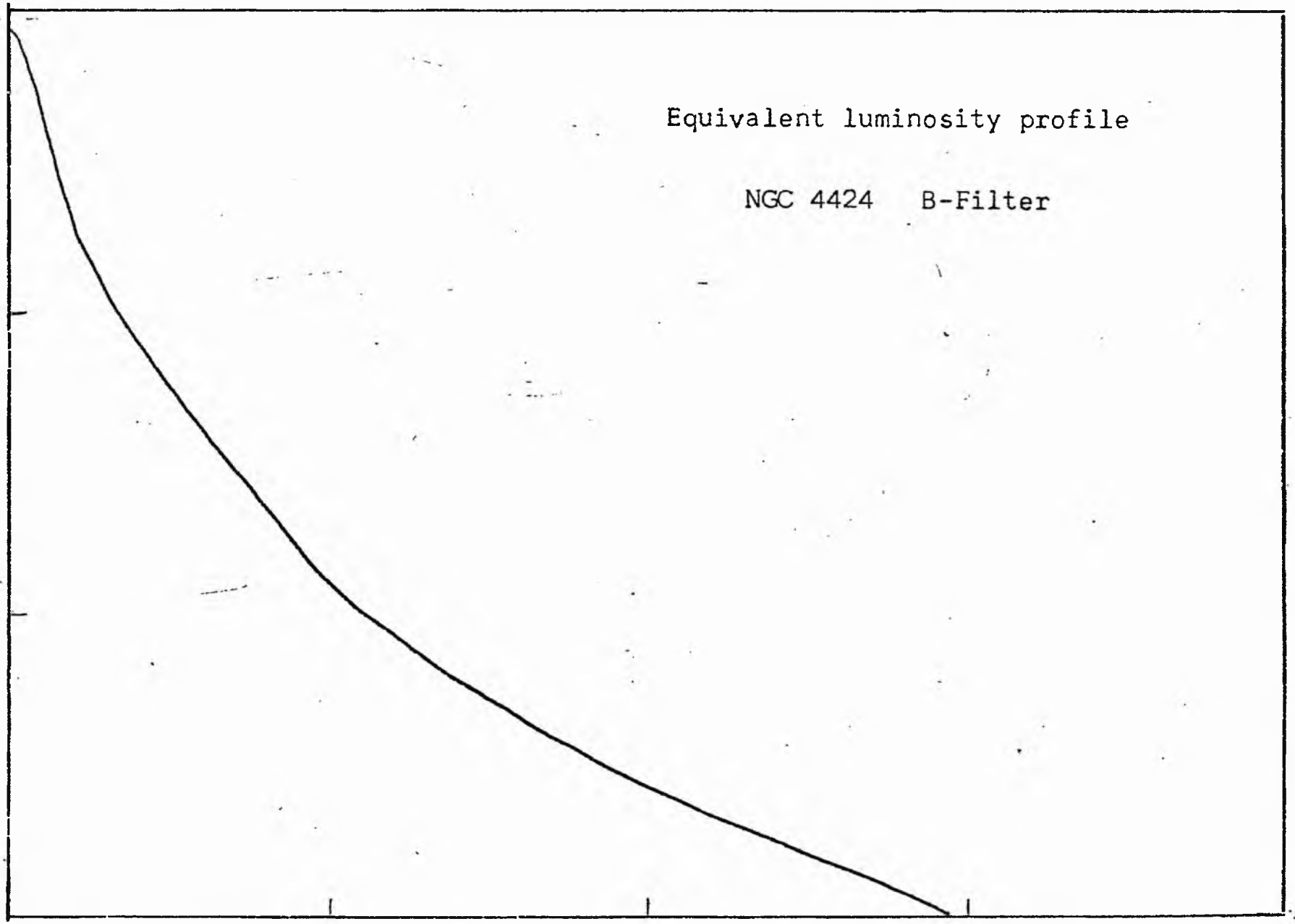
Equivalent luminosity profile
NGC 4424 B-Filter

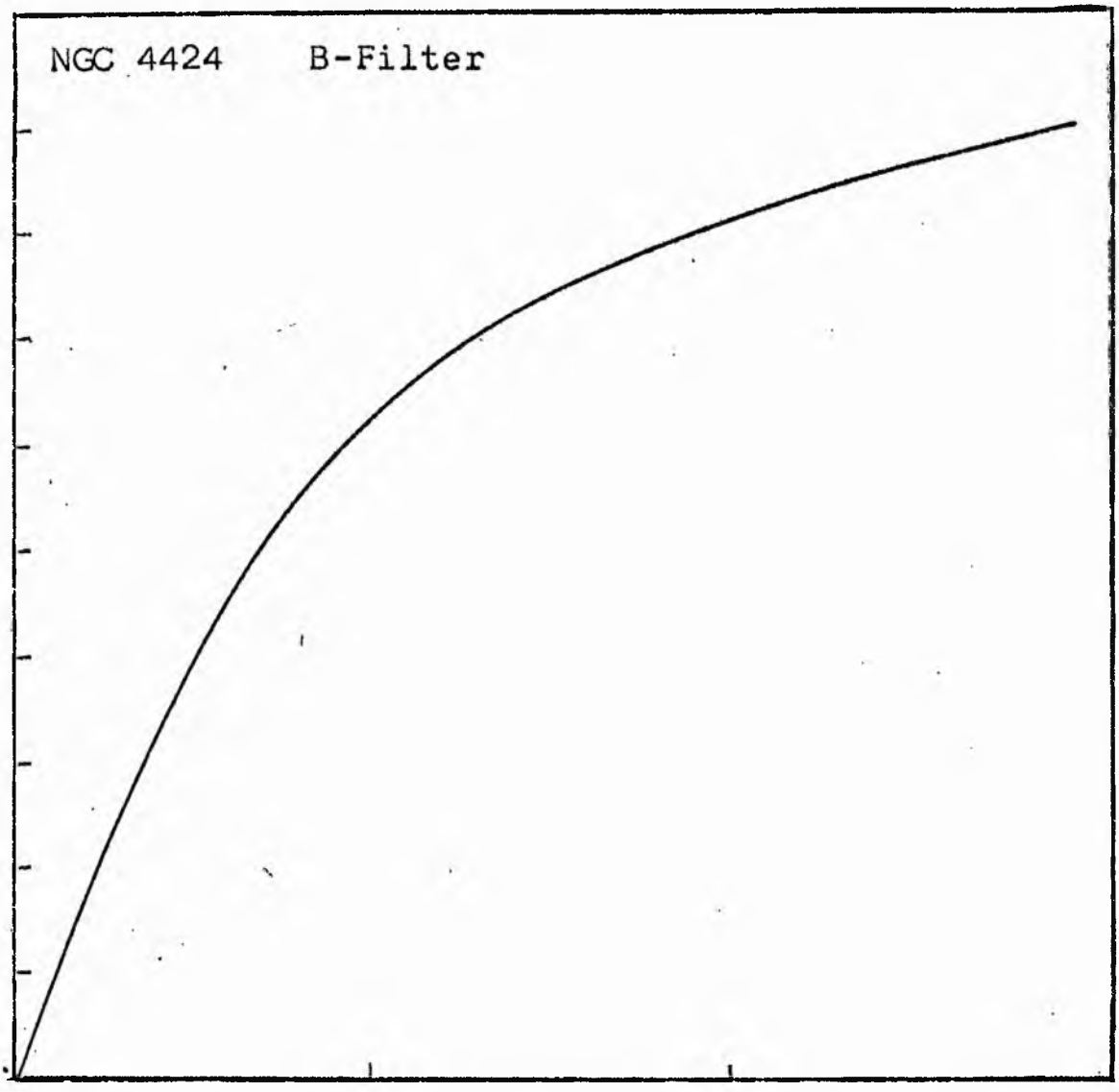

Relative integrated luminosity k(r) versus equivalent radius r*.

MEAN LUMINOSITY DISTRIBUTION IN NGC 4424
B COLOUR

LOG I	I	$\bar{I}$	R	AREA	ΔA	P	ΣP	K(R)	ρ	LOG J	μ
0.88	7.586		0.0	0.0			0.0	0.0	0.0	1.352	19.65
		6.948			49.51	344.0090					
0.80	6.310		3.97	49.51			344.01	0.05	0.12	1.272	19.85
		5.661			21.67	122.6486					
0.70	5.012		4.76	71.18			466.66	0.07	0.14	1.172	20.10
		4.496			31.61	142.1195					
0.60	3.981		5.72	102.79			608.78	0.09	0.17	1.072	20.35
		3.572			42.05	150.1976					
0.50	3.162		6.79	144.84			758.97	0.11	0.20	0.972	20.60
		2.837			61.28	173.8551					
0.40	2.512		8.10	206.12			932.83	0.13	0.24	0.872	20.85
		2.254			106.78	240.6456					
0.30	1.995		9.98	312.90			1173.47	0.17	0.30	0.772	21.10
		1.790			117.15	209.7053					
0.20	1.585		11.70	430.05			1383.18	0.20	0.35	0.672	21.35
		1.422			218.68	310.9382					
0.10	1.259		14.37	648.73			1694.12	0.24	0.43	0.572	21.60
		1.129			281.76	318.2366					
0.00	1.000		17.21	930.49			2012.35	0.29	0.51	0.472	21.85
		0.897			352.68	316.4075					
-0.10	0.794		20.21	1263.16			2328.76	0.33	0.60	0.372	22.10
		0.713			400.49	285.4031					
-0.20	0.631		23.15	1683.65			2614.17	0.38	0.69	0.272	22.35
		0.566			552.61	312.8145					
-0.30	0.501		26.68	2236.25			2926.98	0.42	0.79	0.172	22.60
		0.450			699.64	314.5918					
-0.40	0.398		30.57	2935.90			3241.57	0.47	0.91	0.072	22.85
		0.357			868.70	310.2705					
-0.50	0.316		34.80	3804.59			3551.84	0.51	1.03	-0.028	23.10
		0.284			684.24	194.1237					
-0.60	0.251		37.80	4488.83			3745.97	0.54	1.12	-0.128	23.35
		0.225			843.84	190.1650					
-0.70	0.200		41.20	5332.66			3936.13	0.57	1.22	-0.228	23.60
		0.179			944.52	169.0766					
-0.80	0.158		44.70	6277.18			4105.20	0.59	1.32	-0.328	23.85
		0.142			1639.75	233.1584					
-0.90	0.126		50.20	7916.94			4338.36	0.62	1.49	-0.428	24.10
		0.113			2578.61	291.2451					
-1.00	0.100		57.80	10495.55			4629.60	0.67	1.71	-0.528	24.35
		0.090			2052.72	184.1633					
-1.10	0.079		63.20	12548.27			4813.76	0.69	1.87	-0.628	24.60
		0.071			3199.39	228.0032					
-1.20	0.063		70.80	15747.66			5041.76	0.72	2.10	-0.728	24.85
		0.057			2637.72	149.3150					
-1.30	0.050		76.50	18385.39			5191.07	0.75	2.27	-0.828	25.10
		0.045			4152.67	186.7248					
-1.40	0.040		84.70	22538.05			5377.80	0.77	2.51	-0.928	25.35
		0.036			4926.54	175.9612					
-1.50	0.032		93.50	27464.59			5553.76	0.80	2.77	-1.028	25.60
		0.028			4709.84	133.6232					
-1.60	0.025		101.20	32174.43			5687.38	0.82	3.00	-1.128	25.85
		0.023			9156.64	206.3539					
-1.70	0.020		114.70	41331.07			5893.73	0.85	3.40	-1.228	26.10
		0.018			7442.65	133.2309					
-1.80	0.016		124.60	48773.72			6026.96	0.87	3.69	-1.328	26.35
		0.014			9162.38	130.2825					
-1.90	0.013		135.80	57936.10			6157.24	0.88	4.02	-1.428	26.60
		0.011			9213.65	104.0663					
-2.00	0.010		146.20	67149.75			6261.30	0.90	4.33	-1.528	26.85
- ∞							6961.00	(1)			∞

PHOTOMETRIC PARAMETERS OF NGC 4424

B-FILTER

Total luminosity ..... L_T = 1.93

Total apparent magnitude ..... m_T = 12.24

Apparent central surface brightness ..... μ_o = 19.65

Major axis at threshold ..... $2a_m$ = 5.94

Minor axis at threshold ..... $2b_m$ = 3.85

Major axis at μ=25.0 mag sec^{-2} ..... 2a(25) = 3.68

Luminosity within μ=25.0 mag sec^{-2} ..... k(25) = 0.74

Gradient of exponential component ..... G(a) = -0.89

Equivalent gradient of exponential comp..... G(r*) = -0.67

Equivalent gradient of reduced exp. comp..... G(ρ) = -0.96

Parameters at k = ¼ :

- Semi-major axis ..... a_1 = 0.38
- Axis ratio ..... b/a = 0.48
- Equivalent radius ..... r_1* = 0.25
- Surface brightness ..... μ_1 = 21.65

Parameters at k = ½(effective) :

- Semi-major axis ..... a_e = 1.11
- Axis ratio ..... b/a = 0.32
- Equivalent radius ..... r_e* = 0.56
- Surface brightness ..... μ_e = 23.04
- Mean surface brightness ..... μ_e' = 12.94

Parameters at k = ¾ :

- Semi-major axis ..... a_3 = 1.87
- Axis ratio ..... b/a = 0.51
- Equivalent radius ..... r_3* = 1.30
- Surface brightness ..... μ_3 = 25.10

Concentration indices ..... C_{21} = 2.29, C_{32} = 2.30

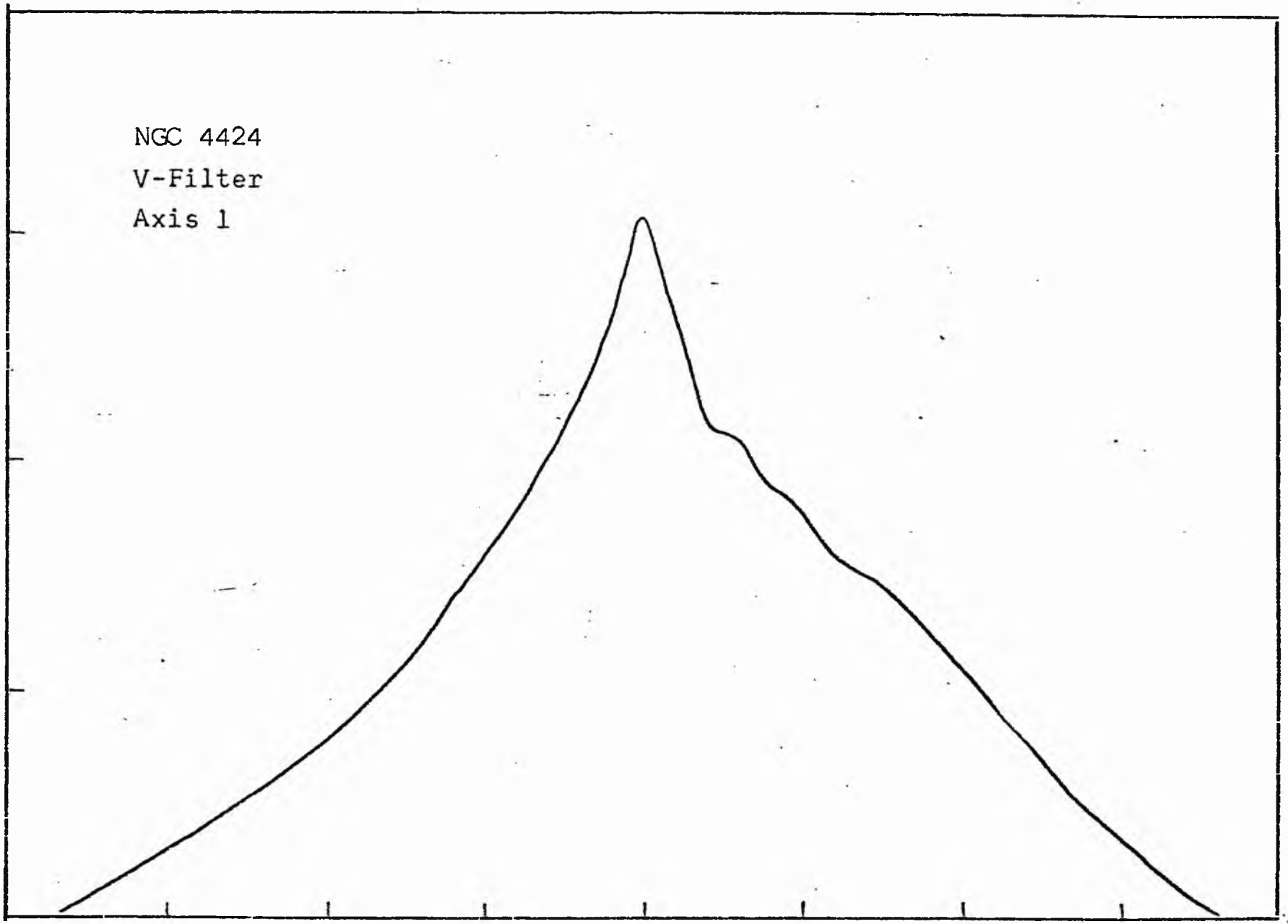
NGC 4424
V-Filter
Axis 1

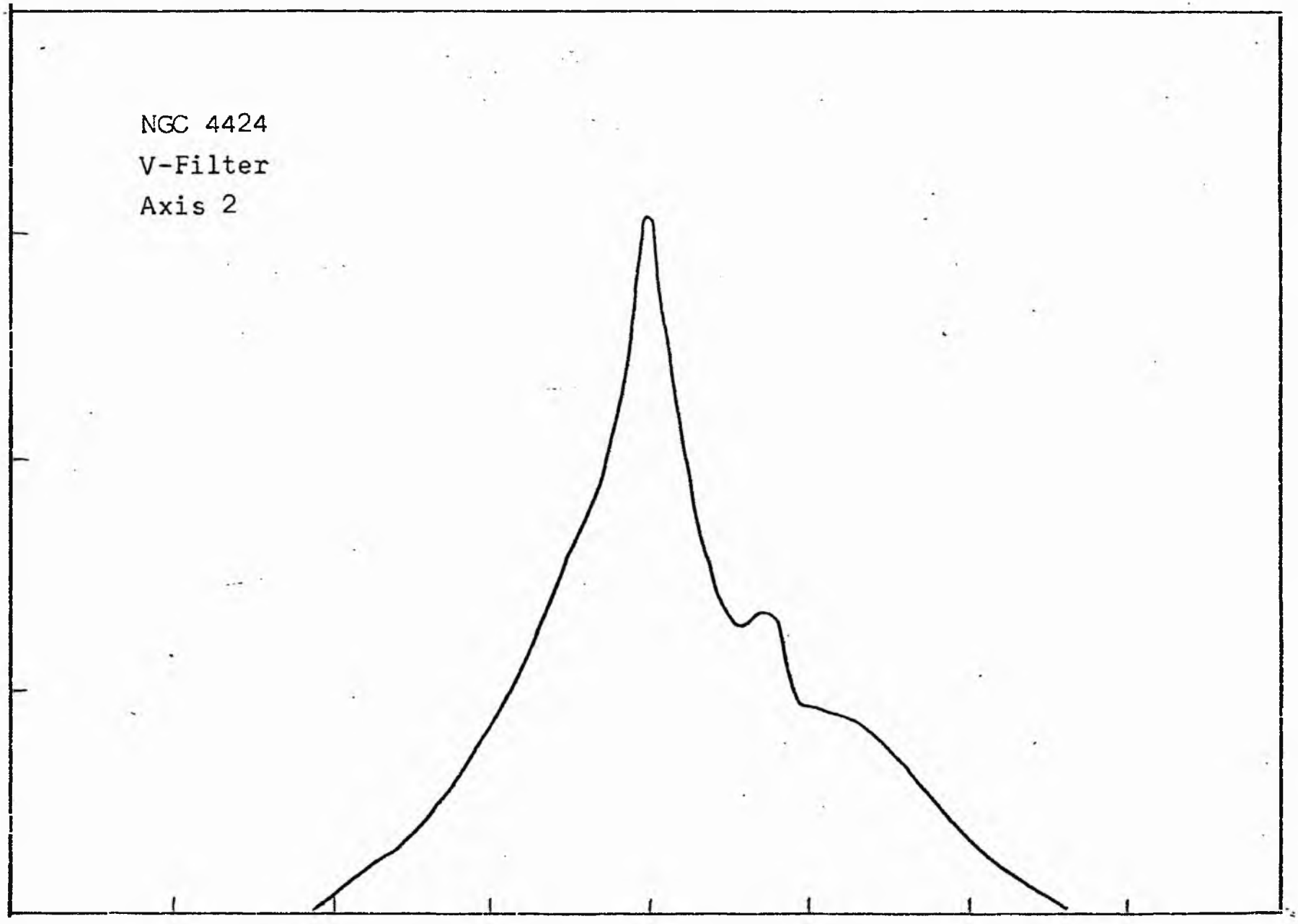
NGC 4424
V-Filter
Axis 2

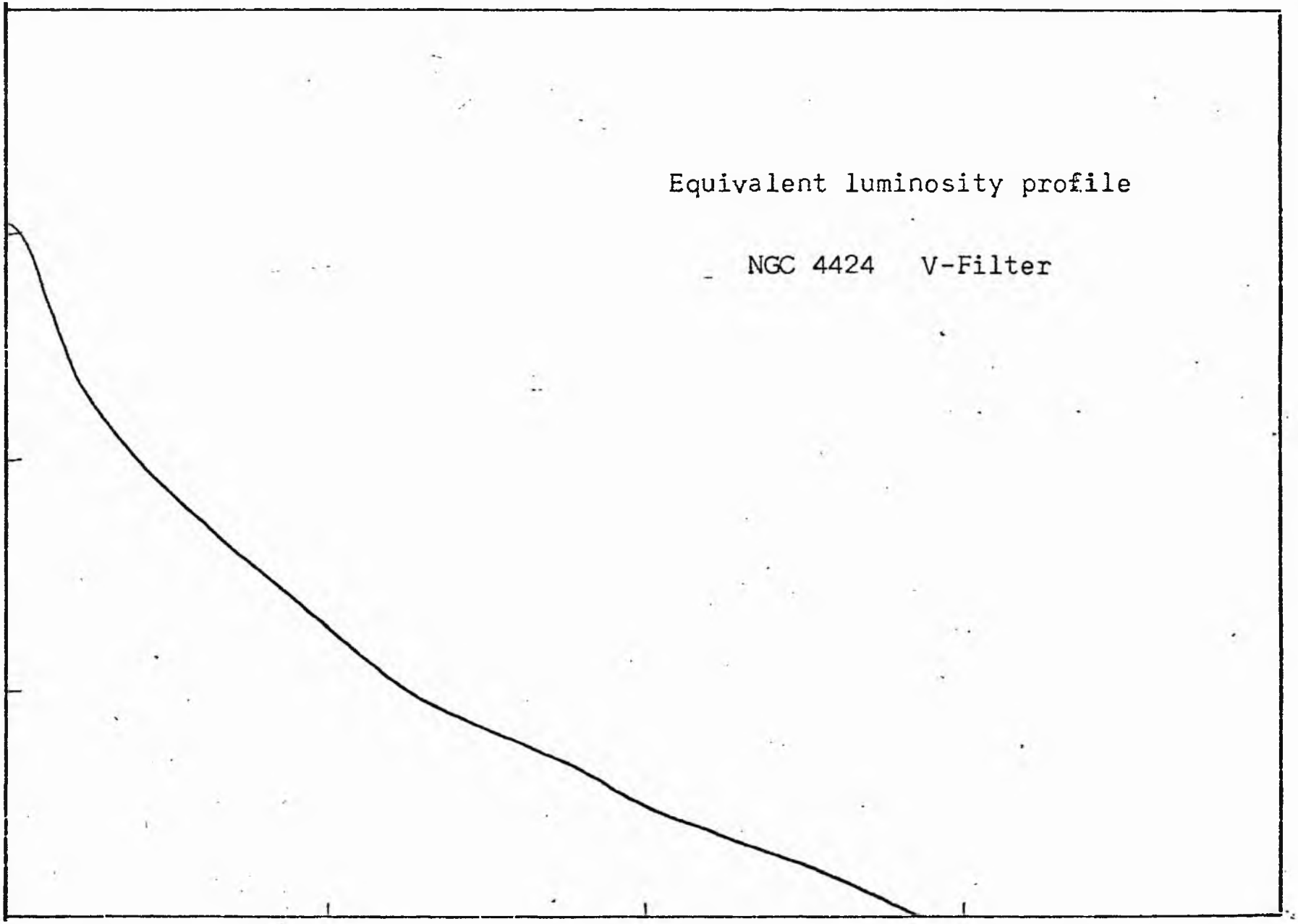
Equivalent luminosity profile
NGC 4424 V-Filter

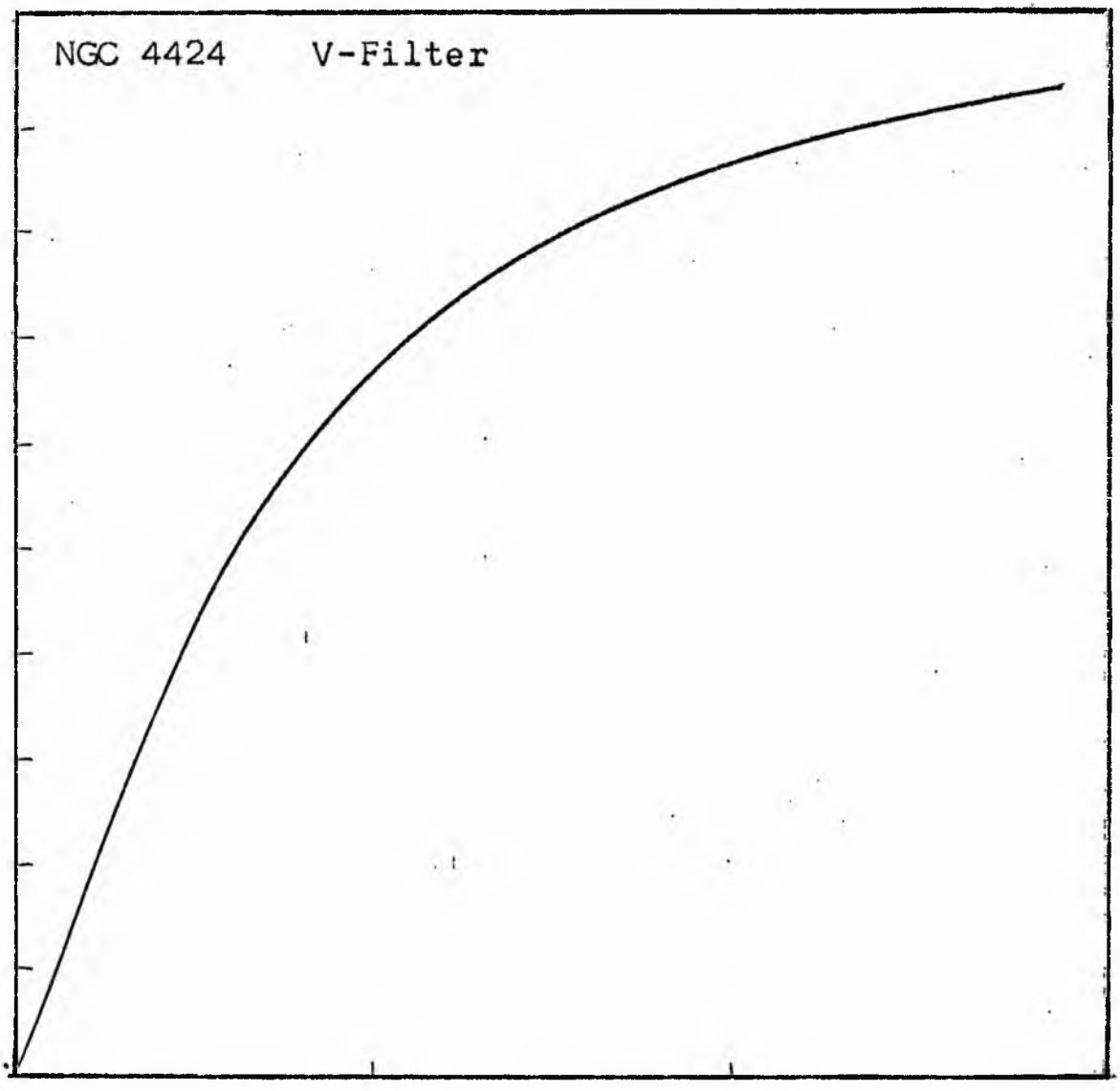

Relative integrated luminosity k(r) versus equivalent radius r*.

MEAN LUMINOSITY DISTRIBUTION IN NGC 4424
V COLOUR

LOG I	I	$\bar{I}$	R	AREA	ΔA	P	ΣP	K(R)	ρ	LOG J	μ
1.03	10.715		0.0	0.0			0.0	0.0	0.0	1.324	18.91
		10.358			28.46	294.8091					
1.00	10.000		3.01	28.46			294.81	0.03	0.10	1.294	18.99
		8.972			34.31	307.8047					
0.90	7.943		4.47	62.77			602.61	0.07	0.14	1.194	19.24
		7.126			20.87	148.7640					
0.80	6.310		5.16	83.65			751.38	0.08	0.17	1.094	19.49
		5.661			54.86	310.5740					
0.70	5.012		6.64	138.51			1061.95	0.12	0.21	0.994	19.74
		4.496			59.05	265.5039					
0.60	3.981		7.93	197.56			1327.46	0.15	0.25	0.894	19.99
		3.572			72.41	258.6152					
0.50	3.162		9.27	269.97			1586.07	0.18	0.30	0.794	20.24
		2.837			69.83	198.1089					
0.40	2.512		10.40	339.79			1784.18	0.20	0.33	0.694	20.49
		2.254			130.10	293.1958					
0.30	1.995		12.23	469.90			2077.38	0.23	0.39	0.594	20.74
		1.790			237.90	425.8667					
0.20	1.585		15.01	707.80			2503.24	0.28	0.48	0.494	20.99
		1.422			292.06	415.2817					
0.10	1.259		17.84	999.86			2918.52	0.32	0.57	0.394	21.24
		1.129			359.32	405.8347					
0.00	1.000		20.80	1359.18			3324.36	0.37	0.67	0.294	21.49
		0.897			375.77	337.1255					
-0.10	0.794		23.50	1734.94			3661.48	0.41	0.75	0.194	21.74
		0.713			585.91	417.5469					
-0.20	0.631		27.18	2320.86			4079.03	0.45	0.87	0.094	21.99
		0.566			802.33	454.1753					
-0.30	0.501		31.53	3123.19			4533.20	0.50	1.01	-0.006	22.24
		0.450			1050.74	472.4631					
-0.40	0.398		36.45	4173.93			5005.66	0.56	1.17	-0.106	22.49
		0.357			1352.02	482.8965					
-0.50	0.316		41.94	5525.94			5488.56	0.61	1.34	-0.206	22.74
		0.284			1410.88	400.2786					
-0.60	0.251		46.99	6936.82			5888.84	0.65	1.50	-0.306	22.99
		0.225			854.45	192.5569					
-0.70	0.200		49.80	7791.27			6081.39	0.67	1.59	-0.406	23.24
		0.179			801.89	143.5449					
-0.80	0.158		52.30	8593.16			6224.93	0.69	1.67	-0.506	23.49
		0.142			1506.71	214.2411					
-0.90	0.126		56.70	10099.87			6439.17	0.71	1.81	-0.606	23.74
		0.113			1743.80	196.9566					
-1.00	0.100		61.40	11843.68			6636.12	0.74	1.96	-0.706	23.99
		0.090			4669.32	418.9158					
-1.10	0.079		72.50	16513.00			7055.04	0.78	2.32	-0.806	24.24
		0.071			3044.07	216.9343					
-1.20	0.063		78.90	19557.07			7271.97	0.81	2.52	-0.906	24.49
		0.057			3949.12	223.5498					
-1.30	0.050		86.50	23506.18			7495.52	0.83	2.77	-1.006	24.74
		0.045			3257.94	146.4934					
-1.40	0.040		92.30	26764.12			7642.01	0.85	2.95	-1.106	24.99
		0.036			2856.09	102.0111					
-1.50	0.032		97.10	29620.21			7744.02	0.86	3.11	-1.206	25.24
		0.028			4686.77	132.9686					
-1.60	0.025		104.50	34306.98			7876.98	0.87	3.34	-1.306	25.49
		0.023			8112.18	182.8160					
-1.70	0.020		116.20	42419.16			8059.80	0.89	3.72	-1.406	25.74
		0.018			9860.09	176.5054					
-1.80	0.016		129.00	52279.25			8236.30	0.91	4.13	-1.506	25.99
		0.014			6685.31	95.0604					
-1.90	0.013		137.00	58964.56			8331.36	0.92	4.38	-1.606	26.24
		0.011			7269.75	82.1104					
-2.00	0.010		145.20	66234.31			8413.47	0.93	4.64	-1.706	26.49
							9013.00	(1)			
$-\infty$											∞

PHOTOMETRIC PARAMETERS OF NGC 4424

V-FILTER

Total luminosity	L_T	= 2.50
Total apparent magnitude	m_T	= 11.60
Apparent central surface brightness	μ_o	= 18.91
Major axis at threshold	$2a_m$	= 5.76
Minor axis at threshold	$2b_m$	= 3.81
Major axis at μ=25.0 mag sec^{-2}	2a(25)	= 4.11
Luminosity within μ=25.0 mag sec^{-2}	k(25)	= 0.85
Gradient of exponential component	G(a)	= -0.69
Equivalent gradient of exponential comp.	G(r*)	= -0.83
Equivalent gradient of reduced exp. comp.	G(ρ)	= -0.77
Parameters at k = ¼ :		
Semi-major axis	a_1	= 0.31
Axis ratio	b/a	= 0.72
Equivalent radius	r_1*	= 0.22
Surface brightness	μ_1	= 20.84
Parameters at k = ½(effective) :		
Semi-major axis	a_e	= 0.88
Axis ratio	b/a	= 0.44
Equivalent radius	r_e*	= 0.52
Surface brightness	μ_e	= 22.24
Mean surface brightness	μ_e'	= 12.15
Parameters at k = ¾ :		
Semi-major axis	a_3	= 1.76
Axis ratio	b/a	= 0.45
Equivalent radius	r_3*	= 1.07
Surface brightness	μ_3	= 24.06
Concentration indices	C_{21}	= 2.34
	C_{32}	= 2.06

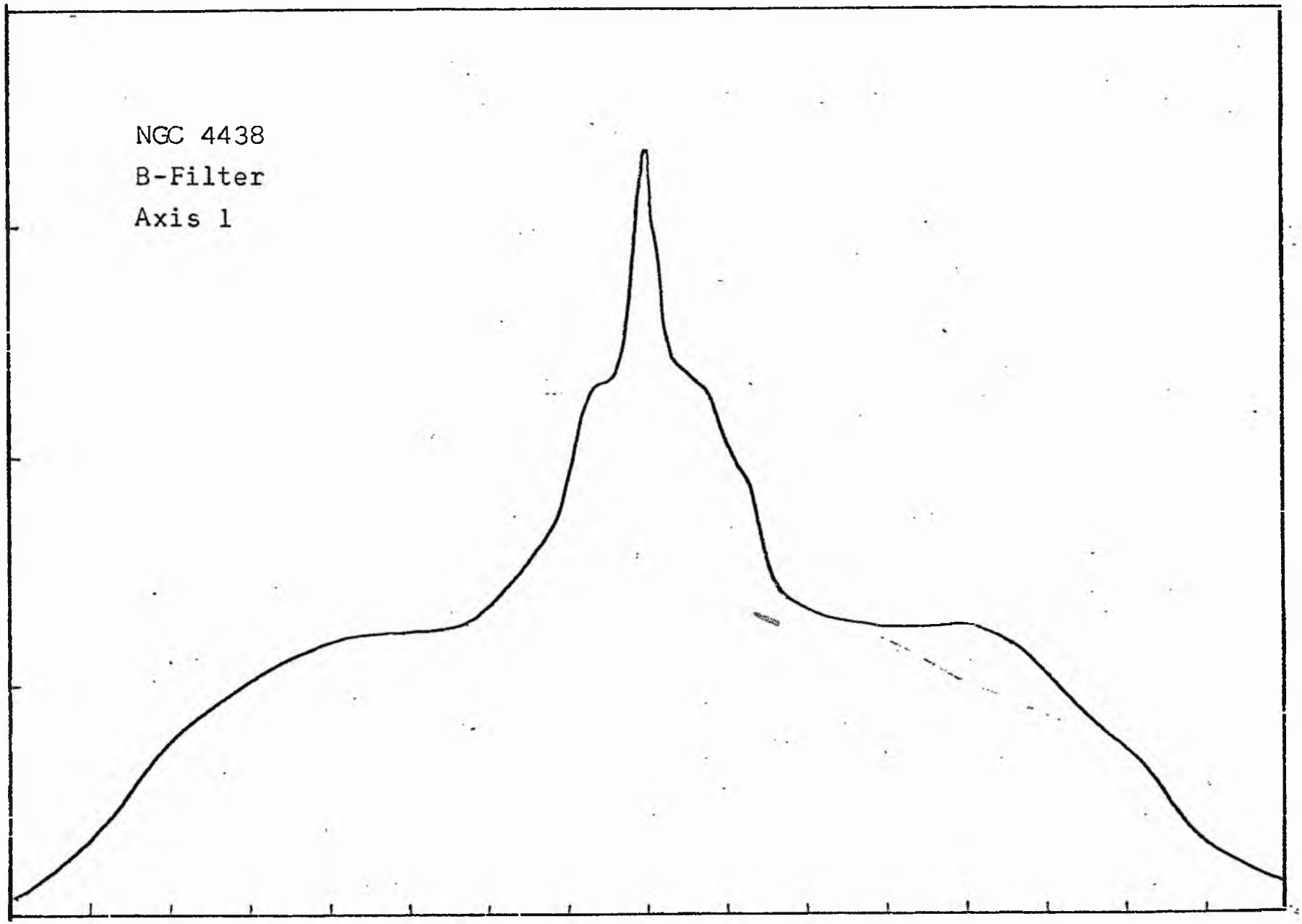
NGC 4438
B-Filter
Axis 1

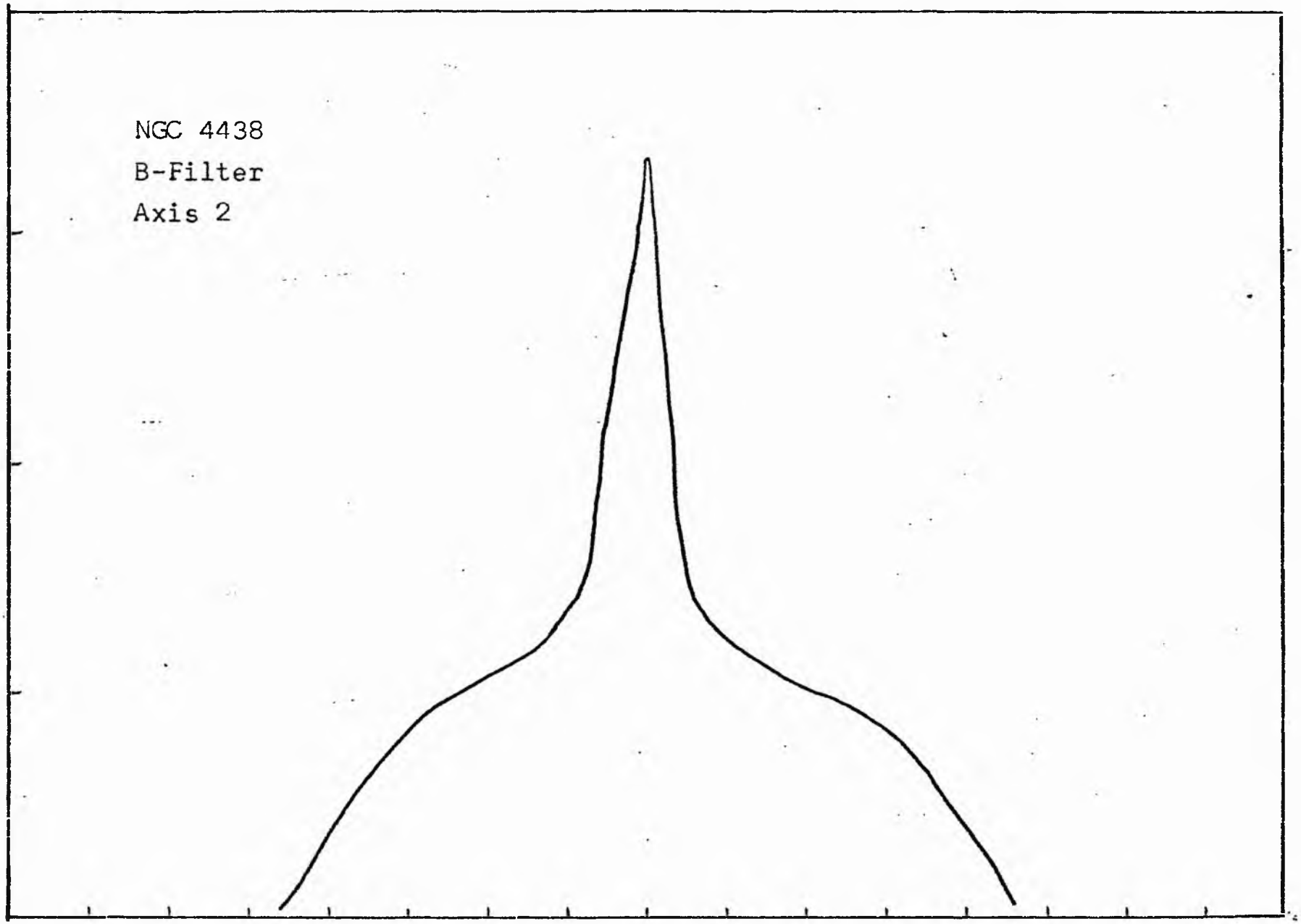
NGC 4438
B-Filter
Axis 2

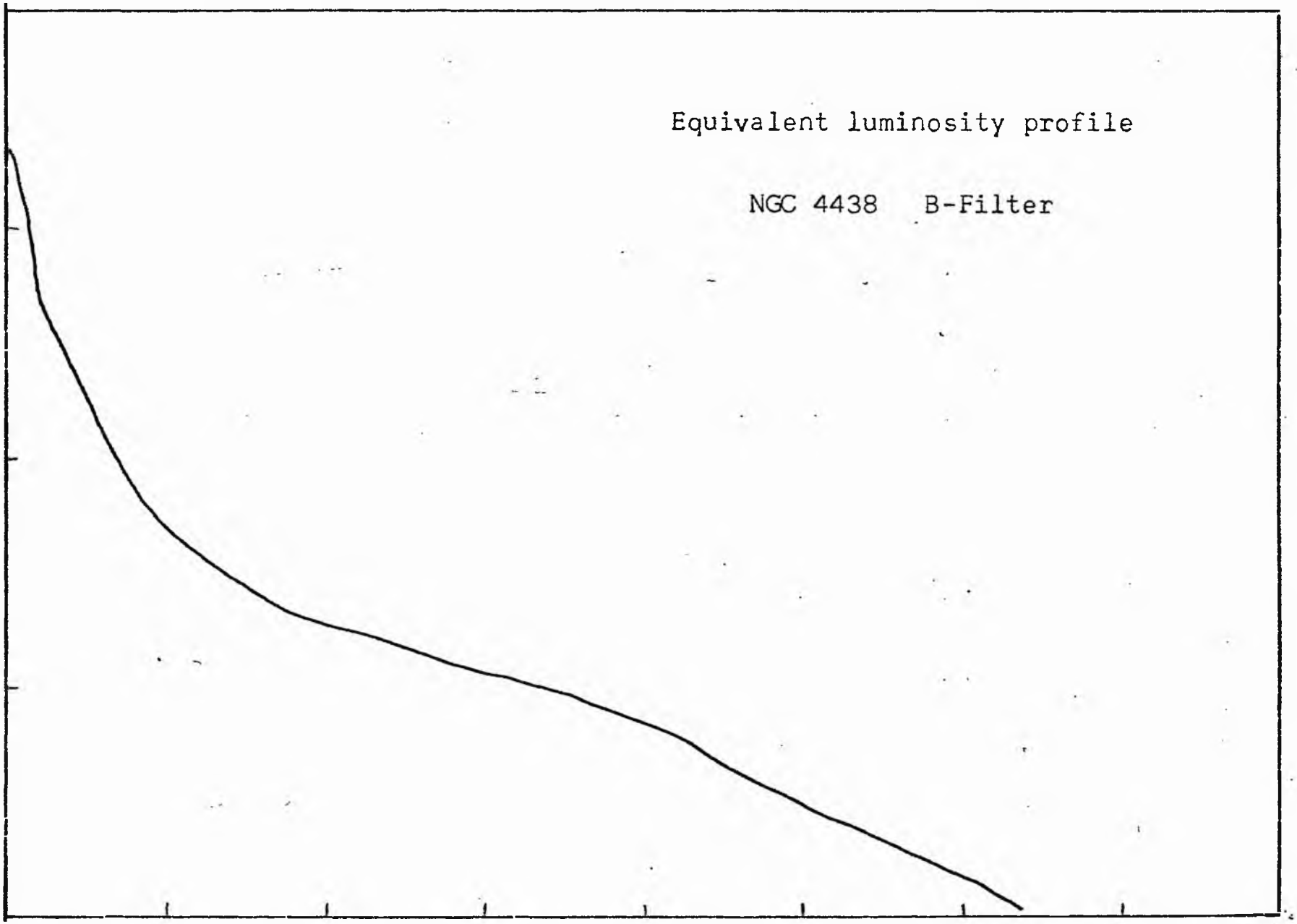
Equivalent luminosity profile
NGC 4438 B-Filter

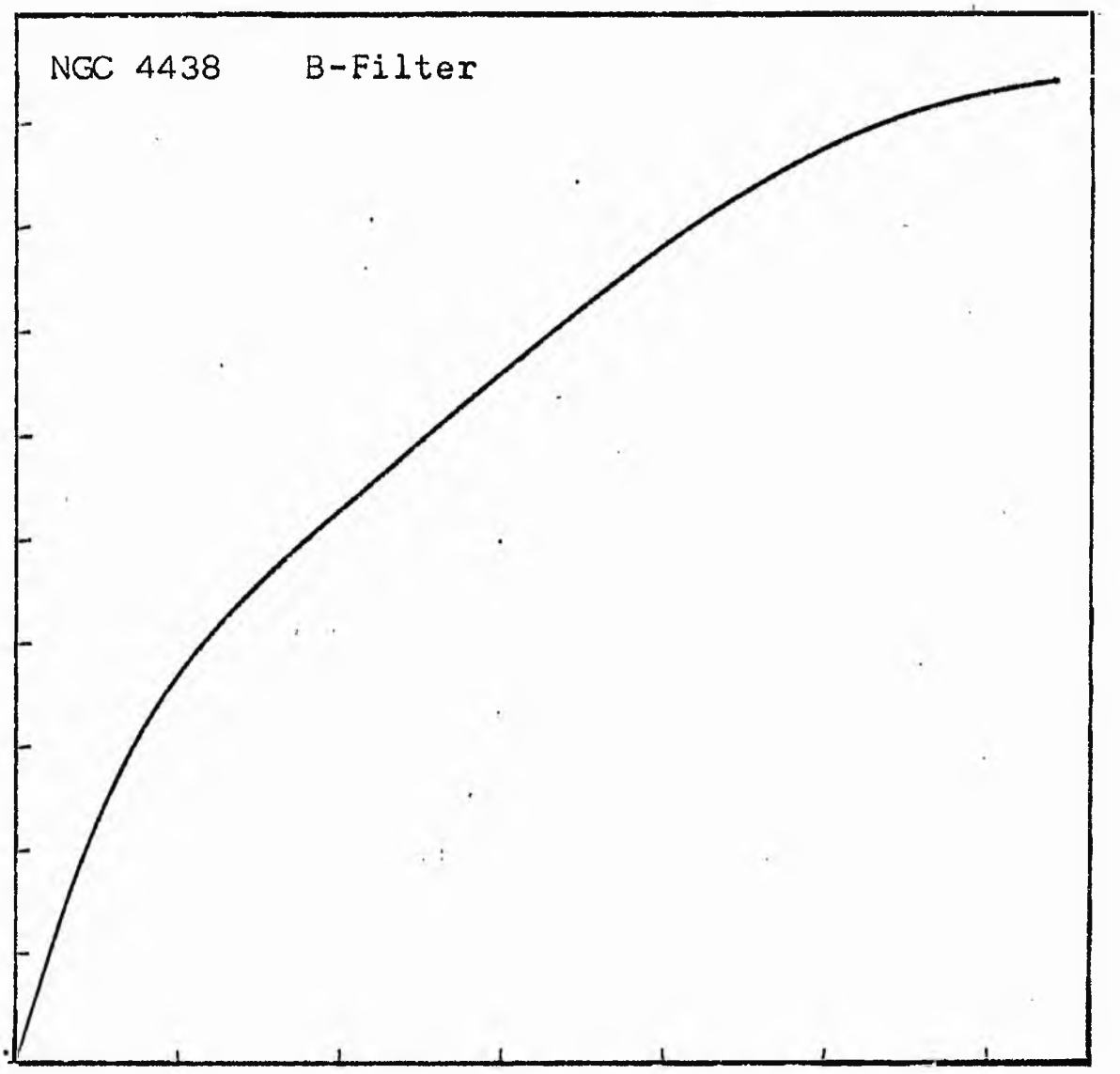

Relative integrated luminosity k(r) versus equivalent radius r*.

MEAN LUMINOSITY DISTRIBUTION IN NGC 4438
B COLOUR

LOG I	I	$\bar{I}$	R	AREA	ΔA	P	ΣP	R(R)	ρ	LOG μ	μ
1.35	22.387		0.0	0.0			0.0	0.0	0.0	2.028	18.97
		21.170			21.24	449.5876					
1.30	19.953		2.60	21.24			449.59	0.01	0.03	1.978	19.10
		17.901			48.16	862.1099					
1.20	15.849		4.70	69.40			1311.70	0.03	0.05	1.878	19.35
		14.219			47.50	675.4167					
1.10	12.589		6.10	116.90			1987.11	0.05	0.07	1.778	19.60
		11.295			32.67	369.0225					
1.00	10.000		6.90	149.57			2356.14	0.06	0.08	1.678	19.85
		8.972			61.67	553.2742					
0.90	7.943		8.20	211.24			2909.41	0.07	0.09	1.578	20.10
		7.126			96.67	688.8848					
0.80	6.310		9.90	307.91			3598.30	0.09	0.11	1.478	20.35
		5.661			114.83	649.9927					
0.70	5.012		11.60	422.73			4248.29	0.11	0.13	1.378	20.60
		4.496			108.20	486.5007					
0.60	3.981		13.00	530.93			4734.79	0.12	0.15	1.278	20.85
		3.572			544.28	1943.9873					
0.50	3.162		18.50	1075.21			6678.77	0.17	0.21	1.178	21.10
		2.837			168.89	479.1548					
0.40	2.512		19.90	1244.10			7157.92	0.18	0.22	1.078	21.35
		2.254			672.55	1515.6440					
0.30	1.995		24.70	1916.65			8673.56	0.22	0.28	0.978	21.60
		1.790			954.30	1708.2639					
0.20	1.585		30.23	2870.95			10381.82	0.27	0.34	0.878	21.85
		1.422			392.45	558.0227					
0.10	1.259		32.23	3263.40			10939.84	0.28	0.36	0.778	22.10
		1.129			673.92	760.7095					
-0.00	1.000		35.40	3936.92			11700.55	0.30	0.40	0.678	22.35
		0.897			480.95	431.4866					
-0.10	0.794		37.50	4417.86			12132.04	0.31	0.42	0.578	22.60
		0.713			1283.37	914.5796					
-0.20	0.631		42.60	5701.23			13046.61	0.33	0.48	0.478	22.85
		0.566			1567.18	887.1365					
-0.30	0.501		48.10	7268.41			13933.75	0.36	0.54	0.378	23.10
		0.450			2831.46	1273.1538					
-0.40	0.398		56.70	10099.87			15206.90	0.39	0.63	0.278	23.35
		0.357			4641.27	1657.7051					
-0.50	0.316		68.50	14741.14			16864.60	0.43	0.76	0.178	23.60
		0.284			3885.37	1102.3081					
-0.60	0.251		77.00	18626.50			17966.91	0.46	0.86	0.078	23.85
		0.225			8662.12	1952.0696					
-0.70	0.200		93.20	27288.62			19918.97	0.51	1.04	-0.022	24.10
		0.179			11209.99	2006.6709					
-0.80	0.158		110.70	38498.61			21925.64	0.56	1.24	-0.122	24.35
		0.142			16822.61	2392.0178					
-0.90	0.126		132.70	55321.22			24317.66	0.62	1.48	-0.222	24.60
		0.113			32714.84	3695.0176					
-1.00	0.100		167.40	88036.06			28012.67	0.72	1.87	-0.322	24.85
		0.090			18904.50	1696.0454					
-1.10	0.079		184.50	106940.56			29708.71	0.76	2.06	-0.422	25.10
		0.071			29500.56	2102.3411					
-1.20	0.063		208.40	136441.12			31811.05	0.82	2.33	-0.522	25.35
		0.057			16719.75	946.4614					
-1.30	0.050		220.60	153160.87			32757.52	0.84	2.46	-0.622	25.60
		0.045			23895.37	1074.4534					
-1.40	0.040		237.40	177056.25			33831.97	0.87	2.65	-0.722	25.85
		0.036			21340.62	762.2219					
-1.50	0.032		251.30	198396.87			34594.19	0.89	2.80	-0.822	26.10
		0.028			16103.37	456.8691					
-1.60	0.025		261.30	214500.25			35051.05	0.90	2.92	-0.922	26.35
		0.023			21529.75	485.1931					
-1.70	0.020		274.10	236030.00			35536.25	0.91	3.06	-1.022	26.60
		0.018			34593.87	619.2634					
-1.80	0.016		293.50	270623.87			36155.51	0.93	3.28	-1.122	26.85
		0.014			32648.00	464.2300					
-1.90	0.013		310.70	303271.87			36619.73	0.94	3.47	-1.222	27.10
		0.011			14818.12	167.3673					
-2.00	0.010		318.20	318090.00			36787.10	0.94	3.55	-1.322	27.35
$-\infty$							38987.00	(1)			∞

PHOTOMETRIC PARAMETERS OF NGC 4438

B-FILTER

Total luminosity ..... L_T = 10.83

Total apparent magnitude ..... m_T = 10.86

Apparent central surface brightness ..... μ_o = 18.97

Major axis at threshold ..... $2a_m$ = 14.15

Minor axis at threshold ..... $2b_m$ = 7.85

Major axis at μ=25.0 mag sec^{-2} ..... 2a(25) = 8.70

Luminosity within μ=25.0 mag sec^{-2} ..... k(25) = 0.74

Gradient of exponential component ..... G(a) = -0.40

Equivalent gradient of exponential comp..... G(r*) = -0.33

Equivalent gradient of reduced exp. comp..... G(ρ) = -0.53

Parameters at k = ¼ :

- Semi-major axis ..... a_1 = 0.68
- Axis ratio ..... b/a = 0.54
- Equivalent radius ..... r_1* = 0.47
- Surface brightness ..... μ_1 = 21.75

Parameters at k = ½(effective) :

- Semi-major axis ..... a_e = 1.97
- Axis ratio ..... b/a = 0.42
- Equivalent radius ..... r_e* = 1.50
- Surface brightness ..... μ_e = 24.05
- Mean surface brightness ..... μ_e' = 13.74

Parameters at k = ¾ :

- Semi-major axis ..... a_3 = 4.43
- Axis ratio ..... b/a = 0.47
- Equivalent radius ..... r_3* = 2.99
- Surface brightness ..... μ_3 = 25.04

Concentration indices ..... C_{21} = 3.19, C_{32} = 2.00

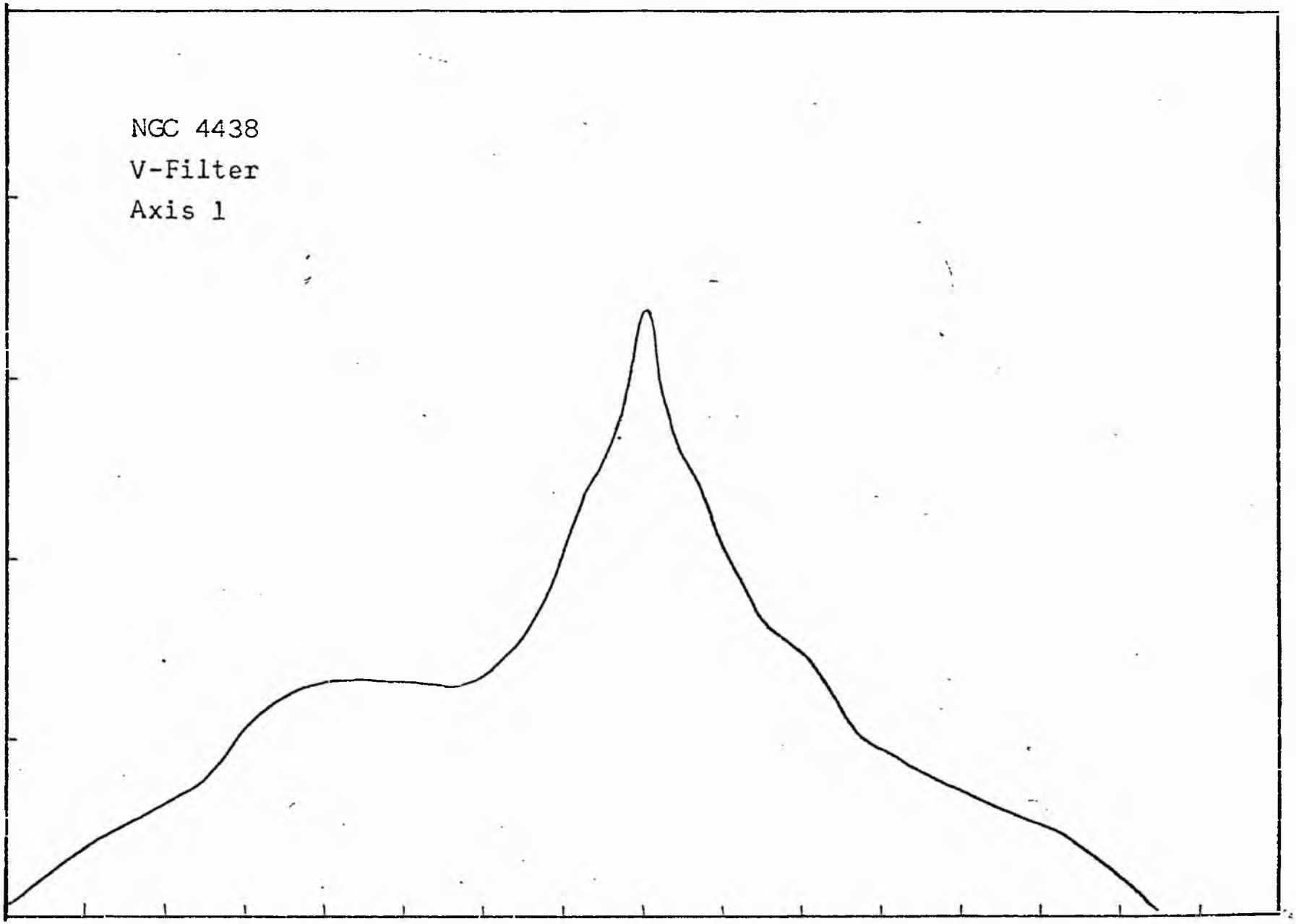
NGC 4438
V-Filter
Axis 1

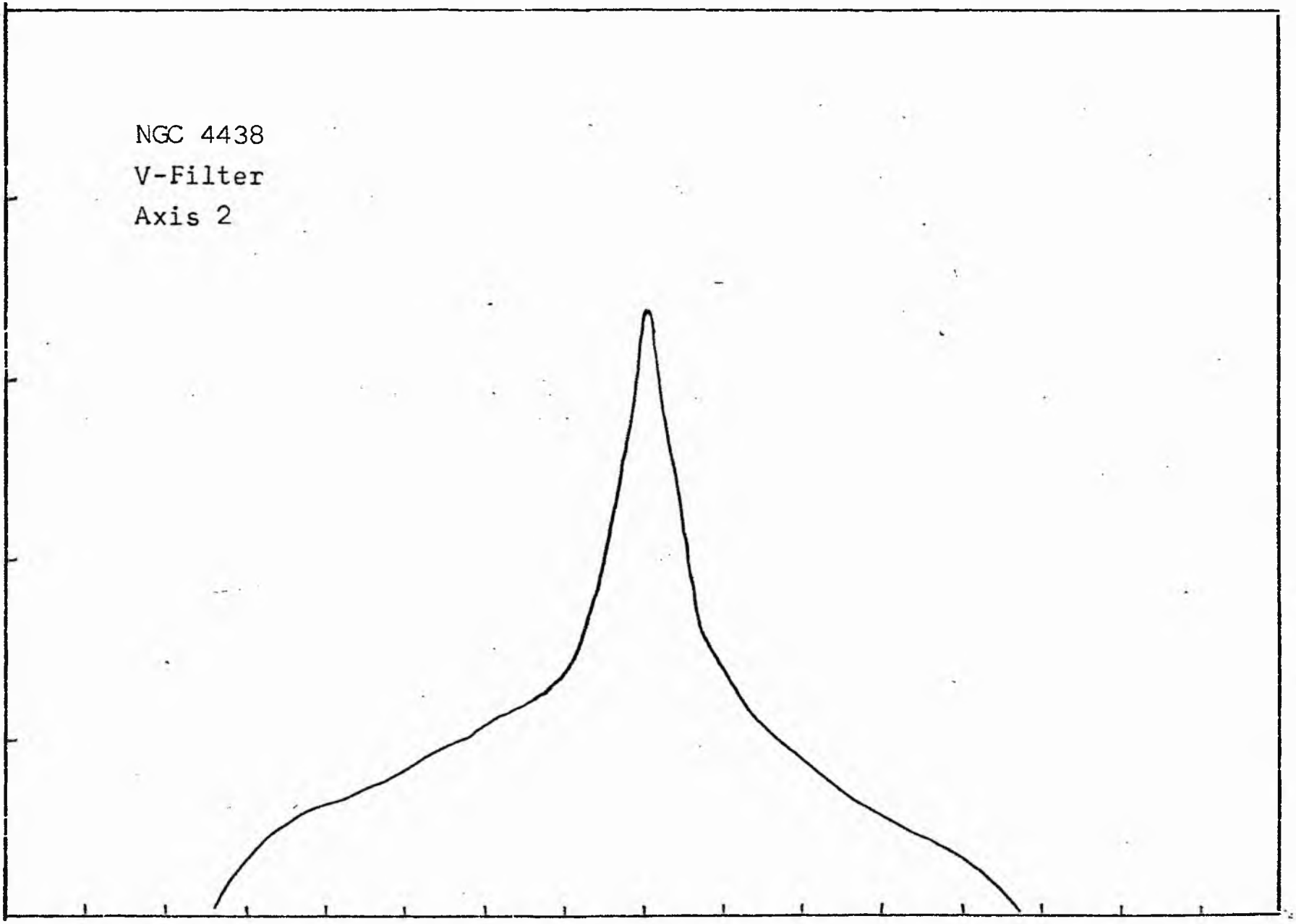
NGC 4438
V-Filter
Axis 2

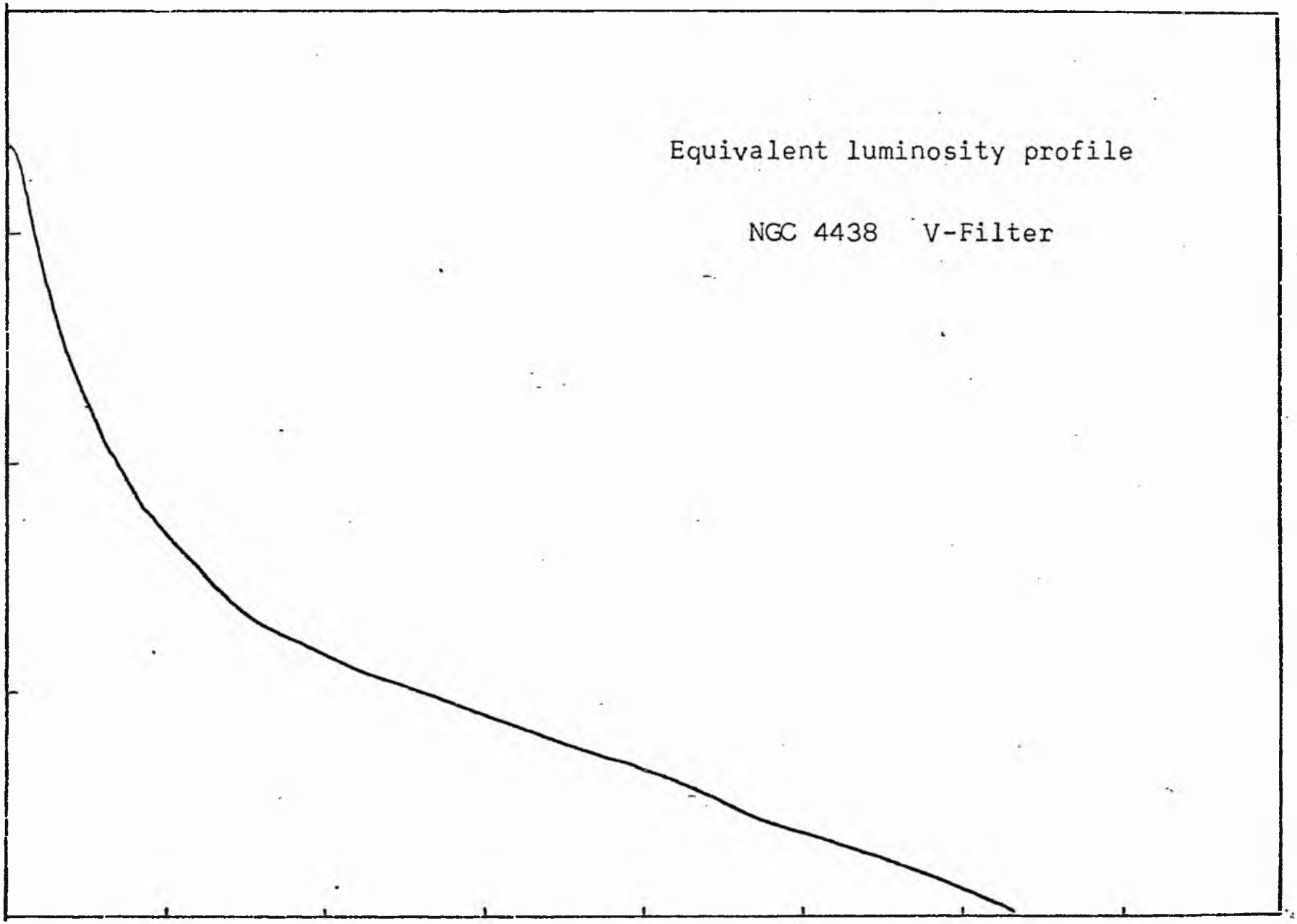
Equivalent luminosity profile
NGC 4438 V-Filter

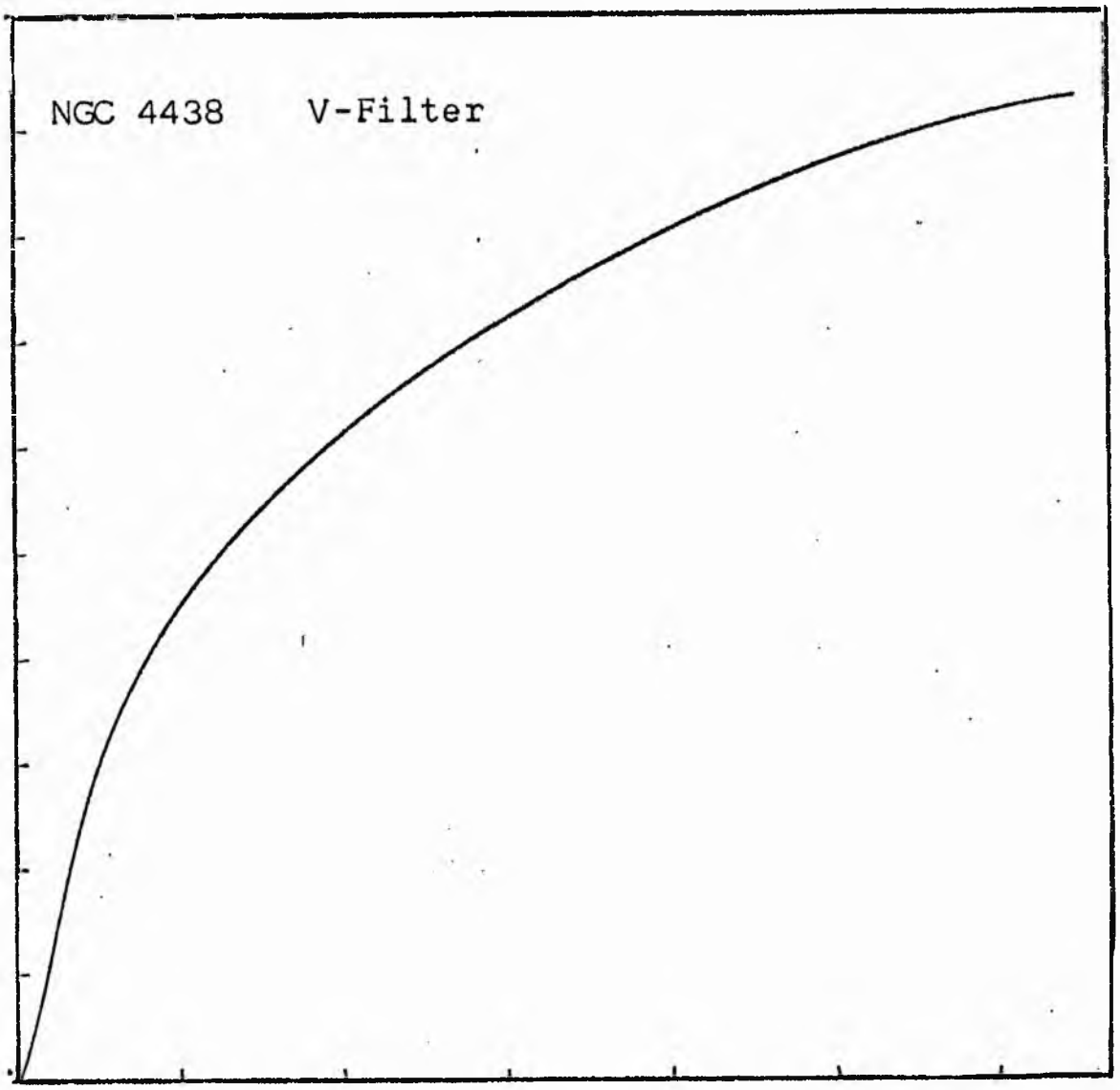

Relative integrated luminosity k(r) versus equivalent radius r*.

MEAN LUMINOSITY DISTRIBUTION IN NGC 4438
V COLOUR

LOG I	I	$\bar{I}$	R	AREA	ΔA	P	ΣP	K(R)	ρ_i	LOG J	μ
1.37	23.442		0.0	0.0			0.0	0.0	0.0	1.812	18.09
		21.697			66.48	1442.3586					
1.30	19.953		4.60	66.48			1442.36	0.04	0.08	1.742	18.27
		17.901			42.88	767.6321					
1.20	15.849		5.90	109.36			2209.99	0.06	0.10	1.642	18.52
		14.219			40.21	571.7815					
1.10	12.589		6.90	149.57			2781.77	0.08	0.11	1.542	18.77
		11.295			118.65	1340.1045					
1.00	10.000		9.24	268.22			4121.87	0.11	0.15	1.442	19.02
		8.972			93.48	838.6565					
0.90	7.943		10.73	361.70			4960.53	0.13	0.18	1.342	19.27
		7.126			151.41	1079.0132					
0.80	6.310		12.78	513.11			6039.54	0.16	0.21	1.242	19.52
		5.661			230.01	1302.0461					
0.70	5.012		15.38	743.13			7341.59	0.20	0.25	1.142	19.77
		4.496			277.01	1245.5720					
0.60	3.981		18.02	1020.14			8587.16	0.23	0.30	1.042	20.02
		3.572			201.56	719.8948					
0.50	3.162		19.72	1221.70			9307.05	0.25	0.32	0.942	20.27
		2.837			392.86	1114.5703					
0.40	2.512		22.67	1614.55			10421.62	0.28	0.37	0.842	20.52
		2.254			402.71	907.5339					
0.30	1.995		25.34	2017.26			11329.15	0.31	0.42	0.742	20.77
		1.790			579.46	1037.2722					
0.20	1.585		28.75	2596.72			12366.42	0.34	0.47	0.642	21.02
		1.422			721.58	1026.0242					
0.10	1.259		32.50	3318.31			13392.45	0.36	0.53	0.542	21.27
		1.129			574.25	648.5925					
-0.00	1.000		35.20	3892.56			14041.04	0.38	0.58	0.442	21.52
		0.897			836.91	750.8477					
-0.10	0.794		38.80	4729.47			14791.88	0.40	0.64	0.342	21.77
		0.713			1160.66	827.1365					
-0.20	0.631		43.30	5890.14			15619.02	0.42	0.71	0.242	22.02
		0.566			2185.29	1237.0298					
-0.30	0.501		50.70	8075.43			16856.04	0.46	0.83	0.142	22.27
		0.450			2639.16	1186.6863					
-0.40	0.398		58.40	10714.59			18042.73	0.49	0.96	0.042	22.52
		0.357			2233.92	797.8809					
-0.50	0.316		64.20	12948.50			18840.61	0.51	1.05	-0.058	22.77
		0.284			3022.37	857.4695					
-0.60	0.251		71.30	15970.87			19698.07	0.53	1.17	-0.158	23.02
		0.225			5359.78	1207.8633					
-0.70	0.200		82.40	21330.65			20905.94	0.57	1.35	-0.258	23.27
		0.179			6843.42	1225.0232					
-0.80	0.158		94.70	28174.07			22130.96	0.60	1.55	-0.358	23.52
		0.142			11445.45	1627.4363					
-0.90	0.126		112.30	39619.52			23758.39	0.65	1.84	-0.458	23.77
		0.113			12174.52	1375.0657					
-1.00	0.100		128.40	51794.04			25133.45	0.68	2.10	-0.558	24.02
		0.090			16277.46	1460.3562					
-1.10	0.079		147.20	68071.50			26593.81	0.72	2.41	-0.658	24.27
		0.071			20913.75	1490.4067					
-1.20	0.063		168.30	88985.25			28084.21	0.76	2.76	-0.758	24.52
		0.057			18768.31	1062.4250					
-1.30	0.050		185.20	107753.56			29146.64	0.79	3.03	-0.858	24.77
		0.045			26990.56	1213.6282					
-1.40	0.040		207.10	134744.12			30360.26	0.82	3.39	-0.958	25.02
		0.036			32894.37	1174.8867					
-1.50	0.032		231.00	167638.50			31535.15	0.86	3.79	-1.058	25.27
		0.028			37124.50	1053.2603					
-1.60	0.025		255.30	204763.00			32588.41	0.88	4.18	-1.158	25.52
		0.023			27664.56	623.4470					
-1.70	0.020		272.00	232427.56			33211.85	0.90	4.46	-1.258	25.77
		0.018			28148.69	503.8884					
-1.80	0.016		288.00	260576.25			33715.74	0.92	4.72	-1.358	26.02
		0.014			29947.81	425.8354					
-1.90	0.013		304.10	290524.06			34141.57	0.93	4.98	-1.458	26.27
		0.011			25171.44	284.3054					
-2.00	0.010		317.00	315695.50			34425.87	0.93	5.19	-1.558	26.52
$-\infty$							36825.00	(1)			∞

PHOTOMETRIC PARAMETERS OF NGC 4438

V-FILTER

Total luminosity ..... L_T = 10.23

Total apparent magnitude ..... m_T = 10.10

Apparent central surface brightness ..... μ_o = 18.09

Major axis at threshold ..... $2a_m$ = 12.68

Minor axis at threshold ..... $2b_m$ = 8.60

Major axis at μ=25.0 mag sec^{-2} ..... $2a(25)$ = 8.58

Luminosity within μ=25.0 mag sec^{-2} ..... $k(25)$ = 0.82

Gradient of exponential component ..... $G(a)$ = -0.31

Equivalent gradient of exponential comp..... $G(r^*)$ = -0.32

Equivalent gradient of reduced exp. comp..... $G(\rho)$ = -0.33

Parameters at k = ¼ :

- Semi-major axis ..... a_1 = 0.57
- Axis ratio ..... b/a = 0.56
- Equivalent radius ..... r_1^* = 0.32
- Surface brightness ..... μ_1 = 20.27

Parameters at k = ½(effective) :

- Semi-major axis ..... a_e = 1.38
- Axis ratio ..... b/a = 0.43
- Equivalent radius ..... r_e^* = 1.02
- Surface brightness ..... μ_e = 22.65
- Mean surface brightness ..... μ_e' = 12.14

Parameters at k = ¾ :

- Semi-major axis ..... a_3 = 3.75
- Axis ratio ..... b/a = 0.59
- Equivalent radius ..... r_3^* = 2.69
- Surface brightness ..... μ_3 = 24.46

Concentration indices ..... C_{21} = 3.13, C_{32} = 2.64

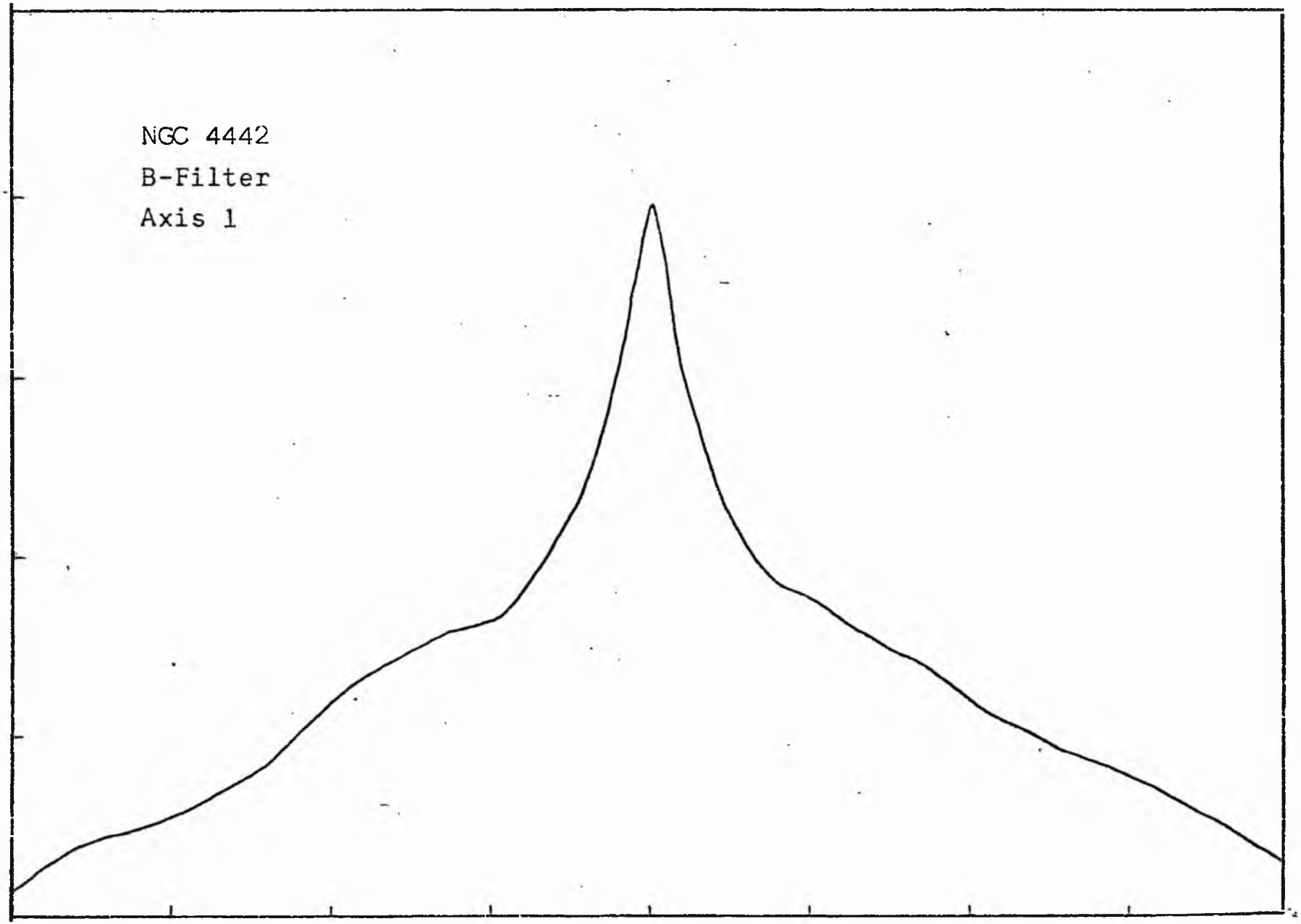
NGC 4442
B-Filter
Axis 1

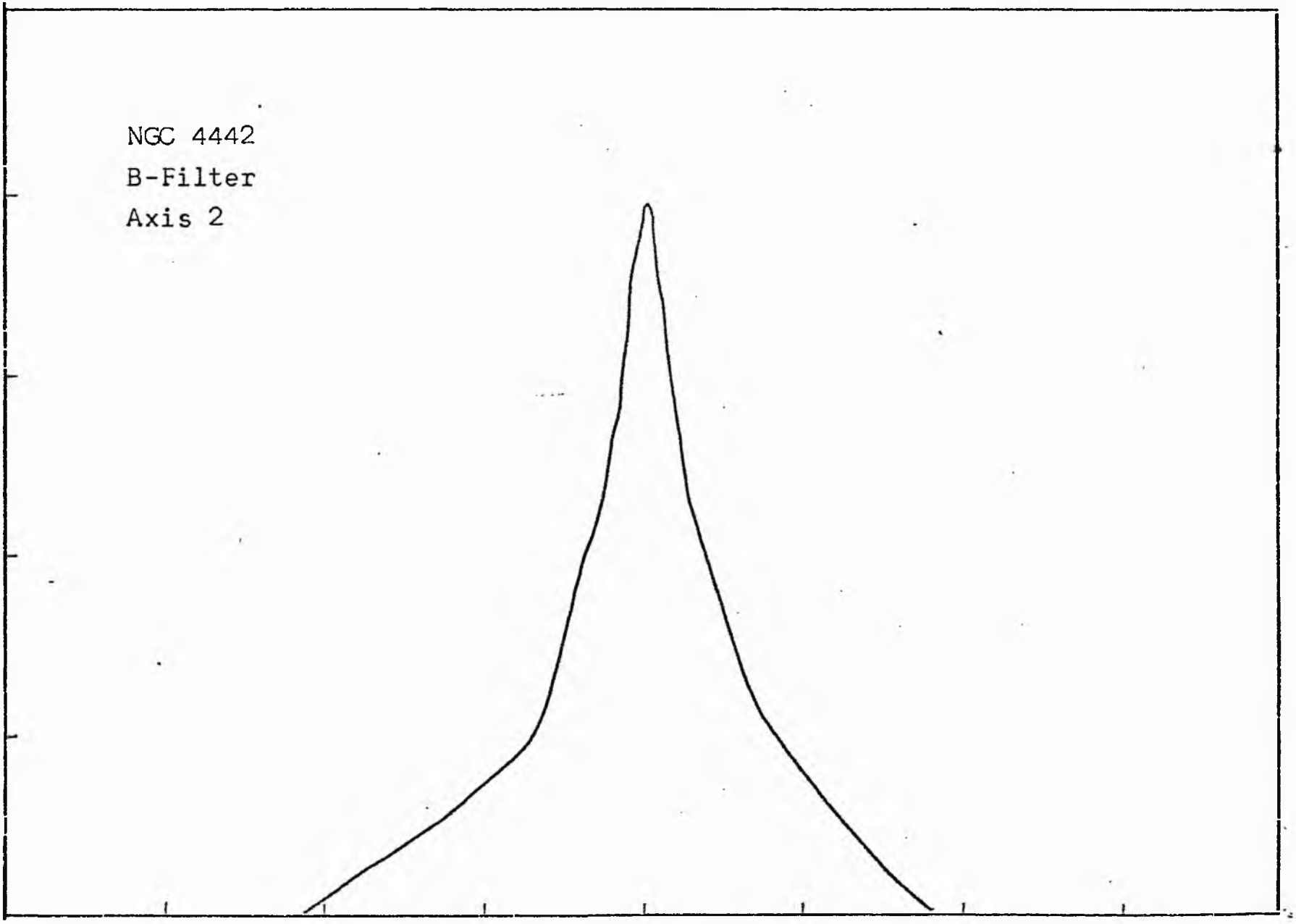
NGC 4442
B-Filter
Axis 2

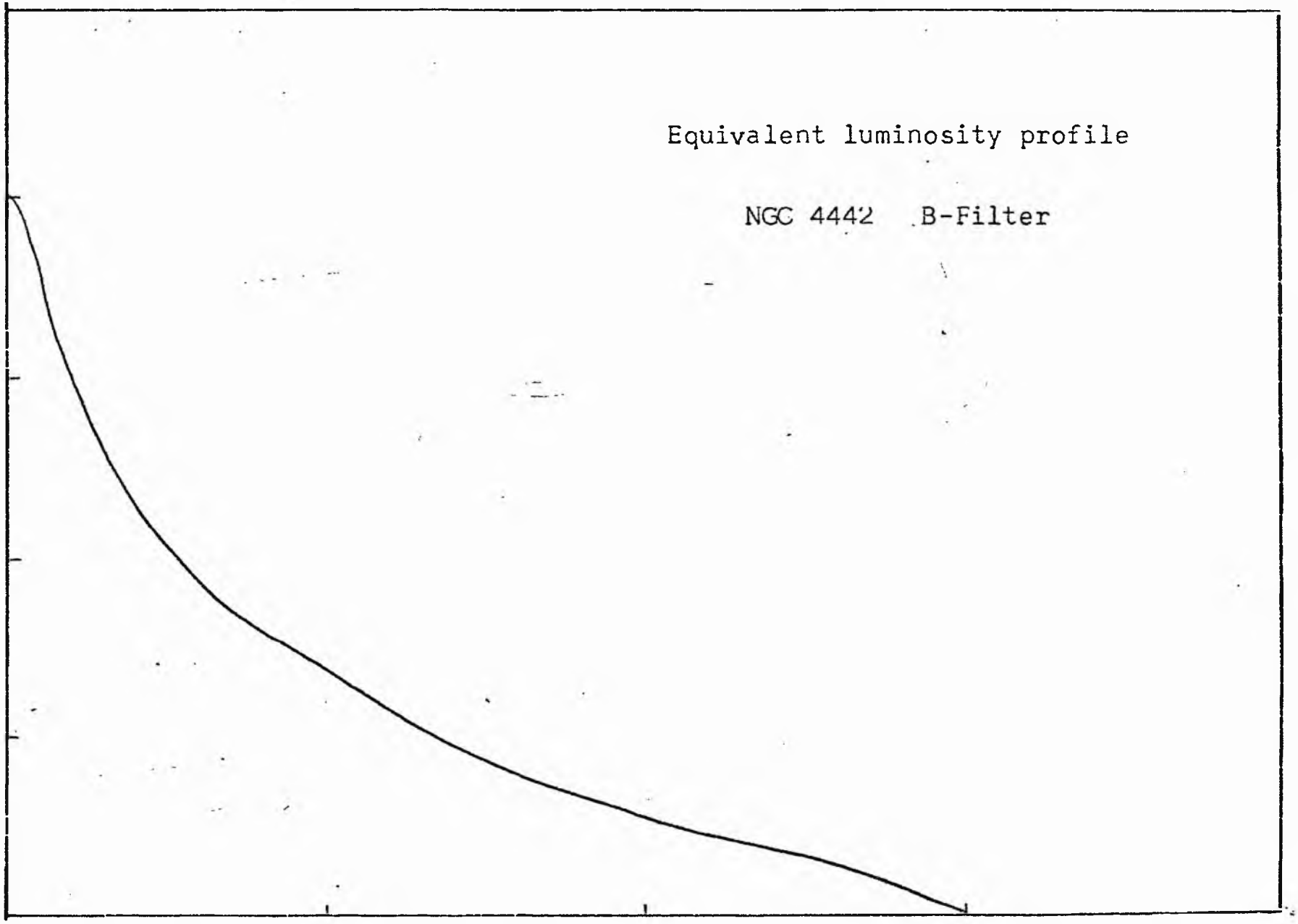
Equivalent luminosity profile
NGC 4442 B-Filter

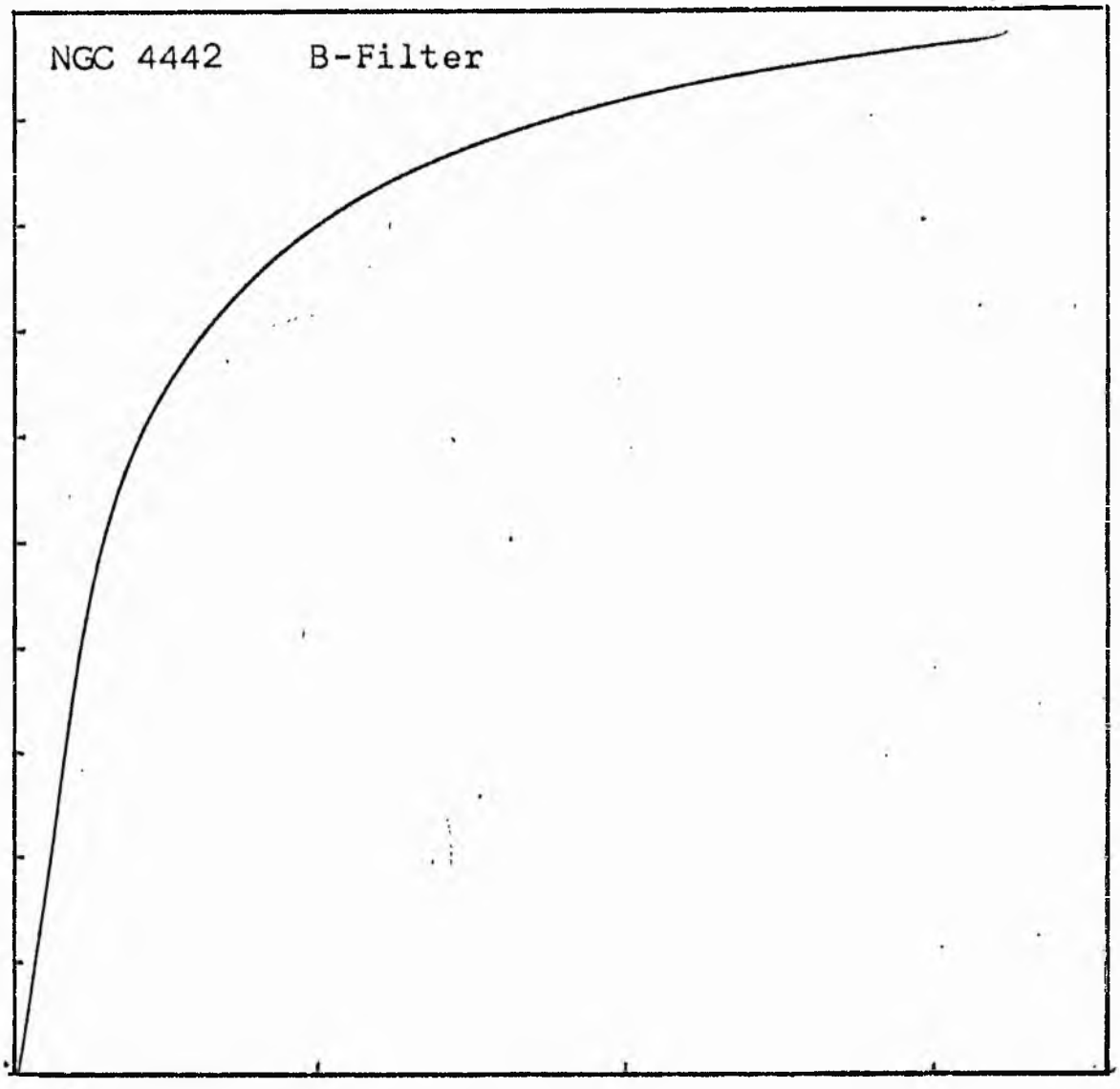

Relative integrated luminosity k(r) versus equivalent radius r*.

MEAN LUMINOSITY DISTRIBUTION IN NGC 4442
B COLOUR

LOG I	I	T	R	AREA	ΔA	P	ΣP	K(R)	ρ	LOG J	μ
1.94	87.096		0.0	0.0			0.0	0.0	0.0	1.326	17.17
		83.265			2.01	167.4131					
1.90	79.433		0.80	2.01			167.41	0.01	0.06	1.286	17.27
		71.264			5.06	360.4517					
1.80	63.096		1.50	7.07			527.86	0.03	0.11	1.186	17.52
		56.607			17.56	994.1040					
1.70	50.119		2.80	24.63			1521.97	0.09	0.21	1.086	17.77
		44.965			10.21	458.9409					
1.60	39.811		3.33	34.84			1980.91	0.12	0.24	0.986	18.02
		35.717			28.78	1027.9399					
1.50	31.623		4.50	63.62			3008.85	0.18	0.33	0.886	18.27
		28.371			18.10	913.3813					
1.40	25.119		5.10	81.71			3522.23	0.21	0.37	0.786	18.52
		22.536			27.65	623.0200					
1.30	19.952		5.90	109.36			4145.25	0.24	0.43	0.686	18.77
		17.901			35.91	642.7830					
1.20	15.849		6.80	145.27			4788.03	0.28	0.50	0.586	19.02
		14.219			60.85	865.2629					
1.10	12.589		8.10	206.12			5653.29	0.33	0.59	0.486	19.27
		11.295			61.52	694.8560					
1.00	10.000		9.23	267.64			6348.15	0.37	0.68	0.386	19.52
		8.972			92.04	825.7388					
0.90	7.943		10.70	359.68			7173.89	0.42	0.78	0.286	19.77
		7.126			85.20	607.1660					
0.80	6.310		11.90	444.88			7781.05	0.46	0.87	0.186	20.02
		5.661			61.83	349.9792					
0.70	5.012		12.70	506.71			8131.03	0.48	0.93	0.086	20.27
		4.496			91.58	411.7717					
0.60	3.981		13.80	598.28			8542.80	0.50	1.01	-0.014	20.52
		3.572			118.03	421.5605					
0.50	3.162		15.10	716.31			8964.36	0.53	1.11	-0.114	20.77
		2.837			138.98	394.3064					
0.40	2.512		16.50	855.30			9358.66	0.55	1.21	-0.214	21.02
		2.254			185.32	417.6333					
0.30	1.995		18.20	1040.62			9776.29	0.58	1.33	-0.314	21.27
		1.790			331.66	593.6882					
0.20	1.585		20.90	1372.28			10369.98	0.61	1.53	-0.414	21.52
		1.422			362.67	515.6753					
0.10	1.259		23.50	1734.94			10885.65	0.64	1.72	-0.514	21.77
		1.129			244.29	275.9131					
-0.00	1.000		25.10	1979.23			11161.56	0.66	1.84	-0.614	22.02
		0.897			413.90	371.3372					
-0.10	0.794		27.60	2393.14			11532.90	0.68	2.02	-0.714	22.27
		0.713			548.52	390.8977					
-0.20	0.631		30.60	2941.66			11923.79	0.70	2.24	-0.814	22.52
		0.566			479.53	271.4492					
-0.30	0.501		33.00	3421.19			12195.24	0.72	2.42	-0.914	22.77
		0.450			1308.28	588.2595					
-0.40	0.398		38.80	4729.47			12783.50	0.75	2.84	-1.014	23.02
		0.357			891.74	318.4990					
-0.50	0.316		42.30	5621.21			13102.00	0.77	3.10	-1.114	23.27
		0.284			1496.87	424.6729					
-0.60	0.251		47.60	7118.09			13526.67	0.80	3.49	-1.214	23.52
		0.225			1475.07	332.4158					
-0.70	0.200		52.30	8593.16			13859.08	0.82	3.83	-1.314	23.77
		0.179			1578.09	282.4885					
-0.80	0.158		56.90	10171.25			14141.57	0.83	4.17	-1.414	24.02
		0.142			1251.86	178.0019					
-0.90	0.126		60.30	11423.11			14319.57	0.84	4.42	-1.514	24.27
		0.113			2137.54	241.4258					
-1.00	0.100		65.70	13560.65			14561.00	0.86	4.82	-1.614	24.52
		0.090			3922.80	351.9385					
-1.10	0.079		74.60	17483.45			14912.93	0.88	5.47	-1.714	24.77
		0.071			3230.44	230.2144					
-1.20	0.063		81.20	20713.89			15143.14	0.89	5.95	-1.814	25.02
		0.057			3947.47	223.4552					
-1.30	0.050		88.60	24661.37			15366.60	0.91	6.49	-1.914	25.27
		0.045			4472.78	201.1174					
-1.40	0.040		96.30	29134.15			15567.71	0.92	7.06	-2.014	25.52
		0.036			8672.05	309.7378					
-1.50	0.032		109.70	37806.20			15877.45	0.94	8.04	-2.114	25.77
		0.028			6831.55	193.8172					
-1.60	0.025		119.20	44637.75			16071.27	0.95	8.74	-2.214	26.02
		0.023			5555.34	125.1943					
-1.70	0.020		126.40	50193.09			16196.46	0.95	9.27	-2.314	26.27
		0.018			6808.24	121.8735					
-1.80	0.016		134.70	57001.33			16318.33	0.96	9.87	-2.414	26.52
		0.014			6613.68	94.0412					
-1.90	0.013		142.30	63615.01			16412.37	0.97	10.43	-2.514	26.77
		0.011			7353.80	83.0591					
-2.00	0.010		150.30	70968.81			16495.43	0.97	11.02	-2.614	27.02
-∞							16975.00	(1)			∞

PHOTOMETRIC PARAMETERS OF NGC 4442

B-FILTER

Total luminosity ..... L_T = 4.72

Total apparent magnitude ..... m_T = 11.45

Apparent central surface brightness ..... μ_o = 17.17

Major axis at threshold ..... $2a_m$ = 9.47

Minor axis at threshold ..... $2b_m$ = 3.28

Major axis at μ=25.0 mag sec^{-2} ..... 2a(25) = 4.43

Luminosity within μ=25.0 mag sec^{-2} ..... k(25) = 0.89

Gradient of exponential component ..... G(a) = -0.51

Equivalent gradient of exponential comp. .... G(r*) = -0.81

Equivalent gradient of reduced exp. comp. .... G(ρ) = -1.41

Parameters at k = ¼ :

- Semi-major axis ..... a_1 = 0.15
- Axis ratio ..... b/a = 0.55
- Equivalent radius ..... r_1* = 0.10
- Surface brightness ..... μ_1 = 18.83

Parameters at k = ½(effective) :

- Semi-major axis ..... a_e = 0.28
- Axis ratio ..... b/a = 0.59
- Equivalent radius ..... r_e* = 0.23
- Surface brightness ..... μ_e = 20.52
- Mean surface brightness ..... μ_e' = 10.25

Parameters at k = ¾ :

- Semi-major axis ..... a_3 = 1.08
- Axis ratio ..... b/a = 0.41
- Equivalent radius ..... r_3* = 0.64
- Surface brightness ..... μ_3 = 23.02

Concentration indices ..... C_{21} = 2.26, C_{32} = 2.80

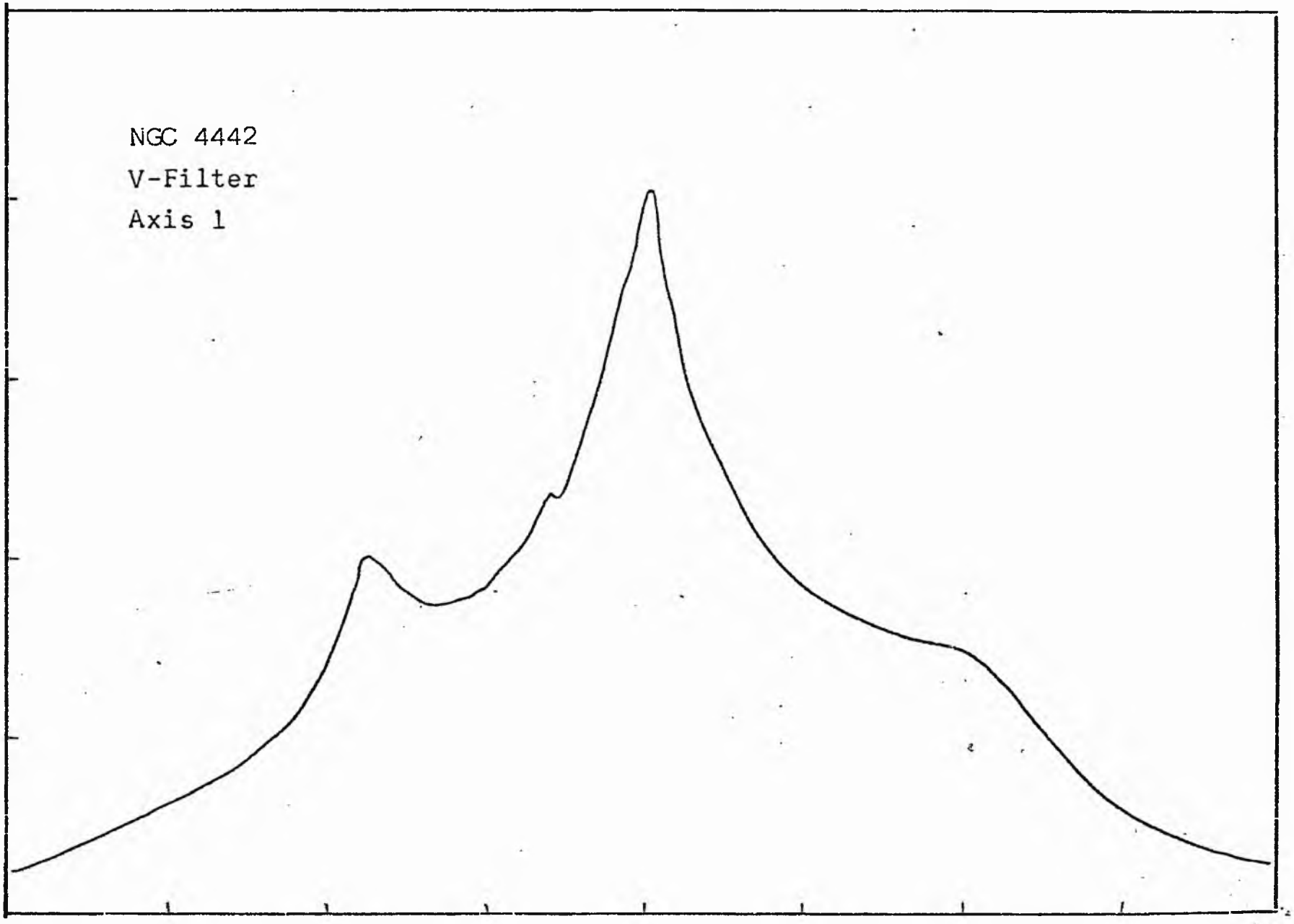
NGC 4442
V-Filter
Axis 1

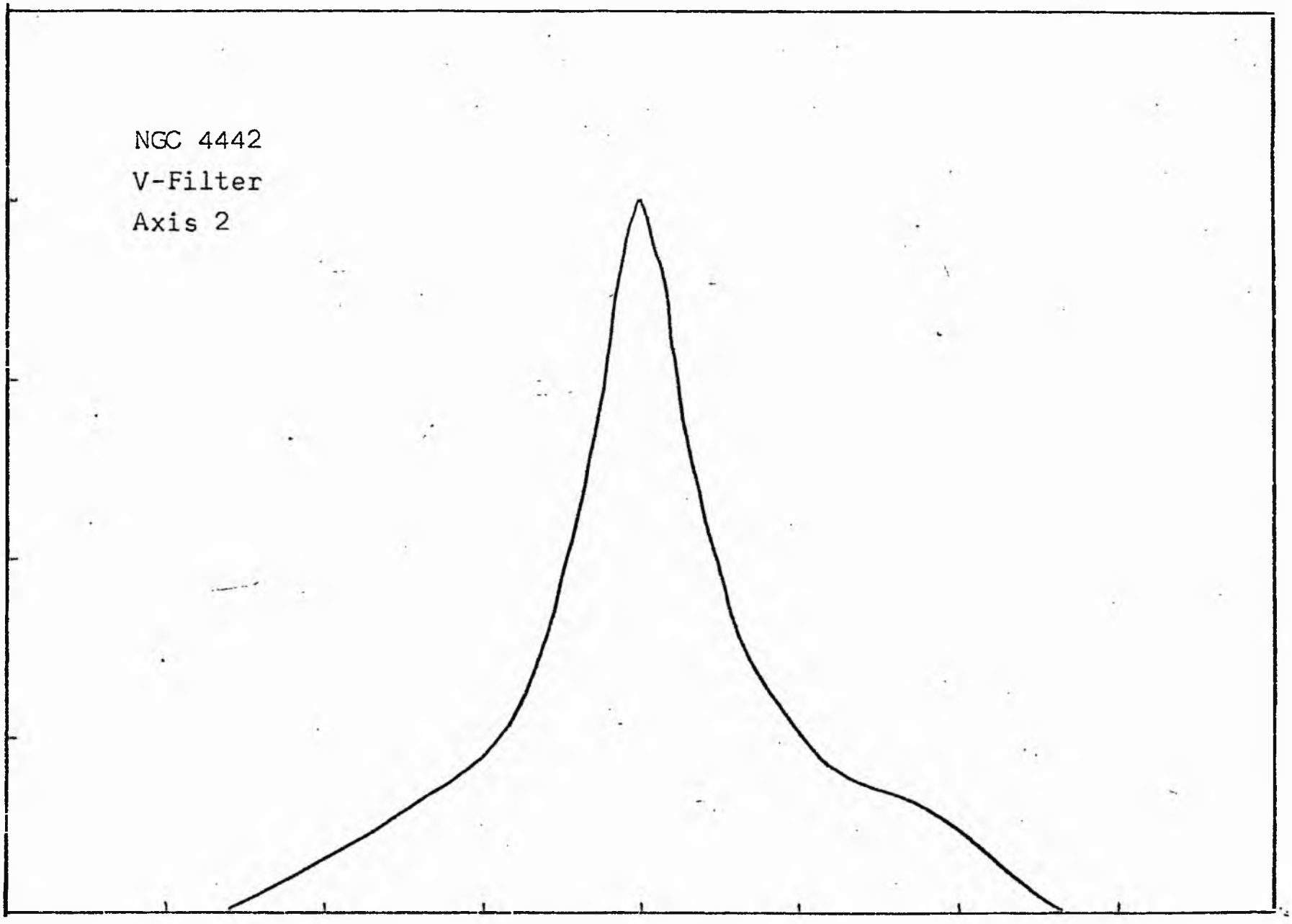
NGC 4442
V-Filter
Axis 2

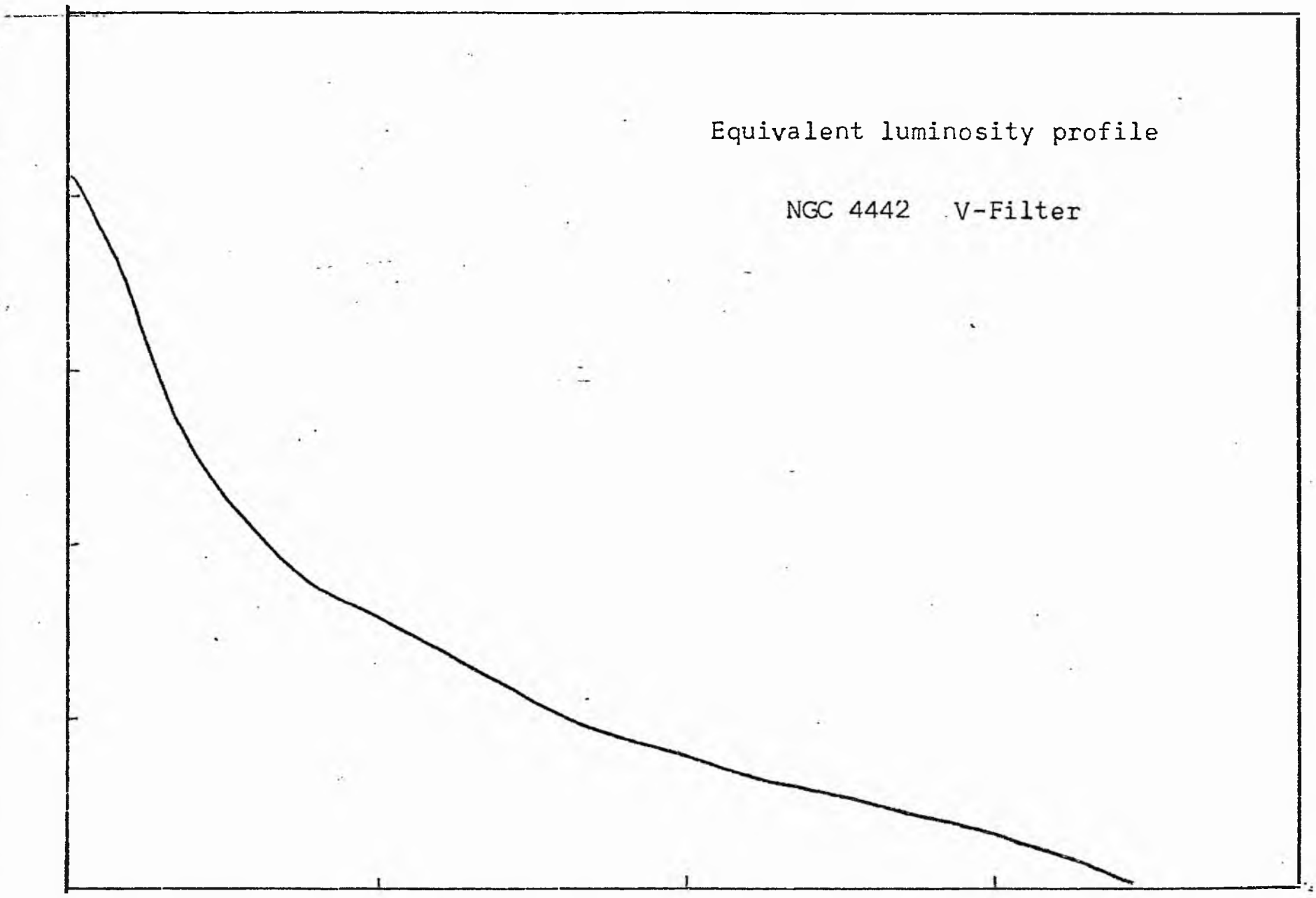
Equivalent luminosity profile
NGC 4442 V-Filter

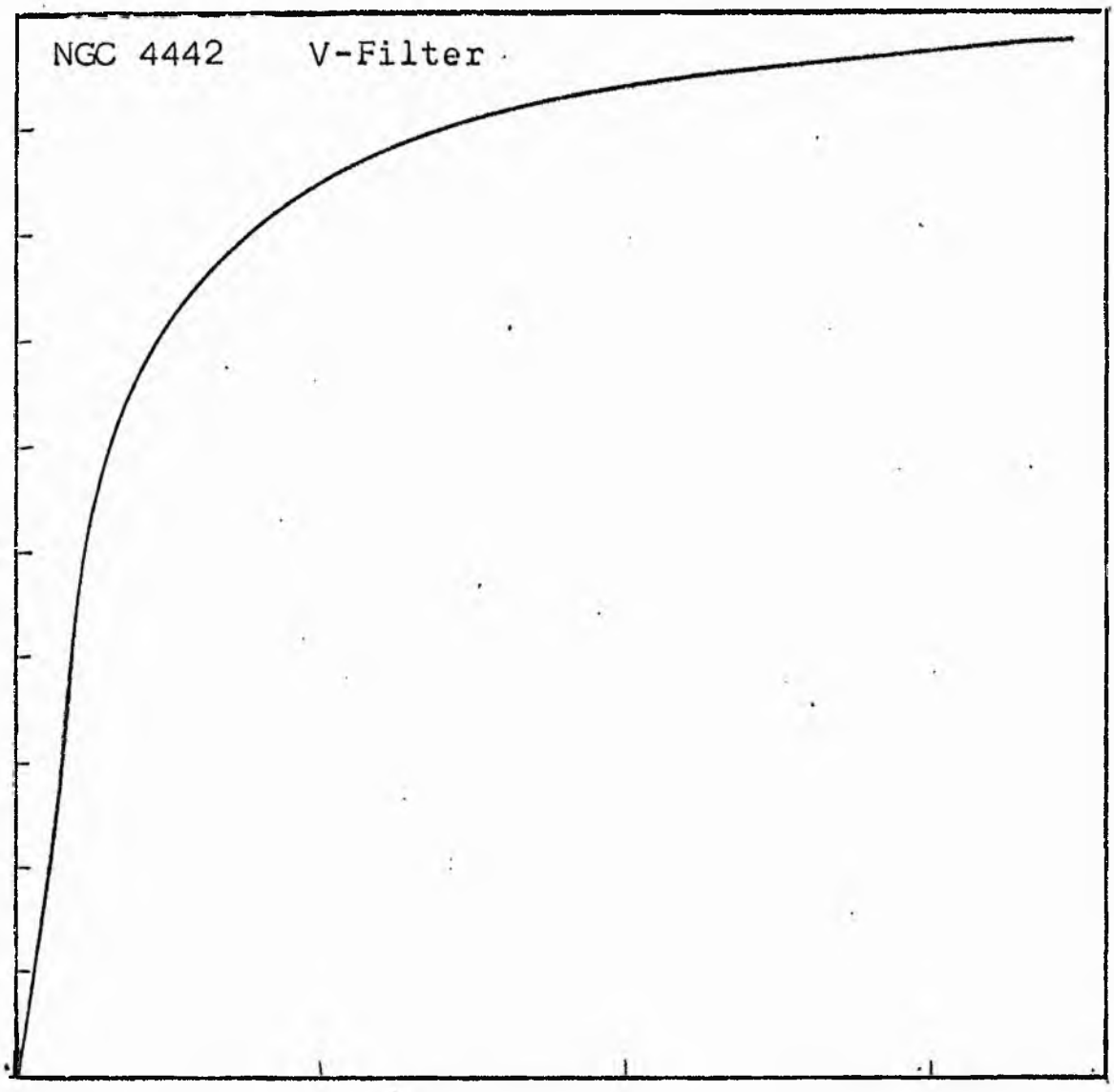

Relative integrated luminosity k(r) versus equivalent radius r*.

MEAN LUMINOSITY DISTRIBUTION IN NGC 4442
V COLOUR

LOG I	I	$\bar{I}$	R	AREA	ΔA	P	ΣP	K(R)	ρ	LOG J	μ
2.05	112.202		0.0	0.0			0.0	0.0	0.0	0.863	16.63
		106.101			5.31	563.3193					
2.00	100.000		1.30	5.31			563.32	0.02	0.11	0.813	16.76
		89.716			24.88	2232.2678					
1.90	79.433		3.10	30.19			2795.59	0.08	0.25	0.713	17.01
		71.264			25.23	1797.7783					
1.80	63.096		4.20	55.42			4593.36	0.13	0.34	0.613	17.26
		56.607			39.62	2242.5193					
1.70	50.119		5.50	95.03			6835.88	0.20	0.45	0.513	17.51
		44.965			37.70	1695.1250					
1.60	39.811		6.50	132.73			8531.00	0.25	0.53	0.413	17.76
		35.717			25.64	915.6077					
1.50	31.623		7.10	158.37			9446.61	0.28	0.58	0.313	18.01
		28.371			137.22	3893.1541					
1.40	25.119		9.70	295.59			13339.76	0.39	0.79	0.213	18.26
		22.536			112.69	2539.5132					
1.30	19.952		11.40	408.28			15879.27	0.47	0.93	0.113	18.51
		17.901			59.31	1061.7454					
1.20	15.849		12.20	467.59			16941.02	0.50	0.99	0.013	18.76
		14.219			71.53	1017.1428					
1.10	12.589		13.10	539.13			17958.16	0.53	1.06	-0.087	19.01
		11.295			40.23	454.4060					
1.00	10.000		13.58	579.36			18412.56	0.54	1.10	-0.187	19.26
		8.972			105.99	950.8630					
0.90	7.943		14.77	685.35			19363.42	0.57	1.20	-0.287	19.51
		7.126			166.84	1188.9761					
0.80	6.310		16.47	852.19			20552.39	0.60	1.34	-0.387	19.76
		5.661			171.35	969.9448					
0.70	5.012		18.05	1023.54			21522.33	0.63	1.47	-0.487	20.01
		4.496			182.10	818.8230					
0.60	3.981		19.59	1205.64			22341.15	0.65	1.59	-0.587	20.26
		3.572			171.89	613.9395					
0.50	3.162		20.94	1377.53			22955.09	0.67	1.70	-0.687	20.51
		2.837			229.91	652.2559					
0.40	2.512		22.62	1607.44			23607.34	0.69	1.84	-0.787	20.76
		2.254			278.30	627.1670					
0.30	1.995		24.50	1885.74			24234.51	0.71	1.99	-0.887	21.01
		1.790			332.11	594.5012					
0.20	1.585		26.57	2217.85			24829.01	0.73	2.16	-0.987	21.26
		1.422			438.82	623.9595					
0.10	1.259		29.08	2656.67			25452.96	0.75	2.36	-1.087	21.51
		1.129			540.24	610.1770					
-0.00	1.000		31.90	3196.91			26063.14	0.76	2.59	-1.187	21.76
		0.897			245.04	219.8433					
-0.10	0.794		33.10	3441.96			26282.98	0.77	2.69	-1.287	22.01
		0.713			1236.46	881.1477					
-0.20	0.631		38.59	4678.42			27164.12	0.80	3.14	-1.387	22.26
		0.566			1925.90	1090.1919					
-0.30	0.501		45.85	6604.32			28254.32	0.83	3.73	-1.487	22.51
		0.450			1215.14	546.3809					
-0.40	0.398		49.89	7819.46			28800.70	0.84	4.05	-1.587	22.76
		0.357			1239.91	442.8540					
-0.50	0.316		53.70	9059.37			29243.55	0.86	4.36	-1.687	23.01
		0.284			1436.18	407.4521					
-0.60	0.251		57.80	10495.55			29651.00	0.87	4.70	-1.787	23.26
		0.225			1697.87	382.6262					
-0.70	0.200		62.30	12193.43			30033.62	0.88	5.06	-1.887	23.51
		0.179			2078.07	371.9878					
-0.80	0.158		67.40	14271.49			30405.61	0.89	5.48	-1.987	23.76
		0.142			1699.38	241.6353					
-0.90	0.126		71.30	15970.87			30647.24	0.90	5.79	-2.087	24.01
		0.113			3388.41	382.7058					
-1.00	0.100		78.50	19359.28			31029.94	0.91	6.38	-2.187	24.26
		0.090			3499.22	313.9360					
-1.10	0.079		85.30	22858.50			31343.87	0.92	6.93	-2.287	24.51
		0.071			5256.11	374.5715					
-1.20	0.063		94.60	28114.61			31718.45	0.93	7.69	-2.387	24.76
		0.057			7384.40	418.0098					
-1.30	0.050		106.30	35499.00			32136.45	0.94	8.64	-2.487	25.01
		0.045			5472.51	246.0698					
-1.40	0.040		114.20	40971.51			32382.52	0.95	9.28	-2.587	25.26
		0.036			8351.77	298.2983					
-1.50	0.032		125.30	49323.28			32680.82	0.96	10.18	-2.687	25.51
		0.028			10331.91	293.1255					
-1.60	0.025		137.80	59655.19			32973.94	0.97	11.20	-2.787	25.76
		0.023			7311.00	164.7594					
-1.70	0.020		146.00	66966.19			33138.70	0.97	11.86	-2.887	26.01
		0.018			8705.44	155.8350					
-1.80	0.016		155.20	75671.62			33294.53	0.98	12.61	-2.987	26.26
		0.014			10169.50	144.6021					
-1.90	0.013		165.30	85841.12			33439.13	0.98	13.43	-3.087	26.51
		0.011			7099.75	80.1897					
-2.00	0.010		172.00	92940.87			33519.32	0.98	13.98	-3.187	26.76
- ∞							34139.00	(1)			∞

PHOTOMETRIC PARAMETERS OF NGC 4442

V-FILTER

Total luminosity ..... L_T = 9.48

Total apparent magnitude ..... m_T = 10.43

Apparent central surface brightness ..... μ_o = 16.63

Major axis at threshold ..... $2a_m$ = 7.41

Minor axis at threshold ..... $2b_m$ = 4.48

Major axis at μ=25.0 mag sec^{-2} ..... 2a(25) = 4.95

Luminosity within μ=25.0 mag sec^{-2} ..... k(25) = 0.94

Gradient of exponential component ..... G(a) = -0.62

Equivalent gradient of exponential comp..... G(r*) = -0.89

Equivalent gradient of reduced exp. comp..... G(ρ) = -0.99

Parameters at k = ¼ :

- Semi-major axis ..... a_1 = 0.12
- Axis ratio ..... b/a = 0.65
- Equivalent radius ..... r_1* = 0.11
- Surface brightness ..... μ_1 = 17.76

Parameters at k = ½(effective) :

- Semi-major axis ..... a_e = 0.23
- Axis ratio ..... b/a = 0.61
- Equivalent radius ..... r_e* = 0.21
- Surface brightness ..... μ_e = 18.76
- Mean surface brightness ..... μ_e' = 9.03

Parameters at k = ¾ :

- Semi-major axis ..... a_3 = 0.63
- Axis ratio ..... b/a = 0.55
- Equivalent radius ..... r_3* = 0.50
- Surface brightness ..... μ_3 = 21.51

Concentration indices ..... C_{21} = 1.89, C_{32} = 2.42

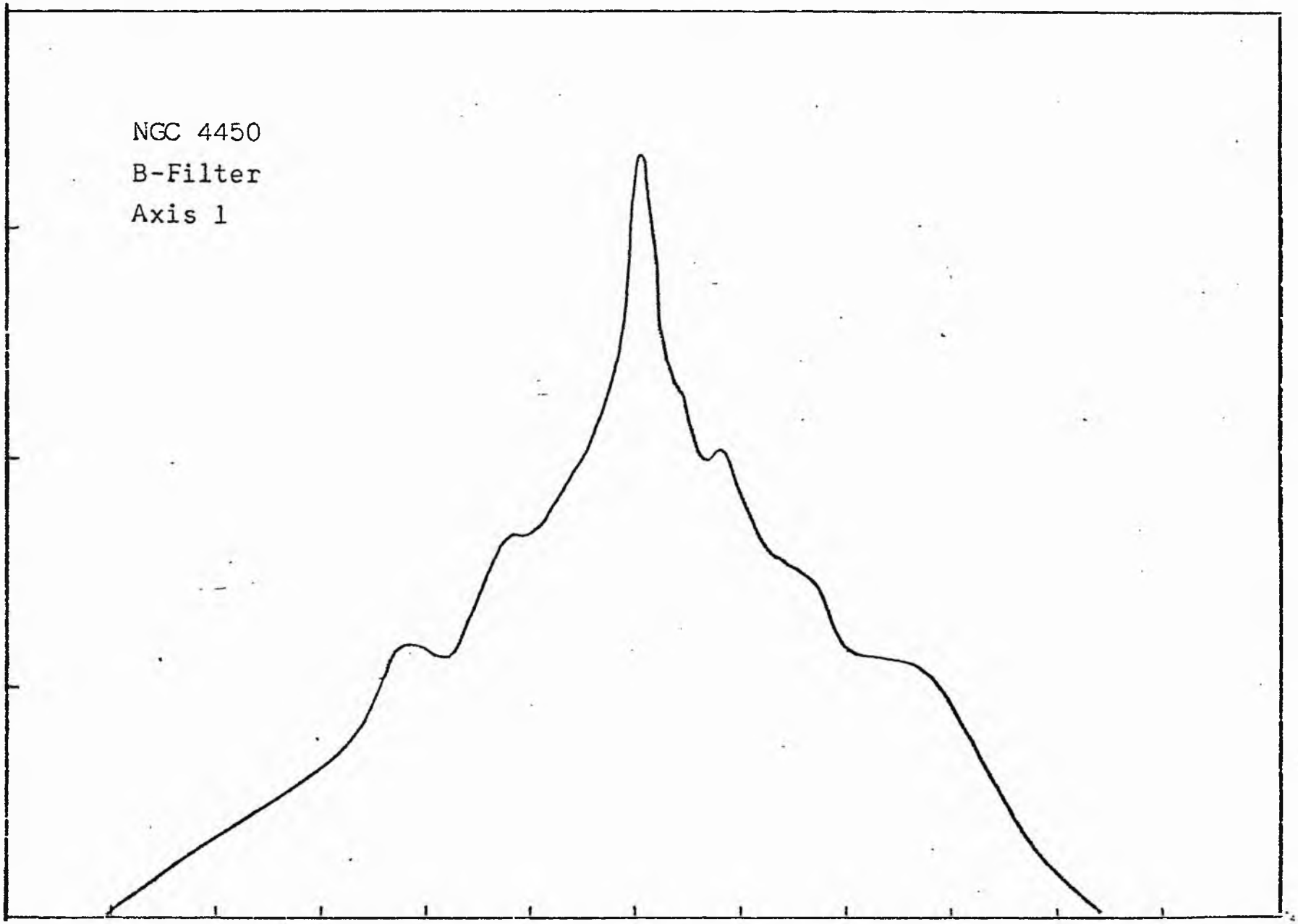
NGC 4450
B-Filter
Axis 1

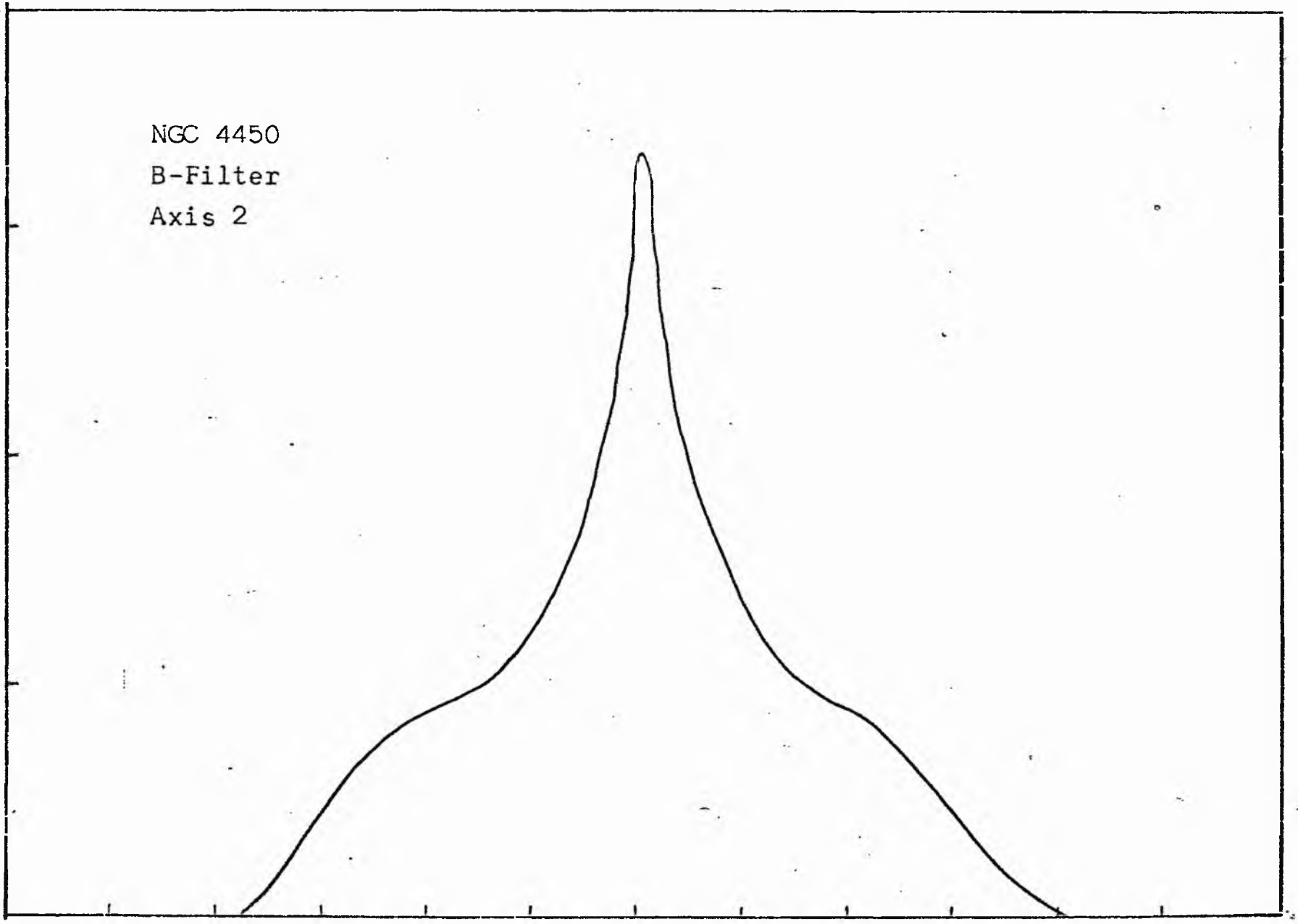
NGC 4450
B-Filter
Axis 2

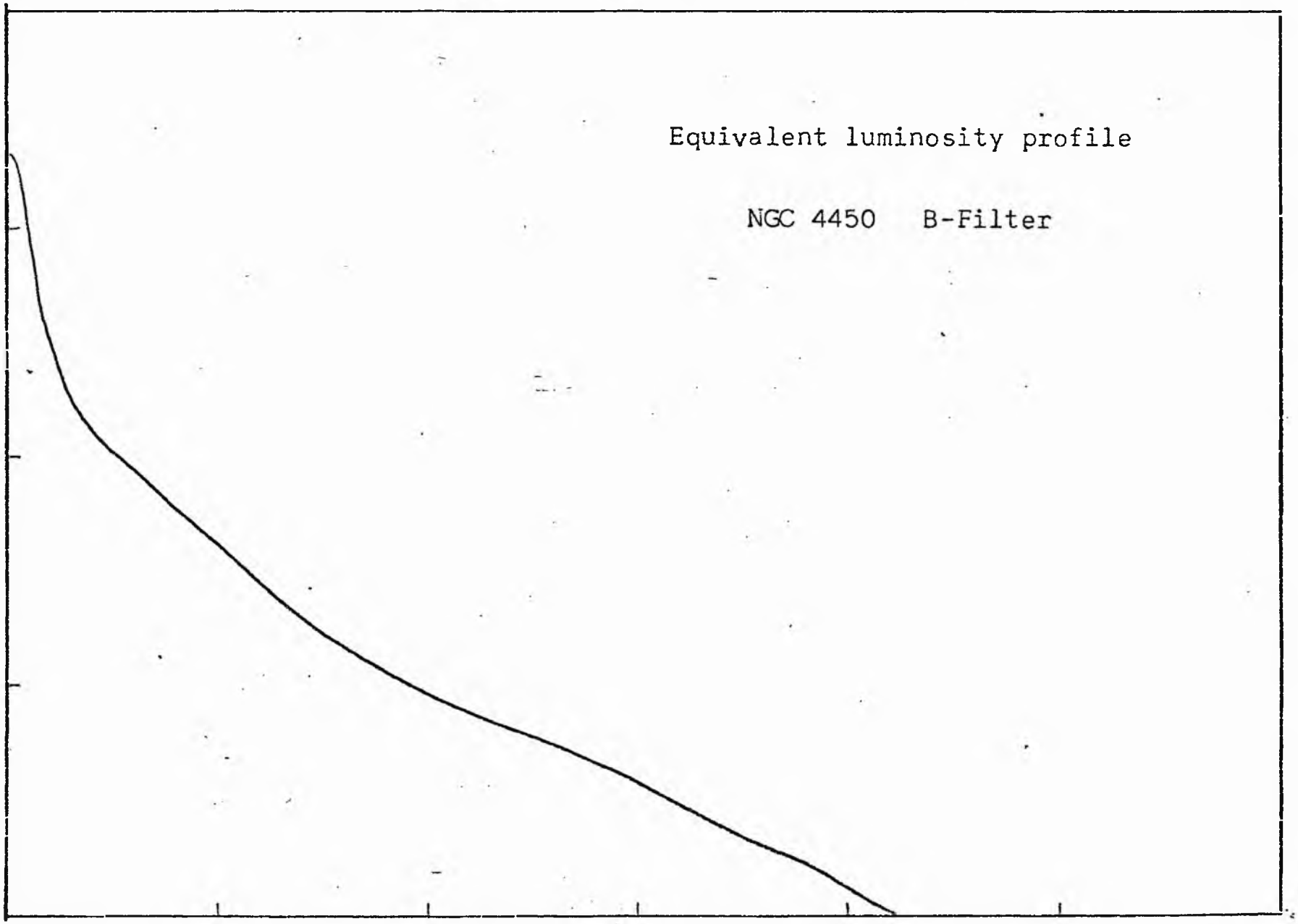
Equivalent luminosity profile
NGC 4450 B-Filter

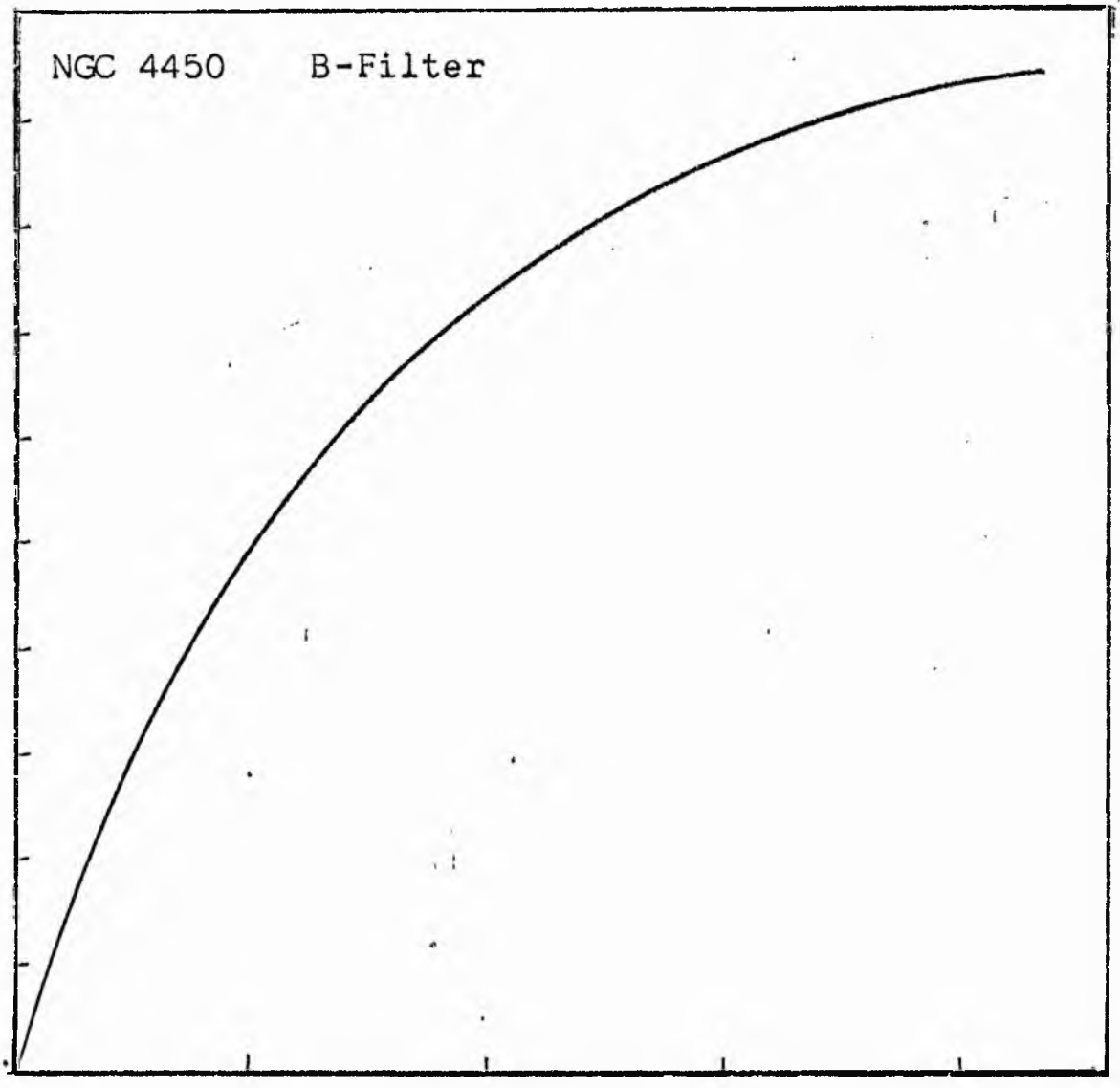

Relative integrated luminosity k(r) versus equivalent radius r*.

MEAN LUMINOSITY DISTRIBUTION IN NGC 4450
B COLOUR

LOG I	I	T	R	AREA	ΔA	P	ΣP	K(R)	ρ	LOG J	μ
1.31	20.417		0.0	0.0			0.0	0.0	0.0	1.709	18.17
		20.185			18.10	365.2583					
1.30	19.953		2.40	18.10			365.26	0.02	0.05	1.699	18.20
		17.901			27.51	492.4146					
1.20	15.849		3.81	45.60			857.67	0.05	0.08	1.599	18.45
		14.219			6.95	98.8108					
1.10	12.589		4.09	52.55			956.48	0.05	0.08	1.499	18.70
		11.295			31.09	351.1926					
1.00	10.000		5.16	83.65			1307.68	0.07	0.10	1.399	18.95
		8.972			39.07	350.5356					
0.90	7.943		6.25	122.72			1658.21	0.09	0.13	1.299	19.20
		7.126			18.31	130.4671					
0.80	6.310		6.70	141.03			1788.68	0.10	0.14	1.199	19.45
		5.661			43.31	245.1500					
0.70	5.012		7.66	184.33			2033.84	0.11	0.16	1.099	19.70
		4.496			97.41	437.9814					
0.60	3.981		9.47	281.74			2471.82	0.14	0.19	0.999	19.95
		3.572			60.02	214.3608					
0.50	3.162		10.43	341.76			2686.18	0.15	0.21	0.899	20.20
		2.837			73.72	209.1427					
0.40	2.512		11.50	415.48			2895.32	0.16	0.23	0.799	20.45
		2.254			292.33	658.7751					
0.30	1.995		15.01	767.80			3554.10	0.20	0.30	0.699	20.70
		1.790			284.23	508.7874					
0.20	1.585		17.77	992.03			4062.88	0.23	0.36	0.599	20.95
		1.422			140.89	200.3344					
0.10	1.259		18.99	1132.92			4263.21	0.24	0.39	0.499	21.20
		1.129			925.95	1045.8254					
-0.00	1.000		25.60	2058.87			5309.04	0.30	0.52	0.399	21.45
		0.897			1358.18	1218.5024					
-0.10	0.794		32.98	3417.05			6527.54	0.37	0.67	0.299	21.70
		0.713			967.89	689.7549					
-0.20	0.631		37.36	4384.93			7217.29	0.41	0.76	0.199	21.95
		0.566			1497.04	847.4319					
-0.30	0.501		43.27	5881.98			8064.72	0.46	0.88	0.099	22.20
		0.450			1759.82	791.2981					
-0.40	0.398		49.32	7641.80			8856.02	0.50	1.00	-0.001	22.45
		0.357			2010.69	718.1519					
-0.50	0.316		55.43	9652.49			9574.17	0.54	1.13	-0.101	22.70
		0.284			2346.00	665.5769					
-0.60	0.251		61.80	11998.49			10239.74	0.58	1.25	-0.201	22.95
		0.225			2828.85	637.5005					
-0.70	0.200		68.70	14827.34			10877.24	0.61	1.39	-0.301	23.20
		0.179			2933.76	525.1643					
-0.80	0.158		75.19	17761.09			11402.41	0.64	1.53	-0.401	23.45
		0.142			3419.67	486.2454					
-0.90	0.126		82.11	21180.77			11888.65	0.67	1.67	-0.501	23.70
		0.113			8195.91	925.6973					
-1.00	0.100		96.70	29376.68			12814.34	0.72	1.96	-0.601	23.95
		0.090			7743.40	694.7104					
-1.10	0.079		108.70	37120.08			13509.05	0.76	2.21	-0.701	24.20
		0.071			12518.62	892.1326					
-1.20	0.063		125.70	49638.70			14401.18	0.81	2.55	-0.801	24.45
		0.057			9153.80	518.1729					
-1.30	0.050		136.80	58792.50			14919.35	0.84	2.78	-0.901	24.70
		0.045			9556.75	429.7180					
-1.40	0.040		147.50	68349.25			15349.07	0.87	2.99	-1.001	24.95
		0.036			5770.19	206.0935					
-1.50	0.032		153.60	74119.44			15555.16	0.88	3.12	-1.101	25.20
		0.028			10583.00	300.2505					
-1.60	0.025		164.20	84702.44			15855.41	0.90	3.33	-1.201	25.45
		0.023			13943.06	314.2200					
-1.70	0.020		177.20	98645.50			16169.62	0.91	3.60	-1.301	25.70
		0.018			12982.31	232.3959					
-1.80	0.016		188.50	111627.81			16402.02	0.93	3.83	-1.401	25.95
		0.014			9429.31	134.0778					
-1.90	0.013		196.30	121057.12			16536.09	0.93	3.98	-1.501	26.20
		0.011			17883.19	201.9864					
-2.00	0.010		210.30	138940.31			16738.08	0.95	4.27	-1.601	26.45
$-\infty$							17698.00	(1)			∞

PHOTOMETRIC PARAMETERS OF NGC 4450

B-FILTER

Total luminosity	L_T	= 4.92
Total apparent magnitude	m_T	= 10.86
Apparent central surface brightness	μ_o	= 18.17
Major axis at threshold	$2a_m$	= 7.70
Minor axis at threshold	$2b_m$	= 6.05
Major axis at μ=25.0 mag sec^{-2}	2a(25)	= 5.28
Luminosity within μ=25.0 mag sec^{-2}	k(25)	= 0.87
Gradient of exponential component	G(a)	= -0.78
Equivalent gradient of exponential comp.	G(r*)	= -0.63
Equivalent gradient of reduced exp. comp.	G(ρ)	= -0.44
Parameters at k = ¼ :		
Semi-major axis	a_1	= 0.43
Axis ratio	b/a	= 0.81
Equivalent radius	r_1*	= 0.33
Surface brightness	μ_1	= 21.25
Parameters at k = ½(effective) :		
Semi-major axis	a_e	= 0.94
Axis ratio	b/a	= 0.65
Equivalent radius	r_e*	= 0.82
Surface brightness	μ_e	= 22.45
Mean surface brightness	μ_e'	= 12.41
Parameters at k = ¾ :		
Semi-major axis	a_3	= 2.15
Axis ratio	b/a	= 0.75
Equivalent radius	r_3*	= 1.74
Surface brightness	μ_3	= 24.14
Concentration indices	C_{21}	= 2.47
	C_{32}	= 2.12

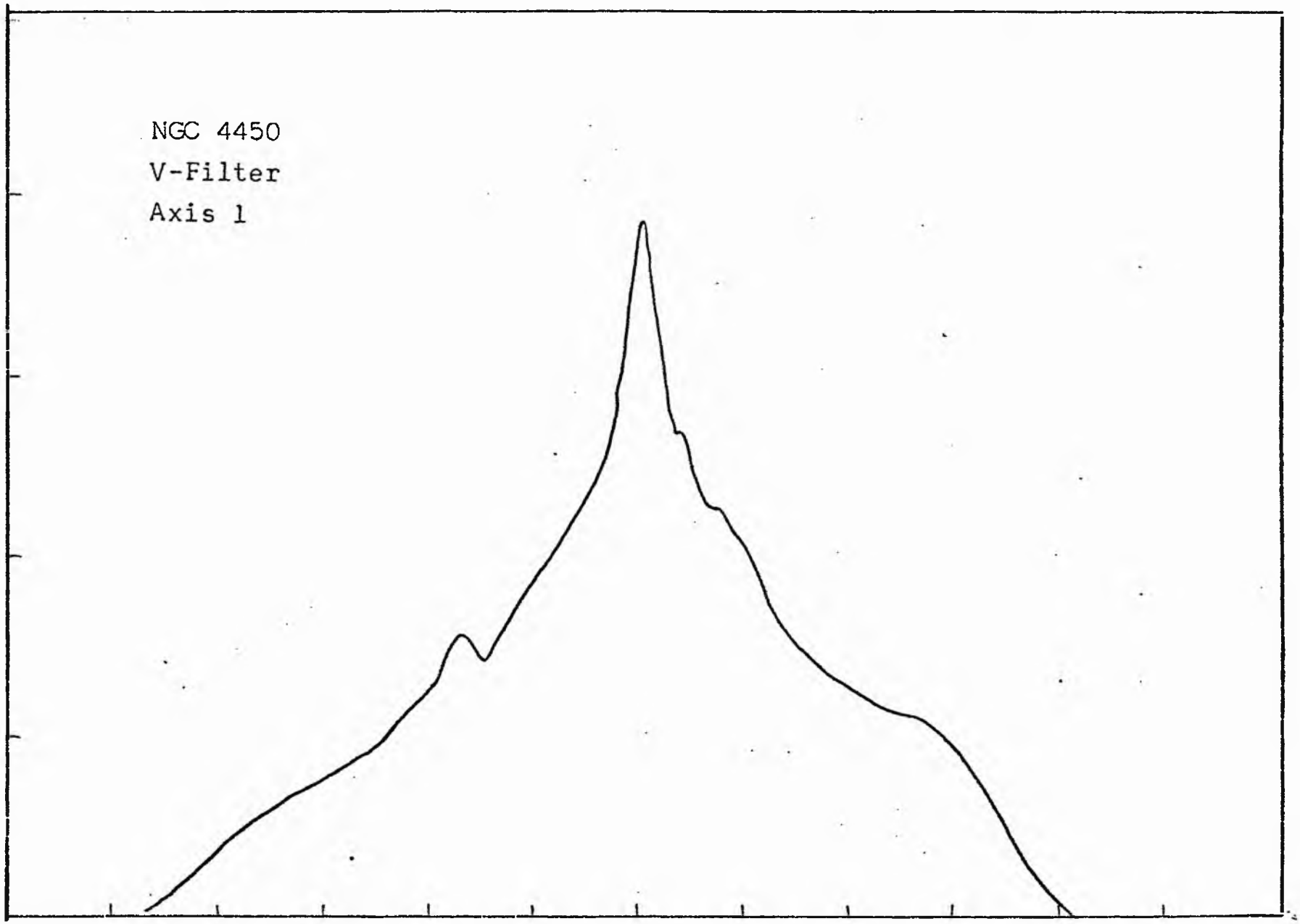
NGC 4450
V-Filter
Axis 1

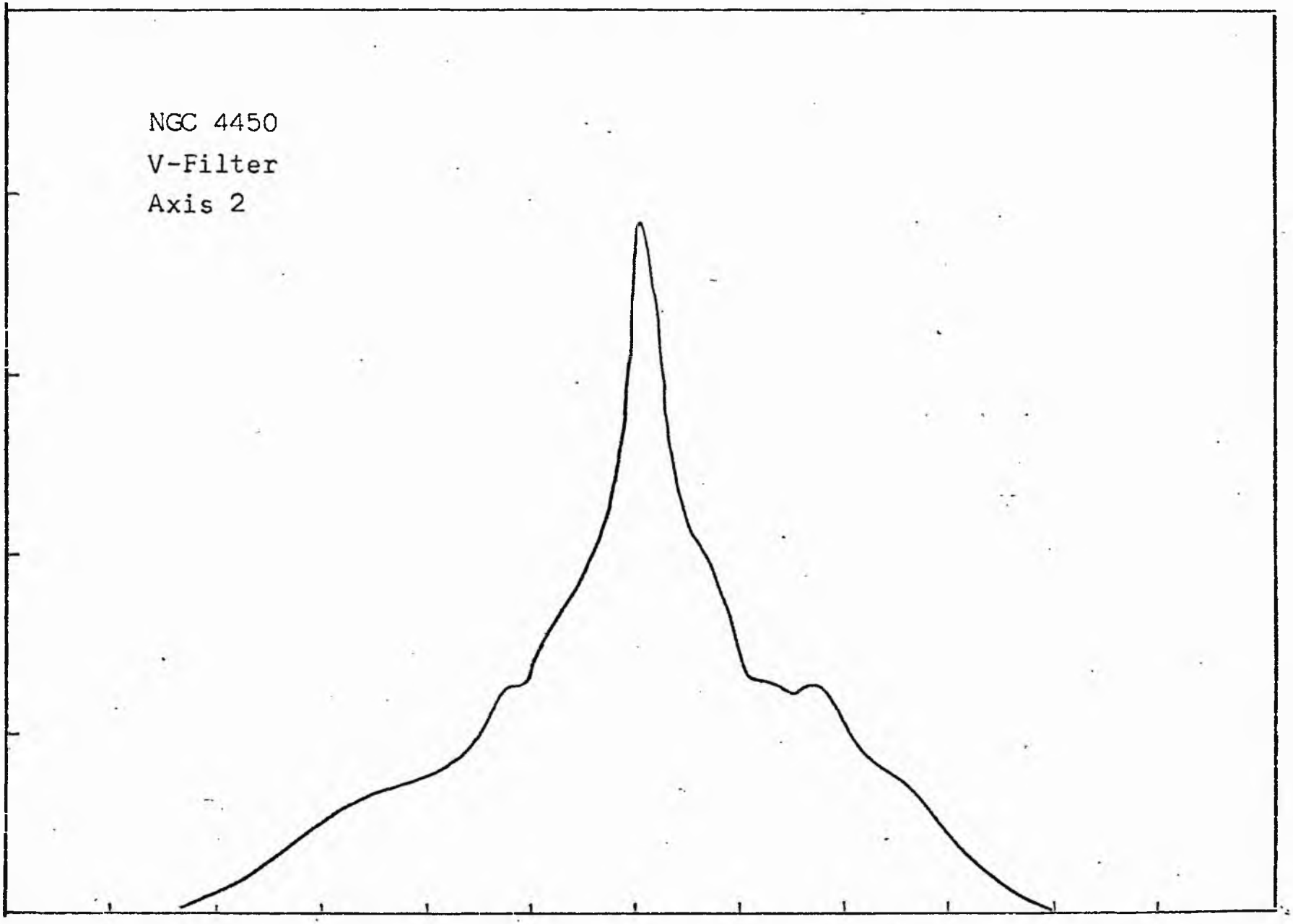
NGC 4450
V-Filter
Axis 2

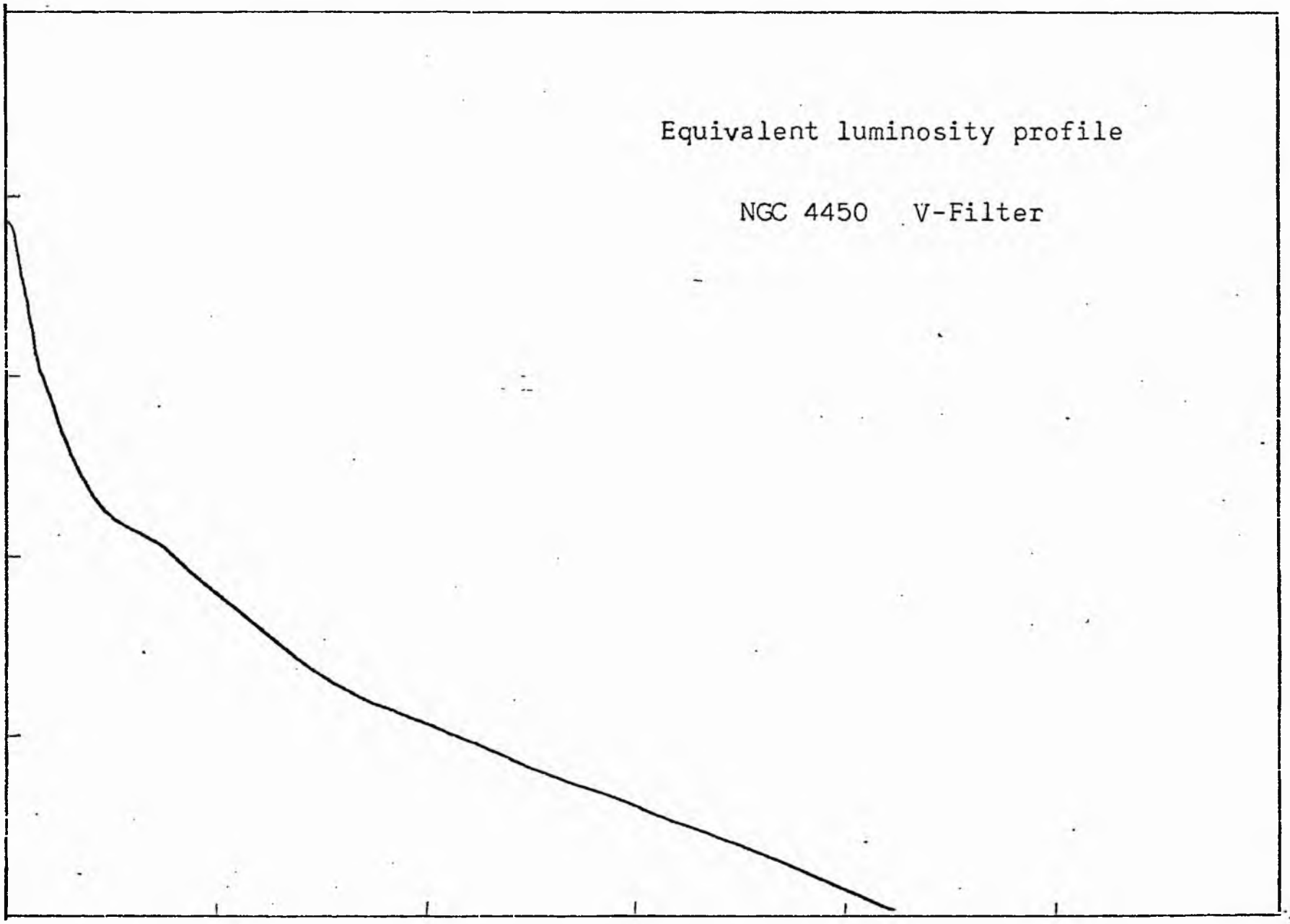
Equivalent luminosity profile
NGC 4450 V-Filter

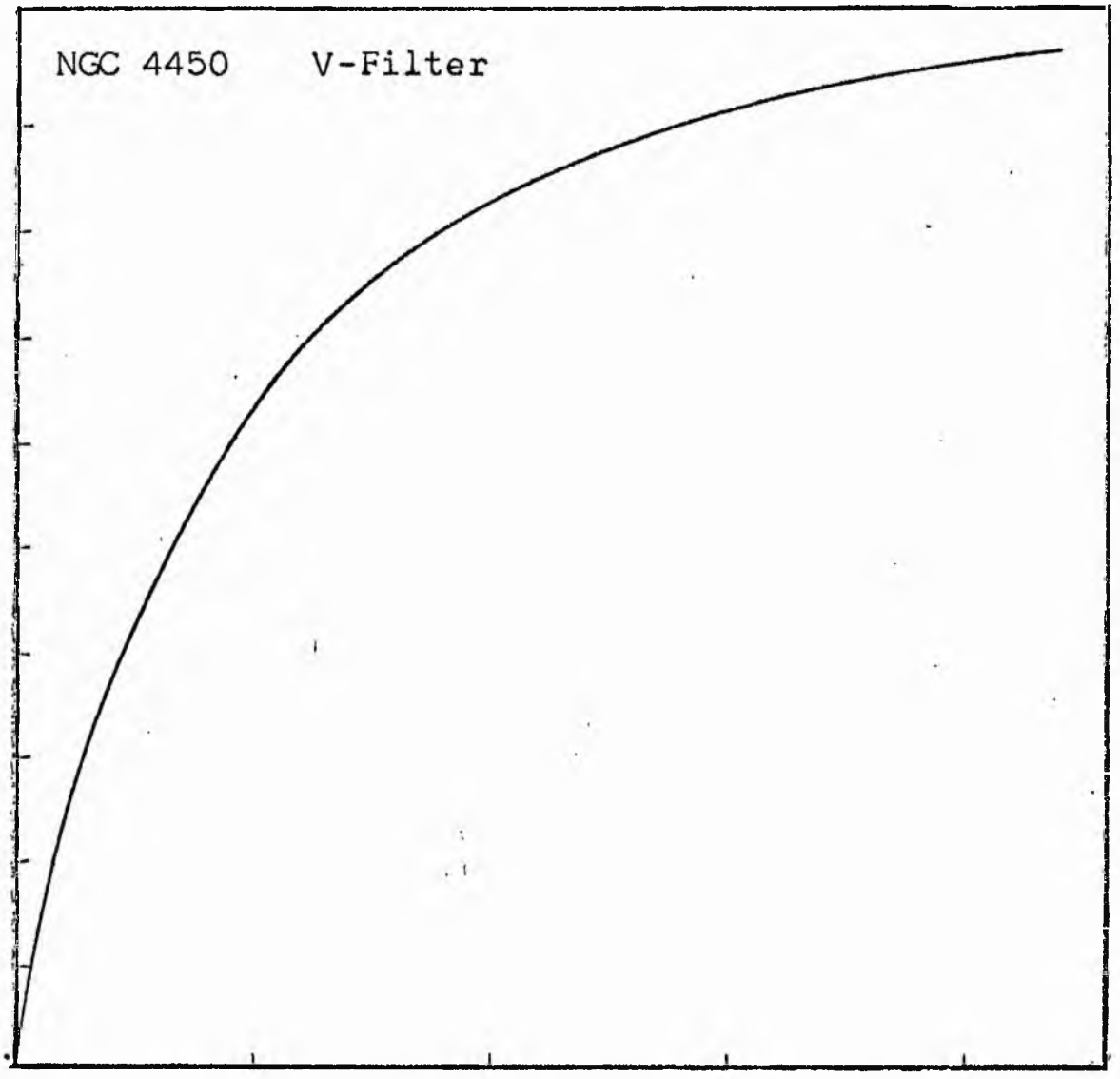

Relative integrated luminosity k(r) versus equivalent radius r*.

MEAN LUMINOSITY DISTRIBUTION IN NGC 4450
V COLOUR

LOG I	I	$\bar{I}$	R	AREA	ΔA	P	ΣP	K(R)	ρ	LOG J	μ
1.83	67.608		0.0	0.0			0.0	0.0	0.0	1.803	16.50
		65.352			4.52	295.6448					
1.80	63.096		1.20	4.52			295.64	0.01	0.03	1.773	16.58
		56.607			18.38	1040.3425					
1.70	50.119		2.70	22.90			1335.99	0.05	0.07	1.673	16.83
		44.965			15.58	700.6516					
1.60	39.811		3.50	38.48			2036.64	0.08	0.10	1.573	17.08
		35.717			16.93	604.7939					
1.50	31.623		4.20	55.42			2641.43	0.10	0.12	1.473	17.33
		28.371			11.06	313.7344					
1.40	25.119		4.60	66.48			2955.17	0.11	0.13	1.373	17.58
		22.536			28.56	643.5515					
1.30	19.952		5.50	95.03			3598.72	0.14	0.15	1.273	17.83
		17.901			33.65	602.2930					
1.20	15.849		6.40	128.68			4201.01	0.16	0.18	1.173	18.08
		14.219			25.26	359.1492					
1.10	12.589		7.00	153.94			4560.16	0.17	0.19	1.073	18.33
		11.295			73.04	824.9751					
1.00	10.000		8.50	226.98			5385.13	0.20	0.23	0.973	18.58
		8.972			62.55	561.1621					
0.90	7.943		9.60	289.53			5946.29	0.23	0.27	0.873	18.83
		7.126			39.25	279.6924					
0.80	6.310		10.23	328.78			6225.98	0.24	0.28	0.773	19.08
		5.661			81.66	462.2295					
0.70	5.012		11.43	410.43			6688.21	0.25	0.32	0.673	19.33
		4.496			136.13	612.0957					
0.60	3.981		13.19	546.56			7309.30	0.28	0.36	0.573	19.58
		3.572			203.34	726.2727					
0.50	3.162		15.45	749.91			8026.57	0.31	0.43	0.473	19.83
		2.837			210.01	595.8049					
0.40	2.512		17.48	959.91			8622.38	0.33	0.48	0.373	20.08
		2.254			180.18	406.0371					
0.30	1.995		19.05	1140.09			9028.41	0.34	0.53	0.273	20.33
		1.790			594.85	1064.8284					
0.20	1.585		23.50	1734.94			10093.24	0.38	0.65	0.173	20.58
		1.422			1071.79	1523.9792					
0.10	1.259		29.89	2806.74			11617.22	0.44	0.83	0.073	20.83
		1.129			1806.44	2040.2957					
-0.00	1.000		38.32	4613.18			13657.51	0.52	1.06	-0.027	21.08
		0.897			1819.43	1632.3118					
-0.10	0.794		45.25	6432.61			15289.82	0.58	1.25	-0.127	21.33
		0.713			1899.68	1353.7864					
-0.20	0.631		51.50	8332.29			16643.61	0.63	1.42	-0.227	21.58
		0.566			1067.64	604.3550					
-0.30	0.501		54.70	9399.93			17247.96	0.66	1.51	-0.327	21.83
		0.450			1241.40	558.1875					
-0.40	0.398		58.20	10641.32			17806.14	0.68	1.61	-0.427	22.08
		0.357			1552.10	554.3564					
-0.50	0.316		62.30	12193.43			18360.50	0.70	1.72	-0.527	22.33
		0.284			1816.71	515.4136					
-0.60	0.251		66.78	14010.14			18875.91	0.72	1.84	-0.627	22.58
		0.225			3304.98	744.7971					
-0.70	0.200		74.24	17315.12			19620.71	0.75	2.05	-0.727	22.83
		0.179			4067.34	728.0815					
-0.80	0.158		82.50	21382.46			20348.79	0.77	2.28	-0.827	23.08
		0.142			4948.48	703.6240					
-0.90	0.126		91.55	26330.94			21052.41	0.80	2.53	-0.927	23.33
		0.113			5970.78	674.3738					
-1.00	0.100		101.40	32301.72			21726.78	0.83	2.80	-1.027	23.58
		0.090			4818.36	432.2839					
-1.10	0.079		108.70	37120.08			22159.06	0.84	3.00	-1.127	23.83
		0.071			7968.17	567.8445					
-1.20	0.063		119.80	45088.25			22726.90	0.86	3.31	-1.227	24.08
		0.057			11828.48	669.5764					
-1.30	0.050		134.60	56916.73			23396.48	0.89	3.72	-1.327	24.33
		0.045			11710.83	526.5742					
-1.40	0.040		147.80	68627.56			23923.05	0.91	4.08	-1.427	24.58
		0.036			7826.19	279.5264					
-1.50	0.032		156.00	76453.75			24202.57	0.92	4.31	-1.527	24.83
		0.028			8145.56	231.0969					
-1.60	0.025		164.10	84599.31			24433.67	0.93	4.53	-1.627	25.08
		0.023			9642.94	217.3117					
-1.70	0.020		173.20	94242.25			24650.98	0.94	4.78	-1.727	25.33
		0.018			16086.56	287.9636					
-1.80	0.016		187.40	110328.81			24938.94	0.95	5.17	-1.827	25.58
		0.014			12585.44	178.9548					
-1.90	0.013		197.80	122914.25			25117.89	0.95	5.46	-1.927	25.83
		0.011			16952.56	191.4745					
-2.00	0.010		211.00	139866.81			25309.36	0.96	5.83	-2.027	26.08
$-\infty$							26309.00	(1)			∞

PHOTOMETRIC PARAMETERS OF NGC 4450

V-FILTER

Total luminosity ..... L_T = 7.31

Total apparent magnitude ..... m_T = 10.03

Apparent central surface brightness ..... μ_o = 16.50

Major axis at threshold ..... $2a_m$ = 7.61

Minor axis at threshold ..... $2b_m$ = 6.32

Major axis at μ=25.0 mag sec^{-2} ..... 2a(25) = 6.20

Luminosity within μ=25.0 mag sec^{-2} ..... k(25) = 0.93

Gradient of exponential component ..... G(a) = -0.71

Equivalent gradient of exponential comp..... G(r*) = -0.68

Equivalent gradient of reduced exp. comp..... G(ρ) = -0.37

Parameters at k = ¼ :

- Semi-major axis ..... a_1 = 0.32
- Axis ratio ..... b/a = 0.53
- Equivalent radius ..... r_1* = 0.19
- Surface brightness ..... μ_1 = 19.33

Parameters at k = ½(effective) :

- Semi-major axis ..... a_e = 0.76
- Axis ratio ..... b/a = 0.51
- Equivalent radius ..... r_e* = 0.60
- Surface brightness ..... μ_e = 21.00
- Mean surface brightness ..... μ_e' = 10.93

Parameters at k = ¾ :

- Semi-major axis ..... a_3 = 1.61
- Axis ratio ..... b/a = 0.63
- Equivalent radius ..... r_3* = 1.26
- Surface brightness ..... μ_3 = 22.83

Concentration indices ..... C_{21} = 3.25, C_{32} = 2.08

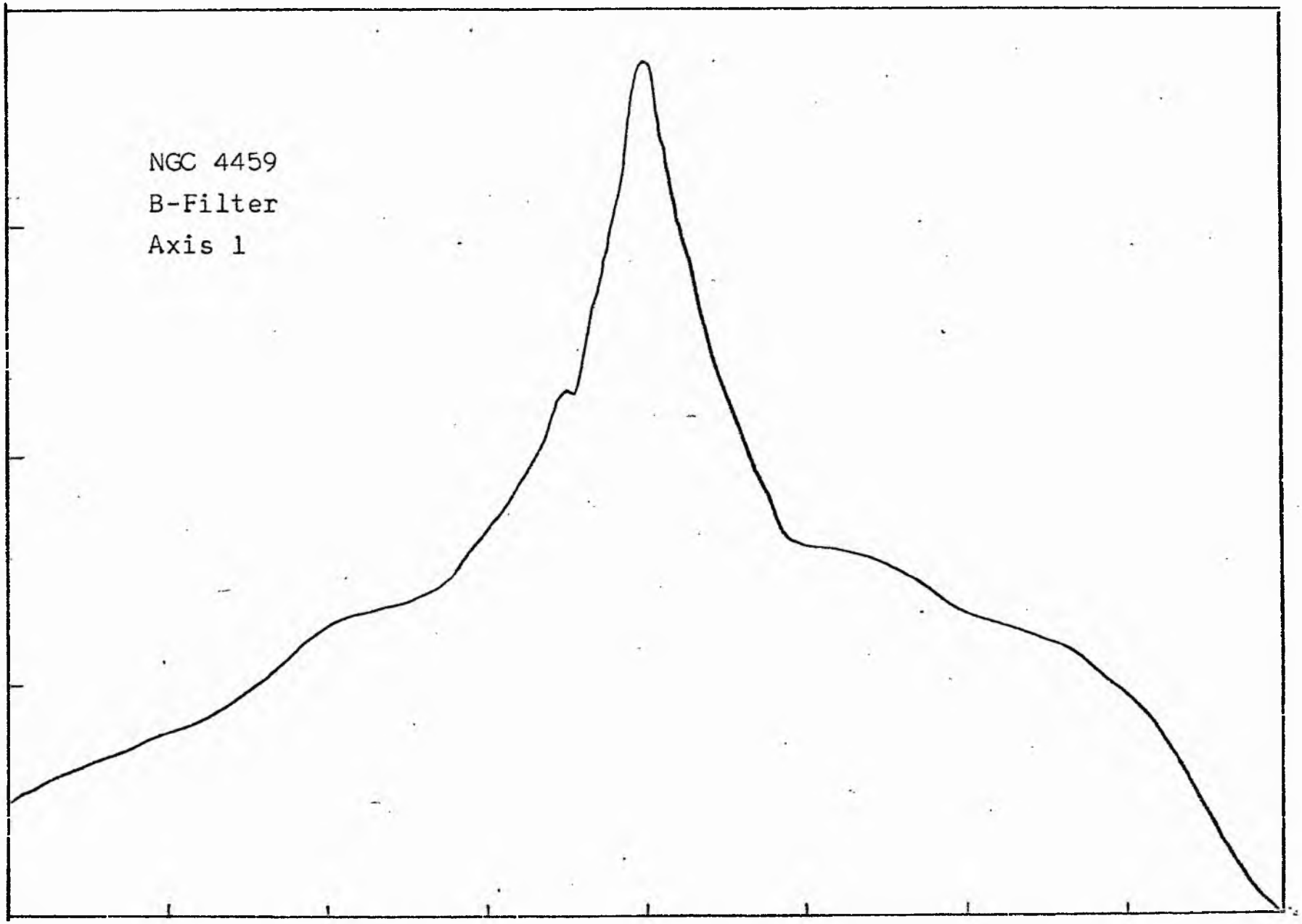
NGC 4459
B-Filter
Axis 1

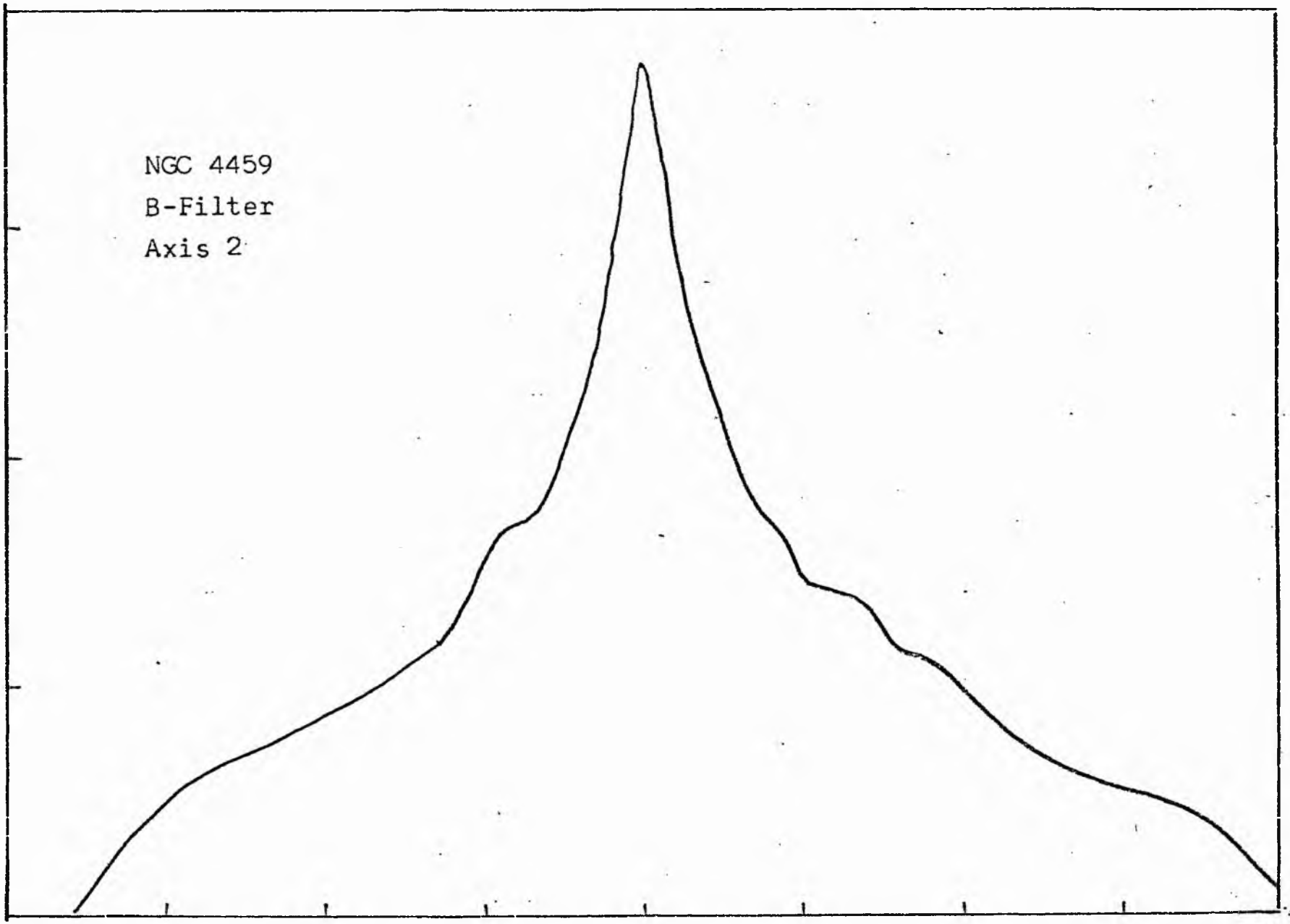
NGC 4459
B-Filter
Axis 2

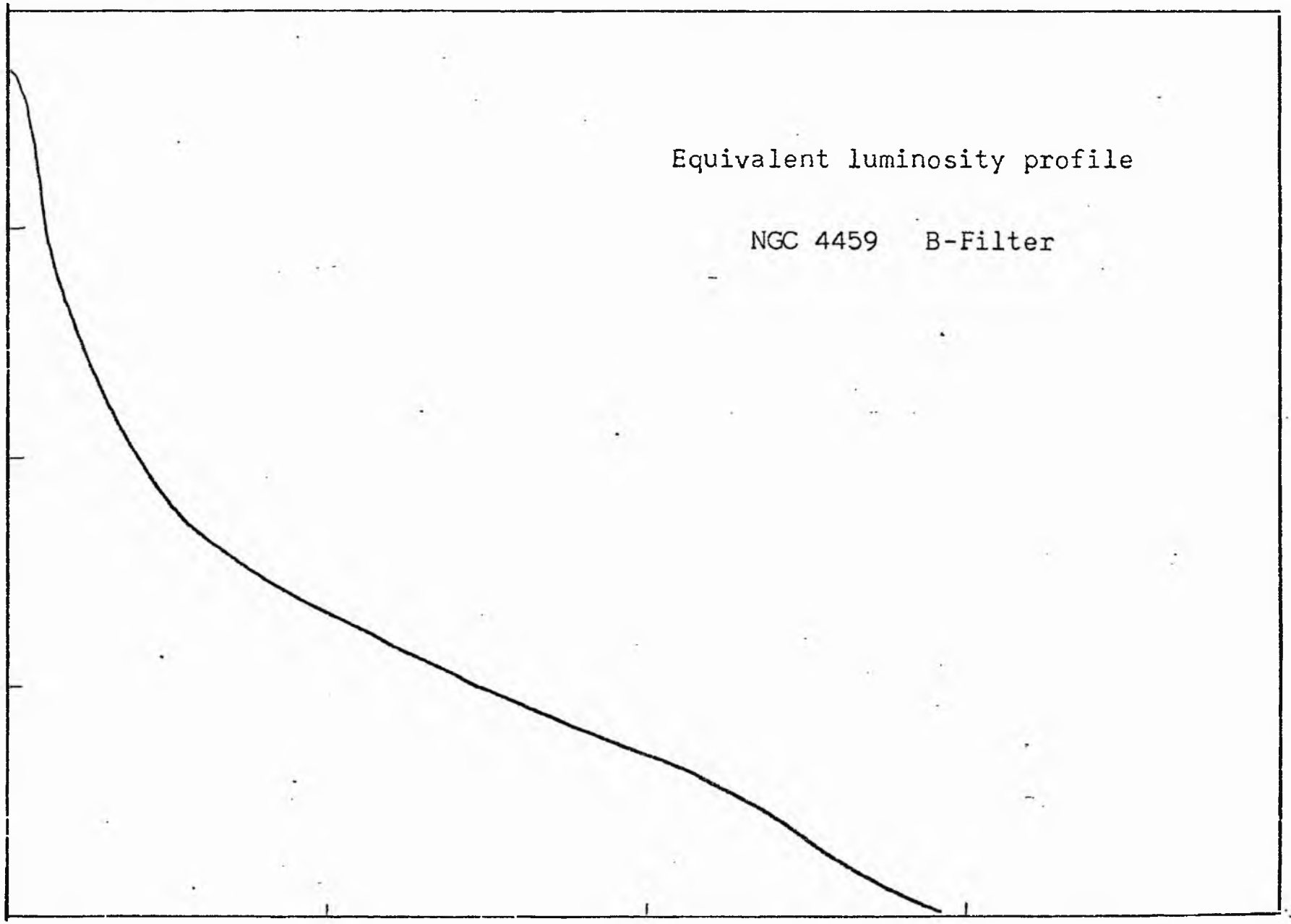
Equivalent luminosity profile
NGC 4459 B-Filter

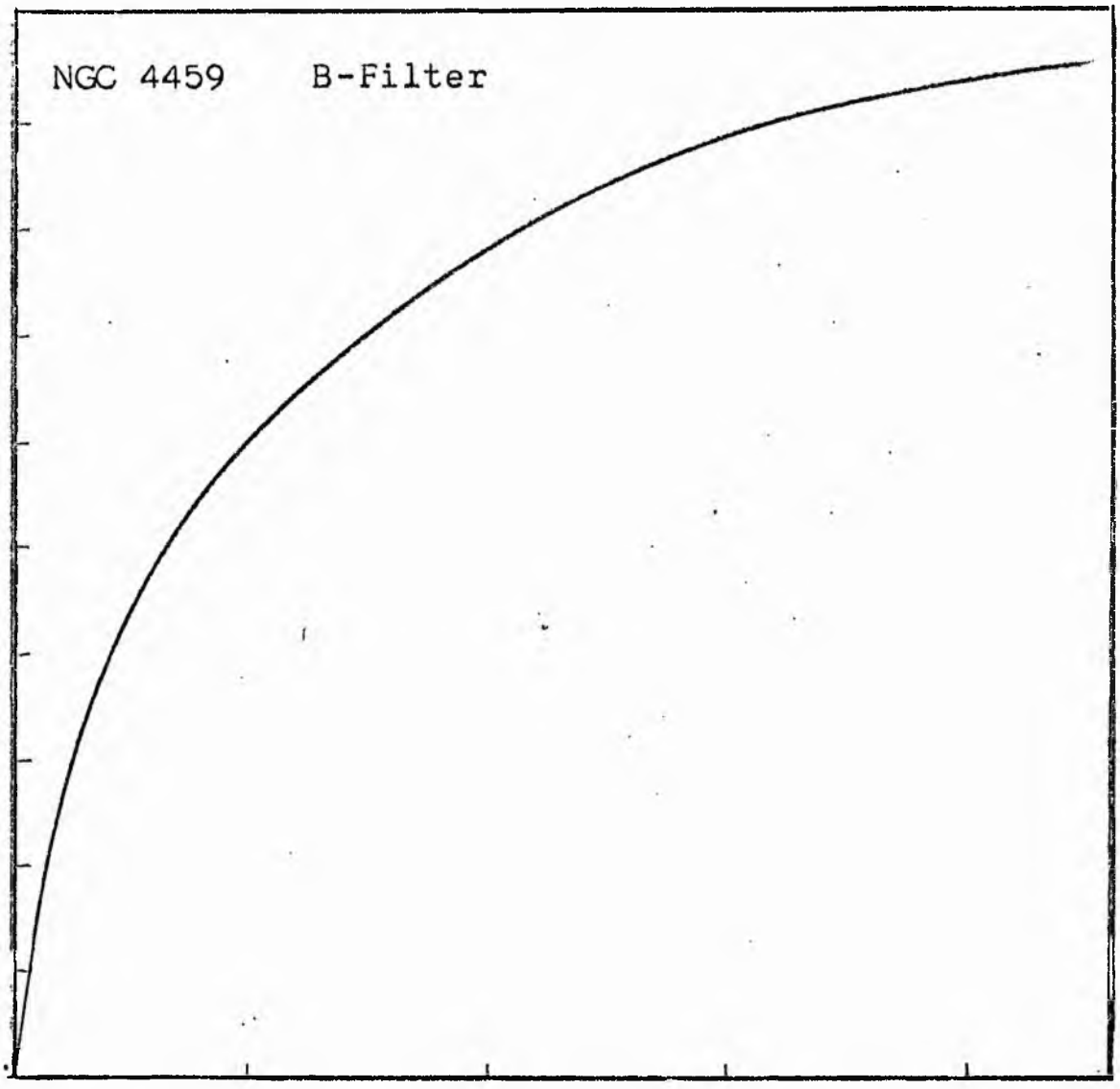

Relative integrated luminosity k(r) versus equivalent radius r*.

MEAN LUMINOSITY DISTRIBUTION IN NGC 4459
B COLOUR

LOG I	I	T	R	AREA	ΔA	P	ΣP	K(R)	ρ	LOG J	μ
1.68	47.863		0.0	0.0			0.0	0.0	0.0	1.722	18.32
		43.837			23.24	1018.8870					
1.60	39.811		2.72	23.24			1018.89	0.04	0.09	1.642	18.52
		35.717			42.94	1533.8381					
1.50	31.623		4.59	66.19			2552.73	0.09	0.14	1.542	18.77
		28.371			28.85	818.3777					
1.40	25.119		5.50	95.03			3371.10	0.12	0.17	1.442	19.02
		22.536			26.90	606.2336					
1.30	19.953		6.23	121.93			3977.34	0.14	0.20	1.342	19.27
		17.901			43.65	781.3918					
1.20	15.849		7.26	165.59			4758.73	0.17	0.23	1.242	19.52
		14.219			66.23	941.6731					
1.10	12.589		8.59	231.81			5700.40	0.20	0.27	1.142	19.77
		11.295			78.59	887.6223					
1.00	10.000		9.94	310.40			6588.02	0.23	0.31	1.042	20.02
		8.972			71.12	638.0181					
0.90	7.943		11.02	381.52			7226.04	0.26	0.35	0.942	20.27
		7.126			100.76	718.0266					
0.80	6.310		12.39	482.27			7944.06	0.28	0.39	0.842	20.52
		5.661			172.79	978.1245					
0.70	5.012		14.44	655.66			8922.18	0.32	0.45	0.742	20.77
		4.496			147.17	661.7578					
0.60	3.981		15.98	802.24			9583.94	0.34	0.50	0.642	21.02
		3.572			195.38	697.8318					
0.50	3.162		17.82	997.62			10281.77	0.36	0.56	0.542	21.27
		2.837			251.49	713.4875					
0.40	2.512		19.94	1249.11			10995.25	0.39	0.63	0.442	21.52
		2.254			378.29	852.5063					
0.30	1.995		22.76	1627.40			11847.75	0.42	0.71	0.342	21.77
		1.790			545.61	976.6729					
0.20	1.585		26.30	2173.01			12824.43	0.45	0.83	0.242	22.02
		1.422			560.97	797.6375					
0.10	1.259		29.50	2733.97			13622.06	0.48	0.93	0.142	22.27
		1.129			296.80	335.2190					
-0.00	1.000		31.06	3030.77			13957.28	0.49	0.98	0.042	22.52
		0.897			769.45	690.3230					
-0.10	0.794		34.78	3800.22			14647.60	0.52	1.09	-0.058	22.77
		0.713			1091.52	777.8599					
-0.20	0.631		39.46	4891.74			15425.46	0.55	1.24	-0.158	23.02
		0.566			1472.81	833.7122					
-0.30	0.501		45.01	6364.55			16259.17	0.58	1.41	-0.258	23.27
		0.450			1974.21	887.6926					
-0.40	0.398		51.52	8338.76			17146.86	0.61	1.62	-0.358	23.52
		0.357			2582.30	922.3083					
-0.50	0.316		58.96	10921.05			18069.17	0.64	1.85	-0.458	23.77
		0.284			4384.09	1244.0254					
-0.60	0.251		69.80	15305.95			19313.19	0.68	2.19	-0.558	24.02
		0.225			5407.95	1218.7158					
-0.70	0.200		81.20	20713.09			20531.91	0.73	2.55	-0.658	24.27
		0.179			4902.92	877.6575					
-0.80	0.158		90.30	25616.82			21409.56	0.76	2.84	-0.758	24.52
		0.142			6684.91	950.5293					
-0.90	0.126		101.40	32301.72			22360.09	0.79	3.18	-0.858	24.77
		0.113			3464.96	391.3525					
-1.00	0.100		106.70	35766.68			22751.44	0.81	3.35	-0.958	25.02
		0.090			8273.91	742.3042					
-1.10	0.079		118.40	44040.59			23493.74	0.83	3.72	-1.058	25.27
		0.071			11698.30	833.6699					
-1.20	0.063		133.20	55738.89			24327.41	0.86	4.18	-1.158	25.52
		0.057			12610.36	713.8379					
-1.30	0.050		147.50	68349.25			25041.25	0.89	4.63	-1.258	25.77
		0.045			15941.00	716.7842					
-1.40	0.040		163.80	84290.25			25758.03	0.91	5.14	-1.358	26.02
		0.036			9083.37	324.4297					
-1.50	0.032		172.40	93373.62			26082.46	0.92	5.41	-1.458	26.27
		0.028			8753.50	248.3454					
-1.60	0.025		180.30	102127.12			26330.80	0.93	5.66	-1.558	26.52
		0.023			12121.56	273.1702					
-1.70	0.020		190.70	114248.69			26603.97	0.94	5.99	-1.658	26.77
		0.018			10662.12	190.8618					
-1.80	0.016		199.40	124910.81			26794.83	0.95	6.26	-1.758	27.02
		0.014			16684.75	237.2441					
-1.90	0.013		212.30	141595.56			27032.07	0.96	6.67	-1.858	27.27
		0.011			12816.50	144.7591					
-2.00	0.010		221.70	154412.06			27176.83	0.96	6.96	-1.958	27.52
-∞							28226.00	(1)			∞

PHOTOMETRIC PARAMETERS OF NGC 4459

B-FILTER

Total luminosity ..... L_T = 7.84

Total apparent magnitude ..... m_T = 11.39

Apparent central surface brightness ..... μ_o = 18.32

Major axis at threshold ..... $2a_m$ = 7.97

Minor axis at threshold ..... $2b_m$ = 6.18

Major axis at μ=25.0 mag sec^{-2} ..... 2a(25) = 4.43

Luminosity within μ=25.0 mag sec^{-2} ..... k(25) = 0.81

Gradient of exponential component ..... G(a) = -0.69

Equivalent gradient of exponential comp. .... G(r*) = -0.55

Equivalent gradient of reduced exp. comp. .... G(ρ) = -0.30

Parameters at k = ¼ :

- Semi-major axis ..... a_1 = 0.22
- Axis ratio ..... b/a = 0.69
- Equivalent radius ..... r_1* = 0.18
- Surface brightness ..... μ_1 = 20.19

Parameters at k = ½(effective) :

- Semi-major axis ..... a_e = 0.58
- Axis ratio ..... b/a = 0.69
- Equivalent radius ..... r_e* = 0.53
- Surface brightness ..... μ_e = 22.60
- Mean surface brightness ..... μ_e' = 11.99

Parameters at k = ¾ :

- Semi-major axis ..... a_3 = 1.93
- Axis ratio ..... b/a = 0.57
- Equivalent radius ..... r_3* = 1.46
- Surface brightness ..... μ_3 = 24.44

Concentration indices ..... C_{21} = 2.97, C_{32} = 2.75

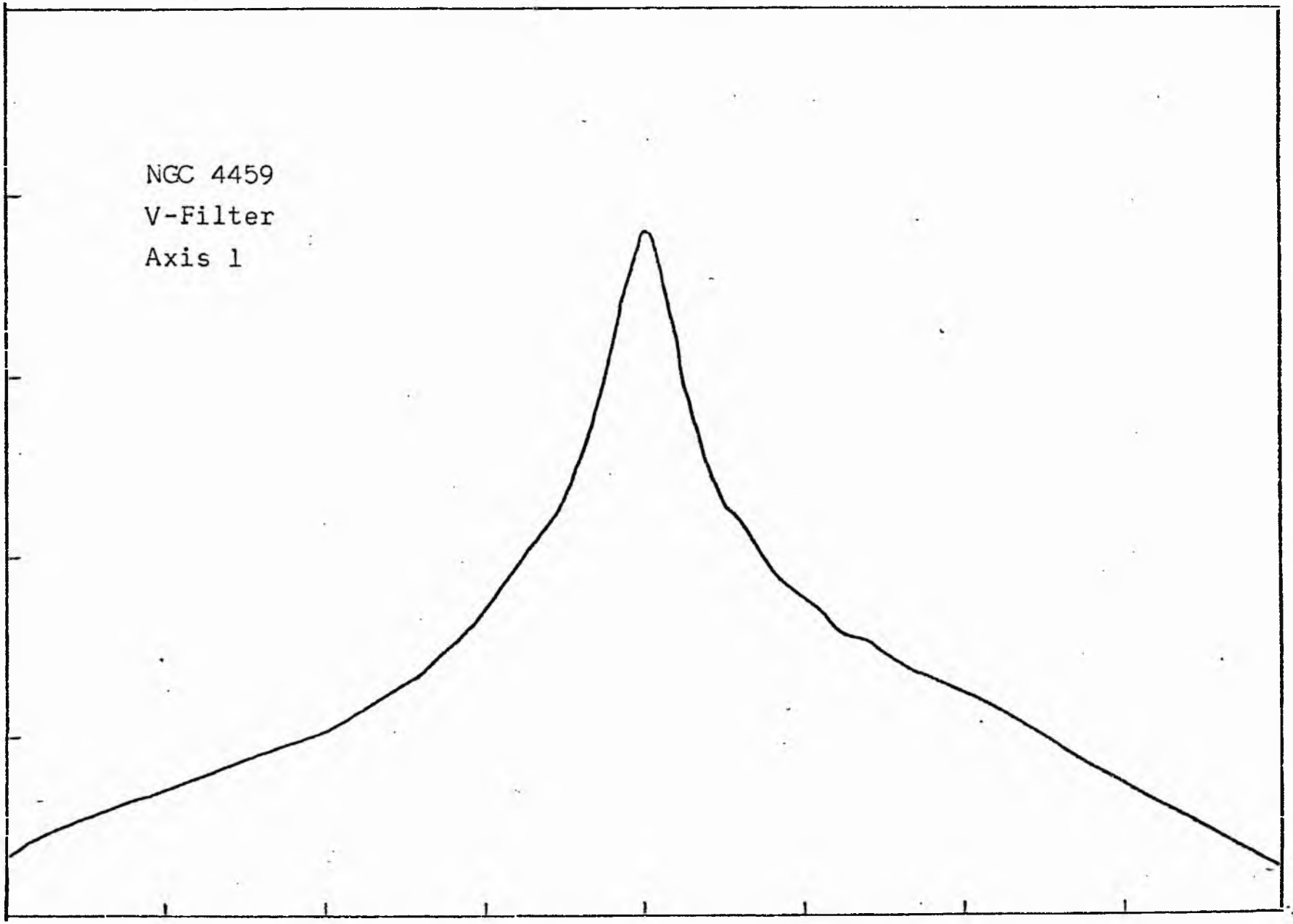
NGC 4459
V-Filter
Axis 1

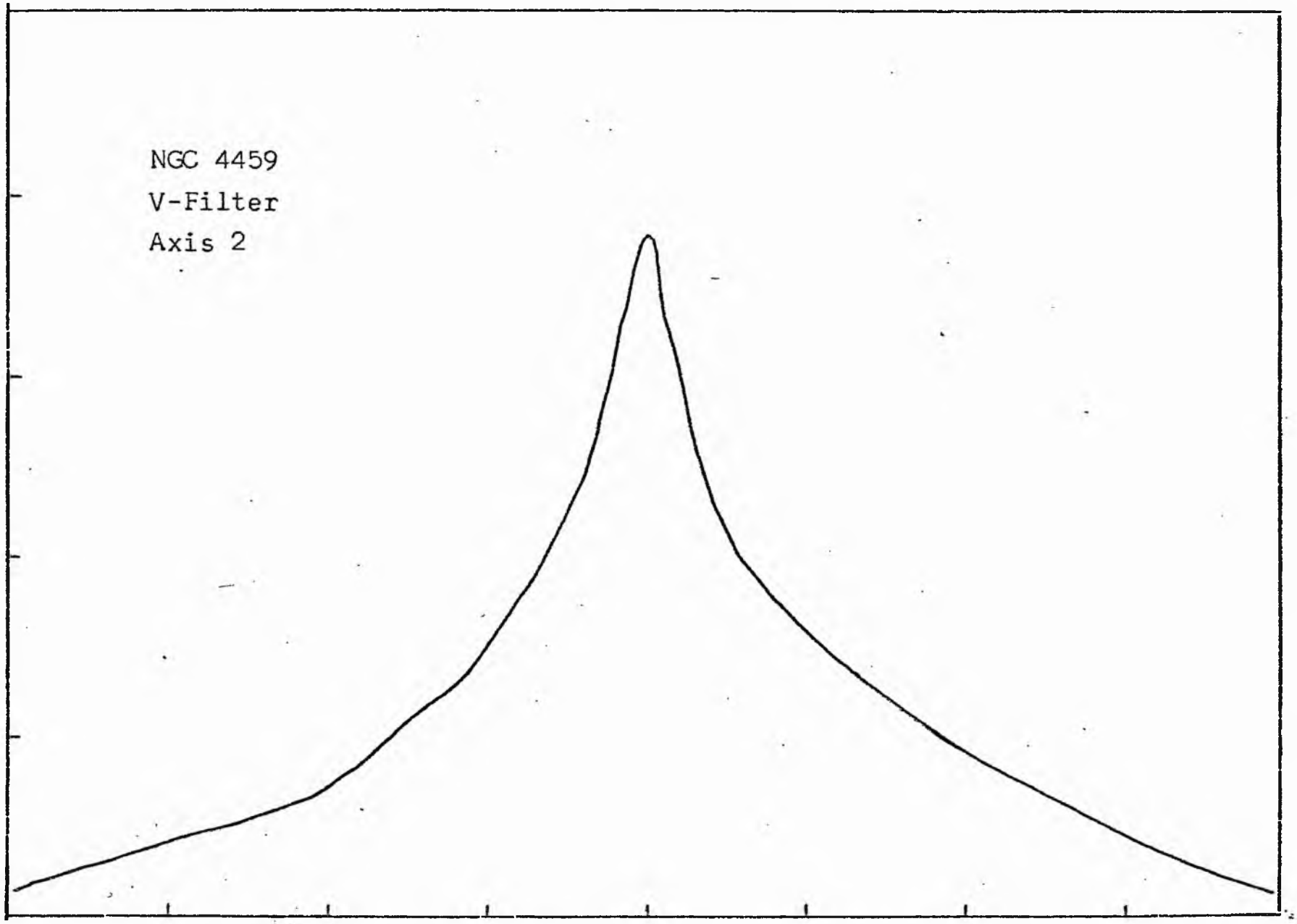
NGC 4459
V-Filter
Axis 2

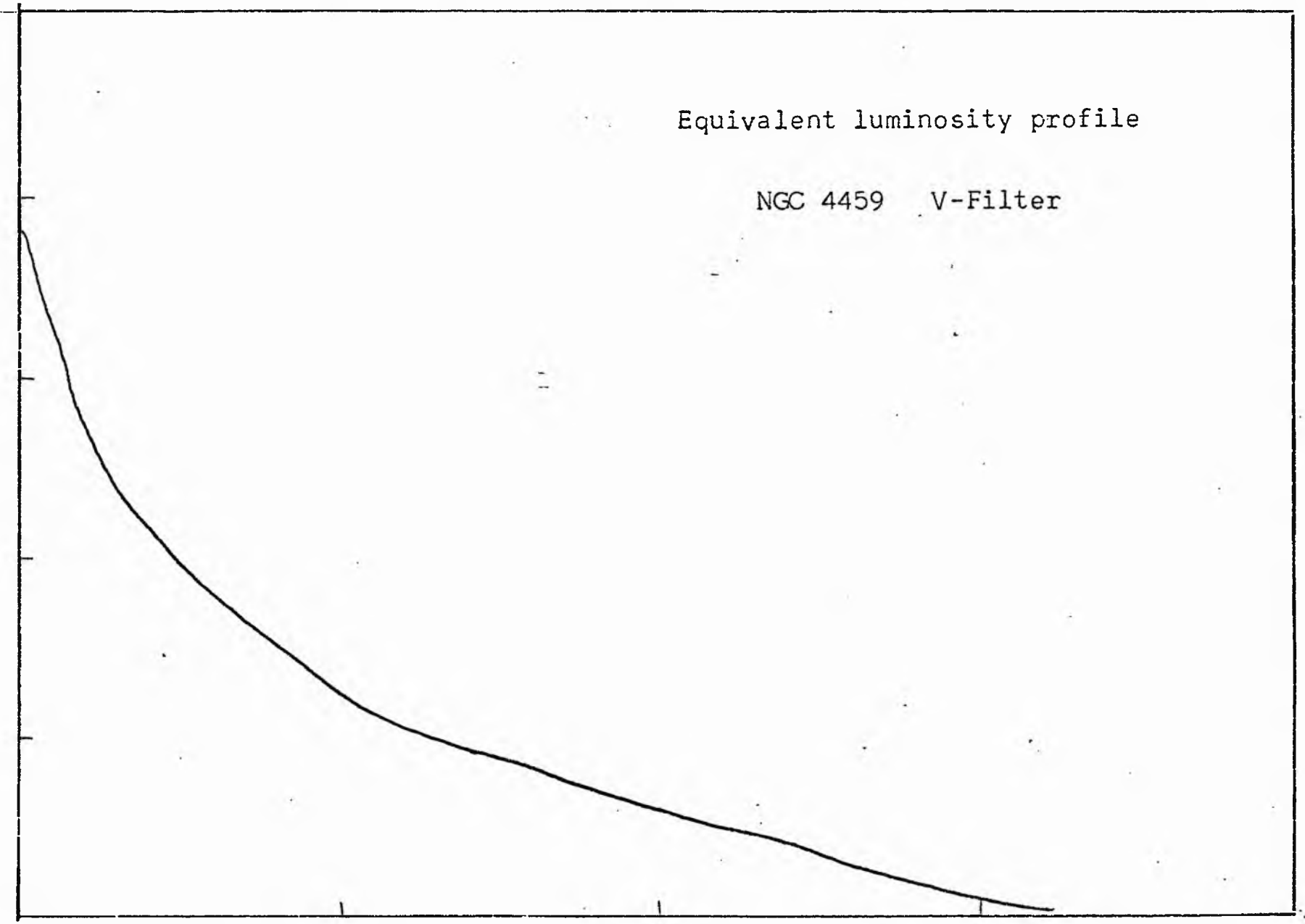
Equivalent luminosity profile
NGC 4459 V-Filter

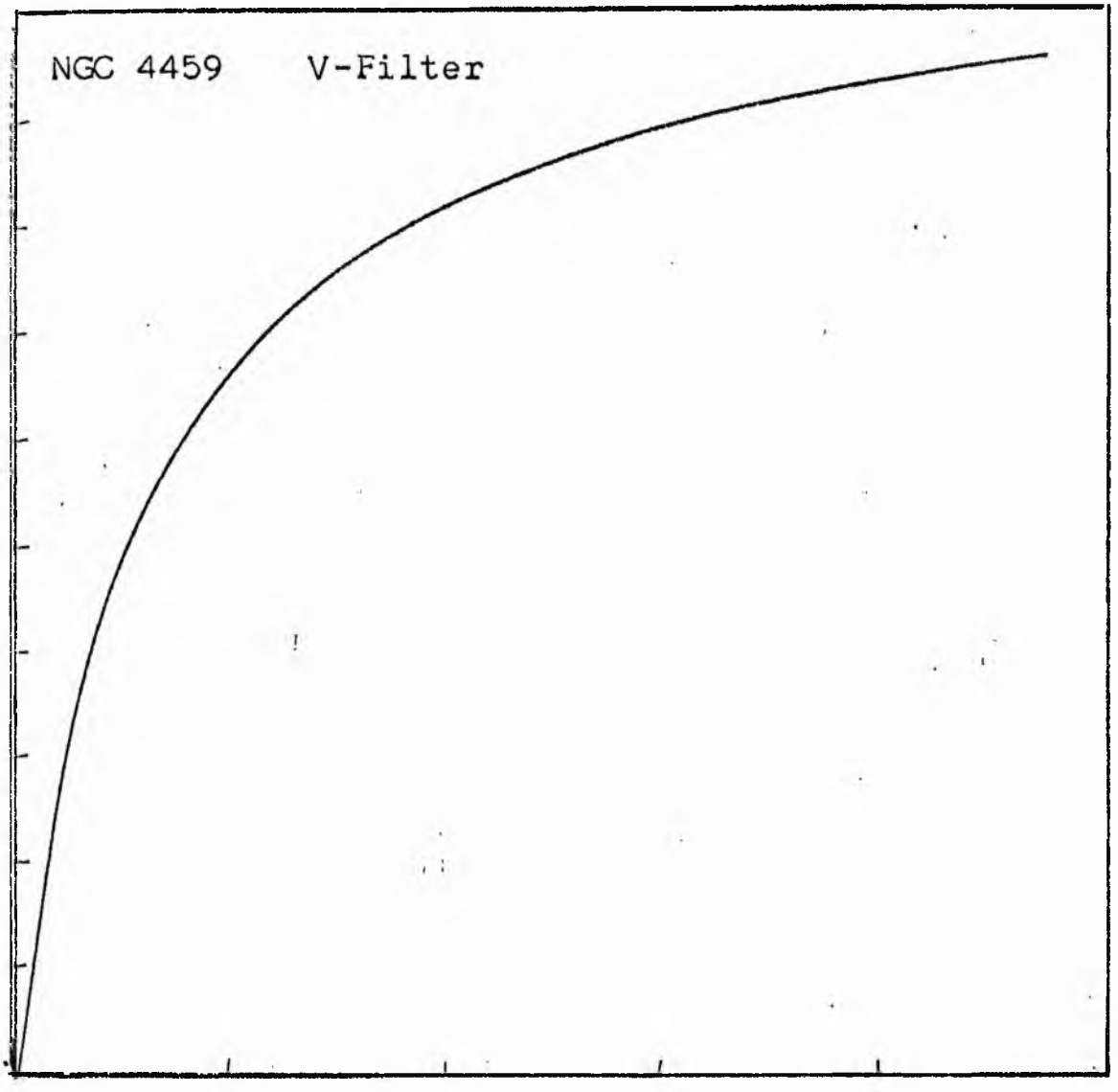

Relative integrated luminosity k(r) versus equivalent radius r*.

MEAN LUMINOSITY DISTRIBUTION IN NGC 4459
V COLOUR

LOG I	I	$\bar{I}$	R	AREA	ΔA	P	ΣP	K(R)	ρ	LUG J	μ
1.78	60.256		0.0	0.0			0.0	0.0	0.0	1.535	17.30
		55.187			5.31	293.0049					
1.70	50.119		1.30	5.31			293.00	0.01	0.05	1.455	17.50
		44.965			21.11	949.2708					
1.60	39.811		2.90	26.42			1242.28	0.04	0.11	1.355	17.75
		35.717			29.00	1035.6716					
1.50	31.623		4.20	55.42			2277.95	0.08	0.16	1.255	18.00
		28.371			39.62	1123.9216					
1.40	25.119		5.50	95.03			3401.87	0.12	0.20	1.155	18.25
		22.536			48.53	1093.6560					
1.30	19.953		6.76	143.56			4495.52	0.15	0.25	1.055	18.50
		17.901			68.71	1229.9409					
1.20	15.849		8.22	212.27			5725.46	0.20	0.31	0.955	18.75
		14.219			84.54	1202.0774					
1.10	12.589		9.72	296.81			6927.54	0.24	0.36	0.855	19.00
		11.295			68.27	771.0435					
1.00	10.000		10.78	365.08			7698.58	0.26	0.40	0.755	19.25
		8.972			81.30	729.3723					
0.90	7.943		11.92	446.38			8427.95	0.29	0.44	0.655	19.50
		7.126			155.38	1107.3020					
0.80	6.310		13.84	601.76			9535.25	0.33	0.51	0.555	19.75
		5.661			177.55	1005.0735					
0.70	5.012		15.75	779.31			10540.32	0.36	0.58	0.455	20.00
		4.496			177.31	797.2671					
0.60	3.981		17.45	956.62			11337.59	0.39	0.65	0.355	20.25
		3.572			169.15	604.1472					
0.50	3.162		18.93	1125.77			11941.73	0.41	0.70	0.255	20.50
		2.837			318.33	903.1304					
0.40	2.512		21.44	1444.10			12844.86	0.44	0.80	0.155	20.75
		2.254			385.11	867.8638					
0.30	1.995		24.13	1829.21			13712.72	0.47	0.90	0.055	21.00
		1.790			769.32	1377.1282					
0.20	1.585		28.76	2598.53			15089.85	0.52	1.07	-0.045	21.25
		1.422			592.38	842.3013					
0.10	1.259		31.87	3190.91			15932.15	0.55	1.18	-0.145	21.50
		1.129			513.77	580.2825					
-0.00	1.000		34.34	3704.68			16512.43	0.57	1.27	-0.245	21.75
		0.897			968.89	869.2522					
-0.10	0.794		38.57	4673.57			17381.68	0.60	1.43	-0.345	22.00
		0.713			1262.91	899.9966					
-0.20	0.631		43.47	5936.48			18281.68	0.63	1.61	-0.445	22.25
		0.566			1621.88	918.0984					
-0.30	0.501		49.05	7558.36			19199.77	0.66	1.82	-0.545	22.50
		0.450			2052.39	922.8457					
-0.40	0.398		55.31	9610.75			20122.62	0.69	2.05	-0.645	22.75
		0.357			1876.86	670.3501					
-0.50	0.316		60.47	11487.61			20792.96	0.71	2.24	-0.745	23.00
		0.284			1879.71	533.2871					
-0.60	0.251		65.23	13367.32			21326.25	0.73	2.42	-0.845	23.25
		0.225			2114.57	476.5332					
-0.70	0.200		70.20	15481.89			21802.78	0.75	2.60	-0.945	23.50
		0.179			3047.96	545.6064					
-0.80	0.158		76.80	18529.85			22348.39	0.77	2.85	-1.045	23.75
		0.142			4922.00	699.8616					
-0.90	0.126		86.40	23451.86			23048.25	0.79	3.21	-1.145	24.00
		0.113			7152.56	807.8521					
-1.00	0.100		98.70	30604.41			23856.10	0.82	3.66	-1.245	24.25
		0.090			5633.10	505.3804					
-1.10	0.079		107.40	36237.51			24361.48	0.84	3.99	-1.345	24.50
		0.071			7654.43	545.4068					
-1.20	0.063		118.20	43891.94			24906.96	0.85	4.39	-1.445	24.75
		0.057			12014.45	680.1050					
-1.30	0.050		133.40	55906.39			25587.06	0.88	4.95	-1.545	25.00
		0.045			8066.78	362.7212					
-1.40	0.040		142.70	63973.16			25949.78	0.89	5.30	-1.645	25.25
		0.036			12774.90	456.2795					
-1.50	0.032		156.30	76748.06			26406.06	0.91	5.80	-1.745	25.50
		0.028			21008.75	596.0388					
-1.60	0.025		176.40	97756.81			27002.09	0.93	6.55	-1.845	25.75
		0.023			11280.56	254.2176					
-1.70	0.020		186.30	109037.37			27256.31	0.94	6.91	-1.945	26.00
		0.018			21831.31	390.8003					
-1.80	0.016		204.10	130868.69			27647.11	0.95	7.57	-2.045	26.25
		0.014			21599.31	307.1252					
-1.90	0.013		220.30	152468.00			27954.23	0.96	8.17	-2.145	26.50
		0.011			16625.06	187.7758					
-2.00	0.010		232.00	169093.06			28142.00	0.97	8.61	-2.245	26.75
- ∞							29142.00	(1)			∞

PHOTOMETRIC PARAMETERS OF NGC 4459

V-FILTER

Total luminosity	L_T	= 8.09
Total apparent magnitude	m_T	= 10.59
Apparent central surface brightness	μ_o	= 17.30
Major axis at threshold	$2a_m$	= 7.71
Minor axis at threshold	$2b_m$	= 6.99
Major axis at μ=25.0 mag sec^{-2}	2a(25)	= 4.37
Luminosity within μ=25.0 mag sec^{-2}	k(25)	= 0.88
Gradient of exponential component	G(a)	= -0.65
Equivalent gradient of exponential comp.	G(r*)	= -0.56
Equivalent gradient of reduced exp. comp.	G(ρ)	= -0.21
Parameters at k = ¼ :		
Semi-major axis	a_1	= 0.23
Axis ratio	b/a	= 0.92
Equivalent radius	r_1*	= 0.17
Surface brightness	μ_1	= 19.12
Parameters at k = ½(effective) :		
Semi-major axis	a_e	= 0.42
Axis ratio	b/a	= 0.97
Equivalent radius	r_e*	= 0.45
Surface brightness	μ_e	= 21.15
Mean surface brightness	μ_e'	= 10.84
Parameters at k = ¾ :		
Semi-major axis	a_3	= 1.43
Axis ratio	b/a	= 0.69
Equivalent radius	r_3*	= 1.18
Surface brightness	μ_3	= 23.50
Concentration indices	C_{21}	= 2.64
	C_{32}	= 2.63

PHOTOGRAPHIC SURFACE PHOTOMETRY OF GALAXIES

IN THE VIRGO CLUSTER

by

Christopher W. Fraser

VOLUME THREE

PHOTOMETRIC DATA FOR GALAXIES

NGC 4661 to NGC 4762

EXPLANATORY NOTES FOR USE WITH THE PHOTOMETRIC DATA

The data for each galaxy occupy twelve pages, divided equally between the B and the V colours. The galaxies are listed in increasing order of NGC identification numbers and each page may be described as follows:-

1. Luminosity profile of major axis. The y-axis denotes log I, with the value of log I = -2.00 at the origin. Each division on the y-axis represents a value of +1.00 in log I. For the x-axis, which denotes distance r, the centre of the galaxy is plotted at the centre of the axis. Each division represents 50 arc sec.

2. Luminosity profile of minor axis. The units for the x and y axes are as before.

3. Equivalent luminosity profile. The y-axis denotes increasing log I, each division representing an integer value from a minimum at the origin of log I = -2.00. The distance r is given on the x-axis, from zero at the origin and increasing by 50 arc sec per division.

4. Relative integrated luminosity curve k(r) is plotted as ordinate, each positive division in y

representing a value of 0.1, and r*, as in case 3, denotes increasing distance r*, in 50 arc sec steps.

5. Table of mean luminosity distribution. The areas in column 5 are expressed in square seconds of arc, and in the last column, μ is in mag sec^{-2}.

6. Table of photometric parameters. The units are as follows:-

a. The total luminosity is expressed in sky units per square minute.

b. The apparent central surface brightness is in mag. per square second, as are the surface brightnesses at k = $\frac{1}{4}$, $\frac{1}{2}$ and $\frac{3}{4}$.

c. The major axis and minor axis at threshold together with the major axis at μ = 25.0 mag.sec^{-2}, and the semi-major axis measurements at k = $\frac{1}{4}$, $\frac{1}{2}$ and $\frac{3}{4}$, are expressed in minutes of arc.

d. The gradient of the exponential component G(a) = d log I/da is expressed per minute of arc, as is the equivalent gradient of the exponential component G(r*) = d log I/dr*.

e. The mean surface brightness is in magnitudes per square minute.

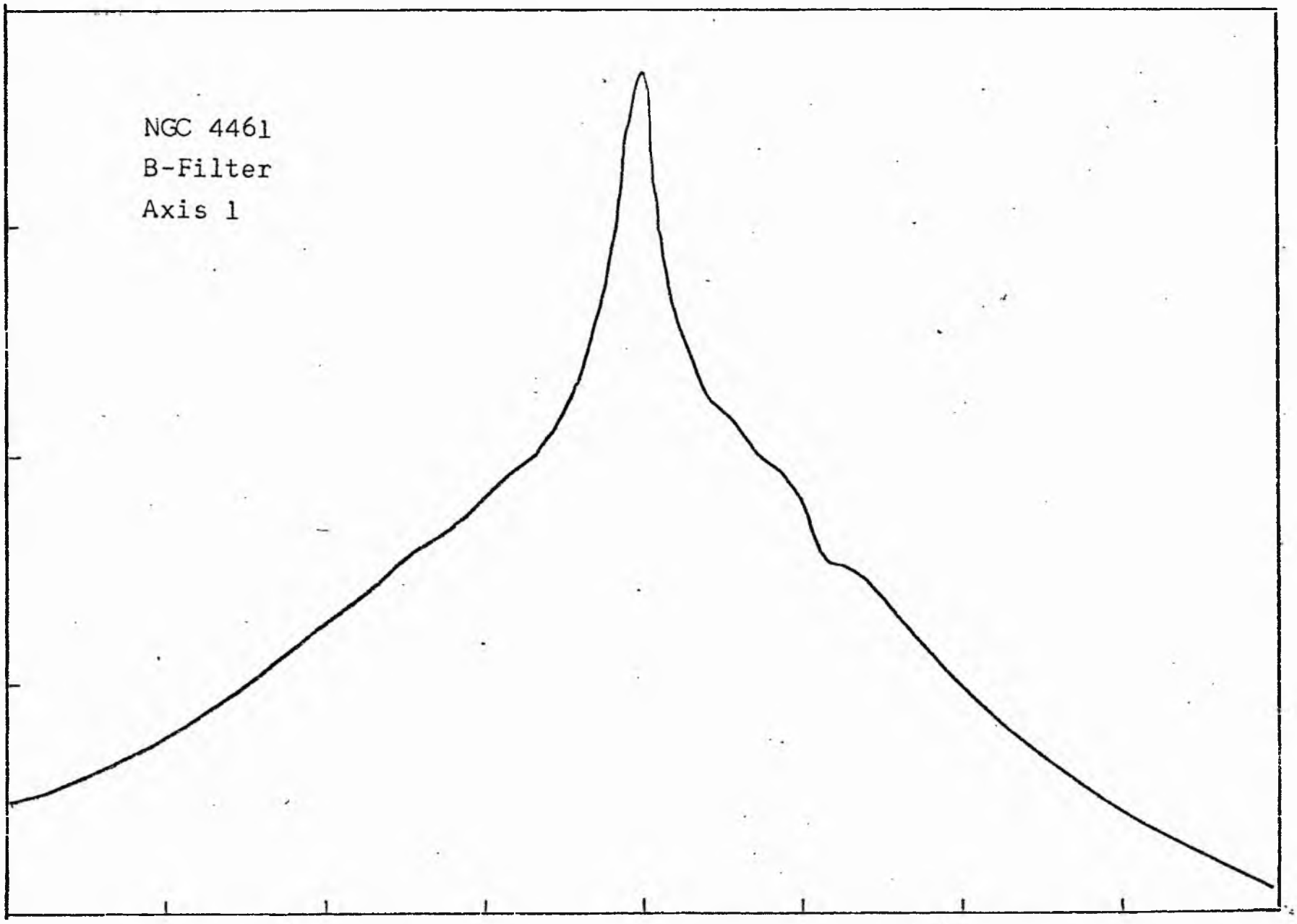
NGC 4461
B-Filter
Axis 1

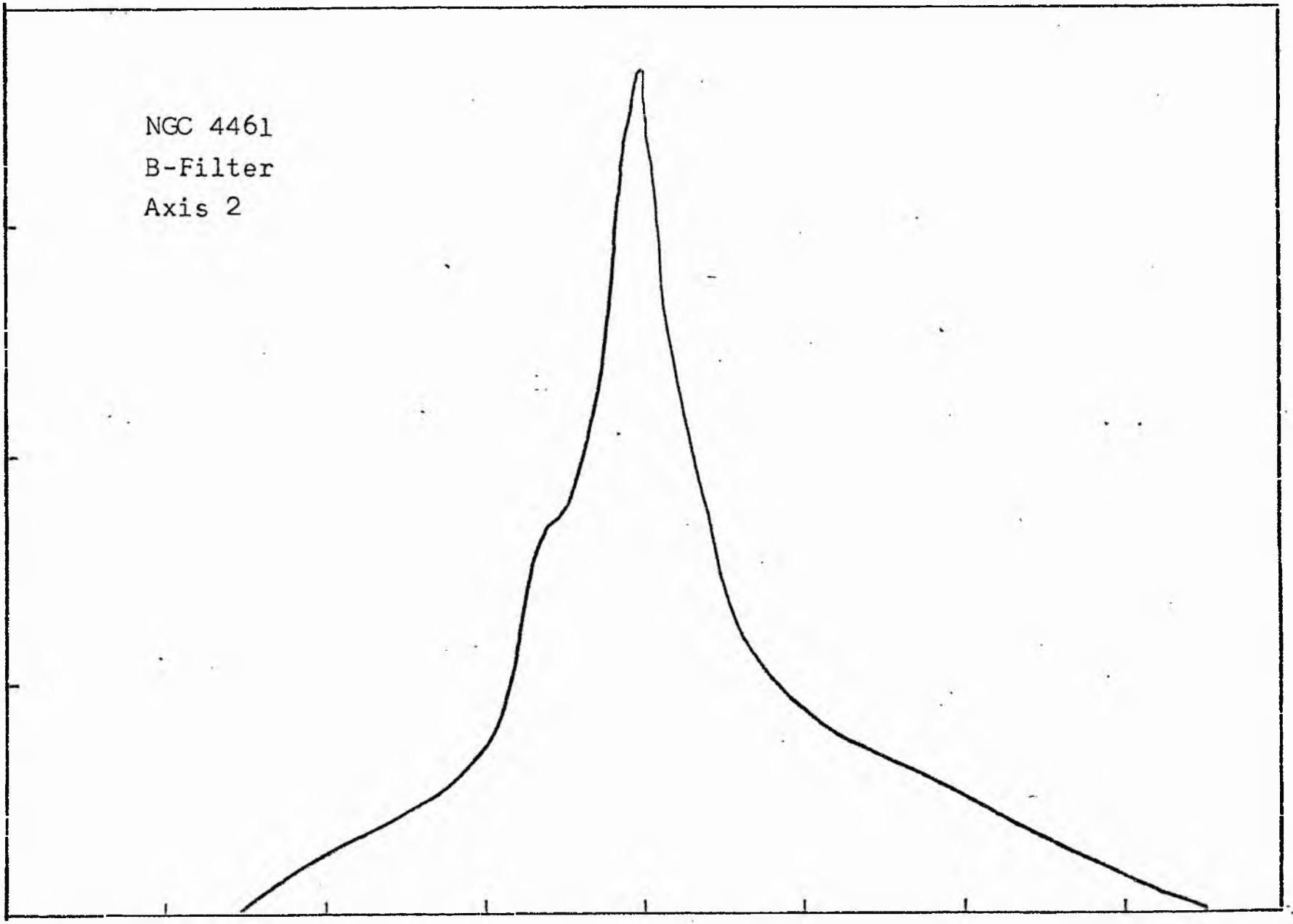
NGC 4461
B-Filter
Axis 2

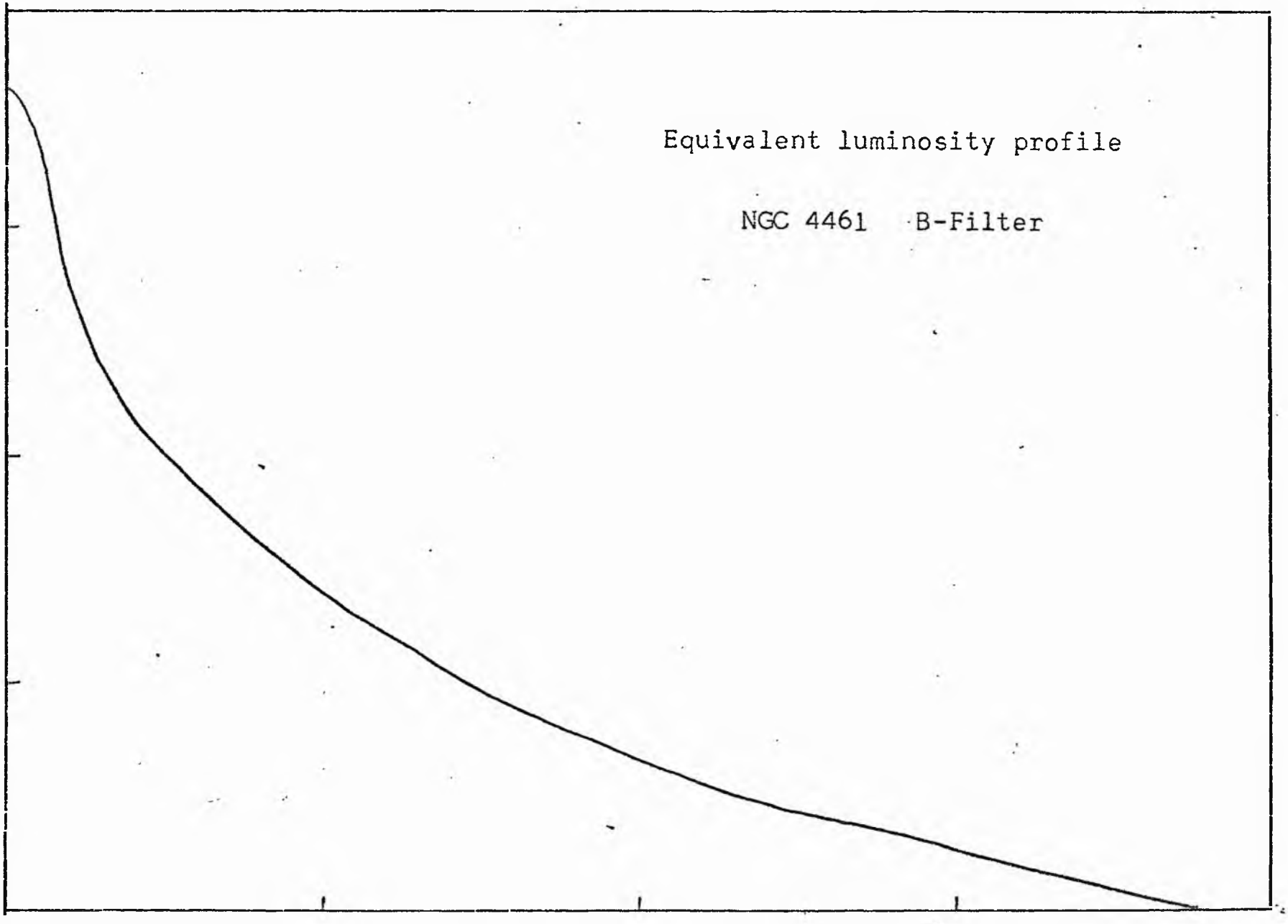
Equivalent luminosity profile
NGC 4461 B-Filter

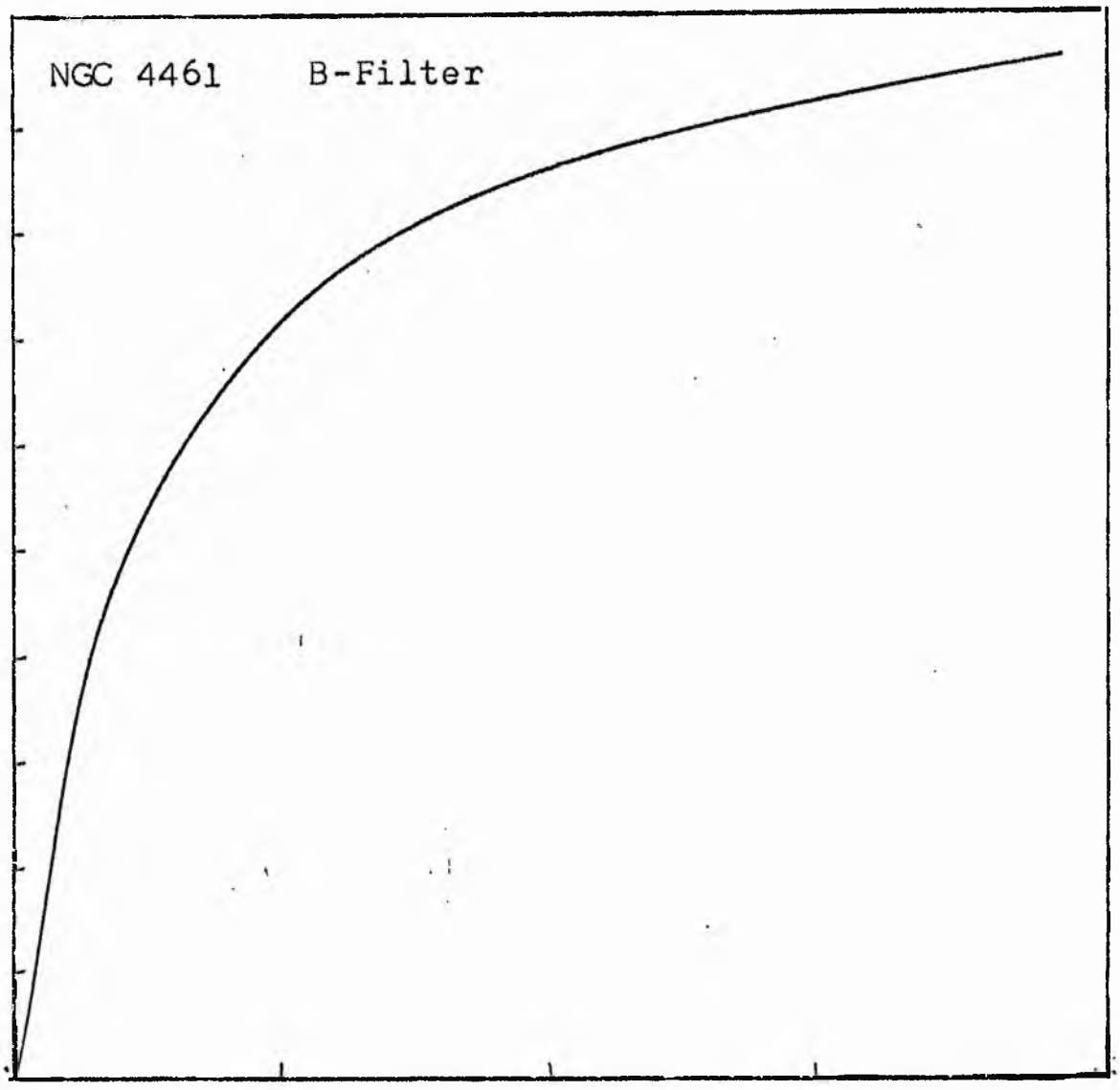

Relative integrated luminosity k(r) versus equivalent radius r*.

MEAN LUMINOSITY DISTRIBUTION IN NGC 4461
B COLOUR

LOG I	I	$\bar{I}$	R	AREA	ΔA	P	ΣP	K(R)	ρ	LOG J	μ
1.65	44.668		0.0	0.0			0.0	0.0	0.0	1.481	18.35
		42.239			20.43	862.8760					
1.60	39.811		2.55	20.43			862.88	0.05	0.12	1.431	18.48
		35.717			9.76	348.6830					
1.50	31.623		3.10	30.19			1211.56	0.07	0.15	1.331	18.73
		28.371			48.66	1380.6200					
1.40	25.119		5.01	78.85			2592.18	0.15	0.24	1.231	18.98
		22.536			25.38	571.8699					
1.30	19.953		5.76	104.23			3164.05	0.19	0.27	1.131	19.23
		17.901			44.04	788.3992					
1.20	15.849		6.87	148.27			3952.45	0.23	0.32	1.031	19.48
		14.219			37.99	540.2031					
1.10	12.589		7.70	186.27			4492.65	0.26	0.36	0.931	19.73
		11.295			31.73	358.3379					
1.00	10.000		8.33	217.99			4850.99	0.29	0.39	0.831	19.98
		8.972			33.10	296.9209					
0.90	7.943		8.94	251.09			5147.91	0.30	0.42	0.731	20.23
		7.126			79.62	567.4055					
0.80	6.310		10.26	330.71			5715.31	0.34	0.48	0.631	20.48
		5.661			56.37	319.0798					
0.70	5.012		11.10	387.08			6034.39	0.35	0.52	0.531	20.73
		4.496			80.52	362.0493					
0.60	3.981		12.20	467.59			6396.43	0.38	0.57	0.431	20.98
		3.572			89.79	320.7136					
0.50	3.162		13.32	557.39			6717.14	0.39	0.63	0.331	21.23
		2.837			158.93	450.8828					
0.40	2.512		15.10	716.31			7168.03	0.42	0.71	0.231	21.48
		2.254			256.82	578.7683					
0.30	1.995		17.60	973.14			7746.79	0.46	0.83	0.131	21.73
		1.790			325.31	582.3242					
0.20	1.585		20.33	1298.45			8329.12	0.49	0.96	0.031	21.98
		1.422			414.42	589.2625					
0.10	1.259		23.35	1712.87			8918.38	0.52	1.10	-0.069	22.23
		1.129			531.78	600.6211					
-0.00	1.000		26.73	2244.64			9519.00	0.56	1.26	-0.169	22.48
		0.897			628.21	563.6013					
-0.10	0.794		30.24	2872.85			10082.60	0.59	1.43	-0.269	22.73
		0.713			752.42	536.2046					
-0.20	0.631		33.97	3625.27			10618.80	0.62	1.60	-0.369	22.98
		0.566			892.10	504.9924					
-0.30	0.501		37.92	4517.37			11123.79	0.65	1.79	-0.469	23.23
		0.450			1048.17	471.3035					
-0.40	0.398		42.09	5565.54			11595.09	0.68	1.98	-0.569	23.48
		0.357			1221.52	436.2852					
-0.50	0.316		46.48	6787.06			12031.38	0.71	2.19	-0.669	23.73
		0.284			1409.87	399.9902					
-0.60	0.251		51.08	8196.93			12431.37	0.73	2.41	-0.769	23.98
		0.225			1306.38	294.4019					
-0.70	0.200		55.00	9503.32			12725.77	0.75	2.59	-0.869	24.23
		0.179			1321.64	236.5823					
-0.80	0.158		58.70	10824.95			12962.35	0.76	2.77	-0.969	24.48
		0.142			2777.00	394.8625					
-0.90	0.126		65.80	13601.95			13357.21	0.78	3.10	-1.069	24.73
		0.113			1879.94	212.3313					
-1.00	0.100		70.20	15481.89			13569.54	0.80	3.31	-1.169	24.98
		0.090			2568.56	230.4415					
-1.10	0.079		75.80	18050.45			13799.98	0.81	3.57	-1.269	25.23
		0.071			5673.62	404.3259					
-1.20	0.063		86.90	23724.07			14204.30	0.83	4.10	-1.369	25.48
		0.057			5410.08	306.2498					
-1.30	0.050		96.30	29134.15			14510.55	0.85	4.54	-1.469	25.73
		0.045			6632.53	298.2305					
-1.40	0.040		106.70	35766.68			14808.78	0.87	5.03	-1.569	25.98
		0.036			8871.07	316.8469					
-1.50	0.032		119.20	44637.75			15125.62	0.89	5.62	-1.669	26.23
		0.028			13011.45	391.8442					
-1.60	0.025		136.40	58449.20			15517.46	0.91	6.43	-1.769	26.48
		0.023			11016.68	248.2706					
-1.70	0.020		148.70	69465.87			15765.73	0.93	7.01	-1.869	26.73
		0.018			12169.75	217.8496					
-1.80	0.016		161.20	81635.62			15983.58	0.94	7.60	-1.969	26.98
		0.014			17232.62	245.0345					
-1.90	0.013		177.40	98868.25			16228.61	0.95	8.36	-2.069	27.23
		0.011			14901.62	168.3100					
-2.00	0.010		190.30	113769.87			16396.92	0.96	8.97	-2.169	27.48
$-\infty$							17016.00	(1)			∞

PHOTOMETRIC PARAMETERS OF NGC 4461

B-FILTER

Total luminosity	L_T	= 4.73
Total apparent magnitude	m_T	= 11.90
Apparent central surface brightness	μ_o	= 18.35
Major axis at threshold	$2a_m$	= 7.53
Minor axis at threshold	$2b_m$	= 5.22
Major axis at μ=25.0 mag sec^{-2}	2a(25)	= 3.85
Luminosity within μ=25.0 mag sec^{-2}	k(25)	= 0.80
Gradient of exponential component	G(a)	= -0.85
Equivalent gradient of exponential comp.	G(r*)	= -0.65
Equivalent gradient of reduced exp. comp.	G(ρ)	= -0.53
Parameters at k = ¼ :		
Semi-major axis	a_1	= 0.13
Axis ratio	b/a	= 0.88
Equivalent radius	r_1*	= 0.12
Surface brightness	μ_1	= 19.65
Parameters at k = ½(effective) :		
Semi-major axis	a_e	= 0.46
Axis ratio	b/a	= 0.72
Equivalent radius	r_e*	= 0.35
Surface brightness	μ_e	= 22.06
Mean surface brightness	μ_e'	= 11.60
Parameters at k = ¾ :		
Semi-major axis	a_3	= 1.42
Axis ratio	b/a	= 0.39
Equivalent radius	r_3*	= 0.93
Surface brightness	μ_3	= 24.23
Concentration indices	C_{21}	= 2.90
	C_{32}	= 2.62

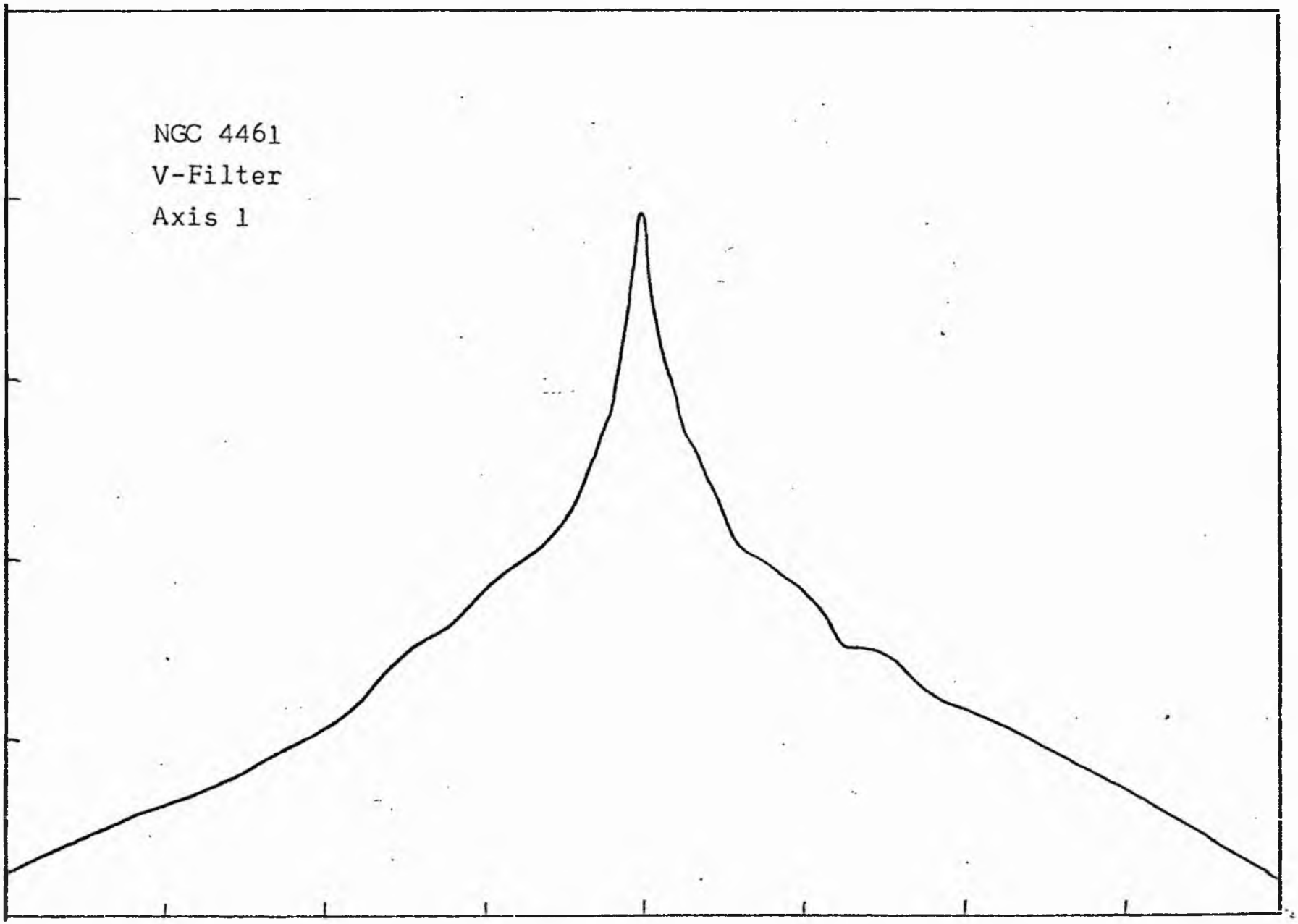
NGC 4461
V-Filter
Axis 1

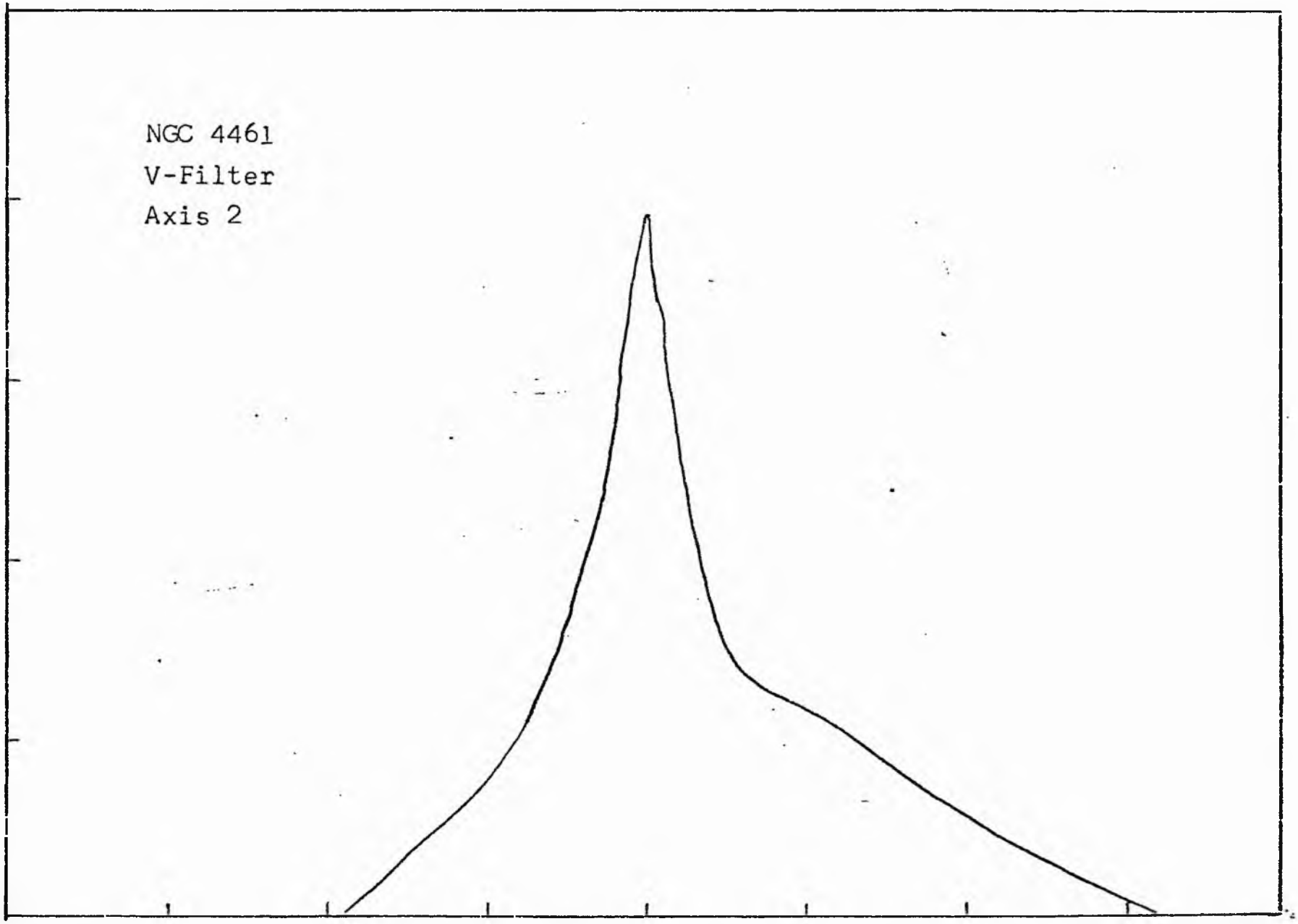
NGC 4461
V-Filter
Axis 2

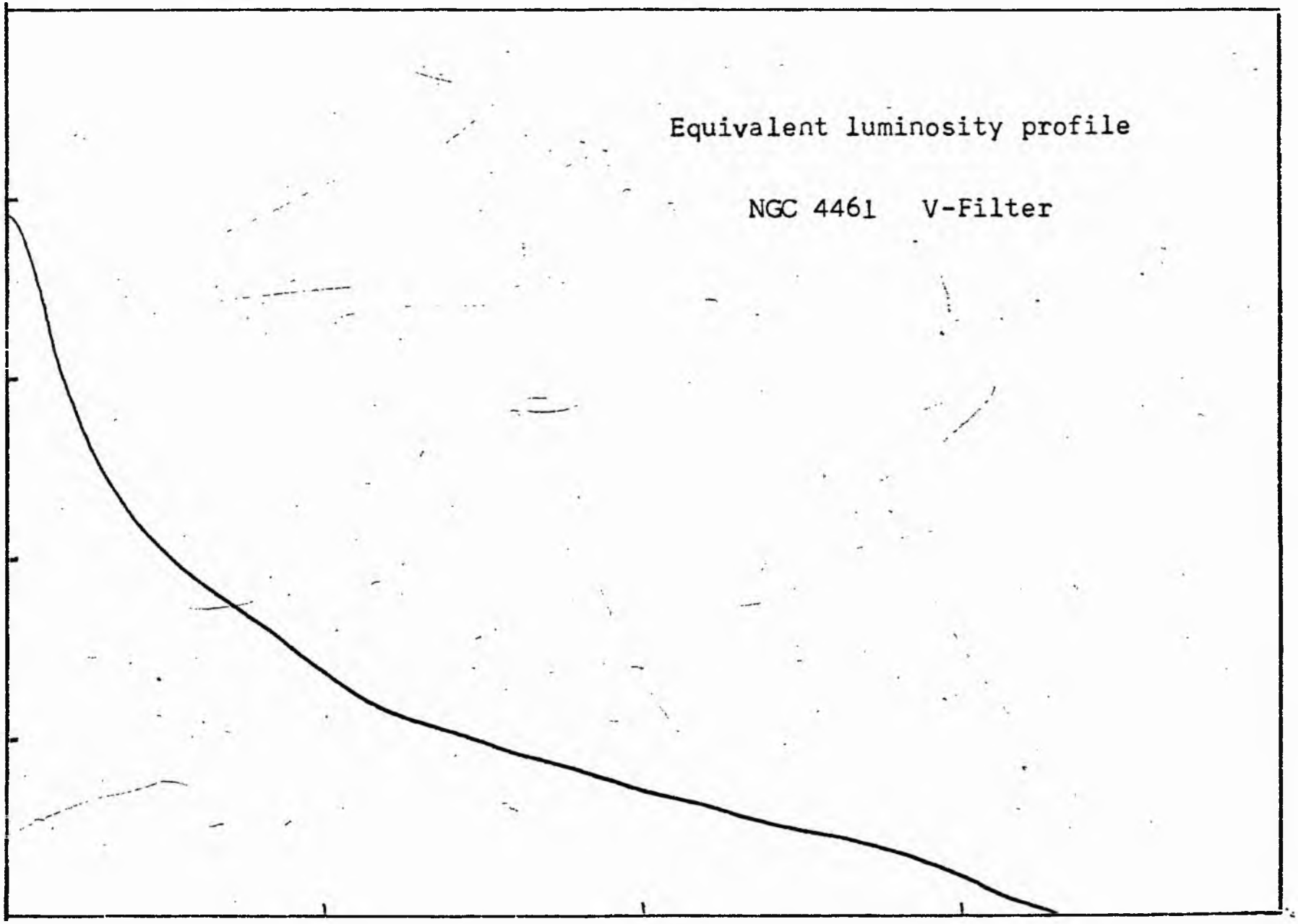
Equivalent luminosity profile
NGC 4461 V-Filter

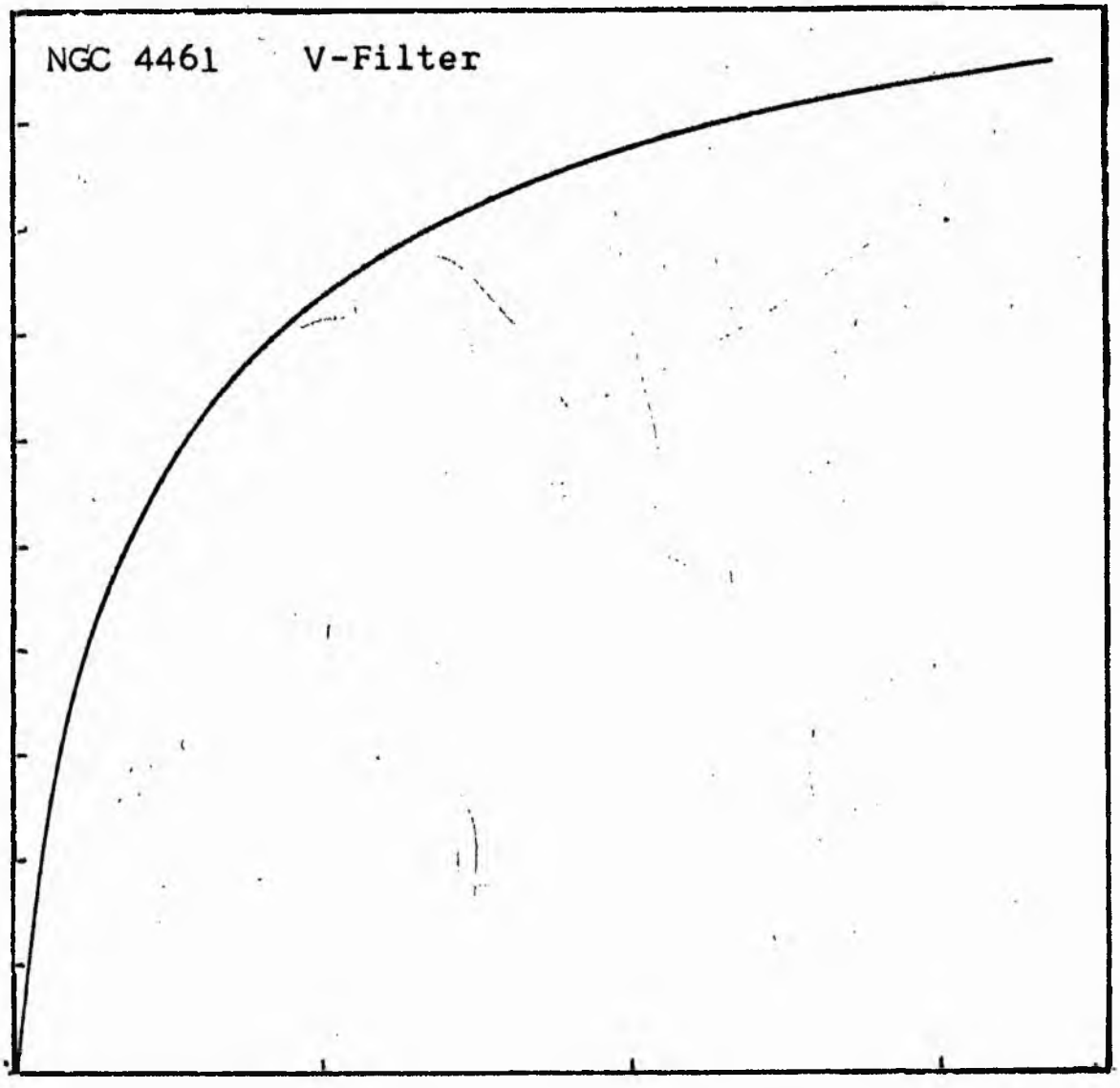

Relative integrated luminosity k(r) versus equivalent radius r*.

MEAN LUMINOSITY DISTRIBUTION IN NGC 4461
V COLOUR

LOG I	I	$\bar{I}$	R	AREA	ΔA	P	ΣP	K(R)	ρ	LOG J	μ
1.86	72.444		0.0	0.0			0.0	0.0	0.0	1.616	17.11
		67.770			2.01	136.2587					
1.80	63.096		0.80	2.01			136.26	0.01	0.04	1.556	17.26
		56.607			9.33	528.1736					
1.70	50.119		1.90	11.34			664.43	0.04	0.10	1.456	17.51
		44.965			20.83	936.5549					
1.60	39.811		3.20	32.17			1600.99	0.09	0.18	1.356	17.76
		35.717			23.25	830.3306					
1.50	31.623		4.20	55.42			2431.32	0.14	0.23	1.256	18.01
		28.371			26.30	746.0095					
1.40	25.119		5.10	81.71			3177.33	0.19	0.28	1.156	18.26
		22.536			28.76	648.1462					
1.30	19.952		5.93	110.47			3825.47	0.23	0.33	1.056	18.51
		17.901			34.79	622.8245					
1.20	15.849		6.80	145.27			4448.30	0.26	0.38	0.956	18.76
		14.219			41.00	582.9475					
1.10	12.589		7.70	186.27			5031.24	0.30	0.42	0.856	19.01
		11.295			30.16	340.6345					
1.00	10.000		8.30	216.42			5371.87	0.32	0.46	0.756	19.26
		8.972			61.17	548.7617					
0.90	7.943		9.40	277.59			5920.64	0.35	0.52	0.656	19.51
		7.126			70.09	499.4878					
0.80	6.310		10.52	347.68			6420.12	0.38	0.58	0.556	19.76
		5.661			53.47	302.6692					
0.70	5.012		11.30	401.15			6722.79	0.40	0.62	0.456	20.01
		4.496			81.12	364.7610					
0.60	3.981		12.39	482.27			7087.55	0.42	0.68	0.356	20.26
		3.572			86.05	307.3386					
0.50	3.162		13.45	568.32			7394.88	0.44	0.74	0.256	20.51
		2.837			136.65	387.6924					
0.40	2.512		14.98	704.97			7782.57	0.46	0.83	0.156	20.76
		2.254			189.11	426.1755					
0.30	1.995		16.87	894.09			8208.75	0.48	0.93	0.056	21.01
		1.790			260.41	466.1562					
0.20	1.585		19.17	1154.50			8674.90	0.51	1.06	-0.044	21.26
		1.422			348.11	494.9817					
0.10	1.259		21.87	1502.61			9169.88	0.54	1.21	-0.144	21.51
		1.129			471.89	532.9800					
-0.00	1.000		25.07	1974.50			9702.86	0.57	1.38	-0.244	21.76
		0.897			580.83	521.0999					
-0.10	0.794		28.52	2555.34			10223.96	0.60	1.57	-0.344	22.01
		0.713			718.20	511.8130					
-0.20	0.631		32.28	3273.53			10735.77	0.63	1.78	-0.444	22.26
		0.566			884.37	500.6145					
-0.30	0.501		36.38	4157.91			11236.38	0.66	2.01	-0.544	22.51
		0.450			1069.15	480.7363					
-0.40	0.398		40.79	5227.05			11717.12	0.69	2.25	-0.644	22.76
		0.357			1285.41	459.1023					
-0.50	0.316		45.53	6512.46			12176.22	0.72	2.51	-0.744	23.01
		0.284			938.42	266.2361					
-0.60	0.251		48.70	7450.88			12442.45	0.73	2.69	-0.844	23.26
		0.225			1440.57	324.6421					
-0.70	0.200		53.20	8891.46			12767.09	0.75	2.93	-0.944	23.51
		0.179			611.86	109.5269					
-0.80	0.158		55.00	9503.32			12876.62	0.76	3.03	-1.044	23.76
		0.142			4473.27	636.0547					
-0.90	0.126		66.70	13976.59			13512.67	0.80	3.68	-1.144	24.01
		0.113			2856.81	322.6646					
-1.00	0.100		73.20	16833.40			13835.34	0.82	4.04	-1.244	24.26
		0.090			4342.21	389.5657					
-1.10	0.079		82.10	21175.61			14224.90	0.84	4.53	-1.344	24.51
		0.071			4554.82	324.5950					
-1.20	0.063		90.50	25730.43			14549.49	0.86	4.99	-1.444	24.76
		0.057			8053.28	455.8730					
-1.30	0.050		103.70	33783.71			15005.36	0.89	5.72	-1.544	25.01
		0.045			5906.41	265.5801					
-1.40	0.040		112.40	39690.12			15270.94	0.90	6.20	-1.644	25.26
		0.036			5247.71	187.4316					
-1.50	0.032		119.60	44937.84			15458.37	0.91	6.60	-1.744	25.51
		0.028			7991.83	226.7354					
-1.60	0.025		129.80	52929.67			15685.11	0.93	7.16	-1.844	25.76
		0.023			6379.70	143.7719					
-1.70	0.020		137.40	59309.37			15828.87	0.93	7.58	-1.944	26.01
		0.018			8762.13	156.8498					
-1.80	0.016		147.20	68071.50			15985.72	0.94	8.12	-2.044	26.26
		0.014			10752.75	152.8954					
-1.90	0.013		158.40	78824.25			16138.62	0.95	8.74	-2.144	26.51
		0.011			9001.56	101.6702					
-2.00	0.010		167.20	87825.81			16240.29	0.96	9.22	-2.244	26.76
$-\infty$							16940.00	(1)			∞

PHOTOMETRIC PARAMETERS OF NGC 4461
V-FILTER

Total luminosity	L_T	= 4.71
Total apparent magnitude	m_T	= 10.62
Apparent central surface brightness	μ_o	= 17.11
Major axis at threshold	$2a_m$	= 7.18
Minor axis at threshold	$2b_m$	= 4.32
Major axis at μ=25.0 mag sec^{-2}	2a(25)	= 4.43
Luminosity within μ=25.0 mag sec^{-2}	k(25)	= 0.89
Gradient of exponential component	G(a)	= -0.68
Equivalent gradient of exponential comp.	G(r*)	= -0.77
Equivalent gradient of reduced exp. comp.	G(ρ)	= -0.48
Parameters at k = ¼ :		
Semi-major axis	a_1	= 0.15
Axis ratio	b/a	= 0.67
Equivalent radius	r_1*	= 0.11
Surface brightness	μ_1	= 18.68
Parameters at k = ½(effective) :		
Semi-major axis	a_e	= 0.41
Axis ratio	b/a	= 0.63
Equivalent radius	r_e*	= 0.30
Surface brightness	μ_e	= 21.18
Mean surface brightness	μ_e'	= 9.97
Parameters at k = ¾ :		
Semi-major axis	a_3	= 1.32
Axis ratio	b/a	= 0.37
Equivalent radius	r_3*	= 0.87
Surface brightness	μ_3	= 23.51
Concentration indices	C_{21}	= 2.79
	C_{32}	= 2.88

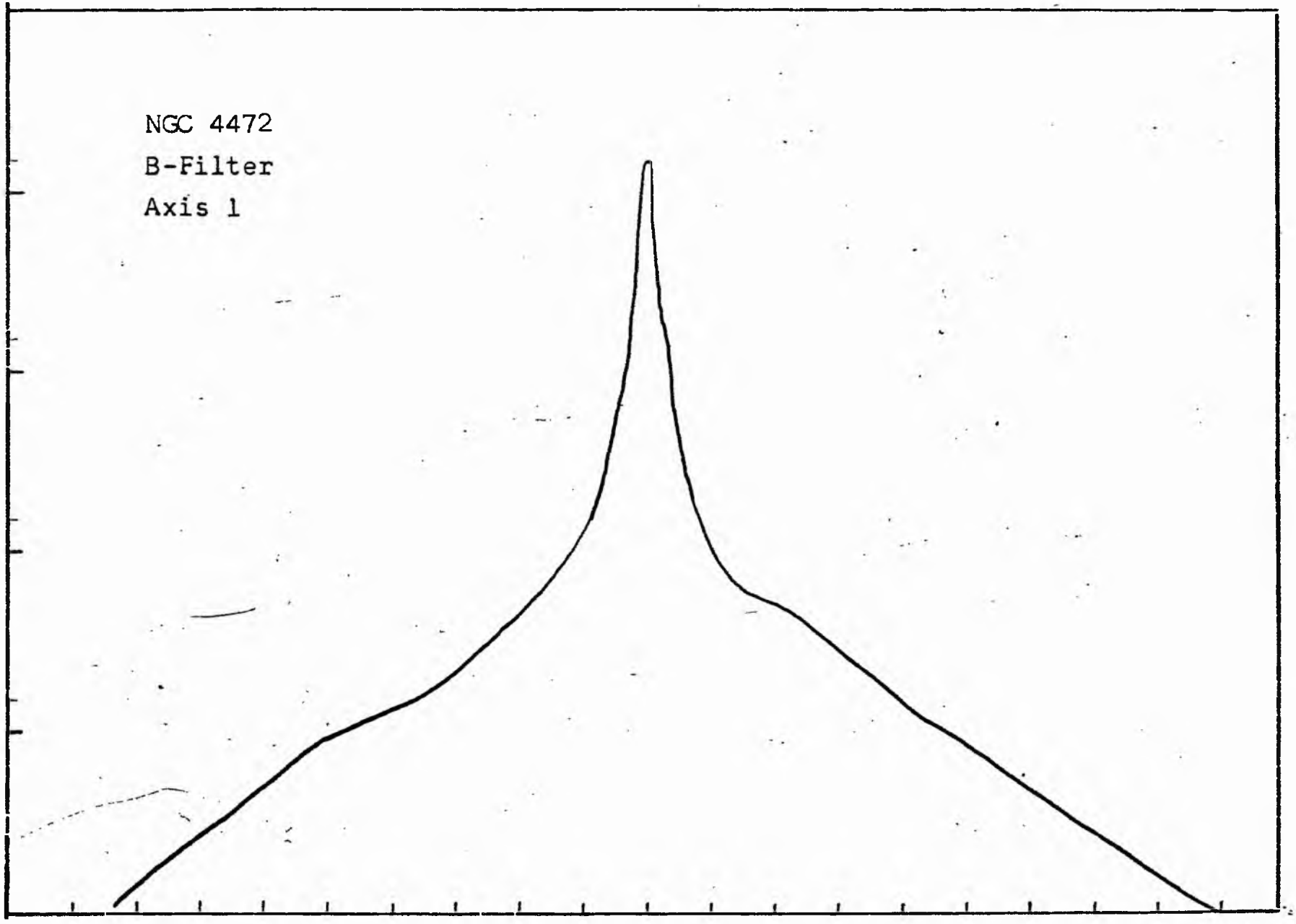
NGC 4472
B-Filter
Axis 1

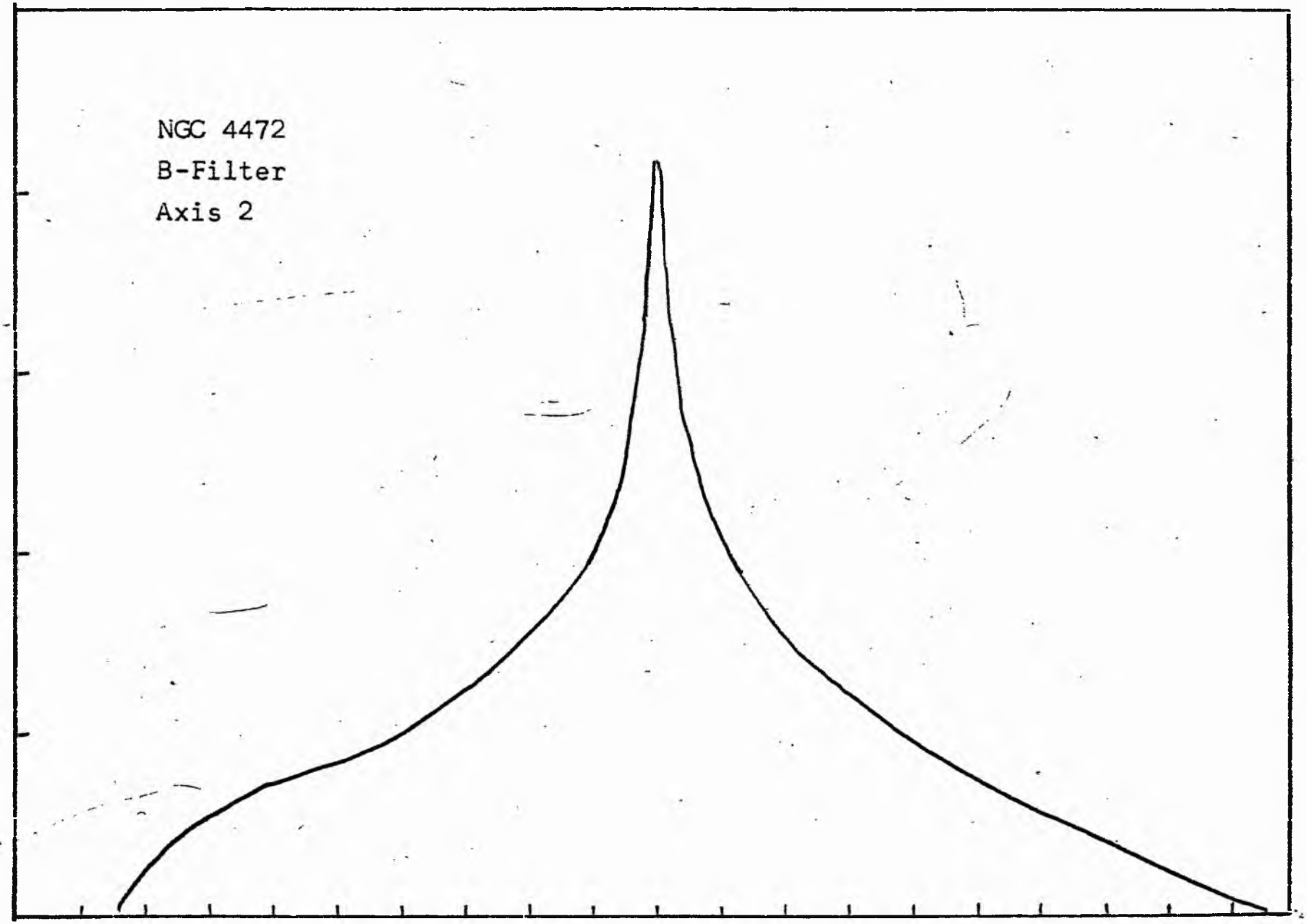
NGC 4472
B-Filter
Axis 2

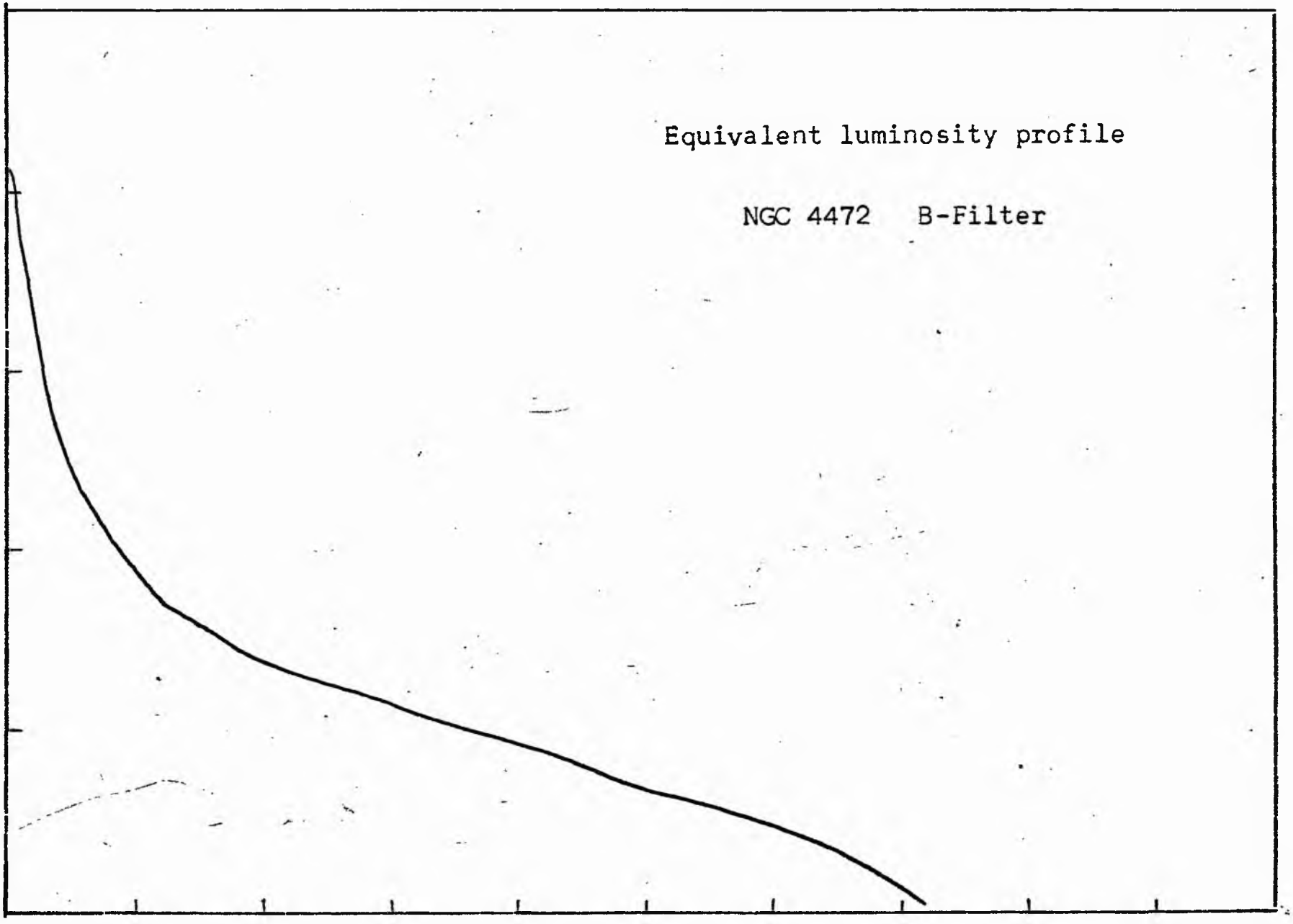
Equivalent luminosity profile
NGC 4472 B-Filter

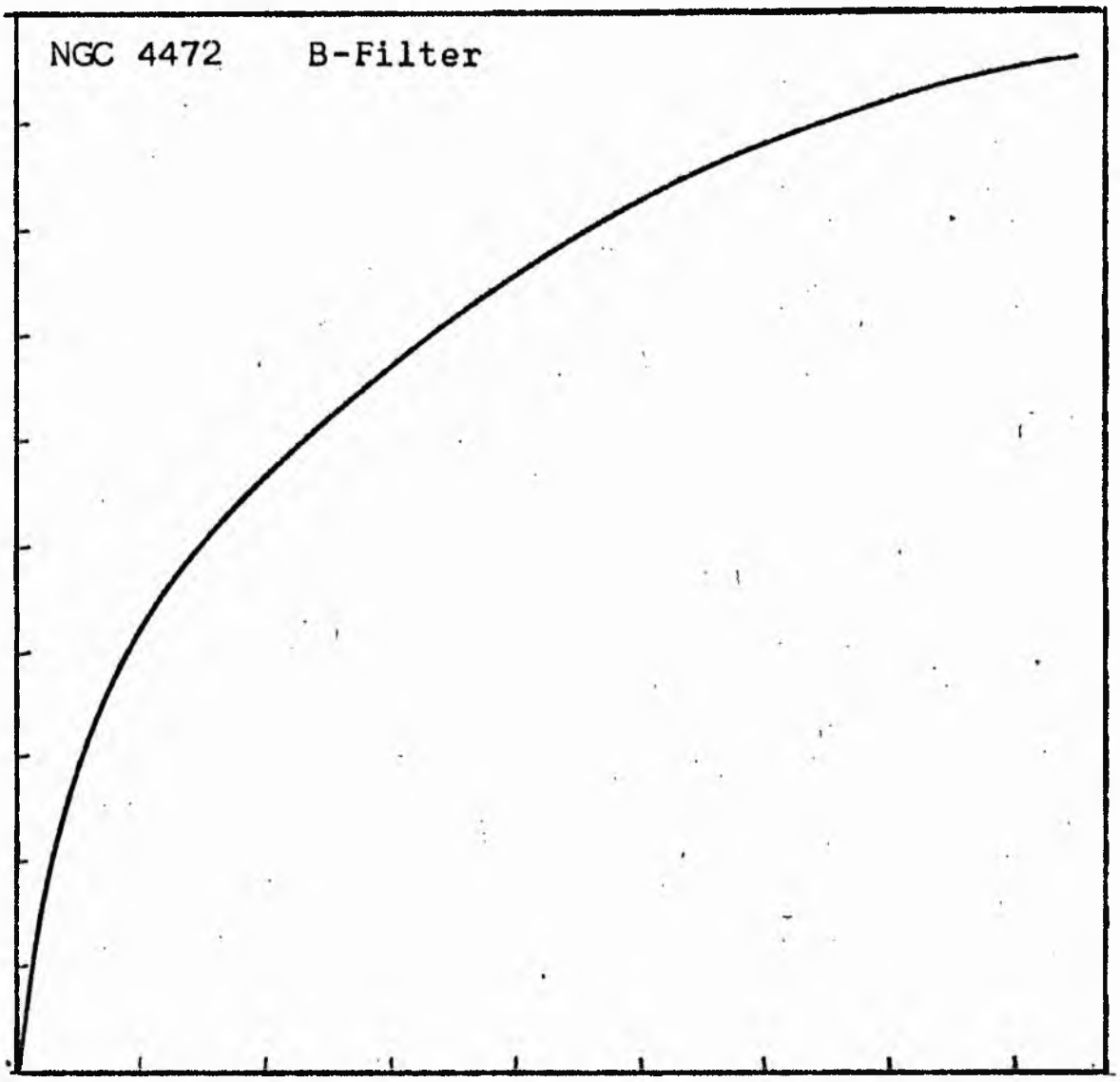

Relative integrated luminosity k(r) versus equivalent radius r*.

MEAN LUMINOSITY DISTRIBUTION IN NGC 4472
B COLOUR

LOG I	I	$\bar{I}$	R	AREA	ΔA	P	ΣP	K(R)	ρ	LOG μ	μ
2.02	104.713		0.0	0.0			0.0	0.0	0.0	2.339	16.69
		102.356			2.01	205.7993					
2.00	100.000		0.80	2.01			205.80	0.00	0.01	2.319	16.74
		89.716			9.33	837.1006					
1.90	79.433		1.90	11.34			1042.90	0.01	0.03	2.219	16.99
		71.264			34.02	2424.6511					
1.80	63.096		3.80	45.36			3467.55	0.04	0.05	2.119	17.24
		56.607			39.58	2240.7383					
1.70	50.119		5.20	84.95			5708.29	0.06	0.07	2.019	17.49
		44.965			39.74	1786.9429					
1.60	39.811		6.30	124.69			7495.23	0.08	0.08	1.919	17.74
		35.717			64.49	2303.3396					
1.50	31.623		7.76	189.18			9798.57	0.11	0.10	1.819	17.99
		28.371			67.56	1916.6294					
1.40	25.119		9.04	256.74			11715.20	0.13	0.12	1.719	18.24
		22.536			74.62	1681.5374					
1.30	19.952		10.27	331.35			13396.73	0.15	0.14	1.619	18.49
		17.901			124.01	2234.2594					
1.20	15.849		12.05	456.17			15630.98	0.18	0.16	1.519	18.74
		14.219			235.69	3351.2979					
1.10	12.589		14.84	691.86			18982.28	0.21	0.20	1.419	18.99
		11.295			22.56	254.7969					
1.00	10.000		15.08	714.42			19237.08	0.22	0.20	1.319	19.24
		8.972			188.17	1688.1655					
0.90	7.943		16.95	902.59			20925.24	0.23	0.23	1.219	19.49
		7.126			397.14	2030.1548					
0.80	6.310		20.34	1299.73			23755.39	0.27	0.27	1.119	19.74
		5.661			118.90	673.0564					
0.70	5.012		21.25	1418.63			24428.45	0.27	0.28	1.019	19.99
		4.496			359.40	1616.0271					
0.60	3.981		23.79	1778.03			26044.47	0.29	0.32	0.919	20.24
		3.572			649.92	2321.2791					
0.50	3.162		27.80	2427.95			28365.75	0.32	0.37	0.819	20.49
		2.837			667.57	1093.9258					
0.40	2.512		31.39	3095.51			30259.68	0.34	0.42	0.719	20.74
		2.254			654.61	1475.2056					
0.30	1.995		34.55	3750.12			31734.88	0.36	0.46	0.619	20.99
		1.790			1055.23	1888.9260					
0.20	1.585		39.11	4805.35			33623.80	0.38	0.52	0.519	21.24
		1.422			1499.95	2132.7703					
0.10	1.259		44.80	6305.30			35756.57	0.40	0.60	0.419	21.49
		1.129			1978.52	2234.6479					
-0.00	1.000		51.35	8283.82			37991.22	0.43	0.68	0.319	21.74
		0.897			2570.66	2306.2900					
-0.10	0.794		58.78	10854.48			40297.51	0.45	0.78	0.219	21.99
		0.713			3286.04	2341.7532					
-0.20	0.631		67.09	14140.52			42639.26	0.48	0.89	0.119	22.24
		0.566			2932.89	1660.2136					
-0.30	0.501		73.72	17073.40			44299.47	0.50	0.98	0.019	22.49
		0.450			6178.03	2777.9138					
-0.40	0.398		86.03	23251.43			47077.38	0.53	1.14	-0.081	22.74
		0.357			9050.29	3232.4492					
-0.50	0.316		101.40	32301.72			50309.83	0.56	1.35	-0.181	22.99
		0.284			15769.95	4474.0352					
-0.60	0.251		123.70	48071.67			54783.86	0.61	1.65	-0.281	23.24
		0.225			14209.25	3202.1411					
-0.70	0.200		140.80	62280.93			57986.00	0.65	1.87	-0.381	23.49
		0.179			22266.82	3985.9104					
-0.80	0.158		164.05	84547.75			61971.91	0.69	2.18	-0.481	23.74
		0.142			24958.37	3548.8323					
-0.90	0.126		186.70	109506.12			65520.75	0.73	2.48	-0.581	23.99
		0.113			39657.94	4479.1914					
-1.00	0.100		217.90	149164.06			69999.94	0.78	2.90	-0.681	24.24
		0.090			41339.19	3708.7096					
-1.10	0.079		246.25	190503.25			73708.69	0.83	3.28	-0.781	24.49
		0.071			32502.31	2316.2476					
-1.20	0.063		266.43	223005.56			76024.87	0.85	3.55	-0.881	24.74
		0.057			30204.06	1709.7659					
-1.30	0.050		283.90	253209.62			77734.62	0.87	3.78	-0.981	24.99
		0.045			26431.01	1188.4993					
-1.40	0.040		298.35	279641.44			78923.06	0.88	3.97	-1.081	25.24
		0.036			67601.25	2417.3577					
-1.50	0.032		332.50	347322.69			81340.37	0.91	4.43	-1.181	25.49
		0.028			67257.19	1908.1467					
-1.60	0.025		363.27	414579.87			83248.50	0.93	4.83	-1.281	25.74
		0.023			47750.06	1076.0076					
-1.70	0.020		383.62	462329.94			84324.56	0.94	5.11	-1.381	25.99
		0.018			35135.56	628.9573					
-1.80	0.016		397.93	497465.50			84953.50	0.95	5.30	-1.481	26.24
		0.014			29940.75	425.7332					
-1.90	0.013		409.73	527406.25			85379.19	0.96	5.45	-1.581	26.49
		0.011			22819.37	257.7383					
-2.00	0.010		418.50	550225.62			85636.87	0.96	5.57	-1.681	26.74
$-\infty$							89276.00	(1)			∞

PHOTOMETRIC PARAMETERS OF NGC 4472

B-FILTER

Total luminosity	L_T	= 24.80
Total apparent magnitude	m_T	= 9.36
Apparent central surface brightness	μ_o	= 16.69
Major axis at threshold	$2a_m$	= 13.70
Minor axis at threshold	$2b_m$	= 13.71
Major axis at μ=25.0 mag sec^{-2}	2a(25)	= 10.08
Luminosity within μ=25.0 mag sec^{-2}	k(25)	= 0.87
Gradient of exponential component	G(a)	= -0.28
Equivalent gradient of exponential comp.	G(r*)	= -0.27
Equivalent gradient of reduced exp. comp.	G(ρ)	= -0.32
Parameters at k = ¼ :		
Semi-major axis	a_1	= 0.38
Axis ratio	b/a	= 0.97
Equivalent radius	r_1*	= 0.31
Surface brightness	μ_1	= 19.61
Parameters at k = ½(effective) :		
Semi-major axis	a_e	= 1.33
Axis ratio	b/a	= 0.98
Equivalent radius	r_e*	= 1.25
Surface brightness	μ_e	= 22.49
Mean surface brightness	μ_e'	= 11.84
Parameters at k = ¾ :		
Semi-major axis	a_3	= 3.80
Axis ratio	b/a	= 0.81
Equivalent radius	r_3*	= 3.27
Surface brightness	μ_3	= 24.09
Concentration indices	C_{21}	= 4.04
	C_{32}	= 2.61

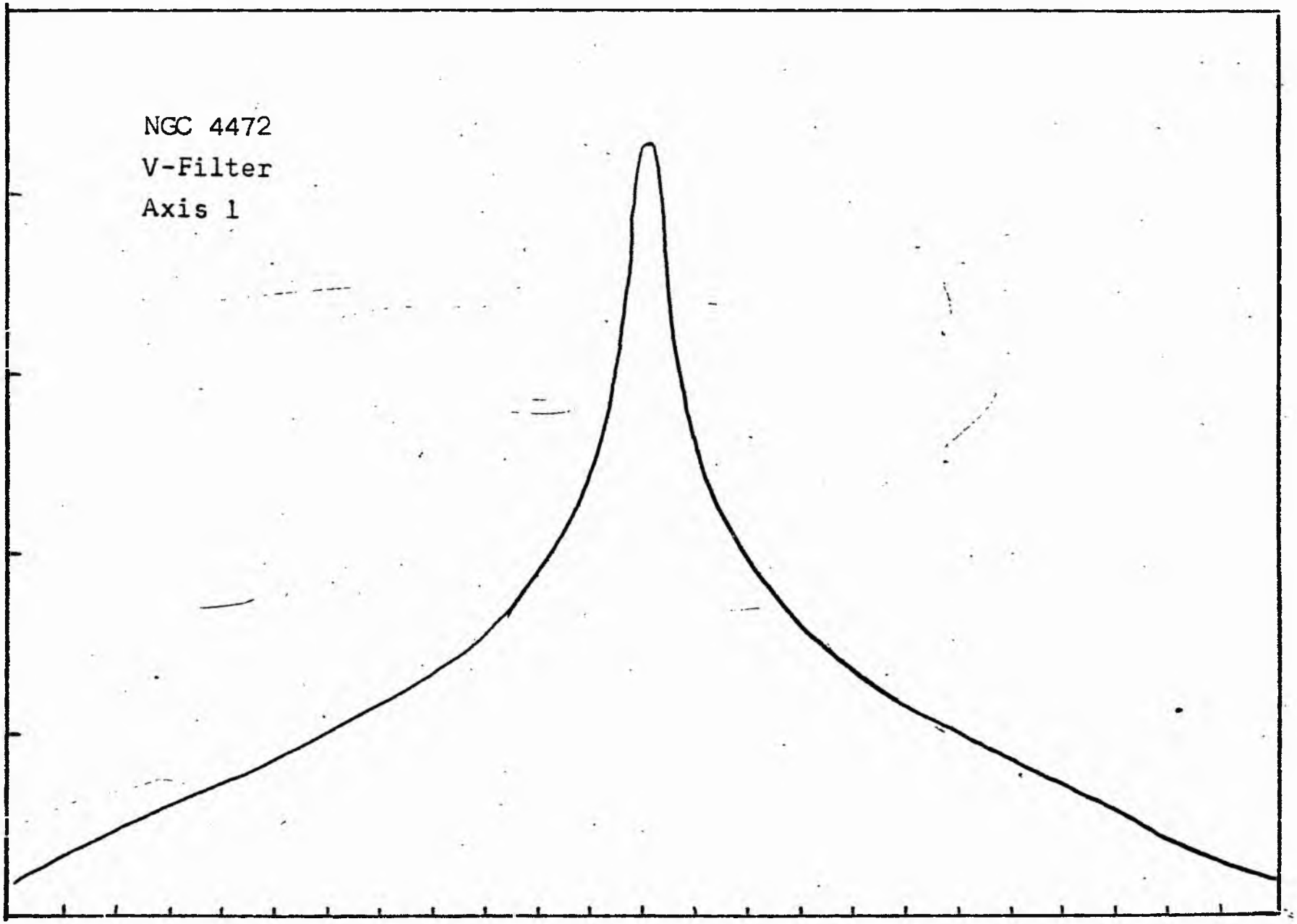
NGC 4472
V-Filter
Axis 1

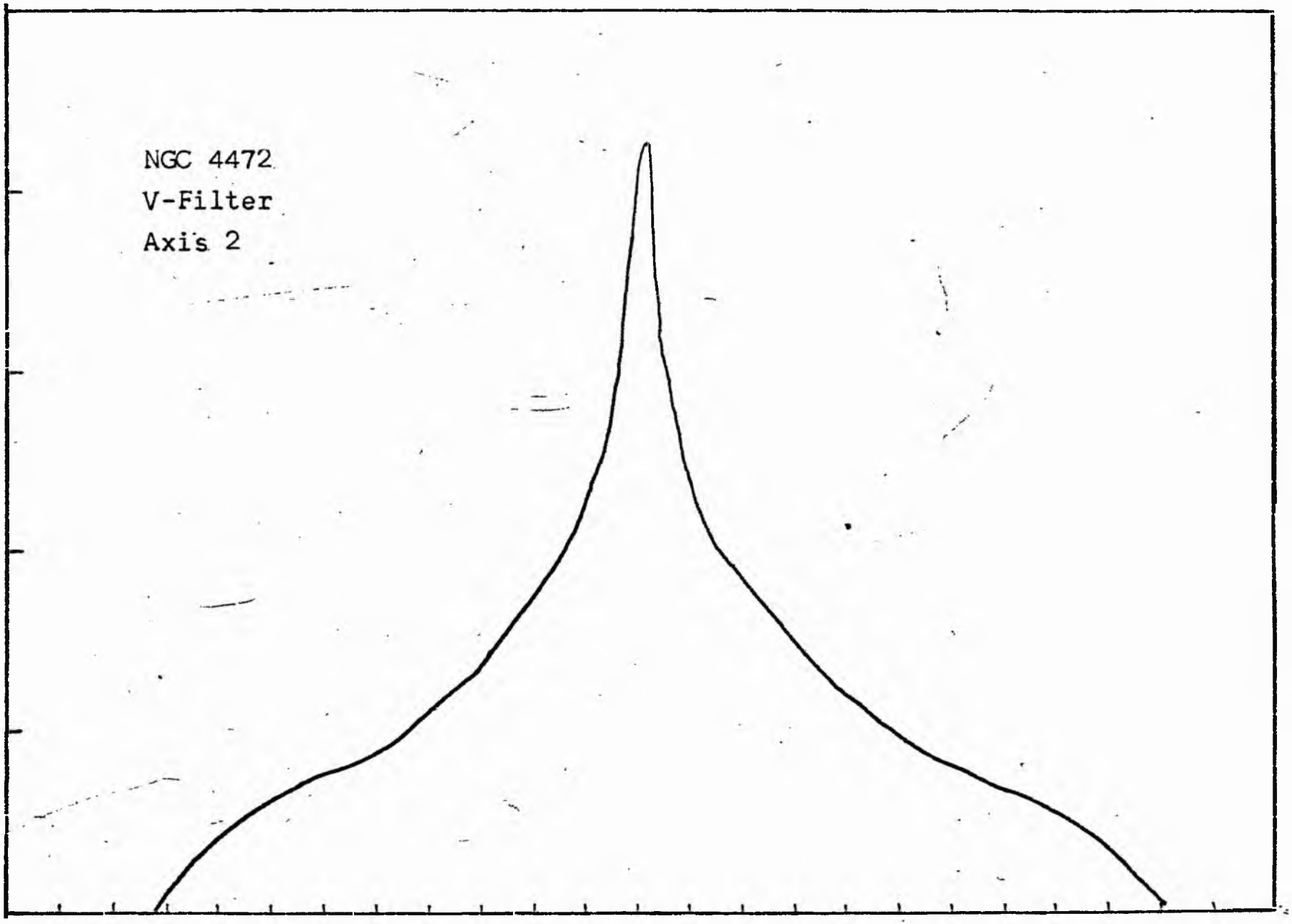
NGC 4472
V-Filter
Axis 2

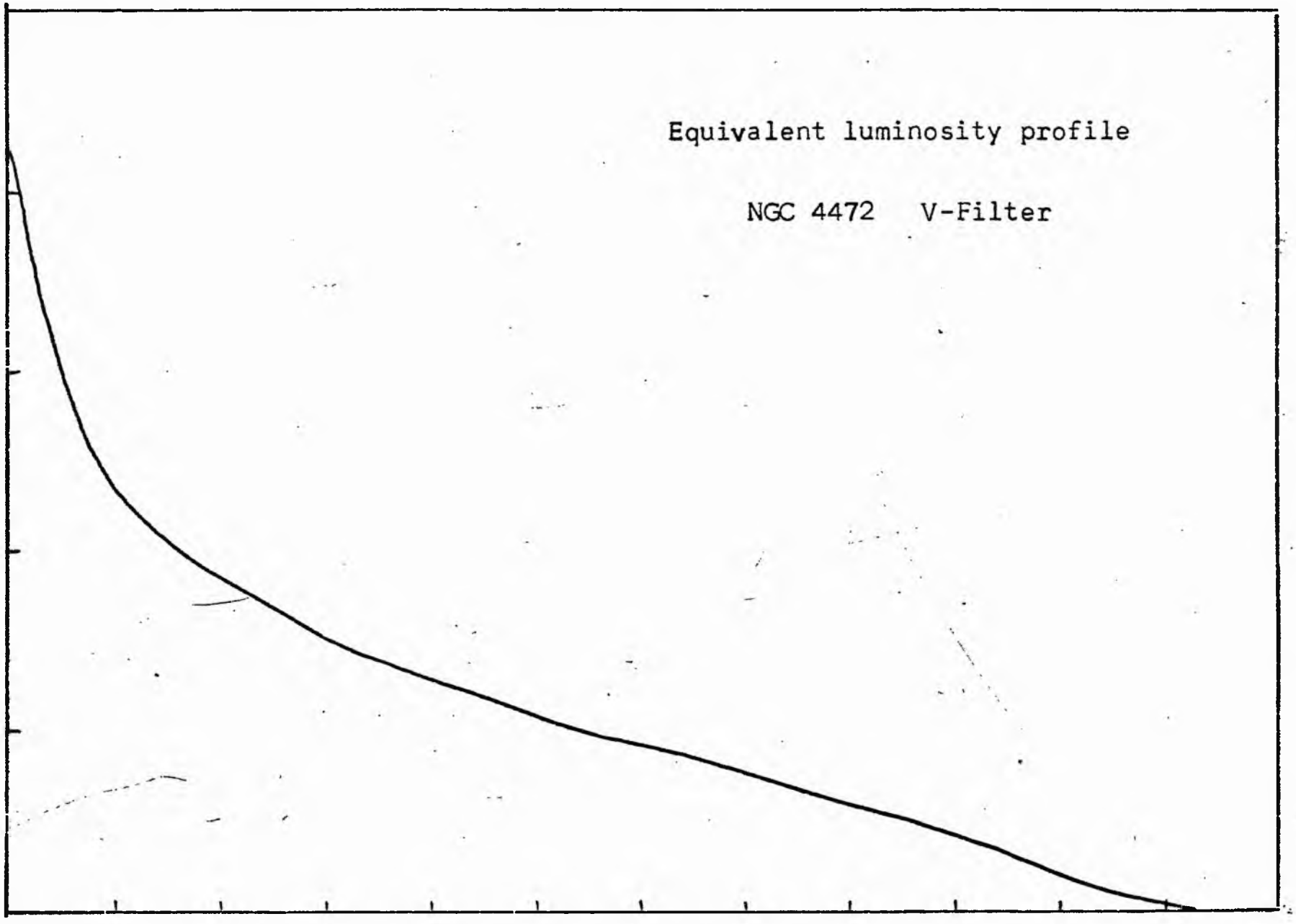
Equivalent luminosity profile
NGC 4472 V-Filter

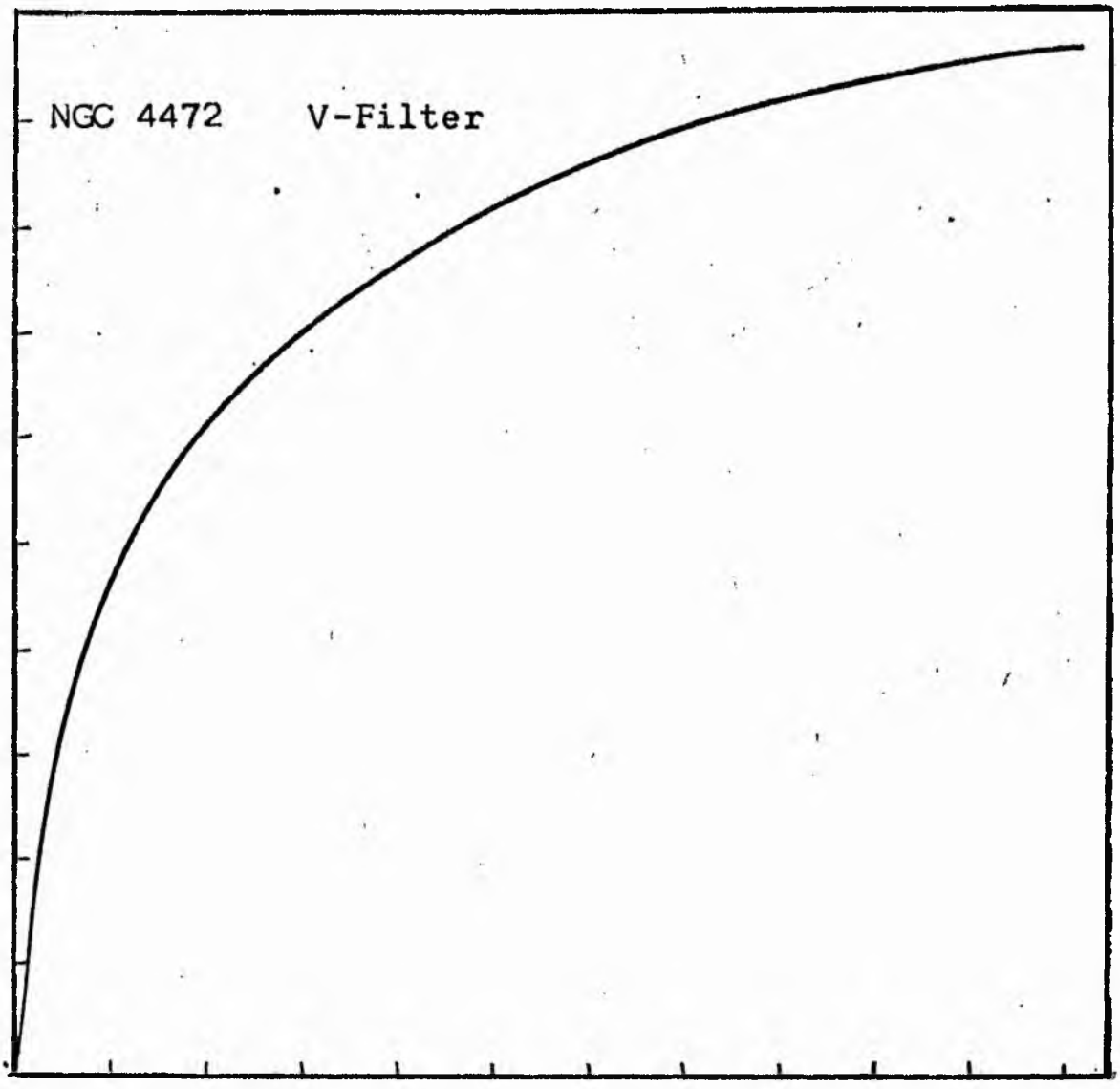

Relative integrated luminosity k(r) versus equivalent radius r*.

MEAN LUMINOSITY DISTRIBUTION IN NGC 4472
V COLOUR

LOG I	I	$\bar{I}$	R	AREA	ΔA	P	ΣP	K(R)	ρ	LOG J	μ_A
2.24	173.780		0.0	0.0			0.0	0.0	0.0	2.000	16.05
		166.135			4.52	751.5742					
2.20	158.489		1.20	4.52			751.57	0.00	0.02	1.960	16.15
		142.191			23.75	3377.0891					
2.10	125.892		3.00	28.27			4128.66	0.02	0.05	1.860	16.40
		112.946			27.14	3065.7312					
2.00	100.000		4.20	55.42			7194.39	0.04	0.07	1.760	16.65
		89.716			61.48	5515.8359					
1.90	79.433		6.10	116.90			12710.23	0.07	0.11	1.660	16.90
		71.264			99.53	7092.5937					
1.80	63.095		8.30	216.42			19802.82	0.10	0.15	1.560	17.15
		56.607			123.37	6983.6055					
1.70	50.118		10.40	339.79			26786.43	0.14	0.19	1.460	17.40
		44.964			75.68	3402.9622					
1.60	39.810		11.50	415.48			30189.39	0.16	0.21	1.360	17.65
		35.717			300.84	10744.9102					
1.50	31.623		15.10	716.31			40934.30	0.21	0.27	1.260	17.90
		28.371			218.51	6199.1328					
1.40	25.119		17.25	934.82			47133.43	0.24	0.31	1.160	18.15
		22.536			362.35	8165.7422					
1.30	19.952		20.32	1297.17			55299.17	0.29	0.36	1.060	18.40
		17.901			269.32	4820.9414					
1.20	15.849		22.33	1566.49			60120.11	0.31	0.40	0.960	18.65
		14.219			319.25	4539.4609					
1.10	12.589		24.50	1885.74			64659.57	0.33	0.44	0.860	18.90
		11.295			370.67	4186.5820					
1.00	10.000		26.80	2256.42			68846.12	0.36	0.48	0.760	19.15
		8.972			309.69	2778.3657					
0.90	7.943		28.58	2566.10			71624.44	0.37	0.51	0.660	19.40
		7.126			557.08	3969.9746					
0.80	6.310		31.53	3123.19			75594.37	0.39	0.56	0.560	19.65
		5.661			463.77	2625.2510					
0.70	5.012		33.79	3586.96			78219.62	0.40	0.60	0.460	19.90
		4.496			932.80	4194.2734					
0.60	3.981		37.93	4519.76			82413.87	0.43	0.68	0.360	20.15
		3.572			1416.72	5060.0078					
0.50	3.162		43.47	5936.48			87473.87	0.45	0.77	0.260	20.40
		2.837			1486.89	4218.3750					
0.40	2.512		48.61	7423.36			91692.25	0.47	0.87	0.160	20.65
		2.254			980.26	2209.0710					
0.30	1.995		51.72	8403.62			93901.31	0.49	0.92	0.060	20.90
		1.790			2606.52	4665.8320					
0.20	1.585		59.20	11010.15			98567.12	0.51	1.06	-0.040	21.15
		1.422			3886.33	5525.9531					
0.10	1.259		68.86	14896.48			104093.06	0.54	1.23	-0.140	21.40
		1.129			6114.39	6905.9023					
-0.00	1.000		81.78	21010.86			110998.94	0.57	1.46	-0.240	21.65
		0.897			6213.38	5574.3711					
-0.10	0.794		93.09	27224.25			116573.25	0.60	1.66	-0.340	21.90
		0.713			7128.70	5080.1680					
-0.20	0.631		104.57	34352.95			121653.37	0.63	1.86	-0.440	22.15
		0.566			8073.51	4570.1445					
-0.30	0.501		116.21	42426.46			126223.50	0.65	2.07	-0.540	22.40
		0.450			7251.74	3260.6963					
-0.40	0.398		125.75	49678.20			129484.19	0.67	2.24	-0.640	22.65
		0.357			11239.05	4014.1892					
-0.50	0.316		139.25	60917.25			133498.37	0.69	2.48	-0.740	22.90
		0.284			21907.68	6215.3359					
-0.60	0.251		162.37	82824.94			139713.69	0.72	2.89	-0.840	23.15
		0.225			32842.00	7401.1289					
-0.70	0.200		191.88	115666.94			147114.81	0.76	3.42	-0.940	23.40
		0.179			33743.69	6040.3320					
-0.80	0.158		218.08	149410.62			153155.12	0.79	3.89	-1.040	23.65
		0.142			24201.94	3441.2686					
-0.90	0.126		235.08	173612.56			156596.37	0.81	4.19	-1.140	23.90
		0.113			47738.75	5391.8711					
-1.00	0.100		265.44	221351.31			161988.19	0.84	4.73	-1.240	24.15
		0.090			65762.56	5899.9453					
-1.10	0.079		302.31	287113.87			167888.12	0.87	5.39	-1.340	24.40
		0.071			51200.69	3648.7642					
-1.20	0.063		328.16	338314.56			171536.87	0.89	5.85	-1.440	24.65
		0.057			72394.31	4098.0273					
-1.30	0.050		361.57	410708.87			175634.87	0.91	6.45	-1.540	24.90
		0.045			86206.87	3876.2585					
-1.40	0.040		397.71	496915.75			179511.12	0.93	7.09	-1.640	25.15
		0.036			80645.69	2880.3987					
-1.50	0.032		428.77	577561.44			182391.50	0.94	7.64	-1.740	25.40
		0.028			59148.12	1678.0820					
-1.60	0.025		450.19	636709.56			184069.56	0.95	8.03	-1.840	25.65
		0.023			50345.37	1134.5728					
-1.70	0.020		467.65	687054.94			185204.12	0.96	8.34	-1.940	25.90
		0.018			71155.75	1273.7478					
-1.80	0.016		491.27	758210.69			186477.81	0.96	8.76	-2.040	26.15
		0.014			86056.06	1223.6448					
-1.90	0.013		518.40	844266.75			187701.44	0.97	9.24	-2.140	26.40
		0.011			79681.37	899.5247					
-2.00	0.010		542.30	923908.12			188600.94	0.98	9.67	-2.240	26.65
- ∞							193350.00	(1)			∞

PHOTOMETRIC PARAMETERS OF NGC 4472

V-FILTER

Total luminosity ..... L_T = 53.7

Total apparent magnitude ..... m_T = 8.43

Apparent central surface brightness ..... μ_o = 16.05

Major axis at threshold ..... $2a_m$ = 22.03

Minor axis at threshold ..... $2b_m$ = 15.98

Major axis at μ=25.0 mag sec^{-2} ..... 2a(25) = 13.83

Luminosity within μ=25.0 mag sec^{-2} ..... k(25) = 0.92

Gradient of exponential component ..... G(a) = -0.21

Equivalent gradient of exponential comp..... G(r*) = -0.23

Equivalent gradient of reduced exp. comp..... G(ρ) = -0.21

Parameters at k = ¼ :

- Semi-major axis ..... a_1 = 0.38
- Axis ratio ..... b/a = 0.90
- Equivalent radius ..... r_1* = 0.29
- Surface brightness ..... μ_1 = 18.20

Parameters at k = ½(effective) :

- Semi-major axis ..... a_e = 1.17
- Axis ratio ..... b/a = 0.75
- Equivalent radius ..... r_e* = 0.93
- Surface brightness ..... μ_e = 21.02
- Mean surface brightness ..... μ_e' = 10.27

Parameters at k = ¾ :

- Semi-major axis ..... a_3 = 3.53
- Axis ratio ..... b/a = 0.74
- Equivalent radius ..... r_3* = 3.05
- Surface brightness ..... μ_3 = 23.34

Concentration indices ..... C_{21} = 3.17, C_{32} = 3.27

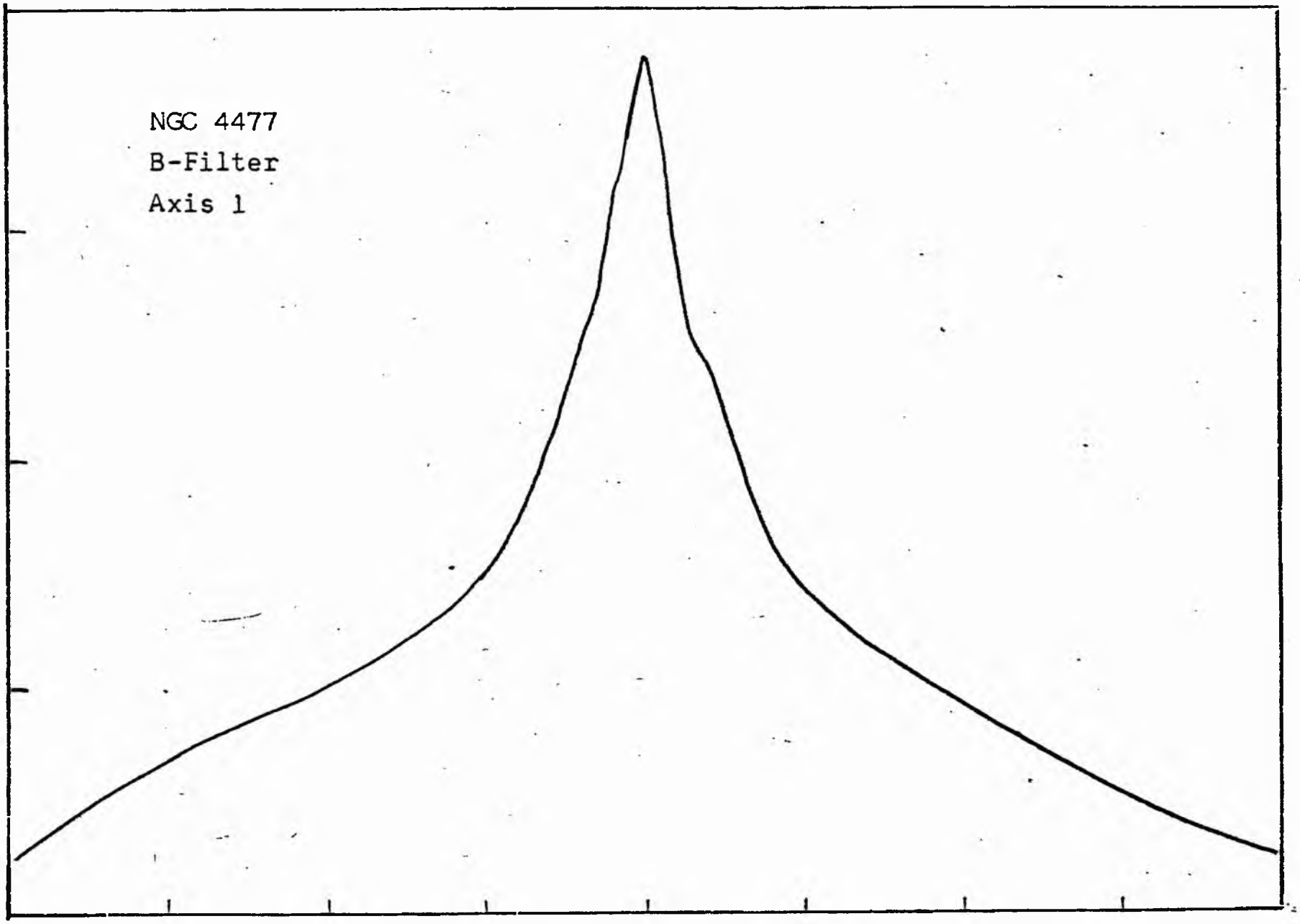
NGC 4477
B-Filter
Axis 1

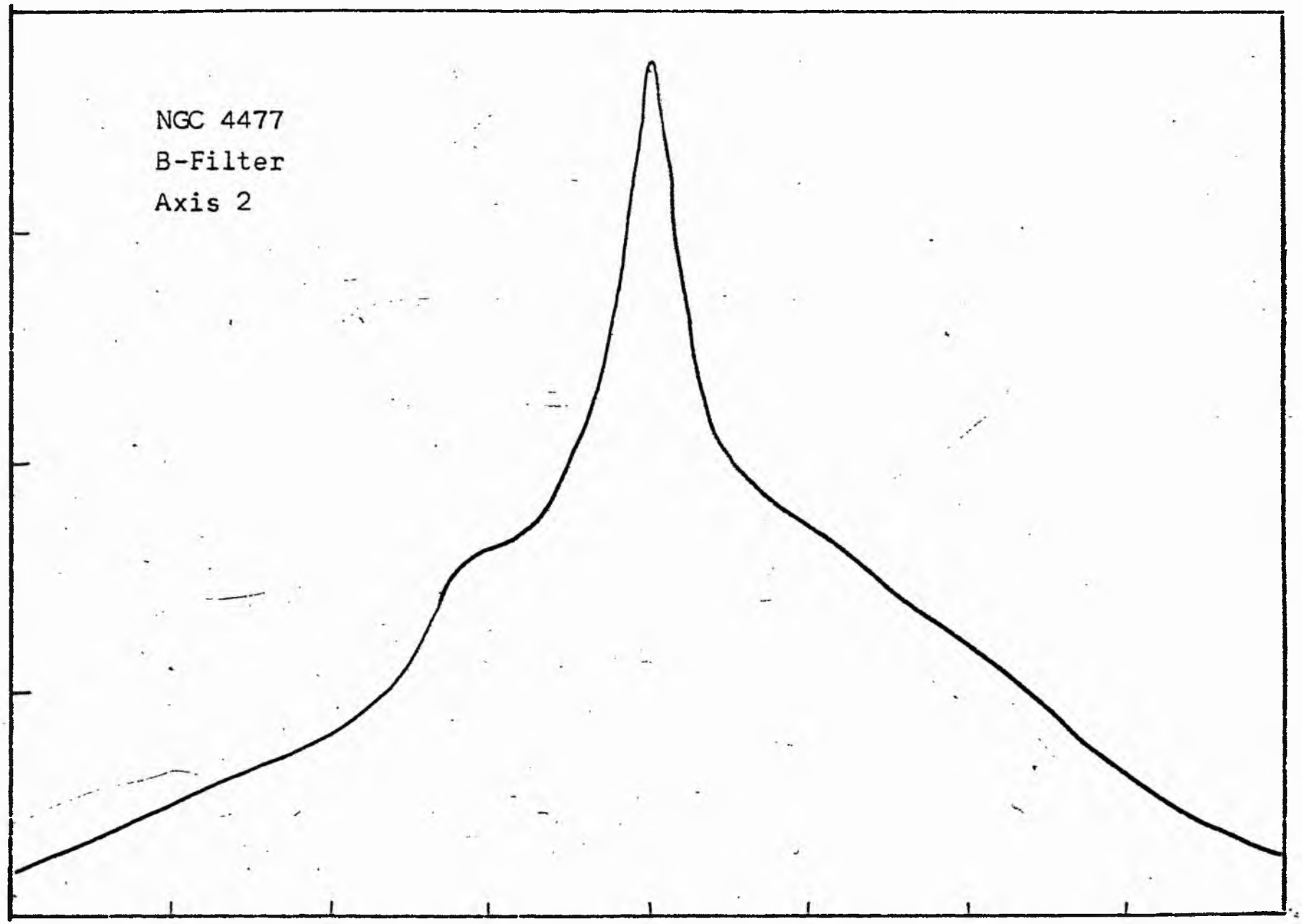
NGC 4477
B-Filter
Axis 2

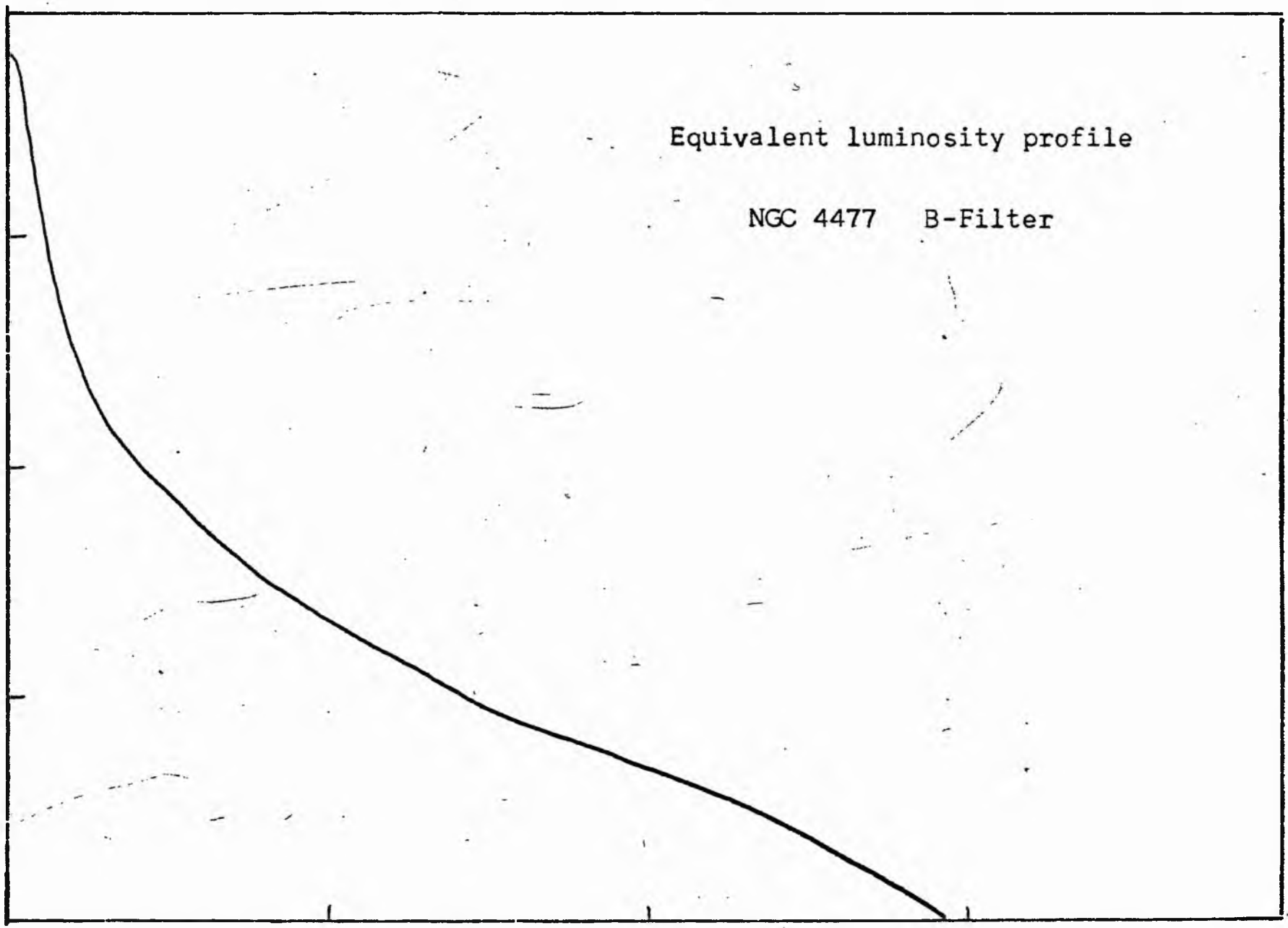
Equivalent luminosity profile
NGC 4477 B-Filter

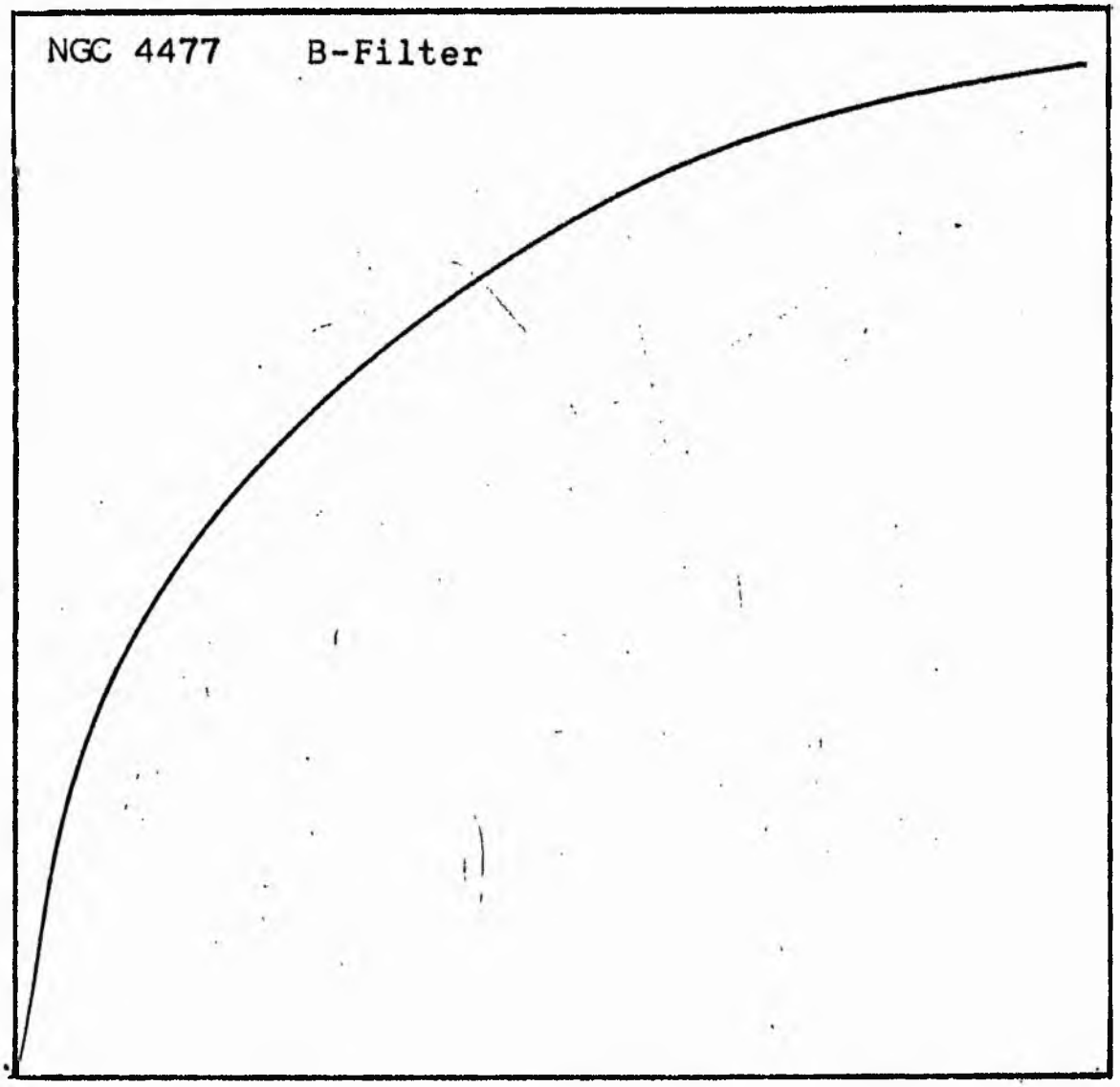

Relative integrated luminosity k(r) versus equivalent radius r*.

MEAN LUMINOSITY DISTRIBUTION IN NGC 4477
B COLOUR

LOG I	I	T	R	AREA	ΔA	P	ΣP	K(R)	ρ	LOG J	μ
1.77	-58.884		0.0	0.0			0.0	0.0	0.0	1.942	17.81
		54.501			13.85	755.0859					
1.70	50.119		2.10	13.85			755.09	0.03	0.05	1.872	17.99
		44.965			4.24	190.7020					
1.60	39.811		2.40	18.10			945.79	0.04	0.06	1.772	18.24
		35.717			39.99	1428.3972					
1.50	31.623		4.30	58.09			2374.19	0.09	0.11	1.672	18.49
		28.371			11.31	320.8660					
1.40	25.119		4.70	69.40			2695.05	0.11	0.12	1.572	18.74
		22.536			36.29	817.7146					
1.30	19.953		5.80	105.68			3512.77	0.14	0.15	1.472	18.99
		17.901			52.68	943.0896					
1.20	15.849		7.10	158.37			4455.85	0.17	0.19	1.372	19.24
		14.219			47.75	678.9888					
1.10	12.589		8.10	206.12			5134.84	0.20	0.21	1.272	19.49
		11.295			42.73	482.5676					
1.00	10.000		8.90	248.85			5617.41	0.22	0.23	1.172	19.74
		8.972			65.31	585.9663					
0.90	7.943		10.00	314.16			6203.37	0.24	0.26	1.072	19.99
		7.126			86.99	619.9292					
0.80	6.310		11.30	401.15			6823.30	0.27	0.30	0.972	20.24
		5.661			89.72	507.8989					
0.70	5.012		12.50	490.87			7331.20	0.29	0.33	0.872	20.49
		4.496			98.77	444.1216					
0.60	3.981		13.70	589.65			7775.32	0.30	0.36	0.772	20.74
		3.572			107.82	385.0933					
0.50	3.162		14.90	697.46			8160.41	0.32	0.39	0.672	20.99
		2.837			157.83	447.7847					
0.40	2.512		16.50	855.30			8608.19	0.34	0.43	0.572	21.24
		2.254			231.57	521.8467					
0.30	1.995		18.60	1086.86			9130.03	0.36	0.49	0.472	21.49
		1.790			298.58	534.4761					
0.20	1.585		21.00	1385.44			9664.50	0.38	0.55	0.372	21.74
		1.422			484.94	689.5298					
0.10	1.259		24.40	1870.38			10354.03	0.40	0.64	0.272	21.99
		1.129			717.32	810.1819					
-0.00	1.000		28.70	2587.70			11164.21	0.44	0.75	0.172	22.24
		0.897			1173.29	1052.6274					
-0.10	0.794		34.60	3760.99			12216.84	0.48	0.91	0.072	22.49
		0.713			1165.53	830.6016					
-0.20	0.631		39.60	4926.52			13047.44	0.51	1.04	-0.028	22.74
		0.566			1463.51	828.4495					
-0.30	0.501		45.10	6390.03			13875.89	0.54	1.18	-0.128	22.99
		0.450			2335.09	1049.9600					
-0.40	0.398		52.70	8725.11			14925.84	0.58	1.38	-0.228	23.24
		0.357			2509.34	896.2505					
-0.50	0.316		59.80	11234.45			15822.09	0.62	1.57	-0.328	23.49
		0.284			2326.20	659.9580					
-0.60	0.251		65.70	13560.65			16482.05	0.64	1.72	-0.428	23.74
		0.225			5503.81	1240.3203					
-0.70	0.200		77.90	19064.46			17722.37	0.69	2.04	-0.528	23.99
		0.179			4659.61	834.1028					
-0.80	0.158		86.90	23724.07			18556.47	0.72	2.28	-0.628	24.24
		0.142			4212.50	598.9763					
-0.90	0.126		94.30	27936.57			19155.45	0.75	2.47	-0.728	24.49
		0.113			6778.70	765.6257					
-1.00	0.100		105.12	34715.26			19921.07	0.78	2.75	-0.828	24.74
		0.090			8216.51	737.1543					
-1.10	0.079		116.90	42931.77			20658.22	0.81	3.06	-0.928	24.99
		0.071			11890.30	847.3528					
-1.20	0.063		132.10	54822.07			21505.57	0.84	3.46	-1.028	25.24
		0.057			15882.55	899.0681					
-1.30	0.050		150.02	70704.62			22404.64	0.87	3.93	-1.128	25.49
		0.045			12079.56	543.1553					
-1.40	0.040		162.33	82784.19			22947.79	0.89	4.25	-1.228	25.74
		0.036			8542.69	305.1182					
-1.50	0.032		170.50	91326.87			23252.91	0.91	4.46	-1.328	25.99
		0.028			9941.12	282.0393					
-1.60	0.025		179.54	101268.00			23534.95	0.92	4.70	-1.428	26.24
		0.023			8003.62	180.3688					
-1.70	0.020		186.50	109271.62			23715.32	0.92	4.88	-1.528	26.49
		0.018			20700.94	370.5657					
-1.80	0.016		203.40	129972.56			24085.88	0.94	5.33	-1.628	26.74
		0.014			14842.56	211.0497					
-1.90	0.013		214.70	144815.12			24296.93	0.95	5.62	-1.728	26.99
		0.011			12958.19	146.3594					
-2.00	0.010		224.10	157773.31			24443.29	0.95	5.87	-1.828	27.24
-∞							25643.00	(1)			∞

PHOTOMETRIC PARAMETERS OF NGC 4477

B-FILTER

Total luminosity	L_T	= 7.12
Total apparent magnitude	m_T	= 11.22
Apparent central surface brightness	μ_o	= 17.81
Major axis at threshold	$2a_m$	= 7.44
Minor axis at threshold	$2b_m$	= 7.21
Major axis at μ=25.0 mag sec^{-2}	2a(25)	= 3.67
Luminosity within μ=25.0 mag sec^{-2}	k(25)	= 0.81
Gradient of exponential component	G(a)	= -0.62
Equivalent gradient of exponential comp.	G(r*)	= -0.53
Equivalent gradient of reduced exp. comp.	G(ρ)	= -0.40
Parameters at k = ¼ :		
Semi-major axis	a_1	= 0.18
Axis ratio	b/a	= 0.81
Equivalent radius	r_1*	= 0.17
Surface brightness	μ_1	= 20.07
Parameters at k = ½(effective) :		
Semi-major axis	a_e	= 0.62
Axis ratio	b/a	= 0.86
Equivalent radius	r_e*	= 0.64
Surface brightness	μ_e	= 22.67
Mean surface brightness	μ_e'	= 12.21
Parameters at k = ¾ :		
Semi-major axis	a_3	= 1.46
Axis ratio	b/a	= 0.97
Equivalent radius	r_3*	= 1.59
Surface brightness	μ_3	= 24.49
Concentration indices	C_{21}	= 3.67
	C_{32}	= 2.50

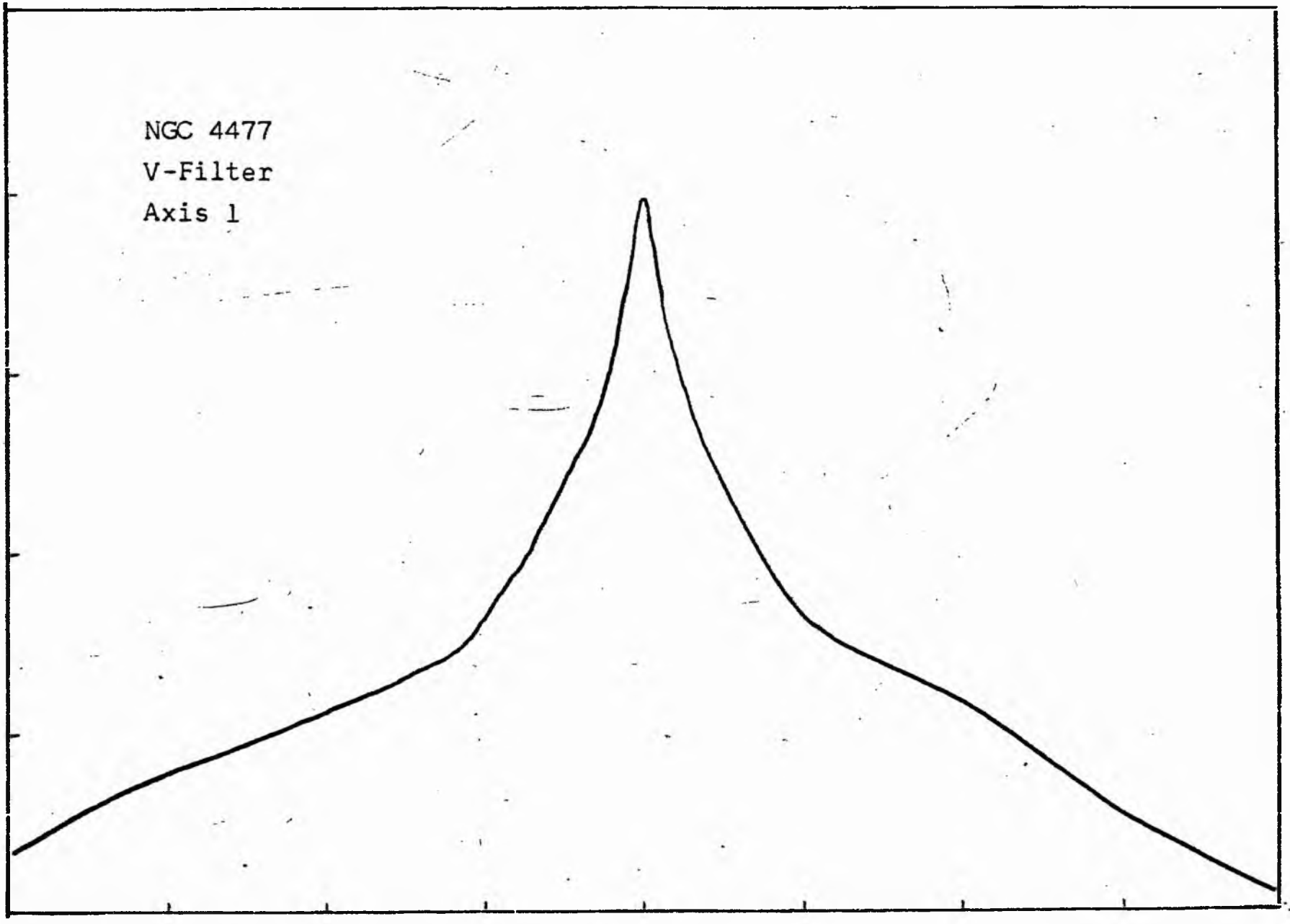
NGC 4477
V-Filter
Axis 1

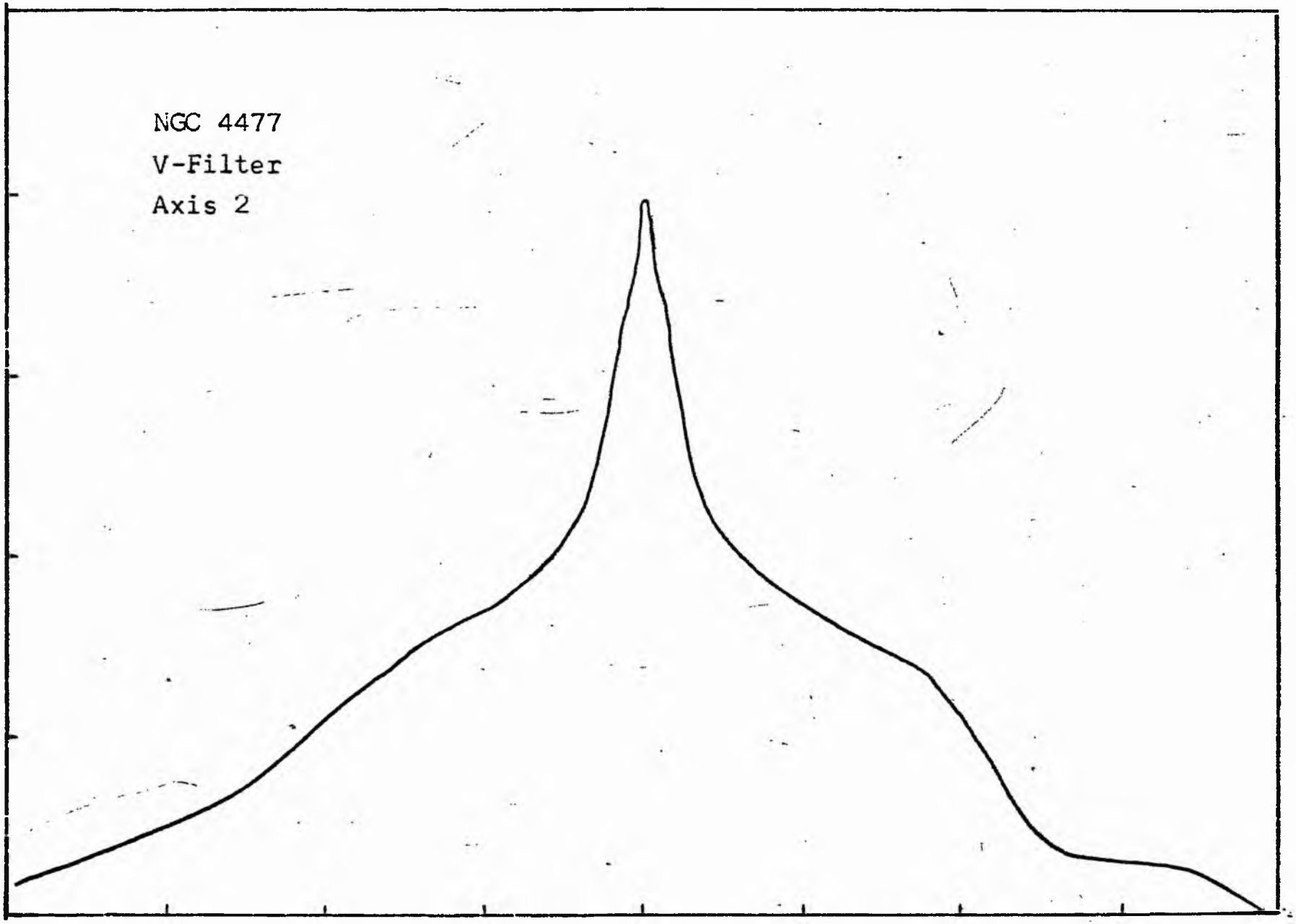
NGC 4477
V-Filter
Axis 2

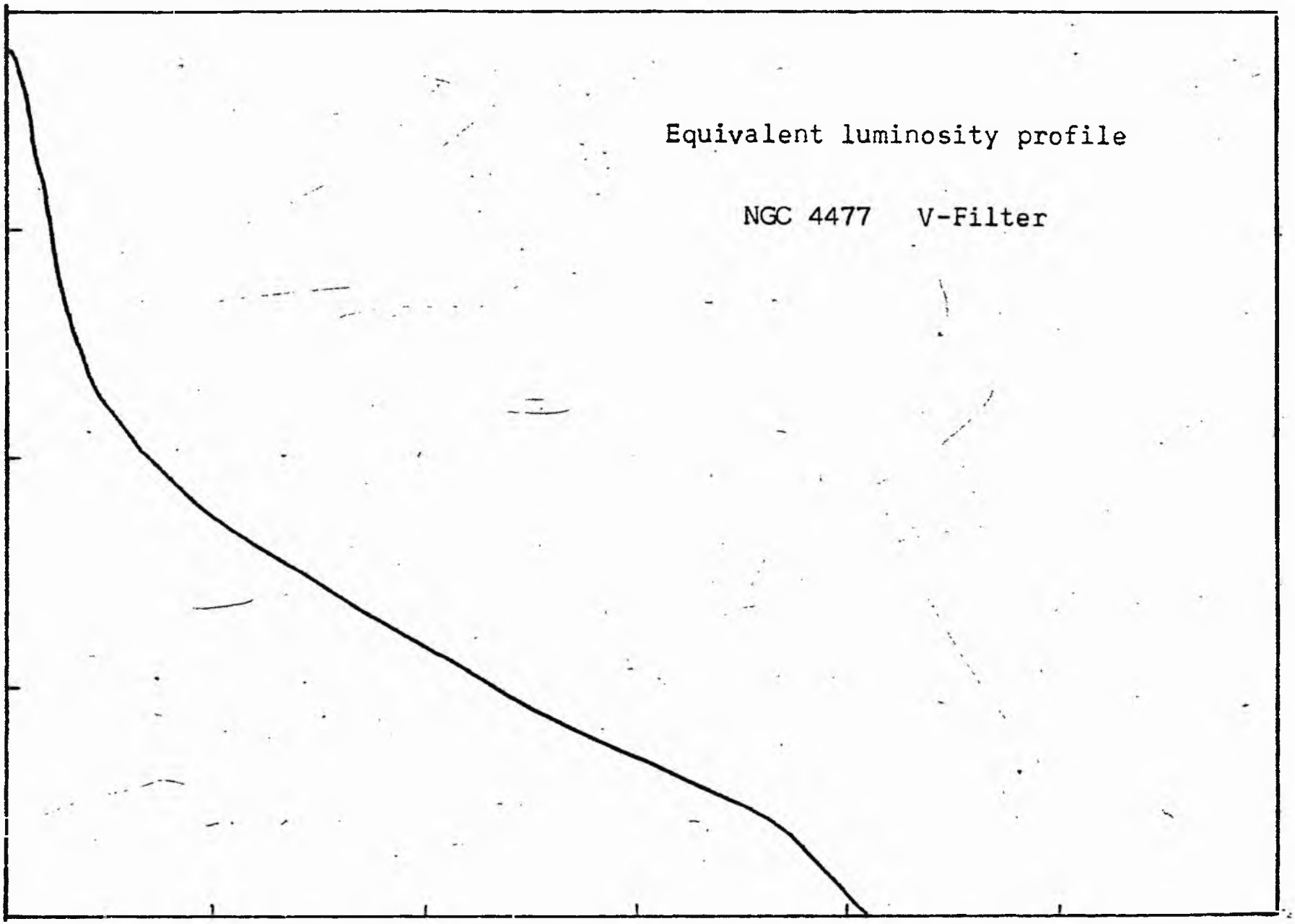
Equivalent luminosity profile
NGC 4477 V-Filter

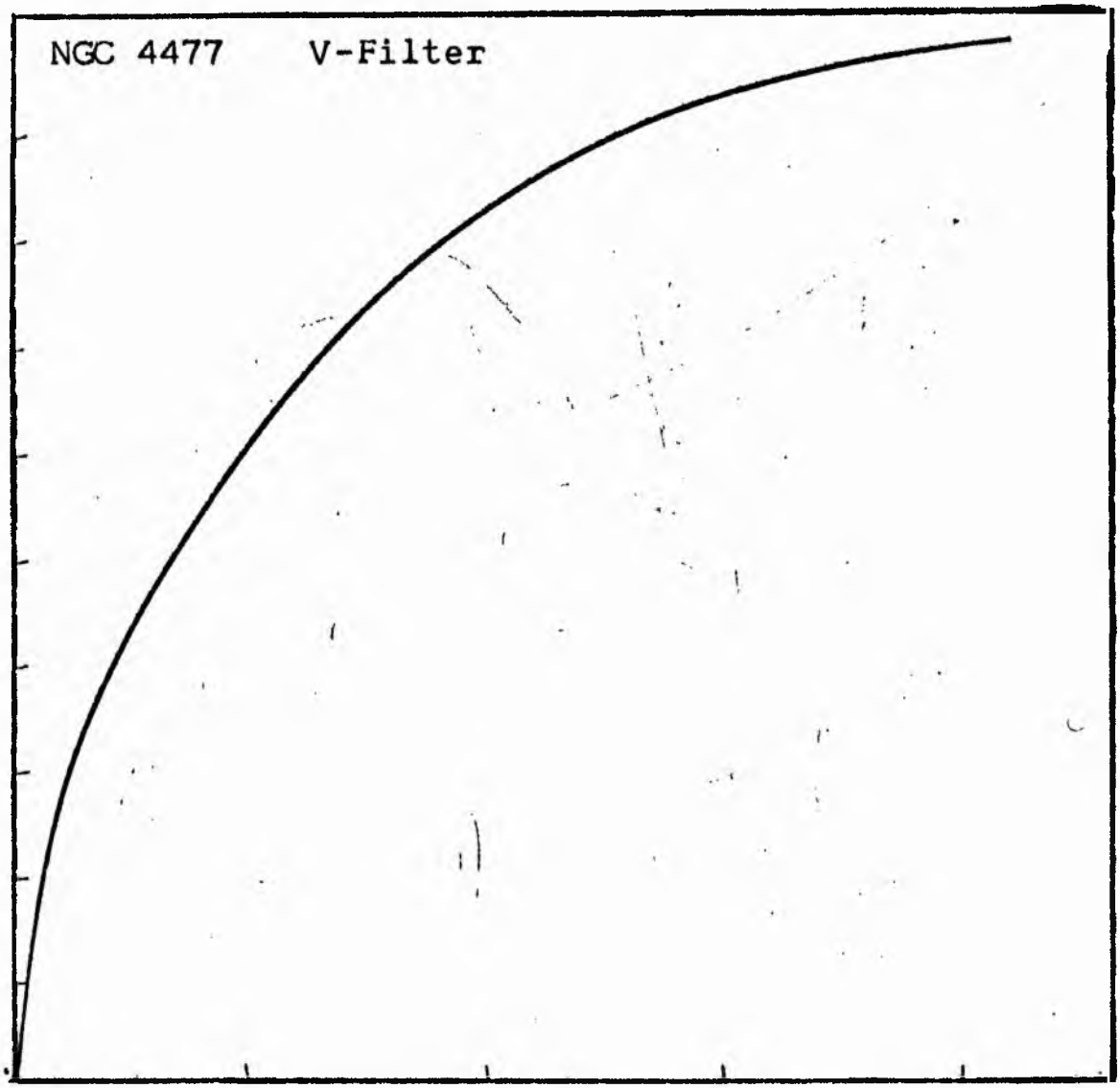

Relative integrated luminosity k(r) versus equivalent radius r*.

MEAN LUMINOSITY DISTRIBUTION IN NGC 4477
V COLOUR

LOG I	I	$\bar{I}$	R	AREA	ΔA	P	ΣP	K(R)	ρ	LOG J	μ_J
1.88	75.858		0.0	0.0			0.0	0.0	0.0	1.910	16.77
		69.477			2.01	139.6909					
1.80	63.096		0.80	2.01			139.69	0.00	0.02	1.830	16.97
		56.607			8.17	462.3740					
1.70	50.119		1.80	10.18			602.06	0.02	0.05	1.730	17.22
		44.965			21.99	988.8218					
1.60	39.811		3.20	32.17			1590.89	0.05	0.09	1.630	17.47
		35.717			34.31	1225.2996					
1.50	31.623		4.60	66.48			2816.19	0.10	0.13	1.530	17.72
		28.371			28.56	810.1843					
1.40	25.119		5.50	95.03			3626.37	0.13	0.16	1.430	17.97
		22.536			21.87	492.7512					
1.30	19.952		6.10	116.90			4119.12	0.14	0.17	1.330	18.22
		17.901			99.53	1781.5737					
1.20	15.849		8.30	216.42			5900.69	0.20	0.24	1.230	18.47
		14.219			43.73	621.8064					
1.10	12.589		9.10	260.16			6522.50	0.23	0.26	1.130	18.72
		11.295			60.32	681.2698					
1.00	10.000		10.10	320.47			7203.77	0.25	0.29	1.030	18.97
		8.972			87.81	787.7717					
0.90	7.943		11.40	408.28			7991.54	0.28	0.33	0.930	19.22
		7.126			74.77	532.8386					
0.80	6.310		12.40	483.05			8524.37	0.29	0.35	0.830	19.47
		5.661			98.02	554.8457					
0.70	5.012		13.60	581.07			9079.21	0.31	0.39	0.730	19.72
		4.496			116.40	523.3669					
0.60	3.981		14.90	697.46			9602.58	0.33	0.42	0.630	19.97
		3.572			127.01	453.6479					
0.50	3.162		16.20	824.48			10056.22	0.35	0.46	0.530	20.22
		2.837			187.75	532.6560					
0.40	2.512		17.95	1012.23			10588.87	0.37	0.51	0.430	20.47
		2.254			268.40	604.8481					
0.30	1.995		20.19	1280.62			11193.72	0.39	0.58	0.330	20.72
		1.790			346.77	620.7490					
0.20	1.585		22.76	1627.40			11814.47	0.41	0.65	0.230	20.97
		1.422			679.82	966.6294					
0.10	1.259		27.10	2307.22			12781.10	0.44	0.77	0.130	21.22
		1.129			1176.46	1328.7612					
-0.00	1.000		33.30	3483.68			14109.86	0.49	0.95	0.030	21.47
		0.897			1336.43	1198.9893					
-0.10	0.794		39.17	4820.11			15308.84	0.53	1.12	-0.070	21.72
		0.713			1655.21	1179.5659					
-0.20	0.631		45.40	6475.32			16488.41	0.57	1.29	-0.170	21.97
		0.566			1760.17	996.3772					
-0.30	0.501		51.20	8235.49			17484.78	0.60	1.46	-0.270	22.22
		0.450			3825.21	1719.9819					
-0.40	0.398		61.96	12060.70			19204.76	0.66	1.77	-0.370	22.47
		0.357			4085.37	1459.1506					
-0.50	0.316		71.69	16146.07			20663.91	0.71	2.04	-0.470	22.72
		0.284			4161.68	1180.6951					
-0.60	0.251		80.40	20307.75			21844.60	0.75	2.29	-0.570	22.97
		0.225			4087.14	921.0618					
-0.70	0.200		88.12	24394.89			22765.66	0.79	2.51	-0.670	23.22
		0.179			3334.70	596.9333					
-0.80	0.158		93.95	27729.59			23362.59	0.81	2.68	-0.770	23.47
		0.142			4102.38	583.3179					
-0.90	0.126		100.66	31831.97			23945.91	0.83	2.87	-0.870	23.72
		0.113			4210.10	475.5127					
-1.00	0.100		107.11	36042.07			24421.42	0.84	3.05	-0.970	23.97
		0.090			9536.79	855.6028					
-1.10	0.079		120.45	45578.86			25277.02	0.87	3.43	-1.070	24.22
		0.071			9742.36	694.2805					
-1.20	0.063		132.70	55321.22			25971.30	0.90	3.78	-1.170	24.47
		0.057			12380.84	700.8442					
-1.30	0.050		146.80	67702.06			26672.14	0.92	4.19	-1.270	24.72
		0.045			8692.87	390.8726					
-1.40	0.040		155.94	76394.94			27063.01	0.93	4.45	-1.370	24.97
		0.036			19267.31	688.1667					
-1.50	0.032		174.50	95662.25			27751.18	0.96	4.98	-1.470	25.22
		0.028			6498.87	184.3789					
-1.60	0.025		180.33	102161.12			27935.55	0.96	5.14	-1.570	25.47
		0.023			5011.44	112.9369					
-1.70	0.020		184.70	107172.56			28048.49	0.97	5.27	-1.670	25.72
		0.018			6836.62	122.3816					
-1.80	0.016		190.50	114009.19			28170.87	0.97	5.43	-1.770	25.97
		0.014			6186.12	87.9617					
-1.90	0.013		195.60	120195.31			28258.83	0.98	5.58	-1.870	26.22
		0.011			8629.62	97.4692					
-2.00	0.010		202.30	128824.94			28356.30	0.98	5.77	-1.970	26.47
∞							28956.00	(1)			∞

PHOTOMETRIC PARAMETERS OF NGC 4477

V-FILTER

Total luminosity	L_T	= 8.04
Total apparent magnitude	m_T	= 10.32
Apparent central surface brightness	μ_o	= 16.77
Major axis at threshold	$2a_m$	= 6.86
Minor axis at threshold	$2b_m$	= 6.52
Major axis at μ=25.0 mag sec^{-2}	2a(25)	= 5.20
Luminosity within μ=25.0 mag sec^{-2}	k(25)	= 0.93
Gradient of exponential component	G(a)	= -0.73
Equivalent gradient of exponential comp.	G(r*)	= -0.65
Equivalent gradient of reduced exp. comp.	G(ρ)	= -0.38
Parameters at k = ¼ :		
Semi-major axis	a_1	= 0.21
Axis ratio	b/a	= 0.99
Equivalent radius	r_1*	= 0.17
Surface brightness	μ_1	= 18.97
Parameters at k = ½(effective) :		
Semi-major axis	a_e	= 0.61
Axis ratio	b/a	= 0.92
Equivalent radius	r_e*	= 0.58
Surface brightness	μ_e	= 21.53
Mean surface brightness	μ_e'	= 11.12
Parameters at k = ¾ :		
Semi-major axis	a_3	= 1.26
Axis ratio	b/a	= 1.03
Equivalent radius	r_3*	= 1.32
Surface brightness	μ_3	= 22.97
Concentration indices	C_{21}	= 3.45
	C_{32}	= 2.26

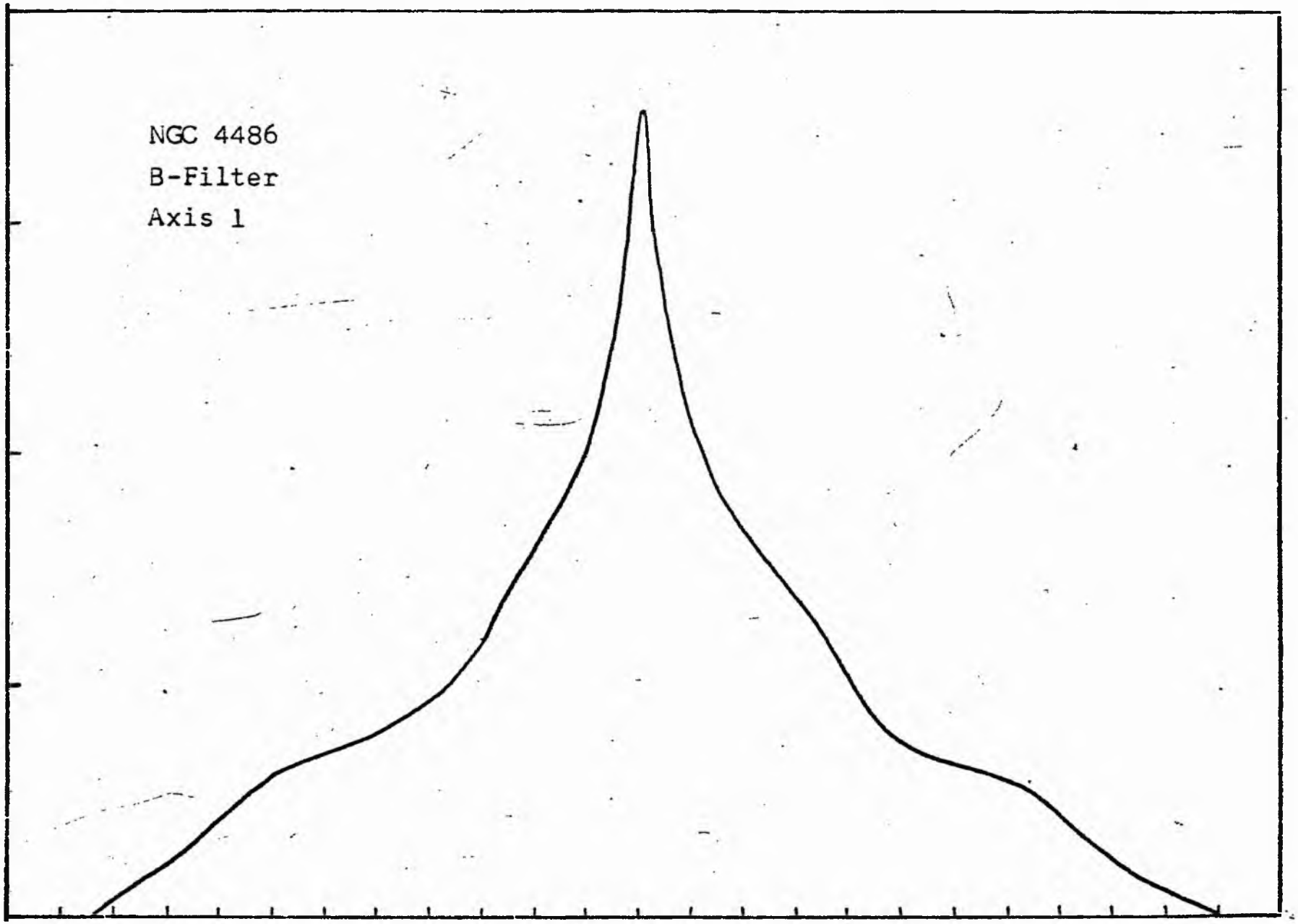
NGC 4486
B-Filter
Axis 1

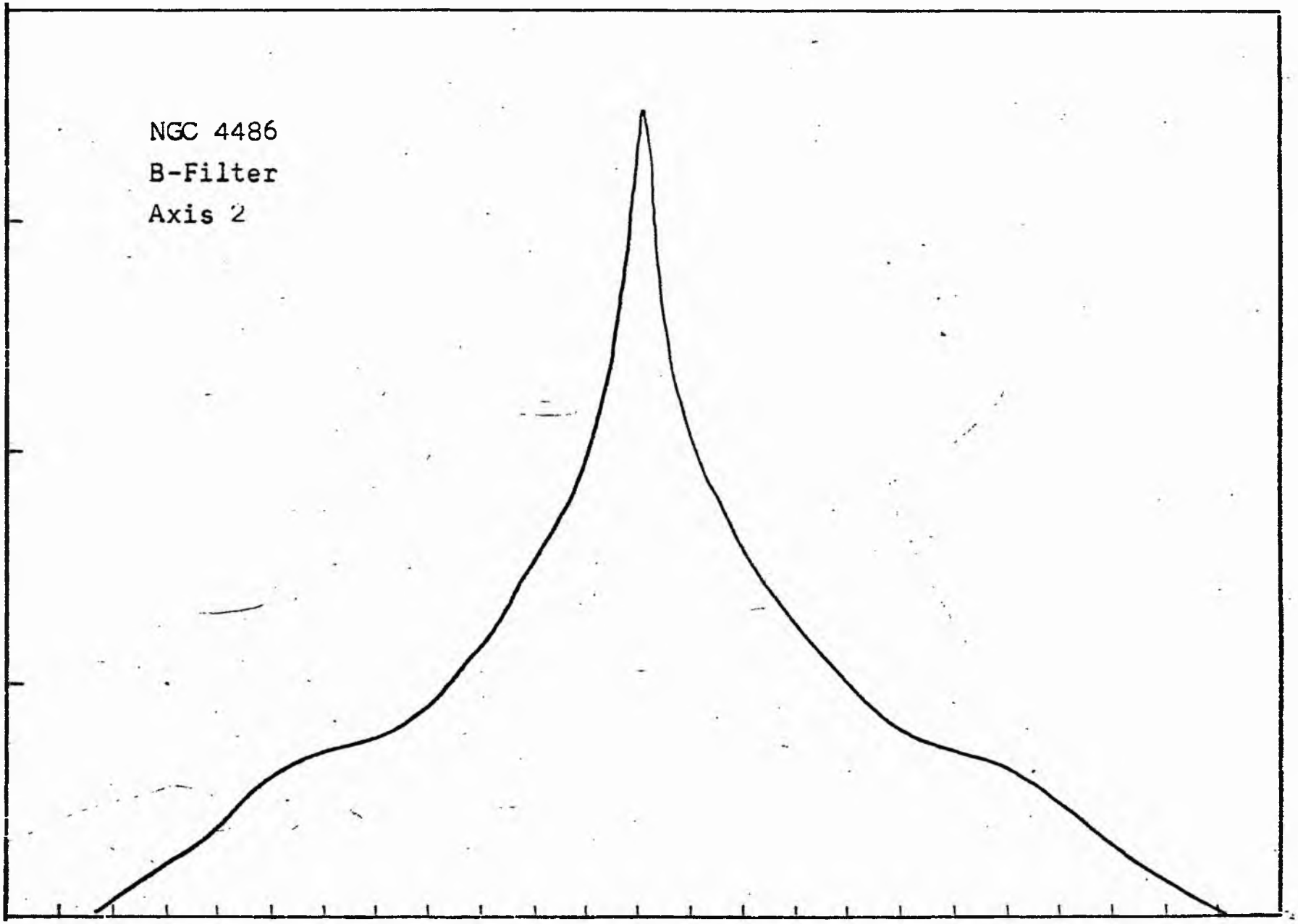
NGC 4486
B-Filter
Axis 2

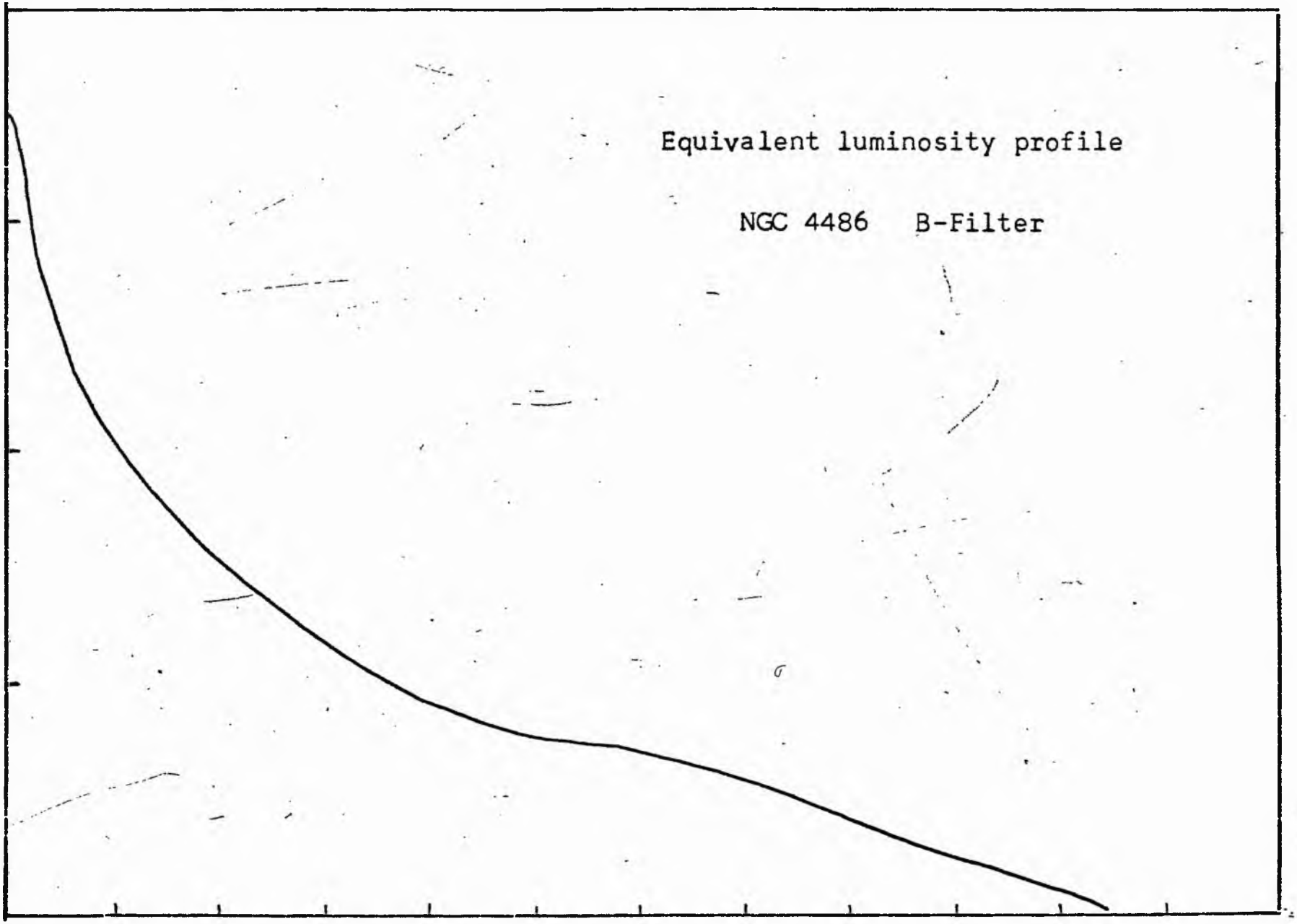
Equivalent luminosity profile
NGC 4486 B-Filter
σ

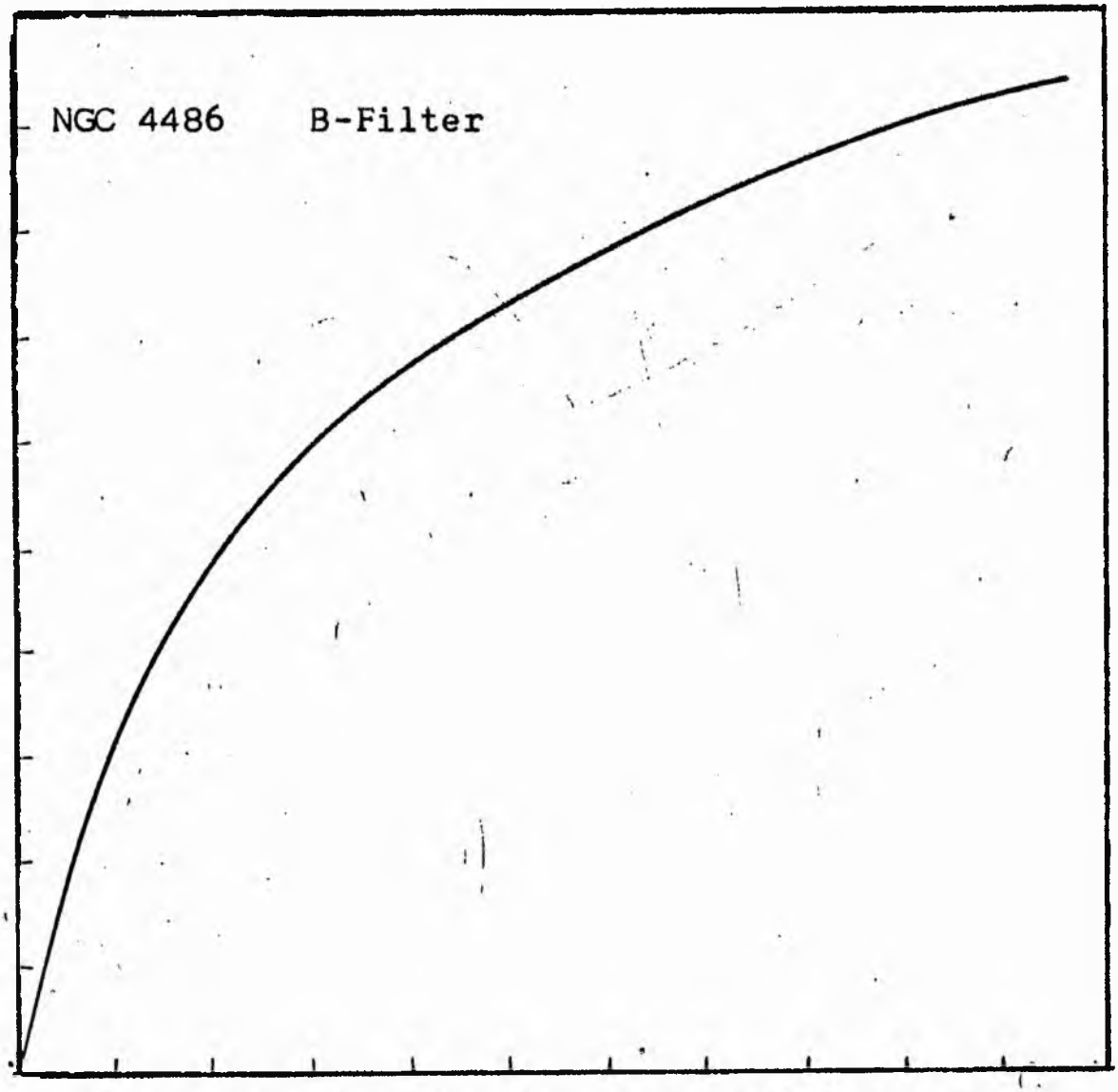

Relative integrated luminosity k(r) versus equivalent radius r*.

B COLCUR

LOG I	I	Ī	R	AREA	ΔA	P	ΣP	K(R)	ρ	LOG J	α
1.43	26.915		0.0	0.0			0.0	0.0	0.0	1.833	18.43
		26.017			58.90	1532.4402					
1.40	25.119		4.33	58.90			1532.44	0.02	0.04	1.803	18.51
		22.536			103.51	2332.5947					
1.30	19.953		7.19	162.41			3865.03	0.04	0.07	1.703	18.76
		17.901			110.48	1977.6392					
1.20	15.849		9.32	272.89			5842.67	0.06	0.09	1.603	19.01
		14.219			156.43	2224.3042					
1.10	12.589		11.69	429.32			8066.97	0.09	0.11	1.503	19.26
		11.295			195.26	2205.4043					
1.00	10.000		14.10	624.58			10272.37	0.11	0.14	1.403	19.51
		8.972			164.70	1657.0632					
0.90	7.943		16.05	809.28			11929.44	0.13	0.16	1.303	19.76
		7.126			277.58	1978.1682					
0.80	6.310		18.60	1086.86			13907.61	0.15	0.18	1.203	20.01
		5.661			269.70	1526.6997					
0.70	5.012		20.78	1356.57			15434.30	0.17	0.20	1.103	20.26
		4.496			437.94	1969.1885					
0.60	3.981		23.90	1794.51			17403.49	0.19	0.23	1.003	20.51
		3.572			540.03	1928.8147					
0.50	3.162		27.26	2334.54			19332.30	0.21	0.27	0.903	20.76
		2.837			717.73	2036.2593					
0.40	2.512		31.17	3052.27			21368.56	0.23	0.31	0.803	21.01
		2.254			1016.97	2291.8044					
0.30	1.995		35.99	4069.24			23660.36	0.26	0.35	0.703	21.26
		1.790			1594.58	2854.4138					
0.20	1.585		42.46	5663.82			26514.77	0.29	0.42	0.603	21.51
		1.422			1839.17	2615.1267					
0.10	1.259		48.87	7502.99			29129.90	0.32	0.48	0.503	21.76
		1.129			1941.66	2193.0305					
-0.00	1.000		54.83	9444.66			31322.93	0.34	0.54	0.403	22.01
		0.897			3372.52	3205.1267					
-0.10	0.794		64.37	13017.18			34528.05	0.38	0.63	0.303	22.26
		0.713			5720.75	4076.8423					
-0.20	0.631		77.23	18737.93			38604.89	0.42	0.76	0.203	22.51
		0.566			6340.33	3593.6016					
-0.30	0.501		89.36	25086.26			42198.49	0.46	0.88	0.103	22.76
		0.450			7209.09	3241.5413					
-0.40	0.398		101.39	32295.35			45440.03	0.50	1.00	0.003	23.01
		0.357			9165.54	3273.6248					
-0.50	0.316		114.88	41460.89			48713.65	0.53	1.13	-0.097	23.26
		0.284			11346.51	3219.0918					
-0.60	0.251		129.65	52807.40			51932.74	0.57	1.27	-0.197	23.51
		0.225			8179.85	1843.3857					
-0.70	0.200		139.33	60987.25			53776.12	0.59	1.37	-0.297	23.76
		0.179			11233.62	2010.9021					
-0.80	0.158		151.62	72220.87			55787.02	0.61	1.49	-0.397	24.01
		0.142			15374.00	2186.0396					
-0.90	0.126		166.98	87594.87			57973.06	0.64	1.64	-0.497	24.26
		0.113			19995.87	2258.4583					
-1.00	0.100		185.06	107590.75			60231.52	0.66	1.82	-0.597	24.51
		0.090			26620.44	2388.2922					
-1.10	0.079		206.69	134211.19			62619.81	0.69	2.03	-0.697	24.76
		0.071			42979.31	3062.8967					
-1.20	0.063		237.49	177190.50			65682.69	0.72	2.33	-0.797	25.01
		0.057			124638.44	7055.4570					
-1.30	0.050		309.96	301828.94			72738.12	0.80	3.04	-0.897	25.26
		0.045			83675.69	3762.4695					
-1.40	0.040		350.30	385504.62			76500.56	0.84	3.44	-0.997	25.51
		0.036			58758.81	2098.6855					
-1.50	0.032		376.05	444263.44			78599.19	0.86	3.69	-1.097	25.76
		0.028			45084.62	1279.0972					
-1.60	0.025		394.67	489348.06			79878.25	0.88	3.88	-1.197	26.01
		0.023			77834.69	1754.0781					
-1.70	0.020		424.90	567182.75			81632.31	0.90	4.17	-1.297	26.26
		0.018			99024.19	1772.6282					
-1.80	0.016		460.50	666206.94			83404.94	0.92	4.52	-1.397	26.51
		0.014			102193.31	1453.1125					
-1.90	0.013		494.56	768400.25			84858.00	0.93	4.86	-1.497	26.76
		0.011			64019.94	723.0901					
-2.00	0.010		514.75	832420.19			85581.06	0.94	5.06	-1.597	27.01
$-\infty$							91099.00	(1)			∞

PHOTOMETRIC PARAMETERS OF NGC 4486

B-FILTER

Total luminosity ..... L_T = 25.31

Total apparent magnitude ..... m_T = 9.62

Apparent central surface brightness ..... μ_o = 18.43

Major axis at threshold ..... $2a_m$ = 17.68

Minor axis at threshold ..... $2b_m$ = 17.20

Major axis at μ=25.0 mag sec^{-2} ..... 2a(25) = 7.82

Luminosity within μ=25.0 mag sec^{-2} ..... k(25) = 0.72

Gradient of exponential component ..... G(a) = -0.22

Equivalent gradient of exponential comp.... G(r*) = -0.21

Equivalent gradient of reduced exp. comp.... G(ρ) = -0.29

Parameters at k = ¼ :

- Semi-major axis ..... a_1 = 0.65
- Axis ratio ..... b/a = 0.90
- Equivalent radius ..... r_1* = 0.56
- Surface brightness ..... μ_1 = 21.18

Parameters at k = ½(effective) :

- Semi-major axis ..... a_e = 1.82
- Axis ratio ..... b/a = 0.84
- Equivalent radius ..... r_e* = 1.70
- Surface brightness ..... μ_e = 23.01
- Mean surface brightness ..... μ_e' = 12.77

Parameters at k = ¾ :

- Semi-major axis ..... a_3 = 4.36
- Axis ratio ..... b/a = 0.99
- Equivalent radius ..... r_3* = 4.41
- Surface brightness ..... μ_3 = 25.10

Concentration indices ..... C_{21} = 2.99, C_{32} = 2.60

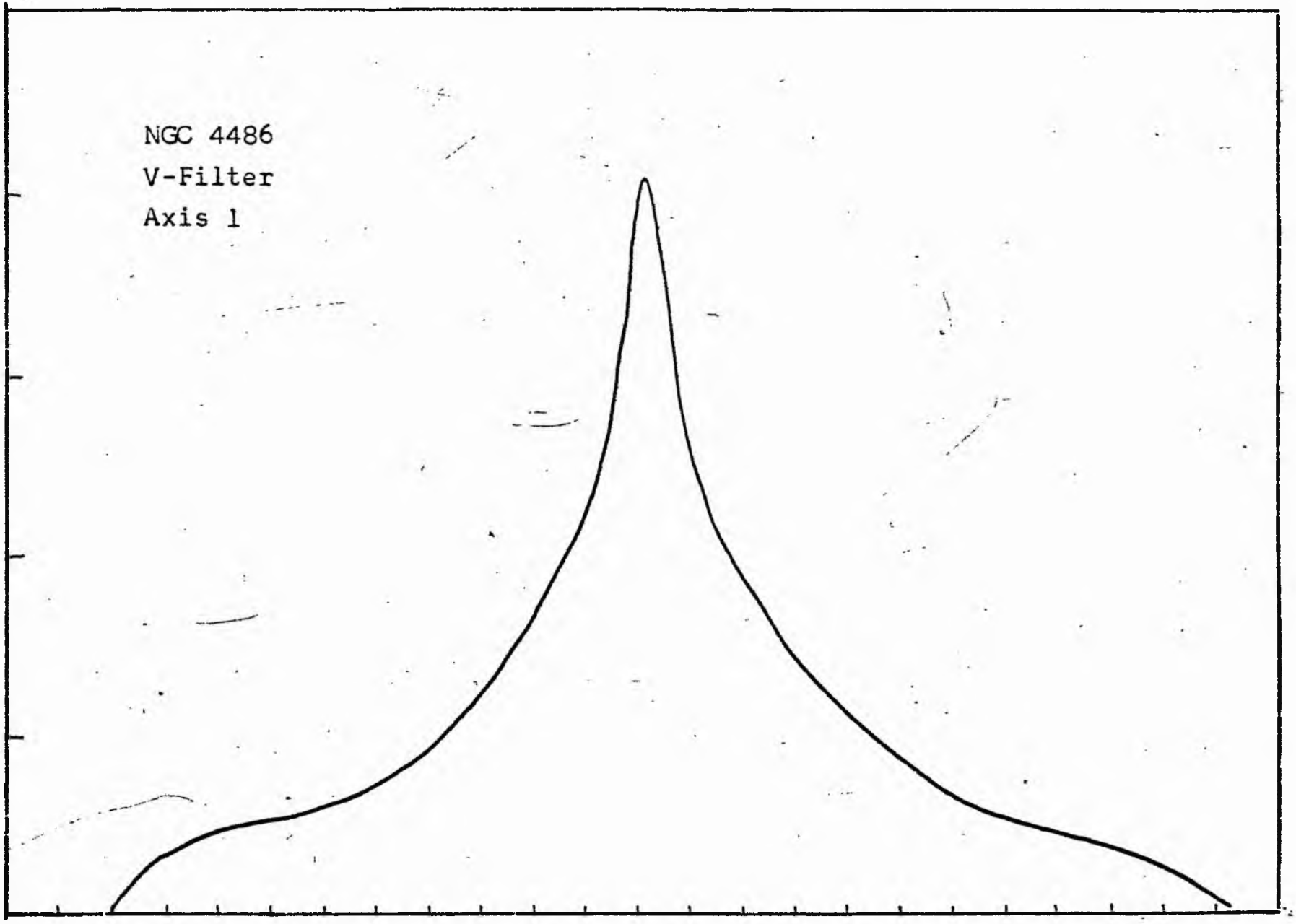
NGC 4486
V-Filter
Axis 1

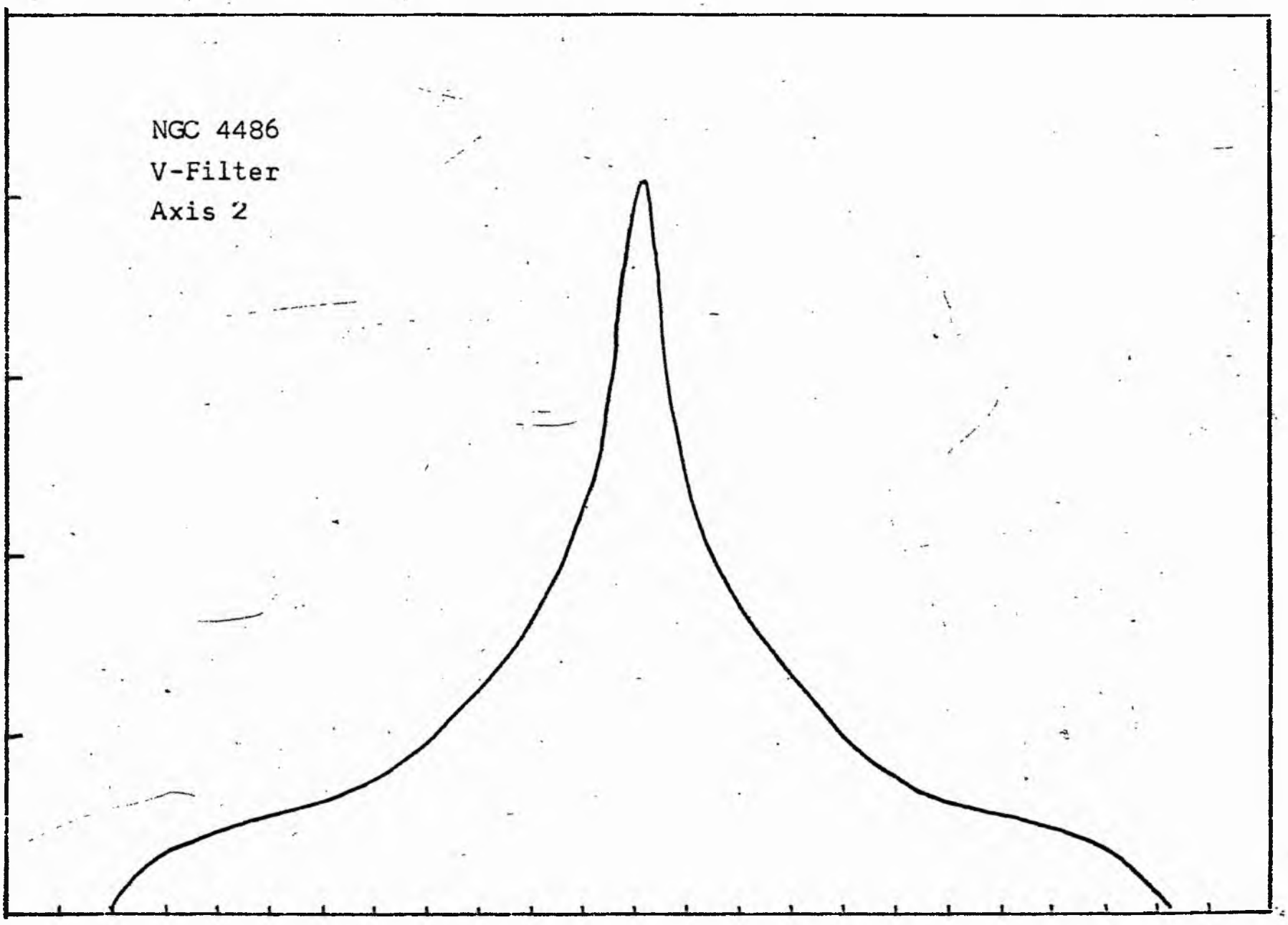
NGC 4486
V-Filter
Axis 2

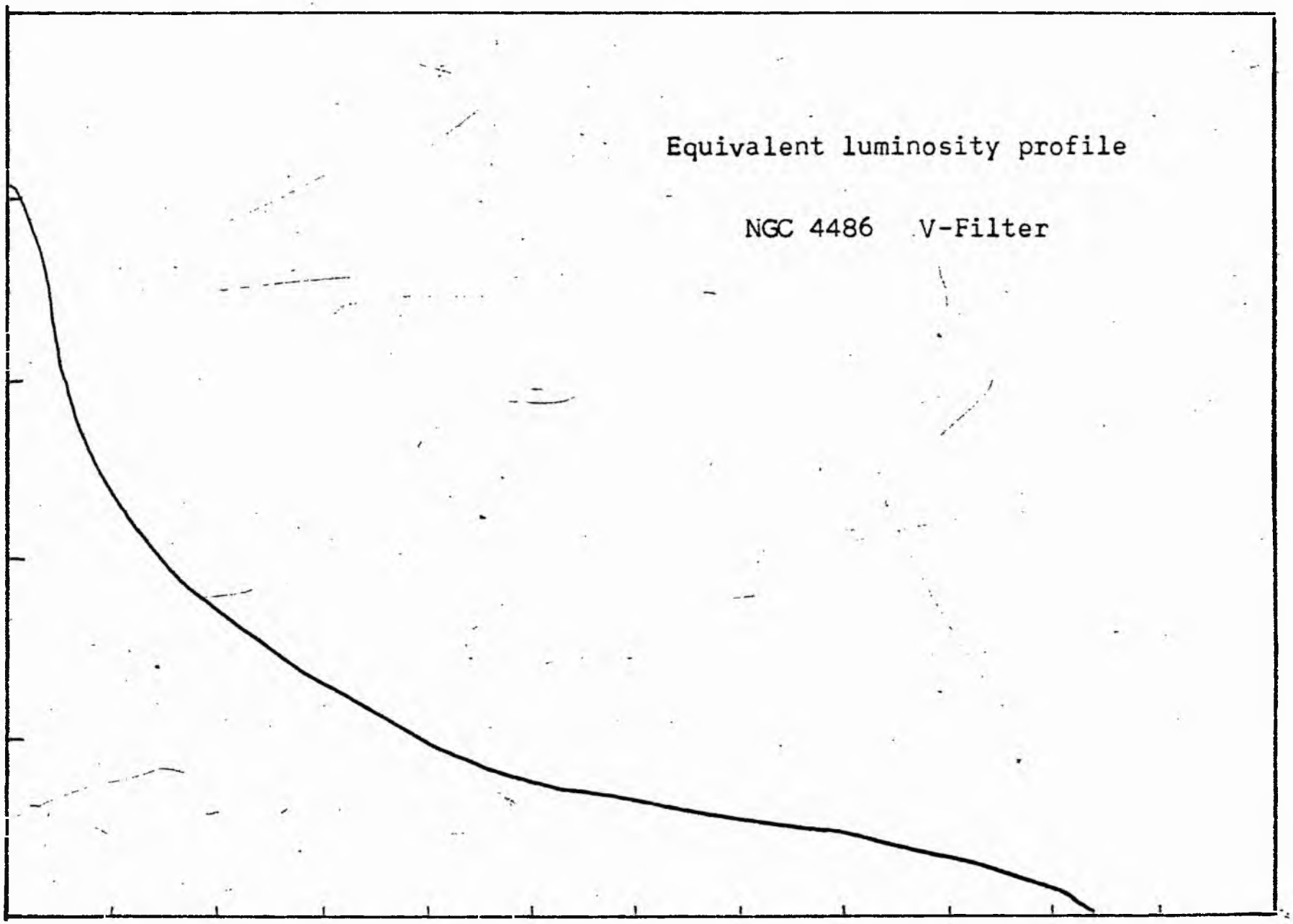
Equivalent luminosity profile
NGC 4486 V-Filter

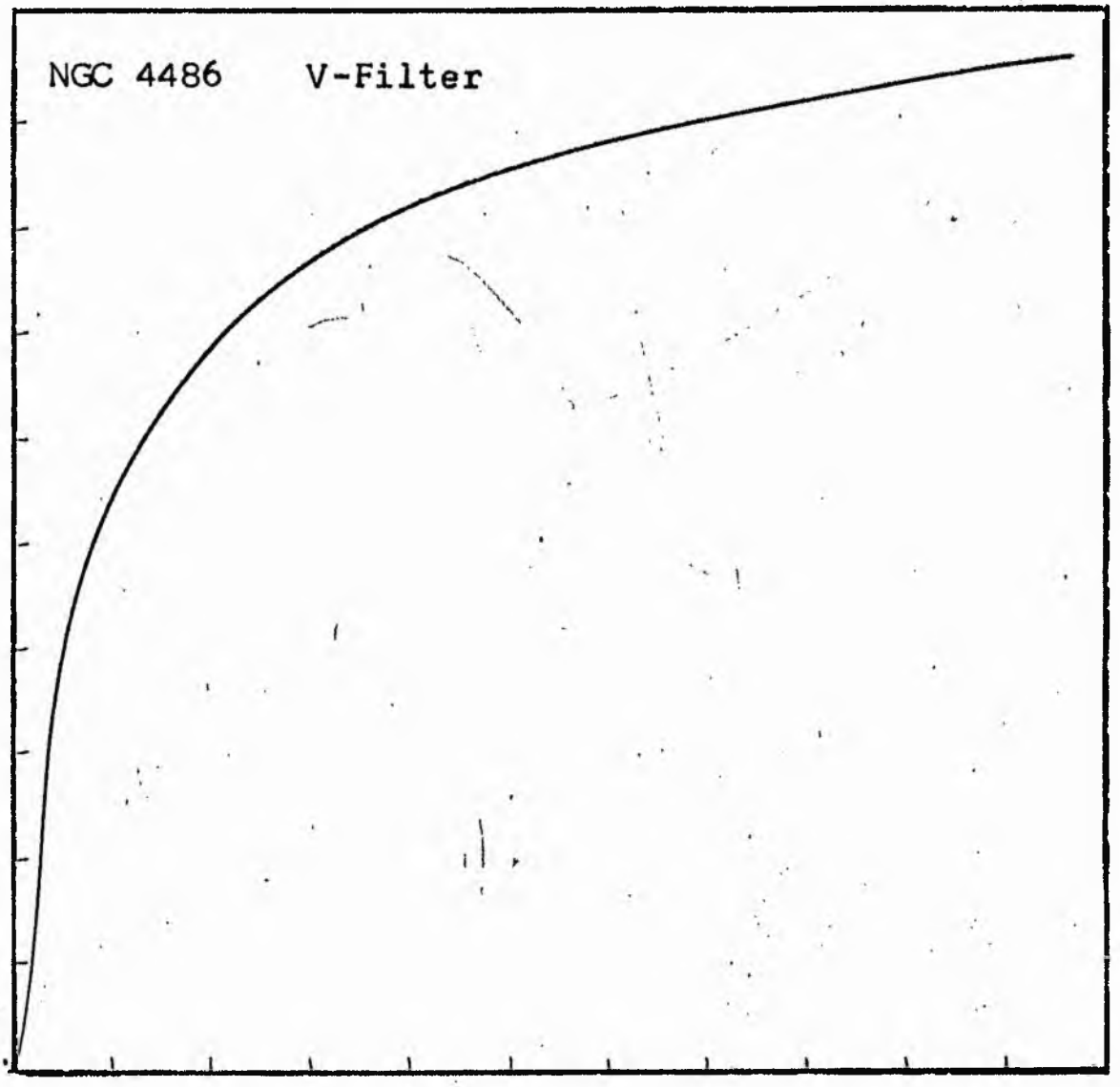

Relative integrated luminosity k(r) versus equivalent radius r*.

MEAN LUMINOSITY DISTRIBUTION IN NGC 4486
V COLOUR

LOG I	I	$\bar{I}$	R	AREA	ΔA	p	Σp	K(R)	ρ	LOG J	μ
2.02	104.713		0.0	0.0			0.0	0.0	0.0	1.438	16.67
		102.356			21.24	2173.7571					
2.00	100.000		2.60	21.24			2173.76	0.01	0.07	1.418	16.72
		89.716			42.38	3802.1877					
1.90	79.433		4.50	63.62			5975.94	0.04	0.12	1.318	16.97
		71.264			73.23	5218.7070					
1.80	63.096		6.60	136.85			11194.65	0.07	0.18	1.218	17.22
		56.607			202.95	11488.2187					
1.70	50.119		10.40	339.79			22682.87	0.15	0.28	1.118	17.47
		44.965			248.13	11157.0859					
1.60	39.811		13.68	587.93			33839.95	0.22	0.37	1.018	17.72
		35.717			216.32	7726.3125					
1.50	31.623		16.00	804.25			41566.27	0.27	0.44	0.918	17.97
		28.371			161.17	4572.3867					
1.40	25.119		17.53	965.41			46138.65	0.30	0.48	0.818	18.22
		22.536			155.61	3506.7007					
1.30	19.952		18.89	1121.02			49645.35	0.33	0.52	0.718	18.47
		17.901			305.63	5470.9102					
1.20	15.849		21.31	1426.65			55116.26	0.36	0.58	0.618	18.72
		14.219			206.48	2935.8789					
1.10	12.589		22.80	1633.12			58052.14	0.38	0.62	0.518	18.97
		11.295			314.69	3554.3174					
1.00	10.000		24.90	1947.82			61606.46	0.41	0.68	0.418	19.22
		8.972			445.32	3995.2180					
0.90	7.943		27.60	2393.14			65601.62	0.43	0.75	0.318	19.47
		7.126			491.12	3499.9358					
0.80	6.310		30.30	2884.26			69101.50	0.46	0.83	0.218	19.72
		5.661			532.79	3015.9253					
0.70	5.012		32.98	3417.05			72117.37	0.48	0.90	0.118	19.97
		4.496			677.11	3044.5596					
0.60	3.981		36.10	4094.15			75161.87	0.50	0.98	0.018	20.22
		3.572			708.74	2531.3748					
0.50	3.162		39.10	4802.89			77693.19	0.51	1.07	-0.082	20.47
		2.837			1133.58	3216.0413					
0.40	2.512		43.47	5936.48			80909.19	0.53	1.19	-0.182	20.72
		2.254			1662.00	3745.4224					
0.30	1.995		49.18	7598.48			84654.56	0.56	1.34	-0.282	20.97
		1.790			1994.89	3570.9905					
0.20	1.585		55.26	9593.37			88225.50	0.58	1.51	-0.382	21.22
		1.422			2443.98	3475.0928					
0.10	1.259		61.90	12037.36			91700.56	0.61	1.69	-0.482	21.47
		1.129			2963.15	3346.7415					
-0.00	1.000		69.10	15000.50			95047.25	0.63	1.88	-0.582	21.72
		0.897			2907.36	2608.3596					
-0.10	0.794		75.50	17907.86			97655.56	0.65	2.06	-0.682	21.97
		0.713			4470.82	3186.0730					
-0.20	0.631		84.40	22378.68			100841.62	0.67	2.30	-0.782	22.22
		0.566			6333.45	3585.1660					
-0.30	0.501		95.60	28712.13			104426.75	0.69	2.61	-0.882	22.47
		0.450			7660.47	3444.4849					
-0.40	0.398		107.60	36372.60			107871.19	0.71	2.94	-0.982	22.72
		0.357			9928.06	3545.9565					
-0.50	0.316		121.40	46300.66			111417.12	0.74	3.31	-1.082	22.97
		0.284			9683.59	2749.0000					
-0.60	0.251		133.50	55990.25			114166.12	0.75	3.64	-1.182	23.22
		0.225			10701.00	2411.5339					
-0.70	0.200		145.70	66691.25			116577.62	0.77	3.97	-1.282	23.47
		0.179			14035.37	2512.4260					
-0.80	0.158		160.30	80726.62			119090.00	0.79	4.37	-1.382	23.72
		0.142			12322.31	1752.1099					
-0.90	0.126		172.10	93048.94			120842.06	0.80	4.69	-1.482	23.97
		0.113			21799.62	2462.1733					
-1.00	0.100		191.20	114848.56			123304.19	0.81	5.22	-1.582	24.22
		0.090			23827.62	2137.7209					
-1.10	0.079		210.10	138676.19			125441.87	0.83	5.73	-1.682	24.47
		0.071			26936.50	1919.6050					
-1.20	0.063		229.60	165612.69			127361.44	0.84	6.26	-1.782	24.72
		0.057			43341.87	2453.4602					
-1.30	0.050		257.90	208954.56			129814.87	0.86	7.04	-1.882	24.97
		0.045			54524.75	2451.6907					
-1.40	0.040		289.60	263479.31			132266.56	0.87	7.90	-1.982	25.22
		0.036			138709.56	4954.2617					
-1.50	0.032		357.80	402188.87			137220.81	0.91	9.76	-2.082	25.47
		0.028			131854.00	3740.8164					
-1.60	0.025		412.30	534042.87			140961.62	0.93	11.25	-2.182	25.72
		0.023			116059.12	2615.4895					
-1.70	0.020		454.90	650102.00			143577.06	0.95	12.41	-2.282	25.97
		0.018			39453.25	706.2478					
-1.80	0.016		468.50	689555.25			144283.25	0.95	12.78	-2.382	26.22
		0.014			75865.00	1078.7390					
-1.90	0.013		493.60	765420.25			145361.94	0.96	13.46	-2.482	26.47
		0.011			66837.94	754.9158					
-2.00	0.010		514.70	832258.19			146116.81	0.97	14.04	-2.582	26.72
- ∞							151316.00	(1)			∞

PHOTOMETRIC PARAMETERS OF NGC 4486

V-FILTER

Total luminosity	L_T	= 42.03
Total apparent magnitude	m_T	= 8.77
Apparent central surface brightness	μ_o	= 16.67
Major axis at threshold	$2a_m$	= 17.33
Minor axis at threshold	$2b_m$	= 17.21
Major axis at μ=25.0 mag sec^{-2}	2a(25)	= 9.03
Luminosity within μ=25.0 mag sec^{-2}	k(25)	= 0.86
Gradient of exponential component	G(a)	= -0.23
Equivalent gradient of exponential comp.	G(r*)	= -0.25
Equivalent gradient of reduced exp. comp.	G(ρ)	= -0.21
Parameters at k = ¼ :		
Semi-major axis	a_1	= 0.31
Axis ratio	b/a	= 0.95
Equivalent radius	r_1*	= 0.25
Surface brightness	μ_1	= 17.87
Parameters at k = ½(effective) :		
Semi-major axis	a_e	= 0.70
Axis ratio	b/a	= 0.98
Equivalent radius	r_e*	= 0.61
Surface brightness	μ_e	= 20.22
Mean surface brightness	μ_e'	= 9.67
Parameters at k = ¾ :		
Semi-major axis	a_3	= 2.37
Axis ratio	b/a	= 0.96
Equivalent radius	r_3*	= 2.17
Surface brightness	μ_3	= 23.22
Concentration indices	C_{21}	= 2.47
	C_{32}	= 3.56

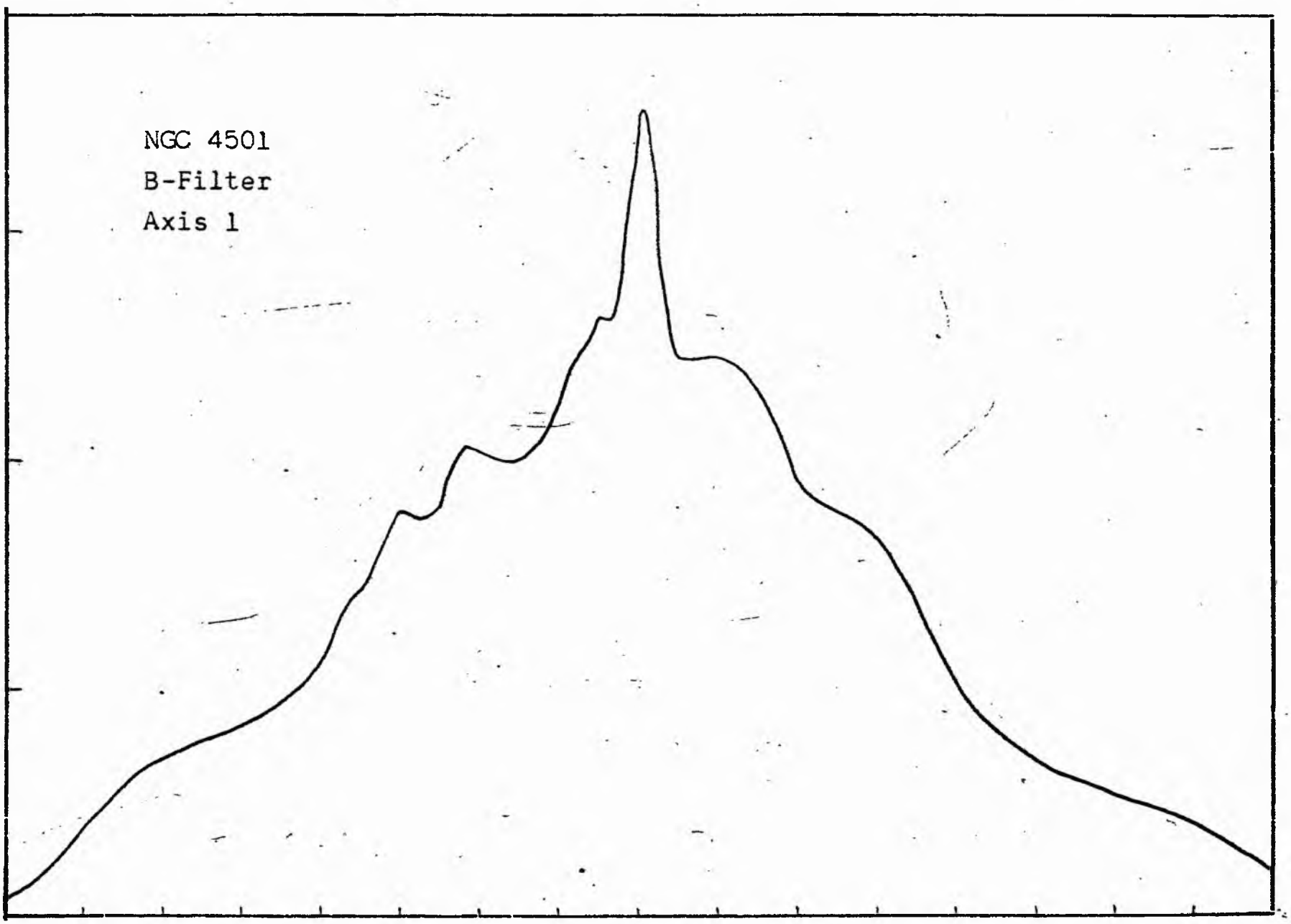
NGC 4501
B-Filter
Axis 1

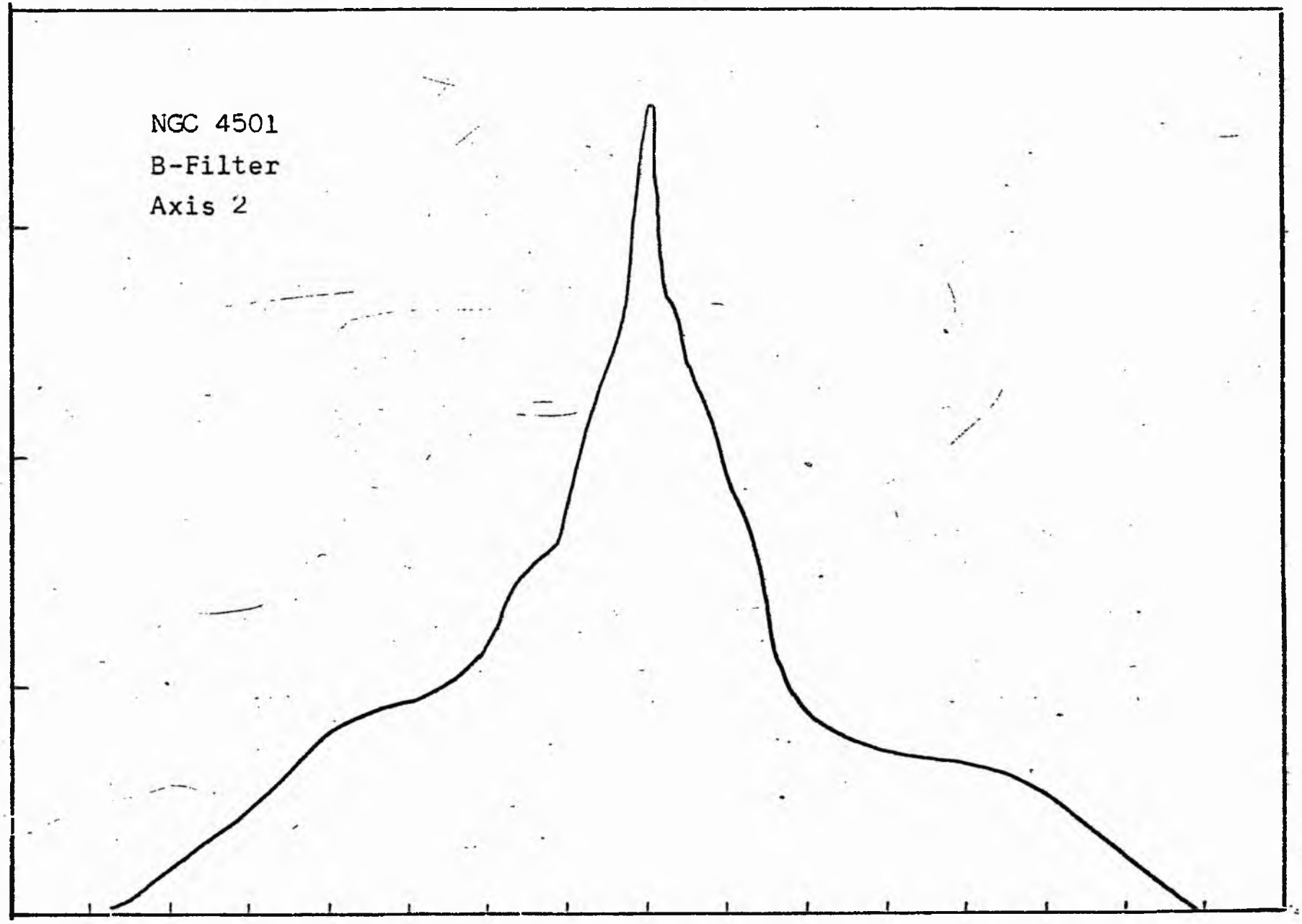
NGC 4501
B-Filter
Axis 2

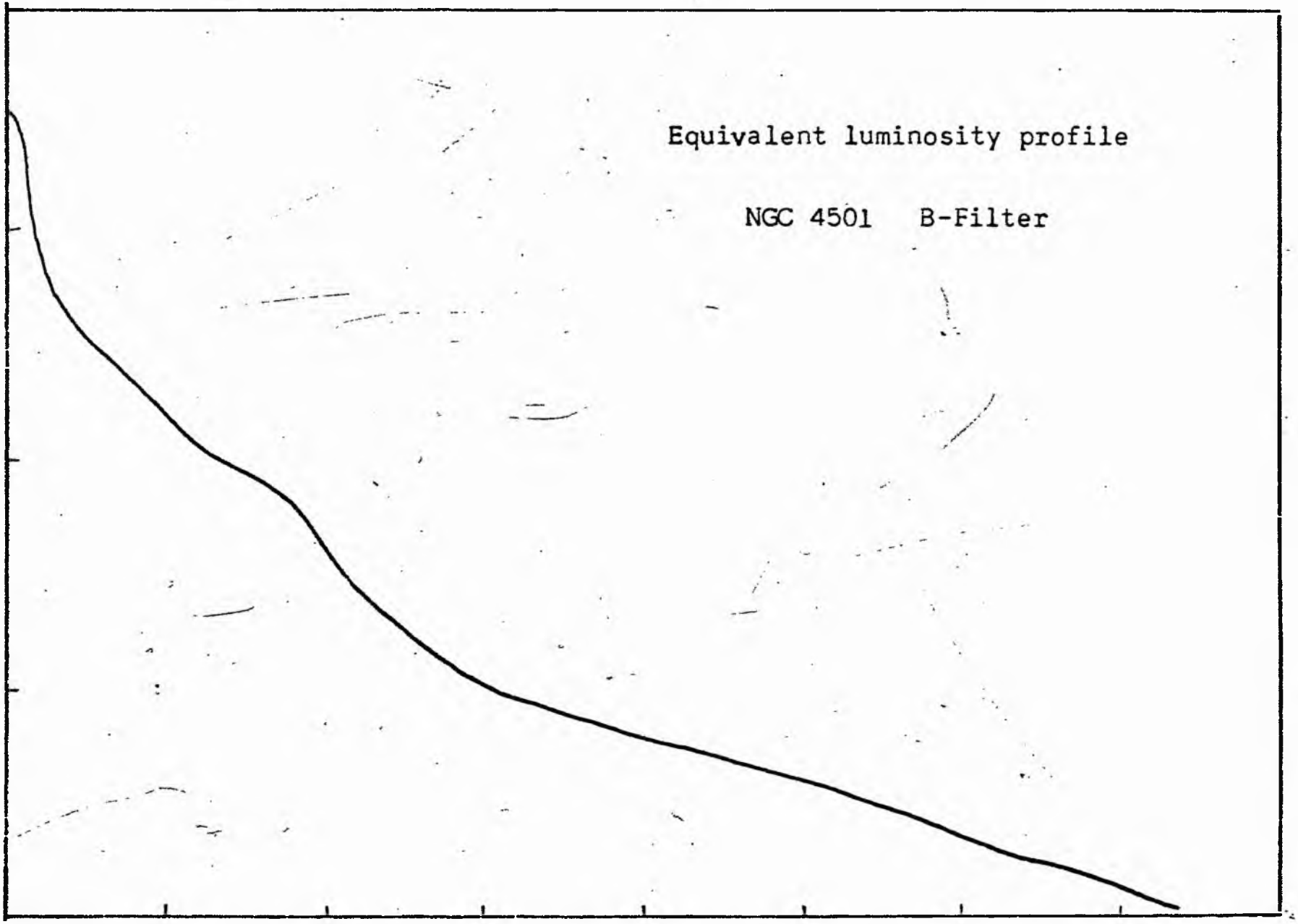
Equivalent luminosity profile
NGC 4501 B-Filter

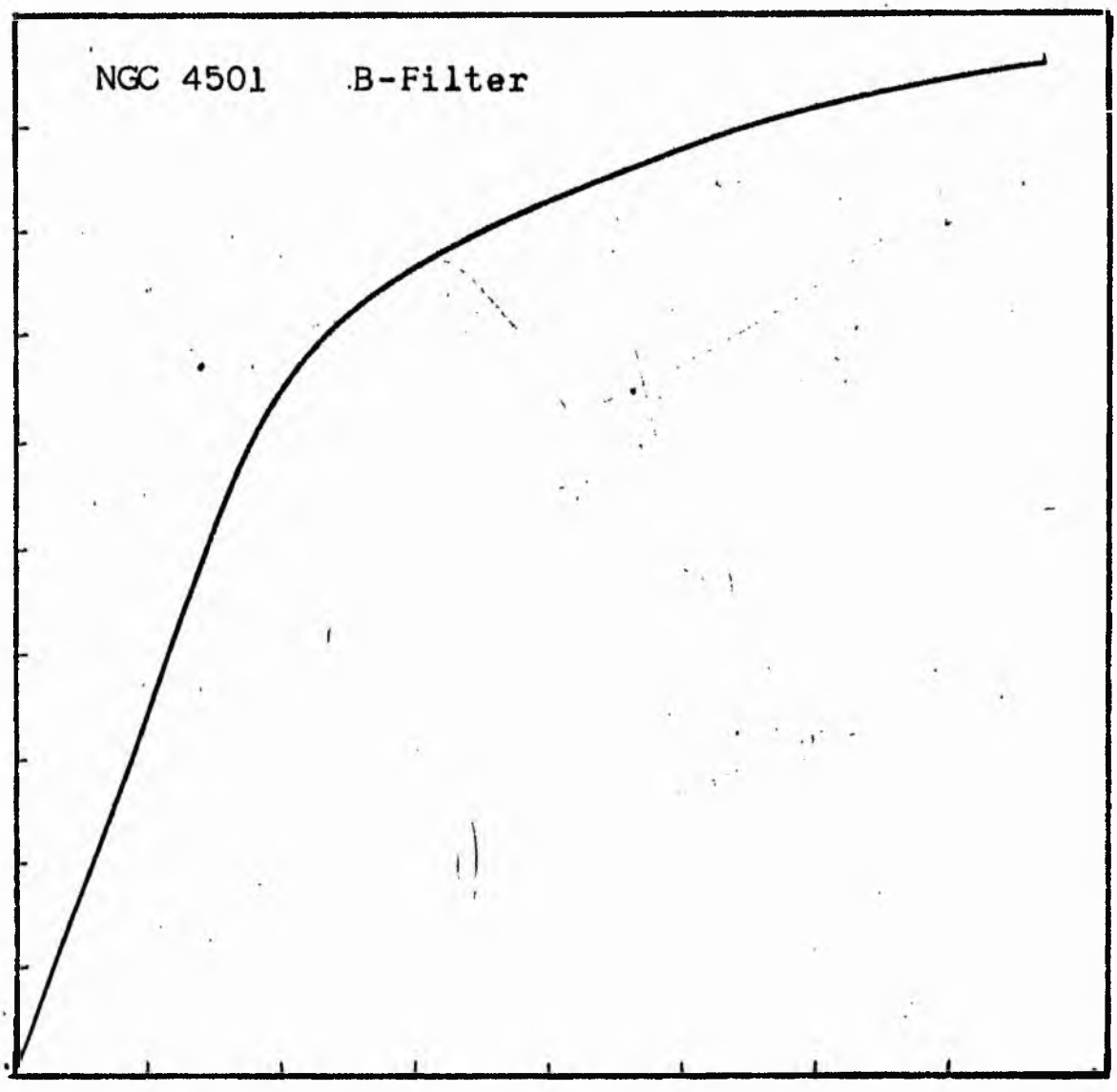

Relative integrated luminosity k(r) versus equivalent radius r*.

B COLOUR

LOG I	I	T	R	AREA	ΔA	P	Σ P	K(R)	ρ	LOG J	J
1.52	33.113		0.0	0.0			0.0	0.0	0.0	1.549	18.37
		32.360			24.45	791.5398					
1.50	31.623		2.79	24.45			791.54	0.01	0.04	1.529	18.42
		28.371			13.37	379.4055					
1.40	25.119		3.47	37.83			1170.95	0.02	0.05	1.429	18.67
		22.536			25.79	581.1880					
1.30	19.953		4.50	63.62			1752.13	0.03	0.07	1.329	18.92
		17.901			42.07	753.0098					
1.20	15.849		5.80	105.68			2505.14	0.04	0.09	1.229	19.17
		14.219			61.73	877.7737					
1.10	12.589		7.30	167.42			3382.92	0.05	0.11	1.129	19.42
		11.295			59.56	672.7576					
1.00	10.000		8.50	226.98			4055.67	0.06	0.13	1.029	19.67
		8.972			119.38	1071.0344					
0.90	7.943		10.50	346.36			5126.71	0.08	0.16	0.929	19.92
		7.126			13.32	94.9259					
0.80	6.310		10.70	359.68			5221.63	0.08	0.16	0.829	20.17
		5.661			319.19	1806.8162					
0.70	5.012		14.70	678.87			7028.45	0.11	0.22	0.729	20.42
		4.496			396.34	1782.1399					
0.60	3.981		18.50	1075.21			8810.58	0.13	0.27	0.629	20.67
		3.572			473.09	1686.7251					
0.50	3.162		22.20	1548.30			10500.30	0.16	0.33	0.529	20.92
		2.837			2799.16	7941.4023					
0.40	2.512		37.20	4347.46			18441.71	0.28	0.55	0.429	21.17
		2.254			1353.77	3050.8201					
0.30	1.995		42.60	5701.23			21492.52	0.33	0.63	0.329	21.42
		1.790			2027.59	3629.5256					
0.20	1.585		49.60	7728.82			25122.05	0.38	0.73	0.229	21.67
		1.422			1263.21	1796.1597					
0.10	1.259		53.50	8992.02			26918.26	0.41	0.79	0.129	21.92
		1.129			3900.07	4404.9648					
-0.00	1.000		64.06	12892.09			31323.17	0.48	0.95	0.029	22.17
		0.897			7511.76	6739.2578					
-0.10	0.794		80.59	20403.85			38062.43	0.58	1.14	-0.071	22.42
		0.713			3648.97	2600.4065					
-0.20	0.631		87.50	24052.82			40662.83	0.62	1.30	-0.171	22.67
		0.566			3824.53	2164.9543					
-0.30	0.501		94.20	27877.35			42827.79	0.65	1.39	-0.271	22.92
		0.450			2479.50	1114.8994					
-0.40	0.398		98.30	30356.86			43942.68	0.67	1.46	-0.371	23.17
		0.357			3426.85	1223.9570					
-0.50	0.316		103.70	33783.71			45166.64	0.69	1.54	-0.471	23.42
		0.284			3336.37	946.5537					
-0.60	0.251		108.70	37120.08			46113.19	0.70	1.61	-0.571	23.67
		0.225			4572.12	1030.3604					
-0.70	0.200		115.20	41692.20			47143.55	0.72	1.71	-0.671	23.92
		0.179			6426.11	1150.3218					
-0.80	0.158		123.76	48118.32			48293.87	0.74	1.83	-0.771	24.17
		0.142			8519.67	1211.4175					
-0.90	0.126		134.27	56637.98			49505.29	0.76	1.99	-0.871	24.42
		0.113			9596.33	1083.8689					
-1.00	0.100		145.20	66234.31			50589.15	0.77	2.15	-0.971	24.67
		0.090			24643.12	2210.8948					
-1.10	0.079		170.08	90877.44			52800.05	0.81	2.52	-1.071	24.92
		0.071			27969.75	1993.2485					
-1.20	0.063		194.50	118847.19			54793.29	0.84	2.88	-1.171	25.17
		0.057			37002.94	2094.6399					
-1.30	0.050		222.73	155850.12			56887.93	0.87	3.30	-1.271	25.42
		0.045			35970.50	1617.4102					
-1.40	0.040		247.10	191820.62			58505.34	0.89	3.66	-1.371	25.67
		0.036			39582.44	1413.7639					
-1.50	0.032		271.40	231403.06			59919.10	0.91	4.02	-1.471	25.92
		0.028			43106.94	1222.9883					
-1.60	0.025		295.60	274510.00			61142.09	0.93	4.38	-1.571	26.17
		0.023			40588.00	914.6890					
-1.70	0.020		316.70	315098.00			62056.78	0.95	4.69	-1.671	26.42
		0.018			24951.12	446.6489					
-1.80	0.016		329.00	340049.12			62503.43	0.95	4.87	-1.771	26.67
		0.014			56092.75	797.5969					
-1.90	0.013		355.10	396141.87			63301.02	0.97	5.26	-1.871	26.92
		0.011			46587.25	526.1921					
-2.00	0.010		375.40	442729.12			63827.21	0.97	5.56	-1.971	27.17
$-\infty$							65527.00	(1)			∞

PHOTOMETRIC PARAMETERS OF NGC 4501

B-FILTER

Total luminosity ..... L_T = 18.20

Total apparent magnitude ..... m_T = 10.13

Apparent central surface brightness ..... μ_o = 18.37

Major axis at threshold ..... $2a_m$ = 13.30

Minor axis at threshold ..... $2b_m$ = 11.40

Major axis at μ=25.0 mag sec^{-2} ..... 2a(25) = 7.55

Luminosity within μ=25.0 mag sec^{-2} ..... k(25) = 0.83

Gradient of exponential component ..... G(a) = -0.40

Equivalent gradient of exponential comp..... G(r*) = -0.35

Equivalent gradient of reduced exp. comp..... G(ρ) = -0.89

Parameters at k = ¼ :

- Semi-major axis ..... a_1 = 0.68
- Axis ratio ..... b/a = 0.56
- Equivalent radius ..... r_1* = 0.56
- Surface brightness ..... μ_1 = 21.12

Parameters at k = ½(effective) :

- Semi-major axis ..... a_e = 1.56
- Axis ratio ..... b/a = 0.46
- Equivalent radius ..... r_e* = 1.13
- Surface brightness ..... μ_e = 22.22
- Mean surface brightness ..... μ_e' = 12.39

Parameters at k = ¾ :

- Semi-major axis ..... a_3 = 2.91
- Axis ratio ..... b/a = 0.53
- Equivalent radius ..... r_3* = 2.18
- Surface brightness ..... μ_3 = 24.49

Concentration indices ..... C_{21} = 2.02, C_{32} = 1.94

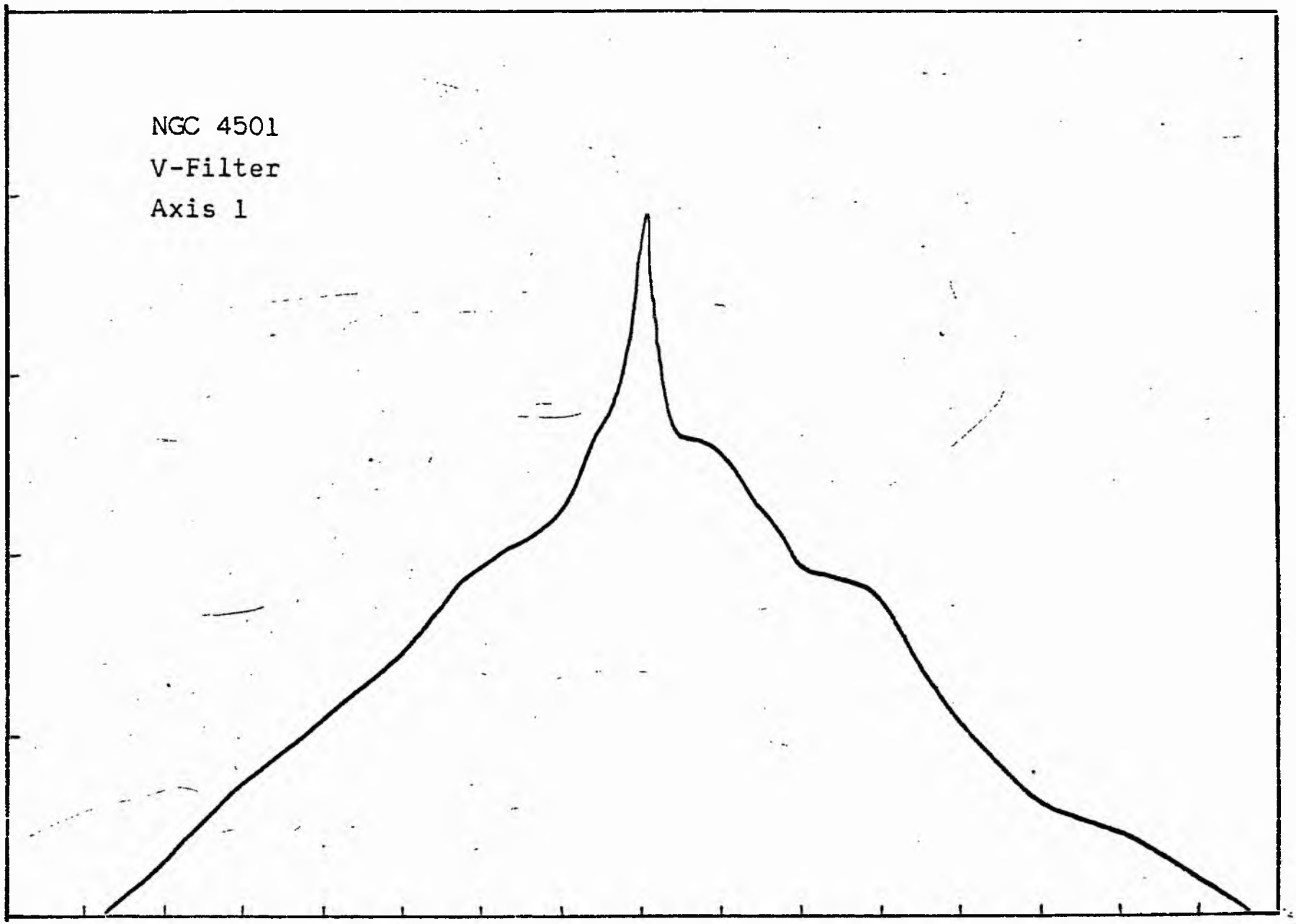
NGC 4501
V-Filter
Axis 1

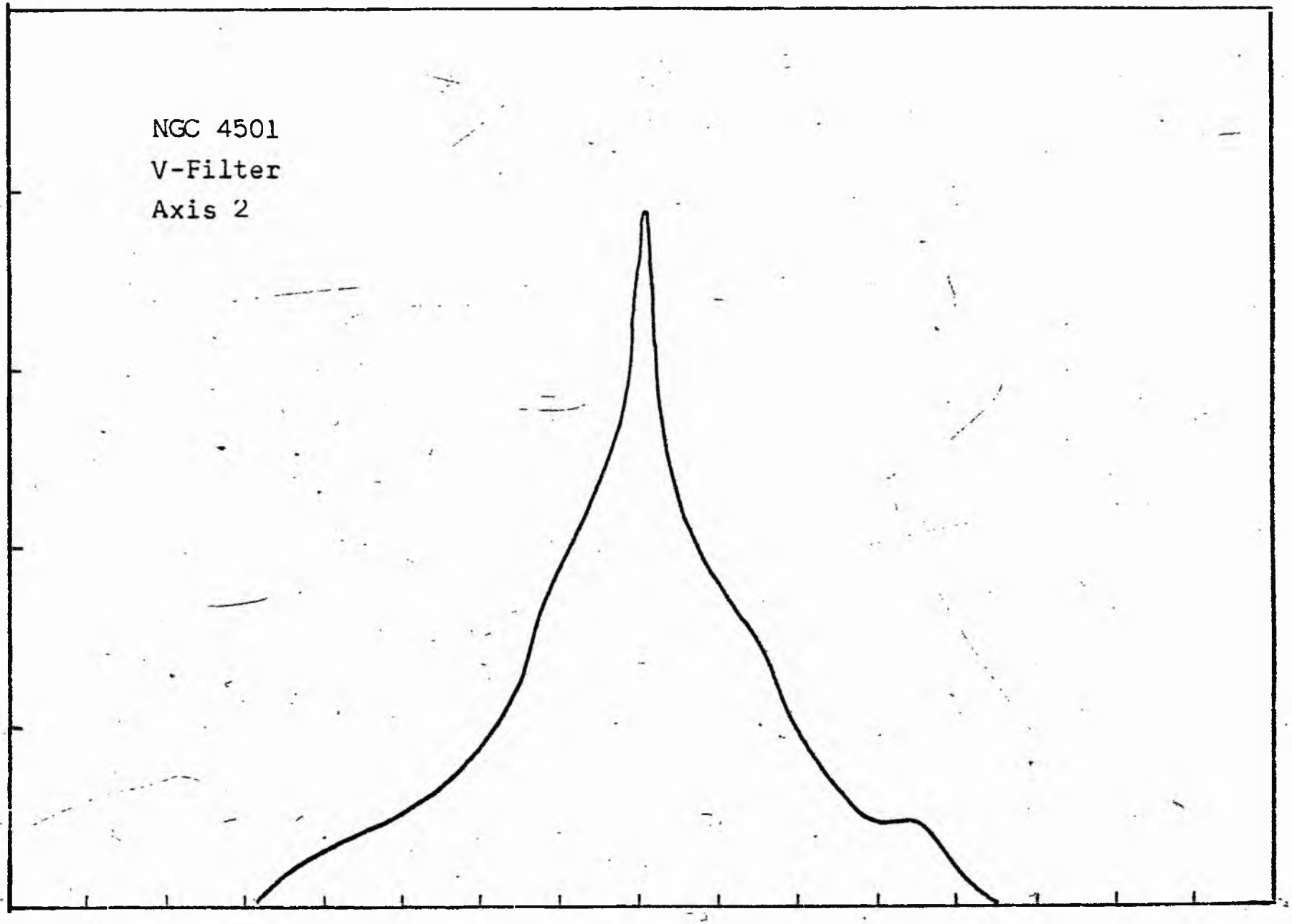
NGC 4501
V-Filter
Axis 2

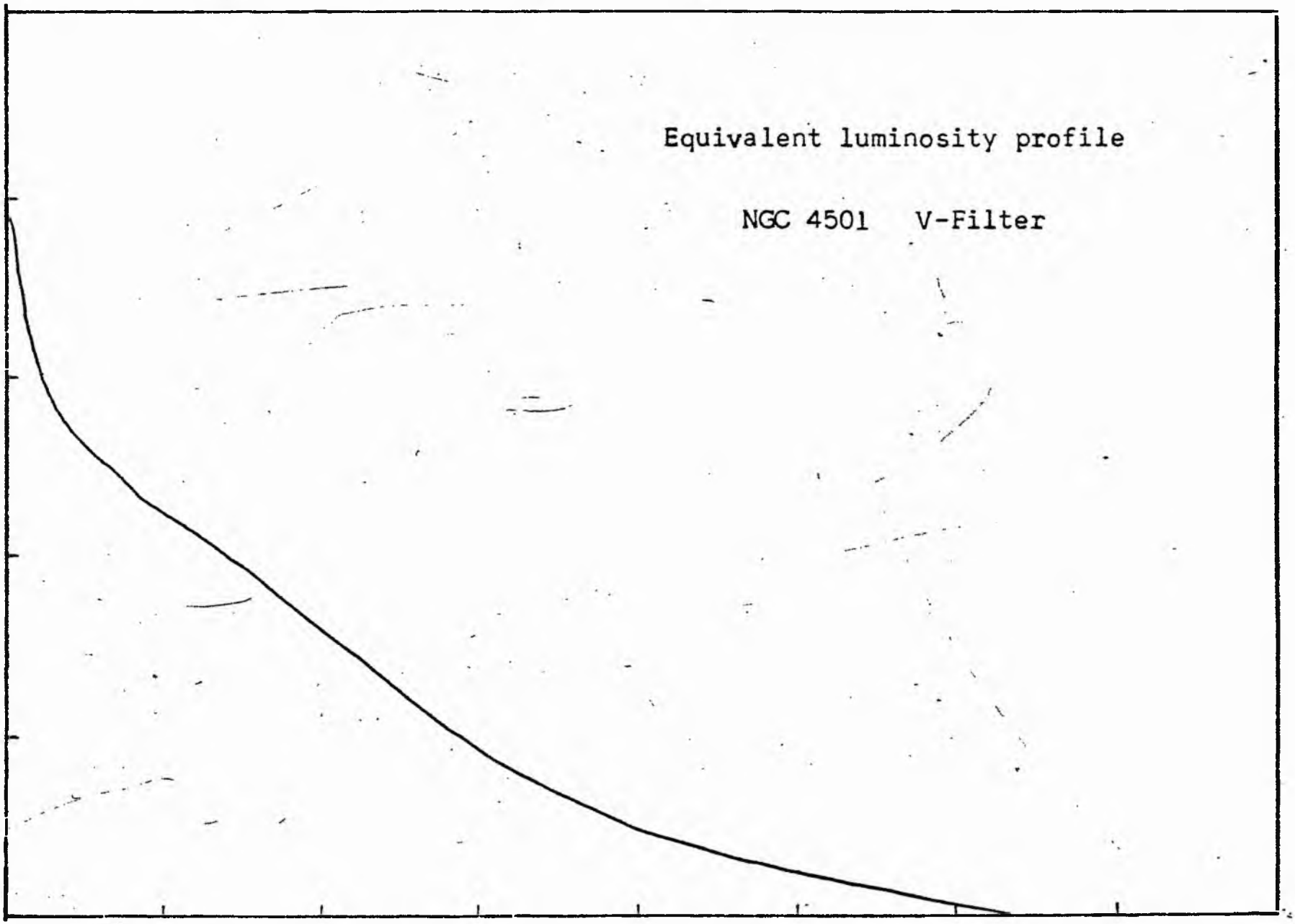
Equivalent luminosity profile
NGC 4501 V-Filter

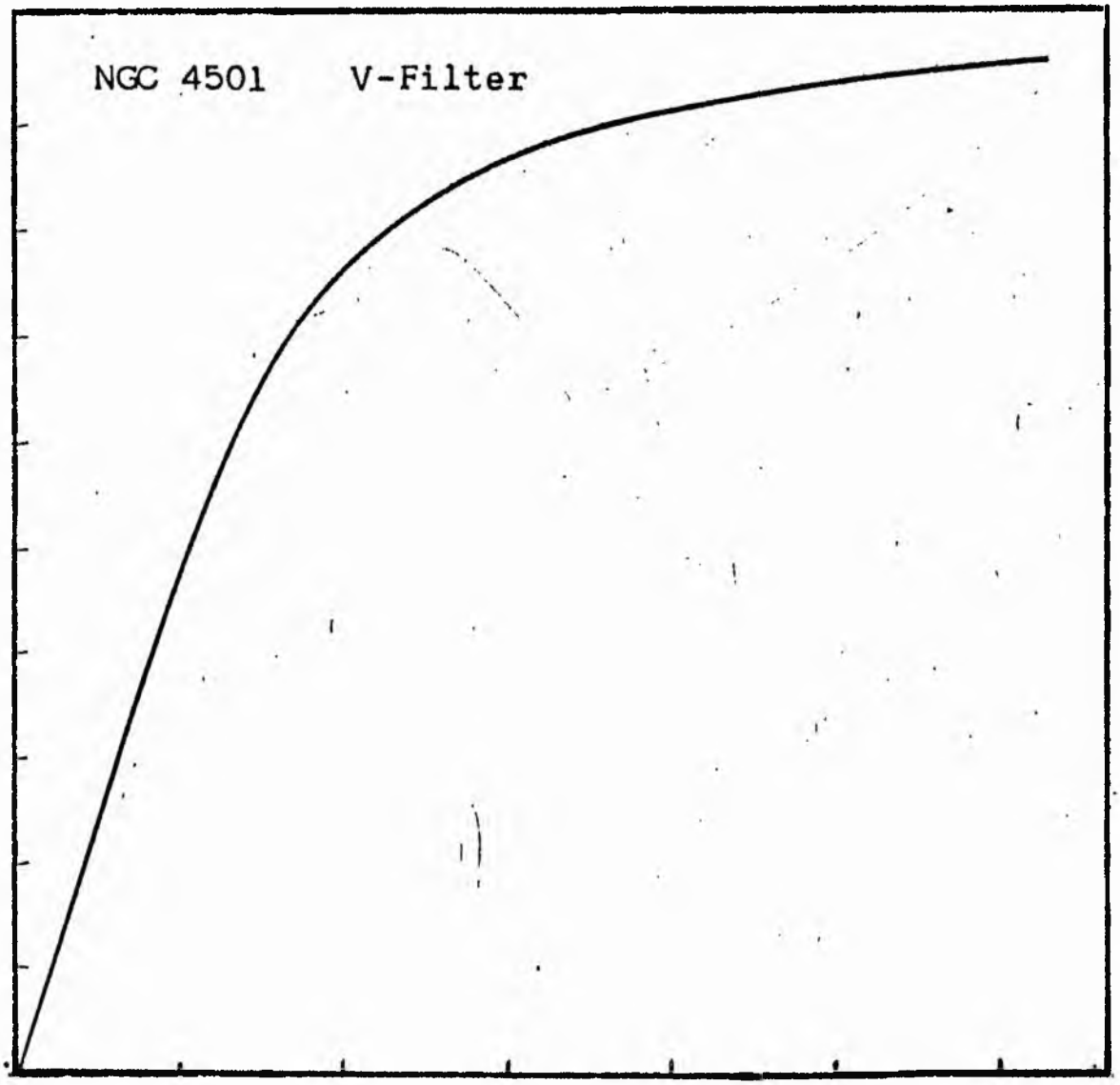

Relative integrated luminosity k(r) versus equivalent radius r*.

MEAN LUMINOSITY DISTRIBUTION IN NGC 4501
V COLOUR

LOG I	I	$\bar{I}$	R	AREA	ΔA	P	ΣP	K(R)	ρ	LOG J	μ
1.91	81.283		0.0	0.0			0.0	0.0	0.0	1.739	16.80
		80.358			1.13	90.8825					
1.90	79.433		0.60	1.13			90.88	0.00	0.01	1.729	16.83
		71.264			5.03	358.2124					
1.80	63.096		1.40	6.16			449.09	0.01	0.03	1.629	17.08
		56.607			7.70	435.6990					
1.70	50.119		2.10	13.85			884.79	0.01	0.04	1.529	17.33
		44.965			12.57	565.0410					
1.60	39.811		2.90	26.42			1449.83	0.02	0.05	1.429	17.58
		35.717			14.29	510.5420					
1.50	31.623		3.60	40.72			1960.38	0.03	0.07	1.329	17.83
		28.371			14.70	417.1230					
1.40	25.119		4.20	55.42			2377.50	0.04	0.08	1.229	18.08
		22.536			26.30	592.5759					
1.30	19.952		5.10	81.71			2970.08	0.05	0.09	1.129	18.33
		17.901			81.15	1452.5913					
1.20	15.849		7.20	162.86			4422.66	0.07	0.13	1.029	18.58
		14.219			48.38	687.9214					
1.10	12.589		8.20	211.24			5110.58	0.08	0.15	0.929	18.83
		11.295			122.05	1378.5061					
1.00	10.000		10.30	333.29			6489.09	0.11	0.19	0.829	19.08
		8.972			60.79	545.3794					
0.90	7.943		11.20	394.08			7034.46	0.12	0.21	0.729	19.33
		7.126			147.52	1051.2766					
0.80	6.310		13.13	541.60			8085.74	0.13	0.24	0.629	19.58
		5.661			396.47	2244.3059					
0.70	5.012		17.28	938.07			10330.04	0.17	0.32	0.529	19.83
		4.496			596.31	2681.2683					
0.60	3.981		22.10	1534.38			13011.31	0.22	0.41	0.429	20.08
		3.572			1368.95	4889.3984					
0.50	3.162		30.40	2903.33			17900.71	0.30	0.56	0.329	20.33
		2.837			771.20	2187.9385					
0.40	2.512		34.20	3674.53			20088.64	0.33	0.63	0.229	20.58
		2.254			672.93	1516.4768					
0.30	1.995		37.20	4347.46			21605.12	0.36	0.69	0.129	20.83
		1.790			4082.18	7307.3711					
0.20	1.585		51.80	8429.64			28912.49	0.48	0.96	0.029	21.08
		1.422			2358.46	3353.4873					
0.10	1.259		58.60	10788.10			32265.98	0.54	1.08	-0.071	21.33
		1.129			2362.88	2668.7644					
-0.00	1.000		64.70	13150.98			34934.74	0.58	1.20	-0.171	21.58
		0.897			2927.60	2626.5166					
-0.10	0.794		71.54	16078.57			37561.25	0.62	1.32	-0.271	21.83
		0.713			5200.33	3705.9507					
-0.20	0.631		82.30	21278.90			41267.20	0.69	1.52	-0.371	22.08
		0.566			3271.26	1851.7549					
-0.30	0.501		88.40	24550.16			43118.96	0.72	1.63	-0.471	22.33
		0.450			4222.08	1898.4343					
-0.40	0.398		95.70	28772.24			45017.39	0.75	1.77	-0.571	22.58
		0.357			2958.63	1056.7190					
-0.50	0.316		100.50	31730.87			46074.11	0.77	1.86	-0.671	22.83
		0.284			4331.40	1228.8455					
-0.60	0.251		107.14	36062.27			47302.95	0.79	1.98	-0.771	23.08
		0.225			5153.56	1161.3862					
-0.70	0.200		114.54	41215.83			48464.34	0.81	2.12	-0.871	23.33
		0.179			6089.45	1090.0520					
-0.80	0.158		122.71	47305.28			49554.39	0.82	2.27	-0.971	23.58
		0.142			7160.48	1018.1484					
-0.90	0.126		131.67	54465.76			50572.54	0.84	2.43	-1.071	23.83
		0.113			8293.82	936.7510					
-1.00	0.100		141.34	62759.58			51509.29	0.86	2.61	-1.171	24.08
		0.090			5589.67	501.4834					
-1.10	0.079		147.50	68349.25			52010.77	0.86	2.72	-1.271	24.33
		0.071			6447.31	459.4617					
-1.20	0.063		154.30	74796.56			52470.23	0.87	2.85	-1.371	24.58
		0.057			11981.87	678.2598					
-1.30	0.050		166.20	86778.44			53148.48	0.88	3.07	-1.471	24.83
		0.045			14444.44	649.4902					
-1.40	0.040		179.50	101222.87			53797.97	0.89	3.32	-1.571	25.08
		0.036			16283.81	581.6055					
-1.50	0.032		193.40	117506.69			54379.58	0.90	3.57	-1.671	25.33
		0.028			28118.94	797.7593					
-1.60	0.025		215.30	145625.62			55177.34	0.92	3.98	-1.771	25.58
		0.023			40952.56	922.9001					
-1.70	0.020		243.70	186578.19			56100.23	0.93	4.50	-1.871	25.83
		0.018			22700.56	406.3599					
-1.80	0.016		258.10	209278.75			56506.59	0.94	4.77	-1.971	26.08
		0.014			36318.56	516.4207					
-1.90	0.013		279.60	245597.31			57023.01	0.95	5.17	-2.071	26.33
		0.011			44926.75	507.4351					
-2.00	0.010		304.10	290524.06			57530.45	0.96	5.62	-2.171	26.58
- ∞							60130.00	(1)			∞

PHOTOMETRIC PARAMETERS OF NGC 4501

V-FILTER

Total luminosity	L_T	= 16.70
Total apparent magnitude	m_T	= 9.63
Apparent central surface brightness	μ_o	= 16.80
Major axis at threshold	$2a_m$	= 12.38
Minor axis at threshold	$2b_m$	= 8.26
Major axis at μ=25.0 mag sec^{-2}	2a(25)	= 8.37
Luminosity within μ=25.0 mag sec^{-2}	k(25)	= 0.88
Gradient of exponential component	G(a)	= -0.48
Equivalent gradient of exponential comp.	G(r*)	= -0.64
Equivalent gradient of reduced exp. comp.	G(ρ)	= -0.76
Parameters at k = ¼ :		
Semi-major axis	a_1	= 0.53
Axis ratio	b/a	= 0.31
Equivalent radius	r_1*	= 0.43
Surface brightness	μ_1	= 20.18
Parameters at k = ½(effective) :		
Semi-major axis	a_e	= 1.21
Axis ratio	b/a	= 0.26
Equivalent radius	r_e*	= 0.90
Surface brightness	μ_e	= 21.16
Mean surface brightness	μ_e'	= 11.38
Parameters at k = ¾ :		
Semi-major axis	a_3	= 2.47
Axis ratio	b/a	= 0.46
Equivalent radius	r_3*	= 1.60
Surface brightness	μ_3	= 22.58
Concentration indices	C_{21}	= 2.11
	C_{32}	= 1.77

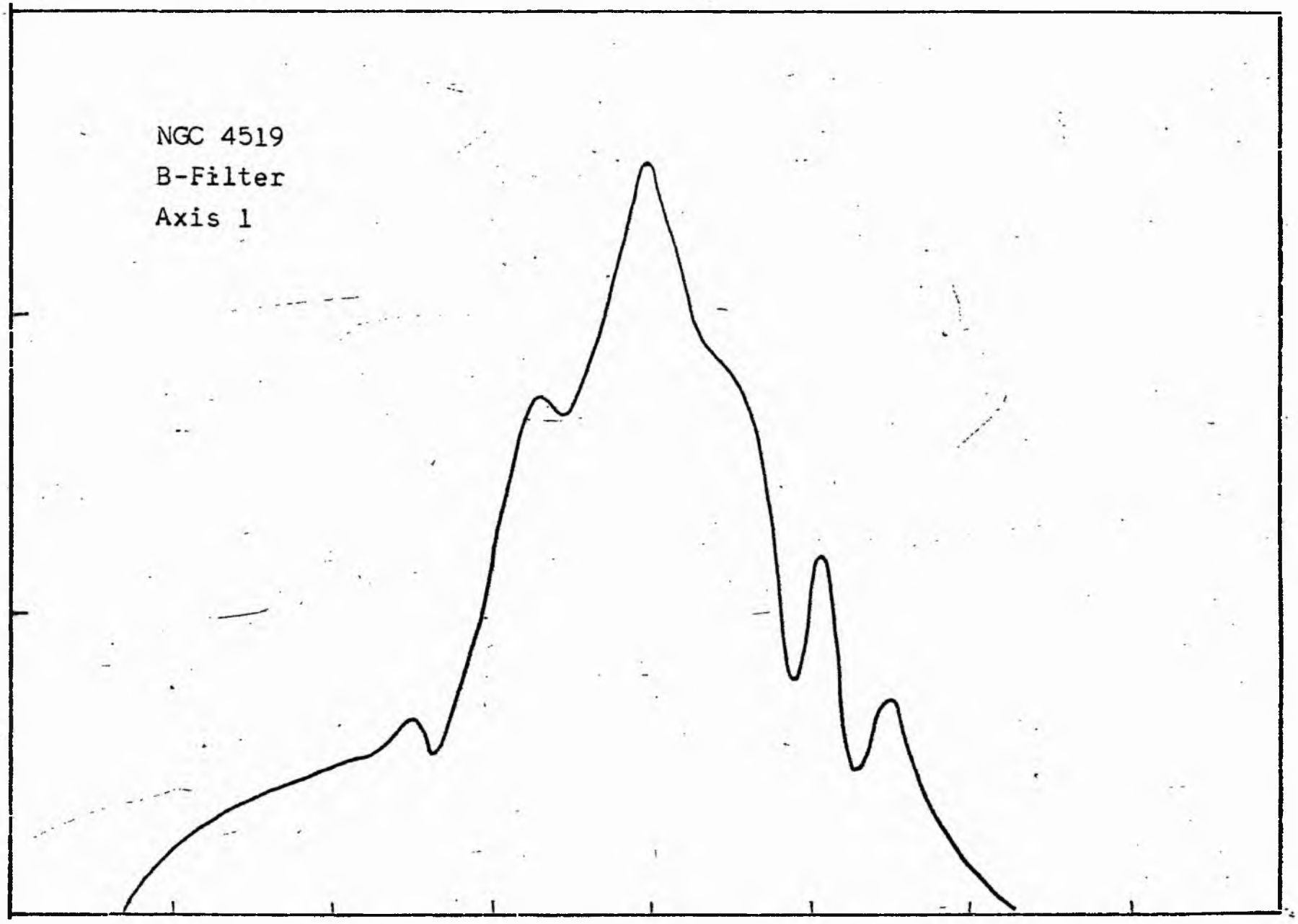
NGC 4519
B-Filter
Axis 1

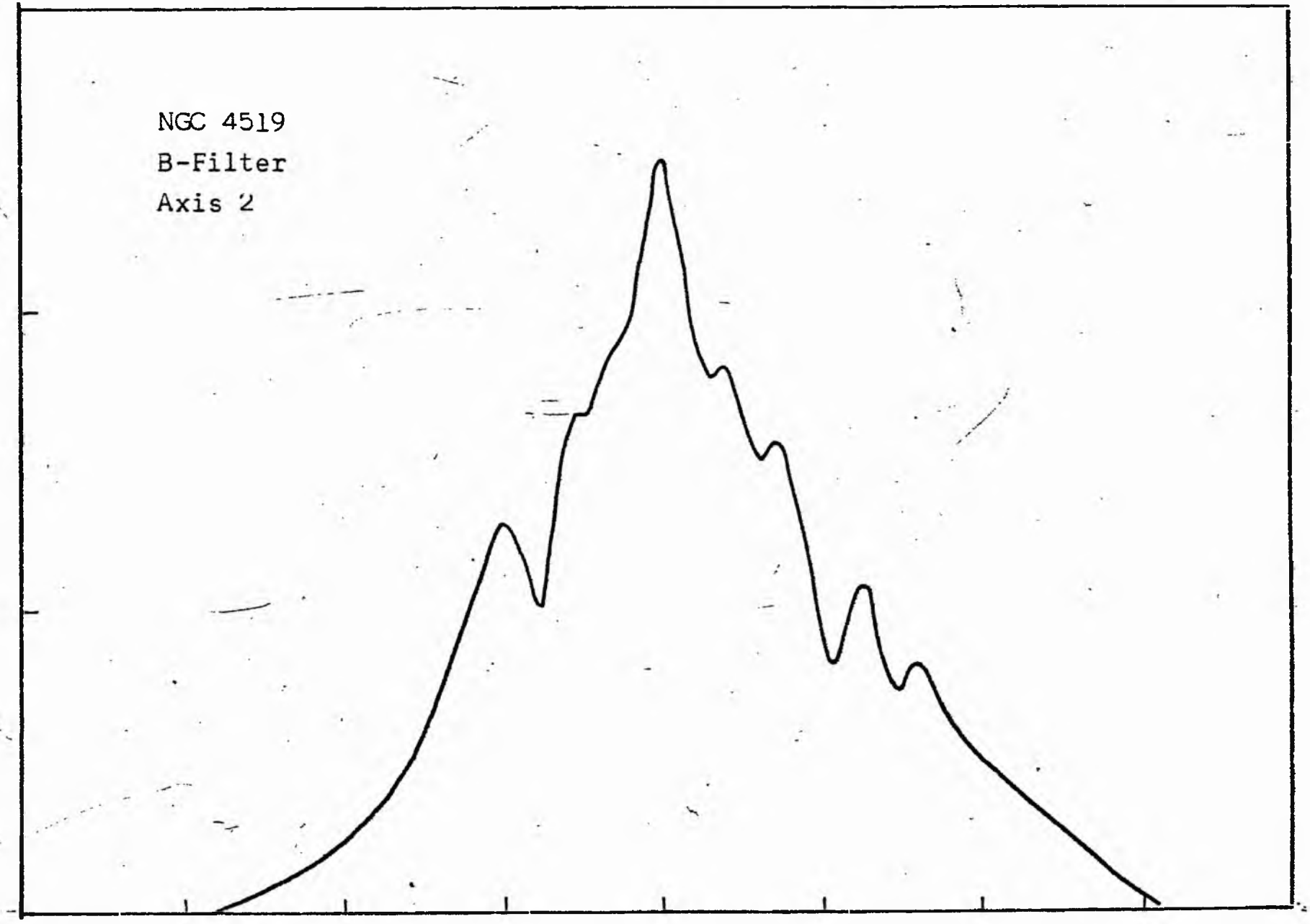
NGC 4519
B-Filter
Axis 2

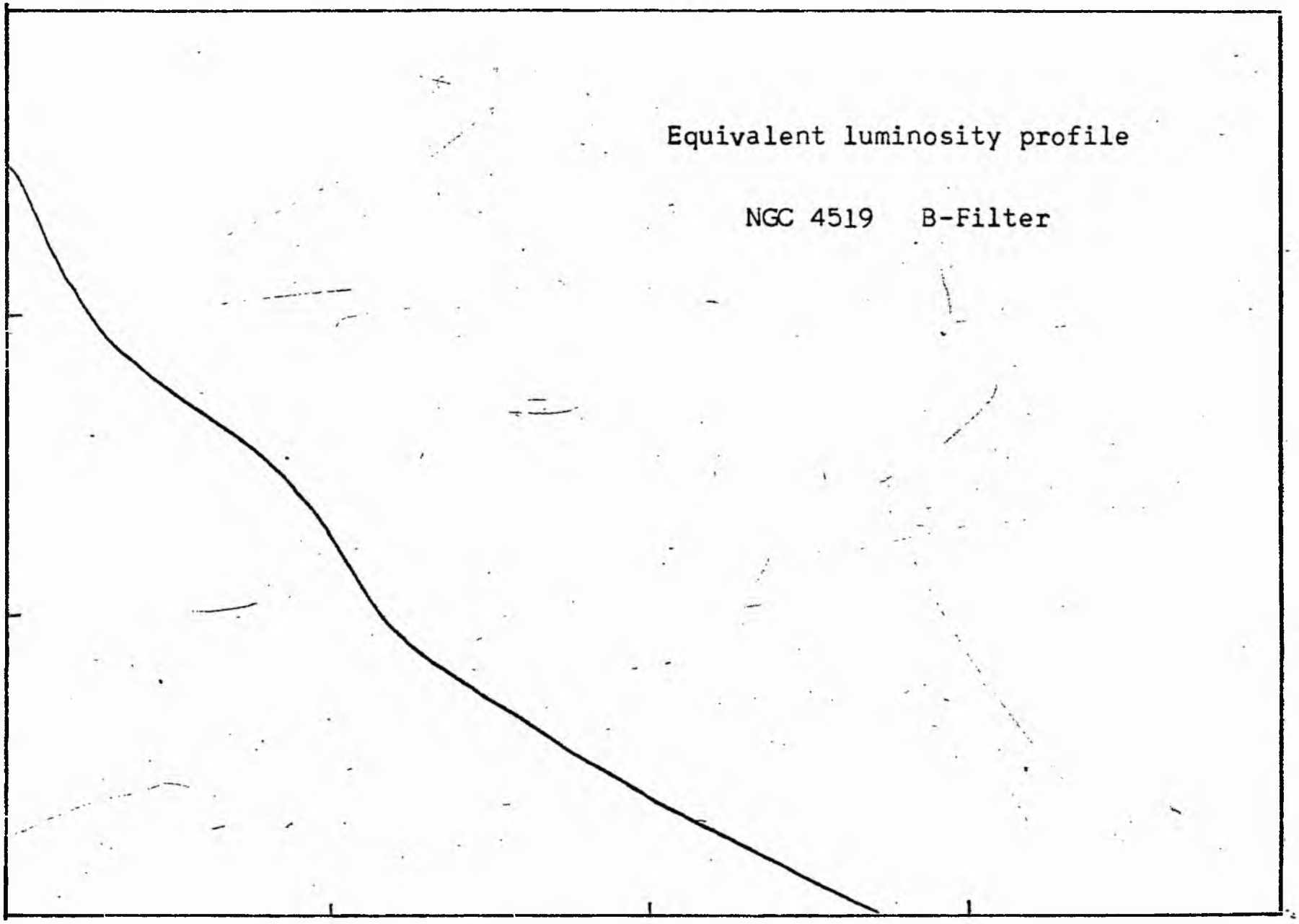
Equivalent luminosity profile
NGC 4519 B-Filter

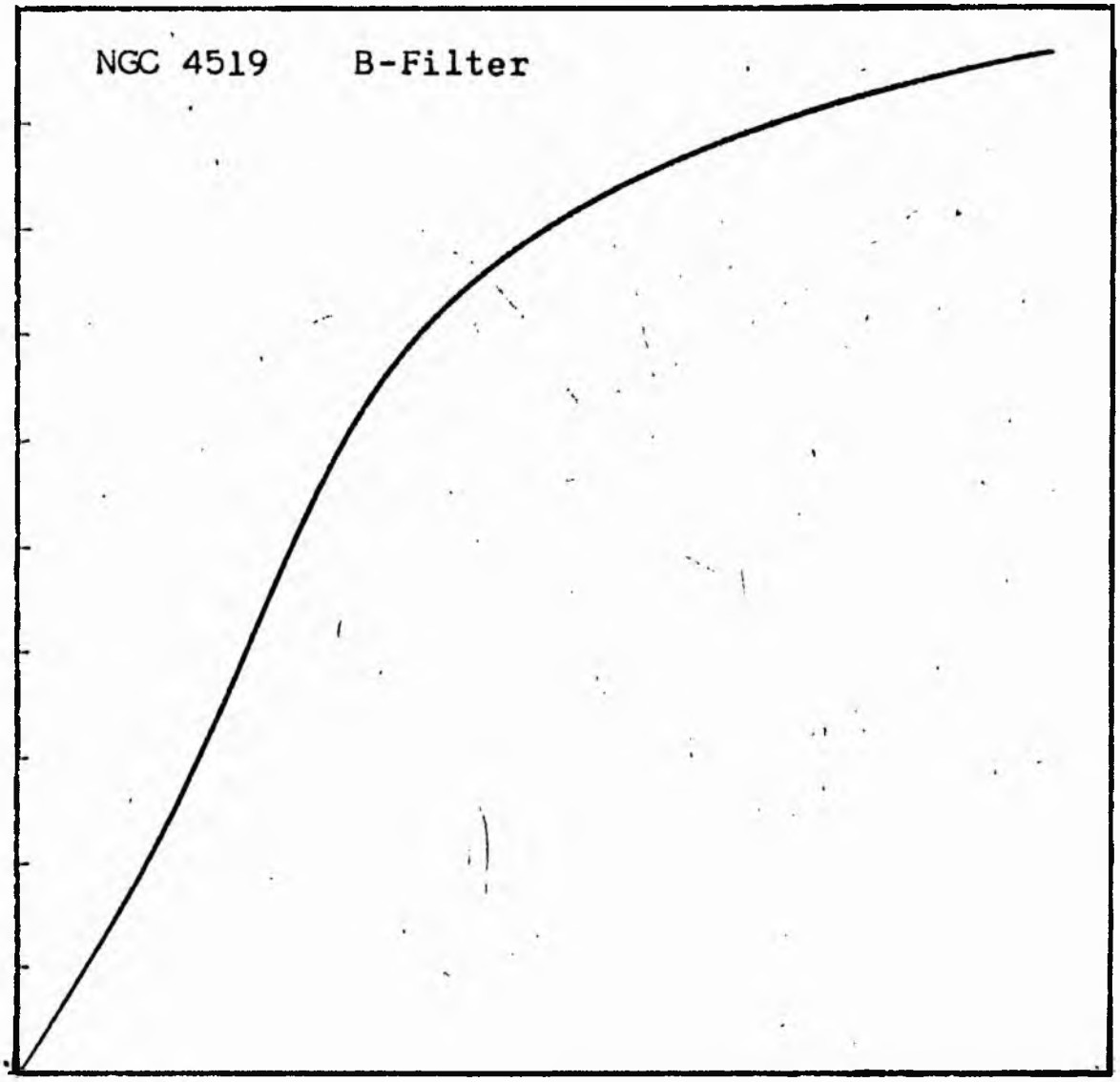

Relative integrated luminosity k(r) versus equivalent radius r*.

MEAN LUMINOSITY DISTRIBUTION IN NGC 4919
B COLOUR

LOG I	I	$\bar{I}$	R	AREA	ΔA	P	ΣP	K(R)	Q	LOG J	M
0.46	2.884		0.0	0.0			0.0	0.0	0.0	0.919	20.53
		2.698			45.13	121.7484					
0.40	2.512		3.79	45.13			121.75	0.02	0.10	0.859	20.68
		2.254			51.29	115.5956					
0.30	1.995		5.54	96.42			237.34	0.04	0.14	0.759	20.93
		1.790			66.44	118.9322					
0.20	1.585		7.20	162.86			356.28	0.06	0.19	0.659	21.18
		1.422			91.04	129.4558					
0.10	1.259		8.99	253.90			485.73	0.08	0.24	0.559	21.43
		1.129			146.54	165.5073					
0.00	1.000		11.29	400.44			651.24	0.11	0.30	0.459	21.68
		0.897			337.86	303.1174					
-0.10	0.794		15.33	738.30			954.36	0.16	0.40	0.359	21.93
		0.713			581.95	414.7239					
-0.20	0.631		20.50	1320.25			1369.08	0.23	0.54	0.259	22.18
		0.566			1185.16	670.8840					
-0.30	0.501		28.24	2505.41			2039.96	0.35	0.74	0.159	22.43
		0.450			1270.81	571.4167					
-0.40	0.398		34.67	3776.22			2611.38	0.45	0.91	0.059	22.68
		0.357			1394.60	498.1055					
-0.50	0.316		40.57	5170.82			3109.49	0.53	1.06	-0.041	22.93
		0.284			1447.91	410.7854					
-0.60	0.251		45.90	6618.73			3520.27	0.60	1.20	-0.141	23.18
		0.225			1166.28	262.8303					
-0.70	0.200		49.78	7785.02			3783.10	0.65	1.30	-0.241	23.43
		0.179			821.30	147.0187					
-0.80	0.158		52.34	8606.31			3930.12	0.67	1.37	-0.341	23.68
		0.142			1004.43	142.8215					
-0.90	0.126		55.31	9610.75			4072.94	0.70	1.45	-0.441	23.93
		0.113			1067.18	120.5337					
-1.00	0.100		58.30	10677.92			4193.47	0.72	1.53	-0.541	24.18
		0.090			2021.70	181.3799					
-1.10	0.079		63.58	12699.62			4374.85	0.75	1.66	-0.641	24.43
		0.071			2479.41	176.6941					
-1.20	0.063		69.51	15179.04			4551.54	0.78	1.82	-0.741	24.68
		0.057			3009.80	170.3772					
-1.30	0.050		76.09	18188.84			4721.92	0.81	1.99	-0.841	24.93
		0.045			3626.01	163.0433					
-1.40	0.040		83.33	21814.85			4884.96	0.84	2.18	-0.941	25.18
		0.036			4631.27	165.4150					
-1.50	0.032		91.75	26446.12			5050.37	0.87	2.40	-1.041	25.43
		0.028			4831.72	137.0808					
-1.60	0.025		99.78	31277.84			5187.45	0.89	2.61	-1.141	25.68
		0.023			5345.32	120.4619					
-1.70	0.020		107.97	36623.17			5307.91	0.91	2.82	-1.241	25.93
		0.018			5898.27	105.5846					
-1.80	0.016		116.34	42521.43			5413.50	0.93	3.04	-1.341	26.18
		0.014			6471.74	92.0233					
-1.90	0.013		124.88	48993.18			5505.52	0.94	3.27	-1.441	26.43
		0.011			8857.65	100.0451					
-2.00	0.010		135.70	57850.82			5605.56	0.96	3.55	-1.541	26.68
$-\infty$							5835.00	(1)			∞

PHOTOMETRIC PARAMETERS OF NGC 4519

B-FILTER

Total luminosity	L_T	= 1.62
Total apparent magnitude	m_T	= 12.26
Apparent central surface brightness	μ_o	= 20.53
Major axis at threshold	$2a_m$	= 4.35
Minor axis at threshold	$2b_m$	= 4.26
Major axis at μ=25.0 mag sec^{-2}	2a(25)	= 2.47
Luminosity within μ=25.0 mag sec^{-2}	k(25)	= 0.82
Gradient of exponential component	G(a)	= -1.21
Equivalent gradient of exponential comp.	G(r*)	= -0.96
Equivalent gradient of reduced exp. comp.	G(ρ)	= -0.81
Parameters at k = ¼ :		
Semi-major axis	a_1	= 0.35
Axis ratio	b/a	= 0.41
Equivalent radius	r_1*	= 0.36
Surface brightness	μ_1	= 22.22
Parameters at k = ½(effective) :		
Semi-major axis	a_e	= 0.65
Axis ratio	b/a	= 0.82
Equivalent radius	r_e*	= 0.64
Surface brightness	μ_e	= 22.83
Mean surface brightness	μ_e'	= 13.26
Parameters at k = ¾ :		
Semi-major axis	a_3	= 0.95
Axis ratio	b/a	= 1.12
Equivalent radius	r_3*	= 1.06
Surface brightness	μ_3	= 24.43
Concentration indices	C_{21}	= 1.77
	C_{32}	= 1.66

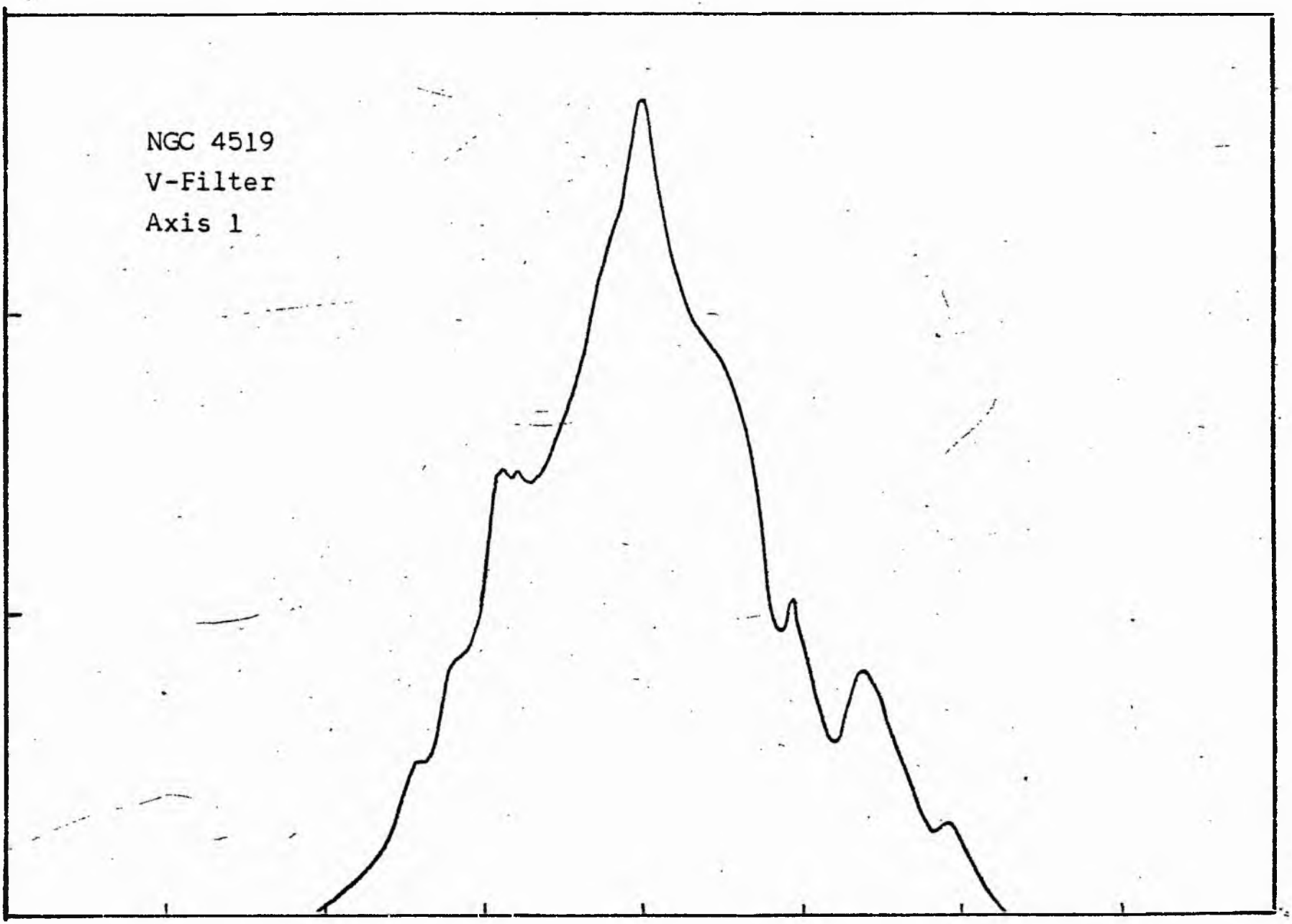
NGC 4519
V-Filter
Axis 1

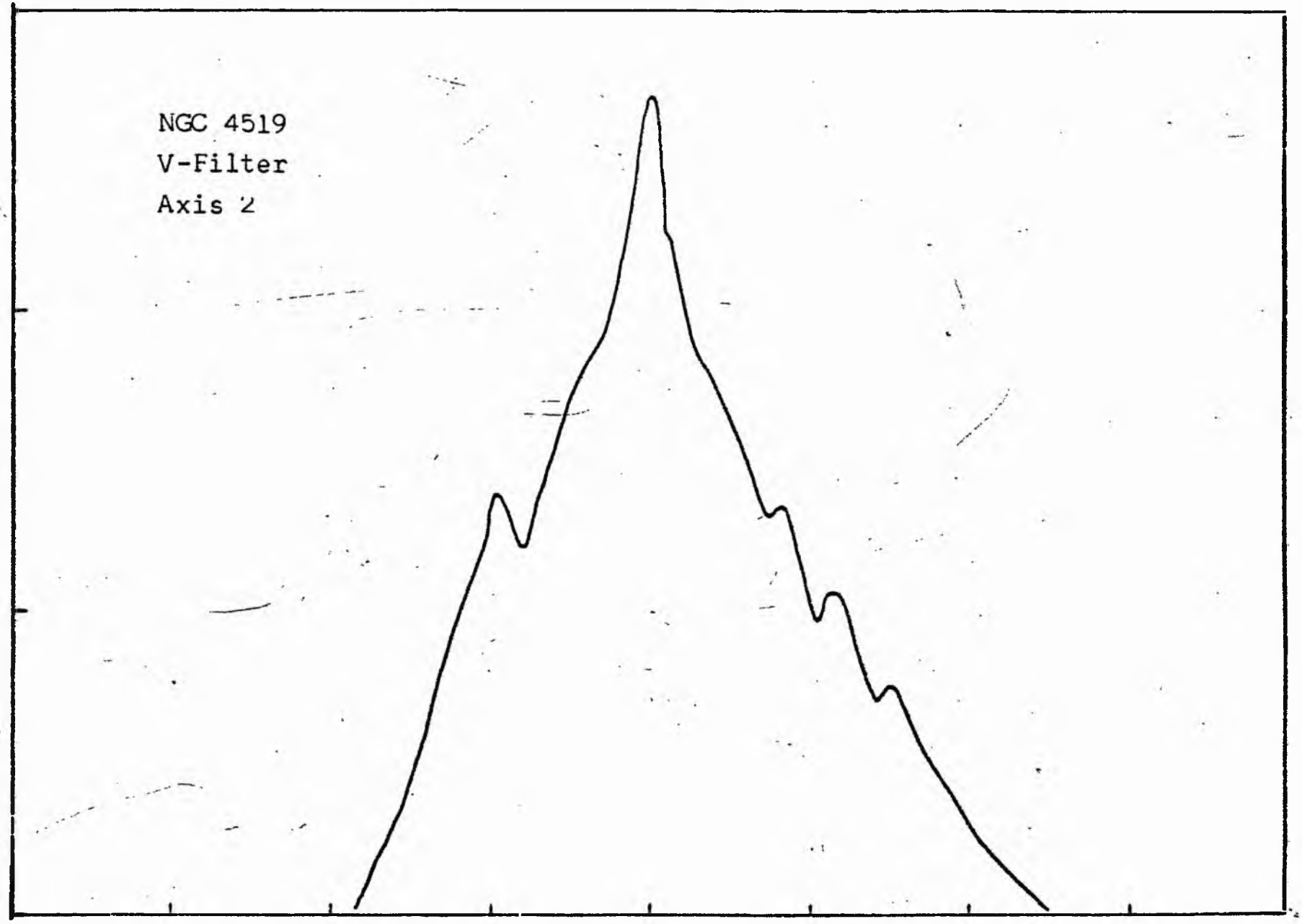
NGC 4519
V-Filter
Axis 2

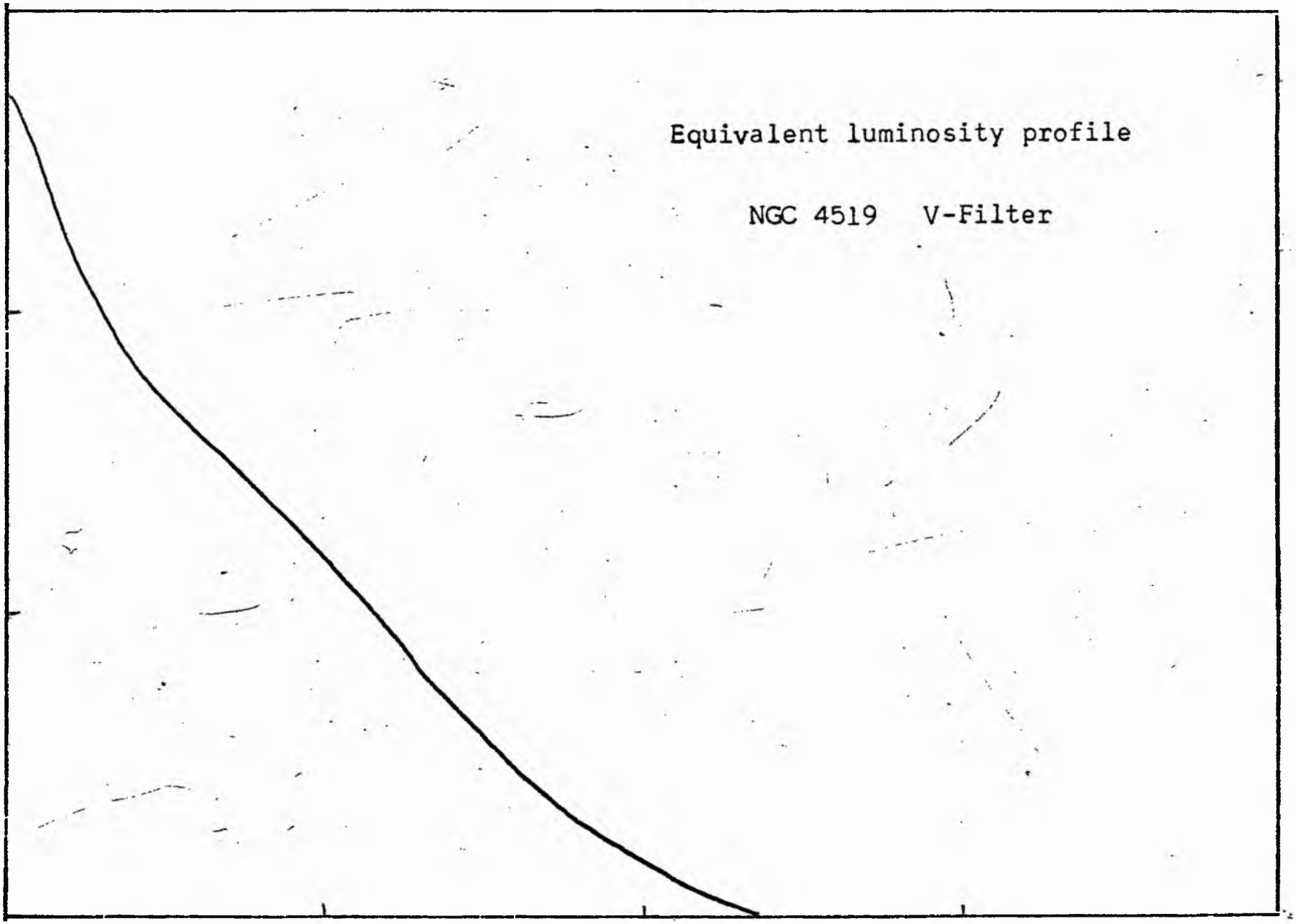
Equivalent luminosity profile
NGC 4519 V-Filter

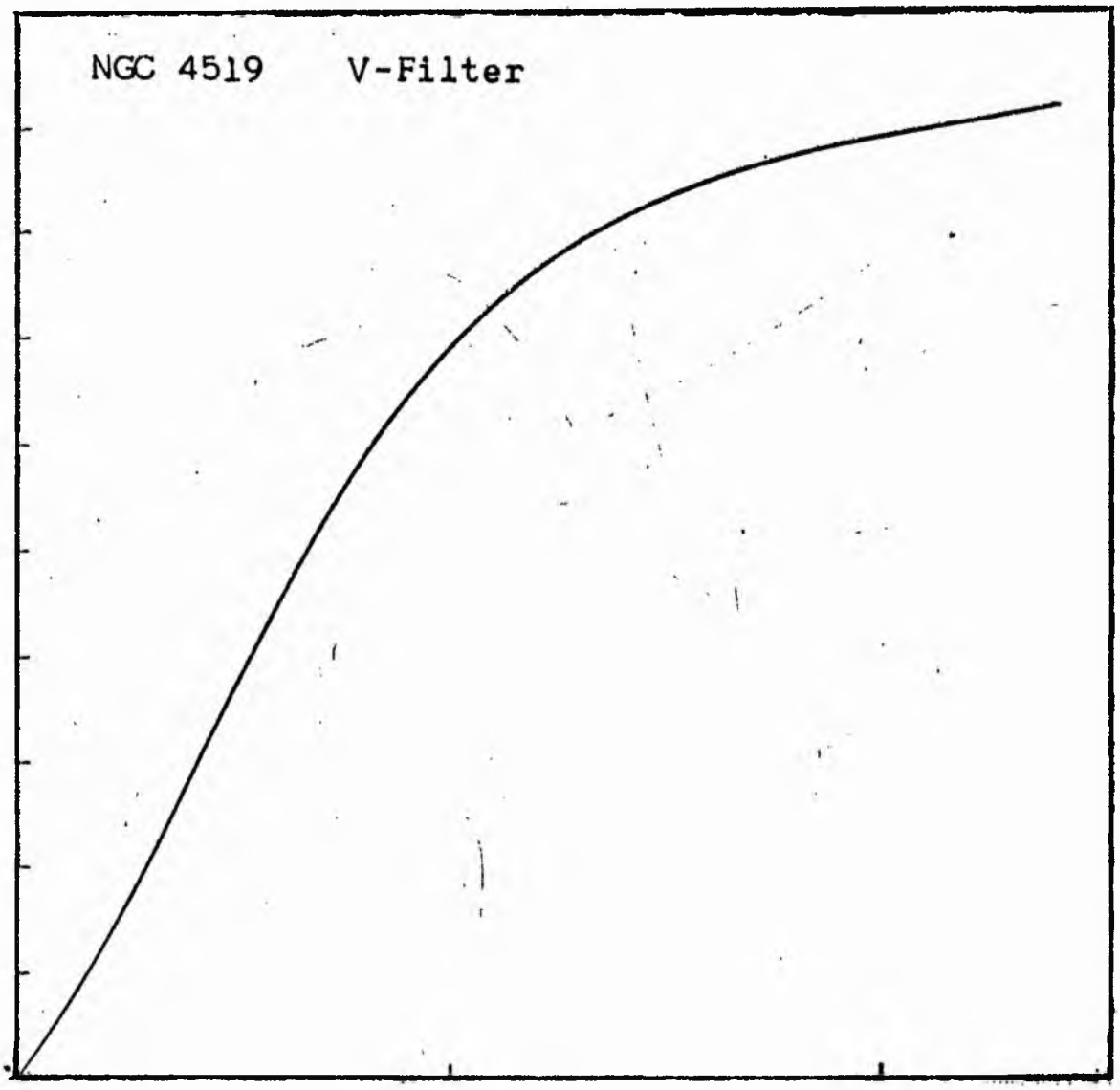

Relative integrated luminosity k(r) versus equivalent radius r*.

MEAN LUMINOSITY DISTRIBUTION IN NGC 4519
V COLOUR

LOG I	I	$\bar{I}$	R	AREA	ΔA	P	ΣP	K(R)	ρ	LOG J	μ
0.69	4.898		0.0	0.0			0.0	0.0	0.0	1.123	19.35
		4.439			32.17	142.8159					
0.60	3.981		3.20	32.17			142.82	0.03	0.10	1.033	19.58
		3.572			27.28	97.4240					
0.50	3.162		4.35	59.45			240.24	0.04	0.13	0.933	19.83
		2.837			59.76	169.5520					
0.40	2.512		6.16	119.21			409.79	0.07	0.18	0.833	20.08
		2.254			62.73	141.3591					
0.30	1.995		7.61	181.94			551.15	0.10	0.23	0.733	20.33
		1.790			77.08	137.9733					
0.20	1.585		9.08	259.01			689.12	0.12	0.27	0.633	20.58
		1.422			97.31	138.3720					
0.10	1.259		10.65	356.33			827.50	0.15	0.32	0.533	20.83
		1.129			278.93	315.0398					
0.00	1.000		14.22	635.26			1142.54	0.20	0.43	0.433	21.08
		0.897			388.28	348.3513					
-0.10	0.794		18.05	1023.54			1490.89	0.27	0.54	0.333	21.33
		0.713			524.76	373.9700					
-0.20	0.631		22.20	1548.30			1864.86	0.33	0.67	0.233	21.58
		0.566			777.68	440.2241					
-0.30	0.501		27.21	2325.98			2305.08	0.41	0.82	0.133	21.83
		0.450			850.92	382.6128					
-0.40	0.398		31.80	3176.90			2687.69	0.48	0.95	0.033	22.08
		0.357			987.86	352.8333					
-0.50	0.316		36.41	4164.77			3040.53	0.54	1.09	-0.067	22.33
		0.284			1118.82	317.4199					
-0.60	0.251		41.01	5283.59			3357.95	0.60	1.23	-0.167	22.58
		0.225			1254.64	282.7429					
-0.70	0.200		45.62	6538.23			3640.69	0.65	1.37	-0.267	22.83
		0.179			1391.32	249.0583					
-0.80	0.158		50.24	7929.55			3889.75	0.69	1.51	-0.367	23.08
		0.142			1521.99	216.4138					
-0.90	0.126		54.85	9451.55			4106.16	0.73	1.65	-0.467	23.33
		0.113			1248.36	140.9982					
-1.00	0.100		58.36	10699.91			4247.16	0.76	1.75	-0.567	23.58
		0.090			1407.55	126.2806					
-1.10	0.079		62.08	12107.46			4373.43	0.78	1.86	-0.667	23.83
		0.071			1585.60	112.9970					
-1.20	0.063		66.02	13693.06			4486.43	0.80	1.98	-0.767	24.08
		0.057			1788.83	101.2609					
-1.30	0.050		70.20	15481.89			4587.69	0.82	2.11	-0.867	24.33
		0.045			2001.56	90.0001					
-1.40	0.040		74.60	17483.45			4677.69	0.83	2.24	-0.967	24.58
		0.036			2242.52	80.0959					
-1.50	0.032		79.24	19725.97			4757.78	0.85	2.38	-1.067	24.83
		0.028			2493.90	70.7545					
-1.60	0.025		84.10	22219.87			4828.54	0.86	2.52	-1.167	25.08
		0.023			5303.49	119.5191					
-1.70	0.020		93.60	27523.36			4948.05	0.88	2.81	-1.267	25.33
		0.018			3616.71	64.7426					
-1.80	0.016		99.56	31140.07			5012.79	0.89	2.99	-1.367	25.58
		0.014			5980.01	85.0312					
-1.90	0.013		108.70	37120.08			5097.82	0.91	3.26	-1.467	25.83
		0.011			3279.42	37.0403					
-2.00	0.010		113.40	40399.50			5134.86	0.91	3.40	-1.567	26.08
- ∞							5614.00	(1)			∞

PHOTOMETRIC PARAMETERS OF NGC 4519

V-FILTER

Total luminosity ..... L_T = 1.56

Total apparent magnitude ..... m_T = 11.71

Apparent central surface brightness ..... μ_o = 19.35

Major axis at threshold ..... $2a_m$ = 3.71

Minor axis at threshold ..... $2b_m$ = 3.64

Major axis at μ=25.0 mag sec^{-2} ..... 2a(25) = 2.66

Luminosity within μ=25.0 mag sec^{-2} ..... k(25) = 0.85

Gradient of exponential component ..... G(a) = -1.06

Equivalent gradient of exponential comp..... G(r*) = -1.17

Equivalent gradient of reduced exp. comp..... G(ρ) = -0.76

Parameters at k = ¼ :

- Semi-major axis ..... a_1 = 0.33
- Axis ratio ..... b/a = 0.65
- Equivalent radius ..... r_1* = 0.28
- Surface brightness ..... μ_1 = 21.15

Parameters at k = ½(effective) :

- Semi-major axis ..... a_e = 0.53
- Axis ratio ..... b/a = 0.91
- Equivalent radius ..... r_e* = 0.56
- Surface brightness ..... μ_e = 22.16
- Mean surface brightness ..... μ_e' = 12.41

Parameters at k = ¾ :

- Semi-major axis ..... a_3 = 0.78
- Axis ratio ..... b/a = 1.19
- Equivalent radius ..... r_3* = 0.96
- Surface brightness ..... μ_3 = 23.50

Concentration indices ..... C_{21} = 1.95, C_{32} = 1.72

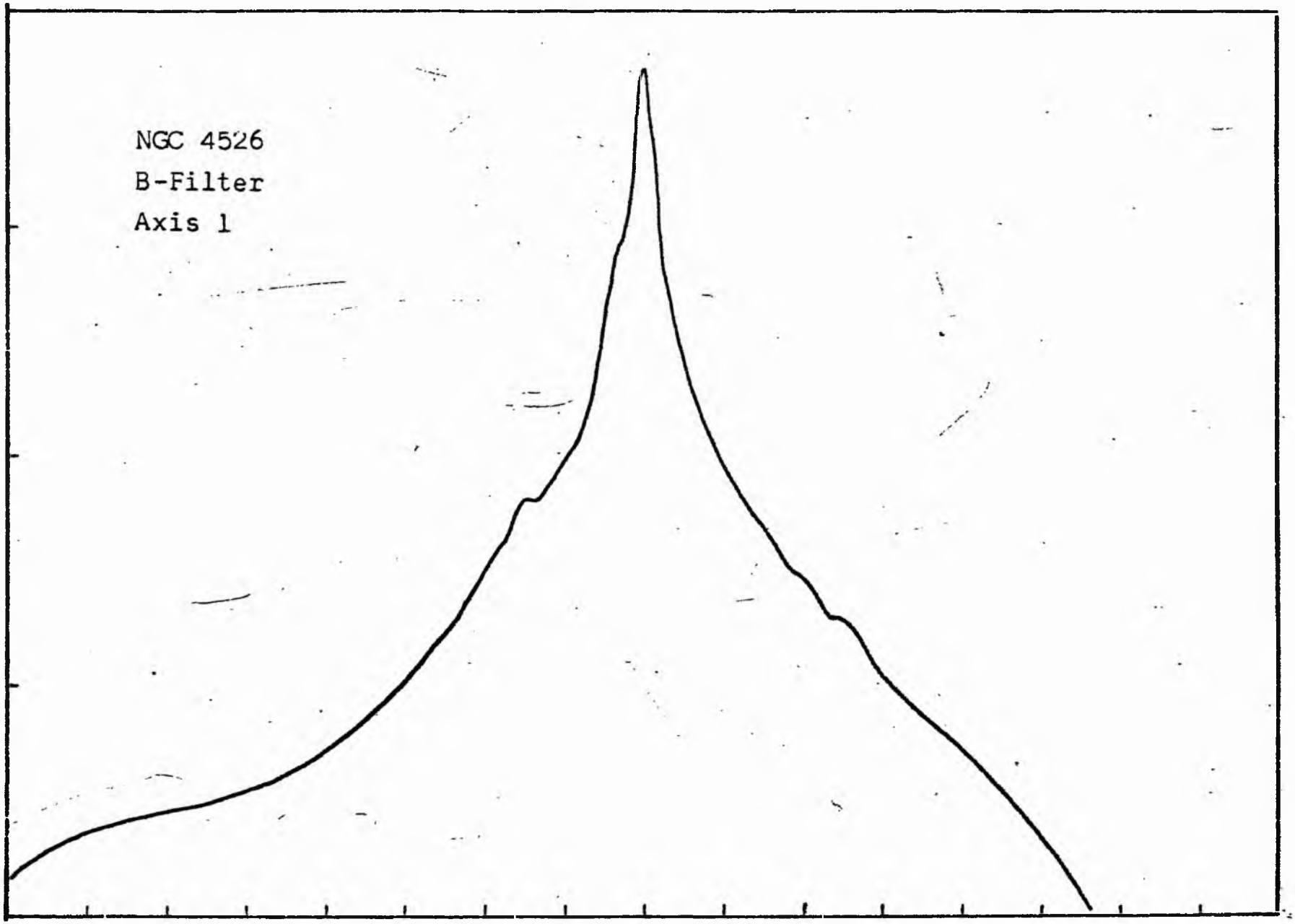
NGC 4526
B-Filter
Axis 1

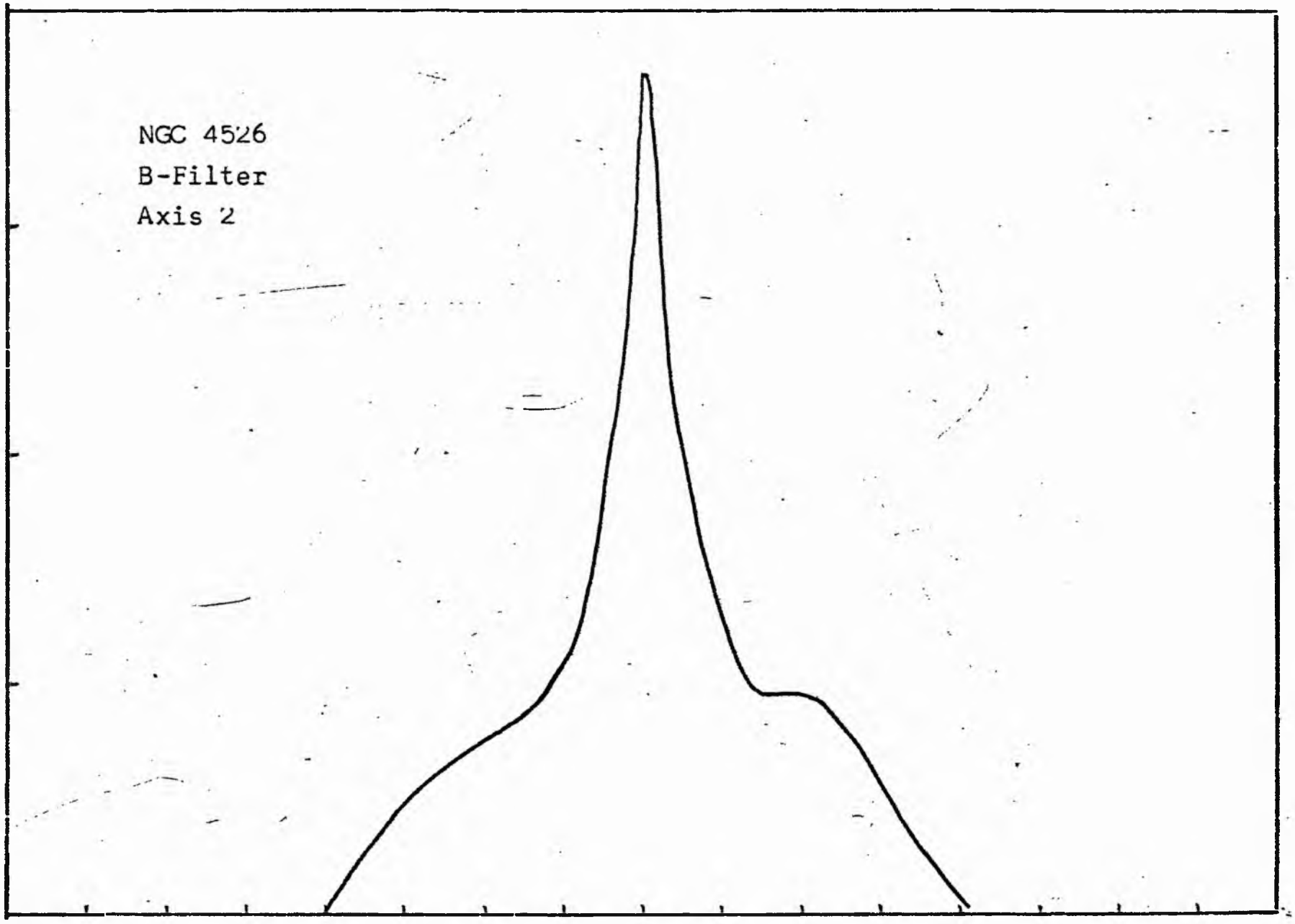
NGC 4526
B-Filter
Axis 2

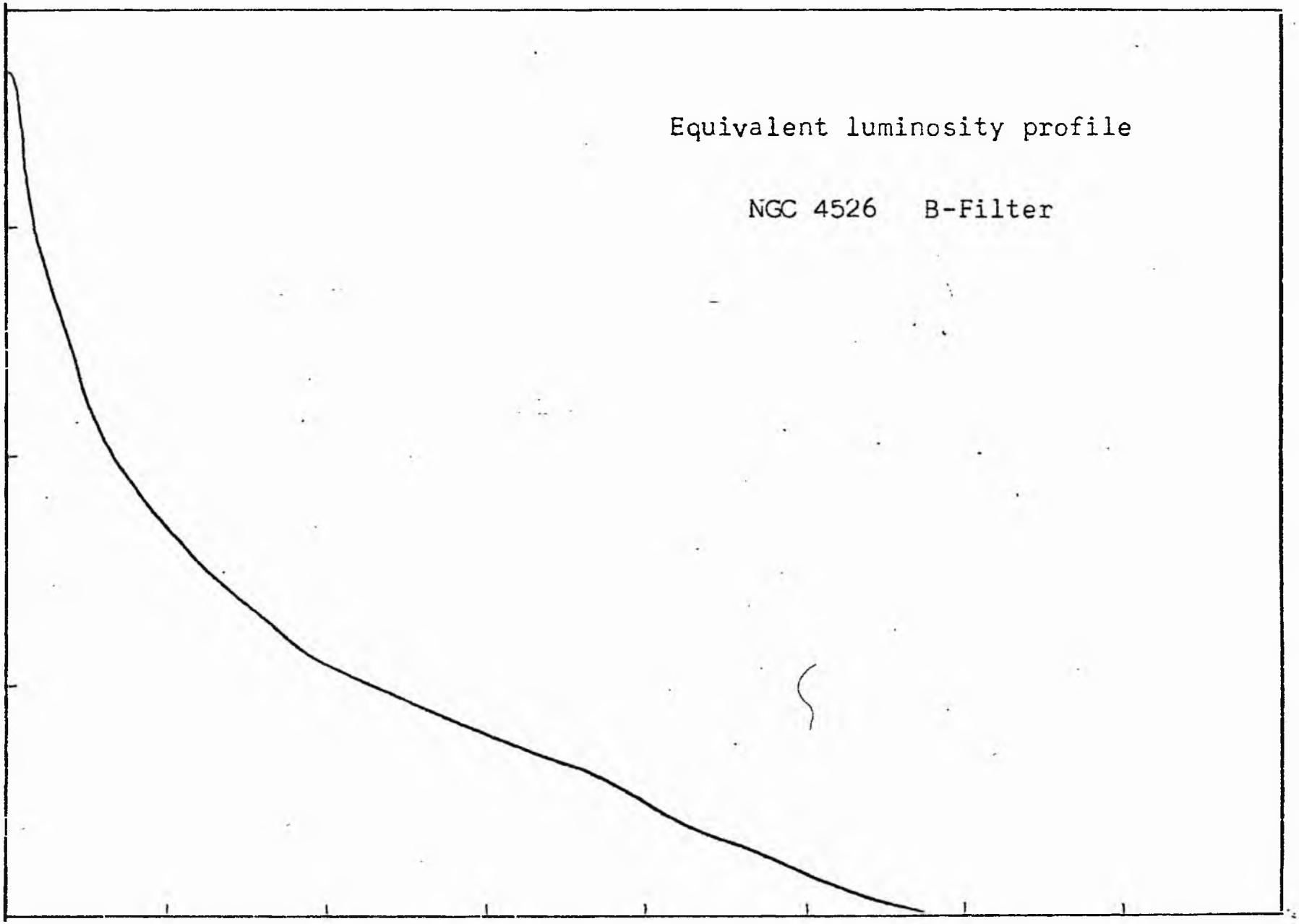
Equivalent luminosity profile
NGC 4526 B-Filter

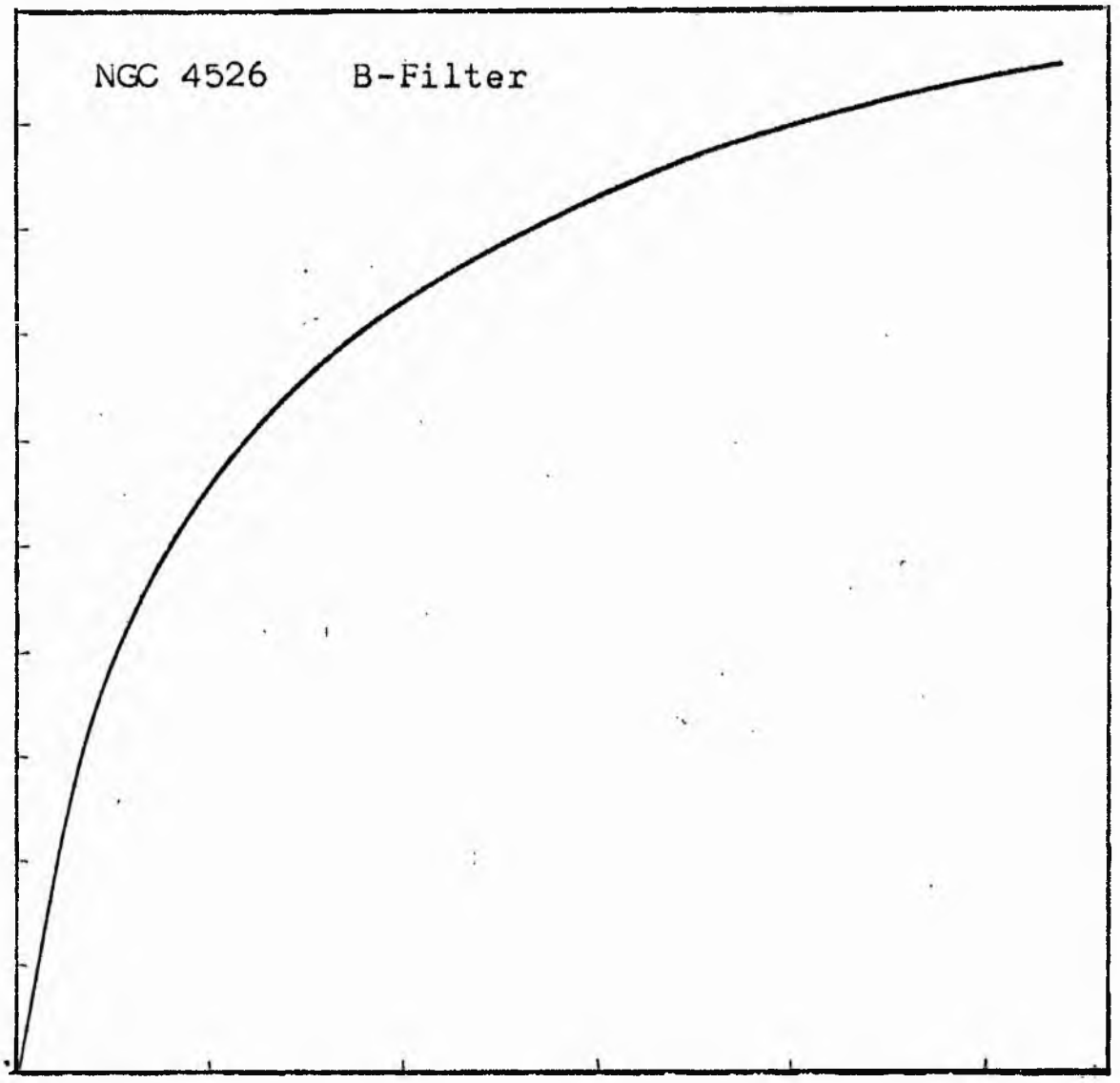

Relative integrated luminosity k(r) versus equivalent radius r*.

MEAN LUMINOSITY DISTRIBUTION IN NGC 4526
B COLOUR

LOG I	I	$\bar{I}$	R	AREA	ΔA	P	ΣP	K(R)	ρ	LOG J	Δμ
1.66	45.709		0.0	0.0			0.0	0.0	0.0	1.748	17.68
		42.780			31.97	1366.9917					
1.60	39.811		3.19	31.97			1366.99	0.04	0.08	1.688	17.83
		35.717			26.39	942.5388					
1.50	31.623		4.31	58.36			2309.53	0.07	0.11	1.588	18.08
		28.371			40.16	1139.4209					
1.40	25.119		5.60	98.52			3448.95	0.11	0.15	1.488	18.33
		22.536			22.24	501.2488					
1.30	19.953		6.20	120.76			3950.20	0.12	0.16	1.388	18.58
		17.901			51.27	917.7822					
1.20	15.849		7.40	172.03			4867.98	0.15	0.19	1.288	18.83
		14.219			60.32	857.6702					
1.10	12.589		8.60	232.35			5725.65	0.17	0.23	1.188	19.08
		11.295			69.37	783.4624					
1.00	10.000		9.80	301.72			6509.11	0.20	0.26	1.088	19.33
		8.972			57.96	520.0142					
0.90	7.943		10.70	359.68			7029.12	0.21	0.28	0.988	19.58
		7.126			208.64	1486.8552					
0.80	6.310		13.45	568.32			8515.97	0.26	0.35	0.888	19.83
		5.661			240.96	1363.9939					
0.70	5.012		16.05	809.28			9879.96	0.30	0.42	0.788	20.08
		4.496			189.46	851.8843					
0.60	3.981		17.83	998.74			10731.85	0.33	0.47	0.688	20.33
		3.572			147.34	526.2651					
0.50	3.162		19.10	1146.08			11258.11	0.34	0.50	0.588	20.58
		2.837			306.12	868.4775					
0.40	2.512		21.50	1452.20			12126.59	0.37	0.56	0.488	20.83
		2.254			312.40	704.0110					
0.30	1.995		23.70	1764.60			12830.59	0.39	0.62	0.388	21.08
		1.790			491.81	880.3823					
0.20	1.585		26.80	2256.42			13710.97	0.42	0.70	0.288	21.33
		1.422			774.35	1101.0535					
0.10	1.259		31.06	3030.77			14812.02	0.45	0.81	0.188	21.58
		1.129			686.87	775.7842					
-0.00	1.000		34.40	3717.63			15587.80	0.48	0.90	0.088	21.83
		0.897			987.50	885.9409					
-0.10	0.794		38.70	4705.13			16473.74	0.50	1.01	-0.012	22.08
		0.713			1319.07	940.0239					
-0.20	0.631		43.79	6024.20			17413.77	0.53	1.15	-0.112	22.33
		0.566			1814.07	1026.8921					
-0.30	0.501		49.95	7838.28			18440.66	0.56	1.31	-0.212	22.58
		0.450			2172.73	976.9558					
-0.40	0.398		56.45	10011.00			19417.61	0.59	1.48	-0.312	22.83
		0.357			2636.74	941.7529					
-0.50	0.316		63.45	12647.74			20359.36	0.62	1.66	-0.412	23.08
		0.284			3287.31	932.6338					
-0.60	0.251		71.22	15935.05			21291.99	0.65	1.87	-0.512	23.33
		0.225			3910.59	881.2778					
-0.70	0.200		79.48	19845.65			22173.27	0.68	2.08	-0.612	23.58
		0.179			1433.25	256.5625					
-0.80	0.158		82.30	21278.90			22429.83	0.69	2.16	-0.712	23.83
		0.142			8037.04	1142.7903					
-0.90	0.126		96.60	29315.95			23572.62	0.72	2.53	-0.812	24.08
		0.113			8835.68	997.9539					
-1.00	0.100		110.20	38151.62			24570.57	0.75	2.89	-0.912	24.33
		0.090			17169.59	1540.3916					
-1.10	0.079		132.70	55321.22			26110.96	0.80	3.48	-1.012	24.58
		0.071			14144.66	1008.0076					
-1.20	0.063		148.70	69465.87			27118.97	0.83	3.90	-1.112	24.83
		0.057			16271.44	921.0815					
-1.30	0.050		165.20	85737.31			28040.05	0.86	4.33	-1.212	25.08
		0.045			15485.56	696.3054					
-1.40	0.040		179.50	101222.87			28736.35	0.88	4.71	-1.312	25.33
		0.036			12786.31	456.6873					
-1.50	0.032		190.50	114009.19			29193.04	0.89	4.99	-1.412	25.58
		0.028			14815.75	420.3372					
-1.60	0.025		202.50	128824.94			29613.37	0.90	5.31	-1.512	25.83
		0.023			32203.50	725.7346					
-1.70	0.020		226.40	161028.44			30339.11	0.93	5.94	-1.612	26.08
		0.018			22196.31	397.3342					
-1.80	0.016		241.50	183224.75			30736.44	0.94	6.33	-1.712	26.33
		0.014			27028.31	384.3215					
-1.90	0.013		258.70	210253.06			31120.76	0.95	6.78	-1.812	26.58
		0.011			8868.87	100.1717					
-2.00	0.010		264.10	219121.94			31220.93	0.95	6.92	-1.912	26.83
$-\infty$							32730.00	(1)			∞

PHOTOMETRIC PARAMETERS OF NGC 4526

B-FILTER

Total luminosity ..... L_T = 9.09

Total apparent magnitude ..... m_T = 10.54

Apparent central surface brightness ..... μ_o = 17.68

Major axis at threshold ..... $2a_m$ = 12.38

Minor axis at threshold ..... $2b_m$ = 6.58

Major axis at μ=25.0 mag sec^{-2} ..... 2a(25) = 6.54

Luminosity within μ=25.0 mag sec^{-2} ..... k(25) = 0.85

Gradient of exponential component ..... G(a) = -0.48

Equivalent gradient of exponential comp..... G(r*) = -0.44

Equivalent gradient of reduced exp. comp..... G(ρ) = -0.25

Parameters at k = ¼ :

- Semi-major axis ..... a_1 = 0.28
- Axis ratio ..... b/a = 0.59
- Equivalent radius ..... r_1* = 0.21
- Surface brightness ..... μ_1 = 19.78

Parameters at k = ½(effective) :

- Semi-major axis ..... a_e = 0.88
- Axis ratio ..... b/a = 0.43
- Equivalent radius ..... r_e* = 0.64
- Surface brightness ..... μ_e = 22.08
- Mean surface brightness ..... μ_e' = 11.54

Parameters at k = ¾ :

- Semi-major axis ..... a_3 = 2.43
- Axis ratio ..... b/a = 0.58
- Equivalent radius ..... r_3* = 1.83
- Surface brightness ..... μ_3 = 24.33

Concentration indices ..... C_{21} = 2.97, C_{32} = 2.88

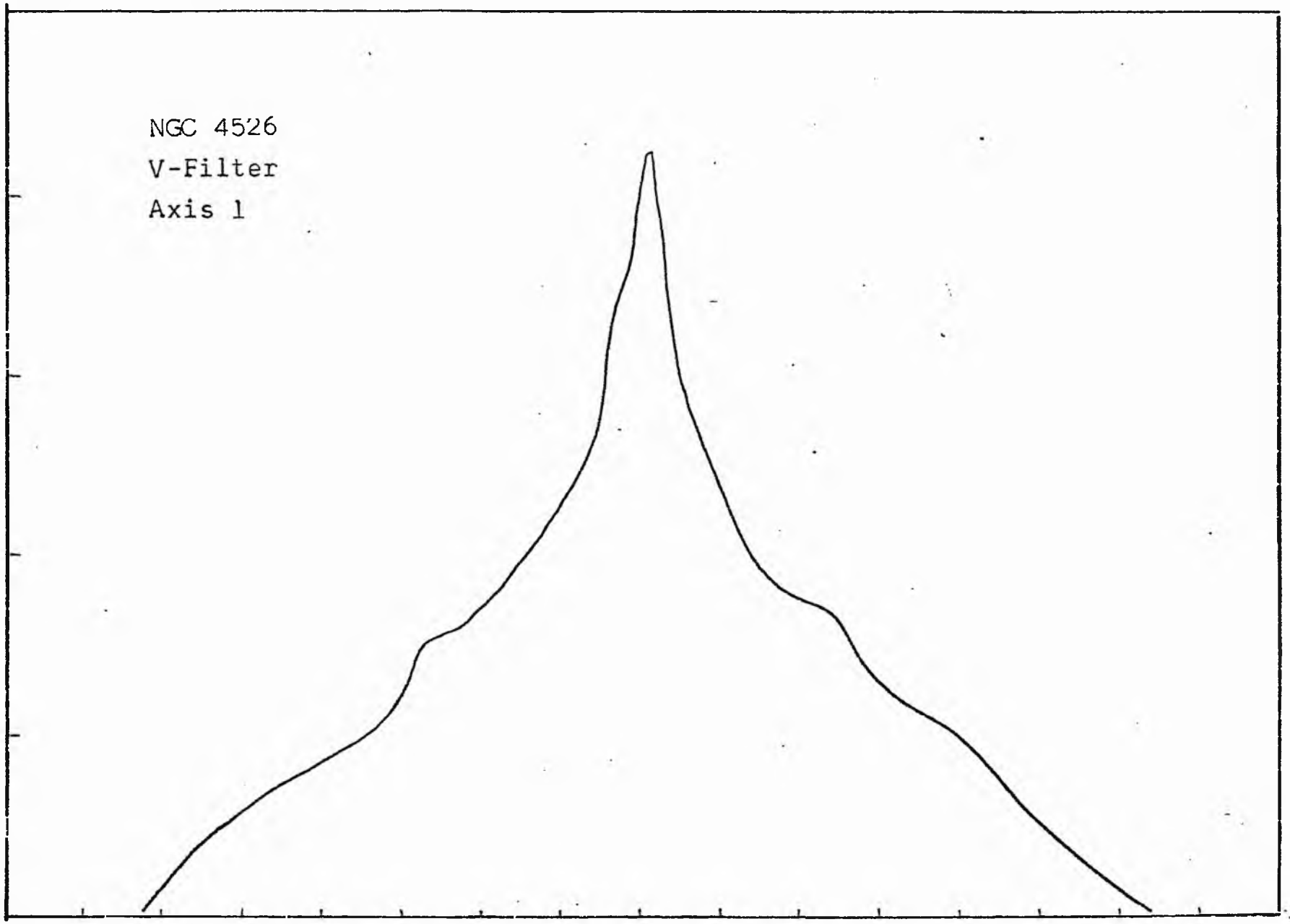
NGC 4526
V-Filter
Axis 1

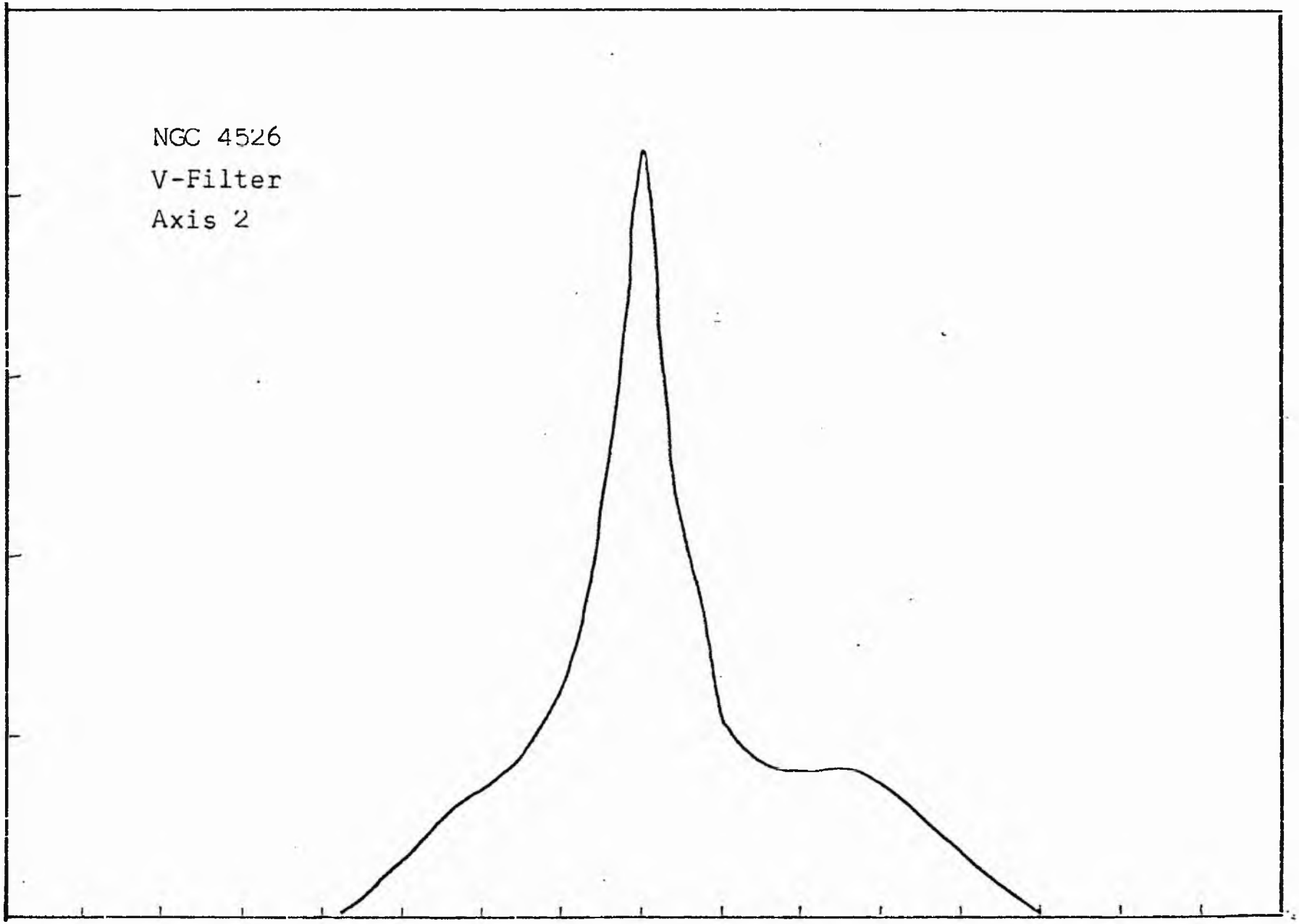
NGC 4526
V-Filter
Axis 2

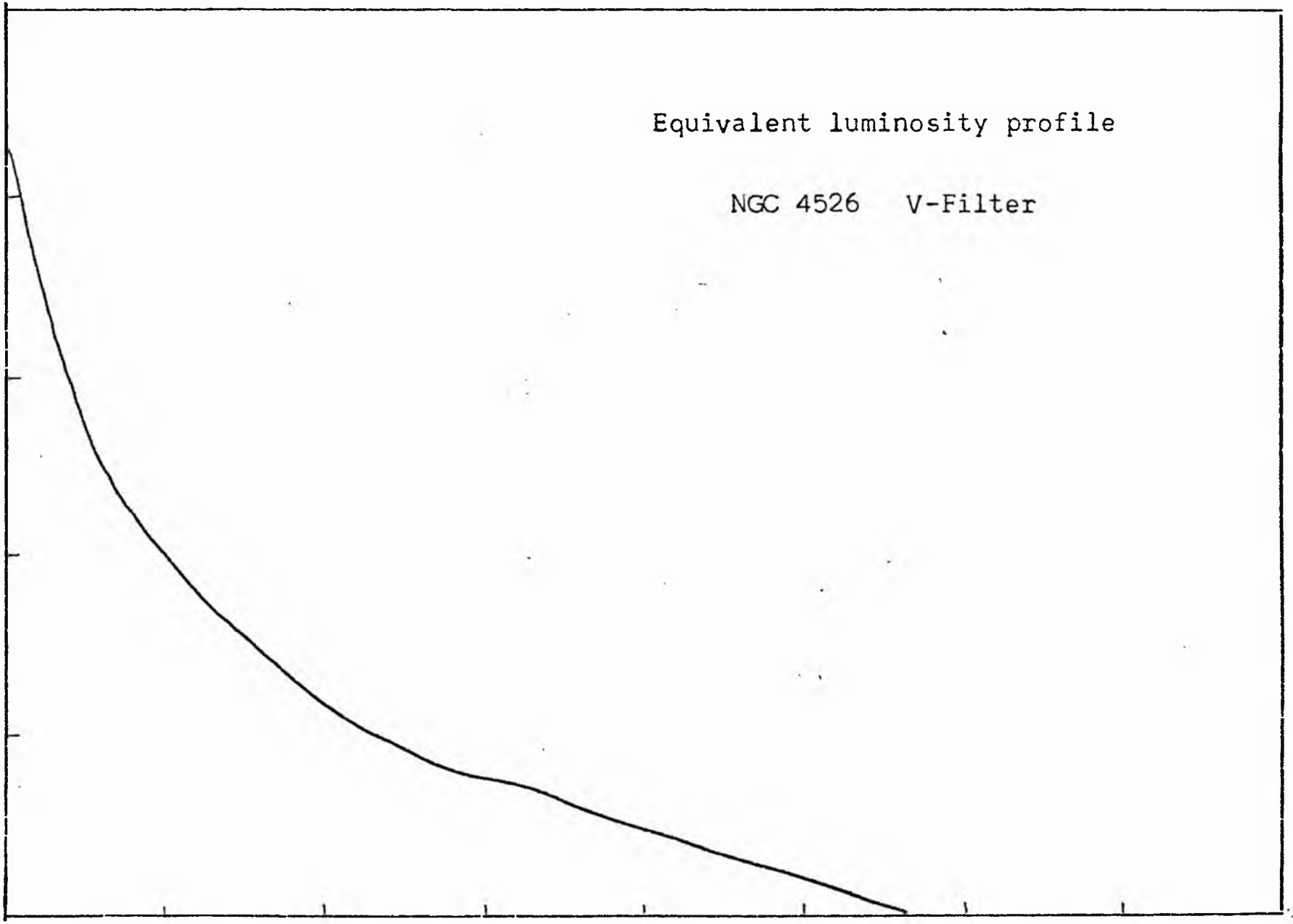
Equivalent luminosity profile
NGC 4526 V-Filter

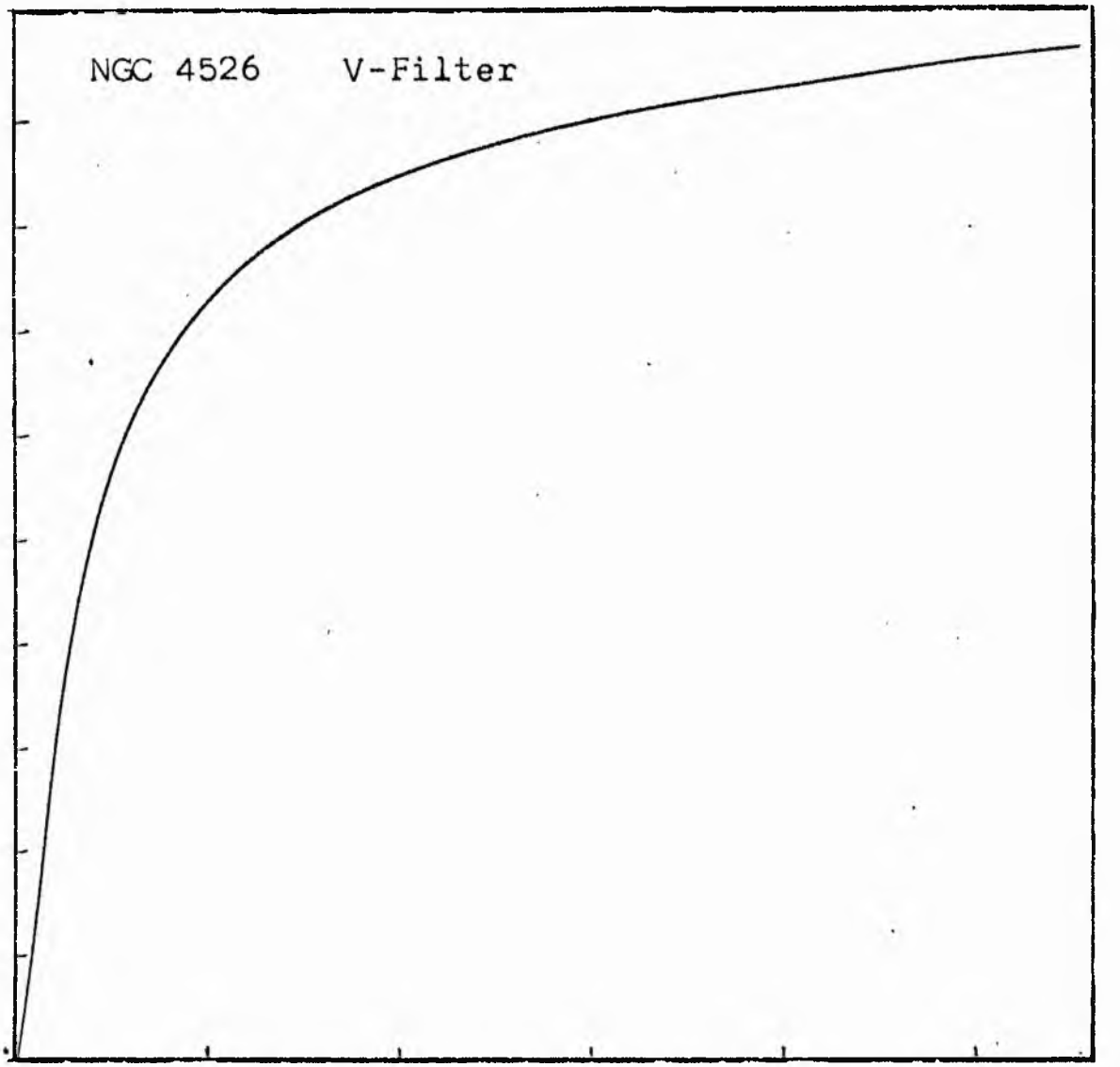

Relative integrated luminosity k(r) versus equivalent radius r*.

MEAN LUMINOSITY DISTRIBUTION IN NGC 4526
V COLOUR

LOG I	I	$\bar{I}$	R	AREA	ΔA	P	ΣP	K(R)	ρ	LOG J	μ
2.11	128.825		0.0	0.0			0.0	0.0	0.0	1.186	16.38
		127.359			0.13	16.0043					
2.10	125.892		0.20	0.13			16.00	0.00	0.01	1.176	16.41
		112.946			6.94	784.1753					
2.00	100.000		1.50	7.07			800.18	0.01	0.08	1.076	16.66
		89.716			40.72	3652.7949					
1.90	79.433		3.90	47.78			4452.97	0.07	0.20	0.976	16.91
		71.264			61.58	4388.0937					
1.80	63.095		5.90	109.36			8841.07	0.14	0.31	0.876	17.16
		56.607			49.01	2774.2422					
1.70	50.118		7.10	158.37			11615.31	0.18	0.37	0.776	17.41
		44.964			68.61	3085.1208					
1.60	39.810		8.50	226.98			14700.43	0.23	0.44	0.676	17.66
		35.717			103.73	3704.7900					
1.50	31.623		10.26	330.71			18405.21	0.29	0.53	0.576	17.91
		28.371			56.37	1599.1851					
1.40	25.119		11.10	387.08			20004.40	0.31	0.58	0.476	18.16
		22.536			111.68	2516.8513					
1.30	19.952		12.60	498.76			22521.25	0.35	0.65	0.376	18.41
		17.901			208.10	3725.1074					
1.20	15.849		15.00	706.86			26246.35	0.41	0.78	0.276	18.66
		14.219			237.74	3380.4265					
1.10	12.589		17.34	944.60			29626.78	0.47	0.90	0.176	18.91
		11.295			73.28	827.6233					
1.00	10.000		18.00	1017.88			30454.40	0.48	0.93	0.076	19.16
		8.972			206.30	1850.8223					
0.90	7.943		19.74	1224.18			32305.22	0.51	1.02	-0.024	19.41
		7.126			301.89	2151.3674					
0.80	6.310		22.04	1526.06			34456.59	0.54	1.14	-0.124	19.66
		5.661			268.44	1519.5693					
0.70	5.012		23.90	1794.51			35976.15	0.56	1.24	-0.224	19.91
		4.496			229.13	1030.2656					
0.60	3.981		25.38	2023.64			37006.42	0.58	1.32	-0.324	20.16
		3.572			483.55	1727.0662					
0.50	3.162		28.25	2507.19			38733.48	0.61	1.46	-0.424	20.41
		2.837			550.96	1563.1135					
0.40	2.512		31.20	3058.15			40296.59	0.63	1.62	-0.524	20.66
		2.254			599.21	1350.3486					
0.30	1.995		34.12	3657.36			41646.94	0.65	1.77	-0.624	20.91
		1.790			550.99	986.3008					
0.20	1.585		36.60	4208.35			42633.24	0.67	1.90	-0.724	21.16
		1.422			944.65	1343.1917					
0.10	1.259		40.50	5153.00			43976.43	0.69	2.10	-0.824	21.41
		1.129			1288.14	1454.8926					
-0.00	1.000		45.28	6441.14			45431.32	0.71	2.35	-0.924	21.66
		0.897			1955.99	1754.8296					
-0.10	0.794		51.70	8397.13			47186.15	0.74	2.68	-1.024	21.91
		0.713			1831.40	1305.1230					
-0.20	0.631		57.06	10228.53			48491.27	0.76	2.96	-1.124	22.16
		0.566			1992.31	1127.7817					
-0.30	0.501		62.37	12220.84			49619.05	0.78	3.23	-1.224	22.41
		0.450			2046.42	920.1577					
-0.40	0.398		67.39	14267.26			50539.21	0.79	3.49	-1.324	22.66
		0.357			2483.45	887.0010					
-0.50	0.316		73.02	16750.71			51426.21	0.81	3.78	-1.424	22.91
		0.284			2485.45	705.1375					
-0.60	0.251		78.25	19236.17			52131.35	0.82	4.06	-1.524	23.16
		0.225			2762.33	622.5068					
-0.70	0.200		83.68	21998.50			52753.85	0.83	4.34	-1.624	23.41
		0.179			2551.66	456.7632					
-0.80	0.158		88.40	24550.16			53210.61	0.84	4.58	-1.724	23.66
		0.142			10217.97	1452.8909					
-0.90	0.126		105.20	34768.13			54663.50	0.86	5.45	-1.824	23.91
		0.113			3522.09	397.8042					
-1.00	0.100		110.40	38290.22			55061.30	0.86	5.72	-1.924	24.16
		0.090			16117.62	1446.0071					
-1.10	0.079		131.60	54407.85			56507.31	0.89	6.82	-2.024	24.41
		0.071			13941.40	993.5195					
-1.20	0.063		147.50	68349.25			57500.83	0.90	7.64	-2.124	24.66
		0.057			17180.56	972.5405					
-1.30	0.050		165.00	85529.81			58473.37	0.92	8.55	-2.224	24.91
		0.045			20139.37	905.5591					
-1.40	0.040		183.40	105669.19			59378.93	0.93	9.51	-2.324	25.16
		0.036			25199.50	900.0432					
-1.50	0.032		204.10	130868.69			60278.97	0.95	10.58	-2.424	25.41
		0.028			12466.31	353.6797					
-1.60	0.025		213.60	143335.00			60632.65	0.95	11.07	-2.524	25.66
		0.023			20120.81	453.4382					
-1.70	0.020		228.10	163455.81			61086.09	0.96	11.82	-2.624	25.91
		0.018			26506.25	474.4841					
-1.80	0.016		245.90	189962.06			61560.57	0.97	12.74	-2.724	26.16
		0.014			21919.69	311.6794					
-1.90	0.013		259.70	211881.75			61872.24	0.97	13.46	-2.824	26.41
		0.011			24320.62	274.6938					
-2.00	0.010		274.20	236202.37			62146.93	0.98	14.21	-2.924	26.66
- ∞							63706.00	1.1			∞

PHOTOMETRIC PARAMETERS OF NGC 4526
V-FILTER

Total luminosity ..... L_T = 17.70
Total apparent magnitude ..... m_T = 9.65
Apparent central surface brightness ..... μ_o = 16.38
Major axis at threshold ..... $2a_m$ = 10.38
Minor axis at threshold ..... $2b_m$ = 7.98
Major axis at μ=25.0 mag sec^{-2} ..... 2a(25) = 7.81
Luminosity within μ=25.0 mag sec^{-2} ..... k(25) = 0.92
Gradient of exponential component ..... G(a) = -0.52
Equivalent gradient of exponential comp. .... G(r*) = -0.42
Equivalent gradient of reduced exp. comp. .... G(ρ) = -0.35

Parameters at k = ¼ :

- Semi-major axis ..... a_1 = 0.23
- Axis ratio ..... b/a = 0.57
- Equivalent radius ..... r_1* = 0.15
- Surface brightness ..... μ_1 = 17.75

Parameters at k = ½(effective) :

- Semi-major axis ..... a_e = 0.47
- Axis ratio ..... b/a = 0.52
- Equivalent radius ..... r_e* = 0.32
- Surface brightness ..... μ_e = 19.34
- Mean surface brightness ..... μ_e' = 9.15

Parameters at k = ¾ :

- Semi-major axis ..... a_3 = 1.40
- Axis ratio ..... b/a = 0.44
- Equivalent radius ..... r_3* = 0.90
- Surface brightness ..... μ_3 = 22.04

Concentration indices ..... C_{21} = 2.13, C_{32} = 2.80

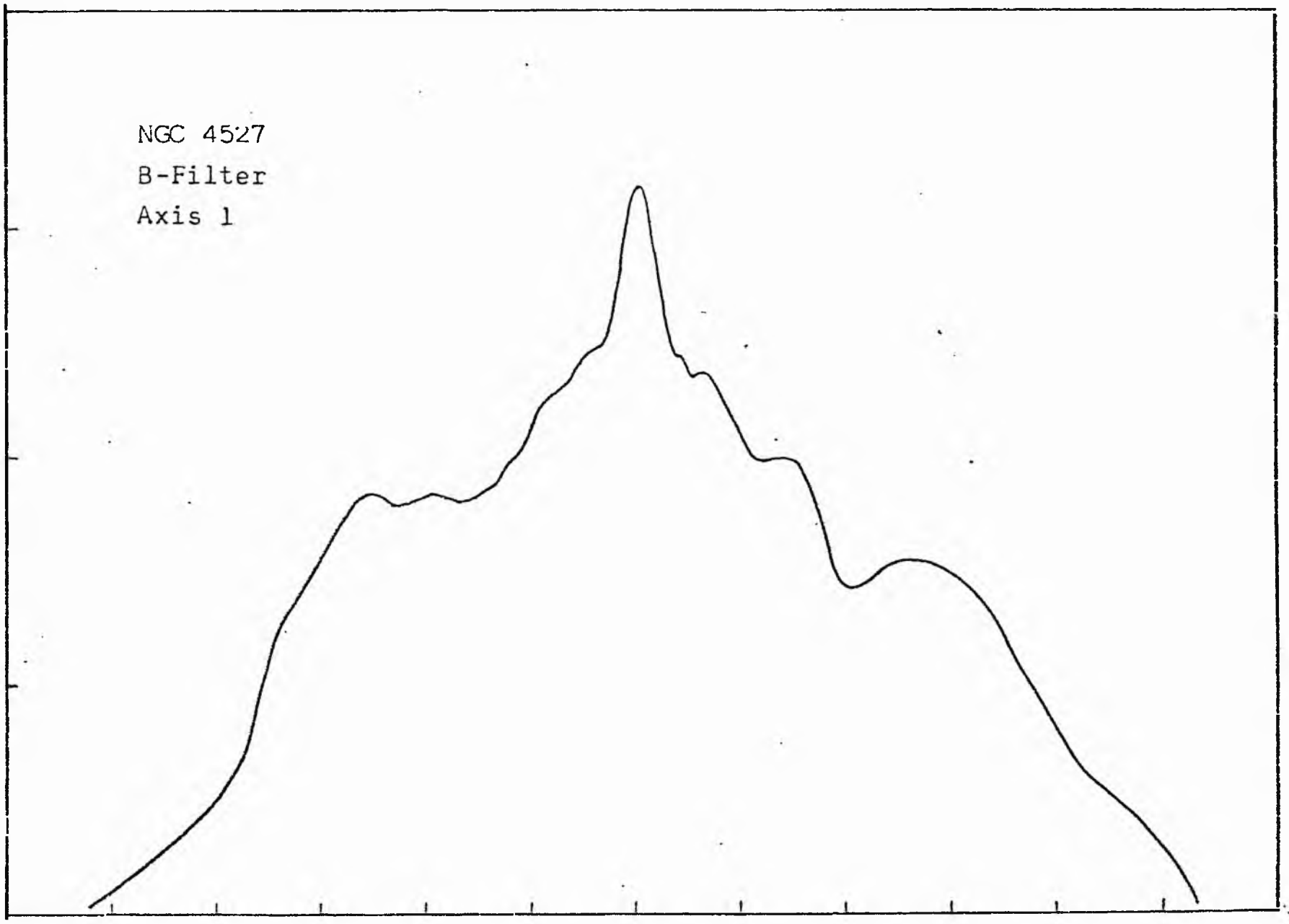
NGC 4527
B-Filter
Axis 1

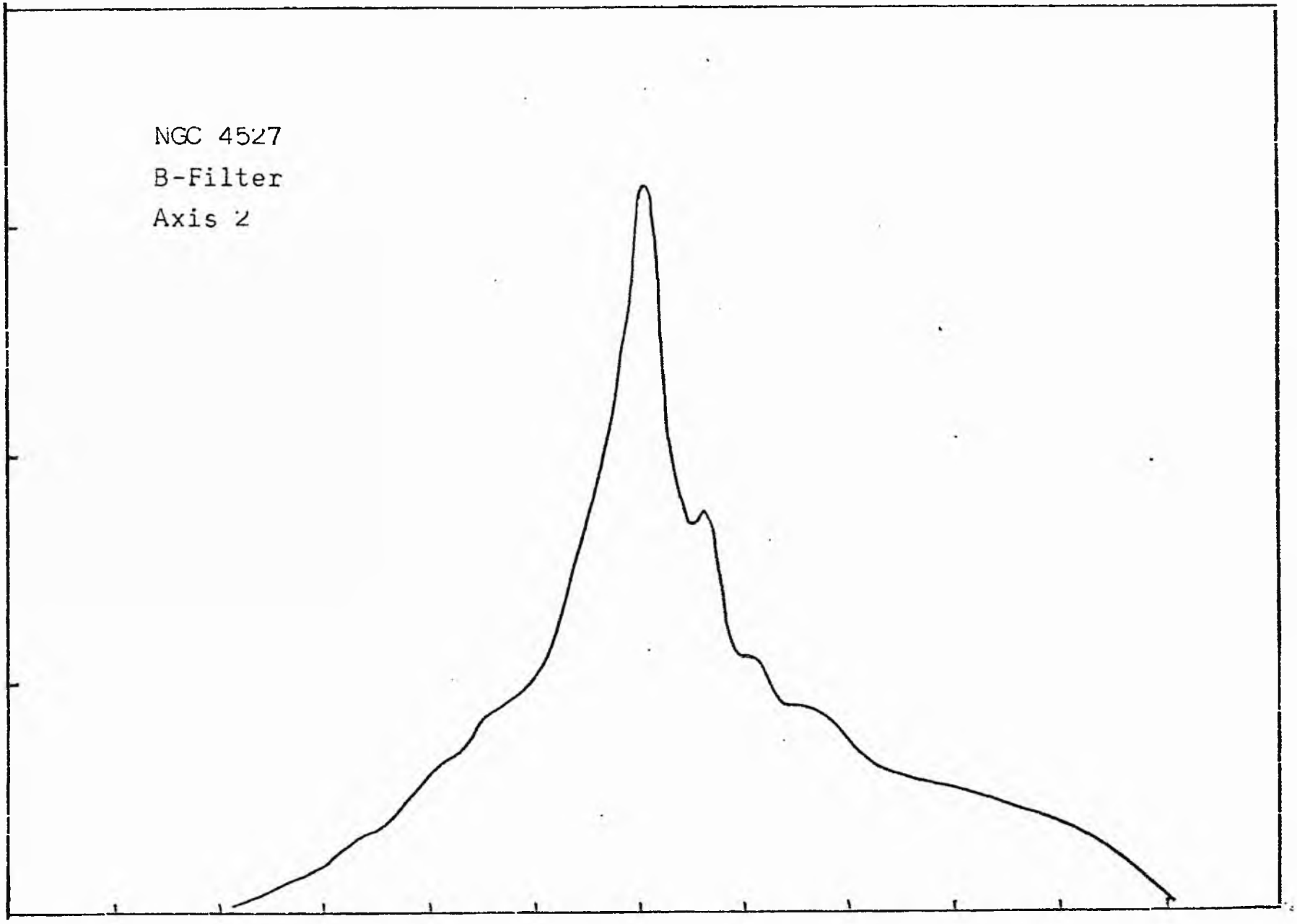
NGC 4527
B-Filter
Axis 2

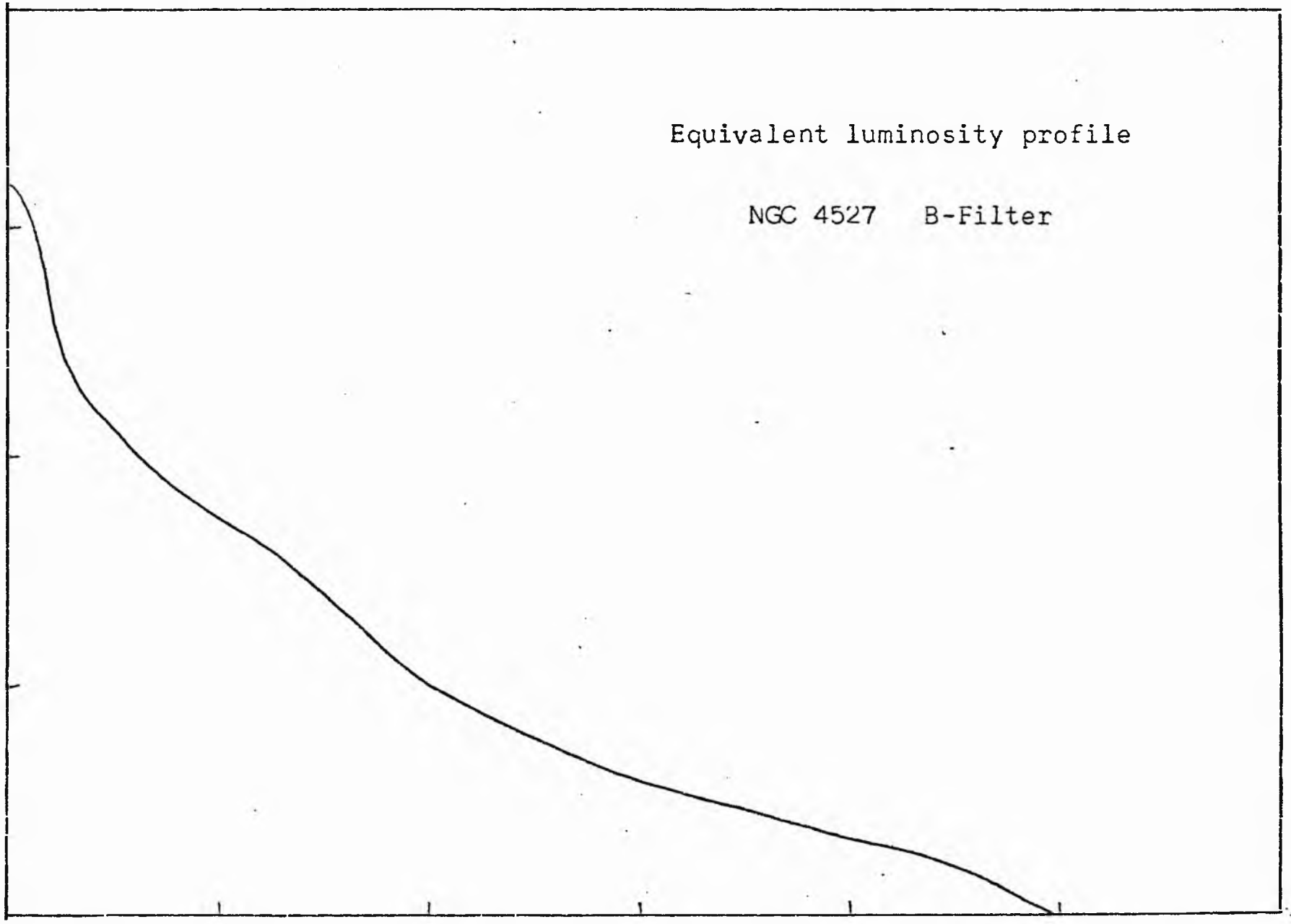
Equivalent luminosity profile
NGC 4527 B-Filter

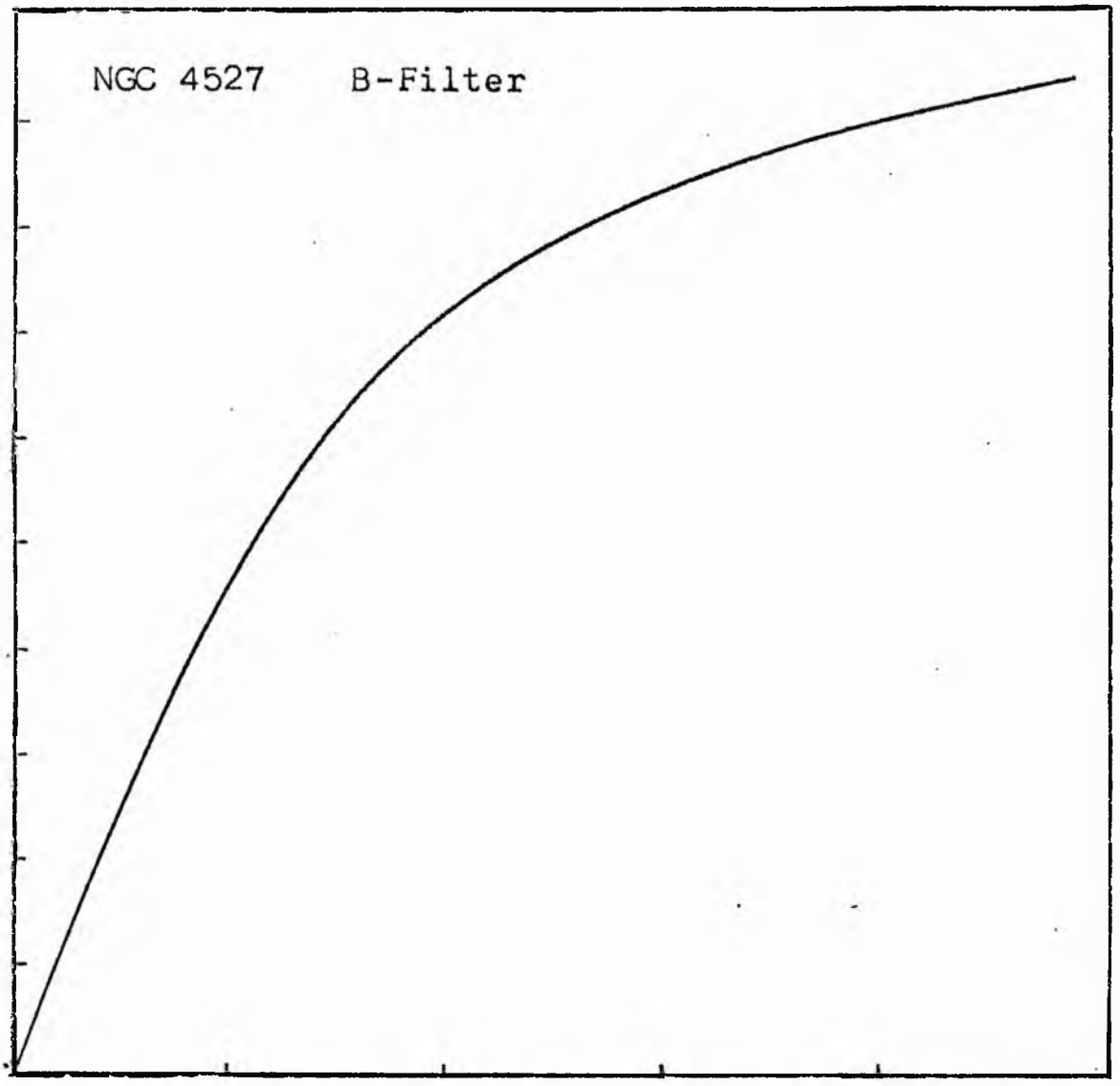

Relative integrated luminosity k(r) versus equivalent radius r*.

B COLOUR

LOG I	I	Ī	R	AREA	ΔA	P	ΣP	KINI	ρ	LOG J	JJ
1.17	14.791		0.0	0.0			0.0	0.0	0.0	1.490	19.28
		13.690			31.97	437.6616					
1.10	12.589		3.19	31.97			437.66	0.02	0.06	1.420	19.46
		11.295			84.93	959.2446					
1.00	10.000		6.10	116.90			1396.91	0.06	0.11	1.320	19.71
		8.972			45.96	412.3496					
0.90	7.943		7.20	162.86			1809.26	0.08	0.13	1.220	19.96
		7.126			58.81	419.1084					
0.80	6.310		8.40	221.67			2228.36	0.10	0.16	1.120	20.21
		5.661			16.12	91.2303					
0.70	5.012		8.70	237.79			2319.59	0.10	0.16	1.020	20.46
		4.496			82.69	371.7969					
0.60	3.981		10.10	320.47			2691.39	0.12	0.19	0.920	20.71
		3.572			109.58	391.3794					
0.50	3.162		11.70	430.05			3082.77	0.14	0.22	0.820	20.96
		2.837			134.05	380.3152					
0.40	2.512		13.40	564.10			3463.09	0.15	0.25	0.720	21.21
		2.254			258.34	582.1868					
0.30	1.995		16.18	822.44			4045.27	0.18	0.30	0.620	21.46
		1.790			756.70	1354.5457					
0.20	1.585		22.42	1579.14			5399.82	0.24	0.42	0.520	21.71
		1.422			712.78	1013.5020					
0.10	1.259		27.01	2291.92			6413.32	0.29	0.50	0.420	21.96
		1.129			492.33	556.0637					
-0.00	1.000		29.77	2784.24			6969.38	0.31	0.56	0.320	22.21
		0.897			1230.91	1104.3259					
-0.10	0.794		35.75	4015.15			8073.70	0.36	0.67	0.220	22.46
		0.713			2158.54	1538.2661					
-0.20	0.631		44.33	6173.69			9611.97	0.43	0.83	0.120	22.71
		0.566			2357.15	1334.3157					
-0.30	0.501		52.11	8530.84			10946.28	0.49	0.97	0.020	22.96
		0.450			2778.89	1249.5217					
-0.40	0.398		60.00	11309.73			12195.80	0.54	1.12	-0.080	23.21
		0.357			3212.71	1147.4746					
-0.50	0.316		67.99	14522.44			13343.27	0.60	1.27	-0.180	23.46
		0.284			2778.69	788.3379					
-0.60	0.251		74.21	17301.13			14131.61	0.63	1.38	-0.280	23.71
		0.225			2905.71	654.8247					
-0.70	0.200		80.20	20206.85			14786.43	0.66	1.50	-0.380	23.96
		0.179			2866.54	513.1335					
-0.80	0.158		85.70	23073.39			15299.57	0.68	1.60	-0.480	24.21
		0.142			3690.73	524.7891					
-0.90	0.126		92.30	26764.12			15824.36	0.71	1.72	-0.580	24.46
		0.113			3840.29	433.7463					
-1.00	0.100		98.70	30604.41			16258.10	0.73	1.84	-0.680	24.71
		0.090			10438.87	936.5391					
-1.10	0.079		114.30	41043.29			17194.64	0.77	2.13	-0.780	24.96
		0.071			7261.84	517.5112					
-1.20	0.063		124.00	48305.13			17712.15	0.79	2.31	-0.880	25.21
		0.057			8950.40	506.6587					
-1.30	0.050		135.00	57255.53			18218.80	0.81	2.52	-0.980	25.46
		0.045			6986.90	314.1653					
-1.40	0.040		143.00	64242.43			18532.97	0.83	2.67	-1.080	25.71
		0.036			20976.63	749.2212					
-1.50	0.032		164.70	85219.06			19282.19	0.86	3.07	-1.180	25.96
		0.028			16908.06	479.6990					
-1.60	0.025		180.30	102127.12			19761.88	0.88	3.36	-1.280	26.21
		0.023			26189.31	590.2009					
-1.70	0.020		202.10	128316.44			20352.08	0.91	3.77	-1.380	26.46
		0.018			20710.75	370.7422					
-1.80	0.016		217.80	149027.19			20722.82	0.93	4.06	-1.480	26.71
		0.014			16297.06	231.7321					
-1.90	0.013		229.40	165324.25			20954.55	0.94	4.28	-1.580	26.96
		0.011			25256.31	285.2642					
-2.00	0.010		246.30	190580.56			21239.82	0.95	4.59	-1.680	27.21
- ∞							22389.00	(1)			∞

PHOTOMETRIC PARAMETERS OF NGC 4527

B-FILTER

Total luminosity	L_T	= 6.22
Total apparent magnitude	m_T	= 11.33
Apparent central surface brightness	μ_o	= 19.28
Major axis at threshold	$2a_m$	= 8.77
Minor axis at threshold	$2b_m$	= 7.65
Major axis at μ=25.0 mag sec^{-2}	2a(25)	= 6.05
Luminosity within μ=25.0 mag sec^{-2}	k(25)	= 0.77
Gradient of exponential component	G(a)	= -0.53
Equivalent gradient of exponential comp.	G(r*)	= -0.59
Equivalent gradient of reduced exp. comp.	G(ρ)	= -0.76

Parameters at k = ¼ :

Semi-major axis	a_1	= 0.80
Axis ratio	b/a	= 0.31
Equivalent radius	r_1*	= 0.39
Surface brightness	μ_1	= 21.76

Parameters at k = ½(effective) :

Semi-major axis	a_e	= 1.81
Axis ratio	b/a	= 0.28
Equivalent radius	r_e*	= 0.89
Surface brightness	μ_e	= 23.01
Mean surface brightness	μ_e'	= 13.07

Parameters at k = ¾ :

Semi-major axis	a_3	= 2.88
Axis ratio	b/a	= 0.39
Equivalent radius	r_3*	= 1.79
Surface brightness	μ_3	= 24.83
Concentration indices	C_{21}	= 2.30
	C_{32}	= 2.00

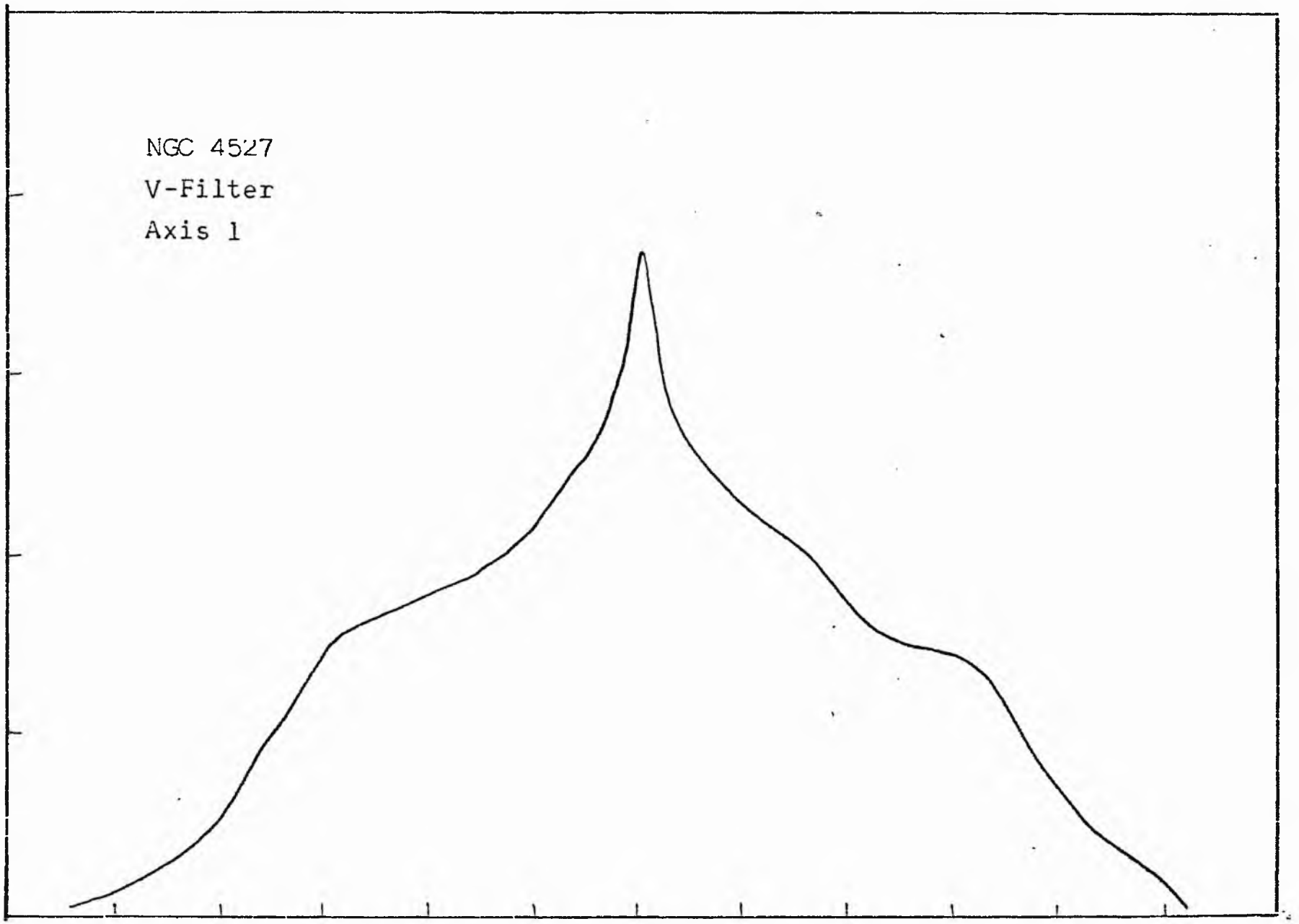
NGC 4527
V-Filter
Axis 1

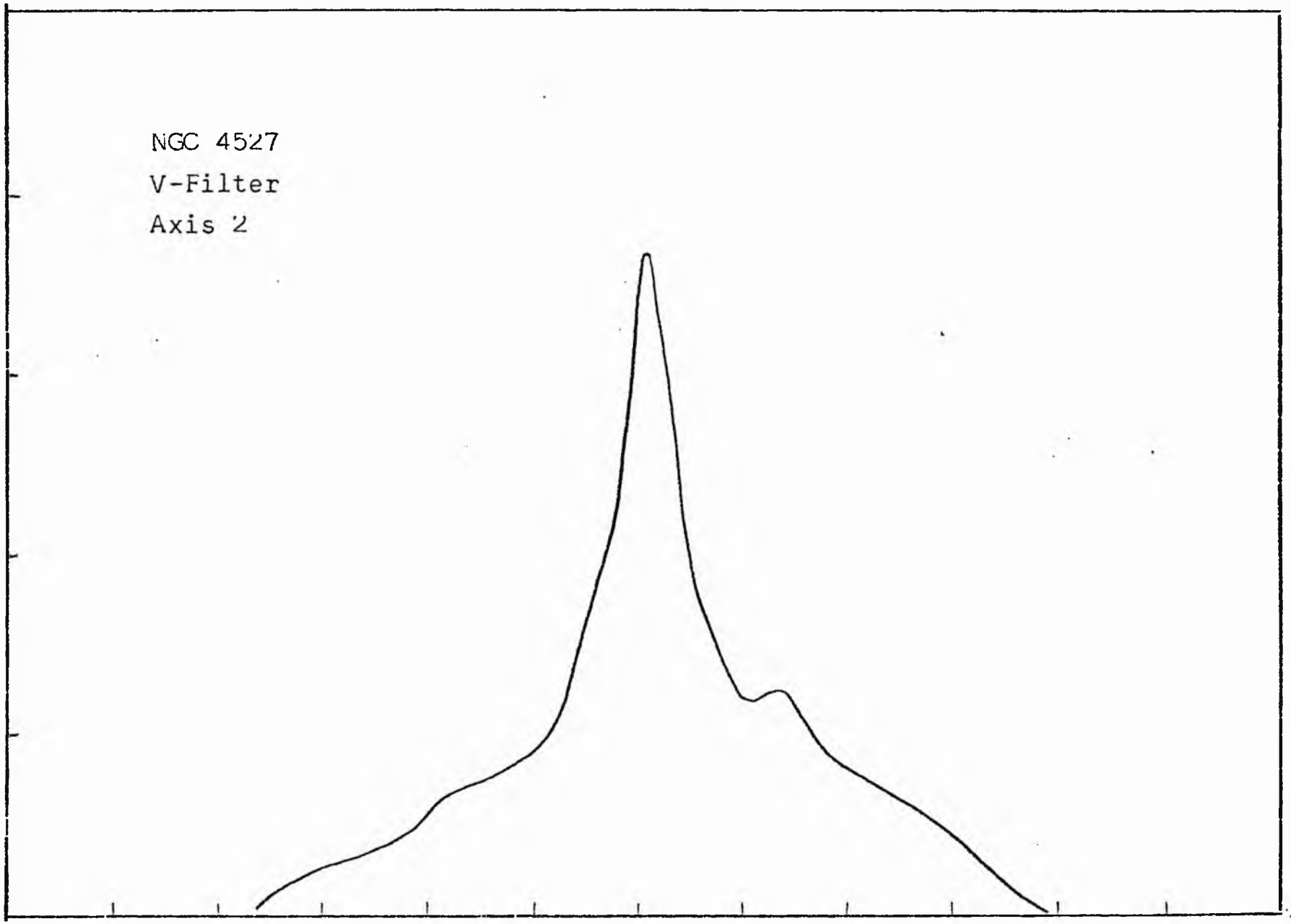
NGC 4527
V-Filter
Axis 2

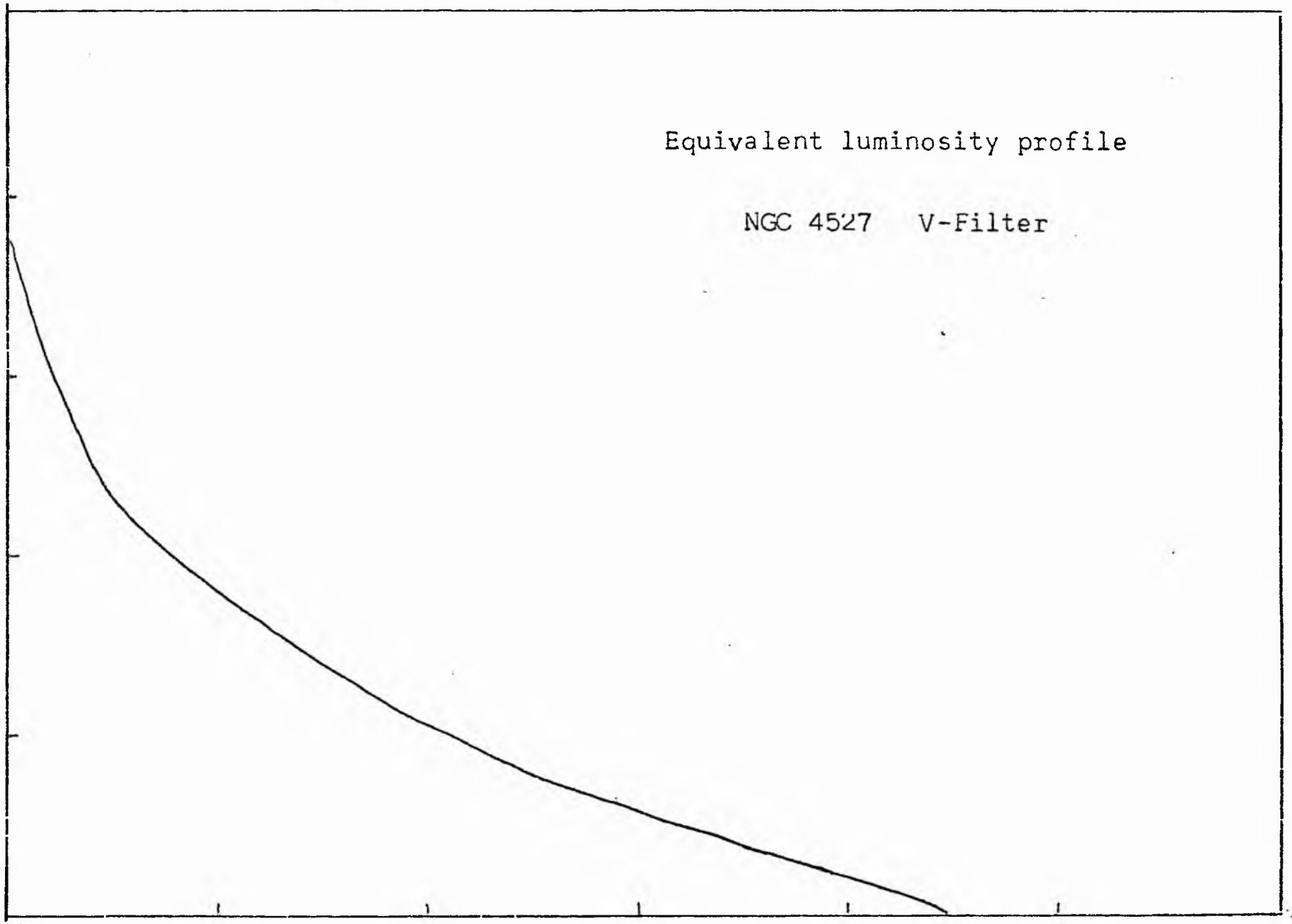
Equivalent luminosity profile
NGC 4527 V-Filter

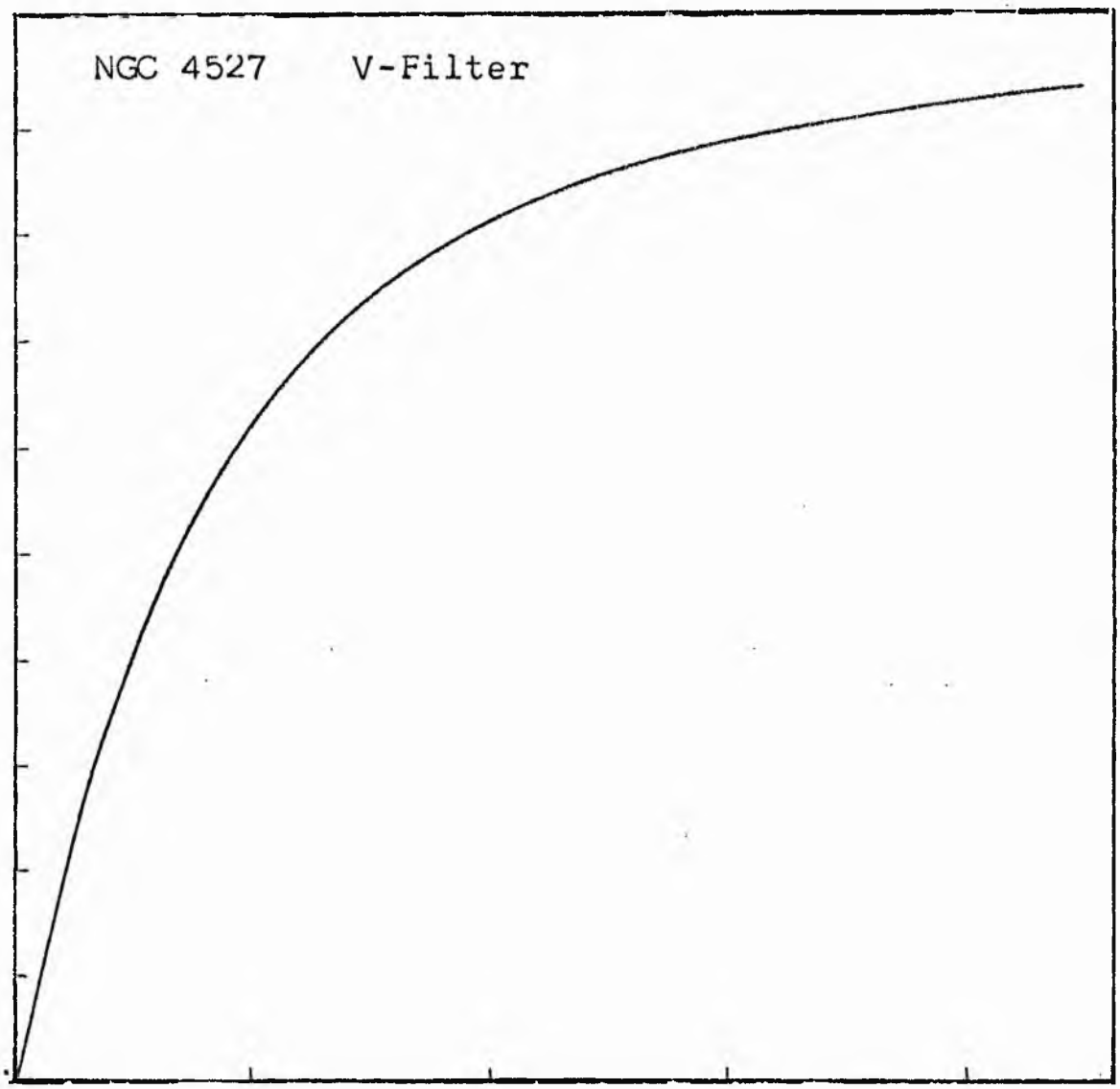

Relative integrated luminosity k(r) versus equivalent radius r*.

MEAN LUMINOSITY DISTRIBUTION IN NGC 4527
V COLOUR

LOG I	I	$\bar{I}$	R	AREA	Δ A	P	Σ P	K(R)	ρ	LOG J	μ
1.65	44.668		0.0	0.0			0.0	0.0	0.0	1.537	17.65
		42.239			7.07	298.5730					
1.60	39.811		1.50	7.07			298.57	0.01	0.04	1.487	17.78
		35.717			11.03	393.8469					
1.50	31.623		2.40	18.10			692.42	0.02	0.07	1.387	18.03
		28.371			22.62	641.7307					
1.40	25.119		3.60	40.72			1334.15	0.04	0.11	1.287	18.28
		22.536			28.68	646.3843					
1.30	19.953		4.70	69.40			1980.53	0.07	0.14	1.187	18.53
		17.901			107.32	1921.0459					
1.20	15.849		7.50	176.71			3901.58	0.13	0.22	1.087	18.78
		14.219			50.27	714.7253					
1.10	12.589		8.50	226.98			4616.30	0.15	0.25	0.987	19.03
		11.295			132.70	1498.7966					
1.00	10.000		10.70	359.68			6115.10	0.20	0.32	0.887	19.28
		8.972			94.97	852.0591					
0.90	7.943		12.03	454.65			6967.16	0.23	0.36	0.787	19.53
		7.126			124.71	888.7102					
0.80	6.310		13.58	579.36			7855.86	0.26	0.41	0.687	19.78
		5.661			159.90	905.1699					
0.70	5.012		15.34	739.27			8761.03	0.29	0.46	0.587	20.03
		4.496			203.16	913.4766					
0.60	3.981		17.32	942.42			9674.51	0.32	0.52	0.487	20.28
		3.572			210.87	753.1663					
0.50	3.162		19.16	1153.29			10427.67	0.35	0.57	0.387	20.53
		2.837			372.77	1057.5725					
0.40	2.512		22.04	1526.06			11485.24	0.38	0.66	0.287	20.78
		2.254			515.15	1160.9297					
0.30	1.995		25.49	2041.22			12646.17	0.42	0.76	0.187	21.03
		1.790			716.90	1283.3025					
0.20	1.585		29.63	2758.12			13929.47	0.46	0.89	0.087	21.28
		1.422			854.36	1214.8147					
0.10	1.259		33.91	3612.48			15144.29	0.51	1.02	-0.013	21.53
		1.129			1107.25	1250.5940					
-0.00	1.000		38.76	4719.73			16394.88	0.55	1.16	-0.113	21.78
		0.897			1348.57	1209.8862					
-0.10	0.794		43.95	6068.30			17604.76	0.59	1.32	-0.213	22.03
		0.713			1496.22	1066.2671					
-0.20	0.631		49.07	7564.53			18671.03	0.62	1.47	-0.313	22.28
		0.566			1701.84	963.3574					
-0.30	0.501		54.31	9266.36			19634.38	0.65	1.63	-0.413	22.53
		0.450			1926.80	866.3765					
-0.40	0.398		59.69	11193.16			20500.76	0.68	1.79	-0.513	22.78
		0.357			2157.77	770.6816					
-0.50	0.316		65.19	13350.93			21271.44	0.71	1.96	-0.613	23.03
		0.284			2410.08	683.7573					
-0.60	0.251		70.83	15761.02			21955.19	0.73	2.12	-0.713	23.28
		0.225			2667.65	601.1729					
-0.70	0.200		76.59	18428.67			22556.36	0.75	2.30	-0.813	23.53
		0.179			2948.61	527.8210					
-0.80	0.158		82.49	21377.27			23084.18	0.77	2.47	-0.913	23.78
		0.142			5934.78	843.8682					
-0.90	0.126		93.24	27312.05			23928.05	0.80	2.80	-1.013	24.03
		0.113			5855.51	661.3560					
-1.00	0.100		102.75	33167.56			24589.41	0.82	3.08	-1.113	24.28
		0.090			5595.80	502.0344					
-1.10	0.079		111.08	38763.37			25091.44	0.84	3.33	-1.213	24.53
		0.071			6046.80	430.9207					
-1.20	0.063		119.43	44810.17			25522.36	0.85	3.58	-1.313	24.78
		0.057			10352.74	586.0403					
-1.30	0.050		132.51	55162.91			26108.39	0.87	3.97	-1.413	25.03
		0.045			7472.40	335.9951					
-1.40	0.040		141.20	62635.31			26444.39	0.88	4.24	-1.513	25.28
		0.036			12549.50	448.2290					
-1.50	0.032		154.70	75184.81			26892.61	0.90	4.64	-1.613	25.53
		0.028			14861.00	421.6211					
-1.60	0.025		169.30	90045.81			27314.23	0.91	5.08	-1.713	25.78
		0.023			15393.06	346.8962					
-1.70	0.020		183.20	105438.87			27661.13	0.92	5.49	-1.813	26.03
		0.018			17724.12	317.2778					
-1.80	0.016		198.00	123163.00			27978.41	0.93	5.94	-1.913	26.28
		0.014			19367.87	275.3960					
-1.90	0.013		213.00	142530.87			28253.80	0.94	6.39	-2.013	26.53
		0.011			12857.81	145.2257					
-2.00	0.010		222.40	155388.69			28399.02	0.95	6.67	-2.113	26.78
- ∞							29979.00	(1)			∞

PHOTOMETRIC PARAMETERS OF NGC 4527

V-FILTER

Total luminosity	L_T	= 8.33
Total apparent magnitude	m_T	= 10.59
Apparent central surface brightness	μ_o	= 17.65
Major axis at threshold	$2a_m$	= 8.24
Minor axis at threshold	$2b_m$	= 5.52
Major axis at μ=25.0 mag sec^{-2}	2a(25)	= 6.28
Luminosity within μ=25.0 mag sec^{-2}	k(25)	= 0.87
Gradient of exponential component	G(a)	= -0.68
Equivalent gradient of exponential comp.	G(r*)	= -0.63
Equivalent gradient of reduced exp. comp.	G(ρ)	= -0.63

Parameters at k = ¼ :

Semi-major axis	a_1	= 0.21
Axis ratio	b/a	= 0.59
Equivalent radius	r_1*	= 0.22
Surface brightness	μ_1	= 19.70

Parameters at k = ½(effective) :

Semi-major axis	a_e	= 0.85
Axis ratio	b/a	= 0.33
Equivalent radius	r_e*	= 0.56
Surface brightness	μ_e	= 21.48
Mean surface brightness	μ_e'	= 11.34

Parameters at k = ¾ :

Semi-major axis	a_3	= 2.70
Axis ratio	b/a	= 0.24
Equivalent radius	r_3*	= 1.26
Surface brightness	μ_3	= 23.53
Concentration indices	C_{21}	= 2.58
	C_{32}	= 2.27

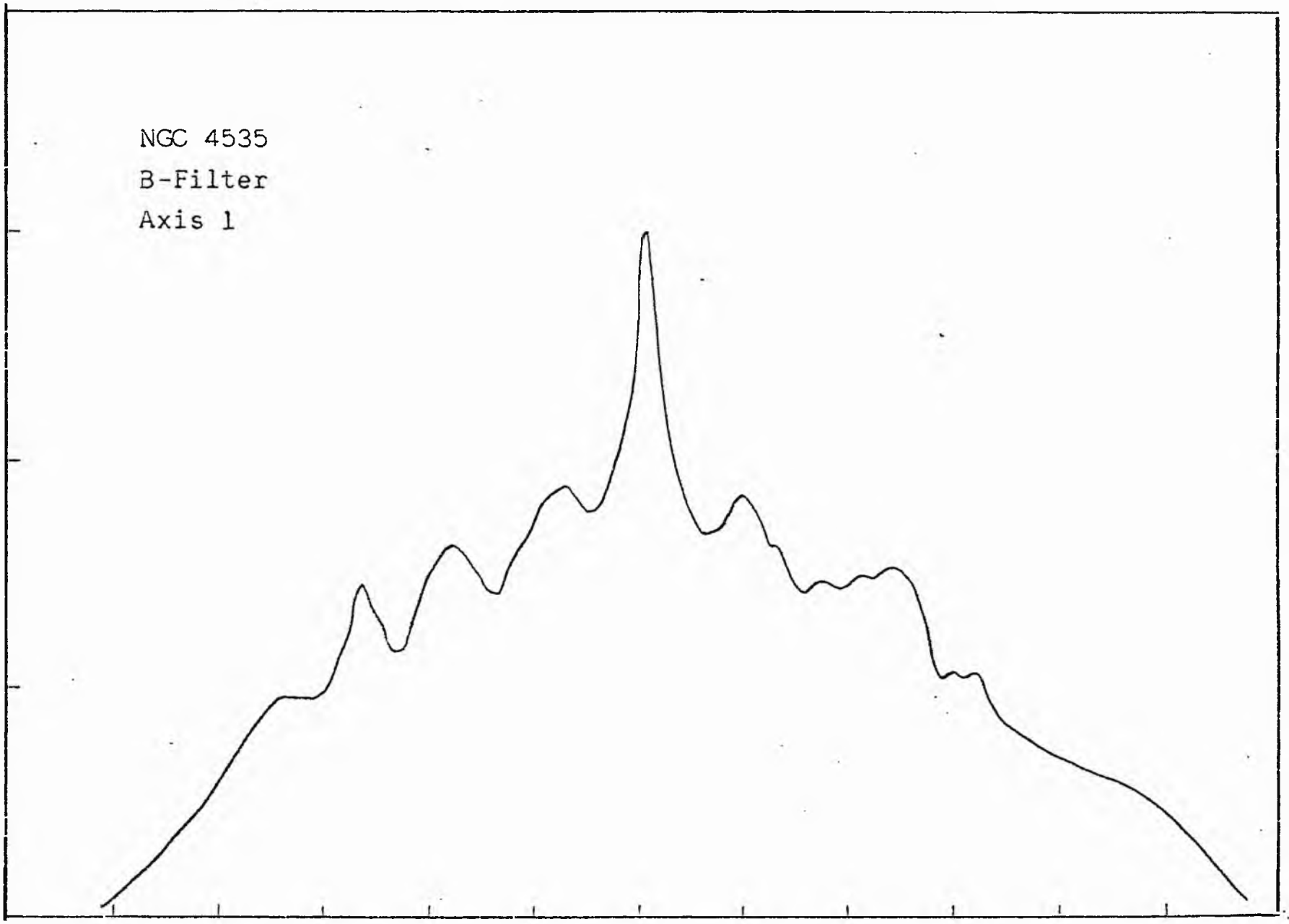
NGC 4535
B-Filter
Axis 1

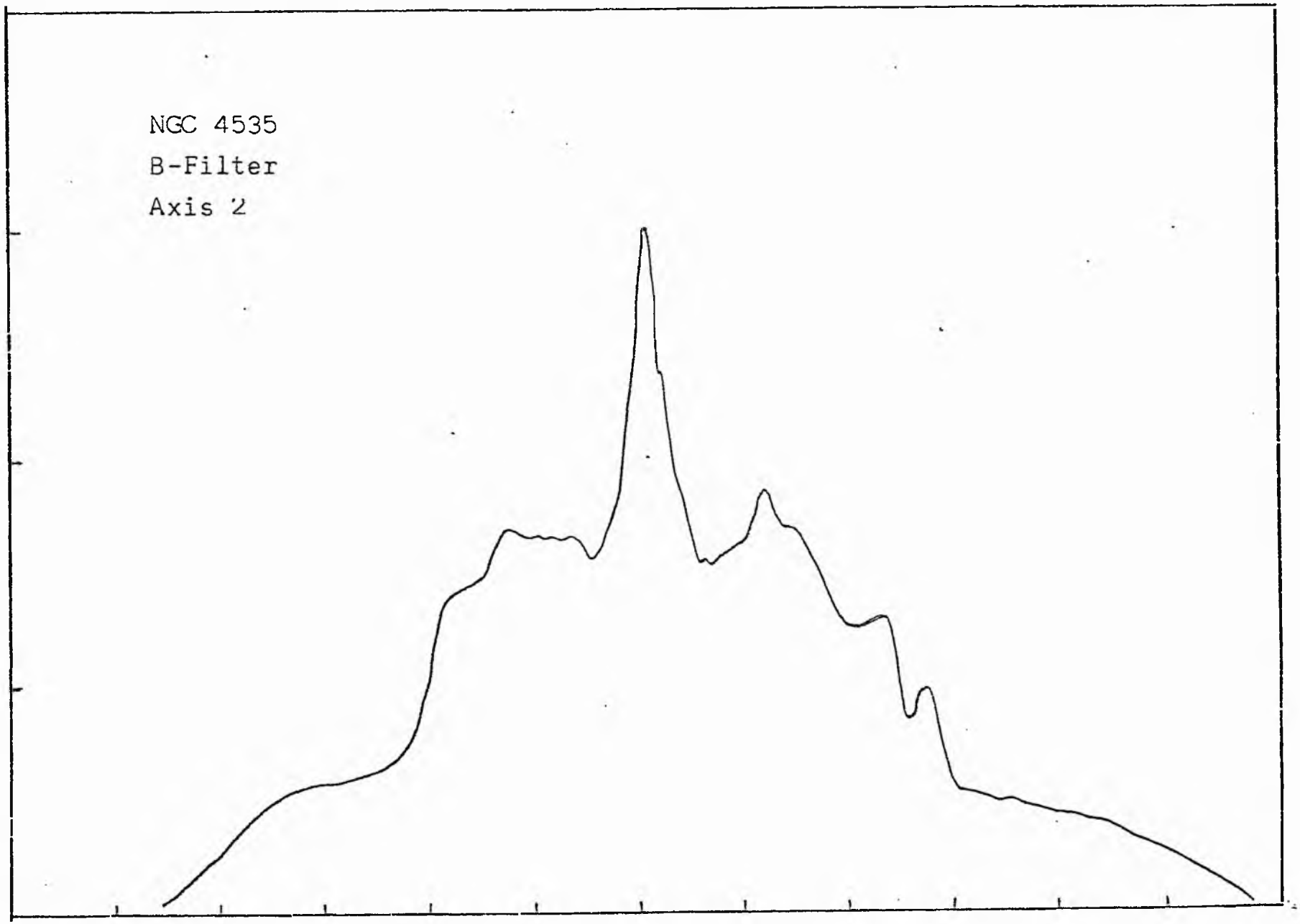
NGC 4535
B-Filter
Axis 2

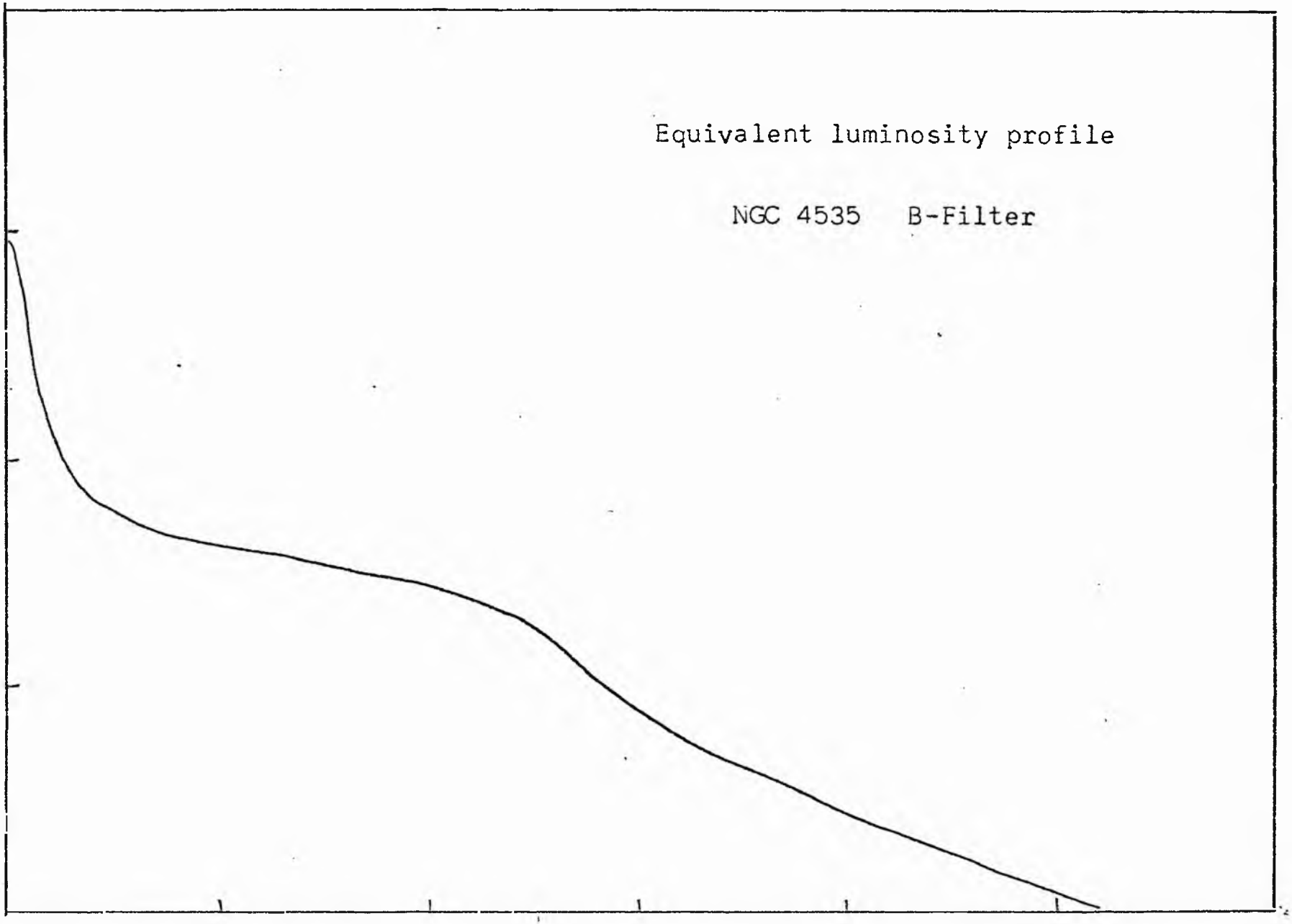
Equivalent luminosity profile
NGC 4535 B-Filter

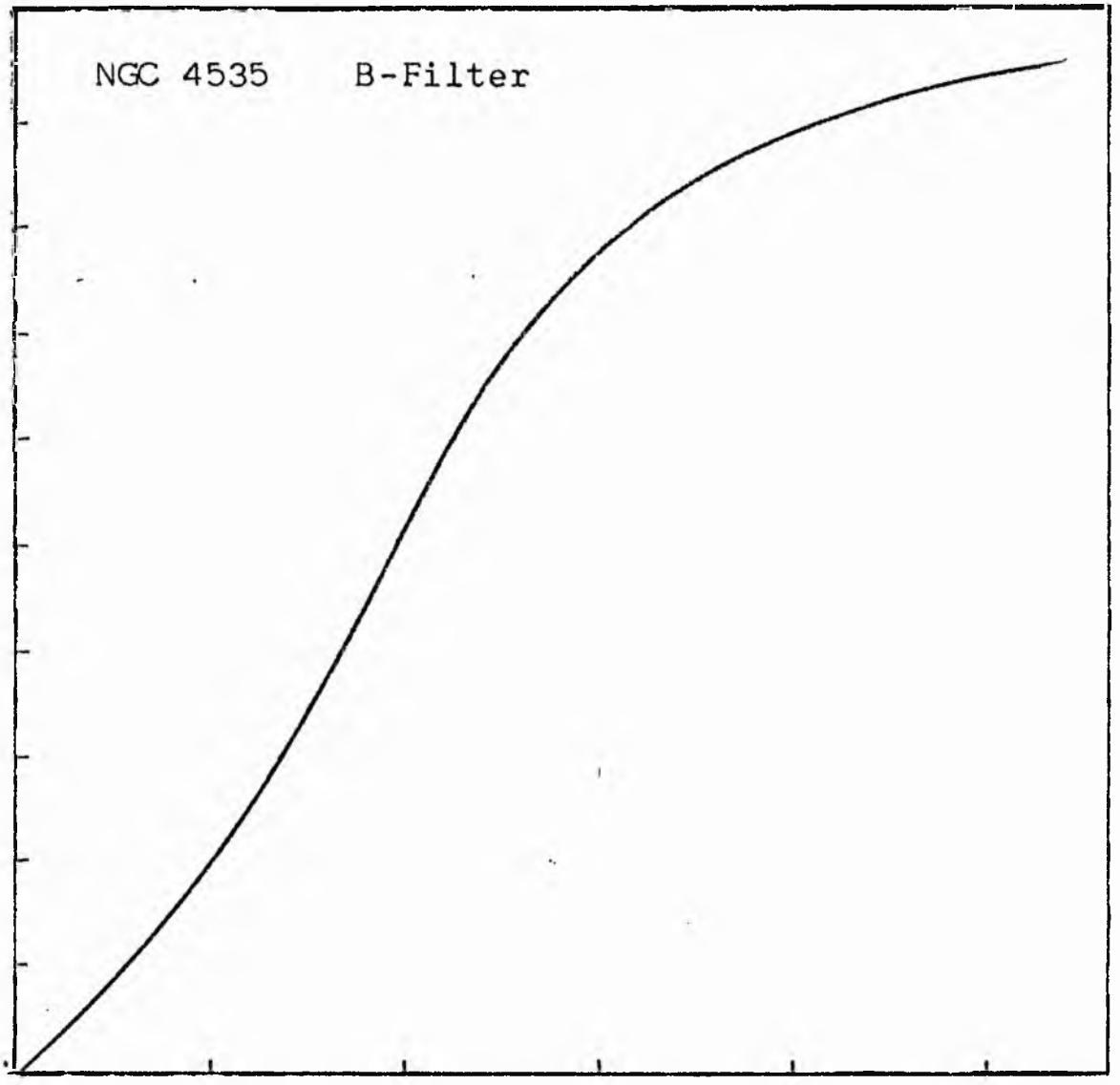

Relative integrated luminosity k(r) versus equivalent radius r*.

B COLOUR

LOG I	I	I	R	AREA	ΔA	P	ΣP	KIRI	ρ	LOG J	μ
0.92	8.318		0.0	0.0			0.0	0.0	0.0	1.465	19.16
		8.130			10.41	84.6071					
0.90	7.943		1.02	10.41			84.61	0.00	0.02	1.445	19.21
		7.126			10.18	72.5650					
0.80	6.310		2.56	20.59			157.17	0.01	0.03	1.345	19.46
		5.661			7.12	40.3209					
0.70	5.012		2.97	27.71			197.49	0.01	0.03	1.245	19.71
		4.496			17.89	80.4509					
0.60	3.981		3.81	45.60			277.94	0.01	0.04	1.145	19.96
		3.572			23.20	82.8797					
0.50	3.162		4.68	68.81			360.82	0.01	0.05	1.045	20.21
		2.837			16.14	45.7912					
0.40	2.512		5.20	84.95			406.61	0.02	0.05	0.945	20.46
		2.254			65.93	148.5692					
0.30	1.995		6.93	150.87			555.18	0.02	0.07	0.845	20.71
		1.790			95.74	171.3805					
0.20	1.585		8.86	246.61			726.56	0.03	0.09	0.745	20.96
		1.422			99.75	141.8311					
0.10	1.259		10.50	346.36			868.39	0.04	0.11	0.645	21.21
		1.129			201.03	227.0566					
0.00	1.000		13.20	547.39			1095.45	0.04	0.14	0.545	21.46
		0.897			131.40	117.9553					
-0.10	0.794		14.70	678.87			1213.41	0.05	0.16	0.445	21.71
		0.713			1100.65	784.3738					
-0.20	0.631		23.80	1779.52			1997.78	0.08	0.25	0.345	21.96
		0.566			2661.93	1506.8462					
-0.30	0.501		37.60	4441.45			3504.63	0.14	0.40	0.245	22.21
		0.450			6199.87	2787.7571					
-0.40	0.398		58.20	10641.32			6292.38	0.26	0.62	0.145	22.46
		0.357			12485.94	4459.5742					
-0.50	0.316		85.80	23127.27			10751.96	0.44	0.91	0.045	22.71
		0.284			10610.84	3010.3860					
-0.60	0.251		103.63	33738.11			13762.34	0.56	1.10	-0.055	22.96
		0.225			9120.24	2055.3174					
-0.70	0.200		116.80	42858.35			15817.66	0.65	1.23	-0.155	23.21
		0.179			6661.94	1192.5410					
-0.80	0.158		125.55	49520.29			17010.20	0.70	1.33	-0.255	23.46
		0.142			7202.09	1024.0730					
-0.90	0.126		134.37	56722.38			18034.27	0.74	1.42	-0.355	23.71
		0.113			3210.21	362.5815					
-1.00	0.100		138.12	59932.59			18396.84	0.75	1.46	-0.455	23.96
		0.090			7889.41	707.8118					
-1.10	0.079		146.93	67822.00			19104.65	0.78	1.55	-0.555	24.21
		0.071			9763.12	695.7646					
-1.20	0.063		157.15	77585.12			19800.41	0.81	1.66	-0.655	24.46
		0.057			13004.06	736.1279					
-1.30	0.050		169.81	90589.19			20536.54	0.84	1.80	-0.755	24.71
		0.045			12264.25	551.4622					
-1.40	0.040		180.94	102853.44			21088.00	0.86	1.91	-0.855	24.96
		0.036			12127.31	433.1516					
-1.50	0.032		191.31	114980.75			21521.15	0.88	2.02	-0.955	25.21
		0.028			18374.69	521.3098					
-1.60	0.025		206.03	133355.44			22042.46	0.90	2.18	-1.055	25.46
		0.023			24488.25	551.8667					
-1.70	0.020		224.15	157843.69			22594.32	0.92	2.37	-1.155	25.71
		0.018			19242.37	344.4575					
-1.80	0.016		237.42	177086.06			22938.78	0.94	2.51	-1.255	25.96
		0.014			14889.87	211.7234					
-1.90	0.013		247.20	191975.94			23150.50	0.95	2.61	-1.355	26.21
		0.011			18765.25	211.9496					
-2.00	0.010		259.00	210741.19			23362.45	0.96	2.74	-1.455	26.46
$-\infty$							24442.00	(1)			∞

PHOTOMETRIC PARAMETERS OF NGC 4535

B-FILTER

Total luminosity	L_T	= 6.79
Total apparent magnitude	m_T	= 10.49
Apparent central surface brightness	μ_o	= 19.16
Major axis at threshold	$2a_m$	= 9.37
Minor axis at threshold	$2b_m$	= 8.85
Major axis at μ=25.0 mag sec^{-2}	2a(25)	= 6.95
Luminosity within μ=25.0 mag sec^{-2}	k(25)	= 0.87
Gradient of exponential component	G(a)	= -0.41
Equivalent gradient of exponential comp.	G(r*)	= -0.47
Equivalent gradient of reduced exp. comp.	G(ρ)	= -0.79
Parameters at k = ¼ :		
Semi-major axis	a_1	= 0.96
Axis ratio	b/a	= 0.74
Equivalent radius	r_1*	= 0.94
Surface brightness	μ_1	= 22.44
Parameters at k = ½(effective) :		
Semi-major axis	a_e	= 1.61
Axis ratio	b/a	= 0.78
Equivalent radius	r_e*	= 1.58
Surface brightness	μ_e	= 22.83
Mean surface brightness	μ_e'	= 13.48
Parameters at k = ¾ :		
Semi-major axis	a_3	= 2.68
Axis ratio	b/a	= 0.73
Equivalent radius	r_3*	= 2.29
Surface brightness	μ_3	= 23.96
Concentration indices	C_{21}	= 1.66
	C_{32}	= 1.45

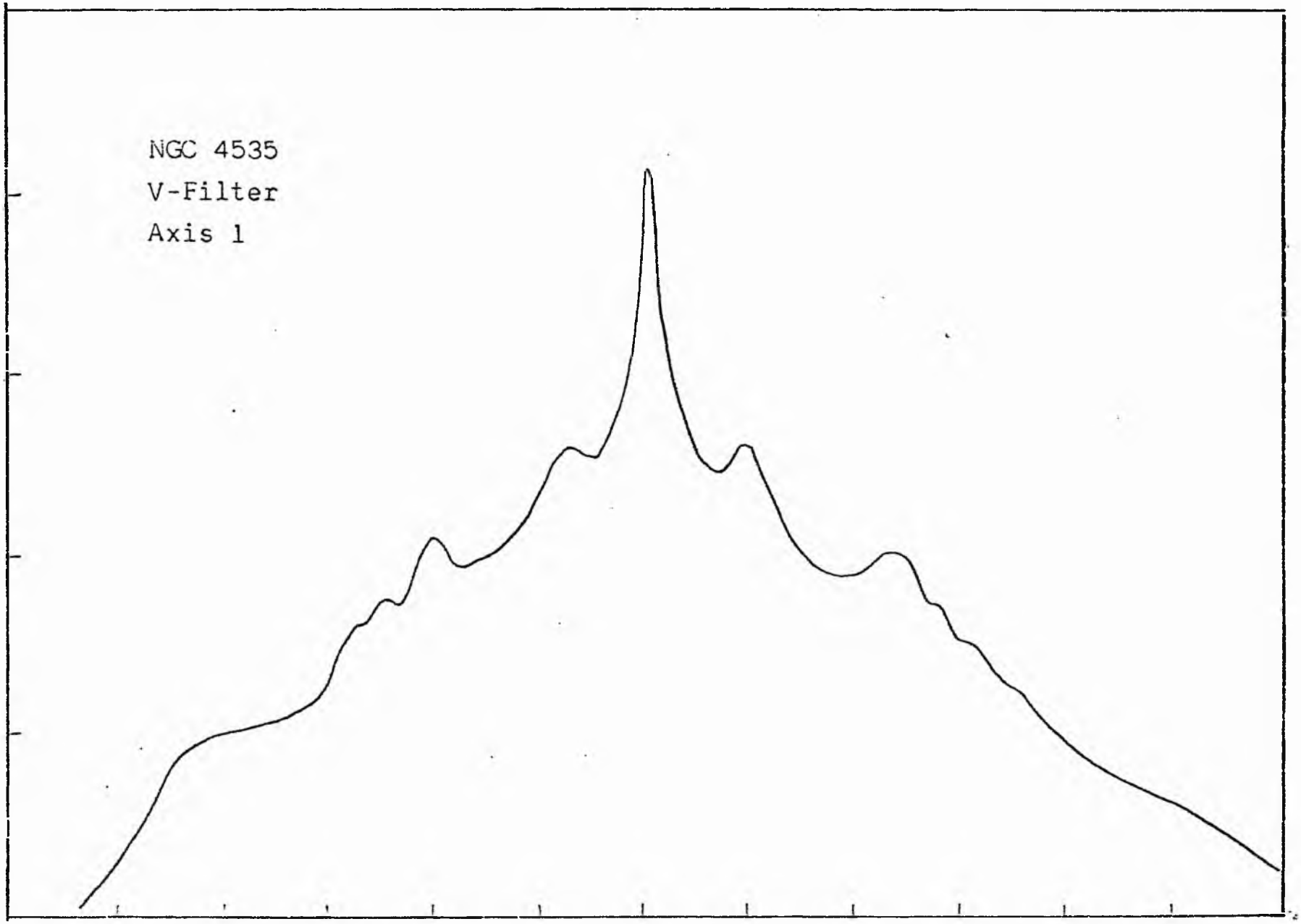
NGC 4535
V-Filter
Axis 1

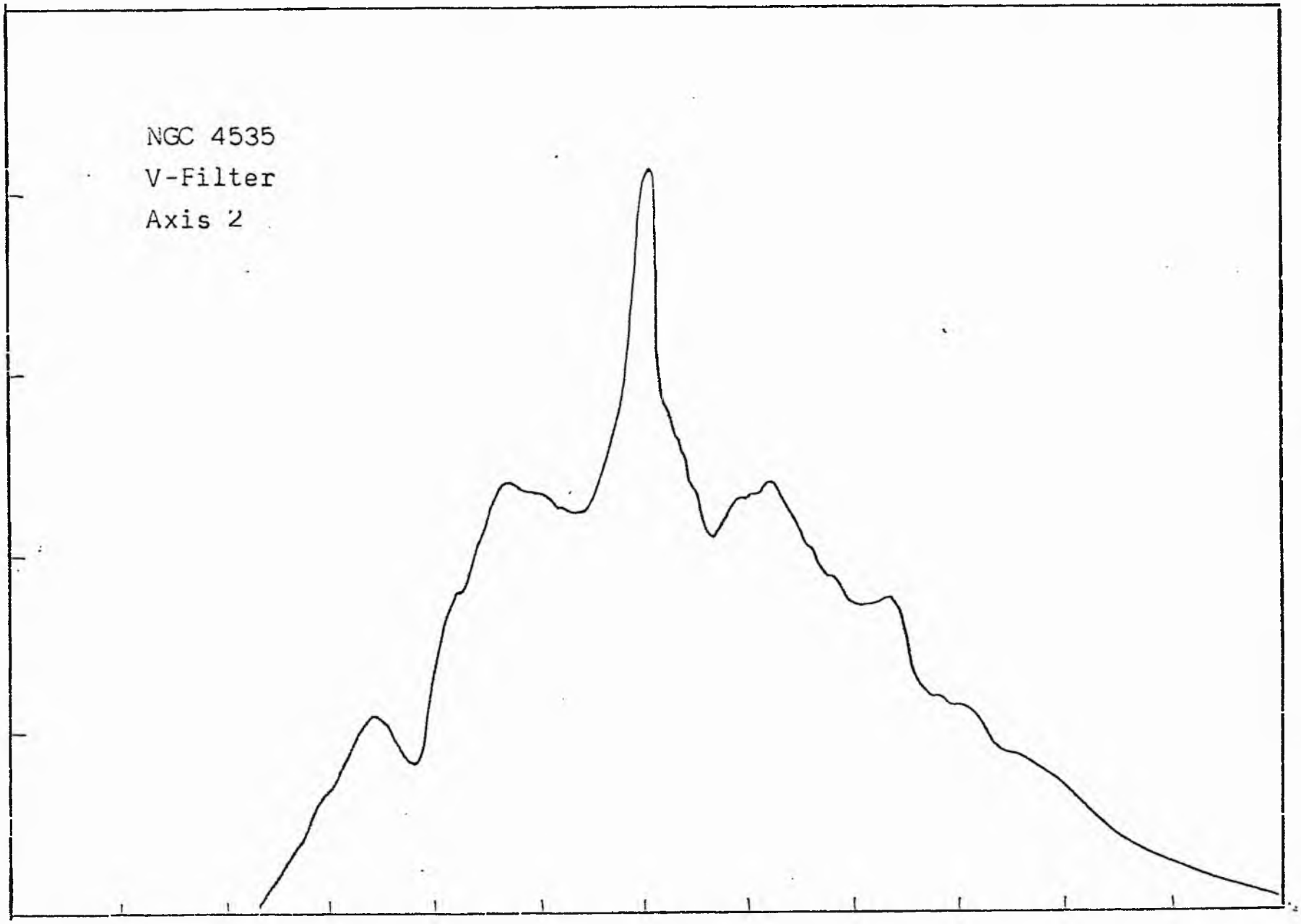
NGC 4535
V-Filter
Axis 2

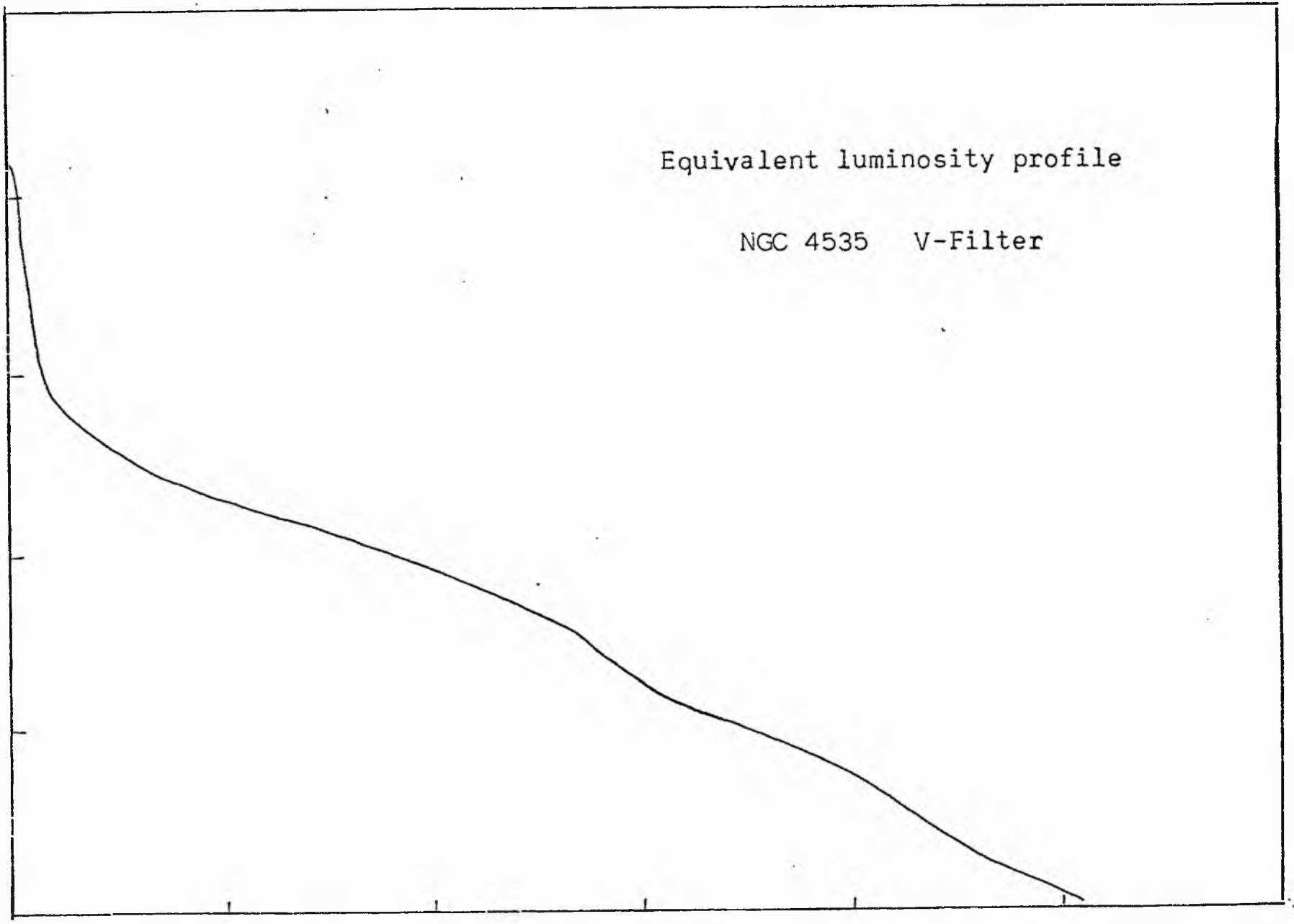
Equivalent luminosity profile
NGC 4535 V-Filter

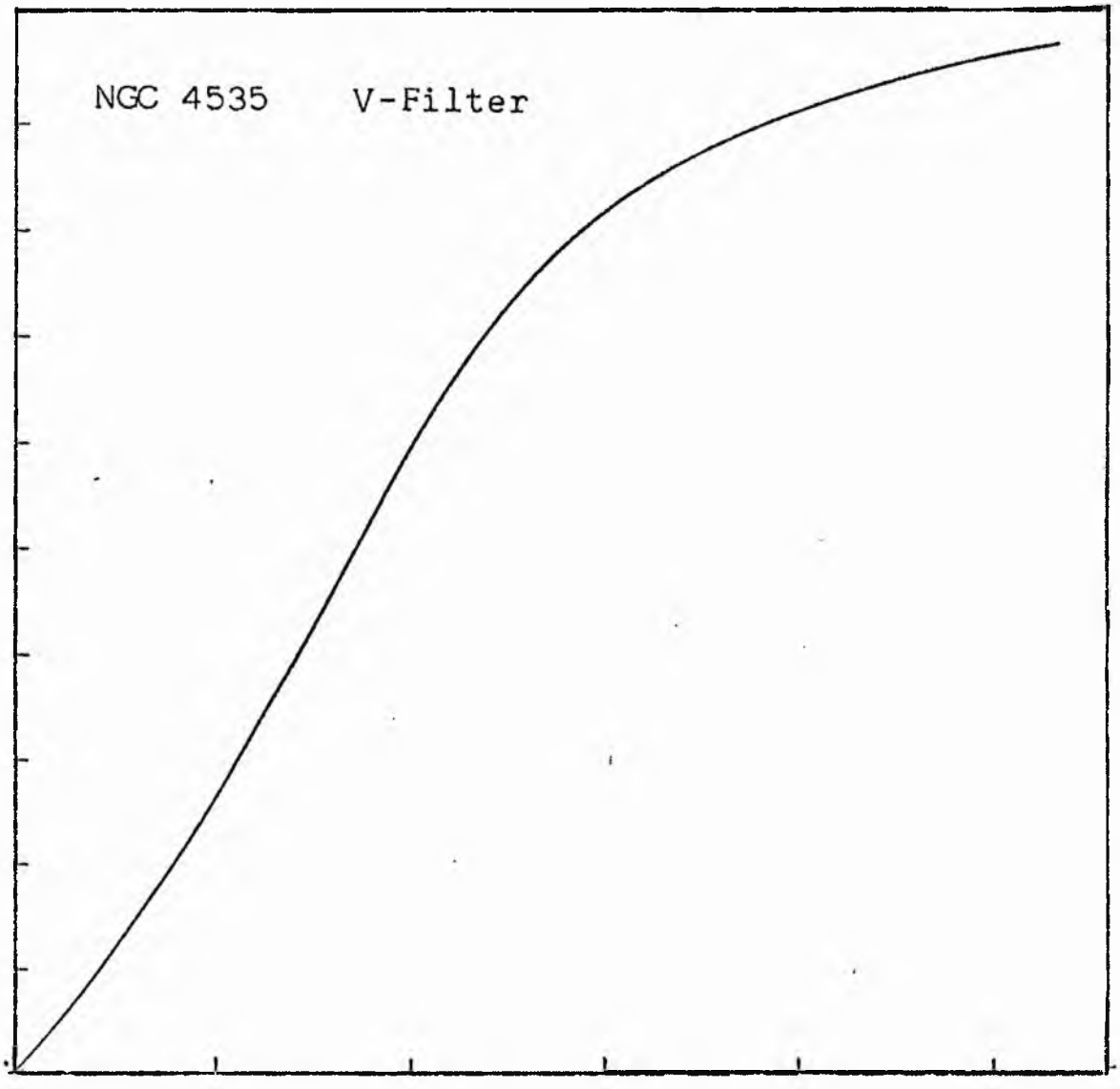

Relative integrated luminosity k(r) versus equivalent radius r*.

MEAN LUMINOSITY DISTRIBUTION IN NGC 4535
V COLOUR

LOG I	I	$\bar{I}$	R	AREA	ΔA	P	ΣP	K(R)	ρ	LOG μ	μ
1.23	16.982		0.0	0.0			0.0	0.0	0.0	1.617	17.98
		16.416			10.41	170.8248					
1.20	15.849		1.82	10.41			170.82	0.01	0.02	1.587	18.06
		14.219			10.02	142.5033					
1.10	12.589		2.55	20.43			313.33	0.01	0.03	1.487	18.31
		11.295			15.89	179.4555					
1.00	10.000		3.40	36.32			492.78	0.02	0.04	1.387	18.56
		8.972			16.49	147.9719					
0.90	7.943		4.10	52.81			640.75	0.02	0.05	1.287	18.81
		7.126			13.67	97.3892					
0.80	6.310		4.60	66.48			738.14	0.02	0.05	1.187	19.06
		5.661			15.24	86.2506					
0.70	5.012		5.10	81.71			824.39	0.03	0.06	1.087	19.31
		4.496			55.13	247.9125					
0.60	3.981		6.60	136.85			1072.31	0.03	0.08	0.987	19.56
		3.572			49.42	176.5022					
0.50	3.162		7.70	186.27			1248.81	0.04	0.09	0.887	19.81
		2.837			35.41	100.4488					
0.40	2.512		8.40	221.67			1349.26	0.04	0.10	0.787	20.06
		2.254			61.86	139.4011					
0.30	1.995		9.50	283.53			1488.66	0.05	0.11	0.687	20.31
		1.790			358.99	642.4502					
0.20	1.585		14.30	642.42			2131.11	0.07	0.17	0.587	20.56
		1.422			716.75	1019.1565					
0.10	1.259		20.80	1359.18			3150.27	0.10	0.25	0.487	20.81
		1.129			1246.58	1407.9678					
-0.00	1.000		28.80	2605.76			4558.23	0.14	0.34	0.387	21.06
		0.897			2050.86	1839.9607					
-0.10	0.794		38.50	4656.62			6398.19	0.20	0.46	0.287	21.31
		0.713			3643.33	2596.3921					
-0.20	0.631		51.40	8299.96			8994.58	0.28	0.61	0.187	21.56
		0.566			7940.84	4495.0820					
-0.30	0.501		71.90	16240.79			13489.66	0.41	0.85	0.087	21.81
		0.450			7048.48	3169.3306					
-0.40	0.398		86.10	23289.28			16658.99	0.51	1.02	-0.013	22.06
		0.357			7067.58	2524.3093					
-0.50	0.316		98.30	30356.86			19183.30	0.59	1.16	-0.113	22.31
		0.284			9262.67	2627.8960					
-0.60	0.251		112.30	39619.52			21811.19	0.67	1.33	-0.213	22.56
		0.225			9075.95	2045.3342					
-0.70	0.200		124.50	48695.48			23856.52	0.73	1.47	-0.313	22.81
		0.179			8221.25	1471.6687					
-0.80	0.158		134.60	56916.73			25328.19	0.78	1.59	-0.413	23.06
		0.142			3433.13	488.1604					
-0.90	0.126		138.60	60349.86			25816.35	0.79	1.64	-0.513	23.31
		0.113			4613.36	521.0615					
-1.00	0.100		143.80	64963.22			26337.41	0.81	1.70	-0.613	23.56
		0.090			11392.53	1022.0979					
-1.10	0.079		155.90	76355.75			27359.51	0.84	1.85	-0.713	23.81
		0.071			16153.31	1151.1567					
-1.20	0.063		171.60	92509.06			28510.66	0.87	2.03	-0.813	24.06
		0.057			15710.50	889.3303					
-1.30	0.050		185.60	108219.56			29399.99	0.90	2.20	-0.913	24.31
		0.045			14682.31	660.1887					
-1.40	0.040		197.79	122901.87			30060.18	0.92	2.34	-1.013	24.56
		0.036			13120.50	468.6240					
-1.50	0.032		208.08	136022.37			30528.80	0.94	2.47	-1.113	24.81
		0.028			3552.94	100.8005					
-1.60	0.025		210.78	139575.31			30629.60	0.94	2.50	-1.213	25.06
		0.023			12560.69	283.0669					
-1.70	0.020		220.06	152136.00			30912.66	0.95	2.61	-1.313	25.31
		0.018			16505.44	295.4631					
-1.80	0.016		231.69	168641.44			31208.12	0.96	2.74	-1.413	25.56
		0.014			20965.44	298.1128					
-1.90	0.013		245.67	189606.87			31506.23	0.97	2.91	-1.513	25.81
		0.011			13076.12	147.6918					
-2.00	0.010		254.00	202683.00			31653.93	0.97	3.01	-1.613	26.06
- ∞							32593.00	(1)			∞

PHOTOMETRIC PARAMETERS OF NGC 4535

V-FILTER

Total luminosity	L_T	= 9.05
Total apparent magnitude	m_T	= 9.78
Apparent central surface brightness	μ_o	= 17.98
Major axis at threshold	$2a_m$	= 10.07
Minor axis at threshold	$2b_m$	= 7.97
Major axis at μ=25.0 mag sec^{-2}	2a(25)	= 8.57
Luminosity within μ=25.0 mag sec^{-2}	k(25)	= 0.94
Gradient of exponential component	G(a)	= -0.45
Equivalent gradient of exponential comp.	G(r*)	= -0.50
Equivalent gradient of reduced exp. comp.	G(ρ)	= -0.75
Parameters at k = ¼ :		
Semi-major axis	a_1	= 0.85
Axis ratio	b/a	= 0.92
Equivalent radius	r_1*	= 0.78
Surface brightness	μ_1	= 21.46
Parameters at k = ½(effective) :		
Semi-major axis	a_e	= 1.36
Axis ratio	b/a	= 0.93
Equivalent radius	r_e*	= 1.41
Surface brightness	μ_e	= 22.03
Mean surface brightness	μ_e'	= 12.52
Parameters at k = ¾ :		
Semi-major axis	a_3	= 2.23
Axis ratio	b/a	= 0.85
Equivalent radius	r_3*	= 2.14
Surface brightness	μ_3	= 22.91
Concentration indices	C_{21}	= 1.79
	C_{32}	= 1.52

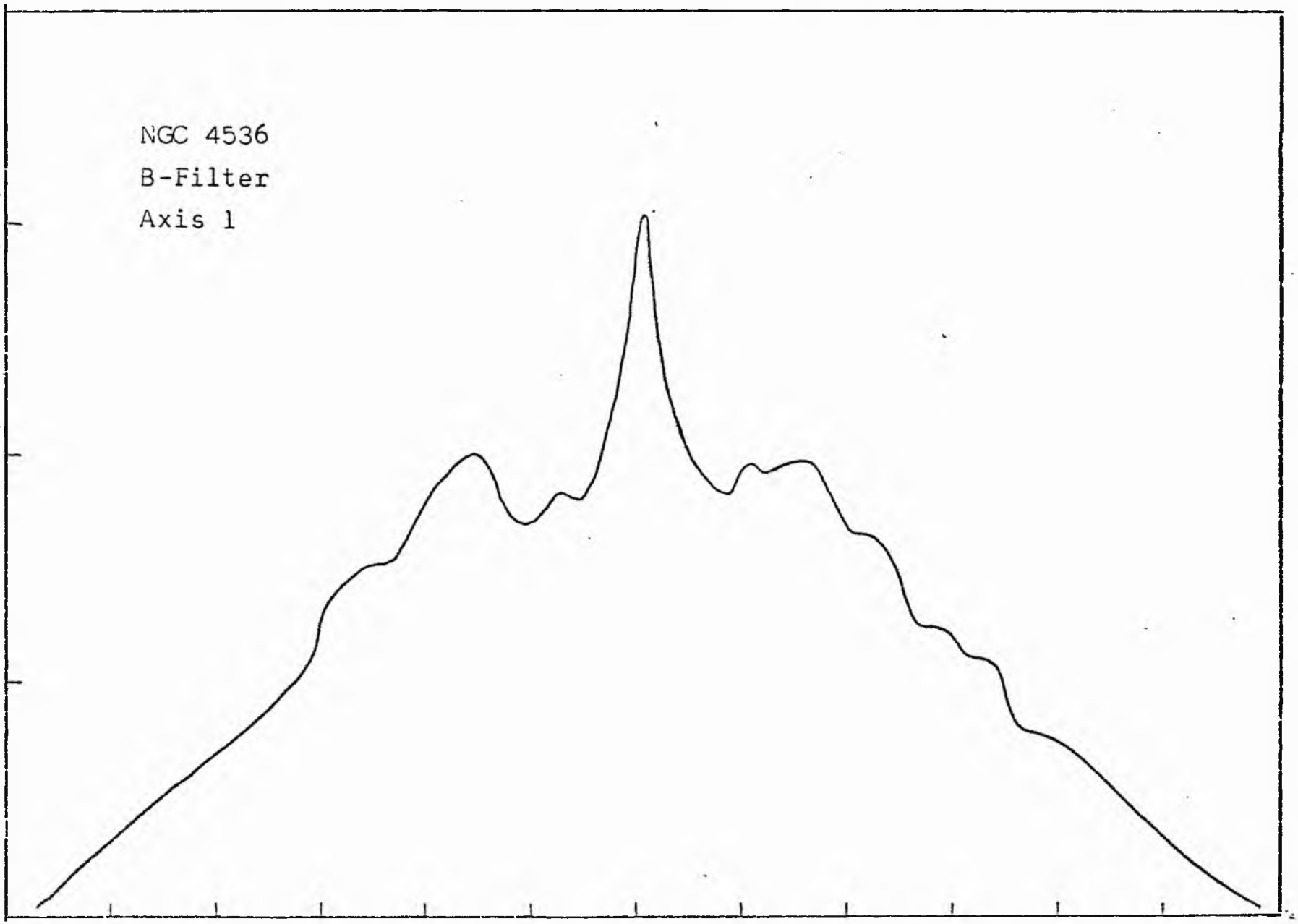
NGC 4536
B-Filter
Axis 1

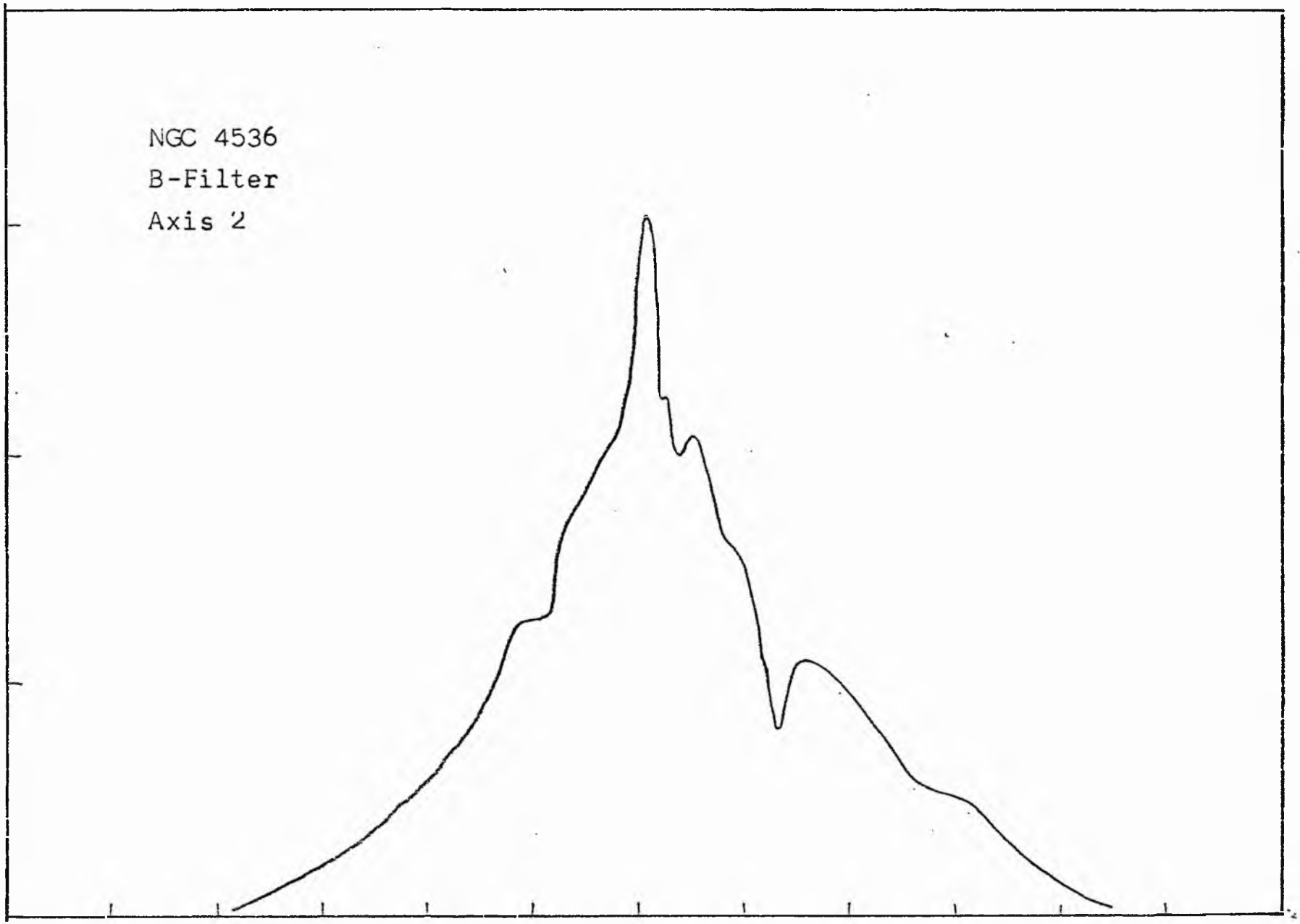
NGC 4536
B-Filter
Axis 2

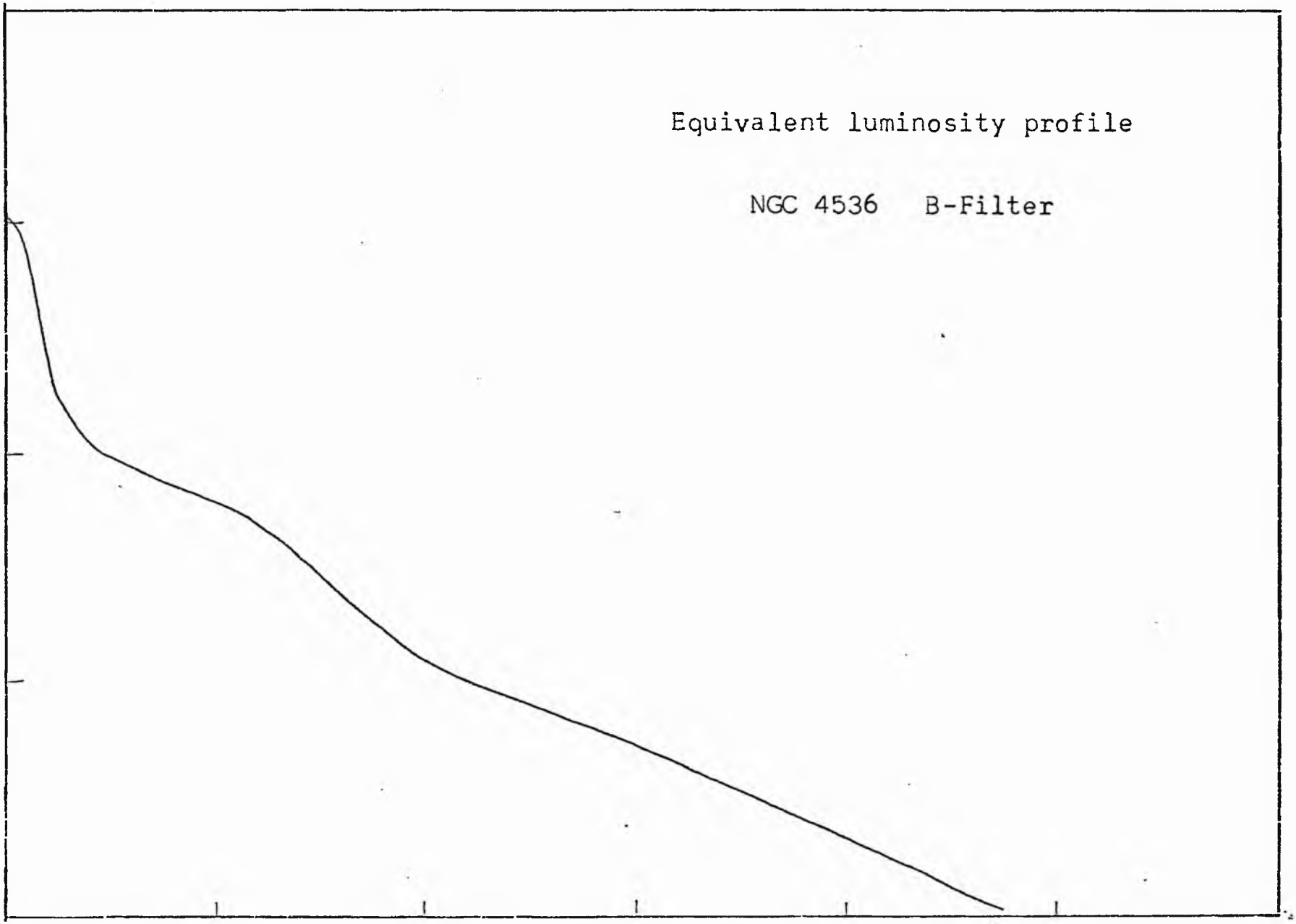
Equivalent luminosity profile
NGC 4536 B-Filter

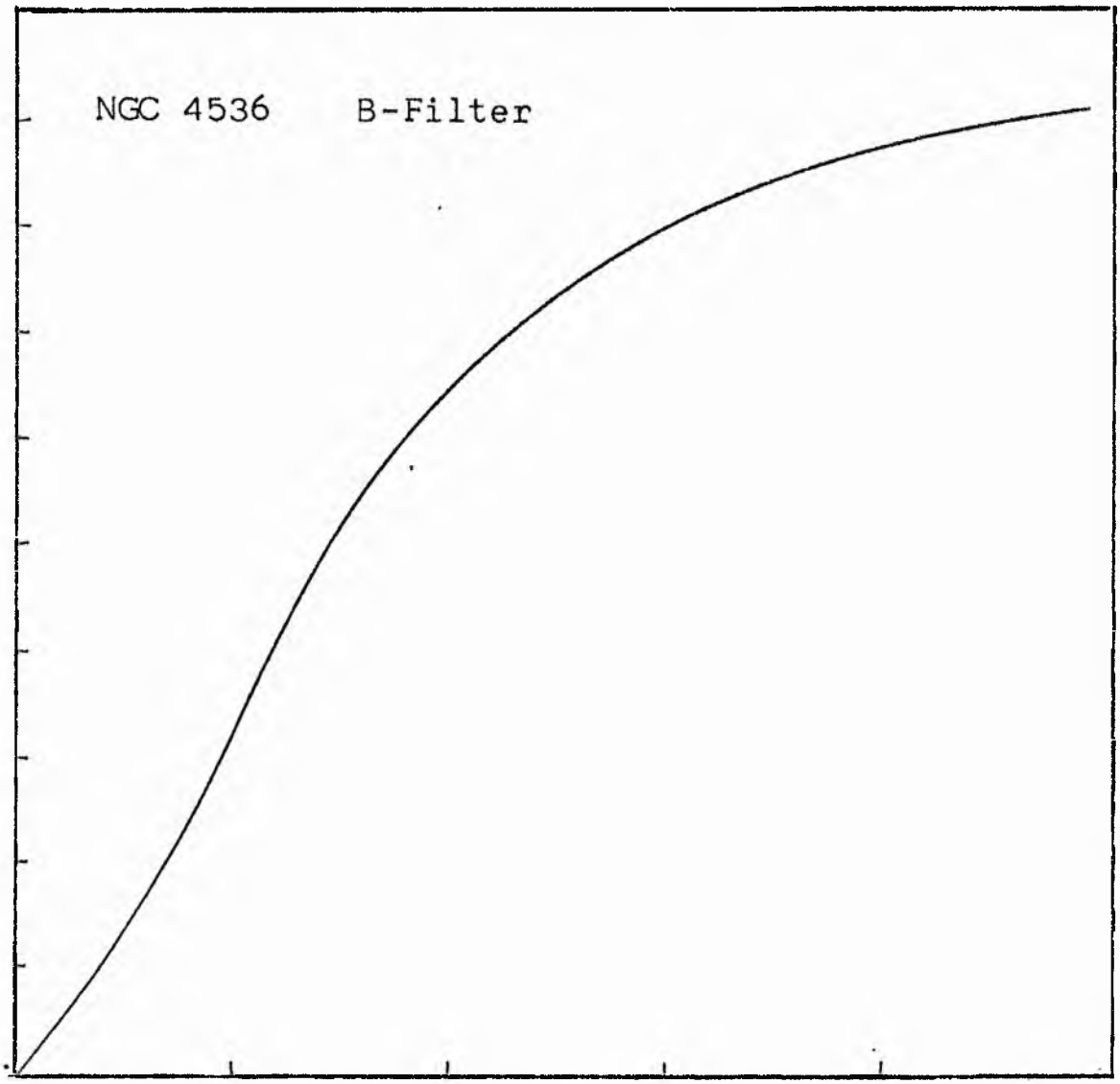

Relative integrated luminosity k(r) versus equivalent radius r*.

LOG I	I	$\bar{I}$	R	AREA	ΔA	P	ΣP	K(R)	ρ	LOG J	μ
0.98	9.550		0.0	0.0			0.0	0.0	0.0	1.402	19.48
		8.747			70.29	614.7676					
0.90	7.943		4.73	70.29			614.77	0.03	0.07	1.322	19.68
		7.126			2.10	14.9350					
0.80	6.310		4.80	72.38			629.70	0.03	0.07	1.222	19.93
		5.661			38.98	209.3140					
0.70	5.012		5.90	109.36			839.02	0.03	0.09	1.122	20.18
		4.496			67.36	302.8633					
0.60	3.981		7.50	176.71			1141.88	0.05	0.11	1.022	20.43
		3.572			19.35	69.1196					
0.50	3.162		7.90	196.07			1211.00	0.05	0.12	0.922	20.68
		2.837			10.05	28.5214					
0.40	2.512		8.10	206.12			1239.52	0.05	0.12	0.822	20.93
		2.254			120.73	272.0767					
0.30	1.995		10.20	326.85			1511.60	0.06	0.15	0.722	21.18
		1.790			195.94	350.7498					
0.20	1.585		12.90	522.79			1862.35	0.08	0.19	0.622	21.43
		1.422			395.84	562.8486					
0.10	1.259		17.10	918.63			2425.20	0.10	0.25	0.522	21.68
		1.129			1108.20	1251.6672					
0.00	1.000		25.40	2026.83			3676.88	0.15	0.37	0.422	21.93
		0.897			3228.46	2896.4573					
-0.10	0.794		40.90	5255.29			6573.32	0.27	0.60	0.322	22.18
		0.713			4110.30	2929.1775					
-0.20	0.631		54.60	9365.59			9502.50	0.39	0.80	0.222	22.43
		0.566			1790.11	1013.3293					
-0.30	0.501		59.59	11155.69			10515.82	0.44	0.87	0.122	22.68
		0.450			2795.77	1257.1091					
-0.40	0.398		66.64	13951.46			11772.93	0.49	0.97	0.022	22.93
		0.357			4385.88	1566.4963					
-0.50	0.316		76.40	18337.34			13339.43	0.55	1.12	-0.078	23.18
		0.284			2941.56	834.5464					
-0.60	0.251		82.30	21278.90			14173.97	0.59	1.20	-0.178	23.43
		0.225			2828.92	637.5186					
-0.70	0.200		87.60	24107.82			14811.48	0.61	1.28	-0.278	23.68
		0.179			2540.45	454.7660					
-0.80	0.158		92.10	26648.27			15266.24	0.63	1.35	-0.378	23.93
		0.142			8252.18	1173.3865					
-0.90	0.126		105.40	34900.45			16439.62	0.68	1.54	-0.478	24.18
		0.113			10037.39	1133.6882					
-1.00	0.100		119.60	44937.84			17573.31	0.73	1.75	-0.578	24.43
		0.090			6856.21	615.1160					
-1.10	0.079		128.40	51794.04			18188.43	0.75	1.88	-0.678	24.68
		0.071			9517.55	678.2642					
-1.20	0.063		139.70	61311.60			18866.69	0.78	2.04	-0.778	24.93
		0.057			11558.53	654.2998					
-1.30	0.050		152.30	72870.12			19520.98	0.81	2.23	-0.878	25.18
		0.045			13074.87	587.9121					
-1.40	0.040		165.40	85945.00			20108.89	0.83	2.42	-0.978	25.43
		0.036			11933.75	426.2380					
-1.50	0.032		176.51	97878.75			20535.13	0.85	2.58	-1.078	25.68
		0.028			14781.87	419.3777					
-1.60	0.025		189.37	112660.62			20954.50	0.87	2.77	-1.178	25.93
		0.023			10751.31	242.2914					
-1.70	0.020		198.20	123411.94			21196.79	0.88	2.90	-1.278	26.18
		0.018			19212.62	343.9250					
-1.80	0.016		213.07	142624.56			21540.71	0.89	3.12	-1.378	26.43
		0.014			18403.87	261.6899					
-1.90	0.013		226.40	161028.44			21802.40	0.90	3.31	-1.478	26.68
		0.011			27699.62	312.8613					
-2.00	0.010		245.10	188728.06			22115.26	0.92	3.58	-1.578	26.93
$-\infty$							24135.00	(1)			∞

PHOTOMETRIC PARAMETERS OF NGC 4536

B-FILTER

Total luminosity	L_T	= 6.70
Total apparent magnitude	m_T	= 10.96
Apparent central surface brightness	μ_o	= 19.48
Major axis at threshold	$2a_m$	= 9.75
Minor axis at threshold	$2b_m$	= 7.06
Major axis at μ=25.0 mag sec^{-2}	2a(25)	= 6.64
Luminosity within μ=25.0 mag sec^{-2}	k(25)	= 0.79
Gradient of exponential component	G(a)	= -0.44
Equivalent gradient of exponential comp.	G(r*)	= -0.57
Equivalent gradient of reduced exp. comp.	G(ρ)	= -0.67

Parameters at k = ¼ :

Semi-major axis	a_1	= 0.90
Axis ratio	b/a	= 0.41
Equivalent radius	r_1*	= 0.64
Surface brightness	μ_1	= 22.14

Parameters at k = ½(effective) :

Semi-major axis	a_e	= 1.93
Axis ratio	b/a	= 0.31
Equivalent radius	r_e*	= 1.14
Surface brightness	μ_e	= 22.98
Mean surface brightness	μ_e'	= 13.24

Parameters at k = ¾ :

Semi-major axis	a_3	= 2.92
Axis ratio	b/a	= 0.41
Equivalent radius	r_3*	= 2.12
Surface brightness	μ_3	= 24.68

Concentration indices	C_{21}	= 1.79
	C_{32}	= 1.86

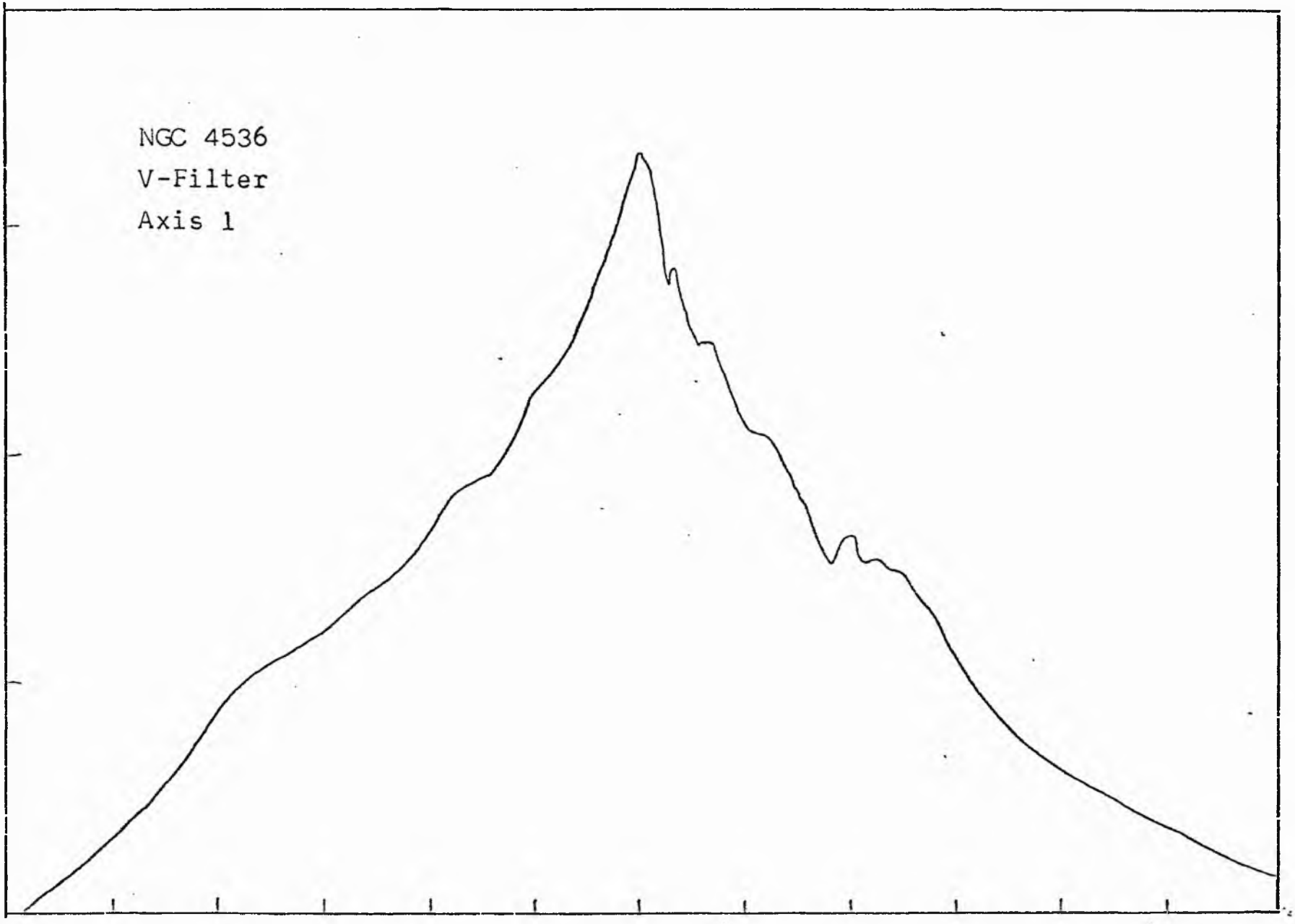
NGC 4536
V-Filter
Axis 1

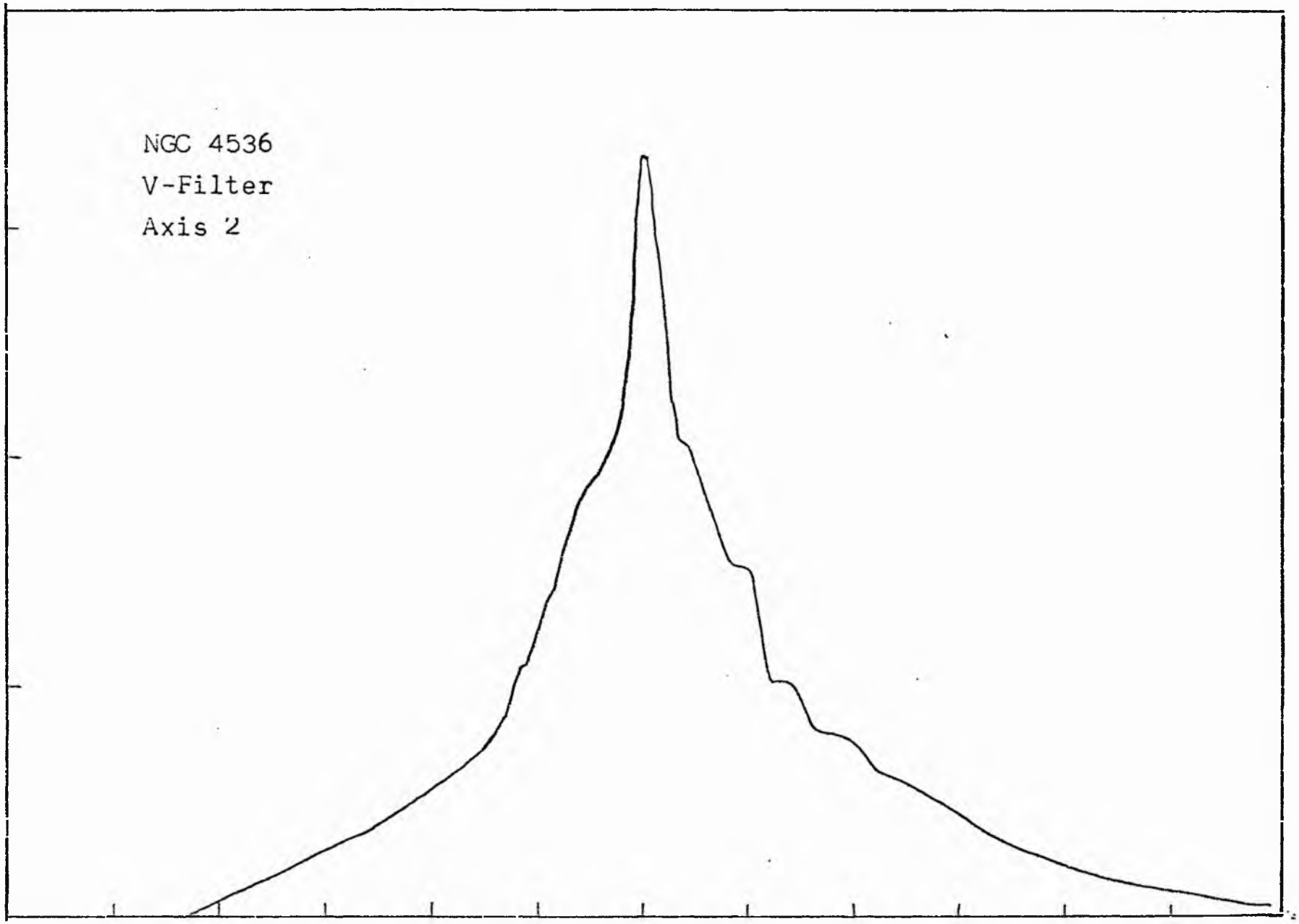
NGC 4536
V-Filter
Axis 2

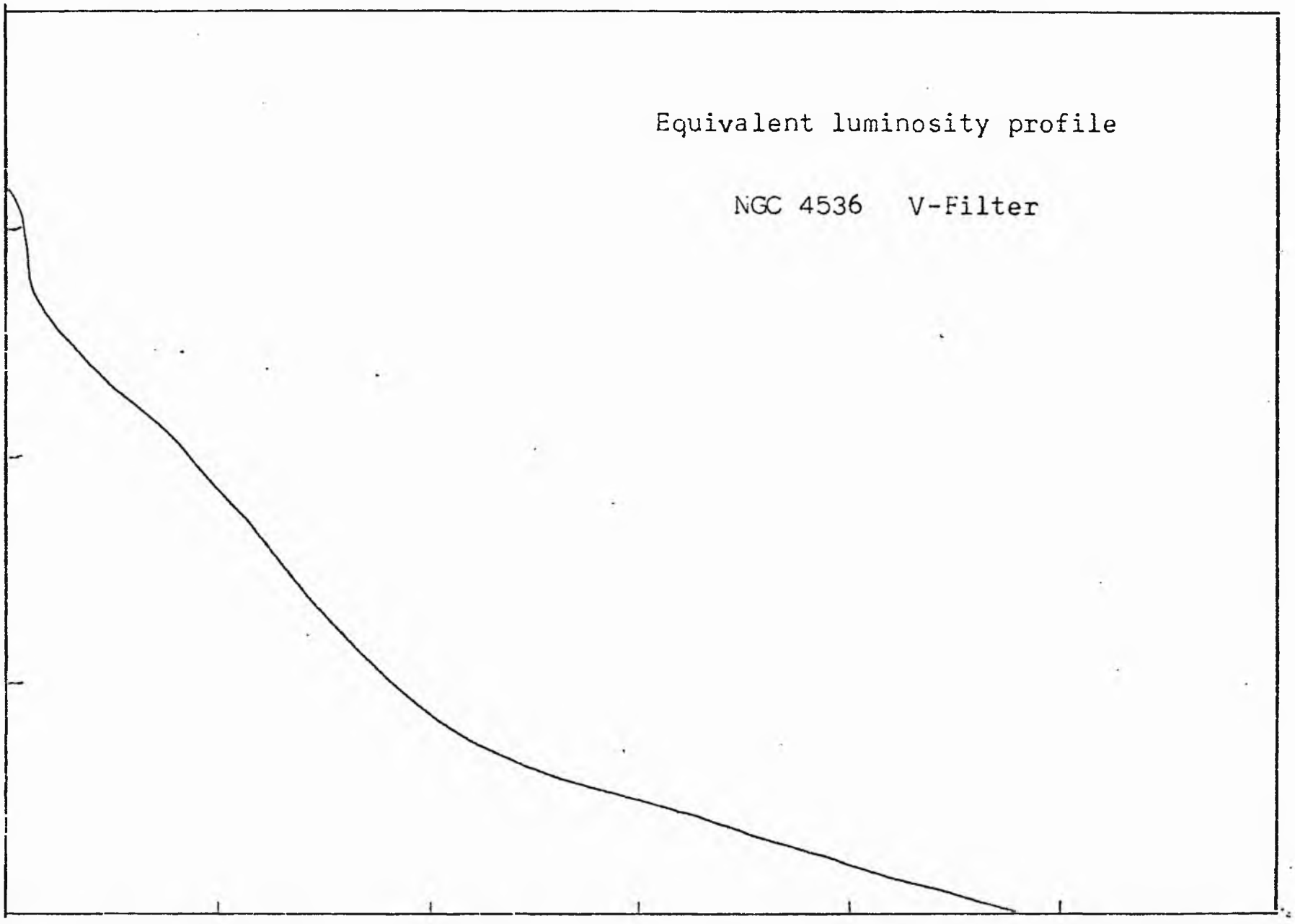
Equivalent luminosity profile
NGC 4536 V-Filter

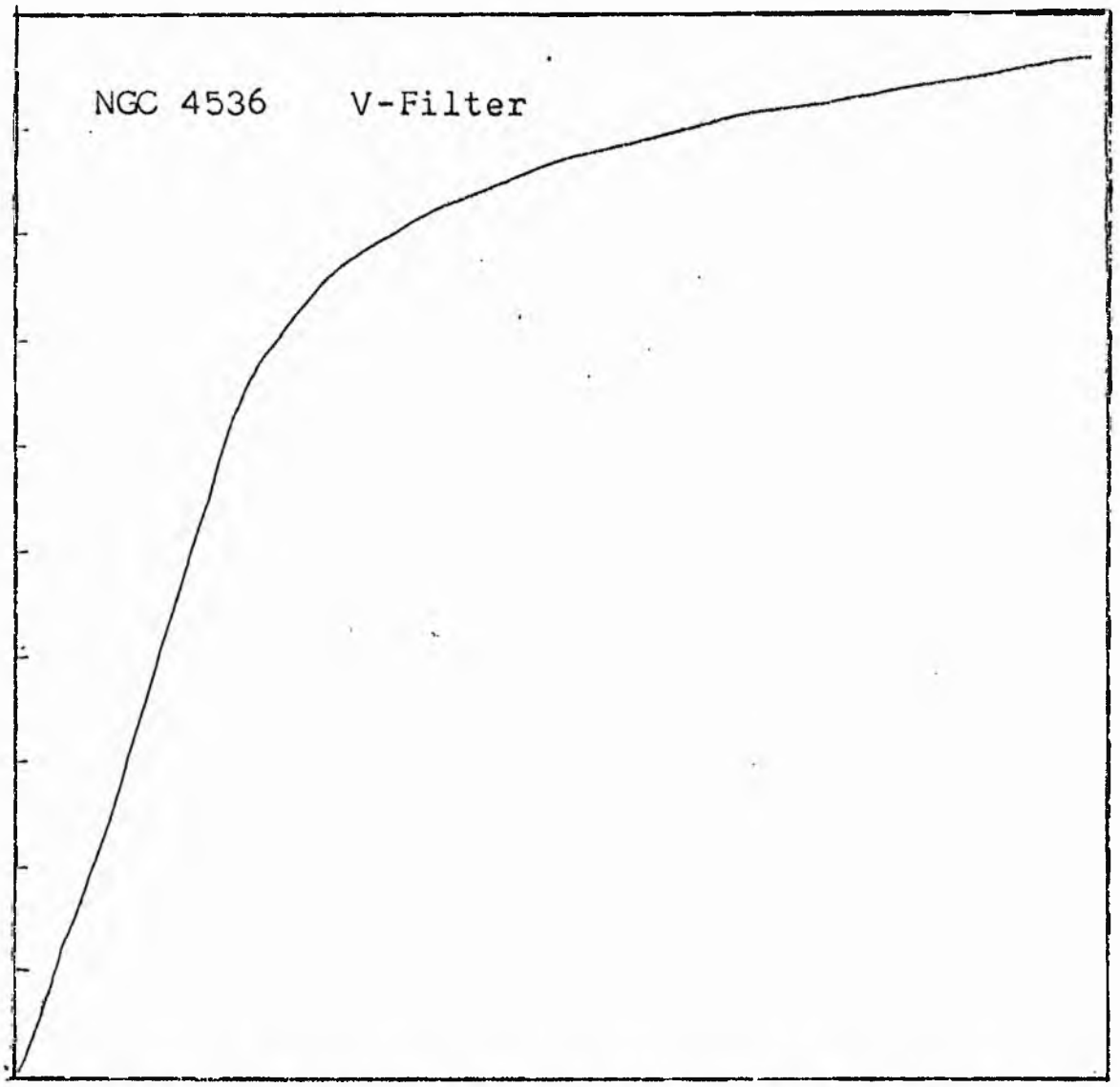

Relative integrated luminosity k(r) versus equivalent radius r*.

MEAN LUMINOSITY DISTRIBUTION IN NGC 4536
V COLOUR

LOG I	I	$\bar{I}$	R	AREA	ΔA	P	ΣP	K(R)	ρ	LOG J	μ
1.26	18.197		0.0	0.0			0.0	0.0	0.0	1.059	18.60
		17.023			66.48	1131.6184					
1.20	15.849		4.60	66.48			1131.62	0.03	0.11	0.999	18.75
		14.219			83.10	1181.5354					
1.10	12.589		6.90	149.57			2313.15	0.07	0.16	0.899	19.00
		11.295			36.69	414.4421					
1.00	10.000		7.70	186.27			2727.60	0.08	0.18	0.799	19.25
		8.972			19.85	178.1302					
0.90	7.943		8.10	206.12			2905.73	0.08	0.19	0.699	19.50
		7.126			42.73	304.4810					
0.80	6.310		8.90	248.85			3210.21	0.09	0.21	0.599	19.75
		5.661			59.06	334.3311					
0.70	5.012		9.90	307.91			3544.54	0.10	0.23	0.499	20.00
		4.496			361.75	1626.6169					
0.60	3.981		14.60	669.66			5171.15	0.15	0.34	0.399	20.25
		3.572			729.00	2603.7644					
0.50	3.162		21.10	1398.67			7774.91	0.22	0.50	0.299	20.50
		2.837			1225.22	3476.0488					
0.40	2.512		28.90	2623.89			11250.96	0.32	0.68	0.199	20.75
		2.254			1607.49	3622.5967					
0.30	1.995		36.70	4231.38			14873.55	0.43	0.87	0.099	21.00
		1.790			1416.45	2535.5449					
0.20	1.585		42.40	5647.82			17409.10	0.50	1.00	-0.001	21.25
		1.422			1174.33	1669.7869					
0.10	1.259		46.60	6822.15			19078.88	0.55	1.10	-0.101	21.50
		1.129			1126.36	1272.1748					
-0.00	1.000		50.30	7948.51			20351.05	0.59	1.19	-0.201	21.75
		0.897			1798.25	1613.3240					
-0.10	0.794		55.70	9746.76			21964.37	0.63	1.32	-0.301	22.00
		0.713			1300.62	926.8745					
-0.20	0.631		59.30	11047.37			22891.25	0.66	1.40	-0.401	22.25
		0.566			1303.13	737.6667					
-0.30	0.501		62.70	12350.51			23628.91	0.68	1.48	-0.501	22.50
		0.450			1668.03	750.0237					
-0.40	0.398		66.80	14018.54			24378.93	0.70	1.58	-0.601	22.75
		0.357			2403.46	858.4395					
-0.50	0.316		72.30	16422.00			25237.37	0.73	1.71	-0.701	23.00
		0.284			2937.28	833.3311					
-0.60	0.251		78.50	19359.28			26070.70	0.75	1.85	-0.801	23.25
		0.225			2597.18	585.2930					
-0.70	0.200		83.60	21956.46			26655.99	0.77	1.97	-0.901	23.50
		0.179			2482.74	444.4302					
-0.80	0.158		88.20	24439.20			27100.42	0.78	2.08	-1.001	23.75
		0.142			3497.37	497.2939					
-0.90	0.126		94.30	27936.57			27597.71	0.79	2.23	-1.101	24.00
		0.113			3228.52	364.6497					
-1.00	0.100		99.60	31165.09			27962.36	0.80	2.35	-1.201	24.25
		0.090			7751.97	695.4792					
-1.10	0.079		111.30	38917.06			28657.84	0.82	2.63	-1.301	24.50
		0.071			6851.20	488.2468					
-1.20	0.063		120.70	45768.26			29146.09	0.84	2.85	-1.401	24.75
		0.057			12680.94	717.8350					
-1.30	0.050		136.40	58449.20			29863.92	0.86	3.22	-1.501	25.00
		0.045			13372.11	601.2756					
-1.40	0.040		151.20	71821.31			30465.19	0.88	3.57	-1.601	25.25
		0.036			16214.75	579.1414					
-1.50	0.032		167.40	88036.06			31044.33	0.89	3.95	-1.701	25.50
		0.028			21001.31	595.8289					
-1.60	0.025		186.30	109037.37			31640.16	0.91	4.40	-1.801	25.75
		0.023			19660.31	443.0637					
-1.70	0.020		202.40	128697.69			32083.22	0.92	4.78	-1.901	26.00
		0.018			32330.75	578.7515					
-1.80	0.016		226.40	161028.44			32661.97	0.94	5.35	-2.001	26.25
		0.014			37368.44	531.3511					
-1.90	0.013		251.30	198396.87			33193.32	0.95	5.93	-2.101	26.50
		0.011			38840.12	438.6899					
-2.00	0.010		274.80	237237.00			33632.01	0.97	6.49	-2.201	26.75
$-\infty$							34782.00	(1)			∞

PHOTOMETRIC PARAMETERS OF NGC 4536

V-FILTER

Total luminosity	L_T	= 9.66
Total apparent magnitude	m_T	= 10.40
Apparent central surface brightness	μ_o	= 18.60
Major axis at threshold	$2a_m$	= 10.37
Minor axis at threshold	$2b_m$	= 8.18
Major axis at μ=25.0 mag sec^{-2}	2a(25)	= 6.34
Luminosity within μ=25.0 mag sec^{-2}	k(25)	= 0.86
Gradient of exponential component	G(a)	= -0.57
Equivalent gradient of exponential comp.	G(r*)	= -0.52
Equivalent gradient of reduced exp. comp.	G(ρ)	= -0.80
Parameters at k = ¼ :		
Semi-major axis	a_1	= 0.43
Axis ratio	b/a	= 0.21
Equivalent radius	r_1*	= 0.38
Surface brightness	μ_1	= 20.57
Parameters at k = ½(effective) :		
Semi-major axis	a_e	= 0.81
Axis ratio	b/a	= 0.19
Equivalent radius	r_e*	= 0.71
Surface brightness	μ_e	= 21.25
Mean surface brightness	μ_e'	= 11.65
Parameters at k = ¾ :		
Semi-major axis	a_3	= 2.05
Axis ratio	b/a	= 0.39
Equivalent radius	r_3*	= 1.31
Surface brightness	μ_3	= 23.25
Concentration indices	C_{21}	= 1.82
	C_{32}	= 1.86

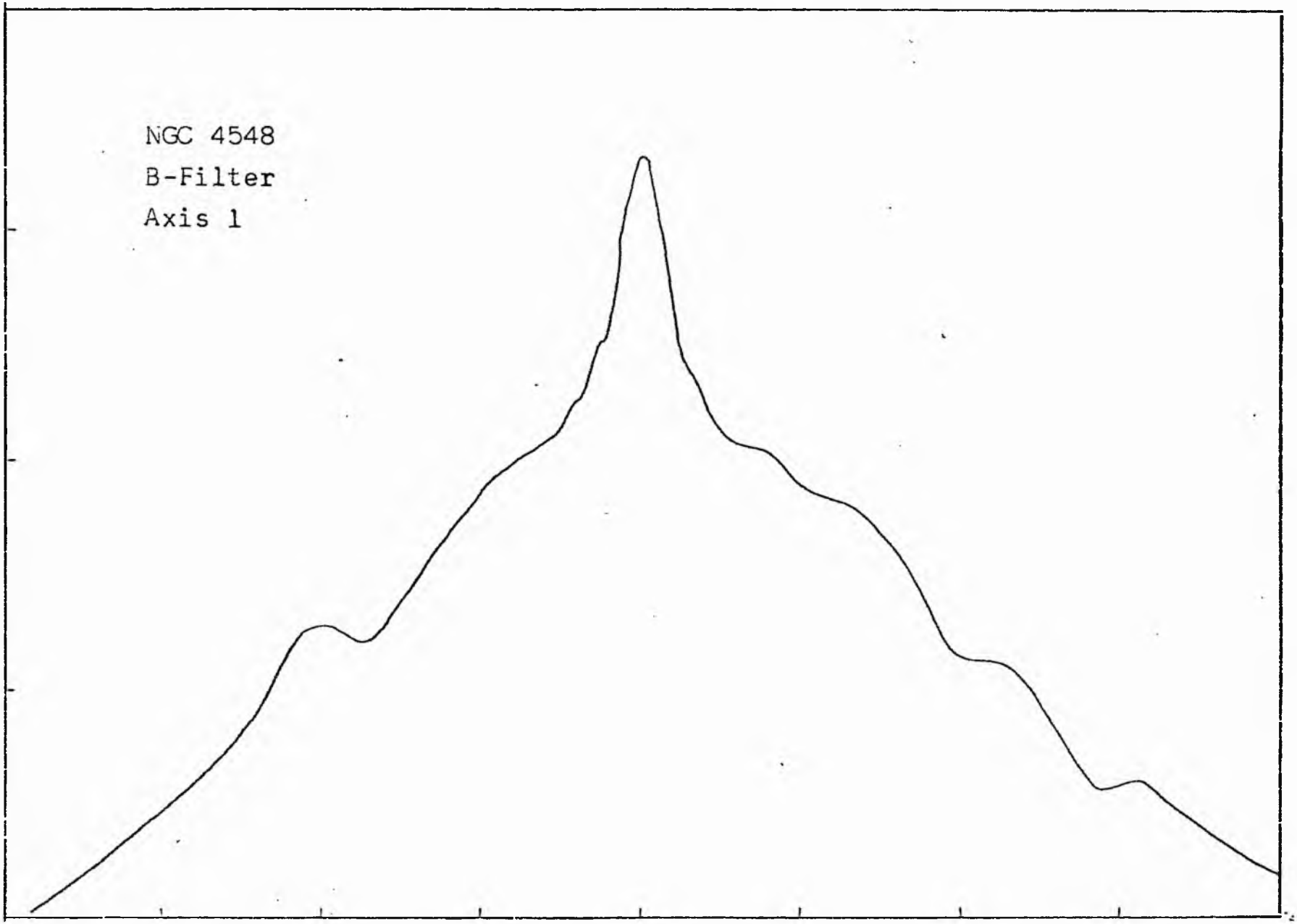
NGC 4548
B-Filter
Axis 1

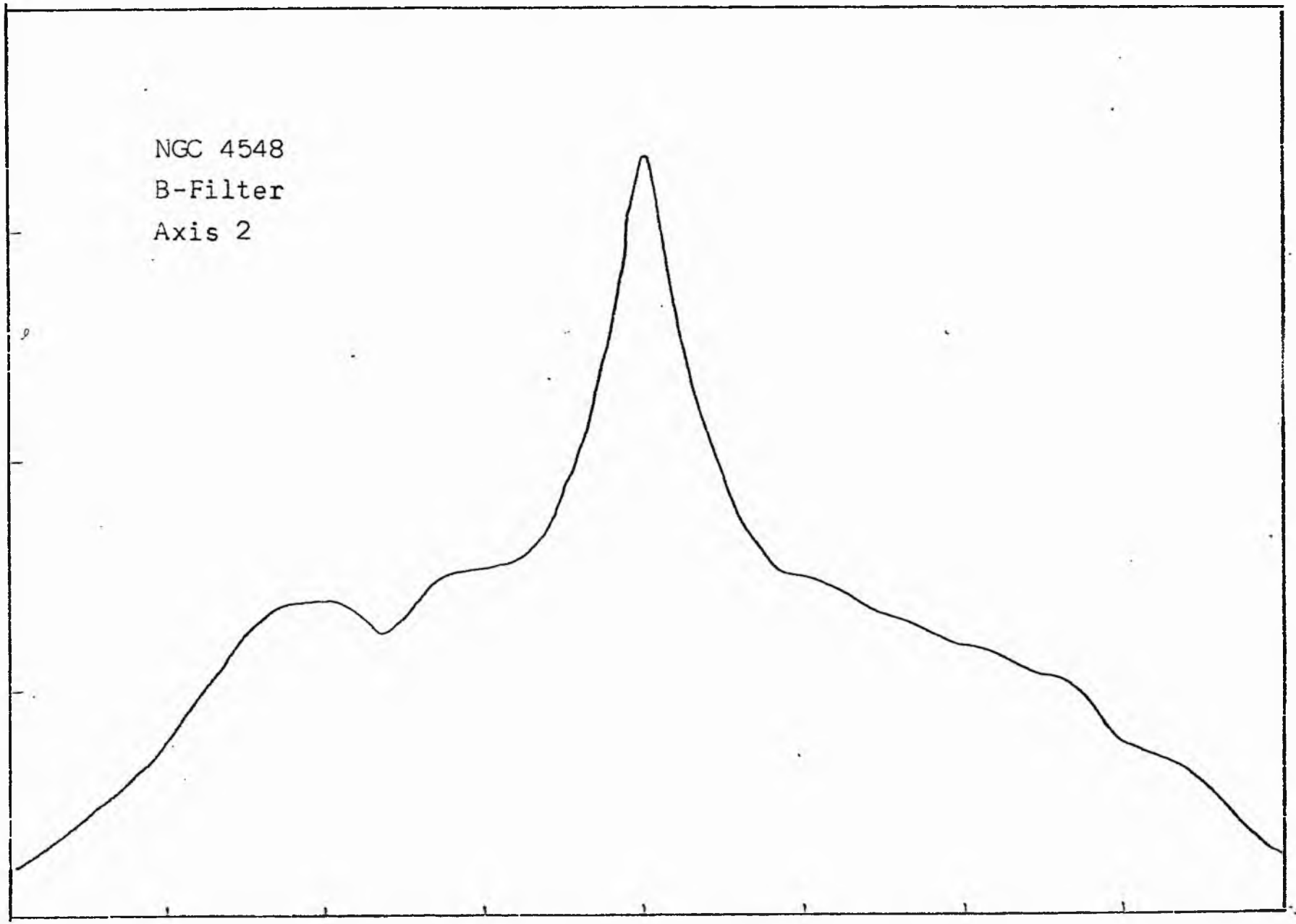
NGC 4548
B-Filter
Axis 2

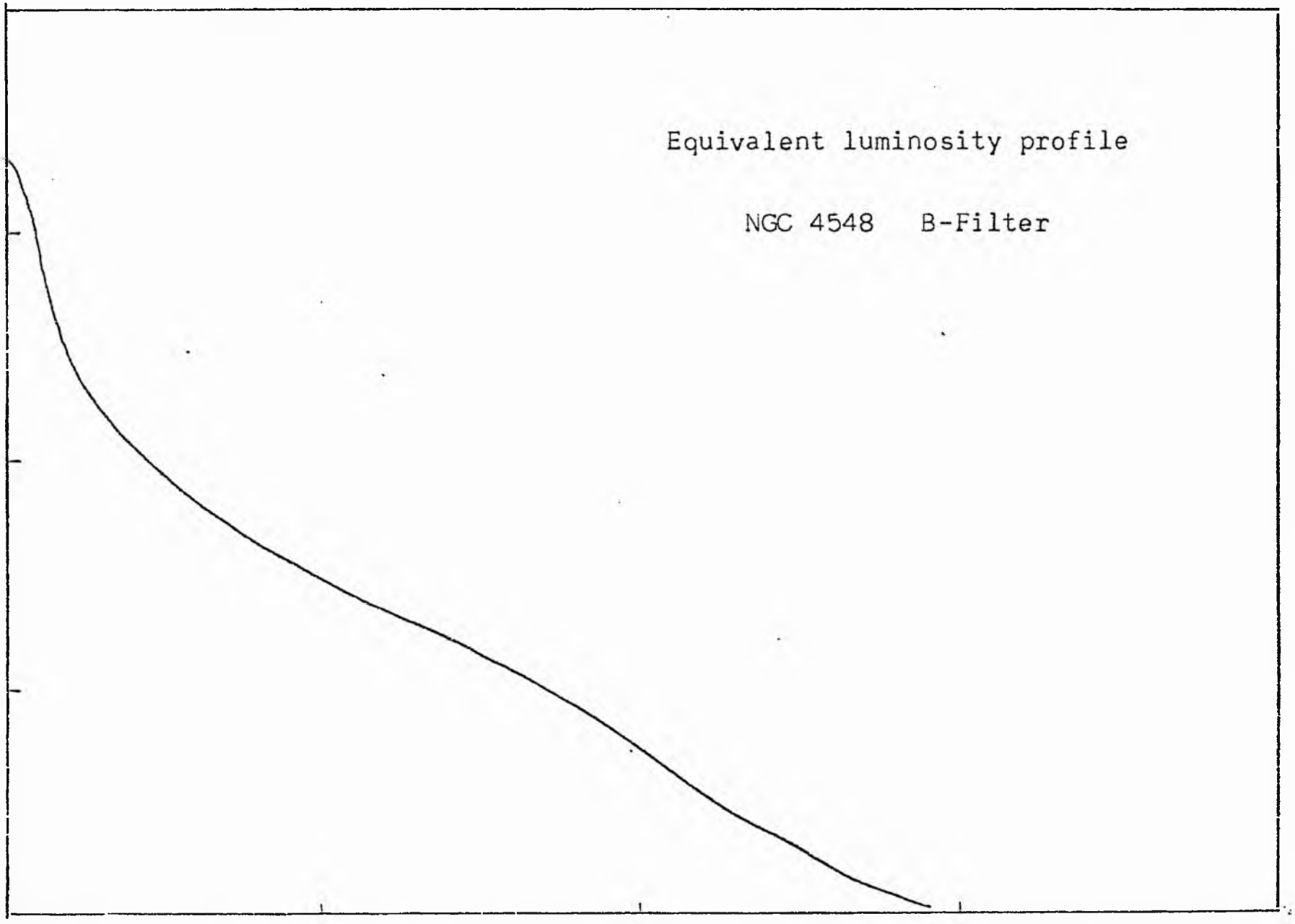
Equivalent luminosity profile
NGC 4548 B-Filter

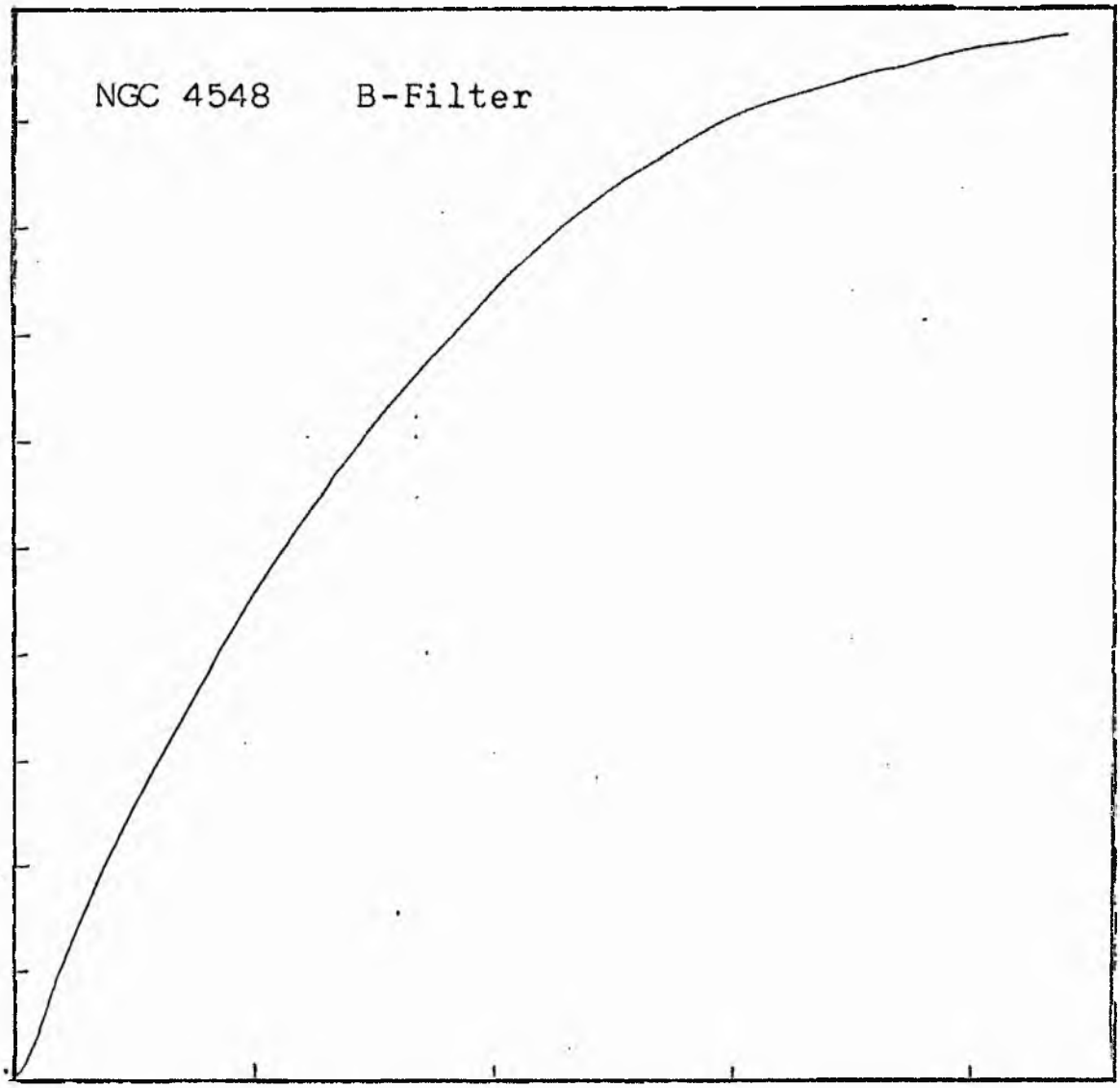

Relative integrated luminosity k(r) versus equivalent radius r*.

MEAN LUMINOSITY DISTRIBUTION IN NGC 4548
B COLOUR

LOG I	I	$\bar{I}$	R	AREA	ΔA	P	ΣP	KIRI	ρ	LOG J	μ
1.29	19.498		0.0	0.0			0.0	0.0	0.0	1.637	18.72
		17.674			38.48	680.1626					
1.20	15.849		3.50	38.48			680.16	0.03	0.06	1.547	18.95
		14.219			30.91	439.5576					
1.10	12.589		4.70	69.40			1119.72	0.04	0.09	1.447	19.20
		11.295			55.29	624.5010					
1.00	10.000		6.30	124.69			1744.22	0.07	0.11	1.347	19.45
		8.972			33.68	302.1493					
0.90	7.943		7.10	158.37			2046.37	0.08	0.13	1.247	19.70
		7.126			95.98	398.9055					
0.80	6.310		8.26	214.34			2445.27	0.09	0.15	1.147	19.95
		5.661			85.93	486.1648					
0.70	5.012		9.77	299.87			2929.44	0.11	0.18	1.047	20.20
		4.496			92.80	417.2764					
0.60	3.981		11.18	392.88			3346.71	0.13	0.20	0.947	20.45
		3.572			153.06	548.6738					
0.50	3.162		13.10	545.73			3893.39	0.15	0.24	0.847	20.70
		2.837			189.68	530.1421					
0.40	2.512		15.30	735.42			4431.53	0.17	0.28	0.747	20.95
		2.254			289.26	651.8616					
0.30	1.995		18.06	1024.67			5083.39	0.20	0.33	0.647	21.20
		1.790			511.10	914.9067					
0.20	1.585		22.11	1535.77			5998.29	0.23	0.40	0.547	21.45
		1.422			1079.04	1534.3022					
0.10	1.259		28.85	2614.82			7532.59	0.29	0.52	0.447	21.70
		1.129			1674.41	1891.1772					
-0.00	1.000		36.95	4289.22			9423.77	0.36	0.67	0.347	21.95
		0.897			1387.95	1245.2136					
-0.10	0.794		42.51	5677.17			10668.98	0.41	0.77	0.247	22.20
		0.713			1136.20	809.7061					
-0.20	0.631		46.57	6813.37			11478.68	0.44	0.85	0.147	22.45
		0.566			1658.64	938.9077					
-0.30	0.501		51.93	8472.01			12417.59	0.48	0.94	0.047	22.70
		0.450			3811.62	1713.8843					
-0.40	0.398		62.53	12283.63			14131.47	0.55	1.14	-0.053	22.95
		0.357			4660.33	1664.5178					
-0.50	0.316		73.44	16943.96			15795.99	0.61	1.33	-0.153	23.20
		0.284			5572.82	1581.0554					
-0.60	0.251		84.66	22516.78			17377.04	0.67	1.54	-0.253	23.45
		0.225			6714.26	1513.1084					
-0.70	0.200		96.46	29231.04			18890.15	0.73	1.75	-0.353	23.70
		0.179			6851.43	1226.4602					
-0.80	0.158		107.17	36082.47			20116.61	0.78	1.95	-0.453	23.95
		0.142			7276.37	1034.6343					
-0.90	0.126		117.48	43358.84			21151.24	0.82	2.13	-0.553	24.20
		0.113			7152.43	807.8401					
-1.00	0.100		126.80	50511.27			21959.08	0.85	2.30	-0.653	24.45
		0.090			6999.00	627.9260					
-1.10	0.079		135.30	57510.27			22587.00	0.87	2.46	-0.753	24.70
		0.071			5507.10	392.4604					
-1.20	0.063		141.63	63017.37			22979.46	0.89	2.57	-0.853	24.95
		0.057			7423.57	420.2285					
-1.30	0.050		149.74	70440.94			23399.69	0.90	2.72	-0.953	25.20
		0.045			8184.44	368.0125					
-1.40	0.040		158.20	78625.37			23767.70	0.92	2.87	-1.053	25.45
		0.036			9000.94	321.4858					
-1.50	0.032		167.01	87626.31			24089.18	0.93	3.03	-1.153	25.70
		0.028			7707.31	218.6644					
-1.60	0.025		174.20	95333.62			24307.85	0.94	3.17	-1.253	25.95
		0.023			12536.31	282.5176					
-1.70	0.020		185.30	107869.94			24590.36	0.95	3.37	-1.353	26.20
		0.018			10977.25	196.5033					
-1.80	0.016		194.50	118847.19			24786.86	0.96	3.53	-1.453	26.45
		0.014			17463.00	248.3108					
-1.90	0.013		208.30	136310.19			25035.17	0.97	3.78	-1.553	26.70
		0.011			12853.87	145.1815					
-2.00	0.010		217.90	149164.06			25180.35	0.97	3.96	-1.653	26.95
$-\infty$							25875.00	(1)			∞

PHOTOMETRIC PARAMETERS OF NGC 4548

B-FILTER

Total luminosity	L_T	= 7.19
Total apparent magnitude	m_T	= 10.90
Apparent central surface brightness	μ_o	= 18.72
Major axis at threshold	$2a_m$	= 7.02
Minor axis at threshold	$2b_m$	= 6.94
Major axis at μ=25.0 mag sec^{-2}	$2a(25)$	= 5.23
Luminosity within μ=25.0 mag sec^{-2}	$k(25)$	= 0.89
Gradient of exponential component	$G(a)$	= -0.76
Equivalent gradient of exponential comp.	$G(r^*)$	= -0.70
Equivalent gradient of reduced exp. comp.	$G(\rho)$	= -0.62

Parameters at k = ¼ :

Semi-major axis	a_1	= 0.28
Axis ratio	b/a	= 1.16
Equivalent radius	r_1^*	= 0.40
Surface brightness	μ_1	= 21.52

Parameters at k = ½(effective) :

Semi-major axis	a_e	= 0.92
Axis ratio	b/a	= 0.56
Equivalent radius	r_e^*	= 0.92
Surface brightness	μ_e	= 22.77
Mean surface brightness	μ_e'	= 12.70

Parameters at k = ¾ :

Semi-major axis	a_3	= 1.55
Axis ratio	b/a	= 1.05
Equivalent radius	r_3^*	= 1.68
Surface brightness	μ_3	= 23.80

Concentration indices	C_{21}	= 2.28
	C_{32}	= 1.83

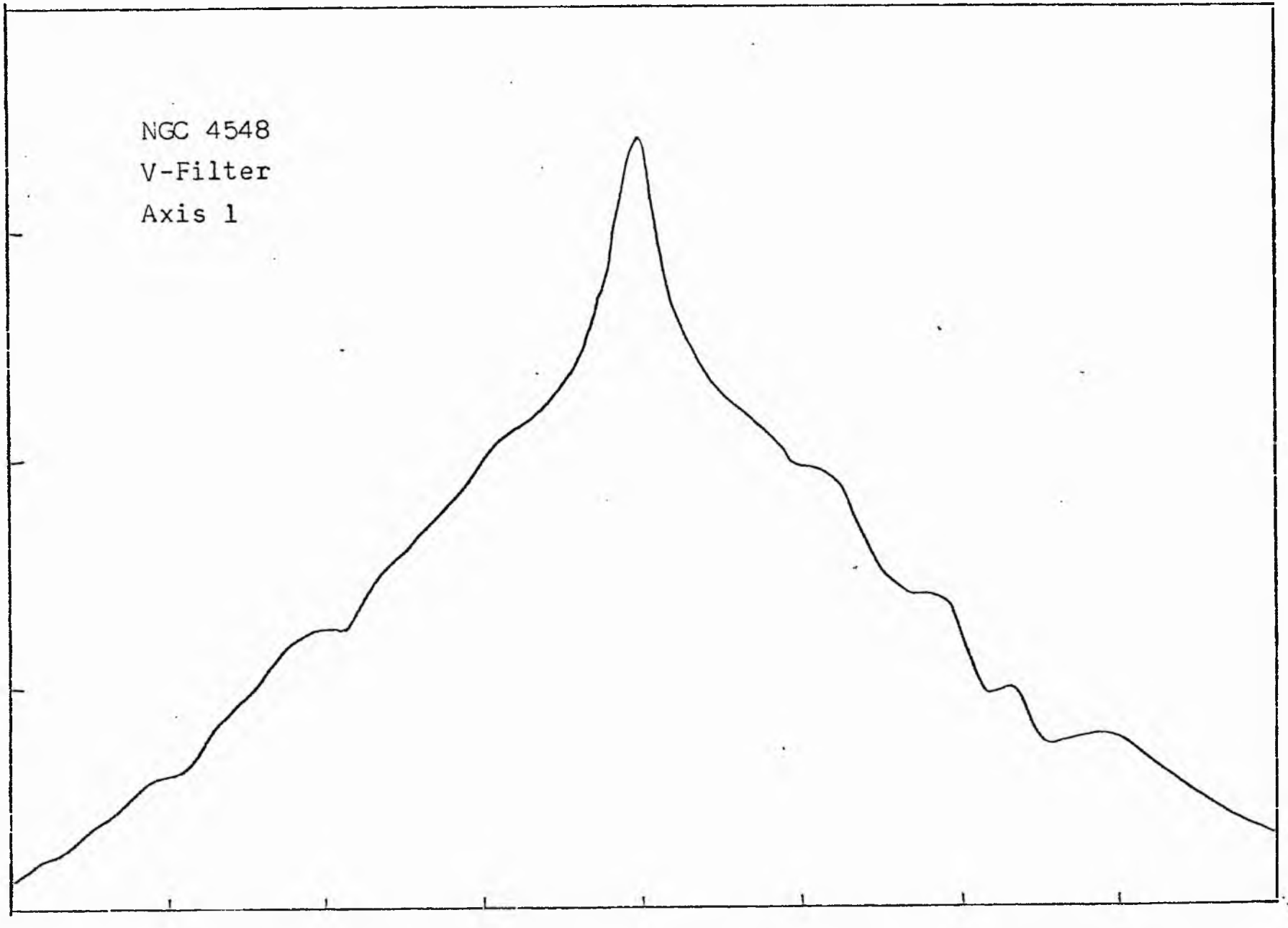
NGC 4548
V-Filter
Axis 1

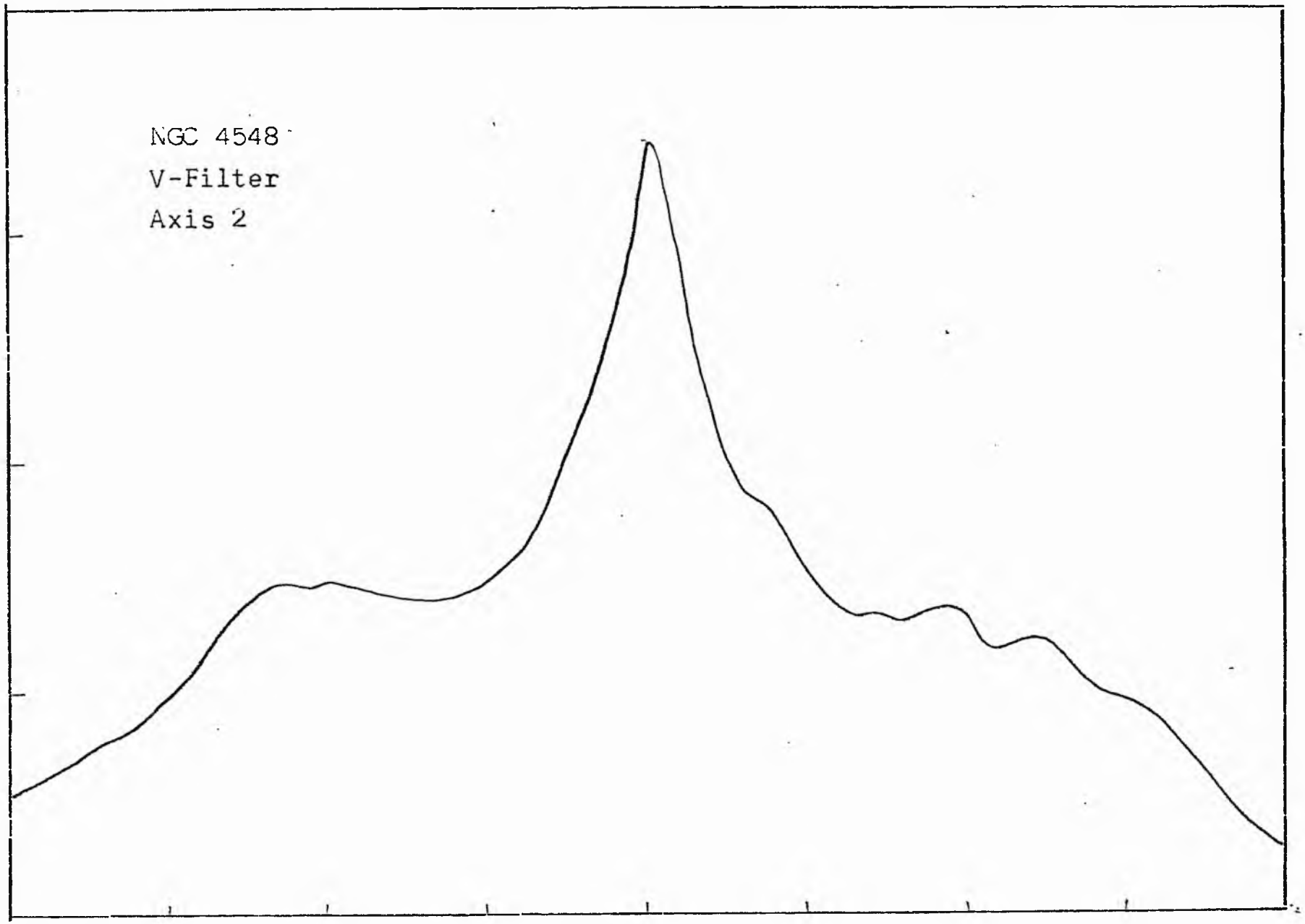
NGC 4548
V-Filter
Axis 2

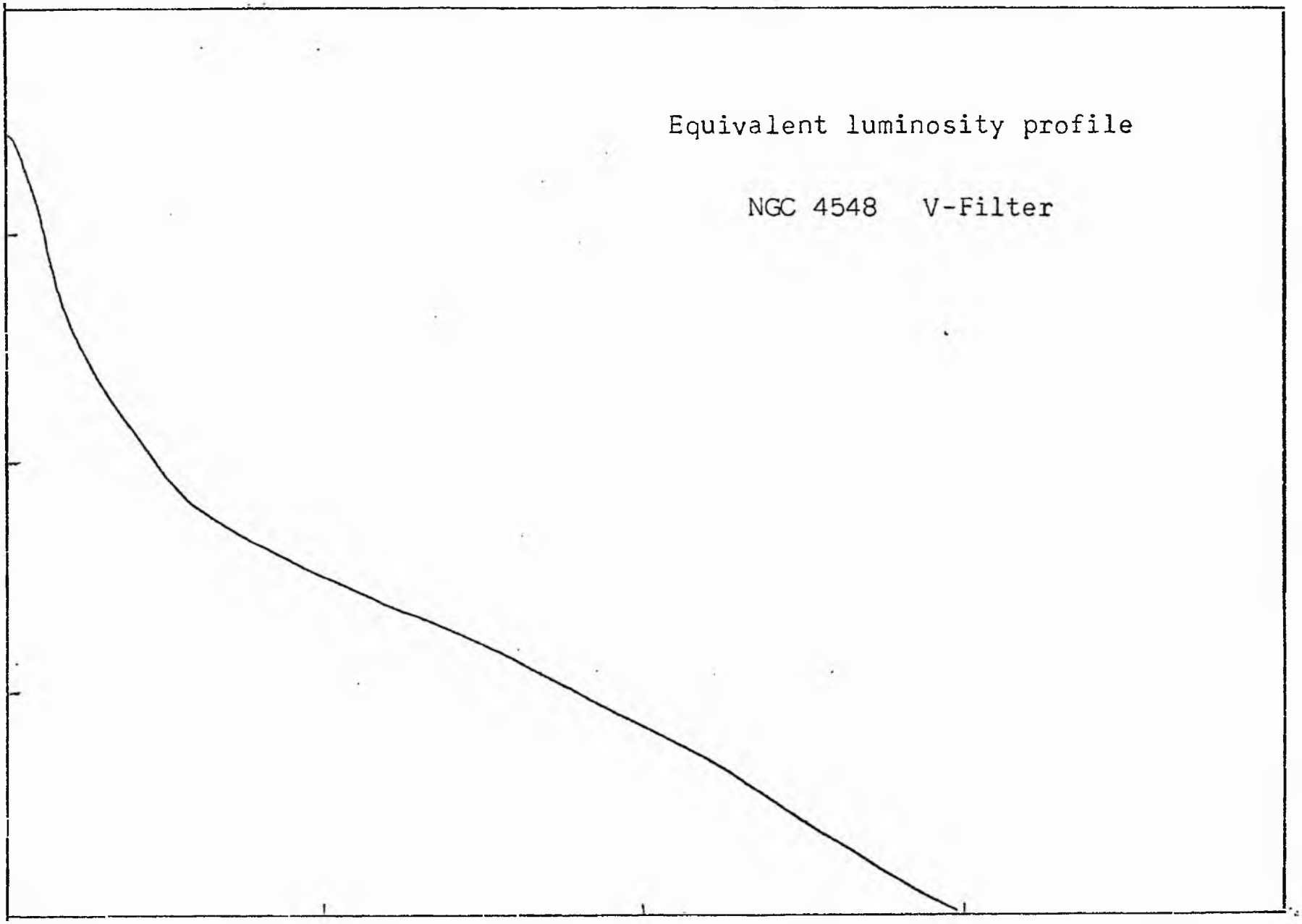
Equivalent luminosity profile
NGC 4548 V-Filter

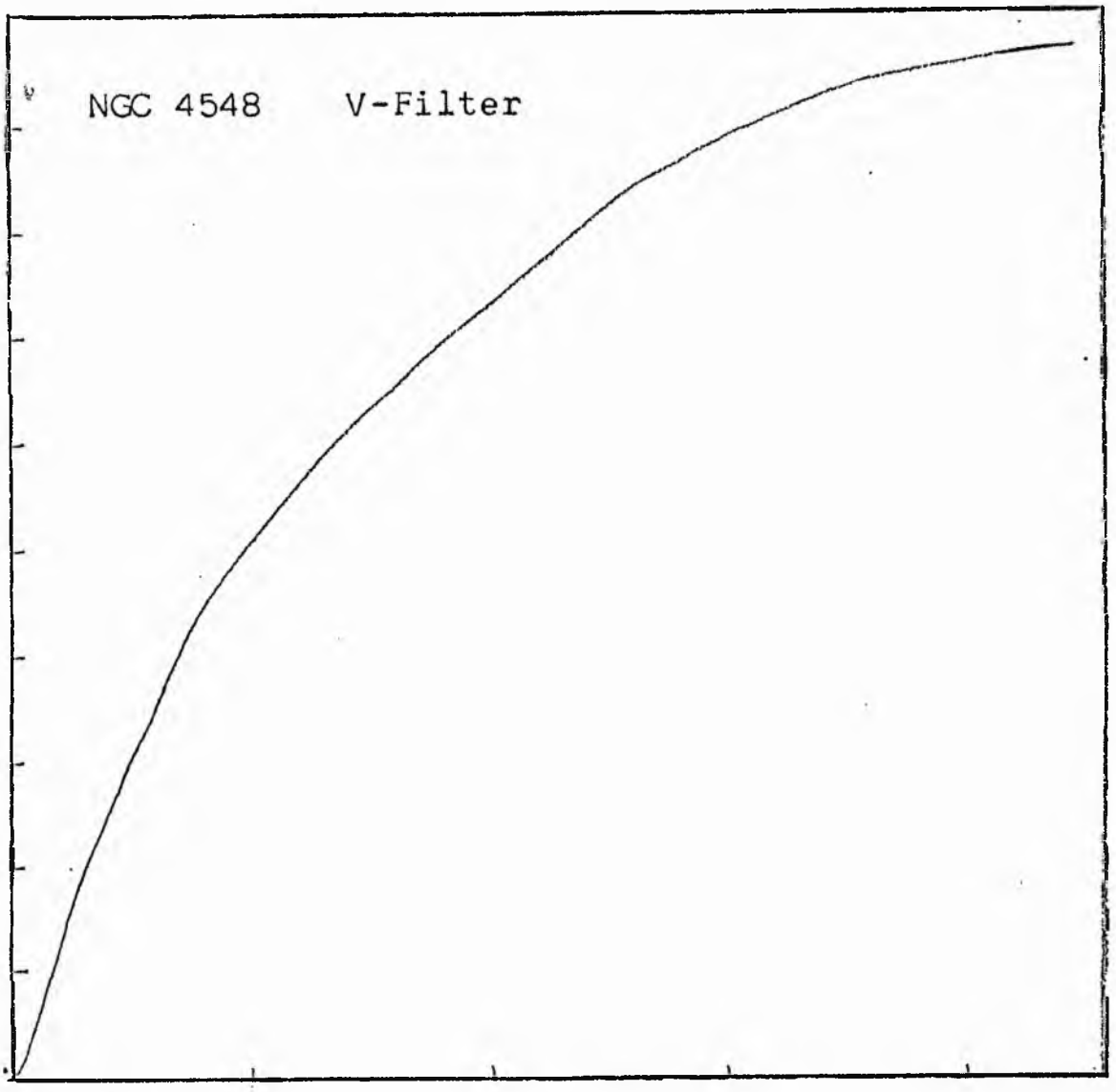

Relative integrated luminosity k(r) versus equivalent radius r*.

MEAN LUMINOSITY DISTRIBUTION IN NGC 4548
V COLOUR

LOG I	I	$\bar{I}$	R	AREA	ΔA	P	ΣP	K(R)	ρ	LOG J	μ
1.37	23.442		0.0	0.0			0.0	0.0	0.0	1.630	17.83
		21.697			52.81	1145.8430					
1.30	19.953		4.10	52.81			1145.84	0.04	0.08	1.560	18.01
		17.901			28.90	517.3779					
1.20	15.849		5.10	81.71			1663.22	0.06	0.10	1.460	18.26
		14.219			42.98	611.0918					
1.10	12.589		6.30	124.69			2274.31	0.08	0.13	1.360	18.51
		11.295			56.77	641.1770					
1.00	10.000		7.60	181.46			2915.49	0.10	0.15	1.260	18.76
		8.972			53.06	476.0354					
0.90	7.943		8.64	234.52			3391.53	0.12	0.17	1.160	19.01
		7.126			100.07	713.1270					
0.80	6.310		10.32	334.59			4104.65	0.14	0.21	1.060	19.26
		5.661			106.56	693.2227					
0.70	5.012		11.85	441.15			4797.87	0.16	0.24	0.960	19.51
		4.496			180.77	812.8462					
0.60	3.981		14.07	621.93			5520.71	0.19	0.28	0.860	19.76
		3.572			167.31	597.5872					
0.50	3.162		15.85	789.24			6118.30	0.21	0.31	0.760	20.01
		2.837			396.79	1125.7200					
0.40	2.512		19.43	1186.03			7244.02	0.25	0.39	0.660	20.26
		2.254			679.75	1531.8696					
0.30	1.995		24.37	1865.78			8775.89	0.30	0.48	0.560	20.51
		1.790			838.61	1501.1775					
0.20	1.585		29.34	2704.39			10277.06	0.35	0.58	0.460	20.76
		1.422			716.80	1019.2222					
0.10	1.259		33.00	3421.19			11296.28	0.38	0.66	0.360	21.01
		1.129			810.18	915.0701					
-0.00	1.000		36.70	4231.38			12211.35	0.41	0.73	0.260	21.26
		0.897			586.27	525.9749					
-0.10	0.794		39.16	4817.64			12737.32	0.43	0.78	0.160	21.51
		0.713			1010.09	719.8284					
-0.20	0.631		43.07	5827.73			13457.15	0.46	0.86	0.060	21.76
		0.566			3483.04	1971.6479					
-0.30	0.501		54.44	9310.77			15428.79	0.52	1.08	-0.040	22.01
		0.450			3118.65	1402.2900					
-0.40	0.398		62.90	12429.43			16831.08	0.57	1.25	-0.140	22.26
		0.357			4065.35	1452.0066					
-0.50	0.316		72.46	16494.77			18283.09	0.62	1.44	-0.240	22.51
		0.284			5163.30	1464.8687					
-0.60	0.251		83.03	21658.08			19747.95	0.67	1.65	-0.340	22.76
		0.225			6563.62	1479.1577					
-0.70	0.200		94.78	28221.70			21227.11	0.72	1.88	-0.440	23.01
		0.179			7746.40	1386.6626					
-0.80	0.158		107.00	35968.10			22613.77	0.77	2.13	-0.540	23.26
		0.142			9792.57	1392.4116					
-0.90	0.126		120.69	45760.66			24006.18	0.81	2.40	-0.640	23.51
		0.113			8498.46	959.8689					
-1.00	0.100		131.42	54259.12			24966.05	0.85	2.61	-0.740	23.76
		0.090			11865.69	1064.5479					
-1.10	0.079		145.08	66124.81			26030.59	0.88	2.88	-0.840	24.01
		0.071			8613.56	613.8406					
-1.20	0.063		154.24	74738.37			26644.43	0.90	3.06	-0.940	24.26
		0.057			10480.69	593.2842					
-1.30	0.050		164.70	85219.06			27237.71	0.92	3.27	-1.040	24.51
		0.045			4826.75	217.0344					
-1.40	0.040		169.30	90045.81			27454.75	0.93	3.36	-1.140	24.76
		0.036			7711.00	275.4133					
-1.50	0.032		176.40	97756.81			27730.16	0.94	3.50	-1.240	25.01
		0.028			8836.25	250.6935					
-1.60	0.025		184.20	106593.06			27980.85	0.95	3.66	-1.340	25.26
		0.023			11156.81	251.4293					
-1.70	0.020		193.60	117749.87			28232.27	0.96	3.85	-1.440	25.51
		0.018			10947.81	195.9764					
-1.80	0.016		202.40	128697.69			28428.25	0.97	4.02	-1.540	25.76
		0.014			11567.12	164.4759					
-1.90	0.013		211.30	140264.81			28592.72	0.97	4.20	-1.640	26.01
		0.011			12757.37	144.0916					
-2.00	0.010		220.70	153022.19			28736.81	0.98	4.39	-1.740	26.26
-∞							29456.00	(1)			∞

PHOTOMETRIC PARAMETERS OF NGC 4548

V-FILTER

Total luminosity	L_T	= 7.19
Total apparent magnitude	m_T	= 10.90
Apparent central surface brightness	μ_o	= 18.72
Major axis at threshold	$2a_m$	= 7.02
Minor axis at threshold	$2b_m$	= 6.94
Major axis at μ=25.0 mag sec^{-2}	2a(25)	= 5.23
Luminosity within μ=25.0 mag sec^{-2}	k(25)	= 0.89
Gradient of exponential component	G(a)	= -0.76
Equivalent gradient of exponential comp.	G(r*)	= -0.70
Equivalent gradient of reduced exp. comp.	G(ρ)	= -0.63
Parameters at k = ¼ :		
Semi-major axis	a_1	= 0.28
Axis ratio	b/a	= 1.16
Equivalent radius	r_1*	= 0.40
Surface brightness	μ_1	= 21.52
Parameters at k = ½(effective) :		
Semi-major axis	a_e	= 0.92
Axis ratio	b/a	= 0.56
Equivalent radius	r_e*	= 0.92
Surface brightness	μ_e	= 22.77
Mean surface brightness	μ_e'	= 12.70
Parameters at k = ¾ :		
Semi-major axis	a_3	= 1.55
Axis ratio	b/a	= 1.05
Equivalent radius	r_3*	= 1.68
Surface brightness	μ_3	= 23.80
Concentration indices	C_{21}	= 2.28
	C_{32}	= 1.83

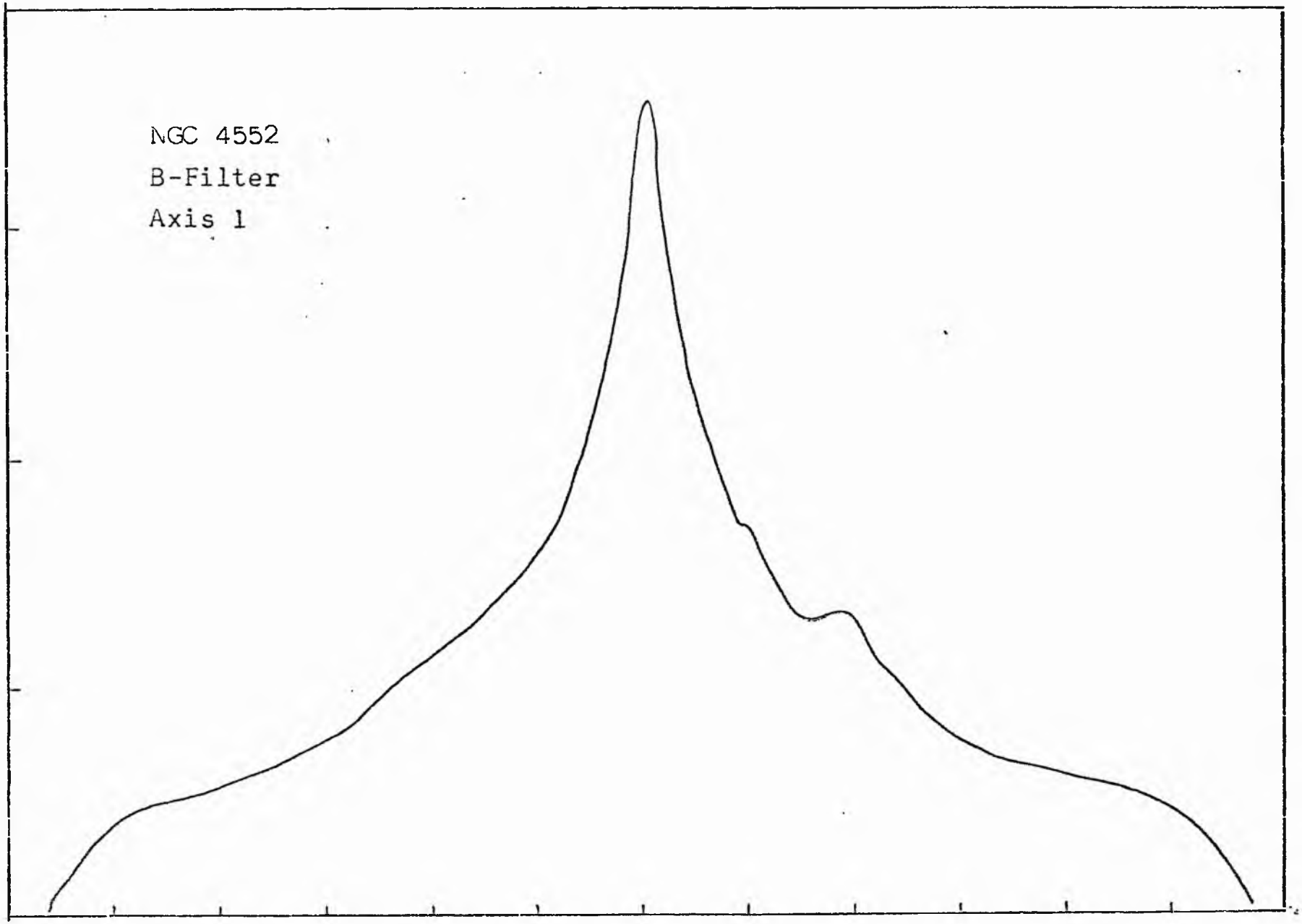
NGC 4552
B-Filter
Axis 1

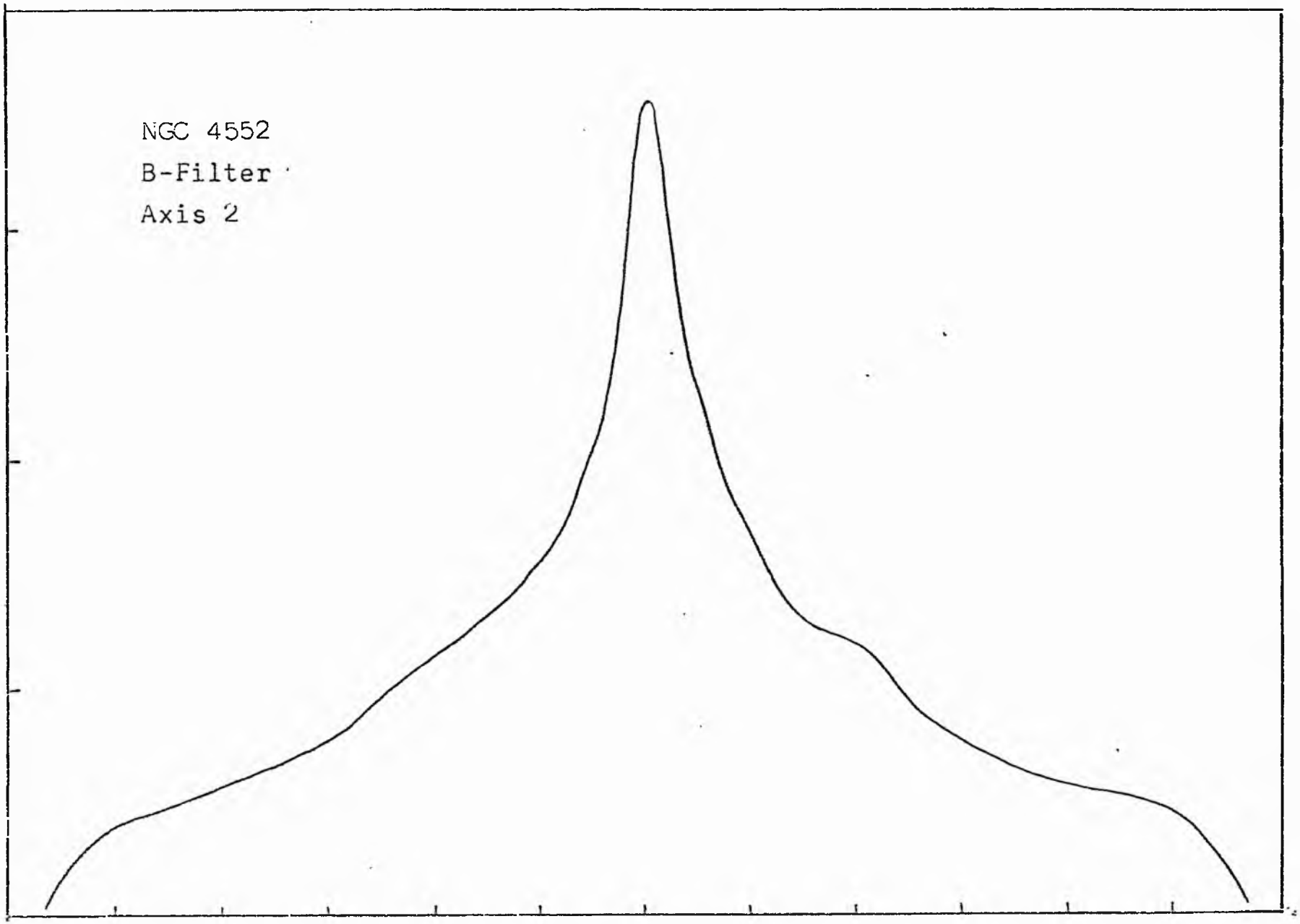
NGC 4552
B-Filter
Axis 2

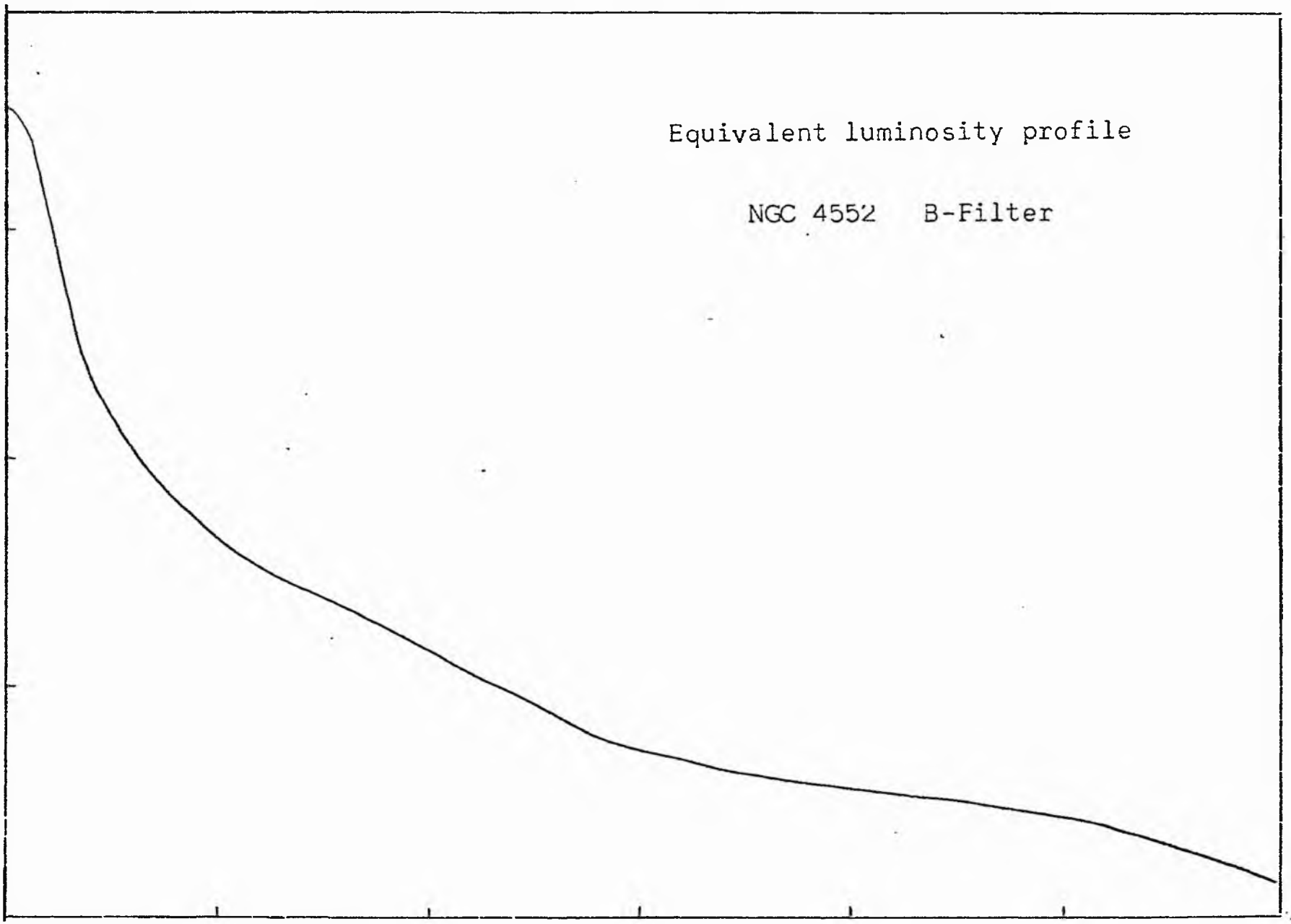
Equivalent luminosity profile
NGC 4552 B-Filter

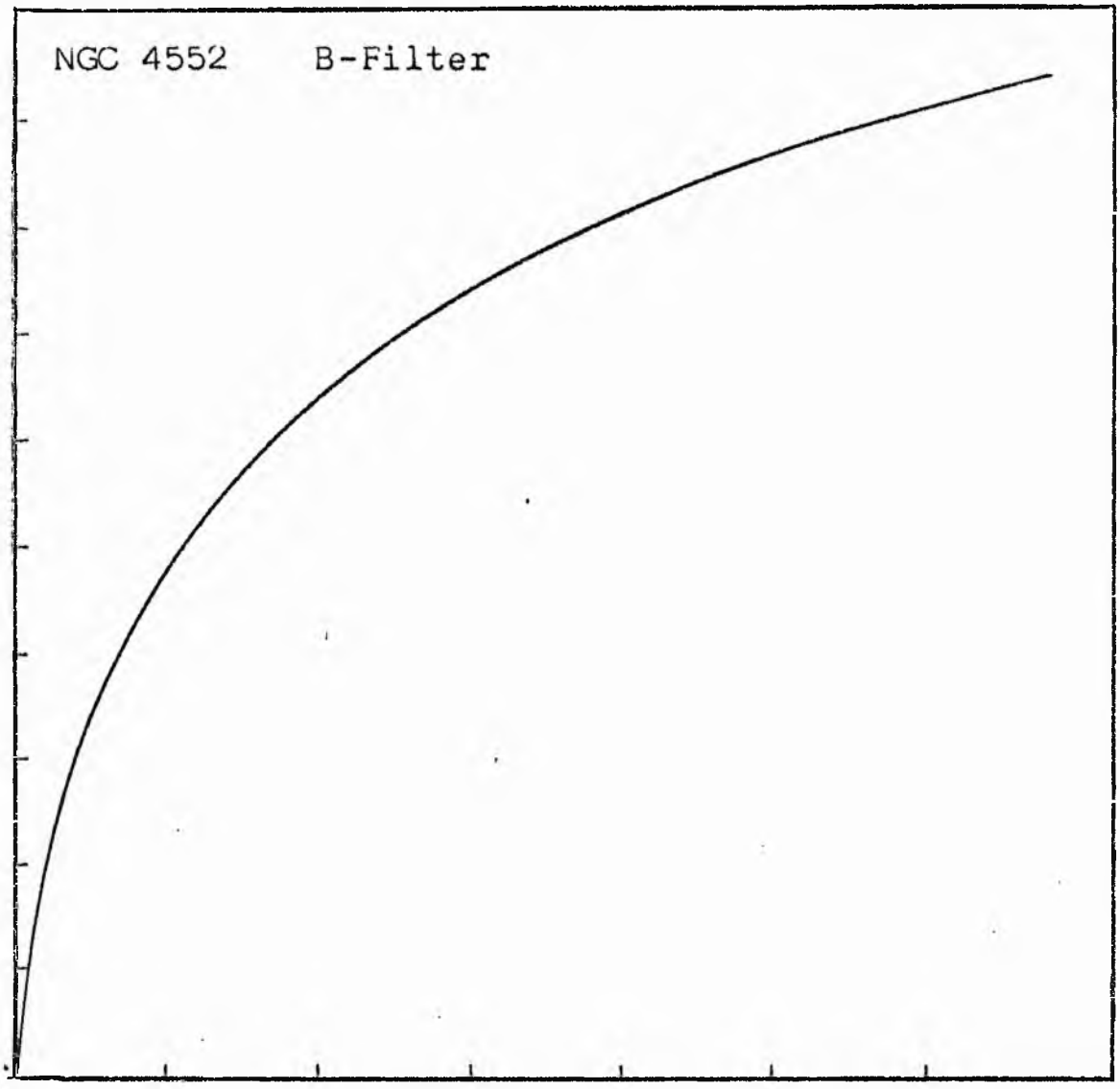

Relative integrated luminosity k(r) versus equivalent radius r*.

MEAN LUMINOSITY DISTRIBUTION IN NGC 4552
B COLOUR

LOG I	I	$\bar{I}$	R	AREA	ΔA	P	ΣP	K(R)	ρ	LOG J	μ
1.54	34.674		0.0	0.0			0.0	0.0	0.0	1.950	18.14
		33.148			40.04	1327.2302					
1.50	31.623		3.57	40.04			1327.23	0.04	0.06	1.910	18.24
		28.371			67.84	1924.7229					
1.40	25.119		5.86	107.88			3251.95	0.09	0.10	1.810	18.49
		22.536			42.99	968.8911					
1.30	19.953		6.93	150.87			4220.84	0.12	0.12	1.710	18.74
		17.901			48.68	871.4446					
1.20	15.849		7.97	199.56			5092.29	0.14	0.14	1.610	18.99
		14.219			70.99	1009.4395					
1.10	12.589		9.28	270.55			6101.72	0.17	0.16	1.510	19.24
		11.295			71.86	811.6792					
1.00	10.000		10.44	342.41			6913.40	0.19	0.18	1.410	19.49
		8.972			46.06	413.2170					
0.90	7.943		11.12	388.47			7326.61	0.20	0.19	1.310	19.74
		7.126			77.59	552.9451					
0.80	6.310		12.18	466.06			7879.55	0.22	0.21	1.210	19.99
		5.661			132.22	748.4690					
0.70	5.012		13.80	598.28			8628.02	0.24	0.24	1.110	20.24
		4.496			166.25	747.5500					
0.60	3.981		15.60	764.54			9375.57	0.26	0.27	1.010	20.49
		3.572			86.62	309.3682					
0.50	3.162		16.46	851.16			9684.94	0.27	0.29	0.910	20.74
		2.837			306.96	870.8689					
0.40	2.512		19.20	1158.12			10555.80	0.29	0.33	0.810	20.99
		2.254			334.89	754.7029					
0.30	1.995		21.80	1493.01			11310.50	0.31	0.38	0.710	21.24
		1.790			486.23	870.3779					
0.20	1.585		25.10	1979.23			12180.88	0.34	0.44	0.610	21.49
		1.422			626.53	890.8613					
0.10	1.259		28.80	2605.76			13071.74	0.36	0.50	0.510	21.74
		1.129			774.09	874.3010					
-0.00	1.000		32.80	3379.85			13946.04	0.39	0.57	0.410	21.99
		0.897			1132.76	1016.2729					
-0.10	0.794		37.90	4512.61			14962.31	0.41	0.66	0.310	22.24
		0.713			1002.79	714.6311					
-0.20	0.631		41.90	5515.41			15676.94	0.43	0.73	0.210	22.49
		0.566			1453.93	823.0266					
-0.30	0.501		47.10	6969.34			16499.96	0.46	0.82	0.110	22.74
		0.450			3166.19	1423.6658					
-0.40	0.398		56.80	10135.53			17923.62	0.50	0.99	0.010	22.99
		0.357			3186.75	1138.2007					
-0.50	0.316		65.12	13322.28			19061.82	0.53	1.13	-0.090	23.24
		0.284			3529.52	1001.3516					
-0.60	0.251		73.24	16851.80			20063.18	0.56	1.27	-0.190	23.49
		0.225			6670.68	1503.2852					
-0.70	0.200		86.53	23522.48			21566.46	0.60	1.50	-0.290	23.74
		0.179			8791.99	1573.8315					
-0.80	0.158		101.42	32314.47			23140.29	0.64	1.76	-0.390	23.99
		0.142			5381.52	765.2024					
-0.90	0.126		109.54	37696.00			23905.49	0.66	1.90	-0.490	24.24
		0.113			6404.14	723.3228					
-1.00	0.100		118.48	44100.13			24628.81	0.68	2.05	-0.590	24.49
		0.090			7556.86	677.9749					
-1.10	0.079		128.23	51656.99			25306.78	0.70	2.22	-0.690	24.74
		0.071			9575.62	682.4011					
-1.20	0.063		139.61	61232.61			25989.18	0.72	2.42	-0.790	24.99
		0.057			10228.14	578.9880					
-1.30	0.050		150.82	71460.75			26568.16	0.74	2.62	-0.890	25.24
		0.045			47423.12	2132.3765					
-1.40	0.040		194.53	118883.87			28700.54	0.80	3.37	-0.990	25.49
		0.036			50078.00	1788.6333					
-1.50	0.032		231.91	168961.87			30489.17	0.84	4.02	-1.090	25.74
		0.028			36539.62	1036.6667					
-1.60	0.025		255.76	205501.50			31525.84	0.87	4.44	-1.190	25.99
		0.023			30580.37	689.1575					
-1.70	0.020		274.13	236081.87			32214.99	0.89	4.75	-1.290	26.24
		0.018			25109.56	449.4851					
-1.80	0.016		288.34	261191.44			32664.48	0.91	5.00	-1.390	26.49
		0.014			42373.19	602.5149					
-1.90	0.013		310.85	303564.62			33266.99	0.92	5.39	-1.490	26.74
		0.011			28469.94	321.5613					
-2.00	0.010		325.10	332034.56			33588.55	0.93	5.64	-1.590	26.99
$-\infty$							36088.00	(1)			∞

PHOTOMETRIC PARAMETERS OF NGC 4552
B-FILTER

Total luminosity ..... L_T = 10.02
Total apparent magnitude ..... m_T = 10.63
Apparent central surface brightness ..... μ_o = 18.14
Major axis at threshold ..... $2a_m$ = 9.47
Minor axis at threshold ..... $2b_m$ = 9.33
Major axis at μ=25.0 mag sec^{-2} ..... $2a(25)$ = 4.95
Luminosity within μ=25.0 mag sec^{-2} ..... $k(25)$ = 0.72
Gradient of exponential component ..... $G(a)$ = -0.38
Equivalent gradient of exponential comp..... $G(r^*)$ = -0.43
Equivalent gradient of reduced exp. comp..... $G(\rho)$ = -----

Parameters at k = ¼ :

Semi-major axis ..... a_1 = 0.26
Axis ratio ..... b/a = 0.93
Equivalent radius ..... r_1^* = 0.25
Surface brightness ..... μ_1 = 20.36

Parameters at k = ½(effective) :

Semi-major axis ..... a_e = 0.94
Axis ratio ..... b/a = 0.96
Equivalent radius ..... r_e^* = 0.96
Surface brightness ..... μ_e = 22.99
Mean surface brightness ..... μ_e' = 12.54

Parameters at k = ¾ :

Semi-major axis ..... a_3 = 2.92
Axis ratio ..... b/a = 0.94
Equivalent radius ..... r_3^* = 2.68
Surface brightness ..... μ_3 = 25.28

Concentration indices ..... C_{21} = 3.92, C_{32} = 2.79

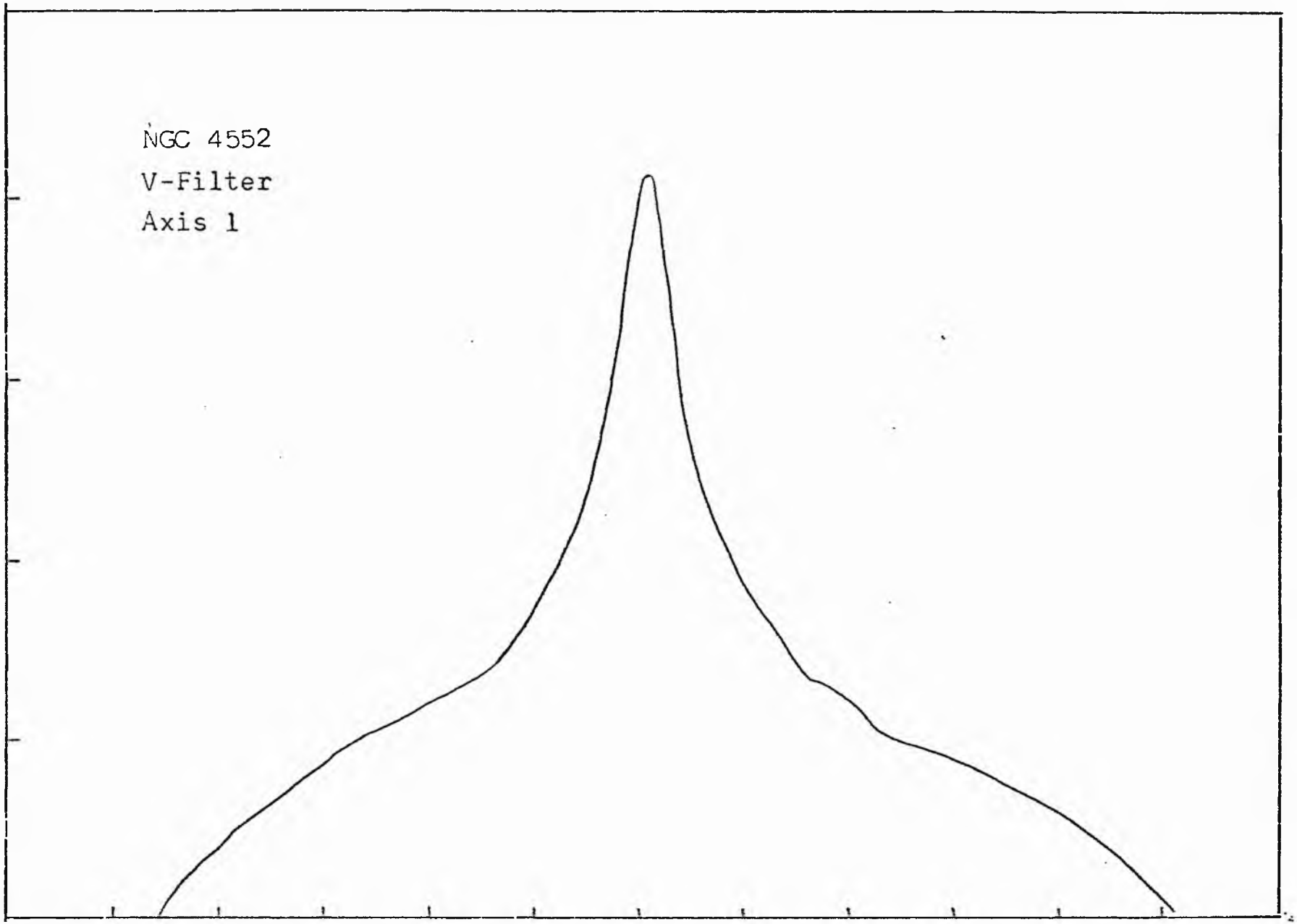
NGC 4552
V-Filter
Axis 1

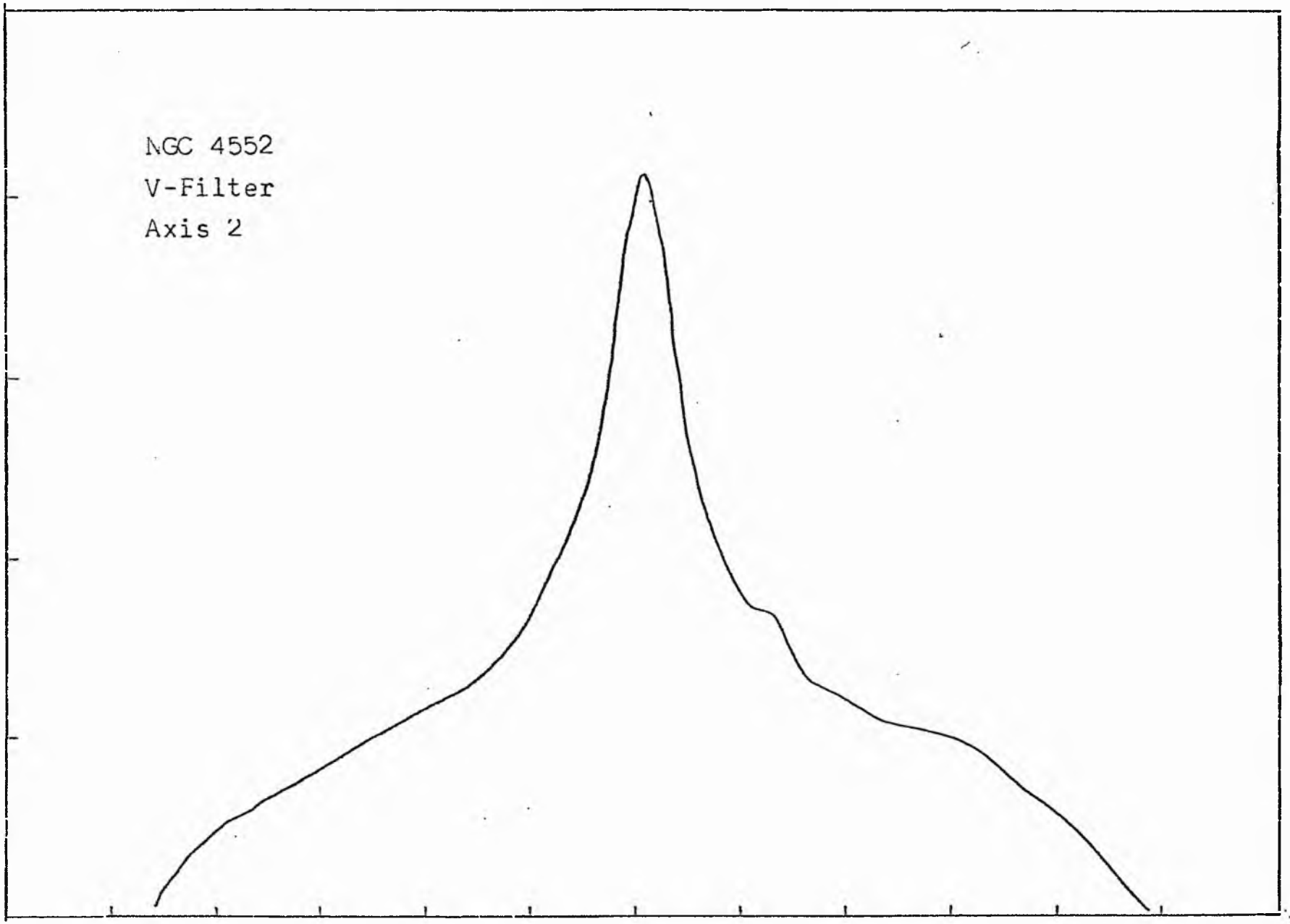
NGC 4552
V-Filter
Axis 2

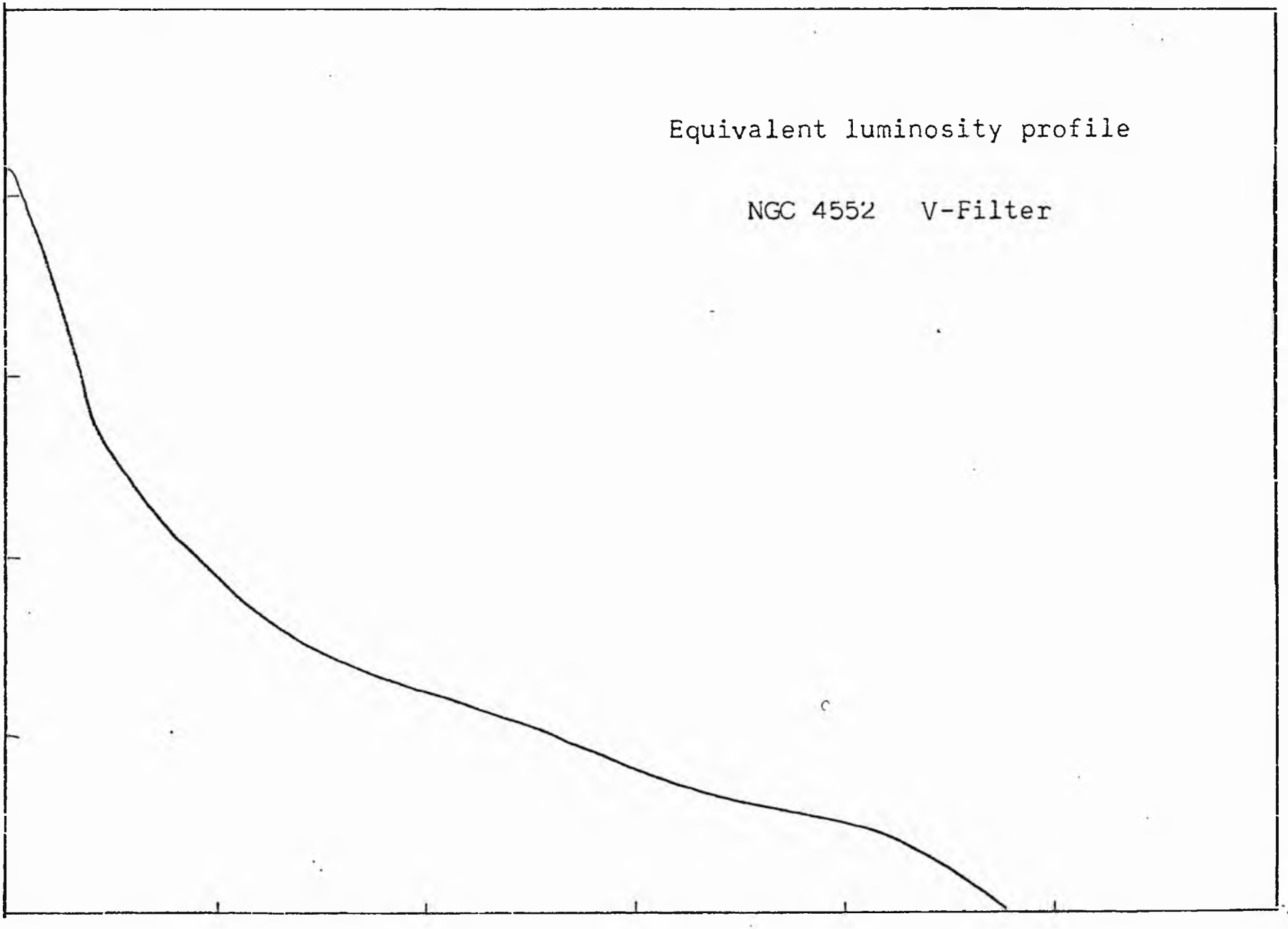
Equivalent luminosity profile
NGC 4552 V-Filter

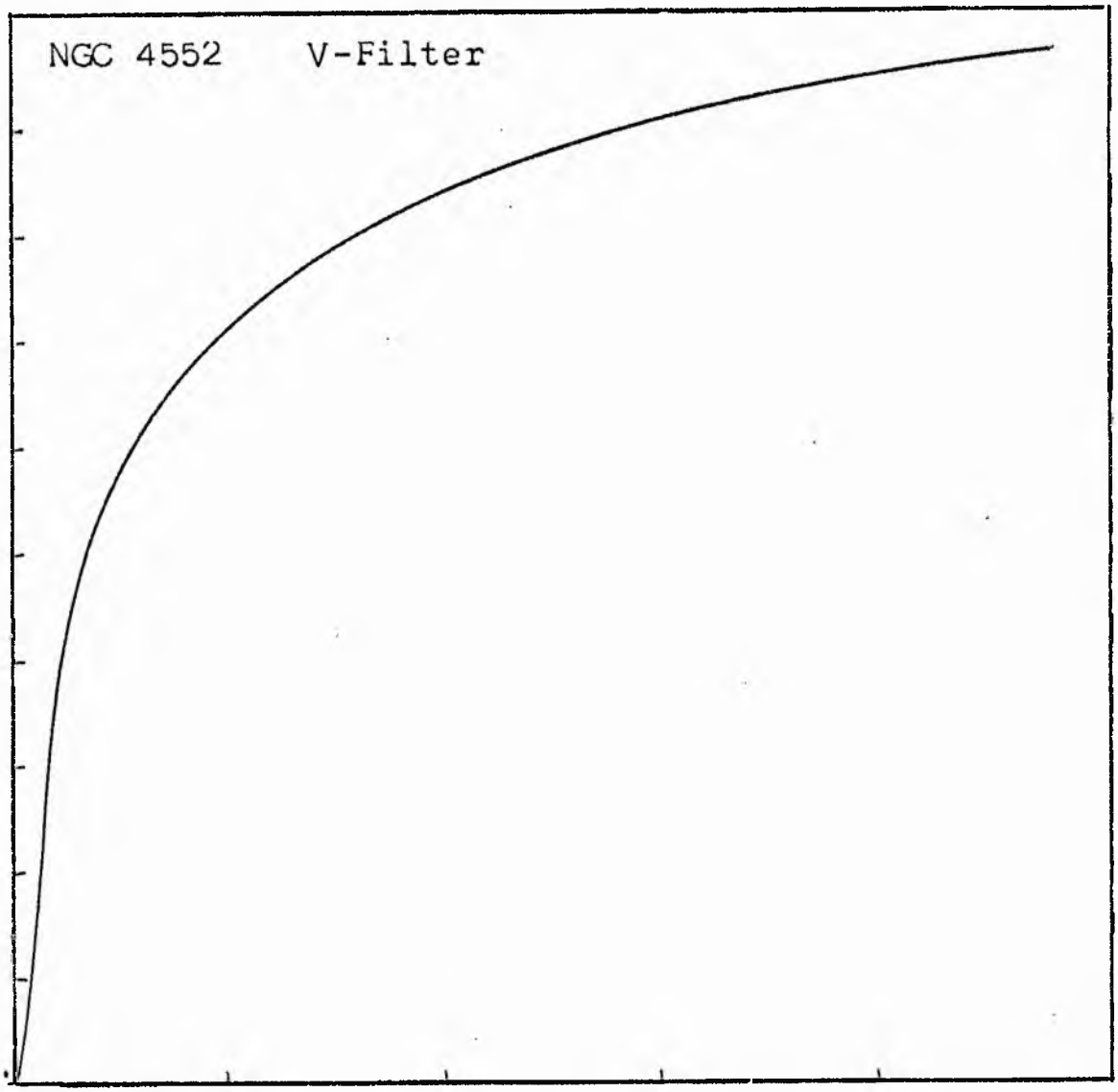

Relative integrated luminosity k(r) versus equivalent radius r*.

MEAN LUMINOSITY DISTRIBUTION IN NGC 4552
V COLOUR

LOG I	I	$\bar{I}$	R	AREA	ΔA	P	Σ P	K(R)	ρ	LOG J	μ
2.12	131.826		0.0	0.0			0.0	0.0	0.0	1.357	16.56
		128.859			8.04	1036.3445					
2.10	125.892		1.60	8.04			1036.34	0.02	0.09	1.337	16.61
		112.946			37.32	4215.3828					
2.00	100.000		3.80	45.36			5251.73	0.09	0.22	1.237	16.86
		89.716			36.35	3261.0178					
1.90	79.433		5.10	81.71			8512.74	0.15	0.30	1.137	17.11
		71.264			39.05	2782.8618					
1.80	63.095		6.20	120.76			11295.60	0.20	0.37	1.037	17.36
		56.607			46.65	2640.8630					
1.70	50.118		7.30	167.42			13936.46	0.24	0.43	0.937	17.61
		44.964			64.94	2919.8440					
1.60	39.810		8.60	232.35			16856.30	0.29	0.51	0.837	17.86
		35.717			114.01	4071.9841					
1.50	31.623		10.50	346.36			20928.29	0.36	0.62	0.737	18.11
		28.371			54.79	1554.4058					
1.40	25.119		11.30	401.15			22482.69	0.39	0.67	0.637	18.36
		22.536			36.29	817.7114					
1.30	19.952		11.80	437.44			23300.40	0.40	0.70	0.537	18.61
		17.901			53.44	956.5818					
1.20	15.849		12.50	490.87			24256.98	0.42	0.74	0.437	18.86
		14.219			133.71	1901.1594					
1.10	12.589		14.10	624.58			26158.13	0.45	0.83	0.337	19.11
		11.295			156.71	1769.9841					
1.00	10.000		15.77	781.29			27928.11	0.48	0.93	0.237	19.36
		8.972			43.19	387.4521					
0.90	7.943		16.20	824.48			28315.56	0.49	0.96	0.137	19.61
		7.126			211.57	1507.7373					
0.80	6.310		18.16	1036.05			29823.30	0.52	1.07	0.037	19.86
		5.661			229.40	1298.5393					
0.70	5.012		20.07	1265.45			31121.84	0.54	1.18	-0.063	20.11
		4.496			162.54	730.8416					
0.60	3.981		21.32	1427.99			31852.68	0.55	1.26	-0.163	20.36
		3.572			315.83	1128.0239					
0.50	3.162		23.56	1743.81			32980.70	0.57	1.39	-0.263	20.61
		2.837			512.60	1454.2776					
0.40	2.512		26.80	2256.42			34434.98	0.59	1.58	-0.363	20.86
		2.254			639.28	1440.6521					
0.30	1.995		30.36	2895.70			35875.62	0.62	1.79	-0.463	21.11
		1.790			787.43	1409.5549					
0.20	1.585		34.24	3683.13			37285.18	0.64	2.02	-0.563	21.36
		1.422			1009.85	1435.9016					
0.10	1.259		38.65	4692.98			38721.08	0.67	2.28	-0.663	21.61
		1.129			1032.37	1166.0088					
-0.00	1.000		42.69	5725.35			39887.09	0.69	2.52	-0.763	21.86
		0.897			1126.12	1010.3025					
-0.10	0.794		46.70	6851.46			40897.39	0.71	2.75	-0.863	22.11
		0.713			1220.78	869.9697					
-0.20	0.631		50.69	8072.24			41767.36	0.72	2.99	-0.963	22.36
		0.566			1503.78	851.2405					
-0.30	0.501		55.21	9576.02			42618.59	0.74	3.26	-1.063	22.61
		0.450			3179.59	1429.6790					
-0.40	0.398		63.72	12755.61			44048.27	0.76	3.76	-1.163	22.86
		0.357			2726.28	973.7307					
-0.50	0.316		70.20	15481.89			45022.00	0.78	4.14	-1.263	23.11
		0.284			5797.01	1644.6462					
-0.60	0.251		82.30	21278.90			46666.64	0.81	4.85	-1.363	23.36
		0.225			7915.79	1783.8667					
-0.70	0.200		96.40	29194.69			48450.51	0.84	5.68	-1.463	23.61
		0.179			5112.29	915.1328					
-0.80	0.158		104.50	34306.98			49365.64	0.85	6.16	-1.563	23.86
		0.142			6664.53	947.6282					
-0.90	0.126		114.20	40971.51			50313.27	0.87	6.73	-1.663	24.11
		0.113			11008.25	1243.3320					
-1.00	0.100		128.63	51979.77			51556.60	0.89	7.58	-1.763	24.36
		0.090			1998.96	179.3386					
-1.10	0.079		131.08	53978.73			51736.93	0.89	7.73	-1.863	24.61
		0.071			12969.09	924.2285					
-1.20	0.063		145.98	66947.81			52660.16	0.91	8.61	-1.963	24.86
		0.057			24883.25	1408.5669					
-1.30	0.050		170.97	91831.06			54068.73	0.93	10.08	-2.063	25.11
		0.045			21711.75	976.2603					
-1.40	0.040		190.11	113542.81			55044.98	0.95	11.21	-2.163	25.36
		0.036			14786.37	528.1206					
-1.50	0.032		202.11	128329.19			55573.10	0.96	11.92	-2.263	25.61
		0.028			13827.19	392.2888					
-1.60	0.025		212.72	142156.37			55965.39	0.97	12.54	-2.363	25.86
		0.023			4662.12	105.0647					
-1.70	0.020		216.18	146818.50			56070.45	0.97	12.75	-2.463	26.11
		0.018			9676.06	173.2097					
-1.80	0.016		223.19	156494.56			56243.66	0.97	13.16	-2.563	26.36
		0.014			9580.06	136.2204					
-1.90	0.013		229.92	166074.62			56379.87	0.97	13.56	-2.663	26.61
		0.011			9493.12	107.2219					
-2.00	0.010		236.40	175567.75			56487.09	0.98	13.94	-2.763	26.86
- ∞							57888.00	(1)			∞

PHOTOMETRIC PARAMETERS OF NGC 4552

V-FILTER

Total luminosity	L_T	= 16.08
Total apparent magnitude	m_T	= 9.95
Apparent central surface brightness	μ_o	= 16.56
Major axis at threshold	$2a_m$	= 8.12
Minor axis at threshold	$2b_m$	= 7.97
Major axis at μ=25.0 mag sec^{-2}	2a(25)	= 5.89
Luminosity within μ=25.0 mag sec^{-2}	k(25)	= 0.92
Gradient of exponential component	G(a)	= -0.48
Equivalent gradient of exponential comp.	G(r*)	= -0.54
Equivalent gradient of reduced exp. comp.	G(ρ)	= -----

Parameters at k = ¼ :

Semi-major axis	a_1	= 0.16
Axis ratio	b/a	= 0.86
Equivalent radius	r_1*	= 0.13
Surface brightness	μ_1	= 17.66

Parameters at k = ½(effective) :

Semi-major axis	a_e	= 0.27
Axis ratio	b/a	= 0.91
Equivalent radius	r_e*	= 0.28
Surface brightness	μ_e	= 19.69
Mean surface brightness	μ_e'	= 9.20

Parameters at k = ¾ :

Semi-major axis	a_3	= 1.02
Axis ratio	b/a	= 0.93
Equivalent radius	r_3*	= 1.00
Surface brightness	μ_3	= 22.73

Concentration indices ..... C_{21} = 2.25, C_{32} = 3.53

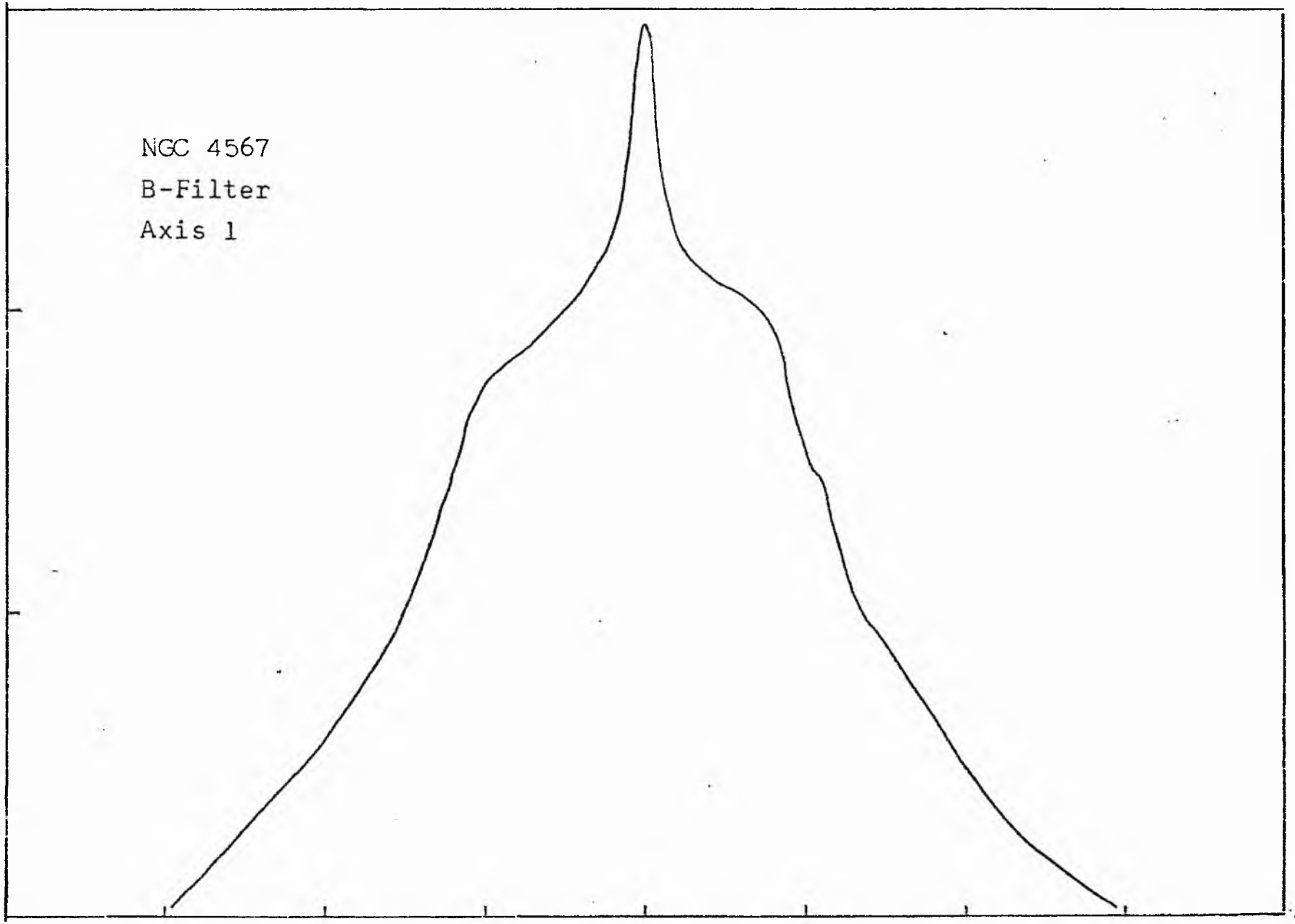
NGC 4567
B-Filter
Axis 1

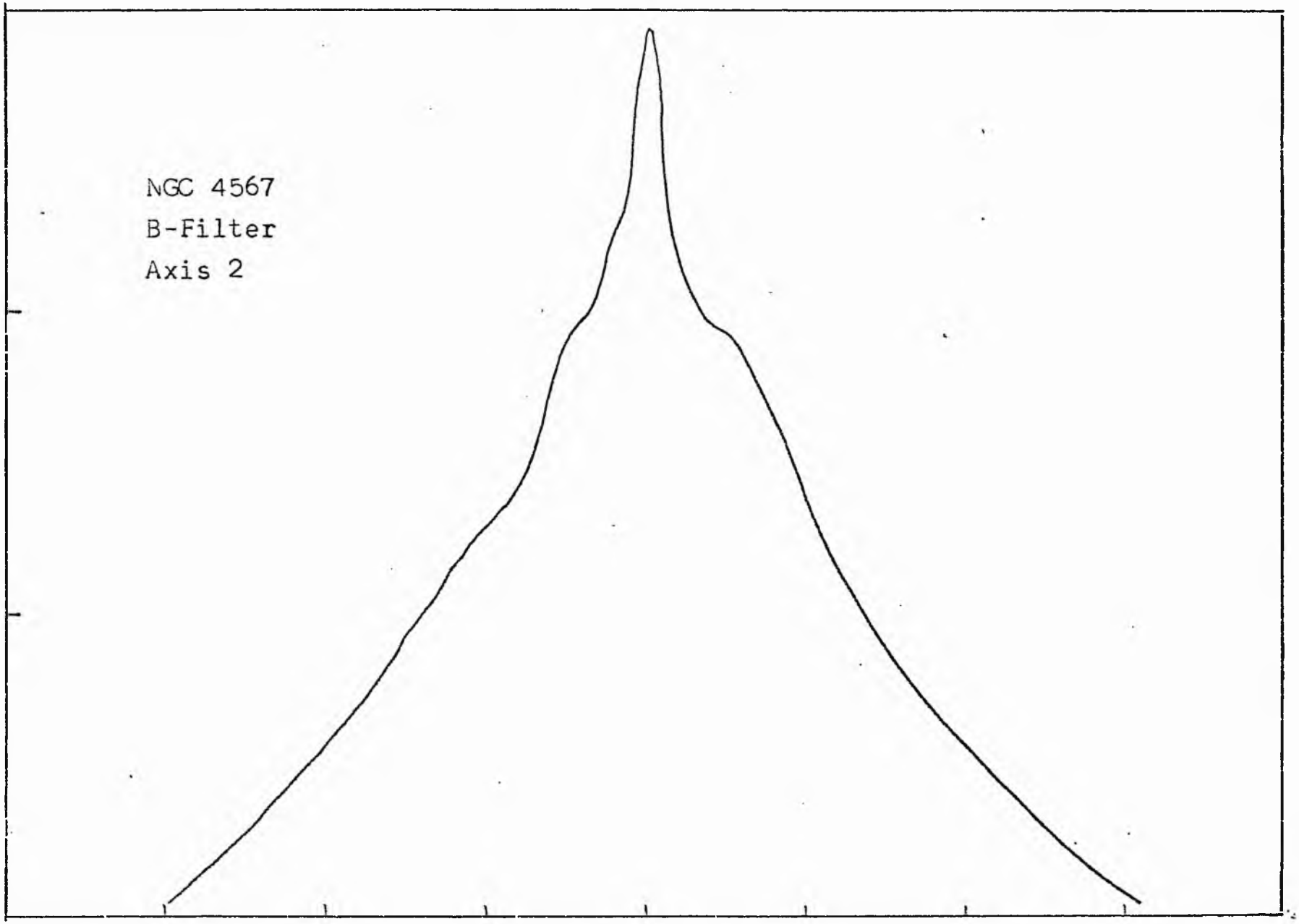
NGC 4567
B-Filter
Axis 2

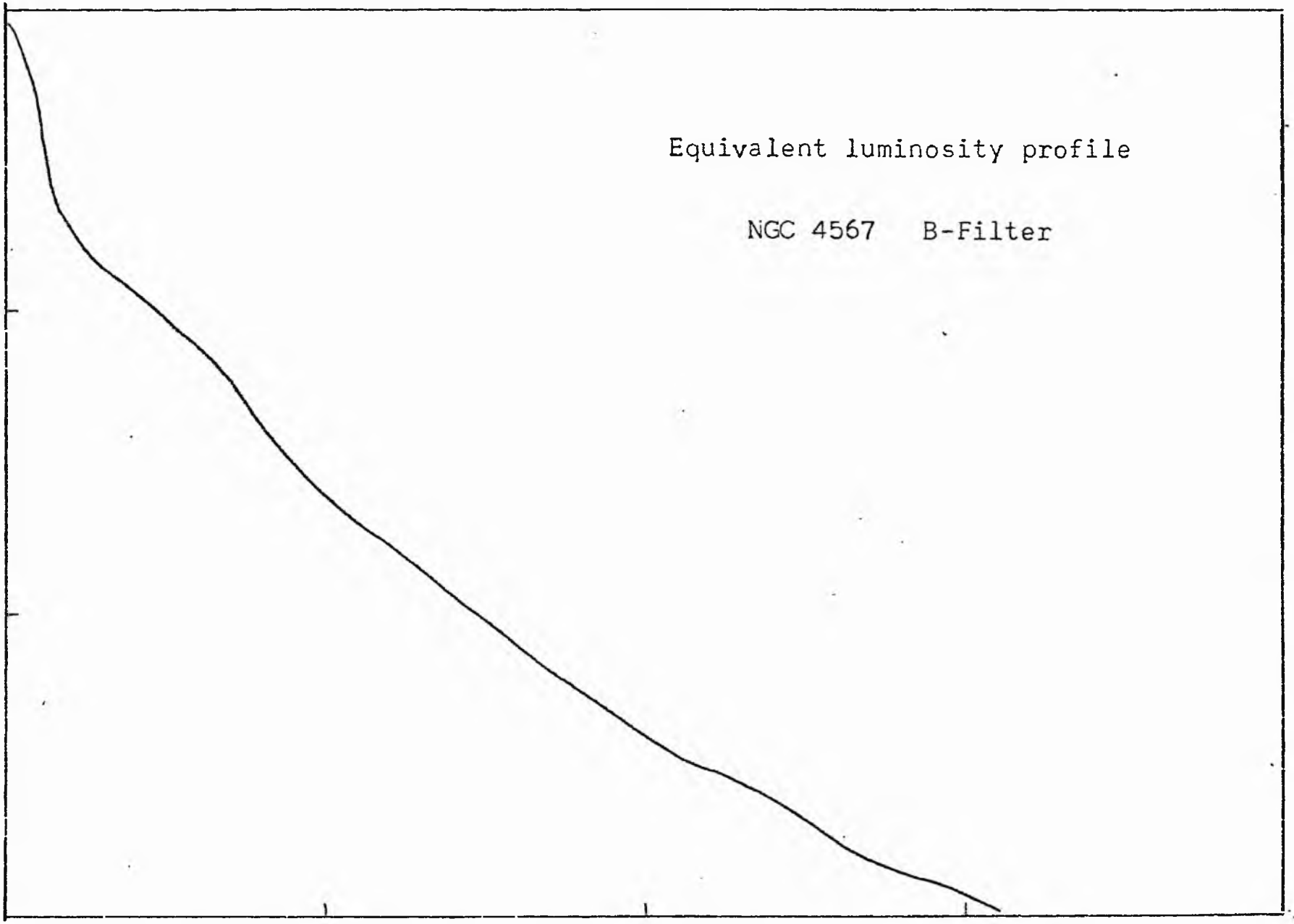
Equivalent luminosity profile
NGC 4567 B-Filter

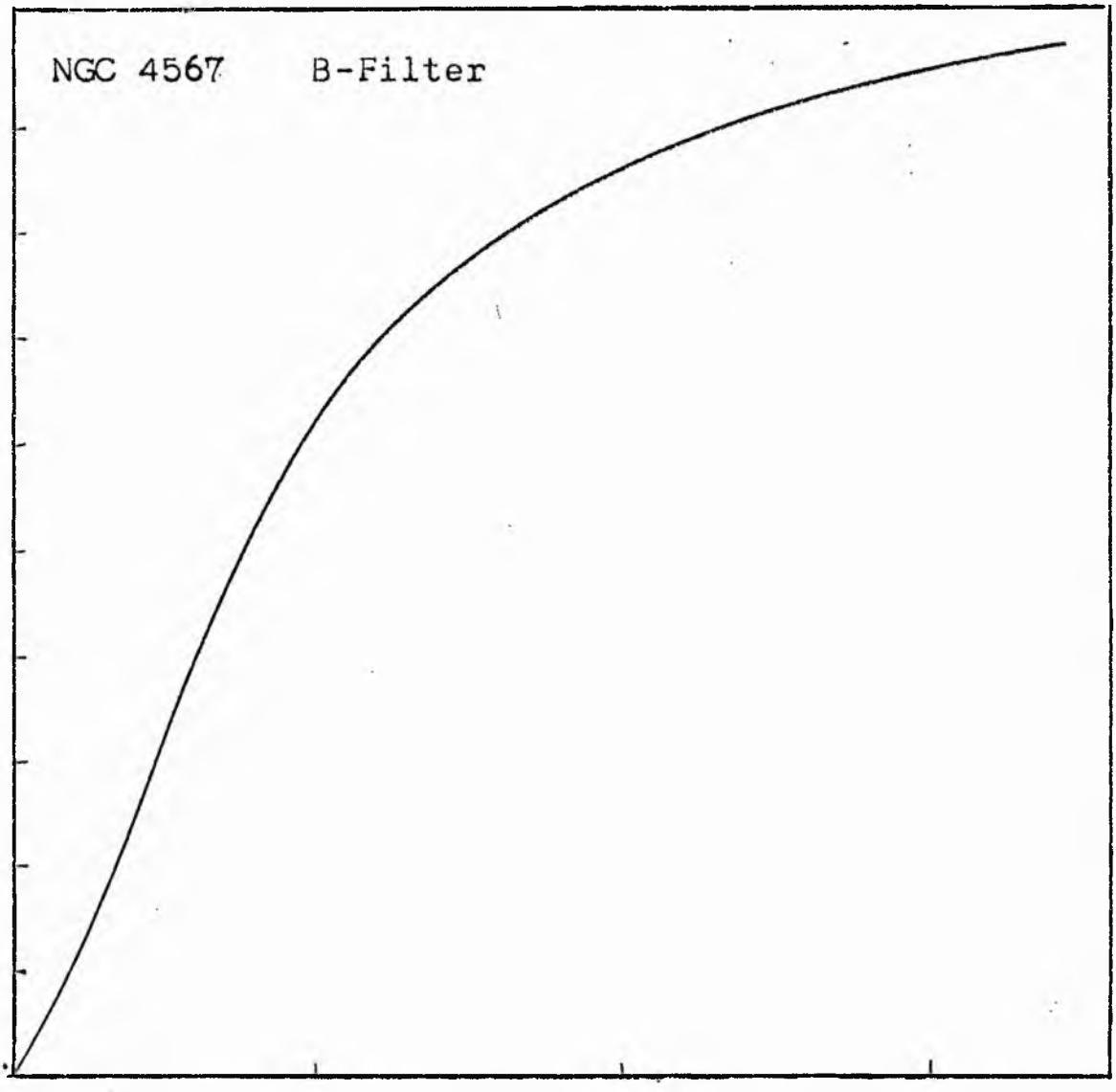

Relative integrated luminosity k(r) versus equivalent radius r*.

MEAN LUMINOSITY DISTRIBUTION IN NGC 4567
B COLOUR

LOG I	I	$\bar{I}$	R	AREA	ΔA	P	ΣP	K(R)	ρ	LOG J	μ
0.94	8.710		0.0	0.0			0.0	0.0	0.0	1.241	19.60
		8.326			16.62	138.3774					
0.90	7.943		2.30	16.62			138.38	0.01	0.06	1.201	19.70
		7.126			28.75	204.8531					
0.80	6.310		3.80	45.36			343.23	0.04	0.10	1.101	19.95
		5.661			24.03	136.0452					
0.70	5.012		4.70	69.40			479.28	0.05	0.13	1.001	20.20
		4.496			12.31	55.3740					
0.60	3.981		5.10	81.71			534.65	0.06	0.14	0.901	20.45
		3.572			46.97	167.7503					
0.50	3.162		6.40	128.68			702.40	0.08	0.17	0.801	20.70
		2.837			43.35	122.9987					
0.40	2.512		7.40	172.03			825.40	0.09	0.20	0.701	20.95
		2.254			44.39	100.0379					
0.30	1.995		8.30	216.42			925.44	0.10	0.23	0.601	21.20
		1.790			129.94	232.5961					
0.20	1.585		10.50	346.36			1158.03	0.12	0.29	0.501	21.45
		1.422			508.94	723.6641					
0.10	1.259		16.50	855.30			1881.70	0.20	0.45	0.401	21.70
		1.129			763.53	862.3811					
0.00	1.000		22.70	1618.83			2744.08	0.29	0.62	0.301	21.95
		0.897			1005.06	901.7021					
-0.10	0.794		28.90	2623.89			3645.78	0.39	0.79	0.201	22.20
		0.713			797.31	568.1948					
-0.20	0.631		33.00	3421.19			4213.97	0.45	0.90	0.101	22.45
		0.566			810.18	458.6228					
-0.30	0.501		36.70	4231.38			4672.59	0.50	1.00	0.001	22.70
		0.450			820.33	368.8584					
-0.40	0.398		40.10	5051.71			5041.45	0.54	1.09	-0.099	22.95
		0.357			703.18	251.1546					
-0.50	0.316		42.80	5754.89			5292.60	0.57	1.17	-0.199	23.20
		0.284			691.93	196.3075					
-0.60	0.251		45.30	6446.82			5488.91	0.59	1.23	-0.299	23.45
		0.225			2578.84	581.1614					
-0.70	0.200		53.60	9025.66			6070.07	0.65	1.46	-0.399	23.70
		0.179			2397.45	429.1619					
-0.80	0.158		60.30	11423.11			6499.23	0.70	1.64	-0.499	23.95
		0.142			2511.61	357.1284					
-0.90	0.126		66.60	13934.72			6856.35	0.73	1.81	-0.599	24.20
		0.113			2715.21	306.6731					
-1.00	0.100		72.80	16649.93			7163.02	0.77	1.98	-0.699	24.45
		0.090			3056.14	274.1870					
-1.10	0.079		79.20	19706.07			7437.21	0.80	2.16	-0.799	24.70
		0.071			3152.43	224.6565					
-1.20	0.063		85.30	22858.50			7661.86	0.82	2.32	-0.899	24.95
		0.057			3501.21	198.1947					
-1.30	0.050		91.60	26359.71			7860.05	0.84	2.49	-0.999	25.20
		0.045			3689.11	165.8811					
-1.40	0.040		97.80	30048.82			8025.93	0.86	2.66	-1.099	25.45
		0.036			8102.80	289.4080					
-1.50	0.032		110.20	38151.62			8315.34	0.89	3.00	-1.199	25.70
		0.028			3903.27	110.7400					
-1.60	0.025		115.70	42054.89			8426.08	0.90	3.15	-1.299	25.95
		0.023			8138.20	183.4023					
-1.70	0.020		126.40	50193.09			8609.48	0.92	3.44	-1.399	26.20
		0.018			4049.52	72.4904					
-1.80	0.016		131.40	54242.61			8681.97	0.93	3.58	-1.499	26.45
		0.014			13828.89	196.6370					
-1.90	0.013		147.20	68071.50			8878.61	0.95	4.01	-1.599	26.70
		0.011			6434.50	72.6763					
-2.00	0.010		154.00	74506.00			8951.28	0.96	4.19	-1.699	26.95
$-\infty$							9351.00	(1)			∞

PHOTOMETRIC PARAMETERS OF NGC 4567

B-FILTER

Total luminosity ..... L_T = 2.60

Total apparent magnitude ..... m_T = 12.04

Apparent central surface brightness ..... μ_o = 19.60

Major axis at threshold ..... $2a_m$ = 4.95

Minor axis at threshold ..... $2b_m$ = 4.75

Major axis at μ=25.0 mag sec^{-2} ..... 2a(25) = 3.12

Luminosity within μ=25.0 mag sec^{-2} ..... k(25) = 0.83

Gradient of exponential component ..... G(a) = -1.18

Equivalent gradient of exponential comp..... G(r*) = -0.89

Equivalent gradient of reduced exp. comp..... G(ρ) = -0.84

Parameters at k = ¼ :

- Semi-major axis ..... a_1 = 0.37
- Axis ratio ..... b/a = 0.82
- Equivalent radius ..... r_1* = 0.33
- Surface brightness ..... μ_1 = 21.81

Parameters at k = ½(effective) :

- Semi-major axis ..... a_e = 0.81
- Axis ratio ..... b/a = 0.73
- Equivalent radius ..... r_e* = 0.61
- Surface brightness ..... μ_e = 22.70
- Mean surface brightness ..... μ_e' = 12.96

Parameters at k = ¾ :

- Semi-major axis ..... a_3 = 1.24
- Axis ratio ..... b/a = 0.89
- Equivalent radius ..... r_3* = 1.16
- Surface brightness ..... μ_3 = 24.32

Concentration indices ..... C_{21} = 1.85, C_{32} = 1.90

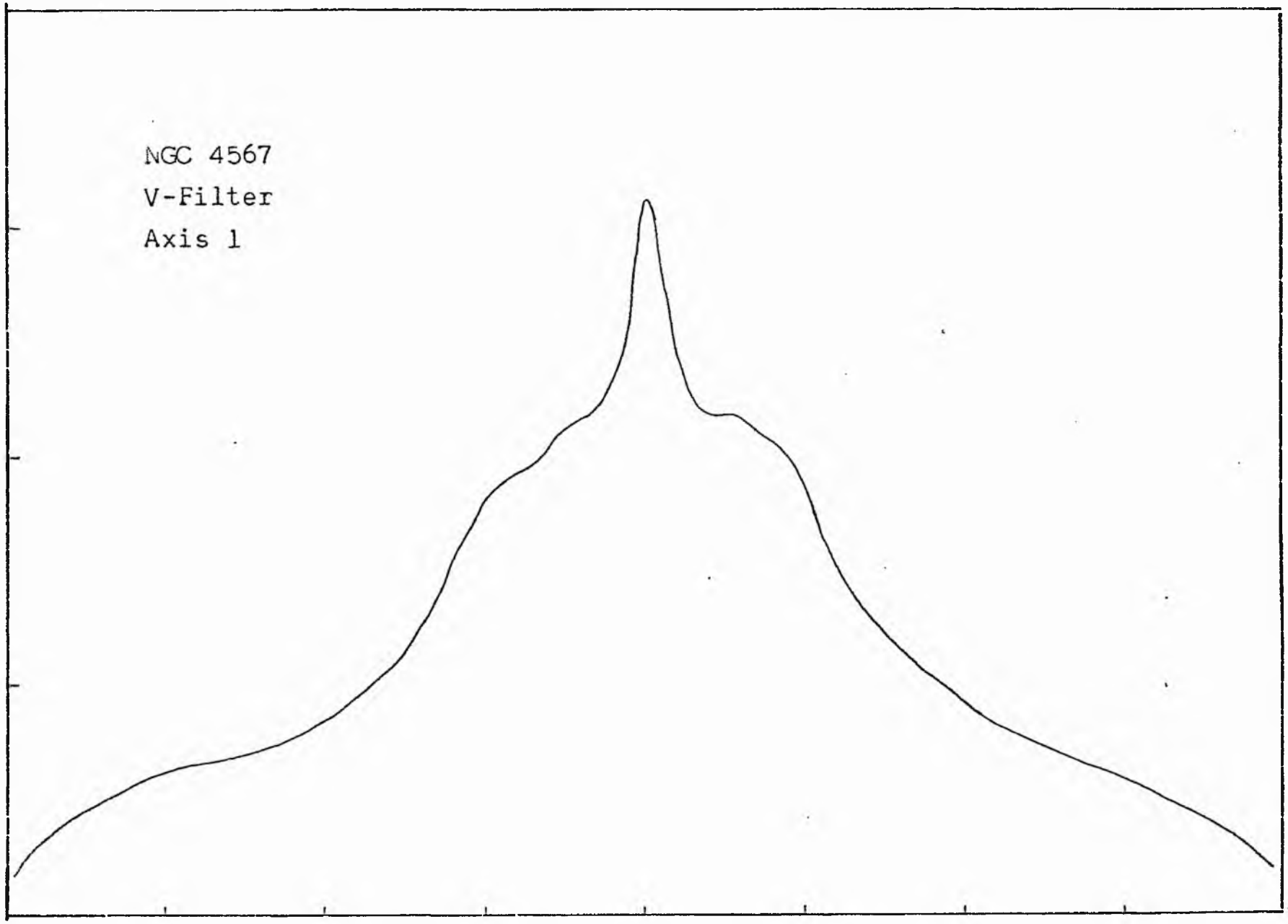
NGC 4567
V-Filter
Axis 1

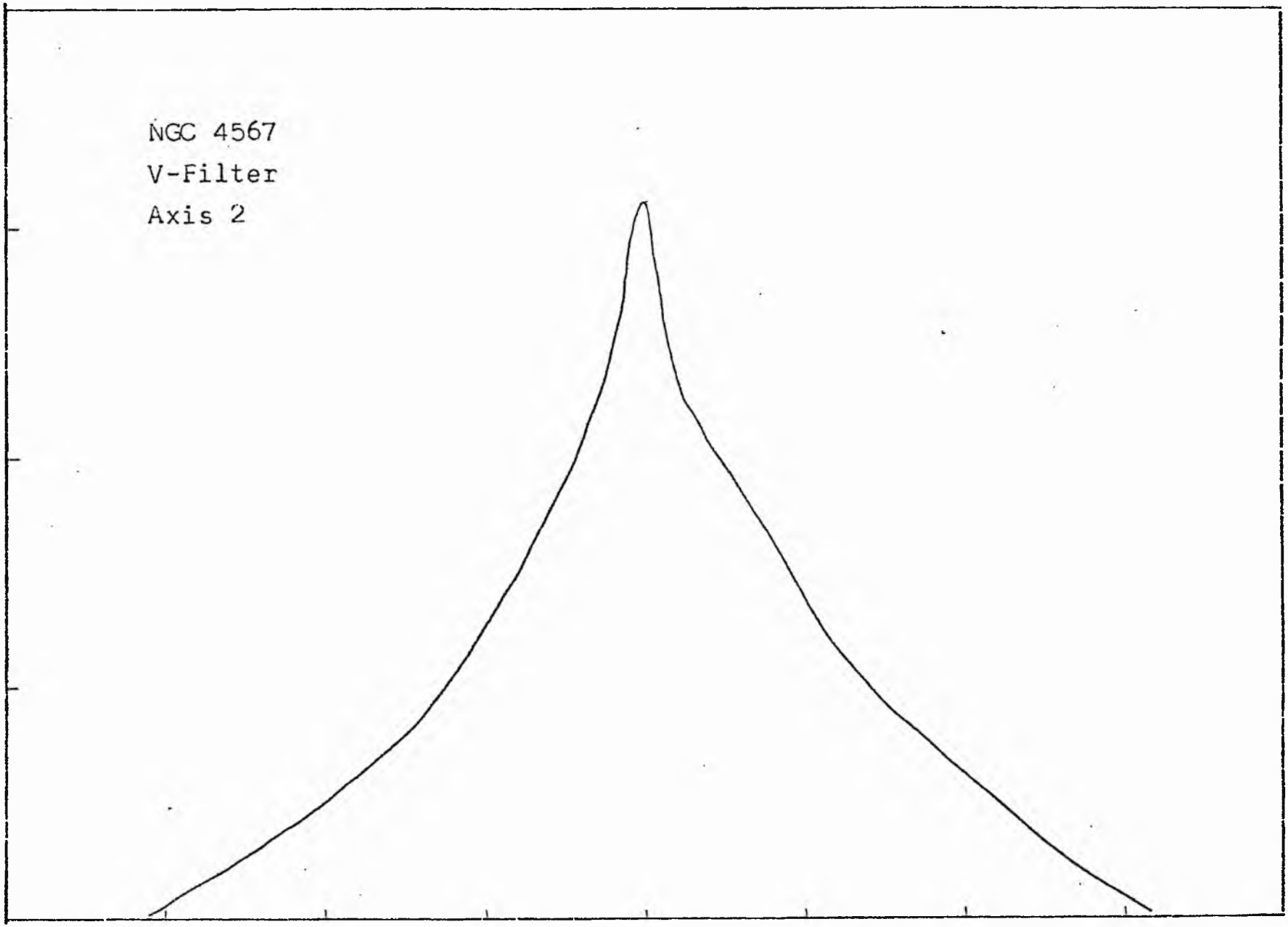
NGC 4567
V-Filter
Axis 2

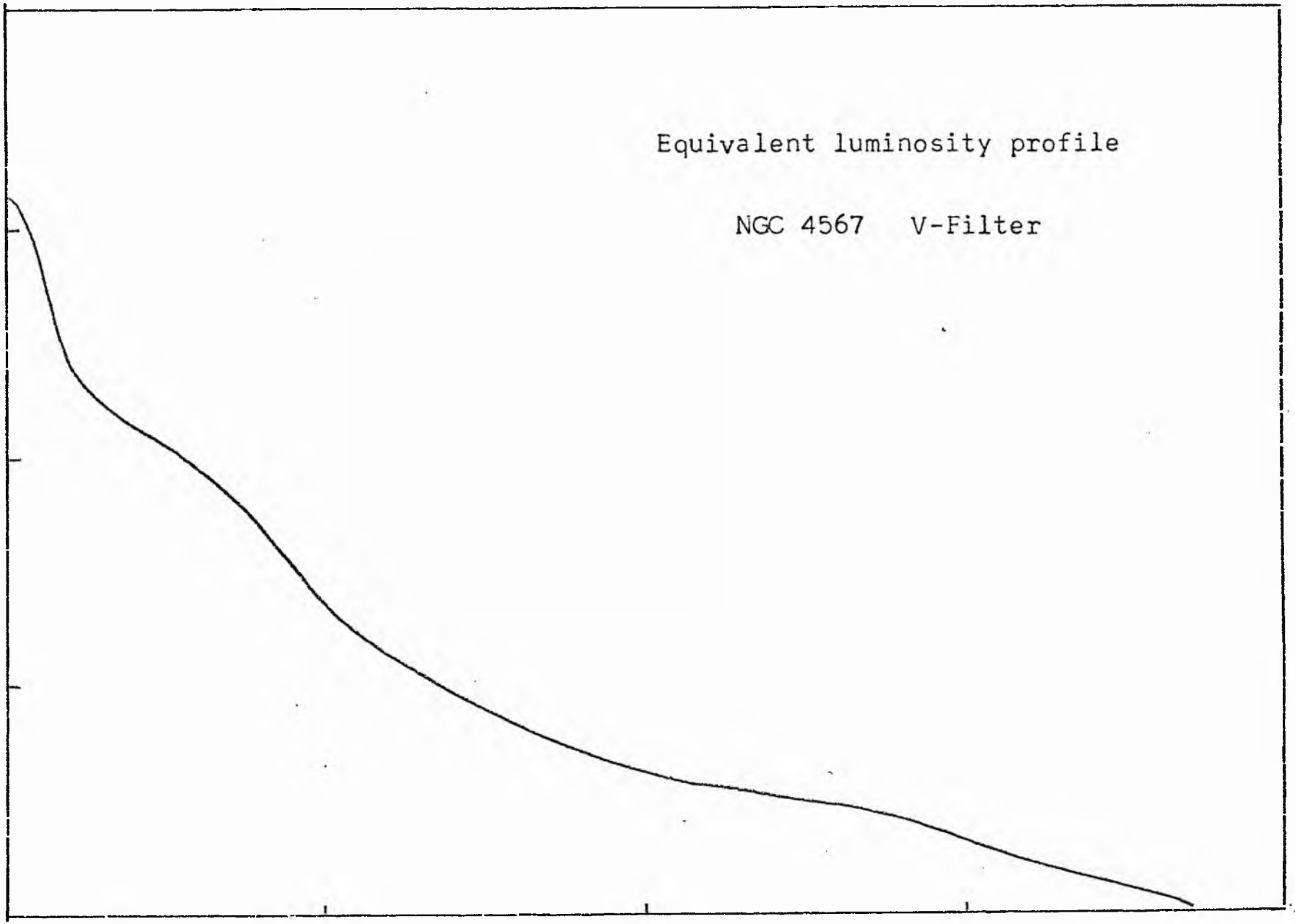
Equivalent luminosity profile
NGC 4567 V-Filter

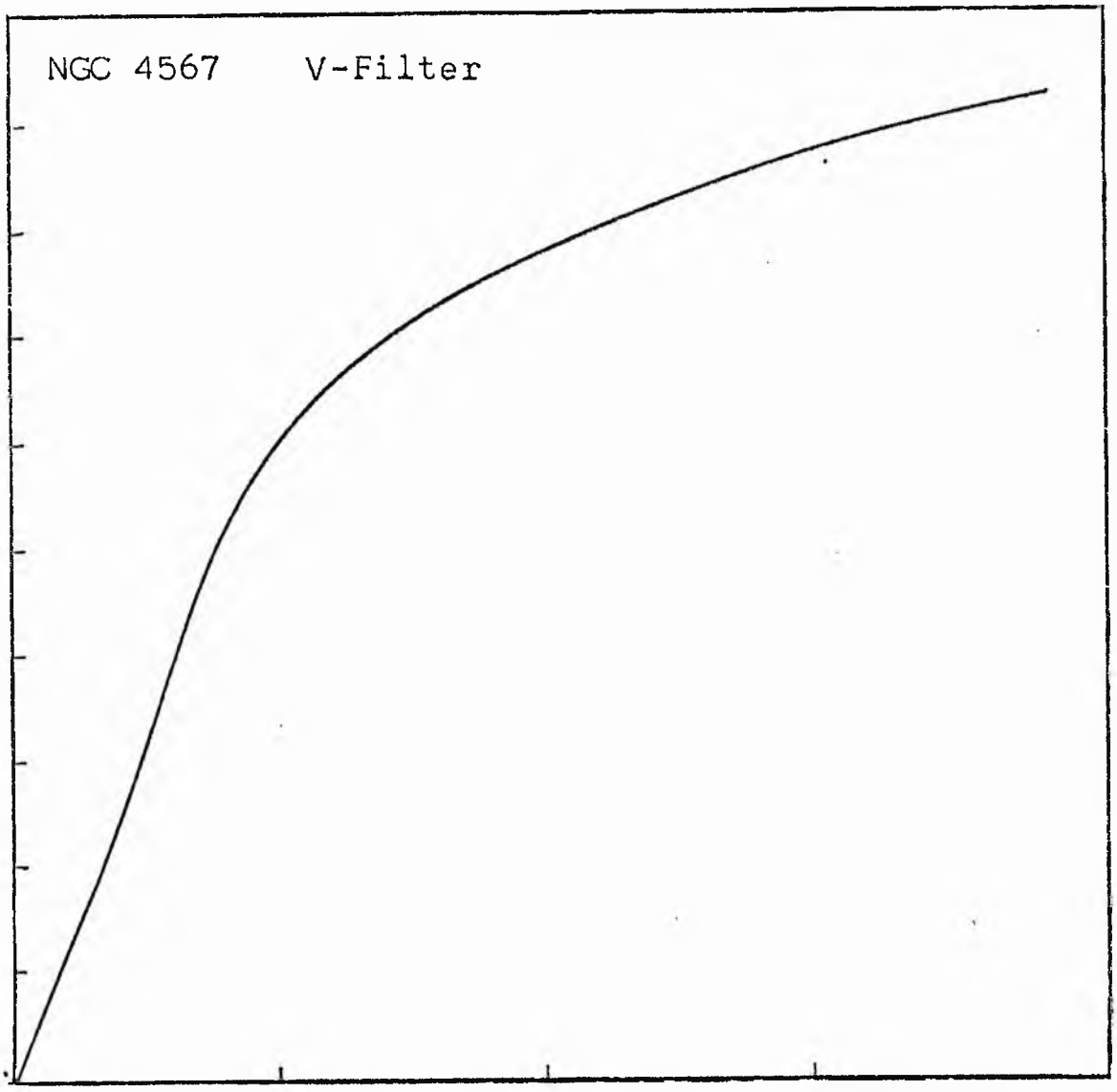

Relative integrated luminosity k(r) versus equivalent radius r*.

MEAN LUMINOSITY DISTRIBUTION IN NGC 4567
V COLOUR

LOG I	I	$\bar{I}$	R	AREA	ΔA	P	ΣP	K(R)	ρ	LOG J	μ
1.14	13.804		0.0	0.0			0.0	0.0	0.0	1.340	18.55
		13.197			16.62	219.3131					
1.10	12.589		2.30	16.62			219.31	0.02	0.06	1.300	18.65
		11.295			26.39	298.0576					
1.00	10.000		3.70	43.01			517.37	0.04	0.10	1.200	18.90
		8.972			12.41	111.3312					
0.90	7.943		4.20	55.42			628.70	0.05	0.11	1.100	19.15
		7.126			20.01	142.6137					
0.80	6.310		4.90	75.43			771.32	0.06	0.13	1.000	19.40
		5.661			53.25	301.4329					
0.70	5.012		6.40	128.68			1072.75	0.09	0.17	0.900	19.65
		4.496			34.18	153.6917					
0.60	3.981		7.20	162.86			1226.44	0.10	0.20	0.800	19.90
		3.572			38.20	136.4441					
0.50	3.162		8.00	201.06			1362.88	0.11	0.22	0.700	20.15
		2.837			88.47	250.9881					
0.40	2.512		9.60	289.53			1613.87	0.13	0.26	0.600	20.40
		2.254			233.26	525.6753					
0.30	1.995		12.90	522.79			2139.55	0.17	0.35	0.500	20.65
		1.790			439.32	786.4172					
0.20	1.585		17.50	962.11			2925.96	0.23	0.48	0.400	20.90
		1.422			772.83	1098.8958					
0.10	1.259		23.50	1734.94			4024.86	0.32	0.64	0.300	21.15
		1.129			798.94	902.3687					
-0.00	1.000		28.40	2533.88			4927.23	0.39	0.77	0.200	21.40
		0.897			784.43	703.7578					
-0.10	0.794		32.50	3318.31			5630.98	0.45	0.89	0.100	21.65
		0.713			913.07	650.6931					
-0.20	0.631		36.70	4231.38			6281.68	0.50	1.00	0.000	21.90
		0.566			596.12	337.4451					
-0.30	0.501		39.20	4827.50			6619.12	0.53	1.07	-0.100	22.15
		0.450			793.72	356.8933					
-0.40	0.398		42.30	5621.21			6976.01	0.56	1.15	-0.200	22.40
		0.357			939.97	335.7263					
-0.50	0.316		45.70	6561.18			7311.73	0.58	1.25	-0.300	22.65
		0.284			767.80	217.8315					
-0.60	0.251		48.30	7328.98			7529.56	0.60	1.32	-0.400	22.90
		0.225			1696.68	382.3594					
-0.70	0.200		53.60	9025.66			7911.92	0.63	1.46	-0.500	23.15
		0.179			1652.26	295.7668					
-0.80	0.158		58.30	10677.92			8207.68	0.65	1.59	-0.600	23.40
		0.142			1949.89	277.2573					
-0.90	0.126		63.40	12627.82			8484.94	0.68	1.73	-0.700	23.65
		0.113			1941.65	219.3025					
-1.00	0.100		68.10	14569.47			8734.24	0.69	1.86	-0.800	23.90
		0.090			3719.90	333.7366					
-1.10	0.079		76.30	18289.37			9037.97	0.72	2.08	-0.900	24.15
		0.071			3562.16	253.8554					
-1.20	0.063		83.40	21851.53			9291.82	0.74	2.27	-1.000	24.40
		0.057			6620.85	374.7888					
-1.30	0.050		95.20	28472.38			9666.61	0.77	2.59	-1.100	24.65
		0.045			9748.51	438.3406					
-1.40	0.040		110.30	38220.89			10104.95	0.80	3.00	-1.200	24.90
		0.036			12210.75	436.1306					
-1.50	0.032		126.70	50431.63			10541.08	0.84	3.45	-1.300	25.15
		0.028			12026.37	341.2004					
-1.60	0.025		141.00	62458.01			10882.28	0.87	3.84	-1.400	25.40
		0.023			11661.43	262.8013					
-1.70	0.020		153.60	74119.44			11145.08	0.89	4.18	-1.500	25.65
		0.018			11099.62	198.6940					
-1.80	0.016		164.70	85219.06			11343.77	0.90	4.49	-1.600	25.90
		0.014			12426.87	176.7009					
-1.90	0.013		176.30	97645.94			11520.47	0.92	4.80	-1.700	26.15
		0.011			14574.87	164.6198					
-2.00	0.010		189.00	112220.81			11685.09	0.93	5.15	-1.800	26.40
$-\infty$							12565.00	(1)			∞

PHOTOMETRIC PARAMETERS OF NGC 4567

V-FILTER

Total luminosity	L_T	= 3.49
Total apparent magnitude	m_T	= 11.15
Apparent central surface brightness	μ_o	= 18.55
Major axis at threshold	$2a_m$	= 6.43
Minor axis at threshold	$2b_m$	= 5.28
Major axis at μ=25.0 mag sec^{-2}	2a(25)	= 5.30
Luminosity within μ=25.0 mag sec^{-2}	k(25)	= 0.81
Gradient of exponential component	G(a)	= -0.76
Equivalent gradient of exponential comp.	G(r*)	= -0.91
Equivalent gradient of reduced exp. comp.	G(ρ)	= -0.91
Parameters at k = ¼ :		
Semi-major axis	a_1	= 0.31
Axis ratio	b/a	= 0.89
Equivalent radius	r_1*	= 0.32
Surface brightness	μ_1	= 20.96
Parameters at k = ½(effective) :		
Semi-major axis	a_e	= 0.82
Axis ratio	b/a	= 0.76
Equivalent radius	r_e*	= 0.62
Surface brightness	μ_e	= 21.90
Mean surface brightness	μ_e'	= 12.11
Parameters at k = ¾ :		
Semi-major axis	a_3	= 1.77
Axis ratio	b/a	= 0.76
Equivalent radius	r_3*	= 1.46
Surface brightness	μ_3	= 24.48
Concentration indices	C_{21}	= 1.96
	C_{32}	= 2.38

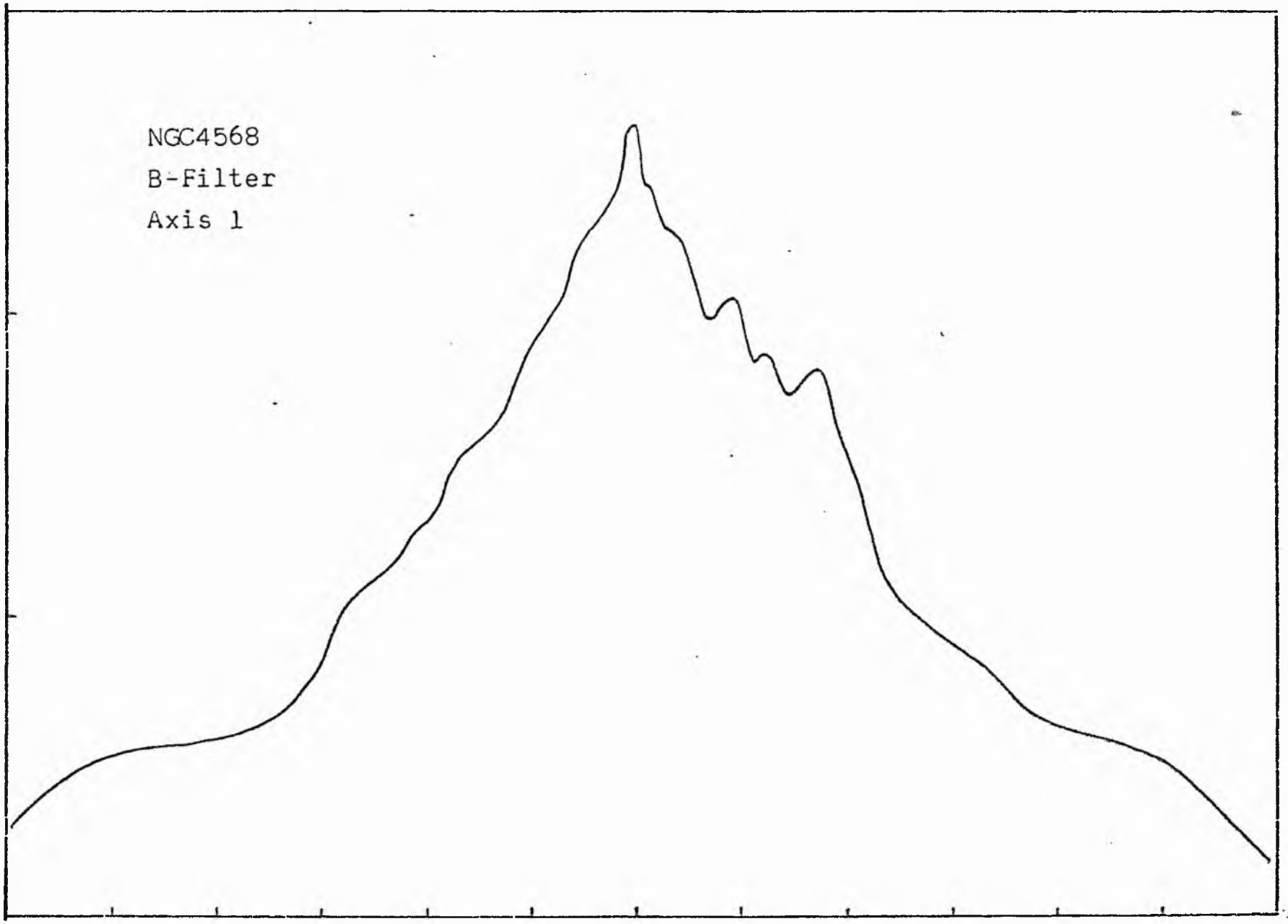
NGC4568
B-Filter
Axis 1

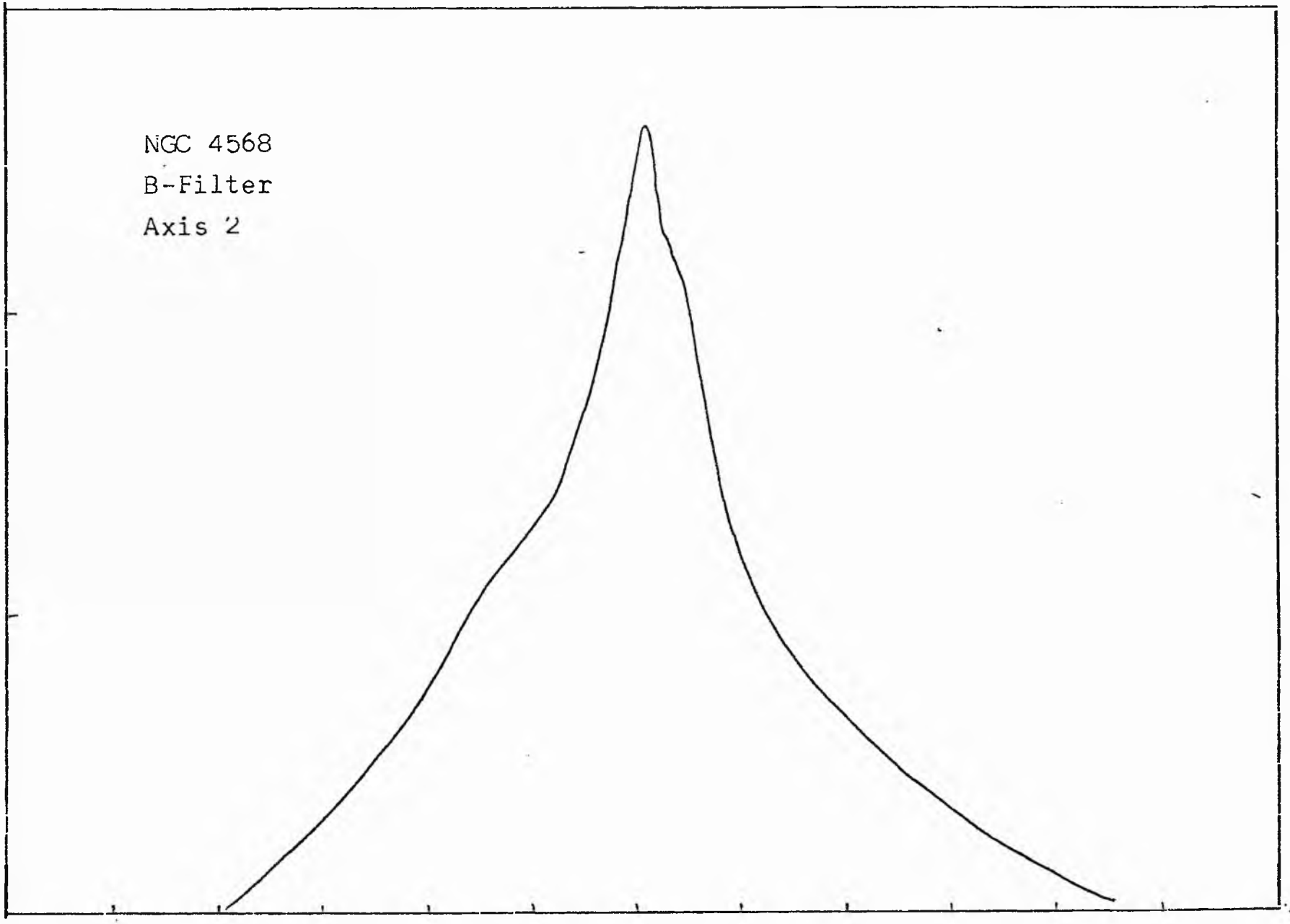
NGC 4568
B-Filter
Axis 2

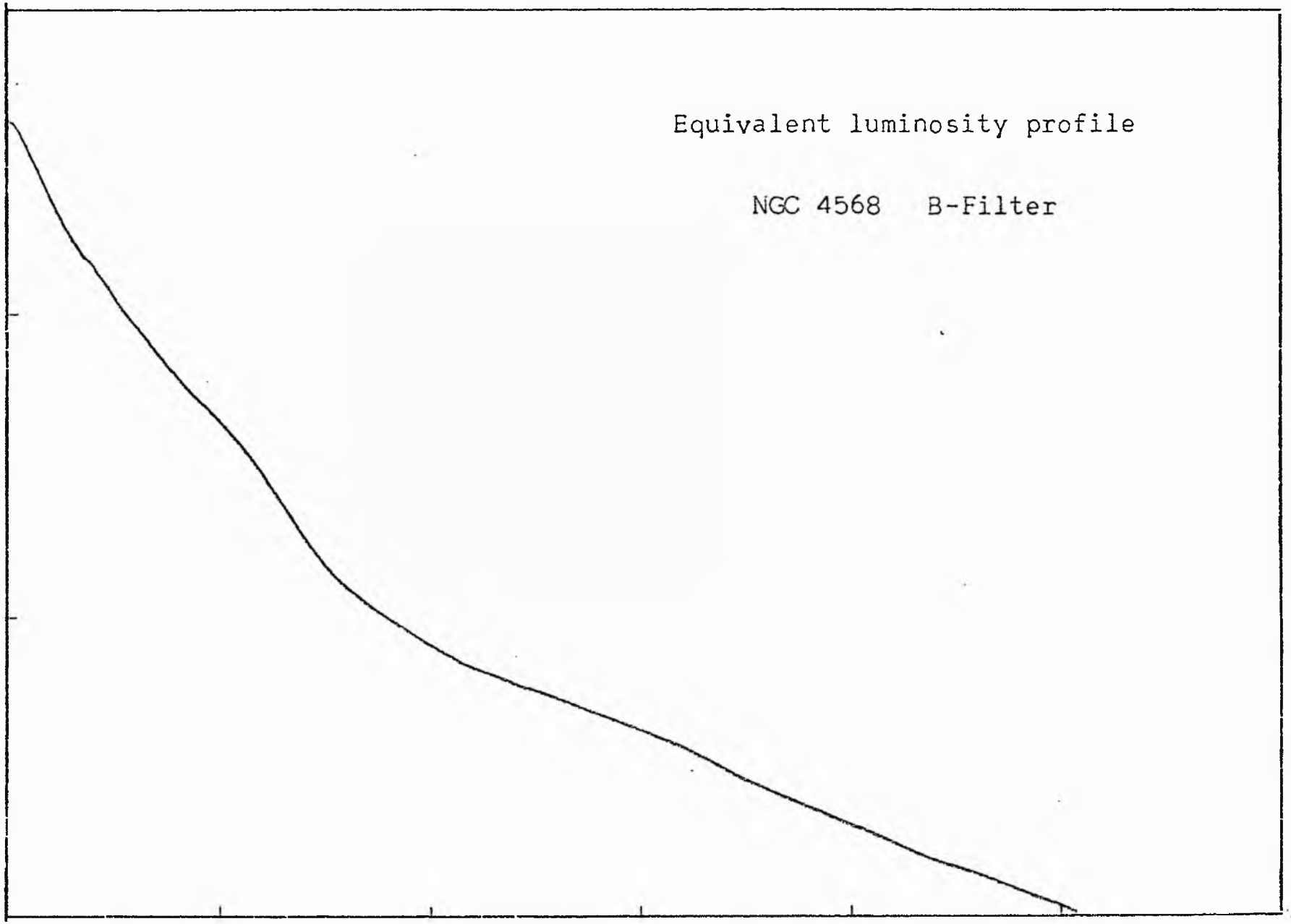
Equivalent luminosity profile
NGC 4568 B-Filter

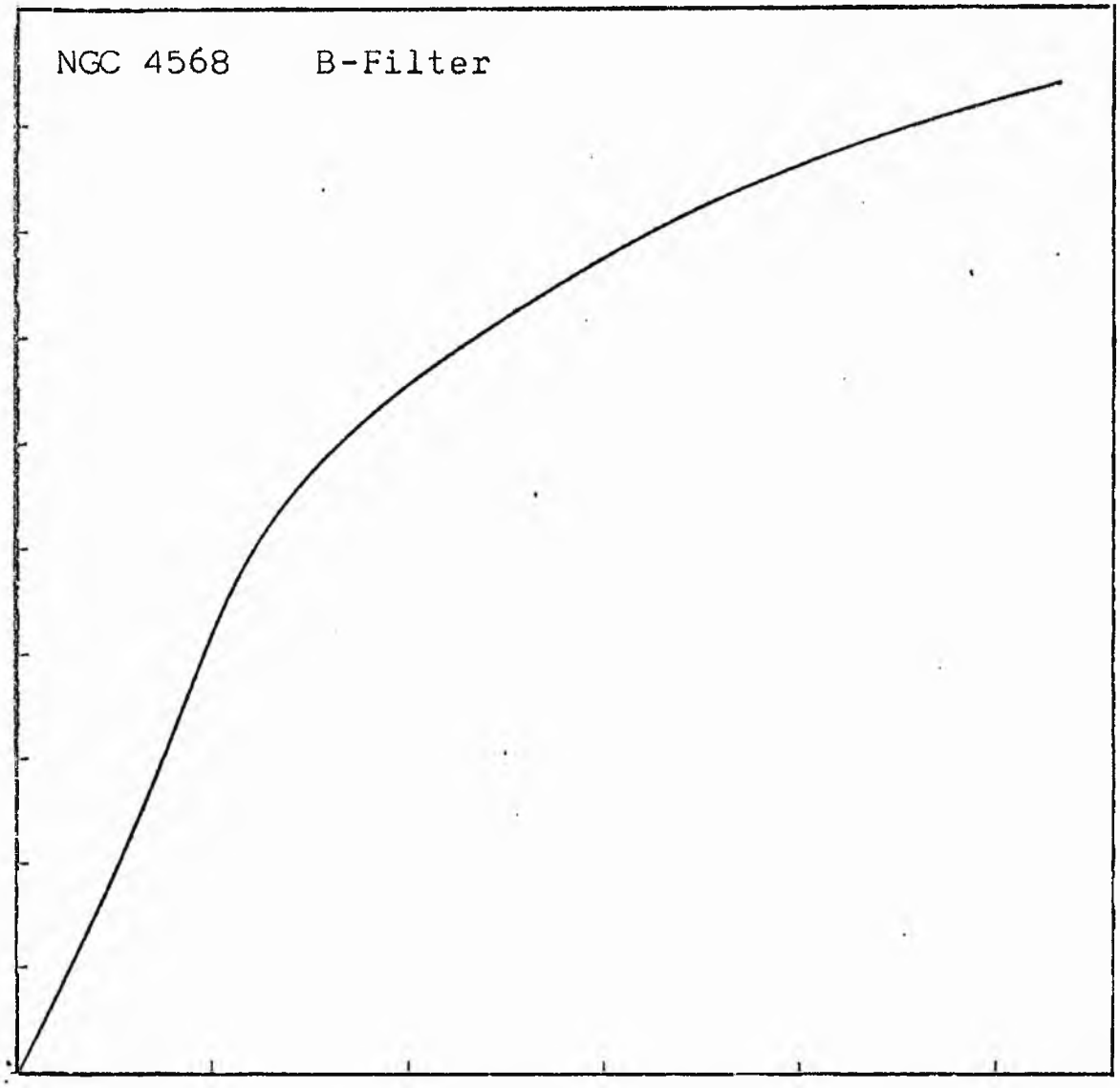

Relative integrated luminosity k(r) versus equivalent radius r*.

MEAN LUMINOSITY DISTRIBUTION IN NGC 4568
B COLOUR

LOG I	I	T	R	AREA	ΔA	P	ΣP	K(R)	ρ	LOG J	μ
0.61	4.074		0.0	0.0			0.0	0.0	0.0	1.134	20.50
		4.027			14.66	59.0318					
0.60	3.981		2.16	14.66			59.03	0.00	0.04	1.124	20.53
		3.572			57.72	206.1741					
0.50	3.162		4.80	72.38			265.21	0.02	0.08	1.024	20.78
		2.837			165.40	469.2668					
0.40	2.512		8.70	237.79			734.47	0.04	0.14	0.924	21.03
		2.254			45.74	103.0817					
0.30	1.995		9.50	283.53			837.55	0.05	0.16	0.824	21.28
		1.790			551.16	986.6184					
0.20	1.585		16.30	834.69			1824.17	0.11	0.27	0.724	21.53
		1.422			561.33	798.1575					
0.10	1.259		21.08	1396.02			2622.33	0.15	0.35	0.624	21.78
		1.129			911.20	1029.1650					
0.00	1.000		27.10	2307.22			3651.50	0.21	0.45	0.524	22.03
		0.897			956.18	857.0542					
-0.10	0.794		32.23	3263.40			4509.35	0.26	0.53	0.424	22.28
		0.713			1512.51	1077.8770					
-0.20	0.631		38.99	4775.91			5587.22	0.32	0.64	0.324	22.53
		0.566			2315.29	1310.6235					
-0.30	0.501		47.51	7091.20			6897.84	0.40	0.78	0.224	22.78
		0.450			2113.84	950.4027					
-0.40	0.398		54.13	9205.04			7848.32	0.45	0.89	0.124	23.03
		0.357			1954.39	698.0466					
-0.50	0.316		59.60	11159.43			8546.37	0.49	0.98	0.024	23.28
		0.284			1628.23	461.9417					
-0.60	0.251		63.80	12787.66			9008.31	0.52	1.05	-0.076	23.53
		0.225			1399.26	315.3335					
-0.70	0.200		67.20	14186.92			9323.64	0.54	1.11	-0.176	23.78
		0.179			1783.96	319.3425					
-0.80	0.158		71.30	15970.87			9642.98	0.56	1.17	-0.276	24.03
		0.142			2947.04	419.0420					
-0.90	0.126		77.60	18917.91			10062.02	0.58	1.28	-0.376	24.28
		0.113			5079.96	573.7629					
-1.00	0.100		87.40	23997.87			10635.78	0.61	1.44	-0.476	24.53
		0.090			6482.65	581.6011					
-1.10	0.079		98.50	30480.52			11217.38	0.65	1.62	-0.576	24.78
		0.071			9139.00	651.2859					
-1.20	0.063		112.30	39619.52			11868.66	0.68	1.85	-0.676	25.03
		0.057			16959.42	960.0286					
-1.30	0.050		134.20	56578.95			12828.69	0.74	2.21	-0.776	25.28
		0.045			14768.12	664.0469					
-1.40	0.040		150.70	71347.06			13492.74	0.78	2.48	-0.876	25.53
		0.036			15535.81	554.8918					
-1.50	0.032		166.30	86882.87			14047.63	0.81	2.74	-0.976	25.78
		0.028			16494.19	467.9570					
-1.60	0.025		181.40	103377.06			14515.59	0.84	2.99	-1.076	26.03
		0.023			22286.62	502.2500					
-1.70	0.020		200.00	125663.69			15017.84	0.87	3.30	-1.176	26.28
		0.018			23363.50	418.2290					
-1.80	0.016		217.80	149027.19			15436.06	0.89	3.59	-1.276	26.53
		0.014			25058.37	356.3113					
-1.90	0.013		235.40	174085.56			15792.37	0.91	3.88	-1.376	26.78
		0.011			22263.94	251.4660					
-2.00	0.010		250.00	196349.50			16043.84	0.93	4.12	-1.476	27.03
- ∞							17343.00	(1)			∞

PHOTOMETRIC PARAMETERS OF NGC 4568

B-FILTER

Total luminosity	L_T	= 4.82
Total apparent magnitude	m_T	= 11.50
Apparent central surface brightness	μ_o	= 20.50
Major axis at threshold	$2a_m$	= 11.02
Minor axis at threshold	$2b_m$	= 7.17
Major axis at μ=25.0 mag sec^{-2}	2a(25)	= 4.77
Luminosity within μ=25.0 mag sec^{-2}	k(25)	= 0.67
Gradient of exponential component	G(a)	= -0.41
Equivalent gradient of exponential comp.	G(r*)	= -0.38
Equivalent gradient of reduced exp. comp.	G(ρ)	= -1.05

Parameters at k = ¼ :

Semi-major axis	a_1	= 0.63
Axis ratio	b/a	= 0.53
Equivalent radius	r_1*	= 0.53
Surface brightness	μ_1	= 22.23

Parameters at k = ½(effective) :

Semi-major axis	a_e	= 1.59
Axis ratio	b/a	= 0.38
Equivalent radius	r_e*	= 1.01
Surface brightness	μ_e	= 23.36
Mean surface brightness	μ_e'	= 13.52

Parameters at k = ¾ :

Semi-major axis	a_3	= 2.74
Axis ratio	b/a	= 0.53
Equivalent radius	r_3*	= 2.31
Surface brightness	μ_3	= 25.34
Concentration indices	C_{21}	= 1.95
	C_{32}	= 2.28

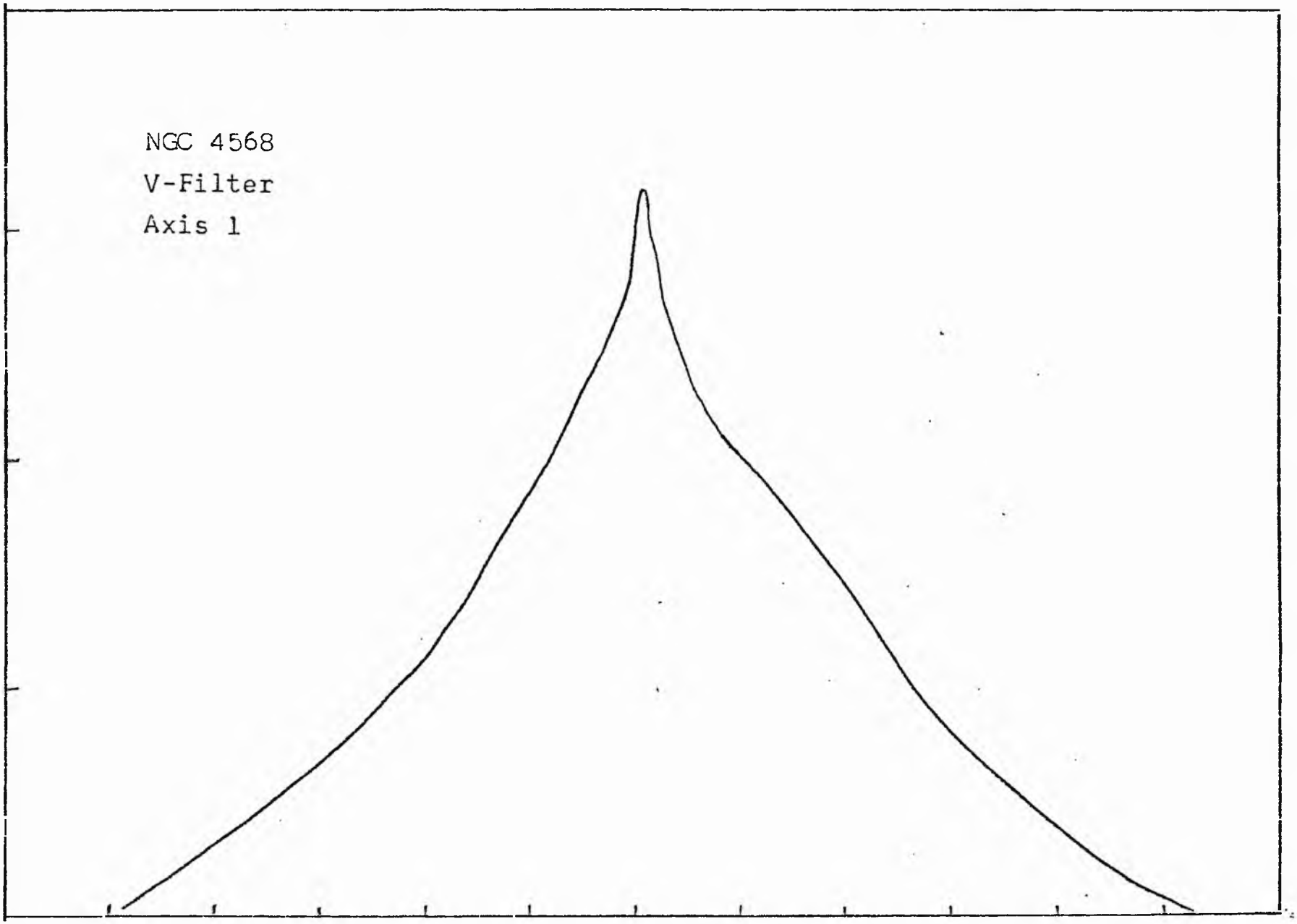
NGC 4568
V-Filter
Axis 1

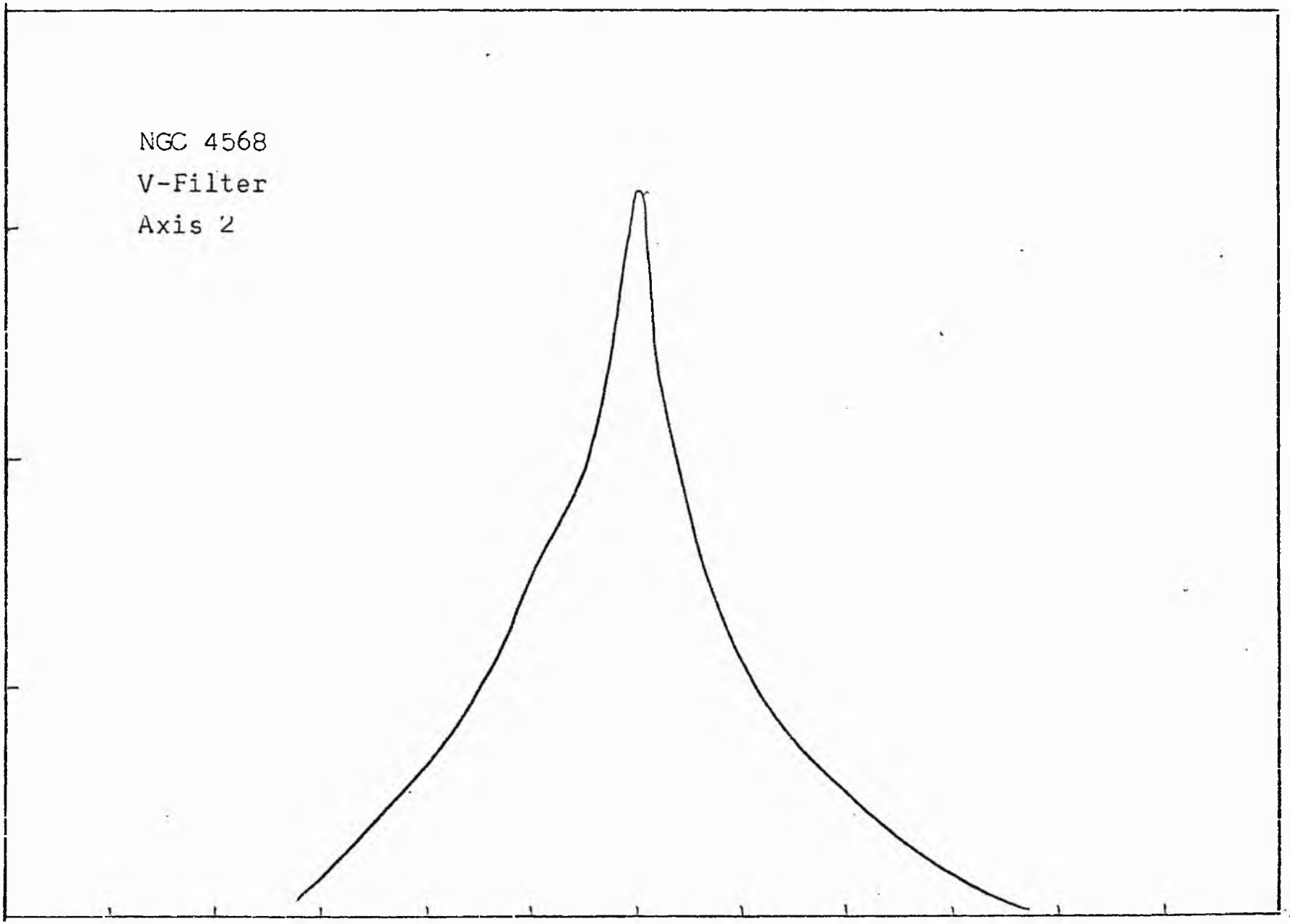
NGC 4568
V-Filter
Axis 2

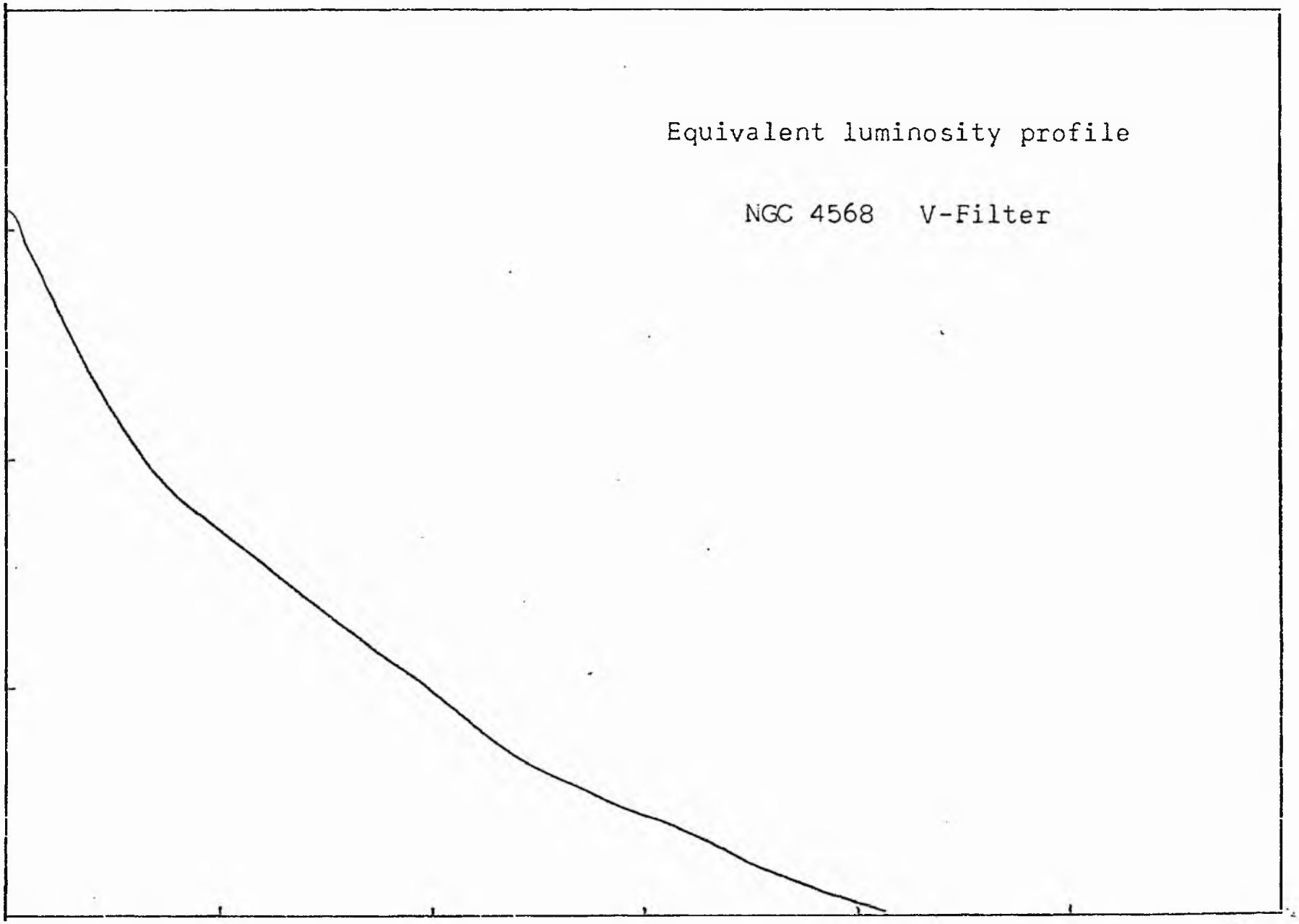
Equivalent luminosity profile
NGC 4568 V-Filter

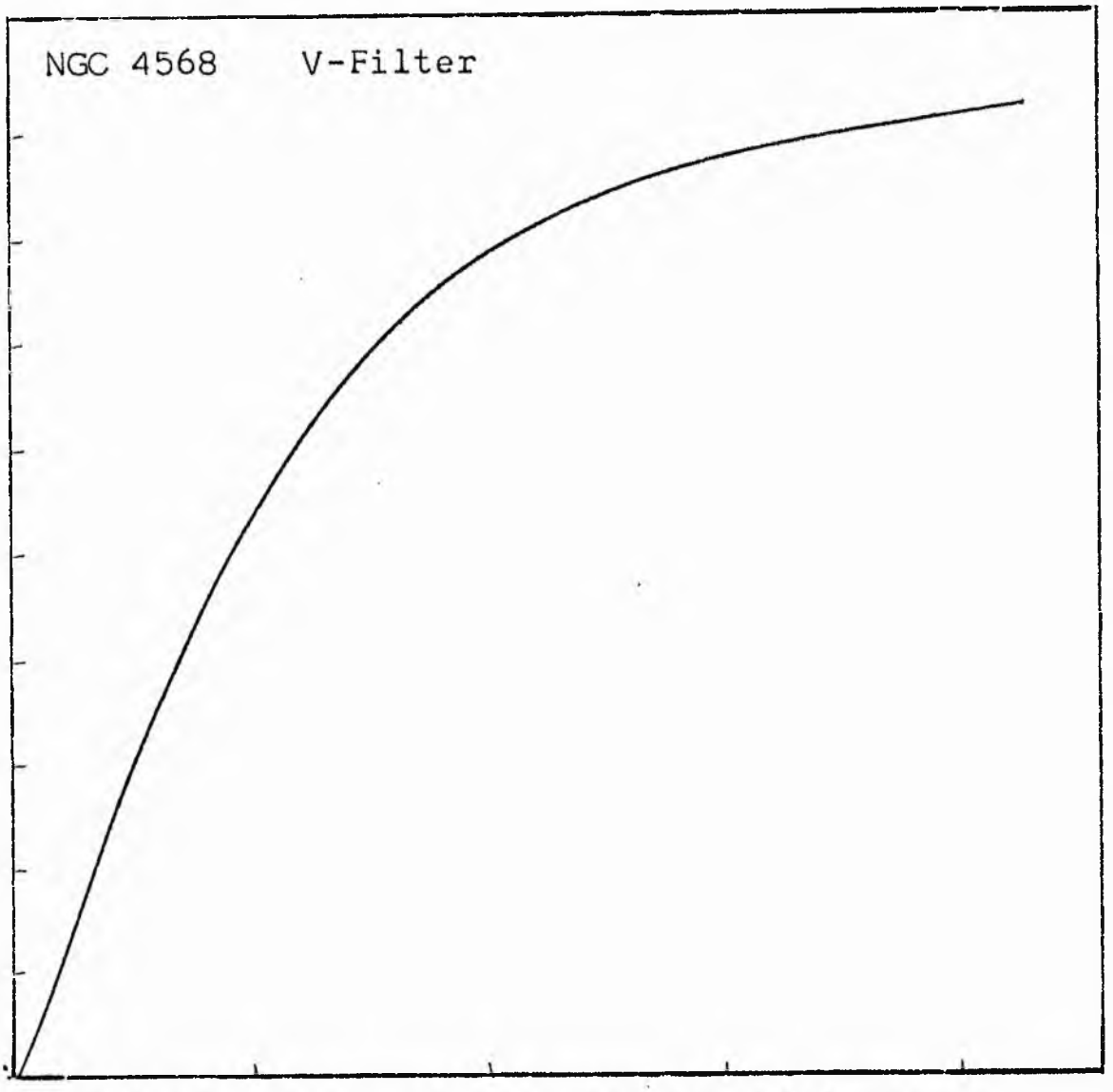

Relative integrated luminosity k(r) versus equivalent radius r*.

MEAN LUMINOSITY DISTRIBUTION IN NGC 4568
V COLOUR

LOG I	I	$\bar{I}$	R	AREA	ΔA	P	ΣP	K(R)	ρ	LOG J	μ
1.09	12.303		0.0	0.0			0.0	0.0	0.0	1.314	18.76
		11.151			34.21	301.5081					
1.00	10.000		3.30	34.21			381.51	0.02	0.07	1.224	19.01
		8.972			21.21	190.2499					
0.90	7.943		4.20	55.42			571.76	0.03	0.09	1.124	19.26
		7.126			116.62	831.0547					
0.80	6.310		7.40	172.03			1432.81	0.07	0.16	1.024	19.51
		5.661			60.32	341.4465					
0.70	5.012		8.60	232.35			1744.26	0.08	0.19	0.924	19.76
		4.496			183.12	823.4092					
0.60	3.981		11.50	415.48			2567.67	0.12	0.25	0.824	20.01
		3.572			200.28	715.3228					
0.50	3.162		14.00	615.75			3282.99	0.16	0.30	0.724	20.26
		2.837			403.25	1144.0659					
0.40	2.512		18.01	1019.01			4427.05	0.21	0.39	0.624	20.51
		2.254			279.44	629.7388					
0.30	1.995		20.33	1298.45			5056.79	0.25	0.44	0.524	20.76
		1.790			488.56	874.5615					
0.20	1.585		23.85	1787.01			5931.35	0.29	0.52	0.424	21.01
		1.422			623.51	886.5681					
0.10	1.259		27.70	2410.51			6817.92	0.33	0.60	0.324	21.26
		1.129			587.17	663.1870					
0.00	1.000		30.89	2997.68			7481.10	0.36	0.67	0.224	21.51
		0.897			1210.67	1086.1663					
-0.10	0.794		36.60	4208.35			8567.27	0.42	0.79	0.124	21.76
		0.713			2004.40	1428.4236					
-0.20	0.631		44.47	6212.75			9995.69	0.48	0.96	0.024	22.01
		0.566			2184.38	1236.5166					
-0.30	0.501		51.70	8397.13			11232.20	0.54	1.12	-0.076	22.26
		0.450			2299.12	1033.7927					
-0.40	0.398		58.35	10696.25			12265.99	0.59	1.26	-0.176	22.51
		0.357			1867.91	667.1589					
-0.50	0.316		63.24	12564.16			12933.15	0.63	1.37	-0.276	22.76
		0.284			2895.68	821.5293					
-0.60	0.251		70.15	15459.84			13754.68	0.67	1.52	-0.376	23.01
		0.225			3438.57	774.9089					
-0.70	0.200		77.56	18898.41			14529.58	0.70	1.68	-0.476	23.26
		0.179			3374.34	604.0342					
-0.80	0.158		84.20	22272.75			15133.61	0.73	1.82	-0.576	23.51
		0.142			3914.59	556.6196					
-0.90	0.126		91.30	26187.34			15690.23	0.76	1.97	-0.676	23.76
		0.113			3067.96	346.5154					
-1.00	0.100		96.50	29255.30			16036.74	0.78	2.09	-0.776	24.01
		0.090			2286.42	205.1298					
-1.10	0.079		100.20	31541.71			16241.87	0.79	2.17	-0.876	24.26
		0.071			2896.70	206.4317					
-1.20	0.063		104.70	34438.41			16448.30	0.80	2.26	-0.976	24.51
		0.057			9156.96	518.3528					
-1.30	0.050		117.80	43595.37			16966.65	0.82	2.55	-1.076	24.76
		0.045			5806.67	261.0969					
-1.40	0.040		125.40	49402.04			17227.75	0.84	2.71	-1.176	25.01
		0.036			10860.78	387.9148					
-1.50	0.032		138.50	60262.82			17615.66	0.85	2.99	-1.276	25.26
		0.028			12607.30	357.6829					
-1.60	0.025		152.30	72870.12			17973.34	0.87	3.29	-1.376	25.51
		0.023			12348.94	278.2954					
-1.70	0.020		164.70	85219.06			18251.63	0.89	3.56	-1.476	25.76
		0.018			16150.44	289.1089					
-1.80	0.016		179.63	101369.50			18540.74	0.90	3.88	-1.576	26.01
		0.014			18580.12	264.1960					
-1.90	0.013		195.40	119949.62			18804.93	0.91	4.22	-1.676	26.26
		0.011			23385.37	264.1328					
-2.00	0.010		213.60	143335.00			19069.07	0.92	4.62	-1.776	26.51
$-\infty$							20619.00	(1)			∞

PHOTOMETRIC PARAMETERS OF NGC 4568
V-FILTER

Total luminosity	L_T	= 5.73
Total apparent magnitude	m_T	= 10.72
Apparent central surface brightness	μ_o	= 18.78
Major axis at threshold	$2a_m$	= 8.03
Minor axis at threshold	$2b_m$	= 5.68
Major axis at μ=25.0 mag sec^{-2}	2a(25)	= 5.61
Luminosity within μ=25.0 mag sec^{-2}	k(25)	= 0.84
Gradient of exponential component	G(a)	= -0.57
Equivalent gradient of exponential comp.	G(r*)	= -0.60
Equivalent gradient of reduced exp. comp.	G(ρ)	= -0.74
Parameters at k = ¼ :		
Semi-major axis	a_1	= 0.43
Axis ratio	b/a	= 0.62
Equivalent radius	r_1*	= 0.35
Surface brightness	μ_1	= 20.76
Parameters at k = ½(effective) :		
Semi-major axis	a_e	= 0.97
Axis ratio	b/a	= 0.57
Equivalent radius	r_e*	= 0.77
Surface brightness	μ_e	= 22.09
Mean surface brightness	μ_e'	= 12.15
Parameters at k = ¾ :		
Semi-major axis	a_3	= 1.87
Axis ratio	b/a	= 0.49
Equivalent radius	r_3*	= 1.47
Surface brightness	μ_3	= 23.68
Concentration indices	C_{21}	= 2.23
	C_{32}	= 1.91

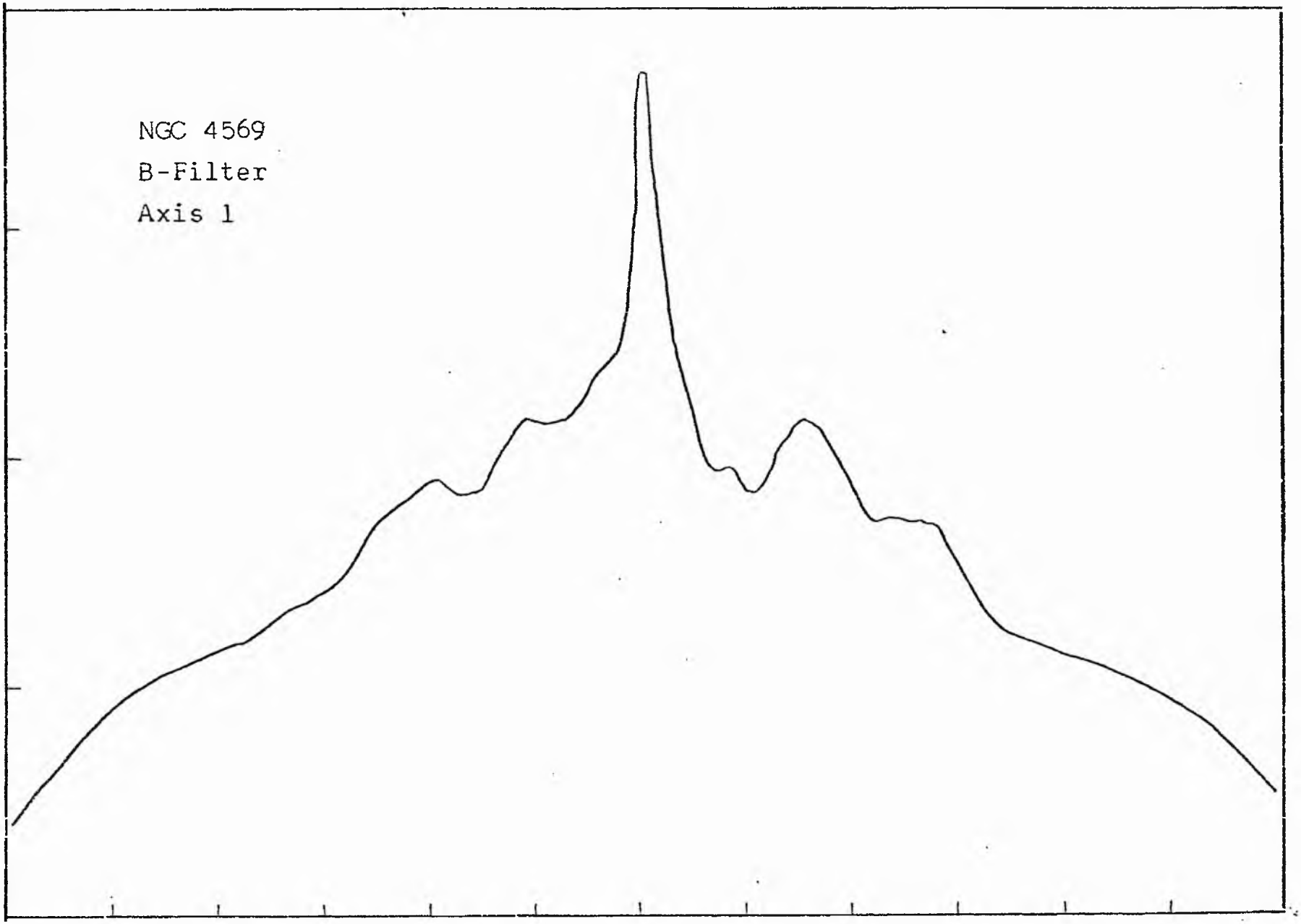
NGC 4569
B-Filter
Axis 1

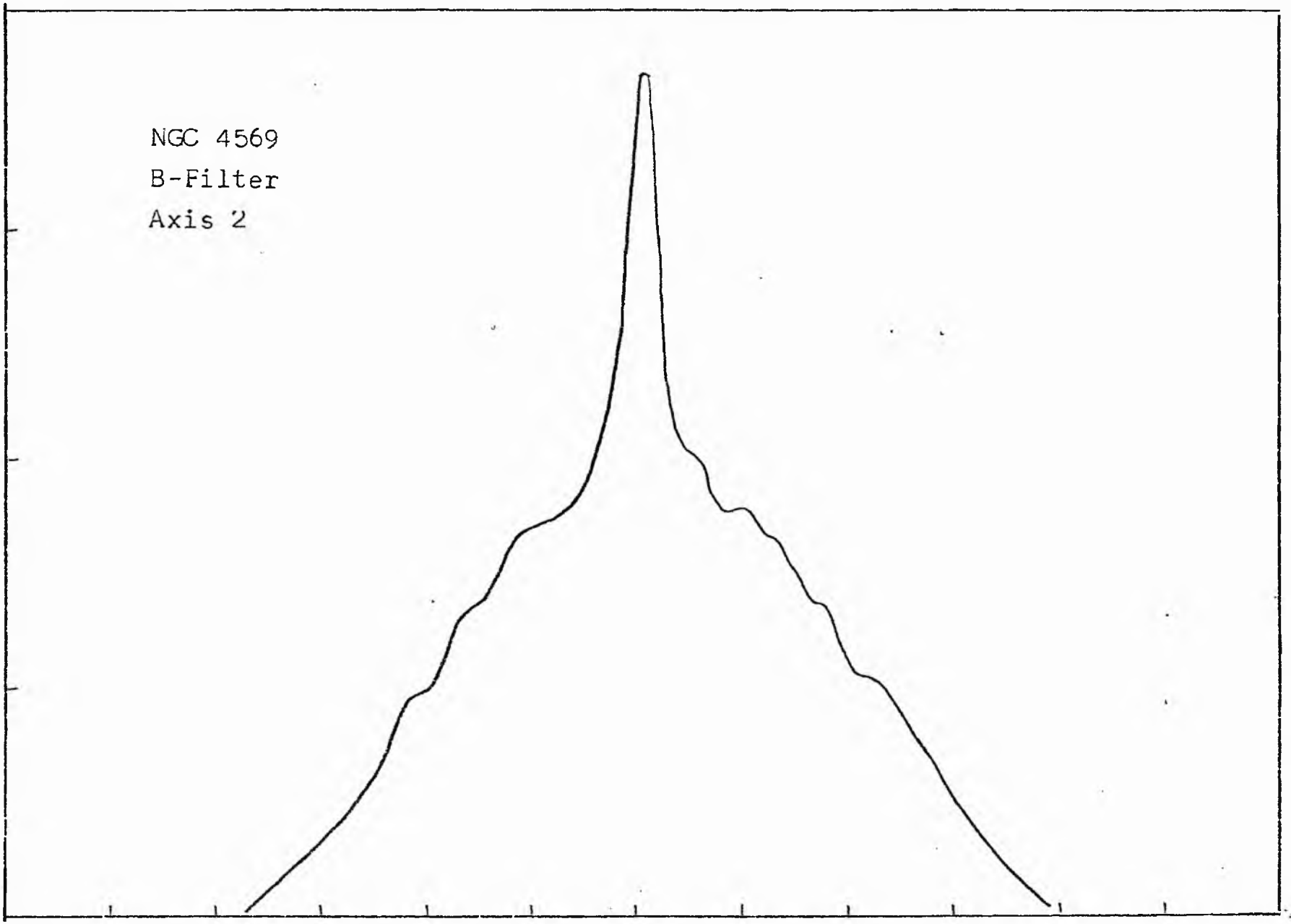
NGC 4569
B-Filter
Axis 2

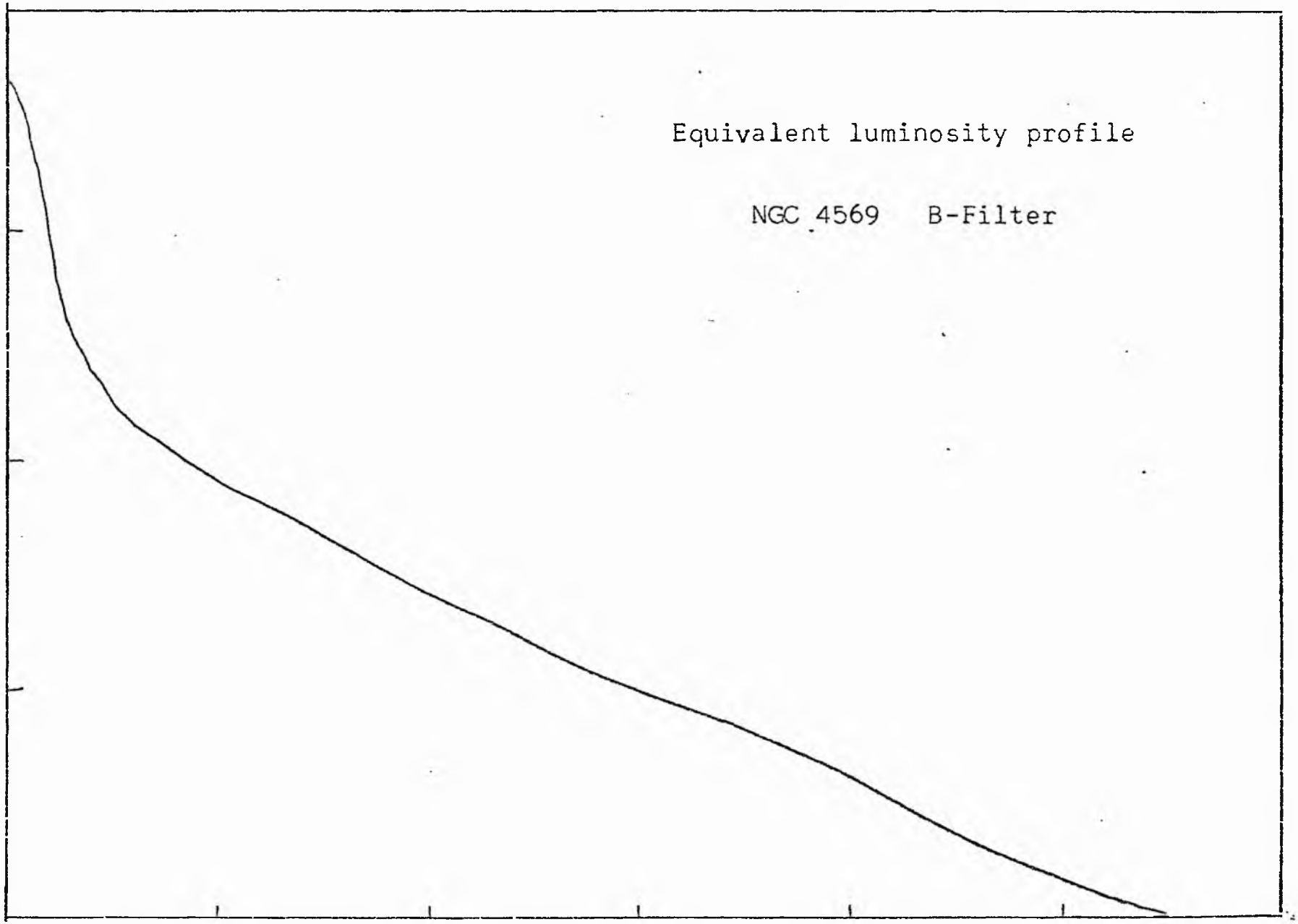
Equivalent luminosity profile
NGC 4569 B-Filter

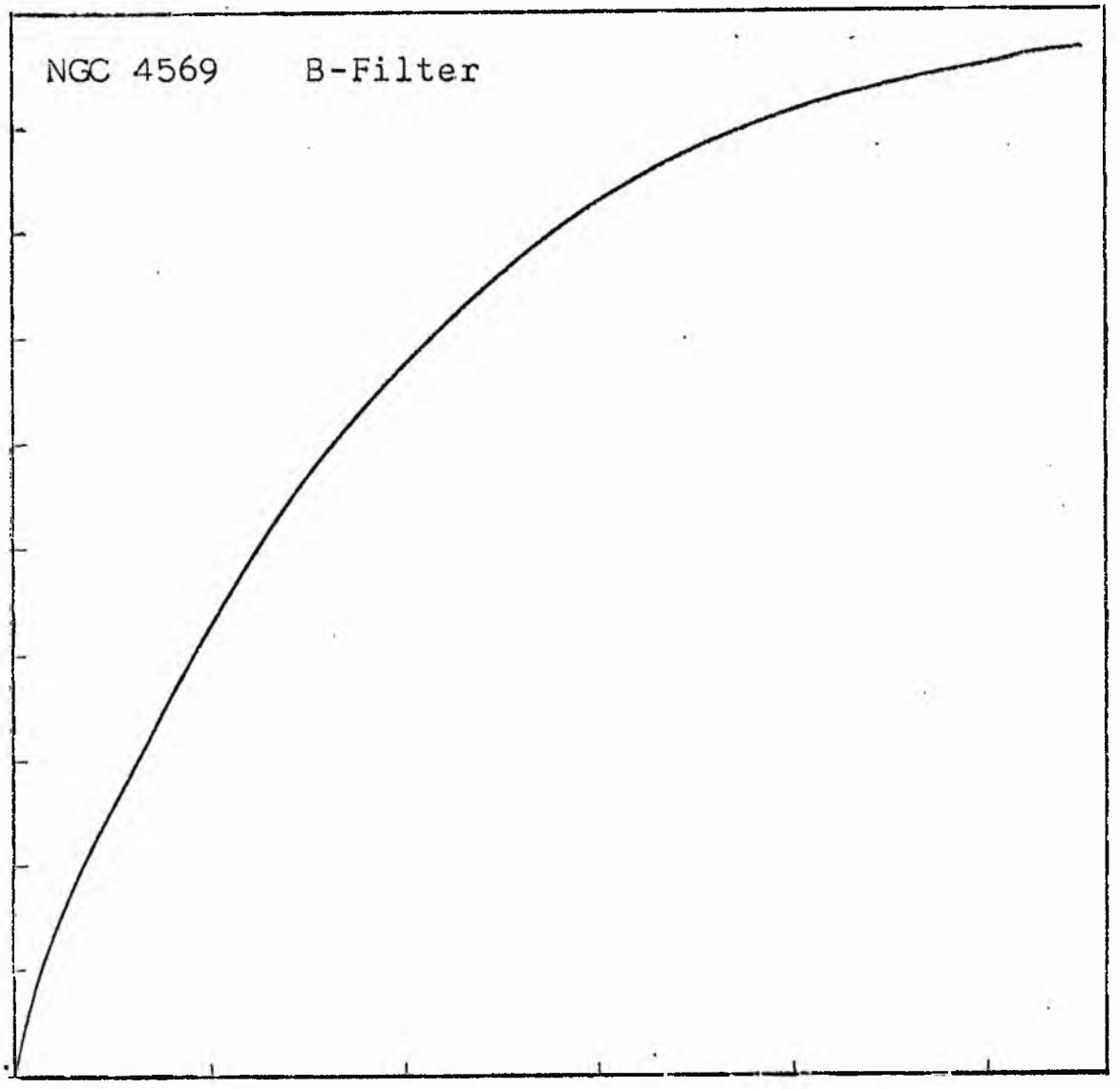

Relative integrated luminosity k(r) versus equivalent radius r*.

MEAN LUMINOSITY DISTRIBUTION IN NGC 4569
B COLOUR

LOG I	I	$\bar{I}$	R	AREA	ΔA	P	ΣP	K(R)	ρ	LOG J	μ
1.58	38.019		0.0	0.0			0.0	0.0	0.0	1.807	17.73
		34.821			34.84	1213.0464					
1.50	31.623		3.33	34.84			1213.05	0.03	0.05	1.727	17.93
		28.371			20.58	583.8950					
1.40	25.119		4.20	55.42			1796.94	0.05	0.07	1.627	18.18
		22.536			57.68	1299.8516					
1.30	19.953		6.00	113.10			3096.79	0.08	0.09	1.527	18.43
		17.901			11.59	207.5130					
1.20	15.849		6.30	124.69			3304.31	0.08	0.10	1.427	18.68
		14.219			38.17	542.7463					
1.10	12.589		7.20	162.86			3847.05	0.10	0.11	1.327	18.93
		11.295			30.20	431.4729					
1.00	10.000		8.00	201.06			4278.52	0.11	0.13	1.227	19.18
		8.972			42.22	378.8071					
0.90	7.943		8.80	243.28			4657.33	0.12	0.14	1.127	19.43
		7.126			46.24	329.5947					
0.80	6.310		9.60	289.53			4986.88	0.13	0.15	1.027	19.68
		5.661			70.15	397.1086					
0.70	5.012		10.70	359.68			5383.99	0.14	0.17	0.927	19.93
		4.496			187.71	844.0305					
0.60	3.981		13.20	547.39			6228.02	0.16	0.21	0.827	20.18
		3.572			236.88	846.0410					
0.50	3.162		15.80	784.27			7074.05	0.18	0.25	0.727	20.43
		2.837			105.58	299.5486					
0.40	2.512		16.83	889.85			7373.60	0.19	0.26	0.627	20.68
		2.254			456.29	1028.2788					
0.30	1.995		20.70	1346.14			8401.88	0.24	0.32	0.527	20.93
		1.790			927.15	1659.6597					
0.20	1.585		26.90	2273.29			10061.54	0.25	0.42	0.427	21.18
		1.422			1379.79	1961.9248					
0.10	1.259		34.10	3653.07			12023.46	0.30	0.53	0.327	21.43
		1.129			1968.14	2222.9355					
-0.00	1.000		42.30	5621.21			14246.39	0.36	0.66	0.227	21.68
		0.897			2939.12	2636.8662					
-0.10	0.794		52.20	8560.34			16883.25	0.43	0.82	0.127	21.93
		0.713			3244.79	2312.3689					
-0.20	0.631		61.30	11805.12			19195.62	0.49	0.96	0.027	22.18
		0.566			3765.10	2131.3108					
-0.30	0.501		70.40	15570.22			21326.93	0.54	1.10	-0.073	22.43
		0.450			3284.35	1476.7959					
-0.40	0.398		77.47	18854.57			22803.72	0.58	1.22	-0.173	22.68
		0.357			5022.62	1793.9126					
-0.50	0.316		87.18	23877.20			24597.63	0.62	1.37	-0.273	22.93
		0.284			6085.66	1726.5481					
-0.60	0.251		97.66	29962.86			26324.18	0.67	1.53	-0.373	23.18
		0.225			7307.63	1646.8252					
-0.70	0.200		108.92	37270.48			27971.00	0.71	1.71	-0.473	23.43
		0.179			8687.56	1555.1372					
-0.80	0.158		120.95	45958.04			29526.14	0.75	1.90	-0.573	23.68
		0.142			12748.55	1812.7246					
-0.90	0.126		136.70	58706.59			31338.86	0.79	2.14	-0.673	23.93
		0.113			14546.79	1643.0042					
-1.00	0.100		152.70	73253.37			32981.87	0.83	2.40	-0.773	24.18
		0.090			12587.75	1129.3286					
-1.10	0.079		165.30	85841.12			34111.20	0.86	2.59	-0.873	24.43
		0.071			15269.00	1088.1367					
-1.20	0.063		179.40	101110.12			35199.33	0.89	2.81	-0.973	24.68
		0.057			5482.94	310.3748					
-1.30	0.050		184.20	106593.06			35509.70	0.90	2.89	-1.073	24.93
		0.045			14340.75	644.8303					
-1.40	0.040		196.20	120933.81			36154.53	0.91	3.08	-1.173	25.18
		0.036			13810.31	493.2622					
-1.50	0.032		207.10	134744.12			36647.79	0.93	3.25	-1.273	25.43
		0.028			12917.75	366.4897					
-1.60	0.025		216.80	147661.87			37014.28	0.94	3.40	-1.373	25.68
		0.023			15650.69	352.7029					
-1.70	0.020		228.00	163312.56			37366.98	0.94	3.58	-1.473	25.93
		0.018			17643.19	315.8298					
-1.80	0.016		240.00	180955.75			37682.81	0.95	3.77	-1.573	26.18
		0.014			30436.50	432.7842					
-1.90	0.013		259.40	211392.25			38115.59	0.96	4.07	-1.673	26.43
		0.011			22233.06	251.1173					
-2.00	0.010		272.70	233625.31			38366.71	0.97	4.28	-1.773	26.68
- ∞							39566.00	(1)			∞

PHOTOMETRIC PARAMETERS OF NGC 4569

B-FILTER

Total luminosity	L_T	= 10.99
Total apparent magnitude	m_T	= 10.19
Apparent central surface brightness	μ_o	= 17.73
Major axis at threshold	$2a_m$	= 12.76
Minor axis at threshold	$2b_m$	= 6.28
Major axis at μ=25.0 mag sec^{-2}	2a(25)	= 8.89
Luminosity within μ=25.0 mag sec^{-2}	k(25)	= 0.90
Gradient of exponential component	G(a)	= -0.43
Equivalent gradient of exponential comp.	G(r*)	= -0.53
Equivalent gradient of reduced exp. comp.	G(ρ)	= -0.70
Parameters at k = ¼ :		
Semi-major axis	a_1	= 0.57
Axis ratio	b/a	= 0.56
Equivalent radius	r_1*	= 0.44
Surface brightness	μ_1	= 21.18
Parameters at k = ½(effective) :		
Semi-major axis	a_e	= 1.73
Axis ratio	b/a	= 0.38
Equivalent radius	r_e*	= 1.06
Surface brightness	μ_e	= 22.23
Mean surface brightness	μ_e'	= 12.31
Parameters at k = ¾ :		
Semi-major axis	a_3	= 2.77
Axis ratio	b/a	= 0.55
Equivalent radius	r_3*	= 2.03
Surface brightness	μ_3	= 23.68
Concentration indices	C_{21}	= 2.43
	C_{32}	= 1.92

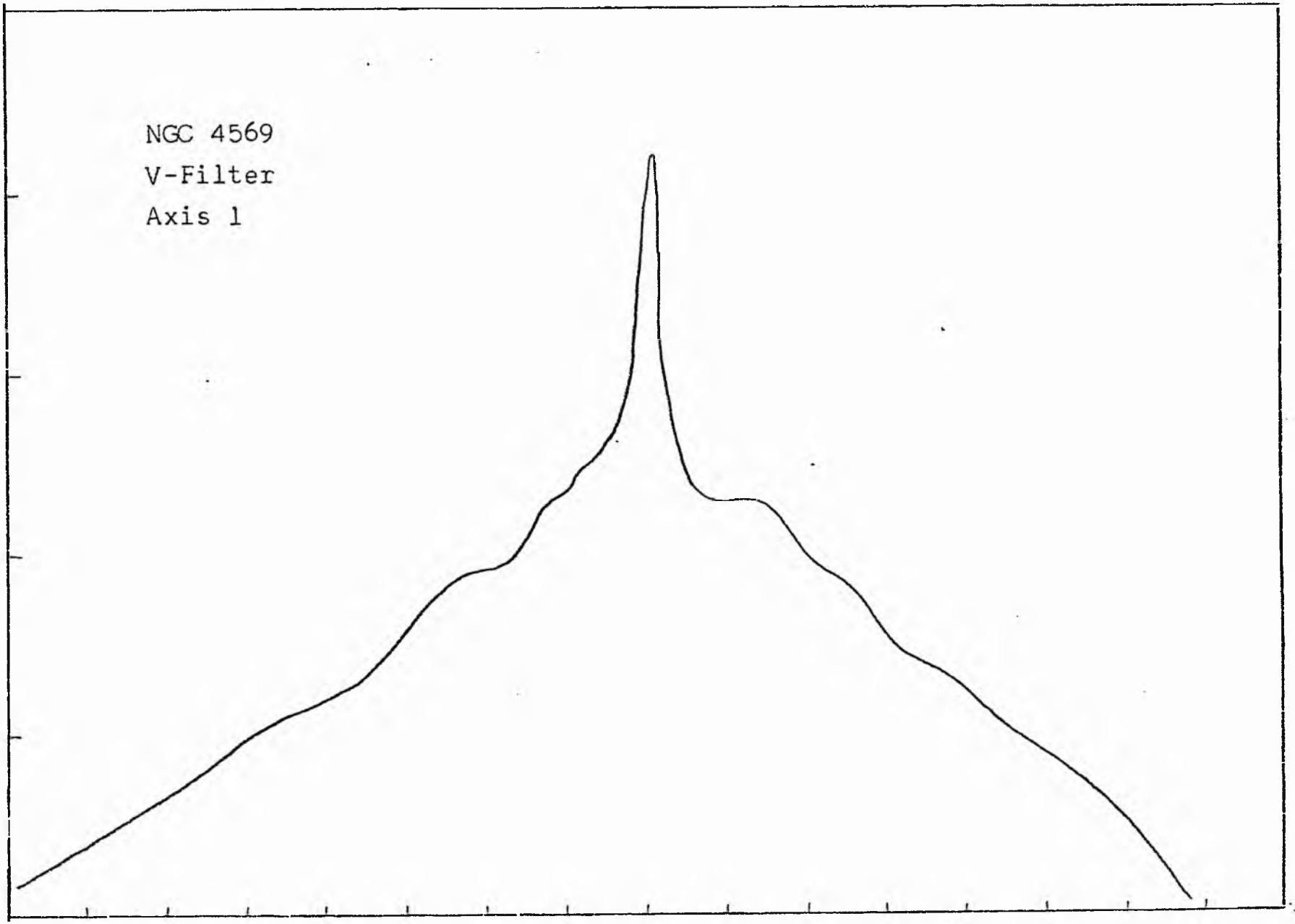
NGC 4569
V-Filter
Axis 1

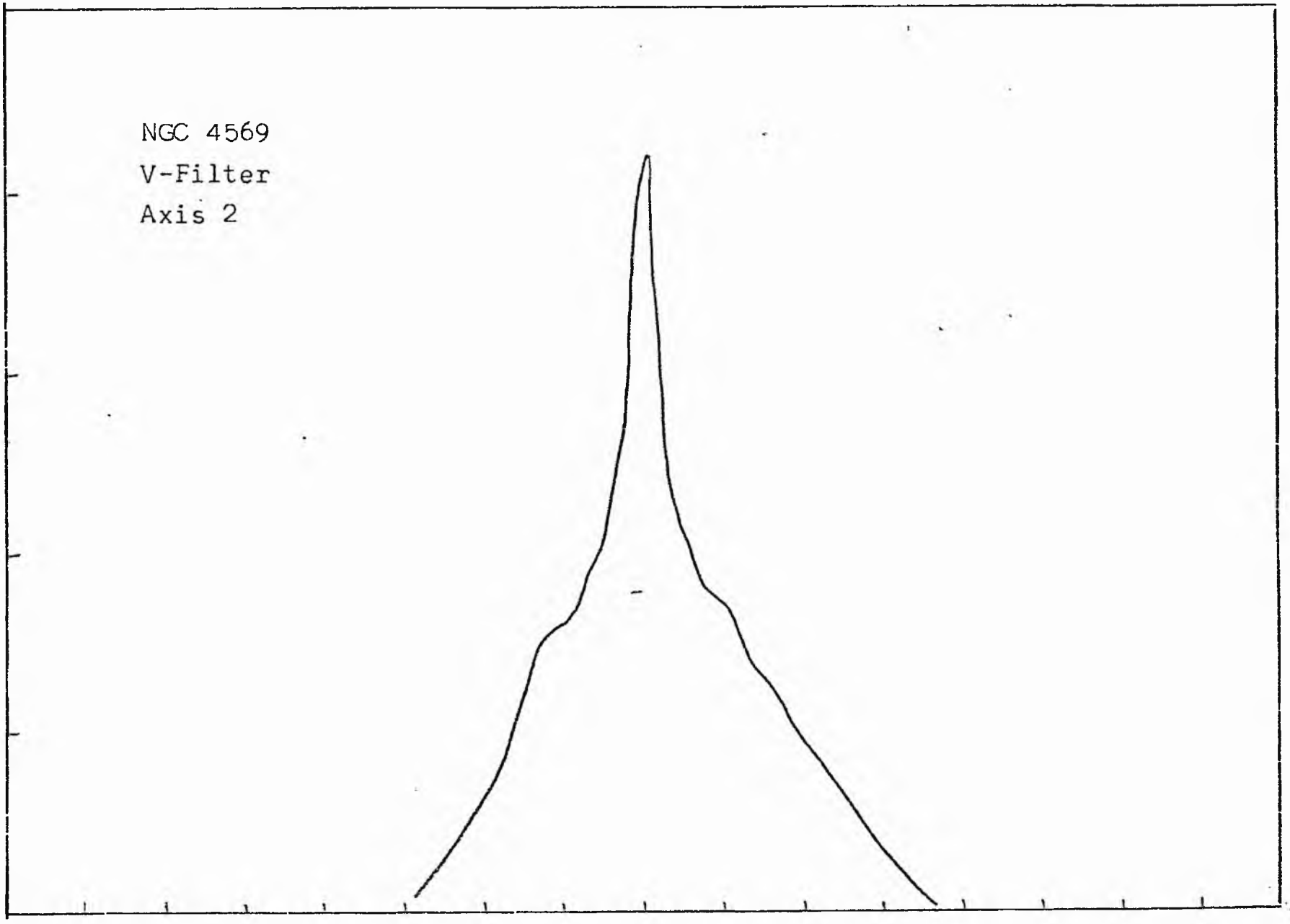
NGC 4569
V-Filter
Axis 2

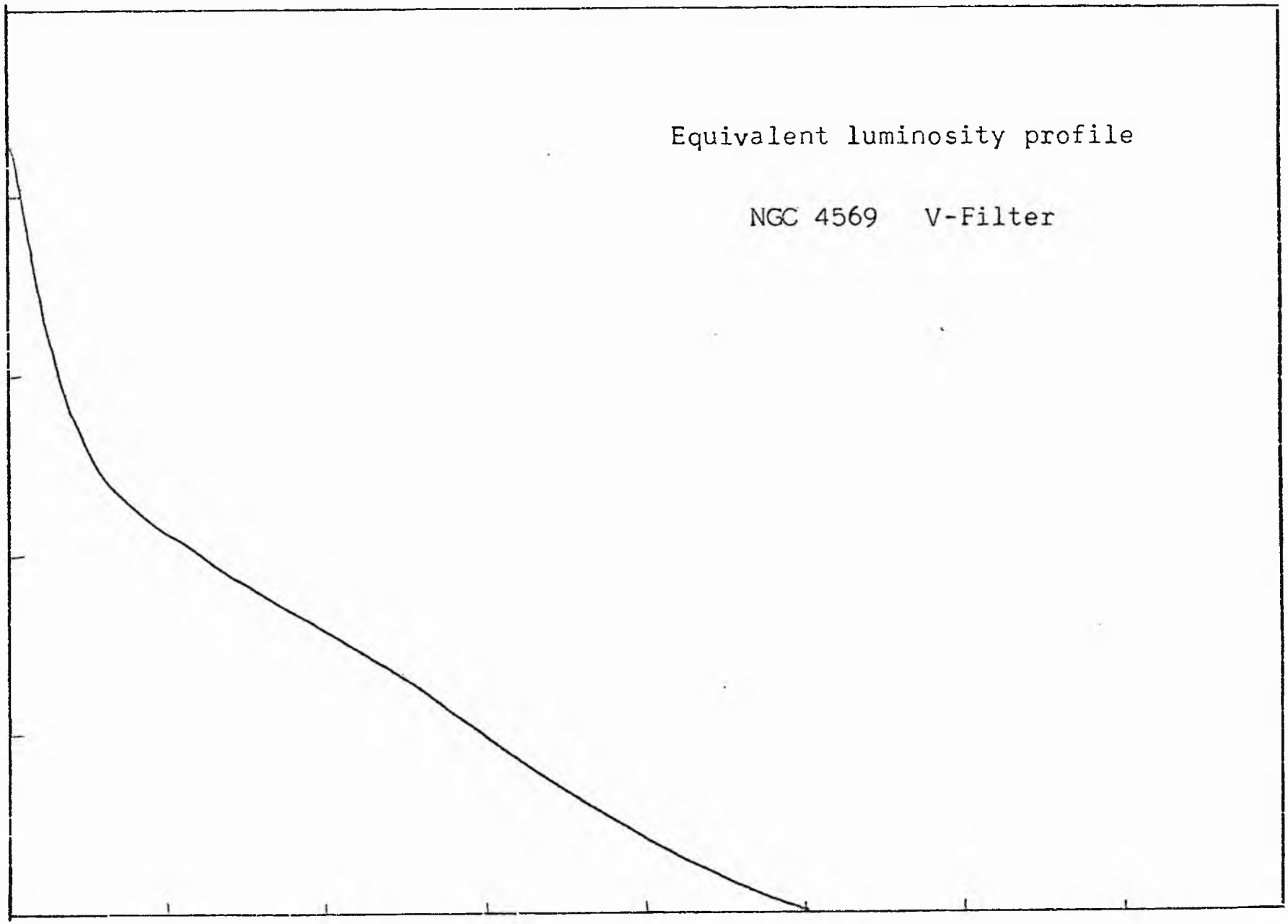
Equivalent luminosity profile
NGC 4569 V-Filter

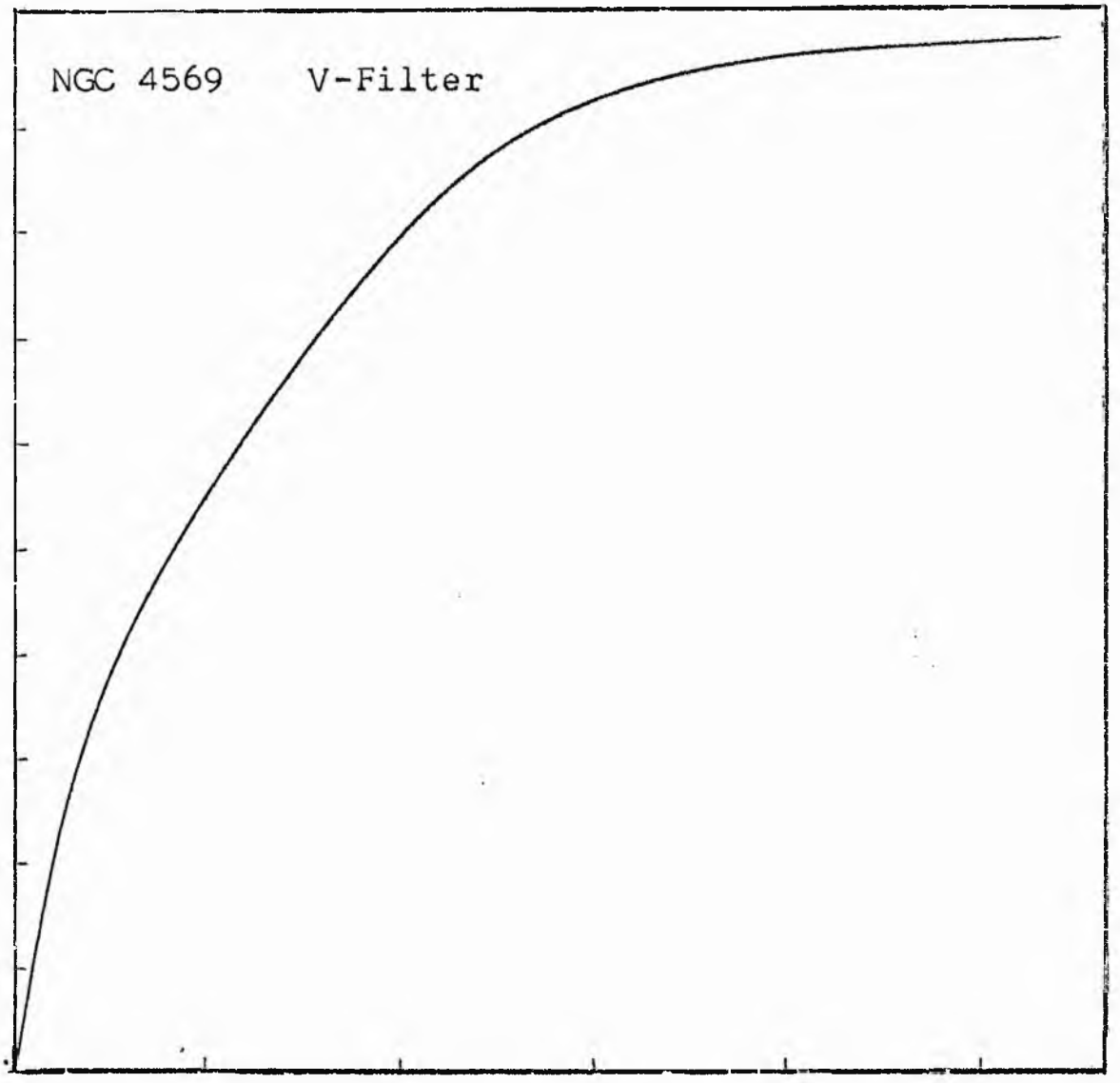

Relative integrated luminosity k(r) versus equivalent radius r*.

MEAN LUMINOSITY DISTRIBUTION IN NGC 4569
V COLOUR

LOG I	I	$\bar{I}$	R	AREA	ΔA	P	ΣP	K(R)	ρ	LOG J	μ
2.17	147.911		0.0	0.0			0.0	0.0	0.0	1.972	16.25
		153.200			4.52	693.0591					
2.20	158.489		1.20	4.52			693.06	0.01	0.03	2.002	16.18
		142.191			5.65	804.0604					
2.10	125.892		1.80	10.18			1497.13	0.02	0.04	1.902	16.43
		112.946			7.92	894.1729					
2.00	100.000		2.40	18.10			2391.30	0.04	0.06	1.802	16.68
		89.716			12.10	1085.1277					
1.90	79.433		3.10	30.19			3476.43	0.05	0.08	1.702	16.93
		71.264			15.17	1081.3521					
1.80	63.095		3.80	45.36			4557.78	0.07	0.09	1.602	17.18
		56.607			12.72	720.2346					
1.70	50.118		4.30	58.09			5278.01	0.08	0.11	1.502	17.43
		44.964			62.67	2818.1375					
1.60	39.810		6.20	120.76			8096.15	0.12	0.15	1.402	17.68
		35.717			51.27	1831.2126					
1.50	31.623		7.40	172.03			9927.36	0.15	0.18	1.302	17.93
		28.371			65.75	1865.4685					
1.40	25.119		8.70	237.79			11792.82	0.18	0.21	1.202	18.18
		22.536			63.93	1440.7290					
1.30	19.952		9.80	301.72			13233.55	0.20	0.24	1.102	18.43
		17.901			128.33	2297.2578					
1.20	15.849		11.70	430.05			15530.81	0.24	0.29	1.002	18.68
		14.219			76.65	1089.9502					
1.10	12.589		12.70	506.71			16620.76	0.25	0.31	0.902	18.93
		11.295			172.16	1944.4563					
1.00	10.000		14.70	678.87			18565.21	0.28	0.36	0.802	19.18
		8.972			182.66	1638.7688					
0.90	7.943		16.56	861.53			20203.98	0.31	0.41	0.702	19.43
		7.126			156.35	1114.1802					
0.80	6.310		18.00	1017.88			21318.16	0.33	0.44	0.602	19.68
		5.661			289.53	1638.9214					
0.70	5.012		20.40	1307.40			22957.07	0.35	0.50	0.502	19.93
		4.496			387.90	1744.1709					
0.60	3.981		23.23	1695.31			24701.24	0.38	0.57	0.402	20.18
		3.572			236.90	846.1121					
0.50	3.162		24.80	1932.20			25547.35	0.39	0.61	0.302	20.43
		2.837			750.11	2128.1084					
0.40	2.512		29.22	2682.32			27675.46	0.42	0.72	0.202	20.68
		2.254			1122.28	2529.1091					
0.30	1.995		34.80	3804.59			30204.56	0.46	0.86	0.102	20.93
		1.790			1340.40	2413.7246					
0.20	1.585		40.50	5153.00			32618.29	0.50	1.00	0.002	21.18
		1.422			2763.94	3930.0371					
0.10	1.259		50.20	7916.94			36548.32	0.56	1.24	-0.098	21.43
		1.129			2871.16	3242.8367					
-0.00	1.000		58.60	10780.10			39791.16	0.61	1.44	-0.198	21.68
		0.897			3568.22	3201.2478					
-0.10	0.794		67.60	14356.32			42992.40	0.66	1.66	-0.298	21.93
		0.713			5499.34	3919.0247					
-0.20	0.631		79.50	19855.65			46911.43	0.72	1.96	-0.398	22.18
		0.566			5084.84	2878.3586					
-0.30	0.501		89.10	24940.49			49789.78	0.76	2.19	-0.498	22.43
		0.450			5354.64	2407.6758					
-0.40	0.398		98.20	30295.13			52197.46	0.80	2.42	-0.598	22.68
		0.357			5807.54	2074.2463					
-0.50	0.316		107.20	36102.67			54271.70	0.83	2.64	-0.698	22.93
		0.284			5952.23	1688.6816					
-0.60	0.251		115.70	42054.69			55960.38	0.86	2.85	-0.798	23.18
		0.225			6094.52	1373.4341					
-0.70	0.200		123.80	48149.41			57333.82	0.88	3.05	-0.898	23.43
		0.179			6341.16	1135.1077					
-0.80	0.158		131.70	54490.57			58468.92	0.89	3.24	-0.998	23.68
		0.142			9303.39	1322.8477					
-0.90	0.126		142.50	63793.97			59791.77	0.92	3.51	-1.098	23.93
		0.113			4833.59	545.9321					
-1.00	0.100		147.80	68627.56			60337.70	0.92	3.64	-1.198	24.18
		0.090			6557.25	588.2896					
-1.10	0.079		154.70	75184.81			60925.99	0.93	3.81	-1.298	24.43
		0.071			6552.12	466.9304					
-1.20	0.063		161.30	81736.94			61392.92	0.94	3.97	-1.398	24.68
		0.057			11528.37	652.5872					
-1.30	0.050		172.30	93265.31			62045.50	0.95	4.24	-1.498	24.93
		0.045			9088.56	408.6636					
-1.40	0.040		180.50	102353.87			62454.16	0.96	4.44	-1.598	25.18
		0.036			12254.56	437.6926					
-1.50	0.032		191.00	114608.44			62891.86	0.96	4.70	-1.698	25.43
		0.028			11936.44	338.6467					
-1.60	0.025		200.70	126544.87			63230.50	0.97	4.94	-1.798	25.68
		0.023			20572.62	463.6204					
-1.70	0.020		216.40	147117.50			63694.12	0.97	5.33	-1.898	25.93
		0.018			21538.56	385.5583					
-1.80	0.016		231.70	160656.06			64079.67	0.98	5.70	-1.998	26.18
		0.014			17922.12	254.8376					
-1.90	0.013		243.70	186578.19			64334.51	0.98	6.00	-2.098	26.43
		0.011			13400.75	151.3573					
-2.00	0.010		252.30	199978.94			64485.86	0.99	6.21	-2.198	26.68
- ∞							65345.00	(1)			∞

PHOTOMETRIC PARAMETERS OF NGC 4569
V-FILTER

Total luminosity	L_T	= 18.15
Total apparent magnitude	m_T	= 9.62
Apparent central surface brightness	μ_o	= 16.25
Major axis at threshold	$2a_m$	= 12.65
Minor axis at threshold	$2b_m$	= 5.77
Major axis at μ=25.0 mag sec^{-2}	2a(25)	= 8.75
Luminosity within μ=25.0 mag sec^{-2}	k(25)	= 0.95
Gradient of exponential component	G(a)	= -0.46
Equivalent gradient of exponential comp.	G(r*)	= -0.46
Equivalent gradient of reduced exp. comp.	G(ρ)	= -0.48
Parameters at k = ¼ :		
Semi-major axis	a_1	= 0.22
Axis ratio	b/a	= 0.82
Equivalent radius	r_1*	= 0.21
Surface brightness	μ_1	= 18.93
Parameters at k = ½(effective) :		
Semi-major axis	a_e	= 1.08
Axis ratio	b/a	= 0.34
Equivalent radius	r_e*	= 0.68
Surface brightness	μ_e	= 21.18
Mean surface brightness	μ_e'	= 10.76
Parameters at k = ¾ :		
Semi-major axis	a_3	= 2.36
Axis ratio	b/a	= 0.47
Equivalent radius	r_3*	= 1.44
Surface brightness	μ_3	= 22.36
Concentration indices	C_{21}	= 3.27
	C_{32}	= 2.13

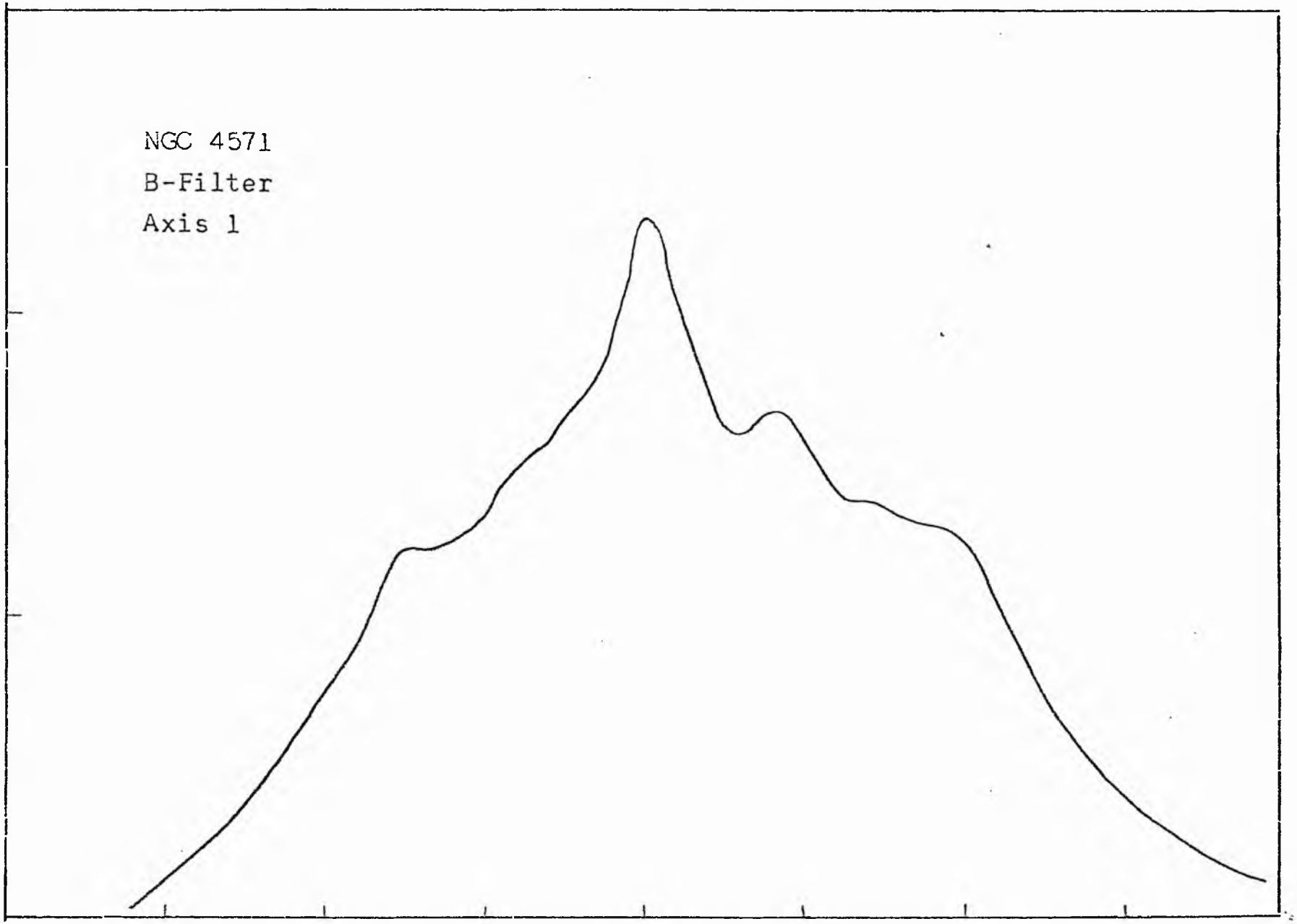
NGC 4571
B-Filter
Axis 1

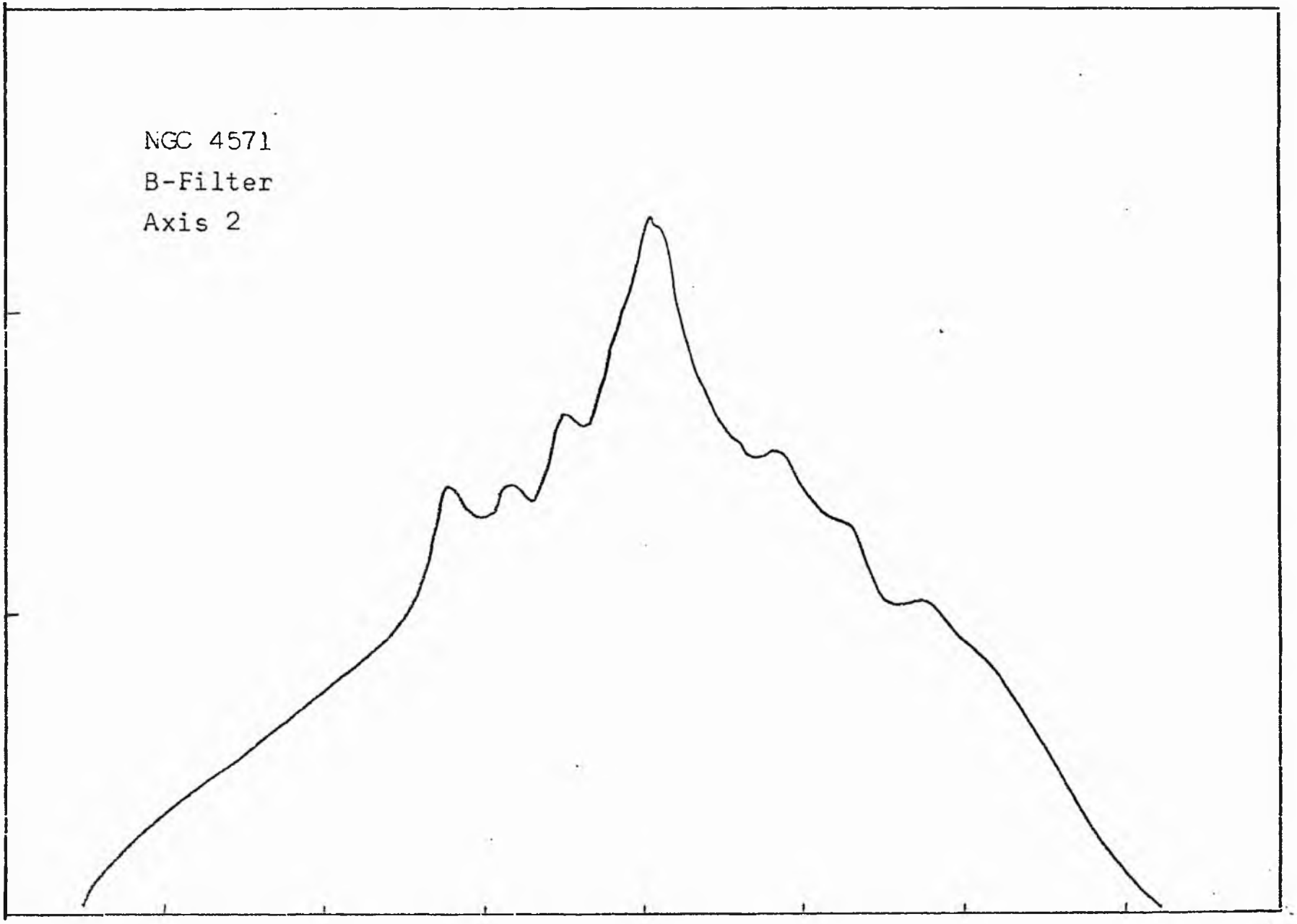
NGC 4571
B-Filter
Axis 2

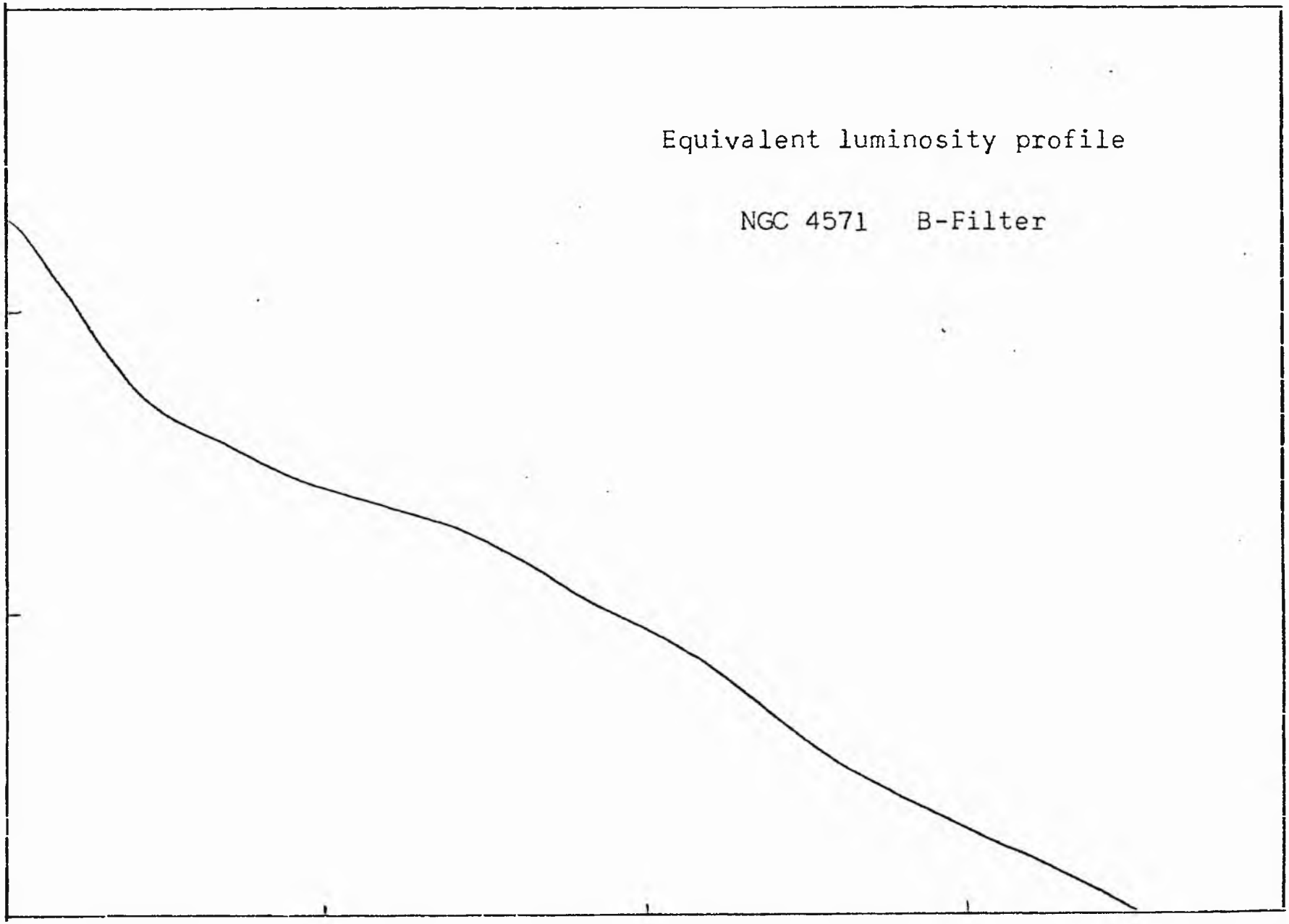
Equivalent luminosity profile
NGC 4571 B-Filter

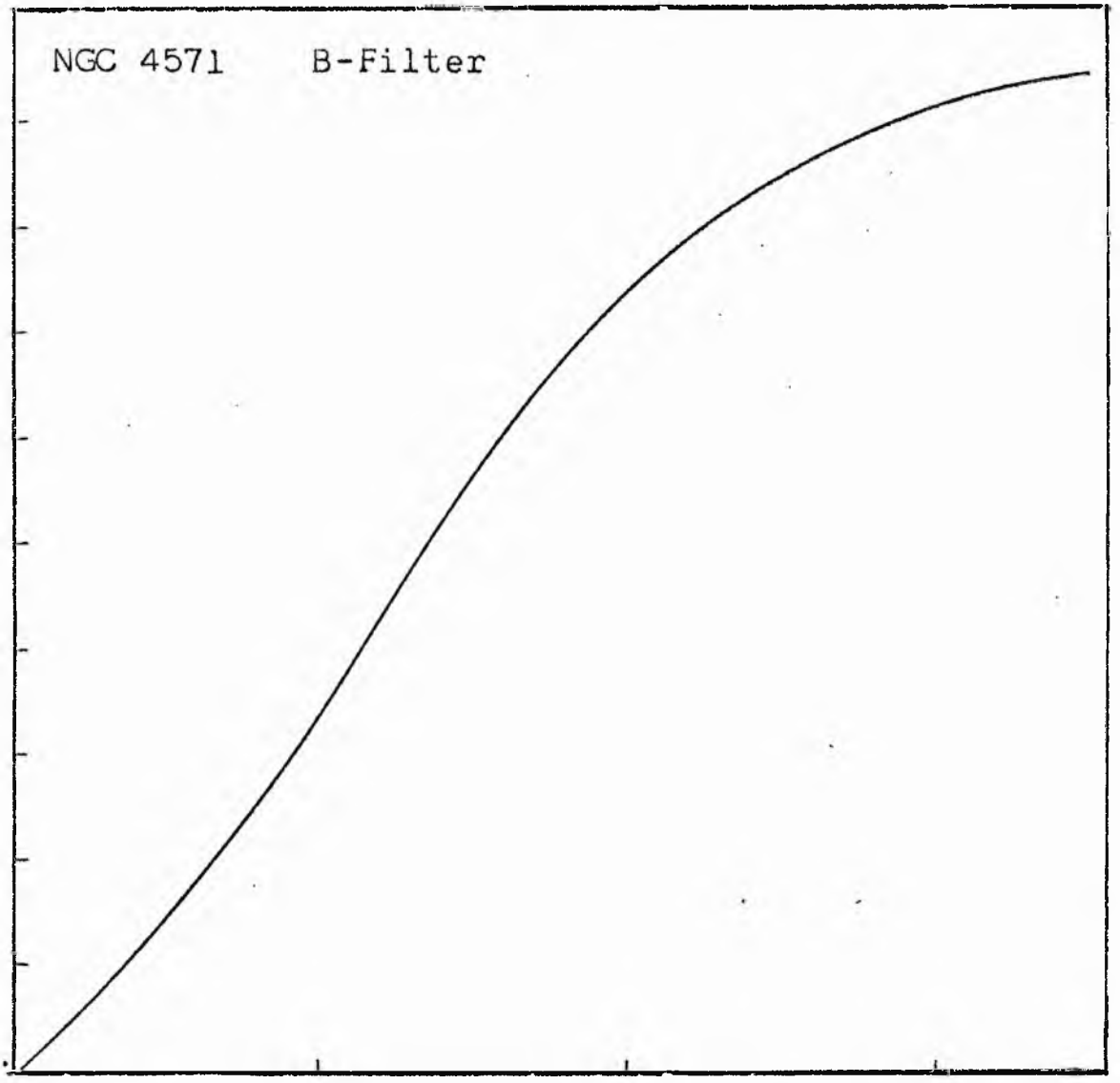

Relative integrated luminosity k(r) versus equivalent radius r*.

MEAN LUMINOSITY DISTRIBUTION IN NGC 4571
B COLOUR

LOG I	I	$\bar{I}$	R	AREA	ΔA	P	ΣP	K(R)	ρ	LOG J	μ
0.23	1.698		0.0	0.0			0.0	0.0	0.0	0.942	21.06
		1.642			56.21	92.2761					
0.20	1.585		4.23	56.21			92.28	0.01	0.06	0.912	21.14
		1.422			165.46	235.2671					
0.10	1.259		8.40	221.67			327.54	0.03	0.12	0.812	21.39
		1.129			131.32	148.3193					
0.00	1.000		10.60	352.99			475.86	0.05	0.16	0.712	21.64
		0.897			194.40	174.4103					
-0.10	0.794		13.20	547.39			650.27	0.07	0.20	0.612	21.89
		0.713			328.77	234.2936					
-0.20	0.631		16.70	876.16			884.57	0.09	0.25	0.512	22.14
		0.566			277.14	156.8789					
-0.30	0.501		19.16	1153.29			1041.44	0.11	0.28	0.412	22.39
		0.450			1416.40	636.8811					
-0.40	0.398		28.60	2569.70			1678.33	0.18	0.42	0.312	22.64
		0.357			1824.64	651.7009					
-0.50	0.316		37.40	4394.33			2330.03	0.24	0.56	0.212	22.89
		0.284			4284.48	1215.5444					
-0.60	0.251		52.56	8678.82			3545.57	0.37	0.76	0.112	23.14
		0.225			4993.50	1125.3242					
-0.70	0.200		65.97	13672.32			4670.89	0.49	0.98	0.012	23.39
		0.179			4612.25	825.6299					
-0.80	0.158		76.29	18284.57			5496.52	0.57	1.13	-0.088	23.64
		0.142			5237.91	744.7832					
-0.90	0.126		86.53	23522.48			6241.30	0.65	1.28	-0.188	23.89
		0.113			6097.73	688.7170					
-1.00	0.100		97.10	29620.21			6930.02	0.72	1.44	-0.288	24.14
		0.090			5353.11	480.2627					
-1.10	0.079		105.51	34973.33			7410.28	0.77	1.57	-0.388	24.39
		0.071			4886.46	348.2312					
-1.20	0.063		112.64	39859.79			7758.51	0.81	1.67	-0.488	24.64
		0.057			312.01	17.6622					
-1.30	0.050		113.08	40171.80			7776.17	0.81	1.68	-0.588	24.89
		0.045			5407.05	243.1275					
-1.40	0.040		120.45	45578.86			8019.30	0.84	1.79	-0.688	25.14
		0.036			6854.49	244.8214					
-1.50	0.032		129.19	52433.34			8264.12	0.86	1.92	-0.788	25.39
		0.028			8501.40	241.1934					
-1.60	0.025		139.27	60934.74			8505.31	0.89	2.07	-0.888	25.64
		0.023			7136.76	160.8336					
-1.70	0.020		147.20	68071.50			8666.14	0.91	2.19	-0.988	25.89
		0.018			7697.69	137.7960					
-1.80	0.016		155.30	75769.19			8803.93	0.92	2.31	-1.088	26.14
		0.014			11532.12	163.9782					
-1.90	0.013		166.70	87301.31			8967.91	0.94	2.47	-1.188	26.39
		0.011			8065.12	91.0937					
-2.00	0.010		174.23	95366.44			9059.00	0.95	2.59	-1.288	26.64
$-\infty$							9569.00	(1)			∞

PHOTOMETRIC PARAMETERS OF NGC 4571

B-FILTER

Total luminosity	L_T	= 2.66
Total apparent magnitude	m_T	= 12.01
Apparent central surface brightness	μ_o	= 21.06
Major axis at threshold	$2a_m$	= 6.28
Minor axis at threshold	$2b_m$	= 5.80
Major axis at μ=25.0 mag sec^{-2}	2a(25)	= 3.86
Luminosity within μ=25.0 mag sec^{-2}	k(25)	= 0.83
Gradient of exponential component	G(a)	= -0.68
Equivalent gradient of exponential comp.	G(r*)	= -0.73
Equivalent gradient of reduced exp. comp.	G(ρ)	= -0.78
Parameters at k = ¼ :		
Semi-major axis	a_1	= 0.71
Axis ratio	b/a	= 0.79
Equivalent radius	r_1*	= 0.64
Surface brightness	μ_1	= 22.90
Parameters at k = ½(effective) :		
Semi-major axis	a_e	= 1.13
Axis ratio	b/a	= 0.84
Equivalent radius	r_e*	= 1.12
Surface brightness	μ_e	= 23.42
Mean surface brightness	μ_e'	= 14.21
Parameters at k = ¾ :		
Semi-major axis	a_3	= 1.63
Axis ratio	b/a	= 0.94
Equivalent radius	r_3*	= 1.69
Surface brightness	μ_3	= 24.29
Concentration indices	C_{21}	= 1.76
	C_{32}	= 1.50

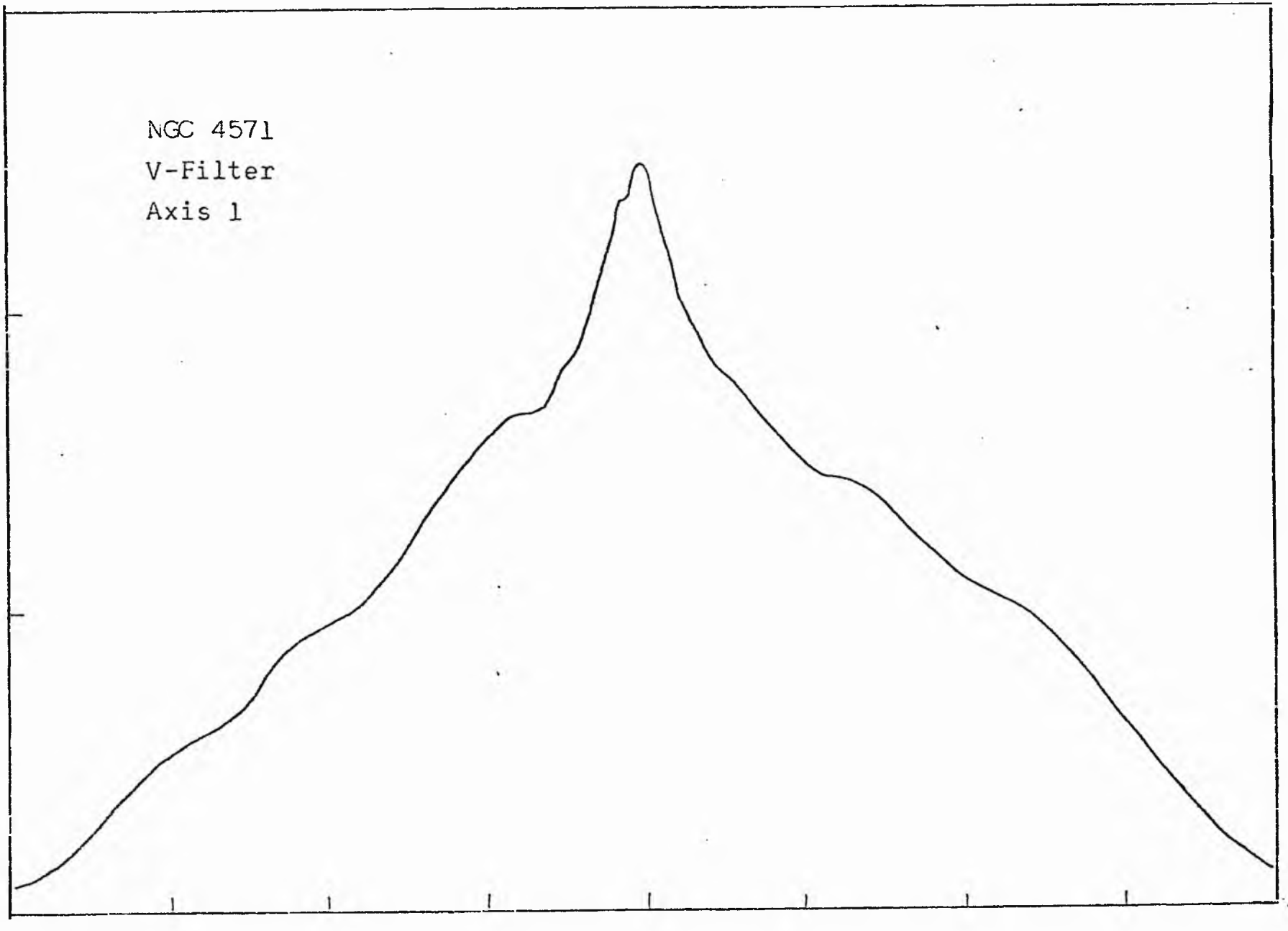
NGC 4571
V-Filter
Axis 1

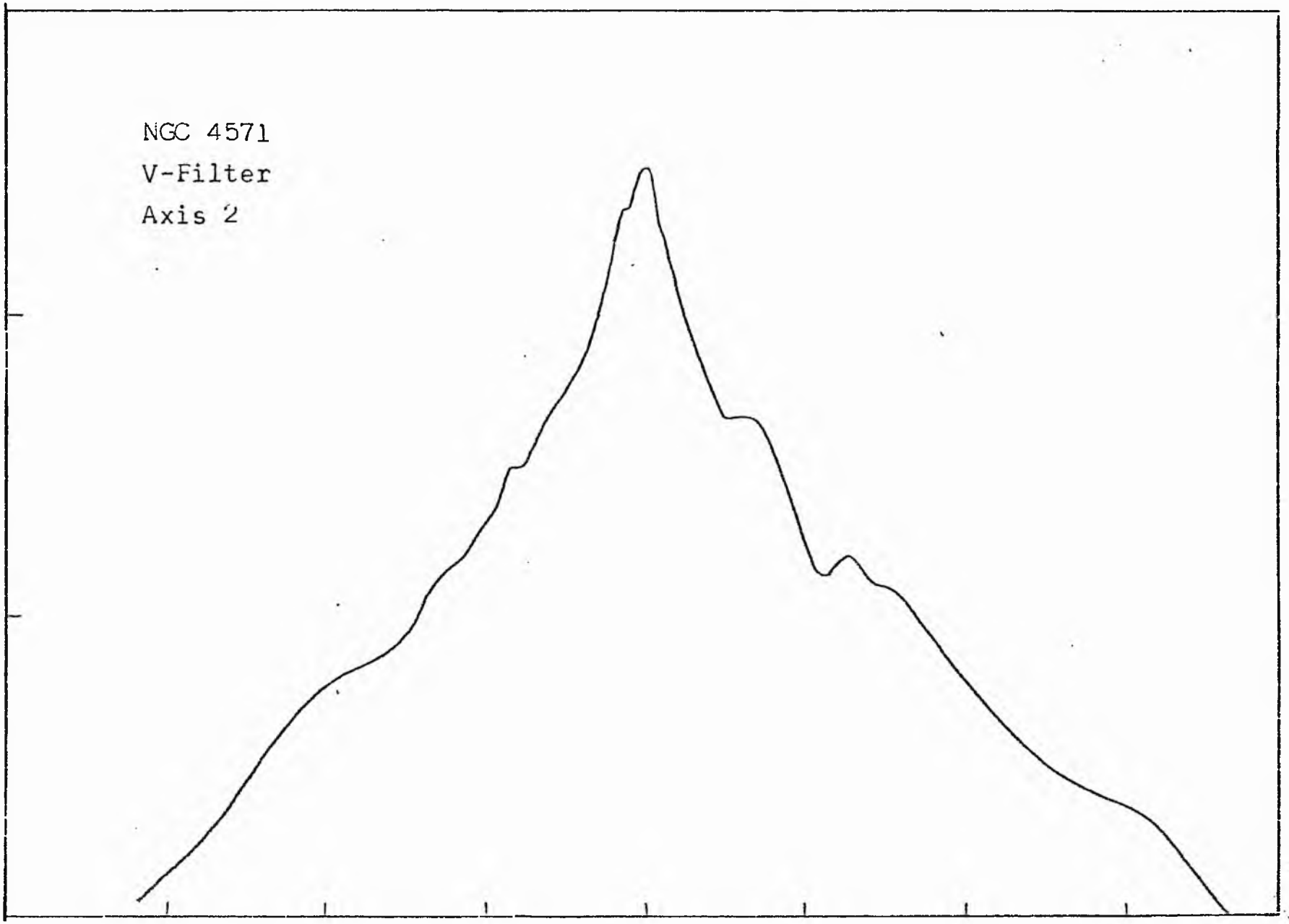
NGC 4571
V-Filter
Axis 2

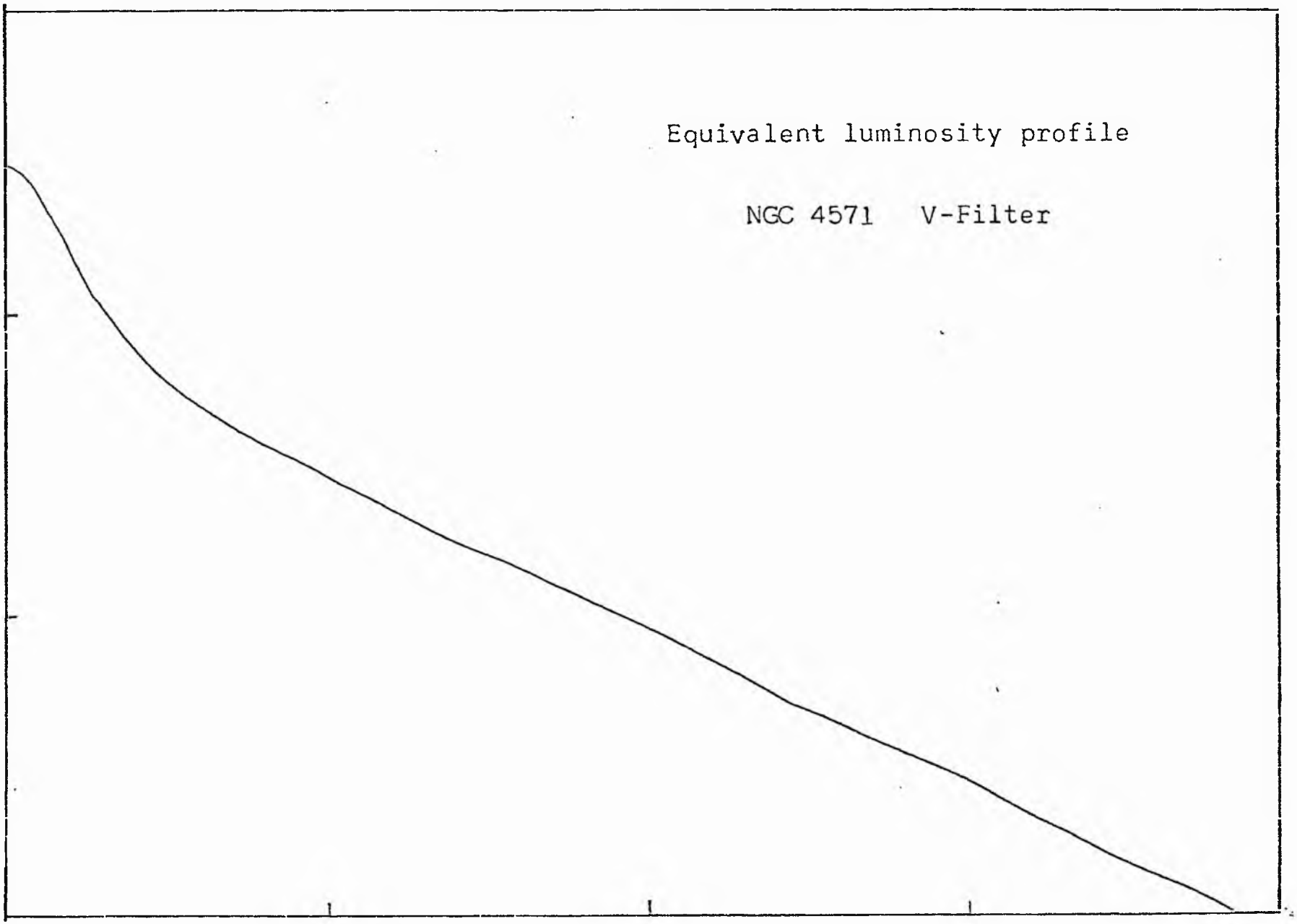
Equivalent luminosity profile
NGC 4571 V-Filter

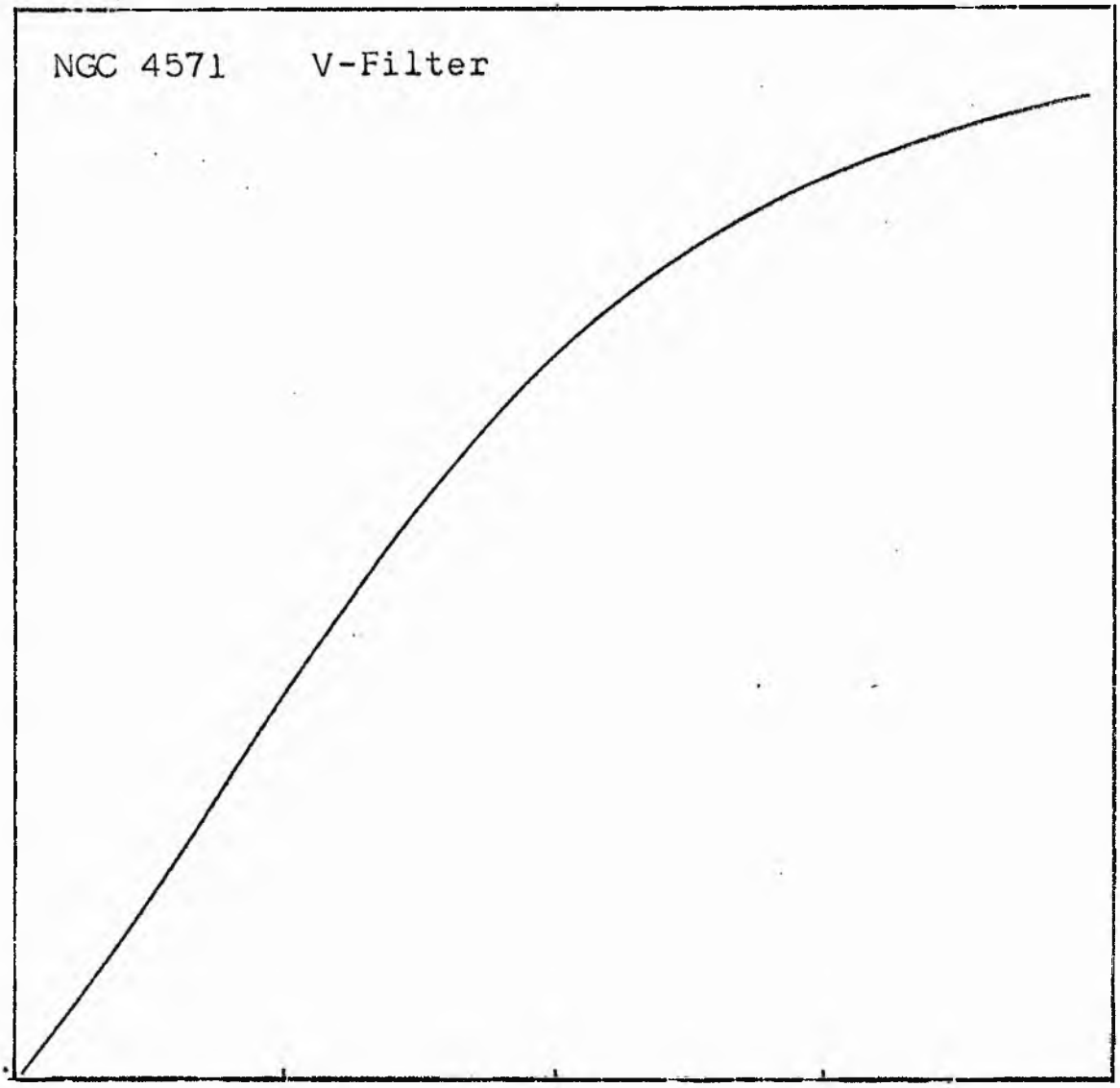

Relative integrated luminosity k(r) versus equivalent radius r*.

MEAN LUMINOSITY DISTRIBUTION IN NGC 4571
V COLOUR

LOG I	I	$\bar{I}$	R	AREA	ΔA	P	ΣP	K(R)	P	LOG J	μ
0.43	2.692		0.0	0.0			0.0	0.0	0.0	1.189	20.14
		2.602			45.84	119.2712					
0.40	2.512		3.82	45.84			119.27	0.01	0.06	1.159	20.22
		2.254			78.45	176.7949					
0.30	1.995		6.29	124.29			296.07	0.03	0.09	1.059	20.47
		1.793			106.44	190.5352					
0.20	1.585		8.57	230.73			486.60	0.04	0.12	0.959	20.72
		1.422			142.52	202.6484					
0.10	1.259		10.90	373.25			689.25	0.06	0.16	0.859	20.97
		1.129			212.95	240.5244					
0.00	1.000		13.66	586.21			929.77	0.08	0.20	0.759	21.22
		0.897			269.09	241.4190					
-0.10	0.794		16.50	855.30			1171.19	0.10	0.24	0.659	21.47
		0.713			547.35	390.0635					
-0.20	0.631		21.13	1402.65			1561.26	0.14	0.31	0.559	21.72
		0.566			892.67	505.3135					
-0.30	0.501		27.03	2295.31			2066.57	0.18	0.39	0.459	21.97
		0.450			1379.22	620.1621					
-0.40	0.398		34.20	3674.53			2686.73	0.24	0.50	0.359	22.22
		0.357			2270.14	810.8220					
-0.50	0.316		43.50	5944.68			3497.55	0.31	0.63	0.259	22.47
		0.284			3462.12	982.2329					
-0.60	0.251		54.72	9406.80			4479.79	0.40	0.80	0.159	22.72
		0.225			3169.29	714.2227					
-0.70	0.200		63.27	12576.08			5194.01	0.46	0.92	0.059	22.97
		0.179			4041.84	723.5212					
-0.80	0.158		72.73	16617.92			5917.53	0.53	1.06	-0.041	23.22
		0.142			5071.46	721.1165					
-0.90	0.126		83.09	21689.38			6638.64	0.59	1.21	-0.141	23.47
		0.113			6699.31	756.6633					
-1.00	0.100		95.06	28388.70			7395.30	0.66	1.38	-0.241	23.72
		0.090			6458.79	579.4597					
-1.10	0.079		105.32	34847.48			7974.76	0.71	1.53	-0.341	23.97
		0.071			5452.32	388.5564					
-1.20	0.063		113.26	40299.80			8363.31	0.74	1.65	-0.441	24.22
		0.057			7376.29	417.5525					
-1.30	0.050		123.19	47676.09			8780.86	0.78	1.79	-0.541	24.47
		0.045			8818.56	396.5256					
-1.40	0.040		134.10	56494.65			9177.39	0.82	1.95	-0.641	24.72
		0.036			10471.54	374.0112					
-1.50	0.032		146.00	66966.19			9551.39	0.85	2.12	-0.741	24.97
		0.028			7762.50	220.2301					
-1.60	0.025		154.23	74728.69			9771.62	0.87	2.24	-0.841	25.22
		0.023			9561.56	215.4789					
-1.70	0.020		163.80	84290.25			9987.10	0.89	2.38	-0.941	25.47
		0.018			9843.19	176.2025					
-1.80	0.016		173.10	94133.44			10163.30	0.90	2.52	-1.041	25.72
		0.014			13853.00	196.9793					
-1.90	0.013		185.40	107986.44			10360.27	0.92	2.69	-1.141	25.97
		0.011			15550.00	175.6336					
-2.00	0.010		198.30	123536.44			10535.91	0.94	2.88	-1.241	26.22
$-\infty$							11255.00	(1)			∞

PHOTOMETRIC PARAMETERS OF NGC 4571

V-FILTER

Total luminosity	L_T	= 3.13
Total apparent magnitude	m_T	= 11.09
Apparent central surface brightness	μ_o	= 20.14
Major axis at threshold	$2a_m$	= 6.93
Minor axis at threshold	$2b_m$	= 6.04
Major axis at μ=25.0 mag sec^{-2}	2a(25)	= 5.05
Luminosity within μ=25.0 mag sec^{-2}	k(25)	= 0.85
Gradient of exponential component	G(a)	= -0.53
Equivalent gradient of exponential comp.	G(r*)	= -0.62
Equivalent gradient of reduced exp. comp.	G(ρ)	= +0.72

Parameters at k = ¼ :

Semi-major axis	a_1	= 0.72
Axis ratio	b/a	= 0.77
Equivalent radius	r_1*	= 0.60
Surface brightness	μ_1	= 22.25

Parameters at k = ½(effective) :

Semi-major axis	a_e	= 1.32
Axis ratio	b/a	= 0.76
Equivalent radius	r_e*	= 1.15
Surface brightness	μ_e	= 23.11
Mean surface brightness	μ_e'	= 13.39

Parameters at k = ¾ :

Semi-major axis	a_3	= 2.18
Axis ratio	b/a	= 0.75
Equivalent radius	r_3*	= 1.92
Surface brightness	μ_3	= 24.28
Concentration indices	C_{21}	= 1.93
	C_{32}	= 1.67

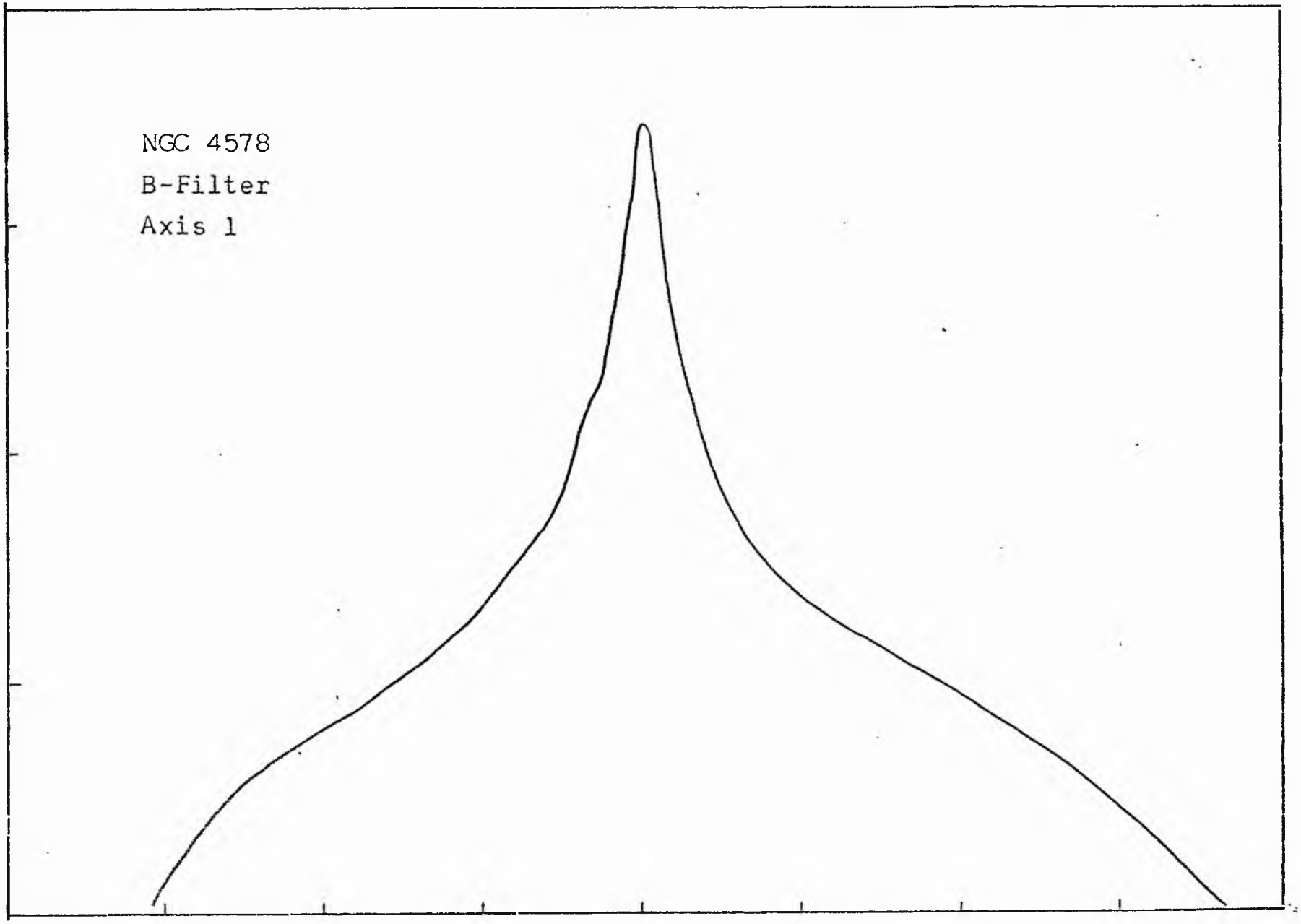
NGC 4578
B-Filter
Axis 1

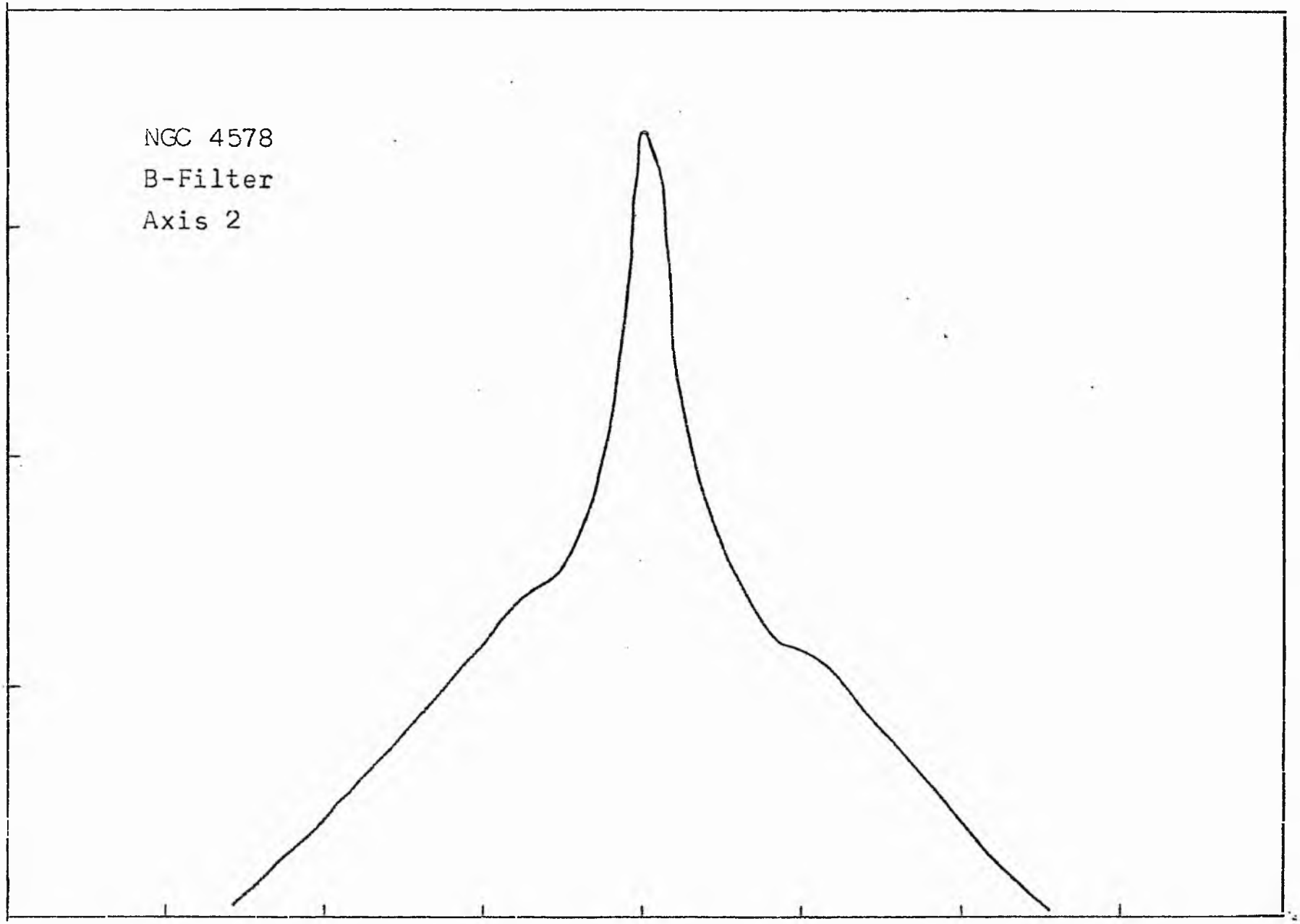
NGC 4578
B-Filter
Axis 2

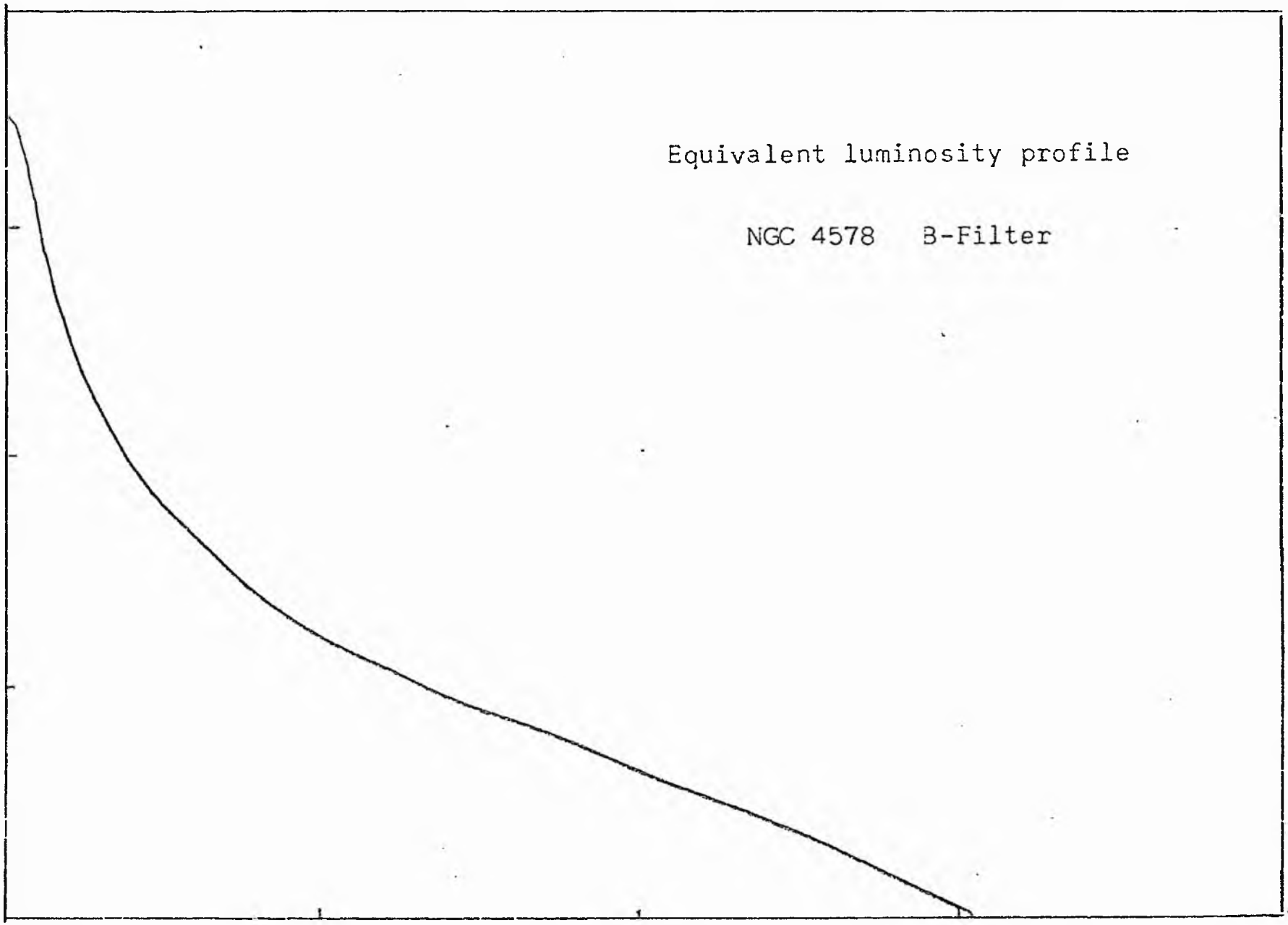
Equivalent luminosity profile
NGC 4578 B-Filter

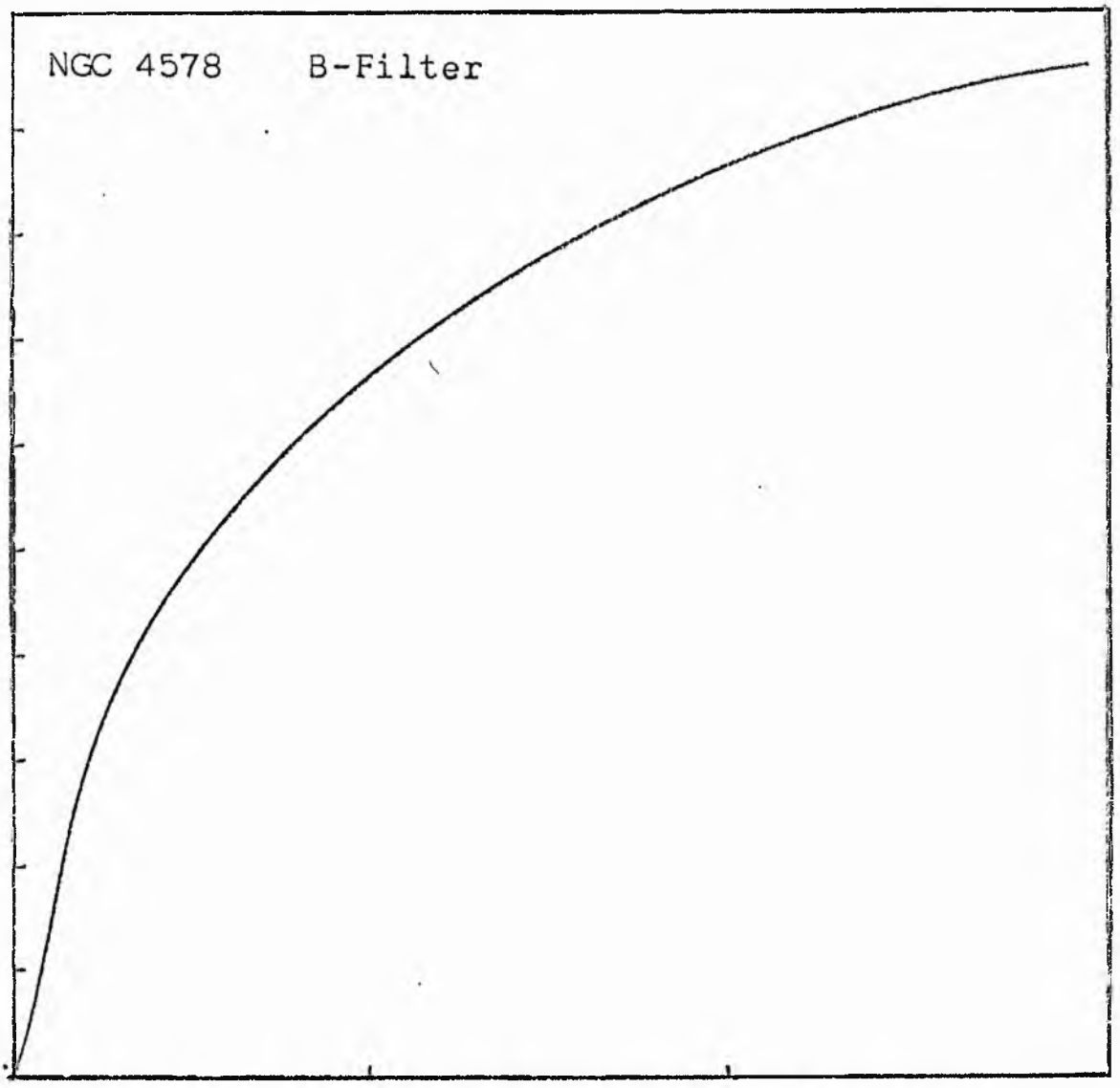

Relative integrated luminosity k(r) versus equivalent radius r*.

MEAN LUMINOSITY DISTRIBUTION IN NGC 4578
B COLOUR

LOG I	I	T	R	AREA	ΔA	P	ΣP	K(R)	ρ	LOG J	μ
1.43	26.915		0.0	0.0			0.0	0.0	0.0	1.717	18.61
		26.017			24.45	636.2332					
1.40	25.119		2.79	24.45			636.23	0.07	0.11	1.667	18.69
		22.536			14.03	316.1765					
1.30	19.953		3.50	38.48			952.41	0.10	0.14	1.567	18.94
		17.901			19.60	350.9167					
1.20	15.849		4.30	58.09			1303.33	0.14	0.17	1.487	19.19
		14.219			17.34	246.5811					
1.10	12.589		4.90	75.43			1549.91	0.16	0.19	1.387	19.44
		11.295			16.16	182.7371					
1.00	10.000		5.40	91.61			1732.64	0.18	0.21	1.287	19.69
		8.972			33.08	296.7891					
0.90	7.943		6.30	124.69			2029.43	0.21	0.24	1.187	19.94
		7.126			33.68	240.0022					
0.80	6.310		7.10	158.37			2269.44	0.24	0.28	1.087	20.19
		5.661			16.35	103.8566					
0.70	5.012		7.50	176.71			2373.29	0.25	0.29	0.987	20.44
		4.496			55.64	250.1717					
0.60	3.981		8.60	232.35			2623.46	0.28	0.33	0.887	20.69
		3.572			45.24	161.5782					
0.50	3.162		9.40	277.59			2785.04	0.29	0.36	0.787	20.94
		2.837			62.20	176.4794					
0.40	2.512		10.40	339.79			2961.52	0.31	0.40	0.687	21.19
		2.254			75.68	170.5526					
0.30	1.995		11.50	415.48			3132.07	0.33	0.45	0.587	21.44
		1.790			272.66	488.0786					
0.20	1.585		14.80	688.13			3620.15	0.38	0.57	0.487	21.69
		1.422			86.24	122.6205					
0.10	1.259		15.70	774.37			3742.77	0.39	0.61	0.387	21.94
		1.129			209.86	237.0260					
-0.00	1.000		17.70	984.23			3979.79	0.42	0.69	0.287	22.19
		0.897			297.67	267.0542					
-0.10	0.794		20.20	1281.89			4246.85	0.45	0.78	0.187	22.44
		0.713			365.59	260.5320					
-0.20	0.631		22.90	1647.48			4507.38	0.47	0.89	0.087	22.69
		0.566			509.03	288.1479					
-0.30	0.501		26.20	2156.51			4795.52	0.50	1.02	-0.013	22.94
		0.450			689.80	310.1650					
-0.40	0.398		30.10	2846.31			5105.69	0.54	1.17	-0.113	23.19
		0.357			871.32	311.2068					
-0.50	0.316		34.40	3717.63			5416.89	0.57	1.34	-0.213	23.44
		0.284			1134.52	321.8716					
-0.60	0.251		39.30	4852.15			5738.76	0.60	1.53	-0.313	23.69
		0.225			1425.03	321.1406					
-0.70	0.200		44.70	6277.18			6059.90	0.64	1.74	-0.413	23.94
		0.179			1451.63	259.8530					
-0.80	0.158		49.60	7728.82			6319.75	0.66	1.93	-0.513	24.19
		0.142			3059.28	435.0012					
-0.90	0.126		58.60	10788.10			6754.75	0.71	2.27	-0.613	24.44
		0.113			2896.68	327.1689					
-1.00	0.100		66.00	13684.78			7081.92	0.74	2.56	-0.713	24.69
		0.090			4845.07	434.6829					
-1.10	0.079		76.80	18529.85			7516.60	0.79	2.98	-0.813	24.94
		0.071			4489.71	319.9570					
-1.20	0.063		85.60	23019.57			7836.56	0.82	3.32	-0.913	25.19
		0.057			5154.51	291.7832					
-1.30	0.050		94.70	28174.07			8128.34	0.85	3.68	-1.013	25.44
		0.045			4000.35	179.8754					
-1.40	0.040		101.20	32174.43			8308.21	0.87	3.93	-1.113	25.69
		0.036			5700.73	203.6126					
-1.50	0.032		109.80	37875.15			8511.82	0.89	4.26	-1.213	25.94
		0.028			4909.84	139.2973					
-1.60	0.025		116.70	42785.00			8651.12	0.91	4.53	-1.313	26.19
		0.023			6853.70	154.4547					
-1.70	0.020		125.70	49638.70			8805.57	0.93	4.88	-1.413	26.44
		0.018			7193.50	128.7706					
-1.80	0.016		134.50	56832.20			8934.34	0.94	5.22	-1.513	26.69
		0.014			7590.05	107.9249					
-1.90	0.013		143.20	64422.25			9042.27	0.95	5.56	-1.613	26.94
		0.011			5324.25	60.1361					
-2.00	0.010		149.00	69746.50			9102.40	0.96	5.78	-1.713	27.19
-∞							9517.00	(1)			∞

PHOTOMETRIC PARAMETERS OF NGC 4578

B-FILTER

Total luminosity	L_T	= 2.64
Total apparent magnitude	m_T	= 12.24
Apparent central surface brightness	μ_o	= 18.61
Major axis at threshold	$2a_m$	= 5.77
Minor axis at threshold	$2b_m$	= 4.25
Major axis at μ=25.0 mag sec^{-2}	2a(25)	= 3.88
Luminosity within μ=25.0 mag sec^{-2}	k(25)	= 0.80
Gradient of exponential component	G(a)	= -0.63
Equivalent gradient of exponential comp.	G(r*)	= -0.83
Equivalent gradient of reduced exp. comp.	G(ρ)	= -0.36
Parameters at k = ¼ :		
Semi-major axis	a_1	= 0.16
Axis ratio	b/a	= 0.80
Equivalent radius	r_1*	= 0.13
Surface brightness	μ_1	= 20.44
Parameters at k = ½(effective) :		
Semi-major axis	a_e	= 0.55
Axis ratio	b/a	= 0.70
Equivalent radius	r_e*	= 0.43
Surface brightness	μ_e	= 22.94
Mean surface brightness	μ_e'	= 12.38
Parameters at k = ¾ :		
Semi-major axis	a_3	= 1.51
Axis ratio	b/a	= 0.66
Equivalent radius	r_3*	= 1.12
Surface brightness	μ_3	= 24.74
Concentration indices	C_{21}	= 3.42
	C_{32}	= 2.61

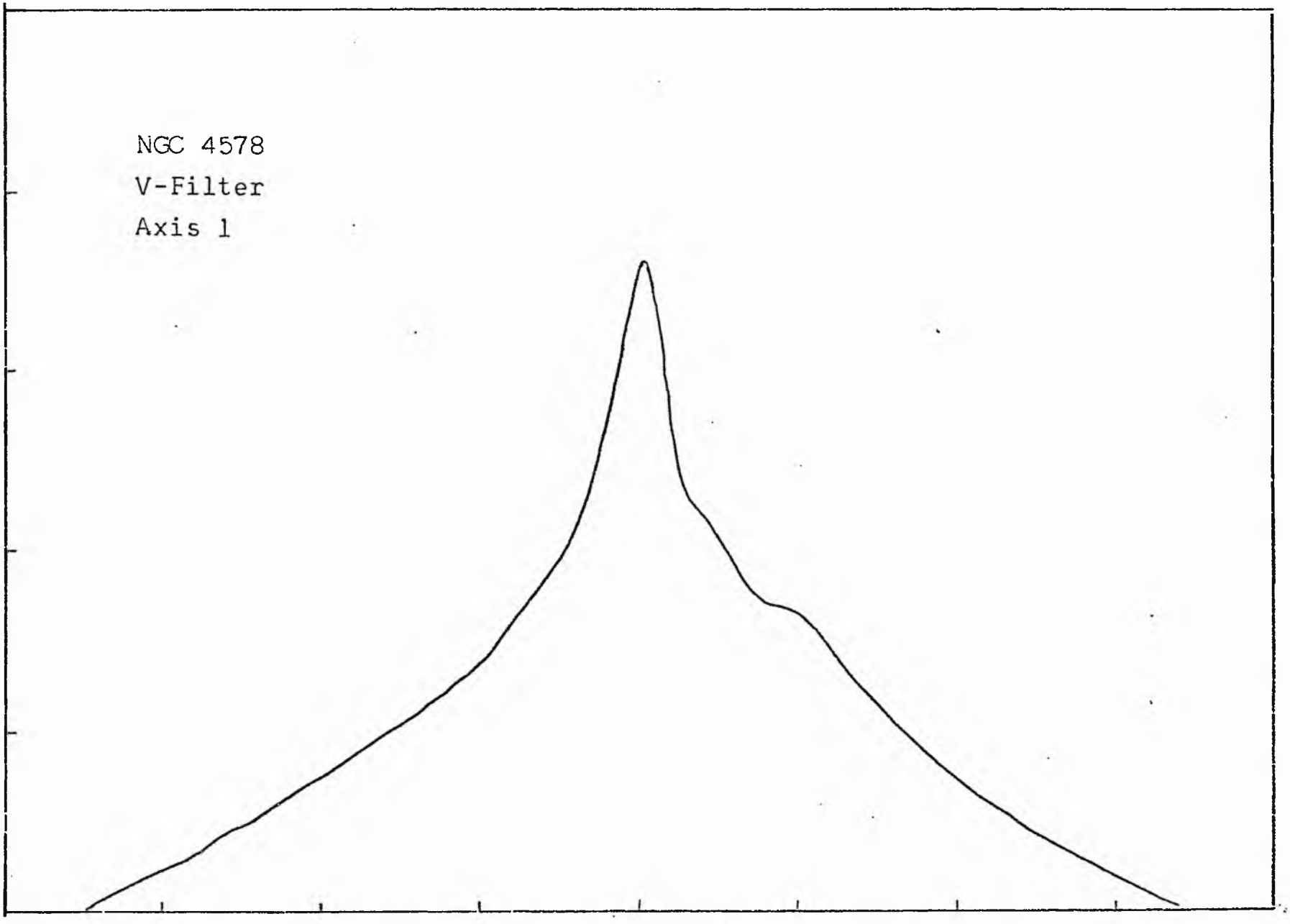
NGC 4578
V-Filter
Axis 1

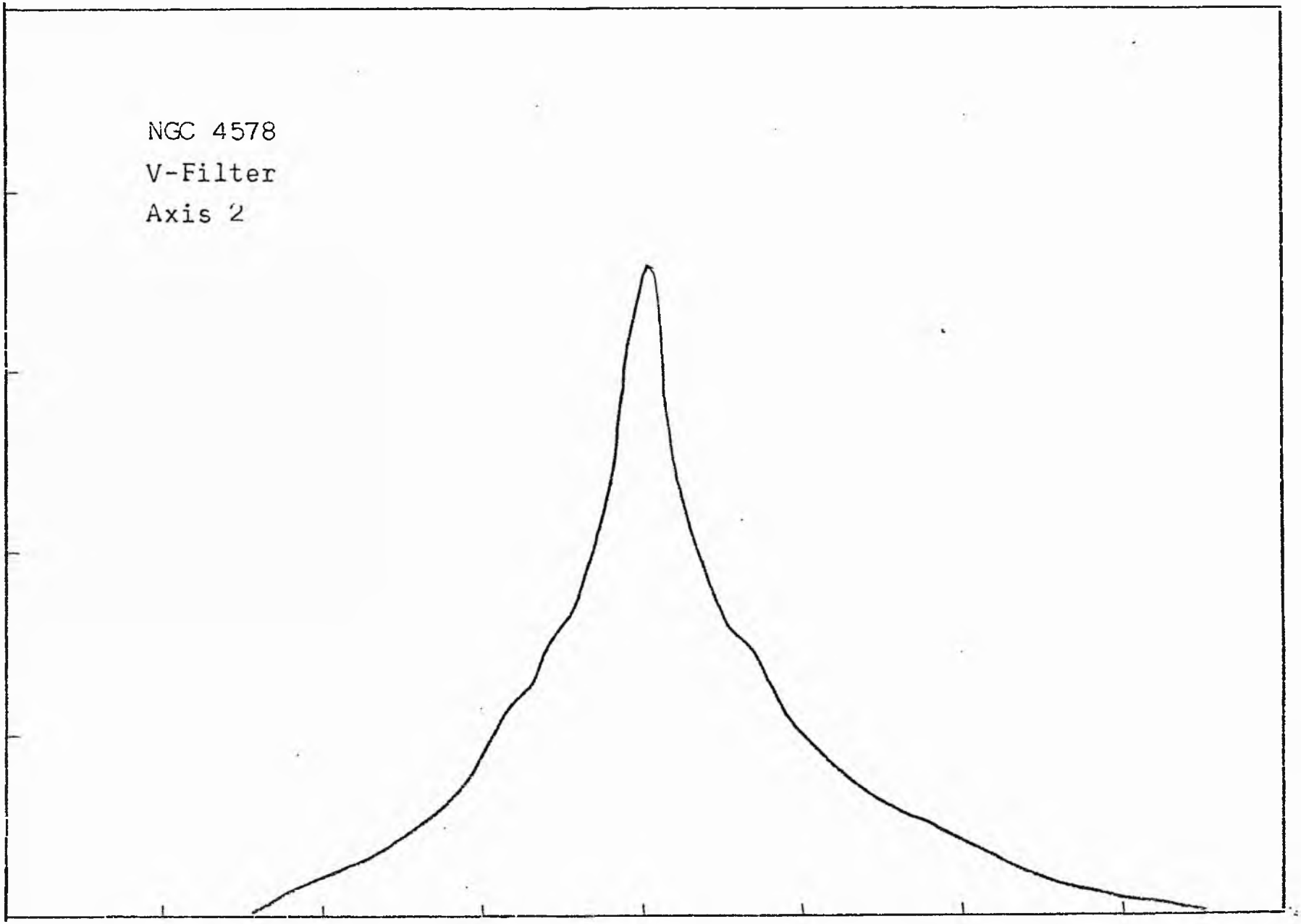
NGC 4578
V-Filter
Axis 2

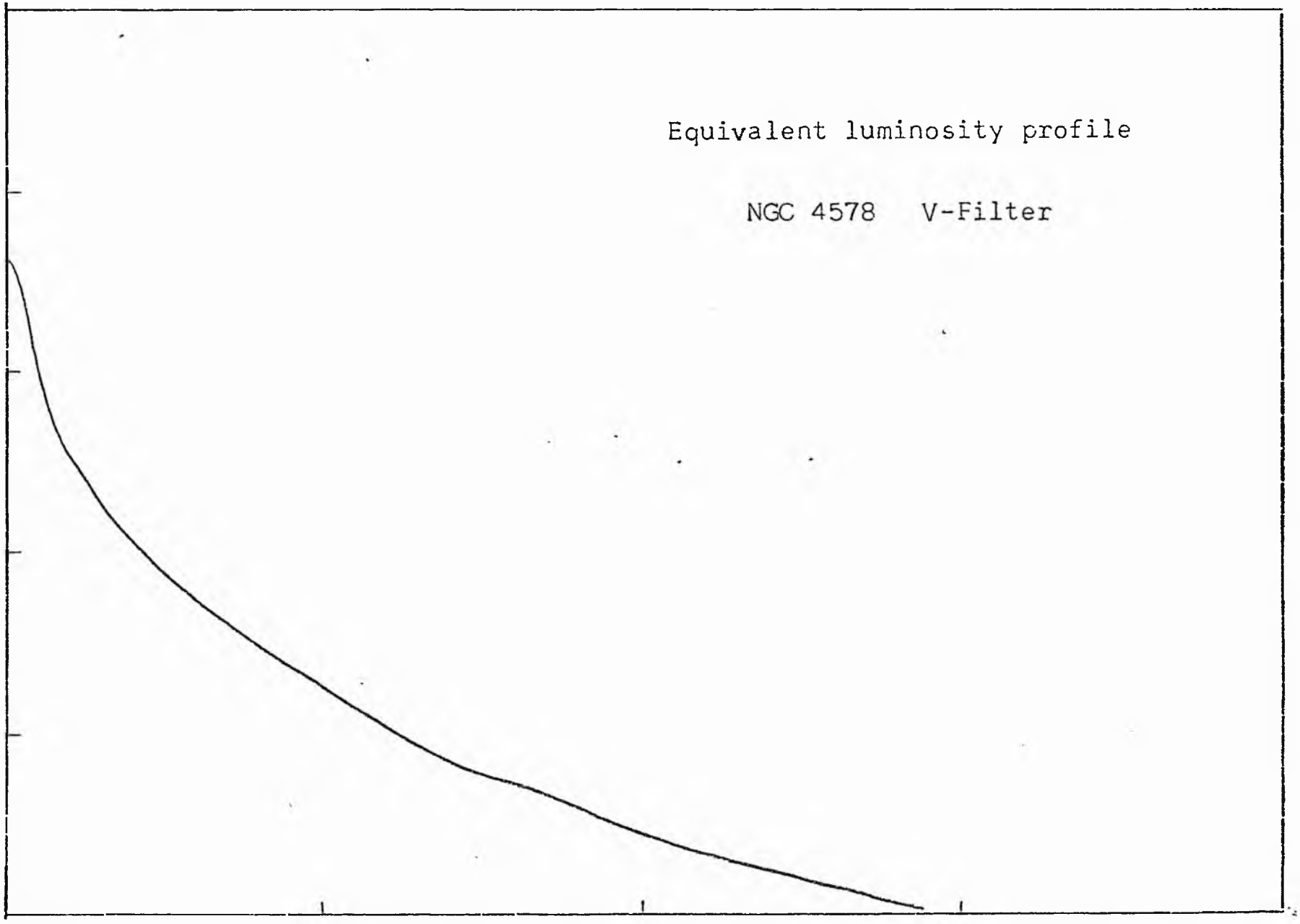
Equivalent luminosity profile
NGC 4578 V-Filter

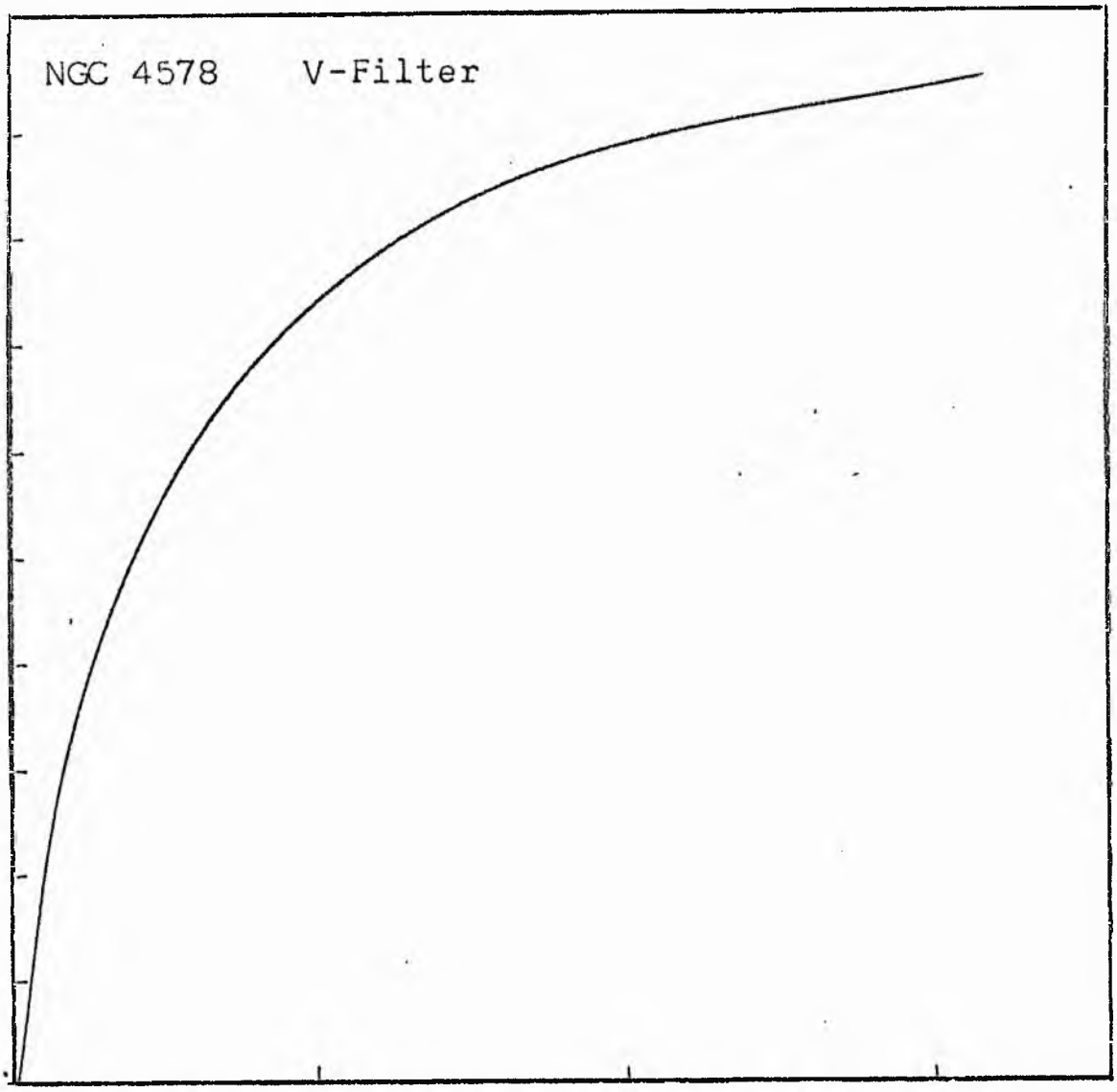

Relative integrated luminosity k(r) versus equivalent radius r*.

MEAN LUMINOSITY DISTRIBUTION IN NGC 4578
V COLOUR

LOG I	I	I	R	AREA	A	P	P	K(R)	I	LOG J	J
1.56	36.308		0.0	0.0			0.0	0.0	0.0	1.573	17.48
		33.965			4.52	153.6551					
1.50	31.623		1.20	4.52			153.66	0.01	0.06	1.513	17.63
		28.371			18.38	521.4570					
1.40	25.119		2.70	22.90			675.06	0.06	0.13	1.413	17.88
		22.536			23.11	653.1067					
1.30	19.953		3.70	43.01			1128.17	0.11	0.18	1.313	18.13
		17.901			41.94	750.7607					
1.20	15.849		5.20	84.95			1878.93	0.18	0.25	1.213	18.38
		14.219			31.95	454.2981					
1.10	12.589		6.10	116.90			2333.23	0.22	0.30	1.113	18.63
		11.295			28.37	320.4104					
1.00	10.000		6.80	145.27			2653.64	0.25	0.33	1.013	18.88
		8.972			26.77	240.1374					
0.90	7.943		7.40	172.03			2893.78	0.28	0.36	0.913	19.13
		7.126			24.03	171.2704					
0.80	6.310		7.90	196.07			3065.05	0.29	0.38	0.813	19.38
		5.661			41.72	236.1665					
0.70	5.012		8.70	237.79			3301.21	0.31	0.42	0.713	19.63
		4.496			45.74	205.6744					
0.60	3.981		9.50	283.53			3506.89	0.33	0.46	0.613	19.88
		3.572			56.27	200.9627					
0.50	3.162		10.40	339.79			3707.85	0.35	0.50	0.513	20.13
		2.837			61.36	174.0699					
0.40	2.512		11.30	401.15			3881.92	0.37	0.55	0.413	20.38
		2.254			105.56	237.8807					
0.30	1.995		12.70	536.71			4119.80	0.39	0.62	0.313	20.63
		1.790			172.16	308.1777					
0.20	1.585		14.70	678.87			4427.97	0.42	0.71	0.213	20.88
		1.422			283.25	402.7488					
0.10	1.259		17.50	962.11			4830.72	0.46	0.85	0.113	21.13
		1.129			332.50	375.5498					
-0.00	1.000		20.30	1294.62			5206.27	0.50	0.98	0.013	21.38
		0.897			295.81	265.3933					
-0.10	0.794		22.50	1590.43			5471.66	0.52	1.09	-0.087	21.63
		0.713			500.74	356.8447					
-0.20	0.631		25.80	2091.17			5828.59	0.56	1.25	-0.187	21.88
		0.566			680.00	384.9272					
-0.30	0.501		29.70	2771.17			6213.43	0.59	1.44	-0.287	22.13
		0.450			989.82	445.0688					
-0.40	0.398		34.60	3760.99			6658.49	0.63	1.68	-0.387	22.38
		0.357			1190.44	425.1863					
-0.50	0.316		39.70	4951.43			7083.68	0.68	1.93	-0.487	22.63
		0.284			1495.39	424.2546					
-0.60	0.251		45.30	6446.82			7507.93	0.72	2.20	-0.587	22.88
		0.225			1004.06	226.2716					
-0.70	0.200		48.70	7450.88			7734.20	0.74	2.36	-0.687	23.13
		0.179			1574.78	281.8975					
-0.80	0.158		53.60	9025.66			8016.09	0.76	2.60	-0.787	23.38
		0.142			1109.86	157.8122					
-0.90	0.126		56.80	10135.53			8173.90	0.78	2.75	-0.887	23.63
		0.113			1061.39	119.8801					
-1.00	0.100		59.70	11196.92			8293.78	0.79	2.90	-0.987	23.88
		0.090			1751.59	157.1461					
-1.10	0.079		64.20	12948.50			8450.93	0.81	3.11	-1.087	24.13
		0.071			3473.50	247.5368					
-1.20	0.063		72.30	16422.00			8698.46	0.83	3.51	-1.187	24.38
		0.057			3583.77	202.8681					
-1.30	0.050		79.80	20005.77			8931.33	0.85	3.87	-1.287	24.63
		0.045			2906.35	130.6838					
-1.40	0.040		85.40	22912.12			9032.01	0.86	4.14	-1.387	24.88
		0.036			4965.23	177.3427					
-1.50	0.032		94.20	27877.35			9239.35	0.88	4.57	-1.487	25.13
		0.028			5000.31	141.8640					
-1.60	0.025		102.30	32877.66			9351.21	0.89	4.96	-1.587	25.38
		0.023			8922.12	180.7861					
-1.70	0.020		114.10	40899.79			9532.00	0.91	5.53	-1.687	25.63
		0.018			10572.07	189.2503					
-1.80	0.016		128.00	51471.86			9721.25	0.93	6.21	-1.787	25.88
		0.014			7837.51	111.4436					
-1.90	0.013		137.40	59309.37			9832.69	0.94	6.66	-1.887	26.13
		0.011			11565.07	130.6247					
-2.00	0.010		150.20	70874.44			9961.31	0.95	7.28	-1.987	26.38
- ∞							10493.00	(1)			∞

PHOTOMETRIC PARAMETERS OF NGC 4578

V-FILTER

Total luminosity	L_T	= 2.91
Total apparent magnitude	m_T	= 11.33
Apparent central surface brightness	μ_o	= 17.48
Major axis at threshold	$2a_m$	= 5.42
Minor axis at threshold	$2b_m$	= 4.95
Major axis at μ=25.0 mag sec^{-2}	2a(25)	= 3.76
Luminosity within μ=25.0 mag sec^{-2}	k(25)	= 0.87
Gradient of exponential component	G(a)	= -0.81
Equivalent gradient of exponential comp.	G(r*)	= -0.92
Equivalent gradient of reduced exp. comp.	G(ρ)	= -0.46

Parameters at k = ¼ :

Semi-major axis	a_1	= 0.12
Axis ratio	b/a	= 1.00
Equivalent radius	r_1*	= 0.11
Surface brightness	μ_1	= 18.88

Parameters at k = ½(effective) :

Semi-major axis	a_e	= 0.37
Axis ratio	b/a	= 0.73
Equivalent radius	r_e*	= 0.34
Surface brightness	μ_e	= 21.38
Mean surface brightness	μ_e'	= 10.98

Parameters at k = ¾ :

Semi-major axis	a_3	= 1.11
Axis ratio	b/a	= 0.59
Equivalent radius	r_3*	= 0.85
Surface brightness	μ_3	= 23.25

Concentration indices	C_{21}	= 3.06
	C_{32}	= 2.47

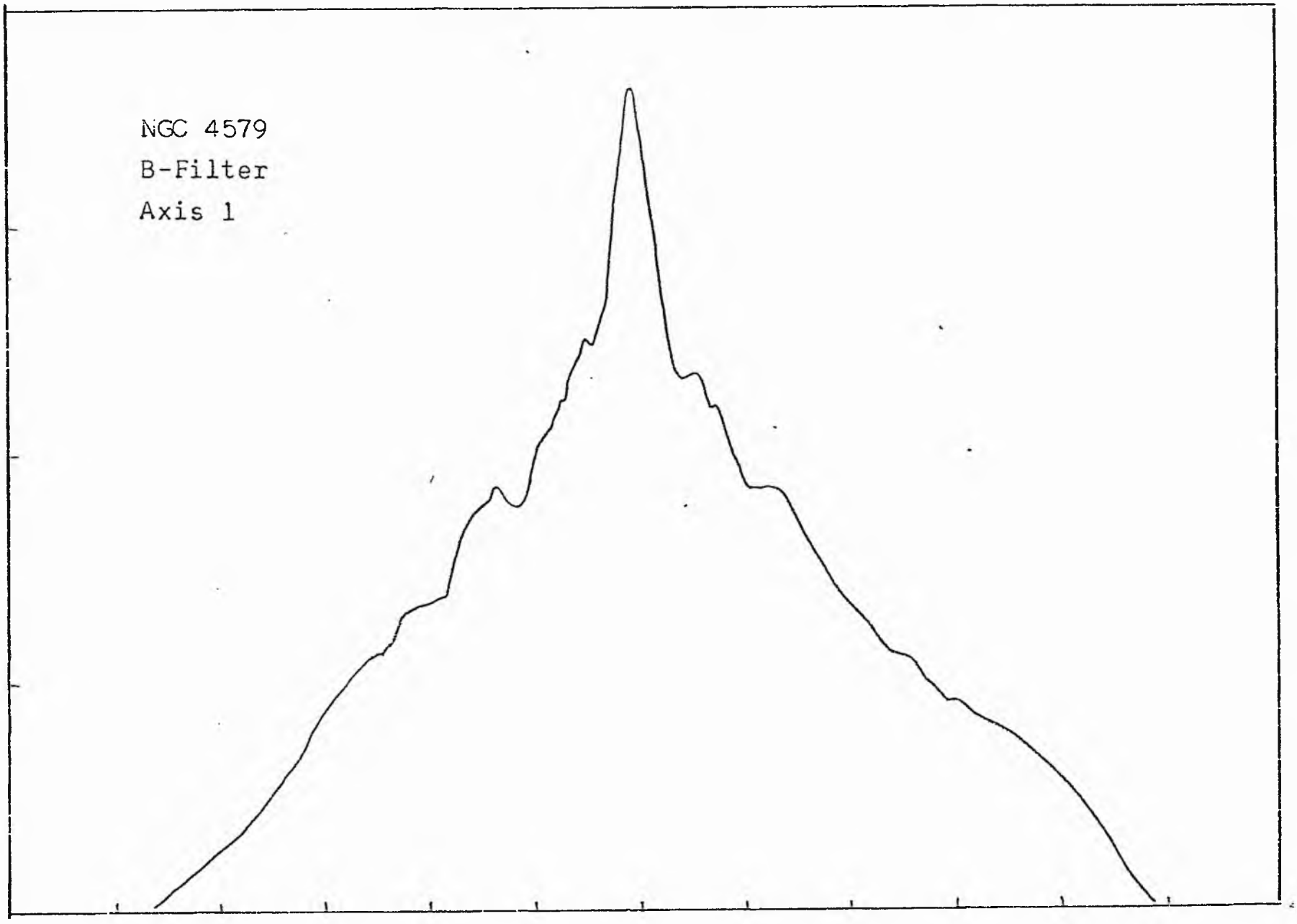
NGC 4579
B-Filter
Axis 1

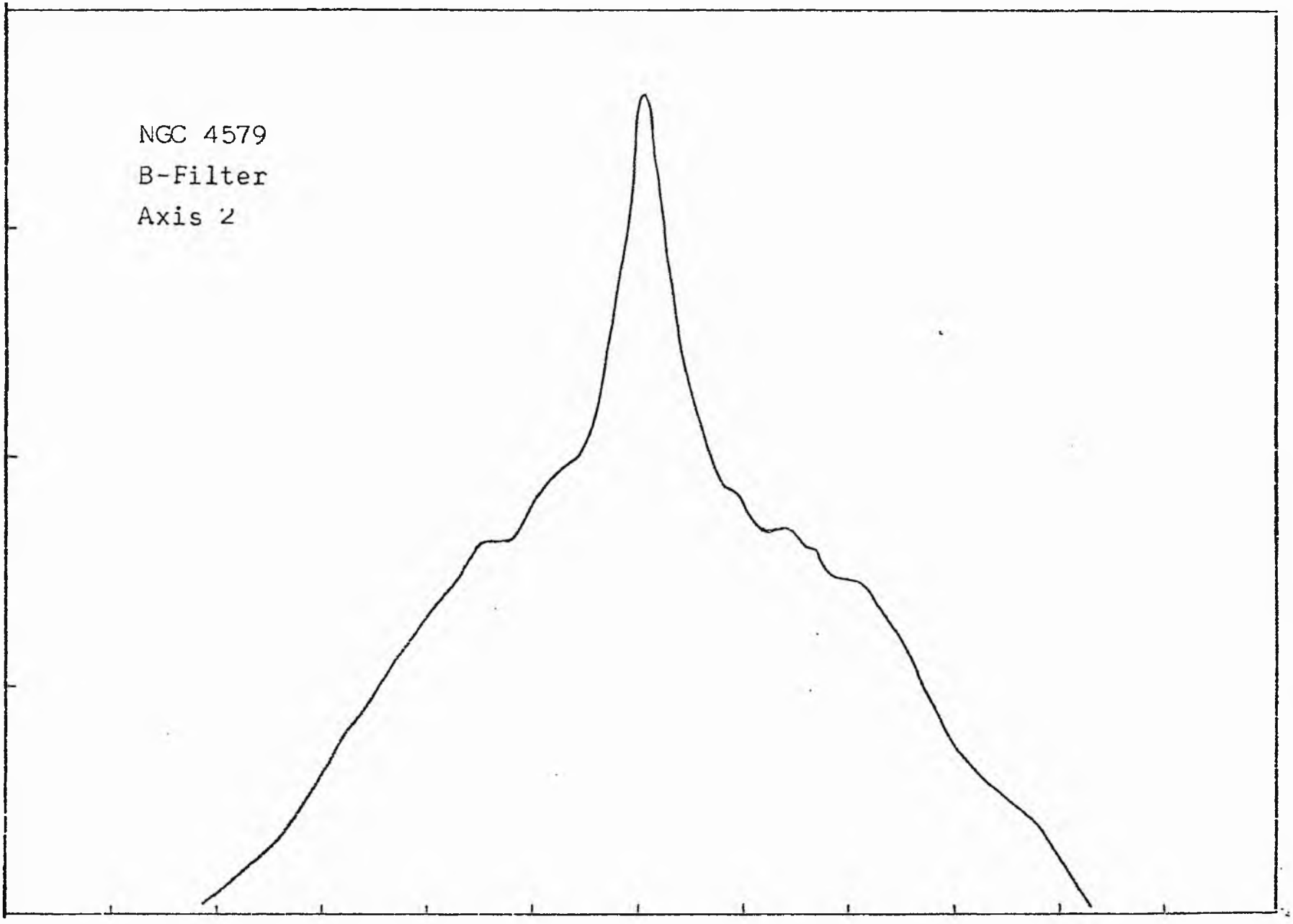
NGC 4579
B-Filter
Axis 2

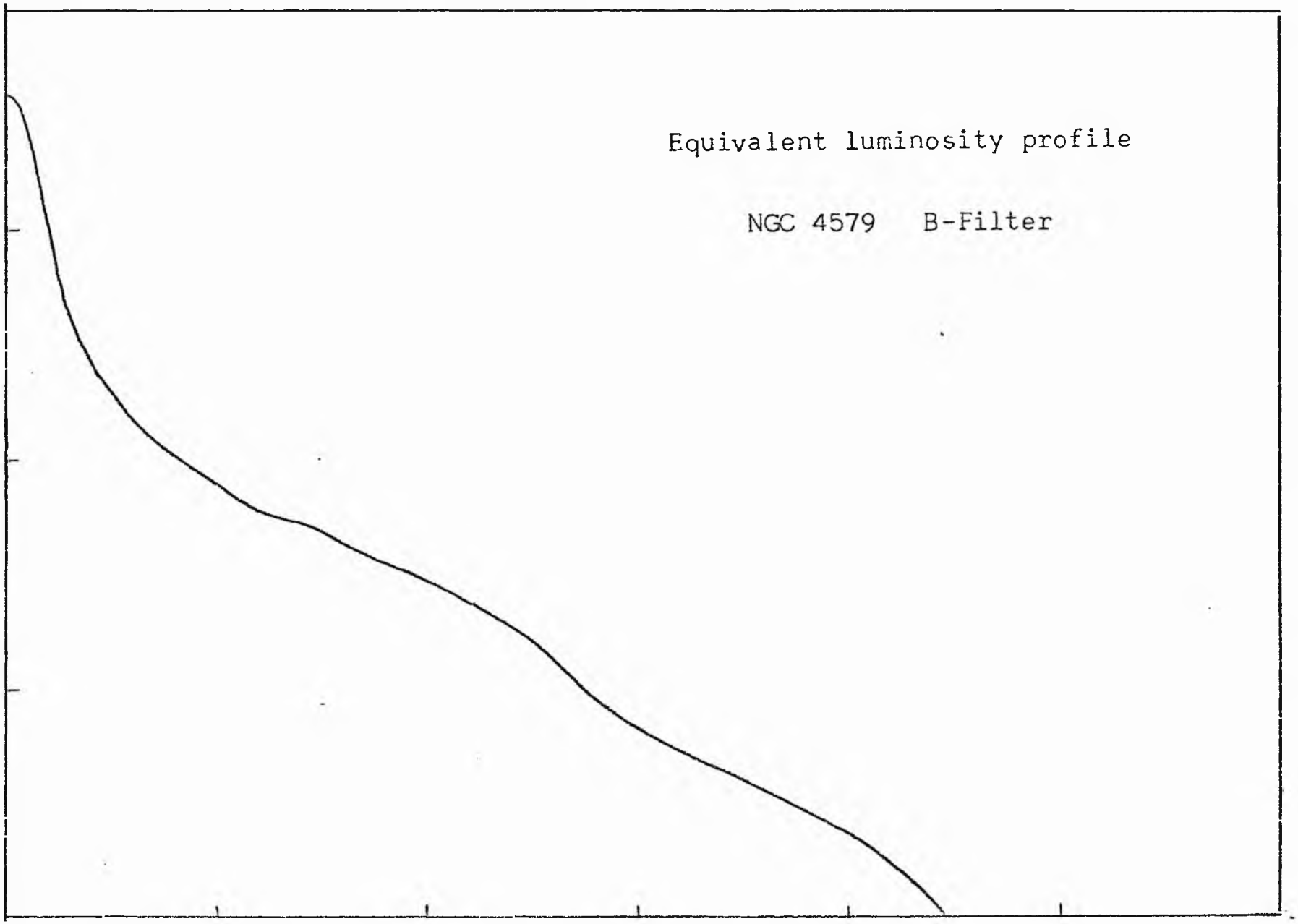
Equivalent luminosity profile
NGC 4579 B-Filter

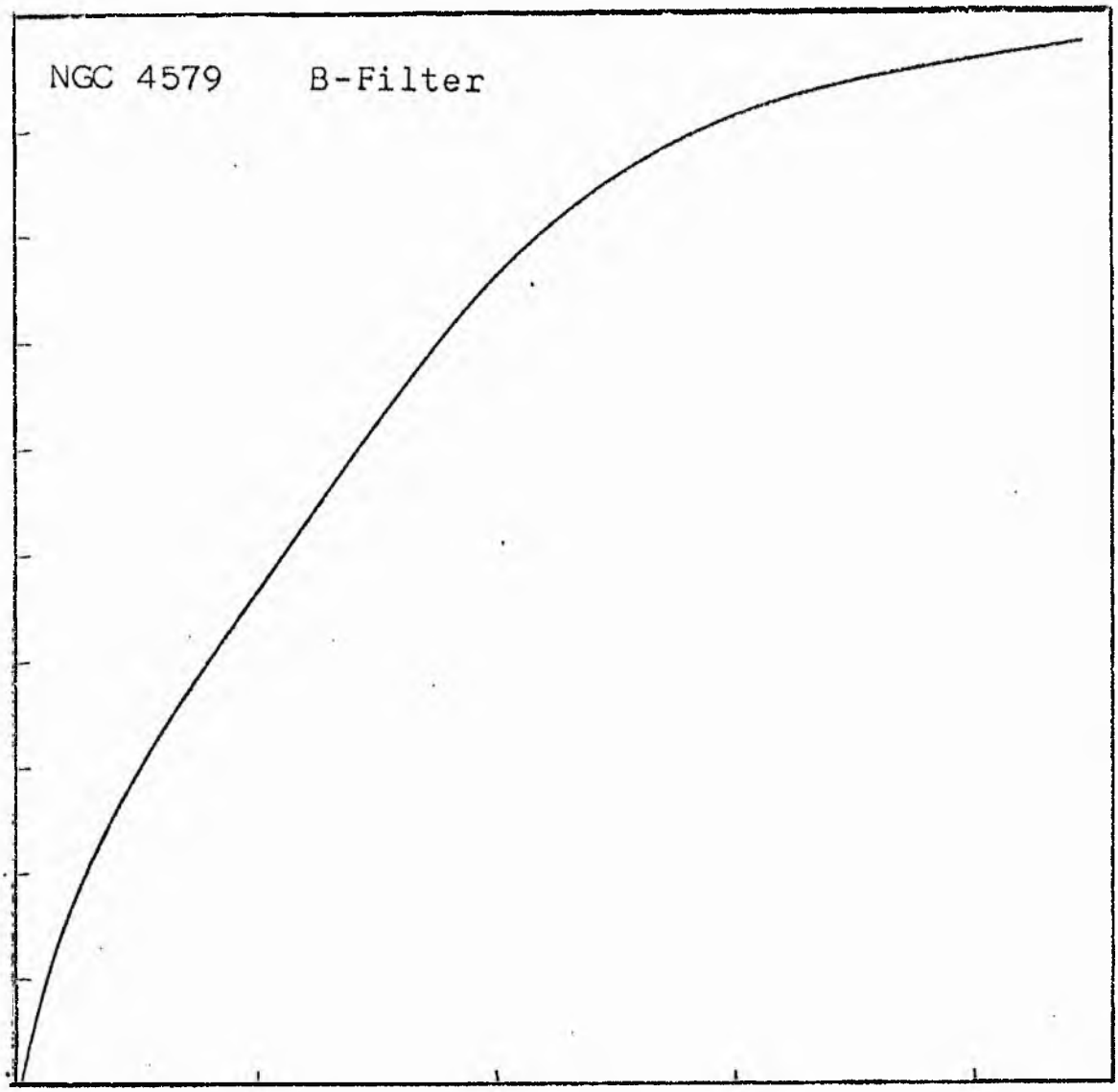

Relative integrated luminosity k(r) versus equivalent radius r*.

MEAN LUMINOSITY DISTRIBUTION IN NGC 4579
B COLOUR

LOG I	I	I	R	AREA	ΔA	P	ΣP	KENI	ρ	LOG J	JJ
1.56	36.308		0.0	0.0			0.0	0.0	0.0	1.728	17.69
		33.965			34.00	1154.9854					
1.50	31.623		3.29	34.00			1154.99	0.03	0.06	1.668	18.14
		28.371			21.41	607.4961					
1.40	25.119		4.20	55.42			1762.48	0.05	0.07	1.568	18.39
		22.536			26.30	592.5781					
1.30	19.953		5.10	81.71			2355.06	0.06	0.09	1.468	18.64
		17.901			109.42	1958.7275					
1.20	15.849		7.80	191.13			4313.79	0.11	0.14	1.368	18.89
		14.219			35.85	509.6904					
1.10	12.589		8.50	226.98			4823.47	0.13	0.15	1.268	19.14
		11.295			56.55	638.6912					
1.00	10.000		9.50	283.53			5462.16	0.14	0.17	1.168	19.39
		8.972			56.27	504.7949					
0.90	7.943		10.40	339.79			5966.95	0.15	0.19	1.068	19.64
		7.126			82.94	591.0510					
0.80	6.310		11.60	422.73			6558.00	0.17	0.21	0.968	19.89
		5.661			132.98	752.7795					
0.70	5.012		13.30	555.72			7310.78	0.19	0.24	0.868	20.14
		4.496			180.60	722.1235					
0.60	3.981		15.10	716.31			8032.90	0.21	0.27	0.768	20.39
		3.572			245.80	877.9087					
0.50	3.162		17.50	962.11			8910.81	0.23	0.31	0.668	20.64
		2.837			397.06	1126.4990					
0.40	2.512		20.80	1359.18			10037.30	0.26	0.37	0.568	20.89
		2.254			495.90	1117.5444					
0.30	1.995		24.30	1855.08			11154.85	0.29	0.43	0.468	21.14
		1.790			469.20	839.8979					
0.20	1.585		27.20	2324.27			11994.74	0.31	0.49	0.368	21.39
		1.422			953.31	1355.5225					
0.10	1.259		32.30	3277.59			13350.26	0.35	0.58	0.268	21.64
		1.129			1673.84	1870.5344					
-0.00	1.000		39.70	4951.43			15240.79	0.40	0.71	0.168	21.89
		0.897			2560.77	2297.4272					
-0.10	0.794		48.90	7512.20			17538.27	0.46	0.87	0.068	22.14
		0.713			3647.23	2599.1650					
-0.20	0.631		59.60	11159.43			20137.38	0.52	1.06	-0.032	22.39
		0.566			6305.28	3569.2339					
-0.30	0.501		74.56	17464.71			23706.61	0.62	1.33	-0.132	22.64
		0.450			6133.95	2758.1067					
-0.40	0.398		86.67	23598.66			26464.72	0.69	1.55	-0.232	22.89
		0.357			6782.91	2622.6277					
-0.50	0.316		98.34	30381.57			28887.34	0.75	1.76	-0.332	23.14
		0.284			7335.08	2001.0173					
-0.60	0.251		109.57	37716.65			30968.36	0.80	1.96	-0.432	23.39
		0.225			4753.62	1071.2625					
-0.70	0.200		116.27	42470.27			32039.62	0.83	2.08	-0.532	23.64
		0.179			4511.75	807.6360					
-0.80	0.158		122.29	46982.02			32847.25	0.85	2.18	-0.632	23.89
		0.142			3521.28	500.6934					
-0.90	0.126		126.79	50503.30			33347.95	0.87	2.26	-0.732	24.14
		0.113			6777.67	765.5117					
-1.00	0.100		135.03	57280.97			34113.46	0.89	2.41	-0.832	24.39
		0.090			5044.21	452.5483					
-1.10	0.079		140.85	62325.18			34566.00	0.90	2.51	-0.932	24.64
		0.071			9372.70	667.9402					
-1.20	0.063		151.07	71697.87			35233.94	0.91	2.70	-1.032	24.89
		0.057			13707.56	775.9492					
-1.30	0.050		164.88	85405.44			36009.89	0.93	2.94	-1.132	25.14
		0.045			12595.31	566.3469					
-1.40	0.040		176.62	98000.75			36576.23	0.95	3.15	-1.232	25.39
		0.036			11388.06	406.7468					
-1.50	0.032		186.60	109388.81			36982.98	0.96	3.33	-1.332	25.64
		0.028			8848.12	251.0304					
-1.60	0.025		194.00	118236.94			37234.01	0.97	3.46	-1.432	25.89
		0.023			9559.44	215.4310					
-1.70	0.020		201.69	127796.37			37449.44	0.97	3.60	-1.532	26.14
		0.018			8972.25	160.6119					
-1.80	0.016		208.65	136768.62			37610.05	0.98	3.72	-1.632	26.39
		0.014			8289.37	117.8687					
-1.90	0.013		214.88	145058.00			37727.91	0.98	3.84	-1.732	26.64
		0.011			7493.06	84.6324					
-2.00	0.010		220.36	152551.06			37812.54	0.98	3.93	-1.832	26.89
							38542.00	(1)			∞

PHOTOMETRIC PARAMETERS OF NGC 4579

B-FILTER

Total luminosity	L_T	= 10.71
Total apparent magnitude	m_T	= 10.42
Apparent central surface brightness	μ_o	= 17.99
Major axis at threshold	$2a_m$	= 8.02
Minor axis at threshold	$2b_m$	= 6.75
Major axis at μ=25.0 mag sec^{-2}	2a(25)	= 5.38
Luminosity within μ=25.0 mag sec^{-2}	k(25)	= 0.92
Gradient of exponential component	G(a)	= -0.54
Equivalent gradient of exponential comp.	G(r*)	= -0.59
Equivalent gradient of reduced exp. comp.	G(ρ)	= -0.64

Parameters at k = ¼ :

Semi-major axis	a_1	= 0.32
Axis ratio	b/a	= 0.94
Equivalent radius	r_1*	= 0.33
Surface brightness	μ_1	= 20.81

Parameters at k = ½(effective) :

Semi-major axis	a_e	= 0.92
Axis ratio	b/a	= 0.89
Equivalent radius	r_e*	= 0.93
Surface brightness	μ_e	= 22.31
Mean surface brightness	μ_e'	= 12.26

Parameters at k = ¾ :

Semi-major axis	a_3	= 1.56
Axis ratio	b/a	= 0.91
Equivalent radius	r_3*	= 1.64
Surface brightness	μ_3	= 23.14
Concentration indices	C_{21}	= 2.86
	C_{32}	= 1.76

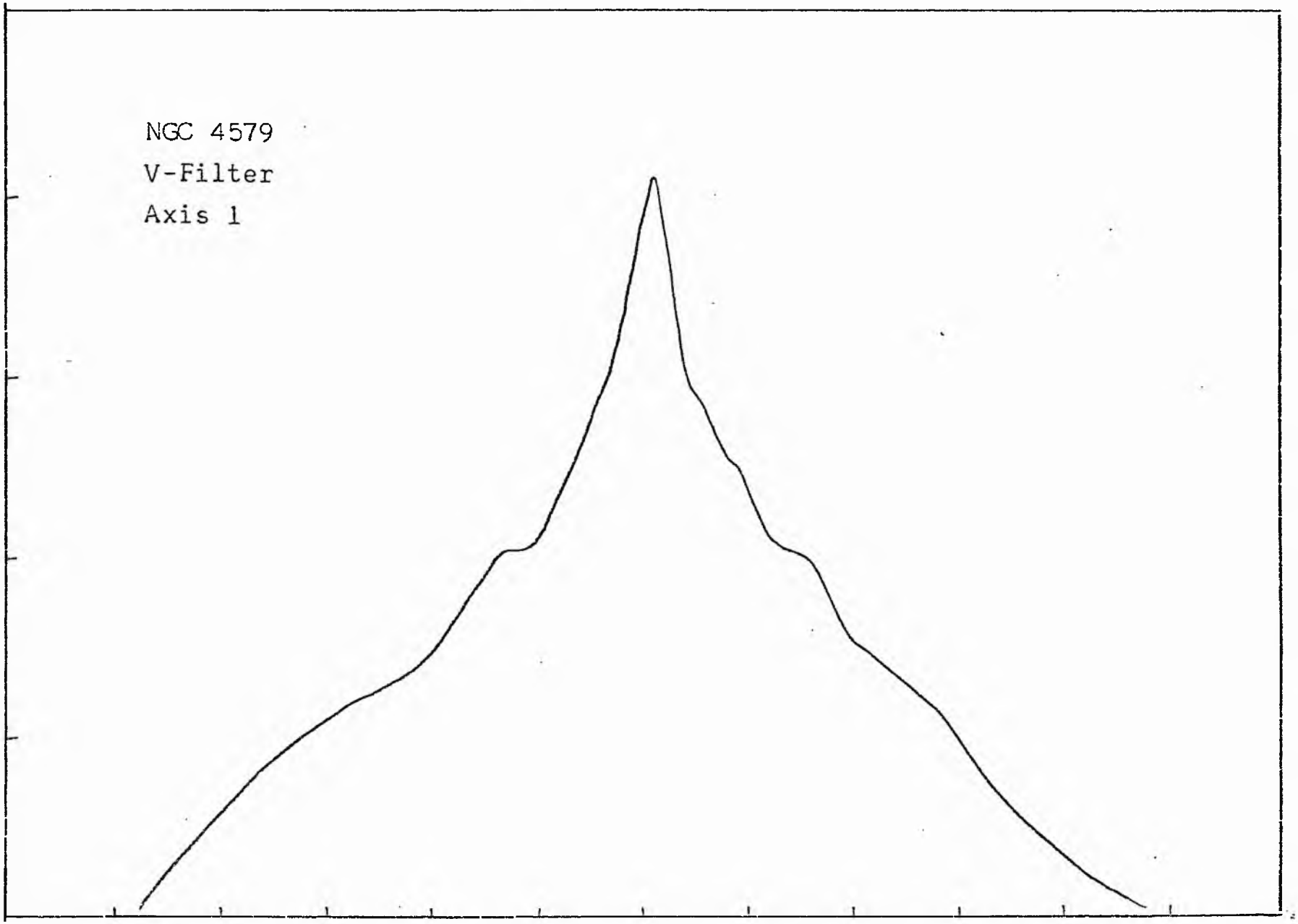
NGC 4579
V-Filter
Axis 1

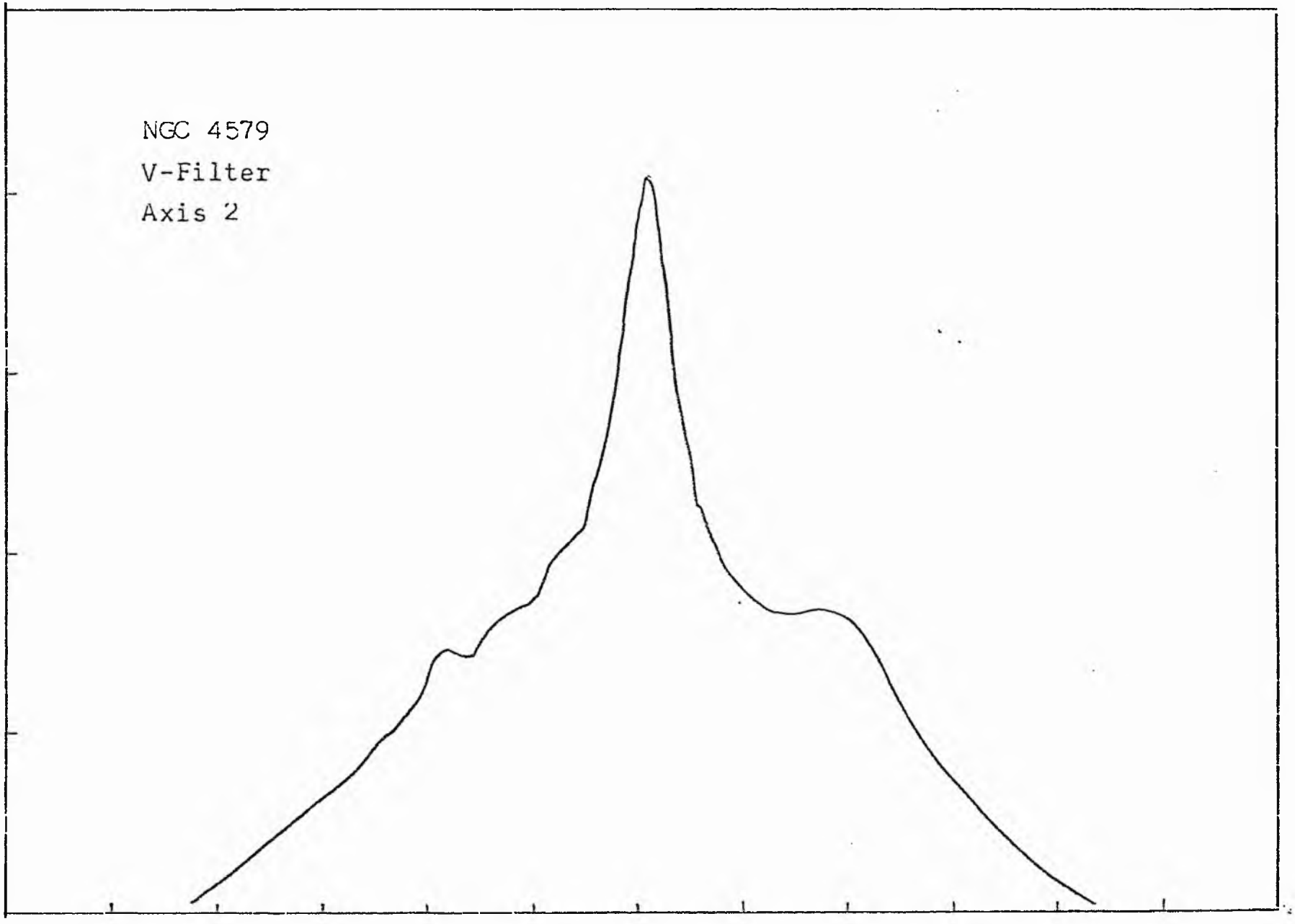
NGC 4579
V-Filter
Axis 2

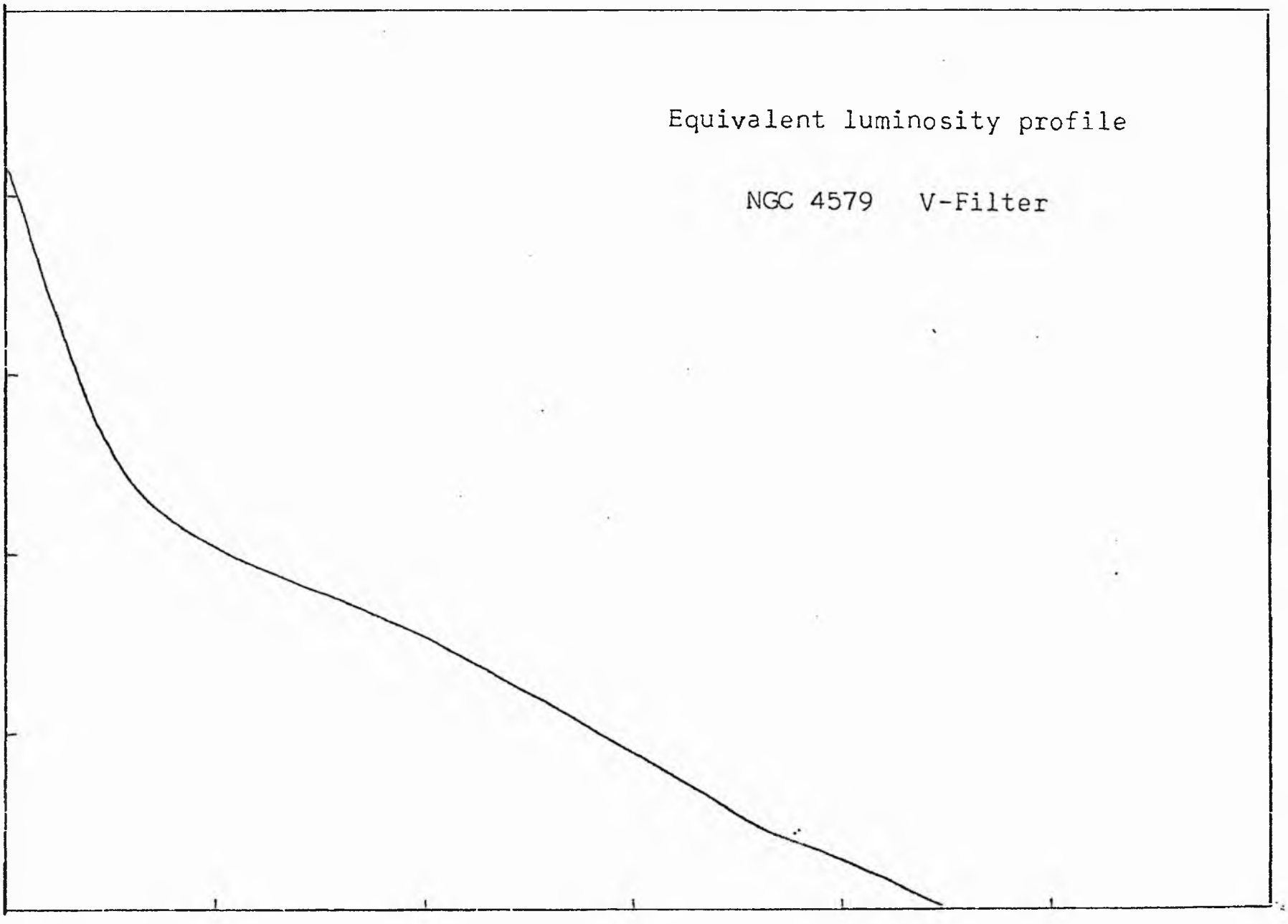
Equivalent luminosity profile
NGC 4579 V-Filter

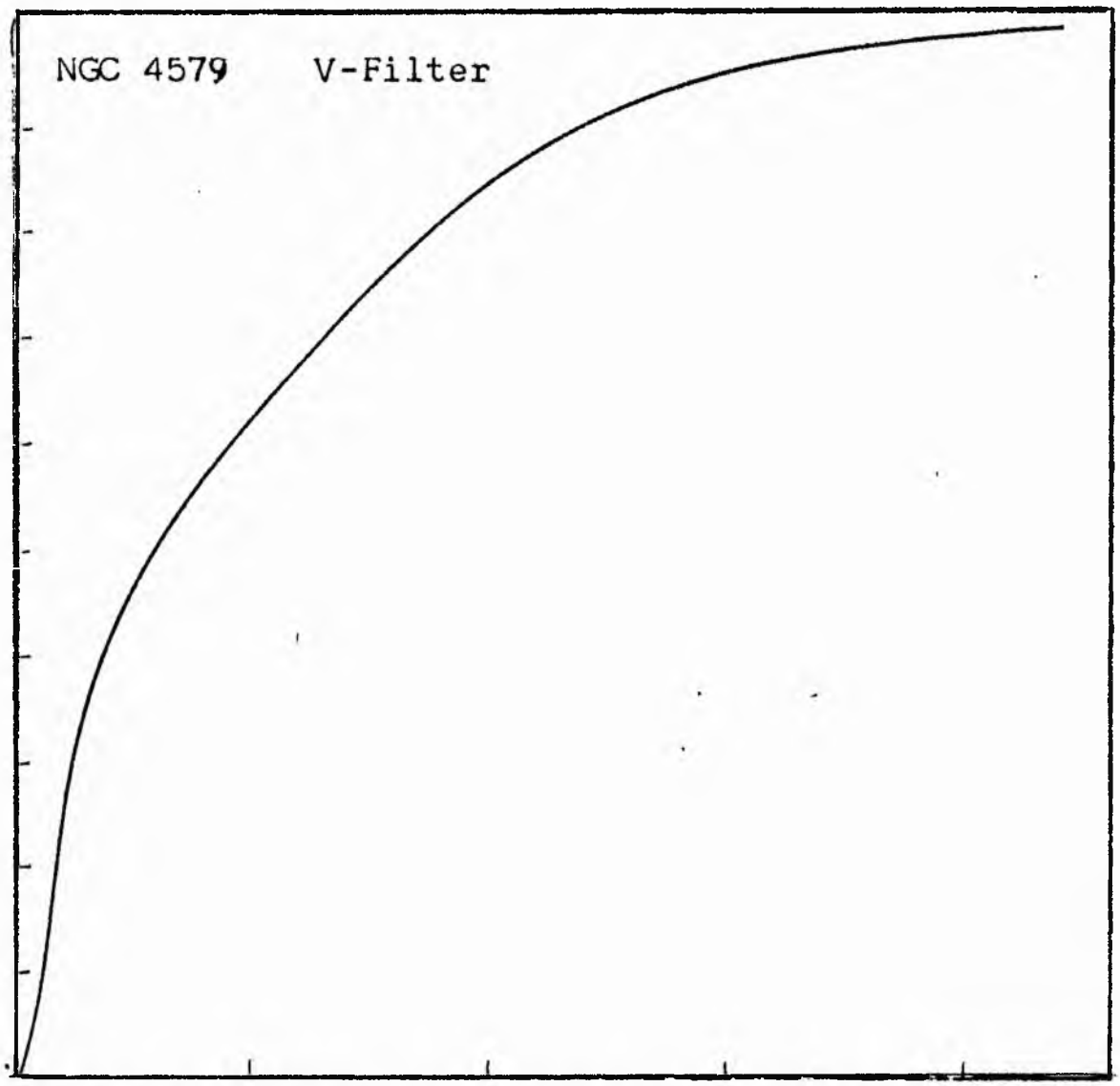

Relative integrated luminosity k(r) versus equivalent radius r*.

MEAN LUMINOSITY DISTRIBUTION IN NGC 4579
V COLOUR

LOG I	I	$\bar{I}$	R	AREA	ΔA	P	ΣP	K(R)	ρ	LOG J	μ
2.08	120.226		0.0	0.0			0.0	0.0	0.0	1.737	16.37
		110.113			4.52	498.1396					
2.00	100.000		1.20	4.52			498.14	0.01	0.04	1.657	16.57
		89.716			20.11	1803.8523					
1.90	79.433		2.80	24.63			2301.99	0.04	0.10	1.557	16.82
		71.264			16.08	1146.2812					
1.80	63.096		3.60	40.72			3448.27	0.06	0.13	1.457	17.07
		56.607			20.68	1623.6462					
1.70	50.119		4.70	69.40			5071.92	0.09	0.17	1.357	17.32
		44.965			32.67	1469.1069					
1.60	39.811		5.70	102.07			6541.02	0.11	0.20	1.257	17.57
		35.717			130.28	4653.2227					
1.50	31.623		8.60	232.35			11194.25	0.19	0.30	1.157	17.82
		28.371			114.01	3234.4961					
1.40	25.119		10.50	346.36			14428.74	0.25	0.37	1.057	18.07
		22.536			60.49	1363.1616					
1.30	19.952		11.38	406.85			15791.90	0.27	0.40	0.957	18.32
		17.901			84.02	1504.0828					
1.20	15.849		12.50	490.87			17295.98	0.30	0.44	0.857	18.57
		14.219			133.71	1901.1633					
1.10	12.589		14.10	624.58			19197.14	0.33	0.50	0.757	18.82
		11.295			63.55	717.8171					
1.00	10.000		14.80	688.13			19914.96	0.35	0.52	0.657	19.07
		8.972			146.55	1314.8162					
0.90	7.943		16.30	834.69			21229.77	0.37	0.57	0.557	19.32
		7.126			311.40	2219.1155					
0.80	6.310		19.10	1146.08			23448.89	0.41	0.67	0.457	19.57
		5.661			306.12	1732.8357					
0.70	5.012		21.50	1452.20			25181.72	0.44	0.76	0.357	19.82
		4.496			297.54	1337.8628					
0.60	3.981		23.60	1749.74			26519.58	0.46	0.83	0.257	20.07
		3.572			277.09	989.6643					
0.50	3.162		25.40	2026.83			27509.24	0.48	0.89	0.157	20.32
		2.837			179.35	508.8401					
0.40	2.512		26.50	2206.18			28018.08	0.49	0.93	0.057	20.57
		2.254			602.43	1357.6118					
0.30	1.995		29.90	2808.61			29375.69	0.51	1.05	-0.043	20.82
		1.790			974.15	1743.7830					
0.20	1.585		34.70	3782.76			31119.47	0.54	1.22	-0.143	21.07
		1.422			1706.35	2426.2571					
0.10	1.259		41.80	5489.11			33545.73	0.58	1.47	-0.243	21.32
		1.129			1931.20	2181.2061					
-0.00	1.000		48.60	7420.31			35726.93	0.62	1.71	-0.343	21.57
		0.897			2930.48	2629.0994					
-0.10	0.794		57.40	10350.79			38356.03	0.67	2.02	-0.443	21.82
		0.713			4911.34	3510.0039					
-0.20	0.631		69.70	15262.12			41856.03	0.73	2.45	-0.543	22.07
		0.566			4593.53	2600.2495					
-0.30	0.501		79.50	19855.65			44456.28	0.77	2.80	-0.643	22.32
		0.450			5140.86	2311.5571					
-0.40	0.398		89.20	24996.51			46767.83	0.81	3.14	-0.743	22.57
		0.357			5298.62	1892.4812					
-0.50	0.316		98.20	30295.13			48660.31	0.85	3.46	-0.843	22.82
		0.284			5538.61	1571.3401					
-0.60	0.251		106.80	35833.74			50231.65	0.87	3.76	-0.943	23.07
		0.225			5786.11	1303.9336					
-0.70	0.200		115.10	41619.85			51535.59	0.90	4.05	-1.043	23.32
		0.179			5754.86	1030.1575					
-0.80	0.158		122.80	47374.70			52565.74	0.91	4.32	-1.143	23.57
		0.142			5881.70	836.3196					
-0.90	0.126		130.20	53256.41			53402.06	0.93	4.59	-1.243	23.82
		0.113			5450.18	615.5745					
-1.00	0.100		136.70	58706.59			54017.63	0.94	4.81	-1.343	24.07
		0.090			8443.16	757.4871					
-1.10	0.079		146.20	67149.75			54775.12	0.95	5.15	-1.443	24.32
		0.071			7840.81	558.7683					
-1.20	0.063		154.50	74990.56			55333.88	0.96	5.44	-1.543	24.57
		0.057			6746.37	381.8931					
-1.30	0.050		161.30	81736.94			55715.77	0.97	5.68	-1.643	24.82
		0.045			4624.25	207.9281					
-1.40	0.040		165.80	86361.19			55923.70	0.97	5.84	-1.743	25.07
		0.036			8098.81	289.2637					
-1.50	0.032		173.40	94460.00			56212.96	0.98	6.11	-1.843	25.32
		0.028			8860.12	251.3697					
-1.60	0.025		181.35	103320.12			56464.33	0.98	6.39	-1.943	25.57
		0.023			15734.94	354.5999					
-1.70	0.020		194.67	119055.06			56818.93	0.99	6.86	-2.043	25.82
		0.018			6219.37	111.3323					
-1.80	0.016		199.69	125274.44			56930.26	0.99	7.03	-2.143	26.07
		0.014			10225.50	145.3984					
-1.90	0.013		207.68	135499.94			57075.65	0.99	7.31	-2.243	26.32
		0.011			9679.62	109.3287					
-2.00	0.010		214.97	145179.56			57184.98	0.99	7.57	-2.343	26.57
- ∞							57579.00	(1)			∞

PHOTOMETRIC PARAMETERS OF NGC 4579

V-FILTER

Total luminosity	L_T	= 15.99
Total apparent magnitude	m_T	= 9.67
Apparent central surface brightness	μ_o	= 16.37
Major axis at threshold	$2a_m$	= 7.97
Minor axis at threshold	$2b_m$	= 6.95
Major axis at μ=25.0 mag sec^{-2}	2a(25)	= 5.62
Luminosity within μ=25.0 mag sec^{-2}	k(25)	= 0.97
Gradient of exponential component	G(a)	= -0.67
Equivalent gradient of exponential comp.	G(r*)	= -0.73
Equivalent gradient of reduced exp. comp.	G(ρ)	= -0.34

Parameters at k = ¼ :

Semi-major axis	a_1	= 0.20
Axis ratio	b/a	= 0.83
Equivalent radius	r_1*	= 0.17
Surface brightness	μ_1	= 18.07

Parameters at k = ½(effective) :

Semi-major axis	a_e	= 0.75
Axis ratio	b/a	= 0.51
Equivalent radius	r_e*	= 0.47
Surface brightness	μ_e	= 20.69
Mean surface brightness	μ_e'	= 10.02

Parameters at k = ¾ :

Semi-major axis	a_3	= 1.37
Axis ratio	b/a	= 0.71
Equivalent radius	r_3*	= 1.25
Surface brightness	μ_3	= 22.19
Concentration indices	C_{21}	= 2.71
	C_{32}	= 2.63

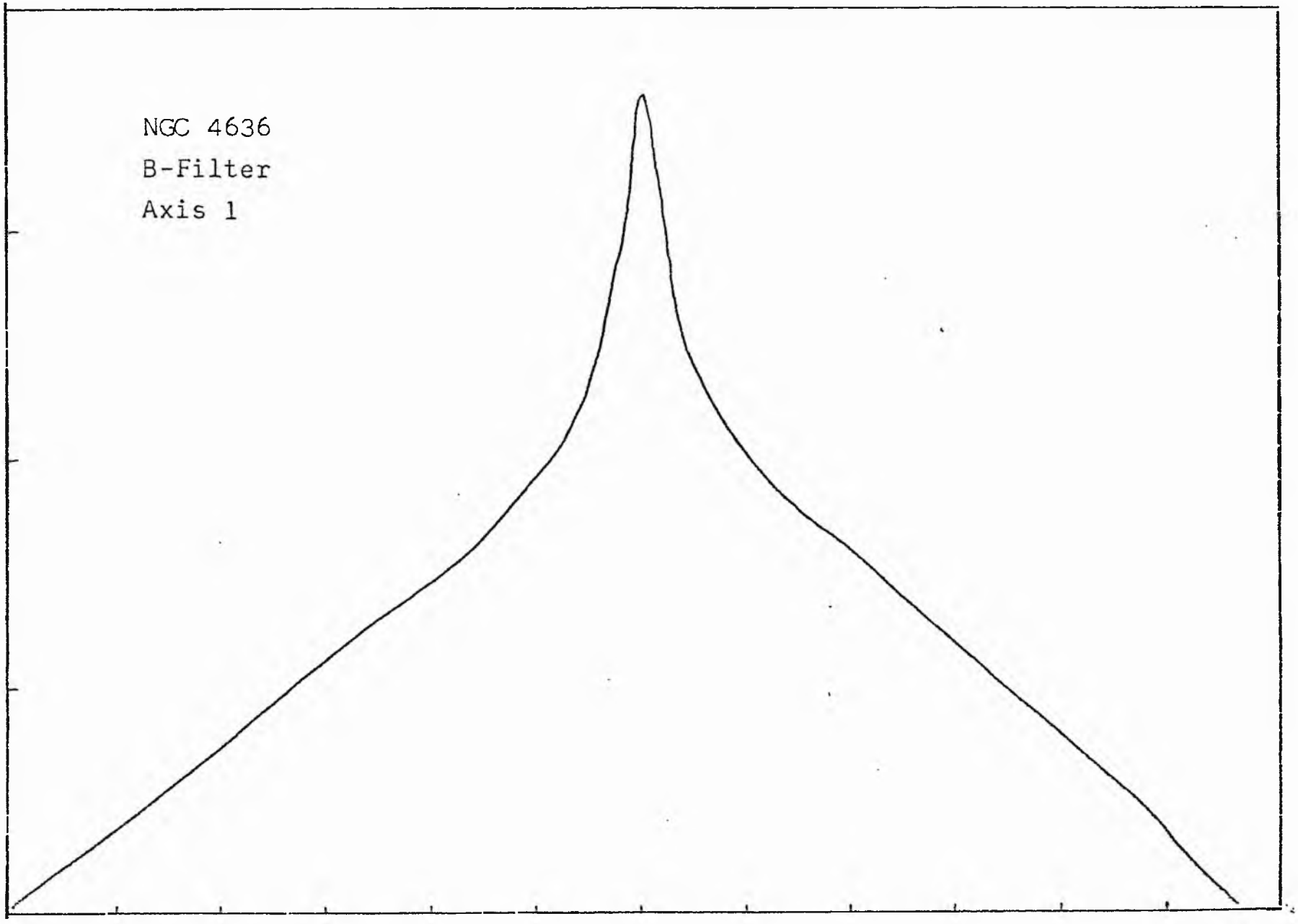
NGC 4636
B-Filter
Axis 1

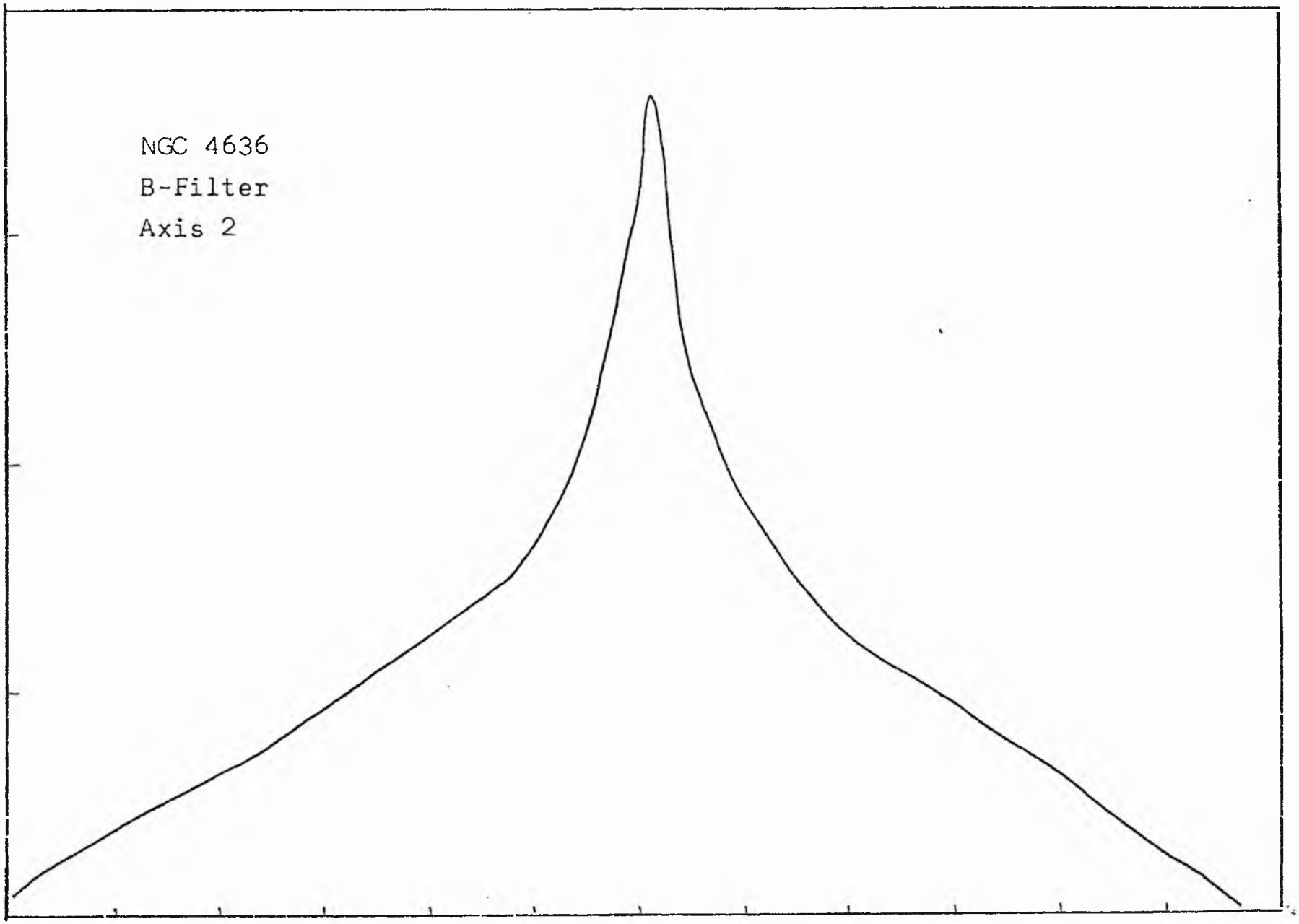
NGC 4636
B-Filter
Axis 2

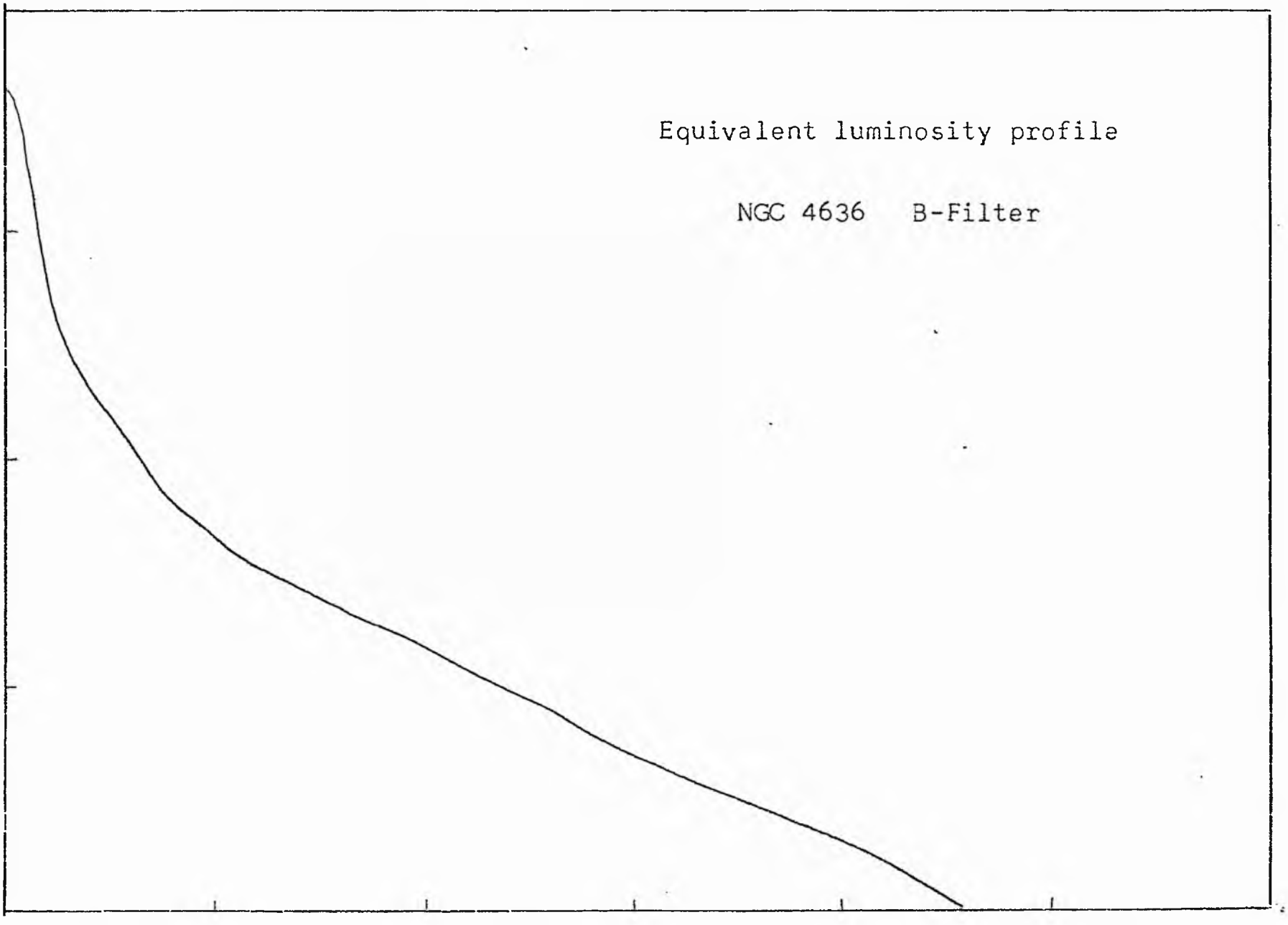
Equivalent luminosity profile
NGC 4636 B-Filter

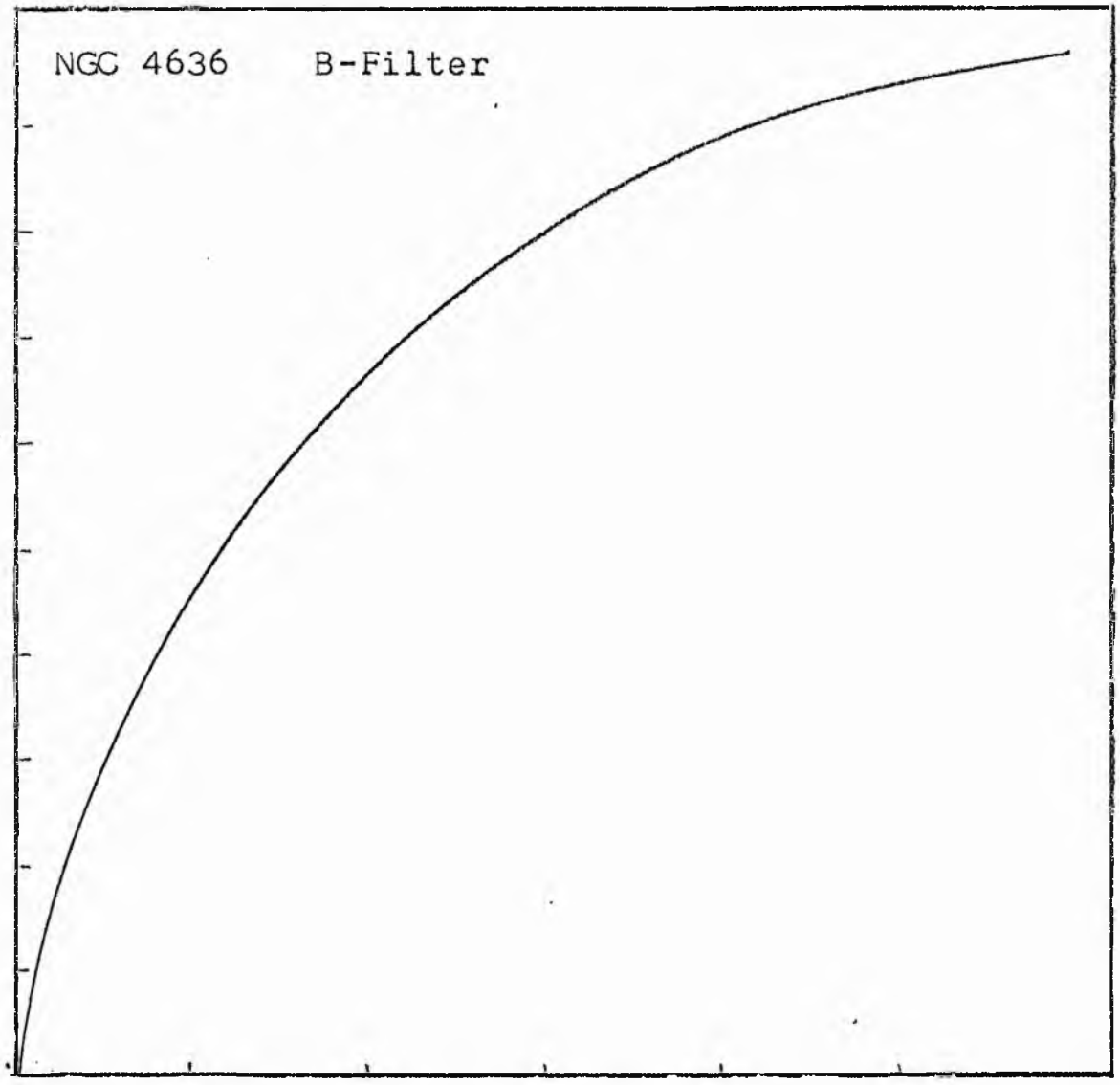

Relative integrated luminosity k(r) versus equivalent radius r*.

MEAN LUMINOSITY DISTRIBUTION IN NGC 6636
B COLOUR

LOG I	I	$\bar{I}$	R	AREA	ΔA	P	ΣP	KIRJ	ρ	LOG J	μ
1.57	37.154		0.0	0.0			0.0	0.0	0.0	1.829	18.24
		34.388			69.40	2386.4597					
1.50	31.623		4.70	69.40			2386.46	0.05	0.08	1.759	18.42
		28.371			63.33	1796.8506					
1.40	25.119		6.50	132.73			4183.31	0.09	0.11	1.659	18.67
		22.536			34.68	781.6079					
1.30	19.953		7.30	167.42			4964.91	0.11	0.13	1.559	18.92
		17.901			49.01	877.2942					
1.20	15.849		8.30	216.42			5842.21	0.13	0.14	1.459	19.17
		14.219			67.10	954.1582					
1.10	12.589		9.50	283.53			6796.36	0.15	0.16	1.359	19.42
		11.295			49.76	562.0513					
1.00	10.000		10.30	333.29			7358.41	0.16	0.18	1.259	19.67
		8.972			134.30	1204.9128					
0.90	7.943		12.20	467.59			8563.32	0.19	0.21	1.159	19.92
		7.126			202.07	1440.0134					
0.80	6.310		14.60	669.66			10003.34	0.22	0.25	1.059	20.17
		5.661			144.67	818.9265					
0.70	5.012		16.10	814.33			10822.26	0.24	0.28	0.959	20.42
		4.496			125.92	566.1724					
0.60	3.981		17.30	940.25			11388.43	0.25	0.30	0.859	20.67
		3.572			111.84	399.4558					
0.50	3.162		18.30	1052.09			11787.89	0.26	0.32	0.759	20.92
		2.837			406.88	1154.3345					
0.40	2.512		21.55	1458.96			12942.22	0.28	0.37	0.659	21.17
		2.254			742.23	1672.6599					
0.30	1.995		26.47	2201.19			14614.87	0.32	0.46	0.559	21.42
		1.790			898.27	1607.9612					
0.20	1.585		31.41	3099.46			16222.84	0.35	0.55	0.459	21.67
		1.422			1051.60	1495.2742					
0.10	1.259		36.35	4151.05			17718.11	0.39	0.63	0.359	21.92
		1.129			1259.55	1422.6113					
-0.00	1.000		41.50	5410.61			19140.72	0.42	0.72	0.259	22.17
		0.897			1588.36	1425.0146					
-0.10	0.794		47.20	6998.96			20565.73	0.45	0.82	0.159	22.42
		0.713			2094.18	1492.3977					
-0.20	0.631		53.80	9093.14			22058.12	0.48	0.93	0.059	22.67
		0.566			2367.89	1340.3909					
-0.30	0.501		60.40	11461.03			23398.52	0.51	1.05	-0.041	22.92
		0.450			3683.09	1656.0872					
-0.40	0.398		69.43	15144.12			25054.60	0.55	1.20	-0.141	23.17
		0.357			5113.14	1826.2417					
-0.50	0.316		80.30	20257.26			26880.84	0.59	1.39	-0.241	23.42
		0.284			8334.87	2364.6653					
-0.60	0.251		95.40	28592.12			29245.50	0.64	1.66	-0.341	23.67
		0.225			12379.39	2789.7812					
-0.70	0.200		114.20	40971.51			32035.29	0.70	1.98	-0.441	23.92
		0.179			12694.71	2272.4473					
-0.80	0.158		130.70	53666.22			34307.73	0.75	2.27	-0.541	24.17
		0.142			11695.16	1662.9424					
-0.90	0.126		144.24	65361.38			35970.67	0.79	2.50	-0.641	24.42
		0.113			11357.25	1282.7578					
-1.00	0.100		156.27	76718.62			37253.43	0.82	2.71	-0.741	24.67
		0.090			10300.12	924.0911					
-1.10	0.079		166.43	87018.75			38177.52	0.84	2.89	-0.841	24.92
		0.071			14395.94	1025.9185					
-1.20	0.063		179.67	101414.69			39203.44	0.86	3.12	-0.941	25.17
		0.057			18007.56	1019.3611					
-1.30	0.050		194.97	119422.25			40222.80	0.88	3.38	-1.041	25.42
		0.045			21081.62	947.9333					
-1.40	0.040		211.48	140503.87			41170.73	0.90	3.67	-1.141	25.67
		0.036			24489.06	874.6746					
-1.50	0.032		229.17	164992.94			42045.40	0.92	3.98	-1.241	25.92
		0.028			27573.62	782.2920					
-1.60	0.025		247.58	192566.56			42827.69	0.94	4.30	-1.341	26.17
		0.023			23216.25	523.2000					
-1.70	0.020		262.08	215782.81			43350.89	0.95	4.55	-1.441	26.42
		0.018			17893.94	320.3186					
-1.80	0.016		272.73	233676.75			43671.20	0.96	4.73	-1.541	26.67
		0.014			19212.00	273.1802					
-1.90	0.013		283.72	252888.75			43944.38	0.96	4.92	-1.641	26.92
		0.011			18251.12	206.1422					
-2.00	0.010		293.78	271139.87			44150.52	0.97	5.10	-1.741	27.17
$-\infty$							45700.00	(1)			∞

PHOTOMETRIC PARAMETERS OF NGC 4636

B-FILTER

Total luminosity	L_T	= 12.70
Total apparent magnitude	m_T	= 10.52
Apparent central surface brightness	μ_o	= 18.24
Major axis at threshold	$2a_m$	= 10.20
Minor axis at threshold	$2b_m$	= 9.97
Major axis at μ=25.0 mag sec^{-2}	2a(25)	= 6.17
Luminosity within μ=25.0 mag sec^{-2}	k(25)	= 0.85
Gradient of exponential component	G(a)	= -0.42
Equivalent gradient of exponential comp.	G(r*)	= -0.41
Equivalent gradient of reduced exp. comp.	G(ρ)	= -0.41

Parameters at k = ¼ :

Semi-major axis	a_1	= 0.42
Axis ratio	b/a	= 0.44
Equivalent radius	r_1*	= 0.29
Surface brightness	μ_1	= 20.67

Parameters at k = ½(effective) :

Semi-major axis	a_e	= 1.17
Axis ratio	b/a	= 0.60
Equivalent radius	r_e*	= 0.96
Surface brightness	μ_e	= 22.75
Mean surface brightness	μ_e'	= 12.43

Parameters at k = ¾ :

Semi-major axis	a_3	= 2.35
Axis ratio	b/a	= 0.73
Equivalent radius	r_3*	= 2.17
Surface brightness	μ_3	= 24.17
Concentration indices	C_{21}	= 3.31
	C_{32}	= 2.26

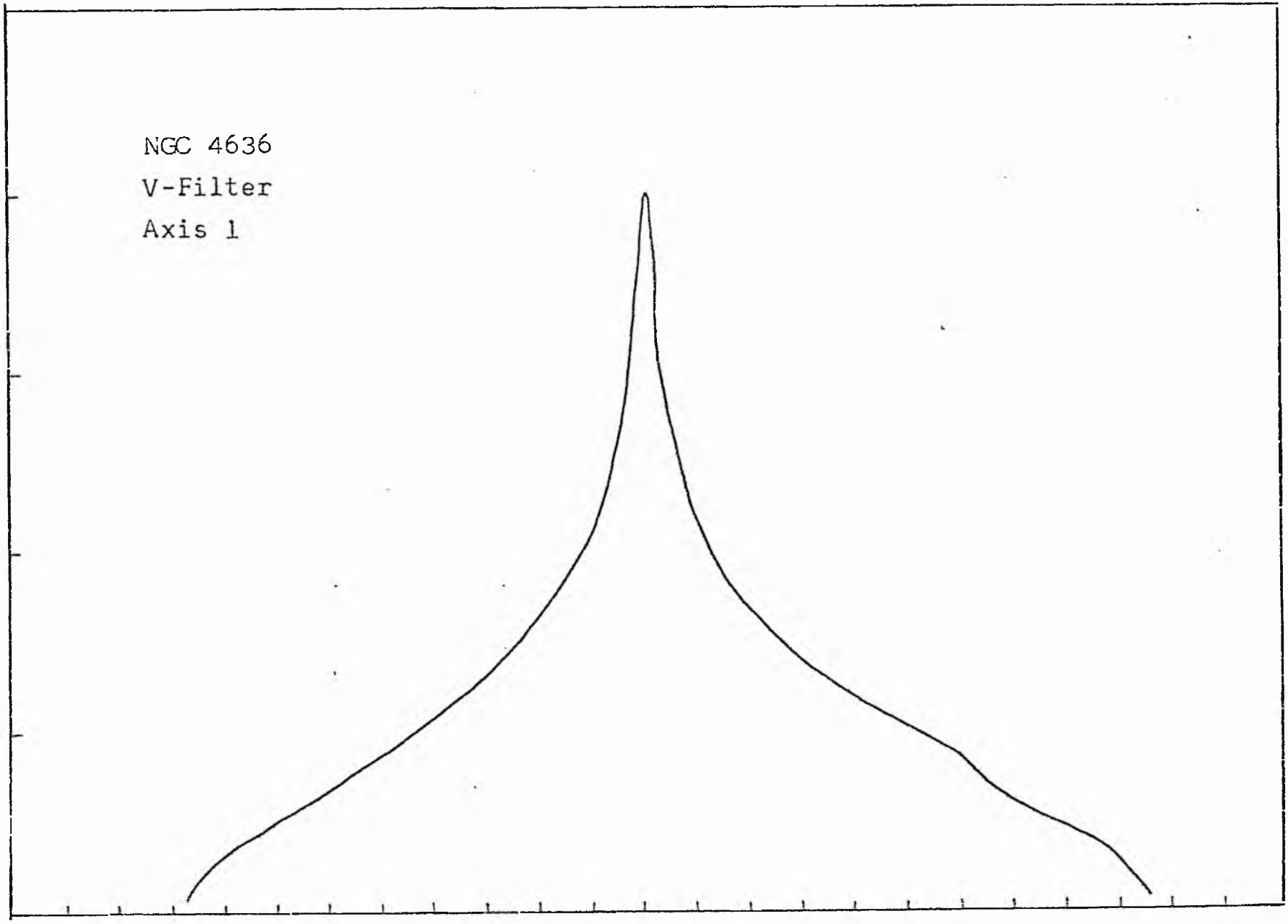
NGC 4636
V-Filter
Axis 1

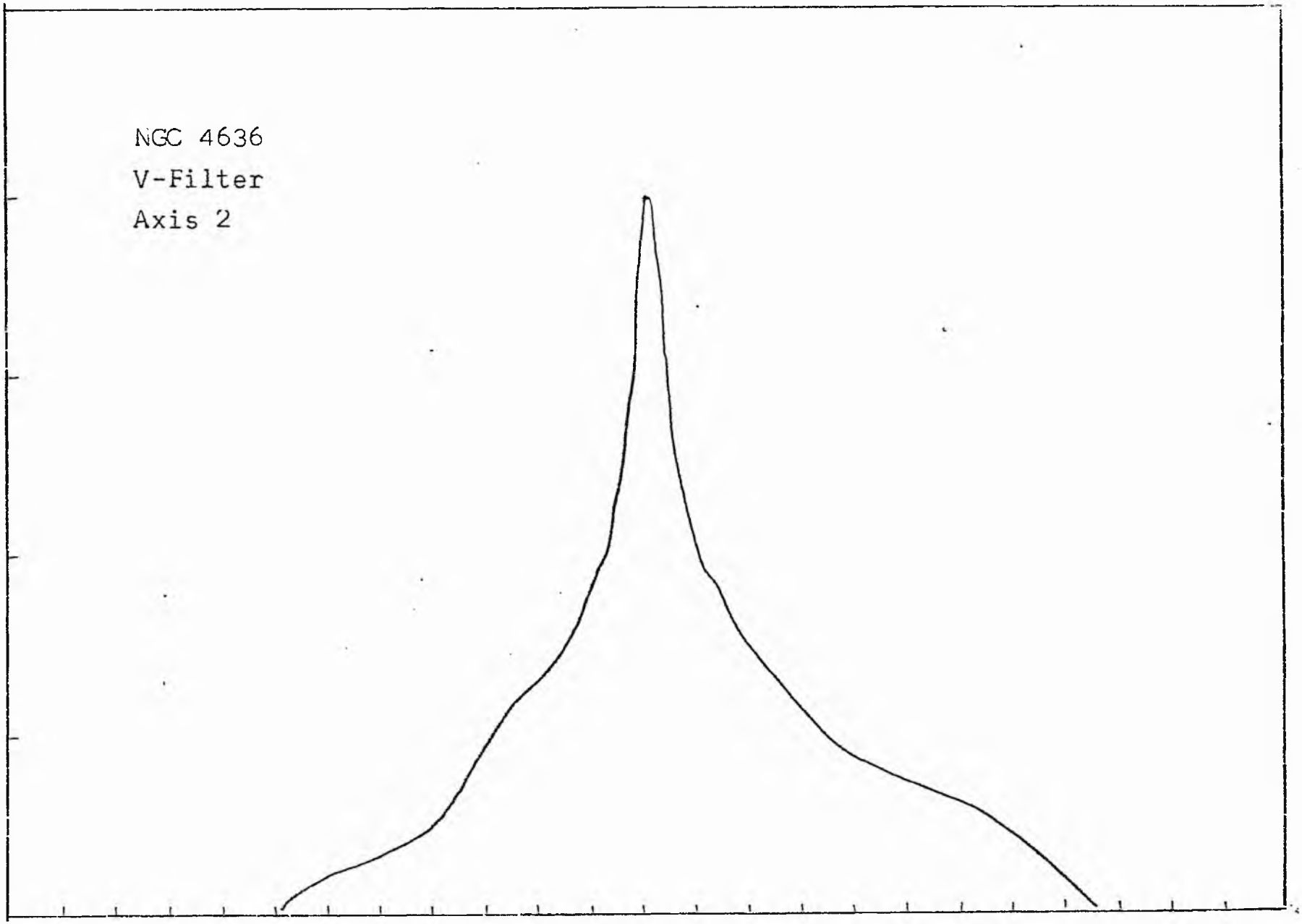
NGC 4636
V-Filter
Axis 2

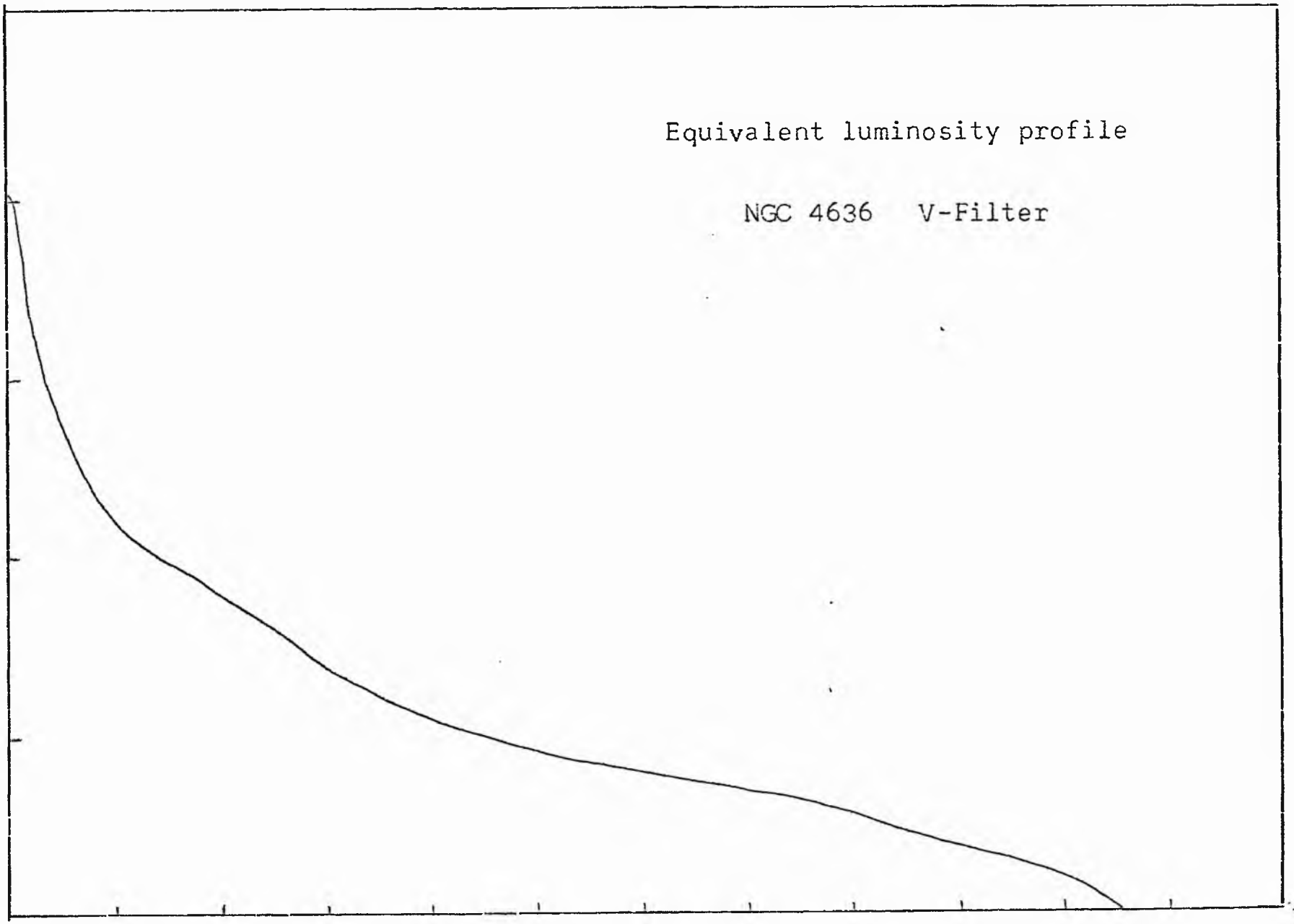
Equivalent luminosity profile
NGC 4636 V-Filter

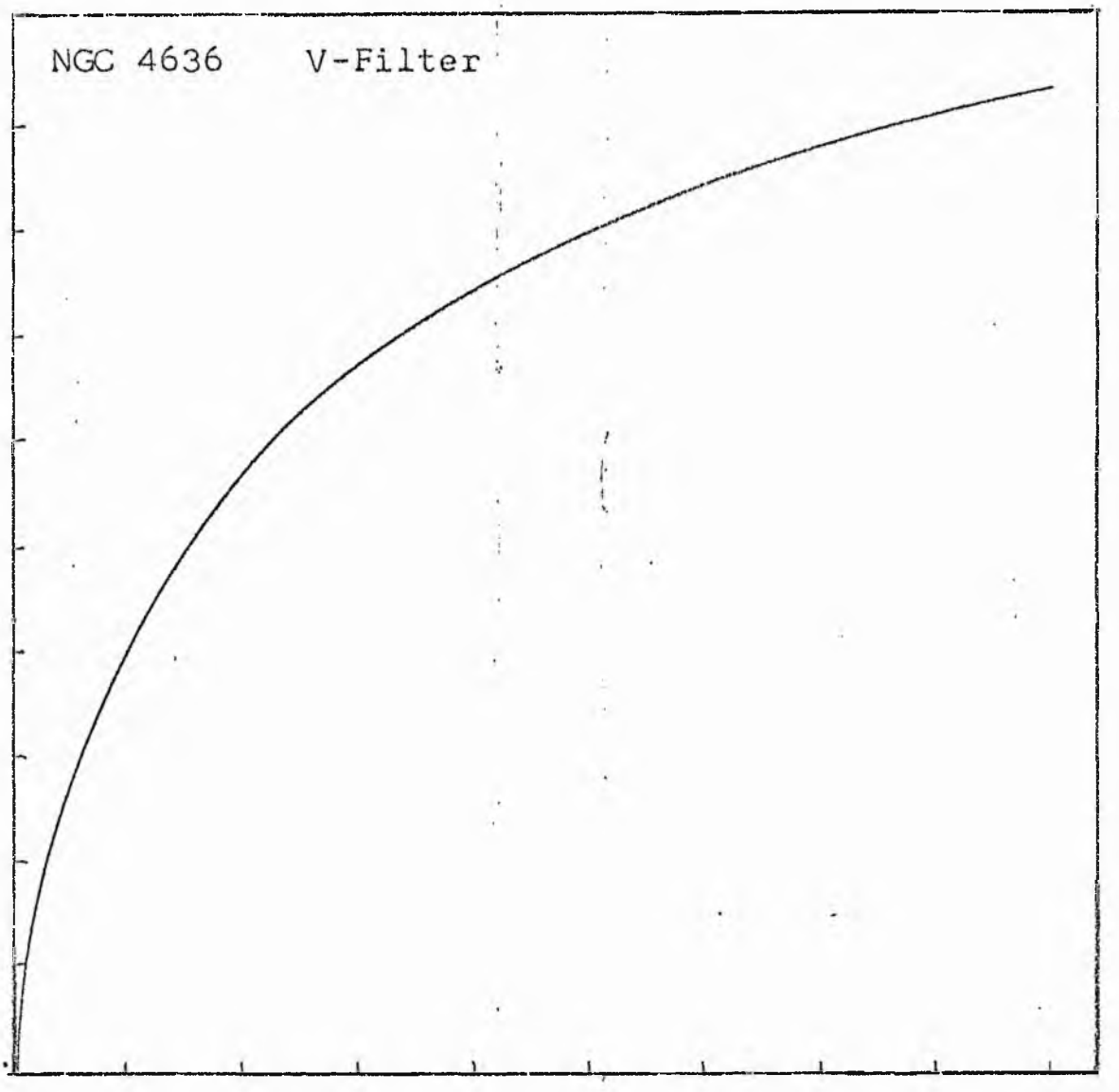

Relative integrated luminosity k(r) versus equivalent radius r*.

MEAN LUMINOSITY DISTRIBUTION IN NGC 4636
V COLOUR

LOG I	I	$\bar{I}$	R	AREA	ΔA	P	ΣP	K(R)	ρ	LOG J	μ
1.96	91.201		0.0	0.0			0.0	0.0	0.0	2.120	16.91
		85.317			6.16	525.3394					
1.90	79.433		1.40	6.16			525.34	0.01	0.02	2.060	17.06
		71.264			39.21	2794.0588					
1.80	63.096		3.80	45.36			3319.40	0.04	0.05	1.960	17.31
		56.607			42.88	2427.4648					
1.70	50.119		5.30	88.25			5746.86	0.07	0.07	1.860	17.56
		44.965			24.85	1117.3718					
1.60	39.811		6.00	113.10			6864.23	0.08	0.08	1.760	17.81
		35.717			68.36	2441.6226					
1.50	31.623		7.60	181.46			9305.85	0.11	0.10	1.660	18.06
		28.371			34.97	992.0071					
1.40	25.119		8.30	216.42			10297.86	0.12	0.11	1.560	18.31
		22.536			67.10	1512.2349					
1.30	19.952		9.50	283.53			11810.09	0.14	0.12	1.460	18.56
		17.901			62.83	1124.7341					
1.20	15.849		10.50	346.36			12934.82	0.15	0.14	1.360	18.81
		14.219			160.35	2279.9658					
1.10	12.589		12.70	506.71			15214.79	0.18	0.17	1.260	19.06
		11.295			200.15	2260.6118					
1.00	10.000		15.00	706.86			17475.39	0.20	0.20	1.160	19.31
		8.972			117.62	1055.2363					
0.90	7.943		16.20	824.48			18530.63	0.21	0.21	1.060	19.56
		7.126			137.63	980.8325					
0.80	6.310		17.50	962.11			19511.46	0.22	0.23	0.960	19.81
		5.661			278.24	1575.0276					
0.70	5.012		19.87	1240.35			21086.49	0.24	0.26	0.860	20.06
		4.496			468.11	2104.8452					
0.60	3.981		23.32	1708.47			23191.33	0.27	0.31	0.760	20.31
		3.572			539.54	1927.0420					
0.50	3.162		26.75	2248.01			25118.37	0.29	0.35	0.660	20.56
		2.837			573.77	1627.8274					
0.40	2.512		29.97	2821.78			26746.20	0.31	0.39	0.560	20.81
		2.254			758.81	1710.0251					
0.30	1.995		33.76	3580.59			28456.22	0.33	0.44	0.460	21.06
		1.790			409.89	733.7314					
0.20	1.585		35.64	3990.48			29189.95	0.34	0.47	0.360	21.31
		1.422			1839.95	2616.2263					
0.10	1.259		43.08	5830.43			31806.17	0.37	0.57	0.260	21.56
		1.129			4134.51	4669.7422					
-0.00	1.000		56.32	9964.95			36475.91	0.42	0.74	0.160	21.81
		0.897			4896.95	4393.3320					
-0.10	0.794		68.78	14861.89			40869.25	0.47	0.90	0.060	22.06
		0.713			5689.05	4054.2358					
-0.20	0.631		80.88	20550.95			44923.48	0.52	1.06	-0.040	22.31
		0.566			6399.08	3622.3167					
-0.30	0.501		92.62	26950.03			48545.80	0.56	1.22	-0.140	22.56
		0.450			4907.25	2206.5178					
-0.40	0.398		100.70	31857.29			50752.31	0.59	1.32	-0.240	22.81
		0.357			4542.36	1622.3738					
-0.50	0.316		107.64	36399.65			52374.68	0.60	1.41	-0.340	23.06
		0.284			7886.79	2237.5315					
-0.60	0.251		118.73	44286.43			54612.21	0.63	1.56	-0.440	23.31
		0.225			9232.06	2080.5010					
-0.70	0.200		130.52	53518.50			56692.71	0.65	1.72	-0.540	23.56
		0.179			6435.54	1510.0186					
-0.80	0.158		140.43	61954.04			58202.73	0.67	1.85	-0.640	23.81
		0.142			17728.46	2520.8105					
-0.90	0.126		159.26	79682.50			60723.54	0.70	2.09	-0.740	24.06
		0.113			24745.81	2794.9324					
-1.00	0.100		182.32	104428.31			63518.47	0.73	2.40	-0.840	24.31
		0.090			23064.06	2069.2170					
-1.10	0.079		201.45	127492.37			65587.62	0.76	2.65	-0.940	24.56
		0.071			44455.12	3168.0537					
-1.20	0.063		233.95	171947.50			68755.62	0.79	3.07	-1.040	24.81
		0.057			73649.81	4169.1055					
-1.30	0.050		279.60	245597.31			72924.69	0.84	3.67	-1.140	25.06
		0.045			49665.25	2233.1846					
-1.40	0.040		306.57	295262.56			75157.81	0.87	4.03	-1.240	25.31
		0.036			32577.37	1163.5596					
-1.50	0.032		323.04	327839.94			76321.31	0.88	4.25	-1.340	25.56
		0.028			68079.31	1931.4712					
-1.60	0.025		355.00	395919.25			78252.75	0.90	4.67	-1.440	25.81
		0.023			73208.69	1649.8191					
-1.70	0.020		386.43	469127.94			79902.56	0.92	5.08	-1.540	26.06
		0.018			70264.87	1257.8030					
-1.80	0.016		414.36	539392.81			81160.31	0.94	5.45	-1.640	26.31
		0.014			17505.00	248.9070					
-1.90	0.013		421.03	556897.81			81409.19	0.94	5.53	-1.740	26.56
		0.011			27662.50	312.4402					
-2.00	0.010		431.36	584560.31			81721.62	0.94	5.67	-1.840	26.81
- ∞							86721.00	(1)			∞

PHOTOMETRIC PARAMETERS OF NGC 4636

V-FILTER

Total luminosity ..... L_T = 24.09

Total apparent magnitude ..... m_T = 9.46

Apparent central surface brightness ..... μ_o = 16.91

Major axis at threshold ..... $2a_m$ = 15.37

Minor axis at threshold ..... $2b_m$ = 13.41

Major axis at μ=25.0 mag sec^{-2} ..... 2a(25) = 10.27

Luminosity within μ=25.0 mag sec^{-2} ..... k(25) = 0.83

Gradient of exponential component ..... G(a) = -0.23

Equivalent gradient of exponential comp..... G(r*) = -0.26

Equivalent gradient of reduced exp. comp..... G(ρ) = -0.74

Parameters at k = ¼ :

- Semi-major axis ..... a_1 = 0.48
- Axis ratio ..... b/a = 0.86
- Equivalent radius ..... r_1* = 0.35
- Surface brightness ..... μ_1 = 20.14

Parameters at k = ½(effective) :

- Semi-major axis ..... a_e = 1.38
- Axis ratio ..... b/a = 0.72
- Equivalent radius ..... r_e* = 1.27
- Surface brightness ..... μ_e = 22.21
- Mean surface brightness ..... μ_e' = 11.97

Parameters at k = ¾ :

- Semi-major axis ..... a_3 = 4.17
- Axis ratio ..... b/a = 0.70
- Equivalent radius ..... r_3* = 3.27
- Surface brightness ..... μ_3 = 24.48

Concentration indices ..... C_{21} = 3.66, C_{32} = 2.58

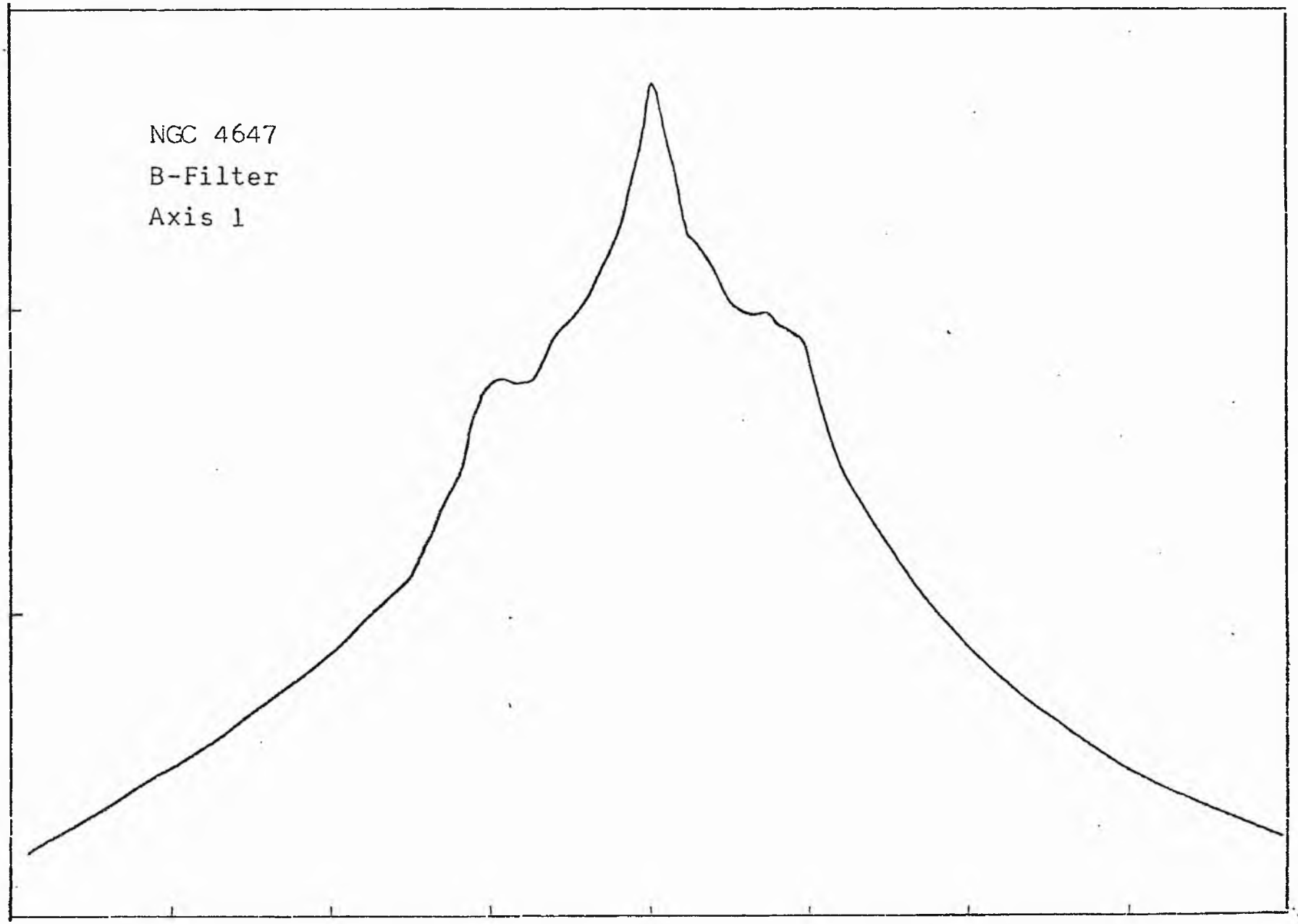
NGC 4647
B-Filter
Axis 1

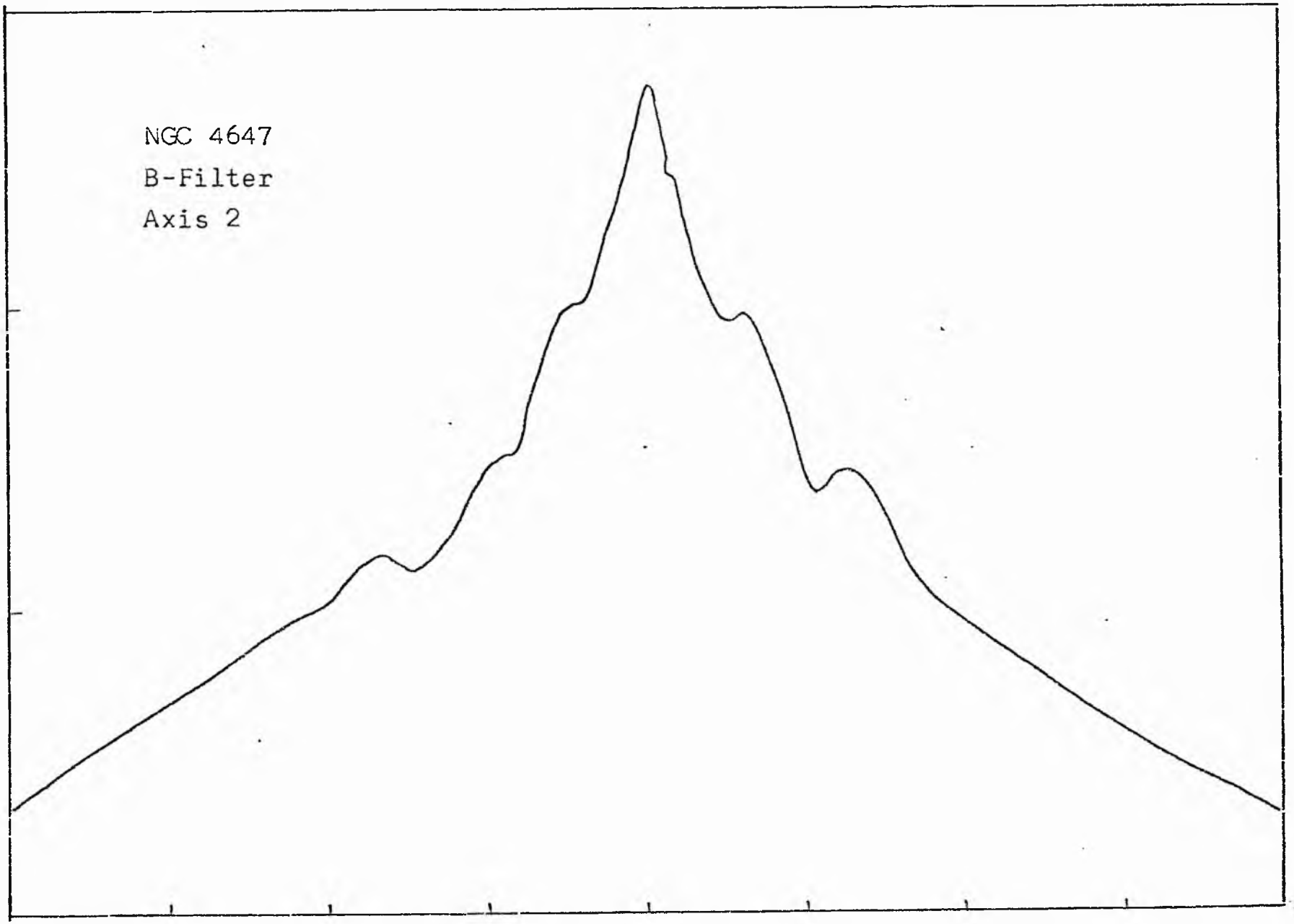
NGC 4647
B-Filter
Axis 2

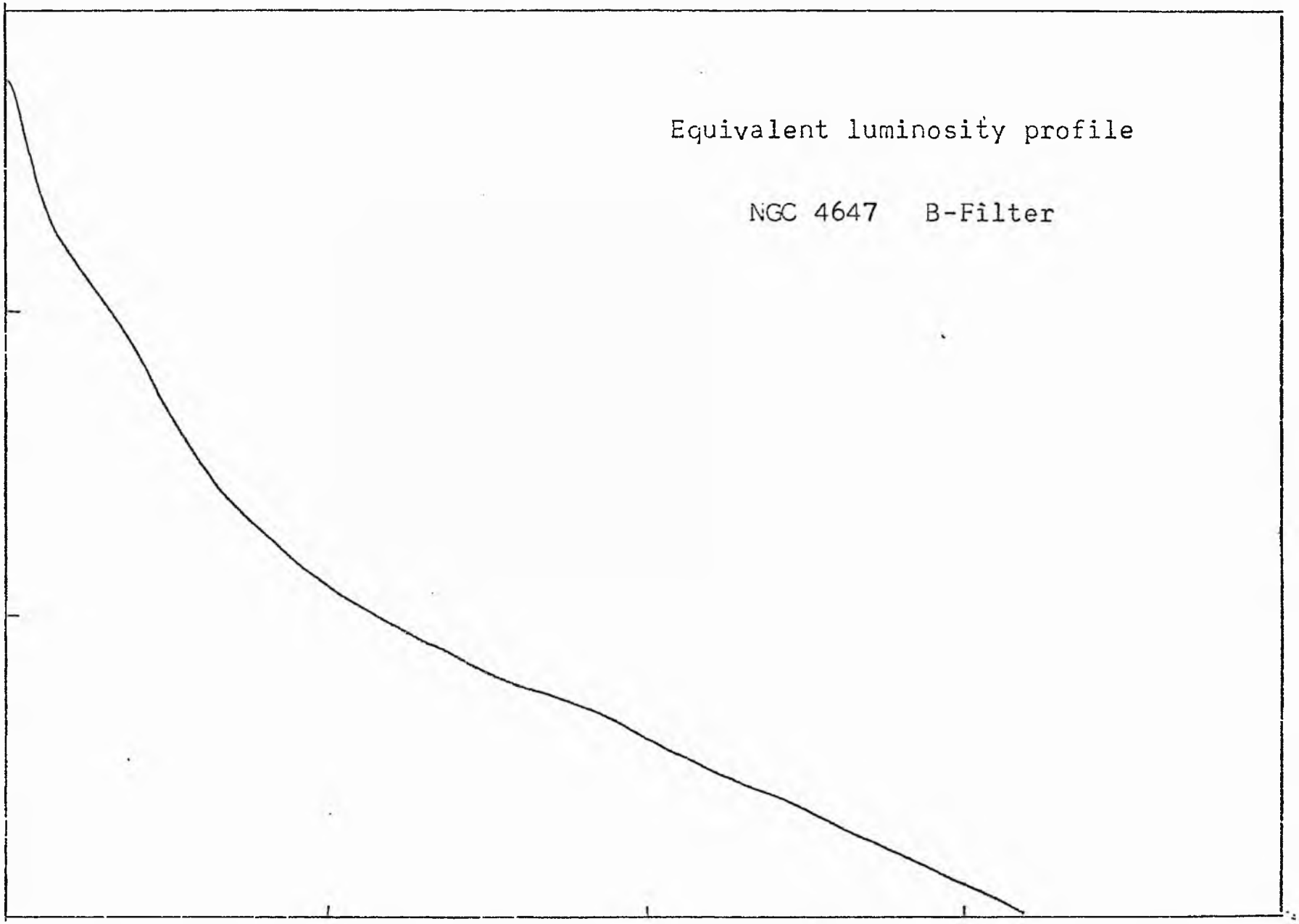
Equivalent luminosity profile
NGC 4647 B-Filter

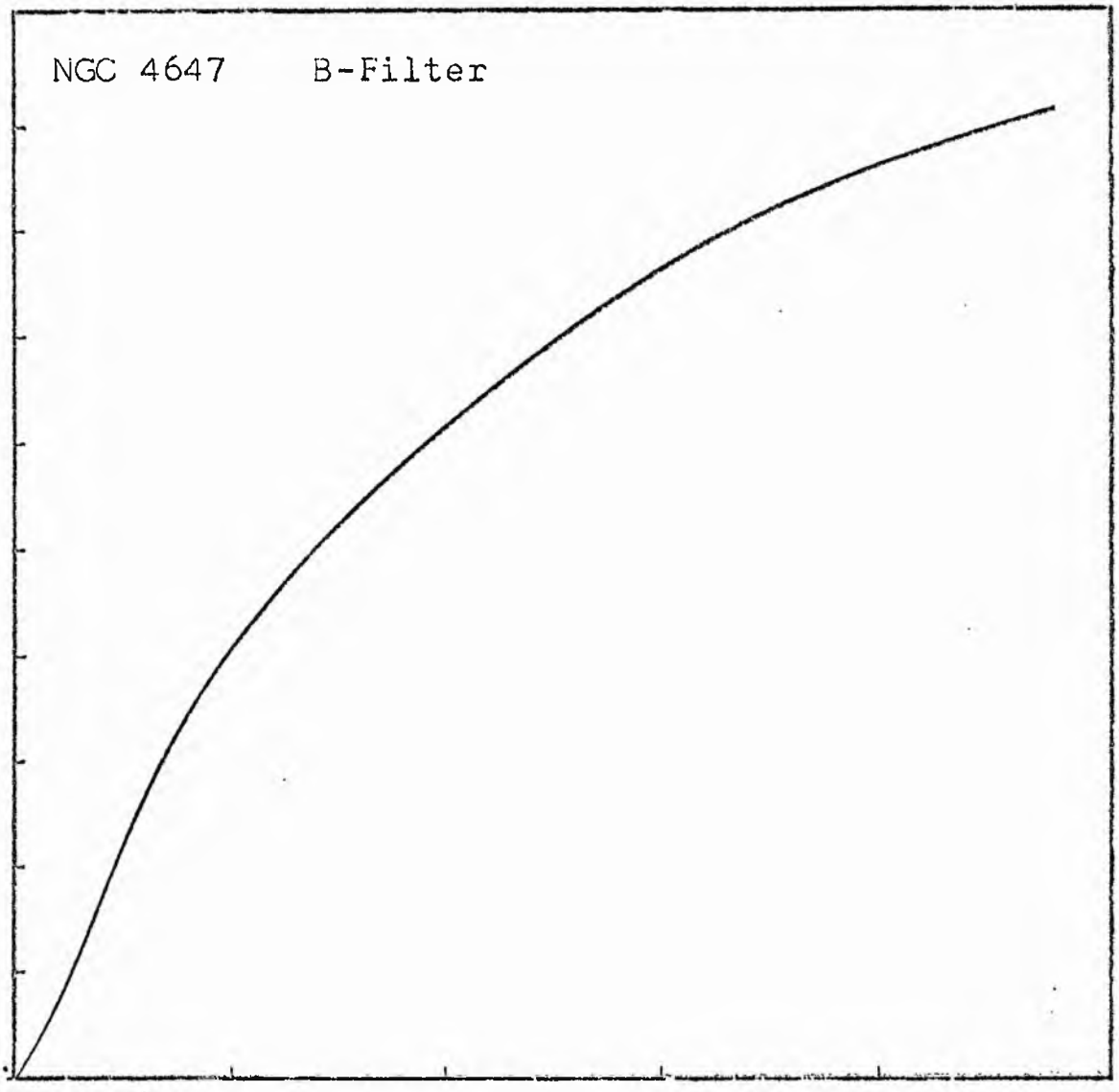

Relative integrated luminosity k(r) versus equivalent radius r*.

MEAN LUMINOSITY DISTRIBUTION IN NGC 4647
B COLOUR

LOG I	I	$\bar{I}$	R	AREA	ΔA	P	ΣP	K(R)	ρ	LOG J	μ
0.74	5.495		0.0	0.0			0.0	0.0	0.0	1.597	20.29
		5.254			11.82	62.1174					
0.70	5.012		1.94	11.82			62.12	0.00	0.03	1.557	20.39
		4.496			55.23	248.3475					
0.60	3.981		4.62	67.06			310.46	0.02	0.07	1.457	20.64
		3.572			19.21	68.5947					
0.50	3.162		5.24	86.26			379.06	0.03	0.08	1.357	20.89
		2.837			106.35	301.7148					
0.40	2.512		7.83	192.61			680.77	0.05	0.11	1.257	21.14
		2.254			134.24	302.5276					
0.30	1.995		10.20	326.85			983.30	0.07	0.15	1.157	21.39
		1.790			205.71	368.2419					
0.20	1.585		13.02	532.56			1351.54	0.09	0.19	1.057	21.64
		1.422			506.91	720.7834					
0.10	1.259		18.19	1039.48			2072.33	0.14	0.26	0.957	21.89
		1.129			889.61	1004.7852					
0.00	1.000		24.78	1929.09			3077.11	0.21	0.36	0.857	22.14
		0.897			801.18	718.7861					
-0.10	0.794		29.48	2730.26			3795.90	0.26	0.43	0.757	22.39
		0.713			541.24	385.7107					
-0.20	0.631		32.27	3271.50			4181.61	0.29	0.47	0.657	22.64
		0.566			763.89	432.4158					
-0.30	0.501		35.84	4035.39			4614.02	0.32	0.52	0.557	22.89
		0.450			893.61	401.8103					
-0.40	0.398		39.61	4929.00			5015.83	0.35	0.57	0.457	23.14
		0.357			1015.67	362.7654					
-0.50	0.316		43.50	5944.68			5378.59	0.37	0.63	0.357	23.39
		0.284			1233.36	349.9133					
-0.60	0.251		47.80	7178.03			5728.50	0.40	0.69	0.257	23.64
		0.225			2744.50	618.4934					
-0.70	0.200		56.20	9922.53			6347.00	0.44	0.81	0.157	23.89
		0.179			2586.07	462.9265					
-0.80	0.158		63.10	12508.59			6809.92	0.47	0.91	0.057	24.14
		0.142			4694.77	667.5537					
-0.90	0.126		74.00	17203.36			7477.47	0.52	1.07	-0.043	24.39
		0.113			7069.86	798.5159					
-1.00	0.100		87.90	24273.22			8275.99	0.58	1.27	-0.143	24.64
		0.090			6083.63	545.8027					
-1.10	0.079		98.30	30356.86			8821.79	0.61	1.42	-0.243	24.89
		0.071			9333.27	665.1311					
-1.20	0.063		112.40	39690.12			9486.92	0.66	1.63	-0.343	25.14
		0.057			15464.47	875.4055					
-1.30	0.050		132.50	55154.59			10362.32	0.72	1.92	-0.443	25.39
		0.045			15154.72	681.4324					
-1.40	0.040		149.60	70309.31			11043.75	0.77	2.16	-0.543	25.64
		0.036			9413.25	336.2134					
-1.50	0.032		159.30	79722.56			11379.96	0.79	2.30	-0.643	25.89
		0.028			18034.25	511.6511					
-1.60	0.025		176.40	97756.81			11891.61	0.83	2.55	-0.743	26.14
		0.023			13634.25	307.2612					
-1.70	0.020		188.30	111391.06			12198.87	0.85	2.72	-0.843	26.39
		0.018			16925.37	302.9810					
-1.80	0.016		202.10	128316.44			12501.85	0.87	2.92	-0.943	26.64
		0.014			24567.12	349.3269					
-1.90	0.013		220.60	152883.56			12851.17	0.89	3.19	-1.043	26.89
		0.011			23576.56	266.2922					
-2.00	0.010		237.00	176460.12			13117.46	0.91	3.43	-1.143	27.14
$-\infty$							14367.00	(1)			∞

PHOTOMETRIC PARAMETERS OF NGC 4647

B-FILTER

Total luminosity	L_T	= 3.99
Total apparent magnitude	m_T	= 11.75
Apparent central surface brightness	μ_o	= 20.29
Major axis at threshold	$2a_m$	= 7.03
Minor axis at threshold	$2b_m$	= 7.13
Major axis at μ=25.0 mag sec^{-2}	2a(25)	= 3.37
Luminosity within μ=25.0 mag sec^{-2}	k(25)	= 0.64
Gradient of exponential component	G(a)	= -0.74
Equivalent gradient of exponential comp.	G(r*)	= -0.30
Equivalent gradient of reduced exp. comp.	G(ρ)	= -0.46

Parameters at k = ¼ :

Semi-major axis	a_1	= 0.57
Axis ratio	b/a	= 0.82
Equivalent radius	r_1*	= 0.47
Surface brightness	μ_1	= 22.34

Parameters at k = ½(effective) :

Semi-major axis	a_e	= 1.25
Axis ratio	b/a	= 1.05
Equivalent radius	r_e*	= 1.15
Surface brightness	μ_e	= 24.29
Mean surface brightness	μ_e'	= 14.04

Parameters at k = ¾ :

Semi-major axis	a_3	= 2.15
Axis ratio	b/a	= 0.98
Equivalent radius	r_3*	= 2.38
Surface brightness	μ_3	= 25.54

Concentration indices	C_{21}	= 2.46
	C_{32}	= 2.06

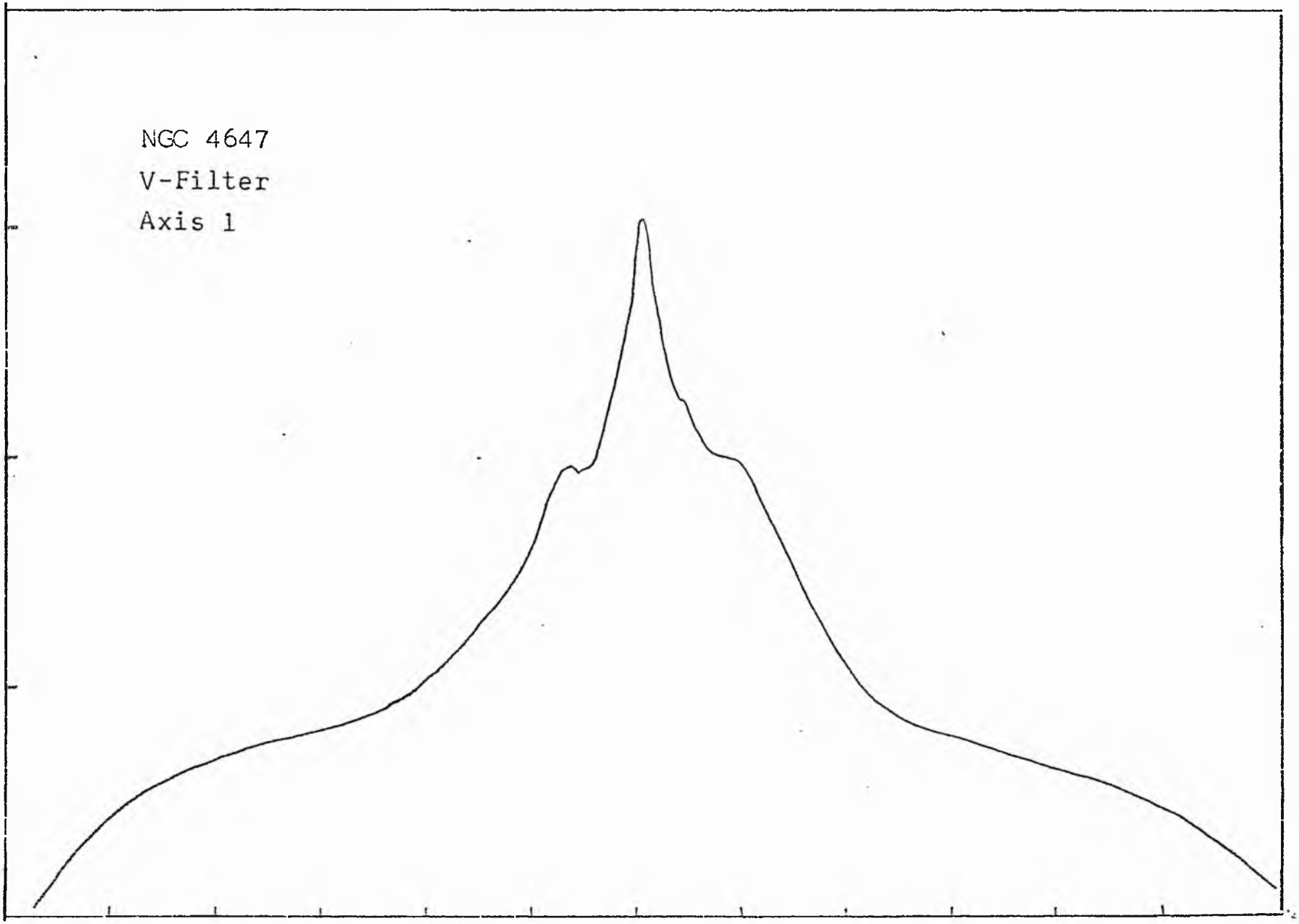
NGC 4647
V-Filter
Axis 1

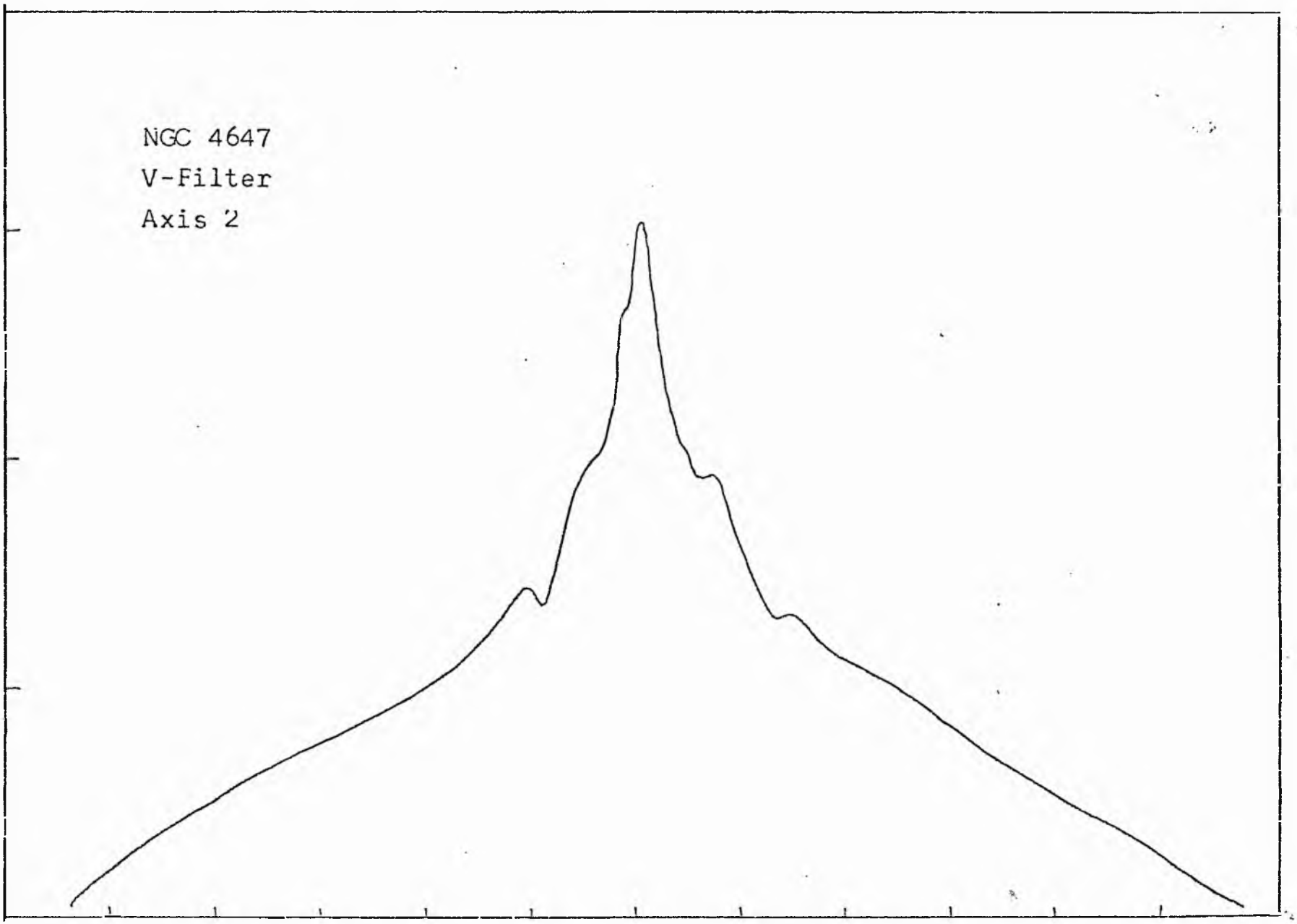
NGC 4647
V-Filter
Axis 2

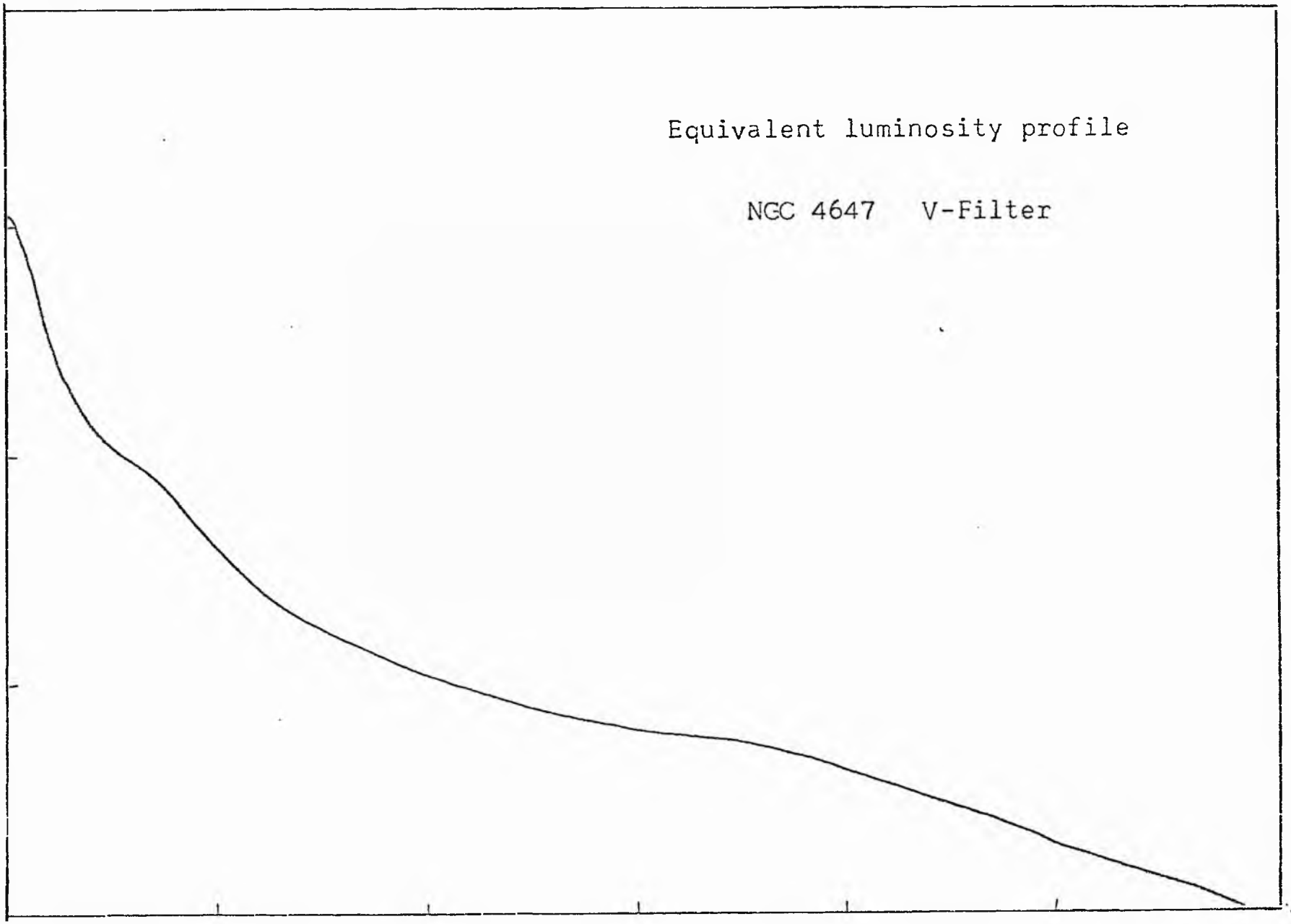
Equivalent luminosity profile
NGC 4647 V-Filter

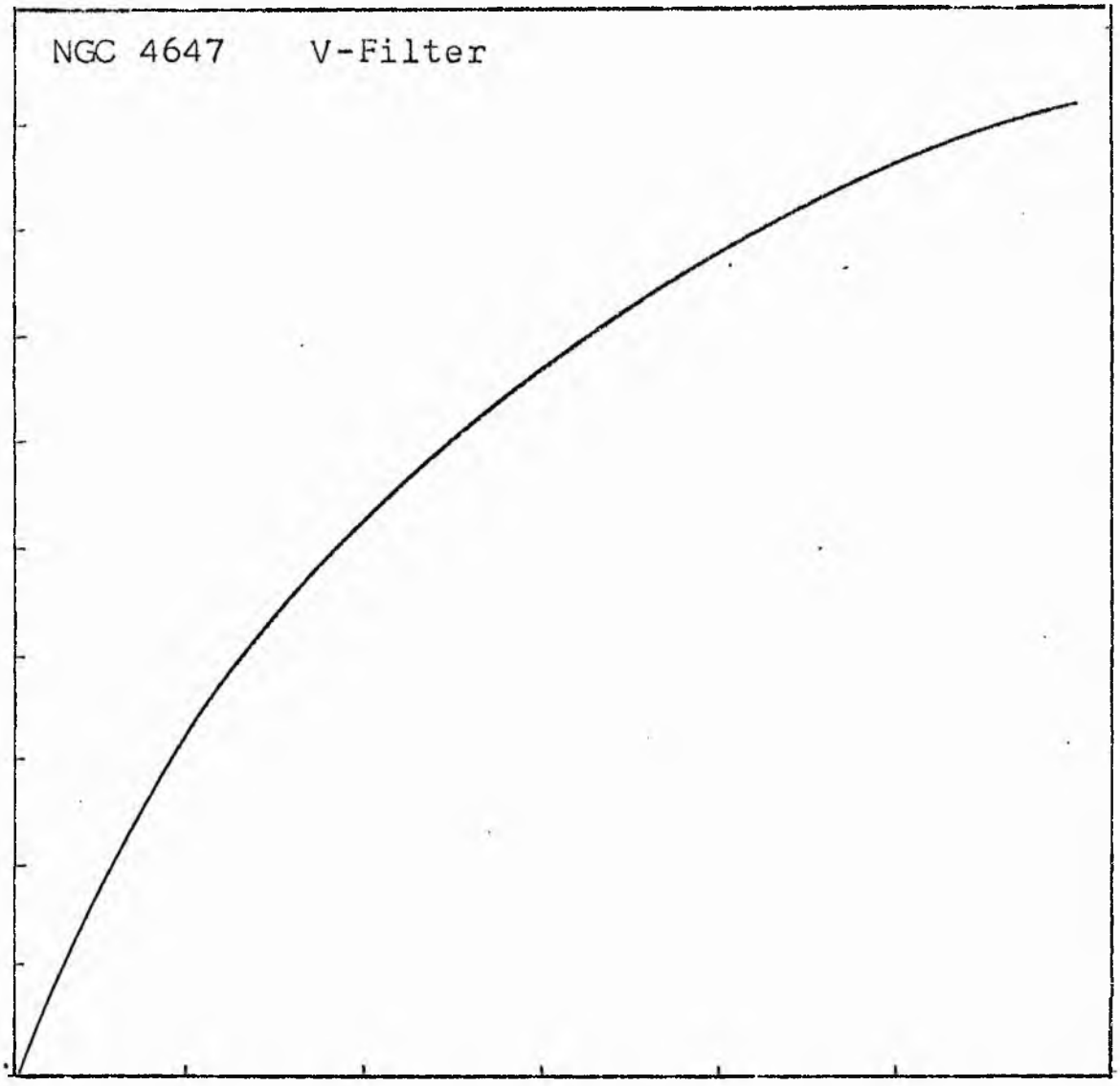

Relative integrated luminosity k(r) versus equivalent radius r*.

MEAN LUMINOSITY DISTRIBUTION IN NGC 4647
V COLOUR

LOG I	I	$\bar{I}$	R	AREA	Δ A	P	ΣP	K(R)	ρ	LOG J	μ
1.06	11.482		0.0	0.0			0.0	0.0	0.0	1.924	19.17
		10.741			18.55	199.2494					
1.00	10.000		2.43	18.55			199.25	0.01	0.03	1.864	19.32
		8.972			34.26	307.3621					
0.90	7.943		4.10	52.81			506.61	0.02	0.05	1.764	19.57
		7.126			22.62	161.1962					
0.80	6.310		4.90	75.43			667.81	0.03	0.05	1.664	19.82
		5.661			16.18	91.5858					
0.70	5.012		5.40	91.61			759.39	0.03	0.06	1.564	20.07
		4.496			124.82	561.2290					
0.60	3.981		8.30	216.42			1320.62	0.05	0.09	1.464	20.32
		3.572			67.10	239.6746					
0.50	3.162		9.50	283.53			1560.30	0.06	0.10	1.364	20.57
		2.837			69.46	197.0657					
0.40	2.512		10.60	352.99			1757.36	0.07	0.12	1.264	20.82
		2.254			190.26	428.7712					
0.30	1.995		13.15	543.25			2186.13	0.09	0.14	1.164	21.07
		1.790			382.92	685.4504					
0.20	1.585		17.17	926.17			2871.58	0.12	0.19	1.064	21.32
		1.422			682.69	970.7268					
0.10	1.259		22.63	1698.86			3842.31	0.16	0.25	0.964	21.57
		1.129			1167.91	1319.1082					
0.00	1.000		29.73	2776.77			5161.42	0.21	0.33	0.864	21.82
		0.897			962.51	863.5330					
-0.10	0.794		34.50	3739.28			6024.95	0.25	0.38	0.764	22.07
		0.713			1014.61	723.0518					
-0.20	0.631		38.90	4753.89			6748.00	0.28	0.43	0.664	22.32
		0.566			1122.66	635.5046					
-0.30	0.501		43.25	5876.54			7383.50	0.31	0.48	0.564	22.57
		0.450			1513.27	680.4363					
-0.40	0.398		48.50	7389.81			8063.94	0.34	0.53	0.464	22.82
		0.357			2217.46	792.0059					
-0.50	0.316		55.30	9607.27			8855.94	0.37	0.61	0.364	23.07
		0.284			1815.84	515.1694					
-0.60	0.251		60.30	11423.11			9371.11	0.39	0.66	0.264	23.32
		0.225			4503.00	1014.7856					
-0.70	0.200		71.20	15926.11			10385.89	0.43	0.78	0.164	23.57
		0.179			5560.16	995.3130					
-0.80	0.158		82.70	21486.26			11381.21	0.47	0.91	0.064	23.82
		0.142			7225.87	1027.4553					
-0.90	0.126		95.60	28712.13			12408.66	0.52	1.05	-0.036	24.07
		0.113			11544.98	1303.9656					
-1.00	0.100		113.20	40257.12			13712.62	0.57	1.25	-0.136	24.32
		0.090			15064.10	1351.5010					
-1.10	0.079		132.70	55321.22			15064.12	0.63	1.46	-0.236	24.57
		0.071			21525.09	1533.9763					
-1.20	0.063		156.40	76846.31			16598.10	0.69	1.72	-0.336	24.82
		0.057			19584.94	1108.6550					
-1.30	0.050		175.20	96431.25			17706.75	0.74	1.93	-0.436	25.07
		0.045			24625.87	1107.3030					
-1.40	0.040		196.30	121057.12			18814.05	0.78	2.16	-0.536	25.32
		0.036			26468.56	945.3787					
-1.50	0.032		216.70	147525.69			19759.43	0.82	2.39	-0.636	25.57
		0.028			20693.87	587.1077					
-1.60	0.025		231.40	168219.56			20346.53	0.85	2.55	-0.736	25.82
		0.023			24222.62	545.8806					
-1.70	0.020		247.50	192442.19			20892.41	0.87	2.73	-0.836	26.07
		0.018			30513.12	546.2151					
-1.80	0.016		266.40	222955.31			21438.62	0.89	2.93	-0.936	26.32
		0.014			14800.00	210.4454					
-1.90	0.013		275.10	237755.31			21649.07	0.90	3.03	-1.036	26.57
		0.011			43106.19	486.8752					
-2.00	0.010		299.00	280861.50			22135.95	0.92	3.29	-1.136	26.82
- ∞							24065.00	(1)			∞

PHOTOMETRIC PARAMETERS OF NGC 4647

V-FILTER

Total luminosity	L_T	= 6.69
Total apparent magnitude	m_T	= 10.87
Apparent central surface brightness	μ_o	= 19.17
Major axis at threshold	$2a_m$	= 10.27
Minor axis at threshold	$2b_m$	= 9.37
Major axis at μ=25.0 mag sec^{-2}	2a(25)	= 5.33
Luminosity within μ=25.0 mag sec^{-2}	k(25)	= 0.73
Gradient of exponential component	G(a)	= -0.29
Equivalent gradient of exponential comp.	G(r*)	= -0.30
Equivalent gradient of reduced exp. comp.	G(ρ)	= -0.50
Parameters at k = ¼ :		
Semi-major axis	a_1	= 0.51
Axis ratio	b/a	= 0.98
Equivalent radius	r_1*	= 0.57
Surface brightness	μ_1	= 22.07
Parameters at k = ½(effective) :		
Semi-major axis	a_e	= 1.38
Axis ratio	b/a	= 1.05
Equivalent radius	r_e*	= 1.51
Surface brightness	μ_e	= 23.97
Mean surface brightness	μ_e'	= 13.76
Parameters at k = ¾ :		
Semi-major axis	a_3	= 3.38
Axis ratio	b/a	= 0.88
Equivalent radius	r_3*	= 3.02
Surface brightness	μ_3	= 25.13
Concentration indices	C_{21}	= 2.64
	C_{32}	= 2.00

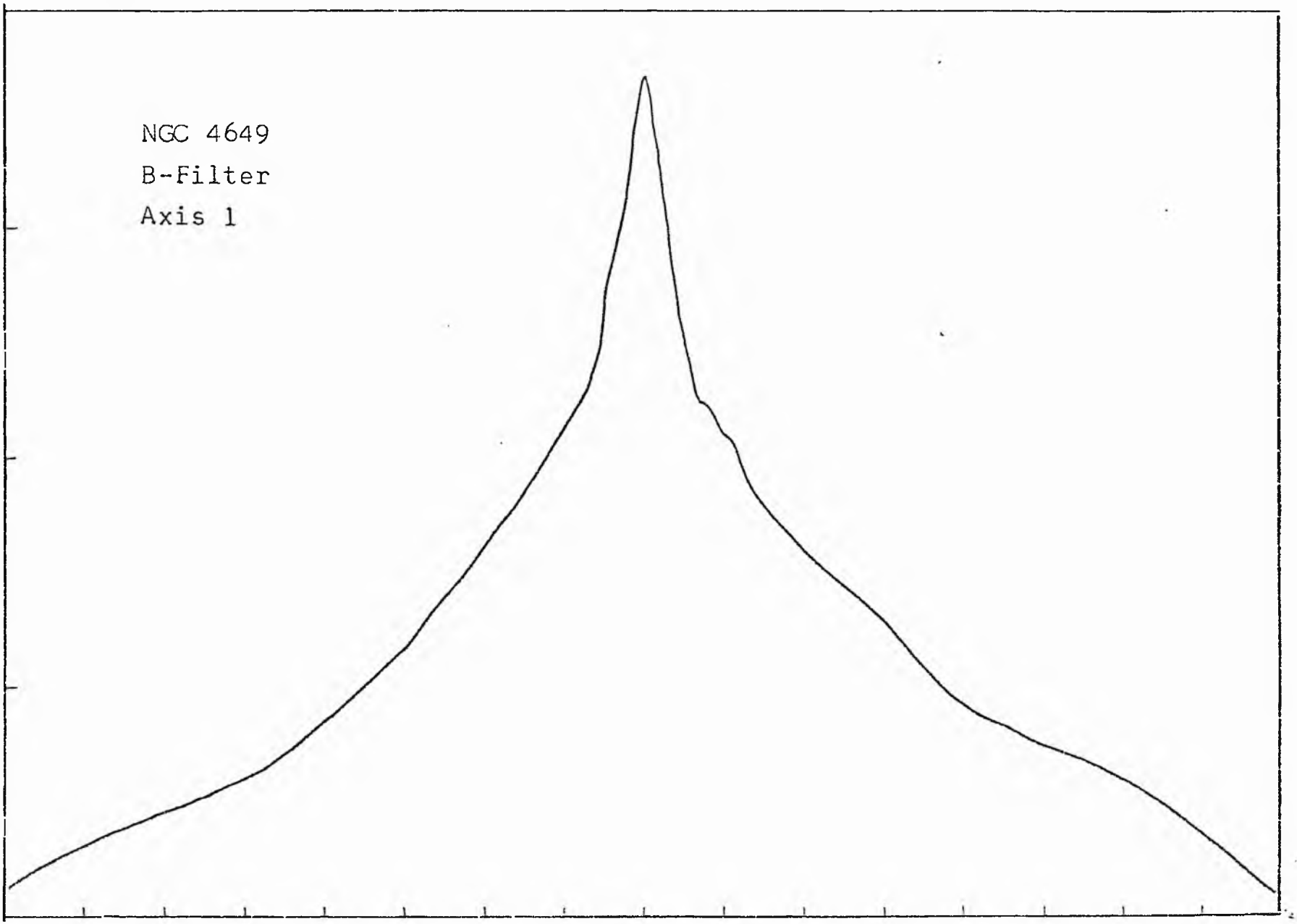
NGC 4649
B-Filter
Axis 1

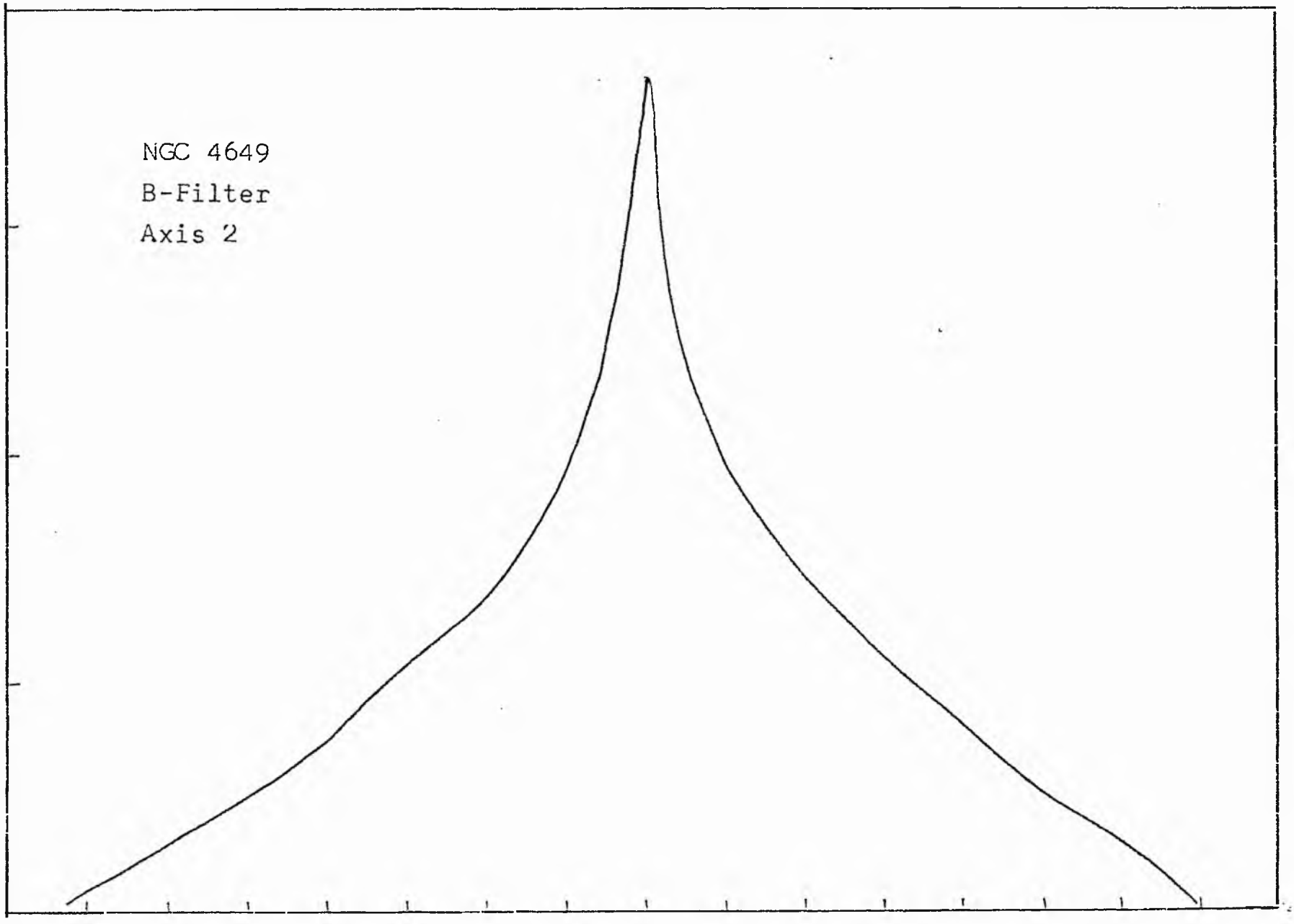
NGC 4649
B-Filter
Axis 2

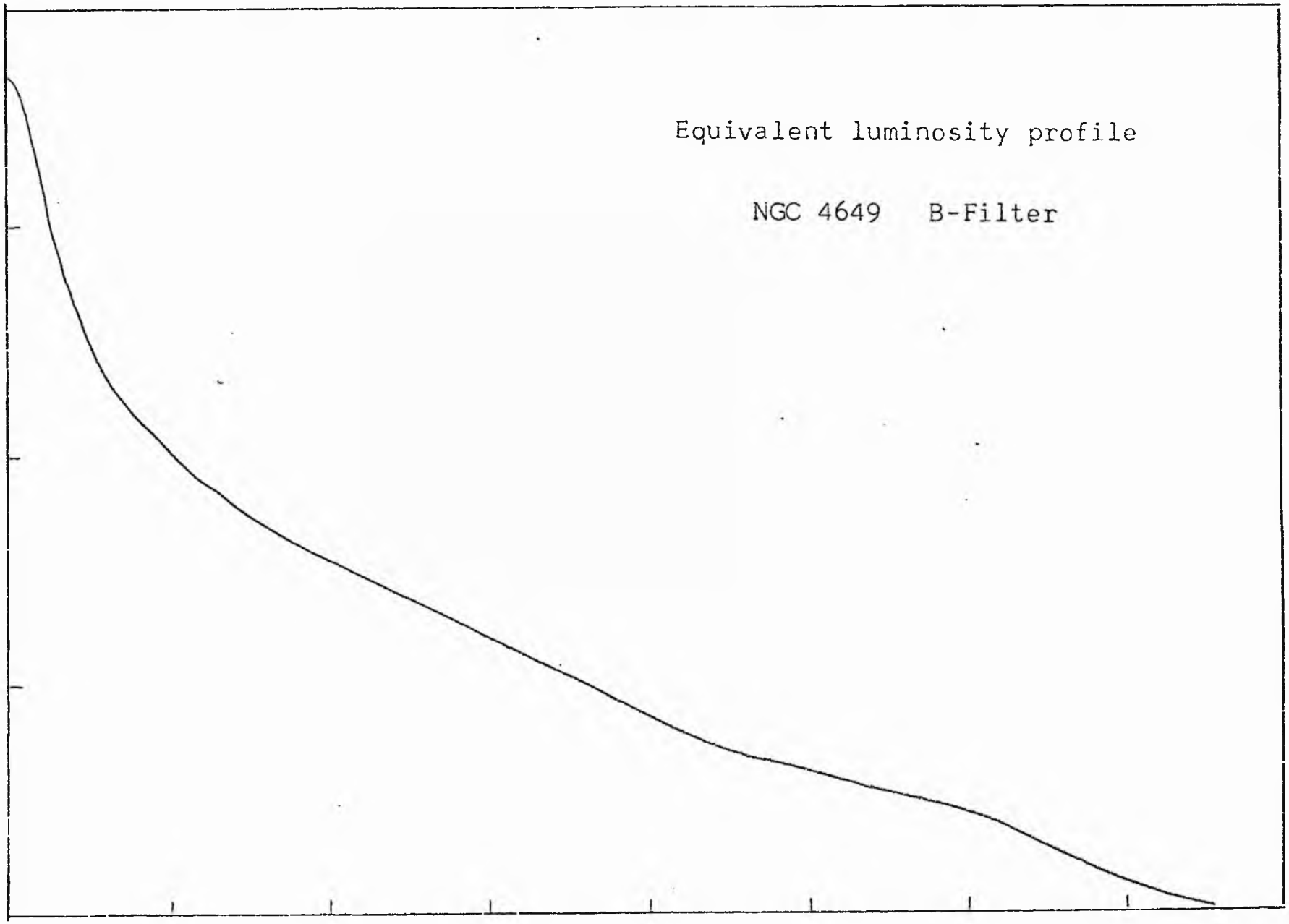
Equivalent luminosity profile
NGC 4649 B-Filter

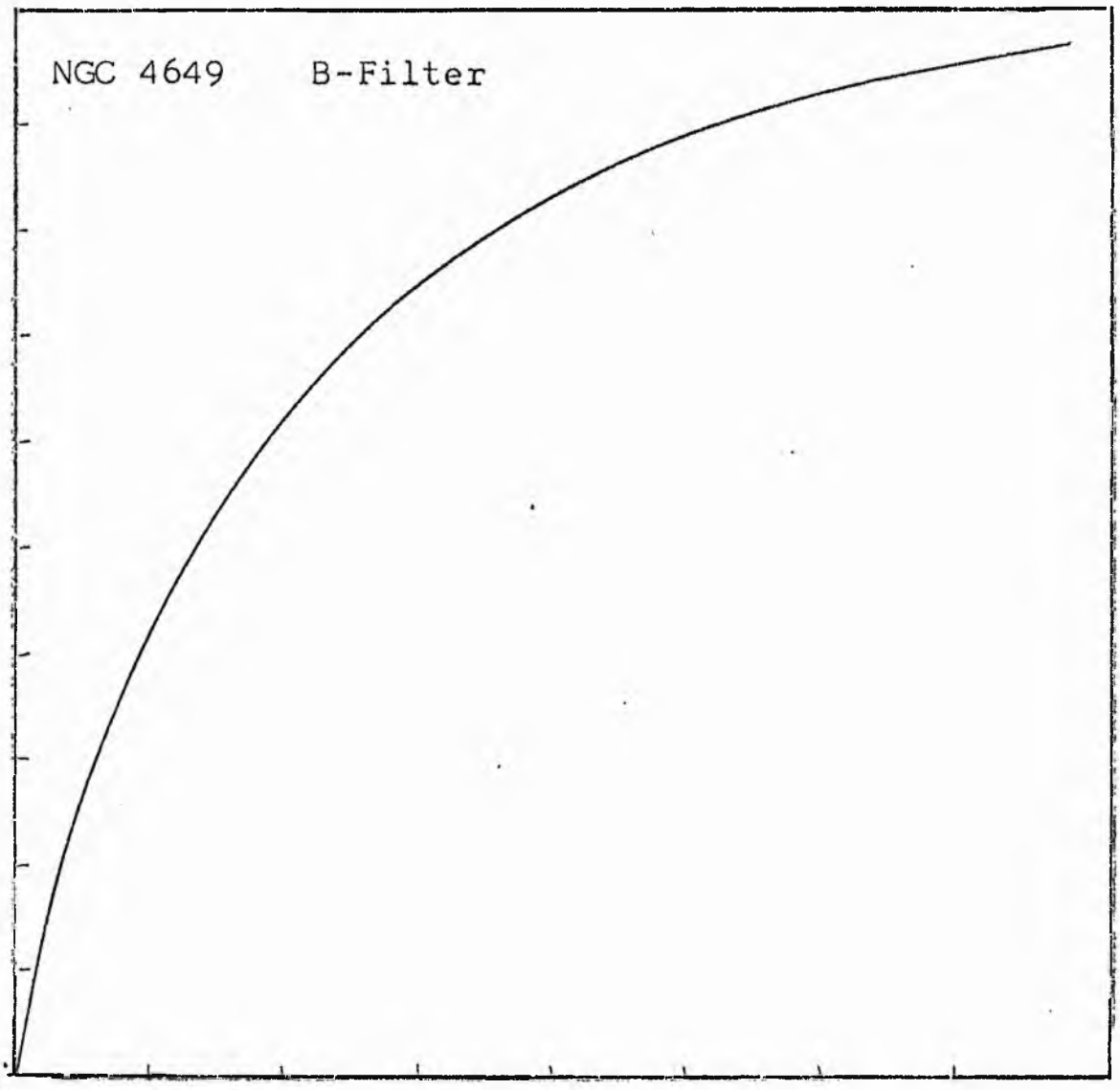

Relative integrated luminosity k(r) versus equivalent radius r*.

MEAN LUMINOSITY DISTRIBUTION IN NGC 4649
B COLOUR

LOG I	I	T	R	AREA	Δ A	P	Σ P	K(R)	ρ	LOG J	μ
1.66	45.709		0.0	0.0			0.0	0.0	0.0	1.829	17.83
		42.760			35.47	1516.5723					
1.60	39.811		3.36	35.47			1516.57	0.02	0.05	1.769	17.98
		35.717			31.01	1107.5291					
1.50	31.623		4.60	66.48			2624.10	0.04	0.07	1.669	18.23
		28.371			78.79	2235.3621					
1.40	25.119		6.80	145.27			4859.46	0.07	0.10	1.569	18.48
		22.536			92.52	2084.9983					
1.30	19.953		8.70	237.79			6944.46	0.10	0.13	1.469	18.73
		17.901			95.50	1709.5947					
1.20	15.849		10.30	333.29			8654.09	0.12	0.15	1.369	18.98
		14.219			111.59	1586.6899					
1.10	12.589		11.90	444.88			10240.74	0.15	0.17	1.269	19.23
		11.295			127.67	1442.0247					
1.00	10.000		13.50	572.56			11682.76	0.17	0.20	1.169	19.48
		8.972			153.28	1375.1487					
0.90	7.943		15.20	725.83			13057.91	0.19	0.22	1.069	19.73
		7.126			203.57	1450.7517					
0.80	6.310		17.20	929.41			14508.66	0.21	0.25	0.969	19.98
		5.661			265.16	1501.1150					
0.70	5.012		19.50	1194.59			16009.77	0.23	0.28	0.869	20.23
		4.496			395.84	1779.8767					
0.60	3.981		22.50	1590.43			17789.65	0.25	0.33	0.769	20.48
		3.572			436.40	1556.6604					
0.50	3.162		25.40	2026.83			19346.31	0.27	0.37	0.669	20.73
		2.837			787.42	2233.7744					
0.40	2.512		29.93	2814.25			21582.28	0.31	0.44	0.569	20.98
		2.254			929.36	2094.3762					
0.30	1.995		34.52	3743.62			23676.66	0.34	0.50	0.469	21.23
		1.790			1032.29	1847.8716					
0.20	1.585		38.89	4775.91			25524.53	0.36	0.57	0.369	21.48
		1.422			1577.33	2242.8110					
0.10	1.259		44.97	6353.24			27767.34	0.39	0.66	0.269	21.73
		1.129			2095.94	2367.2747					
-0.00	1.000		51.86	8449.18			30134.61	0.43	0.76	0.169	21.98
		0.897			3141.24	2818.1953					
-0.10	0.794		60.74	11590.42			32952.80	0.47	0.89	0.069	22.23
		0.711			4663.93	3323.7024					
-0.20	0.631		71.93	16254.36			36276.50	0.51	1.05	-0.031	22.48
		0.566			5586.70	3162.4583					
-0.30	0.501		83.38	21841.05			39438.96	0.56	1.22	-0.131	22.73
		0.450			6901.12	3103.6574					
-0.40	0.398		95.65	28742.18			42542.02	0.60	1.40	-0.231	22.98
		0.357			8200.54	2928.9531					
-0.50	0.316		108.44	36942.71			45470.97	0.64	1.58	-0.331	23.23
		0.284			10362.57	2939.9333					
-0.60	0.251		122.71	47305.28			48410.90	0.69	1.79	-0.431	23.48
		0.225			12427.86	2800.6997					
-0.70	0.200		137.89	59733.14			51211.60	0.73	2.01	-0.531	23.73
		0.179			8282.86	1482.6902					
-0.80	0.158		147.14	68016.00			52694.29	0.75	2.15	-0.631	23.98
		0.142			13346.37	1897.7263					
-0.90	0.126		160.93	81362.37			54592.01	0.77	2.35	-0.731	24.23
		0.113			12651.44	1428.9280					
-1.00	0.100		172.99	94013.81			56020.93	0.79	2.52	-0.831	24.48
		0.090			15586.19	1378.3342					
-1.10	0.079		186.78	109600.00			57419.27	0.81	2.73	-0.931	24.73
		0.071			19632.37	1399.0854					
-1.20	0.063		202.82	129232.37			58818.35	0.83	2.96	-1.031	24.98
		0.057			22516.75	1274.6118					
-1.30	0.050		219.78	151749.12			60092.96	0.85	3.21	-1.131	25.23
		0.045			50264.12	2260.1172					
-1.40	0.040		253.58	202013.25			62353.07	0.88	3.70	-1.231	25.48
		0.036			49273.31	1759.8894					
-1.50	0.032		282.82	251286.56			64112.96	0.91	4.13	-1.331	25.73
		0.028			48869.62	1386.4790					
-1.60	0.025		309.10	300156.19			65499.44	0.93	4.51	-1.431	25.98
		0.023			29838.87	672.4456					
-1.70	0.020		324.10	329995.06			66171.87	0.94	4.73	-1.531	26.23
		0.018			19944.00	357.0156					
-1.80	0.016		333.75	349939.06			66528.87	0.94	4.87	-1.631	26.48
		0.014			60111.25	854.7351					
-1.90	0.013		361.28	410050.31			67383.56	0.95	5.27	-1.731	26.73
		0.011			61679.50	696.6541					
-2.00	0.010		387.50	471729.81			68080.19	0.96	5.66	-1.831	26.98
- ∞							70580.00	(1)			∞

PHOTOMETRIC PARAMETERS OF NGC 4649

B-FILTER

Total luminosity	L_T	= 19.60
Total apparent magnitude	m_T	= 9.86
Apparent central surface brightness	μ_o	= 17.83
Major axis at threshold	$2a_m$	= 13.67
Minor axis at threshold	$2b_m$	= 12.10
Major axis at μ=25.0 mag sec^{-2}	2a(25)	= 8.17
Luminosity within μ=25.0 mag sec^{-2}	k(25)	= 0.83
Gradient of exponential component	G(a)	= -0.30
Equivalent gradient of exponential comp.	G(r*)	= -0.35
Equivalent gradient of reduced exp. comp.	G(ρ)	= +0.54

Parameters at k = ¼ :

Semi-major axis	a_1	= 0.49
Axis ratio	b/a	= 0.90
Equivalent radius	r_1*	= 0.37
Surface brightness	μ_1	= 20.48

Parameters at k = ½(effective) :

Semi-major axis	a_e	= 1.30
Axis ratio	b/a	= 0.82
Equivalent radius	r_e*	= 1.14
Surface brightness	μ_e	= 22.42
Mean surface brightness	μ_e'	= 12.14

Parameters at k = ¾ :

Semi-major axis	a_3	= 2.61
Axis ratio	b/a	= 0.86
Equivalent radius	r_3*	= 2.48
Surface brightness	μ_3	= 23.98

Concentration indices	C_{21}	= 3.08
	C_{32}	= 2.17

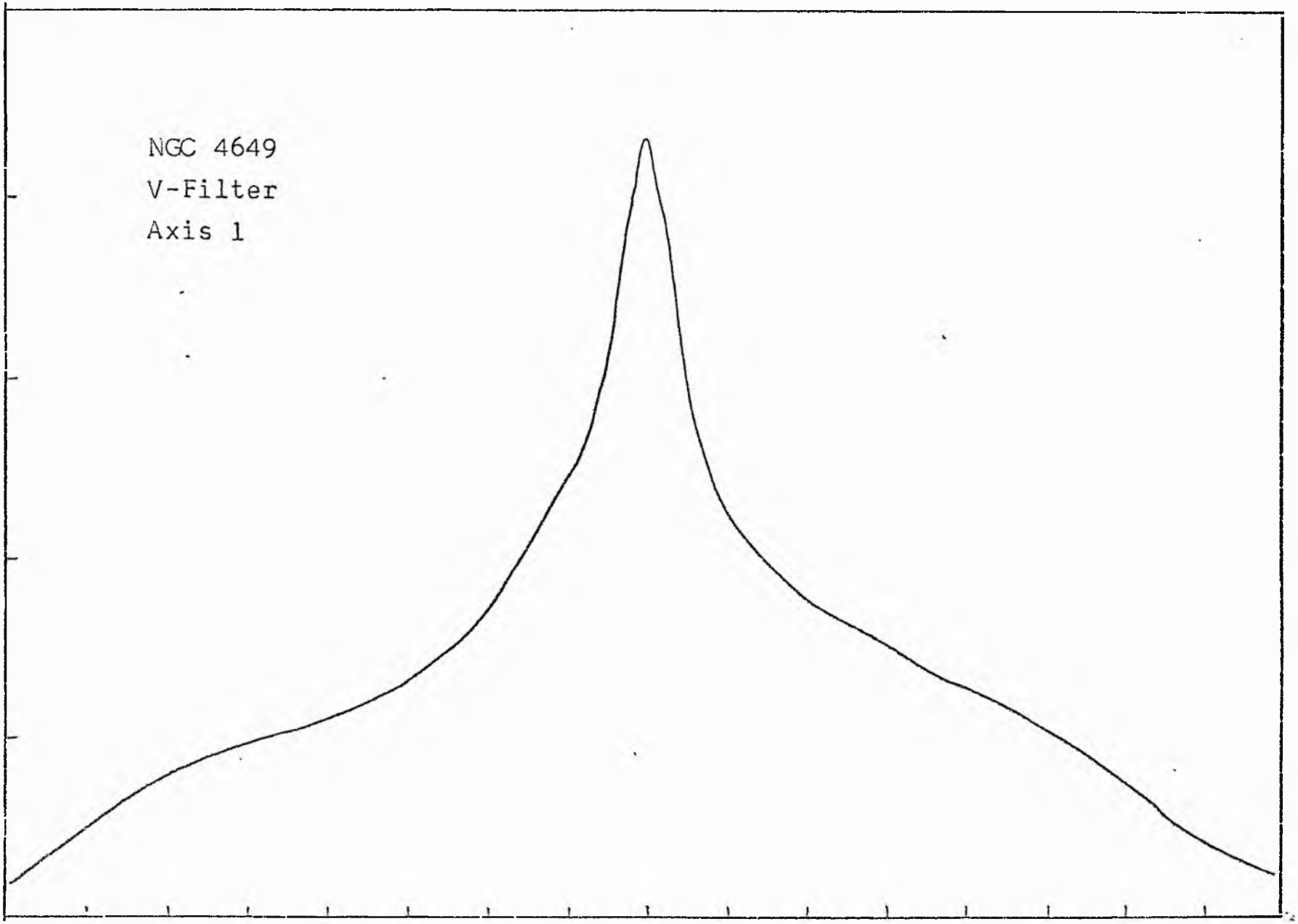
NGC 4649
V-Filter
Axis 1

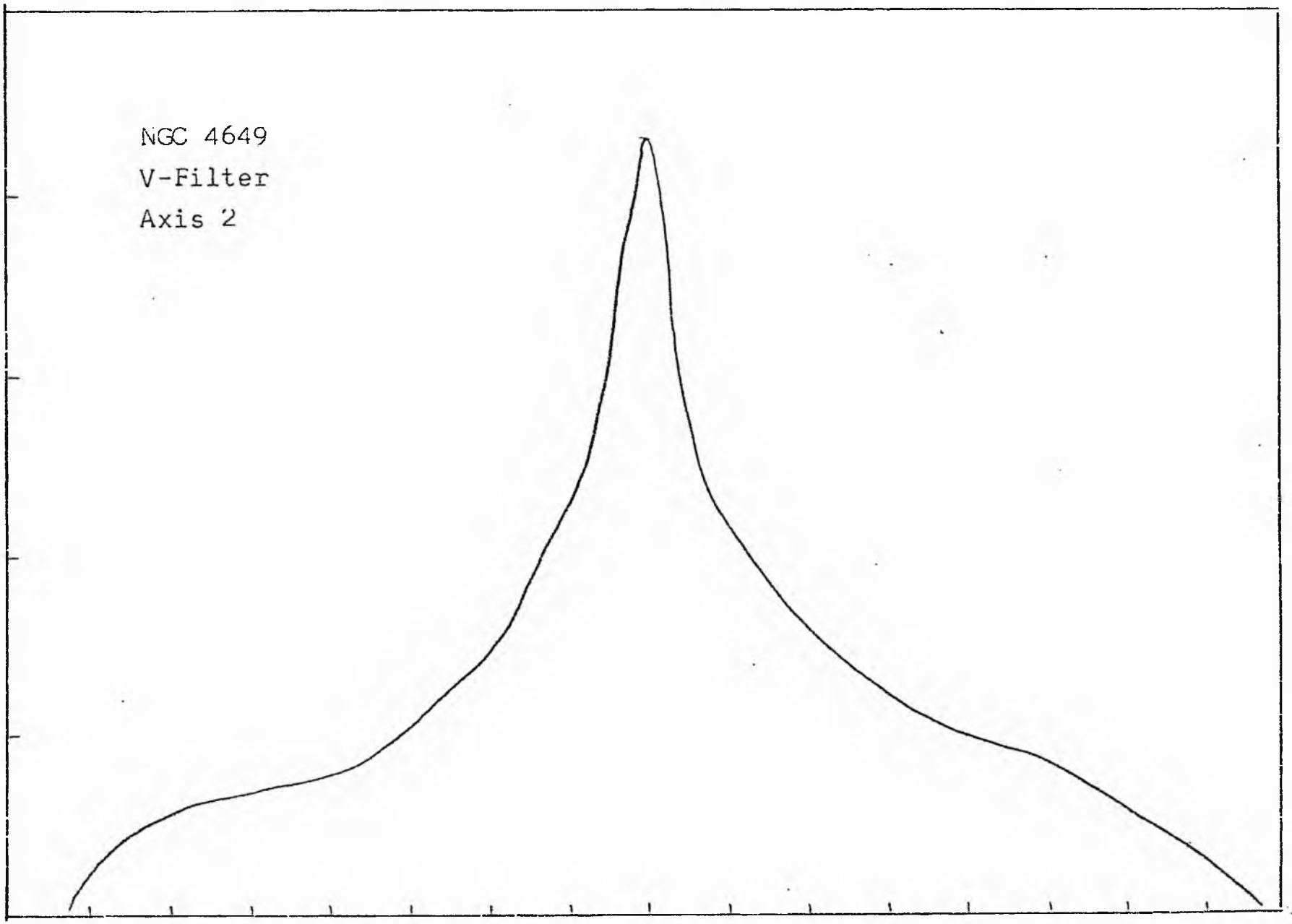
NGC 4649
V-Filter
Axis 2

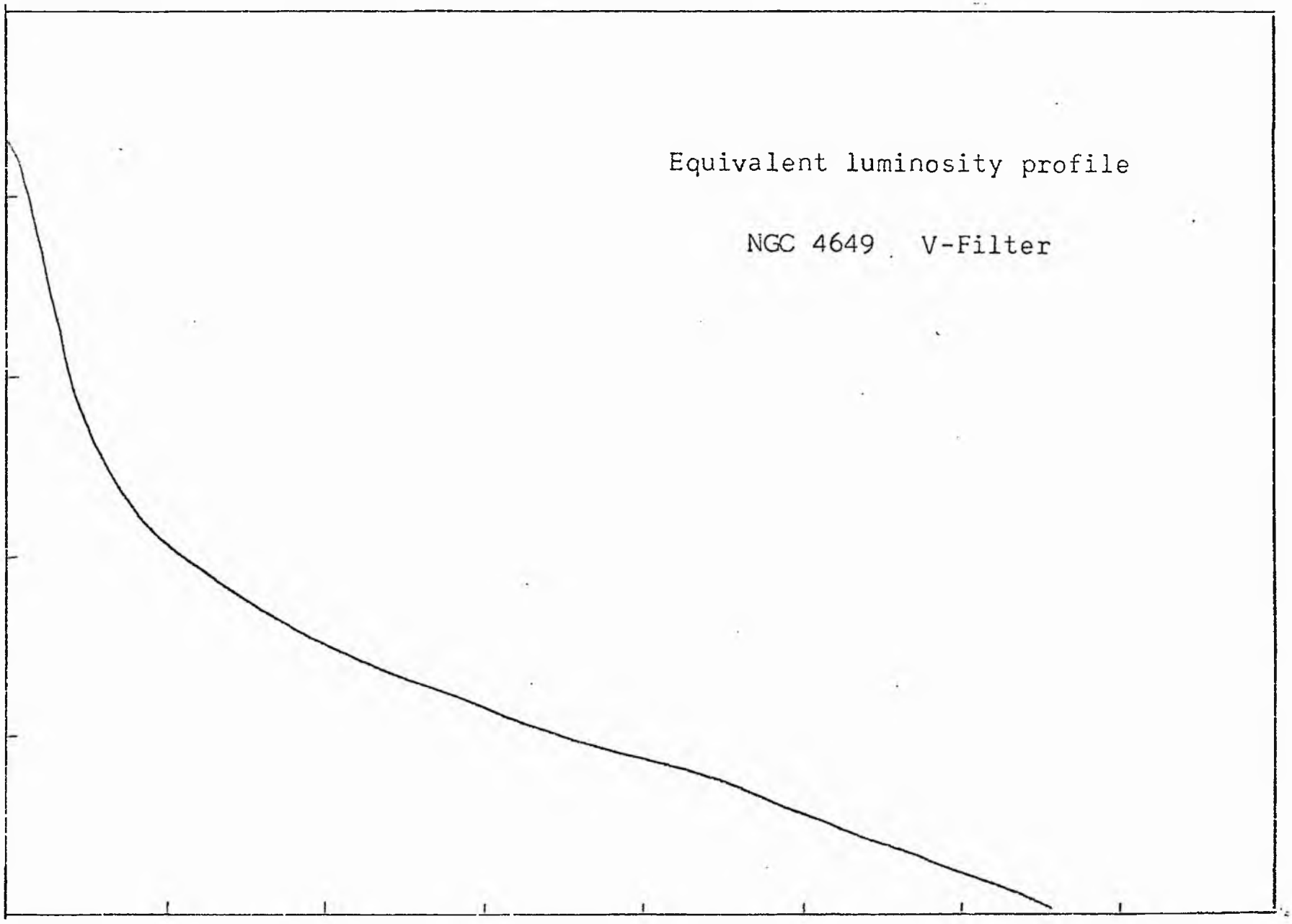
Equivalent luminosity profile
NGC 4649 V-Filter

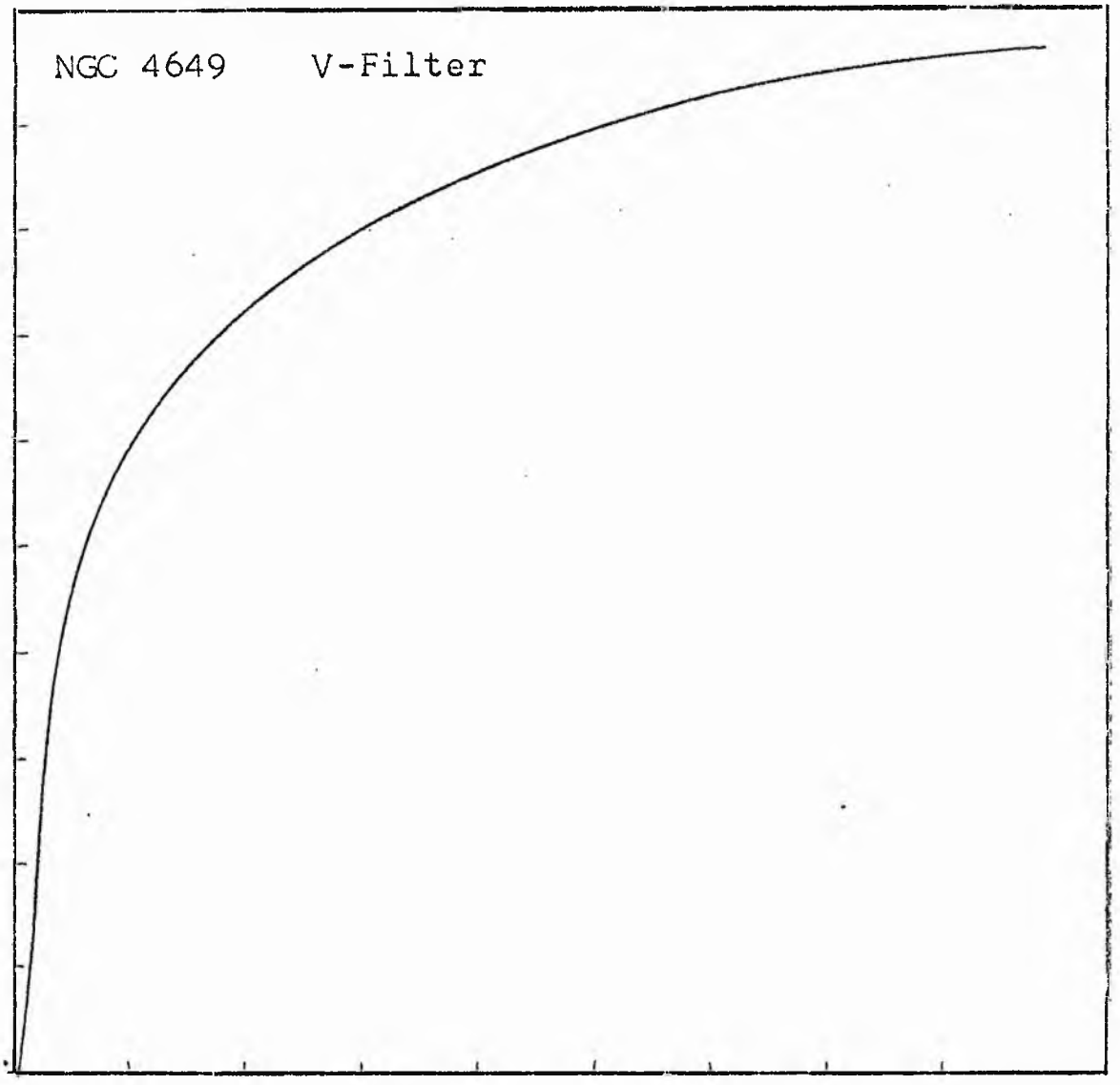

Relative integrated luminosity k(r) versus equivalent radius r*.

MEAN LUMINOSITY DISTRIBUTION IN NGC 4649
V COLOUR

LOG I	I	$\bar{I}$	R	AREA	ΔA	P	ΣP	KIRI	ρ	LOG ϑ	μ
2.28	190.546		0.0	0.0			0.0	0.0	0.0	1.491	16.22
		174.517			8.04	1403.5513					
2.20	158.489		1.60	8.04			1403.55	0.01	0.05	1.411	16.42
		142.191			47.38	6736.3047					
2.10	125.892		4.20	55.42			8139.86	0.05	0.14	1.311	16.67
		112.946			89.85	10148.1445					
2.00	100.000		6.80	145.27			18288.00	0.12	0.23	1.211	16.92
		89.716			76.40	6854.6328					
1.90	79.433		8.40	221.67			25142.63	0.16	0.29	1.111	17.17
		71.264			124.69	8885.8984					
1.80	63.095		10.50	346.36			34028.53	0.22	0.36	1.011	17.42
		56.607			128.93	7298.3828					
1.70	50.118		12.30	475.29			41326.91	0.27	0.42	0.911	17.67
		44.964			137.82	6197.1992					
1.60	39.810		13.97	613.12			47524.11	0.31	0.48	0.811	17.92
		35.717			122.30	4368.1016					
1.50	31.623		15.30	735.42			51892.21	0.34	0.52	0.711	18.17
		28.371			226.70	6431.5430					
1.40	25.119		17.50	962.11			58323.76	0.38	0.60	0.611	18.42
		22.536			124.75	2811.3320					
1.30	19.952		18.60	1086.86			61135.09	0.39	0.63	0.511	18.67
		17.901			95.50	1709.5964					
1.20	15.849		19.40	1182.37			62844.68	0.41	0.66	0.411	18.92
		14.219			264.43	3759.9468					
1.10	12.589		21.46	1446.80			66604.62	0.43	0.73	0.311	19.17
		11.295			405.23	4576.8242					
1.00	10.000		24.28	1852.03			71181.44	0.46	0.83	0.211	19.42
		8.972			163.65	1468.1516					
0.90	7.943		25.33	2015.67			72649.56	0.47	0.86	0.111	19.67
		7.126			608.22	4334.3633					
0.80	6.310		28.90	2623.89			76983.87	0.50	0.99	0.011	19.92
		5.661			674.03	3815.4514					
0.70	5.012		32.40	3297.92			80799.31	0.52	1.11	-0.089	20.17
		4.496			683.61	3073.7993					
0.60	3.981		35.60	3981.53			83873.06	0.54	1.22	-0.189	20.42
		3.572			507.30	1811.8987					
0.50	3.162		37.80	4488.83			85684.94	0.55	1.29	-0.289	20.67
		2.837			974.05	2763.4458					
0.40	2.512		41.70	5462.88			88448.37	0.57	1.42	-0.389	20.92
		2.254			1069.62	2410.4382					
0.30	1.995		45.60	6532.50			90858.81	0.59	1.56	-0.489	21.17
		1.790			1702.99	3048.4583					
0.20	1.585		51.20	8235.49			93907.25	0.61	1.75	-0.589	21.42
		1.422			2187.55	3110.4751					
0.10	1.259		57.60	10423.05			97017.69	0.63	1.97	-0.689	21.67
		1.129			3038.70	3432.0684					
-0.00	1.000		65.46	13461.75			100449.75	0.65	2.23	-0.789	21.92
		0.897			4017.02	3603.8887					
-0.10	0.794		74.59	17478.77			104053.62	0.67	2.55	-0.889	22.17
		0.713			5022.06	3578.8997					
-0.20	0.631		84.63	22500.82			107632.50	0.70	2.89	-0.989	22.42
		0.566			6301.50	3567.0671					
-0.30	0.501		95.75	28802.32			111199.56	0.72	3.27	-1.089	22.67
		0.450			7807.29	3510.4924					
-0.40	0.398		107.95	36609.61			114710.00	0.74	3.69	-1.189	22.92
		0.357			9637.67	3442.2336					
-0.50	0.316		121.33	46247.28			118152.19	0.76	4.14	-1.289	23.17
		0.284			11501.26	3262.9756					
-0.60	0.251		135.58	57748.54			121415.12	0.78	4.63	-1.389	23.42
		0.225			18538.71	4177.8008					
-0.70	0.200		155.83	76287.25			125592.87	0.81	5.32	-1.489	23.67
		0.179			25296.81	4528.2891					
-0.80	0.158		179.82	101584.06			130121.12	0.84	6.14	-1.589	23.92
		0.142			22214.19	3158.6309					
-0.90	0.126		198.51	123798.25			133279.75	0.86	6.78	-1.689	24.17
		0.113			29251.69	3303.8445					
-1.00	0.100		220.72	153049.94			136583.56	0.88	7.53	-1.789	24.42
		0.090			46137.19	4139.2383					
-1.10	0.079		251.80	199187.12			140722.75	0.91	8.60	-1.889	24.67
		0.071			35140.94	2504.2825					
-1.20	0.063		273.11	234328.06			143227.00	0.92	9.32	-1.989	24.92
		0.057			32034.25	1813.3638					
-1.30	0.050		291.18	266362.31			145040.31	0.94	9.94	-2.089	25.17
		0.045			32145.75	1445.4211					
-1.40	0.040		308.25	298508.06			146485.69	0.95	10.52	-2.189	25.42
		0.036			32200.31	1150.0891					
-1.50	0.032		324.45	330708.37			147635.75	0.95	11.08	-2.289	25.67
		0.028			39456.87	1119.4246					
-1.60	0.025		343.26	370165.25			148755.12	0.96	11.72	-2.389	25.92
		0.023			35809.62	816.9983					
-1.70	0.020		359.48	405974.87			149562.06	0.97	12.27	-2.489	26.17
		0.018			54957.87	983.7922					
-1.80	0.016		383.04	460932.75			150545.81	0.97	13.08	-2.589	26.42
		0.014			32714.75	465.1763					
-1.90	0.013		396.40	493647.50			151010.94	0.98	13.53	-2.689	26.67
		0.011			75673.31	854.7068					
-2.00	0.010		425.70	569320.81			151865.62	0.98	14.53	-2.789	26.92
$-\infty$							154865.00	(1)			∞

PHOTOMETRIC PARAMETERS OF NGC 4649

V-FILTER

Total luminosity	L_T	= 43.01
Total apparent magnitude	m_T	= 8.94
Apparent central surface brightness	μ_o	= 16.22
Major axis at threshold	$2a_m$	= 15.37
Minor axis at threshold	$2b_m$	= 12.56
Major axis at μ=25.0 mag sec^{-2}	2a(25)	= 9.65
Luminosity within μ=25.0 mag sec^{-2}	k(25)	= 0.93
Gradient of exponential component	G(a)	= -0.31
Equivalent gradient of exponential comp.	G(r*)	= -0.32
Equivalent gradient of reduced exp. comp.	G(ρ)	= -----

Parameters at k = ¼ :

Semi-major axis	a_1	= 0.20
Axis ratio	b/a	= 0.83
Equivalent radius	r_1*	= 0.19
Surface brightness	μ_1	= 17.57

Parameters at k = ½(effective) :

Semi-major axis	a_e	= 0.35
Axis ratio	b/a	= 0.91
Equivalent radius	r_e*	= 0.49
Surface brightness	μ_e	= 19.92
Mean surface brightness	μ_e'	= 9.39

Parameters at k = ¾ :

Semi-major axis	a_3	= 2.43
Axis ratio	b/a	= 0.57
Equivalent radius	r_3*	= 1.89
Surface brightness	μ_3	= 23.04
Concentration indices	C_{21}	= 2.52
	C_{32}	= 3.87

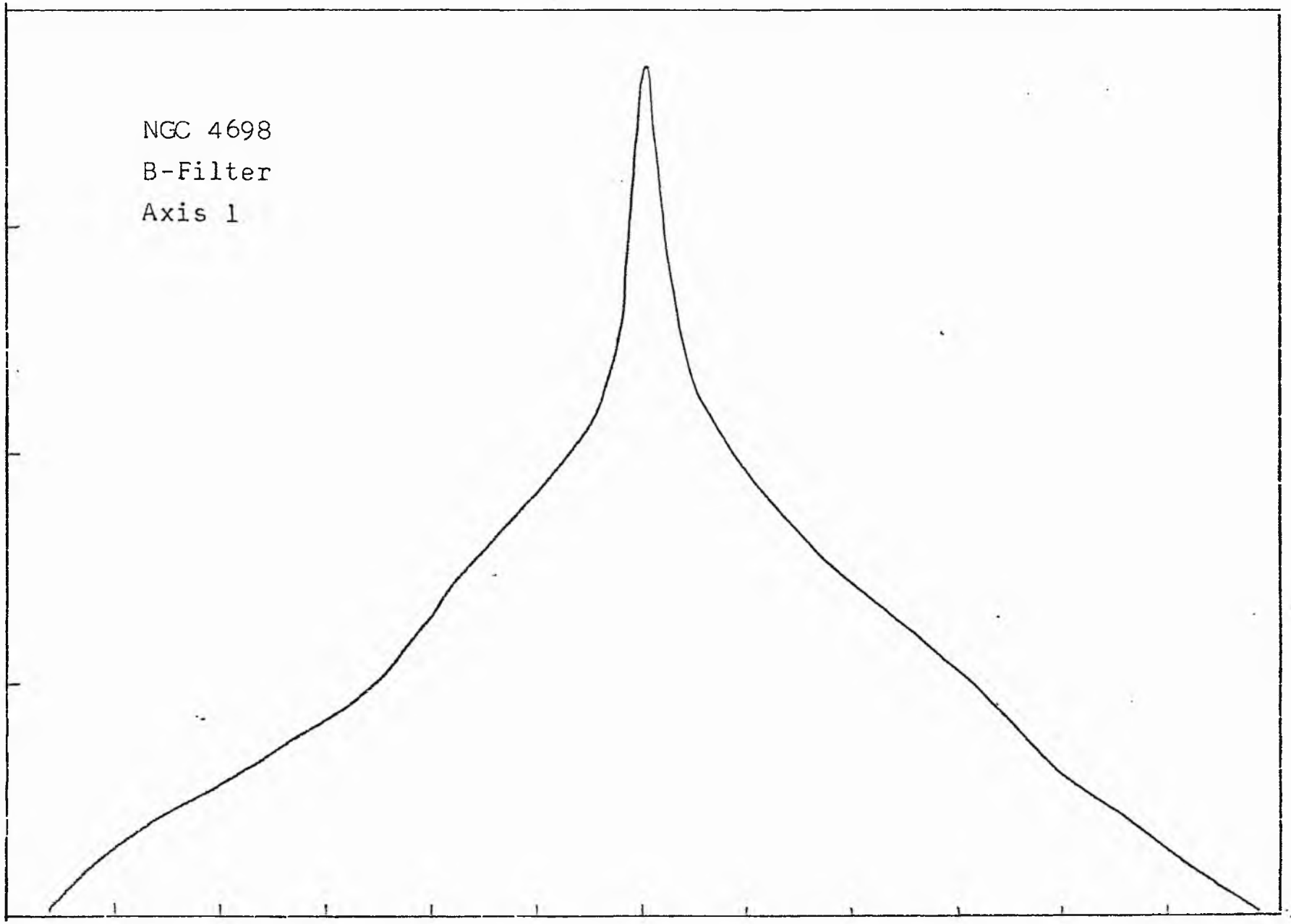
NGC 4698
B-Filter
Axis 1

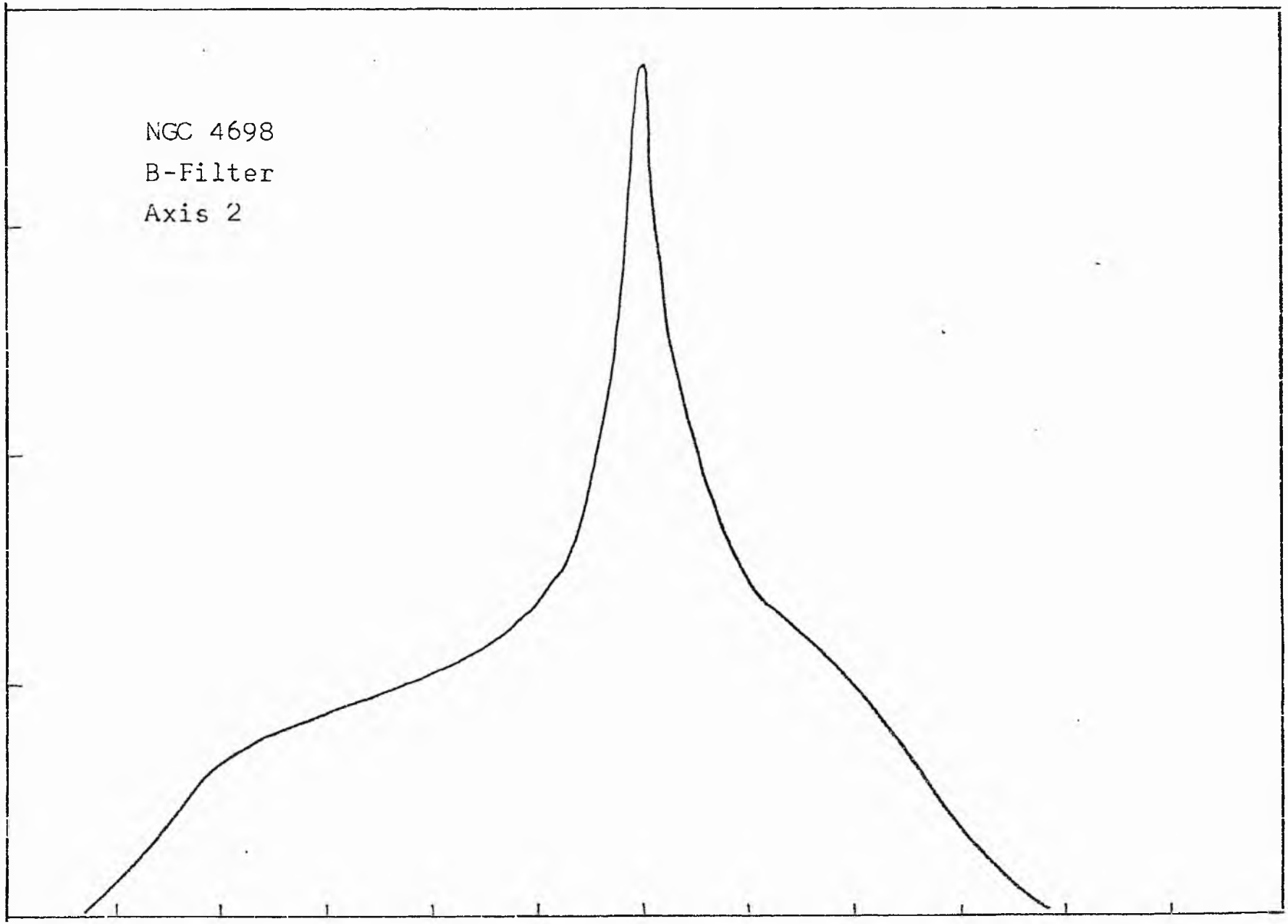
NGC 4698
B-Filter
Axis 2

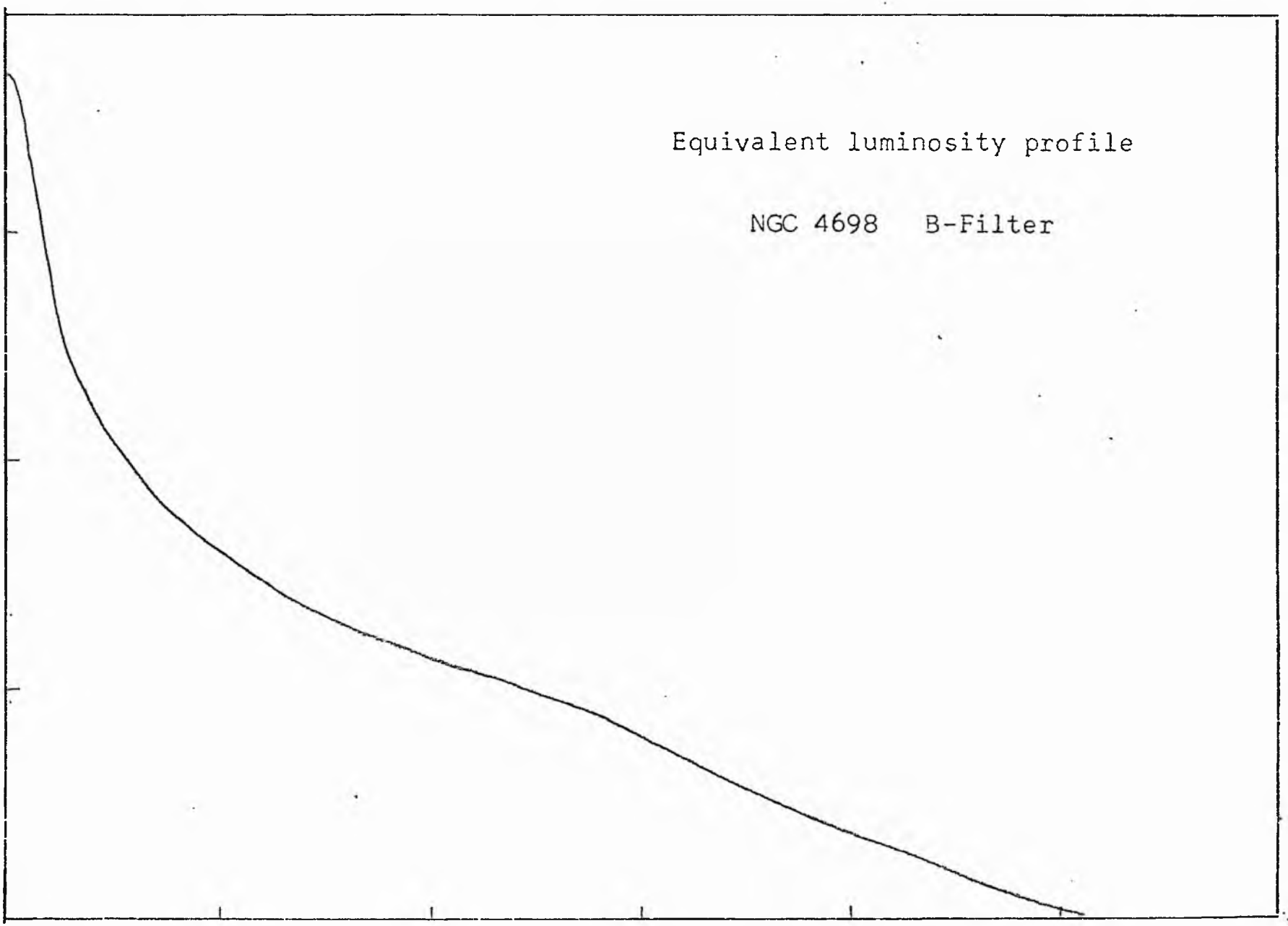
Equivalent luminosity profile
NGC 4698 B-Filter

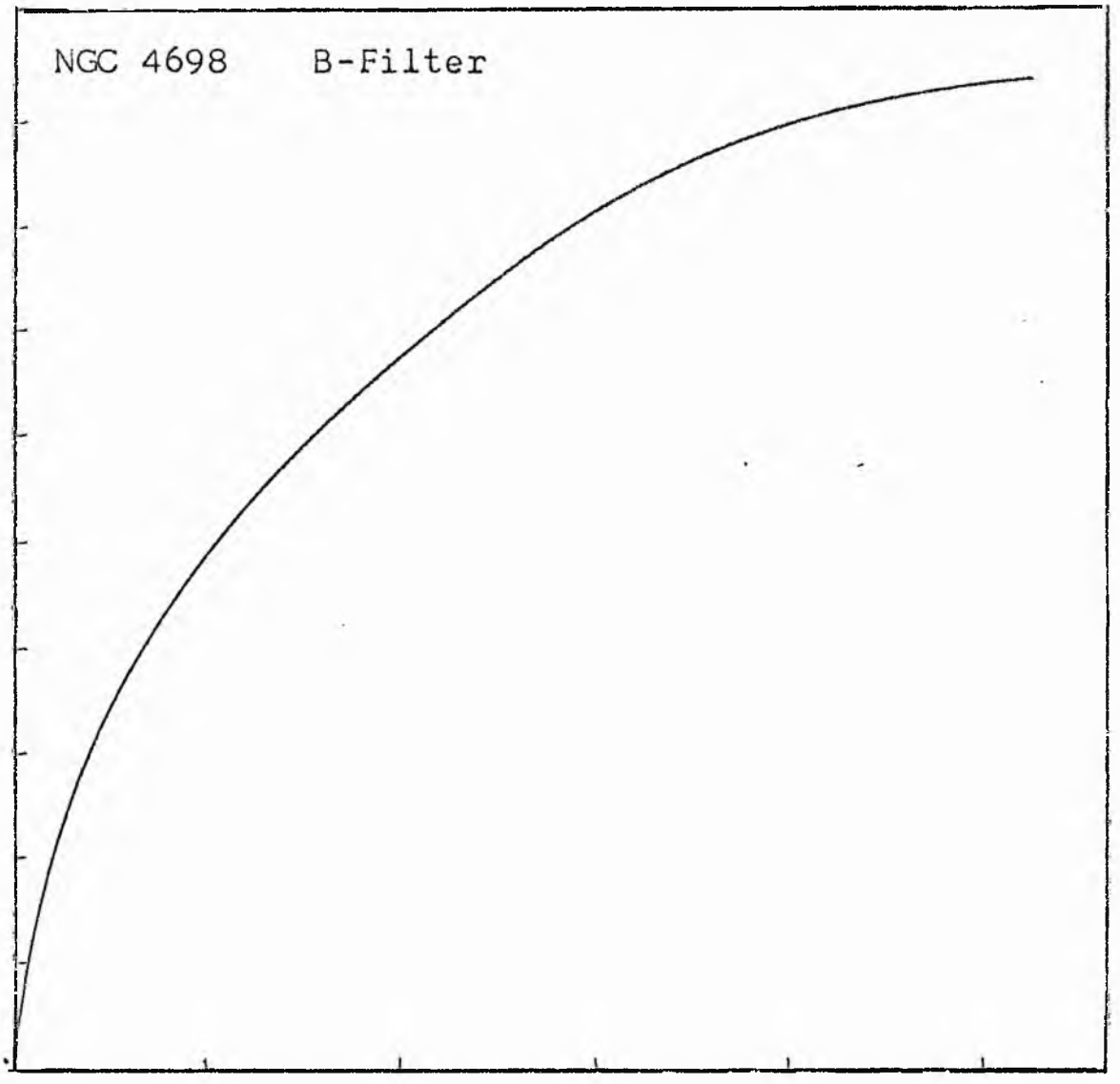

Relative integrated luminosity k(r) versus equivalent radius r*.

MEAN LUMINOSITY DISTRIBUTION IN NGC 4698
B COLOUR

LOG I	I	$\bar{I}$	R	AREA	ΔA	P	ΣP	K(R)	ρ	LOG J	μ
1.69	48.978		0.0	0.0			0.0	0.0	0.0	2.121	18.22
		44.394			30.78	1366.3591					
1.60	39.811		3.13	30.78			1366.36	0.05	0.06	2.031	18.45
		35.717			20.50	732.1187					
1.50	31.623		4.04	51.28			2098.48	0.08	0.08	1.931	18.70
		28.371			9.55	270.8093					
1.40	25.119		4.40	60.82			2369.29	0.09	0.09	1.831	18.95
		22.536			37.70	849.5745					
1.30	19.953		5.60	98.52			3218.86	0.12	0.11	1.731	19.20
		17.901			26.17	468.4514					
1.20	15.849		6.30	124.69			3687.31	0.13	0.12	1.631	19.45
		14.219			33.68	478.8660					
1.10	12.589		7.10	158.37			4166.18	0.15	0.14	1.531	19.70
		11.295			47.75	539.3398					
1.00	10.000		8.10	206.12			4705.52	0.17	0.16	1.431	19.95
		8.972			77.41	694.4783					
0.90	7.943		9.50	283.53			5399.99	0.19	0.18	1.331	20.20
		7.126			62.83	447.7651					
0.80	6.310		10.50	346.36			5847.75	0.21	0.20	1.231	20.45
		5.661			54.79	310.1450					
0.70	5.012		11.30	401.15			6157.90	0.22	0.22	1.131	20.70
		4.496			89.72	403.4385					
0.60	3.981		12.50	490.87			6561.34	0.24	0.24	1.031	20.95
		3.572			178.79	638.5688					
0.50	3.162		14.60	669.66			7199.90	0.26	0.28	0.931	21.20
		2.837			217.02	615.6987					
0.40	2.512		16.80	886.68			7815.60	0.28	0.33	0.831	21.45
		2.254			223.68	504.0801					
0.30	1.995		18.80	1110.36			8319.68	0.30	0.36	0.731	21.70
		1.790			382.65	684.9617					
0.20	1.585		21.80	1493.01			9004.64	0.32	0.42	0.631	21.95
		1.422			630.71	896.8054					
0.10	1.259		26.00	2123.72			9901.44	0.36	0.50	0.531	22.20
		1.129			914.86	1033.2954					
-0.00	1.000		31.10	3038.58			10934.73	0.39	0.60	0.431	22.45
		0.897			920.61	825.9382					
-0.10	0.794		35.50	3959.19			11760.67	0.42	0.69	0.331	22.70
		0.713			134.96	96.1781					
-0.20	0.631		36.10	4094.15			11856.85	0.43	0.70	0.231	22.95
		0.566			1084.32	613.8003					
-0.30	0.501		40.60	5178.47			12470.64	0.45	0.79	0.131	23.20
		0.450			2303.04	1035.5486					
-0.40	0.398		48.80	7481.51			13506.19	0.49	0.94	0.031	23.45
		0.357			3677.93	1313.6296					
-0.50	0.316		59.60	11159.43			14819.82	0.53	1.15	-0.069	23.70
		0.284			3538.69	1003.9517					
-0.60	0.251		68.40	14698.12			15823.77	0.57	1.32	-0.169	23.95
		0.225			5157.53	1162.2827					
-0.70	0.200		79.50	19855.65			16986.05	0.61	1.54	-0.269	24.20
		0.179			6274.35	1123.1523					
-0.80	0.158		91.20	26130.00			18109.20	0.65	1.77	-0.369	24.45
		0.142			13560.12	1928.1189					
-0.90	0.126		112.40	39690.12			20037.32	0.72	2.18	-0.469	24.70
		0.113			13158.02	1486.1448					
-1.00	0.100		129.70	52848.14			21523.46	0.78	2.51	-0.569	24.95
		0.090			7414.68	665.2168					
-1.10	0.079		138.50	60262.82			22188.68	0.80	2.68	-0.669	25.20
		0.071			10046.49	715.9551					
-1.20	0.063		149.60	70309.31			22904.63	0.83	2.90	-0.769	25.45
		0.057			10820.69	612.5295					
-1.30	0.050		160.70	81130.00			23517.16	0.85	3.11	-0.869	25.70
		0.045			9440.50	424.8501					
-1.40	0.040		169.80	90578.50			23942.01	0.86	3.29	-0.969	25.95
		0.036			6956.75	248.4735					
-1.50	0.032		176.20	97535.25			24190.48	0.87	3.41	-1.069	26.20
		0.028			21067.69	597.7109					
-1.60	0.025		194.30	118602.94			24788.19	0.89	3.76	-1.169	26.45
		0.023			23126.06	521.1663					
-1.70	0.020		212.40	141729.00			25309.36	0.91	4.11	-1.269	26.70
		0.018			17314.12	309.9385					
-1.80	0.016		225.00	159043.12			25619.29	0.92	4.35	-1.369	26.95
		0.014			33865.81	481.5454					
-1.90	0.013		247.80	192908.94			26100.84	0.94	4.80	-1.469	27.20
		0.011			16856.75	190.3927					
-2.00	0.010		258.40	209765.69			26291.23	0.95	5.30	-1.569	27.45
- ∞							27721.00	(1)			∞

PHOTOMETRIC PARAMETERS OF NGC 4698

B-FILTER

Total luminosity ..... L_T = 7.70

Total apparent magnitude ..... m_T = 11.34

Apparent central surface brightness ..... μ_o = 18.22

Major axis at threshold ..... $2a_m$ = 9.32

Minor axis at threshold ..... $2b_m$ = 7.40

Major axis at μ=25.0 mag sec^{-2} ..... 2a(25) = 5.30

Luminosity within μ=25.0 mag sec^{-2} ..... k(25) = 0.78

Gradient of exponential component ..... G(a) = -0.50

Equivalent gradient of exponential comp..... G(r*) = -0.52

Equivalent gradient of reduced exp. comp..... G(ρ) = -0.48

Parameters at k = ¼ :

- Semi-major axis ..... a_1 = 0.22
- Axis ratio ..... b/a = 0.92
- Equivalent radius ..... r_1* = 0.23
- Surface brightness ..... μ_1 = 21.09

Parameters at k = ½(effective) :

- Semi-major axis ..... a_e = 1.28
- Axis ratio ..... b/a = 0.48
- Equivalent radius ..... r_e* = 0.85
- Surface brightness ..... μ_e = 23.51
- Mean surface brightness ..... μ_e' = 12.98

Parameters at k = ¾ :

- Semi-major axis ..... a_3 = 2.16
- Axis ratio ..... b/a = 0.65
- Equivalent radius ..... r_3* = 1.99
- Surface brightness ..... μ_3 = 24.82

Concentration indices ..... C_{21} = 3.77, C_{32} = 2.34

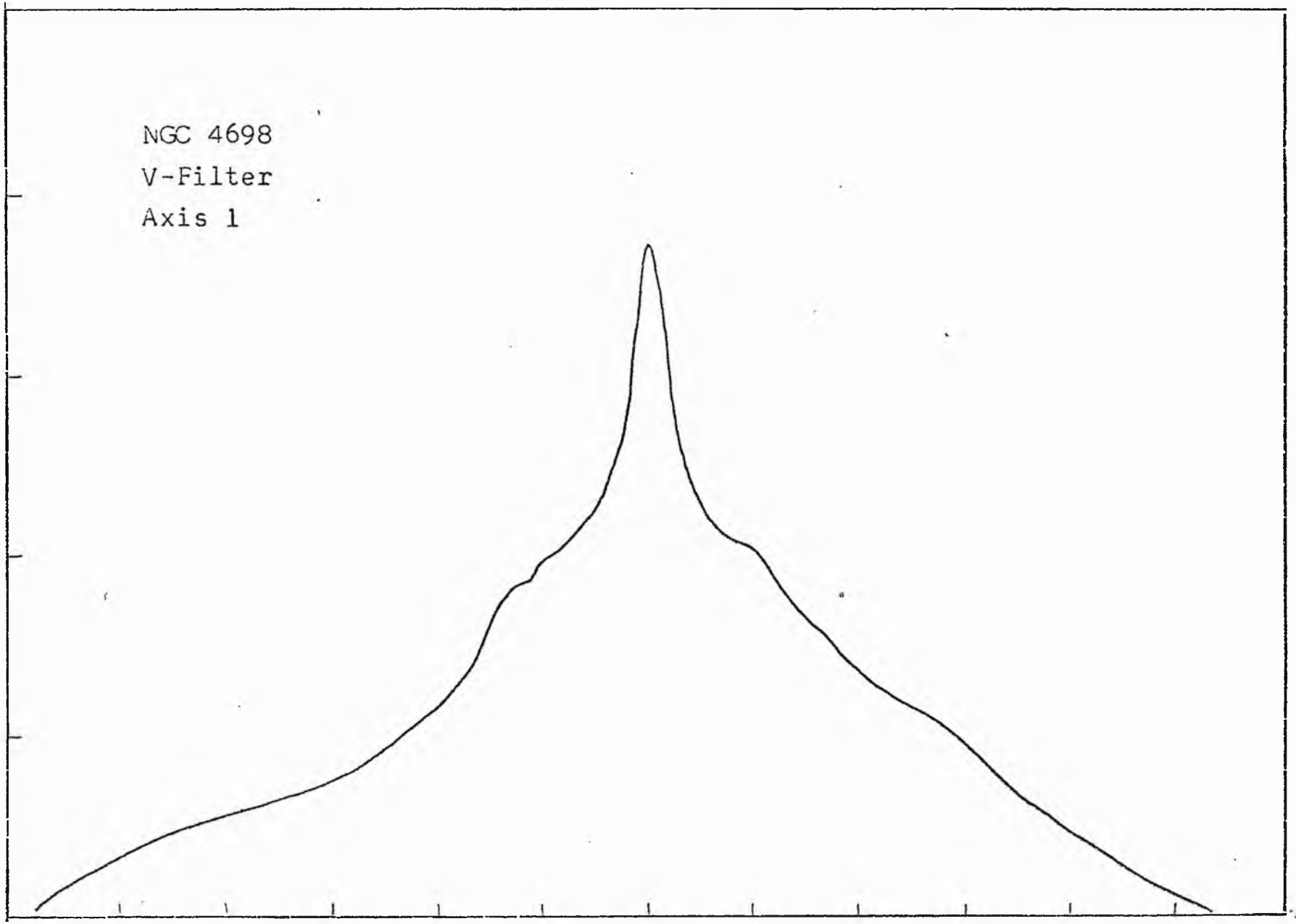
NGC 4698
V-Filter
Axis 1

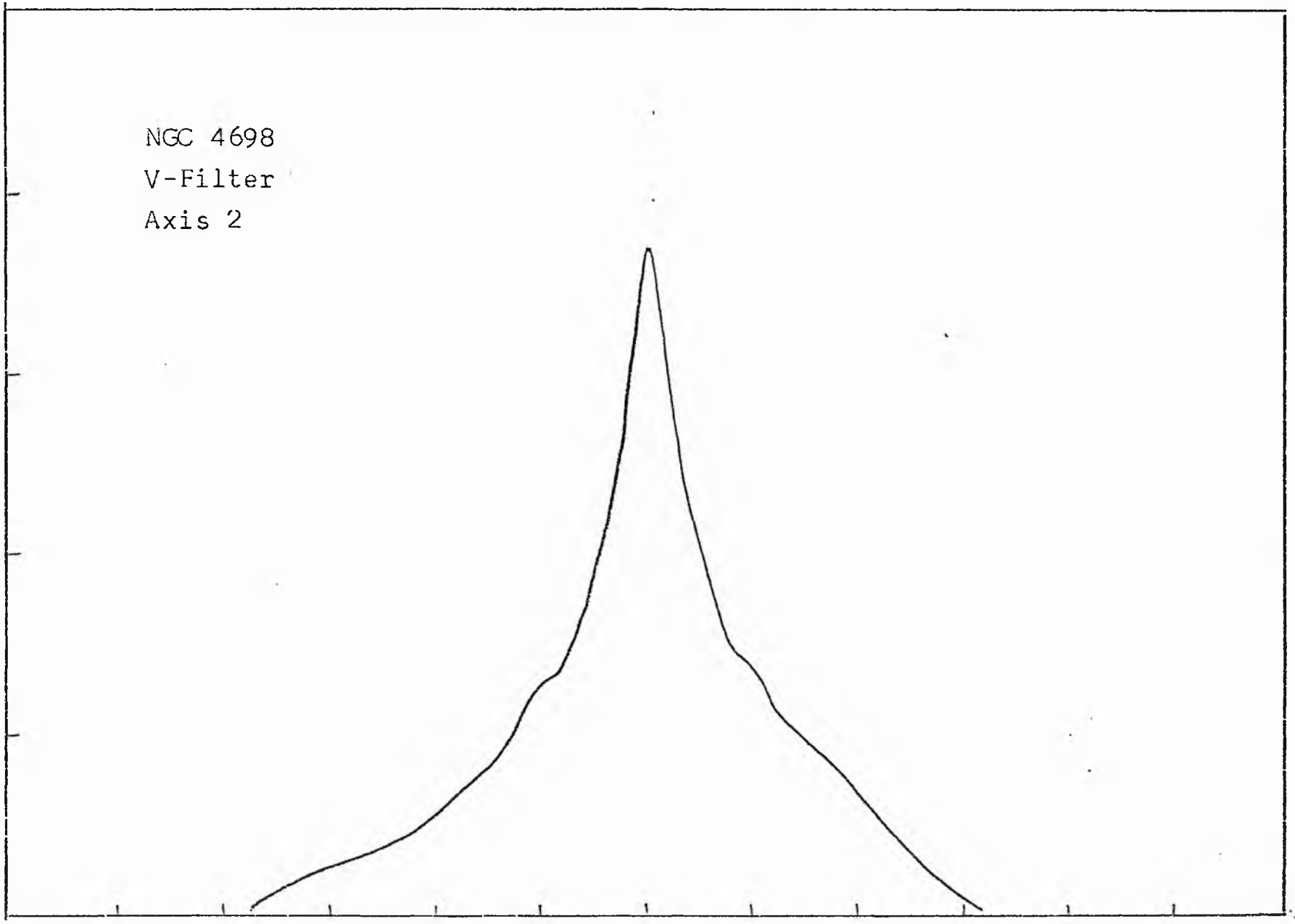
NGC 4698
V-Filter
Axis 2

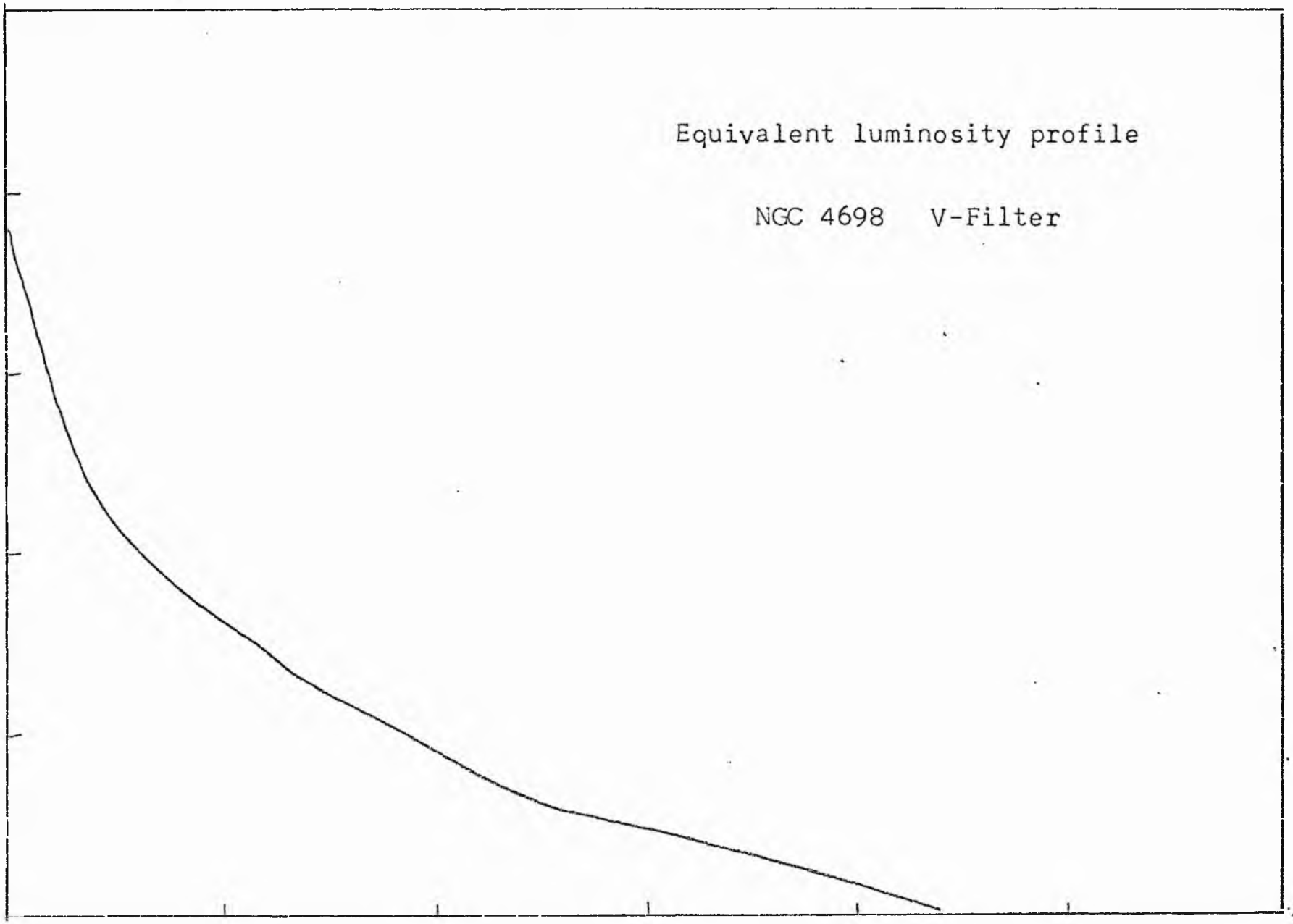
Equivalent luminosity profile
NGC 4698 V-Filter

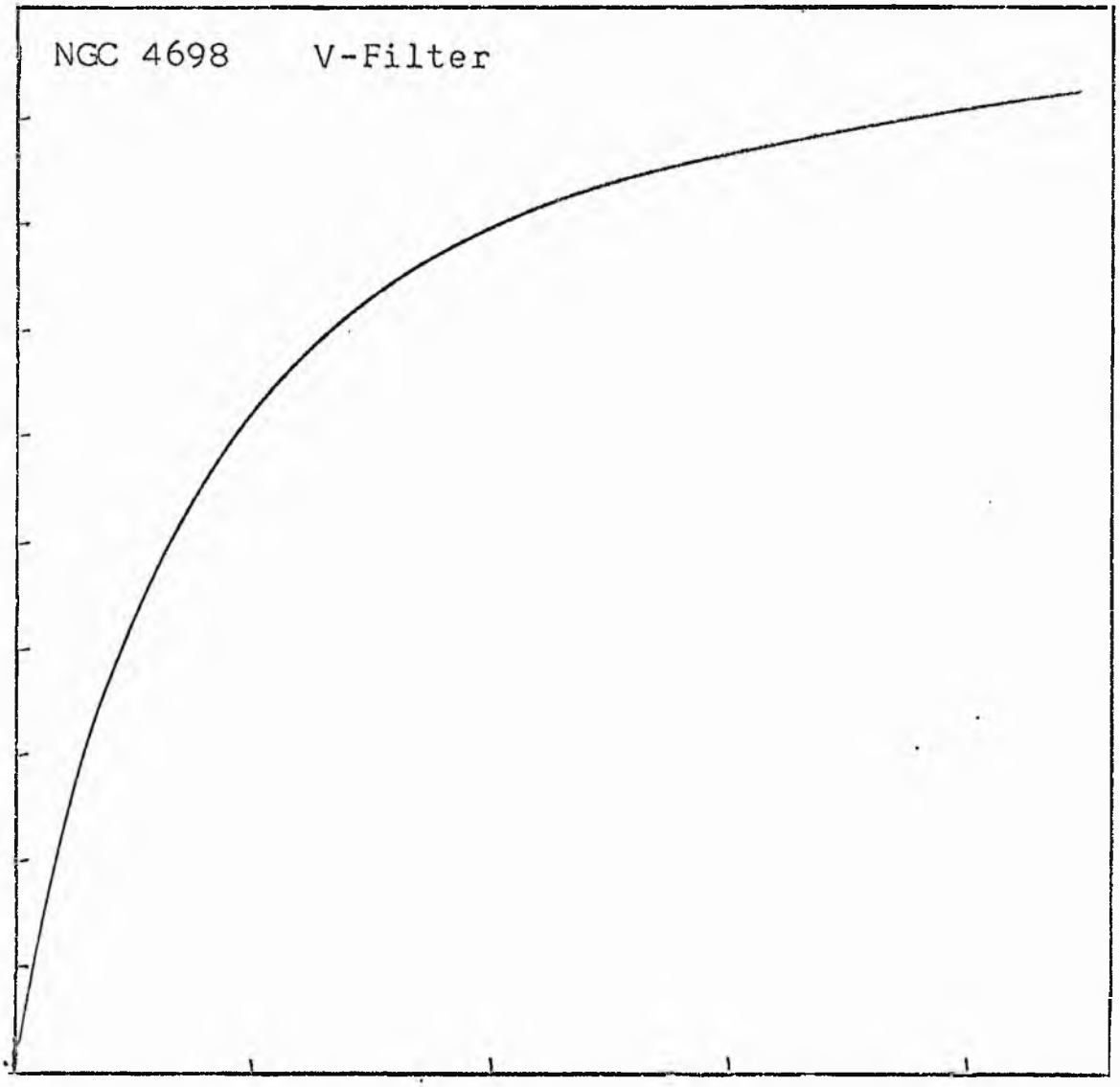

Relative integrated luminosity k(r) versus equivalent radius r*.

MEAN LUMINOSITY DISTRIBUTION IN NGC 4698
V COLOUR

LOG I	I	$\bar{I}$	R	AREA	ΔA	P	Σ P	K(R)	ρ	LOG J	μ
1.71	51.286		0.0	0.0			0.0	0.0	0.0	1.654	17.22
		50.702			0.50	25.4858					
1.70	50.119		0.40	0.50			25.49	0.00	0.01	1.644	17.25
		44.965			6.57	295.2346					
1.60	39.811		1.50	7.07			320.72	0.01	0.05	1.544	17.50
		35.717			6.79	242.3673					
1.50	31.623		2.10	13.85			563.09	0.02	0.07	1.444	17.75
		28.371			24.63	698.7739					
1.40	25.119		3.50	38.48			1261.86	0.05	0.11	1.344	18.00
		22.536			46.46	1047.0996					
1.30	19.953		5.20	84.95			2308.96	0.10	0.16	1.244	18.25
		17.901			51.90	929.0298					
1.20	15.849		6.60	136.85			3237.99	0.14	0.21	1.144	18.50
		14.219			69.27	984.9810					
1.10	12.589		8.10	206.12			4222.97	0.18	0.26	1.044	18.75
		11.295			65.60	740.8799					
1.00	10.000		9.30	271.72			4963.85	0.21	0.29	0.944	19.00
		8.972			61.58	552.4290					
0.90	7.943		10.30	333.29			5516.27	0.24	0.32	0.844	19.25
		7.126			60.79	433.2114					
0.80	6.310		11.20	394.08			5949.48	0.26	0.35	0.744	19.50
		5.661			104.68	592.5481					
0.70	5.012		12.60	498.76			6542.03	0.28	0.40	0.644	19.75
		4.496			161.76	727.3481					
0.60	3.981		14.50	660.52			7269.38	0.31	0.46	0.544	20.00
		3.572			123.75	441.9824					
0.50	3.162		15.80	784.27			7711.36	0.33	0.50	0.444	20.25
		2.837			199.96	567.3052					
0.40	2.512		17.70	984.23			8278.66	0.36	0.56	0.344	20.50
		2.254			198.14	446.5200					
0.30	1.995		19.40	1182.37			8725.18	0.38	0.61	0.244	20.75
		1.790			523.17	936.5078					
0.20	1.585		23.30	1705.54			9661.69	0.42	0.73	0.144	21.00
		1.422			1009.93	1436.0193					
0.10	1.259		29.40	2715.47			11097.71	0.48	0.93	0.044	21.25
		1.129			1002.17	1131.9043					
-0.00	1.000		34.40	3717.63			12229.61	0.53	1.08	-0.056	21.50
		0.897			987.50	885.9409					
-0.10	0.794		38.70	4705.13			13115.55	0.56	1.22	-0.156	21.75
		0.713			147.02	104.7747					
-0.20	0.631		39.30	4852.15			13220.32	0.57	1.24	-0.256	22.00
		0.566			1119.89	633.9336					
-0.30	0.501		43.60	5972.04			13854.25	0.60	1.37	-0.356	22.25
		0.450			1540.16	692.5271					
-0.40	0.398		48.90	7512.20			14546.78	0.63	1.54	-0.456	22.50
		0.357			1991.11	711.1577					
-0.50	0.316		55.00	9503.32			15257.93	0.66	1.73	-0.556	22.75
		0.284			2495.17	737.8977					
-0.60	0.251		61.80	11998.49			15965.83	0.69	1.95	-0.656	23.00
		0.225			1978.10	445.7781					
-0.70	0.200		66.70	13976.59			16411.61	0.71	2.10	-0.756	23.25
		0.179			4553.26	815.0659					
-0.80	0.158		76.80	18529.85			17226.67	0.74	2.42	-0.856	23.50
		0.142			2749.05	390.8884					
-0.90	0.126		82.30	21278.90			17617.55	0.76	2.59	-0.956	23.75
		0.113			4394.68	496.3613					
-1.00	0.100		90.40	25673.59			18113.91	0.78	2.85	-1.056	24.00
		0.090			4930.83	442.3752					
-1.10	0.079		98.70	30604.41			18556.29	0.80	3.11	-1.156	24.25
		0.071			3702.57	263.8604					
-1.20	0.063		104.50	34306.98			18820.15	0.81	3.29	-1.256	24.50
		0.057			6163.80	348.9160					
-1.30	0.050		113.50	40470.79			19169.06	0.82	3.58	-1.356	24.75
		0.045			7600.89	341.7725					
-1.40	0.040		123.70	48071.67			19510.83	0.84	3.90	-1.456	25.00
		0.036			15901.49	567.9517					
-1.50	0.032		142.70	63973.16			20078.78	0.86	4.50	-1.556	25.25
		0.028			17662.46	501.1913					
-1.60	0.025		161.20	81635.62			20579.88	0.88	5.08	-1.656	25.50
		0.023			16010.31	360.8066					
-1.70	0.020		176.30	97645.94			20940.68	0.90	5.56	-1.756	25.75
		0.018			16123.94	288.6331					
-1.80	0.016		190.30	113769.87			21229.32	0.91	6.00	-1.856	26.00
		0.014			22671.25	322.3674					
-1.90	0.013		208.40	136441.12			21551.68	0.93	6.57	-1.956	26.25
		0.011			16858.56	190.4132					
-2.00	0.010		220.90	153299.69			21742.09	0.93	6.96	-2.056	26.50
$-\infty$							23262.00	(1)			∞

PHOTOMETRIC PARAMETERS OF NGC 4698

V -FILTER

Total luminosity	L_T	= 6.46
Total apparent magnitude	m_T	= 10.60
Apparent central surface brightness	μ_o	= 17.22
Major axis at threshold	$2a_m$	= 9.25
Minor axis at threshold	$2b_m$	= 6.05
Major axis at μ=25.0 mag sec^{-2}	2a(25)	= 5.67
Luminosity within μ=25.0 mag sec^{-2}	k(25)	= 0.84
Gradient of exponential component	G(a)	= -0.23
Equivalent gradient of exponential comp.	G(r*)	= -0.54
Equivalent gradient of reduced exp. comp.	G(ρ)	= -0.47

Parameters at k = ¼ :

Semi-major axis	a_1	= 0.21
Axis ratio	b/a	= 0.92
Equivalent radius	r_1*	= 0.19
Surface brightness	μ_1	= 19.37

Parameters at k = ½(effective) :

Semi-major axis	a_e	= 0.80
Axis ratio	b/a	= 0.56
Equivalent radius	r_e*	= 0.53
Surface brightness	μ_e	= 21.35
Mean surface brightness	μ_e'	= 11.22

Parameters at k = ¾ :

Semi-major axis	a_3	= 1.83
Axis ratio	b/a	= 0.52
Equivalent radius	r_3*	= 1.33
Surface brightness	μ_3	= 23.62
Concentration indices	C_{21}	= 2.91
	C_{32}	= 2.51

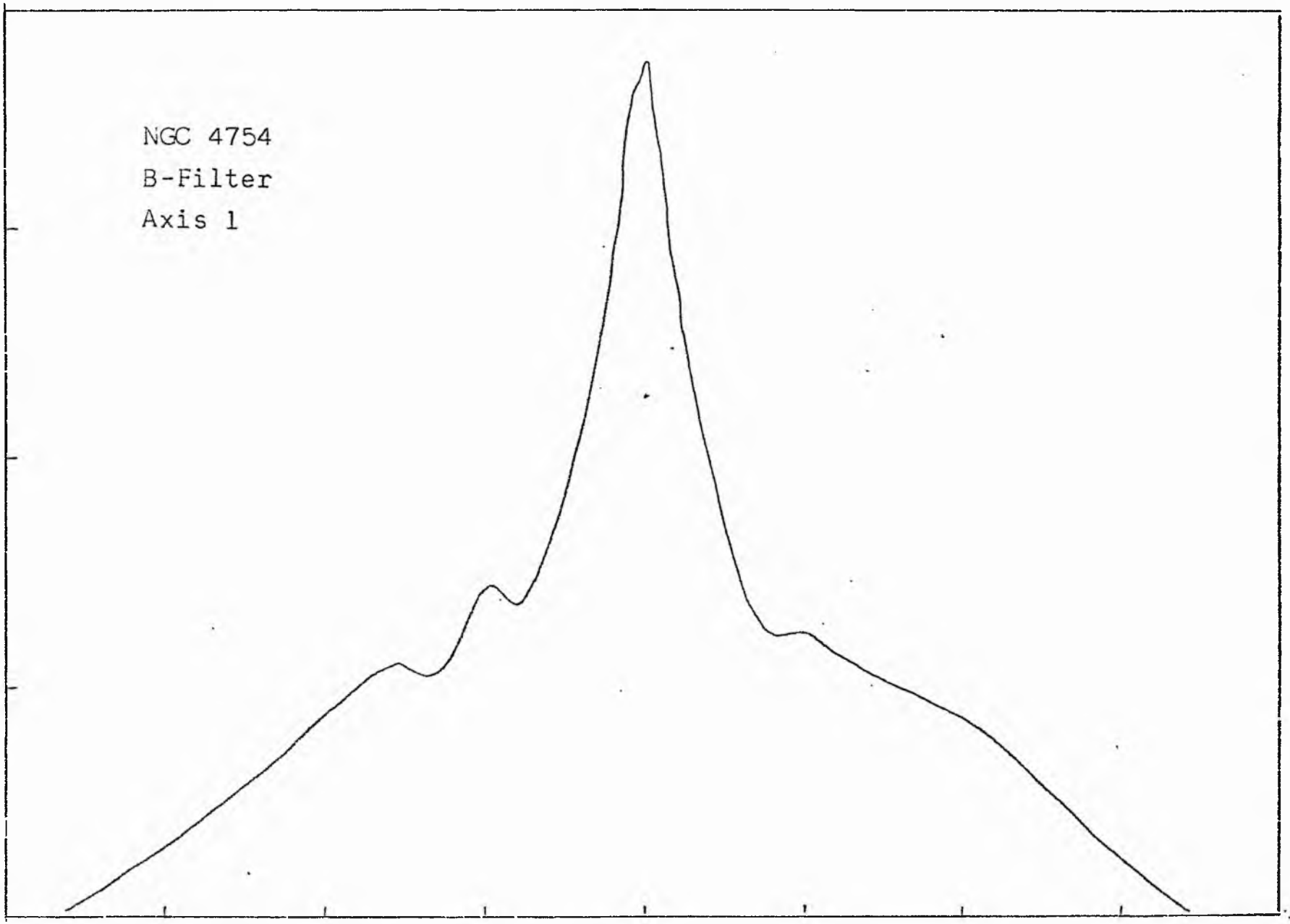
NGC 4754
B-Filter
Axis 1

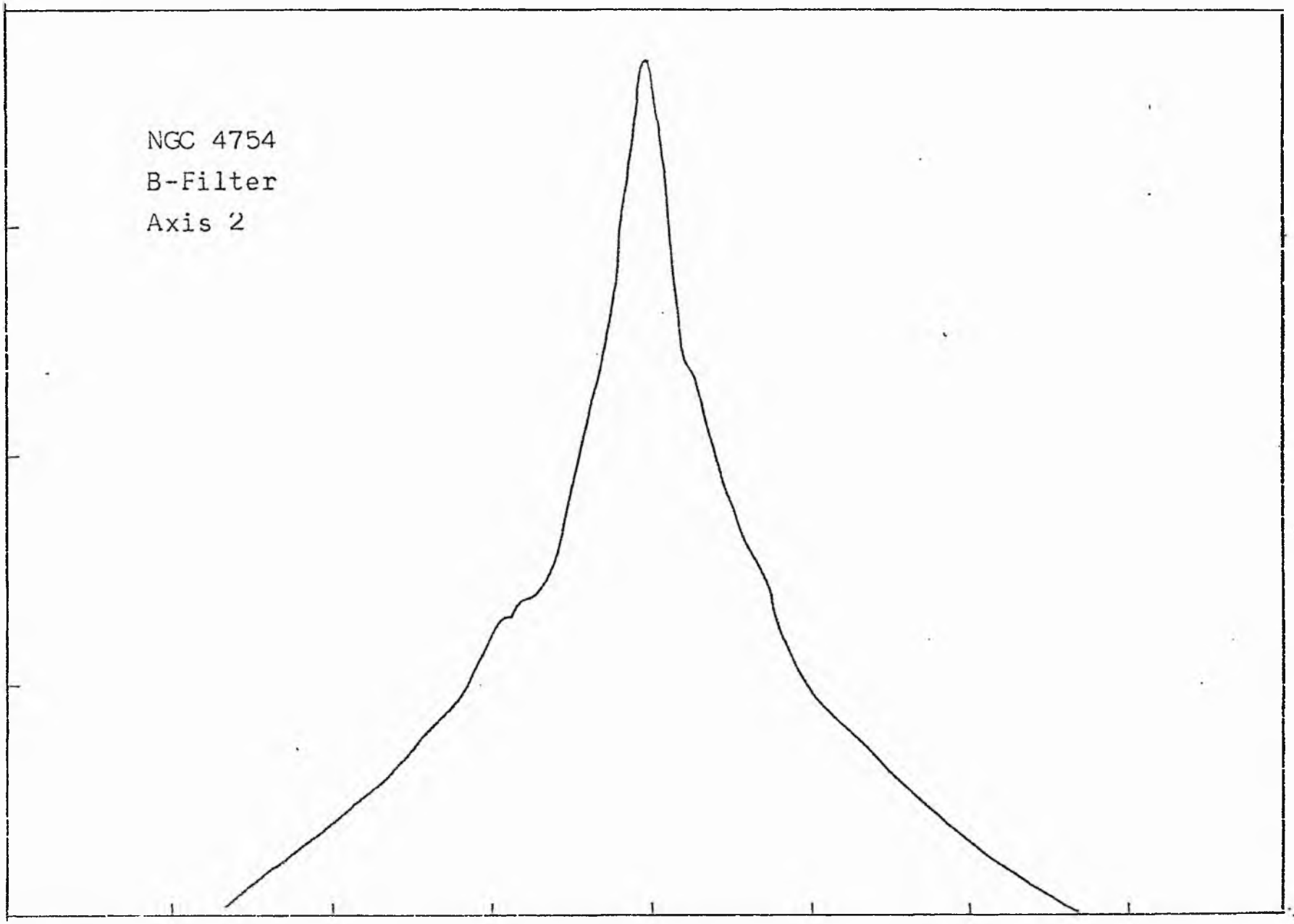
NGC 4754
B-Filter
Axis 2

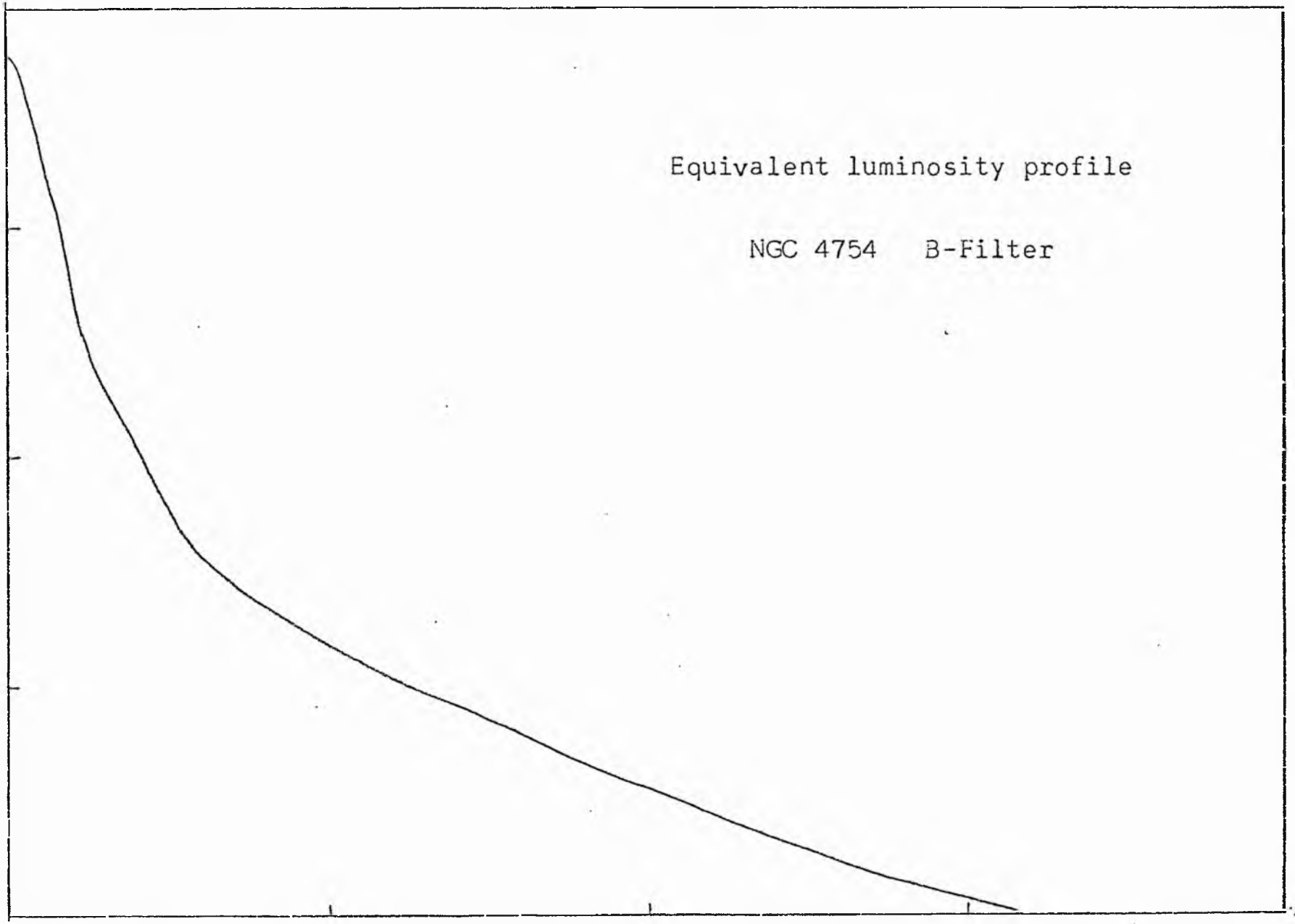
Equivalent luminosity profile
NGC 4754 B-Filter

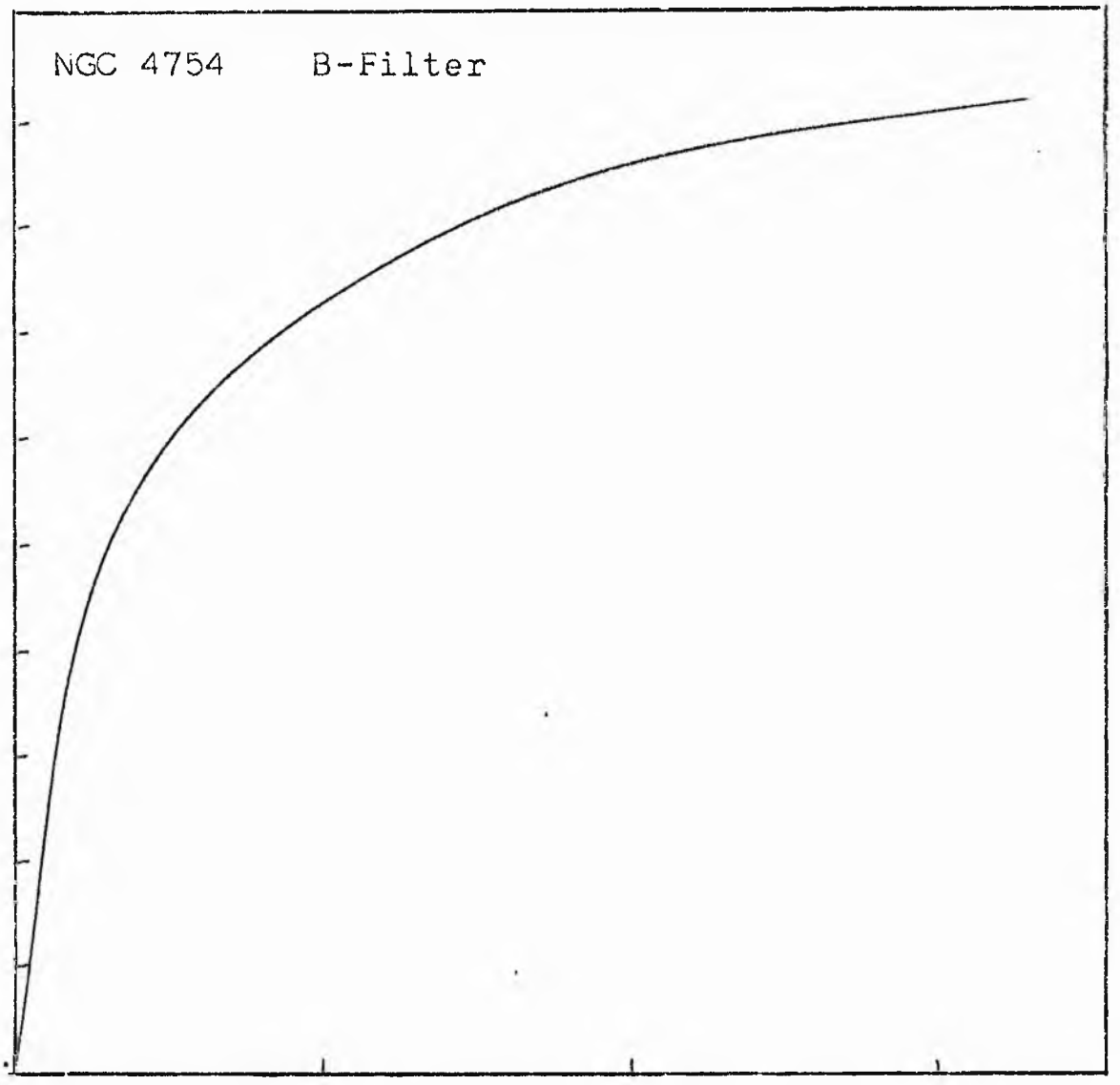

Relative integrated luminosity k(r) versus equivalent radius r*.

MEAN LUMINOSITY DISTRIBUTION IN NGC 4754
B COLOUR

LOG I	I	T	R	AREA	ΔA	P	ΣP	K(R)	ρ	LOG J	μ
1.72	52.481		0.0	0.0			0.0	0.0	0.0	1.411	17.45
		51.300			12.69	651.1128					
1.70	50.119		2.01	12.69			651.11	0.05	0.13	1.391	17.50
		44.965			10.04	451.4690					
1.60	39.811		2.69	22.73			1102.58	0.08	0.17	1.291	17.75
		35.717			5.73	204.6656					
1.50	31.623		3.01	28.46			1307.25	0.10	0.19	1.191	18.00
		28.371			32.08	910.1875					
1.40	25.119		4.39	60.55			2217.43	0.16	0.28	1.091	18.25
		22.536			31.40	707.6965					
1.30	19.953		5.41	91.95			2925.13	0.21	0.34	0.991	18.50
		17.901			40.38	722.7534					
1.20	15.849		6.49	132.32			3647.88	0.27	0.41	0.891	18.75
		14.219			32.81	466.4661					
1.10	12.589		17.25	165.13			4114.35	0.30	0.46	0.791	19.00
		11.295			58.66	662.5039					
1.00	10.000		8.44	223.79			4776.85	0.35	0.54	0.691	19.25
		8.972			39.81	357.1609					
0.90	7.943		9.16	263.60			5134.01	0.37	0.58	0.591	19.50
		7.126			1.73	12.3233					
0.80	6.310		9.19	265.33			5146.33	0.38	0.58	0.491	19.75
		5.661			40.10	226.9818					
0.70	5.012		9.86	305.42			5373.31	0.39	0.63	0.391	20.00
		4.496			72.64	326.6113					
0.60	3.981		10.97	378.06			5699.92	0.42	0.70	0.291	20.25
		3.572			138.27	493.8386					
0.50	3.162		12.82	516.33			6193.76	0.45	0.81	0.191	20.50
		2.837			123.40	350.1033					
0.40	2.512		14.27	639.73			6543.86	0.48	0.91	0.091	20.75
		2.254			152.50	343.6628					
0.30	1.995		15.88	792.23			6887.52	0.50	1.01	-0.009	21.00
		1.790			189.78	339.7126					
0.20	1.585		17.68	982.01			7227.23	0.53	1.12	-0.109	21.25
		1.422			282.18	401.2349					
0.10	1.259		20.06	1264.19			7628.46	0.56	1.27	-0.209	21.50
		1.129			295.29	333.5212					
-0.00	1.000		22.28	1559.48			7961.98	0.58	1.42	-0.309	21.75
		0.897			303.24	272.0527					
-0.10	0.794		24.35	1862.72			8234.04	0.60	1.55	-0.409	22.00
		0.713			100.78	71.8174					
-0.20	0.631		25.00	1963.50			8305.85	0.61	1.59	-0.509	22.25
		0.566			71.32	40.3725					
-0.30	0.501		25.45	2034.82			8346.22	0.61	1.62	-0.609	22.50
		0.450			612.73	275.5117					
-0.40	0.398		29.03	2647.55			8621.73	0.63	1.84	-0.709	22.75
		0.357			928.80	331.7354					
-0.50	0.316		33.74	3576.35			8953.47	0.65	2.14	-0.809	23.00
		0.284			1347.68	382.3472					
-0.60	0.251		39.59	4924.03			9335.81	0.68	2.52	-0.909	23.25
		0.225			1889.34	425.7751					
-0.70	0.200		46.57	6813.37			9761.59	0.71	2.96	-1.009	23.50
		0.179			2579.68	461.7808					
-0.80	0.158		54.68	9393.05			10223.36	0.75	3.47	-1.109	23.75
		0.142			2105.96	299.4478					
-0.90	0.126		60.50	11499.02			10522.81	0.77	3.84	-1.209	24.00
		0.113			2185.76	246.8728					
-1.00	0.100		66.00	13684.78			10769.68	0.79	4.19	-1.309	24.25
		0.090			2828.22	253.7372					
-1.10	0.079		72.50	16513.00			11023.41	0.80	4.61	-1.409	24.50
		0.071			1394.87	99.4041					
-1.20	0.063		75.50	17907.86			11122.82	0.81	4.80	-1.509	24.75
		0.057			5598.32	316.9055					
-1.30	0.050		86.50	23506.18			11439.72	0.83	5.50	-1.609	25.00
		0.045			6053.06	272.1748					
-1.40	0.040		97.00	29559.25			11711.89	0.85	6.16	-1.709	25.25
		0.036			5473.77	195.5062					
-1.50	0.032		105.60	35033.02			11907.39	0.87	6.71	-1.809	25.50
		0.028			7751.98	219.9312					
-1.60	0.025		116.70	42785.00			12127.32	0.88	7.42	-1.909	25.75
		0.023			6932.71	156.2348					
-1.70	0.020		125.80	49717.71			12283.56	0.90	7.99	-2.009	26.00
		0.018			8988.88	160.9092					
-1.80	0.016		136.70	58706.59			12444.46	0.91	8.69	-2.109	26.25
		0.014			9364.91	133.1617					
-1.90	0.013		147.20	68071.50			12577.62	0.92	9.35	-2.209	26.50
		0.011			12353.25	139.5268					
-2.00	0.010		160.00	80424.75			12717.15	0.93	10.17	-2.309	26.75
∞							13717.00	(1)			∞

PHOTOMETRIC PARAMETERS OF NGC 4754

B-FILTER

Total luminosity ..... L_T = 3.81

Total apparent magnitude ..... m_T = 11.43

Apparent central surface brightness ..... μ_o = 17.45

Major axis at threshold ..... $2a_m$ = 5.68

Minor axis at threshold ..... $2b_m$ = 4.37

Major axis at μ=25.0 mag sec^{-2} ..... 2a(25) = 3.53

Luminosity within μ=25.0 mag sec^{-2} ..... k(25) = 0.83

Gradient of exponential component ..... G(a) = -0.67

Equivalent gradient of exponential comp..... G(r*) = -0.62

Equivalent gradient of reduced exp. comp..... G(ρ) = -0.23

Parameters at k = ¼ :

- Semi-major axis ..... a_1 = 0.15
- Axis ratio ..... b/a = 0.77
- Equivalent radius ..... r_1* = 0.10
- Surface brightness ..... μ_1 = 18.67

Parameters at k = ½(effective) :

- Semi-major axis ..... a_e = 0.28
- Axis ratio ..... b/a = 0.88
- Equivalent radius ..... r_e* = 0.26
- Surface brightness ..... μ_e = 21.00
- Mean surface brightness ..... μ_e' = 10.50

Parameters at k = ¾ :

- Semi-major axis ..... a_3 = 0.96
- Axis ratio ..... b/a = 0.81
- Equivalent radius ..... r_3* = 0.93
- Surface brightness ..... μ_3 = 23.75

Concentration indices ..... C_{21} = 2.56, C_{32} = 3.55

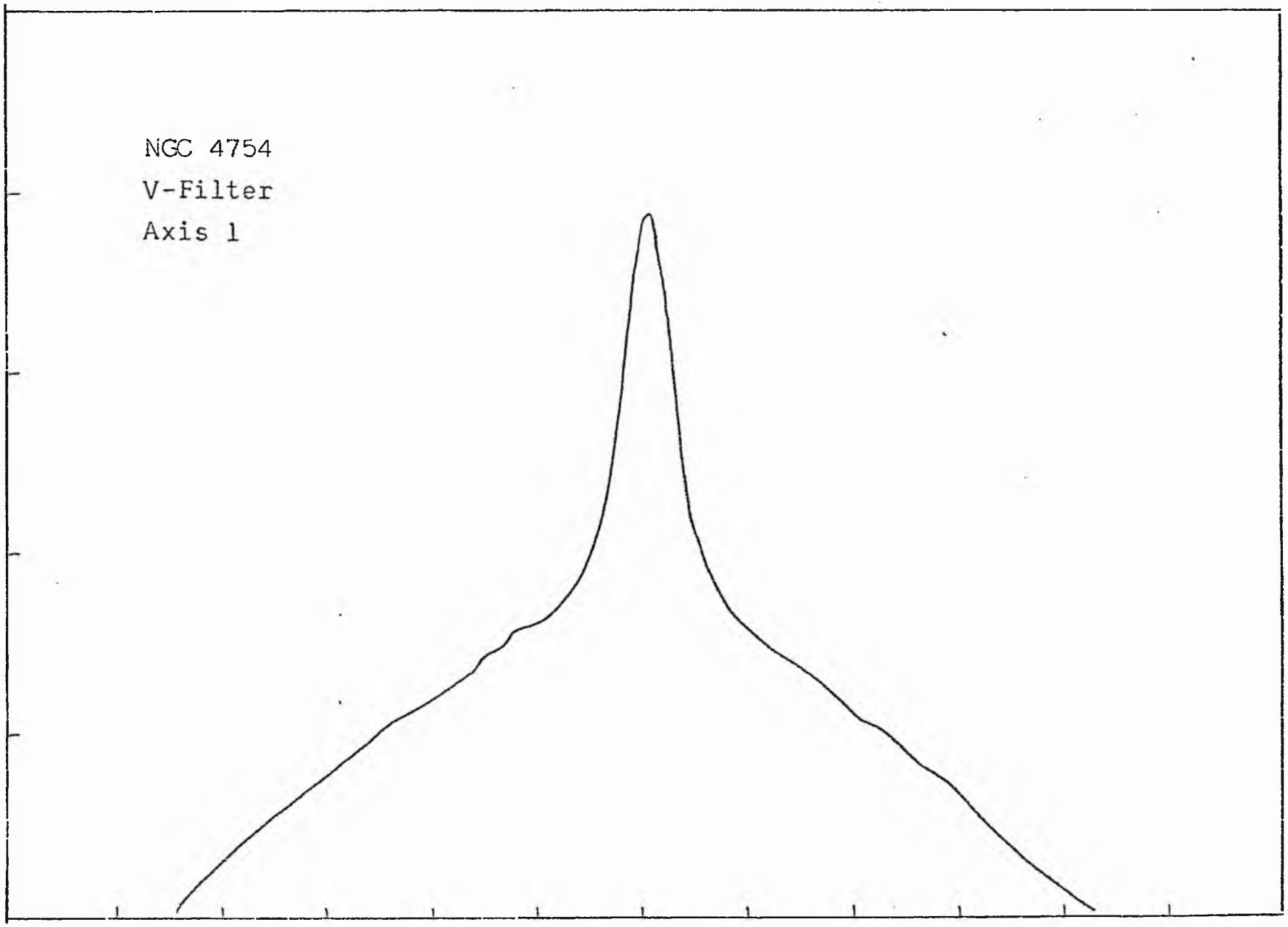
NGC 4754
V-Filter
Axis 1

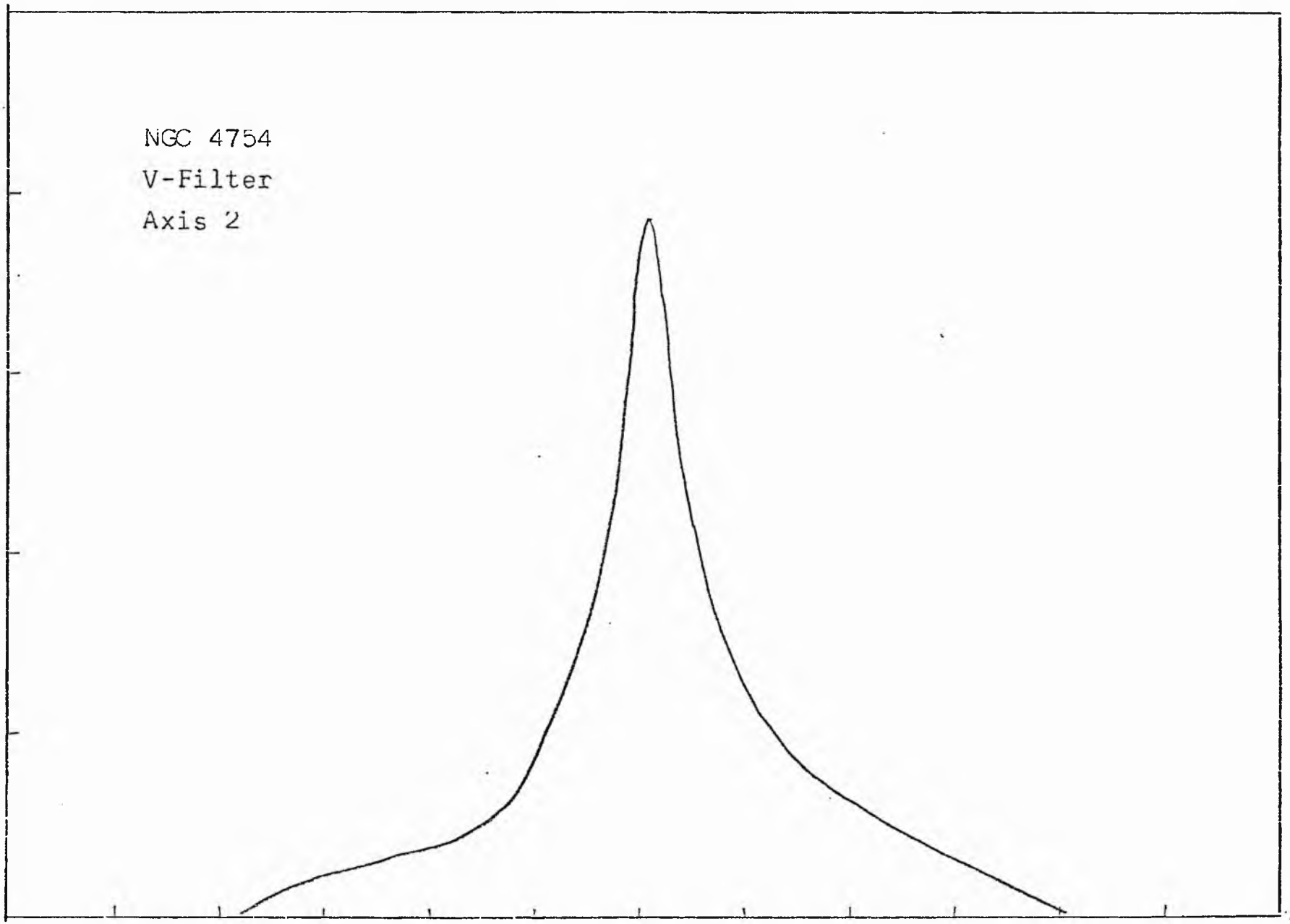
NGC 4754
V-Filter
Axis 2

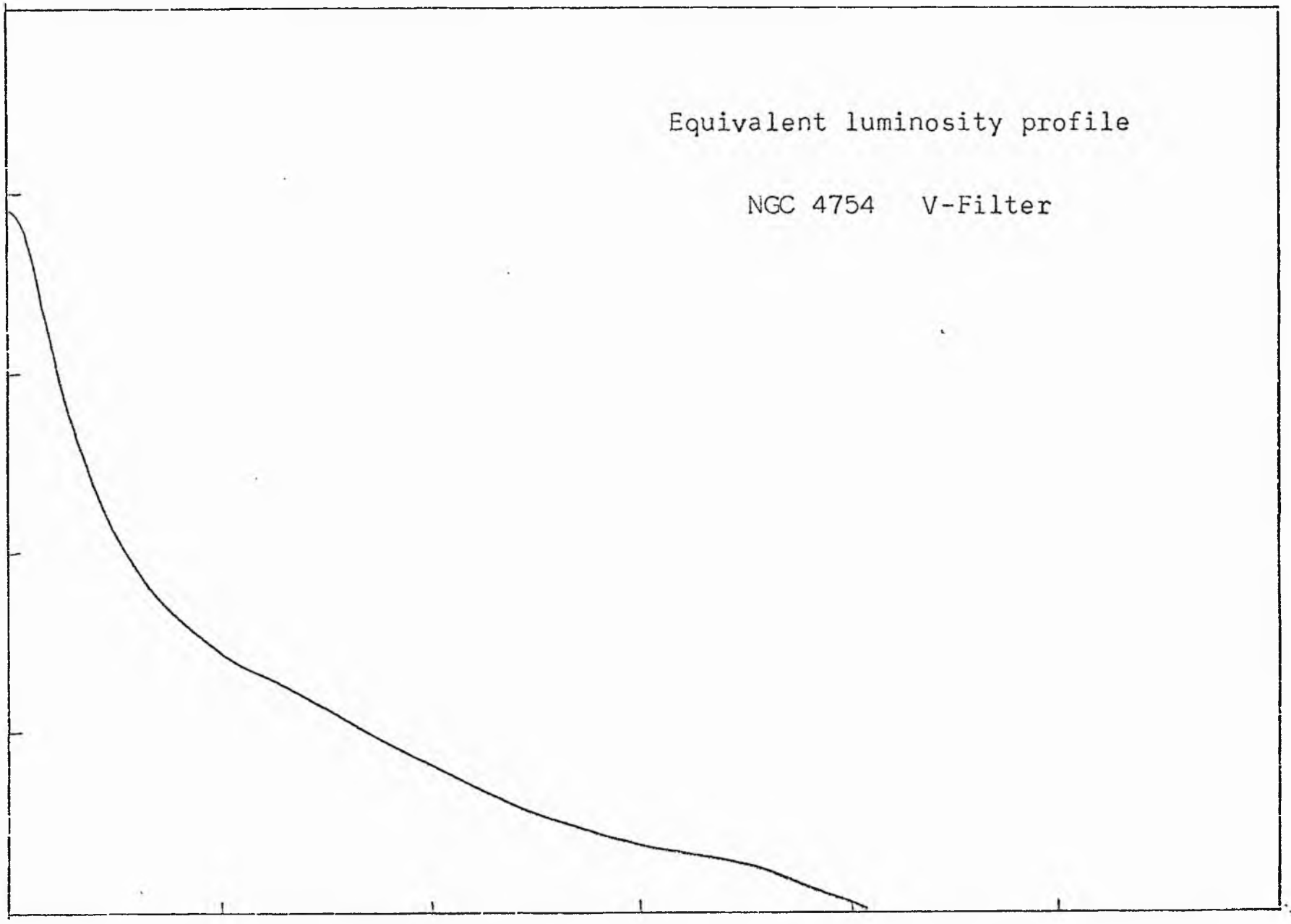
Equivalent luminosity profile
NGC 4754 V-Filter

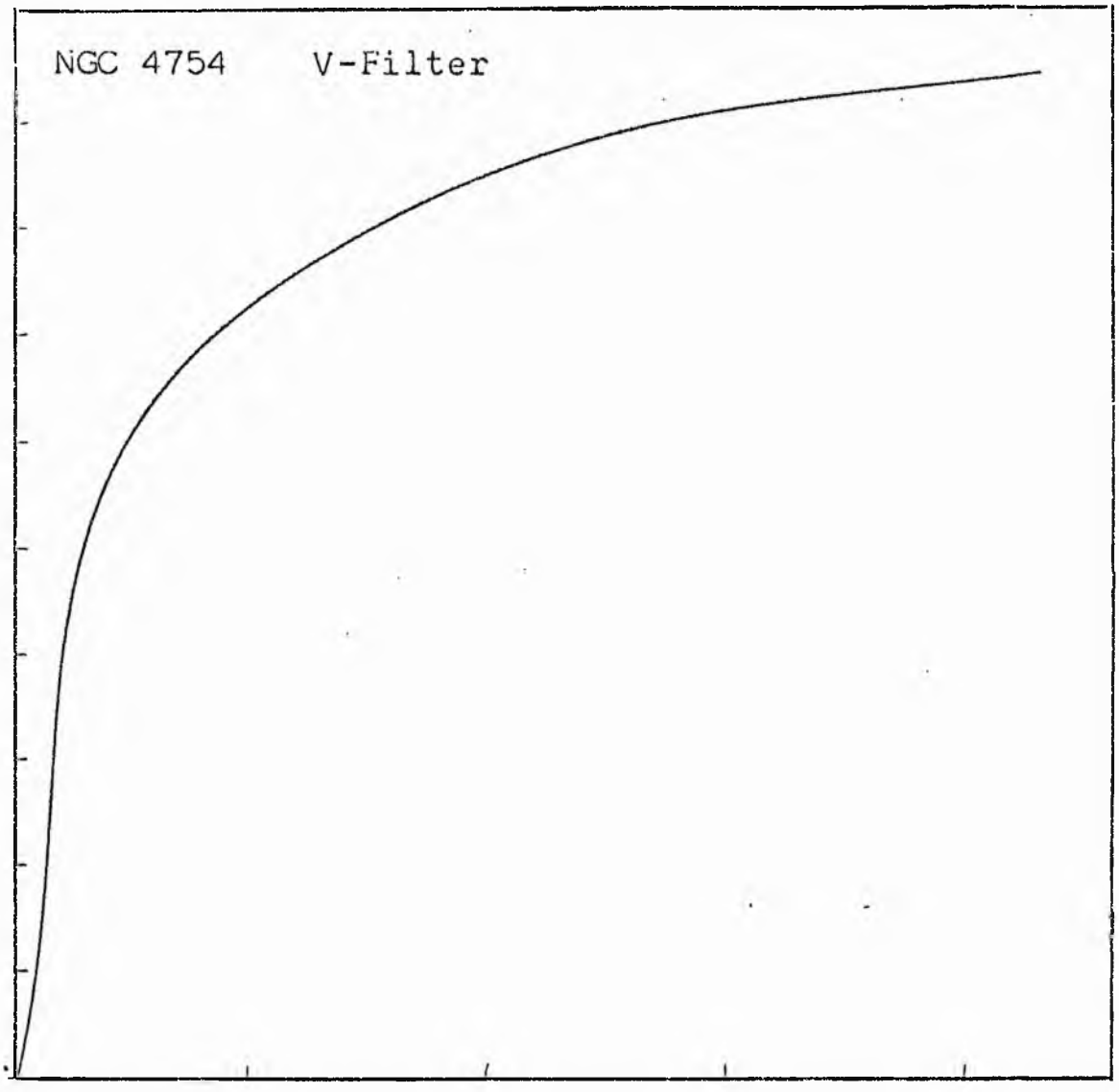

Relative integrated luminosity k(r) versus equivalent radius r*.

MEAN LUMINOSITY DISTRIBUTION IN NGC 4754
V COLOUR

LOG I	I	$\bar{I}$	R	AREA	Δ A	P	Σ P	K(R)	ρ	LOG J	μ
1.84	69.183		0.0	0.0			0.0	0.0	0.0	1.060	16.91
		66.139			13.85	916.3210					
1.80	63.096		2.10	13.85			916.32	0.03	0.15	1.020	17.01
		56.607			33.93	1920.6331					
1.70	50.119		3.90	47.78			2836.95	0.11	0.28	0.920	17.26
		44.965			24.60	1106.0662					
1.60	39.811		4.80	72.38			3943.02	0.15	0.34	0.820	17.51
		35.717			48.38	1727.9888					
1.50	31.623		6.20	120.76			5671.01	0.22	0.44	0.720	17.76
		28.371			109.43	3104.6870					
1.40	25.119		8.56	230.20			8775.69	0.34	0.61	0.620	18.01
		22.536			26.54	598.0959					
1.30	19.952		9.04	256.74			9373.79	0.36	0.64	0.520	18.26
		17.901			9.17	164.1213					
1.20	15.849		9.20	265.90			9537.91	0.36	0.65	0.420	18.51
		14.219			47.00	668.2849					
1.10	12.589		9.98	312.90			10206.19	0.39	0.71	0.320	18.76
		11.295			95.38	1077.2427					
1.00	10.000		11.40	408.28			11283.43	0.43	0.81	0.220	19.01
		8.972			139.11	1248.0332					
0.90	7.943		13.20	547.39			12531.46	0.48	0.93	0.120	19.26
		7.126			65.72	468.3794					
0.80	6.310		13.97	613.12			12999.84	0.50	0.99	0.020	19.51
		5.661			83.41	472.1743					
0.70	5.012		14.89	696.53			13472.01	0.51	1.05	-0.080	19.76
		4.496			97.70	439.2871					
0.60	3.981		15.90	794.23			13911.30	0.53	1.12	-0.180	20.01
		3.572			81.93	292.6343					
0.50	3.162		16.70	876.16			14203.93	0.54	1.18	-0.280	20.26
		2.837			210.71	597.7837					
0.40	2.512		18.60	1086.86			14801.71	0.57	1.32	-0.380	20.51
		2.254			325.09	732.6152					
0.30	1.995		21.20	1411.96			15534.32	0.59	1.50	-0.480	20.76
		1.790			293.58	525.5286					
0.20	1.585		23.30	1705.54			16059.85	0.61	1.65	-0.580	21.01
		1.422			180.20	256.2312					
0.10	1.259		24.50	1885.74			16316.08	0.62	1.73	-0.680	21.26
		1.129			189.25	213.7479					
-0.00	1.000		25.70	2074.99			16529.83	0.63	1.82	-0.780	21.51
		0.897			458.89	411.6985					
-0.10	0.794		28.40	2533.88			16941.52	0.65	2.01	-0.880	21.76
		0.713			583.36	415.7271					
-0.20	0.631		31.50	3117.25			17357.25	0.66	2.23	-0.980	22.01
		0.566			819.67	463.9895					
-0.30	0.501		35.40	3936.92			17821.24	0.68	2.50	-1.080	22.26
		0.450			1014.51	456.1697					
-0.40	0.398		39.70	4951.43			18277.41	0.70	2.81	-1.180	22.51
		0.357			1353.87	483.5540					
-0.50	0.316		44.80	6305.30			18760.96	0.72	3.17	-1.280	22.76
		0.284			3026.02	858.5013					
-0.60	0.251		54.50	9331.32			19619.46	0.75	3.86	-1.380	23.01
		0.225			2940.53	662.6655					
-0.70	0.200		62.50	12271.84			20282.12	0.77	4.42	-1.480	23.26
		0.179			2641.95	472.9258					
-0.80	0.158		68.90	14913.79			20755.05	0.79	4.87	-1.580	23.51
		0.142			2522.84	358.7219					
-0.90	0.126		74.50	17436.62			21113.77	0.81	5.27	-1.680	23.76
		0.113			8293.80	936.7493					
-1.00	0.100		90.50	25730.43			22050.51	0.84	6.40	-1.780	24.01
		0.090			2981.70	267.5066					
-1.10	0.079		95.60	28712.13			22318.02	0.85	6.76	-1.880	24.26
		0.071			2265.49	161.4482					
-1.20	0.063		99.30	30977.62			22479.46	0.86	7.02	-1.980	24.51
		0.057			6074.19	343.8423					
-1.30	0.050		108.60	37051.81			22823.30	0.87	7.68	-2.080	24.76
		0.045			4785.27	215.1684					
-1.40	0.040		115.40	41837.08			23038.47	0.88	8.16	-2.180	25.01
		0.036			13317.51	475.6587					
-1.50	0.032		132.50	55154.59			23514.12	0.90	9.37	-2.280	25.26
		0.028			14779.22	419.2998					
-1.60	0.025		149.20	69933.81			23933.42	0.91	10.56	-2.380	25.51
		0.023			23873.62	538.0120					
-1.70	0.020		172.80	93807.44			24471.43	0.93	12.22	-2.480	25.76
		0.018			8319.69	148.9297					
-1.80	0.016		180.30	102127.12			24620.36	0.94	12.76	-2.580	26.01
		0.014			16964.62	241.2233					
-1.90	0.013		194.70	119091.75			24861.59	0.95	13.77	-2.680	26.26
		0.011			16826.12	190.0464					
-2.00	0.010		208.00	135917.87			25051.63	0.96	14.71	-2.780	26.51
$-\infty$							26181.00	(1)			∞

PHOTOMETRIC PARAMETERS OF NGC 4754

V-FILTER

Total luminosity	L_T	= 7.27
Total apparent magnitude	m_T	= 10.46
Apparent central surface brightness	μ_o	= 16.91
Major axis at threshold	$2a_m$	= 7.28
Minor axis at threshold	$2b_m$	= 6.48
Major axis at μ=25.0 mag sec^{-2}	2a(25)	= 5.41
Luminosity within μ=25.0 mag sec^{-2}	k(25)	= 0.88
Gradient of exponential component	G(a)	= -0.50
Equivalent gradient of exponential comp.	G(r*)	= -0.51
Equivalent gradient of reduced exp. comp.	G(ρ)	= -0.17
Parameters at k = ¼ :		
Semi-major axis	a_1	= 0.13
Axis ratio	b/a	= 0.93
Equivalent radius	r_1*	= 0.11
Surface brightness	μ_1	= 17.82
Parameters at k = ½(effective) :		
Semi-major axis	a_e	= 0.25
Axis ratio	b/a	= 0.93
Equivalent radius	r_e*	= 0.24
Surface brightness	μ_e	= 19.51
Mean surface brightness	μ_e'	= 9.36
Parameters at k = ¾ :		
Semi-major axis	a_3	= 1.21
Axis ratio	b/a	= 0.49
Equivalent radius	r_3*	= 0.91
Surface brightness	μ_3	= 23.01
Concentration indices	C_{21}	= 2.05
	C_{32}	= 3.87

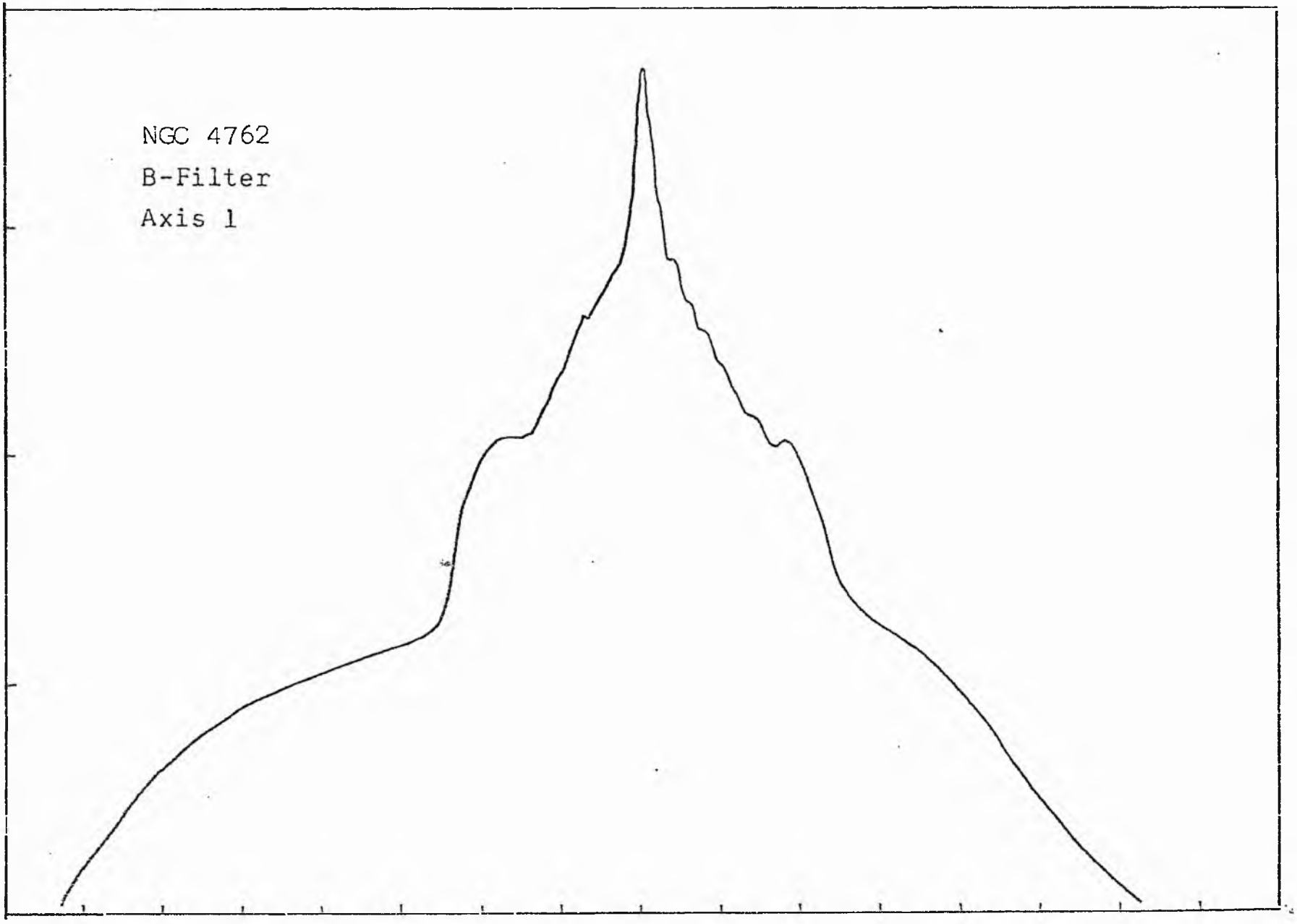
NGC 4762
B-Filter
Axis 1

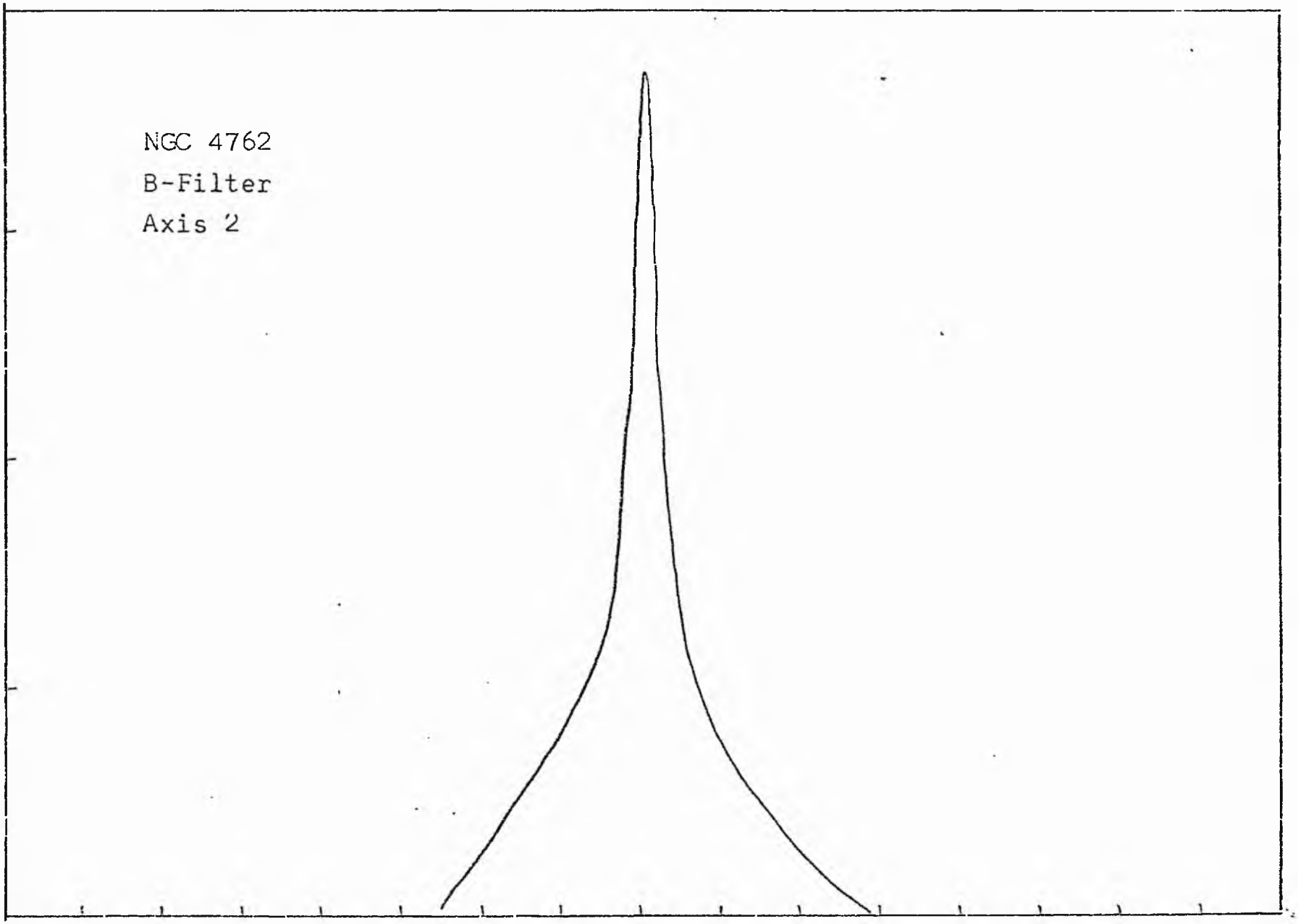
NGC 4762
B-Filter
Axis 2

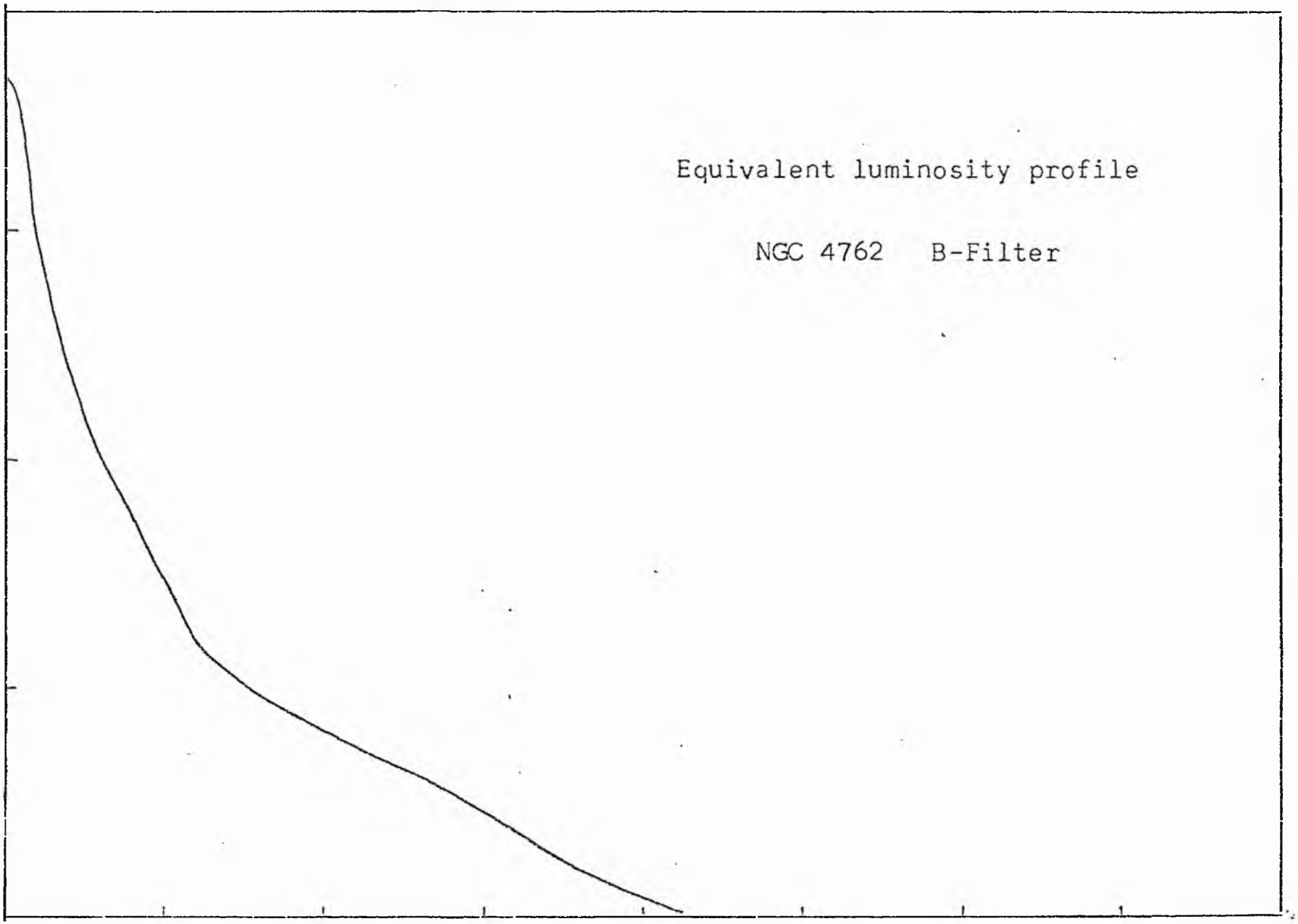
Equivalent luminosity profile
NGC 4762 B-Filter

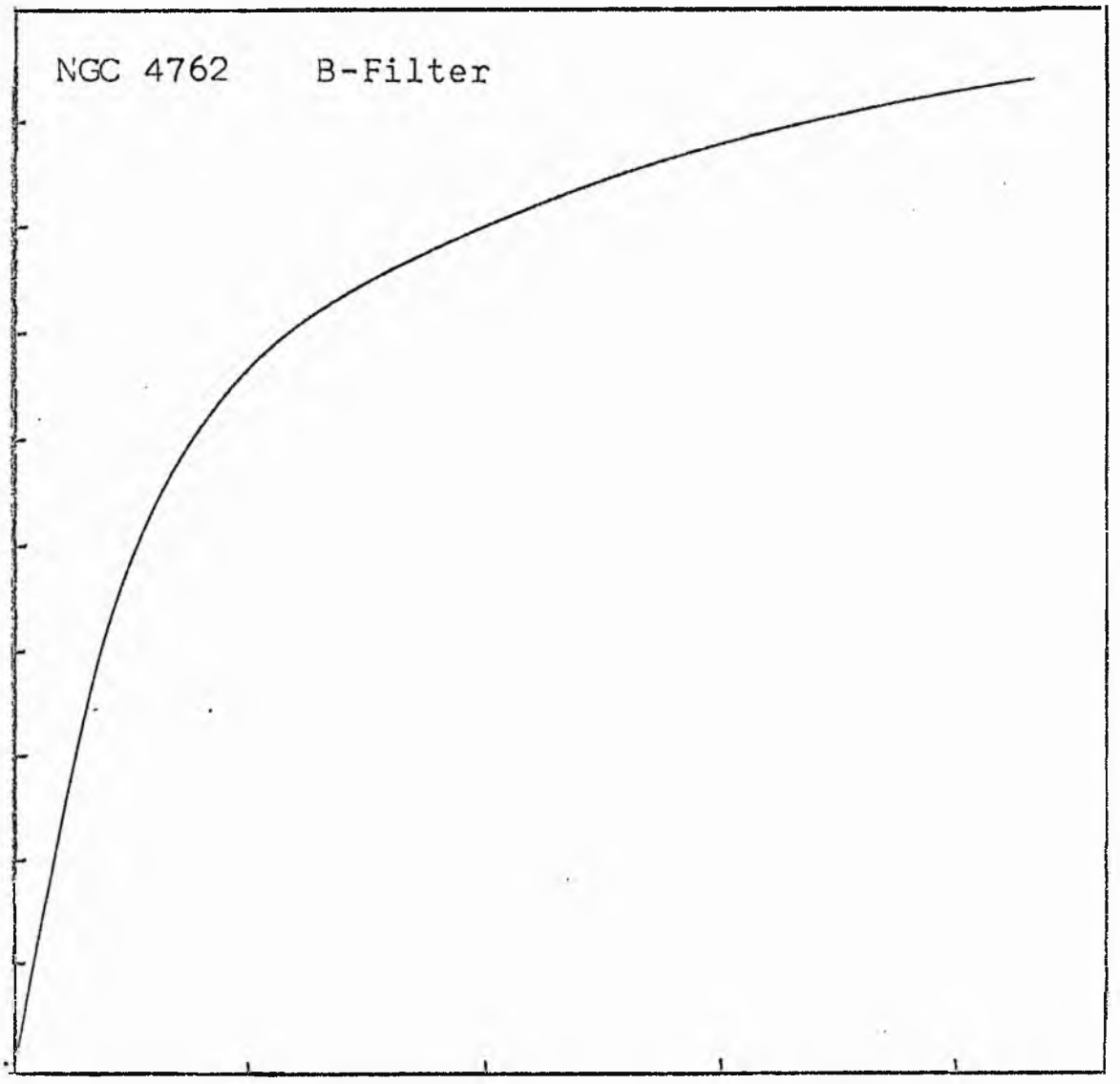

Relative integrated luminosity k(r) versus equivalent radius r*.

MEAN LUMINOSITY DISTRIBUTION IN NGC 4762
B COLOUR

LOG I	I	$\bar{I}$	R	AREA	ΔA	P	ΣP	K(R)	ρ'	LOG J	μ
1.65	44.668		0.0	0.0			0.0	0.0	0.0	1.518	17.73
		42.239			16.05	677.7734					
1.60	39.811		2.26	16.05			677.77	0.03	0.08	1.468	17.86
		35.717			16.33	583.0850					
1.50	31.623		3.21	32.37			1260.86	0.06	0.12	1.368	18.11
		28.371			39.11	1109.5520					
1.40	25.119		4.77	71.48			2370.41	0.12	0.18	1.268	18.36
		22.536			16.77	377.8552					
1.30	19.953		5.30	88.25			2748.27	0.14	0.20	1.168	18.61
		17.901			13.82	247.4418					
1.20	15.849		5.70	102.07			2995.71	0.15	0.21	1.068	18.86
		14.219			7.29	103.6350					
1.10	12.589		5.90	109.36			3099.34	0.15	0.22	0.968	19.11
		11.295			128.43	1450.5408					
1.00	10.000		8.70	237.79			4549.88	0.22	0.32	0.868	19.36
		8.972			11.06	99.2115					
0.90	7.943		8.90	248.85			4649.09	0.23	0.33	0.768	19.61
		7.126			97.52	694.9297					
0.80	6.310		10.50	346.36			5344.02	0.26	0.39	0.668	19.86
		5.661			144.51	818.0442					
0.70	5.012		12.50	490.87			6162.07	0.30	0.47	0.568	20.11
		4.496			107.41	482.9670					
0.60	3.981		13.80	598.28			6645.03	0.33	0.51	0.468	20.36
		3.572			185.98	664.2646					
0.50	3.162		15.80	784.27			7309.29	0.36	0.59	0.368	20.61
		2.837			299.09	848.5488					
0.40	2.512		18.57	1083.36			8157.84	0.40	0.69	0.268	20.86
		2.254			211.26	476.0789					
0.30	1.995		20.30	1294.62			8633.92	0.42	0.76	0.168	21.11
		1.790			381.77	683.3879					
0.20	1.585		23.10	1676.38			9317.30	0.46	0.86	0.068	21.36
		1.422			839.68	1193.9485					
0.10	1.259		28.30	2516.07			10511.25	0.52	1.06	-0.032	21.61
		1.129			761.52	860.1055					
-0.00	1.000		32.30	3277.59			11371.36	0.56	1.20	-0.132	21.86
		0.897			703.94	631.5437					
-0.10	0.794		35.60	3981.53			12002.90	0.59	1.33	-0.232	22.11
		0.713			365.93	260.7764					
-0.20	0.631		37.20	4347.46			12263.67	0.60	1.39	-0.332	22.36
		0.566			780.12	441.6028					
-0.30	0.501		40.40	5127.58			12705.27	0.62	1.51	-0.432	22.61
		0.450			817.10	367.4038					
-0.40	0.398		43.50	5944.68			13072.68	0.64	1.62	-0.532	22.86
		0.357			1054.29	376.5559					
-0.50	0.316		47.20	6998.96			13449.23	0.66	1.76	-0.632	23.11
		0.284			1076.46	305.4006					
-0.60	0.251		50.70	8075.43			13754.63	0.68	1.89	-0.732	23.36
		0.225			1290.16	290.7451					
-0.70	0.200		54.60	9365.59			14045.37	0.69	2.04	-0.832	23.61
		0.179			1422.51	254.6396					
-0.80	0.158		58.60	10788.10			14300.01	0.70	2.19	-0.932	23.86
		0.142			2772.55	394.2300					
-0.90	0.126		65.70	13560.65			14694.23	0.72	2.45	-1.032	24.11
		0.113			4489.80	507.1045					
-1.00	0.100		75.80	18050.45			15201.34	0.75	2.83	-1.132	24.36
		0.090			5947.42	533.5798					
-1.10	0.079		87.40	23997.87			15734.91	0.77	3.26	-1.232	24.61
		0.071			7733.00	551.0862					
-1.20	0.063		100.50	31730.87			16286.00	0.80	3.75	-1.332	24.86
		0.057			10542.40	596.7766					
-1.30	0.050		116.00	42273.27			16882.77	0.83	4.33	-1.432	25.11
		0.045			12465.84	560.5242					
-1.40	0.040		132.00	54739.11			17443.30	0.86	4.92	-1.532	25.36
		0.036			9054.86	323.4111					
-1.50	0.032		142.50	63793.97			17766.71	0.87	5.32	-1.632	25.61
		0.028			5671.91	160.9175					
-1.60	0.025		148.70	69465.87			17927.62	0.88	5.55	-1.732	25.86
		0.023			17940.25	404.2996					
-1.70	0.020		166.80	87406.12			18331.92	0.90	6.22	-1.832	26.11
		0.018			19186.94	343.4636					
-1.80	0.016		184.20	106593.06			18675.38	0.92	6.87	-1.932	26.36
		0.014			13602.25	193.4134					
-1.90	0.013		195.60	120195.31			18868.79	0.93	7.30	-2.032	26.61
		0.011			16507.81	186.4515					
-2.00	0.010		208.60	136703.12			19055.24	0.94	7.78	-2.132	26.86
- ∞							20355.00	(1)			∞

PHOTOMETRIC PARAMETERS OF NGC 4762

B-FILTER

Total luminosity	L_T	= 5.65
Total apparent magnitude	m_T	= 11.09
Apparent central surface brightness	μ_o	= 17.73
Major axis at threshold	$2a_m$	= 11.01
Minor axis at threshold	$2b_m$	= 4.06
Major axis at μ=25.0 mag sec^{-2}	2a(25)	= 7.92
Luminosity within μ=25.0 mag sec^{-2}	k(25)	= 0.82
Gradient of exponential component	G(a)	= -0.44
Equivalent gradient of exponential comp.	G(r*)	= -0.48
Equivalent gradient of reduced exp. comp.	G(ρ)	= -0.84

Parameters at k = ¼ :

Semi-major axis	a_1	= 0.30
Axis ratio	b/a	= 0.44
Equivalent radius	r_1*	= 0.17
Surface brightness	μ_1	= 19.78

Parameters at k = ½(effective) :

Semi-major axis	a_e	= 1.12
Axis ratio	b/a	= 0.25
Equivalent radius	r_e*	= 0.45
Surface brightness	μ_e	= 21.53
Mean surface brightness	μ_e'	= 11.34

Parameters at k = ¾ :

Semi-major axis	a_3	= 2.83
Axis ratio	b/a	= 0.26
Equivalent radius	r_3*	= 1.29
Surface brightness	μ_3	= 24.36
Concentration indices	C_{21}	= 2.71
	C_{32}	= 2.88

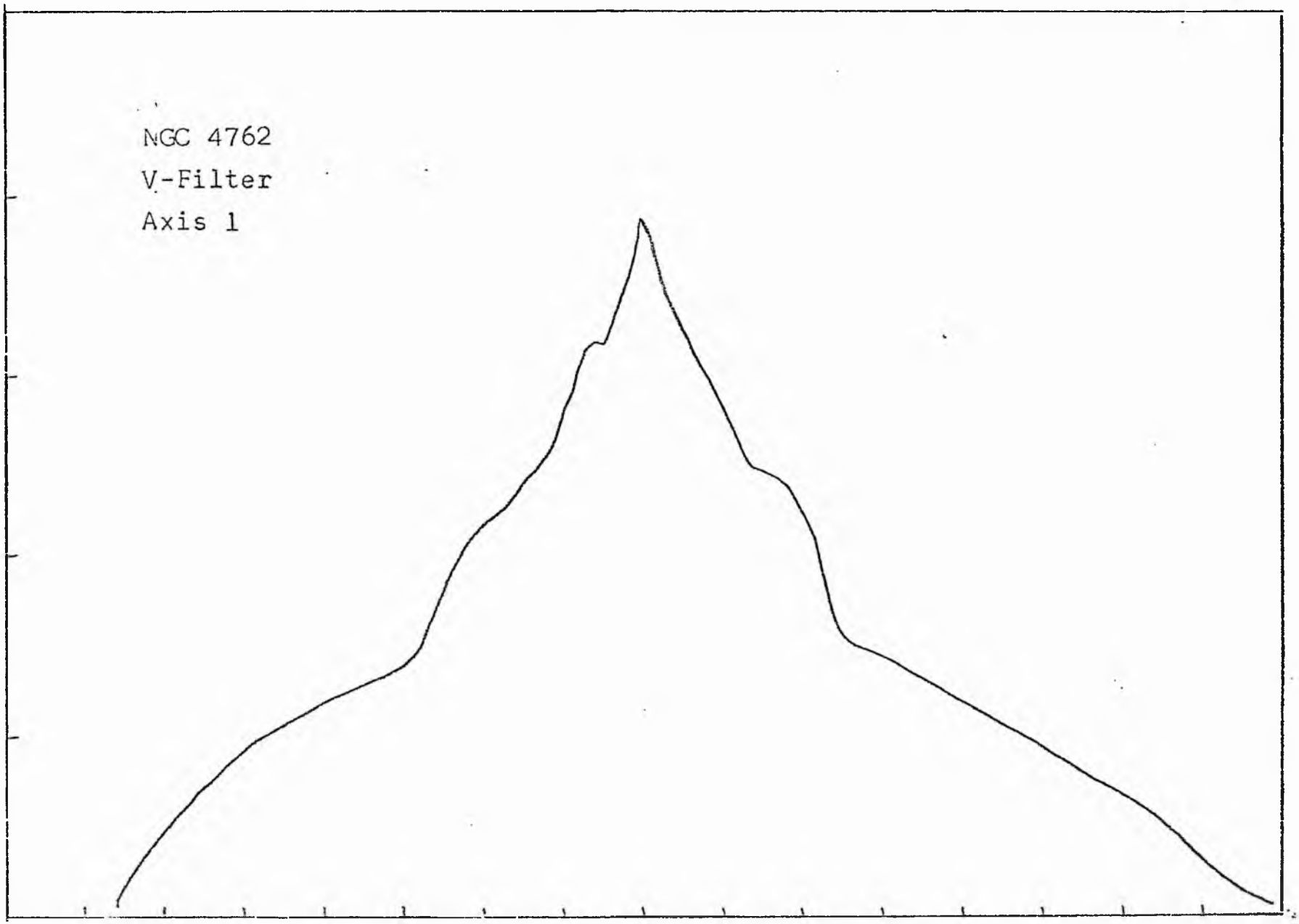
NGC 4762
V-Filter
Axis 1

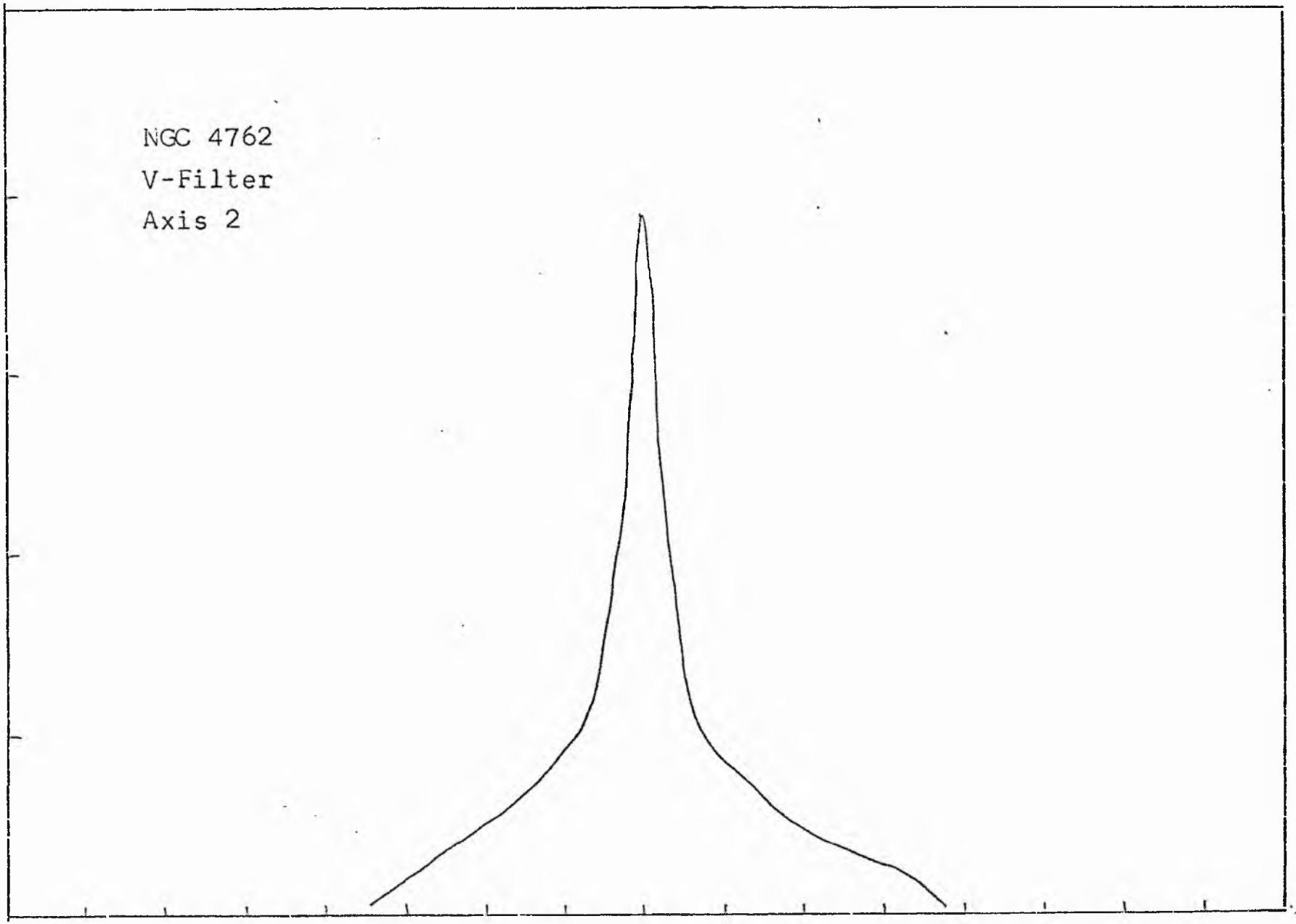
NGC 4762
V-Filter
Axis 2

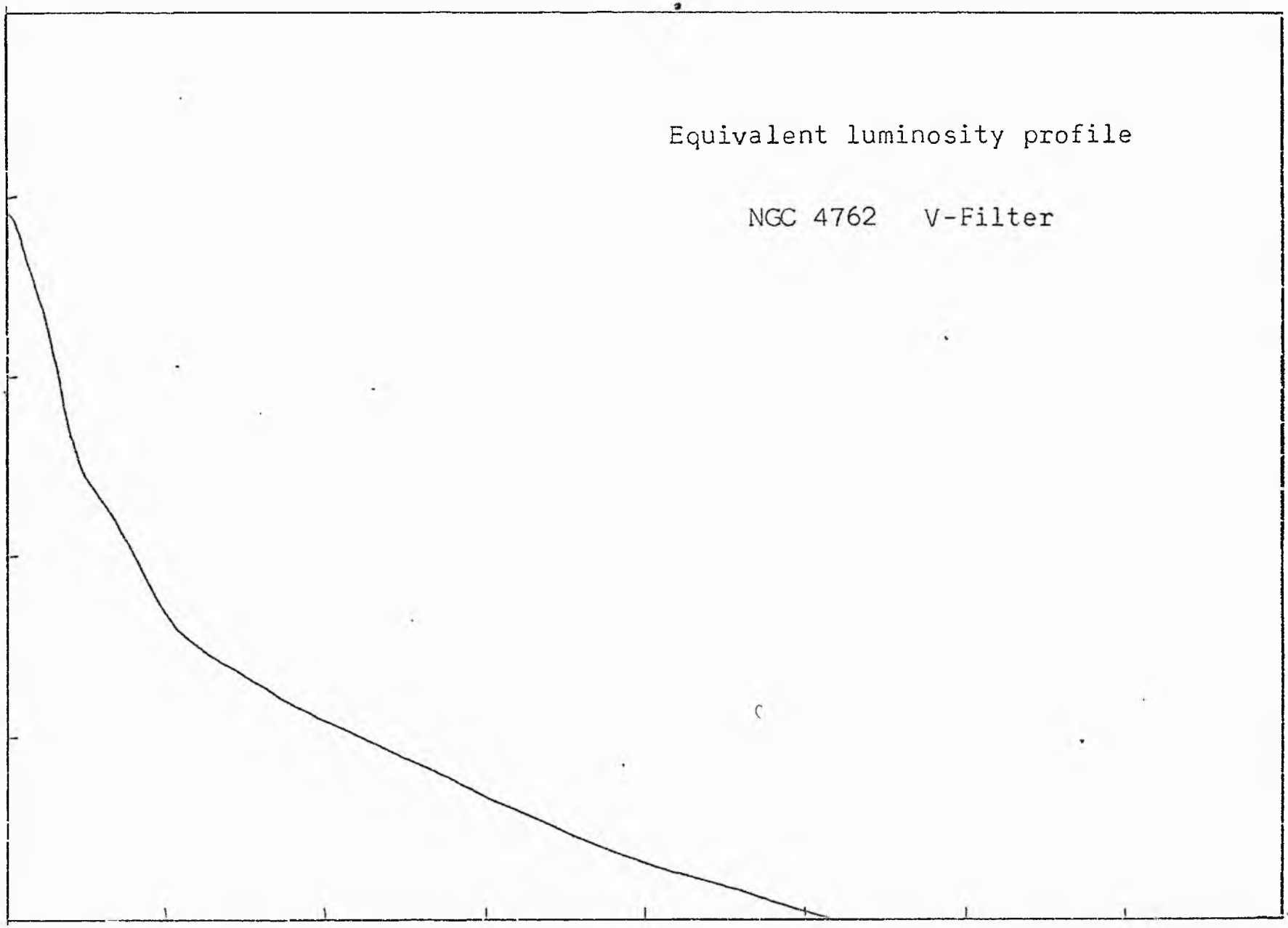
Equivalent luminosity profile
NGC 4762 V-Filter

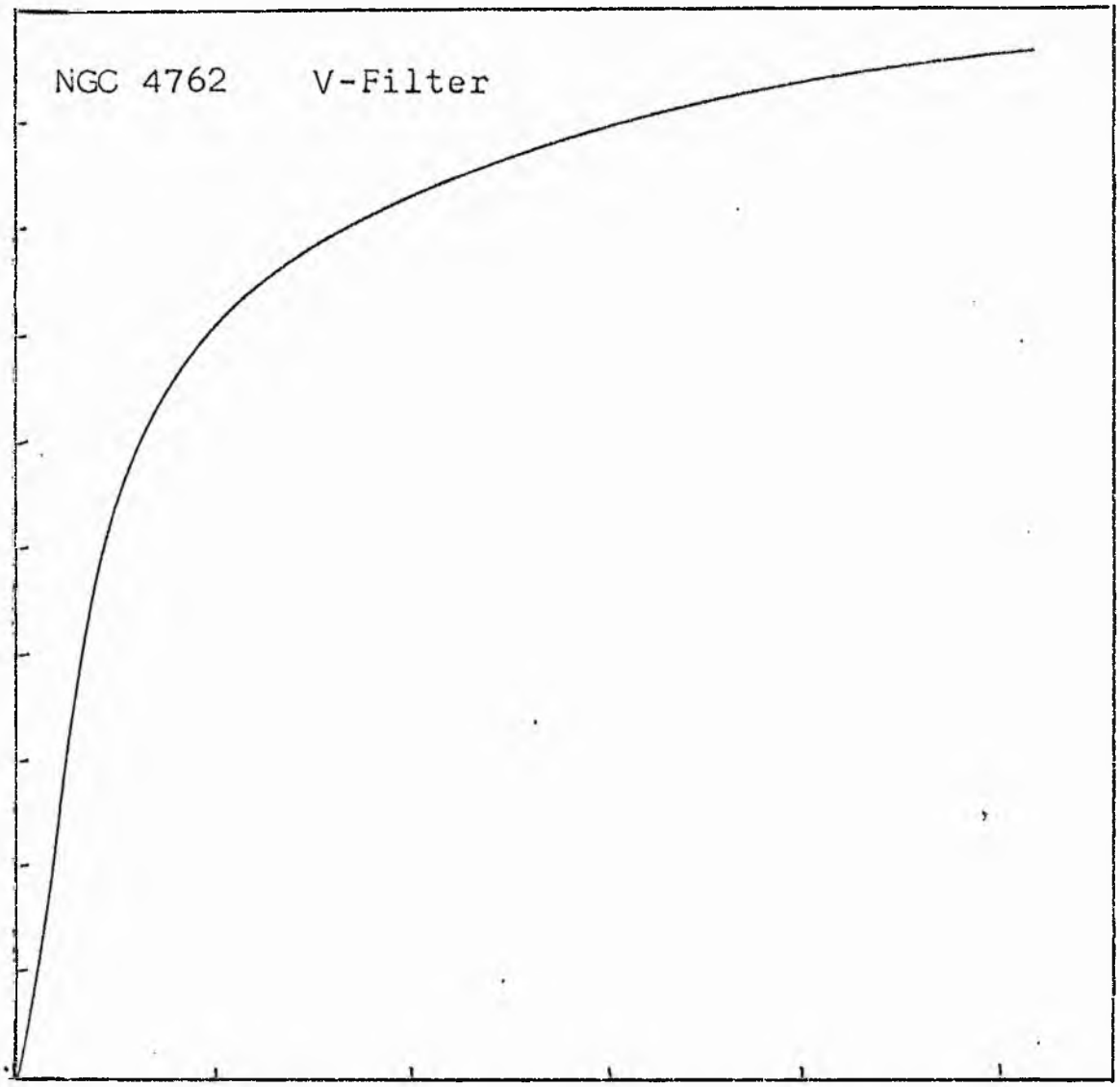

Relative integrated luminosity k(r) versus equivalent radius r*.

MEAN LUMINOSITY DISTRIBUTION IN NGC 4762
V COLOUR

LOG I	I	$\bar{I}$	R	AREA	ΔA	P	ΣP	K(R)	ρ	LOG J	μ
1.82	66.069		0.0	0.0			0.0	0.0	0.0	1.395	17.33
		64.582			4.52	292.1638					
1.80	63.096		1.20	4.52			292.16	0.01	0.06	1.375	17.38
		56.607			18.38	1040.3425					
1.70	50.119		2.70	22.90			1332.51	0.03	0.12	1.275	17.63
		44.965			29.91	1344.7964					
1.60	39.811		4.10	52.81			2677.30	0.07	0.19	1.175	17.88
		35.717			38.80	1385.7571					
1.50	31.623		5.40	91.61			4063.06	0.10	0.25	1.075	18.13
		28.371			191.92	5444.8906					
1.40	25.119		9.50	283.53			9507.95	0.24	0.44	0.975	18.38
		22.536			62.83	1415.9573					
1.30	19.952		10.50	346.36			10923.91	0.27	0.48	0.875	18.63
		17.901			47.72	854.2314					
1.20	15.849		11.20	394.08			11778.14	0.29	0.51	0.775	18.88
		14.219			170.02	2417.5525					
1.10	12.589		13.40	564.10			14195.69	0.35	0.61	0.675	19.13
		11.295			133.36	1506.2444					
1.00	10.000		14.90	697.46			15701.93	0.39	0.68	0.575	19.38
		8.972			76.91	689.9692					
0.90	7.943		15.70	774.37			16391.90	0.41	0.72	0.475	19.63
		7.126			187.74	1337.9165					
0.80	6.310		17.50	962.11			17729.81	0.44	0.80	0.375	19.88
		5.661			252.16	1427.3982					
0.70	5.012		19.66	1214.27			19157.21	0.48	0.90	0.275	20.13
		4.496			38.59	173.5398					
0.60	3.981		19.97	1252.87			19330.75	0.48	0.92	0.175	20.38
		3.572			128.62	459.3723					
0.50	3.162		20.97	1381.48			19790.12	0.49	0.96	0.075	20.63
		2.837			693.51	1967.5161					
0.40	2.512		25.70	2074.99			21757.63	0.54	1.18	-0.025	20.88
		2.254			905.25	2040.0295					
0.30	1.995		30.80	2980.24			23797.66	0.59	1.41	-0.125	21.13
		1.790			715.81	1281.3489					
0.20	1.585		34.30	3696.05			25079.01	0.62	1.57	-0.225	21.38
		1.422			628.07	893.0486					
0.10	1.259		37.10	4324.12			25972.05	0.64	1.70	-0.325	21.63
		1.129			652.29	736.7263					
-0.00	1.000		39.80	4976.40			26708.78	0.66	1.83	-0.425	21.88
		0.897			408.16	366.1838					
-0.10	0.794		41.40	5384.56			27074.96	0.67	1.90	-0.525	22.13
		0.713			1119.32	797.6699					
-0.20	0.631		45.50	6503.88			27872.63	0.69	2.09	-0.625	22.38
		0.566			674.15	381.6138					
-0.30	0.501		47.80	7178.03			28254.24	0.70	2.19	-0.725	22.63
		0.450			770.48	346.4402					
-0.40	0.398		50.30	7948.51			28600.68	0.71	2.31	-0.825	22.88
		0.357			1833.27	654.7812					
-0.50	0.316		55.80	9781.78			29255.46	0.73	2.56	-0.925	23.13
		0.284			3288.03	932.8345					
-0.60	0.251		64.50	13069.81			30188.29	0.75	2.96	-1.025	23.38
		0.225			4980.64	1122.4172					
-0.70	0.200		75.80	18050.45			31310.71	0.78	3.48	-1.125	23.63
		0.179			6112.45	1094.1692					
-0.80	0.158		87.70	24162.90			32404.87	0.80	4.02	-1.225	23.88
		0.142			3951.71	561.8933					
-0.90	0.126		94.60	28114.61			32966.77	0.82	4.34	-1.325	24.13
		0.113			7384.40	834.0356					
-1.00	0.100		106.30	35499.00			33800.80	0.84	4.87	-1.425	24.38
		0.090			10877.98	975.9292					
-1.10	0.079		121.50	46376.98			34776.73	0.86	5.57	-1.525	24.63
		0.071			13278.21	946.2595					
-1.20	0.063		137.80	59655.19			35722.98	0.89	6.32	-1.625	24.88
		0.057			5037.27	285.1455					
-1.30	0.050		143.50	64692.46			36008.13	0.89	6.58	-1.725	25.13
		0.045			8273.41	372.0115					
-1.40	0.040		152.40	72965.87			36380.14	0.90	6.99	-1.825	25.38
		0.036			16654.94	594.8611					
-1.50	0.032		168.90	89620.81			36975.00	0.92	7.75	-1.925	25.63
		0.028			18715.37	530.9719					
-1.60	0.025		185.70	108336.19			37505.96	0.93	8.52	-2.025	25.88
		0.023			22532.50	507.7886					
-1.70	0.020		204.10	130868.69			38013.75	0.94	9.36	-2.125	26.13
		0.018			23961.56	428.9329					
-1.80	0.016		222.00	154830.25			38442.68	0.95	10.18	-2.225	26.38
		0.014			21183.37	331.2104					
-1.90	0.013		236.70	176013.62			38743.89	0.96	10.85	-2.325	26.63
		0.011			20335.87	229.6881					
-2.00	0.010		250.00	196349.50			38973.57	0.97	11.46	-2.425	26.88
$-\infty$							40323.00	(1)			∞

PHOTOMETRIC PARAMETERS OF NGC 4762

V-FILTER

Total luminosity	L_T	= 11.20
Total apparent magnitude	m_T	= 10.37
Apparent central surface brightness	μ_o	= 17.33
Major axis at threshold	$2a_m$	= 11.60
Minor axis at threshold	$2b_m$	= 6.03
Major axis at μ=25.0 mag sec^{-2}	2a(25)	= 8.64
Luminosity within μ=25.0 mag sec^{-2}	k(25)	= 0.89
Gradient of exponential component	G(a)	= -0.57
Equivalent gradient of exponential comp.	G(r*)	= -0.44
Equivalent gradient of reduced exp. comp.	G(ρ)	= -0.74
Parameters at k = ¼ :		
Semi-major axis	a_1	= 0.31
Axis ratio	b/a	= 0.37
Equivalent radius	r_1*	= 0.17
Surface brightness	μ_1	= 18.46
Parameters at k = ½(effective) :		
Semi-major axis	a_e	= 1.16
Axis ratio	b/a	= 0.21
Equivalent radius	r_e*	= 0.36
Surface brightness	μ_e	= 20.68
Mean surface brightness	μ_e'	= 10.15
Parameters at k = ¾ :		
Semi-major axis	a_3	= 2.59
Axis ratio	b/a	= 0.22
Equivalent radius	r_3*	= 1.08
Surface brightness	μ_3	= 23.38
Concentration indices	C_{21}	= 2.20
	C_{32}	= 2.98